VOLUME 27 / NUMBER 17
SEPTEMBER 8, 1989
ACC. NOS. N89-23406 TO N89-24260

STAR
AN ABSTRACT JOURNAL

Scientific and Technical Aerospace Reports

PRODUCED BY THE
SCIENTIFIC AND TECHNICAL
INFORMATION
DIVISION

NASA

NATIONAL AERONAUTICS AND SPACE ADMINISTRATION

WHAT YOU CAN DO FOR *STAR*

All users of this abstract service are urged to forward reports to be considered for announcement in *STAR*. This will aid NASA in its efforts to provide the fullest possible coverage of all scientific and technical publications that might support aeronautics and space research and development. If you have prepared relevant reports (other than those that you will transmit to NASA, DoD, or DOE through the usual contract- or grant-reporting channels), please send them for consideration to the NASA Scientific and Technical Information Facility, P.O. Box 8757, BWI Airport, Maryland 21240.

Reprints of journal articles, book chapters, and conference papers are also welcome. These will be considered for announcement in *STAR's* companion journal, *International Aerospace Abstracts*.

You may specify a particular source to be included in a report announcement if you wish; otherwise the report will be placed on public sale at the National Technical Information Service. Copyrighted publications will be announced but not distributed or sold.

PURCHASE OF *STAR*

The semimonthly issues are available to registered users on annual subscription for $99.00 from the NASA Scientific and Technical Information Facility, ATTN: Registration Services, P.O. Box 8757, BWI Airport, MD 21240. *STAR* is publically available on annual subscription for $99.00 from the Superintendent of Documents, U.S. Government Printing Office, Washington, DC 20402.

PUBLISHED BY:

UNITED STATES GOVERNMENT
NATIONAL AERONAUTICS AND SPACE ADMINISTRATION
SCIENTIFIC AND TECHNICAL INFORMATION DIVISION
Scientific and Technical Aerospace Reports, Volume 27, is prepared by the NASA Scientific and Technical Information Facility operated for the National Aeronautics and Space Administration by RMS Associates.

The Administrator of the National Aeronautics and Space Administration has determined that the publication of this periodical is necessary in the transaction of the public business required by law of this Agency. Use of funds for printing this periodical has been approved by the Director of the Office of Management and Budget through March 22, 1989.

US ISSN 0036-8741

INTRODUCTION

Scientific and Technical Aerospace Reports (STAR) is a major component of a comprehensive National Aeronautics and Space Administration information system covering aeronautics, space, and supporting disciplines. *STAR* is issued on the 8th and 23rd of each month and announces current publications of the following types:

- NASA, NASA contractor, and NASA grantee reports
- Reports issued by other U.S. Government Agencies, domestic and foreign institutions, universities, and private firms
- Translations in report form
- NASA-owned patents and patent applications
- Other U.S. Government Agency and foreign patents and patent applications
- Domestic and foreign dissertations and theses

Journal, book, and conference literature, cover-to-cover journal translations, and certain foreign dissertations are announced in a companion journal, *International Aerospace Abstracts (IAA),* available on subscription from the American Institute of Aeronautics and Astronautics, Technical Information Service, 555 West 57th Street, 12th Floor, New York, New York 10019.

SUBJECT SCOPE

Subject scope of *STAR,* and *IAA* includes all aspects of aeronautics and space research and development, supporting basic and applied research, and applications. Aerospace aspects of earth resources, energy development, conservation, oceanography, environmental protection, urban transportation, and other topics of high national priority are also covered.

OTHER NASA PUBLICATIONS

Other NASA publications and information services are described in the publication, *The NASA Scientific and Technical Information System ... and How to Use It,* available without charge from the NASA Scientific and Technical Information Facility, P.O. Box 8757, BWI Airport, Maryland 21240.

HOW TO USE *STAR* SUBJECT CATEGORIES

STAR is categorized by 10 major subject divisions divided into 76 specific subject categories and one general category/division. The major subject divisions are listed in the Table of Contents, together with a note for each that defines its scope and provides any cross-references. For example:

AERONAUTICS

Includes aeronautics (general); aerodynamics; air transportation and safety; aircraft communications and navigation; aircraft design, testing and performance; aircraft instrumentation; aircraft propulsion and power; aircraft stability and control; and research and support facililties (air).

For related information see also *Astronautics.*

Each major division is further divided into as many as nine specific categories, which are identified by category numbers.

Abstracts in *STAR* are grouped by specific category, the categories appearing in sequential order. Category breaks in the abstract section are identified by the category number and title, and a scope note. Cross-references to other categories are provided as appropriate. For example:

02 AERODYNAMICS

Includes aerodynamics of bodies, combinations, wings, rotors, and control surfaces; and internal flow in ducts and turbomachinery.

For related information see also *34 Fluid Mechanics and Heat Transfer.*

CROSS-REFERENCES

Individual *STAR* abstracts are not ordinarily cross-referenced, except for certain conference reports or book translations that have had separate abstracts written for their component papers or chapters. Citations and abstracts of the components follow immediately after those of the parent document. When the subject content of a component differs sufficiently from the general content of the parent, a cross-reference citation also is printed at the end of the category to which it normally would have been assigned if it were independent.

DOCUMENTS ON MICROFICHE

Documents on microfiche(1) are designated by a pound sign (#) following the accession number. The pound sign is used without regard to the source or quality of the microfiche.

AVAILABILITIES

One or more sources from which a document announced in *STAR* is available to the public is given in each citation. The most commonly indicated sources and their acronyms or abbreviations are listed below. If the publication is available from a source other than those listed, the publisher and his address will be displayed on the availability line or in combination with the corporate source line.

Avail: NTIS. Sold by the National Technical Information Service. Prices for hard copy (HC) and microfiche (MF) are indicated by a price code following the letters HC or MF in the *STAR* citation. Current values for the price codes are given in the tables on page vii.

Initially distributed microfiche under the NTIS SRIM (Selected Research in Microfiche) is available at greatly reduced unit prices. For this service and for information concerning subscription to NASA printed reports, consult the NTIS Subscription Section, Springfield, Va. 22161.

NOTE ON ORDERING DOCUMENTS: When ordering NASA publications (those followed by the * symbol), use the N accession number. NASA patent applications (only the specifications are offered) should be ordered by the US-Patent-Appl-SN number. Non-NASA publications (no asterisk) should be ordered by the AD, PB, or other *report number* shown on the last line of the citation, not by the N accession number. It is also advisable to cite the title and other bibliographic identification.

Avail: SOD (or GPO). Sold by the Superintendent of Documents, U.S. Government Printing Office, in hard copy. The current price and order number are given following the availability line. (NTIS will fill microfiche requests, as indicated above, for those documents identified by a # symbol.)

(1) A microfiche is a transparent sheet of film, 105 by 148 mm in size, containing as many as 60 to 98 pages of information reduced to micro images (not to exceed 26:1 reduction).

Avail: BLL (formerly NLL): British Library Lending Division, Boston Spa, Wetherby, Yorkshire, England. Photocopies available from this organization at the price shown. (If none is given, inquiry should be addressed to the BLL.)

Avail: DOE Depository Libraries. Organizations in U.S. cities and abroad that maintain collections of Department of Energy reports, usually in microfiche form, are listed in *Energy Research Abstracts.* Services available from the DOE and its depositories are described in a booklet, *DOE Technical Information Center - Its Functions and Services* (TID-4660), which may be obtained without charge from the DOE Technical Information Center.

Avail: ESDU. Pricing information on specific data, computer programs, and details on ESDU topic categories can be obtained from ESDU International Ltd. Requesters in North America should use the Virginia address while all other requesters should use the London address, both of which are on page vi.

Avail: Fachinformationszentrum, Karlsruhe. Sold by the Fachinformationszentrum Energie, Physik, Mathematik GMBH, Eggenstein Leopoldshafen, Federal Republic of Germany, at the price shown in deutschmarks (DM).

Avail: HMSO. Publications of Her Majesty's Stationery Office are sold in the U.S. by Pendragon House, Inc. (PHI), Redwood City, California. The U.S. price (including a service and mailing charge) is given, or a conversion table may be obtained from PHI.

Avail: NASA Public Document Rooms. Documents so indicated may be examined at or purchased from the National Aeronautics and Space Administration, Public Documents Room (Room 126), 600 Independence Ave., S.W., Washington, D.C. 20546, or public document rooms located at each of the NASA research centers, the NASA Space Technology Laboratories, and the NASA Pasadena Office at the Jet Propulsion Laboratory.

Avail: Univ. Microfilms. Documents so indicated are dissertations selected from *Dissertation Abstracts* and are sold by University Microfilms as xerographic copy (HC) and microfilm. All requests should cite the author and the Order Number as they appear in the citation.

Avail: US Patent and Trademark Office. Sold by Commissioner of Patents and Trademarks, U.S. Patent and Trademark Office, at the standard price of $1.50 each, postage free. (See discussion of NASA patents and patent applications below.)

Avail: (US Sales Only). These foreign documents are available to users within the United States from the National Technical Information Service (NTIS). They are available to users outside the United States through the International Nuclear Information Service (INIS) representative in their country, or by applying directly to the issuing organization.

Avail: USGS. Originals of many reports from the U.S. Geological Survey, which may contain color illustrations, or otherwise may not have the quality of illustrations preserved in the microfiche or facsimile reproduction, may be examined by the public at the libraries of the USGS field offices whose addresses are listed in this Introduction. The libraries may be queried concerning the availability of specific documents and the possible utilization of local copying services, such as color reproduction.

Avail: Issuing Activity, or Corporate Author, or no indication of availability. Inquiries as to the availability of these documents should be addressed to the organization shown in the citation as the corporate author of the document.

NASA PATENTS AND PATENT APPLICATIONS

Patents and patent applications owned by NASA are announced in *STAR* under appropriate subject categories and are referenced in the *STAR* indexes. In the Report/Accession Number Index, patents are indexed by the NASA Case Number (which appears in lieu of the report number in other indexes), the U.S. Patent Number, the U.S. Patent Application Serial Number, and the U.S. Patent Class. Patent applications for which patents have not yet been issued are indexed by the NASA Case Number and the U.S. Patent Application Serial Number.

NASA *patent application specifications* are sold in paper copy by the National Technical Information Service at price code A02. Microfiche are sold at price code A01. The US-Patent-Appl-SN- number should be used in ordering either paper copy or microfiche from NTIS. Printed copies of *patents* (which are not microfiched) are available for purchase at $1.50 per copy from:

Commissioner of Patents and Trademarks
U.S. Patent and Trademark Office
Washington, D.C. 20231

When ordering patents, the U.S. Patent Number should be used, and payment must be remitted in advance, preferably by money order or check payable to the Commissioner of Patents and Trademarks. Prepaid purchase coupons for ordering are also available from the Patent and Trademark Office. The patents and patent applications announced in *STAR* are owned by NASA and are available for royalty-free licensing. Requests for licensing terms and further information should be addressed to:

Associate General Counsel for Intellectual Property/Code GP
National Aeronautics and Space Administration
Washington, D.C. 20546

ELIGIBILITY AND REGISTRATION FOR NASA INFORMATION PRODUCTS AND SERVICES

A variety of services is available to organizations of the following types that have registered with NASA to receive specific services or products:

1. NASA offices, research centers, contractors, subcontractors, grantees, and consultants;
2. Other U.S. Government agencies and their contractors;
3. Libraries in the United States that have arrangements with NASA to maintain collections of NASA documents for public reference;
4. Other organizations in the United States having a need for NASA documents in work related to aeronautics and space research;
5. Organizations abroad that have established reciprocal document exchange arrangements with NASA.

Only the central service points or central points of document acquisition and control within qualified organizations are eligible to register for NASA products and services. Domestic organizations that may be eligible to receive various classes of NASA publications and services should address their requests for registration or for further information to:

NASA Scientific and Technical Information Facility
ATTN: Registration Services
Post Office Box 8757
BWI Airport, Maryland 21240

Organizations abroad should direct requests to Manager, International STI Activities, NTT, NASA Headquarters, Washington, D.C. 20546.

AVAILABILITY OF *STAR* ABSTRACTS ON MICROFICHE

Microfiche of the abstract sections of this issue and other issues of *STAR* are available on annual subscription from NTIS as PB89-911300, Attn: Subscriptions, 5285 Port Royal Road, Springfield, Virginia 22161. Annual subscription rates are $70.00 North America; $140.00 foreign. Abstract sections for previous years retroactive to 1964 are available at the current rates. Microfiche for individual *STAR* issue abstract sections are not available.

PUBLIC COLLECTIONS OF NASA DOCUMENTS

DOMESTIC: NASA and NASA-sponsored documents and a large number of aerospace publications are available to the public for reference purposes at the library maintained by the American Institute of Aeronautics and Astronautics, Technical Information Service, 555 West 57th Street, 12th Floor, New York, New York 10019

EUROPEAN: An extensive collection of NASA and NASA-sponsored publications is maintained by the British Library Lending Division, Boston Spa, Wetherby, Yorkshire, England for public access. The British Library Lending Division also has available many of the non-NASA publications cited in *STAR*. European requesters may purchase facsimile copy or microfiche of NASA and NASA-sponsored documents, those identified by both the symbols # and * from ESA - Information Retrieval Service European Space Agency, 8-10 rue Mario-Nikis, 75738 Paris CEDEX 15, France.

FEDERAL DEPOSITORY LIBRARY PROGRAM

In order to provide the general public with greater access to U.S. Government publications, Congress established the Federal Depository Library Program under the Government Printing Office (GPO), with 50 regional depositories responsible for permanent retention of material, inter-library loan, and reference services. At least one copy of nearly every NASA and NASA-sponsored publication, either in printed or microfiche format, is received and retained by the 50 regional depositories. A list of the regional GPO libraries, arranged alphabetically by state, appears on the inside back cover. These libraries are *not* sales outlets. A local library can contact a Regional Depository to help locate specific reports, or direct contact may be made by an individual.

ADDRESSES OF ORGANIZATIONS

American Institute of Aeronautics and Astronautics
Technical Information Service
555 West 57th Street, 12th Floor
New York, New York 10019

British Library Lending Division,
Boston Spa, Wetherby, Yorkshire,
England

Commissioner of Patents and Trademarks
U.S. Patent and Trademark Office
Washington, D.C. 20231

Department of Energy
Technical Information Center
P.O. Box 62
Oak Ridge, Tennessee 37830

ESA-Information Retrieval Service
ESRIN
Via Galileo Galilei
00044 Frascati (Rome) Italy

ESDU International
P.O. Box 1633
Manassas, Virginia 22110

ESDU International, Ltd.
251-259 Regent Street
London, W1R 7AD, England

Fachinformationszentrum Energie, Physik, Mathematik GMBH
7514 Eggenstein Leopoldshafen
Federal Republic of Germany

Her Majesty's Stationery Office
P.O. Box 569, S.E. 1
London, England

NASA Scientific and Technical Information Facility
P.O. Box 8757
B.W.I. Airport, Maryland 21240

National Aeronautics and Space Administration
Scientific and Technical Information Division (NTT)
Washington, D.C. 20546

National Technical Information Service
5285 Port Royal Road
Springfield, Virginia 22161

Pendragon House, Inc.
899 Broadway Avenue
Redwood City, California 94063

Superintendent of Documents
U.S. Government Printing Office
Washington, D.C. 20402

University Microfilms
A Xerox Company
300 North Zeeb Road
Ann Arbor, Michigan 48106

University Microfilms, Ltd.
Tylers Green
London, England

U.S. Geological Survey Library
National Center - MS 950
12201 Sunrise Valley Drive
Reston, Virginia 22092

U.S. Geological Survey Library
2255 North Gemini Drive
Flagstaff, Arizona 86001

U.S. Geological Survey
345 Middlefield Road
Menlo Park, California 94025

U.S. Geological Survey Library
Box 25046
Denver Federal Center, MS914
Denver, Colorado 80225

NTIS PRICE SCHEDULES

(Effective January 1, 1989)

Schedule A
STANDARD PRICE DOCUMENTS AND MICROFICHE

PRICE CODE	NORTH AMERICAN PRICE	FOREIGN PRICE
A01	$ 6.95	$13.90
A02	10.95	21.90
A03	13.95	27.90
A04-A05	15.95	31.90
A06-A09	21.95	43.90
A10-A13	28.95	57.90
A14-A17	36.95	73.90
A18-A21	42.95	85.90
A22-A25	49.95	99.90
A99	*	*
NO1	55.00	70.00
NO2	55.00	80.00

Schedule E
EXCEPTION PRICE DOCUMENTS AND MICROFICHE

PRICE CODE	NORTH AMERICAN PRICE	FOREIGN PRICE
E01	$ 9.00	18.00
E02	11.50	23.00
E03	13.00	26.00
E04	15.50	31.00
E05	17.50	35.00
E06	20.50	41.00
E07	23.00	46.00
E08	25.50	51.00
E09	28.00	56.00
E10	31.00	62.00
E11	33.50	67.00
E12	36.50	73.00
E13	39.00	78.00
E14	42.50	85.00
E15	46.00	92.00
E16	50.50	101.00
E17	54.50	109.00
E18	59.00	118.00
E19	65.50	131.00
E20	76.00	152.00
E99	*	*

*Contact NTIS for price quote.

IMPORTANT NOTICE

NTIS Shipping and Handling Charges

U.S., Canada, Mexico — ADD $3.00 per TOTAL ORDER

All Other Countries — ADD $4.00 per TOTAL ORDER

Exceptions — Does NOT apply to:

ORDERS REQUESTING NTIS RUSH HANDLING
ORDERS FOR SUBSCRIPTION OR STANDING ORDER PRODUCTS *ONLY*

NOTE: Each additional delivery address on an order requires a separate shipping and handling charge.

VOLUME 27 NUMBER 17 / SEPTEMBER 8, 1989

TABLE OF CONTENTS

AERONAUTICS

Includes aeronautics (general); aerodynamics; air transportation and safety; aircraft communications and navigation; aircraft design, testing and performance; aircraft instrumentation; aircraft propulsion and power; aircraft stability and control; and research and support facilities (air).

For related information see also *Astronautics.*

01 AERONAUTICS (GENERAL) 2363

02 AERODYNAMICS 2363

Includes aerodynamics of bodies, combinations, wings, rotors, and control surfaces; and internal flow in ducts and turbomachinery.

For related information see also *34 Fluid Mechanics and Heat Transfer*

03 AIR TRANSPORTATION AND SAFETY 2368

Includes passenger and cargo air transport operations; and aircraft accidents.

For related information see also *16 Space Transportation* and *85 Urban Technology and Transportation.*

04 AIRCRAFT COMMUNICATIONS AND NAVIGATION 2368

Includes digital and voice communication with aircraft; air navigation systems (satellite and ground based); and air traffic control.

For related information see also *17 Space Communications, Spacecraft Communications, Command and Tracking* and *32 Communications and Radar.*

05 AIRCRAFT DESIGN, TESTING AND PERFORMANCE 2370

Includes aircraft simulation technology.

For related information see also *18 Spacecraft Design, Testing and Performance* and *39 Structural Mechanics.* For land transportation vehicles see *85 Urban Technology and Transportation.*

06 AIRCRAFT INSTRUMENTATION 2373

Includes cockpit and cabin display devices; and flight instruments.

For related information see also *19 Spacecraft Instrumentation* and *35 Instrumentation and Photography.*

07 AIRCRAFT PROPULSION AND POWER 2373

Includes prime propulsion systems and systems components, e.g., gas turbine engines and compressors; and onboard auxiliary power plants for aircraft.

For related information see also *20 Spacecraft Propulsion and Power, 28 Propellants and Fuels,* and *44 Energy Production and Conversion.*

08 AIRCRAFT STABILITY AND CONTROL 2374

Includes aircraft handling qualities; piloting; flight controls; and autopilots.

For related information see also *05 Aircraft Design, Testing and Performance.*

09 RESEARCH AND SUPPORT FACILITIES (AIR) 2375

Includes airports, hangars and runways; aircraft repair and overhaul facilities; wind tunnels; shock tubes; and aircraft engine test stands.

For related information see also *14 Ground Support Systems and Facilities (Space).*

ASTRONAUTICS

Includes astronautics (general); astrodynamics; ground support systems and facilities (space); launch vehicles and space vehicles; space transportation; space communications, spacecraft communications, command and tracking; spacecraft design, testing and performance; spacecraft instrumentation; and spacecraft propulsion and power.

For related information see also *Aeronautics*

12 ASTRONAUTICS (GENERAL) 2376

For extraterrestrial exploration see *91 Lunar and Planetary Exploration.*

13 ASTRODYNAMICS 2378

Includes powered and free-flight trajectories; and orbital and launching dynamics.

14 GROUND SUPPORT SYSTEMS AND FACILITIES (SPACE) 2379

Includes launch complexes, research and production facilities; ground support equipment, e.g., mobile transporters; and simulators.

For related information see also *09 Research and Support Facilities (Air).*

15 LAUNCH VEHICLES AND SPACE VEHICLES 2379

Includes boosters; operating problems of launch/space vehicle systems; and reusable vehicles.

For related information see also *20 Spacecraft Propulsion and Power.*

16 SPACE TRANSPORTATION 2379

Includes passenger and cargo space transportation, e.g., shuttle operations; and space rescue techniques.

For related information see also *03 Air Transportation and Safety* and *18 Spacecraft Design, Testing and Performance.* For space suits see *54 Man/System Technology and Life Support.*

17 SPACE COMMUNICATIONS, SPACECRAFT COMMUNICATIONS, COMMAND AND TRACKING N.A.

Includes telemetry; space communications networks; astronavigation and guidance; and radio blackout.

For related information see also *04 Aircraft Communications and Navigation* and *32 Communications and Radar.*

18 SPACECRAFT DESIGN, TESTING AND PERFORMANCE 2380

Includes satellites; space platforms; space stations; spacecraft systems and components such as thermal and environmental controls; and attitude controls.

For life support systems see *54 Man/System Technology and Life Support.* For related information see also *05 Aircraft Design, Testing and Performance, 39 Structural Mechanics,* and *16 Space Transportation.*

19 SPACECRAFT INSTRUMENTATION 2382

For related information see also *06 Aircraft Instrumentation* and *35 Instrumentation and Photography.*

20 SPACECRAFT PROPULSION AND POWER 2382

Includes main propulsion systems and components, e.g. rocket engines; and spacecraft auxiliary power sources.

For related information see also *07 Aircraft Propulsion and Power, 28 Propellants and Fuels, 44 Energy Production and Conversion,* and *15 Launch Vehicles and Space Vehicles.*

CHEMISTRY AND MATERIALS

Includes chemistry and materials (general); composite materials; inorganic and physical chemistry; metallic materials; nonmetallic materials; propellants and fuels; and materials processing.

23 CHEMISTRY AND MATERIALS (GENERAL) 2385

24 COMPOSITE MATERIALS 2398

Includes physical, chemical, and mechanical properties of laminates and other composite materials.

For ceramic materials see *27 Nonmetallic Materials.*

25 INORGANIC AND PHYSICAL CHEMISTRY 2401

Includes chemical analysis, e.g., chromatography; combustion theory; electrochemistry; and photochemistry.

For related information see also *77 Thermodynamics and Statistical Physics.*

26 METALLIC MATERIALS 2404

Includes physical, chemical, and mechanical properties of metals, e.g., corrosion; and metallurgy.

27 NONMETALLIC MATERIALS 2409

Includes physical, chemical, and mechanical properties of plastics, elastomers, lubricants, polymers, textiles, adhesives, and ceramic materials.

For composite materials see *24 Composite Materials.*

28 PROPELLANTS AND FUELS 2416

Includes rocket propellants, igniters and oxidizers; their storage and handling procedures; and aircraft fuels.

For related information see also *07 Aircraft Propulsion and Power, 20 Spacecraft Propulsion and Power,* and *44 Energy Production and Conversion.*

29 MATERIALS PROCESSING 2418

Includes space-based development of products and processes for commercial application.

For biological materials see *55 Space Biology.*

ENGINEERING

Includes engineering (general); communications and radar; electronics and electrical engineering; fluid mechanics and heat transfer; instrumentation and photography; lasers and masers; mechanical engineering; quality assurance and reliability; and structural mechanics.

For related information see also *Physics.*

31 ENGINEERING (GENERAL) 2419

Includes vacuum technology; control engineering; display engineering; cryogenics; and fire prevention.

32 COMMUNICATIONS AND RADAR 2421

Includes radar; land and global communications; communications theory; and optical communications.

For related information see also *04 Aircraft Communications and Navigation* and *17 Space Communications, Spacecraft Communications, Command and Tracking.* For search and rescue see *03 Air Transportation and Safety,* and *16 Space Transportation.*

33 ELECTRONICS AND ELECTRICAL ENGINEERING 2428

Includes test equipment and maintainability; components, e.g., tunnel diodes and transistors; microminiaturization; and integrated circuitry.

For related information see also *60 Computer Operations and Hardware* and *76 Solid-State Physics.*

34 FLUID MECHANICS AND HEAT TRANSFER 2431

Includes boundary layers; hydrodynamics; fluidics; mass transfer and ablation cooling.

For related information see also *02 Aerodynamics* and *77 Thermodynamics and Statistical Physics.*

35 INSTRUMENTATION AND PHOTOGRAPHY 2438

Includes remote sensors; measuring instruments and gages; detectors; cameras and photographic supplies; and holography.

For aerial photography see *43 Earth Resources and Remote Sensing.* For related information see also *06 Aircraft Instrumentation* and *19 Spacecraft Instrumentation.*

36 LASERS AND MASERS 2440

Includes parametric amplifiers.

For related information see also *76 Solid-State Physics.*

37 MECHANICAL ENGINEERING 2443

Includes auxiliary systems (nonpower); machine elements and processes; and mechanical equipment.

38 QUALITY ASSURANCE AND RELIABILITY 2445

Includes product sampling procedures and techniques; and quality control.

39 STRUCTURAL MECHANICS 2446

Includes structural element design and weight analysis; fatigue; and thermal stress.

For applications see *05 Aircraft Design, Testing and Performance* and *18 Spacecraft Design, Testing and Performance.*

GEOSCIENCES

Includes geosciences (general); earth resources and remote sensing; energy production and conversion; environment pollution; geophysics; meteorology and climatology; and oceanography.

For related information see also *Space Sciences.*

42 GEOSCIENCES (GENERAL) **N.A.**

43 EARTH RESOURCES AND REMOTE SENSING **2453**

Includes remote sensing of earth resources by aircraft and spacecraft; photogrammetry; and aerial photography.

For instrumentation see *35 Instrumentation and Photography.*

44 ENERGY PRODUCTION AND CONVERSION **2459**

Includes specific energy conversion systems, e.g., fuel cells; global sources of energy; geophysical conversion; and windpower.

For related information see also *07 Aircraft Propulsion and Power, 20 Spacecraft Propulsion and Power,* and *28 Propellants and Fuels.*

45 ENVIRONMENT POLLUTION **2460**

Includes atmospheric, noise, thermal, and water pollution.

46 GEOPHYSICS **2461**

Includes aeronomy; upper and lower atmosphere studies; ionospheric and magnetospheric physics; and geomagnetism.

For space radiation see *93 Space Radiation.*

47 METEOROLOGY AND CLIMATOLOGY **2464**

Includes weather forecasting and modification.

48 OCEANOGRAPHY **2465**

Includes biological, dynamic, and physical oceanography; and marine resources.

For related information see also *43 Earth Resources and Remote Sensing.*

LIFE SCIENCES

Includes life sciences (general); aerospace medicine; behavioral sciences; man/system technology and life support; and space biology.

51 LIFE SCIENCES (GENERAL) **2466**

52 AEROSPACE MEDICINE **2468**

Includes physiological factors; biological effects of radiation; and effects of weightlessness on man and animals.

53 BEHAVIORAL SCIENCES **2470**

Includes psychological factors; individual and group behavior; crew training and evaluation; and psychiatric research.

54 MAN/SYSTEM TECHNOLOGY AND LIFE SUPPORT **2471**

Includes human engineering; biotechnology; and space suits and protective clothing.

For related information see also *16 Space Transportation.*

55 SPACE BIOLOGY **N.A.**

Includes exobiology; planetary biology; and extraterrestrial life.

MATHEMATICAL AND COMPUTER SCIENCES

Includes mathematical and computer sciences (general); computer operations and hardware; computer programming and software; computer systems; cybernetics; numerical analysis; statistics and probability; systems analysis; and theoretical mathematics.

59 MATHEMATICAL AND COMPUTER SCIENCES (GENERAL) **N.A.**

60 COMPUTER OPERATIONS AND HARDWARE **2473**

Includes hardware for computer graphics, firmware, and data processing.

For components see *33 Electronics and Electrical Engineering.*

61 COMPUTER PROGRAMMING AND SOFTWARE **2474**

Includes computer programs, routines, algorithms, and specific applications, e.g., CAD/CAM.

62 COMPUTER SYSTEMS **2477**

Includes computer networks and special application computer systems.

63 CYBERNETICS **2479**

Includes feedback and control theory, artificial intelligence, robotics and expert systems.

For related information see also *54 Man/System Technology and Life Support.*

64 NUMERICAL ANALYSIS **2480**

Includes iteration, difference equations, and numerical approximation.

65 STATISTICS AND PROBABILITY **2484**

Includes data sampling and smoothing; Monte Carlo method; and stochastic processes.

66 SYSTEMS ANALYSIS **2485**

Includes mathematical modeling; network analysis; and operations research.

67 THEORETICAL MATHEMATICS **2486**

Includes topology and number theory.

PHYSICS

Includes physics (general); acoustics; atomic and molecular physics; nuclear and high-energy physics; optics; plasma physics; solid-state physics; and thermodynamics and statistical physics.

For related information see also *Engineering.*

70 PHYSICS (GENERAL) **2486**

For precision time and time interval (PTTI) see *35 Instrumentation and Photography;* for geophysics, astrophysics or solar physics see *46 Geophysics, 90 Astrophysics,* or *92 Solar Physics.*

71 ACOUSTICS 2487
Includes sound generation, transmission, and attenuation.
For noise pollution see *45 Environment Pollution.*

72 ATOMIC AND MOLECULAR PHYSICS 2488
Includes atomic structure, electron properties, and molecular spectra.

73 NUCLEAR AND HIGH-ENERGY PHYSICS 2488
Includes elementary and nuclear particles; and reactor theory.
For space radiation see *93 Space Radiation.*

74 OPTICS 2489
Includes light phenomena and optical devices.
For lasers see *36 Lasers and Masers.*

75 PLASMA PHYSICS 2490
Includes magnetohydrodynamics and plasma fusion.
For ionospheric plasmas see *46 Geophysics.* For space plasmas see *90 Astrophysics.*

76 SOLID-STATE PHYSICS 2493
Includes superconductivity.
For related information see also *33 Electronics and Electrical Engineering* and *36 Lasers and Masers.*

77 THERMODYNAMICS AND STATISTICAL PHYSICS 2499
Includes quantum mechanics; theoretical physics; and Bose and Fermi statistics.
For related information see also *25 Inorganic and Physical Chemistry* and *34 Fluid Mechanics and Heat Transfer.*

SOCIAL SCIENCES

Includes social sciences (general); administration and management; documentation and information science; economics and cost analysis; law, political science, and space policy; and urban technology and transportation.

80 SOCIAL SCIENCES (GENERAL) N.A.
Includes educational matters.

81 ADMINISTRATION AND MANAGEMENT 2499
Includes management planning and research.

82 DOCUMENTATION AND INFORMATION SCIENCE 2500
Includes information management; information storage and retrieval technology; technical writing; graphic arts; and micrography.
For computer documentation see *61 Computer Programming and Software.*

83 ECONOMICS AND COST ANALYSIS N.A.
Includes cost effectiveness studies.

84 LAW, POLITICAL SCIENCE AND SPACE POLICY N.A.
Includes NASA appropriation hearings; aviation law; space law and policy; international law; international cooperation; and patent policy.

85 URBAN TECHNOLOGY AND TRANSPORTATION 2501
Includes applications of space technology to urban problems; technology transfer; technology assessment; and surface and mass transportation.
For related information see *03 Air Transportation and Safety, 16 Space Transportation,* and *44 Energy Production and Conversion.*

SPACE SCIENCES

Includes space sciences (general); astronomy; astrophysics; lunar and planetary exploration; solar physics; and space radiation.
For related information see also *Geosciences.*

88 SPACE SCIENCES (GENERAL) 2502

89 ASTRONOMY 2502
Includes radio, gamma-ray, and infrared astronomy; and astrometry.

90 ASTROPHYSICS 2503
Includes cosmology; celestial mechanics; space plasmas; and interstellar and interplanetary gases and dust.
For related information see also *75 Plasma Physics.*

91 LUNAR AND PLANETARY EXPLORATION 2505
Includes planetology; and manned and unmanned flights.
For spacecraft design or space stations see *18 Spacecraft Design, Testing and Performance.*

92 SOLAR PHYSICS 2505
Includes solar activity, solar flares, solar radiation and sunspots.
For related information see *93 Space Radiation.*

93 SPACE RADIATION 2506
Includes cosmic radiation; and inner and outer earth's radiation belts.
For biological effects of radiation see *52 Aerospace Medicine.* For theory see *73 Nuclear and High-Energy Physics.*

GENERAL

Includes aeronautical, astronautical, and space science related histories, biographies, and pertinent reports too broad for categorization; histories or broad overviews of NASA programs.

99 GENERAL N.A.

Note: N.A. means that no abstracts were assigned to this category for this issue.

SUBJECT INDEX I-1
PERSONAL AUTHOR INDEX I-59
CORPORATE SOURCE INDEX I-67
CONTRACT NUMBER INDEX I-79
REPORT/ACCESSION NUMBER INDEX I-81

TYPICAL CITATION AND ABSTRACT

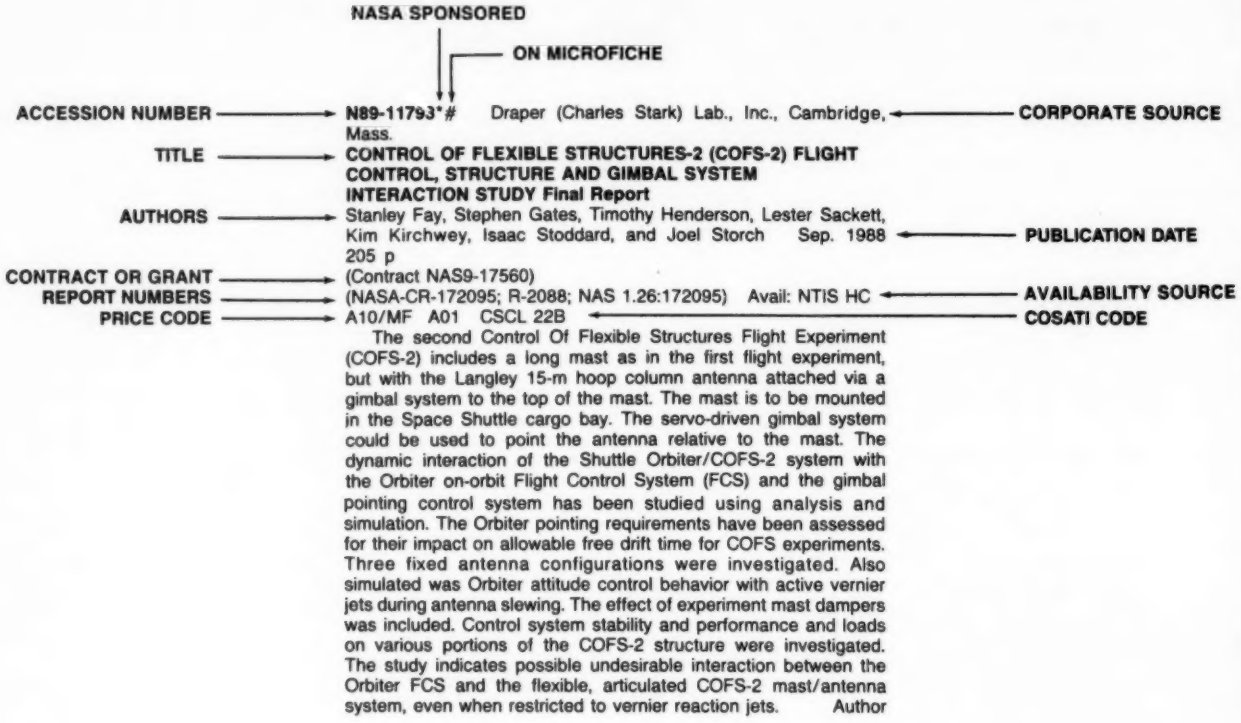
NASA SPONSORED
ON MICROFICHE
ACCESSION NUMBER
N89-11793*# Draper (Charles Stark) Lab., Inc., Cambridge, Mass.
CORPORATE SOURCE
TITLE
CONTROL OF FLEXIBLE STRUCTURES-2 (COFS-2) FLIGHT CONTROL, STRUCTURE AND GIMBAL SYSTEM INTERACTION STUDY Final Report
AUTHORS
Stanley Fay, Stephen Gates, Timothy Henderson, Lester Sackett, Kim Kirchwey, Isaac Stoddard, and Joel Storch Sep. 1988
PUBLICATION DATE
205 p
CONTRACT OR GRANT
(Contract NAS9-17560)
REPORT NUMBERS
(NASA-CR-172095; R-2088; NAS 1.26:172095) Avail: NTIS HC
AVAILABILITY SOURCE
PRICE CODE
A10/MF A01 CSCL 22B
COSATI CODE
The second Control Of Flexible Structures Flight Experiment (COFS-2) includes a long mast as in the first flight experiment, but with the Langley 15-m hoop column antenna attached via a gimbal system to the top of the mast. The mast is to be mounted in the Space Shuttle cargo bay. The servo-driven gimbal system could be used to point the antenna relative to the mast. The dynamic interaction of the Shuttle Orbiter/COFS-2 system with the Orbiter on-orbit Flight Control System (FCS) and the gimbal pointing control system has been studied using analysis and simulation. The Orbiter pointing requirements have been assessed for their impact on allowable free drift time for COFS experiments. Three fixed antenna configurations were investigated. Also simulated was Orbiter attitude control behavior with active vernier jets during antenna slewing. The effect of experiment mast dampers was included. Control system stability and performance and loads on various portions of the COFS-2 structure were investigated. The study indicates possible undesirable interaction between the Orbiter FCS and the flexible, articulated COFS-2 mast/antenna system, even when restricted to vernier reaction jets. Author

VOLUME 27 NUMBER 17 / SEPTEMBER 8, 1989

Scientific and Technical Aerospace Reports

A Semimonthly Publication of the National Aeronautics and Space Administration

01 AERONAUTICS (GENERAL)

N89-23406*# National Aeronautics and Space Administration, Washington, DC.
NASA AERONAUTICS RESEARCH AND TECHNOLOGY Annual Report
1986 60 p Original doc. contains color illustrations
(NASA-EP-259; NAS 1.19:259) Avail: NTIS HC A04/MF A01 CSCL 01B

The technical accomplishments and research highlights of 1986 are featured, along with information on possible areas of future research. These include hypersonic, supersonic, high performance, subsonic, and rotorcraft vehicle technology. Fundamental disciplinary research areas discussed include aerodynamics, propulsion, materials and structures, information sciences and human factors, and flight systems/safety. A description of the NASA organization and facilities is given. A.D.

N89-23407# Horizons Technology, Inc., Oakton, VA.
AN ANALYSIS OF ELECTRONIC AIDS TO MAINTENANCE (EAM) FOR THE LIGHT HELICOPTER FAMILY (LHX) Final Report, Sep. 1985 - May 1987
Edward W. Frederickson, John W. Lindquist, and Julie B. Lemen Jan. 1989 85 p
(Contract DAAG09-85-G-0035)
(AD-A205440; ARI-RN-89-09) Avail: NTIS HC A05/MF A01 CSCL 01/3

Substantial savings in maintenance manpower and training time, special tools, test equipment, and the storage and handling of repair parts have been predicted for weapons systems that incorporate electronic aids to maintenance (EAM) in their design. Performance deficiencies of weapon system's EAM could have serious consequences to both system availability and MPT (Manpower, Personnel, and Training) requirements. This report provides an overview of contemporary EAM technology. It identifies failures or inadequacies for EAM used in recent weapons systems and projects the results of EAM performance for the Light Helicopter Family (LHX). It also identifies MPT-related solutions relevant to the use of EAM in the LHX program. GRA

02 AERODYNAMICS

Includes aerodynamics of bodies, combinations, wings, rotors, and control surfaces; and internal flow in ducts and turbomachinery.

For related information see also *34 Fluid Mechanics and Heat Transfer.*

N89-23408# National Aerospace Lab., Tokyo (Japan).
TRANSONIC OPERATIONAL CHARACTERISTICS AND PERFORMANCE
Akira Koike, Keisuke Asai, Nobuyuki Hosoe, Toshio Karasawa, Hisashi Suenaga, Susumu Mitsubori, and Koichi Suzuki Mar. 1988 33 p In JAPANESE; ENGLISH summary
(NAL-TR-968; ISSN-0389-4010) Avail: NTIS HC A03/MF A01

Two turbine-powered simulators (TPSs) manufactured by Tech Development Inc. (Model 1079A), clad with nacelles of a generic configuration, are subjected to test in the NAL 2 x 2 m Transonic Wind Tunnel up to a Mach number of 0.8 in order to obtain data needed for use of the TPSs in a high-speed wind tunnel test of the NAT STOL research airplane ASKA. The TPSs are placed on top of a strut erected on the balance turn-table of the test-section floor so that the aerodynamic forces acting on the nacelle-strut system can be measured. Operational characteristics are obtained by measuring the TPS fan rotational speed as a function of the turbine-drive air pressure, and by observing the variation of the temperatures at the bearings supporting the TPS rotational part. Acceleration levels due to vibration are also measured. Instrumentation includes the total pressure-and temperature distributions within the fan and turbine nozzle flows to derive the TPS/nacelle performance represented by the fan pressure ratio, the mass flow through the fan and the magnitude of the thrust generated by the TPS/nacelle system. Author

N89-23409# National Aerospace Lab., Tokyo (Japan).
NUMERICAL SIMULATION OF HYPERSONIC FLOW AROUND A SPACE PLANE. 1: BASIC DEVELOPMENT
Yukimitsu Yamamoto and Shin Kubo May 1988 23 p In JAPANESE; ENGLISH summary
(NAL-TR-976T; ISSN-0389-4010) Avail: NTIS HC A03/MF A01

Thomas and Van Leer's flux-split upwind TVD scheme was applied to the hypersonic flow around a space plane proposed by National Aerospace Laboratory (NAL). Thin-layer Navier-Stokes equations in a finite volume formulation are solved by using an implicit approximately factored ADI algorithm. Numerical computations are performed for a Mach number of 7.0 and Reynolds number of 1.3 x 10(7) at angles of attack up to 30 degrees. Numerical results are compared with experimental data obtained from the hypersonic wind tunnel tests at NAL. Through these comparisons, it is demonstrated that the present TVD Navier-Stokes code has excellent capabilities for evaluating total aerodynamic performance and investigating severe aerodynamic heating, which are of great significance in the design of a space plane configuration. In the analysis, a modified Yee-Harten's TVD scheme is also developed and applied. Numerical calculations were carried out by using two schemes for free stream = 10.0 at alpha = 0 deg and almost the same pressure contours were obtained. Author

N89-23410*# National Aeronautics and Space Administration. Langley Research Center, Hampton, VA.
COMPUTING INDUCED VELOCITY PERTURBATIONS DUE TO A HELICOPTER FUSELAGE IN A FREE STREAM
John D. Berry and Susan L. Althoff Jun. 1989 65 p
(DA Proj. 1L1-62211-A-47-A)
(NASA-TM-4113; L-16533; NAS 1.15:4113; AVSCOM-TR-89-B-001) Avail: NTIS HC A04/MF A01 CSCL 01A

The velocity field of a representative helicopter fuselage in a free stream is computed. Perturbation velocities due to the fuselage are computed in a plan above the location of the helicopter rotor (rotor removed). The velocity perturbations computed by a source-panel model of the fuselage are compared with experimental measurements taken with a laser velocimeter. Three paneled fuselage models are studied: fuselage shape, fuselage shape with hub shape, and a body of revolution. The velocity perturbations

computed for both fuselage shape models agree well with the measured velocity field except in the close vicinity of the rotor hub. In the hub region, without knowing the extent of separation, modeling of the effective source shape is difficult. The effects of the fuselage perturbations are not well-predicted with a simplified ellipsoid fuselage. The velocity perturbations due to the fuselage at the plane of the measurements have magnitudes of less than 8 percent of free-stream velocity. The velocity perturbations computed by the panel method are tabulated for the same locations at which previously reported rotor-inflow velocity measurements were made. Author

N89-23411*# Old Dominion Univ., Norfolk, VA.
EXPERIMENTAL STUDY OF PRESSURE AND HEATING RATE ON A SWEPT CYLINDRICAL LEADING EDGE RESULTING FROM SWEPT SHOCK WAVE INTERFERENCE M.S. Thesis
Christopher E. Glass Apr. 1989 164 p Sponsored by NASA
(NASA-CR-185326; NAS 1.26:185326) Avail: NTIS HC
A08/MF A01 CSCL 01A

The effects of cylindrical leading edge sweep on surface pressure and heat transfer rate for swept shock wave interference were investigated. Experimental tests were conducted in the Calspan 48-inch Hypersonic Shock Tunnel at a nominal Mach number of 8, nominal unit Reynolds number of 1.5 x 10 to the 6th power per foot, leading edge and incident shock generator sweep angles of 0, 15, and 30 deg, and incident shock generator angle-of-attack fixed at 12.5 deg. Detailed surface pressure and heat transfer rate on the cylindircal leading edge of a swept shock wave interference model were measured at the region of the maximum surface pressure and heat transfer rate. Results show that pressure and heat transfer rate on the cylindrical leading edge of the shock wave interference model were reduced as the sweep was increased over the range of tested parameters. Peak surface pressure and heat transfer rate on the cylinder were about 10 and 30 times the undisturbed flow stagnation point value, respectively, for the 0 deg sweep test. A comparison of the 15 and 30 deg swept results with the 0 deg swept results showed that peak pressure was reduced about 13 percent and 44 percent, respectively, and peak heat transfer rate was reduced about 7 percent and 27 percent, respectively. Author

N89-23412*# National Aeronautics and Space Administration. Langley Research Center, Hampton, VA.
TRANSONIC AERODYNAMIC CHARACTERISTICS OF A PROPOSED ASSURED CREW RETURN CAPABILITY (ACRC) LIFTING-BODY CONFIGURATION
George M. Ware Jul. 1989 76 p
(NASA-TM-4117; L-16561; NAS 1.15:4117) Avail: NTIS HC
A05/MF A01 CSCL 01A

The investigation was conducted in the Calspan 8-Ft Transonic wind tunnel at Mach numbers from 0.6 to 1.2. The 0.07-scale model had a low aspect ratio body with a flat undersurface. A center fin and two tip fins were mounted on the aft upper body. The tip fins were rolled outboard 40 deg from the vertical. Elevon surfaces made up the trailing edges of the outboard fins and body flaps were located on the upper and lower aft fuselage. Results of the investigation indicated that the model was longitudinally and laterally stable about a center-of-gravity position of 0.54 body length. The maximum trimmed lift-drag ratio was about 3.1 at M = 0.6. The small center fin contributed only a small positive increment to lateral stability but was effective as a yaw control device. Protuberances on the forebody had little effect on the aerodynamic characteristics of the configuration. The model with pitch controls undeflected had desirable longitudinal trim characteristics. Author

N89-23413*# National Aeronautics and Space Administration. Lewis Research Center, Cleveland, OH.
NUMERICAL SOLUTION OF PERIODIC VORTICAL FLOWS ABOUT A THIN AIRFOIL
James R. Scott and Hafiz M. Atassi (Notre Dame Univ., IN.) 1989 12 p Presented at the 24th Thermophysics Conference, Buffalo, NY, 12-14 Jun. 1989; sponsored by the AIAA
(NASA-TM-101998; E-4703; NAS 1.15:101998) Avail: NTIS HC
A03/MF A01 CSCL 01A

A numerical method is developed for computing periodic, three-dimensional, vortical flows around isolated airfoils. The unsteady velocity is split into a vortical component which is a known function of the upstream flow conditions and the Lagrangian coordinates of the mean flow, and an irrotational field whose potential satisfies a nonconstant-coefficient, inhomogeneous, convective wave equation. Solutions for thin airfoils at zero degrees incidence to the mean flow are presented in this paper. Using an elliptic coordinate transformation, the computational domain is transformed into a rectangle. The Sommerfeld radiation condition is applied to the unsteady pressure on the grid line corresponding to the far field boundary. The results are compared with a Possio solver, and it is shown that for maximum accuracy the grid should depend on both the Mach number and reduced frequency. Finally, in order to assess the range of validity of the classical thin airfoil approximation, results for airfoils with zero thickness are compared with results for airfoils with small thickness. Author

N89-23414*# Continuum Dynamics, Inc., Princeton, NJ.
ENHANCEMENTS TO A NEW FREE WAKE HOVER ANALYSIS
Todd R. Quackenbush and Daniel A. Wachspress Apr. 1989 41 p
(Contract NAS2-12810)
(NASA-CR-177523; NAS 1.26:177523) Avail: NTIS HC
A03/MF A01 CSCL 01A

The results of three distinct efforts whose common goal was to enhance the applicability and utility of the EHPIC (Evaluation of Hover Performance using Influence Coefficients) free wake hover performance prediction program are summarized. The primary task in this three-part effort revolved around the addition of an image wake to the original version of the EHPIC analysis to permit exploration of the effect of ground proximity on rotor performance. Representative calculations were carried out to test the adequacy of the current ground effect model and the comparisons obtained with existing full-scale helicopter performance data was encouraging. The second task undertaken involved exploiting a capability that has been latent in the influence coefficient solution method since the original work on this topic. The modified EHPIC code can now undertake wake stability analyses for converged solutions using an existing eigensystem analysis package. Sample calculations are shown that illustrate some of the many possible applications of this capability. Finally, the EHPIC code was extensively rewritten to take advantage of the vector processing capabilities of CRAY-type supercomputers. Test runs on the NASA CRAY X-MP have shown that the modified version of the EHPIC code runs four to five times faster than the original version designed for serial processing machines. Author

N89-23415*# National Aeronautics and Space Administration. Langley Research Center, Hampton, VA.
STATUS OF SONIC BOOM METHODOLOGY AND UNDERSTANDING
Christine M. Darden, Clemans A. Powell, Wallace D. Hayes, Albert R. George, and Allan D. Pierce (Pennsylvania State Univ., University Park.) Washington Jun. 1989 32 p Presented at the Sonic Boom Workshop, Hampton, VA, Jan. 1988
(NASA-CP-3027; L-16567; NAS 1.55:3027) Avail: NTIS HC
A03/MF A01 CSCL 01A

In January 1988, approximately 60 representatives of industry, academia, government, and the military gathered at NASA-Langley for a 2 day workshop on the state-of-the-art of sonic boom physics, methodology, and understanding. The purpose of the workshop was to assess the sonic boom area, to determine areas where additional sonic boom research is needed, and to establish some strategies and priorities in this sonic boom research. Attendees included many internationally recognized sonic boom experts who had been very active in the Supersonic Transport (SST) and Supersonic Cruise Aircraft Research Programs of the 60's and 70's. Summaries of the assessed state-of-the-art and the research

needs in theory, minimization, atmospheric effects during propagation, and human response are given. Author

N89-23416*# National Aeronautics and Space Administration. Lewis Research Center, Cleveland, OH.
AVERAGE-PASSAGE SIMULATION OF COUNTER-ROTATING PROPFAN PROPULSION SYSTEMS AS APPLIED TO CRUISE MISSILES
Richard A. Mulac, Jon C. Schneider (McDonnell-Douglas Astronautics Co., Saint Louis, MO.), and John J. Adamczyk 1989 12 p Prepared for presentation at the 25th Joint Propulsion Conference, Monterey, CA, 10-12 Jul. 1989; sponsored by AIAA, ASME, SAE, and ASEE
(NASA-TM-102043; E-4791; NAS 1.15:102043; AIAA-89-2943) Avail: NTIS HC A03/MF A01 CSCL 01A

Counter-rotating propfan (CRP) propulsion technologies are currently being evaluated as cruise missile propulsion systems. The aerodynamic integration concerns associated with this application are being addressed through the computational modeling of the missile body-propfan flowfield interactions. The work described in this paper consists of a detailed analysis of the aerodynamic interactions between the control surfaces and the propfan blades through the solution of the average-passage equation system. Two baseline configurations were studied, the control fins mounted forward of the counter-rotating propeller and the control fins mounted aft of the counter-rotating propeller. In both cases, control fin-propfan separation distance and control fin deflection angle were varied. Author

N89-23417*# National Aeronautics and Space Administration. Lewis Research Center, Cleveland, OH.
THE LOW FREQUENCY OSCILLATION IN THE FLOW OVER A NACA0012 AIRFOIL WITH AN ICED LEADING EDGE
K. B. M. Q. Zaman and M. G. Potapczuk 1989 16 p Presented at the Conference on Low Reynolds Number Aerodynamics, Notre Dame, IN, 5-7 Jun. 1989; sponsored by Notre Dame Univ.
(NASA-TM-102018; E-4727; NAS 1.15:102018) Avail: NTIS HC A03/MF A01 CSCL 01A

The unusually low frequency oscillation in the wake of an airfoil is explored experimentally as well as computationally for a NACA0012 airfoil with a glaze ice accretion at the leading edge. Experimentally, flow oscillations were observed at low frequencies that correspond to a Strouhal number of about 0.02. This occurred in the angle of attack range of 8 to 9 deg, near the onset of static stall for this airfoil. With a Navier-Stokes computation, limit-cycle oscillations in the flow and in the aerodynamic forces were also observed at low Strouhal numbers. However, the occurrence of the oscillation is found to depend on the turbulence model in use as well as the Reynolds number. Author

N89-23418*# California Univ., Davis. Div. of Aeronautical Science and Engineering.
HIGH ANGLE-OF-ATTACK AERODYNAMIC CHARACTERISTICS OF CRESCENT AND ELLIPTIC WINGS Final Report
C. P. vanDam May 1989 38 p
(Grant NAG1-732)
(NASA-CR-184992; NAS 1.26:184992) Avail: NTIS HC A03/MF A01 CSCL 01A

Static longitudinal and lateral-directional forces and moments were measured for elliptic- and crescent-wing models at high angles-of-attack in the NASA Langley 14 by 22-Ft Subsonic Tunnel. The forces and moments were obtained for an angle-of-attack range including stall and post-stall conditions at a Reynolds number based on the average wing chord of about 1.8 million. Flow-visualization photographs using a mixture of oil and titanium-dioxide were also taken for several incidence angles. The force and moment data and the flow-visualization results indicated that the crescent wing model with its highly swept tips produced much better high angle-of-attack aerodynamic characteristics than the elliptic model. Leading-edge separation-induced vortex flow over the highly swept tips of the crescent wing is thought to produce this improved behavior at high angles-of-attack. The unique planform design could result in safer and more efficient low-speed airplanes. Author

N89-23419 California Univ., Davis.
A NUMERICAL SCHEME TO SOLVE UNSTEADY AND VARIABLE DENSITY LOW MACH NUMBER FLOWS Ph.D. Thesis
Mohamed Ahmed Fahmy Soliman 1988 141 p
Avail: Univ. Microfilms Order No. DA8821727

A numerical scheme is developed to solve unsteady low Mach number flows which are subject to large density gradients due to heat addition. The ultimate object is to use that scheme in solving the diffusion flame flow over a porous sphere. The system of equations which are solved for such a flow are the two-dimension unsteady continuity, momentum, energy, species and the equation of state. The conservation equations were iterated inside every time step until convergence. An approximate fractional step scheme is used with a regular grid for the simultaneous solution of the continuity and momentum equations. An approximate technique is used to avoid the decoupling problem in the resulting Poission equation for the pressure. The use of a direct solver to solve the Poission equation for pressure is essential in such unsteady solutions to keep the computational cost down. The scheme was used first to obtain the unsteady solutions for three different flows over both a cylinder and a sphere in incompressible flow, incompressible flow with injection at the wall and a hot flow over a cold wall. The scheme is then used to compute the ignition of a diffusion flame flow resulting from the flow of hot air over a porous sphere from which methane is injected. The diffusion flame flow results were obtained using two different sizes for the sphere with 0.5 cm show a thin envelope flame at the upstream side of the flow field, while the results obtained using a sphere with 0.1 cm show a thick wake flame ignite at the downstream side of the flow field. The results obtained for the larger sphere show that to continue the computation an adaptive grid has to be used to resolve the steep gradients at the thin flame. Dissert. Abstr.

N89-23420# Stanford Univ., CA. Thermosciences Div.
AN EXPERIMENTAL STUDY OF THE EFFECT OF STREAMWISE VORTICES ON UNSTEADY TURBULENT BOUNDARY-LAYER SEPARATION
W. W. Humphreys and W. C. Reynolds 9 Dec. 1988 273 p
(Contract F49620-86-K-0020)
(AD-A205462; TF-42; AFOSR-89-0275TR) Avail: NTIS HC A12/MF A01 CSCL 01/3

This experiment studied the effect of streamwise vortices on unsteady turbulent boundary-layer separation. The objectives were to document the flow field, to characterize the time response of the boundary layer, and to understand the actual mechanisms by which the streamwise vortices modify boundary-layer behavior. A new configuration for non-obtrusive three-component Laser Doppler Anemometry (LDA) determined the phase averaged velocity and Reynolds stress components, in an unsteady water tunnel, at a momentum thickness Reynolds number of 1840. The streamwise vortices were created by three pairs of half-delta wing vortex generators, while the boundary-layer separation was controlled through impulsively initiated opposite-wall suction, which created a strong adverse pressure gradient. The time response of the freestream velocity demonstrates that convection is the primary mechanism by which vortex generators modify the response of the boundary layer. There is an initial fast response throughout the boundary layer which is unaffected by the presence of vortex generators, followed by a slow or convective response, the magnitude of which is substantially modified by the presence of the vortex generators. GRA

N89-23421# Texas Univ., Austin. Dept. of Aerospace Engineering and Engineering Mechanics.
EFFECTS OF INITIAL CONDITIONS ON THE DEVELOPMENT OF SUPERSONIC TURBULENT FREE SHEAR LAYERS Final Report, 1 Feb. 1987 - 31 Oct. 1988

D. S. Dolling and Y. R. Shau 20 Feb. 1989 37 p
(Contract N00014-87-K-0128)
(AD-A205607) Avail: NTIS HC A03/MF A01 CSCL 21/2

A start has been made on studying the effects of initial conditions on the development of supersonic turbulent shear layers. The shear layer model and its air supply system have been designed and constructed. Tuning of the air supply control system as well as basic hardware validation were performed. Most of the required instrumentation has been designed and built. Pitot pressure measurements of the undisturbed shear layer have been taken and documented, these results were used as a baseline for the comparison of cases with shock wave impingement. Two types of disturbance have been tested; those generated by shock wave/boundary layer interaction; and those caused by shock wave/shear layer interaction. In the preliminary testing, pitot pressure measurements for the shear layer with disturbance were made only at two streamwise stations. At the last measurement station, the shear layer thickness increases substantially when shock wave/boundary layer interaction occurs upstream of the nozzle lip. Qualitatively, the results indicate that the spreading rate can be enhanced using planar shock wave impingement. GRA

N89-23422# Naval Postgraduate School, Monterey, CA.
FLOWFIELD MEASUREMENTS IN THE VORTEX WAKE OF A MISSILE AT HIGH ANGLE OF ATTACK IN TURBULENCE M.S. Thesis
Ming-Hung Lung Dec. 1988 143 p
(AD-A205696) Avail: NTIS HC A07/MF A01 CSCL 20/4

The flowfield downstream of a vertically-launched surface-to-air missile model at an angle of attack of 50 deg and a Reynolds number of 1.1 million was investigated in an NPG wind tunnel. The goal of this thesis is to experimentally validate the pressure measurement system for flowfield variables with elevated levels of turbulence; to determine the location and intensity of the asymmetric vortices in the wake of the VLSAM model at a raised level of freestream turbulence; and to display the asymmetric vortices by velocity mapping and pressure contours. The purpose is to correlate the results with the force measurements of Rabang to provide a greater understanding of the vortex flowfield. The body-only configuration was tested. Two flowfield conditions were treated: the nominal ambient wind tunnel condition, and a condition with grid-generated turbulence of 3.8 percent turbulence intensity and a dissipation length scale of 1.7 inches. The following conclusions were reached: (1) the relative strengths of the asymmetric vortices can be noted by the sharp spike shape in the ambient condition; this condition becomes diffused and becomes fatter in the turbulent condition; (2) the right side vortex has greater strength than the left side one as seen by the diffusion in the total pressure coefficient and static pressure coefficient contours with and without a turbulent condition; (3) an increase in turbulence intensity tends to reduce the strength of the asymmetric nose-generated vortices and pushes the two asymmetric vortices closer together; and (4) cross flow velocities were examined and were found to indicate the behavior denoted by the pressure contours. GRA

N89-23423# Arizona State Univ., Tempe. Dept. of Mechanical and Aerospace Engineering.
DEVELOPMENT OF HARMONIC PANEL METHODS FOR AEROELASTIC APPLICATIONS TO ELASTIC BODIES AND BODY-FIN COMBINATIONS IN SUPERSONIC FLOW Final Report, Jan. 1984 - Dec. 1988
D. D. Liu and Pablo Garcia-Fogeda Jan. 1989 201 p
(Contract DAAG29-84-K-0004)
(AD-A205739; ASU-CR-R-89021; ARO-20928.6-EG) Avail: NTIS HC A10/MF A01 CSCL 20/4

Recent development of several unsteady supersonic methods for computations of airloads for elastic bodies of revolution, asymmetric bodies and body wing configurations are reported. These methods include the Harmonic Potential Panel (HPP) method, the Bundle Triplet Method (BTM) and the combined method of BTM and the Harmonic Gradient Method (HGM) for body wing combinations. All methods are based on the generic Harmonic Gradient (H-G) model, which is essential in providing accurate solutions in the full frequency domain and the low Mach number range. Extensive comparisons of computed results obtained from these methods show good correlations with existing data. Comparison examples range from simple cones and ogive bodies to Saturn SA-1 configuration, to the cylindrical panel membrance and to the NACA wing-body combinations. Cases computed yield steady and unsteady pressures, generalized forces, stability derivatives, aerodynamic dampings and divergence and flutter boundaries for these configurations. The developed methods have been validated with existing theories or measured data. For supersonic aeroelastic analysis, these methods yield results that are accurate and cost-effective, thus rendering them very favorable for technology transfer and industry applications. GRA

N89-23424# Air Force Inst. of Tech., Wright-Patterson AFB, OH. School of Engineering.
NAVIER-STOKES SOLUTION FOR A NACA 0012 AIRFOIL WITH MASS FLUX (FAN) M.S. Thesis
Paul D. Boyles Dec. 1988 140 p
(AD-A205771; AFIT/GAE/AA/88D-02) Avail: NTIS HC A07/MF A01 CSCL 01/1

STOL aircraft use a variety of mechanisms to augment lift. Small fans with vectored exhaust imbedded in an aircraft wing could increase lift and reduce drag. The aim of this thesis is to investigate the two-dimensional effect of a small fan in wing on the flow field and on the lift and drag behavior of a NACA 0012 airfoil. Numerical solutions are obtained for a Mach number of 0.3 and a Reynolds number of one million. The parameters examined are angle of attack, fan ejection angle and suction velocity. The numerical code used is based on the Beam-Warming implicit factorization algorithm for solving the two-dimensional mass-averaged compressible Navier-Stokes equations for viscous, unsteady flows. GRA

N89-23425# Air Force Inst. of Tech., Wright-Patterson AFB, OH. School of Engineering.
INVESTIGATION OF THE FLOWFIELD CREATED BY THE INTERACTION OF A SONIC JET AND A CO-FLOWING SUPERSONIC STREAM M.S. Thesis
Benoit J. Durand Dec. 1988 142 p
(AD-A205823; AFIT/GAE/AA/88D-11) Avail: NTIS HC A07/MF A01 CSCL 20/4

Flowfield characteristics created by a sonic flow expanding freely between two supersonic streams were investigated experimentally using optical and pressure instrumentation. The base flow produced by the expansion of the streams around the base regions is compared to experimental data and theory by Chow. The shear layer created between the sonic and supersonic stream was also studied using Schlieren photographs is examined in an effort to explain the observed flow phenomenon. It was observed that a shear layer crossing a shock wave spreads and increases its turbulence level. However, an undesirable loss in total pressure results which could be undesirable. It appears that Chow's theory on base pressure approximates the characteristics of the flow near the end of the nozzle assembly where the two flows initially interact. The same trends were observed in the behavior of base pressure with increasing secondary total pressure as Chow observed during his experiment. The convective Mach number concept was successfully applied to the sonic injection geometry and it was demonstrated that the convective Mach number decreases drastically as the secondary pressure is increased. This is an indication that the growth rate of the shear layer increases, giving a faster mixing rate. GRA

N89-23426# Stanford Univ., CA.
FLOW CONTROL FOR UNSTEADY AND SEPARATED FLOWS AND TURBULENT MIXING Annual Report, 1 Oct. 1987 - 30 Sep. 1988
J. K. Eaton, Lambertus Hesselink, J. P. Johnston, I. M. Kroo, J. D. Powell, L. Roberts, and W. C. Reynolds 31 Oct. 1988 51 p

(Contract F49620-86-K-0020)
(AD-A205989; AFOSR-89-0232TR) Avail: NTIS HC A04/MF A01 CSCL 01/1

A coordinated set of experimental research projects on flow control is being conducted by a team with experience in fluid mechanics and automatic control. The primary objective of this work is to develop new ways to control flows of technical interest and a generic approach to the design of flow control systems. Included are studies of mixing enhancement by excitation of jets, active control of unsteady turbulent boundary layers and separated flows, and active control of the vortical flow over delta wings using leading-edge blowing. GRA

N89-23427# Air Force Inst. of Tech., Wright-Patterson AFB, OH. School of Engineering.
EJECTOR EFFECTS ON A SUPERSONIC NOZZLE AT LOW ALTITUDE AND MACH NUMBER M.S. Thesis
Christopher A. Seaver Dec. 1988 105 p
(AD-A206049; AFIT/GAE/AA/88D-33) Avail: NTIS HC A06/MF A01 CSCL 01/1

This research involves the study of ejector effects on a supersonic nozzle. A blowdown wind tunnel was used to simulate the launch of an ejector rocket to determine possible thrust augmentation capabilities of such a design. Pressure measurements were made along the mixing chamber during the 42 separate runs which were used to select a specified profile to study the effects the flow has on wall pressures and rocket thrust. Primary airflow was directed to the primary rocket nozzle designed for Mach 3.09. Secondary airflow was directed to a sonic ejector which was adjusted to simulate vehicle Mach number. A vacuum tank was used to provide the environment simulating a reverse trajectory of a launch. GRA

N89-23428# Air Force Inst. of Tech., Wright-Patterson AFB, OH. School of Engineering.
NUMERICAL STUDY OF THE INFLUENCE OF LEADING AND TRAILING EDGE FLAPS ON THE PERFORMANCE OF AIRFOILS M.S. Thesis
Faran Hafeez Mar. 1989 164 p
(AD-A206138; AFIT/GAE/AA/89M-2) Avail: NTIS HC A08/MF A01 CSCL 01/1

The purpose of this study is to develop a code based on the Approximate Navier Stokes (ANS) equations (in the Vorticity Stream Function delta form). The Wortman FX 63-137 airfoil fitted with leading and trailing edge devices has been analyzed at low Reynolds Number (100,000) at various angles of attack and various deflection angles. Results are compared to the experimental data. The agreement is very good at small angles of attack. However, at large angles of attack the disparity is larger, and improvements have been recommended which will resolve this disparity. Overall the present scheme produces very reasonable results, with good repeatability and fast convergence, and has the potential of being developed into an effective design tool. GRA

N89-23429# Bolt, Beranek, and Newman, Inc., Canoga Park, CA.
NOISE AND SONIC BOOM IMPACT TECHNOLOGY. PCBOOM COMPUTER PROGRAM FOR SONIC BOOM RESEARCH, VOLUME 1 Final Report, May 1987 - Oct. 1988
Dwight E. Bishop Oct. 1988 56 p
(Contract F33615-86-C-0530)
(AD-A206290; BBN-6741-Vol-1; HSD-TR-88-014-Vol-1) Avail: NTIS HC A04/MF A01 CSCL 20/1

The PCBOOM computer program, described in this technical report, calculates the location and magnitude of sonic boom overpressures on the ground due to supersonic flight under standard atmosphere and no wind propagation conditions. The program is intended for environmental planners and engineers who may need to estimate the noise impact from individual flights of supersonic military aircraft. The program runs on a Zenith Z-248 personal computer and also should run on most similarly configured IBM-compatible computers. The program contains information for all current military aircraft and allows updating for additional aircraft. The user can select either Quick look computations which assume steady-state flight or detailed ray-tracing calculations which can handle non-steady flight and sonic boom focus conditions. Several types of simple maneuvers can be selected for computations; the program will also handle up to ten connected straight line segments. Flight segments from the MOAOPS library of supersonic combat training flights may also be selected. User-specified output for printer, plotter or screen includes tables of overpressures and graphic display of the sonic boom overpressure footprints on the ground. GRA

N89-23430# Bolt, Beranek, and Newman, Inc., Canoga Park, CA.
NOISE AND SONIC BOOM IMPACT TECHNOLOGY. PCBOOM COMPUTER PROGRAM FOR SONIC BOOM RESEARCH. VOLUME 2: PROGRAM USERS/COMPUTER OPERATIONS MANUAL Final Report, May 1987 - Oct. 1988
Augustine Salvetti and Harry Seidman Oct. 1988 58 p
(Contract F33615-86-C-0530)
(AD-A206291; BBN-6742-Vol-2; HSD-TR-88-014-Vol-2) Avail: NTIS HC A04/MF A01 CSCL 20/1

This report contains the information for both the user and for computer operations. The report provides the user with the information necessary to effectively use PCBOOM. In addition, it provides the computer operations personnel with a description of the computer system and its associated environment. Two other reports provide a technical discussion of the algorithms used and a program maintenance manual. GRA

N89-23431# Nielsen Engineering and Research, Inc., Mountain View, CA.
COMPUTATIONAL STUDY OF HIGH SUPERSONIC FLOW OVER BOATTAILS WITH CENTERED PROPULSIVE JETS Final Report, 1 Nov. 1985 - 31 Oct. 1988
Robert E. Childs 31 Jan. 1989 26 p
(Contract DAAL03-86-C-0002)
(AD-A206364; NEAR-TR-397) Avail: NTIS HC A03/MF A01 CSCL 20/4

The present study concerns the ability to achieve good accuracy in missile after body flow predictions based on the Reynolds-averaged Navier-Stokes equations. The problems of numerical accuracy and turbulence modeling are addressed. By employing grids which were cell clustered and which have grid lines aligned with streamlines in shear layers, it was possible to obtain numerically accurate solutions and to obtain solutions at very high nozzle pressure ratios. The effects on turbulence of high Mach numbers and streamline curvature were examined. It was demonstrated that these phenomena have a significant effect on the turbulence and on the global flow characteristics such as base drag. Changes in base drag on the order of + or - 20 percent for some afterbody flows can be attributed to Mach number and curvature effects. A modified form of the k-epsilon turbulence model which gives good accuracy for flows involving high Mach number and streamline curvature is presented. GRA

N89-23432# Complere, Inc., Palo Alto, CA.
TURBULENT SHEAR STRESS MEASUREMENT IN HYPERSONIC FLOW Final Report, Jun. 1987 - Mar. 1988
F. K. Owen and Wladimiro Calarese Mar. 1989 17 p
(Contract F33615-87-C-3014)
(AD-A206453; WRDC-TR-89-3035) Avail: NTIS HC A03/MF A01 CSCL 01/1

The present report refers to the experimental evaluation of additional shear stress terms which might be significant at high Mach numbers. These terms are necessary to develop accurate empirical turbulence models to be used in Navier-Stokes computational codes. The measurement technique used was the simultaneous employment of hot wire anemometers in conjunction with laser Doppler velocimeters to obtain density-velocity triple correlation terms and compressible shear stress distribution at Mach 6. This diagnostic tool is available for measurements of turbulent hypersonic flows. Comparisons of present laser velocimeter turbulence measurements with previous hot wire results

indicate that significant errors can be incurred in hypersonic flows with the old standard techniques. Results indicate that adequate particle tracking is possible at Mach 6. GRA

N89-23433*# National Aeronautics and Space Administration. Langley Research Center, Hampton, VA.
TRANSONIC NAVIER-STOKES SOLUTIONS OF THREE-DIMENSIONAL AFTERBODY FLOWS
William B. Compton, III, James L. Thomas, William K. Abeyounis, and Mary L. Mason Jul. 1989 62 p
(NASA-TM-4111; L-16516; NAS 1.15:4111) Avail: NTIS HC A04/MF A01 CSCL 01A

The performance of a three-dimensional Navier-Stokes solution technique in predicting the transonic flow past a nonaxisymmetric nozzle was investigated. The investigation was conducted at free-stream Mach numbers ranging from 0.60 to 0.94 and an angle of attack of 0 degrees. The numerical solution procedure employs the three-dimensional, unsteady, Reynolds-averaged Navier-Stokes equations written in strong conservation form, a thin layer assumption, and the Baldwin-Lomax turbulence model. The equations are solved by using the finite-volume principle in conjunction with an approximately factored upwind-biased numerical algorithm. In the numerical procedure, the jet exhaust is represented by a solid sting. Wind-tunnel data with the jet exhaust simulated by high pressure air were also obtained to compare with the numerical calculations. Author

03 AIR TRANSPORTATION AND SAFETY

Includes passenger and cargo air transport operations; and aircraft accidents.

For related information see also *16 Space Transportation* and *85 Urban Technology and Transportation.*

N89-23434# National Transportation Safety Board, Washington, DC. Bureau of Safety Programs.
ANNUAL REVIEW OF AIRCRAFT ACCIDENT DATA, US AIR CARRIER OPERATIONS: CALENDAR YEAR 1986
3 Feb. 1989 101 p
(PB89-151021; NTSB/ARC-89/01) Avail: NTIS HC A06/MF A01 CSCL 01C

The record of aviation accidents involving revenue operations of U.S. Air Carriers including Computer Air Carriers and On Demand Air Taxis for calendar year 1986 is presented. The report is divided into three major sections according to the Federal regulations under which the flight was conducted - 14 CFR 121, 125, 127, Scheduled 14 CFR 135, or Nonscheduled 14 CFR 135. In each section tables describe the losses and characteristics of 1986 accidents to enable comparison with prior years. Author

N89-23435# Computer Resource Management, Inc., Vienna, VA.
NATIONAL AIRSPACE SYSTEM SEARCH AND RESCUE OPERATIONAL CONCEPT (NAS-SR-1329)
William Trent, Rodney Kuhn, and Thomas Pickerell Feb. 1989 50 p
(Contract DTFA01-88-Y-01073)
(DOT/FAA/DS-89/07) Avail: NTIS HC A03/MF A01

A requirement for the National Airspace System (NAS) is to provide for detecting the need for initiating and assisting in search and rescue activities, as identified in the NAS System Requirement Specification. A concept of operations for search and rescue is presented. It describes search and rescue assistance capabilities and shows the relationships between subsystems, facilities, information, and operators/users. It is intended to provide a common perspective for personnel involved in search rescue activities, assist in determining whether the search and rescue procedures meet formal requirements, and support coordination among the organizations involved with search and rescue assistance. Author

N89-23436# National Transportation Safety Board, Washington, DC. Bureau of Accident Investigation.
AIRCRAFT ACCIDENT REPORT: AVAir INC., FLIGHT 3378, FAIRCHILD METRO 3, SA227 AC, N622AV, CARY, NORTH CAROLINA, FEBRUARY 19, 1988
13 Dec. 1988 73 p
(PB88-910412; NTSB/AAR-88/10) Avail: NTIS HC A04/MF A01; HC also available on subscription, North American Continent price $70.00/year, all others write for quote CSCL 01C

On February 19, 1988, an AVAir Inc. Fairchild Metro 3, N622AV, operating as Air Virginia (AVAir) flight 3378, crashed in Cary, North Carolina shortly after it departed runway 23R at Raleigh Durham International Airport (RDU), Morrisville, North Carolina, with 2 flightcrew members and 10 passengers on board. The airplane struck water within 100 feet of the shoreline of a reservoir, about 5,100 feet west of the midpoint of runway 23R. The airplane was destroyed and all 12 persons on board were killed. The National Transportation Safety Board determines that the probable cause of this accident was the failure of the flightcrew to maintain a proper flightpath because of the first officer's inappropriate instrument scan, the captain's inadequate monitoring of the flight, and the flightcrew's response to a perceived fault in the airplane's stall avoidance system. Contributing to the accident was the lack of company response to documented indications of difficulties in the first officer's piloting, and inadequate Federal Aviation Administration surveillance of AVAir. Author

04 AIRCRAFT COMMUNICATIONS AND NAVIGATION

Includes digital and voice communication with aircraft; air navigation systems (satellite and ground based); and air traffic control.

For related information see also *17 Space Communications, Spacecraft Communications, Command and Tracking* and *Communications and Radar.*

N89-23437# Federal Aviation Administration, Atlantic City, NJ.
LORAN C FIELD STRENGTH CONTOURS: CONTIGUOUS US
Frank Garufi May 1989 107 p
(Contract FAA-T0702-N)
(DOT/FAA/CT-TN89/16) Avail: NTIS HC A06/MF A01

The development of Loran C field strength contour plots for the contiguous United States (CONUS) is described. Various plots were developed which show Loran C field strength based on measured data, predicted data, and measured data augmented by predicted data. Measured data were taken from a data base formerly developed by the Federal Aviation Administration (FAA) Technical Center at the Atlantic City International Airport, N.J. Predicted data were generated by the Canadian Loran C propagation model. Field strength contour plots of the CONUS are a result of this project. It is concluded that the contours produced are realistic indicators of Loran C field strength for each of the CONUS transmitters. Also included in this report are atmospheric noise contours of the CONUS and Loran C coverage contours of the CONUS. Author

N89-23438# Federal Aviation Administration, Atlantic City, NJ.
INSTRUMENT LANDING SYSTEM MATHEMATICAL MODELING STUDY FOR ORLANDO INTERNATIONAL AIRPORT RUNWAY 35L LOCALIZER, ORLANDO, FLORIDA. FINAL AIRSIDE DOCKING PLAN (SCHEME 3A)
James D. Rambone and John E. Walls Dec. 1988 30 p
(AD-A205351; DOT/FAA/CT-TN89/4) Avail: NTIS HC A03/MF A01 CSCL 17/7

This Technical Note describes the instrument landing system (ILS) math modeling performed by the Federal Aviation Administration (FAA) Technical Center at the request of the Southern Region. Computed data are presented showing the effects of airside terminals with simulated docked and taxiing aircraft on the performance of an ILS localizer proposed for runway 35L at the Orlando International Airport. The Southern Region is

concerned that reflections from two proposed airside terminals with docked and taxiing aircraft may degrade the localizer course beyond category II/III tolerances. Modeled course structure results indicate that category II/III localizer performance should be obtained with the Wilcox Mark II, 14-element, dual-frequency log periodic antenna and both airside terminals with docked and taxiing aircraft at the currently proposed locations. Computed clearance orbit results indicate satisfactory linearity, course crossover, and signal clearance levels. GRA

N89-23439# Ball Aerospace Systems Div., Boulder, CO.
SYSTEM STUDY: RADIATION HARDENED AUTONOMOUS NAVIGATION Final Report
Charlie Rose 19 Jan. 1989 69 p
(Contract N00014-85-C-2536)
(AD-A205604) Avail: NTIS HC A04/MF A01 CSCL 17/7

The question of whether a beacon tracker, similar to the NRL Rad-Hard Star Tracker, can be successfully used in a Landmark Tracking AutoNav application rests squarely on the accuracies required, the number of beacons available, and their optical characteristics as well as distribution over the surface of the Earth. Basically, we have found that a star tracker can be used in a landmark approach, but only within some rather severe constraints: (1) Beacons can be distributed more-or-less uniformly over the Earth. Restriction to the United States does not seem feasible; (2) Position errors of several kilometers can be tolerated between updates; (3) A very sophisticated orbit propagator is built into the system. There are non-trivial problems associated with this approach to the problem. Most of them stem from the fact that the tracker would be used in a way for which is was not designed nor intended: (1) The beacons twinkle; (2) The light from the beacons is refracted by the atmosphere by varying amounts which can be only partially compensated for; (3) The tracker's field of view is too small; it greatly reduces the number of targets that can be seen, as well as the durations of observations. This results in fewer updates, and necessitates a very sophisticated orbit propagator; (4) The already too few beacons can be obscured by cloud cover. This is, perhaps, the most egregious problem with this approach. GRA

N89-23440# Massachusetts Inst. of Tech., Cambridge. Lab. for Information and Decision Systems.
GENERATION OF ARCHITECTURES FOR DISTRIBUTED INTELLIGENCE SYSTEMS
Alexander H. Levis Feb. 1989 22 p
(Contract N00014-85-K-0519)
(AD-A205783; LIDS-P-1849) Avail: NTIS HC A03/MF A01 CSCL 12/9

An approach to the modeling of discrete event distributed intelligence system is presented that uses ordinary Petri Nets for fixed structure architectures. The model leads to the precise formulation of the problem of generating the complete set of architectures that satisfy a number of resource and design constraints. Two algorithms are presented: The first one (the DFS algorithm) starts with the specification of the desired functionality and generates data flow structures with prescribed redundancy and complexity; then the various functions are allocated to resources; the second one (the Lattice algorithm) starts with a given set of decision making units and obtains the partially ordered sets that contain all the feasible architectures. The resulting architectures can be analyzed to evaluate their performance characteristics. GRA

N89-23441# Microcosm, Inc., Torrance, CA.
AUTONOMOUS NAVIGATION AND CONTROL Final Technical Report, Jun. 1987 - Jun. 1988
Peter D. Noerdlinger and Frank M. Tai Oct. 1988 78 p
(Contract F30602-87-C-0056; ARPA Order 9132)
(AD-A205898; RADC-TR-87-227) Avail: NTIS HC A05/MF A01 CSCL 17/7

The Autonomous Navigation System (ANS) is capable of achieving positioning accuracies of 100 m. to 1.5 km. with straightforward modifications to existing Earth sensing hardware. Because it uses hardware that would be on board the spacecraft for attitude determination, the additional cost for achieving fully autonomous navigation will be quite low. The modifications will allow the sensor to measure the size of the Earth and sense the measurements can be made with a single sensor, including independent redundant observations, many of the principal bias terms can be eliminated or greatly reduced. Additional work is needed to fully develop the cost versus performance of the autonomous navigation model. No new technology is required, although some calibration or bias determination techniques may need to be developed to accommodate the evolving sensor accuracy. The proposed system could have a significant impact on ground operations costs, mission definition and design, survivability, and the potential development of very low cost fully autonomous spacecraft. GRA

N89-23442# Naval Research Lab., Washington, DC. Ionospheric Effects Branch.
IMPACT OF THE GEOPLASMA ON A SPACEBORNE GPS RECEIVER SYSTEM: A PRELIMINARY STUDY
J. M. Goodman 28 Feb. 1989 151 p
(AD-A205965; NRL-MR-6290) Avail: NTIS HC A08/MF A01 CSCL 17/7

It is well known that the most accurate positioning information obtainable from the GPS system, in the traditional application where the receivers are located on or very near to the surface of the earth, i.e., beneath the ionosphere, is achieved through use of the two-frequency method so that the ionospheric component of the ranging error can be removed. However, in an application where a GPS receiver is itself located on a spacecraft orbiting above some of the electron content in the ionosphere and protonosphere, the question as to whether a two-frequency system is necessary may have a different answer. In this preliminary study, the parameters of the latter question are explained and the range of errors which might be experienced by a single-frequency system are estimated. GRA

N89-23443# Air Force Inst. of Tech., Wright-Patterson AFB, OH. School of Engineering.
DEVELOPMENT OF THE EXTENDED KALMAN FILTER FOR THE ADVANCED COMPLETELY INTEGRATED REFERENCE INSTRUMENTATION SYSTEM (CIRIS) M.S. Thesis
Joseph K. Solomon Mar. 1989 160 p
(AD-A206083; AFIT/GE/ENG/89M-8) Avail: NTIS HC A08/MF A01 CSCL 17/7

The Completely Integrated Reference Instrumentation System (CIRIS) was developed by the Central Inertial Guidance Test Facility (CIGTF) at Holloman AFB, NM. The CIRIS system is an inertial navigation system (INS) aided with line-of-sight range and range-rate measurements from surveyed ground transponders. The information from the measurement and INS data is combined using an extended Kalman filter to produce an accurate estimate of the INS position and velocity errors. The accurate CIRIS aircraft position and velocity data is used as a baseline reference to determine the performance capabilities of proposed aircraft navigation systems. The new aircraft navigation systems projected in the next five years will attain accuracies approaching the level of the current CIRIS system. In order to test these systems, the accuracy of CIRIS will be increased through the addition of aiding measurements from the Global Positioning System (GPS). GRA

N89-23444# Royal Signals and Radar Establishment, Malvern (England).
COMPARISON OF INTERPOLATION ALGORITHMS FOR SPEED CONTROL IN AIR TRAFFIC MANAGEMENT
A. J. Budd 17 Aug. 1988 21 p
(AD-A206314; RSRE-MEMO-4131; DRIC-BR-109213) Avail: NTIS HC A03/MF A01 CSCL 17/7

With air traffic movements at a high level, techniques to assist air traffic management using computers are being investigated. One technique in particular being studied is the early adjustment of the speed of arriving aircraft so that the rate of flow near to the airports is closely matched to landing capacity. A Speed Control

Adviser has been developed which allocates a landing time to each inbound aircraft. Once the estimated landing time is known, the speed the aircraft must fly needs to be calculated. This cannot be done directly and interpolation using a suitable polynomial approximation is used. This memorandum investigates four polynomials and examines their effectiveness at providing a good estimate with minimum computations. GRA

N89-23445# Stuttgart Univ. (Germany, F.R.). Fakultaet fuer Luft- und Raumfahrttechnik.
IMPROVEMENT OF NAVIGATION MEASUREMENT PROCEDURES BY THE COMBINED APPLICATION OF CORRELATION TECHNIQUES AND PARAMETER ESTIMATION Ph.D. Thesis [VERBESSERUNG VON NAVIGATIONSMESSVERFAHREN DURCH KOMBINIERTE ANWENDUNG VON KORRELATIONSTECHNIKEN UND PARAMETERSCHAETZUNG]
Manfred Wittig 1987 165 p In GERMAN
(ETN-89-93946) Avail: NTIS HC A08/MF A01

Existing radio navigation methods were generalized by the combined application of correlation techniques and parameter estimation. It is shown that a generally valid structure for the estimation of a parameter of the received signal can be obtained. The application of the general structure of the optimum estimate on the pseudo noise (PN) signal sequence, results in a novel receiver type: the PN-phase-locked-loop (PLL) which has several advantages with respect to the delay-locked-loop, and is suited for very large scale integration. By reducing the ranging measurement to a correlation, the measurement errors expected from frequency instabilities can be quantized, and the frequency instabilities can be reduced. This frequency instability cancellation system is especially suited to stabilize the frequency of lasers and to stabilize tunable high frequency oscillators. ESA

N89-23446# Technische Univ., Delft (Netherlands).
GLOBAL POSITIONING SYSTEM (GPS) POSITIONING AT SEA Thesis [GPS PLAATSBEPALING OP ZEE]
Hans Visser 4 Jul. 1988 110 p In DUTCH
(ETN-89-94145) Avail: NTIS HC A06/MF A01

Positioning using the satellite system NAVSTAR GPS was studied. The satellite system and the orbit calculation are explained. The principles of and the differences between the different types of receivers are described. A computer program for the calculation of a real time filtered position was developed on the HP217 computer. Test calculations using this program are presented and compared with the solutions of other receivers. ESA

05 AIRCRAFT DESIGN, TESTING AND PERFORMANCE

Includes aircraft simulation technology.

For related information see also *18 Spacecraft Design, Testing and Performance* and *39 Structural Mechanics*. For land transportation vehicles see *85 Urban Technology and Transportation*.

N89-23447*# National Aeronautics and Space Administration. Langley Research Center, Hampton, VA.
FLUTTER OF A LOW-ASPECT-RATIO RECTANGULAR WING
Stanley R. Cole Jun. 1989 19 p
(NASA-TM-4116; L-16544; NAS 1.15:4116) Avail: NTIS HC A03/MF A01 CSCL 01C

A flutter test of a low-aspect-ratio rectangular wing was conducted in the Langley Transonic Dynamics Tunnel (TDT). The model used in this flutter test consisted of a rigid wing mounted to the wind-tunnel wall by a flexible, rectangular beam. The flexible support shaft was connected to the wing root and was cantilever mounted to the wind-tunnel wall. The wing had an aspect ratio of 1.5 based on the wing semispan and an NACA 64A010 airfoil shape. The flutter boundary of the model was determined for a Mach number range of 0.5 to 0.97. The shape of the transonic flutter boundary was determined. Actual flutter points were obtained on both the subsonic and supersonic sides of the flutter bucket. The model exhibited a deep transonic flutter bucket over a narrow range of Mach number. At some Mach numbers, the flutter conditions were extrapolated using a subcritical response technique. In addition to the basic configuration, modifications were made to the model structure such that the first bending frequency was changed without significantly affecting the first torsion frequency. The experiment showed that increasing the bending stiffness of the model support shaft through these modifications lowered the flutter dynamic pressure. Flutter analysis was conducted for the basic model as a comparison with the experimental results. This flutter analysis was conducted with subsonic lifting-surface (kernel function) aerodynamics using the k method for the flutter solution. Author

N89-23448*# National Aeronautics and Space Administration. Langley Research Center, Hampton, VA.
HOT-JET SIMULATION IN CRYOGENIC WIND TUNNELS
Keisuke Asai (National Aerospace Lab., Tokyo, Japan) Washington Jul. 1989 49 p
(NASA-RP-1220; L-16564; NAS 1.61:1220) Avail: NTIS HC A03/MF A01 CSCL 01C

In order to evaluate hot jet simulation capability in cryogenic wind tunnel testing, simple theoretical calculations were performed. The similarity parameters, isentropic flow properties, and normal shock relations were calculated for a variety of jet simulation techniques. The results were compared with those estimated for a full scale flight condition. It was shown that the cryogenic wind tunnel testing provides an opportunity for the most accurate hot jet simulation technique. By using a compressed nitrogen gas at ambient or moderately elevated temperatures as a jet gas, most all of the relevant similarity parameters including the jet temperature and velocity ratios and the Reynolds numbers, can be set to the full scale flight values. The only exception is the ratio of specific heats for jet flow. In an attempt to match the ratio of specific heats for the turbojet flow, gases other than pure nitrogen were considered. It was found that a nitrogen/methane mixture at moderately elevated temperature behaves like the real combustion gas. Using this mixture as a jet gas, complete simulation of the full scale turbojet exhaust becomes possible in cryogenic wind tunnels. Author

N89-23449# Aeronautical Research Labs., Melbourne (Australia).
MODELLING AIRCRAFT DYNAMICS Aerodynamics Technical Memo.
C. A. Martin Sep. 1988 21 p
(AD-A204086; ARL-AERO-TM-400; DODA-AR-005-534) Avail: NTIS HC A03/MF A01 CSCL 01/3

A review has been made of the approaches currently under development for the modelling of aircraft flight dynamics at high angles-of-attack. The review is based on current research literature and on discussions held during an overseas visit carried out for the purpose of technical updating in the areas of flight dynamic modelling and parameter estimation. GRA

N89-23450 Kansas Univ., Lawrence.
A CORRELATION STUDY OF X-29A AIRCRAFT AND ASSOCIATED ANALYTICAL DEVELOPMENTS D.E. Thesis
Ali Reza Ahmadi 1988 280 p
Avail: Univ. Microfilms Order No. DA8903074

Contractor results of the structural and zerodynamic analysis of the X-29A aircraft were verified. A brief history and potential advantages of the X-29A aircraft are discussed. The NASA developed computer package, STARS (STructures, Aerodynamics, and Related Systems), which is used in verifying contractor results is discussed. Enhancements of the STARS package are described, particularly the incorporation of the FASTEX computer program into STARS, and the development of a complete computer graphics system. A comparative study of free vibration and aerodynamic analysis of the X-29A aircraft is given. It was shown that the natural frequencies and modeshapes determined analytically by STARS and the contractor compare relatively well with

experimentally determined data. Also included is the formulation and development of the higher-order plane-stress finite dynamic triangular element. Dissert. Abstr.

N89-23451# Aircraft Research and Development Unit, Edinburg (Australia).
FLIGHT TESTING OF THE SOUTHERN CROSS REPLICA AIRCRAFT
N. G. Coulson Sep. 1988 98 p
(AD-A205303; ARDU-TI-953; DODA-AR-003-256) Avail: NTIS HC A05/MF A01 CSCL 01/3

Aircraft Research and Development Unit was tasked to carry out the test flying of a replica of the 1926 Fokker Tri-Motor as flown by Australian aviation pioneer, Sir Charles Kingsford-Smith. The purpose of the test program was, firstly, to ensure safe operation of the aircraft throughout its proposed flight envelope and, secondly, to provide data to allow the issue of a Certificate of Airworthiness or Permit to Fly. The trial included a cockpit and systems assessment as well as an evaluation of the aircraft's flight and ground handling characteristics. Airborne assessments covered stability and control characteristics, stall characteristics, general aircraft performance, asymmetric power characteristics and an evaluation of the aircraft's take-off and landing performance and handling. The flight characteristics of the test aircraft were found to be similar to those expected from an original Fokker VIIb-3M. Consequently, the aircraft could not meet some modern certification requirements. Notwithstanding this the aircraft was found to be generally safe and airworthy provided it was operated by experienced pilots in daylight Visual Meteorological Conditions and that the main recommendations of this report are adopted. GRA

N89-23452# Polytechnic Univ., Farmingdale, NY. Dept. of Aerospace Engineering.
OPTIMUM AEROELASTIC CHARACTERISTICS FOR COMPOSITE SUPERMANEUVERABLE AIRCRAFT Final Technical Report, 1 Jun. 1987 - 31 Sep. 1988
Gabriel A. Oyibo, James Bentson, and T. A. Weisshaar 27 Nov. 1988 136 p
(Contract F49620-87-C-0046)
(AD-A205503; POLY-AE-88-8; AFOSR-89-0127TR) Avail: NTIS HC A07/MF A01 CSCL 01/3

The investigation of an aeroelastically induced constrained warping phenomenon for a composite, supermaneuverable type aircraft wing has continued in this second year of the study. The first year investigation was concentrated mainly on the static phenomena and the search for closed form solutions for free vibration of aircraft wings having constrained warping in the presence of elastic coupling. The wing is analytically modelled as a straight flat laminated plate. Various forms of highly simplified aerodynamic loads are employed in the analysis. The free vibrations and stability aspects of this phenomenon are examined to obtain some physical insights and to determine its importance and/or design implications. Analytical tools employed include an affine transformation concept which was formulated previously (by the present principal investigator) as well a non-dimensionalization scheme. GRA

N89-23453# Analatom, Inc., Sunnyvale, CA.
AN INSTRUMENT FOR THE SIMULTANEOUS MEASUREMENT OF VELOCITY, TEMPERATURE AND DENSITY IN UNSEEDED AIR FLOWS Final Report, 1 Aug. 1988 - 31 Jan. 1989
Gabriel Laufer 31 Jan. 1989 64 p
(Contract F49620-88-C-0126)
(AD-A205588; GL-88-2; AFOSR-89-0310TR) Avail: NTIS HC A04/MF A01 CSCL 22/5

The development and the design of advanced hypersonic vehicles such as the National Aerospace Plane (NASP) or the Space Shuttle will strongly depend on computer simulation mainly because some of the flight conditions experienced by these vehicles will be difficult or prohibitively expensive to create in ground facilities. Computer simulation will be used to reduce the need for expensive test time or will replace those experimental tests which can not be performed. However, computer simulations require validation before their results can be accepted. These validation tests, which must be performed in hypersonic and turbulent air flows, require the simultaneous measurement of air temperature, density and velocity at a high temporal and spatial resolution which will allow to resolve turbulence structures. GRA

N89-23454# Air Force Inst. of Tech., Wright-Patterson AFB, OH. School of Engineering.
PRELIMINARY DESIGN OF A MODULAR UNMANNED RESEARCH VEHICLE. VOLUME 2: SUBSYSTEM TECHNICAL DEVELOPMENT DESIGN STUDY M.S. Thesis
Christopher D. Hall, Richard L. Johnson, Peter J. Lamatsch, Douglas A. McCabe, and Paul J. Mueller, III Dec. 1988 277 p
(AD-A205678; AFIT/GSE/AA/88D-2) Avail: NTIS HC A13/MF A01 CSCL 01/3

This thesis presents the analysis and development of a modular unmanned research vehicle (MURV) to support AFIT's aeronautical research. The MURV is proposed as a test vehicle to permit experimental efforts beyond the restrictions of pure analytical and wind tunnel research, yet less costly and more accessible than full-scale flight tests. A classical systems approach was applied, in concert with a conventional aircraft design process, which emphasized system level needs and objectives in the design of MURV subsystems. Primary design drivers were the need for adequate data acquisition for anticipated experiments, structural and functional modularity to permit simple reconfiguration, and focus on a set of unique experiments relating to fighter-like supermaneuverability. The supermaneuverability experiments dictated that the general arrangement of the MURV baseline design would resemble a typical modern fighter aircraft configuration, the recommended baseline being a turbojet-powered delta wing design with canards, single vertical tail, and control-configured ventral fins. Modularity implications resulted in the design of a flexible, digital flight control system with primary functions distributed between the vehicle and a remote pilot/control ground station and a fuselage design which allows for relocation and replacement of wings and tails or canards. The data acquisition system is fully integrated with the flight control system and the remote ground station. GRA

N89-23455# Air Force Inst. of Tech., Wright-Patterson AFB, OH. School of Engineering.
A METHODOLOGY FOR DETERMINING THE SURVIVABILITY OF FIXED-WING AIRCRAFT AGAINST SMALL ARMS M.S. Thesis
John M. Grover Mar. 1989 119 p
(AD-A205730; AFIT/GST/ENS/89M-05) Avail: NTIS HC A06/MF A01 CSCL 15/3

The purpose of this study was to develop an efficient and effective method of evaluating the survivability of a fixed-wing aircraft against small arms. A computer model was created to predict the probability an aircraft survives given an encounter with a small arms weapon, P(s/e), and the expected number of hits it receives, E(hits). The model was a one-on-one deterministic duel of a small arms weapon and an aircraft. The aircraft was represented on a straight and level flight approaching the weapon at a given velocity, angle, distance, and altitude. The small arms weapon was located at a fixed position, firing at fixed point in front of the aircraft. The weapon orientation varied by normal distributions around the fixed aim point. The bullet trajectories were represented using an interactive technique. Bullet and aircraft intersections were calculated using a sphere to represent the aircraft. All probability distributions were broken into discrete intervals providing the means to maintaining a deterministic model. The results of the model supplied a probability of survival and expected hits for a specific weapon and aircraft with a set velocity, distance away, altitude, and angle of approach. GRA

N89-23456# Air Force Inst. of Tech., Wright-Patterson AFB, OH. School of Engineering.
AN INVESTIGATION INTO THE APPLICATION OF DYNAMIC PROGRAMMING TO DETERMINE OPTIMAL CONTROLS FOR TRACKING A CRUISE MISSILE MANEUVER BY CMMCA (CRUISE MISSILE MISSION CONTROL AIRCRAFT) M.S. Thesis
Leonard G. Heavner Mar. 1989 117 p
(AD-A205970; AFIT/GST/ENS/89M-6) Avail: NTIS HC A06/MF A01 CSCL 12/4

This thesis investigated the application of dynamic programming to determine the optimal control inputs for tracking a cruise missile maneuver by the Cruise Missile Mission Control Aircraft (CMMCA). Conventional dynamic programming and state increment dynamic programming were considered. The objective was to minimize cruise missile deviations from a desired position within the radar sweep cone. Only single turning maneuvers of the cruise missile were investigated in this study. Implementation on a personal computer was attempted. Since time defined the stages for the dynamic programming method, the effect of different time increments was evaluated. The study found state increment dynamic programming difficult to implement. Problems were encountered in the processing of block boundaries. Memory limitations of the FORTRAN compiler prohibited implementation of the dynamic programming technique on the personal computer. The methodology was successfully implemented on a VAX running on the VMS operating system. The model, as formulated, was found to be extremely sensitive to the size of the time increments defining the stages. Widely different controls were computed using three different time increments. A 0.5 minute time increment was determined to provide the best results of the increments investigated. GRA

N89-23457# General Dynamics Corp., Fort Worth, TX.
USAF (US AIR FORCE) DURABILITY DESIGN HANDBOOK: GUIDELINES FOR THE ANALYSIS AND DESIGN OF DURABLE AIRCRAFT STRUCTURES Final Report, Oct. 1984 - Sep. 1987
S. D. Manning and J. N. Yang 20 Feb. 1989 150 p Prepared in cooperation with United Analysis, Inc., Vienna, VA
(Contract F33615-84-C-3208)
(AD-A206286; AFWAL-TR-88-3119) Avail: NTIS HC A07/MF A01 CSCL 11/6

Objectives of this handbook are to: (1) summarize and interpret the essential USAF durability design requirements for metallic airframes; (2) provide durability analysis criteria for economic life and durability-critical parts; (3) provide state-of-the-art durability analysis concepts and methods for determining the initial fatigue quality of fastener holes, the probability of distribution of service time to reach any specified crack size; (4) provide guidelines and design process and for making design tradeoffs. The method accounts for the initial fatigue quality variation, crack growth damage accumulation in a population of structural details (e.g., fastener holes, lugs, fillets, cutouts, etc.), load spectra and structural properties. During manufacturing and assembly, flaws of various types, are produced in structural details. The initial fatigue quality of such details is represented by an Equivalent Initial Flaw Size Distribution (EIFSD). An Equivalent Initial Flaw Size (EIFS) is an artificial crack size which results in an actual crack size at an actual point in time when the initial flaw is grown forward. EIFSs are determined by back-extrapolating fractographic results. GRA

N89-23458# Army Missile Command, Redstone Arsenal, AL. Guidance and Control Directorate.
MISSILE ACTUATOR SIMULATION AND AN INVESTIGATION INTO THE ACCURACY OF RUNGE-KUTTA NUMERICAL INTEGRATION Final Technical Report, for Period Ending Apr. 1988
Scott J. Moody Jul. 1988 51 p
(AD-A206325; AD-E951249; AMSMI/TR-RD-GC-88-14) Avail: NTIS HC A04/MF A01 CSCL 13/7

This report discusses the computer simulation of the ATACMS fin actuators. These subroutines are one of many possible methods of representing actuator behavior in a 6DOF (six Degree Of Freedom) or 5DOF missile simulation. Also included is a section to discuss the accuracy of a version of the Runge-Kutta integration method. This particular simulation was run on a Zenith personal computer with Ryan-McFarland FORTRAN. GRA

N89-23459# Ballistic Research Labs., Aberdeen Proving Ground, MD.
COMPARISON OF COMPUTATIONAL ANALYSIS WITH FLIGHT TESTS OF A 40mm SOLID-FUEL RAMJET PROJECTILE
Michael J. Nusca and Vural Oskay Mar. 1989 43 p
(AD-A206536; BRL-TR-2983) Avail: NTIS HC A03/MF A01 CSCL 19/1

Flight tests of fueled and inert projectiles and a computational analysis of the non-burning internal flowfield have been used to study the performance of 40mm Solid-Fuel Ramjet (SRFJ) projectiles. These projectiles, as originally designed, did not produce detectable thrust in flight. The 40 mm SRFJ is essentially scaled down from a successful 75mm round. Design modifications to the 40 mm SRFJ aimed at reducing the internal velocity and/or increasing internal turbulence yielded slight performance improvements. Alternate solid fuels were found to improve thrust generation. Computational modeling is used to investigate the differences in the non-burning internal flow for 75mm and 40mm SRFJ projectiles. Analysis of internal wall pressures, shock waves and flow separation reveals that the internal flow for the 40 mm geometry can be notably different from that of the 75mm geometry. These differences may have an effect on fuel ignition and burning. However, the computational analysis does not address the effects of projectile axial spin. GRA

N89-23460# Aerospatiale, Toulouse (France). Aircraft Div.
CENTER OF GRAVITY CONTROL ON AIRBUS AIRCRAFT: FUEL, RANGE AND LOADING
Bernard Huber 13 Jun. 1988 38 p Presented at the 47th Annual Conference of the Society of Allied Weight Engineers, Inc., Plymouth, MI, 23-25 May 1988
(Rept-882-111-101; ETN-89-94477) Avail: NTIS HC A03/MF A01

The advantage of an active center of gravity control are described, with reference to the control system by fuel transfer adopted in the A330 and A340 aircraft design. These aircraft can carry fuel in the tailplane in addition to the wing and fuselage tanks. The tail tank has a capacity of 5 tons. The installation results in fuel, range and loading benefits which are detailed in the examples. ESA

N89-23461# Aerospatiale, Toulouse (France).
A330/340 HYDRAULIC SYSTEM
L. Signorelli 1988 37 p Presented at the Vickers 32nd International Aerospace Fluid Power Conference on the Hydraulic Architecture of the A330/A340 Aircraft, Jackson, MS, 11-13 Apr. 1988
(Rept-882-111-102; ETN-89-94478) Avail: NTIS HC A03/MF A01

The Airbus hydraulics design specifications are reviewed. The hydraulic system is basically the same as A300/A310 aircraft, with three fully independent circuits at 3000 psi and mostly the same components used on A310/A30. The description includes details of system layout, flight controls, hydraulic aspects and segregation aspects. Hydraulic fittings, safety aspects and cockpit monitoring are discussed. ESA

N89-23462# Aerospatiale, Chatillon (France). Div. des Engins Tactiques.
PIF-PAF PILOTING OF TACTICAL MISSILES [PILOTAGE PIF-PAF DES MISSILES TACTIQUES]
B. Lazure 1988 13 p In FRENCH
(Rept-882-320-104; ETN-89-94482) Avail: NTIS HC A03/MF A01

A missile piloting system is described, combining a pyrotechnic guidance system creating normal forces near the gravity center and a more classical aerodynamic piloting. The combination is up to 10 times faster than existing systems, and specially adapted

for antimissile defense. Studies of the transversal jet devices and of aerodynamic interferences with the main propulsor are also discussed. ESA

06 AIRCRAFT INSTRUMENTATION

Includes cockpit and cabin display devices; and flight instruments.

For related information see also *19 Spacecraft Instrumentation* and *35 Instrumentation and Photography.*

N89-23463# National Aerospace Lab., Tokyo (Japan).
CHARACTERISTICS OF A FIVE-HOLE SPHERICAL PITOT TUBE
Toshiho Sakai and Toshiharu Inagaki Apr. 1988 25 p In JAPANESE; ENGLISH summary
(NAL-TR-971; ISSN-0389-4010) Avail: NTIS HC A03/MF A01

A five-hole spherical pitot tube produced for experimental purposes was tested for measuring such air data as velocity, angle of attack, sideslip angle and static pressure of aircraft. There are few cases in measuring the static pressure by five-hole spherical pitot tube, although the measurements of airspeed, angle of attack and sideslip-angle are well known. Since the five-hole spherical pitot tube is normally installed at a position far from the lifting surface, one can expect to measure the static pressure without position error. First, wind tunnel tests of the five-hole spherical pitot tube were conducted. The pressure on the surface of the sphere was different from that estimated by theory. Such a difference between theory and practice induced considerable adverse effects on the accuracy of the measured air data. So, by using new revised equations based on the results of the wind tunnel tests, the air data was estimated with much more accuracy. Next, some flight tests were made in order to ascertain position error in free static pressure measurements. The tests were performed under such conditions as level-flight, steady turn, landing and takeoff during the experiments. The static pressure measured by the five-hole spherical pitot tube agreed well with measurements taken with a swivel pitot and the resulting airspeed was shown to be almost the same as that obtained from the position error correction chart, which was made by the speed course method. Author

07 AIRCRAFT PROPULSION AND POWER

Includes prime propulsion systems and systems components, e.g., gas turbine engines and compressors; and onboard auxilliary power plants for aircraft.

For related information see also *20 Spacecraft Propulsion and Power, 28 Propellants and Fuels,* and *44 Energy Production and Conversion.*

N89-23464# National Aerospace Lab., Tokyo (Japan).
EXPERIMENT ON A CYLINDRICAL SCRAMJET COMBUSTOR. 2: SIMULATED FLIGHT MACH NUMBER 6.7
Tomoyuki Komuro, Atsuo Murakami, Kenji Kudou, Goro Masuya, and Nobuo Chinzei Mar. 1988 20 p In JAPANESE; ENGLISH summary
(NAL-TR-969; ISSN-0389-4010) Avail: NTIS HC A03/MF A01

An experimental study was made on a cylindrical scramjet combustor with a rear-facing step in a vitiated air flow. The stagnation temperature and pressure of the vitiated air were 2000 K and 1.0 MPa, respectively. The simulated flight speed was Mach 6.7 at a particular altitude of 40 km. Three different types of fuel injector were used, consisting of two perpendicular schemes and a parallel scheme of fuel injection into the mainstream. Auto-ignition of hydrogen fuel occurred when the air stagnation temperature reached about 1500 K. In all test cases, the flame was anchored on the step. For high air stagnation temperature and low fuel flow rate, however, the flame holding position shifted downstream from the step. At a fuel equivalence ratio of 0.55, mixing efficiency of the parallel injector was higher than that of the perpendicular injectors, but the axial variations in combustion efficiency were almost in the same form for all injectors, except immediately downstream of the injector. In a supersonic combustion mode, significant influence of flight Mach number on mixing was not observed. For a constant inlet Mach number, fuel flow rates at which transition from supersonic to subsonic combustion took place increased nearly in proportion to the stagnation temperature of air. A one-dimensional analysis using the measured pressure distribution served to determine other chemical and fluid mechanical properties. The calculated combustion efficiencies were slightly higher as compared to the experimental data, while the Mach number distributions were in reasonable agreement. Author

N89-23465*# National Aeronautics and Space Administration. Lewis Research Center, Cleveland, OH.
ADVANCES IN COMPUTATIONAL DESIGN AND ANALYSIS OF AIRBREATHING PROPULSION SYSTEMS
John M. Klineberg 1989 19 p Proposed for presentation at the 9th International Symposium on Airbreathing Engines, Athens, Greece, 4-9 Sep. 1989; sponsored by International Society for Air Breathing Engines
(NASA-TM-101987; E-4689; NAS 1.15:101987) Avail: NTIS HC A03/MF A01 CSCL 21E

The development of commercial and military aircraft depends, to a large extent, on engine manufacturers being able to achieve significant increases in propulsion capability through improved component aerodynamics, materials, and structures. The recent history of propulsion has been marked by efforts to develop computational techniques that can speed up the propulsion design process and produce superior designs. The availability of powerful supercomputers, such as the NASA Numerical Aerodynamic Simulator, and the potential for even higher performance offered by parallel computer architectures, have opened the door to the use of multi-dimensional simulations to study complex physical phenomena in propulsion systems that have previously defied analysis or experimental observation. An overview of several NASA Lewis research efforts is provided that are contributing toward the long-range goal of a numerical test-cell for the integrated, multidisciplinary design, analysis, and optimization of propulsion systems. Specific examples in Internal Computational Fluid Mechanics, Computational Structural Mechanics, Computational Materials Science, and High Performance Computing are cited and described in terms of current capabilities, technical challenges, and future research directions. Author

N89-23466*# National Aeronautics and Space Administration. Langley Research Center, Hampton, VA.
METHOD AND SYSTEM FOR MONITORING AND DISPLAYING ENGINE PERFORMANCE PARAMETERS Patent Application
Terence S. Abbott, inventor (to NASA) and Lee H. Person, Jr., inventor (to NASA) 14 Nov. 1988 34 p Sponsored by NASA. Langley Research Center
(NASA-Case-LAR-14049-1; NAS 1.71:LAR-14049-1; US-Patent-Appl-SN-270189) Avail: NTIS HC A03/MF A01 CSCL 21E

The invention is believed a major improvement that will have a broad application in governmental and commercial aviation. It provides a dynamic method and system for monitoring and simultaneously displaying in easily scanned form the available, predicted, and actual thrust of a jet aircraft engine under actual operating conditions. The available and predicted thrusts are based on the performance of a functional model of the aircraft engine under the same operating conditions. Other critical performance parameters of the aircraft engine and functional model are generated and compared, the differences in value being simultaneously displayed in conjunction with the displayed thrust values. Thus, the displayed information permits the pilot to make power adjustments directly while keeping him aware of total performance at a glance of a single display panel. NASA

08 AIRCRAFT STABILITY AND CONTROL

Includes aircraft handling qualities; piloting; flight controls; and autopilots.

For related information see also *05 Aircraft Design, Testing and Performance.*

N89-23467# National Aerospace Lab., Tokyo (Japan).
THE FUNCTIONAL MOCK-UP TEST OF THE FLIGHT CONTROL SYSTEM OF THE NAL QSTOL RESEARCH AIRCRAFT ASKA
Tadao Uchida, Akira Tada, Noriaki Okada, Hiroyuki Yamato, and Toshio Ogawa Apr. 1988 64 p In JAPANESE; ENGLISH summary
(NAL-TR-972; ISSN-0389-4010) Avail: NTIS HC A04/MF A01

The functional mockup test of the flight control system of ASKA with the stability and control augmentation systems is described. The tests made included software verification, simulated failure effects testing, closed loop test, and piloted simulation test. The results show that the functions and performance of the control system are satisfactory for flight safety of ASKA. Author

N89-23468*# National Aeronautics and Space Administration. Langley Research Center, Hampton, VA.
A CLOSED-FORM TRIM SOLUTION YIELDING MINIMUM TRIM DRAG FOR AIRPLANES WITH MULTIPLE LONGITUDINAL-CONTROL EFFECTORS
Kenneth H. Goodrich, Steven M. Sliwa, and Frederick J. Lallman Washington May 1989 30 p
(NASA-TP-2907; L-16484; NAS 1.60:2907) Avail: NTIS HC A03/MF A01 CSCL 01C

Airplane designs are currently being proposed with a multitude of lifting and control devices. Because of the redundancy in ways to generate moments and forces, there are a variety of strategies for trimming each airplane. A linear optimum trim solution (LOTS) is derived using a Lagrange formulation. LOTS enables the rapid calculation of the longitudinal load distribution resulting in the minimum trim drag in level, steady-state flight for airplanes with a mixture of three or more aerodynamic surfaces and propulsive control effectors. Comparisons of the trim drags obtained using LOTS, a direct constrained optimization method, and several ad hoc methods are presented for vortex-lattice representations of a three-surface airplane and two-surface airplane with thrust vectoring. These comparisons show that LOTS accurately predicts the results obtained from the nonlinear optimization and that the optimum methods result in trim drag reductions of up to 80 percent compared to the ad hoc methods. Author

N89-23469*# National Aeronautics and Space Administration. Langley Research Center, Hampton, VA.
SIMULATOR EVALUATION OF A DISPLAY FOR A TAKEOFF PERFORMANCE MONITORING SYSTEM
David B. Middleton, Raghavachari Srivatsan, and Lee H. Person, Jr. Washington May 1989 29 p
(NASA-TP-2908; L-16510; NAS 1.60:2908) Avail: NTIS HC A03/MF A01 CSCL 01C

A Takeoff Performance Monitoring System (TOPMS) has been developed to provide the pilot with graphic and numeric information pertinent to his decision to continue or abort a takeoff. The TOPMS information display consists primarily of a runway graphic overlaid with symbolic status, situation, and advisory information including: (1) current position and airspeed; (2) predicted locations for reaching decision speed (V sub 1) and rotation speed (V sub R); (3) groundroll limit for reaching (V sub R); (4) predicted stop point for an aborted takeoff from current conditions; (5) engine-status flags; and (6) an overall situation advisory flag that recommends continuation or rejection of the takeoff. In this study, 32 experienced multi-engine pilots evaluated the TOPMS on the Langley B-737 real-time research simulator. They rated the system satisfactory - good and judged it to be suitable for implementation on an aircraft. The TOPMS, the TOPMS simulation, and the results of the simulator evaluation are described here. Appendices contain the pilot's prebriefing package (written explanation of the TOPMS--sent to the pilots prior to their visit), evaluation instructions, debriefing questions, and rating criteria (organized into a flow diagram similar to the Cooper-Harper diagram for evaluation of aircraft handling qualities). Author

N89-23470*# Kansas Univ. Center for Research, Inc., Lawrence. Flight Research Lab.
DETAILED DESIGN OF A RIDE QUALITY AUGMENTATION SYSTEM FOR COMMUTER AIRCRAFT Final Report
Reiner Suikat, Kent E. Donaldson, and David R. Downing Washington NASA May 1989 127 p
(Grant NAG1-345)
(NASA-CR-4230; NAS 1.26:4230; KU-FRL-6132-7) Avail: NTIS HC A07/MF A01 CSCL 01C

The design of a Ride Quality Augmentation System (RQAS) for commuter aircraft is documented. The RQAS is designed for a Cessna 402B, an 8 passenger prop twin representative to this class of aircraft. The purpose of the RQAS is the reduction of vertical and lateral accelerations of the aircraft due to atmospheric turbulence by the application of active control. The detailed design of the hardware (the aircraft modifications, the Ride Quality Instrumentation System (RQIS), and the required computer software) is examined. The aircraft modifications, consisting of the dedicated control surfaces and the hydraulic actuation system, were designed at Cessna Aircraft by Kansas University-Flight Research Laboratory. The instrumentation system, which consist of the sensor package, the flight computer, a Data Acquisition System, and the pilot and test engineer control panels, was designed by NASA-Langley. The overall system design and the design of the software, both for flight control algorithms and ground system checkout are detailed. The system performance is predicted from linear simulation results and from power spectral densities of the aircraft response to a Dryden gust. The results indicate that both accelerations are possible. Author

N89-23471*# Boeing Commercial Airplane Co., Seattle, WA.
THE 4D-TECS INTEGRATION FOR NASA TSRV AIRPLANE Final Report
I. Kaminer and P. R. OShaughnessy Washington NASA Jun. 1989 168 p
(Contract NAS1-18027)
(NASA-CR-4231; NAS 1.26:4231) Avail: NTIS HC A08/MF A01 CSCL 01C

The integration of the Total Energy Control System (TECS) concept with 4D navigation is described. This integration was made to increase the operational capacity of modern aircraft and encourage incorporation of this increased capability with the evolving National Airspace System (NAS). Described herein is: 4D smoothing, the basic concepts of TECS, the spoiler integration concept, an algorithm for nulling out time error, speed and altitude profile modes, manual spoiler implementation, 4D logic, and the results of linear and nonlinear analysis. Author

N89-23472# Army Armament Research, Development and Engineering Center, Picatinny Arsenal, NJ. Armament Engineering Directorate.
ANALYTICAL TRANSFER FUNCTIONS IN PARALLEL CONFIGURATIONS Final Report
Michael J. Amoruso, Romel Campbell, and Eugene M. Friedman Mar. 1989 52 p Supersedes ARAED-TR-86041
(AD-A205714; ARAED-TR-89006; ARAED-TR-86041) Avail: NTIS HC A04/MF A01 CSCL 12/1

Piecewise analytical solutions for typical autopilot transfer functions were developed to increase speed of digital simulations of guided munitions over standard numerical integration techniques. The replacement of serial autopilot configurations by equivalent parallel configurations avoids difficulties arising from propagation of signals through a sequential network of widely varying natural frequencies and always leads to a decomposition with readily integrated terms. GRA

N89-23473# Air Force Inst. of Tech., Wright-Patterson AFB, OH. School of Engineering.
FLIGHT CONTROL SYSTEM FOR THE CRCA (CONTROL RECONFIGURABLE COMBAT AIRCRAFT) USING A COMMAND GENERATOR TRACKER WITH PI (PROPORTIONAL-PLUS-INTEGRAL) FEEDBACK AND KALMAN FILTER, VOLUME 1 M.S. Thesis
Steven S. Payson Mar. 1989 154 p
(AD-A205723; AD-E501079; AFIT/GE/ENG/89M-6-Vol-1) Avail: NTIS HC A08/MF A01 CSCL 01/4

This research develops an integrated software design package useful in the synthesis of CGT/PI/KF control systems, and uses this software package to design and evaluate a longitudinal flight control system for the Control Reconfigurable Combat Aircraft (CRCA). The software package, called CGTPIKE and built with MATRIXx commands, allows for the synthesis and evaluation of a Command Generator Tracker (CGT) which provides inputs to the system and acts as a pre-compensator, and a regulator with proportional plus integral (PI) feedback which forces the system outputs to mimic the model output. The software also allows the incorporation of a Kalman filter for estimation of the system states. Certainty equivalence can be invoked by adopting the LQG assumptions, thereby allowing the Kalman filter to be designed independently of the CGT/PI controller. The total CGT/PI/KF controller can then be evaluated and the design refined. CGTPIKF is an interactive, menu-driven CAD package which can be used in the development of any CGT/PI/KF control system, regardless of application. A flight control system was designed for the CRCA air combat mode (ACM) entry using CGTPIKF. This control system was designed to force the aircraft to emulate a first order response in pitch rate. GRA

N89-23474# Department of the Navy, Washington, DC.
ACTUATOR RATE SATURATION COMPENSATOR Patent Application
Shawn T. Donley, inventor (to Navy), Garry L. Gross, inventor (to Navy), and Judith L. Koper, inventor (to Navy) 5 May 1988 13 p Filed 5 May 1988
(AD-D013962; US-Patent-Appl-SN-204152) Avail: NTIS HC A03/MF A01 CSCL 20/3

A device for compensating for actuator rate saturation is disclosed by this patent application. The device is an improvement to a servomechanism of the type wherein a command signal and a position feedback signal from a member being positioned are summed to produce an error signal for driving an actuator to position the member in accordance therewith. The improvement is a means for inverting the error signal when the ratio of the slope of the position feedback signal to the slope of the command signal is less than one and the polarity of the error signal is opposite to the polarity of the slope of the command signal, and the absolute value of the error signal is not increasing. Application of the invention to the flight controls of an aircraft is disclosed. GRA

N89-23475# Air Force Inst. of Tech., Wright-Patterson AFB, OH. School of Engineering.
CONTROL DESIGN OF AN UNSTABLE NON-MINIMUM PHASE AIRCRAFT SUBJECT TO CONTROL SURFACE SATURATION M.S. Thesis
Oliver J. Merwin Mar. 1989 164 p
(AD-A206024; AFIT/GE/ENG/89M-5) Avail: NTIS HC A08/MF A01 CSCL 01/4

This thesis seeks to validate a design technique for the control of unstable aircraft which are subject to limited control authority. It applies the technique to a realistic aircraft model, instead of the simplified models used in the theoretical development, to produce a pitch rate controller for widely spaced regions of the flight envelope. First the aircraft is stabilized by feeding back pitch rate. Then an adjustable command limiter is placed in the input path for the stable effective plant. The saturation level of the limiter, adjusted by a second feedback loop, provides the proper command tracking response when the command limiter is not saturated. The final element is a minor feedback loop around the command limiter to provide a second degree of freedom to ensure the limiter comes out of saturation as quickly as possible. Simulations for step commands ranging from 1 to 5 deg/sec pitch rate show the design is quite successful. The stabilator does not saturate in a manner which causes instability even when responding to extreme commands. Simulations of a pulse command show that the command limiter unsaturates rapidly and the aircraft responds appropriately to a reduced pitch command even when the stabilator is near the limit. The technique applies relatively simple linear design tools to the nonlinear problem of control surface saturation. GRA

N89-23476# Air Force Inst. of Tech., Wright-Patterson AFB, OH. School of Engineering.
MULTIVARIABLE FLIGHT CONTROL DESIGN WITH PARAMETER UNCERTAINTY FOR THE AFTI/F-16 M.S. Thesis
Brian J. Pawlowski Mar. 1989 141 p
(AD-A206068; AFIT/GE/ENG/89M-1) Avail: NTIS HC A07/MF A01 CSCL 01/4

Quantitative Feedback Theory (QFT) techniques are used in the design of a multivariable flight control law for the AFTI/F-16. The techniques were developed by Professor Isaac Horowitz, University of California, Davis, California. The flight control problem involves a multiple input-multiple output (MIMO) plant requiring regulation and control in the presence of parameter uncertainty and disturbances. Based on frequency response fundamentals, the technique uses feedback to achieve closed-loop system response within performance tolerances despite plant uncertainty. The range of uncertainty and the output performance specifications are quantitative parameters in the design process. The MIMO control problem is restructured into a set of two input - single output (multiple input - single output (MISO)) problems where one input is a command input to the system and the other is a disturbance input to be attenuated. The control laws for the MISO problems taken together form the solution of the MIMO problem. To obtain a point of comparison between various design techniques, the identical aircraft model previously developed by Mr. A. Finley Barfield is used in this study. The state space form of the model is converted to the transfer function relationships between the plant input and output variables. GRA

09 RESEARCH AND SUPPORT FACILITIES (AIR)

Includes airports, hangars and runways; aircraft repair and overhaul facilities; wind tunnels; shock tubes; and aircraft engine test stands.

For related information see also *14 Ground Support Systems and Facilities (Space).*

N89-23477# National Aeronautical Lab., Bangalore (India). Propulsion Div.
A RESEARCH FACILITY FOR FILM COOLING INVESTIGATIONS WITH EMPHASIS ON THE INSTRUMENTATION SYSTEM
M. D. Manickam May 1987 46 p
(NAL-TM-PR-8704) Avail: NTIS HC A03/MF A01

The layout and the instrumentation of a facility for film cooling investigation is described. The injectant air is heated and the mainflow air remains at ambient temperature while the temperature ratio between the injectant and the main flow is simulated. The lift-off/attachment characteristics, the nature of streamwise penetration, and the lateral spreading of the injectant film for a discrete hole injection configuration in an accelerating turbine blade passage was studied. Though detailed studies of injectant films in the case of flat plates have been carried out by many researchers, little work has been done on the above topic for the case of actual blades. Many regions remain unexplored in this discrete hole cooling process which is considered promising for turbine blades. The instrumentation system has been geared to obtain details of flow and mixing in the vicinity of the injection holes, including the upstream and the downstream regions. Author

N89-23478*# Polytechnic Univ., Farmingdale, NY. Weber Research Inst.
A CHAMBER EXPERIMENT FOR THE FEASIBILITY STUDY OF AN ARTIFICIAL PLASMA REFLECTOR FOR OTH RADAR APPLICATIONS
S. P. Kuo, Y. S. Zhang, Q. H. Ji, P. E. Miller, and K. K. Tiong [1989] 34 p
(Grant NAG5-1051)
(NASA-CR-184912; NAS 1.26:184912) Avail: NTIS HC A03/MF A01 CSCL 14B

The feasibility of using two intersecting beams for plasma generation in the upper atmosphere as an over-the-horizon radar reflector was investigated. A cube was filled with dry air to a pressure corresponding to the simulated altitude, and two components of a split microwave beam were fed into the cube at right angles. Plasma layers were generated where the two beams intersected. Three critical issues were addressed: (1) reflectivity of the generated plasma layers; (2) propagation of high power microwave pulses; and (3) lifetime of the plasma. A.D.

N89-23479# Swedish Inst. for Materials Testing, Boras.
INVESTIGATIONS ON THE CRACKING BEHAVIOR OF JOINTS IN AIRFIELDS AND ROADS: FIELD INVESTIGATIONS AND LABORATORY SIMULATIONS
S. Linde 1988 27 p
(PB89-141279; SP-RAPP-1988:23; ISBN-91-7848-108-2) Avail: NTIS HC A03/MF A01 CSCL 13B

Cracks in airfield runways and loose debris resulting from the cracks cause severe damage to airplanes and airplane engines. The problem of cracks in airfield runways is examined in a series of field investigations and laboratory simulations. Fundamental parameters studied include: influence of water on adhesion of joint sealants/concrete/bituminous concrete; dessication velocity in concrete; the magnitude and speed of the thermal movement on a number of airfields in different climate zones (for a period of three years); the rheological behavior of the bituminous concrete at different temperatures and mechanical loads, especially with regard to tensile speed; and the behavior of the crack repair compound at different tensile speeds and temperatures. These fundamental parameters were computerized into a dynamic program, a so-called function test. Author

N89-23480# Federal Aviation Administration, Atlantic City, NJ.
HELIPORT NIGHT PARKING AREA CRITERIA TEST PLAN Technical Note, Jan. - Apr. 1989
Marvin S. Plotka and Rosanne M. Weiss Mar. 1989 14 p
(Contract FAA-TO701-R)
(DOT/FAA/CT-TN88/45) Avail: NTIS HC A03/MF A01

This flight test plan describes the methodology to examine the issue of heliport night parking surface separation criteria. Operational measures will be collected at the Federal Aviation Administration (FAA) Technical Center, Atlantic City International Airport, New Jersey, using an instrumented UH-1H helicopter. Flight maneuvers will be conducted at the Technical Center to identify night parking area separation criteria under various wind conditions. Wind velocity and direction data will be collected during night parking operations to determine effects at different locations around the parking area. This data will be used to create a baseline for characterizing heliport night parking area separation criteria. The test development, test equipment, data collection, data reduction, and analysis of flight data are discussed. A schedule for the completion of the associated tasks is presented. Author

N89-23481# Defence Research Establishment Suffield, Ralston (Alberta).
DESIGN OF A CHAMBER FOR CBW AEROSOL STUDIES WITH RELATIVE HUMIDITY AND PARTICLE CONCENTRATION CONTROL
J. Ho Feb. 1989 25 p
(AD-A205623; DRES-SM-1271) Avail: NTIS HC A03/MF A01 CSCL 15/6

An aerosol generating system was integrated into a large chamber to regulate three experimental conditions, temperature, relative humidity (RH) and particle concentration during aerosol studies. A commercial heating and cooling unit was used to control temperature. Control of RH was effected by a polymer-based sensing mechanism coupled to a fogging device. Aerosol particle size and numbers were monitored and controlled by a microcomputer-driven detector coupled to an aerosol generator. The system was able to provide precise and reproducible environmental conditions conducive to aerosol studies. Aerosol concentration control was demonstrated over a range of concentrations suitable for different requirements. Under these conditions, a BW simulant aerosol was stable in terms of viability for an extended period of time. As an illustration of the system's potential application, it was used to demonstrate sampling characteristic similarities between a glass fiber filter and a glass impinger. With the features described, the system has significant utility in aerosol studies involving threat detection and protection. This system is easily adapted to drive a dry powder disseminator to generate different CBW simulant aerosols. GRA

N89-23482# Naval Postgraduate School, Monterey, CA.
AEROTHERMODYNAMIC ANALYSIS OF A COANDA/REFRACTION JET ENGINE TEST FACILITY M.S. Thesis
Andre Maraoui Dec. 1988 140 p
(AD-A205937) Avail: NTIS HC A07/MF A01 CSCL 14/2

A computer model of the Coanda/Refraction Jet Engine Test Cell facility was developed using the PHOENICS computer code. The PHOENICS code was utilized to determine the steady aerothermal characteristics of the test cell during the testing of an F404 gas turbine engine with afterburner in operation. Computer generated aerothermodynamic field variables of pressure, velocity and temperature parameters were compared to operational field test data. Observations regarding compared results as well as system behavior are presented. Additionally, recommendations of the applications of PHOENICS to future modeling projects are made. GRA

N89-23483# Air Force Inst. of Tech., Wright-Patterson AFB, OH. School of Engineering.
DESIGN OF WATER TUNNEL TO MEASURE WALL PRESSURE SIGNATURES DUE TO TUNNEL BLOCKAGE AND WAKE EFFECTS M.S. Thesis
Kurt A. Lautenbach Dec. 1988 127 p
(AD-A206025; AFIT/GAE/AA/88D-20) Avail: NTIS HC A07/MF A01 CSCL 20/4

This thesis describes the design and construction of a new test section for the AFWAL Aero Propulsion Lab six-inch water tunnel in building 18. The new test section has a ten-inch square cross section and is designed to measure wall pressure signatures caused by solid and wake blockage of the flow due to the separation bubble which forms around bluff bodies immersed in the flow. The wall pressure signature for a spherical model is predicted. Applications of the method and associated requirements for instrumentation are discussed. GRA

12 ASTRONAUTICS (GENERAL)

For extraterrestrial exploration see *91 Lunar and Planetary Exploration.*

N89-23484# Joint Publications Research Service, Arlington, VA.
JPRS REPORT: SCIENCE AND TECHNOLOGY. USSR: SPACE
16 Feb. 1989 56 p Transl. into ENGLISH from various Russian articles
(JPRS-USP-89-004) Avail: NTIS HC A04/MF A01

Translations are given of various articles from Soviet journals and periodicals. The general area of concern is science and technology, however some specific areas are: space engineering, manned mission highlights, interplanetary sciences, and life sciences. For individual titles, see N89-23485 through N89-23492.

N89-23485# Joint Publications Research Service, Arlington, VA.
BURAN DIMENSIONS, LANDING SIT FACILITIES c16
M. Rebrov *In its* JPRS Report: Science and Technology. USSR: Space 16 Feb. 1989 p 8 Transl. into ENGLISH from Krasnaya Zvezda (Moscow, USSR), 29 Oct. 1988 p 6 (For primary document see N89-23484 17-12)
Avail: NTIS HC A04/MF A01

The structural dimensions and structural weight of the Soviet Buran spacecraft are given. The landing complex for the Buran is located 12 km from the launching installation. It includes radar equipment, range finders, Kurs and Glissada landing systems, a system for controlling air traffic in the vicinity of Baykonur, special transfer devices, and a 6-story building with an instrument and scanning room on its top story. The landing complex's radar equipment is capable of detecting the returning spaceship at a distance of 400 km and an altitude of 40 km. Displayed on screens in the main control room are data on altitude, distance, azimuth, speed, alignment with the central line of the runway, programmed and actual flight paths, equipment in operation, and information from an escort plane. E.R.

N89-23486# Joint Publications Research Service, Arlington, VA.
DETAILS OF BURAN SHUTTLE FLIGHT Abstract Only c16
M. Rebrov *In its* JPRS Report: Science and Technology. USSR: Space 16 Feb. 1989 p 10-11 Transl. into ENGLISH from Krasnaya Zvezda (Moscow, USSR), 16 Nov. 1988 p 4 (For primary document see N89-23484 17-12)
Avail: NTIS HC A04/MF A01

The test flight of the unmanned reusable spaceship Buran took place on 15 Nov. 1988. This flight was preceded by 6000 tests, including tests of individual structural components. It is reported that the rocket's selfcontained guidance system went into operation at 0536 hrs and emergency protection equipment at 0545 hrs on the day of the launching. After the spaceship's onboard systems had been put into the mode of independent orbital flight, comprehensive tests of the ship's structure, combined engine unit and onboard electronic, communications, automation, actuating and control equipment began. The testing of the Buran proceeded smoothly. E.R.

N89-23487# Joint Publications Research Service, Arlington, VA.
DESIGN FEATURES, FLIGHT MONITORING OF BURAN c16
V. Ovcharov *In its* JPRS Report: Science and Technology. USSR: Space 16 Feb. 1989 p 11-12 Transl. into ENGLISH from Sovetskaya Belorussiya (Minsk, USSR), 16 Nov. 1988 p 4 (For primary document see N89-23484 17-12)
Avail: NTIS HC A04/MF A01

The test flights of the Soviet spacecraft, Buran, is announced. Details are given of the spacecraft's thermal protective ceramic tiles. The launching of the spacecraft was photographed by test pilots. Almost all of the spacecraft systems were in operation while it was flying around the Earth. A brief account is given of the flight and landing. E.R.

N89-23488# Joint Publications Research Service, Arlington, VA.
BURAN DESIGNER SEMENOV INTERVIEWED c16
Yu. Semenov and B. Konovalov *In its* JPRS Report: Science and Technology. USSR: Space 16 Feb. 1989 p 12-15 Transl. into ENGLISH from Izvestiya (Moscow, USSR), 6 Dec. 1988 p 2 (For primary document see N89-23484 17-12)
Avail: NTIS HC A04/MF A01

An interview with the designer, Y. P. Semenov, of the Soviet spacecraft, Buran, is given. He is asked about the use of the spacecraft. An economic justification for reusable spacecraft is given. The question of docking with the Mir space station is raised. The designer is asked to contrast the cost of the Buran with that of the U.S. Space Shuttle. The use of the Soviet rocket, Energiya, by the international rocket community is also raised. E.R.

N89-23489# Joint Publications Research Service, Arlington, VA.
COMMENTARY ON FLIGHT OF BURAN SHUTTLE BY DESIGNERS GLUSHKO AND SEMENOV c16
V. Glushko and Yu. Semenov *In its* JPRS Report: Science and Technology. USSR: Space 16 Feb. 1989 p 15-18 Transl. into ENGLISH from Pravda (Moscow, USSR), 17 Nov. 1988 p 3 (For primary document see N89-23484 17-12)
Avail: NTIS HC A04/MF A01

The flight tests of the Soviet Spacecraft, Buran, is examined with the help of two of its designers. The heat shielding systems, its lift-dray ratio, its control systems, along with its flight tests are briefly reviewed. E.R.

N89-23490# Joint Publications Research Service, Arlington, VA.
BURAN SPACE SHUTTLE DESCRIBED BY ENGINEER c16
Aleksandr Nikitin and Atanas Atanasov *In its* JPRS Report: Science and Technology. USSR: Space 16 Feb. 1989 p 18 Transl. into ENGLISH from Rabotnichesko Delo (Sofia, Bulgaria), 3 Jan. 1989 p 5 (For primary document see N89-23484 17-12)
Avail: NTIS HC A04/MF A01

The Soviet spacecraft, Buran, is examined from the standpoint of its systems engineering. The launching, launching site, electronics, and heat shielding systems are reviewed. E.R.

N89-23491# Joint Publications Research Service, Arlington, VA.
ORBIT PARAMETERS GIVEN c13
In its JPRS Report: Science and Technology. USSR: Space 16 Feb. 1989 p 45 Transl. into ENGLISH from Tass (Moscow, USSR), 29 Jan. 1989 (For primary document see N89-23484 17-12)
Avail: NTIS HC A04/MF A01

The orbit parameters are given for the interplanetary station Phobos. The orbit was changed over to the orbit of Mars' artificial satellite. Comprehensive exploration of the surface, atmosphere, plasma and magnetic envelopes of Mars were carried out from aboard the station in the course of its flight in the elliptical orbit. Navigational measurements of the relative movement of the Martian natural and artificial satellites were made and a number of active maneuvers were carried out to ensure the station's gradual approach to Phobos. E.R.

N89-23492# Joint Publications Research Service, Arlington, VA.
MEDICAL AND BIOLOGICAL SUPPORT FOR A MANNED EXPEDITION TO MARS
O. G. Gazenko and Ye. A. Ilin *In its* JPRS Report: Science and Technology. USSR: Space 16 Feb. 1989 p 47-51 Transl. into ENGLISH from Zemlya i Vselennaya (Moscow, USSR), no. 5, Sep.-Oct. 1988 p 15-20 (For primary document see N89-23484 17-12)
Avail: NTIS HC A04/MF A01

Most, but not all, of the problems involved in the medical and biological support of a Soviet manned expedition to Mars are covered. An attempt, from the standpoint of today's knowledge, is made to present just some of the principal problems that remain to be solved on the road of continued development of outer space. As more knowledge is gained, the perspective about the problem will change. E.R.

N89-23493*# National Aeronautics and Space Administration. John F. Kennedy Space Center, Cocoa Beach, FL.
AGENDA OF THE FOURTH ANNUAL SUMMER CONFERENCE, NASA/USRA UNIVERSITY ADVANCED DESIGN PROGRAM
Jun. 1988 105 p Prepared for presentation at Cocoa Beach, FL, 13-17 Jun. 1988; sponsored in part by AIAA
(Grants NGT-21-002-080; NGT-80001)
(NASA-TM-101750; NAS 1.15:101750) Avail: NTIS HC A06/MF A01 CSCL 22A

Presentations given by the participants at the fourth annual summer conference of the NASA/USRA University Advanced Design Program are summarized. The study topics include potential space and aeronautics projects which could be undertaken during a 20 to 30 year period beginning with the Space Station Initial Operating Configuration (IOC) scheduled for the early to mid-1990's. This includes system design studies for both manned and unmanned endeavors; e.g., lunar launch and landing facilities and operations, variable artificial gravity facility for the Space Station, manned Mars aircraft and delivery system, long term space habitat,

construction equipment for lunar bases, Mars oxygen production system, trans-Pacific high speed civil transport, V/STOL aircraft concepts, etc. A.D.

N89-23494*# Jet Propulsion Lab., California Inst. of Tech., Pasadena.
CURRENT DISTRIBUTION IN A THREE-DIMENSIONAL IC ANALYZED BY A PERTURBATION METHOD. PART 1: A SIMPLE STEADY STATE THEORY
Larry D. Edmonds 1 Oct. 1987 64 p
(NASA-CR-185022; JPL-Publ-87-28-Pt-1; NAS 1.26:185022)
Avail: NTIS HC A04/MF A01 CSCL 22A

The steady state current distribution in a three dimensional integrated circuit is presented. A device physics approach, based on a perturbation method rather than an equivalent lumped circuit approach, is used. The perturbation method allows the various currents to be expressed in terms of elementary solutions which are solutions to very simple boundary value problems. A Simple Steady State Theory is the subtitle because the most obvious limitation of the present version of the analysis is that all depletion region boundary surfaces are treated as equipotential surfaces. This may be an adequate approximation in some applications but it is an obvious weakness in the theory when applied to latched states. Examples that illustrate the use of these analytical methods are not given because they will be presented in detail in the future. Author

13 ASTRODYNAMICS

Includes powered and free-flight trajectories; and orbital and launching dynamics.

N89-23495*# Information and Control Systems, Inc., Hampton, VA.
OPTIMAL AEROASSISTED COPLANAR ORBITAL TRANSFER USING AN ENERGY MODEL
Nesim Halyo and Deborah B. Taylor May 1989 67 p
(Contract NAS1-17493)
(NASA-CR-181778; NAS 1.26:181778; FR-688107) Avail: NTIS HC A04/MF A01 CSCL 22C

The atmospheric portion of the trajectories for the aeroassisted coplanar orbit transfer was investigated. The equations of motion for the problem are expressed using reduced order model and total vehicle energy, kinetic plus potential, as the independent variable rather than time. The order reduction is achieved analytically without an approximation of the vehicle dynamics. In this model, the problem of coplanar orbit transfer is seen as one in which a given amount of energy must be transferred from the vehicle to the atmosphere during the trajectory without overheating the vehicle. An optimal control problem is posed where a linear combination of the integrated square of the heating rate and the vehicle drag is the cost function to be minimized. The necessary conditions for optimality are obtained. These result in a 4th order two-point-boundary-value problem. A parametric study of the optimal guidance trajectory in which the proportion of the heating rate term versus the drag varies is made. Simulations of the guidance trajectories are presented. Author

N89-23496# Air Force Inst. of Tech., Wright-Patterson AFB, OH. School of Engineering.
NUMERICAL STUDY OF ORBITAL TRAJECTORIES ABOUT PHOBOS M.S. Thesis
Robert B. Teets Dec. 1988 67 p
(AD-A205822; AFIT/GSO/AA/88D-16) Avail: NTIS HC A04/MF A01 CSCL 03/3

Orbital trajectories obtained from numerical integration of over two thousands set of initial conditions for equations of motion of a spacecraft in the Mars Phobos system are examined in a Phobos centered rotating coordinate frame. The equations of motion, simplified with the choice of the system of units, are integrated using a Hamming fourth order predictor corrector algorithm. As initial velocity and altitude are varied, trajectories in the orbital plane of Phobos about Mars follow and orderly pattern. A range of initial velocities resulted in orbital trajectories about Phobos at a given altitude. Near the center of this range of initial velocities, termed the orbital window, is a unique initial velocity that resulted in a closed periodic orbit (at a given altitude) in the Phobos centered rotating coordinate frame. Trajectories out of the orbital plane of Phobos about Mars are more complex, three-dimensional (helical shaped) paths that do not remain in an inclined plane, but do exhibit some order. Again there is a range of initial velocities that fall within an orbital window. GRA

N89-23497# Massachusetts Inst. of Tech., Cambridge.
AN IMPROVED STRATEGY FOR DETERMINING EARTH SATELLITE ORBITS BY RADIO Technical Report, 29 Apr. 1986 - 27 May 1988
Charles C. Counselman, III and Richard I. Abbot 27 May 1988 28 p
(Contract F19628-86-K-0009)
(AD-A205826; AFGL-TR-88-0129; SR-1) Avail: NTIS HC A03/MF A01 CSCL 08/5

For satellite orbit determination, the most accurate observable available today is microwave phase, differenced between observing stations and between satellites to cancel both transmitter and receiver related errors. For maximum accuracy, the integer cycle ambiguities of such observations must be resolved. To perform this ambiguity resolution, a bootstrapping strategy is effective. The tracking stations must have a wide ranging progression of spacings. Then, by conventional integrated Doppler processing of the observations from the most widely spaced stations, the orbits can be determined well enough to permit resolution of the ambiguities of the observations from the most closely spaced stations. The resolution of these ambiguities can reduce the uncertainty of the orbit determination enough to enable ambiguity resolution for more widely spaced stations, which will reduce the orbital uncertainty further, and enable ambiguity resolution resolution for still more widely spaced stations, and so on. In a test of this strategy with a total of six tracking stations, both the formal and the actual errors of determining NAVSTAR Global Positioning System satellite orbits were reduced by a factor of two. GRA

N89-23498# Air Force Inst. of Tech., Wright-Patterson AFB, OH. School of Engineering.
CONTINUOUS, LOW THRUST COPLANAR ORBIT TRANSFERS WITH VARYING ECCENTRICITY M.S. Thesis
Gregory L. Beeker Dec. 1988 157 p
(AD-A206022; AFIT/GA/AA/88D-01) Avail: NTIS HC A08/MF A01 CSCL 22/3

The purpose of this study was to investigate the Delta v requirements of a continuous, low thrust spacecraft performing coplanar orbit transfers that are constrained by either constant radius of apogee, perigee, or a combination of the two. The transfers were separated into two timescale problems. The fast timescale involved an optimization of the planar thrust control angle, alpha, to produce the maximum change in eccentricity or semimajor axis over a single revolution. The slow timescale applied the fast timescale results to complete the transfer through many revolutions about the primary body. The constrained radii control laws developed provide optimal circular-to-eccentric and eccentric-to-eccentric orbit transfers. However, when applied to circular-to-circular transfers, the resulting Delta v is nearly twice that obtained using the most optimal continuous thrust control law (alpha = 0), i.e., spiral. Future recommended studies include the development of control laws to provide specified changes in apogee, perigee, and the argument of periapsis. GRA

N89-23491# Joint Publications Research Service, Arlington, VA.
ORBIT PARAMETERS GIVEN
In its JPRS Report: Science and Technology. USSR: Space 16 Feb. 1989 p 45 Transl. into ENGLISH from Tass (Moscow, USSR), 29 Jan. 1989 (For primary document see N89-23484 17-12)
Avail: NTIS HC A04/MF A01

14 GROUND SUPPORT SYSTEMS AND FACILITIES (SPACE)

Includes launch complexes, research and production facilities; ground support equipment, e.g., mobile transporters; and simulators.

For related information see also *09 Research and Support Facilities (Air).*

N89-23499# Illinois Univ., Urbana. Fusion Technology Lab.
ELECTROMAGNETIC RAILGUN HYDROGEN PELLET INJECTOR: PROGRESS AND PROSPECT
Kyekyoon Kim Dec. 1988 10 p Presented at the IAEA Technical Committee Meeting on Pellet Injection and Toroidal Confinement, Gut Ising, Federal Rep. of Germany, 24-26 Oct. 1988
(Contract DE-FG02-84ER-52111)
(DE89-009536; CONF-8810231-9) Avail: NTIS HC A02/MF A01

A two-stage, fuseless, plasma-arc-driven electromagnetic railgun system suitable for hydrogen pellet acceleration has been developed and successfully tested. The first stage is a combination of a hydrogen pellet generator and a gas gun, which is responsible for injecting a medium-velocity hydrogen pellet into the second-stage railgun through a coupling piece. As the pellet enters the railgun, a specially designed arc-initiation scheme electrically breaks down the propellant gas which has followed the pellet from the gas gun into the railgun, thus forming a conducting plasma-arc armature immediately behind the pellet. This arc formation event coincides with the triggering of the main railgun current and allows the plasma-arc armature to subsequently propel the hydrogen pellet to a high velocity. Using this two-stage acceleration scheme with a 1-m-long railgun barrel, solid hydrogen pellet velocities in excess of 2.2 km/s have been achieved for a pellet 3.2 mm in diameter and 4 mm in length. The objectives of this paper are two-fold: first, a critical review of the achievements thus far on the railgun hydrogen-pellet injector and second, a description of the most recent technological developments and their implications for future work, in particular, the prospect of employing a railgun pellet injector for future large devices. DOE

15 LAUNCH VEHICLES AND SPACE VEHICLES

Includes boosters; operating problems of launch/space vehicle systems; and reusable vehicles.

For related information see also *20 Spacecraft Propulsion and Power.*

N89-23500# Office of Technology Assessment, Washington, DC.
REDUCING LAUNCH OPERATIONS COSTS: NEW TECHNOLOGIES AND PRACTICES
Sep. 1988 100 p
(PB89-136402; OTA-TM-ISC-28; LC-88-600539) Avail: NTIS HC A05/MF A01 CSCL 22A

The report discusses the issues of launch operations and how the use of advanced technologies and improved management techniques could reduce the costs of launching payloads.
Author

16 SPACE TRANSPORTATION

Includes passenger and cargo space transportation, e.g., shuttle operations; and space rescue techniques.

For related information see also *03 Air Transportation and Safety* and *18 Spacecraft Design, Testing and Performance.* For space suits see *54 Man/System Technology and Life Support.*

N89-23501*# National Inst. of Standards and Technology, Gaithersburg, MD. Center for Fire Research.
EXPERT SYSTEMS APPLIED TO SPACECRAFT FIRE SAFETY Final Report
Richard L. Smith and Takashi Kashiwagi Jun. 1989 13 p
(NASA Order C-32000-M)
(NASA-CR-182266; E-4812; NAS 1.26:182266) Avail: NTIS HC A03/MF A01 CSCL 22B

Expert systems are problem-solving programs that combine a knowledge base and a reasoning mechanism to simulate a human expert. The development of an expert system to manage fire safety in spacecraft, in particular the NASA Space Station Freedom, is difficult but clearly advantageous in the long-term. Some needs in low-gravity flammability characteristics, ventilating-flow effects, fire detection, fire extinguishment, and decision models, all necessary to establish the knowledge base for an expert system, are discussed.
Author

N89-23502# Aerospatiale Aquitaine, Saint-Medard en Jalles (France).
NOZZLES FOR TEST SYSTEM PLASMA GENERATORS [TUYERES SUR MOYENS D'ESSAIS A GENERATION PLASMA]
Rene Leroux Paris, France 1988 34 p In FRENCH Presented at the 25th Colloque d'Aerodynamique Appliquee, Talence, France, 12-14 Oct. 1988
(Rept-882-430-104; ETN-89-94485) Avail: NTIS HC A03/MF A01

In the frame of developing testing procedures for reentry thermal protection, materials used in missiles and Hermes manned vehicle specifically designed nozzles are described. The nozzles implement plasma generators in hypersonic wind tunnel facilities for up to 7000 K and over 100 bar, the conditions necessary to simulate pressure, thermal flow, and Mach number. The design is already validated by experiment and evolves towards higher enthalpies.
ESA

N89-23485# Joint Publications Research Service, Arlington, VA.
BURAN DIMENSIONS, LANDING SIT FACILITIES
M. Rebrov *In its* JPRS Report: Science and Technology. USSR: Space 16 Feb. 1989 p 8 Transl. into ENGLISH from Krasnaya Zvezda (Moscow, USSR), 29 Oct. 1988 p 6 (For primary document see N89-23484 17-12)
Avail: NTIS HC A04/MF A01

N89-23486# Joint Publications Research Service, Arlington, VA.
DETAILS OF BURAN SHUTTLE FLIGHT Abstract Only
M. Rebrov *In its* JPRS Report: Science and Technology. USSR: Space 16 Feb. 1989 p 10-11 Transl. into ENGLISH from Krasnaya Zvezda (Moscow, USSR), 16 Nov. 1988 p 4 (For primary document see N89-23484 17-12)
Avail: NTIS HC A04/MF A01

N89-23487# Joint Publications Research Service, Arlington, VA.
DESIGN FEATURES, FLIGHT MONITORING OF BURAN
V. Ovcharov *In its* JPRS Report: Science and Technology. USSR: Space 16 Feb. 1989 p 11-12 Transl. into ENGLISH from Sovetskaya Belorussiya (Minsk, USSR), 16 Nov. 1988 p 4 (For primary document see N89-23484 17-12)
Avail: NTIS HC A04/MF A01

N89-23488# Joint Publications Research Service, Arlington, VA.
BURAN DESIGNER SEMENOV INTERVIEWED
Yu. Semenov and B. Konovalov *In its* JPRS Report: Science and Technology. USSR: Space 16 Feb. 1989 p 12-15 Transl.

into ENGLISH from Izvestiya (Moscow, USSR), 6 Dec. 1988 p 2 (For primary document see N89-23484 17-12)
Avail: NTIS HC A04/MF A01

N89-23489# Joint Publications Research Service, Arlington, VA.
COMMENTARY ON FLIGHT OF BURAN SHUTTLE BY DESIGNERS GLUSHKO AND SEMENOV
V. Glushko and Yu. Semenov *In its* JPRS Report: Science and Technology. USSR: Space 16 Feb. 1989 p 15-18 Transl. into ENGLISH from Pravda (Moscow, USSR), 17 Nov. 1988 p 3 (For primary document see N89-23484 17-12)
Avail: NTIS HC A04/MF A01

N89-23490# Joint Publications Research Service, Arlington, VA.
BURAN SPACE SHUTTLE DESCRIBED BY ENGINEER
Aleksandr Nikitin and Atanas Atanasov *In its* JPRS Report: Science and Technology. USSR: Space 16 Feb. 1989 p 18 Transl. into ENGLISH from Rabotnichesko Delo (Sofia, Bulgaria), 3 Jan. 1989 p 5 (For primary document see N89-23484 17-12)
Avail: NTIS HC A04/MF A01

17 SPACE COMM., SPACECRAFT COMM., COMMAND & TRACKING

Includes telemetry; space communications networks; astronavigation and guidance; and radio blackout.

For related information see also *04 Aircraft Communications and Navigation* and *32 Communications and Radar.*

No abstracts in this category.

18 SPACECRAFT DESIGN, TESTING AND PERFORMANCE

Includes satellites; space platforms; space stations; spacecraft systems and components such as thermal and environmental controls; and attitude controls.

For life support systems see *54 Man/System Technology and Life Support.* For related information see also *05 Aircraft Design, Testing and Performance, 39 Structural Mechanics,* and *16 Space Transportation.*

N89-23503*# National Aeronautics and Space Administration. Marshall Space Flight Center, Huntsville, AL.
SPACE STATION CMIF EXTENDED DURATION METABOLIC CONTROL TEST Final Report
Richard G. Schunk, Robert M. Bagdigian, Robyn L. Carrasquillo, Kathryn Y. Ogle, and Paul O. Wieland Mar. 1989 190 p
(NASA-TM-100362; NAS 1.15:100362) Avail: NTIS HC A09/MF A01 CSCL 22B

The Space Station Extended Duration Metabolic Control Test (EMCT) was conducted at the MSFC Core Module Integration Facility. The primary objective of the EMCT was to gather performance data from a partially-closed regenerative Environmental Control and Life Support (ECLS) system functioning under steady-state conditions. Included is a description of the EMCT configuration, a summary of events, a discussion of anomalies that occurred during the test, and detailed results and analysis from individual measurements of water and gas samples taken during the test. A comparison of the physical, chemical, and microbiological methods used in the post test laboratory analyses of the water samples is included. The preprototype ECLS hardware used in the test, providing an overall process description and theory of operation for each hardware item. Analytical results pertaining to a system level mass balance and selected system power estimates are also included. Author

N89-23504# National Aerospace Lab., Tokyo (Japan).
STUDY ON A HIGHLY SENSITIVE ELECTRO-STATIC SUSPENDED ACCELEROMETER (1)
Oct. 1988 20 p In JAPANESE; ENGLISH summary
(NAL-TR-1005; ISSN-0389-4010) Avail: NTIS HC A03/MF A01

An artificial satellite in orbit is not free from accelerations due to external forces such as: gravitational anomalies of the earth's oblateness; gravitational attractions of the sun and the moon; pressure of solar wind; aerodynamic drags. The accelerations are very small; however, they disturb precise position keeping of a satellite, attitude control of a large space system, and also micro-gravity experiments such as International Micro-Gravity Laboratory (IML) in the Space lab. A highly sensitive electro-static suspended accelerometer was studied to measure such disturbances. The device has a hollow vacuum vessel. A non-magnetic metal sphere was suspended at the center of the vessel by means of three-dimensional electro-static fields. A small displacement of the position of the sphere due to external forces induced un-balanced electro-static forces in the fields. The force difference was measured as an electrical output. An analysis of the design of the accelerometer is presented. A series of preliminary experiments were carried out to confirm the analysis by developing a two-axis accelerometer. The experimental result shows good stability for 10(-7)g with a threshold at the 10(-8)g level. Author

N89-23505# Air Force Inst. of Tech., Wright-Patterson AFB, OH. School of Engineering.
AN ANALYSIS OF THE ATTITUDE STABILITY OF A SPACE STATION SUBJECT TO PARAMETRIC EXCITATION OF PERIODIC MASS MOTION M.S. Thesis
Thomas E. Williams Dec. 1988 103 p
(AD-A206009; AFIT/GSO/AA/88D-2) Avail: NTIS HC A06/MF A01 CSCL 22/1

The future space station will contain a mechanism that transports mass across large distances of its surface. Accordingly, this study will derive the equations of attitude motion for a gravity-gradient stabilized space station whose moments of inertia are varying with time. The equations are linearized, after which Hill's Equation is used to determine pitch stability, while the Method of Multiple Scales is used to determine the roll/yaw stability of the system. Results show that for certain frequencies of mass motion, attitude motion can grow boundlessly with time. Consequently, the shape of the classical Lagrange stability region is altered. GRA

N89-23506# Aerospace Corp., El Segundo, CA. Space Sciences Lab.
ON-ORBIT OBSERVATIONS OF SINGLE-EVENT UPSET IN HARRIS HM-6508 RAMSS (RANDOM ACCESS MEMORIES): AN UPDATE
J. B. Blake and R. Mandel 16 Feb. 1989 10 p Prepared in cooperation with Lockheed Missiles and Space Corp., Sunnyvale, CA
(Contract F04701-85-C-0086)
(AD-A206266; TR-0088(3940-05)-5; SD-TR-89-07) Avail: NTIS HC A02/MF A01 CSCL 22/2

The Single Event Upset (SEU) phenomenon has continued to be of great interest to designers of spaceflight hardware. Although a great deal of ground testing has been and continues to be carried out, quantitative on-orbit measurements are very limited. Space measurements are a key part of the effort to ensure that the ground-based testing yields accurate predictions of on-orbit upset rates. Blake and Mandel have published data from two years of flight observations from a subsystem consisting of 384 Harris HM-6508 1K RAMs. This report is an update of that study; the results of 2560 days of observation are presented. A total of 234 SEUs were observed during 2560 days of observation. Thus, the average upset rate per day is (2.62 + or - 0.17) x .0000007 upsets/bit day. GRA

N89-23507# Virginia Univ., Charlottesville. Dept. of Applied Mathematics and Computer Science.
INCREASING THE MARGIN OF STABILITY OF ARBITRARILY FINITE MODES OF FLEXIBLE LARGE SPACE STRUCTURES WITH DAMPING Annual Report, 1 Sep. 1987 - 31 Aug. 1988
I. Lasiecka and R. Triggiani Dec. 1988 13 p
(Grant AF-AFOSR-0321-87)
(AD-A206487; UVA/525683/AM89/102; AFOSR-89-0328TR)
Avail: NTIS HC A03/MF A01 CSCL 22/1

Achievements during this report period include new results for wave equations and plate equations, linear and nonlinear, on the following problems: exact controllability, strong and uniform stabilization, structural damping, quadratic optimal control problem, Riccati equations, and numerical aspects thereof. GRA

N89-23508# Aerospatiale Aquitaine, Saint-Medard en Jalles (France). Lab. des Materiaux.
BREAK DIMENSIONING OF SPACE STRUCTURAL ASSEMBLIES AND ITS EXPERIMENTAL VALIDATION [DIMENSIONNEMENT A RUPTURE D'ASSEMBLAGES STRUCTURAUX SPATIAUX ET VALIDATION EXPERIMENTALE]
Jean-Pierre Maigret and Michel Martin Paris, France 1988 4 p In FRENCH Presented at the 2nd International ADHECOM Congress, Mar. 1989
(Rept-882-430-109; ETN-89-94490) Avail: NTIS HC A02/MF A01

The thermomechanical behavior of adhesive bonded metal to composite assemblies and the characterization of the adhesive systems are studied. Computerized simulation procedures and computing routines are developed using the finite difference method. Thermomechanical complex loadings are considered. The solutions are based on the Goland and Reissner model. The first results are compared to those of the finite elemet method. ESA

N89-23509# Aerospatiale Aquitaine, Saint-Medard en Jalles (France).
COMPOSITES IN COMPLEX ASSEMBLIES [LES COMPOSITES DANS ASSEMBLAGE COMPLEXE]
Michel Vignollet Paris, France 1988 43 p In FRENCH
(Rept-882-430-110; ETN-89-94491) Avail: NTIS HC A03/MF A01

The large diversity of application of composite materials to complex space applications is illustrated describing the design, performance, weight gain, cost, and main mechanical characteristics of many aerospace structural elements actually manufactured. ESA

N89-23510# Aerospatiale, Cannes La Bocca (France).
ASSEMBLING THE ISO THERMAL MODEL WITH ESAT AN
A. Rocaboy Paris, France 1988 9 p
(Rept-882-440-107; ETN-89-94500) Avail: NTIS HC A02/MF A01

The thermal analysis conducted at the ISO satellite system level for the demonstration of the helium cryostat operational lifetime is described. The thermal analysis is performed using separate models for each module of the spacecraft. These submodels are condensed and assembled using the modular structure of ESAT AN and subroutines and through numerical interface specification. Guidelines to be applied in assembling submodels are given. Improvements are suggested. ESA

N89-23511# Aerospatiale, Cannes La Bocca (France).
THE TWO APPROACHES FOR THE THERMAL CONTROL OF THE COLUMBUS RESOURCE MODULE AND POLAR PLATFORM
B. Poulain and S. Aucel Paris, France 1988 9 p
(Rept-882-440-110; ETN-89-94503) Avail: NTIS HC A02/MF A01

The two Columbus architecture systems developed lead to two completely different approaches for the thermal control designs of the Resource Module (RM) and the Polar Platform (PP). The optimized PP thermal control in terms of mass and performance has nevertheless penalties on power budget and servicing mass. The RM thermal control has penalties on mass and performance. Although the two thermal controls are quite different, the selected designs of both are the best compromise which could be achieved at system level. ESA

N89-23512*# Lockheed Missiles and Space Co., Palo Alto, CA. Research and Development Div.
SIRTF TELESCOPE INSTRUMENT CHANGEOUT AND CRYOGEN REPLENISHMENT (STICCR) STUDY Final Report, Nov. 1984 - Aug. 1985
T. C. Nast, D. Frank, C. K. Liu, R. T. Parmley, D. Jaekle, H. Builteman, J. Schmidt, and T. H. K. Frederking (California Univ., Los Angeles.) Aug. 1985 175 p
(Contract NAS2-12051)
(NASA-CR-177380; NAS 1.26:177380; T-4277) Avail: NTIS HC A08/MF A01 CSCL 22B

The Space Infrared Telescope Facility (SIRTF) is a long-life cryogenically cooled space-based telescope for infrared astronomy from 2 to 700 micrometers. SIRTF is currently under study by NASA-ARC (Reference AP) and planned for launch in approximately the mid 1990s. SIRTF will operate as a multiuser facility, initially carrying three instruments at the focal plane. It will be cooled to below 2 K by superfluid liquid helium to achieve radiometric sensitivity limited only by the statistical fluctuations in the natural infrared background radiation over most of its spectral range. The lifetime of the mission will be limited by the lifetime of the liquid helium supply, and baseline is currently to be 2 years. The telescope changes required to allow in-space replenishment of the 4,000-L superfluid helium tank was investigated. A preliminary design for the space services equipment was also developed. The impacts of basing the equipment and servicing on the space station were investigated. Space replenishment and changeout of instruments required changes to the telescope design. Preliminary concepts are presented. Author

N89-23530*# National Aeronautics and Space Administration. Langley Research Center, Hampton, VA.
STRUCTURAL MATERIALS FOR SPACE APPLICATIONS
Darrel R. Tenney *In its* NASA/SDIO Space Environmental Effects on Materials Workshop, Part 1 May 1989 p 25-52 (For primary document see N89-23528 17-23)
Avail: NTIS HC A16/MF A01 CSCL 22B

N89-23536*# National Oceanic and Atmospheric Administration, Boulder, CO. Solar-Terrestrial Physics Div.
TRENDS IN ENVIRONMENTALLY INDUCED SPACECRAFT ANOMALIES
Daniel C. Wilkinson *In* NASA, Langley Research Center, NASA/SDIO Space Environmental Effects on Materials Workshop, Part 1 May 1989 p 123-131 (For primary document see N89-23528 17-23)
Avail: NTIS HC A16/MF A01 CSCL 22B

N89-23541*# National Aeronautics and Space Administration. Lyndon B. Johnson Space Center, Houston, TX.
ATOMIC OXYGEN EFFECTS ON SPACECRAFT MATERIALS: THE STATE OF THE ART OF OUR KNOWLEDGE
Steven L. Koontz *In* NASA, Langley Research Center, NASA/SDIO Space Environmental Effects on Materials Workshop, Part 1 May 1989 p 241-253 (For primary document see N89-23528 17-23)
Avail: NTIS HC A16/MF A01 CSCL 22B

N89-23545*# Aerospace Corp., El Segundo, CA. Materials Sciences Lab.
SPACECRAFT CONTAMINATION EXPERIENCE
E. N. Borson *In* NASA, Langley Research Center, NASA/SDIO Space Environmental Effects on Materials Workshop, Part 1 May 1989 p 331-352 (For primary document see N89-23528 17-23)
Avail: NTIS HC A16/MF A01 CSCL 22B

N89-23550*# Aerospace Corp., El Segundo, CA. Thermal Control Dept.
SPACE VEHICLE THERMAL TESTING: PRINCIPLES, PRACTICES AND EFFECTIVENESS
Donald F. Gluck *In* NASA, Langley Research Center, NASA/SDIO Space Environmental Effects on Materials Workshop, Part 2 May 1989 p 395-424 (For primary document see N89-23547 17-23)
Avail: NTIS HC A12/MF A01 CSCL 22B

N89-23552*# National Aeronautics and Space Administration. Langley Research Center, Hampton, VA.
EFFECTS OF THERMAL CYCLING ON COMPOSITE MATERIALS FOR SPACE STRUCTURES
Stephen S. Tompkins *In its* NASA/SDIO Space Environmental Effects on Materials Workshop, Part 2 May 1989 p 447-470 (For primary document see N89-23547 17-23)
Avail: NTIS HC A12/MF A01 CSCL 22B

N89-23553*# Air Force Geophysics Lab., Hanscom AFB, MA. Space Physics Div.
DIELECTRICS FOR LONG TERM SPACE EXPOSURE AND SPACECRAFT CHARGING: A BRIEFING
A. R. Frederickson *In* NASA, Langley Research Center, NASA/SDIO Space Environmental Effects on Materials Workshop, Part 2 May 1989 p 473-494 (For primary document see N89-23547 17-23)
Avail: NTIS HC A12/MF A01 CSCL 22B

N89-23556*# TRW Space Technology Labs., Redondo Beach, CA. System Integration Lab.
INFLUENCE OF CHARGING ENVIRONMENTS ON SPACECRAFT MATERIALS AND SYSTEM PERFORMANCE
N. John Stevens *In* NASA, Langley Research Center, NASA/SDIO Space Environmental Effects on Materials Workshop, Part 2 May 1989 p 535-542 (For primary document see N89-23547 17-23)
Avail: NTIS HC A12/MF A01 CSCL 22B

N89-23563*# TRW Space Technology Labs., Redondo Beach, CA.
SPACECRAFT CHARGING
N. John Stevens *In* NASA, Langley Research Center, NASA/SDIO Space Environmental Effects on Materials Workshop, Part 2 May 1989 p 577-584 (For primary document see N89-23547 17-23)
Avail: NTIS HC A12/MF A01 CSCL 22B

N89-23568*# TRW Space Technology Labs., Redondo Beach, CA.
WORKING GROUP WRITTEN PRESENTATION: SPACECRAFT CHARGING
N. John Stevens *In* NASA, Langley Research Center, NASA/SDIO Space Environmental Effects on Materials Workshop, Part 2 May 1989 p 609-612 (For primary document see N89-23547 17-23)
Avail: NTIS HC A12/MF A01 CSCL 22B

N89-23898*# I.A.M. Rinaldo Piaggio, Finale Ligure (Italy).
DESIGN AND TESTING OF A DEPLOYABLE, RETRIEVABLE BOOM FOR SPACE APPLICATIONS
P. Becchi and S. DellAmico *In* NASA, Marshall Space Flight Center, The 23rd Aerospace Mechanisms Symposium Mar. 1989 p 101-112 (For primary document see N89-23892 17-39)
Avail: NTIS HC A15/MF A01 CSCL 22B

N89-23905*# National Aeronautics and Space Administration. Langley Research Center, Hampton, VA.
DOUBLE LEAD SPIRAL PLATEN PARALLEL JAW END EFFECTOR
David C. Beals *In* NASA, Marshall Space Flight Center, The 23rd Aerospace Mechanisms Symposium Mar. 1989 p 195-206 (For primary document see N89-23892 17-39)
Avail: NTIS HC A15/MF A01 CSCL 22B

19 SPACECRAFT INSTRUMENTATION

For related information see also *06 Aircraft Instrumentation* and *35 Instrumentation and Photography.*

N89-23513# Naval Research Lab., Washington, DC. Upper Atmospheric Physics Branch.
CO-ALIGNING THE RAIDS (REMOTE ATMOSPHERIC AND IONOSPHERIC DETECTION SYSTEM) INSTRUMENTS Interim Report, Apr. 1987 - Sep. 1988
Dianne K. Prinz 9 Feb. 1989 108 p
(AD-A205456; NRL-MR-6400) Avail: NTIS HC A06/MF A01 CSCL 17/5

The RAIDS (Remote Atmospheric Ionospheric Detection System) experiment consists of eight optical instruments that are to make multi-spectral measurements of emissions from neutral and ionized constituents of the earth's atmosphere from an orbiting satellite in the 1990 time frame. The primary goal of RAIDS is to verify theoretical concepts, developed under an Accelerated Research Initiative, which indicate that optical remote-sensing techniques can be used to obtain ionospheric parameters on a global scale. Seven of the instruments are to be attached to a scan platform, mounted in the satellite so as to scan tangent-ray heights between approx. 75 km and approx. 720 km. GRA

20 SPACECRAFT PROPULSION AND POWER

Includes main propulsion systems and components, e.g., rocket engines; and spacecraft auxilliary power sources.

For related information see also *07 Aircraft Propulsion and Power, 28 Propellants and Fuels, 44 Energy Production and Conversion,* and *15 Launch Vehicles and Space Vehicles.*

N89-23514# National Aerospace Lab., Tokyo (Japan).
STUDY OF THE PBE CYCLE 100kN LH2/LO2 ROCKET ENGINE
Takeshi Kanda, Yoshio Wakamatsu, Ryohei Hashimoto, and Akio Kanmuri Mar. 1988 30 p In JAPANESE; ENGLISH summary
(NAL-TR-965; ISSN-0389-4010) Avail: NTIS HC A03/MF A01

It was previously reported that the PBE (Partial Bleed Expander) cycle LH2/LO2 engine had good performance at a 10 kN-thrust. The PBE cycle LH2/LO2 engine and other low-temperature-cycle engines at a 100 kN-thrust are discussed. The PBE cycle 100 kN engine has the same engine performance as that of the GG (Gas Generator) cycle engine. Among the engines whose thrust chambers are regeneratively cooled, the PBE cycle 100 kN engine has the best performance; start transient simulation analysis showed that the PBE cycle engine can start without trouble. It is not suitable that both the nozzle skirt and the thrust chamber of the PBE cycle 100 kN engine be regeneratively cooled. Author

N89-23515*# Renault Vehicles Industriels (France).
SRB ASCENT AERODYNAMIC HEATING DESIGN CRITERIA REDUCTION STUDY, VOLUME 1 Final Report
W. K. Crain, C. L. Frost, and C. D. Engel 18 Jan. 1989 97 p
(Contract NAS8-35322)
(NASA-CR-183580; NAS 1.26:183580; RTR-090-01) Avail: NTIS HC A05/MF A01 CSCL 21H

An independent set of solid rocket booster (SRB) convective ascent design environments were produced which would serve as a check on the Rockwell IVBC-3 environments used to design the ascent phase of flight. In addition, support was provided for lowering the design environments such that Thermal Protection System (TPS), based on conservative estimates, could be removed leading to a reduction in SRB refurbishment time and cost. Ascent convective heating rates and loads were generated at locations in

the SRB where lowering the thermal environment would impact the TPS design. The ascent thermal environments are documented along with the wind tunnel/flight test data base used as well as the trajectory and environment generation methodology. Methodology, as well as, environment summaries compared to the 1980 Design and Rockwell IVBC-3 Design Environment are presented in this volume, 1. E.R.

N89-23516*# National Aeronautics and Space Administration. Lewis Research Center, Cleveland, OH.

SOLAR DYNAMIC POWER FOR SPACE STATION FREEDOM

Thomas L. Labus, Richard R. Secunde, and Ronald G. Lovely (Rockwell International Corp., Canoga Park, CA.) 1989 24 p Presented at the International Conference on Space Power, Cleveland, OH, 5-7 Jun. 1989; sponsored by the International Astronautical Federation

(NASA-TM-102016; E-4730; NAS 1.15:102016) Avail: NTIS HC A03/MF A01 CSCL 22B

The Space Station Freedom Program is presently planned to consist of two phases. At the completion of Phase 1, Freedom's manned base will consist of a transverse boom with attached manned modules and 75 kW of available electric power supplied by photovoltaic (PV) power sources. In Phase 2, electric power available to the manned base will be increased to 125 kW by the addition of two solar dynamic (SD) power modules, one at each end of the transverse boom. Power for manned base growth beyond Phase 2 will be supplied by additional SD modules. Studies show that SD power for the growth eras will result in life cycle cost savings of $3 to $4 billion when compared to PV-supplied power. In the SD power modules for Space Station Freedom, an offset parabolic concentrator collects and focuses solar energy into a heat receiver. To allow full power operation over the entire orbit, the receiver includes integral thermal energy storage by means of the heat of fusion of a salt mixture. Thermal energy is removed from the receiver and converted to electrical energy by a power conversion unit (PCU) which includes a closed brayton cycle (CBC) heat engine and an alternator. The receiver/PCU/radiator combination will be completely assembled and charged with gas and cooling fluid on Earth before launch to orbit. The concentrator subassemblies will be pre-aligned and stowed in the orbiter bay before launch. On orbit, the receiver/PCU/radiator assembly will be installed as a unit. The pre-aligned concentrator panels will then be latched together and the total concentrator attached to the receiver/PCU/radiator by the astronauts. After final electric connections are made and checkout is complete, the SD power module will be ready for operation. Author

N89-23517*# National Aeronautics and Space Administration. Lewis Research Center, Cleveland, OH.

PHOTOVOLTAIC POWER SYSTEM CONSIDERATIONS FOR FUTURE LUNAR BASES

Dennis J. Flood and Joseph Appelbaum 1989 8 p Presented at International PVSEC-4, Sydney, Australia, 14-17 Feb. 1989; sponsored by The Institution of Radio and Electronics Engineers of Australia and The University of New South Wales

(NASA-TM-102019; E-4744; NAS 1.15:102019) Avail: NTIS HC A02/MF A01 CSCL 10B

The cost of transportation to the lunar surface places a premium on developing ultralightweight power system technology to support the eventual establishment of a lunar base. The photovoltaic technology issues to be addressed by the Surface Power program element of NASA's Project Pathfinder are described. Author

N89-23518*# National Aeronautics and Space Administration. Lewis Research Center, Cleveland, OH.

PRELIMINARY ASSESSMENT OF ROVER POWER SYSTEMS FOR THE MARS ROVER SAMPLE RETURN MISSION

David J. Bents 1989 26 p Presented at the International Conference on Space Power, Cleveland, OH, 5-7 Jun. 1989; sponsored by International Astronautical Federation

(NASA-TM-102003; E-4707; NAS 1.15:102003) Avail: NTIS HC A03/MF A01 CSCL 10B

Four isotope power system concepts were presented and compared on a common basis for application to on-board electrical prime power for an autonomous planetary rover vehicle. A representative design point corresponding to the Mars Rover Sample Return (MRSR) preliminary mission requirements (500 W) was selected for comparison purposes. All systems concepts utilize the General Purpose Heat Source (GPHS) isotope heat source developed by DOE. Two of the concepts employ thermoelectric (TE) conversion: one using the GPHS Radioisotope Thermoelectric Generator (RTG) used as a reference case, the other using an advanced RTG with improved thermoelectric materials. The other two concepts employed are dynamic isotope power systems (DIPS): one using a closed Brayton cycle (CBC) turboalternator, and the other using a free piston Stirling cycle engine/linear alternator (FPSE) with integrated heat source/heater head. Near term technology levels have been assumed for concept characterization using component technology figure-of-merit values taken from the published literature. For example, the CBC characterization draws from the historical test database accumulated from space Brayton cycle subsystems and components from the NASA B engine through the mini-Brayton rotating unit. TE system performance is estimated from Voyager/multihundred Watt (MHW)-RTG flight experience through Mod-RTG performance estimates considering recent advances in TE materials under the DOD/DOE/NASA SP-100 and NASA Committee on Scientific and Technological Information programs. The Stirling DIPS system is characterized from scaled-down Space Power Demonstrator Engine (SPDE) data using the GPHS directly incorporated into the heater head. The characterization/comparison results presented here differ from previous comparison of isotope power (made for Low Earth Orbit (LEO) applications) because of the elevated background temperature on the Martian surface compared to LEO, and the higher sensitivity of dynamic systems to elevated sink temperature. The mass advantage of dynamic systems is significantly reduced for this application due to Mars' elevated background temperature. Author

N89-23519*# Pratt and Whitney Aircraft, West Palm Beach, FL. Government Products Div.

DESIGN, FABRICATION AND TEST OF THE RL10 DERIVATIVE II CHAMBER/PRIMARY NOZZLE Final Report, Nov. 1984 - Nov. 1986

R. W. Marable Apr. 1989 136 p

(Contract NAS3-24738)

(NASA-CR-179595; NAS 1.26:179595; FR-19625) Avail: NTIS HC A07/MF A01 CSCL 21H

The design, fabrication and test of the RL10-II chamber/primary nozzle was accomplished as part of the RL10 Product Improvement Program (PIP). The overall goal of the RL10 PIP was to gain the knowledge and experience necessary to develop new cryogenic upper stage engines to fulfill future NASA requirements. The goal would be reached by producing an RL10 engine designed to be reusable, operate at several thrust levels, and have increased performance. The goals for the chamber/primary nozzle task were: (1) to design a reusable assembly capable of operation at increased mixture ratio and low thrust; (2) to fabricate three assemblies using new or updated techniques where possible; and (3) to test one assembly to verify the design and construction. The design and fabrication phases produced an assembly having improved features such as single piece reinforcing band segments (i.e., Mae West segments) and relocated tube exit braze joints (i.e., hooked tube exit). In addition, a computer program was developed to design the chamber tubes to meet both performance and heat transfer requirements. The test phase showed the specific impulse of the test bed engine system to be as predicted. These results, along with the heat transfer data obtained, sufficiently proved the overall design of the RL10-II recontoured and shortened chamber/primary nozzle assembly. Author

N89-23520*# National Aeronautics and Space Administration. Lewis Research Center, Cleveland, OH.

TEST FACILITY AND PRELIMINARY PERFORMANCE OF A 100 kW CLASS MPD THRUSTER

James S. Sovey, Maris A. Mantenieks, Thomas W. Haag, Paul

Raitano, and James E. Parkes (Sverdrup Technology, Inc., Cleveland, OH.) 1989 21 p Presented at the JANNAF Propulsion Meeting, Cleveland, OH, 23-25 May 1989
(NASA-TM-102021; E-4742; NAS 1.15:102021) Avail: NTIS HC A03/MF A01 CSCL 21C

A 260 kW magnetoplasmadynamic (MPD) thruster test facility was assembled and used to characterize thrusters at power levels up to 130 kW using argon and helium propellants. Sensitivities of discharge characteristics to arc current, mass flow rate, and applied magnetic field were investigated. A thermal efficiency correlation developed by others for low power MPD thrusters defined parametric guidelines to minimize electrode losses in MPD thrusters. Argon and helium results suggest that a parameter defined as the product of arc voltage and the square root of the mass flow rate must exceed .7 V-kg(1/2)-s(-1/2) in order to obtain thermal efficiencies in excess of 60 percent. Author

N89-23521*# Rockwell International Corp., Canoga Park, CA. Rocketdyne Div.
SPACE STATION PROPULSION TEST BED
G. L. Briley and S. A. Evans Jan. 1989 270 p
(Contract NAS8-36418)
(NASA-CR-183615; NAS 1.26:183615; RI/RD89-104) Avail: NTIS HC A12/MF A01 CSCL 21H

A test bed was fabricated to demonstrate hydrogen/oxygen propulsion technology readiness for the intital operating configuration (IOC) space station application. The test bed propulsion module and computer control system were delivered in December 1985, but activation was delayed until mid-1986 while the propulsion system baseline for the station was reexamined. A new baseline was selected with hydrogen/oxygen thruster modules supplied with gas produced by electrolysis of waste water from the space shuttle and space station. As a result, an electrolysis module was designed, fabricated, and added to the test bed to provide an end-to-end simulation of the baseline system. Subsequent testing of the test bed propulsion and electrolysis modules provided an end-to-end demonstration of the complete space station propulsion system, including thruster hot firings using the oxygen and hydrogen generated from electrolysis of water. Complete autonomous control and operation of all test bed components by the microprocessor control system designed and delivered during the program was demonstrated. The technical readiness of the system is now firmly established. Author

N89-23522*# National Aeronautics and Space Administration. Lewis Research Center, Cleveland, OH.
ARCJET NOZZLE DESIGN IMPACTS
Francis M. Curran, Amy J. Sovie (Ohio State Univ., Columbus.), and Thomas W. Haag May 1989 15 p Prepared for presentation at the 1989 JANNAF Propulsion Meeting, Cleveland OH, 23-25 May 1989
(NASA-TM-102050; E-4802; NAS 1.15:102050) Avail: NTIS HC A03/MF A01 CSCL 21H

The effect of nozzle configuration on the operating characteristics of a low power dc arcjet thruster was determined. A conical nozzle with a 30 deg converging angle, a 20 deg diverging angle, and an area ratio of 225 served as the baseline case. Variations on the geometry included bell-shaped contours both up and downstream, and a downstream trumpet-shaped contour. The nozzles were operated over a range of specific power near that anticipated for on-orbit operation. Mass flow rate, thrust, current, and voltage were monitored to provide accurate comparisons between nozzles. The upstream contour was found to have minimal effect on arcjet operation. It was determined that the contour of the divergent section of the nozzle, that serves as the anode, was very important in determining the location of arc attachment, and thus had a significant impact on arcjet performance. The conical nozzle was judged to have the optimal current/voltage characteristics and produced the best performance of the nozzles tested. Author

N89-23523*# Morton Thiokol, Brigham City, UT. Aerospace Group.
QUALIFICATION MOTOR NO. 8 (QM-8), VOLUME 1 Final Test Report
D. M. Garecht Mar. 1989 183 p
(Contract NAS8-30490)
(NASA-CR-183650; NAS 1.26:183650; TWR-17591-Vol-1; Publ-89605-Vol-1) Avail: NTIS HC A09/MF A01 CSCL 09C

All inspection and instrumentation data indicate that the QM-8 static test firing conducted 20 January 1989 was successful. Ambient temperature at T-0 was 28 F. With two flights successfully accomplished, this final test in the redesigned solid rocket motor (RSRM) program certified that the design meets motor performance requirements under extreme cold conditions. This test was a prerequisite to the third flight. The entire test article was cold conditioned at 20 to 25 F for approximately 31 days to assure a maximum propellant mean bulk temperature (PMBT) of 40 F, making it the lowest PMBT in the history of the program. This extreme condition also presented the opportunity to certify critical components at low temperatures. Certification of field joint and igniter heaters, adhesive bondline integrity, flex bearing performance, flight instrumentation performance, RSRM seal performance, and LSC and nozzle plug performance was accomplished. Prior to motor ignition, the field joints were maintained between 75 to 130 F, the igniter-to-case joint was maintained between 75 to 123 F, and the case-to-nozzle joint was maintained between 75 to 120 F. QM-8 was tested with induced side loads to simulate the strut loads experienced during ignition and maximum aerodynamic loading conditions. The ability of the safe and arm device to change position from safe-to-arm and arm-to-safe was certified. Ballistics performance was certified at the lower limits. Values were within specification requirements. Nozzle performance was nominal with typical erosion. The use of Fiberite carbon-cloth phenolic was certified. The water deluge system, CO2 quench, and other test equipment performed as planned during all required test operations. Author

N89-23524# Naval Postgraduate School, Monterey, CA.
CODE OPTIMIZATION OF SPECKLE REDUCTION ALGORITHMS FOR IMAGE PROCESSING OF ROCKET MOTOR HOLOGRAMS M.S. Thesis
Dana S. Kaeser Dec. 1988 88 p
(AD-A205306) Avail: NTIS HC A05/MF A01 CSCL 14/1

This thesis supplements and updates previous research completed in the digital analysis of rocket motor combustion chamber holographic images. In particular this thesis deals with the software code optimization of existing automatic data retrieval algorithms that are used to extract useful particle information from the holograms using a micro-computer based imaging system. Two forms of optimization were accomplished, the application of an optimizing FORTRAN compiler to the existing FORTRAN programs and the complete rewrite of the programs in the C language using an optimizing compiler. The overall results achieved were a reduction in executable program size and a significant decrease in program execution speed. GRA

N89-23525# Hersh Acoustical Engineering, Chatsworth, CA.
FLOW-TURNING LOSSES IN SOLID ROCKET MOTORS Final Report, Jul. 1981 - Mar. 1988
Alan S. Hersh and Jin Tso Mar. 1988 66 p
(Contract F04611-81-C-0041)
(AD-A206099; AFAL-TR-87-095) Avail: NTIS HC A04/MF A01 CSCL 21/8

Results are presented of an experimental and analytical investigation of the flow-turning losses resulting from the injection of ambient air into an acoustically energized duct. Measurements show that acoustic energy is absorbed. In all test cases, however, the sound energies absorbed by the finite admittance duct side walls were significantly larger than that absorbed by the injected flows. One dimensional steady state and transient flow-turning solutions were derived. For the special case of rigid walls and low injection rates, the steady-state solutions showed that the flow-turning losses were approximately equal to 10 Log (1-Mav)

where Mav is the average Mach number across the duct cross-section. The one-dimensional solutions inadequately predicted the measured acoustic energy losses. The transient solutions compared very favorably with Culick's model. Both estimated almost the same decay constants. GRA

N89-23526# Army Missile Command, Redstone Arsenal, AL. Structures Directorate.
A NUMERICAL ROUTINE FOR DEFINING ROCKET EXHAUST CHARACTERISTICS AND IMPINGEMENT EFFECTS Technical Report, for period ending Jun. 1988
Roswell W. Nourse Sep. 1988 90 p
(AD-A206323; AD-E951294; AMSMI/TR-RD-ST-88-7) Avail: NTIS HC A05/MF A01 CSCL 21/2

This report presents a computer method for predicting the thermodynamic properties of decaying rocket exhaust plumes. A momentum integral technique is the chosen method for the program. This method describes accurately the plume parameters of Pitot pressure, total temperature, and velocity at discrete axial and radial locations. An analytical method was determined. An empirical determination of the mixing parameter K was made. Program listings are provided with a description of their use. Also included is a plot program for graphically presenting constant contour lines of pressure, temperature, and velocity within the plume flow field. GRA

N89-23527*# National Aeronautics and Space Administration. Lewis Research Center, Cleveland, OH.
RESULTS FROM BASELINE TESTS OF THE SPRE 1 AND COMPARISON WITH CODE MODEL PREDICTIONS
James E. Cairelli, Steven M. Geng, and Robert C. Skupinski (Sverdrup Technology, Inc., Cleveland, OH.) 1989 14 p Prepared for presentation at the 24th Intersociety Energy Conversion Engineering Conference, Washington, DC, 6-11 Aug. 1989; sponsored in part by IEEE, AIAA, ANS, ASME, SAE, ACS and AIChE
(NASA-TM-102044; E-4792; NAS 1.15:102044) Avail: NTIS HC A03/MF A01 CSCL 10B

The space power research engine (SPRE), a free piston Stirling engine with linear alternator, is being tested at NASA-Lewis as a candidate for high capacity space power. Results are presented of baseline engine tests at design and off-design operating conditions. The test results are compared with code model prediction. Author

N89-23902*# General Dynamics Corp., San Diego, CA. Space Systems Div.
PYRO THRUSTER FOR PERFORMING ROCKET BOOSTER ATTACHMENT, DISCONNECT, AND JETTISON FUNCTIONS
Stephen Hornyak *In* NASA, Marshall Space Flight Center, The 23rd Aerospace Mechanisms Symposium Mar. 1989 p 157-167 (For primary document see N89-23892 17-39)
Avail: NTIS HC A15/MF A01 CSCL 21H

23 CHEMISTRY AND MATERIALS (GENERAL)

N89-23528*# National Aeronautics and Space Administration. Langley Research Center, Hampton, VA.
NASA/SDIO SPACE ENVIRONMENTAL EFFECTS ON MATERIALS WORKSHOP, PART 1
Louis A. Teichman, comp. and Bland A. Stein, comp. Washington May 1989 356 p Workshop held in Hampton, VA, 28 Jun. - 1 Jul. 1988
(NASA-CP-3035-Pt-1; L-16575-Pt-1; NAS 1.55:3035-Pt-1) Avail: NTIS HC A16/MF A01 CSCL 11G

The present state of knowledge regarding space environmental effects on materials is described and the knowledge gaps that prevent informed decisions on the best use of advanced materials in space for long-duration NASA and Strategic Defense Initiative Organization (SDIO) missions are identified. Establishing priorities for future ground-based and space-based materials research was a major goal. The end product was an assessment of the current state-of-the-art in space environmental effects on materials in order to develop a national plan for spaceflight experiments. For individual titles, see N89-23529 through N89-23546.

N89-23529*# National Aeronautics and Space Administration. Lewis Research Center, Cleveland, OH.
OVERVIEW OF ENVIRONMENTAL FACTORS c88
C. K. Purvis *In* NASA, Langley Research Center, NASA/SDIO Space Environmental Effects on Materials Workshop, Part 1 May 1989 p 5-24 (For primary document see N89-23528 17-23)
Avail: NTIS HC A16/MF A01 CSCL 11G

The orbital environment is complex, dynamic, and comprised of both natural and system-induced components. Several environment factors are important for materials. Materials selection/suitability determination requires consideration of each and all factors, including synergisms among them. Understanding and evaluating these effects will require ground testing, modeling, and focused flight experimentation. Author

N89-23530*# National Aeronautics and Space Administration. Langley Research Center, Hampton, VA.
STRUCTURAL MATERIALS FOR SPACE APPLICATIONS c18
Darrel R. Tenney *In its* NASA/SDIO Space Environmental Effects on Materials Workshop, Part 1 May 1989 p 25-52 (For primary document see N89-23528 17-23)
Avail: NTIS HC A16/MF A01 CSCL 22B

The long-term performance of structural materials in the space environment is a key research activity within NASA. The primary concerns for materials in low Earth orbit (LEO) are atomic oxygen erosion and space debris impact. Atomic oxygen studies have included both laboratory exposures in atomic oxygen facilities and flight exposures using the Shuttle. Characterization of atomic oxygen interaction with materials has included surface recession rates, residual mechanical properties, optical property measurements, and surface analyses to establish chemical changes. The Long Duration Exposure Facility (LDEF) is scheduled to be retrieved in 1989 and is expected to provide a wealth of data on atomic oxygen erosion in space. Hypervelocity impact studies have been conducted to establish damage mechanisms and changes in mechanical properties. Samples from LDEF will be analyzed to determine the severity of space debris impact on coatings, films, and composites. Spacecraft placed in geosynchronous Earth orbit (GEO) will be subjected to high doses of ionizing radiation which for long term exposures will exceed the damage threshold of many polymeric materials. Radiation interaction with polymers can result in chain scission and/or cross-linking. The formation of low molecular weight products in the epoxy plasticize the matrix at elevated temperatures and embrittle the matrix at low temperatures. This affects both the matrix-dominated mechanical properties and the dimensional stability of the composite. Embrittlement of the matrix at low temperatures results in enhanced matrix microcracking during thermal cycling. Matrix microcracking changes the coefficient of thermal expansion (CTE) of composite laminates and produces permanent length changes. Residual stress calculations were performed to estimate the conditions necessary for microcrack development in unirradiated and irradiated composites. The effects of UV and electron exposure on the optical properties of transparent polymer films were also examined to establish the optimum chemical structure for good radiation resistance. Thoughts on approaches to establishing accelerated testing procedures are discussed. Author

N89-23531*# Mission Research Corp., San Diego, CA.
RADIATION EFFECTS IN SPACECRAFT ELECTRONICS c33
James P. Raymond *In* NASA, Langley Research Center, NASA/SDIO Space Enviromental Effects on Materials Workshop, Part 1 May 1989 p 53-74 (For primary document see N89-23528 17-23)

(Contract N00014-85-C-2642)
Avail: NTIS HC A16/MF A01 CSCL 09C

Effects on the internal spacecraft electronics due to exposure to the natural and enhanced space radiation environment will be reviewed. The emphasis will be placed on the description of the nature of both the exposure environment and failure mechanisms in semiconductors. Understanding both the system environment and device effects is critical in the use of laboratory simulation environments to obtain the data necessary to design and qualify components for successful application. Author

N89-23532*# Rockwell International Corp., Seal Beach, CA.
ENVIRONMENTAL EFFECTS ON SPACECRAFT MATERIALS
J. W. Haffner *In* NASA, Langley Research Center, NASA/SDIO Space Environmental Effects on Materials Workshop, Part 1 May 1989 p 75-86 (For primary document see N89-23528 17-23)
Avail: NTIS HC A16/MF A01 CSCL 11G

The effects on the natural space environments on materials are presented, which may be used for SDI applications. The current state-of-the-art knowledge of those effects was studied, and a literature search, a questionnaire mailing, and some visits to NASA and Air Force research facilities were performed. Phase 2 will be a study of what materials may be used for SDI applications and to what natural space environments they may be vulnerable. Deficiencies in knowledge of the effects of the natural space environments on these materials are to be identified and recommendations are to be made to eliminate these knowledge deficiencies. Author

N89-23533*# Oak Ridge National Lab., TN.
SURFACE TREATMENT USING METAL FOIL LINER **c24**
Ray Garvey *In* NASA, Langley Research Center, NASA/SDIO Space Enviromental Effects on Materials Workshop, Part 1 May 1989 p 87-99 (For primary document see N89-23528 17-23)
Avail: NTIS HC A16/MF A01 CSCL 11D

A metal foil liner can be used to seal large area surfaces. Characteristics of the two-layer foil liner are discussed. Micrographs for foil-to-foil, foil-to-composite, visible seams, and hidden seams are examined. Author

N89-23534*# National Aeronautics and Space Administration. Langley Research Center, Hampton, VA.
THE LONG DURATION EXPOSURE FACILITY MATERIAL EXPERIMENTS
William H. Kinard and James L. Jones, Jr. *In its* NASA/SDIO Space Environmental Effects on Materials Workshop, Part 1 May 1989 p 101-105 (For primary document see N89-23528 17-23)
Avail: NTIS HC A16/MF A01 CSCL 11G

In the early 1970s, the NASA Office of Aeronautics and Space Technology (OAST) approved the Long Duration Exposure Facility (LDEF) Project. The LDEF project provided NASA and other U.S. and foreign research organizations with opportunities to perform critical technology and science experiments in space using the LDEF and the Space Shuttle. Many of the experiments which were developed and are flying on the first LDEF mission are experiments to investigate the effects of the space environment on materials. An overview is provided for these materials experiments. The LDEF was placed in orbit by the shuttle orbiter Challenger in April 1984, and it was to have been retrieved approximately 1 year later. The Challenger accident, however, has delayed the retrieval more than 4 years. The LDEF retrieval is now manifested on Flight 32 in July 1989. Since the facility and experiments will have been in space almost 5-1/4 years when they are retrieved, they will be a national trove of science and technology data. Author

N89-23535*# Naval Research Lab., Washington, DC.
SOME EXAMPLES OF THE DEGRADATION OF PROPERTIES OF MATERIALS IN SPACE
Frederick E. Betz and Joseph A. Hauser *In* NASA, Langley Research Center, NASA/SDIO Space Environmental Effects on Materials Workshop, Part 1 May 1989 p 109-121 (For primary document see N89-23528 17-23)
Avail: NTIS HC A16/MF A01 CSCL 11G

The space environment effects on the silver teflon covering (solar panels) of two SOLRAD SATELLITES AND NTS-Z are examined to analyze the design requirements for the Shuttle Launch Dispenser (SLD). Author

N89-23536*# National Oceanic and Atmospheric Administration, Boulder, CO. Solar-Terrestrial Physics Div.
TRENDS IN ENVIRONMENTALLY INDUCED SPACECRAFT ANOMALIES **c18**
Daniel C. Wilkinson *In* NASA, Langley Research Center, NASA/SDIO Space Environmental Effects on Materials Workshop, Part 1 May 1989 p 123-131 (For primary document see N89-23528 17-23)
Avail: NTIS HC A16/MF A01 CSCL 22B

The Spacecraft Anomaly Data Base was useful in identifying trends in anomaly occurrence. Trends alone do not provide quantitative testimony to a spacecraft's reliability, but they do indicate areas that command closer study. An in-depth analysis of a specific anomaly can be expensive and difficult without access to the spacecraft. Statistically verified anomaly trends can provide a good reference point to begin anomaly analysis. Many spacecraft experience an increase in anomalies during the period of several days centered on the solar equinox, a period that is also correlated with sun eclipse at geostationary altitude and an increase in major geomagnetic storms. Increase anomaly occurrence can also be seen during the local time interval between midnight and dawn. This local time interval represents a region in Earth's near space that experiences an enhancement in electron plasma density due to a migration from the magnetotail during or following a geomagnetic substorm. Author

N89-23537*# National Aeronautics and Space Administration. Goddard Space Flight Center, Greenbelt, MD.
RETURNED SOLAR MAX HARDWARE DEGRADATION STUDY RESULTS
Jack J. Triolo and Gilbert W. Ousley *In* NASA, Langley Research Center, NASA/SDIO Space Environmental Effects on Materials Workshop, Part 1 May 1989 p 133-159 (For primary document see N89-23528 17-23)
Avail: NTIS HC A16/MF A01 CSCl. 11G

The Solar Maximum Repair Mission returned with the replaced hardware that had been in low Earth orbit for over four years. The materials of this returned hardware gave the aerospace community an opportunity to study the realtime effects of atomic oxygen, solar radiation, impact particles, charged particle radiation, and molecular contamination. The results of these studies are summarized. Author

N89-23538*# National Aeronautics and Space Administration. Goddard Space Flight Center, Greenbelt, MD.
EnviroNET: SPACE ENVIRONMENT FOR STRATEGIC DEFENSE INITIATIVE EXPERIMENTS **c82**
Michael Lauriente *In* NASA, Langley Research Center, NASA/SDIO Space Environmental Effects on Materials Workshop, Part 1 May 1989 p 161-175 (For primary document see N89-23528 17-23)
Avail: NTIS HC A16/MF A01 CSCL 05B

EnviroNET is an operational system available to the Strategic Defense Initiative (SDI) experimenters who have access to a terminal or dial-up port. It is a tail node on Space Physics Analysis Network (SPAN) accessible directly or through the national networks via NPSS. Some of the benefits to using EnviroNET include: validated NASA environmental information and interactive space models; facilitating the payload integration process; easy access to expert assistance; and potential for time and cost savings. Author

N89-23539*# National Aeronautics and Space Administration. Lyndon B. Johnson Space Center, Houston, TX.
ENVIRONMENTAL DEFINITION OF THE EARTH'S NEUTRAL ATMOSPHERE **c45**
James T. Visentine *In* NASA, Langley Research Center, NASA/SDIO Space Environmental Effects on Materials Workshop, Part 1 May 1989 p 179-195 (For primary document see N89-23528 17-23)
Avail: NTIS HC A16/MF A01 CSCL 13B

Although number densities are low at altitudes where spacecraft typically operate, high orbital speeds result in incident fluxes and collisional energies large enough to interact with and degrade material surfaces. Global thermospheric models, when combined with orbital mechanics models, may be used to predict atomic oxygen fluence, or total integrated flux incidence on spacecraft sentences. Fluence predictions, when used with STS materials reactivity measurements, provide reliable estimates of the oxidative effects on spacecraft surfaces. Author

N89-23540*# National Aeronautics and Space Administration. Lewis Research Center, Cleveland, OH.
ATOMIC OXYGEN EFFECTS ON MATERIALS
Bruce A. Banks, Sharon K. Rutledge, Joyce A. Brady, and James E. Merrow (Ohio Univ., Athens.) *In* NASA, Langley Research Center, NASA/SDIO Space Environmental Effects on Materials Workshop, Part 1 May 1989 p 197-239 (For primary document see N89-23528 17-23)
Avail: NTIS HC A16/MF A01 CSCL 11G

Understanding of the basic processes of atomic oxygen interaction is currently at a very elementary level. However, measurement of erosion yields, surface morphology, and optical properties for low fluences have brought about much progress in the past decade. Understanding the mechanisms and those factors that are important for proper simulation of low Earth orbit is at a much lower level of understanding. The ability to use laboratory simulations with confidence to quantifiably address the functional performance and durability of materials in low Earth orbit will be necessary to assure long-term survivability to the natural space environment. Author

N89-23541*# National Aeronautics and Space Administration. Lyndon B. Johnson Space Center, Houston, TX.
ATOMIC OXYGEN EFFECTS ON SPACECRAFT MATERIALS: THE STATE OF THE ART OF OUR KNOWLEDGE **c18**
Steven L. Koontz *In* NASA, Langley Research Center, NASA/SDIO Space Environmental Effects on Materials Workshop, Part 1 May 1989 p 241-253 (For primary document see N89-23528 17-23)
Avail: NTIS HC A16/MF A01 CSCL 22B

In the flight materials exposure data base extensive quantitative data is available from limited exposures in a narrow range of orbital environments. More data is needed in a wider range of environments as well as longer exposure times. Synergistic effects with other environmental factors; polar orbit and higher altitude environments; and real time materials degradation data is needed to understand degradation kinetics and mechanism. Almost no laboratory data exists from high fidelity simulations of the LEO environment. Simulation and test system are under development, and the data base is scanty. Theoretical understanding of hyperthermal atom surface reactions in the LEO environment is not good enough to support development of reliable accelerated test methods. The laser sustained discharge, atom beam sources are the most promising high fidelity simulation-test systems at this time. Author

N89-23542*# National Aeronautics and Space Administration. Lyndon B. Johnson Space Center, Houston, TX.
THE LONG-TERM EFFECTS OF THE MICROMETEOROID AND ORBITAL DEBRIS ENVIRONMENTS ON MATERIALS USED IN SPACE
Burton G. Cour-Palais *In* NASA, Langley Research Center, NASA/SDIO Space Environmental Effects on Materials Workshop, Part 1 May 1989 p 257-280 (For primary document see N89-23528 17-23)
Avail: NTIS HC A16/MF A01 CSCL 11G

The long-term effects of the orbital debris and micrometeoroid environments on materials that are current candidates for use on space vehicles are discussed. In addition, the limits of laboratory testing to determine these effects are defined and the need for space-based data is delineated. The impact effects discussed are divided into primary and secondary surfaces. Primary surfaces are those that are subject to erosion, pitting, the degradation and delamination of optical coatings, perforation of atomic oxygen erosion barriers, vapor coating of optics and the production of secondary ejecta particles. Secondary surfaces are those that are affected by the result of the perforation of primary surfaces, for example, vapor deposition on electronic components and other sensitive equipment, and the production of fragments with damage potential to internal pressurized elements. The material properties and applications that are required to prevent or lessen the effects described, are defined. Author

N89-23543*# National Aeronautics and Space Administration. Lyndon B. Johnson Space Center, Houston, TX.
ORBITAL DEBRIS ENVIRONMENT AND DATA REQUIREMENTS **c88**
Donald J. Kessler *In* NASA, Langley Research Center, NASA/SDIO Space Environmental Effects on Materials Workshop, Part 1 May 1989 p 281-299 (For primary document see N89-23528 17-23)
Avail: NTIS HC A16/MF A01 CSCL 03B

Orbital debris is already a major design consideration for Space Station Freedom and is becoming important to the design of unmanned spacecraft. Mathematical models predict the environment will increase with time. The amount it increases is dependent on future operations in space, and how these operations are conducted. Therefore, it is important to understand the sources of debris and which operations will minimize debris generation. This requires that debris be monitored. Currently, NASA plans to have an operational capability to monitor 1 cm debris at 500 km by 1991. However, there are currently no plans to monitor the environment of smaller debris which will be important to future spacecraft design. Author

N89-23544*# National Aeronautics and Space Administration. Lyndon B. Johnson Space Center, Houston, TX.
MICROPARTICLE IMPACTS IN SPACE: RESULTS FROM SOLAR MAX AND SHUTTLE WITNESS PLATE INSPECTIONS
David S. McKay *In* NASA, Langley Research Center, NASA/SDIO Space Environmental Effects on Materials Workshop, Part 1 May 1989 p 301-327 (For primary document see N89-23528 17-23)
Avail: NTIS HC A16/MF A01 CSCL 11G

The Solar Maximum Satellite developed electronic problems after operating successfully in space for several years. Astronauts on Space Shuttle mission STS-41C retrieved the satellite into the orbiter cargo bay, replaced defective components, and re-deployed the repaired satellite into orbit. The defective components were returned to Earth for study. The space-exposed surfaces were examined. The approach and objectives were to: document morphology of impact; find and analyze projectile residue; classify impact by origin; determine flux distribution; and determine implications for space exposure. The purpose of the shuttle witness plate experiment was to detect impacts from PAM D2 solid rocket motor; determine flux and size distribution of particles; and determine abrasion effects on various conditions. Results are given for aluminum surfaces, copper surfaces, stainless steel surfaces, Inconel surfaces, and quartz glass surfaces. Author

N89-23545*# Aerospace Corp., El Segundo, CA. Materials Sciences Lab.
SPACECRAFT CONTAMINATION EXPERIENCE **c18**
E. N. Borson *In* NASA, Langley Research Center, NASA/SDIO Space Environmental Effects on Materials Workshop, Part 1 May

1989 p 331-352 (For primary document see N89-23528 17-23)
Avail: NTIS HC A16/MF A01 CSCL 22B

Effective contamination control must encompass all aspects of ground and flight from design of the system through the end of mission life. Design systems are needed to minimize sensitivity to contamination, ease of cleaning, and contaminant production. Facilities and procedures are critical to maintaining cleanliness during ground operations. Flight operations should be planned so as to minimize contamination. More data from flights are required to assess the adequacy of designs and operations. Standards and specifications should include contamination control requirements. Author

N89-23546*# Jet Propulsion Lab., California Inst. of Tech., Pasadena.
EFFECTS OF THE CONTAMINATION ENVIRONMENT ON SURFACES AND MATERIALS
Carl R. Maag *In* NASA, Langley Research Center, NASA/SDIO Space Environmental Effects on Materials Workshop, Part 1 May 1989 p 353-364 (For primary document see N89-23528 17-23)
Avail: NTIS HC A16/MF A01 CSCL 11G

In addition to the issues that have always existed, demands are being placed on space systems for increased contamination prevention/control. Optical surveillance sensors are required to detect low radiance targets. This increases the need for very low scatter surfaces in the optical system. Particulate contamination levels typically experienced in today's working environments/habits will most likely compromise these sensors. Contamination (molecular and particulate) can also affect the survivability of space sensors in both the natural and hostile space environments. The effects of di-octyl phthalate (DOP) on sensors are discussed. Author

N89-23547*# National Aeronautics and Space Administration. Langley Research Center, Hampton, VA.
NASA/SDIO SPACE ENVIRONMENTAL EFFECTS ON MATERIALS WORKSHOP, PART 2
Louis A. Teichman, comp. and Bland A. Stein, comp. Washington May 1989 253 p Workshop held in Hampton, VA, 28 Jun. - 1 Jul. 1988
(NASA-CP-3035-Pt-2; L-16575-Pt-2; NAS 1.55:3035-Pt-2) Avail: NTIS HC A12/MF A01 CSCL 11G

The National Aeronautics and Space Administration (NASA) and the Strategic Defense Initiative Organization (SDIO) cosponsored a workshop on Space Environmental Effects on Materials. The joint workshop was designed to inform participants of the present state of knowledge regarding space environmental effects on materials and to identify knowledge gaps that prevent informed decisions on the best use of advanced materials in space for long duration NASA and SDIO missions. Establishing priorities for future ground based and space based materials research was a major goal of the workshop. The end product of the workshop was an assessment of the current state-of-the-art in space environmental effects on materials in order to develop a national plan for spaceflight experiments. For individual titles, see N89-23548 through N89-23568.

N89-23548*# Aerospace Corp., Los Angeles, CA.
THE SPACE PARTICLE ENVIRONMENT **c88**
Alfred L. Vampola *In* NASA, Langley Research Center, NASA/SDIO Space Environmental Effects on Materials Workshop, Part 2 May 1989 p 367-382 (For primary document see N89-23547 17-23)
Avail: NTIS HC A12/MF A01 CSCL 03B

The energetic charged particle environment in the Earth's magnetosphere was studied. An overview is provided of trapped particle morphology, the geometry of the trapping regions, the radiation environmental models, the current status of these models, and future modelling requirements. Author

N89-23549*# Aerospace Corp., El Segundo, CA. Space Sciences Lab.
EFFECTS OF SPACE RADIATION ON ELECTRONIC MICROCIRCUITS **c33**
W. A. Kolasinski *In* NASA, Langley Research Center, NASA/SDIO Space Environmental Effects on Materials Workshop, Part 2 May 1989 p 383-392 (For primary document see N89-23547 17-23)
Avail: NTIS HC A12/MF A01 CSCL 09C

The single event effects or phenomena (SEP), which so far have been observed as events falling on one or another of the SE classes: Single Event Upset (SEU), Single Event Latchup (SEL) and Single Event Burnout (SEB), are examined. Single event upset is defined as a lasting, reversible change in the state of a multistable (usually bistable) electronic circuit such as a flip-flop or latch. In a computer memory, SEUs manifest themselves as unexplained bit flips. Since latchup is in general caused by a single event of short duration, the single event part of the SEL term is superfluous. Nevertheless, it is used customarily to differentiate latchup due to a single heavy charged particle striking a sensitive cell from more ordinary kinds of latchup. Single event burnout (SEB) refers usually to total instantaneous failure of a power FET when struck by a single particle, with the device shorting out the power supply. An unforeseen failure of these kinds can be catastrophic to a space mission, and the possibilities are discussed. Author

N89-23550*# Aerospace Corp., El Segundo, CA. Thermal Control Dept.
SPACE VEHICLE THERMAL TESTING: PRINCIPLES, PRACTICES AND EFFECTIVENESS **c18**
Donald F. Gluck *In* NASA, Langley Research Center, NASA/SDIO Space Environmental Effects on Materials Workshop, Part 2 May 1989 p 395-424 (For primary document see N89-23547 17-23)
Avail: NTIS HC A12/MF A01 CSCL 22B

Component qualification and acceptance temperatures are derived from worst case thermal analyses and analytic uncertainty margin subject to certain specified temperature extremes. Temperature requirements are shown for equipment operation within specification and for survival and turn-on (need not operate within specification, but must not experience any degradation when returned to operational range). Temperature excursions for most equipment are seen to be 20 to 50 C above and below room temperature. Components without active electronics which are mounted outboard, such as solar arrays and antennas, are usually designed to withstand wider temperature excursions, particularly at the cold end. Batteries are tightly controlled at cold temperatures to increase life. Payload components such as extremely accurate clocks for precise navigation are controlled over a relatively narrow temperature range. Author

N89-23551*# National Aeronautics and Space Administration. Langley Research Center, Hampton, VA.
ULTRAVIOLET RADIATION EFFECTS
Wayne S. Slemp *In its* NASA/SDIO Space Environmental Effects on Materials Workshop, Part 2 May 1989 p 425-446 (For primary document see N89-23547 17-23)
Avail: NTIS HC A12/MF A01 CSCL 11G

Solar ultraviolet testing was not developed which will provide highly accelerated (20 to 50X) exposures that correlate to flight test data. Additional studies are required to develop an exposure methodology which will assure that accelerated testing can be used for qualification of materials and coatings for long duration space flight. Some conclusions are listed: Solar UV radiation is present in all orbital environments; Solar UV does not change in flux with orbital altitude; UV radiation can degrade most coatings and polymeric films; Laboratory UV simulation methodology is needed for accelerated testing to 20 UV solar constants; Simulation of extreme UV (below 200 nm) is needed to evaluate requirements for EUV in solar simulation. Author

N89-23552*# National Aeronautics and Space Administration. Langley Research Center, Hampton, VA.
EFFECTS OF THERMAL CYCLING ON COMPOSITE MATERIALS FOR SPACE STRUCTURES **c18**
Stephen S. Tompkins *In its* NASA/SDIO Space Environmental Effects on Materials Workshop, Part 2 May 1989 p 447-470 (For primary document see N89-23547 17-23)
Avail: NTIS HC A12/MF A01 CSCL 22B

The effects of thermal cycling on the thermal and mechanical properties of composite materials that are candidates for space structures are briefly described. The results from a thermal analysis of the orbiting Space Station Freedom is used to define a typical thermal environment and the parameters that cause changes in the thermal history. The interactions of this environment with composite materials are shown and described. The effects of this interaction on the integrity as well as the properties of GR/thermoset, Gr/thermoplastic, Gr/metal and Gr/glass composite materials are discussed. Emphasis is placed on the effects of the interaction that are critical to precision spacecraft. Finally, ground test methodology are briefly discussed. Author

N89-23553*# Air Force Geophysics Lab., Hanscom AFB, MA. Space Physics Div.
DIELECTRICS FOR LONG TERM SPACE EXPOSURE AND SPACECRAFT CHARGING: A BRIEFING **c18**
A. R. Frederickson *In* NASA, Langley Research Center, NASA/SDIO Space Environmental Effects on Materials Workshop, Part 2 May 1989 p 473-494 (For primary document see N89-23547 17-23)
Avail: NTIS HC A12/MF A01 CSCL 22B

Charging of dielectrics is a bulk, not a surface property. Radiation driven charge stops within the bulk and is not quickly conducted to the surface. Very large electric fields develop in the bulk due to this stopped charge. At space radiation levels, it typically requires hours or days for the internal electric fields to reach steady state. The resulting electric fields are large enough to produce electrical failure within the insulator. This type failure is thought to produce nearly all electric discharge anomalies. Radiation also induces bond breakage, creates reactive radicals, displaces atoms and, in general, severely changes the chemistry of the solid state material. Electric fields can alter this process by reacting with charged species, driving them through the solid. Irradiated polymers often lose as much as a percent of their mass, or more, at exposures typical in space. Very different aging or contaminant emission can be induced by the stopped charge electric fields. These radiation effects are detailed. Author

N89-23554*# Jet Propulsion Lab., California Inst. of Tech., Pasadena.
AN OVERVIEW OF CHARGING ENVIRONMENTS
S. B. Gabriel and H. B. Garrett *In* NASA, Langley Research Center, NASA/SDIO Space Environmental Effects on Materials Workshop, Part 2 May 1989 p 495-509 (For primary document see N89-23547 17-23)
Avail: NTIS HC A12/MF A01 CSCL 11G

A brief synopsis of the natural environments that play a role in spacecraft charging is presented. Environments that cause both surface and internal charging are discussed along with the mechanisms involved. The geosynchronous and low altitude regions of the Earth's magnetosphere/ionosphere are considered and simple descriptions of each environment presented. As material properties are critical to the charging process, definition of material properties important to charging, which can be affected by the environment, are also described. Several space experiments are proposed that would help fill the gaps in the knowledge of the performance of materials in a charging environment. Author

N89-23555*# National Aeronautics and Space Administration. Lewis Research Center, Cleveland, OH.
SURFACE PHENOMENA IN PLASMA ENVIRONMENTS **c75**
C. K. Purvis and D. C. Ferguson *In* NASA, Langley Research Center, NASA/SDIO Space Environmental Effects on Materials Workshop, Part 2 May 1989 p 511-534 (For primary document see N89-23547 17-23)
Avail: NTIS HC A12/MF A01 CSCL 20I

Plasma interactions and their effects on materials depend on a number of factors, including the pre-existing environment, the properties of surface materials and the characteristics of the system. An additional dimension is the question of mission: some payloads may be much more sen itive to plasma interactions than others. As an example, a payload whose objective is to measure the ambient environment will be more sensitive to any effects than will a power system. Material specific effects include charging and its associated effects, which can result in short- and long-term damage. Selection of materials for a particular application requires consideration of all factors and assessment of effects due to all causes. Proper selection and suitability determination requires analysis to identify the actual environment combined with testing under exposure to single and combined environment factors.
Author

N89-23556*# TRW Space Technology Labs., Redondo Beach, CA. System Integration Lab.
INFLUENCE OF CHARGING ENVIRONMENTS ON SPACECRAFT MATERIALS AND SYSTEM PERFORMANCE **c18**
N. John Stevens *In* NASA, Langley Research Center, NASA/SDIO Space Environmental Effects on Materials Workshop, Part 2 May 1989 p 535-542 (For primary document see N89-23547 17-23)
Avail: NTIS HC A12/MF A01 CSCL 22B

An overview is presented of potential interactions that can occur on spacecraft operating in space environments. These interactions are discussed in detail. The environment acts on spacecraft in such a way that charging of exterior surfaces occurs. The consequences from this charging then affect system operational performance. Hence, it is the coupling of this exterior charging to system performance that is of concern here. These interactions were first discovered in the spacecraft charging phenomena in which the geomagnetic substorms charged external surfaces to a level that discharges occurred. As a result of the discharge, electronic systems either changed logic state (anomalous switching) or failed. These interactions can occur in all orbits. The type associated with geosynchronous orbits is called passive since the environment provides the charging mechanism. This type can also occur in polar orbits due to auroral charging environments. In low Earth orbits, the thermal plasma alleviates charging environment concerns, but system operations can induce similar effects.
Author

N89-23557*# National Aeronautics and Space Administration. Lyndon B. Johnson Space Center, Houston, TX.
ATOMIC OXYGEN **c72**
Lubert J. Leger and James T. Visentine *In* NASA, Langley Research Center, NASA/SDIO Space Environmental Effects on Materials Workshop, Part 2 May 1989 p 545-552 (For primary document see N89-23547 17-23)
Avail: NTIS HC A12/MF A01 CSCL 20H

The effects of atomic oxygen (AO) on materials in aerospace environments are examined. Materials are categorized according to their susceptibility to AO. The degradation effects of AO are examined to determine which materials are most vulnerable. Classes of spacecraft materials are listed and correlated with a performance category. The spacecraft orbits sensitive to AO interactions are also listed. Correlations are presented of AO effects on materials and of spacecraft glow effects. E.R.

N89-23558*# National Aeronautics and Space Administration. Lyndon B. Johnson Space Center, Houston, TX.
MICROMETEOROIDS AND DEBRIS **c90**
Andrew Potter *In* NASA, Langley Research Center, NASA/SDIO Space Environmental Effects on Materials Workshop, Part 2 May 1989 p 553-557 (For primary document see N89-23547 17-23)
Avail: NTIS HC A12/MF A01 CSCL 03B

The materials with vulnerability to micrometeoroids and space debris are discussed. It is concluded that all materials are vulnerable to hypervelocity impacts and that the importance of these impacts depends on the function of material. It is also concluded that low earth orbits are the most significant region relative to orbital debris. The consequences of aerospace environment effects are discussed. E.R.

N89-23559*# Jet Propulsion Lab., California Inst. of Tech., Pasadena.
CONTAMINATION
Carl R. Maag *In* NASA, Langley Research Center, NASA/SDIO Space Environmental Effects on Materials Workshop, Part 2 May 1989 p 559-563 (For primary document see N89-23547 17-23)
Avail: NTIS HC A12/MF A01 CSCL 11G

Contamination of spacecraft in the aerospace environment is examined. The optical systems, thermal control systems and solar power systems were deemed to be most vulnerable to particle damage. It was decided that all orbits should be considered. Specific issues concern whether there are changes in transmittance of optics and the radiative properties of protective coatings. E.R.

N89-23560*# Aerospace Corp., Los Angeles, CA.
TRAPPED RADIATION
Alfred L. Vampola and Wayne K. Stuckey *In* NASA, Langley Research Center, NASA/SDIO Space Environmental Effects on Materials Workshop, Part 2 May 1989 p 565-568 (For primary document see N89-23547 17-23)
Avail: NTIS HC A12/MF A01 CSCL 11G

The vulnerability of spacecraft materials and components to trapped radiation in aerospace environment is considered along with which orbits the radiation effects are most likely to occur. It seems that the effects on organic polymers are embrittlement, change of modulus and coefficient of expansion; on optics the effects are discoloration and distortion. The effects on integrated circuits are also listed. E.R.

N89-23561*# National Aeronautics and Space Administration. Goddard Space Flight Center, Greenbelt, MD.
TRAPPED PARTICLE FLUX MODELS AT NSSDC/WDC-A-R/S
D. Bilitza, D. M. Sawyer, and J. H. King *In* NASA, Langley Research Center, NASA/SDIO Space Environmental Effects on Materials Workshop, Part 2 May 1989 p 569-572 (For primary document see N89-23547 17-23)
Avail: NTIS HC A12/MF A01 CSCL 11G

The data needed in the future for trapped particle modeling are summarized. A short summary of past and future modeling activities and a list of satellite data that have not yet been considered in the modeling efforts is included. Author

N89-23562*# National Aeronautics and Space Administration. Langley Research Center, Hampton, VA.
SOLAR RADIATION **c92**
Wayne S. Slemp *In its* NASA/SDIO Space Environmental Effects on Materials Workshop, Part 2 May 1989 p 573-575 (For primary document see N89-23547 17-23)
Avail: NTIS HC A12/MF A01 CSCL 03B

The effects of solar radiation in aerospace environments on aerospace systems are examined. It was concluded that most materials degrade to solar radiation. The information available on short term effects on materials provides a limited data base. Flight data on coating degradation seems to be confused by contamination. Other conclusions of data examination are listed. E.R.

N89-23563*# TRW Space Technology Labs., Redondo Beach, CA.
SPACECRAFT CHARGING **c18**
N. John Stevens *In* NASA, Langley Research Center, NASA/SDIO Space Environmental Effects on Materials Workshop, Part 2 May 1989 p 577-584 (For primary document see N89-23547 17-23)
Avail: NTIS HC A12/MF A01 CSCL 22B

The effects of spacecraft charging on spacecraft materials are studied. Spacecraft charging interactions seem to couple environment to system performance through materials. Technology is still developing concerning both environment-driven and operating system-driven interactions. The meeting addressed environment but lacked specific mission requirements, as a result system definition are needed to prioritize interactions. E.R.

N89-23564*# National Aeronautics and Space Administration. Lyndon B. Johnson Space Center, Houston, TX.
WORKING GROUP WRITTEN PRESENTATION: ATOMIC OXYGEN
Lubert J. Leger and James T. Visentine *In* NASA, Langley Research Center, NASA/SDIO Space Environmental Effects on Materials Workshop, Part 2 May 1989 p 587-588 (For primary document see N89-23547 17-23)
Avail: NTIS HC A12/MF A01 CSCL 11G

Earlier Shuttle flight experiments have shown NASA and SDIO spacecraft designed for operation in low-Earth orbit (LEO) must take into consideration the highly oxidative characteristics of the ambient flight environment. Materials most adversely affected by atomic oxygen interactions include organic films, advanced (carbon-based) composites, thermal control coatings, organic-based paints, optical coatings, and thermal control blankets commonly used in spacecraft applications. Earlier results of NASA flight experiments have shown prolonged exposure of sensitive spacecraft materials to the LEO environment will result in degraded systems performance or, more importantly, lead to requirements for excessive on-orbit maintenance, with both conditions contributing significantly to increased mission costs and reduced mission objectives. Flight data obtained from previous Space Shuttle missions and results of the Solar Max recovery mission are limited in terms of atomic oxygen exposure and accuracy of fluence estimates. The results of laboratory studies to investigate the long-term (15 to 30 yrs) effects of AO exposure on spacecraft surfaces are only recently available, and qualitative correlations of laboratory results with flight results have been obtained for only a limited number of materials. The working group recommended the most promising ground-based laboratories now under development be made operational as soon as possible to study the full-life effects of atomic oxygen exposure on spacecraft systems. Author

N89-23565*# National Aeronautics and Space Administration. Lyndon B. Johnson Space Center, Houston, TX.
WORKING GROUP WRITTEN PRESENTATION: METEOROID/ORBITAL DEBRIS EFFECTS ON MATERIALS
Andrew Potter *In* NASA, Langley Research Center, NASA/SDIO Space Environmental Effects on Materials Workshop, Part 2 May 1989 p 589-594 (For primary document see N89-23547 17-23)
Avail: NTIS HC A12/MF A01 CSCL 11G

Low earth orbit (LEO) is the most significant region relative to orbital debris, since the flux of orbital debris peaks in the region from 800 to 1000 kilometers, and the relative velocities of objects in LEO are about 10 kilometers per second. The flux and relative velocities of objects in geosynchronous orbit (GEO) are small, so that debris is not considered to be a problem in GEO. The meteoroid environment is independent of orbit or altitude, so that its effects are the same in LEO and GEO. The effects of orbital debris and meteoroid impacts can be divided into two broad regions: (1) Erosion and pitting; Small particles (less than 100 microns) are very numerous. Impacts from these generally do not lead to penetration of surfaces, but cause pitting and erosion. The Solar Max surfaces were peppered with thousands of tiny impact pits. (2) Catastrophic impacts; Large debris particles are few in number relative to small debris, so that the probability of an impact is low. However, the effects of an impact of a large particle at 10 kilometers per second are devastating. These effects are examined. Author

N89-23566*# National Aeronautics and Space Administration. Langley Research Center, Hampton, VA.
WORKING GROUP WRITTEN PRESENTATION: TRAPPED RADIATION EFFECTS
Alfred L. Vampola, Wayne K. Stuckey, D. Coulter, E. J. Friebele, K. J. Hand, D. A. Hardy, P. Higby, W. A. Kolasinski, R. T. Santoro, and Stephen S. Tompkins (National Aeronautics and Space Administration. Langley Research Center, Hampton, VA.) *In its* NASA/SDIO Space Environmental Effects on Materials Workshop, Part 2 May 1989 p 597-605 (For primary document see N89-23547 17-23)
Avail: NTIS HC A12/MF A01 CSCL 11G

The results of the Trapped Radiation Effects Panel for the Space Environmental Effects on Materials Workshop are presented. The needs of the space community for new data regarding effects of the space environment on materials, including electronics are listed. A series of questions asked of each of the panels at the workshop are addressed. Areas of research which should be pursued to satisfy the requirements for better knowledge of the environment and better understanding of the effects of the energetic charged particle environment on new materials and advanced electronics technology are suggested. Author

N89-23567*# National Aeronautics and Space Administration. Langley Research Center, Hampton, VA.
WORKING GROUP WRITTEN PRESENTATION: SOLAR RADIATION
Wayne S. Slemp *In its* NASA/SDIO Space Environmental Effects on Materials Workshop, Part 2 May 1989 p 607-608 (For primary document see N89-23547 17-23)
Avail: NTIS HC A12/MF A01 CSCL 11G

The members of the Solar Radiation Working Group arrived at two major solar radiation technology needs: (1) generation of a long term flight data base; and (2) development of a standardized UV testing methodology. The flight data base should include 1 to 5 year exposure of optical filters, windows, thermal control coatings, hardened coatings, polymeric films, and structural composites. The UV flux and wavelength distribution, as well as particulate radiation flux and energy, should be measured during this flight exposure. A standard testing methodology is needed to establish techniques for highly accelerated UV exposure which will correlate well with flight test data. Currently, UV can only be accelerated to about 3 solar constants and can correlate well with flight exposure data. With space missions to 30 years, acceleration rates of 30 to 100X are needed for efficient laboratory testing. Author

N89-23568*# TRW Space Technology Labs., Redondo Beach, CA.
WORKING GROUP WRITTEN PRESENTATION: SPACECRAFT CHARGING **c18**
N. John Stevens *In* NASA, Langley Research Center, NASA/SDIO Space Environmental Effects on Materials Workshop, Part 2 May 1989 p 609-612 (For primary document see N89-23547 17-23)
Avail: NTIS HC A12/MF A01 CSCL 22B

A brief listing of the concerns of the working group on spacecraft charging is presented. Brief conclusions for each concern is also given. E.R.

N89-23569# Kernforschungsanlage, Juelich (Germany, F.R.). International Bureau.
THE 8TH GERMAN-YUGOSLAV MEETING ON MATERIALS SCIENCE AND DEVELOPMENT: CERAMICS AND METALS
Drago Kolar, ed., Marija Kosec, ed., and Johanna Krawczynski, ed. 1988 479 p Meeting held in Brdo pri Kranju, Yugoslavia, 18-21 May 1987
(JUEL-Spez-446; ISBN-3-89336-001-8; ETN-89-93956) Copyright Avail: NTIS HC A21/MF A01

Powder synthesis and forming; sintering and microstructure; mechanical properties of ceramics and metals; thermal properties; surfaces and interfaces; and electrical and magnetic properties were discussed. For individual titles, see N89-23570 through N89-23618.

N89-23570# Kernforschungsanlage, Juelich (Germany, F.R.). International Bureau.
MATERIALS SCIENCE COOPERATION IN 1987
Johanna Krawczynski *In its* The 8th German-Yugoslav Meeting on Materials Science and Development: Ceramics and Metals 1988 p 1-8 (For primary document see N89-23569 17-23)
Copyright Avail: NTIS HC A21/MF A01

The European Community programs Basic Research in Industrial Technologies for Europe, and European Research on Advanced Materials are outlined. The Materials Sciences program of the Federal Ministry for Research and Technology of the Federal Republic of Germany is presented. Bilateral German-Yugoslav cooperation in materials sciences is summarized. ESA

N89-23571# Max-Planck-Inst. fuer Metallforschung, Stuttgart (Germany, F.R.). Pulvermetallurgisches Lab.
CERAMIC PROJECT OF THE MAX-PLANCK SOCIETY **c27**
Guenter Petzow *In* Kernforschungsanlage Juelich GmbH, The 8th German-Yugoslav Meeting on Materials Science and Development: Ceramics and Metals 1988 p 9-15 (For primary document see N89-23569 17-23)
Copyright Avail: NTIS HC A21/MF A01

The construction of ceramics laboratories, the establishment of a professor's chair for nonmetallic inorganic materials, and the research program of the project are summarized. The aim of the project is to develop thermally and mechanically highly stressed ceramic materials for engine and turbine components. The program includes production and processing of high purity ceramic powders; microstructural reinforcement of advanced ceramics; study of high temperature properties (1000 to 1500C); and study of thermodynamic phase equilibria in multicomponent ceramic systems. ESA

N89-23572# Karlsruhe Univ. (Germany, F.R.). Inst. fuer Chemische Technik.
SILICON-CARBIDE MADE OF SILICON-ORGANIC COMPOUNDS **c27**
E. Fitzer and Mathias Keuthen *In* Kernforschungsanlage Juelich GmbH, The 8th German-Yugoslav Meeting on Materials Science and Development: Ceramics and Metals 1988 p 19-26 (For primary document see N89-23569 17-23)
Copyright Avail: NTIS HC A21/MF A01

The composition, properties, and applications of an SiC fiber are shown, and a route from hydrido-polysilazane is outlined. The application domains of the resulting continuous SiC fiber in various industries are listed. The synthesis of an SiC precursor and thermal degradation to SiC are described. Experiments on the applicability of the SiC precursor as liquid impregnant, and development of SiC composites are mentioned. ESA

N89-23573# Institut za Nuklearne Nauke Boris Kidric, Belgrade (Yugoslavia). Inst. for Materials.
SLIP CASTING OF FUSED SILICA **c27**
Dusan Kicevic, B. Kostic, and M. Gasic *In* Kernforschungsanlage Juelich GmbH, The 8th German-Yugoslav Meeting on Materials Science and Developement: Ceramics and Metals 1988 p 27-36 (For primary document see N89-23569 17-23)
Copyright Avail: NTIS HC A21/MF A01

It is shown, using slip casting process analysis and experimental results, that the casting rate of fused silica can be increased by vibrocasting, pressure casting, and casting of coarse grain slip. All of these methods yield satisfactory green cast densities, and in certain cases, higher densities than those obtained by prolonged simple drain casting. ESA

N89-23574# Ljubljana Univ. (Yugoslavia).
INJECTION MOLDING OF WHISKER-REINFORCED Al2O3-ZrO2 CERAMICS **c27**
Tomaz Kosmac, D. Gorjan, E. Lutz, and N. Claussen (Technische Univ., Hamburg, Germany, F.R.) *In* Kernforschungsanlage Juelich GmbH, The 8th German-Yugoslav Meeting on Materials Science and Development: Ceramics and Metals 1988 p 37-44

Sponsored by the Research Council of Slovenia, Yugoslavia (For primary document see N89-23569 17-23)
Copyright Avail: NTIS HC A21/MF A01

Injection molding was used to shape SiC whisker reinforced Al2O3-ZrO2 ceramic parts, and the influence of the whiskers was studied. High amounts of organic vehicle are needed to obtain sufficient plasticity in the case of firmly agglomerated powders. The presence of ZrO2 and SiC whiskers has a more pronounced influence on the specific surface area and dry pressing ability of the powder mixture, whereas the paste characteristics are mainly determined by the properties of the major powder mixture constituent. With 10 percent SiC whisker, loading in a paste containing 45 percent of organic vehicle, whisker orientation is seen to depend on shear rate of the paste at the mold gate. ESA

N89-23575# Max-Planck-Inst. fuer Metallforschung, Stuttgart (Germany, F.R.). Inst. fuer Werkstoffwissenschaften.
SINTERING AND HIPing WITH ADDITIVES **c26**
Wolfgang A. Kaysser, Guenter Petzow, and M. Mitkov (Institut za Nuklearne Nauke Boris Kidric, Belgrade, Yugoslavia) *In* Kernforschungsanlage Juelich GmbH, The 8th German-Yugoslav Meeting on Materials Science and Development: Ceramics and Metals 1988 p 47-61 Sponsored in part by Deutsche Forschungsgemeinschart, Bonn, Fed. Republic of Germany (For primary document see N89-23569 17-23)
Copyright Avail: NTIS HC A21/MF A01

The effects of additives on pressureless and pressure assisted sintering are described using examples which cover basic principles of interactions of additives with the host material. Solid state sintering and hot isostatic pressing with a small amount of additives is reviewed, and the process with additives forming a second phase is summarized. Liquid phase sintering, densification, liquid film penetration, and liquid and film migration is described. ESA

N89-23576# Skopje Univ. (Yugoslavia). Faculty of Technology and Metallurgy.
PREPARING AND SINTERING OF YTTRIA-STABILIZED ZIRCONIA **c27**
Blagoj Pavlovski, L. Stojanovska, and B. Jasmakovski *In* Kernforschungsanlage Juelich GmbH, The 8th German-Yugoslav Meeting on Materials Science and Development: Ceramics and Metals 1988 p 63-72 (For primary document see N89-23569 17-23)
Copyright Avail: NTIS HC A21/MF A01

Reactive and homogeneous stabilized zirconia was prepared by coprecipitation from a solution of ZrOCl2 and YCl3. The X-ray diffraction patterns of the dried hydroxide show that the material is amorphous and that it transforms rapidly to a crystalline state at 515C. The calcined powders were cold pressed at 60 MPa and the sintering of the obtained samples was done at 1300 and 1400C. Microstructure and phase composition were examined. The partially stabilized zirconia was tested for resistance to thermal shocks between 1300 and 20C. Results show that samples with 3 mol percent Y2O3 have the best shock resistance. ESA

N89-23577# Technische Hochschule, Aachen (Germany, F.R.). Inst. fuer Gesteinshuettenkunde.
INVESTIGATIONS OF MULLITE-ZIRCONIA COMPOSITES **c27**
Thomas Fandel and W. Kroenert *In* Kernforschungsanlage Juelich GmbH, The 8th German-Yugoslav Meeting on Materials Science and Development: Ceramics and Metals 1988 p 73-80 (For primary document see N89-23569 17-23)
Copyright Avail: NTIS HC A21/MF A01

Mullite-zirconia products were produced by sintering. It is shown that the products obtained from the fused mullite and zirconia powders have good thermal and mechanical properties, especially hot modulus of rupture and thermal shock resistance, for refractory applications. The products are fine grained, nearly dense, with a homogeneous microstructure. Tests show that MgO-PSZ is destabilized in the mullite matrix, but the densification is improved by the formation of a liquid phase. ESA

N89-23578# Kernforschungsanlage, Juelich (Germany, F.R.).
PREPARATION AND THERMAL EXPANSION OF Al2TiO5-TiO5-TiO2 SINTERED BODIES **c27**
Ivan Stamenkovic (Institut za Nuklearne Nauke Boris Kidric, Belgrade, Yugoslavia) and Gerhard Ondracek *In its* The 8th German-Yugoslav Meeting on Materials Science and Development: Ceramics and Metals 1988 p 81-88 (For primary document see N89-23569 17-23)
Copyright Avail: NTIS HC A21/MF A01

The synthesis of Al2TiO5 material in the form of two-phase ceramics was studied in view of its application as a host material in nuclear waste management and in bioceramics. The modifying component was TiO2, chosen because of its high corrosion resistance with respect to nuclear waste materials and its biocompatibility. The whole concentration range between the two phases was studied to assess property changes. The TiO2 particles were considered as a dispersed component in the Al2TiO5 matrix, the composite system having a negative thermal expansion difference of minus 6.4C/deg C at 20 to 1200C. Microstructural analysis of sintered samples shows that samples with the lowest TiO2 content have fairly nonsintered Al2TiO5 matrix, confirming its poor sinterability. However, samples with 35 vol percent TiO2 are characterized by interbonded TiO2 particles due to its sintering temperature lower than Al2TiO5. Theoretical analysis shows that altering the strength ratio and/or strength values and/or elastic moduli of matrix/dispersed component could be tailored to the composite material without matrix cracking. ESA

N89-23579# Technische Hochschule, Aachen (Germany, F.R.).
MICROSTRUCTURE DEVELOPMENT IN ALUMINA **c27**
Piet Reijnen and H. D. Kim *In* Kernforschungsanlage Juelich GmbH, The 8th German-Yugoslav Meeting on Materials Science and Development: Ceramics and Metals 1988 p 91-97 (For primary document see N89-23569 17-23)
Copyright Avail: NTIS HC A21/MF A01

The role of sintering additives on microstructure development in alumina was studied, and the phase relationships in the system Al2O3 (bulk)-MgO-TiO2-Na2O were established using large amounts of impurities in order to be able to detect the phases by X-ray diffraction. The results show that additions of MgO and TiO2 have a strong effect on the sintering of alumina, but the presence of small amounts of Na2O influence considerably the kind of phase formed. All samples containing excess TiO2 beyond stoichiometric composition show enhanced sintering and grain growth, due to the formation of a liquid phase. The Na2O is combined preferentially in the Beta and Beta"" phase as soon as excess MgO is present. ESA

N89-23580# Institut za Nuklearne Nauke Boris Kidric, Belgrade (Yugoslavia).
SINTERING OF CaO AND MgO IN THE PRESENCE OF NONEQUILIBRIUM LIQUID PHASE **c27**
Emilija Kostic, Sandor J. Kiss, and D. Cerovic *In* Kernforschungsanlage Juelich GmbH, The 8th German-Yugoslav Meeting on Materials Science and Development: Ceramics and Metals 1988 p 99-107 (For primary document see N89-23569 17-23)
Copyright Avail: NTIS HC A21/MF A01

The effects of additives forming equilibrium liquid phase at sintering temperatures on inactive alumina powders were tested, using systems CaO with CoO addition, as well as MgO with manganese oxide addition. The densification process is enhanced in CaO-CoO and MgO-MnO systems through the sintering in the presence of transient liquid phase. After sintering at 1700 C, 2 hr, the liquid phase in the CaO-CoO system disappears, but in the MgO-MnO system it is still present. Increased additive amount provokes more pronounced densification, more evident in CaO-CoO system in which material without open porosity is attained. Intense grain growth is observed in both investigated cases, being more evident with CaO-CoO system. Sintering is accompanied by solid solution formation from which during cooling secondary crystalline phases reprecipitate. These secondary phase were observed under

the light microscope. Precipitated phases are very finegrained and they could not be detected by X-ray. Ceramic material based on CaO is more resistant to basic slag attack. ESA

N89-23581# Institut za Nuklearne Nauke Boris Kidric, Belgrade (Yugoslavia).
SINTERING OF Si3N4 IN THE PRESENCE OF ADDITIVES FROM Y2O3-SiO2-Al2O3 SYSTEM **c27**
Snezana Boskovic *In* Kernforschungsanlage Juelich GmbH, The 8th German-Yugoslav Meeting on Materials Science and Development: Ceramics and Metals 1988 p 109-117 (For primary document see N89-23569 17-23)
Copyright Avail: NTIS HC A21/MF A01

Sintering of Si3N4 in the presence of liquid phase from Y2O3-SiO2-Al2O3 system was investigated. Starting composition of liquid phase was varied according to data in the phase diagram of Y2O3-SiO2-Al2O3 system, in order to lower the temperature of liquid formation because it might exibit an influence on the sintering behavior of Si3N4. Densification as well as phase analysis were followed as a function of composition and the amount of liquid phase, both in sintered and in hot pressed samples. Results show that it is possible to synthesize materials from this system by pressureless sintering. Keeping the Y2O3/SiO2 ratio within 2.6 and 1.5 limit, one can synthesize single phase ceramics which can subsequently be heat treated to crystallize the existing glass. Chemical reaction takes place with additives having lower Y2O3/SiO2 ratio, with a negative effect on densification during liquid phase sintering. Additive amount can be kept as low as 15 percent during pressureless sintering because already at 1780 C, open porosity is zero with certain additives. ESA

N89-23582# Center for Research and Development of Materials, Sarajevo (Yugoslavia).
MICROSTRUCTURE DEVELOPMENT IN SiC **c27**
Taric Fetahagic and Drago Kolar (Ljubljana Univ., Yugoslavia) *In* Kernforschungsanlage Juelich GmbH, The 8th German-Yugoslav Meeting on Materials Science and Development: Ceramics and Metals 1988 p 119-128 (For primary document see N89-23569 17-23)
Copyright Avail: NTIS HC A21/MF A01

Microstructure development and grain growth in alpha SiC were examined by analyzing photomicrographs of sintered SiC materials. Activated alpha-SiC powders with boron and carbon additives sinter rapidly to high densities. Typically, densities above 97 percent of the theoretical value may be achieved at 2080 C in less than 30 min. Microstructures of such samples consist of isometric grains with average grain size of 4 microns. The remaining pores are located at grain boundaries. After the high density is achieved, rapid grain growth takes place with linear time dependence and the grain size distribution curve broadens. Above the average 10 micron size, the grain growth rate levels off and large pores appear within the grains. ESA

N89-23583# Karlsruhe Univ. (Germany, F.R.). Inst. fuer Keramik im Maschinenbau.
FATIGUE IN CERAMICS **c27**
Georg Grathwohl *In* Kernforschungsanlage Juelich GmbH, The 8th German-Yugoslav Meeting on Materials Science and Development: Ceramics and Metals 1988 p 131-139 (For primary document see N89-23569 17-23)
Copyright Avail: NTIS HC A21/MF A01

Methods to identify true cyclic fatigue behavior in ceramics, in contrast with static fatigue phenomena, are presented. Results for different ceramic materials are reviewed, and possible cyclic fatigue mechanisms are considered. It is concluded that specific cyclic fatigue mechanisms are active when ceramic components are loaded in a cyclic manner. There may be a difference in the crack growth behavior between a situation with alternating stresses and swelling (e.g., tension-tension) stresses. The relevant fatigue mechanisms are not completely understood and quantitative relations between the controlling microstructural features and the parameters of crack growth kinetics have to be elaborated. Cyclic induced crack extension mechanisms include the participation of residual stresses which enable an additional crack growth step during the unloading phase. Features responsible for the R-curve behavior of ceramics may suffer in a particular way by cyclic stresses. The idea that the compression half-cycle in a tension-compression cycle is irrelevant for crack extension in ceramics may be wrong. Features which can explain additional crack growth when samples are loaded by alternating stresses include elastic mismatch between both crack sides due to anisotropic stress relief during crack growth; asperities in the crack surfaces, and volume increase, e.g., due to phase transformation in the crack zone. ESA

N89-23584# Kernforschungsanlage, Juelich (Germany, F.R.).
YOUNG'S MODULUS OF ELASTICITY: MEASURED VALUES FOR MULTIPHASE METALS AND THEIR CALCULATION VIA THE BOUND CONCEPT **c26**
Gerhard Ondracek and Dirk Windelberg (Technische Univ., Hanover, Germany, F.R.) *In its* The 8th German-Yugoslav Meeting on Materials Science and Development: Ceramics and Metals 1988 p 141-146 (For primary document see N89-23569 17-23)
Copyright Avail: NTIS HC A21/MF A01

It is shown that in predicting elastic properties of two-phase and ceramic materials, in the case of the bound concept, the statistical Monte-Carlo method leads to mathematical difficulties and inappropriate calculations. Mathematical analysis in two dimensions is shown to give good results. For the case of the model concept, an iterative calculation of Young's modulus is outlined. ESA

N89-23585# Max-Planck-Inst. fuer Metallforschung, Stuttgart (Germany, F.R.). Pulvermetallurgisches Lab.
STRENGTHENING OF SILICON NITRIDE CERAMICS **c27**
Peter Greil *In* Kernforschungsanlage Juelich GmbH, The 8th German-Yugoslav Meeting on Materials Science and Development: Ceramics and Metals 1988 p 147-156 (For primary document see N89-23569 17-23)
Copyright Avail: NTIS HC A21/MF A01

Strengthening of Si3N4 ceramics by reduction of defect sizes by controlled processing of multiphase powders and microstructure toughening, mainly by composite formation is described. Physical and chemical contamination of the powders has to be excluded by environment controlled powder processing and manufacturing under clean conditions. In situ composites made by reaction sintering and subsequent devitrification of the glass containing microstructures as well as single phase solid solution formation demonstrate superior thermomechanical properties at temperatures above 1000 C. The precipitation of refractory grain boundary phases offers the possibility to combine good sinterability with improved high temperature properties of multiphase, crystalline Si3N4 ceramics. Particulate and whisker reinforced Si3N4 composites are supposed to achieve high fracture toughness materials with improved reliability. Although this type of composite suffers from weak sinterability resulting in porous microstructures, gas pressure sintering or post-hipping techniques at temperatures above 1800 to 1900 C yield fully dense Si3N4 composites in complex shape. ESA

N89-23586# Ljubljana Univ. (Yugoslavia). Jozef Stefan Inst.
THE WEAR OF CUTTING TOOLS: THE CONTRIBUTION OF ABRASIVE WEAR **c37**
Sasa Novak and Marija Komac *In* Kernforschungsanlage Juelich GmbH, The 8th German-Yugoslav Meeting on Materials Science and Development: Ceramics and Metals 1988 p 157-164 (For primary document see N89-23569 17-23)
Copyright Avail: NTIS HC A21/MF A01

The abrasion resistance of WC and TiC hard metals and ceramics when applied as cutting tools was examined. Diffusion couples were employed to estimate the contribution of chemical interactions at the chip-tool interface. Results show that the plastic deformation and fracture mechanisms cause material removal during abrasive wear. There is no simple relation between wear

and the mechanical properties of the investigated materials.
ESA

N89-23587# Kernforschungszentrum G.m.b.H., Karlsruhe (Germany, F.R.). Inst. fuer Material- und Festkoerperforschung.
ADVANCED LAYER MATERIALS **c27**
H. Holleck and Hans Schulz *In* Kernforschungsanlage Juelich GmbH, The 8th German-Yugoslav Meeting on Materials Science and Development: Ceramics and Metals 1988 p 165-172 (For primary document see N89-23569 17-23)
Copyright Avail: NTIS HC A21/MF A01

The influence of high amounts of interfaces in hard coatings was examined. The preparation and properties of nanodisperse coatings are reviewed. The constitution of sputtered phase transitions is discussed. Tests on the hardness, adherence, toughness, and internal stresses of nanodisperse coatings using continuous and interrupted cutting against plain carbon steel with hard metal substrate are summarized. The introduction of a high amount of phase boundaries in hard coatings is shown to be promising for wear resistant coatings. ESA

N89-23588# Institut za Nuklearne Nauke Boris Kidric, Belgrade (Yugoslavia).
PHASE TRANSFORMATION OF Zr(x)Hf(1-x)O2 IN ALUMINA MATRIX **c27**
Feodor Sigulinski *In* Kernforschungsanlage Juelich GmbH, the 8th German-Yugoslav Meeting on Materials Science and Development: Ceramics and Metals 1988 p 173-177 (For primary document see N89-23569 17-23)
Copyright Avail: NTIS HC A21/MF A01

The A sub s temperature was determined on the basis of dilatometric measurements for different Al2O3+15 v/o (Zr(x)Hf(1-x)O2) compositions. It is demonstrated that A sub s temperature is a manifestation of soft lattice modes. Additional proof was obtained by IR results which confirm that phase transformation (monoclinic - tetragonal) is of soft phonon mode.
ESA

N89-23589# Institut za Nuklearne Nauke Boris Kidric, Belgrade (Yugoslavia).
PREPARATION AND PROPERTIES OF HIGH STRENGTH CARBON FIBERS **c27**
Slobadan Marinkovic, V. Raskovic, Stanko Pejanovic (Belgrade Univ., Yugoslavia), and V. Pavlovic *In* Kernforschungsanlage Juelich GmbH, The 8th German-Yugoslav Meeting on Materials Science and Development: Ceramics and Metals 1988 p 179-184 (For primary document see N89-23569 17-23)
Copyright Avail: NTIS HC A21/MF A01

Research on the process of continuous fabrication of high strength carbon fibers from the PAN precursor is summarized. The obtained fibers are compared with those obtained from another process using acrylic fibers. Properties are generally similar, but the fibers obtained from the first process have lower strength and strain to failure, suggesting that they contain more flaws. ESA

N89-23590# Max-Planck-Inst. fuer Metallforschung, Stuttgart (Germany, F.R.). Pulvermetallurgisches Lab.
THERMAL TRANSPORT IN PRESSURELESS SINTERED ALUMINUM NITRIDE **c27**
Axel Kranzmann, Peter Greil, and Guenter Petzow *In* Kernforschungsanlage Juelich GmbH, The 8th German Yugoslav Meeting on Materials Science and Development: Ceramics and Metals 1988 p 187-194 (For primary document see N89-23569 17-23)
Copyright Avail: NTIS HC A21/MF A01

High purity AlN powders were pressureless sintered in nitrogen at temperatures between 2020 and 2370 K. The powders were sintered with MgO as a sintering additive and without additives, respectively. A maximum sintered density of 3630 kg/cum is obtained by formation of AlN polytypes, 3170 kg/cum with 1 wt percent MgO, and 3210 kg/cum without additives. After sintering, a residual porosity of 2.2 vol percent is detected. A distinct increase of oxygen content is found by wet chemical analysis and XRD resulting in the anisotropic growth of platelike AlN polytypes in the sintered AlN material. The measured quantities of heat conductivity are interpreted with common principles of heat conductivity in single crystals and compared with calculations based upon mixture theory. Both can sufficiently describe the heat transport. ESA

N89-23591# Kernforschungszentrum G.m.b.H., Karlsruhe (Germany, F.R.). Inst. fuer Material- und Festkoerperforschung.
PREPARATION, CHARACTERIZATION AND THERMAL DIFFUSIVITY OF Al2TiO5 **c27**
Milosav Milosevski and Brigitte Schulz *In* Kernforschungsanlage Juelich GmbH, The 8th German-Yugoslav Meeting on Materials Science and Development: Ceramics and Metals 1988 p 195-208 (For primary document see N89-23569 17-23)
Copyright Avail: NTIS HC A21/MF A01

A technique for the preparation and characterization of crack free Al2TiO5 samples was developed. The porosity range of the samples is between 10 and 18 percent. On these crack free samples, the thermal diffusivity was measured with a laser-flash technique. The data follow a temperature relationship as expected for electrical insulators. ESA

N89-23592# Kernforschungszentrum G.m.b.H., Karlsruhe (Germany, F.R.). Inst. fuer Material- und Festkoerperforschung.
DILATOMETRIC ANALYSIS OF Al-, Ba-, Ca-TITANATE **c27**
Milosav Milosevski and Brigitte Schulz *In* Kernforschungsanlage Juelich GmbH, The 8th German-Yugoslav Meeting on Materials Science and Development: Ceramics and Metals 1988 p 209-219 (For primary document see N89-23569 17-23)
Copyright Avail: NTIS HC A21/MF A01

The titanates of aluminum, barium, and calcium were chosen to perform dilatometry with respect to second order transitions and to hysteris effects in thermal expansion. The relative thermal expansion of all three materials was determined, after a detailed study of the method itself. Results were compared wit literature data. Good agreement is obtained for BaTiO3, but Al2TiO3 shows discrepancies. The literature data on CaTiO3 were very old and did not contain enough information on the measuring conditions.
ESA

N89-23593# Technische Hochschule, Aachen (Germany, F.R.). Inst. fuer Gesteinshuettenkunde.
INVESTIGATIONS ON LOW CEMENT AND ULTRA LOW CEMENT REFRACTORY CASTABLES **c27**
Uwe Schuhmacher, W. Kroenert, and A. Seltveit (Norges Tekniske Hoegskole, Trondheim.) *In* Kernforschungsanlage Juelich GmbH, The 8th German-Yugoslav Meeting on Materials Science and Development: Ceramics and Metals 1988 p 221-228 (For primary document see N89-23569 17-23)
Copyright Avail: NTIS HC A21/MF A01

Properties of low cement and ultralow cement high alumina castables (ULCC) were tested, especially the influence of mullite formation on hot modulus of rupture (HMOR) values. Powder and X-ray diffraction analyses were performed. Hot modulus of rupture was measured. Rate of increase for the bending strength for the samples tested on hot and cold modulus of rupture is 0.15 N/mm sq/sec. Low cement castables improve the lack of strength in the temperature range 300 to 900 C compared to ordinary castables. For many applications their maximum operating temperature is restricted due to formation of liquids at higher temperatures. In order to improve the unsatisfactory properties at temperatures higher than 1300 C, the cement content was decreased to a minimum in ultralow cement castables. An addition of reactive alumina combined with cement minimization reduces anorthite and melting phase formation. Mullite formation in ULCC improves strength at temperatures higher than 1300 C. ESA

N89-23594# Kernforschungsanlage, Juelich (Germany, F.R.).
CORROSION OF SILICON CARBIDE CERAMICS AT HIGH TEMPERATURES IN WATER VAPOR-CONTAINING ATMOSPHERES **c27**
Rudiger Foerthmann, E. Gyarmati, and Aristides Naoumidis *In*

its The 8th German-Yugoslav Meeting on Materials Science and Development: Ceramics and Metals 1988 p 231-240 (For primary document see N89-23569 17-23)
Copyright Avail: NTIS HC A21/MF A01

Corrosion tests with different silicon carbide qualities in water and hydrogen containing atmospheres were carried out at 1400C in view of the application of these materials in heat exchanger tubes and chemical reactors. The corrosion of different silicon carbide ceramics in water vapor/hydrogen atmospheres at high temperatures leads to different growth rates and structures of the silicon oxide layers. The growth rate of dense silicon oxide layers on exposed SiSiC specimens is controlled by the oxygen diffusion in the oxide layer. The 4-point bending strength of SSiC and SiSiC is slightly decreased by corrosion in water vapor/hydrogen, but increased if SiSiC is exposed to nitrogen-containing atmospheres. The bending strength of specimens from joined SSiC tubes is not significantly decreased after exposure to water vapor/hydrogen atmospheres at high temperatures. The corrosion of SiSiC and SSiC in sulfur-containing atmospheres is expected to be mostly dependent on the oxygen partial pressure. ESA

N89-23595# Ljubljana Univ. (Yugoslavia). Jozef Stefan Inst.
INVESTIGATION OF ALPHA-SiC HOT CORROSION IN THE PRESENCE OF BASIC SLAG **c27**
Varuzan Kevorkijan, Milos Komac, Taric Fetahagic, and V. Strumberger *In* Kernforschungsanlage Juelich GmbH, The 8th German-Yugoslav Meeting on Materials Science and Development: Ceramics and Metals 1988 p 241-248 (For primary document see N89-23569 17-23)
Copyright Avail: NTIS HC A21/MF A01

A method to manufacture SiC tubes by pressureless sintering of alpha SiC is described. The corrosion of sintered SiC by basic coal slag is discussed. The effect of corrosion on fracture strength and thermal shock resistance of sintered alpha SiC is considered. Hot corrosion mechanisms of sintered alpha-SiC depend on the environment during high temperature exposure. In the case of oxidation in an air atmosphere, a passive SiO2 layer is formed on the surface of specimens which locally penetrates deeper into the SiC matrix. Most probably, these penetrations are associated with chemical or microstructural nonhomogeneities in the substrate. In the case of basic slag coated specimens, a layer of dense packed SiO2 crystals is formed on the slag/SiC interface. However, this layer may either dissolve in the slag matrix, or react due to low oxygen partial pressure with SiC to form gaseous products. Thus slag may come into direct contact with SiC which promotes the formation of metallic silicides. As a consequence of corrosion attack, strength degradation of sintered alpha-SiC may be noted after extended exposure time. In contrast, thermal shock resistance remains unchanged. ESA

N89-23596# Max-Planck-Gesellschaft, Ploen (Germany, F.R.). Fritz-Haber-Inst.
OXYGEN INTERACTION WITH METAL SURFACES: SURFACE SCIENCE APPROACH **c26**
Klaus Wandelt, Petar Pervan, and Milorad Milun (Yugoslav Academy of Sciences and Arts, Zagreb.) *In* Kernforschungsanlage Juelich GmbH, The 8th German-Yugoslav Meeting on Materials Science and Development: Ceramics and Metals 1988 p 249-266 Sponsored by Bundesministerium fuer Forschung und Technologie, Bonn, Fed. Republic of Germany; Bilateral Yugoslav-German Project; Deutsche Forschungsgemeinschaft, Bonn, Fed, Republic of Germany and SIZ za Znanstveni rad SAH Project, Yugoslavia (For primary document see N89-23569 17-23)
(Contracts IAEA-3227; IAEA-4527)
Copyright Avail: NTIS HC A21/MF A01

The surface science approach to the investigation of oxidation processes at molecular level is introduced. Under ultrahigh vacuum conditions, atomically clean metal surfaces are exposed to well defined doses of pure oxygen. The uptake and nature, as well as the reaction kinetics and energetics of the metal-oxygen interaction is studied as a function of external parameters such as exposure, pressure and temperature, and surface composition and structure. Examples of the application of the approach to single component polycrystalline surfaces, two-component crystal surfaces, and two-component polycrystalline samples are described. ESA

N89-23597# Skopje Univ. (Yugoslavia). Faculty of Technology and Metallurgy.
STABILITY AND INSTABILITY OF ANODICALLY FORMED LAYERS ON METALLIC SURFACES **c26**
Ljubomir D. Arsov *In* Kernforschungsanlage Juelich GmbH, The 8th German-Yugoslav Meeting on Materials Science and Development: Ceramics and Metals 1988 p 267-272 (For primary document see N89-23569 17-23)
Copyright Avail: NTIS HC A21/MF A01

Stability and instability of anodic surface layers formed on aluminum, titanium and their alloys was investigated. It is shown that surface color varies with the layer depth and (in the case of titanium) the uniform dissolution of the colored layers is possible. The effect of CuSO4 and NiSO4 on the formation and dissolution of anodic layers on aluminum was also investigated. When the sulfate concentration is increased, kinetic viscosity of the electrolyte becomes higher, hardness of the film generally increases at first and then decreases and the uniformity of the film decreases. ESA

N89-23598# Technische Hochschule, Aachen (Germany, F.R.). Inst. fuer Gesteinshuettenkunde.
THE ADHESION BETWEEN GLASS AND ENAMEL **c27**
Otmar Seide and H. Roecker *In* Kernforschungsanlage Juelich GmbH, The 8th German-Yugoslav Meeting on Materials Science and Development: Ceramics and Metals 1988 p 273-280 (For primary document see N89-23569 17-23)
Copyright Avail: NTIS HC A21/MF A01

Adhesion tests and microscope examinations of enamelled glass were carried out. The investigations show that the adhesion depends on the Si-O-Si-bondings. The critical point of the compound material glass-enamel is not the adhesion between the two compounds itself, but the decrease of the mechanical strength caused by the enamelling. The decrease of the mechanical strength is caused by the nonhomogeneous nature of the enamel layer (e.g., pores, crystallizations, phase separations) and in this case can also be caused by thermal induced tensions in the phase boundary of the compound. Thermal tensions are caused by a change in the coefficient of thermal expansion induced by a diffusion process during baking of the enamel. ESA

N89-23599# Patras Univ. (Greece). Inst. of Physical Metallurgy.
TEMPERATURE DEPENDENCE OF INTERFACIAL ENERGIES BETWEEN SOLID OXIDES AND LIQUID METALS **c26**
Panajotis Nikolopoulos, D. Sotiropoulou, U. Jauch, and Gerhard Ondracek (Kernforschungsanlage, Juelich, Germany, F.R.) *In* Kernforschungsanlage Juelich GmbH, The 8th German-Yogoslav Meeting on Materials Science and Development: Ceramics and Metals 1988 p 281-289 Sponsored by the Deutsche Forschungsgemeinschaft, Bonn, Fed. Republic of Germany (For primary document see N89-23569 17-23)
Copyright Avail: NTIS HC A21/MF A01

Wetting experiments were carried out to determine the temperature functions of the interfacial energies in the Al2O3-Bi, Pb, Cu, Ni, and ZrO2-Cu, Co, Ni systems. Test results and literature data show that, by using an average value for the interfacial energy between ceramic and liquid metals at the metal's melting point, a reasonable approach to wettability in such systems can be obtained. The approach is independent of the type of metal, and is particularly applicable to metals with high melting point and high surface energy. ESA

N89-23600# Belgrade Univ. (Yugoslavia). Lab. for Electron Microanalysis.
CHARACTERIZATION OF A PHASE BOUNDARY IN Ni-Al2O3 SINTERED UNDER PRESSURE **c27**
Miodrag K. Pavicevic, G. Burri, H. Schmid, and R. Gotthard (Ecole Polytechnique Federale de Lausanne, Switzerland) *In* Kernforschungsanlage Juelich GmbH, The 8th German-Yugoslav

Meeting on Materials Science and Development: Ceramics and Metals 1988 p 291-298 (For primary document see N89-23569 17-23)
Copyright Avail: NTIS HC A21/MF A01

The nature of bond in Ni-Al2O3 systems exposed to pressure ranging from 50 to 600 MPa was investigated in vacuum at temperature of 1350C, using electron microexcitation, scanning electron microscope, Auger spectroscopy, photoelectron spectrometry, and TV-transmission electron microscope. The existence of intermetal Ni2Al3 phase was proved only on the basis of properties of X-ray emission spectra of a valent-conductive Al bond. ESA

N89-23601# Technische Univ., Clausthal-Zellerfeld (Germany, F.R.). Fachbereich Metallurgie und Werkstoffwissenschaften.
NEUTRAL PRIMARY BEAM SIMS ANALYSIS OF CERAMIC MATERIALS **c27**
Guenter Borchardt, S. Scherrer, and S. Weber (Ecole des Mines, Nancy, France) *In* Kernforschungsanlage Juelich GmbH, The 8th German-Yugoslav Meeting on Materials Science and Development: Ceramics and Metals 1988 p 299-306 Sponsored in part by the Deutsche Forschungsgemeinschaft, Bonn, Fed. Republic of Germany (For primary document see N89-23569 17-23)
Copyright Avail: NTIS HC A21/MF A01

The utility of surface analysis methods for materials with low room temperature electrical conductivity is discussed, taking secondary ion mass spectrometry (SIMS) as an example. Charge effects and mobile species in the solid are considered. Experimental results on poorly conducting surfaces such as corroded or fresh glass surfaces, oxide scales on silicon nitride, and a bioceramic material demonstrate that even in the most unfavorable case of the rather mobile hydrogen (deuterium) or sodium in glass at room temperature, the resulting electric field in SIMS is too weak to hinder the analysis. ESA

N89-23602# Ljubljana Univ. (Yugoslavia).
MICROSTRUCTURE-PERMEABILITY RELATION IN MnZn FERRITES PREPARED OF IRON OXIDE WITH CHLORINE IMPURITIES **c27**
Heda Intihar, Miha Drofenik, Drago Kolar, and M. Limpel *In* Kernforschungsanlage Juelich GmbH, The 8th German-Yugoslav Meeting on Materials Science and Development: Ceramics and Metals 1988 p 309-316 (For primary document see N89-23569 17-23)
Copyright Avail: NTIS HC A21/MF A01

The influence of small amounts of chlorine on the ferrite microstructure, and consequently the magnetic permeability of MnZn ferrites was studied by varying the sintering temperature and time during the preparation of the ferrites. A very thin layer of chlorine which encloses the ferrite grains during sintering, effectively retards the grain boundary mobility, and retards the promotion of grains with overestimated size and entrapped porosity, which gives rise to the formation of the normal microstructure. The chlorine impurities compensate the influence of a higher amount of impurities Na2O and SiO2, present in samples prepared with Fe2O3 (A), making them less prone to exaggerated grain growth, even at higher temperatures. ESA

N89-23603# Technische Hochschule, Aachen (Germany, F.R.). Inst. fuer Gesteinshuettenkunde.
ELECTRON CONDUCTING CERAMICS AS SENSOR MATERIAL FOR NOISE THERMOMETRY **c27**
Helmut Heinz Haeusser, D. vonMallinckrodt, and H. Brixy (Kernforschungsanlage, Juelich, Germany, F.R.) *In* Kernforschungsanlage Juelich GmbH, The 8th German-Yugoslav Meeting on Materials Science and Development: Ceramics and Metals 1988 p 317-322 (For primary document see N89-23569 17-23)
Copyright Avail: NTIS HC A21/MF A01

The ohmic resistance of LaCrO3 was diminished by substituting Sr, Ca, or Mg for La. It becomes nearly independent of temperature above 600C. While temperature independence is advantageous for noise thermometry, the resistance value is too low. The resistance can be enhanced through a second, electrically nonconducting phase (MgAl2O4). The volume fraction of spinel was varied between 10 and 90 percent, and the resultant effect on resistance was plotted as a temperature function. ESA

N89-23604# Serbian Academy of Sciences and Arts, Belgrade (Yugoslavia). Inst. of Technical Sciences.
MICROSTRUCTURE AND PHASE DEVELOPMENT IN MULTICOMPONENT ZnO BASED VARISTOR CERAMICS **c27**
Olivera Milosevic, Petar Kostic, Lj. Karanovic, V. Petrovic, and Dragoljub Uskokovic *In* Kernforschungsanlage Juelich GmbH, The 8th German-Yugoslav Meeting on Materials Science and Development: Ceramics and Metals 1988 p 323-330 Sponsored by the Republic Committee for the Science of Serbia; the Committee for the Science, Belgrade, Yugoslavia and MINEL (For primary document see N89-23569 17-23)
Copyright Avail: NTIS HC A21/MF A01

Multicomponent varistor ceramics based on ZnO were investigated. Observation shows that the main constituents of microstructure (ZnO grains, spinel, and intergranular phase) are in general independent from the varying composition within the framework of investigated systems. Based on different experimental methods, a hypothetical scheme of microstructure and phase development in such multicomponent systems was derived. Starting from a current-voltage characteristic and a mechanism of a potential barrier formation, as well as from microstructure formation mechanisms, it was established that the requirements for obtainment of highly resistant intergranular layer can be reached through the control of polymorphous transformations of Bi2O3 within an intergranular phase, and by intentional synthesis and stabilization of a cubic gamma-shape. ESA

N89-23605# Yugoslav Academy of Sciences and Arts, Zagreb. Faculty of Natural Sciences.
AMORPHOUS MAGNETS **c70**
Boran Leontic *In* Kernforschungsanlage Juelich GmbH, The 8th German-Yugoslav Meeting on Materials Science and Development: Ceramics and Metals 1988 p 331-339 (For primary document see N89-23569 17-23)
Copyright Avail: NTIS HC A21/MF A01

The theory of ferromagnetism is reviewed, and systems of practical interest are shown. Soft ferromagnetism, anisotropy, and magnetostriction are discussed. Production techniques are mentioned. Application in medium frequency magnetic cores and similar devices where an insulated bulk material is desirable is proposed. ESA

N89-23606# Kernforschungszentrum G.m.b.H., Karlsruhe (Germany, F.R.). Inst. fuer Material- und Festkoerperforschung.
ON THE CORRELATION BETWEEN MICROSTRUCTURE AND MAGNETIC INDUCTION OF POROUS IRON AND IRON-Ni(0.4)Zn(0.6)Fe2O4 COMPOSITES **c26**
Edmund Remane *In* Kernforschungsanlage Juelich GmbH, The 8th German-Yugoslav Meeting on Materials Science and Development: Ceramics and Metals 1988 p 341-349 (For primary document see N89-23569 17-23)
Copyright Avail: NTIS HC A21/MF A01

The dependence of the magnetic induction on the microstructure of sintered iron toroids and sintered iron-NiZn ferrite toroids was investigated. Compacting pressures, sintering temperature, and sintering time were varied over a wide range in order to obtain cores with very different microstructures. The microstructures were characterized by a computerized imaging system. A theory which used the measured microstructural parameters to calculate the induction behavior was applied. Theoretical results are in good agreement with the experimental results. ESA

N89-23607# Karlsruhe Univ. (Germany, F.R.). Nuclear Research Center.
WEAR RESISTANT SINTERED STEEL WITH HIGH CARBIDE CONTENT **c26**
R. Klausmann, R. Oberacker, and Fritz Ernst Thuemmler *In*

Kernforschungsanlage Juelich GmbH, The 8th German-Yugoslav Meeting on Materials Science and Development: Ceramics and Metals 1988 p 353-361 (For primary document see N89-23569 17-23)

Copyright Avail: NTIS HC A21/MF A01

Sintered steels with 10 to 30 vol-percent of special carbides were developed by mechanical alloying, pressing, and liquid phase sintering. The best results are achieved with systems where the carbide phase is added as fine carbide powder, which does not take part in liquid phase formation, but is provided by addition of P or P+C. Especially in Fe-NbC-P and Fe-NbC-P-C systems, very high densification and equal and fine distribution of the carbide phase in the heat treatable matrix are reached. These alloys provide advantages compared with HSS T15 as well as Astaloy E with 2.5 percent C. ESA

N89-23608# Serbian Academy of Sciences and Arts, Belgrade (Yugoslavia). Inst. of Technical Sciences.

PRODUCTION OF METAL POWDERS BY ROTATING ELECTRODE PROCESS **c26**

Miodrag Zdujic, V. Petrovic, L. Nelevic (Titograd Univ., Yugoslavia), and Dragoljub Uskokovic *In* Kernforschungsanlage Juelich GmbH, The 8th German-Yugoslav Meeting on Materials Science and Development: Ceramics and Metals 1988 p 363-370 Sponsored by the Serbian Research Foundation and the Prvi Partizan Hard Metal Factory (For primary document see N89-23569 17-23)

Copyright Avail: NTIS HC A21/MF A01

Metal powders whose thermophysical properties differ considerably were produced by the rotating electrode process. The properties of molybdenum, titanium, and aluminum powders are discussed. Results of theoretical calculations concerning droplet motion and solidification in helium and argon are given. The mean particle size as well as the particle size distribution can be well controlled. The particles are spherical in shape and have no satellites; thus the powders have a high apparent and tap density. For the given material, the solidification structure changes with particle size, being a result of different conditions under which the particles of various diameters are solidified. ESA

N89-23609# Max-Planck-Inst. fuer Metallforschung, Stuttgart (Germany, F.R.). Inst. fuer Werkstoffwissenschaften.

COOLING RATE, UNDERCOOLING AND RAPID SOLIDIFICATION BY ATOMIZATION **c26**

Klaus Rzesnitzek, Wolfgang A. Kaysser, and Guenter Petzow *In* Kernforschungsanlage Juelich GmbH, The 8th German-Yugoslav Meeting on Materials Science and Development: Ceramics and Metals 1988 p 371-378 (For primary document see N89-23569 17-23)

Avail: NTIS HC A21/MF A01

Powder production on a semipilot scale using the gas atomization technique is described. Undercoolings of the droplets smaller than 30 micron by 150 K and more are obtained. The calculation of the cooling rate from thermal data is in good agreement with the dendrite ripening model based on thermodynamical data. The resulting dendritic microstructures are a product of the time the dendrites and the melt are in contact. The gas velocity at the nozzle determines the particle size. During the solidification of the droplet there is only a minor relative velocity between the gas and the particles. So the cooling rate is mainly determined by the type of gas and the droplet diameter. The nucleation conditions normally generate a dendritic microstructure. By cleaning the melt from heterogeneous nuclei, large undercoolings are obtainable and solidification can occur in a segregation free manner. ESA

N89-23610# Max-Planck-Inst. fuer Metallforschung, Stuttgart (Germany, F.R.). Inst. fuer Werkstoffwissenschaften.

MECHANICAL PROPERTIES OF GAS ATOMIZED Cu-Ti AND Cu-Ti-B ALLOYS **c26**

Dusan Bosic, Rainhard Laag, Wolfgang A. Kaysser, and M. Mitkov (Institut za Nuklearne Nauke Boris Kidric, Belgrade, Yugoslavia) *In* Kernforschungsanlage Juelich GmbH, The 8th German-Yugoslav Meeting on Materials Science and Development: Ceramics and Metals 1988 p 379-383 (For primary document see N89-23569 17-23)

Copyright Avail: NTIS HC A21/MF A01

The use of boron additions to improve the mechanical and electrical properties of Cu-Ti was tested. In order to avoid primary precipitation of TiB2 during solidification, and to keep Ti and B in a supersaturated Cu solid solution, the Cu-Ti-B alloys were cooled and solidified rapidly. The supersturated solid solutions were aged to obtain the complete depletion of the Cu solid solution from Ti and B by the precipitation of fine TiB2. Results show that atomization of Cu-Ti-B alloys results in homogeneous microstructures which are free of TiB2 agglomerations. The hardness of the atomized Cu-Ti-B powders increases rapidly during the initial stage of hardening. From the slow formation of Cu4Ti, an equally slow formation of TiB2 can be deduced. The first hardness maximum of the atomized powders results from arranging Ti atoms near to the dislocations in the lattice in a periodical structure. ESA

N89-23611# Technische Univ., Clausthal-Zellerfeld (Germany, F.R.). Inst. fuer Werkstoffkunde und Werkstofftechnik.

MECHANICAL PROPERTIES OF RAPIDLY SOLIDIFIED IRON-BASED ALLOYS **c26**

Barry Leslie Mordike, H. D. Burchards, and Karl Urlich Kainer *In* Kernforschungsanlage Juelich GmbH, The 8th German-Yugoslav Meeting on Materials Science and Development: Ceramics and Metals 1988 p 385-392 (For primary document see N89-23569 17-23)

Copyright Avail: NTIS HC A21/MF A01

High carbon cast irons were produced by combining powder metallurgy and rapid solidification techniques. Alloys were produced in powder form by gas or water atomization and then consolidated by extrusion or hot isostatic processing and submitted to a thermomechanical treatment. The alloys produced show high tensile strength and acceptable ductility. ESA

N89-23612# Max-Planck-Inst. fuer Metallforschung, Stuttgart (Germany, F.R.). Inst. fuer Werkstoffwissenschaften.

INTERMETALLIC PHASES FOR HIGH TEMPERATURE APPLICATIONS **c26**

Rainhard Laag and Wolfgang A. Kaysser *In* Kernforschungsanlage Juelich GmbH, The 8th German-Yugoslav Meeting on Materials Science and Development: Ceramics and Metals 1988 p 395-402 Sponsored by the Deutsche Forschungsgemeinschaft, Bonn, Fed. Republic of Germany (For primary document see N89-23569 17-23)

Avail: NTIS HC A21/MF A01

Attempts to improve the structural properties of iron aluminide and nickel aluminide intermetallics destined for moderate to high temperature applications are discussed. Problems arise with coarse grained intermetallics due to their brittleness, whereas finer grained materials show considerable ductility at room temperature. Solidification experiments show that higher cooling rates increase the microhardness more effectively than higher Al-concentrations or a decrease in the grain size. There is hardly any difference at higher cooling rates between ternary additions of Cr and Ti. At higher cooling rates ternary additions considerably increase the microhardness caused by the increasing amount of Al2Fe precipitates. Due to the precipitation of Al2Fe the predictions of the valency difference model on the influence of microalloying by Cr and Ti in Fe-Al-alloys are not applicable. An increased solidification rate very suitable to produce Fe aluminides with finer microstructure and better properties is found. An improved mechanical behavior due to the absence of Al2Fe precipitations at the grain boundaries in a material with further reduced grain size is expected. ESA

N89-23613# Technische Univ., Clausthal-Zellerfeld (Germany, F.R.).

BEHAVIOR OF METALS DURING HOT ROLLING PROCESSES. PART 1: MATHEMATICAL MODELS **c26**

Paul Funke *In* Kernforschungsanlage Juelich GmbH, The 8th

German-Yugoslav Meeting on Materials Science and Development: Ceramics and Metals 1988 p 403-412 (For primary document see N89-23569 17-23)
Avail: NTIS HC A21/MF A01

Mechanisms encountered during hot deformation of high strength, low alloyed structural steels are reviewed. Indicators of different strengthening and softening mechanisms are summarized. Assumptions that must be included in mathematical models which describe the hot deformation behavior of steels for a hot rolling process in continuous hot strip mills are discussed. ESA

N89-23614# Technische Univ., Clausthal-Zellerfeld (Germany, F.R.). Inst. fuer Werkstoffumformung.
BEHAVIOR OF METALS DURING HOT ROLLING PROCESSES. PART 2: EXPERIMENTAL METHODS FOR FLOW STRESS DETERMINATION AND CALCULATION OF THE TWO-DIMENSIONAL TEMPERATURE-FIELD IN THE ROLL GAP **c26**
Ronald Krengel *In* Kernforschungsanlage Juelich GmbH, The 8th German-Yugoslav Meeting on Materials Science and Development: Ceramics and Metals 1988 p 413-421 (For primary document see N89-23569 17-23)
Copyright Avail: NTIS HC A21/MF A01

An experimental technique to determine the course of the deformation parameters in the roll gap with the aid of the viscoplasticity method is discussed. Parameters are mainly the strain-rate, the strain, and the deformation temperature. The strain rates and strains can be determined in the whole deformation zone by making the metal flow visible with a square grid on a flow plane of the material. The two-dimensional temperature field inside the metal is calculated by a finite difference method. From this analysis the deformation parameters can be obtained to determine the course of the mechanical properties and the structure in the hot rolling process by a subsequent simulation with material tests. ESA

N89-23615# Ljubljana Univ. (Yugoslavia).
INTERFACIAL REACTIONS DURING CLADDING OF STEEL BY HOT ROLLING **c26**
Tatjana Vecko, Radomir Turk, H.-R. Priebe, and Guenter Borchardt (Technische Univ., Clausthal-Zellerfeld, Germany, F.R.) *In* Kernforschungsanlage Juelich GmbH, The 8th German-Yugoslav Meeting on Materials Science and Development: Ceramics and Metals 1988 p 423-430 Sponsored by the Deutsche Akademische Austauschdienst (For primary document see N89-23569 17-23)
Copyright Avail: NTIS HC A21/MF A01

Cladding of commercial steels (tool steel and construction steel) was studied by laboratory hot rolling experiments under the same thermomechanical conditions at which commercial rolling of compound strips is performed, i.e., at a temperature of 1150 C with a degree of deformation of up to 0.5 and a slow cooling rate. The relations between the thermomechanical conditions during hot rolling and the mechanical properties of the compound strip are discussed in terms of the properties of the interfacial layer. The experiments demonstrate that cladding of the two steels is achieved. The moderate tensile strength of the compound material is due to a pure ferrite layer in the contact zone. ESA

N89-23616# Ljubljana Univ. (Yugoslavia).
INFORMATION ABOUT HOT FLOW-STRESS CURVES AND THE RESULTING STRUCTURAL CHANGES **c26**
Ivan Bizjak, Radomir Turk (Technische Univ., Clausthal-Zellerfeld, Germany, F.R.), and Paul Funke *In* Kernforschungsanlage Juelich GmbH, The 8th German-Yugoslav Meeting on Materials Science and Development: Ceramics and Metals 1988 p 431-438 (For primary document see N89-23569 17-23)
Copyright Avail: NTIS HC A21/MF A01

It is shown using experimental data from a tension testing machine that it is possible to apply a numerical method to determine the continuous changes of the necking of tensile bars, to construct a thermomechanical controlled true stress-elongation diagram. Computer programs for the evaluation of all data during the hot tensile test were developed. The results are compared with the running structural changes; interpretation of special effects is improved for hot deformation behavior. ESA

N89-23617# Serbian Academy of Sciences and Arts, Belgrade (Yugoslavia). Dept. of Physical Chemistry.
PHYSICO-MATHEMATICAL INVESTIGATION OF THE CONSOLIDATION OF IRON POWDER **c26**
Ratomir Agatonovic, Rada Novakovic, D. Stefanovic (Nis Univ., Yugoslavia), and M. M. Ristic *In* Kernforschungsanlage Juelich GmbH, The 8th German-Yugoslav Meeting on Materials Science and Development: Ceramics and Metals 1988 p 441-447 (For primary document see N89-23569 17-23)
Copyright Avail: NTIS HC A21/MF A01

It was established that the processes at electron level control the consolidation process of iron powder. A mathematical model connecting the mutual dependence of the pressing pressure, thermoelectromotive force (TEMF) and electron concentration, was developed. The physical essence of the TEMF occurrence during consolidation of iron powder is presented on the basis of this model. ESA

N89-23618# Serbian Academy of Sciences and Arts, Belgrade (Yugoslavia). Dept. of Physical Chemistry.
P-T DIAGRAMS OF TRANSITION ELEMENTS **c26**
Rada Novakovic and M. M. Ristic *In* Kernforschungsanlage Juelich GmbH, The 8th German-Yugoslav Meeting on Materials Science and Development: Ceramics and Metals 1988 p 449-458 (For primary document see N89-23569 17-23)
Copyright Avail: NTIS HC A21/MF A01

The mathematical-physical analysis of phase transformation of transition elements as a function of temperature and pressure was done. The analytical expressions characterizing the phase transformations are obtained. The initial thermodynamic conditions can be defined in advance on the basis of these analytical expressions in order that the desired phase can be obtained. ESA

24 COMPOSITE MATERIALS

Includes physical, chemical, and mechanical properties of laminates and other composite materials.
For ceramic materials see *27 Nonmetallic Materials.*

N89-23619*# Christopher Newport Coll., Newport News, VA. Dept. of Physics.
[AN INVESTIGATION OF THE TEMPERATURE DEPENDENCE OF THE ULTRASONIC PROPERTIES OF AS4/LEXAN AND XAS/LEXAN COMPOSITES] Annual Report, 1 Nov. 1987 - 31 Oct. 1988
B. T. Smith Oct. 1988 9 p
(Grant NAG1-431)
(NASA-CR-184845; NAS 1.26:184845) Avail: NTIS HC A02/MF A01 CSCL 11D

An investigation of the temperature dependence of the ultrasonic properties of AS4/lexan and XAS/lexan composites is summarized. In particular, a technique for determination of velocity and attenuation as a function of temperature, for both the matrix and composite materials is determined. The separation of contributions of the matrix and fiber to ultrasonic propagation and scattering is discussed. Work begun on the characterization of wave propagation in graphite fiber/polymer matrix composites is described. A.D.

N89-23620# Helsinki Univ. of Technology, Espoo (Finland). Materials Processing and Powder Metallurgy Lab.
FABRICATION AND PROPERTIES OF ALUMINA-ZIRCONIA COMPOSITES
Tuija Rytkoenen, Kari Keskinen, and Pekka Lintula (Tampere Univ. of Technology, Finland) 1988 27 p Presented at the 2nd International Conference on Ceramic Powder Processing Science,

Berchtesgaden, Fed. Republic of Germany, 12-14 Oct. 1988
(PB89-147532; TKK-V-B41; ISBN-951-754-658-0;
ISSN-0785-5168) Avail: NTIS HC A03/MF A01 CSCL 11D

The mixing homogeneity of alumina-zirconia composites was studied in the composition range Al2O3 = 0, 20, 40, 60, 80 and 100 vol.-percent. Two commercial starting powders with approximately the same average particle size were used and the results were compared with a composite made from commercially available composite powder. Powders were mixed with a dispersing agent in a ball mill. Shrinkage behavior of the uniaxially pressed composites was followed by an optical dilatometer. Results revealed that the pure end-members densified faster to full density and the addition of the other end-member impaired the densification. Scanning electron microscopy showed that the dispersion homogeneity of these composites was good and no large agglomerates were detected. The grain sizes were relatively fine with no excessive grain growth present. X-ray diffraction analyses revealed the increase of monoclinic ZrO2 - phase content with decreasing ZrO2-content in the composite. Author

N89-23621*# National Aeronautics and Space Administration. Lewis Research Center, Cleveland, OH.
COMPOSITE BLADE STRUCTURAL ANALYZER (COBSTRAN) USER'S MANUAL
Robert A. Aiello Apr. 1989 84 p
(NASA-TM-101461; E-4570; NAS 1.15:101461) Avail: NTIS HC A05/MF A01 CSCL 11D

The installation and use of a computer code, COBSTRAN (COmposite Blade STRuctrual ANalyzer), developed for the design and analysis of composite turbofan and turboprop blades and also for composite wind turbine blades was described. This code combines composite mechanics and laminate theory with an internal data base of fiber and matrix properties. Inputs to the code are constituent fiber and matrix material properties, factors reflecting the fabrication process, composite geometry and blade geometry. COBSTRAN performs the micromechanics, macromechanics and laminate analyses of these fiber composites. COBSTRAN generates a NASTRAN model with equivalent anisotropic homogeneous material properties. Stress output from NASTRAN is used to calculate individual ply stresses, strains, interply stresses, thru-the-thickness stresses and failure margins. Curved panel structures may be modeled providing the curvature of a cross-section is defined by a single value function. COBSTRAN is written in FORTRAN 77. Author

N89-23622*# Sverdrup Technology, Inc., Cleveland, OH.
THEORETICAL ANALYSIS OF COMPATIBILITY OF SEVERAL REINFORCEMENT MATERIALS WITH NiAl AND FeAl MATRICES Final Contractor Report
Ajay K. Misra May 1989 21 p Presented at the 13th Annual Conference on Composites and Advanced Ceramics, Cocoa Beach, FL, 18-20 Jan. 1989; sponsored by Advanced Ceramics Association
(Contract NAS3-25266)
(NASA-CR-182291; E-4796; NAS 1.26:182291) Avail: NTIS HC A03/MF A01 CSCL 11D

Several potential reinforcement materials were assessed for their chemical, coefficient of thermal expansion (CTE), and mechanical compatibility with the intermetallic matrices based on NiAl and FeAl. Among the ceramic reinforcement materials, Al2O3, TiC, and TiB2, appear to be the optimum choices for NiAl and FeAl matrices. However, the problem of CTE mismatch with the matrix needs to be solved for these three reinforcement materials. Beryllium-rich intermetallic compounds can be considered as potential reinforcement materials provided suitable reaction barrier coatings can be developed for these. Based on preliminary thermodynamic calculations, Sc2O3 and TiC appear to be suitable as reaction barrier coatings for the beryllides. Several reaction barrier coatings are also suggested for the currently available SiC fibers. Author

N89-23623*# National Aeronautics and Space Administration. Lewis Research Center, Cleveland, OH.
LIGHT WEIGHT POLYMER MATRIX COMPOSITE MATERIAL Patent Application
Kenneth J. Bowles, inventor (to NASA) and Carl E. Lowell, inventor (to NASA) 5 Dec. 1988 16 p Sponsored by NASA. Lewis Research Center
(NASA-Case-LEW-14734-1; NAS 1.71:LEW-14734-1;
US-Patent-Appl-SN-279624) Avail: NTIS HC A03/MF A01 CSCL 11D

A graphite fiber reinforced polymer matrix is layed up, cured, and thermally aged at about 750 F in the presence of an inert gas. The heat treatment improves the structural integrity and alters the electrical conductivity of the materials. In the preferred embodiment PMR-15 polyimides and Celion-6000 graphite fibers are used. NASA

N89-23624 Rensselaer Polytechnic Inst., Troy, NY.
MODE 2 DELAMINATION FATIGUE RESISTANCE OF COMPOSITES Ph.D. Thesis
Krishna Srinivasan 1988 156 p
Avail: Univ. Microfilms Order No. DA8905213

The search for damage tolerant high performance composites has prompted investigators to substitute tough thermoplastics for the brittle epoxy resins currently in use. However, given the lack of detailed knowledge about the constrained in situ resin deformational behavior, it is difficult to determine the necessary physical and mechanical properties of the neat resin responsible for specific enhancement of laminate properties. A functional understanding of the relationships between neat resin behavior and composite damage tolerance and toughness was sought. Mode II delamination fatigue resistance of thermoplastic and thermoset resin composites was examined using a newly developed clamped edge flawed cantilever geometry. Fully reversed and nonreversed bending stress states were used to characterize the resistance of composite materials to delamination initiation in fatigue. Experimental data were gathered to support a path dependent failure analysis based on viscoelastic matrix constitutive behavior. The role of microstructure and fiber-matrix interface in influencing shear delamination behavior was explored. Electron Microscopy was used to distinguish the mechanisms of critical flaw initiation in these materials. Dissert. Abstr.

N89-23625# Air Force Systems Command, Wright-Patterson AFB, OH. Foreign Technology Div.
CARBON FIBER THERMAL CONDUCTIVITY MEASUREMENT AND ANALYSIS
Jinxian Wei 10 Feb. 1989 18 p Transl. into ENGLISH from Yuhang Xuebao (Peoples Republic of China), no. 1, 1988 p 49-55
(AD-A205682; FTD-ID(RS)T-1075-88) Avail: NTIS HC A03/MF A01 CSCL 11/4

The paper describes the working principle of the laser flash method and the results of measuring the axial thermal conductivity of carbon fibers using the flash method. The relation between heat transfer and carbon fiber microstructure is discussed and the directional effect of the axial thermal conductivity of carbon fibers is suggested. The relation between the thermal conductivity of carbon fibers and that of carbon fiber reinforced composites is discussed and analyzed along with the problem of the anisotropy of carbon fiber reinforced composites. GRA

N89-23626# Naval Air Development Center, Warminster, PA. Air Vehicle and Crew Systems Technology Dept.
ANALYSIS OF THE NAVAIRDEVCEN SELF-PRIMING TOPCOAT ON GRAPHITE/EPOXY COMPOSITES Final Report, Oct. 1986 - Sep. 1987
Anthony T. Eng 15 Aug. 1988 21 p
(AD-A205961; NADC-88102-60) Avail: NTIS HC A03/MF A01 CSCL 11/3

The standard coating system for Navy aircraft consists of an epoxy-polymade primer (MIL-P-2337) under a polyurethane topcoat (MIL-C-83286). In September of 1986, the Naval Air Development Center developed a self-priming (single coating) to replace the

standard Navy aircraft coating system. Equivalent or superior paint properties were achieved with potential material and labor savings. This self-priming topcoat was developed for use on aluminum-skinned aircraft. Since the amount of polymeric composite components used on naval aircraft is rapidly increasing, the current effort was undertaken to determine the compatibility of the self-priming topcoat with graphite/epoxy composite substrates. GRA

N89-23627# Georgia Inst. for Research, Atlanta.
ULTRAFINE MICROSTRUCTURE COMPOSITES PREPARED BY CHEMICAL VAPOR DEPOSITION Annual Report, Jan. - Dec. 1988
W. J. Lackey, Garth B. Freeman, John A. Hanigofsky, John R. Thompson, and Geoving J. Gerard Dec. 1988 46 p
(Contract N00014-87-K-0036)
(AD-A206061; GTRI-A-4699-2) Avail: NTIS HC A03/MF A01 CSCL 11/2

This year we succeeded in preparing dispersed phase composite coatings which consist of a boron nitride matrix containing aluminum nitride. Chemical vapor deposition (CVD) offers an alternate avenue of preparing ceramic composites by simultaneous deposition of multiple phases (i.e., codeposition). The major advantage of preparing dispersed phase ceramic composites by CVD is that mechanical as well as chemical, electrical, optical, and thermal properties of the composites can be favorably tailored by controlling the composite composition and microstructure. Dispersed phase composites containing BN+ALN were deposited by CVD. The phases were either amorphous or crystalline depending on the deposition temperature and reagent concentration. One type of deposit which consisted of a turbostratic BN matrix containing oriented single crystal whiskers of ALN was very hard. A qualitative model based on statistical-mechanical nucleation theory and a hypothesized competition between growth of BN and ALN phases was successful in describing the relationship between operating conditions and the resulting microstructure of dispersed phase ceramic (BN+ALN) composites prepared by CVD. GRA

N89-23628# Geo-Centers, Inc., Fort Washington, MD.
THE DYNAMIC BEHAVIOR OF WATER VAPOR ON ACTIVATED CARBON Technical Report, Feb. 1987 - Jul. 1988
John J. Mahle and David K. Friday Feb. 1989 29 p
(Contract DAAA15-87-D-0007; DA Proj. 1C1-61102-A-71-A)
(AD-A206124; CRDEC-TR-045) Avail: NTIS HC A03/MF A01 CSCL 13/11

Water vapor is present, usually in relatively large concentrations, in many adsorption systems of industrial and military interest. This work develops an approach to predict the dynamic behavior of water vapor on an activated carbon adsorbent. Prior studies have neglected the importance of including the heat balance to account for behavior to high relative humidities. Water vapor isotherms were measured for BPL carbon at 15, 25, and 35 C, and the data were correlated using a modified version of the Antoine Equation first suggested by LeVan. Breakthrough experiments were performed using the following initial bed and feed conditions: (1) 50 percent RH feed to a dry bed, (2) 80 percent RH feed to a bed initially equilibrated at 50 percent RH, and (3) 80 percent RH feed to a dry bed. Two mathematical models were developed to analyze the values predicted using a non-isothermal stage model with a fluid phase mass transfer resistance and a adiabatic equilibrium theory model. GRA

N89-23629# Aerospatiale Aquitaine, Saint-Medard en Jalles (France). Div. Systems Strategiques et Spatiaux.
REENTRY MATERIALS IN THE ATMOSPHERE [LES MATERIAUX DE RENTREE DANS L'ATMOSPHERE]
A. Hordonneau Paris, France 1988 3 p In FRENCH
(Rept-882-430-102; ETN-89-94484) Avail: NTIS HC A02/MF A01

The materials which are currently used for thermal protection of manned vehicle or missile reentry are described and classified. A difference is made between gast reentry (military missiles, 30 sec, 20 Mw/m2, 100 bar) and slow manned vehicles reentry (some tenths of kW and few milibars). The materials discussed include ablative shieldings, low density ceramic foam, hot skin insulating structures, carbon-carbon composite materials and ceramic composites. ESA

N89-23630# Aerospatiale Aquitaine, Saint-Medard en Jalles (France).
COMPOSITE MATERIALS NONDESTRUCTIVE TESTS: CHOICE OF METHODS DEPENDING ON REQUIREMENTS [C.N.D. DES MATERIAUX COMPOSITES: CHOIX DE LA METHODE EN FONCTION DU BESOIN]
P. Barbier Paris, France 1988 11 p In FRENCH
(Rept-882-430-105; ETN-89-94486) Avail: NTIS HC A03/MF A01

Nondestructive tests of high performance composite materials used in the aerospace industry such as carbon epoxy composites are discussed. Thermography, holography, and tomography are studied. It is shown that the optimum choice is very much dependent on the geometry and use of each specimen. It is indicated that the validity of the tests is the main problem to examine. ESA

N89-23631# Aerospatiale Aquitaine, Saint-Medard en Jalles (France).
HIGH PERFORMANCE REFRACTORY COMPOSITE MATERIALS [LES MATERIAUX COMPOSITES REFRACTAIRES A HAUTE PERFORMANCE]
A. Hordonneau Paris, France 1988 8 p In FRENCH
(Rept-882-430-106; ETN-89-94487) Avail: NTIS Hc A02/MF A01

The development of carbon-ceramics thermostructural composites is discussed. These materials are needed for solid propellant rocket engine requirements in missiles and reentry vehicles. The manufacturing procedures are described, including the automatic weaving of fibrous forms and densification techniques. The properties shown include utilization temperature up to 3000 C, mechanical resistance, shock resistance, light weight, resistance to oxidation and erosion, and possibility of manufacturing large objects. ESA

N89-23632# Aerospatiale Aquitaine, Saint-Medard en Jalles (France).
CHALLENGES OF NONDESTRUCTIVE TESTING OF COMPOSITE MATERIALS [NOUVEAUX DEFIS POUR LES CONTROLES NON DESTRUCTIFS DES MATERIAUX COMPOSITES]
C. LeFloch Paris, France 1988 12 p In FRENCH
(Rept-882-430-107; ETN-89-94488) Avail: NTIS HC A03/MF A01

The quality control of composite materials is discussed, pointing out the most popular procedures in actual industrial practice including intermediate process controls; nondestructive control, and acoustic emission to study damaging; macroscopic evaluation tests (fiber rate, porosity rate, morphology); and defect characterization (delamination, impact, adhesion). The development of computer aided control and entirely automatic tests is examined. ESA

N89-23633# Aerospatiale Aquitaine, Saint-Medard en Jalles (France).
THE PROTECTION AGAINST OXIDATION OF CARBON MATERIALS. THERMODYNAMIC AND EXPERIMENTAL STUDY: A LITERATURE SURVEY [LA PROTECTION CONTRE L'OXYDATION DES MATERIAUX CARBONES. ETUDE THERMODYNAMIQUE ET EXPERIMENTALE]
Paris, France 6 Sep. 1988 32 p In FRENCH
(Rept-882-430-108; ETN-89-94489) Avail: NTIS HC A03/MF A01

Oxidation protective coatings proposed for carbon fibers in high temperature environments are reviewed. A thermodynamical analysis of mechanisms and potential of different coating systems is included. The coatings discussed include metals, oxides, B203,

SIC, La203, and multilayer coatings. The best ceramics for protection above 1800 C are HfB2 of mixtures of ZrB2 and Sic.
ESA

N89-23533*# Oak Ridge National Lab., TN.
SURFACE TREATMENT USING METAL FOIL LINER
Ray Garvey *In* NASA, Langley Research Center, NASA/SDIO Space Enviromental Effects on Materials Workshop, Part 1 May 1989 p 87-99 (For primary document see N89-23528 17-23)
Avail: NTIS HC A16/MF A01 CSCL 11D

25 INORGANIC AND PHYSICAL CHEMISTRY

Includes chemical analysis, e.g., chromatography; combustion theory; electrochemistry; and photochemistry.

For related information see also *77 Thermodynamics and Statistical Physics.*.

N89-23634*# Georgia Tech Research Inst., Atlanta.
ELECTRON SPECTROSCOPY FOR CHEMICAL ANALYSIS: SAMPLE ANALYSIS Final Report
W. B. Carter 5 Jan. 1989 60 p
(NASA Order H-98048-B)
(NASA-CR-183568; NAS 1.26:183568) Avail: NTIS HC A04/MF A01 CSCL 07D

Exposure conditions in atomic oxygen (ESCA) was performed on an SSL-100/206 Small Spot Spectrometer. All data were taken with the use of a low voltage electron flood gun and a charge neutralization screen to minimize charging effects on the data. The X-ray spot size and electron flood gun voltage used are recorded on the individual spectra as are the instrumental resolutions. Two types of spectra were obtained for each specimen: (1) general surveys, and (2) high resolution spectra. The two types of data reduction performed are: (1) semiquantitative compositional analysis, and (2) peak fitting. The materials analyzed are: (1) kapton 4, 5, and 6, (2) HDPE 19, 20, and 21, and (3) PVDF 4, 5, and 6.
Author

N89-23635# National Aerospace Lab., Tokyo (Japan).
SPONTANEOUS IGNITION OF ATOMIZED KEROSINE/AIR MIXTURES IN A HIGH PRESSURE FLOWING SYSTEM
Shigeru Hayashi, Hideshi Yamada, Kazuo Shimodaira, Takashi Saitoh, and Shouji Horiuchi Mar. 1988 12 p In JAPANESE; ENGLISH summary
(NAL-TR-966; ISSN-0389-4010) Avail: NTIS HC A03/MF A01

Measurements of spontaneous ignition delay have been conducted for mixtures of atomized kerosine and air at pressures from 1 MPa to 4 MPa under weakly vitiated conditions (18 to 19.3 percent O2). Equivalence ratios are 0.3 and 0.6. The apparatus is comprised of a preburner, a multi venturi fuel injector, a premixing tube of 45.3 mm in diameter and 200 mm in length, and an afterburner. The variation of the equivalence ratio from 0.3 to 0.6 is found to have no appreciable effect on the measured ignition delay. Ignition delay shortens as pressure increases up to 3 MPa. A further increase in pressure does not decrease ignition delay. For pressures up to 3 MPa and inlet air temperatures from 680 to 810 K, ignition delay can be expressed by the following empirical equation: tau (ig) = 2.1 x 10(-6) exp (92 x 10(3)/RT)/P where T is the air temperature, and P is the pressure. The value of E is 92 kJ/mol, which is one half of the values previously reported for kerosine vapor/air mixtures.
Author

N89-23636# California Univ., Berkeley. Dept. of Mechanical Engineering.
FIRE PROPAGATION IN CONCURRENT FLOWS Final Progress Report, 1 Aug. 1987 - 31 Jul. 1988
A. C. Fernandez-Pollo Jan. 1989 67 p
(Grant NANB-7-D0737)
(PB89-151781; NIST-GCR-89-557) Avail: NTIS HC A04/MF A01 CSCL 21B

The effect on the spread of flames of the turbulence intensity of an opposed air flow and a theoretical analysis of the concurrent spread of flames over thin fuels were studied. Both studies are important contributions in the study of the flame spread process. The results of the experimental study show that the flame spread process is significantly affected by the flow turbulence intensity for flames spreading over both thin and thick fuels. For a fixed flow velocity, the spread rate decreases as the turbulent intensity is increased. This appears to be due to the turbulent convective cooling of the fuel surface and gas in the vicinity of the flame front. Also observed is that extinction of the flames occurs at lower velocities as the turbulent intensity increases. The results of the theoretical analysis, which are in good agreement with previous experimental measurements, give detailed information about the flame structure and mechanisms of flame spread. It is shown that the flame length and consequently the rate of flame spread, are strongly dependent on the interaction between the pyrolysis and burn-out fronts.
Author

N89-23637# National Inst. of Standards and Technology, Boulder, CO. Thermophysics Div.
EXPERIMENTAL THERMAL CONDUCTIVITY, THERMAL DIFFUSIVITY AND SPECIFIC HEAT VALUES OF ARGON AND NITROGEN Final Report
H. M. Roder, R. A. Perkins, and C. A. NietodeCastro Oct. 1988 54 p
(PB89-148407; NISTIR-88/3902) Avail: NTIS HC A04/MF A01 CSCL 07D

Experimental measurements of thermal conductivity and thermal diffusivity as obtained in a transient hot-wire apparatus for argon and nitrogen are reported. Values of the specific heat were calculated from these measured values and the density associated with each measurement. The measurements were made at temperatures between 80 and 320 K with pressures between 0.1 and 70 MPa. The density range was 0 to 36 mol/L for argon and 0 to 32 mol/L for nitrogen. The total number of points recorded was 1484 for argon and 1423 for nitrogen.
Author

N89-23638*# Case Western Reserve Univ., Cleveland, OH. Dept. of Mechanical and Aerospace Engineering.
AN EXPERIMENTAL STUDY OF OPPOSED FLOW DIFFUSION FLAME EXTINCTION OVER A THIN FUEL IN MICROGRAVITY M.S. Thesis. Final Report
Paul V. Ferkul Feb. 1989 17 p Sponsored by NASA, Lewis Research Center, Cleveland, OH
(Grant NGT-50088)
(NASA-CR-182185; E-4440; NAS 1.26:182185) Avail: NTIS HC A03/MF A01 CSCL 21B

The flame spread and flame extinction characteristics of a thin fuel burning in a low-speed forced convective environment in microgravity were examined. The flame spread rate was observed to decrease both with decreasing ambient oxygen concentration as well as decreasing free stream velocity. A new mode of flame extinction was observed, caused by either of two means: keeping the free stream velocity constant and decreasing the oxygen concentration, or keeping the oxygen concentration constant and decreasing the free stream velocity. This extinction is called quenching extinction. By combining this data together with a previous microgravity quiescent flame study and normal-gravity blowoff extinction data, a flammability map was constructed with molar percentage oxygen and characteristic relative velocity as coordinates. The Damkohler number is not sufficient to predict flame spread and extinction in the near quench limit region.
Author

N89-23639# National Aerospace Lab., Tokyo (Japan).
BURNING RATE CONSTANT OF FUEL DROPLET UNDER HIGH PRESSURE
Mamoru Takahashi, Takashi Niioka, Junichi Sato, and Masanori Yamakawa Oct. 1988 12 p In JAPANESE; ENGLISH summary
(NAL-TR-1001; ISSN-0389-4010) Avail: NTIS HC A03/MF A01

Droplet combustion behavior under high pressure is presented. Heptane and n-hexadecane droplets suspended by a fine quartz

fiber were burnt in a high pressure air environment of up to 4 MPa. The burning rate constant increased with pressure and reached a maximum around the critical pressure. The same experiments were carried out for high density hydrocarbons (Rho=969 kg/cu m) which were developed recently. Allowing for the effect of density increase, the burning rate of high density hydrocarbons was found to be consistent with the predicted value obtained from heptane or n-hexadecane data and the classical analysis. In an oxygen atmosphere, however, the burning rate decreased by 30 percent from the predicted value. Author

N89-23640# Purdue Univ., West Lafayette, IN. Heat Transfer Lab.
SOLIDIFICATION OF BINARY SUBSTANCES IN RECTANGULAR AND CYLINDRICAL CAVITIES
M. S. Christenson and F. P. Incropera Feb. 1989 130 p
(Contract DE-FG02-87ER-13759)
(DE89-008883; DOE/ER-13759/2) Avail: NTIS HC A07/MF A01

An experimental study of solidification has been performed for binary solutions in rectangular and cylindrical cavities with varying initial concentration and thermal boundary conditions. Solutally driven flows were found to strongly influence solidification rates, localized remelting, and macroscopic solute redistribution. Control of these flows can be effected through selection of the thermal conditions imposed on the solidification process. Comparisons between experimental and numerical results for solidification of a binary NH4Cl-H2O solution is in a rectangular cavity have been made using a newly developed continuum model. Qualitative and quantitative agreement was found to exist and several experimentally unobservable features of the solidification process were highlighted by means of the numerical model. DOE

N89-23641# Illinois Univ., Urbana.
THETA PINCH DISCHARGES FOR SOLIDS VAPORIZATION AND ELEMENTAL CHEMICAL ANALYSIS Progress Report, 1 Dec. 1987 - 2 Feb. 1989
1989 7 p
(Contract DE-FG02-84ER-13218)
(DE89-008888; DOE/ER-13218/23) Avail: NTIS HC A02/MF A01

This period covered is from month 9 to month 22 of the 3 year renewal of the above named project. The goal of the project is to develop the theta pinch discharge as a source for elemental analysis of non-volatile solid materials. The first three years of research resulted in knowledge of how to design a functioning discharge system, and of how to resolve the emission in time to optimize signal-to-background ratio. Sampling was possible on a variety of materials, but was still not sufficient for purposes of universal solids analysis. The first 8 months of current grant saw the beginnings of operation of a discharge system using a 6 F capacitor; this system has operated reliably for the entire year. Total firings of the pinch this year have approached 1000. We have pursued hardware development, studies of sampling, excitation, and vapor propagation, and made our first attempts at doing quantitative analyses. DOE

N89-23642# Northwestern Univ., Evanston, IL. Dept. of Physics and Astronomy.
NMR CHARACTERIZATION OF POROUS STRUCTURES: CERAMICS AND SANDSTONES: RENEWAL PROPOSAL Progress Report, 15 May 1986 - Present
W. P. Halperin Aug. 1988 17 p
(Contract DE-FG02-86ER-45251)
(DE89-009148; DOE/ER-45251/T2) Avail: NTIS HC A03/MF A01

There has recently been considerable attention drawn to the potential for nuclear magnetic resonance (NMR) methods in quantitative non-destructive evaluation of porous structures: notably the characterization of ceramic green bodies, porous glasses, cementitious materials, and natural geological porous solids, such as sandstones and clays. The purpose of the present grant has been to establish these methods and test the theory; to apply them in the characterization of a variety of materials both model porous media and some that are technologically relevant; and very importantly, to explore the limitations of the NMR approach to pore structure determination. The potential of the method resides in the fact that it is non-destructive, quick to perform, covers a wide range of pore size from tens of angstroms to tens of microns, yet it can be applied to relatively small amounts of materials, less than 1 g, without undue constraint as to material type provided that it is non-metallic and not magnetized. Researchers have discovered some important results concerning porous structures that are of fundamental interest to basic science and which put NMR relaxation analysis on solid footing. They have demonstrated important technical applications of NMR. DOE

N89-23643 Georgia Inst. of Tech., Atlanta.
PULSATING CATALYTIC COMBUSTION OF GASEOUS FUELS Ph.D. Thesis
Reuven Gal-Ed 1988 130 p
Avail: Univ. Microfilms Order No. DA8904809

The feasibility of operating catalytic combustors under pulsating conditions and the circumstances under which acoustic pulsations increase the combustion efficiencies and output of catalytic combustors was investigated. An experimental catalytic combustor was developed, and a theoretical model of acoustic motions in non-isothermal, low Mach number duct flow was used to predict the acoustic behavior of the combustor. The effects of pulsations were determined by comparing temperature and species concentration data measured during operation with pulsations at different frequencies and pressure amplitudes to similar data measured during non-pulsating combustion. Experiments conducted with lean mixtures of methane or propane with air revealed that acoustic pulsations affected the temperature distribution along the combustor at flow Reynolds numbers less than 17,500. Excitation of pulsations during methane combustion caused shifts in the location of the combustion, and sometimes the onset or extinction of gas phase reactions. This occurred when several catalyst segments were located in the combustion section between an upstream pressure node and a downstream velocity node, defined here as an in phase location. This is where the acoustic pressure and the gas particle displacements are in phase. Investigation of possible improvements in combustion efficiency was carried out when diffusion processes limited the rate of the heterogeneous reaction and prevented its completion. Burning propane mixtures on a single catalyst segment at an in phase location showed that the excitation of acoustic pulsations increased the combustion efficiency by 10 to 50 percent. The effects of acoustic pulsations on catalytic combustion increased with increased amplitude of pulsations. The lower threshold amplitude at which acoustic effects were noted was near 135 dB. Dissert. Abstr.

N89-23644# Ohio State Univ., Columbus. Dept. of Ceramic Engineering.
STRENGTH AND STRUCTURE OF Ga(1-x)In(x)As ALLOYS Final Report, 1 Sep. 1985 - 30 Nov. 1988
Katherine T. Faber, John P. Hirth, and Dennis Ready 31 Jan. 1989 23 p
(Contract F49620-85-C-0129; ARPA Order 5526)
(AD-A205415; AFOSR-89-0265TR) Avail: NTIS HC A03/MF A01 CSCL 07/2

The role of isovalent dopants in the high temperature deformation of GaAs has been studied in the temperature range 550 to 1150 C. Additions of In, Sb, and B increase the high temperature hardness and the critical resolved shear stress for deformation at a given strain rate and result in lowering the dislocation density of as-grown liquid-encapsulated Czochralski GaAs crystals. Phosphorus, because of its minor influence on the lattice strain, provides little enhancement of the yield stress. The results are consistent with a solute hardening model where the solute atom surrounded tetrahedrally by four Ga or As atoms comprise the hardening cluster. Codoping with In and Si is less effective than the isovalent solutes, In, B, and Sb, and produces softening at high temperatures. Transmission electron microscopy provides evidence consistent with the athermal contribution to the

friction stress arising from a solid solution hardening effect. Cursory studies on solid solution in II-VI compounds, specifically, Cd(1-x)Mn(x)Te, demonstrate similar results. The role of dislocation damage in strained layer superlattices has also been modeled. GRA

N89-23645# Yale Univ., New Haven, CT.
NONLINEAR SPECTROSCOPY OF MULTICOMPONENT DROPLETS AND TWO- AND THREE-DIMENSIONAL MEASUREMENTS IN FLAMES Annual Report, 1 Jan. - 31 Dec. 1988
Richard K. Chang and Marshall B. Long 27 Jan. 1989 17 p
(Grant AF-AFOSR-0100-88; AF Proj. 2308)
(AD-A205449; AFOSR-89-0267TR) Avail: NTIS HC A03/MF A01 CSCL 21/2

Our progress in the area of nonlinear spectroscopy of droplets includes the following: (1) demonstration that shape distortion of totally transparent liquid droplets can result via the electrostrictive force associated with the gradient of the laser intensity, which is greatest at the internal focal spot just within the droplet shadow face; (2) investigation of the quenching of the stimulated Raman scattering from droplets after the high intensity laser has reached the laser-induced breakdown threshold and produced a dense, high temperature plasma which can absorb the stimulated Raman radiation; (3) studies on the dependence of the intensity threshold to generate stimulated Raman scattering on the linewidth of the laser, which can be operated in a single mode or a multimode; and (4) development of a fluorescence imaging technique which is capable of demarcating the liquid phase of the deformed droplet after radiation by a carbon dioxide laser has caused the droplet to undergo vaporization. GRA

N89-23646# Air Force Academy, CO.
VISCOSITY AND CONDUCTANCE OF MEICI/AICI3 MELTS CONTAINING NONAQUEOUS SOLVENTS Technical Report, 1 Sep. 1987 - 1 May 1988
Chester J. Dymek, Jr. and Greg E. Godec 26 May 1988 17 p
(AD-A205468; FJSRL-TR-88-0003) Avail: NTIS HC A03/MF A01 CSCL 10/2

Ionic liquids formed by mixing 1-methyl 3-ethylimidazolium chloride (MEICI) with AICI3 are of interest as electrolytes for batteries. Enhanced conductivities of these melts were observed upon addition of the solvents, benzene, acetonitrile, and dichloromethane. Conductivities and viscosities of these melt/solvent solutions were measured as a function of mole fraction of solvent and found to have similar functional dependence. A model for benzene-ion and ion-ion interactions in the solutions is proposed to explain the variations in the interdependence of conductivity and viscosity in the benzene-melt solutions. GRA

N89-23647# Cincinnati Univ., OH. Dept. of Chemistry.
X-RAY ABSORPTION SPECTROSCOPY OF ELECTROCHEMICALLY GENERATED SPECIES Annual Report, 1 Jan. 1988 - 31 Feb. 1989
Richard C. Elder and William R. Heineman 27 Jan. 1989 5 p
(Grant AF-AFOSR-0089-88; AF Proj. 2303)
(AD-A205572; AFOSR-89-0301TR) Avail: NTIS HC A02/MF A01 CSCL 07/4

Our research concerns the study of the change in the coordination environment and bond length about transition metals in complexes incorporated in a variety of media using EXAFS spectroelectrochemistry. These systems include: Fe(2,2 bipyridine)3(ClO4)2, Ru(2,2bipyridine)3Cl2, and Cu(dimethyl-1,10-phenanthroline)2BF4 in solution at reticulated vitreous carbon electrodes, and incorporated in Nafion films on gold Mylar and colloidal graphite gold Mylar electrodes; K3Fe(CN)6, Co(1,10-phenanthroline, e-disulfonic acid)3Cl3, Fe(2,2bipyridine)3(ClO4)2, and K3Cu(2,9-dimethyl-4,7-diphenyl 1,10-phenanthroline disulfonic acid)2 incorporated in the solid poly-electrolytes poly(dimethyl diallylammonium chloride) and poly(acrylamide) on gold minigrid electrode in a humidistatic cell; and Prussian Blue, KFe(Fe(CN)6), cyanometalate films electrochemically deposited onto gold Mylar electrodes. GRA

N89-23648# Chemical Research and Development Center, Aberdeen Proving Ground, MD.
A USER'S GUIDE TO THE MOLECULAR MODELING, ANALYSIS AND DISPLAY SYSTEM (MMADS), 2ND EDITION Report, Jun. 1986 - Jul. 1988
Joseph M. Leonard and George R. Famini Jan. 1989 110 p
(AD-A205674; CRDEC-TR-030) Avail: NTIS HC A06/MF A01 CSCL 07/4

The Molecular Modeling, Analysis, and Display System (MMADS) provides a chemist's workbench - a users-friendly, integrated suite of programs organized around a common data structure. The guiding principle throughout the development of MMADS has been to provide the user with the largest practical number of programs in an environment conducive to their use. With MMADS, a tool has been constructed that incorporates application programs for quantum, physical, and physical organic chemistry, as well as state-of-the-art molecular graphics routines, in a coherent whole. GRA

N89-23649# Texas A&M Univ., College Station. Dept. of Chemistry.
MEASURING CONDUCTIVITIES OF HIGHLY CONDUCTIVE MEMBRANES
Zhihua Cai, Chao Liu, and Charles R. Martin 28 Mar. 1989 39 p Submitted for publication
(Contract N00014-82-K-0612)
(AD-A206043; TR-34) Avail: NTIS HC A03/MF A01 CSCL 07/4

The theoretical and experimental aspects of an electrochemical approach for evaluating the conductivities of highly conductive membranes are described. The methods developed involve either a current or a potential step at a solid state electrochemical cell. It is assumed, and we prove, that only capacitive currents flow during these current or potential step experiments. The theory for these methods is derived from classical electrochemical theory for current and potential steps at RC circuits. We show that if the conductivity of the system under study is not too high (less than ca. 0.2/ohm/m), the classical theory provides accurate conductivity data. However, we also show that if the conductivity of the system is greater than ca. 0.2/ohm/m, conductivities obtained from the classical expressions are inaccurate. The modified theoretical analysis developed here, however, yields very accurate conductivity data for such highly conductive systems. The modifications of the classical theory entails accounting for the non-ideal wave shape of real potential or current step waveforms. GRA

N89-23650# Texas A&M Univ., College Station. Dept. of Chemistry.
NANO- AND MICROSTRUCTURES IN CHEMISTRY, ELECTROCHEMISTRY, AND MATERIALS SCIENCE
C. R. Martin, M. J. Tierney, I. F. Cheng, L. S. VanDyke, and Zhihua Cai 28 Mar. 1989 7 p
(Contract N00014-82-K-0612)
(AD-A206296; ONR-TR-35) Avail: NTIS HC A02/MF A01 CSCL 07/4

We have recently become interested in the fabrication and characterization of ensembles of nano- and micro-scale structures. In contrast to the majority of the work in this area, our interests do not lie in the microelectronic applications of such structures; rather, we are interested in the possible electrochemical, chemical, optical, and materials applications of nanostructure ensembles. We review these applications and the results of our investigations in this paper. GRA

N89-23651# California Univ., Irvine. Dept. of Mechanical Engineering.
FUNDAMENTAL STUDIES ON SPRAY COMBUSTION AND TURBULENT COMBUSTION Annual Technical Report, 1 Nov. 1987 - 31 Oct. 1988
W. A. Sirignano, G. S. Samuelsen, R. H. Rangel, C.-H. Chiang, and F. Miralles-Wilhelm 6 Feb. 1989 69 p
(Grant AF-AFOSR-0016-86; AF Proj. 2308)

(AD-A206438; AFOSR-89-0436TR) Avail: NTIS HC A04/MF A01 CSCL 21/2

Four major research tasks were performed during the year. Several prototype liquid atomization experimental designs were developed and tested, and the pulse visualization system was demonstrated. A nonlinear theory for liquid sheet deformation has been developed that predicts vortical rollup of the liquid-gas interface and allows for a rough estimate of early ligament dimensions in the atomization process. The turbulent reactive flow study identifies that the mixing and entrainment rates are identical on the high-speed and low-speed sides of a constant-density mixing layer. The formation, merging, and pairing of vortical structures is also predicted. Variable property effects have been included in the vaporizing droplet theory providing significant modifications on drag coefficients, Nusselt number, and Sherwood numbers. Modified correlations for higher transfer numbers are being developed and interacting droplets are considered. GRA

N89-23652# Florida Univ., Gainesville.
SPECTROSCOPIC STUDIES OF METAL-LIGAND-SURFACE INTERACTIONS Final Report, Jan. 1986 - Sep. 1987
C. T. Johnston, W. B. Person, M. T. Vala, T. L. Tipton, and D. A. Stone Oct. 1988 242 p
(Contract F08635-83-C-0136)
(AD-A206460; AFESC/ESL-TR-88-08) Avail: NTIS HC A11/MF A01 CSCL 07/2

A four part program of research on the vibrational spectroscopy of hydrazine, aromatic hydrocarbons, metals and clays and their interactions has been carried out. Vibrational spectra of hydrazine and its deuterated analogs have been obtained in cold rare gas matrices. A theoretical study of the vibrational frequencies and intensities of these systems has been carried out and used to interpret the observed spectra. Hydrazine has been reacted with various metal atoms and ions and their Raman or infrared spectra recorded and interpreted. Finally, the vibrational spectra of specific clay minerals and the effect of adsorbed metal cations and aromatic hydrocarbons were obtained and used to study the interactions between these species. GRA

N89-23653# Stanford Univ., CA. Electronics Lab.
FUNDAMENTAL AND PRACTICAL STUDIES OF METAL CONTACTS ON MERCURY ZINC TELLURIDE Annual Report, 1 Jan. - 31 Dec. 1988
W. E. Spicer 31 Dec. 1988 65 p
(Contract N00014-86-K-0854; ARPA Order 5674)
(AD-A206560) Avail: NTIS HC A04/MF A01 CSCL 07/2

Further understanding the role that the weak Hg-Te bond plays during metal/HgCdTe interface formation has a primary goal of our investigations during this reporting period. Metal/HgCdTe systems in general are highly disruptive, exhibiting a high degree of intermixing of semiconductor substrate components with the overlayer metal. The complexity of the interfaces formed on HgCdTE makes it difficult to isolate the various mechanisms leading to Fermi-level movement in these systems. During this reporting period, we have taken several approaches to investigate these effects under more simplified conditions. We have continued our study of metal/HgCdTe interfaces formed at low temperature, an approach which inhibits metal indiffusion, chemical reaction, and Hg loss, thus leading to a more simplified interface. GRA

N89-23654# Institut Franco-Allemand de Recherches, Saint-Louis (France).
DEVELOPMENT OF A CARS DEVICE FOR A FEASIBILITY STUDY OF DENSITY AND TEMPERATURE MEASUREMENTS AT HIGH TIME DEPENDENT RESOLUTION [AUFBAU EINER CARS-APPARATUR ZUR UNTERSUCHUNG DER DURCHFUEHRBARKEIT VON DICHTE- UND TEMPERATURMESSUNGEN MIT HOHER ZEITAUFLOESUNG]
A. Eichhorn 26 Aug. 1987 40 p In GERMAN
(ISL-R-117/87; ETN-89-94117) Avail: NTIS HC A03/MF A01

A Coherent Anti-Stokes Raman Scattering (CARS) system is developed for a feasibility study of CARS spectroscopy of N2 molecule density and temperature high frequency measurements. Experimental results indicate that the available pulse energy (0.5 mJ) is not sufficient for the given temperature measurements and resolution range wanted. Conversely density measurements with narrow band dye laser are feasible. Possible error sources are surveyed. ESA

26 METALLIC MATERIALS

Includes physical, chemical, and mechanical properties of metals, e.g., corrosion; and metallurgy.

N89-23655# Los Alamos National Lab., NM.
THEORETICAL STUDIES OF NI3AI AND NIAI WITH IMPURITIES
S. P. Chen, A. F. Voter, A. M. Boring, R. C. Albers, and P. J. Hay 1988 7 p Presented at the Fall Meeting of the Materials Research Society, Boston, MA, 28 Nov. 1988
(Contract W-7405-eng-36)
(DE89-006556; LA-UR-89-218; CONF-881155-42) Avail: NTIS HC A02/MF A01

Intermetallic compound has been extensively studied because of their superior properties in strength, low creep rate, and high melting point. But most of the systems have room temperature ductility problems, like Li2 and B2 compounds. Both Li2, Ni3Aland B2NiAl exhibit intergranular fracture mode. Understanding grain boundaries in these materials is of particular importance since intergranular fracture limits the applicability of these otherwise promising material. In an effort trying to understand the fracture mechanism, we have used embedded atom potentials to study the properties of Ni3Al and NiAl. We also consider the effect of boron, sulfur, and nickel segregation on the strength of grain boundaries in Ni3Al and NiAl. DOE

N89-23656# National Aerospace Lab., Amsterdam (Netherlands). Dept. of Materials.
QUENCH SENSITIVITY OF AIRFRAME ALUMINIUM ALLOYS
H. J. Kolkman, W. G. J. tHart, and L. Schra 29 Jan. 1988 11 p Presented at the 8th International Conference on the Strength of Metals and Alloys, Tampere, Finland, 22-26 Aug. 1988
(PB89-146039; NLR-MP-88003-U) Avail: NTIS HC A03/MF A01 CSCL 11F

The quench sensitivity of six precipitation hardened aluminum alloys for aerospace applications was investigated and explained by means of TEM (Transmission Electron Microscopy). The quench sensitivity was mainly caused by the solute depletion associated with heterogeneous precipitation at dispersoids for low quench rates. Author

N89-23657# Helsinki Univ. of Technology, Espoo (Finland). Materials Processing and Powder Metallury Lab.
CRITICAL ASSESSMENT OF THE THERMODYNAMIC PROPERTIES OF ANTIMONY-COPPER ALLOYS
Osmo Teppo and Pekka Taskinen 1988 36 p
(PB89-147524; TKK-V-B40; ISBN-951-754-661-0) Avail: NTIS HC A03/MF A01 CSCL 11F

The phase diagram and the solution thermodynamics of the binary system antimony-copper were critically assessed by using simultaneously experimental thermodynamic and phase diagram information. The thermodynamic model parameters of the solution phases and the Gibbs energies of the intermetallic compounds were optimized by the Lukas program. Author

N89-23658# Academy of Sciences (USSR), Novosibirsk. Inst. Yadernoj Fiziki.
ON STEEL SUPERFICIAL HARDENING BY CONCENTRATED ELECTRON BEAM IN THE AIR
A. F. Vajsman, S. B. Vasserman, M. G. Golkovskij, V. D. Kedo, and R. A. Salimov 1988 31 p In RUSSIAN
(DE88-705781; IYaF-88-73) Avail: NTIS (US Sales Only) HC A03/MF A01

Possibilities of steel superficial hardening by a concentrated

electron beam are studied. Experiments have been conducted since 1985 using the EhLV-6 accelerator with concentrated emission of the beam into atmosphere. Regimes ensuring the hardening and certain characteristic properties of the hardened layer are described. DOE

N89-23659# Pacific Northwest Labs., Richland, WA.
ENVIRONMENT-INDUCED CRACK GROWTH PROCESSES IN NICKEL-BASE ALLOYS
R. H. Jones and S. M. Bruemmer Oct. 1988 95 p Presented at the International Conference on Environment-induced Crack Growth of Metals, Kohler, WI, 5 Oct. 1988
(Contract DE-AC06-76RL-01830)
(DE89-008253; PNL-SA-16273; CONF-8810330-1) Avail: NTIS HC A05/MF A01

Ni-base alloys exhibit excellent corrosion resistance and are used extensively in corrosive applications, although environment-induced crack growth has occurred in several applications. Environment induced crack growth in Ni-base alloys occurs in a number of environments, including water, acidic and basic solutions, and gaseous H. Factors controlling environment-induced crack growth are similar to those in other materials, namely: (1) microstructure/microchemistry, (2) environment, and (3) stress. The critical factors controlling stress corrosion cracking of Ni-base alloys are generally known, but many of the details are not. In some cases, quantitative information is lacking with details limited to knowledge about general susceptibility. The crack growth mode is generally intergranular for aqueous environments and H gas environments. A key difference between environment-induced crack growth in FeCrNi alloys and Ni-base alloys is the susceptibility to cracking in H environments in Ni-base alloys, while FeCrNi alloys exhibit cracking in hydrogen environments only under extreme conditions. This paper presents a comprehensive review of the literature on environment-induced crack growth of Ni-base alloys, and covers both phenomenological observation and mechanistic interpretation. DOE

N89-23660# Kernforschungsanlage, Juelich (Germany, F.R.). Inst. fuer Plasmaphysik.
IONIZATION INVESTIGATION OF SPUTTERED TITANIUM AND OF TITANIUM ION TRANSPORT PROCESS IN AN ARGON DISCHARGE GLOW USING LASER INDUCED FLUORESCENCE Thesis - Ruhr Univ. [UNTERSUCHUNGEN ZUR IONISATION VON ABGESTAEUBTEM TITAN UND ZUM TRANSPORT DER TITANIONEN IN EINER ARGON-GLIMMENTLADUNG MITTELS LASER INDUZIERTER FLUORESZENZ]
Ralf Koppmann Jul. 1988 128 p In GERMAN; ENGLISH summary
(JUEL-2219; ISSN-0366-0885; ETN-89-93964) Avail: NTIS HC A07/MF A01

The ionization mechanism for sputtered titanium and the transport process of the titanium ions were investigated in an argon glow discharge using laser-induced fluorescence spectroscopy. The density profiles of neutral titanium show a maximum near to the cathode and a decrease towards the anode. The shape of the profile can be described by a model considering thermalization and diffusion processes. The density distribution of singly ionized titanium was measured in the axis of a glow discharge. The density profiles of Ti(+) show a maximum located on diffusion dominated side of the corresponding Ti(0)-profile. Towards the cathode the density of Ti(+) decreases rapidly, the decrease towards the anode follows the Ti(0)-profile. The titanium ionization degree of 0.1 leads to the assumption that Penning ionization is the dominant ionization process for the sputtered titanium atoms. From a balance of the Ti(0) and Ti(+) fluxes it is possible to calculate the axial electrical field strength. The results reveal an almost constant field strength of 3V/cm in the positive column and an increase towards the cathode. ESA

N89-23661# Oak Ridge National Lab., TN.
A FIRST-PRINCIPLES CALCULATION OF THE RESISTIVITY AND THERMOPOWER IN STRONG-SCATTERING ALLOYS
Randall H. Brown, Philip B. Allen (State Univ. of New York, Stony Brook.), Donald M. Nicholson, and William H. Butler 1988 6 p Presented at the Fall Meeting of the Materials Research Society, Boston, MA, 28 Nov. 1988
(Contracts DE-AC05-84OR-21400; DE-AC02-76CH-00016)
(DE89-008565; CONF-881155-52) Avail: NTIS HC A02/MF A01

We investigate the concentration and short-range order dependence of the zero-temperature resistivity and thermopower for substitutionally ordered alloys from a first-principles approach. The alloy disorder is simulated by calculating the electronic structure of a large supercell (typically 200 to 250 atoms) with periodic boundary conditions. For the strong-scattering alloys we consider, the electron mean-free path is much less than the supercell dimension, causing artificial effects of periodicity to be negligible. In spite of strong scattering, there is no evidence for localized states near E sub F. The resistivity and thermopower are averaged over several configurations resulting in statistical error bounds of approximately + or - 10%. The concentration-dependent resistivity of substitutional V(1-x)Al(x) alloys agree well with Korringa-Kohn-Rostoker coherent potential approximation (KKR CPA) calculations. This confirms the accuracy of KKR CPA theory. DOE

N89-23662# Pennsylvania State Univ., University Park. Materials Research Lab.
TWIN BOUNDARIES, INTERFACES AND MODULATED STRUCTURES IN MARTENSITES Annual Progress Report No. 4, 1 Jul. 1988 - 30 Jun. 1989
Gerald R. Barsch 15 Mar. 1989 24 p
(Contract DE-FG02-85ER-45214)
(DE89-009064; DOE/ER-45214/T4) Avail: NTIS HC A03/MF A01

A comprehensive theoretical study with concurrent supporting experimental investigations is being carried out on coherent and semicoherent interfaces in ferroelastic martensites, including twin boundaries and twin bands, heterophase parent/product interfaces and inclusions, and transformation precursors. This work is motivated by the need for a new theoretical basis for investigating the martensite nucleation mechanism and for establishing the conditions for nonclassical nucleation. Soliton-like solutions of a dynamic Ginzburg-Landau continuum theory for ferroelastic martensites are being studied in order to determine the strain distribution, strain energy and dynamical behavior for various geometric configurations as a function of the material parameters, temperature and boundary conditions. Model parameters of the theory consist of the second and higher order elastic constants and the harmonic strain gradient coefficients in the parent phase. X-ray measurements of the transformation strain versus temperature, and ultrasonic velocity and attenuation measurements on biaxially stressed crystals in In sub 1-x Tl sub x alloys for determining the second and higher order elastic constants in the single domain tetragonal state and for studying the morphology and the dynamic behavior of the martensite interfaces and transformation precursors are in progress. DOE

N89-23663# Oak Ridge National Lab., TN.
IRON-NIOBIUM-ALUMINUM ALLOY HAVING HIGH-TEMPERATURE CORROSION RESISTANCE Patent Application
Huey S. Hsu, inventor (to DOE) 14 Apr. 1988 13 p
(Contract DE-AC05-84OR-21400)
(DE89-009600; PATENTS-US-A7181630;
US-Patent-Appl-SN-181630) Avail: NTIS HC A03/MF A01

An alloy for use in high temperature sulfur and oxygen containing environments, having aluminum for oxygen resistance, niobium for sulfur resistance and the balance iron, is discussed. DOE

N89-23664*# National Aeronautics and Space Administration. Lewis Research Center, Cleveland, OH.
MACROSEGREGATION AND NUCLEATION IN UNDERCOOLED Pb-Sn ALLOYS

Henry C. deGroh, III May 1989 36 p
(NASA-TM-102023; E-4759; NAS 1.15:102023) Avail: NTIS HC A03/MF A01 CSCL 11F

A technique resulting in large undercoolings in bulk samples (23g) of lead-tin alloys was developed. Samples of Pb-12.5 wt percent Sn, Pb-61 wt percent Sn, and Pb-77 wt percent Sn were processed with undercoolings ranging from 4 to 34 K and with cooling rates varying between 0.04 and 4 K/sec. The nucleation behavior of the Pb-Sn system was found to be nonreciprocal. The solid Sn phase effectively nucleated the Pb phase of the eutectic; however, large undercoolings developed in Sn-rich eutectic liquid in the presence of the solid Pb phase. This phenomenon is believed to be mainly the result of differences in interfacial energies between solid Sn-eutectic liquid, and solid Pb-eutectic liquid rather than lattice misfit between Pb and Sn. Large amounts of segregation developed in the highly undercooled eutectic ingots. This macrosegregation was found to increase as undercooling increases. Macrosegregation in these undercooled eutectic alloys was found to be primarily due to a sink/float mechanism and the nucleation behavior of the alloy. Lead-rich dendrites are the primary phase in the undercooled eutectic system. These dendrites grow rapidly into the undercooled bath and soon break apart due to recalescence and Sn enrichment of the liquid. These fragmented Pb dendrites are then free to settle to the bottom portion of the ingot causing the macrosegregation observed in this study. A eutectic Pb-Sn alloy undercooled 20 K and cooled at 4 K/sec had a composition of about Pb-72 wt percent Sn at the top and 55 percent Sn at the bottom. Author

N89-23665# Carnegie-Mellon Univ., Pittsburgh, PA. Dept. of Metallurgical Engineering and Mate Rials Science.
FUNDAMENTAL STUDIES OF BETA PHASE DECOMPOSITION MODES IN TITANIUM ALLOYS Interim Technical Report, 1 Oct. 1987 - 30 Sep. 1988
H. I. Aaronson, T. Furuhara, and Y. Mou 31 Jan. 1989 39 p
(Grant AF-AFOSR-0303-84; AF Proj. 2306)
(AD-A205296; AFOSR-89-0235TR) Avail: NTIS HC A03/MF A01 CSCL 11/6

An electron microscopy investigation of the interphase boundary structure of (hcp) grain boundary alpha allotriomorphs in a titanium-7.15 W/O chromium alloy has shown that whether these crystals are Burgers or non-Burgers-related with respect to their bounding (bcc) beta matrix grains their interfacial structures are partially coherent. No misfit dislocations are observed at either type of interface. Instead, two types of ledge are present. One type is widely and irregularly spaced and heavily kinked; this appears to be growth ledges. The other type is quite straight and both closely and uniformly spaced; this is likely to be structural ledges. Habit plane measurements on the broad faces of alpha plates support the presence of structural ledges. These ledges have a Burgers vector of a/6 (111) parallel to the terrace plane, indicating that they can perform as significant compensators of misfit dislocations. Studies on the interphase boundary structure of the bcc/hcp massive transformation in a silver-26 A/O aluminum alloy have reached the point where a technique for preparing thin foils in a manner which permits a significant number of interfaces to be imaged has finally been achieved. Studies of this structure have now been inititiated. GRA

N89-23666# Army Armament Research, Development and Engineering Center, Watervliet, NY.
TESTING CHROMIUM ADHESION USING ACOUSTIC EMISSION Final Technical Report
M. E. Todaro and G. P. Capsimalis Feb. 1989 19 p
(AD-A205621; ARCCB-TR-89005) Avail: NTIS HC A03/MF A01 CSCL 11/6

The use of acoustic emission was investigated as a method of characterizing chromium adhesion on steel. The samples used in the study were cylinders cut from the muzzle end of 120 mm gun tubes, plated on the inner surface with chromium, and cut to form split rings. Acoustic emission data was taken during loading of each ring. The results of the study are inconclusive regarding the effectiveness of acoustic emission as a test method for chromium adhesion. GRA

N89-23667# Naval Postgraduate School, Monterey, CA.
THE EFFECT OF WELDING PROCESS ON THE MICROSTRUCTURE OF HY-130 STEEL WELDMENTS M.S. Thesis
Teresa M. McNutt Dec. 1988 76 p
(AD-A205692) Avail: NTIS HC A05/MF A01 CSCL 11/6

HY-130 is a high-strength, low-carbon steel used in the quenched and tempered condition. It is designed for high performance and marine applications where good weldability is a requirement. Optimum welding parameters are currently under investigation. In this study, 1/2 inch (12.7 mm) HY-130 steel weldments produced by submerged arc welding (SAW) and gas metal arc welding (GMAW) processes are compared by means of a systematic microstructural characterization of the base metal, weld metal, and heat affected zone (HAZ). The microstructures are characterized by optical and electron microscopy and microhardness measurements are performed in the weld metal and across the HAZ to relate the microstructure with the microhardness profiles. The weld metal microstructure of both weldments showed a predominantly martensitic structure. The GMAW weld metal had a finer lath martensite structure and contained more retained austenite and twinned martensite. The SAW weld metal had a less defined lath structure which was more bainitic. The microhardness values were higher in the GMAW weld metal. No significant differences in microstructure and hardness were observed in the HAZ of the two weldments. GRA

N89-23668# Applied Research Lab., State College, PA.
FABRICATION OF UNIDIRECTIONAL FIBER REINFORCED 6061 ALUMINUM ALLOY USING HIGH PRESSURE SQUEEZE CASTING M.S. Thesis
Robert J. Sample and Ram B. Bhagat Dec. 1988 119 p
(Contract N00024-85-C-6041)
(AD-A205717; ARL/PSU/TR-88-015) Avail: NTIS HC A06/MF A01 CSCL 11/6

Aluminum alloy castings have been successfully reinforced with unidirectional graphite fibers. The reinforced castings were fabricated using an innovative technique known as high pressure squeeze casting. Previously, squeeze casting has been recognized as a superior metal forming method. The materials fabricated in this study demonstrate the ability of squeeze casting to achieve good fiber distribution and infiltration without the need for pretreatment of the fibers. There was very little observed chemical reaction between the graphite fibers and the aluminum in the as-cast condition. The strength of the reinforced castings increased with increasing fiber volume fraction, although the strengths were generally less than those predicted by rule mixtures. The tensile strengths ranged from 120 MPa for fiber volume fractions of 5 percent to 52 percent, respectively. GRA

N89-23669# Cornell Univ., Ithaca, NY.
SIMPLE ADSORBATES ON TRANSITION METAL SURFACES: A JOINT CHEMICAL AND PHYSICAL APPROACH Final Report, 1 Sep. 1985 - 31 Aug. 1988
Roald Hoffmann and John Wilkins 28 Feb. 1989 15 p
(Contract N00014-82-K-0576)
(AD-A205726; AD-E501079) Avail: NTIS HC A03/MF A01 CSCL 07/2

In this work we have carried out a number of joint chemical and physical studies of metal surfaces, of adsorbates on such surfaces, and their reactions. Several catalytic reactions were studied theoretically, as well as materials problems related to interfaces and overlayers. GRA

N89-23670# Naval Postgraduate School, Monterey, CA.
STRESS RELIEF CRACKING IN COPPER-PRECIPITATION STRENGTHENED HSLA-100 STEEL M.S. Thesis
Steven A. McNutt Dec. 1988 98 p
(AD-A205936) Avail: NTIS HC A05/MF A01 CSCL 11/6

The U.S. Navy is currently developing a new family of high-strength, low-alloy steels which derive a significant portion of their strength from copper precipitation. These highly weldable steels require little or no preheat, resulting in substantial cost savings. The first of these steels, HSLA-80, has been certified for ship construction, but recent studies have indicated some susceptibility to stress relief cracking in weldments. HSLA-100, modification of HSLA-80, is now being considered for several higher-strength naval structures. Stress-relief cracking has not been studied previously in this steel and is the subject of investigation in this work. The steel weldments were loaded below their yield strength, heated to temperature of 550 to 650 C, and permitted to stress relief for one hour. At all temperatures, the steel exhibited susceptibility to stress relief cracking in certain stress ranges. Optical and scanning electron microscopy exhibited intergranular cracking which always traversed the coarse-grained region of the heat affected zone. GRA

N89-23671# Naval Air Development Center, Warminster, PA. Air Vehicle and Crew Systems Technology Dept.
AMBIENT TEMPERATURE PROPERTIES OF PM (POWDER METAL) ALUMINUM-TITANIUM ALLOYS Final Report
William E. Frazier and Michael J. Koczak Jun. 1988 35 p
(AD-A205997; NADC-88067-60) Avail: NTIS HC A03/MF A01 CSCL 11/6

The structure and properties of dispersion strengthened aluminum 4 and 6 weight percent titanium powder alloys were investigated as candidate materials for high temperature performance. Alloy rod was extruded from vacuum hot pressed billets of helium gas atomized, mechanically alloyed, and atomized plus mechanically alloyed powder. Microstructure and mechanical properties were fully characterized to assess the effect of disperoids on alloy strength, ductility, notch toughness, and modulus. The alloys exhibited low density (2.8g/cu cm), high modulus (85 GPa), good ductility (12 percent), and strength equivalent to Al-Fe-Ce alloys, e.g., 120 MPa at 250 to 300 C. GRA

N89-23672# Drexel Univ., Philadelphia, PA. Dept. of Materials Engineering.
SPRAY DEPOSITION: A FUNDAMENTAL STUDY OF DROPLET IMPINGEMENT, SPREADING AND CONSOLIDATION
D. Apelian, A. Lawley, G. Gillen, and P. Mathur Dec. 1988 26 p
(Contract N00014-84-K-0472)
(AD-A206065; TR-4) Avail: NTIS HC A03/MF A01 CSCL 11/6

Spray deposition via the Osprey process is rapidly emerging as an attractive technology to produce net or near-net-shaped components of a variety of alloys. The process is schematically shown. The alloy charge is melted under an inert gas cover in a crucible placed on top of the spray chamber. At the appropriate superheat temperature, the molten metal is allowed to exit through a refractory nozzle at the base of the crucible into the atomizing zone. The stream of molten metal is gas atomized. Subsequently, the liquid droplets accelerate and cool/solidify under the influence of the atomizing gas, and consolidate on the substrate to form a homogeneous deposit. Spray deposition has an intrinsic beneficial component of rapid solidification which results in a fine-scale homogeneous microstructure devoid of macroscopic segregation. Further, the process is capable of high throughput rates in excess of 20 kg/min. Key process parameters are superheat, atomizing gas pressure, the working distance and the substrate motion. Detailed descriptions of the Osprey process are given elsewhere. GRA

N89-23673# Pittsburgh Univ., PA. Dept. of Materials Science and Engineering.
ENVIRONMENTAL EFFECTS IN NIOBIUM BASE ALLOYS AND OTHER SELECTED INTERMETALLIC COMPOUNDS Annual Report No. 1, 1 Nov. 1987 - 31 Oct. 1988
G. H. Meier and A. W. Thompson (Carnegie-Mellon Univ., Pittsburgh, PA.) 15 Dec. 1988 68 p
(Contract F49620-88-C-0013; DARPA Order 6155)
(AD-A206072; AFOSR-89-0366TR) Avail: NTIS HC A04/MF A01 CSCL 11/6

Niobium aluminides and silicides as well as other intermetallic compounds have potential for use in advanced gas turbines where increased operating temperatures are necessary to obtain the targeted performance goals. These materials will be subjected to a variety of environments over a range of temperatures. Two of the principal reactants in these environments are oxygen and hydrogen. This program is concerned with the effects of oxygen and hydrogen on niobium alloys and other selected intermetallic compounds. This program consists of two parts. The investigations involving oxygen are directed toward describing the conditions which must be achieved in order to have a continuous, protective Aluminum Oxide or Silicon dioxide scale developed on niobium-base alloys and compounds, and other selected intermetallics, at temperatures between 600 and 1400 C. The studies concerned with hydrogen effects are directed toward determining solubility limits, hydrogen uptake and permeation rates, and the degree to which hydrogen degrades the mechanical properties of these materials. GRA

N89-23674# Rensselaer Polytechnic Inst., Troy, NY. Dept. of Mechanical Engineering.
STEEL HARDNESS EFFECTS IN BOUNDARY LUBRICATED SLIDING: AN IN-SITU SEM (SCANNING ELECTRON MICROSCOPE) STUDY
W. Holzhauer and S. J. Calabrese 1988 10 p
(Contract DAAL03-86-K-0076)
(AD-A206156; ARO-23525.27-EG) Avail: NTIS HC A02/MF A01 CSCL 11/6

A pin-on cylinder test apparatus was used to perform low speed, steel-on-steel sliding experiments in-situ in a scanning electron microscope (SEM). Through modifications to the SEM, these experiments could be run with a thin film of hydrocarbon oil applied to the sliding surface. Studies have been performed using AISI 4340 steel, both annealed and through hardened, for the pin and cylinder in combinations of soft (annealed)-versus-soft, hard-versus-soft and hard-versus-hard. All three material combinations show a progressive smoothing in the wear track as the number of sliding passes increases, plus agglomeration of wear debris interspersed with oil around the contact. Both of these effects lead to failure of the contacts due to insufficient lubrication. The combinations involving annealed steel fail catastrophically by an apparent third body abrasive mechanism while the failure of the hard versus hard combination involves intermittent plowing, resulting in more localized damage. GRA

N89-23675# Baylor Univ., Waco, TX. Dept. of Chemistry.
CONTROL OF THE COMPOSITION OF ELECTRODEPOSITED ALLOYS BY THE USE OF CERTAIN TYPES OF ADDITIVES Final Report, 1 Aug. 1985 - 31 Dec. 1988
Thomas C. Franklin, Venita Totten, Ali I. Aktan, and Danielle Beu 13 Feb. 1989 61 p
(Contract DAAG29-85-K-0205)
(AD-A206370; ARO-22727.13-CH) Avail: NTIS HC A04/MF A01 CSCL 11/6

Using the principle that additives used in electrodeposition of metals often exert their effect by selectively accelerating or inhibiting one of the competing reactions occurring at the electrode, a study was made to demonstrate the predictable effect of additives that affect the rate of electrode reactions by ion pairing, electron bridging and electrode filming. The effect of these additives was demonstrated by studying their effect on voltammetric measurements, on the current efficiencies for deposition of metals and on the composition of binary alloys. GRA

N89-23676# Naval Research Lab., Washington, DC.
FILMCAL: AN ESR (ELECTRON SPIN RESONANCE) SIMULATION PROGRAM FOR TRANSITION METALS IN PHTHALOCYANINE FILMS Memorandum Report, Jun. - Aug. 1988

M. D. Pace and S. M. Masumura 24 Feb. 1989 28 p (AD-A206441; NRL-MR-6417) Avail: NTIS HC A03/MF A01 CSCL 07/2

A computer program, written in FORTRAN, was developed to simulate ESR spectra of transition metal ions in thin layer phthalocyanine films. The spectral calculation is based on Gaussian distribution of orientations of the molecules plane of the phthalocyanine with respect to the surface of the film. Four 14N hyperfine interactions are included to simulate the coordination site of the transition metal ion. GRA

N89-23575# Max-Planck-Inst. fuer Metallforschung, Stuttgart (Germany, F.R.). Inst. fuer Werkstoffwissenschaften.
SINTERING AND HIPing WITH ADDITIVES
Wolfgang A. Kaysser, Guenter Petzow, and M. Mitkov (Institut za Nuklearne Nauke Boris Kidric, Belgrade, Yugoslavia) *In* Kernforschungsanlage Juelich GmbH, The 8th German-Yugoslav Meeting on Materials Science and Development: Ceramics and Metals 1988 p 47-61 Sponsored in part by Deutsche Forschungsgemeinschart, Bonn, Fed. Republic of Germany (For primary document see N89-23569 17-23)
Copyright Avail: NTIS HC A21/MF A01

N89-23584# Kernforschungsanlage, Juelich (Germany, F.R.).
YOUNG'S MODULUS OF ELASTICITY: MEASURED VALUES FOR MULTIPHASE METALS AND THEIR CALCULATION VIA THE BOUND CONCEPT
Gerhard Ondracek and Dirk Windelberg (Technische Univ., Hanover, Germany, F.R.) *In its* The 8th German-Yugoslav Meeting on Materials Science and Development: Ceramics and Metals 1988 p 141-146 (For primary document see N89-23569 17-23)
Copyright Avail: NTIS HC A21/MF A01

N89-23596# Max-Planck-Gesellschaft, Ploen (Germany, F.R.). Fritz-Haber-Inst.
OXYGEN INTERACTION WITH METAL SURFACES: SURFACE SCIENCE APPROACH
Klaus Wandelt, Petar Pervan, and Milorad Milun (Yugoslav Academy of Sciences and Arts, Zagreb.) *In* Kernforschungsanlage Juelich GmbH, The 8th German-Yugoslav Meeting on Materials Science and Development: Ceramics and Metals 1988 p 249-266 Sponsored by Bundesministerium fuer Forschung und Technologie, Bonn, Fed. Republic of Germany; Bilateral Yugoslav-German Project; Deutsche Forschungsgemeinschaft, Bonn, Fed, Republic of Germany and SIZ za Znanstveni rad SAH Project, Yugoslavia (For primary document see N89-23569 17-23)
(Contracts IAEA-3227; IAEA-4527)
Copyright Avail: NTIS HC A21/MF A01

N89-23597# Skopje Univ. (Yugoslavia). Faculty of Technology and Metallurgy.
STABILITY AND INSTABILITY OF ANODICALLY FORMED LAYERS ON METALLIC SURFACES
Ljubomir D. Arsov *In* Kernforschungsanlage Juelich GmbH, The 8th German-Yugoslav Meeting on Materials Science and Development: Ceramics and Metals 1988 p 267-272 (For primary document see N89-23569 17-23)
Copyright Avail: NTIS HC A21/MF A01

N89-23599# Patras Univ. (Greece). Inst. of Physical Metallurgy.
TEMPERATURE DEPENDENCE OF INTERFACIAL ENERGIES BETWEEN SOLID OXIDES AND LIQUID METALS
Panajotis Nikolopoulos, D. Sotiropoulou, U. Jauch, and Gerhard Ondracek (Kernforschungsanlage, Juelich, Germany, F.R.) *In* Kernforschungsanlage Juelich GmbH, The 8th German-Yogoslav Meeting on Materials Science and Development: Ceramics and Metals 1988 p 281-289 Sponsored by the Deutsche Forschungsgemeinschaft, Bonn, Fed. Republic of Germany (For primary document see N89-23569 17-23)
Copyright Avail: NTIS HC A21/MF A01

N89-23606# Kernforschungszentrum G.m.b.H., Karlsruhe (Germany, F.R.). Inst. fuer Material- und Festkoerperforschung.
ON THE CORRELATION BETWEEN MICROSTRUCTURE AND MAGNETIC INDUCTION OF POROUS IRON AND IRON-Ni(0.4)Zn(0.6)Fe2O4 COMPOSITES
Edmund Remane *In* Kernforschungsanlage Juelich GmbH, The 8th German-Yugoslav Meeting on Materials Science and Development: Ceramics and Metals 1988 p 341-349 (For primary document see N89-23569 17-23)
Copyright Avail: NTIS HC A21/MF A01

N89-23607# Karlsruhe Univ. (Germany, F.R.). Nuclear Research Center.
WEAR RESISTANT SINTERED STEEL WITH HIGH CARBIDE CONTENT
R. Klausmann, R. Oberacker, and Fritz Ernst Thuemmler *In* Kernforschungsanlage Juelich GmbH, The 8th German-Yugoslav Meeting on Materials Science and Development: Ceramics and Metals 1988 p 353-361 (For primary document see N89-23569 17-23)
Copyright Avail: NTIS HC A21/MF A01

N89-23608# Serbian Academy of Sciences and Arts, Belgrade (Yugoslavia). Inst. of Technical Sciences.
PRODUCTION OF METAL POWDERS BY ROTATING ELECTRODE PROCESS
Miodrag Zdujic, V. Petrovic, L. Nelevic (Titograd Univ., Yugoslavia), and Dragoljub Uskokovic *In* Kernforschungsanlage Juelich GmbH, The 8th German-Yugoslav Meeting on Materials Science and Development: Ceramics and Metals 1988 p 363-370 Sponsored by the Serbian Research Foundation and the Prvi Partizan Hard Metal Factory (For primary document see N89-23569 17-23)
Copyright Avail: NTIS HC A21/MF A01

N89-23609# Max-Planck-Inst. fuer Metallforschung, Stuttgart (Germany, F.R.). Inst. fuer Werkstoffwissenschaften.
COOLING RATE, UNDERCOOLING AND RAPID SOLIDIFICATION BY ATOMIZATION
Klaus Rzesnitzek, Wolfgang A. Kaysser, and Guenter Petzow *In* Kernforschungsanlage Juelich GmbH, The 8th German-Yugoslav Meeting on Materials Science and Development: Ceramics and Metals 1988 p 371-378 (For primary document see N89-23569 17-23)
Avail: NTIS HC A21/MF A01

N89-23610# Max-Planck-Inst. fuer Metallforschung, Stuttgart (Germany, F.R.). Inst. fuer Werkstoffwissenschaften.
MECHANICAL PROPERTIES OF GAS ATOMIZED Cu-Ti AND Cu-Ti-B ALLOYS
Dusan Bosic, Rainhard Laag, Wolfgang A. Kaysser, and M. Mitkov (Institut za Nuklearne Nauke Boris Kidric, Belgrade, Yugoslavia) *In* Kernforschungsanlage Juelich GmbH, The 8th German-Yugoslav Meeting on Materials Science and Development: Ceramics and Metals 1988 p 379-383 (For primary document see N89-23569 17-23)
Copyright Avail: NTIS HC A21/MF A01

N89-23611# Technische Univ., Clausthal-Zellerfeld (Germany, F.R.). Inst. fuer Werkstoffkunde und Werkstofftechnik.
MECHANICAL PROPERTIES OF RAPIDLY SOLIDIFIED IRON-BASED ALLOYS
Barry Leslie Mordike, H. D. Burchards, and Karl Urlich Kainer *In* Kernforschungsanlage Juelich GmbH, The 8th German-Yugoslav Meeting on Materials Science and Development: Ceramics and Metals 1988 p 385-392 (For primary document see N89-23569 17-23)
Copyright Avail: NTIS HC A21/MF A01

N89-23612# Max-Planck-Inst. fuer Metallforschung, Stuttgart (Germany, F.R.). Inst. fuer Werkstoffwissenschaften.
INTERMETALLIC PHASES FOR HIGH TEMPERATURE APPLICATIONS
Rainhard Laag and Wolfgang A. Kaysser *In* Kernforschungsanlage

Juelich GmbH, The 8th German-Yugoslav Meeting on Materials Science and Development: Ceramics and Metals 1988 p 395-402 Sponsored by the Deutsche Forschungsgemeinschaft, Bonn, Fed. Republic of Germany (For primary document see N89-23569 17-23)
Avail: NTIS HC A21/MF A01

N89-23613# Technische Univ., Clausthal-Zellerfeld (Germany, F.R.).
BEHAVIOR OF METALS DURING HOT ROLLING PROCESSES. PART 1: MATHEMATICAL MODELS
Paul Funke *In* Kernforschungsanlage Juelich GmbH, The 8th German-Yugoslav Meeting on Materials Science and Development: Ceramics and Metals 1988 p 403-412 (For primary document see N89-23569 17-23)
Avail: NTIS HC A21/MF A01

N89-23614# Technische Univ., Clausthal-Zellerfeld (Germany, F.R.). Inst. fuer Werkstoffumformung.
BEHAVIOR OF METALS DURING HOT ROLLING PROCESSES. PART 2: EXPERIMENTAL METHODS FOR FLOW STRESS DETERMINATION AND CALCULATION OF THE TWO-DIMENSIONAL TEMPERATURE-FIELD IN THE ROLL GAP
Ronald Krengel *In* Kernforschungsanlage Juelich GmbH, The 8th German-Yugoslav Meeting on Materials Science and Development: Ceramics and Metals 1988 p 413-421 (For primary document see N89-23569 17-23)
Copyright Avail: NTIS HC A21/MF A01

N89-23615# Ljubljana Univ. (Yugoslavia).
INTERFACIAL REACTIONS DURING CLADDING OF STEEL BY HOT ROLLING
Tatjana Vecko, Radomir Turk, H.-R. Priebe, and Guenter Borchardt (Technische Univ., Clausthal-Zellerfeld, Germany, F.R.) *In* Kernforschungsanlage Juelich GmbH, The 8th German-Yugoslav Meeting on Materials Science and Development: Ceramics and Metals 1988 p 423-430 Sponsored by the Deutsche Akademische Austauschdienst (For primary document see N89-23569 17-23)
Copyright Avail: NTIS HC A21/MF A01

N89-23616# Ljubljana Univ. (Yugoslavia).
INFORMATION ABOUT HOT FLOW-STRESS CURVES AND THE RESULTING STRUCTURAL CHANGES
Ivan Bizjak, Radomir Turk (Technische Univ., Clausthal-Zellerfeld, Germany, F.R.), and Paul Funke *In* Kernforschungsanlage Juelich GmbH, The 8th German-Yugoslav Meeting on Materials Science and Development: Ceramics and Metals 1988 p 431-438 (For primary document see N89-23569 17-23)
Copyright Avail: NTIS HC A21/MF A01

N89-23617# Serbian Academy of Sciences and Arts, Belgrade (Yugoslavia). Dept. of Physical Chemistry.
PHYSICO-MATHEMATICAL INVESTIGATION OF THE CONSOLIDATION OF IRON POWDER
Ratomir Agatonovic, Rada Novakovic, D. Stefanovic (Nis Univ., Yugoslavia), and M. M. Ristic *In* Kernforschungsanlage Juelich GmbH, The 8th German-Yugoslav Meeting on Materials Science and Development: Ceramics and Metals 1988 p 441-447 (For primary document see N89-23569 17-23)
Copyright Avail: NTIS HC A21/MF A01

N89-23618# Serbian Academy of Sciences and Arts, Belgrade (Yugoslavia). Dept. of Physical Chemistry.
P-T DIAGRAMS OF TRANSITION ELEMENTS
Rada Novakovic and M. M. Ristic *In* Kernforschungsanlage Juelich GmbH, The 8th German-Yugoslav Meeting on Materials Science and Development: Ceramics and Metals 1988 p 449-458 (For primary document see N89-23569 17-23)
Copyright Avail: NTIS HC A21/MF A01

27 NONMETALLIC MATERIALS

Includes physical, chemical, and mechanical properties of plastics, elastomers, lubricants, polymers, textiles, adhesives, and ceramic materials.

For composite materials see *24 Composite Materials.*

N89-23677# National Aeronautical Lab., Bangalore (India). Materials Science Div.
HIGH PRESSURE STUDIES ON INFRARED DETECTOR MATERIALS
T. G. Ramesh and V. Shubha Apr. 1987 25 p
(NAL-TM-MT-8701) Avail: NTIS HC A03/MF A01

The mercury chalcogenides HgTe, Hg(1-x)Cd(x)Te and the lead chalcogenides Pb(1-x)Sn(x)Te have received considerable attention in recent years because of their use in infrared photon detectors. Pressure studies on symmetry induced zero gap semiconductors belonging to the zinc blend family viz., HgSe, HgTe and Hg(1-x)Cd(x)Te and the pressure induced semiconductor-semiconductor transition in Pb(1-x)Sn(x)Te were studied. Although the inverted band model proposed by Groves and Paul (1963) is valid for HgTe, the conclusions of the earlier workers on the pressure induced gamma 6 to gamma 8 crossover are shown to be erroneous. Experimental results show that it is difficult to observe band crossover due to an intervening structural phase transition from zinc blend to cinnabar structure. However, present pressure experiments on the semiconductor alloy system Hg(0.9)Cd(0.1)Te clearly indicate this crossover transition. Thermoelectric power and resistivity data on Pb(0.8)Sn(0.2)Te indicate that the principal energy gap E(g)=E(L6)(-)-E(L6)(+) decreases with pressure resulting in a zero gap state near 35 Kbar pressure. Thermoelectric power (TEP) studies on the alloy system Pb(0.6)Sn(0.4)Te provide direct evidence for a pressure induced L(6)- to L(6)+ crossover transition. Author

N89-23678*# Alfred Univ., NY.
PREPARATION AND EVALUATION OF SILICON NITRIDE MATRICES FOR SILICON NITRIDE-SiC FIBER COMPOSITES M.S. Thesis Final Technical Report
Scott R. Axelson Feb. 1988 63 p
(Contract NCC3-59)
(NASA-CR-184798; NAS 1.26:184798) Avail: NTIS HC A04/MF A01 CSCL 11C

Continuous silicon carbide (SiC) fiber was added to three types of silicon nitride (Si3N4) matrices. Efforts were aimed at producing a dense Si3N4 matrix from reaction-bonded silicon nitride (RBSN) by hot-isostatic-pressing (HIP) and pressureless sintering, and from Si3N4 powder by hot-pressing. The sintering additives utilized were chosen to allow for densification, while not causing severe degradation of the fiber. The ceramic microstructures were evaluated using scanning optical microscopy. Vickers indentation was used to determine the microhardness and fracture toughness values of the matrices. The RBSN matrices in this study did not reach more than 80 percent of theoretical density after sintering at various temperatures, pressures, and additive levels. Hot-pressing Si3N4 powder produced the highest density matrices; hardness and toughness values were within an order of magnitude of the best literature values. The best sintering aid composition chosen included Y2O3, SiO2, and Al2O3 or AlN. Photomicrographs demonstrate a significant reduction of fiber attack by this additive composition. Author

N89-23679# National Inst. of Standards and Technology, Gaithersburg, MD. Ceramics Div.
CERAMIC TRIBOLOGY: METHODOLOGY AND MECHANISMS OF ALUMINA WEAR Final Report
Richard S. Gates, Stephen M. Hsu, and E. Erwin Klaus (Pennsylvania State Univ., University Park.) Sep. 1988 231 p
(PB89-148357; NIST/SP-758; LC-88-600582) Avail: NTIS HC A11/MF A01; also available SOD HC $12.00 as 003-003-02914-9 CSCL 11B

A systematic study that was conducted to develop methods for measuring the tribological properties of ceramic materials under concentrated contacts is described. Step-loading four-ball and

ball-on-three-flat wear tests were developed to provide friction and wear characteristics of ceramic/lubricant combinations under various lubrication conditions. These measurement techniques now enable the studying of the effect of different materials processing parameters, material microstructures, and different lubricants on the friction and wear performance of ceramics. Water was found to react with alumina in a wearing contact to produce lubricous products. A combination of X-ray diffraction and thermogravimetric analysis techniques were used to investigate the kinetics of alumina-water reactions. Author

N89-23680# National Inst. of Standards and Technology, Gaithersburg, MD. Polymers Div.
IN SITU FLUORESCENCE MONITORING OF THE VISCOSITIES OF PARTICLE-FILLED POLYMERS IN FLOW Annual Report
A. J. Bur, F. W. Wang, A. Lee, R. E. Lowry, S. C. Roth, and T. K. Trout Nov. 1988 37 p
(Contract N00014-86-F-0115)
(PB89-146278; NISTIR-88/3892) Avail: NTIS HC A03/MF A01 CSCL 11C

Work during FY 88 focused on three areas: the chemical synthesis of a polymeric chromophore; the design of experiments to measure fluorescence anisotropy and non-Newtonian viscosity as a function of shear rate; and, measuring the equality-of-mix of a two component material using a fluorescence microscope. Significant results from these areas of work are presented. A polymeric chromophore, consisting of anthracene covalently bonded to polybutadiene, was synthesized and characterized by gel permeation chromatography and infrared observations. The number average molecular weight is 12,000 which is above the entanglement molecular weight for polybutadiene. Experiments using the polymeric chromophore as a dopant in a Newtonian fluid, very low molecular weight polybutadiene, show that fluorescence anisotropy correlates with the viscosity, i.e., it remains constant as a function of shear rate. Using a fluorescence microscope, optical transmittance and near neighbor distances between particles were measured in a matrix/particle mixing experiment and correlated these data correlated with fluorescence intensity fluctuations. Author

N89-23681# Clemson Univ., SC. Dept. of Industrial Engineering.
RESEARCH NEEDS IN CERAMIC MACHINING
Eric C. Skaar and W. J. Kennedy, Jr. 1988 26 p
(Grant NSF DMC-86-12943)
(PB89-148191; NSF/ENG-88015) Avail: NTIS HC A03/MF A01 CSCL 11C

A workshop was organized to address three main topics: conventional ceramic machining; nontraditional ceramic machining; and material effects of machining. Attendees recommended research topics ranging from modification of existing machinery to the development of several nontraditional machining methods. They observed that the entire manufacturing process must be examined, and not just the maching step. They placed emphasis on optimization and modeling. GRA

N89-23682# American Optical Co., Southbridge, MA.
FATIGUE-RESISTANT PHOTOCHROMIC PLASTICS
Nori Y. C. Chu 1988 11 p Presented at the International Congress on Optical Science and Engineering, Hamburg, Fed. Republic of Germany, 22 Sep. 1988
(Contract DE-AC03-87SF-17300)
(DE89-007336; CONF-8809123-2) Avail: NTIS HC A03/MF A01

The optical switching properties of a photochromic spirooxazine compound in retrofit polyester film and in poly(vinyl butyral) have been measured. The light fatigue resistance of these two optical switching elements were tested by an accelerated method. The length of photochromic activity of the optical switching elements can be improved by various organonickel and hindered amine light stabilizers. The effectiveness and optimal concentration for each light stabilizer in these host materials has been determined. These two types of light stabilizers act synergistically in improving the light fatigue resistance of the optical switching elements significantly. DOE

N89-23683*# Syracuse Univ., NY. Dept. of Chemical Engineering.
STRUCTURE/PERMEABILITY RELATIONSHIPS OF SILICON-CONTAINING POLYIMIDES
S. A. Stern, R. Vaidyanathan, and J. R. Pratt (PRC Systems Services Co., Hampton, VA.) Washington NASA Jun. 1989 29 p
(Contract NAS1-18000)
(NASA-CR-4237; NAS 1.26:4237) Avail: NTIS HC A03/MF A01 CSCL 11B

The permeability to H2, O2, N2, CO2 and CH4 of three silicone-polyimide random copolymers and two polyimides containing silicon atoms in their backbone chains, was determined at 35.0 C and at pressures up to about 120 psig (approximately 8.2 atm). The copolymers contained different amounts of BPADA-m-PDA and amine-terminated poly (dimethyl siloxane) and also had different numbers of siloxane linkages in their silicone component. The polyimides containing silicon atoms (silicon-modified polyimides) were SiDA-4,4'-ODA and SiDA-p-PDA. The gas permeability and selectivity of the copolymers are more similar to those of their silicone component than of the polyimide component. By contrast, the permeability and selectivity of the silicon-modified polyimides are more similar to those of their parent polyimides, PMDA-4,4'-ODA and SiDA-p-PDA. The substitution of SiDA for the PMDA moiety in a polyimide appears to result in a significant increase in gas permeability, without a correspondingly large decrease in selectivity. The potential usefulness of the above polymers and copolymers as gas separation membranes is discussed. Author

N89-23684# California Univ., Berkeley. Lawrence Berkeley Lab.
ATOMIC IMAGING AND MICROANALYSIS OF CERAMICS
G. Thomas and R. Ramesh Oct. 1988 35 p Presented at the 41st Pacific Coast Regional Meeting of American Ceramic Society, San Francisco, CA, 26-28 Oct. 1988
(Contract DE-AC03-76SF-00098)
(DE89-008172; LBL-26319; CONF-8810195-6) Avail: NTIS HC A03/MF A01

This paper is a short review of electron microscopy techniques, as applied to modern ceramics. Examples that are representative of the significance of modern electron microscopy, methods of atomic resolution imaging, diffraction and spectroscopy in the task of characterizing, and understanding typical ceramic materials are given. DOE

N89-23685# Oak Ridge National Lab., TN. Building Materials Group.
THE THERMAL RESISTANCE OF FLAT POWDER-FILLED EVACUATED PANELS
R. S. Graves, D. W. Yarbrough, and D. L. McElroy 1989 35 p Presented at the 5th International Conference on Thermal Insulation, San Francisco, CA, 27 Feb. - 1 Mar. 1989
(Contract DE-AC05-84OR-21400)
(DE89-008243; CONF-890273-1) Avail: NTIS HC A03

The need to develop high thermal resistance insulations that do not use chlorofluorocarbons has resulted in renewed interest in evacuated powder-filled panel insulations. Evacuated panels containing small diameter milled perlite or silica particles have been studied using a linear heat flow measurement technique. Thermal resistivities (R-value for one-inch of thickness) as high as 19.3 sq ft/h/F/Btu-in. have been observed for silica panels. Thermal measurements completed for a commercially produced evacuated panel containing perlite have shown thermal resistivities from 9.0 to 18.1 sq ft/h/F/Btu-in. Thermal resistance measurements have been repeated to determine changes in thermal performance with time (aging). DOE

N89-23686# Oak Ridge Gaseous Diffusion Plant, TN.
MOLDED BODIES HAVING A HIGH DEGREE OF HARDNESS AND A HIGH DEGREE OF TOUGHNESS FOR MACHINING METALS, CARBIDES, CERAMICS AND GLASSES Patent Application
Volker Heinzel, inventor, Hossein-Ali Keschtkar, inventor, and Ingeborg Schub, inventor 1989 11 p Transl. into ENGLISH of German Patent Application No. 86102025.3 (Pub. 10 Dec. 1986) Filed 18 Feb. 1986 Original document was prepared by Kernforshungzentrum GMbH, Karlsruhe Federal Rep. of Germany)
(Contract DE-AC05-84OT-21400)
(DE89-008820; K/TR-89/1; Int-Patent-Class-C22C2906; Int-Patent-Class-C22C3200) Avail: NTIS HC A03/MF A01

This paper is a European patent application for molded bodies having a degree of hardness and a high degree of toughness for machining metals, carbides, ceramics and glasses. The invention concerns molded bodies having a high degree of hardness and a high degree of toughness for machining metals, carbides, ceramics and glasses, made of sintered boron carbide and a binding metal phase. The goal of the invention is to introduce bodies of this type in which strength, especially toughness, is higher than in molded bodies of pure B4C and which are very well suited for cutting or grinding tools or for applications in which mechanical wear stresses or high surface pressures must be faced, such as in nozzles. DOE

N89-23687# EG and G Mound Applied Technologies, Miamisburg, OH.
EPOXYLITE 8822 HARDNESS STUDY
Mark E. Sterrett, Brian T. Leahy, and Daniel J. Ryan 31 Mar. 1989 16 p
(Contract DE-AC04-88DP-43495)
(DE89-008961; MLM-3581) Avail: NTIS HC A03/MF A01

A study of Epoxylite 8822 was conducted to investigate several properties of the epoxy curing process and their effects on hardness. The epoxy is used in numerous Mound timer programs, and the study was performed to determine the most effective and efficient curing process. The cure time, batch, and day and their interactions were examined to determine their contributions to hardness. Data from the investigation support the feasibility of verification trials using a 12-hr initial cure followed by additional cures to further determine the optimal cure time. DOE

N89-23688# Los Alamos National Lab., NM.
WATER-PROCESSABLE CONDUCTING POLYMERS
Steven P. Armes and Mahmoud Aldissi 1989 6 p Presented at the NATO Advanced Study Institute on Phase Transitions in Soft Condensed Matter, Geilo, Norway, 4-14 Apr. 1989
(Contract W-7405-eng-36)
(DE89-009251; LA-UR-89-1125; CONF-8904138-1) Avail: NTIS HC A02/MF A01

Until recently, most organic conducting polymers suffered from the lack of processability which is a prerequisite for their use in most technological applications. Furthermore, processability is of importance for the study of the polymers' intrinsic properties. Because of the rigid nature of their backbones, processing of most of the initial undoped systems was successful. For doped polymers, the difficulties were even greater because doping causes further aggregation due to increased interchain interaction and certain local geometry changes of the chains. Therefore, we have utilized various methods to achieve processability, directly or indirectly. The discussion is limited to the use of small or polymeric surfactant molecules grafted or physically absorbed onto the conducting polymer chain or particle. Both solutions and colloidal dispersions are the subject of this brief discussion. DOE

N89-23689# Michigan Univ., Ann Arbor. Dept. of Materials Science and Engineering.
THE STRUCTURAL BASIS FOR FATIGUE INITIATION IN GLASSY POLYMERS Progress Report, 1 Aug. 1988 - 28 Feb. 1989
Albert F. Yee and David W. Gidley 28 Feb. 1989 10 p
(Contract DE-FG02-88ER-45366)
(DE89-009292; DOE/ER-45366/1) Avail: NTIS HC A02/MF A01

Experiments have been conducted to quickly establish whether physical aging is indeed accelerated by fatigue loading. Differential Scanning Calorimetry (DSC) experiments were run on a polycarbonate specimen fatigued at 200 to 2000 psi (tension-tension) at 2 Hz for 150,000 cycles and compared with a specimen exposed to an identical thermal history but no mechanical loading. A larger peak is found in the DSC trace of the fatigued specimen. The existence of a peak is typical of glassy materials subjected to physical aging. The larger peak is equivalent to aging for longer periods of time. These results establish clearly the occurrence of fatigue accelerated physical aging. To assess the extent to which this aging retards the shear yielding tendency of the glass, stress relaxation experiments are planned. Preliminary experiments have been performed to establish correct testing procedures. DOE

N89-23690# Los Alamos National Lab., NM.
MICROWAVE PROCESSING OF CERAMICS
Joel D. Katz 1989 10 p Presented at the Industry-University Advanced Materials Conference, Denver, CO, 6-9 Mar. 1989
(Contract W-7405-eng-36)
(DE89-009350; LA-UR-89-995; CONF-890306-1) Avail: NTIS HC A02/MF A01

This paper discusses the following topics on microwave processing of ceramics: microwave-material interactions; anticipated advantage of microwave sintering; ceramic sintering; and ceramic joining. DOE

N89-23691*# National Aeronautics and Space Administration. Lewis Research Center, Cleveland, OH.
UNDERCUTTING OF DEFECTS IN THIN FILM PROTECTIVE COATINGS ON POLYMER SURFACES EXPOSED TO ATOMIC OXYGEN
Sharon K. Rutledge and Judith A. Mihelcic (Cleveland State Univ., OH.) 1989 10 p Presented at the 16th International Conference on Metallurgical Coatings, San Diego, CA, 17-21 Apr. 1989; sponsored by American VAcuum Society
(NASA-TM-101986; E-4686; NAS 1.15:101986) Avail: NTIS HC A02/MF A01 CSCL 11C

Protection for polymeric surfaces is needed to make them durable in the low Earth orbital environment, where oxidation by atomic oxygen is the predominant failure mechanism. Thin film coatings of oxides such as silicon dioxide are viable candidates to provide this protection, but concern has been voiced over the ability of these coatings to protect when defects are present in the coating due to surface anomalies occurring during the deposition process, handling, or micrometeoroid and debris bombardment in low Earth orbit. When a defected coating protecting a polymer substrate is exposed to atomic oxygen, the defect provides a pathway to the underlying polymer allowing oxidation and subsequent undercutting to occur. Defect undercutting was studied for sputter deposited coatings of silicon dioxide on polyimide Kapton. Preliminary results indicate that undercutting may be limited as long as the coating remains intact with the substrate. Therefore, coatings may not need to be defect free to give protection to the underlying surface. Author

N89-23692*# National Aeronautics and Space Administration. Langley Research Center, Hampton, VA.
PROCESSABLE POLYIMIDE ADHESIVE AND MATRIX COMPOSITE RESIN Patent Application
J. Richard Pratt, inventor (to NASA) (PRC Kentron, Inc., Hampton, VA.), Terry L. StClair, inventor (to NASA), and Donald J. Progar, inventor (to NASA) 2 Nov. 1988 15 p Sponsored by NASA. Langley Research Center
(NASA-Case-LAR-14101-1; NAS 1.71:LAR-14101-1; US-Patent-Appl-SN-266045) Avail: NTIS HC A03/MF A01 CSCL 11A

A high temperature polyimide composition prepared by reacting

4,4'-isophthaloyldiphthalic anhydride with metaphenylenediamine is employed to prepare matrix resins, adhesives, films, coatings, moldings, and laminates. NASA

N89-23693*# Salk Institute for Biological Studies, San Diego, CA.
MODEL OF EARLY SELF-REPLICATION BASED ON COVALENT COMPLEMENTARITY FOR A COPOLYMER OF GLYCERATE-3-PHOSPHATE AND GLYCEROL-3-PHOSPHATE
Arthur L. Weber 10 May 1989 11 p
(Grant NsG-7627)
(NASA-CR-182912; NAS 1.26:182912) Avail: NTIS HC A03/MF A01 CSCL 11B

Glyceraldehyde-3-phosphate acts as the substrate in a model of early self-replication of a phosphodiester copolymer of glycerate-3-phosphate and glycerol-3-phosphate. This model of self-replication is based on covalent complementarity in which information transfer is mediated by a single covalent bond, in contrast to multiple weak interactions that establish complementarity in nucleic acid replication. This replication model is connected to contemporary biochemistry through its use of glyceraldehyde-3-phosphate, a central metabolite of glycolysis and photosynthesis. Author

N89-23694# Aerospace Corp., El Segundo, CA. Materials Sciences Lab.
DYNAMIC FATIGUE OF ULTRALOW-EXPANSION GLASS FOR SPACE MIRRORS, REISSUE A
Dana J. Speece 30 Oct. 1988 31 p Supersedes report dated 8 Aug. 1986, AD-A172086 (N87-13551)
(Contract F04701-85-C-0086)
(AD-A205401; TR-0086(6409-11)-1; SD-TR-86-49) Avail: NTIS HC A03/MF A01 CSCL 11/2

Ultralow-expansion (ULE) glass is one of the primary materials used for space mirrors because its SiO2-TiO2 composition has a very low coefficient of thermal expansion. Several problems with cracking of this material in the Defense Satellite Program (DSP) led to the conclusion that insufficient design information was available to ensure reliability of the mirror structure. Accordingly, the Materials Sciences Laboratory of the Aerospace Corporation undertook an investigation into the fracture behavior of ULE glass for space mirrors. Dynamic fatigue experiments were performed on two sets of samples (optically polished and lightly ground) to characterize the fracture behavior of this material in a humid environment. As expected, the flaw size distribution affects the expected lifetime at a given stress and failure probability. In addition, it is shown that the polished material is apparently less sensitive to subcritical crack growth than the unpolished glass. GRA

N89-23695# Army Belvoir Research and Development Center, Fort Belvoir, VA.
CORROSION AND LUBRICITY TESTING OF NONFLAMMABLE USAF FORMULATED CTFE (CHLOROTRIFLUOROETHYLENE) BASE HYDRAULIC FLUID Final Report, May 1986 - Nov. 1987
Jane S. Smith Sep. 1988 21 p
(AD-A205467; BRDEC-2473) Avail: NTIS HC A03/MF A01 CSCL 11/8

The objective of this study was to evaluate the antiwear and anticorrosion properties of the U.S. Air Force's latest nonflammable hydraulic fluid formulation, a chlorotrifluroethylene oligimer containing an antiwear additive and an anticorrosion additive. This formulation, referred to as NFHF, is stable to 135 C. The NFHF was tested according to ASTMD1472 and D1748, the Federal Test Standard 791C Methods 5322.1 and 5308.6, and the corrosion rate evaluation procedure (CREP). The data contained in this report is compared with the chlorotrifluoroethylene with no additives and the present fire resistant hydraulic fluid military specification MIL-H-46170. The antiwear and anticorrosion properties of the formulated NFHF improved over the base fluid with no additives. GRA

N89-23696# Ultrasystems, Inc., Irvine, CA. Chemicals and Materials Research Dept.
HETEROCYCLES BASED ON GROUP 3, 4, AND 5 ELEMENTS PRECURSORS FOR NOVEL GLASSES AND CERAMICS Annual Progress Report, No. 3
K. L. Paciorek, J. H. Nakahara, and R. H. Kratzer 31 May 1988 40 p
(Contract F49620-85-C-0042)
(AD-A205586; AFOSR-89-0281TR) Avail: NTIS HC A03/MF A01 CSCL 11/2

The objective of this program is to explore the feasibility of synthesizing novel heterocyclics from the group of elements consisting of B, C, N, Al, Si, and P, the ultimate goal being the production of processible precursors leading to novel ceramics of unusual properties. The initial efforts under the program were devoted to development of processible preceramic systems leading to aluminum nitride ceramics. This involved the synthesis of novel trimethylsilylamino-substituted aluminum compounds and the study of their reactions. During the current reporting period the investigations of processible precursors of aluminum nitride were further pursued. Work was also directed at identification of processes leading to the formation of processible Al-N-B systems amenable to transformation into AlN.BN ceramics. GRA

N89-23697# Army Lab. Command, Watertown, MA. Material Technology Lab.
ENVIRONMENTAL STRESS CRAZING AND CRACKING OF TRANSPARENT POLYMERS Final Report
Alex J. Hsieh and Janice J. Vanselow Feb. 1989 15 p
(AD-A205624; MTL-TR-89-12) Avail: NTIS HC A03/MF A01 CSCL 11/9

The resistance to crack and growth in polycarbonate and poly(methyl methacrylate) is evaluated with several surface active solvents including a component of the universal chemical warfare decontaminant, DS2. A static dead weight loading apparatus is used for experimentation, and linear elastic fracture mechanics (LEFM) is used to interpret craze initiation and crack propagation via compact tension specimens. Results reflect relationships based on solubility parameters of the solvents and the polymers. Various structural effects due to environmentally induced degradation of these amorphous thermoplastics are illustrated. GRA

N89-23698# Arizona Univ., Tucson. Dept. of Chemistry.
FABRICABLE POLYMERS WITH EXCELLENT HEAT, OXIDATIVE AND HYDROLYTIC STABILITY Final Report, 1 May 1985 - 15 Oct. 1988
H. K. Hall, Jr. 31 Aug. 1988 4 p
(Contract DAAG29-85-K-0110)
(AD-A205627; ARO-22536.5-CH) Avail: NTIS HC A02/MF A01 CSCL 07/6

The study of extremely electrophilic imines was continued. Methyl dicyano-methanimine was synthesized and co-polymerized with p-methoxy styrene. The investigation of the polymerization of benzylidene cyanamide and piralidene cyanamide was continued. GRA

N89-23699# Connecticut Univ., Storrs.
THE MECHANISMS OF BIODEGRADATION OF SYNTHETIC POLYMERS Final Report, 15 Sep. 1985 - 31 Dec. 1988
J. A. Cameron and S. J. Huang 17 Feb. 1989 6 p
(Contract DAAG29-85-K-0222)
(AD-A205628; ARO-22677.11-LS) Avail: NTIS HC A02/MF A01 CSCL 07/6

This research was an attempt to gain a better understanding of the processes involved in the microbial degradation of synthetic polymers. It involved the examination of extracellular and cell associated enzymes capable of cleaving the model polyester, polycaprolactone. An effort was made to compare these enzymes to gain some understanding of their multiplicity and activity. As information was gained regarding the degradation process we attempted the modification of other polymers to render them degradable or more degradable. GRA

N89-23700# United Technologies Research Center, East Hartford, CT.

STUDY OF ADHERENT OXIDE SCALES Annual Report, 1 May 1987 - 31 Dec. 1988

John G. Smeggil 15 Feb. 1989 36 p

(Contract N00014-85-C-0421)

(AD-A205799; UTRC/R89-917259-1) Avail: NTIS HC A03/MF A01 CSCL 07/2

In agreement with previously reported studies involving alumina formers, the bond between a protective chromia scale and a Ni-40 wt. % Cr substrate is intrinsically strong. Segregation of sulfur to this interface weakens that bond. Segregated sulfur has been documented at the scale-metal interface. The sulfur content of the Ni-40 wt. % Cr is more important than yttrium additions regarding scale adherence during cyclic testing. Glow discharge mass spectrometry has been found to reliably and reproducibly differentiate sulfur contents in metal matrices in the low ppm range, i.e., approximately 1 to 50 ppm by weight. In the presence of ambient environments at elevated temperatures, all structural alloys are thermodynamically unstable reacting to form oxide scales. In order for such thermally grown oxide scales to be protective, they must limit the reaction rate between atmospheric oxygen and the substrate alloy. Oxidation rates are limited by scales which exhibit these properties: (1) Slow growth kinetics; (2) Minimal vaporization effects at temperatures of interest; (3) Minimal interaction with molten salts which might be present on hardware surfaces; and (4) Adherence under thermal cycling conditions. For most alloys which form either alumina or chromia scales, the latter most property (oxide scale adherence under thermal cycling conditions) controls service life. GRA

N89-23701# Gordon Research Conferences, Inc., Kingston, RI.

REPORT ON THE PARTIAL SUPPORT OF THE 1988 GORDON CONFERENCE ON POLYMERS (WEST) Final Report, Jan. - Jun. 1988

Alexander M. Cruickshank 25 Jan. 1989 4 p Conference held in Ventura, CA, 4-8 Jan. 1988

(Grant AF-AFOSR-0108-88; AF Proj. 2303)

(AD-A205834; AFOSR-89-0261TR) Avail: NTIS HC A02/MF A01 CSCL 07/6

The technical program of the 1988 Gordon Conference on Polymers (West) came together exactly as outlined in the proposal requesting support. The final program as it occurred is appended. There were sixteen speakers: Seven from the U.S., three from Israel, two from West Germany, and one each from Australia, Canada, Japan and the United Kingdom. While this Gordon Conference has a charter to cover the entire area of polymers, from chemical synthesis to solid-state properties, that is naturally a difficult goal to achieve. The guiding principal in the organization of this particular conference was that this broad coverage could be best achieved if there were a unifying sub-theme running through these different areas. The main sub-theme for this conference was surfaces, interfaces and microstructured polymers. GRA

N89-23702# Department of the Navy, Washington, DC.

AN ELASTOMERIC ELECTRICAL ISOLATION MEMBRANE Patent Application

Victor Marolda, inventor (to Navy) 20 Sep. 1988 14 p Filed 20 Sep. 1988

(AD-D013966; US-Patent-Appl-SN-246703) Avail: NTIS HC A03/MF A01 CSCL 09/1

The present invention relates to elastomeric means for providing electrical connector pin isolation and more particularly to a means for achieving full electrical connection between corresponding pins and sockets of an electrical connector as well as full pin-to-pin electrical isolation while the connector is immersed in a wet environment without requiring removal of the connector from such an environment. Accordingly, it is a general purpose and object of the present invention to provide a means for permitting electrical connectors to be mated underwater such that full electrical isolation is established. Still another object is that such, electrical isolation means exhibit dielectric properties while having a high degree of hydrolytic stability. GRA

N89-23703# Rutgers - The State Univ., New Brunswick, NJ. Dept. of Ceramics.

MECHANICAL BEHAVIOR OF PMMA-IMPREGNATED SILICA GELS

Bennet Abramoff and Lisa C. Klein 27 Feb. 1989 11 p Presented at the Fourth International Conference on Ultrastructure Processing of Ceramics, Glasses and Composites, Tucson, AZ, 19-24 Feb. 1989 Submitted for publication

(Contract N00014-87-K-0529)

(AD-A205975; TR-1) Avail: NTIS HC A03/MF A01 CSCL 07/2

Silica xerogels have been prepared from tetraethylorthosilicate with 50 volume percent open porosity. Methyl methacrylate monomer has been introduced into xerogel monoliths and polymerized with ultraviolet radiation. The fully infiltrated silica gel - PMMA composite has a bulk density of about 1.6 g/cm cubed. The resulting composite is light-weight and optically transparent. Elastic constants have been determined with ultrasonics. Flexure strengths have been measured in 4-point bending. The flexure strength of the composite is over 100 MPa in comparison to 20 MPa for the silica xerogel. The composite is designed for use at or below room temperature. GRA

N89-23704# Princeton Univ., NJ. Dept. of Chemical Engineering.

EFFECT OF PHYSICAL ANNEALING ON THE DYNAMIC MECHANICAL PROPERTIES OF A HIGH T(g) AMINE-CURED EPOXY SYSTEMS Technical Report, 7 Jan. 1988 - 15 Mar. 1989

Guy Wisanrakkit and John K. Gillham Mar. 1989 12 p

(Contract N00014-84-K-0021)

(AD-A205980; TR-19) Avail: NTIS HC A03/MF A01 CSCL 11/9

Physical annealing of a fully cured epoxy system has been investigated using the Torsional Braid Analysis (TBA) technique. The dynamic mechanical properties were monitored during isothermal annealing at sub-Tg temperatures (-30 to 150 C). The properties after annealing were measured vs. temperature and compared with those of the unannealed state. Isothermally, the relative rigidity increased linearly with log time, whereas the logarithmic decrement decreased with time. Temperature-scanning the isothermally annealed material showed a maximum deviation from the unannealed material in the vicinity of the annealing temperature. Effects of sequential annealing at different isothermal temperatures suggested that annealing at different temperatures involves different scales of chain segment relaxation. GRA

N89-23705# Princeton Univ., NJ. Dept. of Chemical Engineering.

THE GLASS TRANSITION TEMPERATURE (Tg) AS A PARAMETER FOR MONITORING THE CURE OF AN AMINE-CURED EPOXY SYSTEM AT CONSTANT HEATING RATES Technical Report No. 17, 7 Jan. 1988 - 15 Feb. 1989

John K. Gillham, Guy Wisanrakkit, and J. B. Enns Feb. 1989 27 p

(Contract N00014-84-K-0021)

(AD-A206098) Avail: NTIS HC A03/MF A01 CSCL 11/9

A continuous heating transformation (CHT) diagram displays the time and temperature of events that a material encounters during the course of continuous heating at different heating rates. For thermosetting systems, these events include gelation, vitrification and devitrification. Analysis of isothermal data for a diglycidyl-type epoxy/tetrafunctional aliphatic amine system, which is initially liquid at room temperature, indicated that kinetic control applied prior to vitrification. The parameters so obtained (i.e., order of reaction, Arrhenius pre-exponential term, and activation energy) together with a relationship between Tg and extent of reaction were used as a basis for modeling the onset of vitrification and devitrification in the CHT diagram. For heating scans from below Tgo (glass transition temperature of the reactants), the initially glassy material will devitrify when the temperature reaches Tgo, except for very low heating rates for which initial devitrification is not encountered. GRA

N89-23706# Florida Univ., Gainesville. Dept. of Chemistry.
DONOR ACCEPTOR POLYMERIZATION CHEMISTRY AS A VEHICLE TO LOW ENERGY CURE OF MATRIX RESINS: EVOLUTION OF THE 2-Tg CONCEPT TO PRODUCE Tg POLYMERS AT AMBIENT TEMPERATURES Final Report, Feb. 1986 - Jul. 1988
K. B. Wagener, G. B. Butler, Choon H. Do, Mike Johnson, and Mark A. Smith Mar. 1989 67 p
(Contract F33615-85-C-5093)
(AD-A206287; AFWAL-TR-88-4249) Avail: NTIS HC A04/MF A01 CSCL 07/6

A recent study conducted by the National Materials Advisory Board has identified a need for matrix resins that can be prepared at ambient or near ambient room temperatures for on site airfoil repair. The research described herein focuses on this problem through the synthesis of network polymers using donor/acceptor polymerization chemistry. The di and tetrafunctional donors used in this study are based on vinyl ether chemistry, and di and tetrafunctional maleimides are the acceptors. Meeting our first objective required the synthesis of the necessary donor and acceptor monomers, and consequently we examined a variety of synthetic approaches to create these compounds. In the case of donor monomers, we selected a palladium assisted vinyl exchange reaction as the best route. Using this chemistry we successfully prepared 15 monomers based on vinyl ether chemistry. GRA

N89-23707# Massachusetts Univ., Amherst. Dept. of Biochemistry.
CELLULAR AND MOLECULAR APPROACHES TO POLYMER SYNTHESIS BY BACTERIA Annual Report, 1 Mar. 1988 - 28 Feb. 1989
R. C. Fuller and Robert W. Lenz 1 Mar. 1989 7 p
(Contract N00014-86-K-0369)
(AD-A206395) Avail: NTIS HC A02/MF A01 CSCL 06/1

During the last year we have concentrated our research in in the following areas: (1) The regulation and optimization of the synthesis and production of poly-Beta-hydroxyalkanoates) (PHA) in Rhodospirillum rubrum and Pseudomonas oleovorans. Oxygen concentration affects cell growth, polymer content and cell yield. (2) The biosynthesis and analysis of functionalized PHA from R. rubrum, Alkaligenes eutrophus and Pseudomonas oleovorans. A remarkable functionalized biopolymer Beta-hyroxy-5-phenylvalerate was produced by Pseudomonas oleovorans. (3) A study was initiated on the production and characterization of biodegradable polymers from Pseudomonas oleovorans. GRA

N89-23708# Carnegie-Mellon Univ., Pittsburgh, PA. Dept. of Chemistry.
MECHANISM OF THE INITIATION OF THE CATIONIC POLYMERIZATION OF STYRENES BY SILANES AND ACTIVATED COVALENT ESTERS
K. Matyjaszewski 23 Mar. 1989 11 p
(Contract N00014-87-K-0116)
(AD-A206502; TR-9) Avail: NTIS HC A03/MF A01 CSCL 07/3

The mechanism of the initiation of the cationic polymerization of styrenes by silanes and activated covalent species has been studied by NMR and SEC. Trimethylsilyl trifluoromethanesulfonate has been used as initiator for the cationic polymerization of styrene. It has been found that silyl triflate does not react directly with styrene but polymerization is initiated by the trace amount of the triflic acid formed by the hydrolysis of trimethylsilyl triflate. Polymer end groups do not contain silyl groups, polymerization is strongly inhibited by hindered pyridine and starts only after pyridine is completely consumed. Hexamethyldisiloxane was found in the reaction products. GRA

N89-23709# Texas Univ., Arlington. Dept. of Chemistry.
ELECTRONIC AND IONIC TRANSPORT IN POLYMERS Quarterly Technical Report No. 14, 1 Jan. - 31 Mar. 1989
Martin Pomerantz, John R. Reynolds, Krishnan Rajeshwar, Dennis S. Marynick, and Timothy D. Shaffer 3 Apr. 1989 6 p
(Contract N00014-86-K-0769)
(AD-A206530) Avail: NTIS HC A02/MF A01 CSCL 07/6

Melt spun fibers of poly(3-decylthiophene) show conductivities of 5 S/cm when doped with FeCl3 and doping has been shown to be uniform across the cross section by EDAX studies. Large polypyrrole/poly(styrene sulfonate) films have been prepared with conductivities of 40 S/cm. The polyelectrolyte increases mechanical integrity and smoothes the morphology compared to poly(pyrrole tosylate). Cyclic voltammetry and scanning electron microscopy has been shown to be useful as a fingerprint tool for the ion composition of polypyrrole membranes. Anion exchange to polypyrrole membranes has been found to be sensitive to the nature of the cation when electrochemically switched. A recently discovered bimechanistic phase transfer catalyzed polythioetherification is being studied. New salen monomers containing terminal alkyl units and unsaturation have been prepared and their polymerization is being studied. GRA

N89-23710# Karlsruhe Univ. (Germany, F.R.). Fakultaet fuer Physik.
METALLICALLY CONDUCTING POLYMERS: THE LIMITING EFFECT OF CONJUGATION DEFECTS ON THE ELECTRICAL CONDUCTIVITY, A POLYACETYLENE EXAMPLE Ph.D. Thesis [METALLISCH LEITENDE POLYMERE: DER BEGRENZENDE EINFLUSS VON KOKONJUGATIONSDEFEKTEN AUF DIE ELEKTRISCHE LEITFAEHIGKEIT, DARGESTELLT AM POLYAZETYLEN]
Dietrich Schaefer-Siebert 1988 120 p In GERMAN
(ETN-89-93950) Avail: NTIS HC A06/MF A01

Properties of the electronic transport processes were investigated in polyacetylene, a representative of electrically conducting polymers. The conductivity of polyacetylene can be understood by a superposition of charge transport along the carbon chains and steps between chains, since, the transport along the chains is limited by the conjugation length. Information about the dependence of the conductivity on the conjugation length was obtained by building defects into the chains. The distributions of the conjugation lengths were determined. A ten times shorter average conjugation length reduces the conductivity by ten orders of magnitude. This effect can be quantitatively explained by a Hopping model. A universal correlation between conductivity at room temperature and temperature dependence of the conductivity was obtained. All the experimental results can be satisfactorily described by the modified Hopping model. ESA

N89-23571# Max-Planck-Inst. fuer Metallforschung, Stuttgart (Germany, F.R.). Pulvermetallurgisches Lab.
CERAMIC PROJECT OF THE MAX-PLANCK SOCIETY
Guenter Petzow *In* Kernforschungsanlage Juelich GmbH, The 8th German-Yugoslav Meeting on Materials Science and Development: Ceramics and Metals 1988 p 9-15 (For primary document see N89-23569 17-23)
Copyright Avail: NTIS HC A21/MF A01

N89-23572# Karlsruhe Univ. (Germany, F.R.). Inst. fuer Chemische Technik.
SILICON-CARBIDE MADE OF SILICON-ORGANIC COMPOUNDS
E. Fitzer and Mathias Keuthen *In* Kernforschungsanlage Juelich GmbH, The 8th German-Yugoslav Meeting on Materials Science and Development: Ceramics and Metals 1988 p 19-26 (For primary document see N89-23569 17-23)
Copyright Avail: NTIS HC A21/MF A01

N89-23573# Institut za Nuklearne Nauke Boris Kidric, Belgrade (Yugoslavia). Inst. for Materials.
SLIP CASTING OF FUSED SILICA
Dusan Kicevic, B. Kostic, and M. Gasic *In* Kernforschungsanlage Juelich GmbH, The 8th German-Yugoslav Meeting on Materials Science and Developement: Ceramics and Metals 1988 p 27-36 (For primary document see N89-23569 17-23)
Copyright Avail: NTIS HC A21/MF A01

N89-23574# Ljubljana Univ. (Yugoslavia).
INJECTION MOLDING OF WHISKER-REINFORCED Al2O3-ZrO2 CERAMICS
Tomaz Kosmac, D. Gorjan, E. Lutz, and N. Claussen (Technische Univ., Hamburg, Germany, F.R.) *In* Kernforschungsanlage Juelich GmbH, The 8th German-Yugoslav Meeting on Materials Science and Development: Ceramics and Metals 1988 p 37-44 Sponsored by the Research Council of Slovenia, Yugoslavia (For primary document see N89-23569 17-23)
Copyright Avail: NTIS HC A21/MF A01

N89-23576# Skopje Univ. (Yugoslavia). Faculty of Technology and Metallurgy.
PREPARING AND SINTERING OF YTTRIA-STABILIZED ZIRCONIA
Blagoj Pavlovski, L. Stojanovska, and B. Jasmakovski *In* Kernforschungsanlage Juelich GmbH, The 8th German-Yugoslav Meeting on Materials Science and Development: Ceramics and Metals 1988 p 63-72 (For primary document see N89-23569 17-23)
Copyright Avail: NTIS HC A21/MF A01

N89-23577# Technische Hochschule, Aachen (Germany, F.R.). Inst. fuer Gesteinshuettenkunde.
INVESTIGATIONS OF MULLITE-ZIRCONIA COMPOSITES
Thomas Fandel and W. Kroenert *In* Kernforschungsanlage Juelich GmbH, The 8th German-Yugoslav Meeting on Materials Science and Development: Ceramics and Metals 1988 p 73-80 (For primary document see N89-23569 17-23)
Copyright Avail: NTIS HC A21/MF A01

N89-23578# Kernforschungsanlage, Juelich (Germany, F.R.).
PREPARATION AND THERMAL EXPANSION OF Al2TiO5-TiO5-TiO2 SINTERED BODIES
Ivan Stamenkovic (Institut za Nuklearne Nauke Boris Kidric, Belgrade, Yugoslavia) and Gerhard Ondracek *In its* The 8th German-Yugoslav Meeting on Materials Science and Development: Ceramics and Metals 1988 p 81-88 (For primary document see N89-23569 17-23)
Copyright Avail: NTIS HC A21/MF A01

N89-23579# Technische Hochschule, Aachen (Germany, F.R.).
MICROSTRUCTURE DEVELOPMENT IN ALUMINA
Piet Reijnen and H. D. Kim *In* Kernforschungsanlage Juelich GmbH, The 8th German-Yugoslav Meeting on Materials Science and Development: Ceramics and Metals 1988 p 91-97 (For primary document see N89-23569 17-23)
Copyright Avail: NTIS HC A21/MF A01

N89-23580# Institut za Nuklearne Nauke Boris Kidric, Belgrade (Yugoslavia).
SINTERING OF CaO AND MgO IN THE PRESENCE OF NONEQUILIBRIUM LIQUID PHASE
Emilija Kostic, Sandor J. Kiss, and D. Cerovic *In* Kernforschungsanlage Juelich GmbH, The 8th German-Yugoslav Meeting on Materials Science and Development: Ceramics and Metals 1988 p 99-107 (For primary document see N89-23569 17-23)
Copyright Avail: NTIS HC A21/MF A01

N89-23581# Institut za Nuklearne Nauke Boris Kidric, Belgrade (Yugoslavia).
SINTERING OF Si3N4 IN THE PRESENCE OF ADDITIVES FROM Y2O3-SiO2-Al2O3 SYSTEM
Snezana Boskovic *In* Kernforschungsanlage Juelich GmbH, The 8th German-Yugoslav Meeting on Materials Science and Development: Ceramics and Metals 1988 p 109-117 (For primary document see N89-23569 17-23)
Copyright Avail: NTIS HC A21/MF A01

N89-23582# Center for Research and Development of Materials, Sarajevo (Yugoslavia).
MICROSTRUCTURE DEVELOPMENT IN SiC
Taric Fetahagic and Drago Kolar (Ljubljana Univ., Yugoslavia) *In* Kernforschungsanlage Juelich GmbH, The 8th German-Yugoslav Meeting on Materials Science and Development: Ceramics and Metals 1988 p 119-128 (For primary document see N89-23569 17-23)
Copyright Avail: NTIS HC A21/MF A01

N89-23583# Karlsruhe Univ. (Germany, F.R.). Inst. fuer Keramik im Maschinenbau.
FATIGUE IN CERAMICS
Georg Grathwohl *In* Kernforschungsanlage Juelich GmbH, The 8th German-Yugoslav Meeting on Materials Science and Development: Ceramics and Metals 1988 p 131-139 (For primary document see N89-23569 17-23)
Copyright Avail: NTIS HC A21/MF A01

N89-23585# Max-Planck-Inst. fuer Metallforschung, Stuttgart (Germany, F.R.). Pulvermetallurgisches Lab.
STRENGTHENING OF SILICON NITRIDE CERAMICS
Peter Greil *In* Kernforschungsanlage Juelich GmbH, The 8th German-Yugoslav Meeting on Materials Science and Development: Ceramics and Metals 1988 p 147-156 (For primary document see N89-23569 17-23)
Copyright Avail: NTIS HC A21/MF A01

N89-23587# Kernforschungszentrum G.m.b.H., Karlsruhe (Germany, F.R.). Inst. fuer Material- und Festkoerperforschung.
ADVANCED LAYER MATERIALS
H. Holleck and Hans Schulz *In* Kernforschungsanlage Juelich GmbH, The 8th German-Yugoslav Meeting on Materials Science and Development: Ceramics and Metals 1988 p 165-172 (For primary document see N89-23569 17-23)
Copyright Avail: NTIS HC A21/MF A01

N89-23588# Institut za Nuklearne Nauke Boris Kidric, Belgrade (Yugoslavia).
PHASE TRANSFORMATION OF Zr(x)Hf(1-x)O2 IN ALUMINA MATRIX
Feodor Sigulinski *In* Kernforschungsanlage Juelich GmbH, the 8th German-Yugoslav Meeting on Materials Science and Development: Ceramics and Metals 1988 p 173-177 (For primary document see N89-23569 17-23)
Copyright Avail: NTIS HC A21/MF A01

N89-23589# Institut za Nuklearne Nauke Boris Kidric, Belgrade (Yugoslavia).
PREPARATION AND PROPERTIES OF HIGH STRENGTH CARBON FIBERS
Slobadan Marinkovic, V. Raskovic, Stanko Pejanovic (Belgrade Univ., Yugoslavia), and V. Pavlovic *In* Kernforschungsanlage Juelich GmbH, The 8th German-Yugoslav Meeting on Materials Science and Development: Ceramics and Metals 1988 p 179-184 (For primary document see N89-23569 17-23)
Copyright Avail: NTIS HC A21/MF A01

N89-23590# Max-Planck-Inst. fuer Metallforschung, Stuttgart (Germany, F.R.). Pulvermetallurgisches Lab.
THERMAL TRANSPORT IN PRESSURELESS SINTERED ALUMINUM NITRIDE
Axel Kranzmann, Peter Greil, and Guenter Petzow *In* Kernforschungsanlage Juelich GmbH, The 8th German-Yugoslav Meeting on Materials Science and Development: Ceramics and Metals 1988 p 187-194 (For primary document see N89-23569 17-23)
Copyright Avail: NTIS HC A21/MF A01

N89-23591# Kernforschungszentrum G.m.b.H., Karlsruhe (Germany, F.R.). Inst. fuer Material- und Festkoerperforschung.
PREPARATION, CHARACTERIZATION AND THERMAL DIFFUSIVITY OF Al2TiO5
Milosav Milosevski and Brigitte Schulz *In* Kernforschungsanlage Juelich GmbH, The 8th German-Yugoslav Meeting on Materials Science and Development: Ceramics and Metals 1988 p 195-208 (For primary document see N89-23569 17-23)
Copyright Avail: NTIS HC A21/MF A01

N89-23592# Kernforschungszentrum G.m.b.H., Karlsruhe (Germany, F.R.). Inst. fuer Material- und Festkoerperforschung.
DILATOMETRIC ANALYSIS OF Al-, Ba-, Ca-TITANATE
Milosav Milosevski and Brigitte Schulz *In* Kernforschungsanlage Juelich GmbH, The 8th German-Yugoslav Meeting on Materials Science and Development: Ceramics and Metals 1988 p 209-219 (For primary document see N89-23569 17-23)
Copyright Avail: NTIS HC A21/MF A01

N89-23593# Technische Hochschule, Aachen (Germany, F.R.). Inst. fuer Gesteinshuettenkunde.
INVESTIGATIONS ON LOW CEMENT AND ULTRA LOW CEMENT REFRACTORY CASTABLES
Uwe Schuhmacher, W. Kroenert, and A. Seltveit (Norges Tekniske Hoegskole, Trondheim.) *In* Kernforschungsanlage Juelich GmbH, The 8th German-Yugoslav Meeting on Materials Science and Development: Ceramics and Metals 1988 p 221-228 (For primary document see N89-23569 17-23)
Copyright Avail: NTIS HC A21/MF A01

N89-23594# Kernforschungsanlage, Juelich (Germany, F.R.).
CORROSION OF SILICON CARBIDE CERAMICS AT HIGH TEMPERATURES IN WATER VAPOR-CONTAINING ATMOSPHERES
Rudiger Foerthmann, E. Gyarmati, and Aristides Naoumidis *In its* The 8th German-Yugoslav Meeting on Materials Science and Development: Ceramics and Metals 1988 p 231-240 (For primary document see N89-23569 17-23)
Copyright Avail: NTIS HC A21/MF A01

N89-23595# Ljubljana Univ. (Yugoslavia). Jozef Stefan Inst.
INVESTIGATION OF ALPHA-SiC HOT CORROSION IN THE PRESENCE OF BASIC SLAG
Varuzan Kevorkijan, Milos Komac, Taric Fetahagic, and V. Strumberger *In* Kernforschungsanlage Juelich GmbH, The 8th German-Yugoslav Meeting on Materials Science and Development: Ceramics and Metals 1988 p 241-248 (For primary document see N89-23569 17-23)
Copyright Avail: NTIS HC A21/MF A01

N89-23598# Technische Hochschule, Aachen (Germany, F.R.). Inst. fuer Gesteinshuettenkunde.
THE ADHESION BETWEEN GLASS AND ENAMEL
Otmar Seide and H. Roecker *In* Kernforschungsanlage Juelich GmbH, The 8th German-Yugoslav Meeting on Materials Science and Development: Ceramics and Metals 1988 p 273-280 (For primary document see N89-23569 17-23)
Copyright Avail: NTIS HC A21/MF A01

N89-23600# Belgrade Univ. (Yugoslavia). Lab. for Electron Microanalysis.
CHARACTERIZATION OF A PHASE BOUNDARY IN Ni-Al2O3 SINTERED UNDER PRESSURE
Miodrag K. Pavicevic, G. Burri, H. Schmid, and R. Gotthard (Ecole Polytechnique Federale de Lausanne, Switzerland) *In* Kernforschungsanlage Juelich GmbH, The 8th German-Yugoslav Meeting on Materials Science and Development: Ceramics and Metals 1988 p 291-298 (For primary document see N89-23569 17-23)
Copyright Avail: NTIS HC A21/MF A01

N89-23601# Technische Univ., Clausthal-Zellerfeld (Germany, F.R.). Fachbereich Metallurgie und Werkstoffwissenschaften.
NEUTRAL PRIMARY BEAM SIMS ANALYSIS OF CERAMIC MATERIALS
Guenter Borchardt, S. Scherrer, and S. Weber (Ecole des Mines, Nancy, France) *In* Kernforschungsanlage Juelich GmbH, The 8th German-Yugoslav Meeting on Materials Science and Development: Ceramics and Metals 1988 p 299-306 Sponsored in part by the Deutsche Forschungsgemeinschaft, Bonn, Fed. Republic of Germany (For primary document see N89-23569 17-23)
Copyright Avail: NTIS HC A21/MF A01

N89-23602# Ljubljana Univ. (Yugoslavia).
MICROSTRUCTURE-PERMEABILITY RELATION IN MnZn FERRITES PREPARED OF IRON OXIDE WITH CHLORINE IMPURITIES
Heda Hitihar, Miha Drofenik, Drago Kolar, and M. Limpel *In* Kernforschungsanlage Juelich GmbH, The 8th German-Yugoslav Meeting on Materials Science and Development: Ceramics and Metals 1988 p 309-316 (For primary document see N89-23569 17-23)
Copyright Avail: NTIS HC A21/MF A01

N89-23603# Technische Hochschule, Aachen (Germany, F.R.). Inst. fuer Gesteinshuettenkunde.
ELECTRON CONDUCTING CERAMICS AS SENSOR MATERIAL FOR NOISE THERMOMETRY
Helmut Heinz Haeusser, D. vonMallinckrodt, and H. Brixy (Kernforschungsanlage, Juelich, Germany, F.R.) *In* Kernforschungsanlage Juelich GmbH, The 8th German-Yugoslav Meeting on Materials Science and Development: Ceramics and Metals 1988 p 317-322 (For primary document see N89-23569 17-23)
Copyright Avail: NTIS HC A21/MF A01

N89-23604# Serbian Academy of Sciences and Arts, Belgrade (Yugoslavia). Inst. of Technical Sciences.
MICROSTRUCTURE AND PHASE DEVELOPMENT IN MULTICOMPONENT ZnO BASED VARISTOR CERAMICS
Olivera Milosevic, Petar Kostic, Lj. Karanovic, V. Petrovic, and Dragoljub Uskokovic *In* Kernforschungsanlage Juelich GmbH, The 8th German-Yugoslav Meeting on Materials Science and Development: Ceramics and Metals 1988 p 323-330 Sponsored by the Republic Committee for the Science of Serbia; the Committee for the Science, Belgrade, Yugoslavia and MINEL (For primary document see N89-23569 17-23)
Copyright Avail: NTIS HC A21/MF A01

28 PROPELLANTS AND FUELS

Includes rocket propellants, igniters, and oxidizers; their storage and handling procedures; and aircraft fuels.

For related information see also *07 Aircraft Propulsion and Power, 20 Spacecraft Propulsion and Power,* and *44 Energy Production and Conversion.*

N89-23711# Florida State Univ., Gainesville. Inst. of Food and Agricultural Sciences.
SORPTION OF SELECTED VOLATILE ORGANIC CONSTITUENTS OF JET FUELS AND SOLVENTS ON NATURAL SORBENTS FROM GAS AND SOLUTIONS PHASES
Final Report, Apr. 1985 - Sep. 1987
P. S. Rao, R. D. Rhue, Clifford T. Johnson, and Richard A. Oguada Aug. 1988 212 p
(Contract F08635-83-C-0136)
(AD-A204073; AFESC/ESL-TR-88-02) Avail: NTIS HC A10/MF A01 CSCL 21/9

Sorption of selected volatile organic constituents (VOC) of jet fuels and solvents on several natural sorbents from the gas and aqueous phases was investigated. The sorbates studied were: trans-1,2-dichloroethylene; 1,2-dichloroethane; trichloroethylene; 1,1,2,2-tetrachloroethane; toluene; ethylbenzene; p-xylene; o-xylene; and cyclohexane. The sorbents used included clays (kaolin, montmorillonite, SAz-1), soils (Webster and Oldsmar), and aquifer materials (Borden and Lula). Sorption from the vapor phase was studied using three techniques; the headspace analysis method, dynamic flow method, and a gas chromatographic method. Sorption of VOC on anhydrous sorbents and sorbents in equilibrium with water at different relative humidities was examined. The energetics of sorption were characterized by measuring VOC sorption at several temperatures. GRA

N89-23712# North Dakota Univ., Grand Forks. Energy and Minerals Research Center.
PRODUCTION OF JET FUELS FROM COAL-DERIVED LIQUIDS. VOLUME 8: HETEROATOM REMOVAL BY CATALYTIC PROCESSING Interim Report, 1 Jan. - 30 Aug. 1988
J. R. Rindt, M. D. Hetland, C. L. Knudson, and W. G. Willson Jan. 1989 99 p
(Contract MIPR-FY1455-86-N-0657; AF Proj. 2480)
(AD-A205470; AFWAL-TR-87-2042-Vol-8) Avail: NTIS HC A05/MF A01 CSCL 21/4

In September 1986, the Fuels Branch of the Aero Propulsion Laboratory at Wright-Patterson Air Force Base, Ohio, commenced an investigation of the potential of the production of jet fuel from the liquid by-products streams produced by the gasification of lignite at the Great Plains Gasification Plant in Beulah, North Dakota. Funding was provided to the Department of Energy (DOE), Pittsburgh Energy Technology Center (PETC), to administer the experimental portion of this effort. This report details the program with the University of North Dakota Energy and Mineral Research Center (UNDEMRC) to study the removal of heteroatoms and the saturation of aromatics found in the Great Plains tar oil stream. UNDEMRC tested a processing approach consisting of multiple-stage hydrogenations. GRA

N89-23713# State Univ. of New York, Binghamton. Dept. of Chemistry.
NOVEL ORGANOBORANES AS INTERMEDIATES FOR CERAMIC PRECURSORS AND HIGH-ENERGY FUELS Final Technical Report, 1 Feb. 1985 - 31 Aug. 1988
John J. Eisch 1 Jan. 1989 27 p
(Grant AF-AFOSR-0108-85; AF Proj. 2303)
(AD-A206101; AFOSR-89-0234TR) Avail: NTIS HC A03/MF A01 CSCL 07/3

This project investigated, as its primary objective, the influence of carbon-boron bonding in unsaturated, cyclic boranes on the energy content of this system. Such insights should aid the choice of the best carbon-boron clusters to be incorporated into high-energy fuels. The synthesis and structural characterization of the following boron-containing carbocycles were undertaken: the borirene or boracyclopropene system, as exemplified by trimesitylborirene; the borole or boracyclopentadiene ring, as represented by pentaarylboroles; the borepin or boracyclo-heptatriene nucleus, as seen in heptaphenylborepin; the 7-borabicyclo 2.2.1 heptadiene system, again typified by its heptararyl derivative; and the 1-boratetrahydronaphthalene derivative, which was the thermal rearrangement product of the borepin. As estimated by chemical reactivity towards heat, oxidants and protolyzing agents, the borirene and borole nuclei display unusual stability and thus can be termed aromatic. The boroles are very reactive and therefore can be said to possess destabilization or be antiaromatic. A rich variety of both thermal and photochemical skeletal rearrangements was uncovered with these boracyclopolyenes, indicating that tricoordinate boron has a pronounced tendency to interact either intermolecularily or intramolecularily, with pi-electrons. GRA

N89-23714# Little (Arthur D.), Inc., Cambridge, MA.
PROPELLANT REUSE/RECOVERY TECHNOLOGY Final Report, Apr. 1986 - Aug. 1988
A. A. Balasco, R. C. Bowen, C. A. Jake, L. H. McDaniel, and M. L. Hundley 31 Aug. 1988 236 p
(Contract DAAK11-85-D-0008)
(AD-A206306; AMXTH-TE-CR-88026) Avail: NTIS HC A11/MF A01 CSCL 19/1

Due primarily to changes in weapon systems, the military has stocks of chemically acceptable propellants which are obsolete. Past disposal practices have been to incinerate or open-burn these stocks; however, extensive research has been conducted in the past at the Radford Army Ammunition plant (RAAP) for the reclamation/reuse of solvent-based obsolete propellants. A literature review indicated that resolvation of propellant and recovery of selected ingredients from propellant via solvent extraction were the optimal reclamation technologies. This study was conducted in order to demonstrate the feasibility of these technologies. The propellant resolvation studies consisted of both laboratory and bench-scale evaluations; furthermore, appropriate hazards analyses of the procedures and equipment used in the evaluations were performed by the RAAP Hazards Analysis Department. Several operating parameters were assessed including resolvation time, propellant/solvent ratio, solvent/solvent ratio, and propellant particle size. GRA

N89-23715# Naval Postgraduate School, Monterey, CA.
AN EXPERIMENTAL INVESTIGATION IN THE BEHAVIOR OF METALLIZED SOLID PROPELLANTS M.S. Thesis
Michael J. Smith Dec. 1988 76 p
(AD-A206510) Avail: NTIS HC A05/MF A01 CSCL 21/9

The combustion behavior of metallized solid propellants at pressures between 100 and 750 psi was investigated using high speed motion pictures together with scanning electron microscope and light diffraction examinations of collected residue. A reduced smoke ZrC propellant and two propellants with low aluminum loadings were utilized. ZrC was observed to agglomerate and ignite on the propellant surface before being ejected. The aluminum did not agglomerate but did ignite on the propellant surface. ZrC was found to burn in part with a detached flame and the flame moved closer to the particle surface as pressure increased. Aluminum particles were observed to burn with similar behavior, but with flames more detached from the particle surface. Increased aluminum loading resulted in smaller particles above the propellant surface, but the flames were further from particle surfaces. GRA

N89-23716# Ballistic Research Labs., Aberdeen Proving Ground, MD.
POLYETHYLENE GLYCOL-POLY(2-METHYL-5-VINYL TETRAZOLE) POLYMER BLEND: A DESENSITIZING BINDER FOR PROPELLANTS AND EXPLOSIVES Final Report, Dec. 1985 - Aug. 1986
Indu B. Mishra and Lawrence Vande Kieft Mar. 1989 39 p
(AD-A206563; BRL-TR-2985) Avail: NTIS HC A03/MF A01 CSCL 19/1

Miscible polymer pairs are formed with an energetic polymer, (Poly(2-Methyl-5-Vinyl Tetrazole), PMVT, and a nonenergetic polymer, polyethylene glycol, PEG, of molecular weight 1000 to 4000. This polymer blend PEG-PMVT is formed from acetonitrile solution upon removal of the solvent. The blend also precipitates when a nonsolvent, hexane, is added to a solution of PEG-PMVT in acetronitrile at or below 0 C. With PEG E1000, blends have been formed with PEG:PMVT of 1:1 to 1:1.8 by weight. This blend has been characterized from its unique glass transition temperature, Tg, as well as formation of transparent films. Interaction between chains in the form of weak C-H. O hydrogen bonding has been identified from infrared spectroscopy. Polymer blends are not formed with PMVT and polypropylene glycol, PPG, with methyl side chains as well as polyols with hydroxy number 3 or more. A blend is formed, however in a narrow regime of temperature with PMVT and glycidylazide polymer, GAP. This polymer blend is found to be a desensitizing energetic binder for propellants and for plastic-bonded explosives in particular. A PBX composition containing 91 percent RDX by weight and 9 percent PEG-PMVT polymer blend has a drop-weight-impact sensitivity better than Comp B. GRA

N89-23717# Ballistic Research Labs., Aberdeen Proving Ground, MD.
CHLORIDE ANALYSIS IN HAN-BASED LIQUID PROPELLANTS BY INDUCTIVELY COUPLED PLASMA SPECTROSCOPY
Madelyn M. Decker Jan. 1989 22 p
(AD-A206564; BRL-TR-2978) Avail: NTIS HC A03/MF A01 CSCL 19/1

Inductively coupled plasma (ICP) spectroscopy was used to determine the chloride content of HAN-based liquid propellants in the parts per million (ppm) range with a detection limit of 1.5 ppm. Chloride is traditionally determined titrimetrically or gravimetrically with a typical precision of 0.01 weight percent (100

ppm). Samples of propellant as formulated and spiked with chloride ions were reacted with a known excess of silver. After the silver chloride precipitate was removed, the remaining silver in solution was analyzed by ICP. This excess metal reaction is necessary in ICP analysis because the instrument is not capable of monitoring emissions from chloride ions. GRA

29 MATERIALS PROCESSING

Includes space-based development of products and processes for commercial applications.

For biological materials see *55 Space Biology.*

N89-23718# Aachener Centrum fuer Erstarrung unter Schwerelosigkeit e.V. (Germany, F.R.).
RESEARCH ACTIVITY REPORT CONCERNING SOLIDIFICATION TECHNOLOGY UNDER MICROGRAVITY [BEWERTUNG DURCHGEFUEHRTER FORSCHUNGSARBEITEN AUF DEM GEBIET DER ERSTARRUNGSTECHNOLOGIEN UNTER SCHWERELOSIGKEIT]
M. Host, T. Kaup, M. Mathes, S. Rex, and G. J. Schmitz Jul. 1987 103 p In GERMAN
(Contract BMFT-FKZ-SLN87-01)
(ETN-89-93988) Avail: NTIS HC A06/MF A01

Materials science research under microgravity and solidification technology results obtained are reported. Solidification phenomena; diffusion; undercooling and nucleation; solidification front dynamics; single crystals; and eutectical solidification; monotectic alloys preparation; and composite materials processing with emphasis on grain formation in liquid phases matrix are discussed. ESA

N89-23719# Deutsche Forschungs- und Versuchsanstalt fuer Luft- und Raumfahrt, Cologne (Germany, F.R.). Inst. fuer Raumsimulation.
SUMMARY OF 1ST SUMMER SCHOOL ON MICROGRAVITY [VORTRAGSKURZFASSUNGEN DER 1. SOMMERSCHULE MIKROGRAVITATION]
G. Otto, ed. Jul. 1987 176 p In ENGLISH and GERMAN Summer school held in Cologne, Fed. Republic of Germany, 13-16 Jul. 1987
(DFVLR-IB-333-87/2; ETN-89-93758) Avail: NTIS HC A09/MF A01

The activities of the Microgravity User Support Center of DFVLR were discussed. The center is involved in space conditions experimentation and in the study of reduced gravity effects on biology, material science, and material processing crystallography, plant growth, and human physiology. Experiment design, hardware, methods and results gained with D1-Mission are presented. For individual titles, see N89-23720 through N89-23732.

N89-23720# Deutsche Forschungs- und Versuchsanstalt fuer Luft- und Raumfahrt, Cologne (Germany, F.R.). Hauptabteilung Projekte und Mikrogravitation.
MISSION CONDITIONS AND HARDWARE CONCEPTS [MISSIONSGELEGENHEITEN UND HARDWARE KONZEPTE]
H. Binnenbruck *In its* Summary of 1st Summer School on Microgravity Jul. 1987 p 1-23 In GERMAN (For primary document see N89-23719 17-29)
Avail: NTIS HC A09/MF A01

The ORBIS mission conditions and technical concepts are described by charts. Drop tower characteristics, dimensions and structures with ejection mechanisms are depicted. The MIKROBA microgravity balloon experiment technical outlines and payload capacities are specified. For KC-135 jet cargo-type aircraft, flight characteristics are indicated. The TEXUS (technological experiment under microgravity) mission sequence, profile, and payload concept are summed up. Orbital flight test shuttle use and main objectives; Spacelab system internal accomodation layout; and EURECA system capabilities, mission profile and payload are overviewed. Microgravity missions with national and ESA-NASA participation conditions are summarized. ESA

N89-23721# Deutsche Forschungs- und Versuchsanstalt fuer Luft- und Raumfahrt, Cologne (Germany, F.R.). Inst. fuer Raumsimulation.
MICROGRAVITY USER SUPPORT CENTER (MUSC) [NUTZERZENTRUM UND NUTZERUNTERSTUETZUNG]
K. Wittmann *In its* Summary of 1st Summer School on Microgravity Jul. 1987 p 25-37 In GERMAN (For primary document see N89-23719 17-29)
Avail: NTIS HC A09/MF A01

The MUSC supports microgravity experiments concerning materials science, biology, medicine, on EURECA and Spacelab shuttles. Main objectives and technical components are described: information and documentation center with data banks and archives; terrestrial models of space station instruments for experiment preparation; control room for experiment supervision and monitoring; and scientific and technical infrastructure for probe characterization, diagnosis, and data processing during and after the missions. ESA

N89-23722# Stuttgart Univ. (Germany, F.R.). Inst. fuer Raumfahrtsysteme.
PAYLOAD EXPERTS IN D1-MISSION [NUTZLASTEXPERTE BEI DER D1-MISSION]
E. Messerschmid *In* DFVLR, Summary of 1st Summer School on Microgravity Jul. 1987 p 39-41 In GERMAN (For primary document see N89-23719 17-29)
Avail: NTIS HC A09/MF A01

Microgravity effects on materials processing, biology and medicine during D1-Mission were studied by ground-based experts in cooperation with the Spacelab astronauts. Experiments in material science concerning liquid phase physics and solidification, and biological effects of microgravity on plant growth and on human physiological reactions are outlined. ESA

N89-23723# Deutsche Forschungs- und Versuchsanstalt fuer Luft- und Raumfahrt, Cologne (Germany, F.R.). Inst. fuer Theoretische Stroemungsmechanisk.
CONVECTION [KONVECTION]
G. S. R. Sarma *In its* Summary of 1st Summer School on Microgravity Jul. 1987 p 43-52 In GERMAN (For primary document see N89-23719 17-29)
Avail: NTIS HC A09/MF A01

Basic features in possible convection types in microgravity are discussed. Characteristic data are analyzed concerning free and forced convection, thermal convection, Marangoni and b-jitter (time dependent acceleration) convection. ESA

N89-23724# Deutsche Forschungs- und Versuchsanstalt fuer Luft- und Raumfahrt, Cologne (Germany, F.R.). Inst. fuer Raumsimulation.
DIFFUSION
G. Otto *In its* Summary of 1st Summer School on Microgravity Jul. 1987 p 53-65 In GERMAN (For primary document see N89-23719 17-29)
Avail: NTIS HC A09/MF A01

Going from general diffusion theory described by Fick's law, diffusion coefficients for gases and liquids are compared for different temperatures. Fick's law is applied to diffusion in liquids and verified with Spacelab experiment results under microgravity. Diffusion mass flow conditions are analyzed on a liquid metal sphere embedded in a matrix. Marangoni convection effects together with thermal transport effect are outlined. ESA

N89-23725# Deutsche Forschungs- und Versuchsanstalt fuer Luft- und Raumfahrt, Cologne (Germany, F.R.). Inst. fuer Raumsimulation.
PHASE TRANSFORMATION [PHASENUEBERGAENGE]
H. Klein *In its* Summary of 1st Summer School on Microgravity Jul. 1987 p 67-73 Partly in ENGLISH and GERMAN (For primary document see N89-23719 17-29)
Avail: NTIS HC A09/MF A01

Microgravity effects on phase transformations of liquid single components are outlined. Phase transformations are characterized

by order parameter of major importance for material structure according to renormalization group theory. Scale behavior and dynamics of cluster diffusion in hydrodynamic regime are indicated. Density distribution near gas/liquid critical point under reduced gravity with divergence of the compressibility is analyzed. ESA

N89-23726# Deutsche Forschungs- und Versuchsanstalt fuer Luft- und Raumfahrt, Cologne (Germany, F.R.). Inst. fuer Raumsimulation.
NUCLEATION AND UNDERCOOLING [KEIMBILDUNG UND UNTERKUEHLUNG]
D. M. Herlach *In its* Summary of 1st Summer School on Microgravity Jul. 1987 p 75-87 In GERMAN (For primary document see N89-23719 17-29)
Avail: NTIS HC A09/MF A01

Quantitative kinetics of phase transformation is analyzed by registration of nucleation rate of a liquid. Nucleation theory developed in vapor phase is enlarged and applied to liquid-solid phase transformation. Basic features of the theory are examined: cluster formation and crystallization of the melt, heterogenic nucleation, nuclei formation rate, embedding of dispersed melt in an inert fluidic medium, and production of solid containerless melts by levitation melting. ESA

N89-23727# Deutsche Forschungs- und Versuchsanstalt fuer Luft- und Raumfahrt, Cologne (Germany, F.R.). Inst. fuer Raumsimulation.
METALLIC SOLIDIFICATION [METALLISCHE ERSTARRUNG]
D. M. Herlach *In its* Summary of 1st Summer School on Microgravity Jul. 1987 p 89-103 In GERMAN (For primary document see N89-23719 17-29)
Avail: NTIS HC A09/MF A01

Thermodynamic considerations for solidification of nonequilibrium state phases are exposed. Undercooling and supercooling temperature effects and solidification kinetics is examined. Grain size distribution depends on undercooling temperature. Experimental methods for undercooling and amorphous embedding are described. A dispersion method for division of heterogen melts in small particles is proposed. An effective method to avoid boundary surface induced nucleation by solidification of the melt in free fall is examined. ESA

N89-23728# Aachener Centrum fuer Erstarrung unter Schwerelosigkeit e.V. (Germany, F.R.).
MODEL SYSTEMS [MODELLSYSTEME]
S. Rex and G. J. Schmitz *In* DFVLR, Summary of 1st Summer School on Microgravity Jul. 1987 p 105-111 In GERMAN (For primary document see N89-23719 17-29)
Avail: NTIS HC A09/MF A01

Dendritic solidification occurring in melting metallurgy is observed on transparent model systems in wind tunnel for metallic alloys. Solidification is visualized by holography for the determination of flow effects under reduced gravity on crystal structures, tensile strength, and conductivity at critical point of liquid/solid phase transformation. A measurement method on transparent model substances by holographic interferometry with determination of temperature and concentration profiles is described. ESA

N89-23729# Deutsche Forschungs- und Versuchsanstalt fuer Luft- und Raumfahrt, Cologne (Germany, F.R.). Inst. fuer Werkstoff-Forschung.
SEMICONDUCTORS AND MONOCRYSTAL GROWTH: COLLECTION OF CHARTS, FORMULAS AND REFERENCES [HALBLEITER UND ZUECHTUNG VON EINKRISTALLEN. ZUSAMMENFASSUNG VON VESENTLICHEN ABBILDUNGEN, FORMELN, REFERENZEN]
B. O. Hildman *In its* Summary of 1st Summer School on Microgravity Jul. 1987 p 113-129 In GERMAN (For primary document see N89-23719 17-29)
Avail: NTIS HC A09/MF A01

Electrical conductivity of semiconductors is analyzed by studying electrical and opto-electronic properties relative to the electrical band structure conditions. Donor and acceptor levels in band models are described for doped semiconductors. The most important crystal growth methods are presented: zone melting process, horizontal and vertical Bridgman process. Reduced gravity effects on crystal growth are indicated. ESA

N89-23730# Freiburg Univ. (Germany, F.R.). Chemisches Lab.
ORGANIC MONOCRYSTALS [ORGANISCHE EINKRISTALLE]
W. Littke *In* DFVLR, Summary of 1st Summer School on Microgravity Jul. 1987 p 131-141 In GERMAN Sponsored by Bundesministerium fuer Forschung und Technologie, Bonn, Fed. Republic of Germany (For primary document see N89-23719 17-29)
Avail: NTIS HC A09/MF A01

Protein crystallization under reduced gravity is studied and an experimental assembly is detailed. To avoid counterdiffusion between protein molecules and salt ions, short time experiments of 6 min are carried out in TEXUS program rockets. Results indicate that under microgravity conditions diffusion processes are laminar, monocrystal sizes are greater, and satisfactory crystal qualities are obtained. Three-dimensional crystallographic data of enzymes are depicted. ESA

N89-23731# Deutsche Forschungs- und Versuchsanstalt fuer Luft- und Raumfahrt, Cologne (Germany, F.R.). Inst. fuer Raumsimulation.
MICROGRAVITY CONDITIONS OF A SPACECRAFT [MIKROGRAVITATIONSBEDINGUNGEN EINES RAUMSFAHRZEUGS]
H. Hamacher *In its* Summary of 1st Summer School on Microgravity Jul. 1987 p 143-167 Partly in ENGLISH and GERMAN (For primary document see N89-23719 17-29)
Avail: NTIS HC A09/MF A01

Methods for simulation of microgravity are described: parabolic flight, ballistic rockets, aircraft and drop towers. Effectiveness for spacecraft design is evaluated. Atmospheric resistance effects, and tidal and rotation effects are indicated for each method. Sensitivity of experiments to accelerations is discussed. ESA

N89-23732# Bonn Univ. (Germany, F.R.). Inst. fuer Botanie.
BIOLOGICAL RESULTS OBTAINED BY D1-MISSION [ERGEBNISSE AUS DEM BEREICH BIOLOGIE AM BEISPIEL DER D1-MISSION]
D. Volkmann *In* DFLVR, Summary of 1st Summer School on Microgravity Jul. 1987 p 171-182 In GERMAN (For primary document see N89-23719 17-29)
Avail: NTIS HC A09/MF A01

Physical environmental factors effects like light and gravity on biological growth, development, and behavior were studied on Spacelab mission D1. Light dependent processes, energy transformation, morphogenesis, and orientation are studied for different types of bacteria and plants. Experiment hardware is presented and results are indicated. ESA

N89-24019*# Florida Univ., Gainesville.
MICROGRAVITY PARTICLE REDUCTION SYSTEM
Vanessa Brandon, Michelle Joslin, Lili Mateo, and Tracey Tubbs *In its* Advanced Space Design Program to the Universities Space Research Association and the National Aeronautics and Space Administration Jun. 1988 20 p (For primary document see N89-24015 17-51)
Avail: NTIS HC A12/MF A01 CSCL 22A

31 ENGINEERING (GENERAL)

Includes vacuum technology; control engineering; display engineering; cryogenics; and fire prevention.

N89-23733# Rocky Research Corp., Boulder City, NV.
SOLID-VAPOR ADSORPTION REFRIGERATION SYSTEM DEVELOPMENT Final Report, Oct. 1987 - Sep. 1988
Uwe Rockenfeller Oct. 1988 98 p

(Contract GRI-5087-233-1583)
(PB89-140859; GRI-88/0273) Avail: NTIS HC A05/MF A01 CSCL 13B

The feasibility of several gas fired refrigeration cycles using ammoniated complex compounds as the working media are described. The cycles take advantage of the coordinative characteristic of complex compound ligand bonds which result in large coordination spheres with only one degree of freedom. The coordinative bond yields refrigerant concentration plateaus of constant pressure which in turn result in high thermal cycle efficiencies and eliminate electrical parasitics and the requirement for moving parts. Media properties of known complex compound materials were verified with respect to vapor pressure equilibria, coordination properties, and thermal stability. An existing computer model was used to predict heat balances and coefficients of performance. Author

N89-23734# Environmental Protection Agency, Ann Arbor, MI. Test and Evaluation Branch.
SAMPLE PREPARATION TECHNIQUES FOR EVALUATING METHANOL AND FORMALDEHYDE EMISSIONS FROM METHANOL FUELED VEHICLES AND ENGINES
William M. Pidgeon and Matthew P. Reed 19 Sep. 1988 19 p
(PB89-136147; EPA/AA/TEB-88/02) Avail: NTIS HC A03/MF A01 CSCL 13F

The wet Chemistry procedures used by the Emission Control Technology Division, Test and Evaluation Branch of the E.P.A. Motor Vehicle Emission Laboratory in evaluating methanol fuels for use in motor vehicles are described. The formaldehyde and methanol wet chemistry procedures used are also described. Included is elution changes, volume measurement, sample contamination issues, preparation procedures and various appendices. Author

N89-23735# National Inst. of Standards and Technology, Gaithersburg, MD. Office of Nondestructive Evaluation.
INTELLIGENT PROCESSING OF MATERIALS
H. Thomas Yolken, ed. and Leonard Mordfin, ed. Jan. 1989 51 p Presented at an Industrial Workshop, 31 Aug. - 1 Sep. 1988
(PB89-151823; NISTIR-89/4024) Avail: NTIS HC A04/MF A01 CSCL 13H

Intelligent processing of materials was established as a major new program area in the Institute for Materials Science and Engineering, National Institute of Standards and Technology (NIST). Some of the generic scientific and technological bases were developed for intelligent processing and, by means of selected pilot or demonstration projects, encouraged American industry to pursue and to adopt this powerful approach to materials processing. In developing the new program, NIST cooperated in organizing two national workshops in 1985 to 1986 to help identify the principal industrial needs in this field of technology and to solicit guidance for program planning activities. On August 30 and September 1, 1988, NIST convened a third workshop in this series. This one was comprised primarily of selected industrial specialists and was designed to define the specific materials processes upon which the NIST program should focus, and to discuss suitable approaches for accomplishing the work. The results of that workshop are documented. Author

N89-23736*# Ohio State Univ., Columbus. ElectroScience Lab.
A METHOD TO DESIGN BLENDED ROLLED EDGES FOR COMPACT RANGE REFLECTORS
Inder J. Gupta and Walter D. Burnside Mar. 1989 42 p
(Grant NsG-1613)
(NASA-CR-184976; NAS 1.26:184976; ESL-719493-6) Avail: NTIS HC A03/MF A01 CSCL 13H

A method to design blended rolled edges for arbitrary rim shape compact range reflectors is presented. The reflectors may be center-fed or offset-fed. The method leads to rolled edges with minimal surface discontinuities. It is shown that the reflectors designed using the prescribed method can be defined analytically using simple expressions. A procedure to obtain optimum rolled edges parameter is also presented. The procedure leads to blended rolled edges that minimize the diffracted fields emanating from the junction between the paraboloid and the rolled edge surface while satisfying certain constraints regarding the reflector size and the minimum operating frequency of the system. Author

N89-23737# Oxford Univ. (England). Dept. of Engineering Science.
THE APPLICATION OF SELF-TUNING CONTROL TECHNIQUES TO A MULTIVARIABLE PROCESS Ph.D. Thesis
F. G. Jota 1988 249 p Sponsored by the Conselho Nacional de Pesquisas, Brazil and the Universities of the United Kingdom Committee of Vice-Chancellors and Principals
(OUEL-1737/88; ETN-89-94214) Avail: NTIS HC A11/MF A01

The application of self tuning control techniques to an air-handling rig is described. Three types of self-tuning controller were implemented on a dedicated distributed microcomputer system: a detuned minimum variance controller, a pole-placement self-tuning controller, and a long range predictive controller. A self-tuning controller cascaded with a fixed-parameter PI controller, two cascaded self-tuning controllers, and a self-tuning controller with no inner-loop were used. The feasibility of single-input single-output self-tuning controllers incorporating feed-forward control action, as opposed to a single multivariable controller, to compensate for interactions between temperature and humidity of the air, is investigated. The performance of the multiloop control scheme is compared with that of its multivariable counterpart. Self-tuning control of the temperature and relative humidity of the supply air using fixed-parameter and self-tuning controllers, and using no inner-loop, was performed; the behavior of the various types of self-tuning controllers under different modes of operation is assessed. A nonlinear digital computer simulation of the experimental air-handling plant was developed and used in the preliminary commissioning and tuning of the control schemes. ESA

N89-23738*# National Aeronautics and Space Administration. Marshall Space Flight Center, Huntsville, AL.
ELECTRODE CARRYING WIRE FOR GTAW WELDING Patent Application
Gene Morgan, inventor (to NASA) and Gerald Dyer, inventor (to NASA) (Rockwell International Corp., Huntsville, AL.) 5 Dec. 1988 8 p
(NASA-Case-MFS-29491-1; NAS 1.71:MFS-29491-1; US-Patent-Appl-SN-279677) Avail: NTIS HC A02/MF A01 CSCL 13B

A welding torch for gas tungsten arc welding apparatus has a hollow tungsten electrode including a ceramic liner and forms the filler metal wire guide. The wire is fed through the tungsten electrode thereby reducing the size of torch to eliminate clearance problems which exist with external wire guides. Since the wire is preheated from the tungsten more wire may be fed into the weld puddle, and the wire will not oxidize because it is always within the shielding gas. NASA

N89-23739*# National Aeronautics and Space Administration. Marshall Space Flight Center, Huntsville, AL.
INTERNAL WIRE GUIDE FOR GTAW WELDING Patent Application
Gene Morgan, inventor (to NASA) and Gerald Dyer, inventor (to NASA) (Rockwell International Corp., Huntsville, AL.) 5 Dec. 1988 8 p Sponsored by NASA. Marshall Space Flight Center
(NASA-Case-MFS-29489-1; NAS 1.71:MFS-29489-1; US-Patent-Appl-SN-279625) Avail: NTIS HC A02/MF A01 CSCL 13B

A welding torch for gas tungsten arc welding apparatus has a filler metal wire guide positioned within the torch, and within the shielding gas nozzle. The wire guide is adjacent to the tungsten electrode and has a ceramic liner through which the wire is fed. This reduces the size of the torch and eliminates the outside clearance problems that exit with external wire guides. Additionally, since the wire is always within the shielding gas, oxidizing of the wire is eliminated. NASA

N89-23740# Army Cold Regions Research and Engineering Lab., Hanover, NH.
RESPONSE OF PAVEMENT TO FREEZE-THAW CYCLES: LEBANON, NEW HAMPSHIRE, REGIONAL AIRPORT
Wendy L. Allen, William F. Quinn, Donald Keller, and Robert A. Eaton Jan. 1989 35 p
(Contract DOT-FA79WA1-059; DA Proj. 4A7-62730-AT-42)
(AD-A205559; CRREL-SR-89-2; DOT/FAA/PS-89/1) Avail: NTIS HC A03/MF A01 CSCL 13/2

In 1978 reconstruction was begun on the runway of the Lebanon Regional Airport, Lebanon, New Hampshire. The runway had experienced severe differential frost heaving and cracking during the previous three winters, which had resulted in closure of the facility during periods of extreme roughness. Temperature sensors were placed within the newly constructed pavement sections, and during the winters of 1979, 1980, and 1982 temperature data were recorded, and level surveys and repeated plate bearing tests were performed in order to provide data for the investigation. The three pavement sections were constructed to investigate the effect of section thickness on the level of frost protection provided. The sections consisted of 4 in. of asphalt concrete, 6 in. of crushed gravel and 22,30 dn 38 in. of well-graded sand subbase material. The 48-in section provided the highest level of frost protection to the subgrade. However, all three pavement sections maintained resilient stiffness values during the spring thaw period on the order of two to three times that of the pavement before reconstruction. Also, frost heave in all sections was reduced to levels that would not cause difficulty for aircraft using the facility. GRA

N89-23741# Army Armament Research, Development and Engineering Center, Watervliet, NY.
HIGH SPEED ABRASIVE BELT GRINDING Final Technical Report
Joseph Bak Jan. 1989 51 p
(AD-A205618; ARCCB-TR-89002) Avail: NTIS HC A04/MF A01 CSCL 13/8

A project was established to reduce current stock removal costs and eliminate finish turning operations of tubes by combining rough stock removal and finish grinding. The first phase was designated for engineering and investigation into the feasibility and application of abrasive belt grinding technology. This information was then used to generate a specification establishing some criteria for design and manufacture of a machine to remove heavy stock and finish tubes using abrasive belt technology. The specification was subsequently used for the acquisition of a machine to perform the tasks. The second phase was designated for testing of the equipment and establishing production parameters. GRA

N89-23742# Air Force Inst. of Tech., Wright-Patterson AFB, OH. School of Engineering.
PARAMETRIC STUDY OF RADIATIVE COOLING OF SOLID ANTIHYDROGEN M.S. Thesis
Michael J. MacLachlan Mar. 1989 56 p
(AD-A206092; AFIT/GNE/ENP/89M-4) Avail: NTIS HC A04/MF A01 CSCL 21/4

A computer model of cryogenic system for storing solid antimatter is used to explore the radiative cooling-power requirements for long-term antimatter storage. If vacuum-chamber pressures as low as 10 to -18th power torr can be reached, and the rest of the large set of assumptions is valid, milligram quantities of solid antimatter could be stored indefinitely at 1.5 K using cooling powers of less than a microwatt. Many of the assumptions made are problematic and need verification, as they could potentially change the results greatly. The system modeled is a sphere of solid anti-parahydrogen at 1.5 K or below levitated in a spherical cryogenic vacuum chamber. The free matter gas in the chamber is assumed to be molecular hydrogen, and sublimation of both matter and antimatter is assumed to be negligible. The antihydrogen is assumed to be in thermal equilibrium, although annihilation-energy deposition is localized and hydrogen's thermal-impulse response time is comparable to the interval between annihilations. A parametric analysis is performed, with system cooling power evaluated over a wide range of pressures and system sizes, as temperature and emissivity are also varied. The cooling-power requirements of storing solid antimatter for extended times may not be an obstacle, if the proper conditions are obtained. However, whether these conditions are indeed possible remains in doubt. GRA

N89-23743# McDonnell Aircraft Co., Saint Louis, MO.
LOW ENERGY CONSUMPTION HYDRAULIC TECHNIQUES Final Technical Report, Aug. 1984 - Apr. 1988
J. B. Greene, J. R. Jeffrey, S. N. Lohe, S. E. Pehowski, and N. J. Pierce 30 Aug. 1988 292 p
(Contract F33615-84-C-2417)
(AD-A206285; AFWAL-TR-88-2062) Avail: NTIS HC A13/MF A01 CSCL 20/4

This report documents the efforts to develop and test low energy consumption hydraulic techniques. Included is a discussion of the efforts to select and analyze a baseline hydraulic system (Phase 1) and conduct trade studies on various candidate design approaches which could reduce weight and power consumption (Phase 2). In addition, the report discusses the development of a test plan (Phase 3) and the results of an endurance test (Phase 4). This program was directed at 8000 psi hydraulic system technology using a nonflammable hydraulic fluid chlorotrifluoroethylene (CTFE) although the concepts developed could be applied to any fluid at any system pressure. The concepts selected for test were variable system pressure, flow augmentation with load recovery valves and overlapped main valves. GRA

N89-23744# Army Research Inst. of Environmental Medicine, Natick, MA.
EVALUATION OF THREE COMMERCIAL MICROCLIMATE COOLING SYSTEMS
Bruce S. Cadarette, Barry S. DeCristofano, Karen N. Speckman, and Michael N. Sawka Nov. 1988 25 p
(AD-A206318; AD-E900858; USARIEM-M19-89) Avail: NTIS HC A03/MF A01 CSCL 13/2

Three commercially available microclimate cooling systems were evaluated for their ability to reduce heat stress in men exercising in a hot environment while wearing high insulative, low permeability clothing. The cooling systems were: (1) ILC Dover Model 19 Coolvest (ILC) (2) LSSI Coolhead(LSSI), and (3) Thermacor Cooling vest (THERM). Endurance Time (ET), Heart Rate (HR), rectal temperature (Tre), mean skin temperature (TSK), Sweating Rate (SR), Rated Perceived Exertion (RPE) and Thermal Sensation (TS) were measured. The subjects self-terminated on all LSSI tests because of headaches. Statistical analyses were performed on data collected at 60 minutes to have values on all subjects. There were no differences in HR, Tre, SR or TS values among the cooling vests. The subjects' TSK was lower (P less than 0.05) for the LSSI than THERM: and RPE values were higher (P less than 0.05) for LSSI than the other two vests. These data suggest an improved physiological response to exercise heat stress with all three commercial systems with the greatest benefit in performance time provided by the ILC cooling system. GRA

32 COMMUNICATIONS AND RADAR

Includes radar; land and global communications; communications theory; and optical communications.

For related information see also *04 Aircraft Communications and Navigation* and *17 Space Communications, Spacecraft Communications, Command and Tracking.* For search and rescue see *03 Air Transportation and Safety,* and *16 Space Transportation.*

N89-23745 British Broadcasting Corp., Kingswood (England). Engineering Div.
INVESTIGATION OF MUTUAL INTERFERENCE BETWEEN DIGITALLY MODULATED SIGNALS

J. D. Newland Dec. 1988 14 p
(BBC-RD-1988/13) Avail: Issuing Activity

The effects of co-channel and adjacent-channel interference on a quaternary phase shift keying (QPSK) modulating system are investigated. From previous theoretical studies an upper and lower error bound is identified. The usefulness of these bounds at predicting the performance of QPSK at various levels of noise and interference is examined. The two error bounds gave a good indication of the error performance for QPSK with single and multiple interferers. The results should also be applicable to other types of digital phase modulation. Author

N89-23746*# National Academy of Sciences - National Research Council, Washington, DC. Space Applications Board.
NASA SPACE COMMUNICATIONS R AND D (RESEARCH AND DEVELOPMENT): ISSUES, DERIVED BENEFITS, AND FUTURE DIRECTIONS
Feb. 1989 73 p
(Contract NASw-4154)
(NASA-CR-184831; NAS 1.26:184831) Avail: NTIS HC A04/MF A01 CSCL 17B

Space communication is making immense strides since ECHO was launched in 1962. It was a simple passive reflector of signals that demonstrated the concept. Today, satellites incorporating transponders, sophisticated high-gain antennas, and stabilization systems provide voice, video, and data communications to millions of people nationally and worldwide. Applications of emerging technology, typified by NASA's Advanced Communications Technology Satellite (ACTS) to be launched in 1992, will use newer portions of the frequency spectrum (the Ka-band at 30/20 GHz), along with antennas and signal-processing that could open yet new markets and services. Government programs, directly or indirectly, are responsible for many space communications accomplishments. They are sponsored and funded in part by NASA and the U.S. Department of Defense since the early 1950s. The industry is growing rapidly and is achieving international preeminence under joint private and government sponsorship. Now, however, the U.S. space communications industry - satellite manufacturers and users, launch services providers, and communications services companies - are being forced to adapt to a different environment. International competition is growing, and terrestrial technologies such as fiber optics are claiming markets until recently dominated by satellites. At the same time, advancing technology is opening up opportunities for new applications and new markets in space exploration, for defense, and for commercial applications of several types. Space communications research, development, and applications (RD and A) programs need to adjust to these realities, be better coordinated and more efficient, and be more closely attuned to commercial markets. The programs must take advantage of RD and A results in other agencies - and in other nations. Author

N89-23747# Alaska Univ., Fairbanks. Geophysical Inst.
HIGH-LATITUDE FIELD-STRENGTH MEASUREMENTS OF STANDARD BROADCAST BAND SKYWAVE TRANSMISSIONS MONITORED AT FAIRBANKS, ALASKA Final Report
Robert D. Hunsucker and Brett S. Delana 18 Oct. 1988 152 p
(Contract FCC-0375)
(PB89-134829; FCC-0375-88) Avail: NTIS HC A08/MF A01 CSCL 20N

In order to achieve the most efficient utilization of the medium frequency (MF) portion of the spectrum, a more accurate method for predicting skywave field strength is essential. Before such a prediction method can be developed, sufficient measurement data from all latitudes and covering all phases of solar activity are needed. The measurements represent different levels of sunspot numbers and considerably enlarges the FCC databank. A wide number of topics affecting MF skywave propagation were discussed including the effects of magnetic storm, effects of sunspot cycle, seasonal and diurnal variations of field strengths and other topics relevant to radio propagation at high latitudes. Author

N89-23748# National Bureau of Standards, Boulder, CO. Electromagnetic Technology Div.
METROLOGY FOR ELECTROMAGNETIC TECHNOLOGY: A BIBLIOGRAPHY OF NBS (NATIONAL BUREAU OF STANDARDS) PUBLICATIONS, JANUARY 1970 - AUGUST 1988
Mary E. DeWeese, ed. Aug. 1988 63 p Supersedes PB88-123682
(PB89-147847; NBSIR-88/3097) Avail: NTIS HC A04/MF A01 CSCL 20N

The bibliography lists the publications of the personnel of the Electromagnetic Technology Division of NBS in the period from January 1970 through publication of the report. A few earlier references that are directly related to the present work of the Division are also included. Author

N89-23749# National Center for Atmospheric Research, Boulder, CO. Atmospheric Technology Div.
DESIGN OF THE ELDORA AIRBORNE DOPPLER RADAR
Peter H. Hildebrand, Charles L. Frush, and Craig Walther Dec. 1988 147 p
(Grant NSF ATM-87-09659)
(PB89-144604; NCAR/TN-325+EDD) Avail: NTIS HC A07/MF A01 CSCL 17I

During the past decade the need for airborne Doppler radars for meteorological research became apparent. Airborne Doppler weather radars can provide quick observation of large-scale storm systems and high resolution observations of small-scale weather phenomena. First serious calls for airborne Doppler weather radars were heard in the 1970's, and by 1982, a prototype airborne Doppler radar was operating aboard the NOAA P-3 aircraft. Tests of that system proved that airborne Doppler radar was indeed a valuable research tool and an observational tool which could open new horizons for atmospheric scientists. Plans are described for building a next-generation airborne Doppler radar system. This system builds upon the excellent beginning of the NOAA P-3 radar. Major areas of improvement will include radar sensitivity and measurement accuracy, scanning technique, and data handling and display. Author

N89-23750# National Inst. of Standards and Technology, Boulder, CO. Electromagnetic Fields Div.
AN ITERATIVE TECHNIQUE TO CORRECT PROBE POSITION ERRORS IN PLANAR NEAR-FIELD TO FAR-FIELD TRANSFORMATIONS
Lorant A. Muth and Richard L. Lewis Oct. 1988 19 p
(PB89-153886; NIST-TN-1323) Avail: NTIS HC A03/MF A01 CSCL 20N

A general theoretical procedure was developed to take into account probe position errors when planar near-field data are transformed to the far field. If the probe position errors are known, measured data can be represented as a Taylor series, whose terms contain the error function and the ideal spectrum of the antenna. Then the ideal spectrum can be solved in terms of the measured data and the measured position errors by inverting the Taylor series. This is complicated by the fact that the derivatives of the ideal data are unknown; that is, can only be approximated by the derivatives of the measured data. This introduces additional computational errors, which must be properly taken into account. The first few terms of the inversion can be easily obtained by simple approximation techniques, where the order of the approximation is easily specified. A more general solution can also be written by formulating the problem as an integral equation and using the method of successive approximations to obtain a general solution. An important criterion that emerges from the condition of convergence of the solution to the integral equation is that the total averaged position error must be less than some fraction of the sampling criterion for the antenna under test. Author

N89-23751# Selenia S.p.A., Rome (Italy). Radar Dept.
BATTLEFIELD RADAR IMAGING THROUGH AIRBORNE MILLIMETRIC WAVE SAR (SYNTHETIC APERTURE RADAR)

U. Carletti, E. DAddio, A. Farina, C. Morabito, R. Pangrazi, and F. A. Studer 1988 27 p Presented at the Symposium on Machine Aided Target Detection and Recognition Shape, Mons, Belgium, 22-23 Nov. 1988
(ETN-89-94228) Avail: NTIS HC A03/MF A01

Airborne synthetic aperture radar (SAR), operating in the millimetric-wave (mmw) region, is discussed with reference to a battlefield surveillance application. The SAR system provides high resolution real-time imaging of the battlefield and moving target detection, under adverse environmental conditions (e.g., weather, dust, smoke, obscurants). The most relevant and original aspects of the system are the band of operation (i.e., mmw in lieu of the more traditional microwave region) and the use of an unmanned platform. The former implies reduced weight and size requirements, thus allowing use of small unmanned platforms. The latter enchances the system operational effectiveness by permitting accomplishment of recognition missions in depth beyond the FEBA. An overall system architecture based on the onboard sensor, the platform, the communication equipment, and a mobile ground station is described. The main areas of ongoing investigation are presented: the simulation of the end-to-end system, and the critical technological issues such as mmw antenna, transmitter, signal processor for image formation and platform attitude errors compensation and detection and imaging of moving targets. ESA

N89-23752# Sandia National Labs., Albuquerque, NM.
AUTOFOCUS OF SAR IMAGERY DEGRADED BY IONOSPHERIC-INDUCED PHASE ERRORS
Charles V. Jakowatz, Jr., Paul H. Eichel, and Dennis C. Ghiglia 1989 7 p Presented at the SPIE Technical Symposium on Aerospace Sensing, Orlando, FL, 27 Mar. 1989
(Contract DE-AC04-76DP-00789)
(DE89-008278; SAND-88-2720C; CONF-890374-1) Avail: NTIS HC A02/MF A01

It has been suggested that synthetic aperture radar (SAR) images obtained from platforms such as SEASAT are subject to potential degradation by ionospheric-induced phase errors. This premise is based upon data from various satellite experiments that indicate large levels of phase scintillation in auroral zone data. Current models for phase errors induced by the ionosphere suggest that the phase error power spectrum is power law. This implies that the resulting phase errors contain significant components up to the Nyquist limit. Traditional sub-aperture based autofocus techniques, designed to correct uncompensated platform motion errors, are inadequate due to their inability to estimate higher order error terms. A new non-parametric phase error correction scheme developed at Sandia National Laboratories, however, has been demonstrated to remove phase errors of arbitrary structure. Consequently, our new algorithm is a viable candidate for correcting ionospheric phase errors. In this paper we show examples of SAR images degraded by simulated ionospheric phase errors. These images demonstrate that such errors cause smearing with complicated sidelobe structure. Restoration of these images via the new algorithm illustrates its superiority to classical sub-aperture based autofocus techniques. DOE

N89-23753*# National Aeronautics and Space Administration. Lewis Research Center, Cleveland, OH.
A SEGMENTED MIRROR ANTENNA FOR RADIOMETERS
S. W. Lee, B. Houshmand, M. Zimmerman (Illinois Univ., Urbana.), and R. Acosta May 1989 40 p
(Grant NAG3-419)
(NASA-TM-102045; E-4793; NAS 1.15:102045) Avail: NTIS HC A03/MF A01 CSCL 20N

An antenna is designed for the radiometer application of the planned NASA Earth Science Geostationary Platforms in the 1990's. The antenna consists of two parts: a regular parabolic dish of 5 meters in diameter which converts the radiation from feeds into a collimated beam, and a movable mirror that redirects the beam to a prescribed scan direction. The mirror is composed of 28 segmented planar conducting plates, mostly one square meter in size. The secondary pattern of the antenna was analyzed based on a physical optics analysis. For frequencies between 50 and 230 GHz, and for a scan range of + or -8 deg (270 beamwidths scan at 230 GHz), the worst calculated beam efficiency is 95 percent. To cover such a wide frequency and scan range, each of the 28 plates is individually controlled for a tilting less than 4 deg, and for a sliding less than 0.5 cm. The sliding is done at discrete steps. At 230 GHz, a step size of 2 mil is sufficient. The plate positions must be reset for each frequency and for each scan direction. Once the position is set, the frequency bandwidth of the antenna is very narrow. Author

N89-23754# Computas Expert Systems A/S, Kokkedal (Denmark).
DIRECT DISSEMINATION OF DATA FROM ESA'S FUTURE IN-ORBIT INFRASTRUCTURE Final Report
Sverre Maudal, Bernt Rognes, Eirik Vefsnmo, Lars Rorhlt, and Agnar Sandvik (Telox Engineering A.S., Oslo, Norway) Paris, France ESA 9 Dec. 1988 268 p
(Contract ESA-7450/87/NL/PP(SC))
(DDD-CP/TE-RE-7450; ESA-CR(P)-2734; ETN-89-94460) Avail: NTIS HC A12/MF A01

An overall information system which permits users on the Earth, equipped with relatively small satellite user terminals to obtain data or telescience services from low Earth orbit satellites by relay through geostationary DRS satellites, based upon their own, prior user requests, is discussed. User requirements, architectural solutions, and a comparative cost analysis of this dispersed system versus a centralized one are considered. Specifications for subsystems are drawn up, and recommendations for the choice of architecture are made. Such a dispersed system is feasible, both for observation, microgravity missions, and interactive telescience operations, and the concept of prior user requests can relieve ESA central authorities of considerable tasks for archiving, storing, and retrieval of space data. ESA

N89-23755# Societe Nationale Industrielle Aerospatiale, Paris (France). Div. Engins Tactiques.
NAVIGATION SHIFT CORRECTION BY RADAR CARTOGRAPHY. OPTIMIZATION AND VALIDATION BY SIMULATION [RECALAGE DE NAVIGATION PAR CARTOGRAPHIE RADAR: OPTIMISATION ET VALIDATION PAR OUTIL DE SIMULATION]
J. P. Guyvarch 1988 12 p In FRENCH
(Rept-882-320-103; ETN-89-94481) Avail: NTIS HC A03/MF A01

The application of millimeter wave radar as navigation aid in ground to ground long distance missile attack systems is discussed. A complete numerical simulation system is described. ESA

N89-23756*# Virginia Polytechnic Inst. and State Univ., Blacksburg. Dept. of Electrical Engineering.
STUDY OF SPREAD SPECTRUM MULTIPLE ACCESS SYSTEMS FOR SATELLITE COMMUNICATIONS WITH OVERLAY ON CURRENT SERVICES: EXECUTIVE SUMMARY
Tri T. Ha and Timothy Pratt Dec. 1987 21 p
(Contract NAS3-24887)
(NASA-CR-180827-Exec-Summ; NAS 1.26:180827-Exec-Summ) Avail: NTIS HC A03/MF A01 CSCL 17B

Two different methods of generating spread spectrum signals for an overlay service are discussed, and the data rate and efficiency which can be achieved while maintaining low interference with existing traffic are examined. B.G.

N89-23757*# Virginia Polytechnic Inst. and State Univ., Blacksburg. Dept. of Electrical Engineering.
STUDY OF SPREAD SPECTRUM MULTIPLE ACCESS SYSTEMS FOR SATELLITE COMMUNICATIONS WITH OVERLAY ON CURRENT SERVICES
Tri T. Ha and Timothy Pratt 1989 255 p
(Contract NAS3-24887)
(NASA-CR-180827; NAS 1.26:180827) Avail: NTIS HC A12/MF A01 CSCL 17B

The feasibility of using spread spectrum techniques to provide a low-cost multiple access system for a very large number of low data terminals was investigated. Two applications of spread spectrum technology to very small aperture terminal (VSAT) satellite communication networks are presented. Two spread spectrum multiple access systems which use a form of noncoherent M-ary FSK (MFSK) as the primary modulation are described and the throughput analyzed. The analysis considers such factors as satellite power constraints and adjacent satellite interference. Also considered is the effect of on-board processing on the multiple access efficiency and the feasibility of overlaying low data rate spread spectrum signals on existing satellite traffic as a form of frequency reuse is investigated. The use of chirp is examined for spread spectrum communications. In a chirp communication system, each data bit is converted into one or more up or down sweeps of frequency, which spread the RF energy across a broad range of frequencies. Several different forms of chirp communication systems are considered, and a multiple-chirp coded system is proposed for overlay service. The mutual interference problem is examined in detail and a performance analysis undertaken for the case of a chirp data channel overlaid on a video channel. Author

N89-23758# Massachusetts Inst. of Tech., Lexington. Lincoln Lab.

ASR-9 WEATHER CHANNEL TEST REPORT, EXECUTIVE S UMMARY

Seth W. Troxel 3 May 1989 29 p Original contains color illustrations

(Contracts DTFA01-80-Y-10546; F19628-85-C-0002) (DOT/FAA/PS-89/6-Exec-Summ; ATC-168-Exec-Summ) Avail: NTIS HC A03/MF A01

The next generation airport surveillance radar, (ASR-9), will be deployed by the FAA at over 100 locations throughout the United States. The system includes a weather channel designed to provide air traffic controller personnel with timely and accurate weather reflectivity information as a supplement to normal aircraft information. Comparisons between data from an ASR-9 in Huntsville, Alabama, recorded during design qualification and testing, and data from two other reference radars, were used as the basis for assessment of ASR-9 weather channel performance. Results suggest that, with the exception of an apparent 3 dB discrepancy between the weather products of the ASR-9 and the reference radars, the ASR-9 weather channel seems to perform according to FAA specifications. Author

N89-23759# Naval Postgraduate School, Monterey, CA.

PERFORMANCE OF RADAR RECEIVERS IN THE PRESENCE OF NOISE AND INTENTIONAL INTERFERENCE M.S. Thesis

Panagiotis G. Mavropoulos Dec. 1988 116 p

(AD-A205328) Avail: NTIS HC A06/MF A01 CSCL 17/9

This thesis is devoted to analyzing the problem of masking a reflected radar signal, in order to degrade the radar receiver's performance. This is to be accomplished by appropriately choosing the Power Spectral Density (PSD) of a power constrained colored noise interference to be generated either by the target itself or by pre-positioned friendly noise makers. The goal in either case is to generate interference signals that result in decreased receiver probability of detection, PD, for a given receiver probability of false alarm, PF. Efforts to identify appropriate PSD's of the power constrained interference were carried out by evaluating the receivers PD as a function of PF for two specific target models. The performance results for the various receivers investigated demonstrate that the noise interference generated by the noise makers can achieve significant levels of degradation, while the target generated noise interference tends to improve rather than degrade the radar receiver's performance. In all cases considered, the sinc squared shaped noise interference PSD is more effective at degrading the receiver performance than any other kink of PSD analyzed. GRA

N89-23760# Naval Postgraduate School, Monterey, CA.

SEA SPIKE MODELING M.S. Thesis

Chin-Chuan Kuo Dec. 1988 94 p

(AD-A205355) Avail: NTIS HC A05/MF A01 CSCL 17/9

In this thesis a clutter voltage model for scattering from the sea surface is developed. A model for the scattering from a whitecap and a wave breaking occurrence model are combined to simulate the back scattered signal from one radar resolution cell. The simulation is performed to obtain the probability density function of sea clutter under different assumptions of wind velocities and wave breaking conditions. Some measured quantities such as the mean clutter voltage and the correlation time are incorporated into this model as parameters. The probability density function depends on the parameters of this model. The obtained probability density functions do not confirm to any familiar simple density function. GRA

N89-23761# Defence Research Establishment Suffield, Ralston (Alberta).

ELECTROMAGNETIC REMOTE SENSING. LOW FREQUENCY ELECTROMAGNETICS

John E. McFee Jan. 1989 136 p

(AD-A205402; DRES-SP-124) Avail: NTIS HC A07/MF A01 CSCL 17/6

A series of lectures are presented on the topic of the location and identification of compact objects by low frequency electromagnetics. These lectures were presented as a portion of two graduate level courses in electrical engineering at the University of Toronto in 1985 and 1987. Magnetostatics, electrostatics and electromagnetic induction techniques are discussed in detail. GRA

N89-23762# Defence Research Establishment Ottawa, (Ontario). Electronics Div.

LINK AVAILABILITY AND RAIN ATTENUATION EXCEEDANCE CHARACTERISTICS FOR EHF (EXTREMELY HIGH FREQUENCY) SATELLITE COMMUNICATIONS WITH ARBITRARY LINK PARAMETERS IN CANADA

S. M. Khanna and D. M. Adams Oct. 1988 186 p

(AD-A205403; DREO-991) Avail: NTIS HC A09/MF A01 CSCL 25/2

The rain attenuation exceedance and the corresponding link availability have been calculated for any location in Canada for a Satcom link in the 10 to 45 GHz range with arbitrary values of the link parameters. Contours, with arbitrary constant values, of these two parameters are also determined for any region in Canada. The effect of site diversity on these results can be studied. The results are presented in different formats to facilitate their use in a system design. The CCIR rain attenuation prediction model, Hodge sits diversity model and long term rain statistics have been used for this work. Following a brief review of the subject, representative rain attenuation exceedance and link availability results are given to a Satcom link at 20, 30 and 44 GHz for a few selected values of the link parameters. GRA

N89-23763# Defence Research Establishment Ottawa, (Ontario).

A STATISTICAL ANALYSIS OF THE OUTPUT SIGNALS OF AN ACOUSTO-OPTIC SPECTRUM ANALYZER FOR CW (CONTINUOUS-WAVE) SIGNALS

Guy J. Farley Oct. 1988 74 p

(AD-A205404; DREO-993) Avail: NTIS HC A04/MF A01 CSCL 17/4

A statistical analysis on the output signals of an acousto-optic spectrum analyzer (AOSA) is performed for the case when the input signal is a continuous-wave (CW). To this end, a statistical model of these output signals is presented as a basis for the different analyses along with some numerical algorithms to calculate the deterministic components on a digital computer. Using this model, the optimum test for the detection of a known frequency is derived and its performance is analyzed. To deal with the unknown frequency situation, a scheme which was easily implemented with a finite impulse response (FIR) filter is presented

and its performance degradation as compared to the case of a known frequency is analyzed. GRA

N89-23764# Naval Research Lab., Washington, DC. Search Radar Branch.
PHASE ACCURACY EXPERIMENTS WITH A DIRECT-SAMPLING COHERENT DETECTOR Final Report
W. M. Waters, G. J. Linde, and B. R. Jarrett 10 Mar. 1989 13 p
(AD-A205458; NRL-9182) Avail: NTIS HC A03/MF A01 CSCL 17/9

The full potential of digital radar and communications signal processing may be realized only after errors in converting received signals to digital sample values are minimized. Coherent methods of analog-to-digital (A/D) conversion that preserve phase information fall into two classes-baseband and direct-sampling methods. As modern A/D converters have become faster, interest in direct-sampling approaches has grown; this report focuses on a direct-sampling digital coherent detector (DCD). The main advantage claimed for direct sampling over baseband detectors is improved phase accuracy. In the baseband case this is due to difficulties in matching separate I and Q channels. Data taken from the DCD demonstrate operation at carrier frequencies to 11.25 MHz with phase errors less than 0.8. At frequencies less than 4 MHz, phase errors are less than 0.3; this corresponds to time-measurement accuracy better than 230 picoseconds. A brief review of the rules of direct sampling proceeds descriptions of the approach, hardware implementation instrumentation test results, and conclusions. GRA

N89-23765# Naval Research Lab., Washington, DC. Radar Div.
RADAR WAVEFORMS DERIVED FROM ORTHOGONAL MATRICES Interim Report
Frank F. Kretschmer, Jr. and Karl Gerlach 14 Feb. 1989 39 p
(AD-A205459; NRL-9080) Avail: NTIS HC A03/MF A01 CSCL 17/9

New polyphase coded sequences are described that may be used to modulate a carrier frequency in pulse compression waveforms. These waveforms have low sidelobes when individual or multiple pulses are appropriately processed. They are related to orthogonal matrices that may be associated with complementary sequences and also with periodic waveforms having autocorrelation functions with constant zero-amplitude GRA

N89-23766*# Naval Ocean Research and Development Activity, Bay Saint Louis, MS.
KRMS (K-BAND RADIOMETRIC MAPPING SYSTEM) SSM/I VALIDATION MARCH 1988 QUICK LOOK REPORT Technical Note, 6-14 Mar. 1988
L. Dennis Farmer, Duane T. Eppler, Bruce Heydlauff, and David Olsen Jan. 1989 44 p Prepared in cooperation with Naval Ocean Research and Development Activity, Hanover, NH and Naval Weapons Center, China Lake, CA
(NASA-CR-185320; NAS 1.26:185320; AD-A205606; NORDA-TN-385) Avail: NTIS HC A03/MF A01 CSCL 17/9

The primary objective of this mission was to provide high-resolution passive microwave imagery in support of the NASA SSM/I sea ice algorithm verification program. Four flights were flown, originating from Eielson AFB, Fairbanks, Alaska, over the Chukchi Sea, the Beaufort Sea, and the Bering Sea. The Ka-band Radiometric Mapping System (KRMS) was flown from 6 to 14 March 1988. Data were collected on each of four days during this period. This report provides the flight and navigation records required to reconstruct the missions. Flight racks, compiled from the primary navigation system, indicate areas of coverage. The system logs provide the sensor settings and pertinent flight data, such as altitude and ground speed. The navigation logs provide specifics as to location of data and time of collection. A flight track chart is provided for each day's mission. Several examples of KRMS imagery are also provided. GRA

N89-23767# Aerospace Medical Research Labs., Wright-Patterson AFB, OH.
INTELLIGIBILITY IN NOISE OF THREE LPC (LINEAR PREDICTIVE CODERS) VOICE CHANNELS WITH ACTIVE NOISE REDUCTION HEADSETS Summary Report, Jun. - Nov. 1988
Charles W. Nixon and Richard L. McKinley 4 Nov. 1988 29 p
(AD-A205613; AAMRL-TR-88-063) Avail: NTIS HC A03/MF A01 CSCL 25/4

Voice communications processed by Linear Predictive Coders (LPC) are vulnerable to degradation by noise. An earlier study demonstrated that the major effect occurs at the listener. Possible mechanisms for this effect range from poor LPC speech quality to the apparent ease of masking LPC speech by noise. The intelligibility of analog systems is increased with improved signal-to-noise ratios at the ear of the listener. The previous study used state-of-the-art communications headsets with passive sound attenuation. The amount of attenuation provided by these headsets has reached a practical limit, consequently the speech-to-noise ratio cannot be increased for wearable devices. Improvements in speech intelligibility provided by the enhanced and high quality LPC vocoders have not eliminated the problem. A prototype Active Noise Reduction (ANR) headset used with the LPC vocoder systems provided active sound attenuation in addition to the passive attenuation of the headset and resulted in reduced noise at the ear. This reduction improved the speech-to-noise ratio which led to improved intelligibility. Current versions of active noise reduction systems have a high potential for markedly reducing the noise masking problem with the vocoders. State-of-the-art active noise reduction has been proven in laboratory and flight tests. This technology should be applied to these vocoder systems and verified in flight demonstrations in the future. GRA

N89-23768# Air Force Inst. of Tech., Wright-Patterson AFB, OH. School of Engineering.
THE EFFECT OF MUTUAL COUPLING ON THE SIDE LOBE PERFORMANCE OF CHEBYSHEV ARRAYS, VOLUME 1 M.S. Thesis
Robert A. Gierard Mar. 1989 247 p
(AD-A205724; AD-E501079; AFIT/GE/ENG/89M-4-Vol-1) Avail: NTIS HC A11/MF A01 CSCL 09/1

This computer analysis assessed the impact of mutual coupling on the side lobe performance of Chebyshev linear arrays as a function array size, scan condition, and the severity of Chebyshev taper. Array elements were horizontal parallel dipoles over a ground plane. Three simple compensation schemes to account for coupling were investigated. A FORTRAN computer program, based upon King-Middleton's modified, zero-order, two-term theory for cylindrical dipoles, was written to calculate the generalized impedance matrix for the linear array, dipole current distributions and the far-field H-plane pattern in the presence of coupling. It is sufficiently general to allow the user of specify, number of dipoles, dipole length and radius, dipole spacing, height above ground plane, frequency, and complex generator voltages driving the array. The results relate side lobe degradation (growth) to array size, scan condition, and desired Chebyshev side lobe level. Additional programs were written to reverse the matrix solution, and solve for generator voltages, which after coupling, produce a base current distribution with a Chebyshev taper. Three simpler compensation schemes then used approximations of the compensated (complex) voltages to drive the array. GRA

N89-23769# Air Force Inst. of Tech., Wright-Patterson AFB, OH. School of Engineering.
ENHANCED TRACKING OF BALLISTIC TARGETS USING FORWARD LOOKING INFRARED MEASUREMENTS M.S. Thesis
David R. Rizzo Mar. 1989 361 p
(AD-A205727; AD-E501079; AFIT/GE/ENG/89M-7) Avail: NTIS HC A16/MF A01 CSCL 17/5

This thesis is an extension of earlier work performed at AFIT towards tracking airborne targets using FLIR measurements. The research has aimed at replacing a standard correlation tracker

with a hybrid Kalman filter/enhanced correlation tracker for implementation in a high energy laser weapon. In this thesis the target trajectory being tracked is modelled as a benign, non-maneuvering, thrusting ballistic missile trajectory at large sensor-to-target ranges. To capture the characteristic shape of the exhaust plume, the plume is modelled as the difference between two bivariate Gaussian functions with elliptical equal intensity contours. As the missile ascends on its thrusting trajectory, the exhaust plume tends to oscillate (pogo) along the direction of the velocity vector. In this thesis, a second-order Gauss-Markov process is used to model the plume's 'pogo' oscillation properties. The ultimate goal is to design a multiple model adaptive filter (MMAF) algorithm composed of elemental filters tuned for varying plume pogo parameters (frequency and amplitude characteristics). This MMAF accounts for atmospheric disturbance effects of the propagating infrared wave fronts, as well as bending/vibrational effects of the optical hardware associated with the FLIR sensor. The bank of filters provide the accurate estimation capability to guide the pointing mechanism of a shared aperture laser/FLIR sensor. GRA

N89-23770# Mitre Corp., Bedford, MA.
AN/TAC-1 DEMULTIPLEXER CIRCUIT CARD ASSEMBLY Final Report
Paul J. Krueger Jan. 1989 80 p
(Contract F19628-86-C-0001)
(AD-A205744; MTR-10362; ESD-TR-88-290) Avail: NTIS HC A05/MF A01 CSCL 17/2

This report describes the design, operation, and testing of the AN/TAC-1 demultiplexer subassembly. It demultiplexes the 6144 kb/s digital data stream received over fiber optic cable or tropo satellite support radio, and converts it into 2 digital groups and 16 digital channels. Timing recovery is accomplished by generating a 18432 kHz master clock synchronized to the incoming data. This master clock is divided modulo two to generate the proper group and loop timing. GRA

N89-23771# Naval Research Lab., Washington, DC. Target Characteristics Branch.
ON THE PROBLEM OF OPTIMAL SIGNAL DETECTION IN DISCRETE-TIME, CORRELATED, NON-GAUSSIAN NOISE Interim Report
K. J. Sangston and B. H. Cantrell 23 Feb. 1989 25 p
(AD-A205859; NRL-9177) Avail: NTIS HC A03/MF A01 CSCL 17/9

Recent results of the detection of signals in discrete-time correlated, non-Gaussian noise in which the univariate statistics and a general covariance structure of the noise are known have been obtained. the results are predicted on the assumption that a solution to the signal detection problem based on knowledge of univariate statistics and a convariance structure is reasonable, even though it is known that in general a non-Gaussian noise process is not completely specified by such information. to examine this issue of reasonableness, we present two general non-Gaussian noise models that are equivalent in these assumed attributes and yet lead to fundamentally different detection structures. This difference in the detection structures indicate the signal detection problem is not adequately formulated without additional knowledge of the structure of the non-Gaussian noise process. We further present a specific radar example to quantify the difference in the detection structures. GRA

N89-23772# Defence Research Establishment Ottawa, (Ontario). Airborne Radar Section.
THE PERFORMANCE OF SPACE-BASED RADARS (SBR) ORBITING ON ELLIPTICAL ORBITS
D. Faubert and M. P. Kerr Dec. 1988 29 p
(AD-A205951; DREO-995) Avail: NTIS HC A03/MF A01 CSCL 17/9

The performance of Space-Based Radars (SBR) orbiting on elliptical orbits is discussed. Their ability to detect air-breathing targets is analyzed as a function of the antenna look angle, the orbital parameters of the satellite, the number of radio pulses transmitted and the peak power of the radar. The results show that the minimum detectable velocities of the SBR tend to degrade as the satellite approaches the apogee of its orbit. Depending on the orbital parameters of the satellite, the advantage of more extended coverage when the satellite is at the apogee of its orbit could be hindered by the poorer performance of the radar. GRA

N89-23773# Columbia Univ., New York, NY. Dept. of Applied Physics and Nuclear Engineering.
INVESTIGATION OF THREE-DIMENSIONAL MESH GENERATION WITH PRECISE CONTROLS Final Report, 30 Sep. 1986 - 26 Sep. 1988
Peter R. Eiseman 31 Jan. 1989 14 p
(Grant AF-AFOSR-0307-86; AF Proj. 2304)
(AD-A205967; AFOSR-89-0319TR) Avail: NTIS HC A03/MF A01 CSCL 20/4

In the grant, a number of accomplishments were made in a variety of ways and in a variety of topics. The ways in which this was achieved were in oral communication with others, in the organization of conferences, in the journal publications, in the direction of graduate studies, and in the computer demonstration of theoretical developments. The topics include a study of shock-vortex interaction and a number of studies in grid generation. Those studies covered algebraic and interactive aspects here converged with the establishment of a powerful control point formulation for arbitrary grid generation. GRA

N89-23774# Aeronautical Systems Div., Wright-Patterson AFB, OH. Human Factors Branch.
AN EVALUATION OF THE F/FB/EF-111 CREW/VOICE MESSAGE SYSTEM Final Report, Dec. 1987 - Jun. 1988
John A. Hassoun, J. M. Barnaba, and E. M. Matheson Jan. 1989 68 p
(AD-A205998; ASD-TR-88-5037) Avail: NTIS HC A04/MF A01 CSCL 25/4

In support of the F/FB/EF-111 Digital Flight Control System Program Office, subjective and performance data were collected in order to provide the government and contractor engineers with information needed in the design of a Voice Message Unit (VMU) interface for the F/FB/EF-111 aircraft. The VMU, one of the new safety of flight systems, is being included as part of the Digital Flight Control Computer. The VMU will be used as a means for alerting crew members to flight critical conditions. The evaluation was comprised of two phases. During the first phase, questionnaire data were collected from a sample of 119 operational F/FB/EF-111 crew members. The second phase of the evaluation involved the mechanization of the VMU interface in an FB-111 simulator, located at the Crew Station Design Facility, for pilots' on-hand experience with the content of the voice messages and the mechanization aspects of the interface. GRA

N89-23775# Air Force Inst. of Tech., Wright-Patterson AFB, OH. School of Engineering.
COUPLED INTEGRAL EQUATION SOLUTION FOR TWO DIMENSIONAL BISTATIC TE SCATTER FROM A CONDUCTING CAVITY-BACKED INFINITE PLANE M.S. Thesis
Ronald R. Fairbanks Dec. 1988 162 p
(AD-A206096; AFIT/MA/GE/88D-1) Avail: NTIS HC A08/MF A01 CSCL 12/2

The purpose of this thesis is to determine the scattered electromagnetic fields and radar cross section from a two-dimensional cavity in a perfectly electric conducting infinite plane. This is accomplished by deriving a coupled set of Fredholm integral equations of the second kind. A set of integral equations outside the cavity and a set of integral equations inside the cavity are coupled together at the interface. The Fredholm integral equations of the second kind for the outside of the cavity use a Green's function with Neumann boundry conditions to avoid an integration over the infinite plane for a transverse electric incident plane wave. An example problem is introduced and numerically solved to test the application of the newly derived equations. GRA

N89-23776# Delta Information Systems, Inc., Horsham, PA.
INVESTIGATION OF OPTICAL COMPRESSION TECHNIQUES FOR DITHER CODING Final Report
Apr. 1988 80 p
(Grant DCA100-7-C-0078; AF Proj. Q011)
(AD-A206140; NCS-TIB-88-5) Avail: NTIS HC A05/MF A01
CSCL 25/3

The purpose of this study was to perform a computer simulation study in which several dither coding techniques were evaluated in order to determine their relative performances in terms of compression and output image quality in reproducing gray scale imagery transmitted over facsimile channels. Gray scale images can be represented in two ways. One method produces gray scale using multilevel pixels (i.e., each pixel can have one of 2 gray level values, where n is the number of bits of resolution of the gray scale employed). The second method simulates gray scale by locally adjusting the ratio of black pels to white pels (dithering), using spatial frequency to give the appearance of gray scale. Although the multilevel approach produces higher quality images, the dithering approach is more compatible with existing facsimile equipments. GRA

N89-23777# Swedish Defence Research Establishment, Linkoeping. Dept. of Information Technology.
ACTIVE RADAR JAMMING
Veine Jernemalm Sep. 1988 37 p In SWEDISH; ENGLISH summary
(FOA-C-30506-3.6; ISSN-0347-3708; ETN-89-94306) Avail: NTIS HC A03/MF A01; Swedish Defence Research Establishment, P.O. Box 1165, S-581 11 Linkoeping, Sweden, 50 Swedish crowns

Active radar jammers are described. In confusion jammers the perturbing action is produced by thermal noise which is intensified, or by a carrier wave modulated by a noise signal, or by a carrier wave which is frequency modulated with a lot of sine waves of different frequencies. There are jammers to be used once, which are fired to the spot or hang from a parachute. Deception jammers (misleading jammers) emit false radar echoes, one or several produced by a repetition system, requiring a certain form of memory. It is shown how to emit varying false distance or velocities, and how to disturb angles in a radar used to guide artillery fire. ESA

N89-23778# Swedish Defence Research Establishment, Linkoeping. Dept. of Information Technology.
COHERENT LASER RADAR
Dietmar Letalick, Ingmar Renhorn, Ove Steinvall, and Anders Widen Dec. 1988 39 p In SWEDISH; ENGLISH summary
(FOA-C-30512-3.1; ISSN-0347-3708; ETN-89-94309) Avail: NTIS HC A03/MF A01; Swedish Defence Research Establishment, P.O. Box 1165, S-581 11 Linkoeping, Sweden, 50 Swedish crowns

The reasons for a broadening and a reflection of the radar beam are analyzed and the atmospheric influence on the return signal is given. The results from investigations of laser radar sensitivity are presented as well as target measurements, and tactical use in a multisensor system is discussed. The coherent laser radar can be used for distance measuring, navigation, target detection, target classification, to guide artillery fire, terrain following, and atmospheric sounding. A disavantage of this radar is its complexity. ESA

N89-23779# Swedish Defence Research Establishment, Linkoeping. Dept. of Information Technology.
LOSSY LAYERS: THEORY AND METHODS OF MEASUREMENT
Ake Berquist Nov. 1988 44 p In SWEDISH; ENGLISH summary
(FOA-C-30513-3.2; ISSN-0347-3708; ETN-89-94310) Avail: NTIS HC A03/MF A01; Swedish Defence Research Establishment, P.O. Box 1165, S-581 11 Linkoeping, Sweden, 50 Swedish crowns

The propagation of electromagnetic waves in a homogenous medium with losses is considered. A method of computing the reflection and transmission properties of plane, lossy layers at various angles of incidence and polarizations is reviewed. Both thick layers with moderate losses and very thin films with high losses are examined. Using the theory, methods of measurement of the permittivity and losses in the materials are proposed. ESA

N89-23780# Aerospatiale, Cannes La Bocca (France).
SMALL UHF MICROSTRIP RADIATING ELEMENT
G. Kossiavas, A. Papiernik (Nice Univ., France), J. P. Boisset, and M. Sauvan Paris, France 1988 4 p In FRENCH; ENGLISH summary
(Rept-882-440-103; ETN-89-94496) Avail: NTIS HC A02/MF A01

A radiating element featuring dimensions inferior to circular or square antennas is presented. The main characteristics are a good impedance matching for coaxial feeds, a relatively narrow bandwidth, and an omnidirectional radiating pattern for linear polarization. The surface reduction rate is three times. ESA

N89-23781# Aerospatiale, Cannes La Bocca (France). Space and Strategic Systems Div.
MECHANICAL/ELECTRICAL DISTORTION MODEL FOR REFLECTOR ANTENNAS
J. P. Boisset, L. Marro, K. Pontoppidan, and P. H. Nielsen (TICRA A/s, Copenhagen, Denmark) Paris, France 1988 6 p
(Rept-882-440-104; ETN-89-94497) Avail: NTIS HC A02/MF A01

A single software package capable of both mechanical and electrical analysis was developed in order to evaluate the reflector profile distortions and/or active skin anisotropy, which have to be assessed during the antenna lifetime. The software performs exhaustive analysis of reflector performance in any environmental conditions and supports and antenna designer during the early definition phase of a satellite program. ESA

N89-23782# Aerospatiale, Cannes La Bocca (France).
TELE-X ANTENNA MODULE THERMAL CONTROL
Alain Lanteri and Bjorn Henning (Telefonaktiebolaget L. M. Ericsson, Moelndal, Sweden) Paris, France 1988 9 p
(Rept-882-440-106; ETN-89-94499) Avail: NTIS HC A02/MF A01

The variable conductance heat pipes which regulate the transmitter feed of the TELE-X satellite, as well as the different tests whereby the thermal design was qualified are described. The extensive thermal analysis conducted in parallel to the development program is discussed. The thermal balance tests demonstrate adequacy of the thermal control concept. ESA

N89-23783# Aerospatiale, Cannes La Bocca (France).
NEAR FIELD TESTING OF THE ELECTRONICALLY DESPUN ANTENNA OF THE METEOSAT SATELLITE
K. vantKlooster, P. Balling (TICRA A/s, Copenhagen, Denmark), J. P. Cadot, and J. P. Moutonnet Paris, France 1988 5 p
(Rept-882-440-108; ETN-89-94501) Avail: NTIS HC A02/MF A01

A near field facility was adapted to test the antennas for the Meteosat Operational Program. Dedicated software was developed for the processing of the measurements. Examples of that processing are given, along with a description of the antenna, the test method, and the software. ESA

N89-23784# Aerospatiale, Cannes La Bocca (France).
ESA-D: AN INTEGRATED SOFTWARE FOR ANTENNA DESIGN AND ANALYSIS
L. Marro, J. P. Boisset, and K. Pontoppidan (TICRA A/s, Copenhagen, Denmark) Paris, France 1988 7 p
(Contract ESTEC-6659/86/NL/PH)
(Rept-882-440-111; ETN-89-94504) Avail: NTIS HC A02/MF A01

The main functional and architectural characteristics of the software are described. The program is intended to address the shortfalls of classical reflector design loop by presenting a single thermal-structural-radioelectrical software allowing full evaluation

of reflector dimensional characteristics in an integrated and interactive way. Either rigid, unfurlable or inflatable types of reflectors can be processed. ESA

N89-23899*# Dornier-Werke G.m.b.H., Friedrichshafen (Germany, F.R.).
DESIGN AND VERIFICATION OF MECHANISMS FOR A LARGE FOLDABLE ANTENNA
Hans Jurgen Luhmann, Carl Christian Etzler, and Rudolf Wagner *In* NASA, Marshall Space Flight Center, The 23rd Aerospace Mechanisms Symposium Mar. 1989 p 113-126 (For primary document see N89-23892 17-39)
Avail: NTIS HC A15/MF A01 CSCL 20N

N89-23910*# Ford Aerospace and Communications Corp., Palo Alto, CA.
DESIGN OF A 60 GHz BEAM WAVEGUIDE ANTENNA POSITIONER
Kenneth S. Emerick *In* NASA, Marshall Space Flight Center, The 23rd Aerospace Mechanisms Symposium Mar. 1989 p 267-278 (For primary document see N89-23892 17-39)
Avail: NTIS HC A15/MF A01 CSCL 20K

33 ELECTRONICS AND ELECTRICAL ENGINEERING

Includes test equipment and maintainability; components, e.g., tunnel diodes and transistors; microminiaturization; and integrated circuitry.

For related information see also *60 Computer Operations and Hardware* and *76 Solid-State Physics.*

N89-23785*# National Aeronautics and Space Administration. Ames Research Center, Moffett Field, CA.
DIGITAL CONTROL OF THE KUIPER AIRBORNE OBSERVATORY TELESCOPE
Ann C. McCormack and Philip K. Snyder Mar. 1989 13 p Presented at the 35th International Instrumentation Symposium (ISA), Orlando, FL, 1-14 May 1989
(NASA-TM-101082; A-89068; NAS 1.15:101082) Avail: NTIS HC A03/MF A01 CSCL 09A

The feasibility of using a digital controller to stabilize a telescope mounted in an airplane is investigated. The telescope is a 30 in. infrared telescope mounted aboard a NASA C-141 aircraft known as the Kuiper Airborne Observatory. Current efforts to refurbish the 14-year-old compensation system have led to considering a digital controller. A typical digital controller is modeled and added into the telescope system model. This model is simulated on a computer to generate the Bode plots and time responses which determine system stability and performance parameters. Important aspects of digital control system hardware are discussed. A summary of the findings shows that a digital control system would result in satisfactory telescope performance. Author

N89-23786# Tennessee Univ., Knoxville. Dept. of Chemistry.
SYNTHESIS OF NOVEL ACID ELECTROLYTES FOR PHOSPHORIC ACID FUEL CELLS Final Report, May 1985 - Oct. 1988
James L. Adcock Nov. 1988 51 p
(Contract GRI-5084-260-1090)
(PB89-148944; GRI-88/0329) Avail: NTIS HC A04/MF A01 CSCL 10A

A 40 millimole per hour scale aerosol direct fluorination reactor was constructed. F-Methyl F-4-methoxybutanoate and F-4-methoxybutanoyl fluoride were synthesized by aerosol direct fluorination of methyl 4-methoxybutanoate. Basic hydrolysis of the perfluorinated derivatives produce sodium F-4 methoxybutanoate which was pyrolyzed to F-3-methoxy-1-propene. Purification and shipment of 33 grams of F-3-methoxy-1-propene followed. Syntheses by analogous methods allowed production and shipment of 5 grams of F-3-ethoxy 1-propene, 18 grams of F-3-(2-methoxy.ethoxy) 1-propene, and 37 grams of F-3,3-dimethyl 1-butene. Eighteen grams of F-2,2-dimethyl 1-chloropropane was produced directly and shipped. As suggested by other contractors, 5 grams of F-3-methoxy 1-iodopropane, and 5 grams of F-3-(2-methoxy.ethoxy) 1-iodopropane were produced by converting the respective precursor acid sodium salts produced for olefin synthesis to the silver salts and pyrolyzing them with iodine. Each of these compounds was prepared for the first time by the aerosol fluorination process during the course of the contract. These samples were provided to other Gas Research Institute (GRI) contractors for synthesis of perfluorinated sulfur (VI) and phosphorous (V) acids. Author

N89-23787# Technische Hogeschool, Delft (Netherlands). Dept. of Geodesy.
PERFORMANCE ANALYSIS OF KALMAN FILTERS
P. J. G. Teunissen and M. A. Salzmann Sep. 1988 24 p
(PB89-146104; Rept-88.2) Avail: NTIS HC A03/MF A01 CSCL 09A

Methods for the analysis of the performance of Kalman filters are considered. The methods are all based on the innovation sequence which has well defined statistical properties if the filter is optimal. Local and global test statistics are presented and discussed. A global slippage test statistic is introduced. This test, which has batch type properties, is given in a recursive form. Author

N89-23788# Loewe Opta G.m.b.H., Kronach (Germany, F.R.).
TUNER FOR THE FIRST INTERMEDIATE FREQUENCY OF RECEIVERS FOR DIRECT SATELLITE RECEPTION Final Report [TUNER FUER DIE ERSTE ZWISCHENFREQUENZ VON EMPFANGSGERAETEN FUER DEN DIREKTSATELLITENENEMPFANG]
Bonno Poppinga and Ulrich Mann 1988 113 p In GERMAN
(Contract BMFT-01-YH-8503-9)
(ETN-89-93766) Avail: NTIS HC A06/MF A01

A tuner for end items of equipment for direct satellite reception, especially color television receivers, was developed. The tuner is suited for the reception of D2-MAC-coded signals as well as of PAL and SECAM television signals. A technical modification makes the tuner also usable for the reception of radio signals in the 900 MHz mobile radio communications range. By cost optimization a cheap solution was obtained, comparable with tuners for terrestrial multistandard reception. The developed tuner has a high reception sensitivity and a compact form suitable for chip component parts, and allows a universal application. ESA

N89-23789# Risberg Power Electronics, Inc., New Berlin, WI.
HIGH ENERGY SEMICONDUCTOR SWITCH Final Report, 24 Feb. 1987 - 24 Feb. 1989
R. L. Risberg 24 Feb. 1989 11 p
(Contract DE-FG01-87CE-15319)
(DE89-007399; DOE/CE-15319/T8) Avail: NTIS HC A03/MF A01

The objective was a controller for electric motors. By operating standard Nema B induction motors at variable speed a great deal of energy is saved. This is especially true in pumping and air conditioning applications. To allow wider use of variable speed AC drives, and to provide improved performance, a better semiconductor switch was sought. This was termed the High Energy Semiconductor Switch. DOE

N89-23790# TeleRobotics International, Inc., Knoxville, TN.
AN APPLICATION SPECIFIC INTEGRATED CIRCUIT FOR DUAL-AXIS MOTION CONTROL
S. D. Zimmermann, P. E. Satterlee, Jr., and D. W. Bouldin (Tennessee Univ., Knoxville.) 1989 7 p Presented at the Southeastcon '89 Conference and Exhibition, Columbia, SC, 9 Apr. 1989
(Contract DE-AC05-86ER-80399)
(DE89-007974; CONF-8904111-5) Avail: NTIS HC A02

An Application Specific Integrated Circuit (ASIC) for dual-axis robotic motion control was designed and developed with Computer Aided Design (CAD) tools. The ASIC provides an all digital dual-axis

Pulse Width Modulated (PWM) amplifier interface. The ASIC layout was produced on a SUN workstation using VLSI design tools. A standard cell library of basic digital functions and an automatic placement and autorouting program was used in the course of the design. The design was implemented in a 2-micron Scalable CMOS (SCMOS) technology through the Metal Oxide Semiconductor Implementation Service (MOSIS). The device was fabricated in both 40-pin ceramic DIP and 44-pin Plastic Leaded Chip Carrier (PLCC) packages. The dual-axis PWM controller chip was designed as part of a complete dual-arm, force-reflecting, master-slave telerobotic manipulator system and provides a 24 KHz PWM drive signal and control for a two-axis, 500-watt amplifier module. The device interfaces to a microprocessor bus and requires only 100 mW of power at 12 MHz operation. DOE

N89-23791*# National Aeronautics and Space Administration. Lewis Research Center, Cleveland, OH.
SEQUENTIALLY EVAPORATED THIN Y-Ba-Co-O SUPERCONDUCTING FILMS ON MICROWAVE SUBSTRATES
G. J. Valco, N. J. Rohrer (Ohio State Univ., Columbus.), J. D. Warner, and K. B. Bhasin 1989 9 p Presented at the Workshop on High Temperature Superconductivity, Huntsville, AL, 23-25 May 1989; cosponsored by the US Army Missile Command, the US Army Strategic Defense Command and the ARO
(Contract NCC3-105)
(NASA-TM-102068; E-4825; NAS 1.15:102068) Avail: NTIS HC A02/MF A01 CSCL 20L

The development of high T sub c superconducting thin films on various microwave substrates is of major interest in space electronic systems. Thin films of YBa2Cu3O(7-Delta) were formed on SrTiO3, MgO, ZrO2 coated Al2O3, and LaAlO3 substrates by multi-layer sequential evaporation and subsequent annealing in oxygen. The technique allows controlled deposition of Cu, BaF2 and Y layers, as well as the ZrO buffer layers, to achieve reproducibility for microwave circuit fabrication. The three layer structure of Cu/BaF2/Y is repeated a minimum of four times. The films were annealed in an ambient of oxygen bubbled through water at temperatures between 850 C and 900 C followed by slow cooling (-2 C/minute) to 450 C, a low temperature anneal, and slow cooling to room temperature. Annealing times ranged from 15 minutes to 5 hrs. at high temperature and 0 to 6 hr. at 450 C. Silver contacts for four probe electrical measurements were formed by evaporation followed with an anneal at 500 C. The films were characterized by resistance-temperature measurements, energy dispersive X-ray spectroscopy, X-ray diffraction, and scanning electron microscopy. Critical transition temperatures ranged from 30 K to 87 K as a function of the substrate, composition of the film, thicknesses of the layers, and annealing conditions. Microwave ring resonator circuits were also patterned on these MgO and LaAlO3 substrates. Author

N89-23792*# National Aeronautics and Space Administration. Lewis Research Center, Cleveland, OH.
MAGNIFICATION OF STARTING TORQUES OF dc MOTORS BY MAXIMUM POWER POINT TRACKERS IN PHOTOVOLTAIC SYSTEMS
Joseph Appelbaum and S. Singer (Colorado Univ., Colorado Springs.) 1989 8 p Proposed for presentation at the 24th Intersociety Energy Conversion Engineering Conference, Washington, DC, 6-11 Aug. 1989; sponsored by IEEE, AIAA, ANS, ASME, SAE, ACS and AIChE
(NASA-TM-102040; E-4741; NAS 1.15:102040) Avail: NTIS HC A02/MF A01 CSCL 09C

Direct current (dc) motors are used in terrestrial photovoltaic (PV) systems such as in water-pumping systems for irrigation and water supply. Direct current motors may also be used for space applications. Simple and low weight systems including dc motors may be of special interest in space where the motors are directly coupled to the solar cell array (with no storage). The system will operate only during times when sufficient insolation is available. An important performance characteristic of electric motors is the starting to rated torque ratio. Different types of dc motors have different starting torque ratios. These ratios are dictated by the size of solar cell array, and the developed motor torque may not be sufficient to overcome the load starting torque. By including a maximum power point tracker (MPPT) in the PV system, the starting to rated torque ratio will increase, the amount of which depends on the motor type. The starting torque ratio is calculated for the permanent magnet, series and shunt excited dc motors when powered by solar cell arrays for two cases: with and without MPPT's. Defining a motor torque magnification by the ratio of the motor torque with an MPPT to the motor torque without an MPPT, a magnification of 3 was obtained for the permanent magnet motor and a magnification of 7 for both the series and shunt motors. The effect of the variation of solar insolation on the motor starting torque was covered. All motor types are less sensitive to insolation variation in systems including MPPT's as compared to systems with MPPT's. The analysis of this paper will assist the PV system designed to determine whether or not to include an MPPT in the system for a specific motor type. Author

N89-23793# Stanford Linear Accelerator Center, CA.
DESIGN OF A 100 M:V X-BAND KLYSTRON
Kenneth Eppley Feb. 1989 4 p Presented at the 13th Particle Accelerator Conference, Chicago, IL, 20 Mar. 1989
(Contract DE-AC03-76SF-00515)
(DE89-008939; SU-SLAC-PUB-4900; CONF-890335-8-Vugraphs)
Avail: NTIS HC A02

Future linear colliders will require klystrons with higher peak power at higher frequency than are currently in use. SLAC is currently designing a 100 MW klystron at 11.4 GHz as a prototype for such a tube. The gun has been designed for 440 kV and 510 amps. Transporting this beam through a 5 mm radius X-band drift tube presents the major design problem. The area convergence ratio of 190 to one is over ten times higher than is found in conventional klystrons. Even with high magnetic fields of 6 to 7 kilogauss careful matching is required to prevent excessive scalloping. Extensive EGUN and CONDOR simulations have been made to optimize the transmission and RF efficiency. The EGUN simulations indicate that better matching is possible by using resonant magnetic focusing. CONDOR calculations indicate efficiencies of 45 percent are possible with a double output cavity. We will discuss the results of the simulations and the status of the experimental program. DOE

N89-23794# Argonne National Lab., IL.
LI/FeS BATTERY DESIGN FOR AN ELECTRIC VAN
A. A. Chilenskas and G. Barlow (Westinghouse Electric Corp., Chardon, OH.) 1989 5 p Presented at the SAE International Congress and Exposition, Detroit, MI, 27 Feb. 1989
(Contract W-31-109-eng-38)
(DE89-009808; CONF-890240-4) Avail: NTIS HC A02/MF A01

Li-alloy/FeS battery designs, based upon a well-characterized 300-Ah cell developed by Westinghouse Oceanic Division have been developed for four electric vans currently under development by the U.S. Department of Energy and the Electric Power Research Institute. Computerized cell models were developed to calculate power, energy, weight, and volume values for a cell while varying key design parameters. Battery specifications and vehicle performance are given for the Chrysler TE Van, GMC G-Van, Ford ETX-II, and the Eaton DSEP. DOE

N89-23795# Naval Postgraduate School, Monterey, CA.
AN EVALUATION OF COPLANAR LINE FOR APPLICATION IN MICROWAVE INTEGRATED CIRCUITRY M.S. Thesis
Jae S. Jeong Dec. 1988 67 p
(AD-A205305) Avail: NTIS HC A04/MF A01 CSCL 09/1

A general study of conductor backed coplanar waveguide is presented. The impedance (Z0) and effective dielectric constant of conductor-backed coplanar waveguide (CBCPW) have been calculated by using a variational method and the boundary point matching method. In this present work only the (TEM) dominant low frequency propagation mode of coplanar line has been considered. Experimental facilities are vector network analyzer (HP8409) and bench-instrument measurements. GRA

N89-23796# Illinois Univ., Urbana. Applied Computation Theory Group.
RECURSIVE GATE-ARRAYS
C. Chiang, S. Maddila, and M. Sarrafzadeh (Northwestern Univ., Evanston, IL.) Dec. 1988 11 p
(Contract N00014-84-C-0149; NSF MIP-87-09074; NSF ECS-84-10902)
(AD-A205335; ACT-104; UILU-ENG-88-2262) Avail: NTIS HC A03/MF A01 CSCL 09/1

The authors propose a regular architecture, called recursive gate-arrays, suitable for circuits with modules of nonuniform size. A set of n (rectangular and L-shaped) modules can be placed in a recursive gate-array. The placement can be obtained in O(n log n) time. GRA

N89-23797# Utah Univ., Salt Lake City. Dept. of Electrical Engineering.
THE EFFECTS OF DIELECTRIC AND METAL LOADING ON THE DISPERSION CHARACTERISTICS FOR CONTRAWOUND HELIX CIRCUITS USED IN HIGH POWER TRAVELING-WAVE TUBES Final Report, Sep. 1985 - Sep. 1987
William N. Cain Oct. 1988 146 p
(Contract F30602-84-C-0153)
(AD-A205345; UTEC-MD-88-050; RADC-TR-88-215) Avail: NTIS HC A07/MF A01 CSCL 20/14

The dispersion characteristics for contrawood helix structures are examined to determine the effects of dielectric and metal loading. The theory developed by Chodorow and Chu is expanded to include the problem of a contrawound helix interposed between two dielectric regions, symmetrically oriented inside a conducting cylinder. Simultaneously analyzed is the single helix oriented in an identical fashion. Numerical results are presented in the form of dispersion diagrams over a wide range of parameters. Interesting behavior found within these diagrams is discussed and, whatever possible, compared to experimental results. GRA

N89-23798# Technical Univ. of Denmark, Lyngby. Lab. of Applied Mathematical Physics.
COHERENCE AND CHAOS PHENOMENA IN JOSEPHSON OSCILLATORS FOR SUPERCONDUCTING ELECTRONICS Final Report, 21 May 1988 - 21 Jan. 1989
P. L. Christiansen, R. D. Paramentier, and O. Skovgaard 25 Jan. 1989 235 p
(Contract DAJA45-85-C-0042; DA Proj. 1L1-61102-BH-57)
(AD-A205469; R/D-4943-PH-01) Avail: NTIS HC A11/MF A01 CSCL 09/1

Work under the present contract has been dedicated to acquiring a detailed understanding of the fundamental mechanisms governing the dynamics of Josephson junction devices, with a view to employing this knowledge in the design of practical Josephson devices. Particular attention has been given to the questions of the interplay between coherence and chaos, and to determining the limits of stability of coherent states. A combination of analytical, computational, and experimental methods has been employed in order to maximize the results obtained. GRA

N89-23799# State Univ. of New York, Albany. Dept. of Electrical and Computer Engineering.
HIGH ELECTRIC FIELD PHENOMENA IN INSULATION Final Report, 15 Nov. 1986 - 14 Nov. 1988
J. R. Laghari and W. J. Sarjeant 15 Jan. 1989 96 p
(Grant AF-AFOSR-0063-87; AF Proj. 2301)
(AD-A205525; AFOSR-89-0266TR) Avail: NTIS HC A05/MF A01 CSCL 20/3

The present study extends previous work to include electron radiation-induced changes in monoisopropyl biphenyl (MIPB)-impregnated polypropylene film as well as the effects of neutron/gamma radiation on dry polypropylene films. Effects that were quite similar were induced by both electron and neutron radiation on the properties of interest of the polypropylene films. Impregnation of the film with MIPB had a mitigatory effect on the degradation of the properties. This report also contains the results of a simultaneous electrical and thermal aging study of a capacitor-grade polypropylene film. The data obtained in this study was fitted to models that will enable realistic prediction of lifetimes under operating conditions. GRA

N89-23800# Massachusetts Inst. of Tech., Cambridge. Artificial Intelligence Lab.
GENERATING CIRCUIT TESTS BY EXPLOITING DESIGNED BEHAVIOR Ph.D. Thesis
Mark H. Shirley Dec. 1988 305 p
(Contract N00014-85-K-0124)
(AD-A206175; AI-TR-1099) Avail: NTIS HC A14/MF A01 CSCL 09/1

Generating tests for sequential devices is one of the hardest problems in designing and manufacturing digital circuits. This task is difficult primarily because internal components are accessible only indirectly, forcing a test generator to use the surrounding components collectively as a probe for detecting faults. This in turn forces the test generator to reason about complex interactions between the behaviors of these surrounding components. Current automated solutions are becoming ineffective as designs grow larger and more complex. Yet, despite the complexity, human experts remain remarkably successful, in part, because they use knowledge from many sources and use a variety of reasoning techniques. This thesis exploits several kinds of expert knowledge about circuits and test generation not used by the current algorithms. First, many test generation problems can be solved efficiently using operation relations, a novel representation of circuit behavior that connects internal component operations with directly executable circuit operations. Operation relations can be computed efficiently for sequential circuits that provide few operations at their interfaces by searching traces of simulated circuit behavior. Second, experts write test programs rather than test vectors because programs are a more readable and compact representation for tests than vectors are. Test programs can be constructed automatically by merging test program fragments using expert supplied goal-refined rules and domain independent planning techniques from artificial intelligence. GRA

N89-23801# Naval Research Lab., Washington, DC. High Power Electromagnetic Radiation Branch.
MEGAVOLT, MULTI-KILOAMP K(SUB)A-BAND GYROTRON OSCILLATOR EXPERIMENT Memorandum Report, Oct. 1987 - Oct. 1988
W. M. Black, S. H. Gold, A. W. Fliflet, D. A. Kirkpatrick, W. M. Manheimer, R. C. Lee, V. L. Granatstein, D. L. Hardesty, A. K. Kinkead, and M. Sucy (JAYCOR, Vienna, VA.) 15 Mar. 1989 30 p
(AD-A206271; NRL-MR-6419) Avail: NTIS HC A03/MF A01 CSCL 09/1

High peak power K sub a band gyrotron oscillator experiment is reported. This experiment operated at 35 GHz in a sub a TE sub 62 mode, using a 1 to 1.35 MeV, multi-kiloamp beam from the VEBA pulseline accelerator. The use of an apertured anode configuration provided improved beam quality compared to earlier experiments that were carried out in a foiless diode geometry. As a result, the peak power has increased to approximately 275 MW with peak efficiencies exceeding 10 percent. The experimental results are in reasonable agreement with the predictions of theory. GRA

N89-23802# Princeton Univ., NJ. Dept. of Electrical Engineering and Computer Science.
NEAR-FAR RESISTANT LINEAR MULTIUSER DETECTION
R. Lupas Jan. 1989 56 p
(Contract DAAL03-87-K-0062; ARPA Order 4989)
(AD-A206363; ARO-24543.9-EL) Avail: NTIS HC A04/MF A01 CSCL 12/9

This dissertation studies linear detectors for Code-Division Multiple-Access channels perturbed by additive white Gaussian noise, under the assumption that the ensemble of user code waveforms is known to the receiver. In particular the near-far problem of Direct-Sequence Spread-Spectrum Multiple-Access channels, i.e., the problem of demodulating a weak transmitter in

the presence of powerful interferers, is solved with a linear receiver. Two multiuser performance measures are used to quantify the performance degradation due to the presence of multiuser interference: The asymptotic efficiency, which is equivalent to bit-error-rate in the low background noise region, and the near-far resistance, which measures a detector's robustness to the near-far problem. Conventional single-user detection in a multiuser channel is not near-far resistant, while the substantially higher performance of the optimum multiuser detector requires exponential complexity in the number of users. We show that the near-far resistance of optimum multiuser detection is achieved by a linear receiver (whose complexity per demodulated bit is only linear in the number of users). The optimum linear detector for worst-case energies - the decorrelating detector - is found, along with existence conditions, which are always satisfied in the models of practical interest. GRA

N89-23803# Aerospace Corp., El Segundo, CA. Electronics Research Lab.
ATTENUATION MEASUREMENT OF VERY LOW-LOSS DIELECTRIC WAVEGUIDES BY THE CAVITY RESONATOR METHOD IN THE MILLIMETER/SUBMILLIMETER WAVELENGTH RANGE
F. I. Shimabukuko and C. Yeh 20 Mar. 1989 33 p Prepared in cooperation with California Univ., Los Angeles
(Contract F04701-85-C-0086)
(AD-A206458; TR-0086A(2925-06)-1; SD-TR-89-10) Avail: NTIS HC A03/MF A01 CSCL 09/1

A dielectric waveguide shorted at both ends is constructed as a cavity resonator. By measuring the Q of this cavity, one can determine the attenuation constant of the guided mode on this dielectric structure. The complex permittivity of the dielectric waveguide material can also be derived from these measurements. Measurement were made at Ka-band for dielectric waveguides constructed of nonpolar, low-loss polymers such as Teflon, polypropylene, polyethylene, polyethylene, and Rexolite. GRA

N89-23804# Swedish Defence Research Establishment, Linkoeping. Dept. of Information Technology.
TRANSMISSION LOSSES IN HOLLOW ALUMINUM OXIDE WAVEGUIDE AT 10.6 MICRONS
Anders Callenas and Ingmar Renhorn Dec. 1988 15 p In SWEDISH; ENGLISH summary
(FOA-C-30518-3.1; ISSN-0347-3708; ETN-89-94311) Avail: NTIS HC A03/MF A01; Swedish Defence Research Establishment, P.O. Box 1165, S-581 11 Linkoeping, Sweden, 50 Swedish crowns

A study on waveguides is reported. The attenuation in the waveguide is the difference between the total transmission loss and the coupling loss which is especially important for carbon dioxide lasers. Five tubes of 19.7 cm length, 4 mm outer diameter, and 2 mm inner diameter were tested. Two of the tubes were polished with diamond paste. The attenuation coefficient in the waveguides are for unpolished tubes 0.5 percent, and 0.2 percent for the polished ones. The tubes were drilled to ensure straightness. The results show that the attenuation is low enough and the tubes of Al2O3, purity 99.7 percent could be used in a carbon dioxide waveguide lasers as a hollow waveguide. ESA

N89-23531*# Mission Research Corp., San Diego, CA.
RADIATION EFFECTS IN SPACECRAFT ELECTRONICS
James P. Raymond *In* NASA, Langley Research Center, NASA/SDIO Space Enviromental Effects on Materials Workshop, Part 1 May 1989 p 53-74 (For primary document see N89-23528 17-23)
(Contract N00014-85-C-2642)
Avail: NTIS HC A16/MF A01 CSCL 09C

N89-23549*# Aerospace Corp., El Segundo, CA. Space Sciences Lab.
EFFECTS OF SPACE RADIATION ON ELECTRONIC MICROCIRCUITS
W. A. Kolasinski *In* NASA, Langley Research Center, NASA/SDIO Space Environmental Effects on Materials Workshop, Part 2 May 1989 p 383-392 (For primary document see N89-23547 17-23)
Avail: NTIS HC A12/MF A01 CSCL 09C

N89-23894*# Sandia National Labs., Albuquerque, NM.
A UNIDIRECTIONAL ROTARY SOLENOID AS APPLIED TO STRONGLINKS
Eugene W. Kenderdine *In* NASA, Marshall Space Flight Center, The 23rd Aerospace Mechanisms Symposium Mar. 1989 p 17-37 (For primary document see N89-23892 17-39)
Avail: NTIS HC A15/MF A01 CSCL 20K

N89-23900*# Honeywell Space and Aviation Systems, Durham, NC.
EDDY CURRENT DAMPER
R. C. Ellis, R. A. Fink, and R. W. Rich *In* NASA, Marshall Space Flight Center, The 23rd Aerospace Mechanisms Symposium Mar. 1989 p 127-137 (For primary document see N89-23892 17-39)
Avail: NTIS HC A15/MF A01 CSCL 09A

N89-23909*# Honeywell, Inc., Phoenix, AZ. Satellite Systems Div.
SIGNAL AND POWER ROLL RING TESTING UPDATE
Dennis W. Smith *In* NASA, Marshall Space Flight Center, The 23rd Aerospace Mechanisms Symposium Mar. 1989 p 255-266 (For primary document see N89-23892 17-39)
Avail: NTIS HC A15/MF A01 CSCL 20K

34 FLUID MECHANICS AND HEAT TRANSFER

Includes boundary layers; hydrodynamics; fluidics; mass transfer; and ablation cooling.

For related information see also *02 Aerodynamics* and *77 Thermodynamics and Statistical Physics.*

N89-23805# National Aeronautical Lab., Bangalore (India). Aerodynamics Div.
FLOSOLVER: A PARALLEL COMPUTER FOR FLUID DYNAMICS
U. N. Sinha, M. D. Deshpande, and V. R. Sarasamma Jun. 1988 31 p
(NAL-TM-AE-8803) Avail: NTIS HC A03/MF A01

The Flosolver parallel computer designed and built at NAL for fluid dynamics problem solving is described. The computer has two nodes each having four processors based on Intel 8086-8087 chips. In each node one of the processors acts as host and has access to a section of the private memory of the remaining three processors through the Multibus. Inter-node communication is done using parallel ports. Synchronization and inter-processor communication is done by passing the message through a global memory. Prior to execution the host processor loads the absolute codes from a disk to the respective processors. Several fluid dynamical problems of practical interest have been programmed on Flosolver using concurrent algorithms, and show that it is comparable in speed with mainframes available in the country. Author

N89-23806# National Aerospace Lab., Tokyo (Japan).
AN EXPERIMENTAL STUDY OF LAMINAR FLOW CONTROL AIRFOIL WITH SUCTION THROUGH PERFORATED SURFACE AT LOW SPEED
Yoji Ishida and Masayoshi Noguchi Mar. 1988 17 p In JAPANESE; ENGLISH summary
(NAL-TR-967; ISSN-0389-4010) Avail: NTIS HC A03/MF A01

An experimental study of a laminar flow control airfoil with suction through a perforated surface at low speed was made. The airfoil section was designed to be a natural laminar flow airfoil which can delay the boundary layer transition as far

downstream as possible. The effects of suction quantity and position of sucked area on transition delay were examined. It was found that a very small amount of suction was able to delay the transition from x/c = 0.674 to 0.913 and to reduce the profile drag about 18 percent compared with the case of zero suction at Rc of 6.7 x 10(5). It was also observed that application of the suction near and downstream of the natural transition point had a very large effect on delaying the transition point; but on the other hand, application upstream of the point had very little effect. Theoretical calculation based on an equivalent uniform suction assumption showed good agreement with the experimental results. Michel's criterion, which was originally developed for layers without suction, has given at least qualitatively correct results even for layers with suction. Author

N89-23807# National Aerospace Lab., Tokyo (Japan).
MECHANISMS OF SECONDARY FLOWS AND LOSSES WITHIN A THREE DIMENSIONAL TURBINE STATOR CASCADE
Atsumasa Yamamoto, Ryoji Yanagi, and Hiroyuki Nouse Apr. 1988 20 p In JAPANESE; ENGLISH summary
(NAL-TR-970T; ISSN-0389-4010) Avail: NTIS HC A03/MF A01

In order to reveal aerodynamic loss mechanisms of turbine blade rows, internal flows of a low speed 3-D turbine stator cascade were measured in detail using five-hole pitot tubes. Flow visualization tests and the cascade endwall static pressure measurements were also made. These test results show that many vortical flows relate to the loss generation but the major process of loss generation in the cascade passage can be explained simply as a migration process in which boundary layer fluids with low energy being developed on the cascade passage walls (i.e., both endwalls and both blade surfaces) migrate onto the blade suction surface near the trailing edge. Complicated flow patterns were seen rather in the vortical flows near the trailing edge and downstream of the cascade: for example, a strong trailing-shedding-vortex occurring downstream of the cascade affects the upstream flow field within the cascade by extremely complicated mechanisms. Effects of blade tip leakage flow on the cascade internal flow and the associated loss are also shown. Author

N89-23808# Texas A&M Univ., College Station. Dept. of Mechanical Engineering.
THREE-DIMENSIONAL LASER ANEMOMETER STUDY OF COMPRESSIBLE FLOW THROUGH ORIFICE PLATES Annual Report, Sep. 1987 - Aug. 1988
Gerald L. Morrison Sep. 1988 91 p
(Contract GRI-5086-260-1340; RF Proj. 5595)
(PB89-145098; GRI-88/0289) Avail: NTIS HC A05/MF A01 CSCL 20D

Two experimental facilities were constructed, one for the measurement of the pressure distributions on the pipe wall upstream and downstream of the orifice plate and on the orifice plate surface and the other for use with a laser Doppler anemometer (LDA) system to measure the complex flow field inside the orifice run. Pressure measurements for Beta = 0.25, 0.50 and 0.75 were performed for a range of Reynolds numbers from 17,700 to 120,000. A five hole Pitot probe and a 3-D laser Doppler anemometer (LDA) were used to measure profiles of the axial and radial velocities downstream of the orifice plate. Both devices showed a large recirculation zone extending approximately 2.5 pipe diameters downstream. The 3-D LDA measurements clearly showed the vena contracta and a secondary recirculation zone near the downstream base of the orifice plate. The 3-D LDA also measured the entire Reynolds stress tensor distribution downstream of a Beta = 0.05 orifice for a Reynolds number of 17,700. Creare, Inc.'s Fluent program was used to predict the flow field inside a Beta = 0.50 orifice flow meter. Using assumed inlet conditions, the agreement between experimental and computed results was good. Author

N89-23809*# National Aeronautics and Space Administration. Lewis Research Center, Cleveland, OH.
ADVANCED COMPUTATIONAL TECHNIQUES FOR HYPERSONIC PROPULSION
Louis A. Povinelli 1989 24 p Proposed for presentation at the 9th International Symposium on Air Breathing Engines, Athens, Greece, 4-9 Sep. 1989; sponsored by AIAA and International Society for Air Breathing Engines
(NASA-TM-102005; E-4711; NAS 1.15:102005) Avail: NTIS HC A03/MF A01 CSCL 20D

Computational Fluid Dynamics (CFD) has played a major role in the resurgence of hypersonic flight, on the premise that numerical methods will allow performance of simulations at conditions for which no ground test capability exists. Validation of CFD methods is being established using the experimental data base available, which is below Mach 8. It is important, however, to realize the limitations involved in the extrapolation process as well as the deficiencies that exist in numerical methods at the present time. Current features of CFD codes are examined for application to propulsion system components. The shortcomings in simulation and modeling are identified and discussed. Author

N89-23810# Nevada Univ., Reno. Dept. of Mechanical Engineering.
FREE SHEAR LAYER AND SWIRL FLOW HEAT TRANSFER ENHANCEMENT Annual Report, Sep. 1987 - Aug. 1988
R. A. Wirtz, M. Greiner, B. Snyder, and R. Turner Sep. 1988 76 p
(Contract GRI-5087-260-1562)
(PB89-145106; GRI-88/0321; GR-104) Avail: NTIS HC A05/MF A01 CSCL 20D

Two wall shape induced convective heat transfer enhancement mechanisms for channel flows are investigated. The first uses transverse grooves in the channel wall to produce unstable free shear layers which cause traveling waves to be superimposed on the channel mean flow, thus augmenting heat transfer. The onset of natural oscillations are observed at a channel Reynolds number of 630, and they persist into the turbulent flow regime. Heat transfer measurements show augmentation for Reynolds numbers between 1500 and 5000. The second technique uses streamline curvature to produce a steady swirling flow in a serpentine channel. Flow visualization shows that the secondary flow consists of pairs of counter-rotating axial rolls which form adjacent to the upper and lower channel boundaries and sweep fluid into the core of the flow. Author

N89-23811# ICI-TENSA Services, Houston, TX.
PROCESS INTEGRATION METHODOLOGY FOR NATURAL GAS-FUELED HEAT PUMPS AND COGENERATION SYSTEMS Final Report, Mar. 1987 - Oct. 1988
Alan P. Rossiter Nov. 1988 338 p
(Contract GRI-5086-233-1459)
(PB89-140867; GRI-88/0165) Avail: NTIS HC A15/MF A01 CSCL 10B

A process integration methodology was developed for analyzing industrial processes, identifying those that will benefit from natural gas fueled heat pumps and cogeneration system as well as novel, process-specific opportunities for further equipment improvements, including performance targets. The development included the writing of software to assist in implementing the methodology and application of the procedures in studies using both literature data and plant operating data. These highlighted potential applications for gas fueled heat pumps in ethylene processes and liquor distilling plants, and slightly less attractive opportunities in a number of other plants. Many of the processes studied showed excellent potentials for cogeneration applications. GRA

N89-23812*# Virginia Polytechnic Inst. and State Univ., Blacksburg. Dept. of Engineering Science and Mechanics.
EFFECT OF WALL COOLING ON THE STABILITY OF COMPRESSIBLE SUBSONIC FLOWS OVER SMOOTH HUMPS AND BACKWARD-FACING STEPS
Ayman A. Al-Maaitah, Ali Nayfeh, H., and Saad A. Ragab

[1989] 35 p
(Contract NAG1-714; N00014-85-K-0011; NR Proj. 4325201)
(NASA-CR-184960; NAS 1.26:184960) Avail: NTIS HC A03/MF A01 CSCL 20D

The effect of wall cooling on the two-dimensional linear stability of subsonic flows over two-dimensional surface imperfections is investigated. Results are presented for flows over smooth humps and backward-facing steps with Mach numbers up to 0.8. The results show that, whereas cooling decreases the viscous instability, it increases the shear-layer instability and hence it increases the growth rates in the separation region. The coexistence of more than one instability mechanism makes a certain degree of wall cooling most effective. For the Mach numbers 0.5 and 0.8, the optimum wall temperatures are about 80 pct and 60 pct of the adiabatic wall temperature, respectively. Increasing the Mach number decreases the effectiveness of cooling slightly and reduces the optimum wall temperature. Author

N89-23813*# National Aeronautics and Space Administration. Lewis Research Center, Cleveland, OH.
ON THE NATURE OF NAVIER-STOKES TURBULENCE Ph.D. Thesis - Case Western Reserve Univ.
Robert G. Deissler (Case Western Reserve Univ., Cleveland, OH.) May 1989 102 p
(NASA-TM-101983; E-4682; NAS 1.15:101983) Avail: NTIS HC A06/MF A01 CSCL 20D

Several turbulent and nonturbulent solutions of the Navier-Stokes equations are obtained. The unaveraged equations are used numerically in conjunction with tools and concepts from nonlinear dynamics, including time series, phase portraits, Poincare sections, largest Liapunov exponents, power spectra, and strange attractors. Initially neighboring solutions for a low-Reynolds-number fully developed turbulence are compared. The solutions, separate exponentially with time, having a positive Liapunov exponent. Thus the turbulence is characterized as chaotic. In a search for solutions which contrast with the turbulent ones, the Reynolds number is reduced. Several qualitatively different flows are noted. These are, fully chaotic, complex period, weakly chaotic, simple periodic, and fixed-point. Of these, only the fully chaotic flows are classified as turbulent. Those flows have both a positive Liapunov exponent and Poincare sections without pattern. By contrast, the weakly chaotic flows have some pattern in their Poincare sections. The fixed-point and periodic flows are nonturbulent, since turbulence, is both time-dependent and aperiodic. Turbulent solutions are obtained in which energy cascades from large to small-scale motions. In general, the spectral energy transfer takes place between wavenumber bands that are considerably separated. The special transfer can occur either as a result of nonlinear turbulence self-interaction or by interaction of turbulence with mean gradients. Turbulent systems are compared with those studied in kinetic theory. The two types of systems are fundamentally different (continuous and dissipative as opposed to discrete and conservative), but there are similarities. For instance, both are nonlinear and show sensitive dependence on initial conditions. Also, the turbulent and molecular stress tensors are identical if the macroscopic velocities for the turbulent stress are replaced by molecular velocities. Author

N89-23814# Technische Univ., Delft (Netherlands).
SOME APPLICATIONS OF THE QUALITATIVE THEORY OF DIFFERENTIAL EQUATIONS IN FLUID DYNAMICS Ph.D. Thesis
Pieter Gerrit Bakker 1988 195 p
(ETN-89-94143) Avail: NTIS HC A09/MF A01

The qualitative theory of differential equations is used along with topological considerations to discuss problems in fluid dynamics and gasdynamics. Special attention is given to the qualitative aspects of flow fields, in particular to the geometry, the shape, and the structural stability of streamline patterns. The theory relies much on critical point analyses and on bifurcations in vector fields. Local solutions of the flow equations are derived to dicuss changes in flow topology in conjuntion with bifurcations of critical points. The theory is applied to inviscid, nonlinear conical flows and steady viscous flows over plane walls. ESA

N89-23815# National Aerospace Lab., Amsterdam (Netherlands). Space Div.
TELESCIENCE AND IMAGE PROCESSING FOR PODI: AN ANALYSIS AND A PROPOSAL FOR A SIMULATION SET-UP
E. A. Kuijpers 24 Dec. 1987 45 p Original contains color illustrations
(Contract NIVR-2405N)
(NLR-TR-88005-U; ETN-89-94198) Avail: NTIS HC A03/MF A01

A prototype optical diagnostic instrument (PODI) for microgravity fluid physics was developed. The instrument consists of a whole field Schlieren and scene observation system combined with a narrow field optical stimulus/observation system which can accommodate various optical diagnostic instruments. An equal beam Twyman-Green interferometer and a moire deflectometer were developed as passengers for the narrow field system. Adding an electronic subsystem with a digitizing capability for camera images makes quantitative analyses possible. Positioning devices and an additional camera enable computer controlled data acquisition and experiment control. For use in a fluid science facility, PODI should be developed taking into account requirements for telescience. Requirements related to communication, on board processing, and ground station processing are discussed. Image processing algorithms for PODI and for which space application should be considered are described. Prototyping is needed to extend PODI with image acquisition and experiment control. Telescience concepts and several image processing algorithms need prototyping also. For prototyping an additional electronic subsystem with image acquisition capabilities is proposed. ESA

N89-23816# Aeronautical Research Inst. of Sweden, Stockholm. Aerodynamics Dept.
OPEN BOUNDARY CONDITIONS FOR THE NAVIER-STOKES EQUATION
Jan Nordstrom 5 May 1988 61 p Sponsored by the Swedish Board for Technical Development
(FFA-145; ETN-89-94225) Avail: NTIS HC A04/MF A01; Almqvist and Wiksell, Bocksellers, Printers, Publishers, Stockholm, Sweden, 100 Swedish crowns

The question of open boundary conditions of in and outflow type for the Navier-Stokes equation is related to that of the boundary condition used for the Euler equations. The continuous and semidiscrete problem are analyzed using the energy method and the Laplace-transform technique. The energy-method is used to derive well-posed boundary conditions for the continuous problem. For the semidiscrete problem the energy-method is used to prove that by using the well-posed boundary conditions for the continuous problem and adding a suitable numerical boundary condition, well-posedness is preserved. By employing the Laplace-transform technique the spectra for different types of boundary conditions are obtained. The spectra are analyzed and it is shown how the choice of boundary conditions strongly affects the convergence to steady-state. One-dimensional Navier-Stokes calculations are performed and the resulting convergence rates agree well with the theoretical analysis. Spectra obtained using in and outflow type of boundary conditions are compared with spectra obtained using periodic boundary conditions, and the choice of time-integration method for the Navier-Stokes equation is discussed. ESA

N89-23817*# Institute for Computer Applications in Science and Engineering, Hampton, VA.
NUMERICAL SIMULATION OF GOERTLER/TOLLMEIN-SCHLICHTING WAVE-INTERACTION Final Report
M. R. Malik and M. Y. Hussaini (High Technology Corp., Hampton, VA.) Mar. 1989 31 p Prepared in cooperation with NASA, Langley Research Center Submitted for publication
(Contract NAS1-18605)

(NASA-CR-181823; ICASE-89-21; NAS 1.26:181823) Avail: NTIS HC A03/MF A01 CSCL 20D

The problem of nonlinear development of Goertler vortices and interaction with Tollmein-Schlichting (TS) waves is considered within the framework of incompressible Navier-Stokes equations which are solved by a Fourier-Chebyshev spectral method. It is shown that two-dimensional waves can be excited in the flow modulated by Goertler vortices. Due to nonlinear effects, this interaction further leads to the development of oblique waves with spanwise wavelength equal to the Goertler vortex wavelength. Interaction is also considered of oblique waves with spanwise wavelength twice that of Goertler vortices. Author

N89-23818*# Analex Corp., Cleveland, OH.
NUMERICAL STUDIES OF THE EFFECTS OF JET-INDUCED MIXING ON LIQUID-VAPOR INTERFACE CONDENSATION Final Report
Chin-Shun Lin Apr. 1989 22 p Presented at the 24th Thermophysics Conference, Buffalo, NY, 12-14 Jun. 1989; sponsored by AIAA
(Contract NAS3-24564)
(NASA-CR-182285; E-4749; NAS 1.26:182285; AIAA-89-1744)
Avail: NTIS HC A03/MF A01 CSCL 20D

Numerical solutions of jet-induced mixing in a partially full cryogenic tank are presented. An axisymmetric laminar jet is discharged from the central part of the tank bottom toward the liquid-vapor interface. Liquid is withdrawn at the same volume flow rate from the outer part of the tank. The jet is at a temperature lower than the interface, which is maintained at a certain saturation temperature. The interface is assumed to be flat and shear-free and the condensation-induced velocity is assumed to be negligibly small compared with radial interface velocity. Finite-difference method is used to solve the nondimensional form of steady state continuity, momentum, and energy equations. Calculations are conducted for jet Reynolds numbers ranging from 150 to 600 and Prandtl numbers ranging from 0.85 to 2.65. The effects of above stated parameters on the condensation Nussett and Stanton numbers which characterize the steady-state interface condensation process are investigated. Detailed analysis to gain a better understanding of the fundamentals of fluid mixing and interface condensation is performed. Author

N89-23819*# National Aeronautics and Space Administration. Ames Research Center, Moffett Field, CA.
EFFECT OF INTERNAL CONVECTION AND INTERNAL RADIATION ON THE STRUCTURAL TEMPERATURES OF SPACE SHUTTLE ORBITER
William L. Ko, Robert D. Quinn, and Leslie Gong Oct. 1988 34 p
(NASA-TM-100414; H-1466; NAS 1.15:100414) Avail: NTIS HC A03/MF A01 CSCL 20D

Structural performance and resizing of the finite-element thermal analysis computer program was used in the reentry heat transfer analysis of the space shuttle orbiter. One midfuselage cross section and one midspan wing segment were selected to study the effects of internal convection and internal radiation on the structural temperatures. The effect of internal convection was found to be more prominent than that of internal radiation in the orbiter thermal analysis. Without these two effects, the calculated structural temperatures at certain stations could be as much as 45 to 90 percent higher than the measured values. By considering internal convection as free convection, the correlation between the predicted and measured structural temperatures could be improved greatly. Author

N89-23820*# National Aeronautics and Space Administration. Ames Research Center, Moffett Field, CA.
A NUMERICAL STUDY OF VISCOUS VORTEX RINGS USING A SPECTRAL METHOD
S. K. Stanaway, B. J. Cantwell (Stanford Univ., CA.), and Philippe R. Spalart Oct. 1988 170 p Previously announced as N89-22572
(NASA-TM-101041; A-88306; NAS 1.15:101041) Avail: NTIS HC A08/MF A01 CSCL 20D

Viscous, axisymmetric vortex rings are investigated numerically by solving the incompressible Navier-Stokes equations using a spectral method designed for this type of flow. The results presented are axisymmetric, but the method is developed to be naturally extended to three dimensions. The spectral method relies on divergence-free basis functions. The basis functions are formed in spherical coordinates using Vector Spherical Harmonics in the angular directions, and Jacobi polynomials together with a mapping in the radial direction. Simulations are performed of a single ring over a wide range of Reynolds numbers (Re approximately equal gamma/nu), 0.001 less than or equal to 1000, and of two interacting rings. At large times, regardless of the early history of the vortex ring, it is observed that the flow approaches a Stokes solution that depends only on the total hydrodynamic impulse, which is conserved for all time. At small times, from an infinitely thin ring, the propagation speeds of vortex rings of varying Re are computed and comparisons are made with the asymptotic theory by Saffman. The results are in agreement with the theory; furthermore, the error is found to be smaller than Saffman's own estimate by a factor square root ((nu x t)/R squared) (at least for Re=0). The error also decreases with increasing Re at fixed core-to-ring radius ratio, and appears to be independent of Re as Re approaches infinity). Following a single ring, with Re=500, the vorticity contours indicate shedding of vorticity into the wake and a settling of an initially circular core to a more elliptical shape, similar to Norbury's steady inviscid vortices. Finally, we consider the case of leapfrogging vortex rings with Re=1000. The results show severe straining of the inner vortex core in the first pass and merging of the two cores during the second pass. Author

N89-23821*# National Aeronautics and Space Administration. Lewis Research Center, Cleveland, OH.
ON THE LAGRANGIAN DESCRIPTION OF UNSTEADY BOUNDARY LAYER SEPARATION. PART 1: GENERAL THEORY
Leon L. VanDommelen and Stephen J. Cowley (Imperial Coll. of Science and Technology, London, England) May 1989 50 p
(NASA-SAA-C-99066-G)
(NASA-TM-102026; E-4770; ICOMP-89-8; NAS 1.15:102026)
Avail: NTIS HC A03/MF A01 CSCL 20D

Although unsteady, high-Reynolds number, laminar boundary layers have conventionally been studied in terms of Eulerian coordinates, a Lagrangian approach may have significant analytical and computational advantages. In Lagrangian coordinates the classical boundary layer equations decouple into a momentum equation for the motion parallel to the boundary, and a hyperbolic continuity equation (essentially a conserved Jacobian) for the motion normal to the boundary. The momentum equations, plus the energy equation if the flow is compressible, can be solved independently of the continuity equation. Unsteady separation occurs when the continuity equation becomes singular as a result of touching characteristics, the condition for which can be expressed in terms of the solution of the momentum equations. The solutions to the momentum and energy equations remain regular. Asymptotic structures for a number of unsteady 3-D separating flows follow and depend on the symmetry properties of the flow. In the absence of any symmetry, the singularity structure just prior to separation is found to be quasi 2-D with a displacement thickness in the form of a crescent shaped ridge. Physically the singularities can be understood in terms of the behavior of a fluid element inside the boundary layer which contracts in a direction parallel to the boundary and expands normal to it, thus forcing the fluid above it to be ejected from the boundary layer. Author

N89-23822 Colorado Univ., Boulder.
COMPUTATION OF DYNAMICS AND CONTROL OF UNSTEADY VORTICAL FLOWS PH.D. Thesis
Kalpana Chawla 1988 147 p
Avail: Univ. Microfilms Order No. DA8902887

In the first part of this work, unsteady, two-dimensional, vortical flows past stationary and oscillating normal plates and airfoil

configurations with stationary and oscillating spoilers are studied using the Discrete-Vortex method. Vortical structures as well as unsteady life and drag were computed for various flow conditions and body configurations. The comparison of force results for the airfoil configurations involving oscillating spoilers with the corresponding stationary cases indicates that there is no appreciable difference between the average values of life and drag. In the second part, computational models are presented for multi-vortex systems in the presence of acoustic waves. Computational models are developed to study the stability of single infinite row of vortices and Karman's infinite, unsymmetric, double row of vortices. Results suggest that acoustic waves of specific wavelengths can be used to destabilize the Karman street manifested in nature, so as to scatter its vortices in an effort to weaken its impact. It is also shown that for vortex systems made up of small number of vortices, redistribution or recombination of vortices by conserving strength of the system and maintaining constant center of vorticity can result in vortex systems with different properties compared to the original systems.

Dissert. Abstr.

N89-23823*# National Aeronautics and Space Administration. Lewis Research Center, Cleveland, OH.

TWO-DIMENSIONAL NUMERICAL SIMULATION OF A STIRLING ENGINE HEAT EXCHANGER

Mounir B. Ibrahim (Cleveland State Univ., OH.), Roy C. Tew, and James E. Dudenhoefer 1989 13 p Prepared for presentation at the 24th Intersociety Energy Conversion Engineering Conference, Washington, DC, 6-11 Aug. 1989; sponsored by IEEE, AIAA, ANS, ASME, SAE, ACS, and AIChE

(NASA-TM-102057; E-4815; NAS 1.15:102057) Avail: NTIS HC A03/MF A01 CSCL 20D

The first phase of an effort to develop multidimensional models of Stirling engine components is described; the ultimate goal is to model an entire engine working space. More specifically, parallel plate and tubular heat exchanger models with emphasis on the central part of the channel (i.e., ignoring hydrodynamic and thermal end effects) are described. The model assumes: laminar, incompressible flow with constant thermophysical properties. In addition, a constant axial temperature gradient is imposed. The governing equations, describing the model, were solved using Crank-Nicloson finite-difference scheme. Model predictions were compared with analytical solutions for oscillating/reversing flow and heat transfer in order to check numerical accuracy. Excellent agreement was obtained for the model predictions with analytical solutions available for both flow in circular tubes and between parallel plates. Also the heat transfer computational results are in good agreement with the heat transfer analytical results for parallel plates.

Author

N89-23824# Ballistic Research Labs., Aberdeen Proving Ground, MD.

DERIVATION OF A GODUNOV ONE DIMENSIONAL FLUID DYNAMICS CODE

Hubert W. Meyer, Jr. Dec. 1988 111 p

(AD-A205463; BRL-TR-2975) Avail: NTIS HC A06/MF A01 CSCL 12/5

This report details the development of a one dimensional code using the Godunov method, which is the first part of a larger effort to develop an axisymmetric fluid dynamics code. The ultimate objective flow field associated with a shaped charge jet, in order to study how and to what extent perturbations of the jet are caused by interactions of the flow field with various target geometries. The report contains detailed derivations of the equations involved in the one dimensionals Godunov method, and the incorporation of these equations into a computer program. Many of these basic relationships are applicable to the axisymmetric code. A shock tube experiment was conducted to test the predictions of the program. The program accurately predicted all aspects of the shock tube flow, being within 2 percent of experimental values for pressure, 6 percent of experimental values for velocity, and 1 percent of theoretical values for density.

GRA

N89-23825# Naval Ocean Systems Center, San Diego, CA.

DRAG AND NOISE MEASUREMENTS ON UNDERWATER VEHICLES WITH A RIBLET SURFACE COATING Professional Paper for period ending Jul. 1989

Marc C. Gillcrist and Laurel W. Reidy Jan. 1989 3 p

(AD-A205500) Avail: NTIS HC A02/MF A01 CSCL 13/10

The purpose of this study was to investigate both the drag and noise reducing effects of riblet surface coatings on marine vehicles. The use of microgrooves, or riblets, for skin friction reduction originated at NASA Langley for aerodynamic applications. Water tunnel tests at the Naval Ocean Systems Center (NOSC), San Diego, have shown that reductions in skin friction of up to 8 percent can be achieved with sharp peaked riblets of appropriate size, when applied to a flat plate in a turbulent boundary layer. It is reasonable to suspect that a reduction in flow noise might accompany the measured reduction in skin friction. In fact, wind tunnel tests on a flat plate, conducted in cooperation with University of California at fullerton, indicate a 2 to 3 dB reduction in noise at the peak in the turbulent boundary layer spectrum when riblets are used. The flat plate laboratory experiments led to the current effort to study hydrodynamic drag and noise reduction on underwater vehicles. Because undersea vehicles are subject to fouling from marine organisms, the effect of biofouling on riblets was also studied.

GRA

N89-23826# Yale Univ., New Haven, CT.

SPECTROMETRIC STUDIES OF GAS PHASE COLLISION PROCESSES Final Report, 1 Aug. 1987 - 31 Jul. 1988

J. B. Fenn 10 Feb. 1989 3 p

(Grant AF-AFOSR-0323-87; AF Proj. 2303)

(AD-A205570; AFOSR-89-0309TR) Avail: NTIS HC A02/MF A01 CSCL 07/4

Measurements have been made of the total radiation intensity from free jets of carbon dioxide and carbon that were excited in the source by a corona discharge. The radiation per molecule, obtained from the ratio of total intensity to source density, increases sharply when source temperature and pressure are such as to produce clustering in a jet of unexcited gas. We believe this enhancement may be due to interaction between aligned dipoles in adjacent cluster molecules. Measurements of the terminal rotational temperature of carbon monoxide and CO2, both pure in admixture with each other and/or argon indicate that CO always relaxes more slowly. There is no evidence of coupling between the rotational modes of the two species.

GRA

N89-23827# Naval Postgraduate School, Monterey, CA.

RAYLEIGH-TAYLOR INSTABILITY OF A VISCOUS FILM OVERLYING A PASSIVE FLUID Technical Report, Jun. 1985 - Apr. 1987

David Canright and Stephen Morris Feb. 1989 54 p

(AD-A205578; NPS53-89-012) Avail: NTIS HC A04/MF A01 CSCL 20/4

To help understand the stability of cold, viscous boundary layers in geophysical contexts such as lava lakes and mantle convection, the following model problem is analyzed: Beneath a shear-free horizontal boundary, a thin layer of very viscous fluid overlies a deep layer of less viscous, less dense fluid. The initial unstable equilibrium is perturbed, and the growth of the disturbance is followed, including the nonlinear effects of large amplitude, by a long-wave analysis. The result shows that, in the final catastrophic growth, the peak thickness of the upper layer approaches infinity inversely proportional to the remaining time. (This conclusion also applies to fluids with power-law rheology.) Thus nonlinear effects greatly enhance growth.

GRA

N89-23828# Virginia Polytechnic Inst. and State Univ., Blacksburg. Dept. of Engineering Science and Mechanics.

THREE-DIMENSIONAL STRUCTURE OF BOUNDARY LAYERS IN TRANSITION TO TURBULENCE Final Report, 1 Mar. 1987 - 30 Jun. 1988

Herbert Thornwald 6 Feb. 1989 12 p

(Contract F49620-87-K-0005)

(AD-A205587; AFOSR-89-0303TR) Avail: NTIS HC A03/MF A01 CSCL 20/4

The Floquet theory of secondary instability in shear flows has been further developed and applied to a variety of flows. The linear theory has been extended to explain and quantitatively analyze the observed combination resonance in boundary layers. Numerical methods for the study of secondary instability in unbounded flows have been developed and applied to the viscous and inviscid mixing layer. The linear theory has been formulated for a variety of spatially periodic flows that include Gortler vortices and oblique waves. Applications await accounting for nonparallel effects. A new approach to analyzing nonparallel flows based on parabolic partial differential equations has been successfully applied to the primary stability problem. A perturbation method has been successfully applied to the primary stability problem. A perturbation method has been developed to reveal the nonlinear interactions that lead to breakdown of the laminar flow. This method permits prediction of the transition location in a given disturbance environment. GRA

N89-23829# Stanford Univ., CA. Dept. of Mechanical Engineering.

BIFURCATING JETS AT HIGH REYNOLDS NUMBERS

D. E. Parekh, A. Leonard, and W. C. Reynolds 7 Dec. 1988 265 p

(Contracts F49620-84-K-0005; F49620-86-K-0020)

(AD-A205718; TF-35; AFOSR-89-0282TR) Avail: NTIS HC A12/MF A01 CSCL 20/4

There is much interest in the use of controlled excitations to manage various types of flows. This work focuses on use of dual-mode forcing to alter dramatically the structure of round turbulent jets. Properly-combined axial and helical excitations can cause a round jet to split into two distinct jets. This Y-shaped jet, known as a bifurcating jet, exhibits spreading angles as high as 80 deg. Vortex rings are formed at the jet exit and propagate along the two branches of the jet. A vortex-filament code was developed for simulating the large-scale features of bifurcating jets. The motion and interaction of the vortex structures in this flow are tracked in a three-dimensional, Lagrangian coordinate system. This simulation showed that inviscid vortex interactions cause the dramatic changes in jet development and that spreading angle increases with axial Strouhal number. The experimental apparatus consists of an acoustically-excited, 2-cm-diameter air jet. The jet evolution is documented by flow visualization at velocities up to 75 m/s, Reynolds numbers up to 100,000, and Mach numbers up to 0.22. Instantaneous and phase-average cross-sections of the jet reveal the effects of forcing amplitude on the structure and spreading angle of axially-excited, helically-excited, and bifurcating jets. GRA

N89-23830# North Carolina Univ., Chapel Hill. Dept. of Mathematics.

NONLINEAR SYSTEMS OF CONSERVATION LAWS Final Report, Jul. 1987 - Sep. 1988

Michael Shearer 21 Nov. 1988 6 p

(Grant AF-AFOSR-0283-87; AF Proj. 2304)

(AD-A205837; AFOSR-89-0076TR) Avail: NTIS HC A02/MF A01 CSCL 12/1

This final report covers research in the following areas: (1) Non-strictly hyperbolic conservation laws: Change of type of equations modelling three phase flow in porous media, solution of Riemann problems; (2) Plastic flow in two dimensions: Linear stability of homogeneous deformations, justification of the quasidynamic approximation; and (3) Glimm's method for the vibrating string' discovery of exact solutions related to a periodic motion. GRA

N89-23831# Nielsen Engineering and Research, Inc., Mountain View, CA.

EXPLOITATION OF MULTIPLE SOLUTIONS OF THE NAVIER-STOKES EQUATIONS TO ACHIEVE RADICALLY IMPROVED FLIGHT Final Report, 1 Aug. 1988 - 31 Jan. 1989

David Nixon, S. C. Caruso, and M. Farshchi 27 Feb. 1989 50 p

(Contract F49620-88-C-0097; AF Proj. 3005)

(AD-A205939; NEAR-TR-398; AFOSR-89-0364TR) Avail: NTIS HC A03/MF A01 CSCL 20/4

It is known that the nonlinear Navier Stokes equations will model most fluid flow of aeronautical interest. The existence and uniqueness of the solutions to the Navier-Stokes equations have not been proven although it is known that in certain cases only the most stable solution is obtained. This present work is concerned with identifying multiple solutions of the Navier-Stokes equations for transonic flow. The objective is to exploit the existence of these solutions rather than avoid them as has been the custom in the past. The present work has shown that the cause of multiple solutions in potential flow is a bifurcation of solutions at a specific Mach number distribution; airfoils can be designed to give such a distribution. It is also found that the presence of entropy and vorticity do not affect the occurrence of phantom solutions. A physical example of a phantom solution is explained by a study of the potential phantom solutions. GRA

N89-23832# Naval Postgraduate School, Monterey, CA.

INVESTIGATION OF INCOMPRESSIBLE CASCADE FLOWS USING A VISCOUS/INVISCID INTERACTIVE CODE M.S. Thesis

Zeev Snir Dec. 1988 135 p

(AD-A205972) Avail: NTIS HC A07/MF A01 CSCL 20/4

A two dimensional, incompressible viscous inviscid interaction computer code, designed to compute cascade flows, was investigated. Comparison of the flow characteristics predicted by the code with experimentally available data indicates that the code predicts reasonably well flow parameters on lightly loaded cascades. However, the code fails to predict correctly the actual boundary layer development and the velocity distribution for highly loaded cascades. It is concluded that further improvement of the code is needed and recommendations are presented to achieve the required improvements. GRA

N89-23833# Scientific Research Associates, Inc., Glastonbury, CT.

COMPUTATION OF FLOW AROUND MANEUVERING SUBMERGED BODIES Final Report

T. R. Govindan, W. R. Briley, and R. Levy Oct. 1988 33 p

(Contract N00167-86-C-0049)

(AD-A205994; SRA-R88-920029-F) Avail: NTIS HC A03/MF A01 CSCL 20/4

Generalized primary/secondary flow equations and a spatial-marching solution algorithm have been used to develop a procedure to compute the three-dimensional viscous flow around a submerged body in maneuver. The primary/secondary flow equations are an approximation to the Navier-Stokes equations for flows in which a primary flow direction can be identified. Important elements of the approximation are a locally specified primary flow direction and a decomposition of the secondary velocity field to identify a small velocity vector for approximations. No approximations are introduced for pressure in this approach. The primary/secondary flow equations are a well-posed initial-value problem in a spatial coordinate nominally aligned with the primary flow direction and are solved by a sequentially decoupled implicit algorithm. The procedure provides an order to two orders-of-magnitude run time advantage over solution of the Navier-Stokes equations. Results are presented for the flow past an unappended submarine hull in drift at a Reynolds number of 16 million and incidence of 20 degrees. These results are consistent with experimental observations and provide a means to compute the complex three-dimensional viscous flow field economically. GRA

N89-23834# Air Force Inst. of Tech., Wright-Patterson AFB, OH. School of Engineering.

TWO-DIMENSIONAL CONFINED JET THRUST VECTOR CONTROL: OPERATING MECHANISMS AND PERFORMANCE M.S. Thesis

Jeffrey L. Caton Mar. 1989 167 p
(AD-A206011; AFIT/GAE/AA/89M-1) Avail: NTIS HC A08/MF A01 CSCL 20/4

An experimental investigation of two-dimensional confined jet thrust vector control nozzles was performed. Thrust vector control was accomplished by using secondary flow injection in the diverging section of the nozzle. Schlieren photographs and video tapes were used to study flow separation and internal shock structures. Nozzle performance parameters were determined for nozzle flow with and without secondary flows. These parameters included nozzles forces, vector angles, thrust efficiencies, and flow switching response times. Vector angles as great as 18 degrees with thrust efficiencies of 0.79 were measured. Several confined jet nozzles with variations in secondary flow port design were tested and results were compared to each other. Converging-diverging nozzles of similar design to the confined jet nozzles were also tested and results were compared to the confined jet nozzle results. Existing prediction models for nozzle side to axial force ratio were evaluated. A model for nozzle total forces based on shock losses that predicted values very close to actual results was developed. GRA

N89-23835# Stanford Univ., CA. Dept. of Mechanical Engineering.
THE DIMENSION OF ATTRACTORS UNDERLYING TURBULENT POISEUILLE FLOW Final Report, 1 Dec. 1987 - 30 Jan. 1989
Laurence Keefe and Parviz Moin 13 Feb. 1989 37 p
(Grant AF-AFOSR-0056-88; AF Proj. 2307)
(AD-A206021; AFOSR-89-0304TR) Avail: NTIS HC A03/MF A01 CSCL 20/4

It is shown that fully developed channel flow is confined to a strange attractor. However, the dimension of the attractor is much larger than dimensions encountered in closed flows such as Benard Convection and Taylor-Couette flow. In addition, we have examined the relationship between turbulent structures and attractor geometry. In the end, what is sought from any theory of turbulence is a universal framework that allows known phenomena to be understood, calculated, and related, and a predictive capability for unknown flows or control measures. Crucial to the erection of such a structure is a knowledge of the fundamental mathematical character of turbulence. The purpose of this research has been to investigate this character to determine if chaos theory and the strange attractor can provide the foundation for such a global theory. GRA

N89-23836# Air Force Inst. of Tech., Wright-Patterson AFB, OH. School of Engineering.
COMPARISON OF SPLIT-FILM AND x-FILM MEASUREMENTS IN 2-D FLOW M.S. Thesis
Timothy E. Fisk Nov. 1988 76 p
(AD-A206023; AFIT/GAE/AA/88D-16) Avail: NTIS HC A05/MF A01 CSCL 20/4

The purpose of these experiments was to compare turbulence measurements using two types of velocity measurement probes: split-film and x-film. The goal is to determine the turbulent flow regimes where the split-film can be used to replace the x-film. The split-film sensor is composed of two independent films supported by a quartz filament. The split-film's larger diameter makes it less sensitive to high frequency fluctuations than the x-film, but is able to measure higher flow angles than the x-film. The objective of this thesis is to compare turbulence measurements of the split-film with the more established x-film over a range of turbulence levels. Results indicate problems using the split-film in regions of low velocity combined with low turbulence (Reynolds number based on film diameter less than 380 and turbulence intensity below 1.5 percent). The split-film provided better turbulence measurements than the x-film when used in regions of high turbulence (10 to 50 percent) with velocity fluctuations greater than 45 deg from the mean. The split-film is not capable of detecting flow reversals, but will give the proper direction of the velocity component normal to the split. This information is helpful because the magnitude of the Reynolds shear stress in reversing flow can still be determined using the split-film, but not the direction (sign). GRA

N89-23837# Iowa State Univ. of Science and Technology, Ames. Dept. of Aerospace Engineering.
THREE DIMENSIONAL HIGH SPEED BOUNDARY LAYER FLOWS Final Report, Sep. 1985 - May 1988
George R. Inger 28 Sep. 1988 61 p
(Grant AF-AFOSR-0357-85; AF Proj. 2307)
(AD-A206145; AFOSR-89-0287TR) Avail: NTIS HC A04/MF A01 CSCL 20/4

This final report summarizes the research results obtained by a two-faceted basic theoretical investigation involving: (1) fundamental analyses of three-dimensional viscous-inviscid interaction effects within high speed turbulent boundary layers, and (2) study of the influence of streamwise vortex arrays on the skin friction within attached or separated laminar layer flows. GRA

N89-23838# Naval Research Lab., Washington, DC. Ocean Technology Program.
TURBULENCE NEAR A FREE SURFACE IN A PLANE JET Interim Report, Oct. 1987 - 14 Mar. 1989
S. E. Ramberg, T. F. Swean, Jr., and M. A. Plesnia 14 Mar. 1989 51 p Prepared in cooperation with Stanford Univ., CA
(AD-A206269; NRL-MR-6367) Avail: NTIS HC A04/MF A01 CSCL 20/4

Laboratory measurements of the turbulent flow in a plane jet issuing at the free surface are reported and analyzed. Single point hot-film data were obtained for mean velocities and turbulent fluctuations of velocity and shear stress in the developing jet to (X sub 1)/(b sub 0) = 240 with an emphasis on the near surface turbulent behavior. Synoptic behavior of the jet resembled that of a 2D wall jet rather than one half of a planar free jet with the free surface represented by the symmetry plane. The effects of jet confinement are to retard the ability of the jet to entrain fluid, to decrease the growth rate of the length scale and to increase the decay rate of the velocity scale. Mean velocity profile similarity is still observed when the data is non-dimensionalized with the reduced scales. Jet momentum will appear to have been lost due to momentum exchange with the return flow. An approximate analysis provides a means to estimate the momentum loss due to limited depth and is shown to correlate well with scale development in several jet configurations for these and prior experiments. One-dimensional turbulence spectra revealed blocking of certain vertical scales as the free surface is approached with a concommitant redistribution of turbulent kinetic energy from the vertical fluctuations to the lateral components. GRA

N89-23839# Princeton Univ., NJ.
MATHEMATICAL ANALYSIS OF STRONG FLUID MECHANICAL EFFECTS IN REACTING AND NONREACTING GASES Final Report, 1 Oct. 1985 - 31 Dec. 1988
Andrew J. Majda 13 Jan. 1989 3 p
(Contract DAAL03-86-K-0003)
(AD-A206336; ARO-22943.12-MA) Avail: NTIS HC A02/MF A01 CSCL 20/4

The research performed under this grant includes mathematical analysis of strong fluid mechanical effects in reacting and nonreacting gases. The following topics have been studied during this three year period: (1) Numerical Modelling of Initiation and Detonation Wave Stability in Multi-D; (2) Enhanced Combustion through Nonlinear Wave Interaction; and (3) New Criteria to Predict Regular Spacing of Reacting Mach Stems. GRA

N89-23840# Institut Franco-Allemand de Recherches, Saint-Louis (France).
ANALOGY BETWEEN EXPLOSIVE WAVE AND FRONT WAVE NEAR CURVED WALLS [DIE ANALOGIE EXPLOSIONSWELLE-KOPFWELLE NAHE GEKRUEMMTEN WAENDEN]
K. W. Naumann 13 Apr. 1987 18 p In GERMAN Presented

at the Fruehjahrstagung der Deustchen Physikalischen Gesellschaft im Fachgremium Kurzzeitphysik, Goettingen, Fed. Republic of Germany, 16-20 Mar. 1987
(ISL-CO-209/87; ETN-89-94109) Avail: NTIS HC A03/MF A01

Three dimensional steady flow field propagation around a curved wall is investigated by means of analogy with a two dimensional non steady state detonation wave. Analytical detonation wave equations are transformed taking in account the shock front surface changes with the detonation wave radius. A family of spiraloid concave contour lines is obtained for which Sakurai distribution functions are applied. For the other contour configurations, a short time energy source is proposed. ESA

N89-23841# Institut Franco-Allemand de Recherches, Saint-Louis (France).
BOUNDARY LAYER AND HEAT TRANSFER BEHIND A PISTON IN A SHOCK TUBE. PART 1: THEORETICAL CONSIDERATIONS OF LAMINAR AND TURBULENT BOUNDARY LAYER BEHIND A PISTON IN A TUBE Final Report [GRENZSCHICHT UND WAERMEUEBERGANG AM FLUGKOLBEN. TEIL 1: THEORETISCHE BETRACHTUNG DER LAMINAREN UND TURBULENTEN GRENZSCHICHT HINTER DEM KOLBEN IM ROHR]
F. Seiler and J. Srulijes 30 Apr. 1987 80 p In GERMAN
(Contract BMVg-T/R-760/F-0007/F-1707)
(ISL-R-111/87-Pt-1; ETN-89-94114) Avail: NTIS HC A05/MF A01

Laminar and turbulent compressible boundary layers behind a piston in a shock tube are studied. The boundary layer behavior is calculated by means of Prandtl equations neglecting time dependent factors. Boundary layer configuration between tube inlet and projectile is obtained by coupling two types of layer: one non steady state of piston type, and the other steady state of plate type. Mass and motion conservation equations are resolved by a Runge-Kutta method for the laminar and turbulent boundary layers determination. Heat flow and boundary layer thickness are calculated in both cases and compared with experimental results. ESA

N89-23842# Institut Franco-Allemand de Recherches, Saint-Louis (France).
BOUNDARY LAYER AND HEAT TRANSFER BEHIND A PISTON IN A SHOCK TUBE. PART 2: EXPERIMENTAL STUDY OF HEAT TRANSFER AT THE PISTON IN A TUBE Final Report [GRENZSCHICHT UND WAERMEUEBERGANG AM FLUGKOLBEN. TEIL 2: EXPERIMENTELLE UNTERSUCHUNG DES WAERMEUEBERGANGS AM KOLBEN IM ROHR]
F. Seiler 16 Jul. 1987 46 p In GERMAN
(Contract BMVg-T/R-760/F-0007/F-1707)
(ISL-R-115/87-Pt-2; ETN-89-94115) Avail: NTIS HC A03/MF A01

By model experiments in shock tube interiors, ballistics before and behind a projectile are simulated. Heat transfer in tube walls and in piston walls with and without air gap are studied by means of compressed air fluid flow. Lengthwise piston splits of 10 to 50 mm length and of 0.5 to 5 mm depth are managed for the demonstration of air gap effects. Results indicate that heat transfer depends on the same manner of split length and depth. Higher gas temperatures increase also this dependance of wall temperature, heat flow in tube wall and heat transfer from split length and depth. ESA

N89-23843# Institut Franco-Allemand de Recherches, Saint-Louis (France).
NUMERICAL SOLUTION OF THE THREE DIMENSIONAL HEAT FLOW EQUATION GENERATED BY A MOVING SOURCE [NUMERISCHE LOESUNG DER DREIDIMENSIONALEN WAERMELEITUNGSGLEICHUNG MIT BEWEGTER WAERMEQUELLE]
M. Schellhorn 24 Jul. 1987 23 p In GERMAN
(ISL-R-116/87; ETN-89-94116) Avail: NTIS HC A03/MF A01

A numerical analysis method for heat conduction in a finite solid heated by a HF-laser beam is described. The three dimensional model takes into account heat source linear motion, material temperature coefficients, phase transformations (fusion, vaporization) heat dissipation and convective loss to an ambiant gas. Heat sources are included into the differential equations so that surface absorption and volume absorption can be considered for opalescent or transparent materials. The model is time dependent and is applied to temperature distribution calculation at welding crown glass with HF-laser beam. ESA

N89-23844# Metraflu, Ecully (France).
A SIMPLE APPROXIMATE METHOD TO EVALUATE THE 3-D AERODYNAMIC FIELD AROUND A STREAMLINE AND TO DETERMINE THE VALIDITY OF THE QUASI-THREE DIMENSIONAL HYPOTHESIS
J.-M. Duchemin and F. Jean (Societe Europeenne de Propulsion, Vernon, France) 1988 8 p Sponsored by CNES, France
(ETN-89-94366) Avail: NTIS HC A02/MF A01

The quasi three dimensional (Q3D) calculation method is described. It is based on the hypothesis of axisymetric surfaces and is widely used in turbomachinery design. An attempt to determine the validity of the method is presented. The model is based on the calculation of the 3D velocity and total pressure field around a streamline in a steady incompressible inviscid flow. It is shown that a first order approximation can lead to accurate and important results. ESA

N89-23845# Aerospatiale, Cannes La Bocca (France). Space and Strategic Systems Div.
THE FLUIDNET DEVELOPMENT AND APPLICATION TO PRELIMINARY SIZING OF FLUID LOOP SYSTEMS
S. Andre, J. N. Chelotti, J. F. Gory, and T. Lafon (Centre National d'Etudes Spatiales, Toulouse, France) Paris, France 1988 8 p
(Rept-882-440-102; ETN-89-94495) Avail: NTIS HC A02/MF A01

An interactive application computer program applicable to preliminary design of fluid loop networks in space thermal control systems is described. The main features are portability, easy implementation, speed, and flexibility. The current version is applied to thermal and hydraulic analysis of single phase fluid loops in steady state. For first application this program is devoted to Hermes thermal control subsystem design. ESA

35 INSTRUMENTATION AND PHOTOGRAPHY

Includes remote sensors; measuring instruments and gages; detectors; cameras and photographic supplies; and holography.

For aerial photography see *43 Earth Resources and Remote Sensing.* For related information see also *06 Aircraft Instrumentation,* and *19 Spacecraft Instrumentation.*

N89-23846# National Inst. of Standards and Technology, Gaithersburg, MD. Temperature and Pressure Div.
LIQUID-IN-GLASS THERMOMETER CALIBRATION SERVICE Final Report
Jacquelyn Wise Sep. 1988 132 p
(PB89-128888; NIST/SP-250/23; LC-88-600580) Avail: NTIS HC A07/MF A01; also available SOD HC $6.00 as 003-003-02891-6 CSCL 14B

A description of the calibration of liquid-in-glass thermometers at the National Bureau of Standards is presented. The calibration equipment and procedures used are discussed in detail. Calculations and stem-temperature corrections are shown and a discussion of the sources of error encountered in calibration and estimates of uncertainties is presented. Author

N89-23847# National Inst. of Standards and Technology, Gaithersburg, MD. Ceramics Div.
DESIGN AND CONSTRUCTION OF A STATE-OF-THE-ART HIGH TEMPERATURE TRIBOMETER Final Report

Jeffrey P. Yellets, Stephen M. Hsu, and E. Erwin Klaus (Pennsylvania State Univ., University Park.) Sep. 1988 215 p (PB89-148332; NIST/SP-755; LC-88-600579) Avail: NTIS HC A10/MF A01; also available SOD HC $11.00 as 003-003-02913-1 CSCL 14B

High temperature ceramic tribology is one of the least understood areas in tribology. The need to understand the mechanisms of friction and wear for ceramic materials is critical. Ceramic materials are being utilized in tool development, bearing design, materials development for low-heat-rejection diesels, automotive gas turbines, Stirling engines, and aerospace applications. The development of a ceramics industry capable of manufacturing high technology wear resistant ceramics is essential in the United States, or the United States will lose a substantial market to an already rapidly growing foreign market. Author

N89-23848 City Univ., London (England).
AUTOMATIC ANALYSIS OF HOLOGRAPHIC INTERFEROGRAMS Ph.D. Thesis
J. C. Hunter 1987 387 p
Avail: Univ. Microfilms Order No. BRDX83290

A technique for producing infinite fringe background holographic interferograms is described. A heat transfer study using fringes to represent isotherms investigated the temperature field and heat transfer distribution over several geometries in a wind tunnel. The fringes represented isotherms. The interferograms were investigated along scan lines that lay essentially perpendicular to the general orientation of the isotherms, and the fringe coordinates were extracted using either a bucket-bin technique or a gradient change algorithm. Results were compared with those of a Large Eddy Simulation, (LES). A compressible flow study investigated the influence of blade incidence upon the flow within low pressure transonic steam turbine blading. Here fringes represented isobars. To simplify the interferograms, a two-dimensional automatic fringe analysis system was devised, involving binarization of the fringe field, followed by detection and tracing of the fringe edges. Fringe coordinates than can by used to produce a map of the complete density distribution. Author

N89-23849# National Technical Systems, Long Beach, CA.
DEVELOPMENT OF AN OPTICAL MULTIGAS DETECTOR Final Report, Jan. 1985 - May 1988
Scott A. Boller Jul. 1988 63 p
(Contract GRI-5084-251-1070)
(PB89-148878; NTS-TR-6005; GRI-88/0245) Avail: NTIS HC A04/MF A01 CSCL 14B

A preproduction model of an optical multigas detector for use as a real-time, portable monitor was developed, demonstrated, field tested, and delivered. The desired operational features of the unit were to be: low cost; portability; small size; light weight, ruggedness; and high sensitivity. This multigas detector was designed for the purpose of detecting gasses related to the use of natural gas in pre-hazardous concentrations. These gasses are methane, carbon monoxide, and nitrogen dioxide. This instrument would facilitate the prevention of hazardous conditions by providing early detection of potentially dangerous gas accumulations. These detectors would also aid in keeping accurate safety records. The chosen detection method is based on spectral absorption of light directed through a chamber where the sample gas is introduced. Electro-optical detectors within the chamber measure light intensity changes due to light absorption at the appropriate wavelength range for each gas. This absorption is a function of gas concentration, light pathlength through the gas, and absorption coefficient for the specific gas. Author

N89-23850*# National Aeronautics and Space Administration. Lewis Research Center, Cleveland, OH.
A VECTOR SCANNING PROCESSING TECHNIQUE FOR PULSED LASER VELOCIMETRY
Mark P. Wernet and Robert V. Edwards (Case Western Reserve Univ., Cleveland, OH.) 1989 19 p Prepared for presentation at the 13th International Congress on Instrumentation in Aerospace Simulation Facilities, Goettingen (Federal Rep. of Germany), 18-21 Sep. 1989; sponsored by IEEE
(NASA-TM-102048; E-4798; NAS 1.15:102048) Avail: NTIS HC A03/MF A01 CSCL 14B

Pulsed laser sheet velocimetry yields nonintrusive measurements of two-dimensional velocity vectors across an extended planar region of a flow. Current processing techniques offer high precision (1 pct) velocity estimates, but can require several hours of processing time on specialized array processors. Under some circumstances, a simple, fast, less accurate (approx. 5 pct), data reduction technique which also gives unambiguous velocity vector information is acceptable. A direct space domain processing technique was examined. The direct space domain processing technique was found to be far superior to any other techniques known, in achieving the objectives listed above. It employs a new data coding and reduction technique, where the particle time history information is used directly. Further, it has no 180 deg directional ambiguity. A complex convection vortex flow was recorded and completely processed in under 2 minutes on an 80386 based PC, producing a 2-D velocity vector map of the flow field. Hence, using this new space domain vector scanning (VS) technique, pulsed laser velocimetry data can be reduced quickly and reasonably accurately, without specialized array processing hardware. Author

N89-23851*# Physical Sciences, Inc., Andover, MA.
HIGH-TEMPERATURE LDV SEED PARTICLE DEVELOPMENT Final Report
Michael B. Frish and Vicky G. Pierce May 1989 33 p
(Contract NAS3-25284)
(NASA-CR-182265; NAS 1.26:182265; PSI-2062/TR-890) Avail: NTIS HC A03/MF A01 CSCL 14B

The feasibility of developing a method for making monodisperse, unagglomerated spherical particles greater than 50 nm in diameter was demonstrated. Carbonaceous particles were made by pyrolyzing ethylene with a pulsed CO2 laser, thereby creating a non-equilibrium mixture of carbon, hydrogen, hydrocarbon vapors, and unpyrolyzed ethylene. Via a complex series of reactions, the carbon and hydrocarbon vapors quickly condensed into the spherical particles. By cooling and dispersing them in a supersonic expansion immediately after their creation, the hot newly-formed spheres were prevented from colliding and coalescing, thus preventing the problem of agglomeration which as plagued other investigators studying laser-simulated particle formation. The cold particles could be left suspended in the residual gases indefinitely without agglomerating. Their uniform sizes and unagglomerated nature were visualized by collecting the particles on filters that were subsequently examined using electron microscopy. It was found the mean particle size can be coarsely controlled by varying the initial ethylene pressure, and can be finely controlled by varying the fluence (energy/unit area) with which the laser irradiates the gas. The motivating application for this research was to manufacture particles that could be used as laser Doppler velocimetry (LDV) seeds in high-temperature high-speed flows. Though the particles made in this program will not evaporate until heated to about 3000 K, and thus could serve as LDV seeds in some applications, they are not ideal when the hot atmosphere is also oxidizing. In that situation, ceramic materials would be preferable. Research performed elsewhere has demonstrated that selected ceramic materials can be manufactured by laser pyrolysis of appropriate supply gases. It is anticipated that, when the same gases are used in conjunction with the rapid cooling technique, unagglomerated spherical ceramic particles can be made with little difficulty. Such particles would also be valuable to manufacturers of ceramic or abrasive products, and this technique may find its greatest commercial potential in those areas. Author

N89-23852*# Arizona Univ., Tucson. Optical Sciences Center.
THE ABSOLUTE RADIOMETRIC CALIBRATION OF THE ADVANCED VERY HIGH RESOLUTION RADIOMETER Final Report, 28 Feb. 1988 - 29 Feb. 1989
P. N. Slater, P. M. Teillet, and Y. Ding 2 Jun. 1989 42 p

(Grant NAG5-859)
(NASA-CR-185057; NAS 1.26:185057) Avail: NTIS HC A03/MF A01 CSCL 14B

The measurement conditions are described for an intensive field campaign at White Sands Missile Range for the calibration of the AVHRRs on NOAA-9, NOAA-10 and NOAA-11, LANDSAT-4 TM and SPOT. Three different methods for calibration of AVHRRs by reference to a ground surface site are reported, and results from these methods are compared. Significant degradations in NOAA-9 and NOAA-10 AVHRR responsivities occurred since prelaunch calibrations were completed. As of February 1988, degradations in NOAA-9 AVHRR responsivities were on the order of 37 percent in channel and 41 percent in channel 2, and for the NOAA-10 AVHRR these degradations were 42 and 59 percent in channels 1 and 2, respectively. Author

N89-23853# Air Force Inst. of Tech., Wright-Patterson AFB, OH. School of Engineering.
A NUMERICAL INVESTIGATION OF THIN-FILM HEAT TRANSFER GAGES M.S. Thesis
Joseph A. Bonafede Mar. 1989 234 p
(AD-A206134; AFIT/GA/AA/88M-1) Avail: NTIS HC A11/MF A01 CSCL 20/13

When using a thin film gage to measure surface heat flux, one typically reduces the data for surface temperature to surface heat flux using a series solution for one-dimensional heat transfer in an initially isothermal, semi-infinite solid. However, the gage may not behave as an initially isothermal, semi-infinite solid due to multidimensional heat transfer and electrical preheating of the gage when the instrumentation is turned on. To evaluate the accuracy of the series solution for use with thin-film gages, the heat transfer in a gage was numerically simulated using a two-dimensional, finite-difference model. The actual geometry of the probe was simplified to reduce the heat transfer to two dimensions. The simulation produced surface temperatures which were used in the series solution to find estimates of surface heat flux. The heat fluxes from the simulation and the series solution were then compared to evaluate the accuracy of the series solution. The analysis provides good insight into the causes of inaccuracies when using the series solution. It also provides some quantitative results which may be helpful for estimating errors in actual laboratory use. GRA

N89-23854# Naval Research Lab., Washington, DC. High Power Electromagnetic Radiation Branch.
OPERATION OF A QUASI-OPTICAL GYROTRON WITH VARIABLE MIRROR SEPARATION Memorandum Report, Jun. - Aug. 1988
A. W. Fliflet, T. A. Hargraeves, W. M. Manheimer, R. P. Fischer, and M. L. Barsanti 10 Mar. 1989 23 p Prepared in cooperation with Mission Research Corp., Newington, VA and JAYCOR, Inc., Vienna, VA
(AD-A206347; NRL-MR-6422) Avail: NTIS HC A03/MF A01 CSCL 09/1

Results from a quasi-optical gyrotron experiment with a 20 to 28 cm mirror separation are presented showing operation from 95 to 130 GHz at powers up to 148 kW and output efficiencies up to 11.5 percent. The output coupling could be varied from 0.4 to 3 percent by changing the mirror separation and operating frequency. Efficiency optimization by variation of output coupling and by tapering the magnetic field has been demonstrated and regions of single-mode operation at powers up to 125 kW have been characterized. GRA

N89-23896*# National Aeronautics and Space Administration. Marshall Space Flight Center, Huntsville, AL.
DESIGN, FABRICATION AND TEST OF A 4750 NEWTON-METER-SECOND DOUBLE GIMBAL CONTROL MOMENT GYROSCOPE
Lewis Cook, Paul Golley, Henning Krome, Joseph Blondin, Charles Gurrisi, and John Kolvek (Allied Signal Corp., Teterboro, NJ.) *In its* The 23rd Aerospace Mechanisms Symposium Mar. 1989 p 59-76 (For primary document see N89-23892 17-39)
Avail: NTIS HC A15/MF A01 CSCL 14B

N89-23903*# Jet Propulsion Lab., California Inst. of Tech., Pasadena.
DESIGN AND DEVELOPMENT OF A HIGH-STIFFNESS, HIGH-RESOLUTION TORQUE SENSOR
Michael M. Socha and Boris J. Lurie *In* NASA, Marshall Space Flight Center, The 23rd Aerospace Mechanisms Symposium Mar. 1989 p 169-180 (For primary document see N89-23892 17-39)
Avail: NTIS HC A15/MF A01 CSCL 14B

36 LASERS AND MASERS

Includes parametric amplifiers.
For related information see also *76 Solid-State Physics.*

N89-23855*# Amerasia Technology, Inc., Westlake Village, CA.
MONOLITHIC GaAs DIGITIZER FOR SPACE-BASED LASER PULSE SPREADING EFFECT Final Technical Report, 1 Feb. - 31 Jul. 1988
Bennig Lao and Edward Staples 1988 23 p
(Contract NAS5-30266)
(NASA-CR-183430; NAS 1.26:183430) Avail: NTIS HC A03/MF A01 CSCL 20E

A 6-bit 1-GHz digitizer was designed to analyze the 1-ns pulse spreading effects in a space based altimeter. The digitizer consisted of four 4-bit flash A/D converters and a 6-bit encoder. Also, the converter utilized four 4-bit converters and a 4-to-6 bit encoder to achieve 6 bit resolution at the 1 GHz sample rate. The design was unique because it utilized only the inverters and NOR gates for the converters and encoder, hence it could be fabricated using the existing state-of-the-art GaAs processing techniques. This GHz digitizer has many commercial applications. It could be applicable to: (1) digital microwave transmission system for the telecommunication industries, (2) pulse monitoring in high kinetic chemical reactions, (3) transient signals in the medical field, and (4) microwave signals in astronomy. Author

N89-23856*# Stanford Univ., CA. Lab. of Physics.
HIGH ENERGY EFFICIENT SOLID STATE LASER SOURCES Final Report, 1 Jun. 1981 - 30 Sep. 1988
Robert L. Byer Mar. 1989 19 p
(Grant NAG1-182)
(NASA-CR-181782; NAS 1.26:181782; Ginzton-4442) Avail: NTIS HC A03/MF A01 CSCL 20E

Recent progress in the development of highly efficient coherent optical sources was reviewed. This work has focused on nonlinear frequency conversion of the highly coherent output of the non-planar ring laser oscillators developed earlier in the program, and includes high efficiency second harmonic generation and the operation of optical parametric oscillators for wavelength diversity and tunability. Author

N89-23857# Los Alamos National Lab., NM.
DIRECT LASER/MATERIALS INTERACTION: LASER ABLATION OF SUPERCONDUCTOR MATERIALS AND LASER WELDING
D. A. Cremers, R. D. Dixon, R. C. Estler (Fort Lewis A&M Coll., Durango, CO.), G. K. Lewis, J. L. Lyman, R. E. Muenchausen, N. S. Nogar, and M. Piltch 1989 28 p Presented at the 6th International Conference on High Temperatures: Chemistry of Inorganic Materials, Gaithersburg, MD, 3-7 Apr. 1989
(Contract W-7405-eng-36)
(DE89-006560; LA-UR-89-300; CONF-890435-1) Avail: NTIS HC A03/MF A01

This paper considers two applications of direct laser/materials interaction, laser ablation of superconductor materials and Nd-YAG laser welding. The laser ablation experiments with 355 nm, 10 ns pulses have demonstrated uniform, thin superconductor films. The film uniformity was improved significantly by rotating both the laser

target and the film support, and by vertically dithering the laser focus. The film stoichiometry does vary with laser fluence, but it is within 10% of the target material at high fluence. Annealing of the thallium-containing films restores lost oxygen. For the welding application we have investigated the conditions that influence the melt depth. High speed photography has shown the plume to consist of a series of regenerated pulses that move in a direction normal to the surface. The time for plume initiation and the laser power threshold for plume formation are dependent on the substrate material. The plume temperatures depended on the welding atmosphere. Temperatures and melt depths are higher for the reactive gases, air, O2, and SF6, than for the nonreactive gases, He, Ar, and N2. DOE

N89-23858# Los Alamos National Lab., NM. Theoretical Div.
VAPORIZATION AND RECONDENSATION IN PROPAGATION AND IMAGING OF LASER BEAMS
A. Zardecki and S. A. W. Gerstl Feb. 1989 11 p Presented at the Society of Photo-Instrumentation Engineers Conference on Applications of Artificial Intelligence, Orlando, FL, 27-31 Mar. 1989
(Contract W-7405-eng-36)
(DE89-008014; LA-UR-89-622; CONF-890358-4) Avail: NTIS HC A03/MF A01

To study the response of a medium to a localized disturbance, the coupled aerosol-beam equations (in which the dominant interactions are diffusive mass transport and conductive energy transport) are solved numerically, thus giving the spatio-temporal behavior of the propagating beam and the irradiated aerosols. In the context of the cloud clearing problem, a deleterious effect of recondensation is assessed. We examine the effect of turbulence on the distribution of droplet sizes during the recondensation. Results relevant to propagation and imaging are given. DOE

N89-23859# Lawrence Livermore National Lab., CA.
PULSE SHAPING ON THE NOVA LASER SYSTEM
J. K. Lawson, D. R. Speck, C. Bibeau, T. L. Weiland, and P. H. Chaffee 6 Feb. 1989 10 p Presented at the CLEO '89: Conference on Lasers and Electro Optics, Baltimore, MD, 24-28 Apr. 1989
(Contract W-7405-eng-48)
(DE89-008026; UCRL-99951; CONF-890423-7) Avail: NTIS HC A02/MF A01

Inertial confinement fusion requires temporally shaped pulses to achieve high gain efficiency. Recently, we demonstrated the ability to produce complex temporal pulse shapes at high power at 0.35 microns on the Nova laser system. DOE

N89-23860*# David Sarnoff Research Center, Princeton, NJ.
HIGH-POWER SINGLE SPATIAL MODE AlGaAs CHANNELED-SUBSTRATE-PLANAR SEMICONDUCTOR DIODE LASERS FOR SPACEBORNE COMMUNICATIONS Final Report, 16 Jul. 1987 - 15 Oct. 1988
J. C. Connolly, D. B. Carlin, and M. Ettenberg Washington NASA Jun. 1989 98 p
(Contract NAS1-17441)
(NASA-CR-4238; NAS 1.26:4238) Avail: NTIS HC A05/MF A01 CSCL 20E

A high power single spatial mode channeled substrate planar AlGaAs semiconductor diode laser was developed. The emission wavelength was optimized at 860 to 880 nm. The operating characteristics (power current, single spatial mode behavior, far field radiation patterns, and spectral behavior) and results of computer modeling studies on the performance of the laser are discussed. Reliability assessment at high output levels is included. Performance results on a new type of channeled substrate planar diode laser incorporating current blocking layers, grown by metalorganic chemical vapor deposition, to more effectively focus the operational current to the lasing region was demonstrated. The optoelectronic behavior and fabrication procedures for this new diode laser are discussed. The highlights include single spatial mode devices with up to 160 mW output at 8600 A, and quantum efficiencies of 70 percent (1 W/amp) with demonstrated operating lifetimes of 10,000 h at 50 mW. Author

N89-23861# Lawrence Livermore National Lab., CA.
EFFECT OF n ON 1 LASER TREATMENT ON DAMAGE THRESHOLD OF SELECTED OPTICAL COATING
John G. Wilder and Ian M. Thomas 28 Feb. 1989 11 p Presented at the Boulder Damage Symposium, Boulder, CO, 3-5 Nov. 1988
(Contract W-7405-eng-48)
(DE89-008830; UCRL-100617; CONF-8810296-4) Avail: NTIS HC A03/MF A01

Laser damage threshold improvement was observed in selected thin film coatings that were repeatedly irradiated by 1.06 micrometers, 16 nsec pulse emitted by a laser with 30 Hz repetition rate. Each sample was first irradiated for one minute at separate sites (1 on 1 testing) to determine the laser damage threshold of the thin film. A separate site was multiply irradiated (n on 1 testing) using a pulse fluence that initially was arbitrarily low, then subsequently raised in a step-wise fashion until damage occurred. Results indicate a significant increase in laser damage threshold of some thin film coatings due to this treatment. DOE

N89-23862# New Mexico Univ., Albuquerque. Center for Advanced Studies.
THE CHIRPED-PULSE FREE-ELECTRON LASER Final Technical Report, Sep. 1987 - Oct. 1988
Gerald T. Moore Jan. 1989 28 p
(Contract DE-FG04-87ER-13788)
(DE89-009041; DOE/ER-13788/T1) Avail: NTIS HC A03/MF A01

This is the final report of a theoretical and numerical investigation into the operation of pulsed free-electron lasers in which the electron energy depends on the time of injection into the wiggler. Such energy chirping over each of a train of electron micropulses injected into an FEL oscillator is expected to give rise to a laser pulse inside the optical resonator with a chirped carrier frequency omega sub s (tau). DOE

N89-23863# California Univ., Berkeley. Lawrence Berkeley Lab. Materials and Chemical Sciences Div.
ULTRA-HIGH RESOLUTION VUV-XUV LASER: APPLICATION TO THE HYPERFINE STUDY OF KRYPTON
A. H. Kung, T. Trickl, E. Cromwell, M. J. J. Varkking, and Y. T. Lee Sep. 1988 6 p Presented at the 4th Topical Meeting on Short Wavelength Coherent Radiation: Generation and Applications, Cape Cod, MA, 26-29 Sep. 1988 Submitted for publication
(Contract DE-AC03-76SF-00098)
(DE89-009059; LBL-26760; CONF-880904-9) Avail: NTIS HC A02/MF A01

A near-transform-limited VUV-XUV laser source with 210 MHz resolution has been constructed and used to study the hyperfine splitting, isotope shift, and lifetime of the three lowest ns (n = 5, 6, 7) Rydberg states of Krypton. DOE

N89-23864# Institute for Defense Analyses, Alexandria, VA.
IDA (INSTITUTE FOR DEFENSE ANALYSES) GAMMA-RAY LASER: INVESTIGATION OF THE FEASIBILITY OF DEVELOPING A LASER USING NUCLEAR TRANSITIONS Final Annual Summary Report, 1 Oct. 1985 - 30 Sep. 1986
Bohdan Balko, Leslie Cohen, and David A. Sparrow Dec. 1988 256 p
(Contract MDA903-84-C-0031)
(AD-A205318; AD-E501074; IDA-P-2004; IDA/HQ-87-31897) Avail: NTIS HC A12/MF A01 CSCL 09/3

This report summarizes the IDA research effort in FY86 investigating the feasibility of developing a gamma-ray laser. GRA

N89-23865# Institute for Defense Analyses, Alexandria, VA.
IDA (INSTITUTE FOR DEFENSE ANALYSES) GAMMA-RAY LASER: INVESTIGATION OF DEVELOPING A LASER USING NUCLEAR TRANSITIONS Final Annual Summary Report, Oct. 1986 - Sep. 1987
Bohdan Balko, Leslie Cohen, David A. Sparrow, and Jeffrey F. Nicoll Dec. 1988 87 p
(Contract MDA903-84-C-0031)
(AD-A205319; AD-E501075; IDA-P-2083; IDA/HQ-87-33002)
Avail: NTIS HC A05/MF A01 CSCL 09/3

This report summarizes the IDA research effort in FY87 in investigating the feasibility of developing a gamma-ray laser. GRA

N89-23866# Texas Univ., Dallas. Center for Quantum Electronics.
PROOF OF THE FEASIBILITY OF COHERENT AND INCOHERENT SCHEMES FOR PUMPING A GAMMA-RAY LASER Quarterly Technical Progress Report, 1 Oct. - 31 Dec. 1988
Carl B. Collins Jan. 1989 78 p
(Contract N00014-86-C-2488)
(AD-A205371; GRL/8803) Avail: NTIS HC A05/MF A01 CSCL 09/3

Recent approaches to the problem of the gamma-ray laser have focused upon upconversion techniques in which metastable nuclei are pumped with long wavelength radiation. At the nuclear level the storage of energy can approach tera-Joules (10(12) J) per liter for thousands of years. However, any plan to use such a resource for a gamma-ray laser poses problems of a broad interdisciplinary nature requiring the fusion of concepts taken from relatively unrelated fields of physics. Since 1978 an approach for the upconversion of longer wavelength radiation incident upon isomeric nuclear populations that can avoid many of the difficulties encountered with traditional concepts of single photon pumping is pursued. Recent experiments have confirmed the general feasibility and have indicated that a gamma-ray laser is feasible if the right combination of energy levels and branching ratios exist in some real material. A laser-grade database of nuclear properties does not yet exist, but the techniques for constructing one have been developed under this contract and are now being utilized. GRA

N89-23867# Optical Society of America, Washington, DC.
SUMMARIES OF PAPERS PRESENTED AT SHORT WAVELENGTH COHERENT RADIATION: GENERATION AND APPLICATIONS TOPICAL MEETING HELD IN CAPE COD, MASSACHUSETTS ON SEPTEMBER 26-29, 1988 Final Report, 9 Mar. 1988 - 1 Mar. 1989
Jarus W. Quinn 1 Mar. 1989 166 p Meeting held in Cape Cod, MA, 26-29 Sep. 1988
(Contract N00014-88-J-1115)
(AD-A205471) Avail: NTIS HC A08/MF A01 CSCL 09/1

The meeting dealt with the development and application of sources of coherent radiation from the extreme ultraviolet to the X-ray spectral region. Closely related areas of interest are multiphoton phenomena, soft X-ray optics, and laser produced plasmas. Topics covered included: Short-wavelength lasers, free electron lasers and undulators, harmonic generation and frequency conversion, short wavelength optics and novel instrumentation, laser plasma radiation sources, multiphoton phenomena, ultrafast short-wavelength sources, applications in spectroscopy, microscopy, and microfabrication, phase coherent applications: Holography and interferometry, and unique applications of short-wavelength sources. GRA

N89-23868# Stanford Univ., CA. Lab. of Physics.
RESEARCH STUDIES ON EXTREME ULTRAVIOLET AND SOFT X-RAY LASERS Final Technical Report, 23 Nov. 1985 - 22 Nov. 1988
S. E. Harris and J. F. Young 24 Feb. 1989 10 p
(Contracts F49620-85-C-0101; MIPR-ARO-106-88)
(AD-A205625; ARO-22842.25-PH) Avail: NTIS HC A02/MF A01 CSCL 09/3

This program consisted of experimental and theoretical studies of the physics, technology, and spectroscopy of extreme ultraviolet (XUV) and soft X-ray lasers. It is a continuation of several predecessor programs. The overall objective of our work is to develop a class of lasers whose wavelengths span the 100 A to 1000 A spectral region. Major accomplishment are summarized and resulting publication listed. GRA

N89-23869# Air Force Systems Command, Wright-Patterson AFB, OH. Foreign Technology Div.
LASER PHOTOELECTRIC EFFECT AT SURFACE OF DISCHARGE CATHODE
Zhenxing Gui, Shunye Zhang, Guirong Shen, and Runwen Wang 24 Jan. 1989 6 p Transl. into ENGLISH from Zhongguo Jiguang (Peoples Republic of China), v. 13, no. 9, 1986 p 590
(AD-A205741; FTD-ID(RS)T-1067-88) Avail: NTIS HC A02/MF A01 CSCL 07/4

The photoelectric effect is produced by a glow discharge cathode irradiated by a continuous Carbon Monoxide laser; this photoelectric effect is not related to the frequency of incident light (that is nonresonant absorption photoelectric current) but is only proportional to the intensity of incident light. Moreover, the photocurrent produced by a unit of light intensity is very sensitive to discharge current, gas composition, and gas pressure. A high temperature photoelectron emission mechanism at the cathode surface is described. GRA

N89-23870# Air Force Inst. of Tech., Wright-Patterson AFB, OH. School of Engineering.
NUMERICAL SIMULATION OF THE DISSOCIATION OF I2 BY O2 (1 DELTA) IN A TWO DIMENSIONAL PARALLEL JET M.S. Thesis
Jeffrey A. Miller Mar. 1989 121 p
(AD-A206137; AFIT/GAE/AA/89M-3) Avail: NTIS HC A06/MF A01 CSCL 09/3

The thin-shear-layer equations are solved for a two dimensional parallel jet of molecular iodine in singlet delta oxygen freestream, to investigate the effect of mixing and water vapor on molecular iodine dissociation in Chemical Oxygen-Iodine Lasers (COIL). Predicting the dissociation of molecular iodine has been identified as the largest source of error in COIL performance modeling. Recent experimental and modeling experience have indicated that much of the problem may be due to the coupled iodine mixing and dissociation process. The numerical code was used to study the combined mixing and dissociation problem. Comparison of a set of 1-D premixed cases and 2-D jet cases with varying jet velocity ratios (and mixing rates) indicates that, imperfect mixing which results in initial regions of high iodine concentration leads to faster dissociation rates. High laser gain, however, does require efficient mixing. The results of both premixed and jet mixed cases with and without water vapor in the oxygen stream demonstrate the strong dependence of the dissociation efficiency (i.e., the penalty paid to dissociate iodine) on both the device geometry and operating conditions which challenges the wisdom of suing empirically determined efficiency factors to predict COIL performance. GRA

N89-23871# Ohio Wesleyan Univ., Delaware. Dept. of Psychology.
FUNCTIONAL ASSESSMENT OF LASER IRRADIATION Final Annual Report, 1 Jul. 1974 - 30 Jun. 1986
David O. Robbins Mar. 1988 30 p
(Contracts DAMD17-81-C-1065; DAMD17-75-C-5008; DA Proj. 3E1-62777-A-878)
(AD-A206230) Avail: NTIS HC A03/MF A01 CSCL 09/3

Exposure of the fovea to intense coherent light can produce either transient or permanent changes in the eye's ability to resolve fine spatial detail. Permanent functional changes can occur in the absence of gross morphological damage and at power densities below the ED50 level. Furthermore, the eye may become increasingly susceptible to damage after repeated low-level exposures which initially produce only transient effects.

Independent of any long-term hazards, laser exposures can also disrupt visual/motor behavior for periods of up to 96 hrs GRA

N89-23872# Naval Research Lab., Washington, DC.
DEVELOPMENT OF HIGH POWER CARM (CYCLOTRON AUTO-RESONANCE MASER) OSCILLATORS Memorandum Report, Oct. 1987 - Oct. 1988
A. W. Fliflet, R. B. McCowan, C. A. Sullivan, D. A. Kirkpatrick, and S. H. Gold 14 Mar. 1989 27 p Prepared in cooperation with Science Applications International Corp., McLean, VA
(AD-A206270; NRL-MR-6388) Avail: NTIS HC A03/MF A01 CSCL 09/3

The Cyclotron Auto-Resonance Maser (CARM) is under investigation at the U.S. Naval Research Laboratory as an efficient source of high power millimeter-wave and submillimeter-wave radiation for applications such as plasma heating, advanced rf accelerators, and space-based radars. A short-pulse 100 GHz CARM oscillator experiment based on a 600 kV, 200 Amp, 50 nsec electron beam is under way. The mode selective, high-Q waveguide cavity with rippled-wall Bragg reflectors is designed to operate in the TE61 mode. A novel code cathode diode is used to produce a high quality annular beam with a momentum pitch ratio of 0.6. The cathode features nonemitting focussing electrodes and an annular velvet emitter. The main objective of the experiment is to demonstrate high efficiency approx. 20 percent at a power of approximately 20 MW. In addition, a long pulse 250 GHz CARM oscillator experiment based on a 500 kV, 100 Amp, 1 microsec MIG-type thermionic cathode electron gun is planned. The design of these experiments and the optimization of CARM oscillator efficiency are discussed. GRA

N89-23913*# National Aeronautics and Space Administration. Langley Research Center, Hampton, VA.
A TWO-AXIS LASER BORESIGHT SYSTEM FOR A SHUTTLE EXPERIMENT
Joseph F. DeLorme *In* NASA, Marshall Space Flight Center, The 23rd Aerospace Mechanisms Symposium Mar. 1989 p 309-318 (For primary document see N89-23892 17-39)
Avail: NTIS HC A15/MF A01 CSCL 20E

37 MECHANICAL ENGINEERING

Includes auxiliary systems (nonpower); machine elements and processes; and mechanical equipment.

N89-23873# National Aerospace Lab., Tokyo (Japan).
STUDY ON A TWIN VALVELESS PULSE BURNER (TEMPERATURE CHARACTERISTICS DURING PULSE COMBUSTION)
Apr. 1988 12 p In JAPANESE; ENGLISH summary
(NAL-TR-973; ISSN-0389-4010) Avail: NTIS HC A03/MF A01

Detailed temperature profiles in a twin valveless pulse combustor were measured using a simplified CARS (coherent anti-Stokes Raman spectroscopy) technique to understand the fundamental pulse combustion process for burner design purpose. Time-and ensemble-averaged temperatures in the combustion chamber were obtained from a constant 20Hz data sampling and a phase locked data sampling, respectively. The CARS method offered a near-real-time, nonintrusive temperature measurement system with high spatial and time resolutions. Results show that very large temperature oscillations of up to 600 K exist near the wall upstream of the combustion chamber, while stable and homogeneous temperature regions were created in other regions. The maximum temperature was found to be lower about 200 to 400 K than the adiabatic flame temperature. From a comparison of one-cycle ensemble data between temperature and heat release rate, a similar tendency was observed, this indicating that fuel-air mixing rate affects significantly the ignition delay time during pulse combustion as described previously. Author

N89-23874# Environmental Protection Agency, Ann Arbor, MI. Control Technology and Applications Branch.
METHANOL VEHICLE CATALYST EVALUATION, PHASE 3
Gregory K. Piotrowski Nov. 1988 24 p
(PB89-136139; EPA/AA/CTAB-88/10) Avail: NTIS HC A03/MF A01 CSCL 13F

The evaluation of two noble metal catalysts is discussed for methanol-fueled vehicles to reduce mobile source emissions. The catalysts were first tested as three-way converters, to oxidize unburned fuel, aldehydes, and carbon monoxide, as well as to reduce oxides of nitrogen emissions. An air pump, which supplied air to the exhaust ahead of the catalyst but downstream of the exhaust oxygen sensor, was then used to evaluate the catalysts in a simulated oxidation mode. Also included are the test vehicle descriptions, the test facilities and analytical methods used, and specifications for each individual test vehicle. Author

N89-23875*# Texas Univ., Austin. Dept. of Mechanical Engineering.
MODELING AND SIMULATION OF A STEWART PLATFORM TYPE PARALLEL STRUCTURE ROBOT Final Report, 1 Dec. 1987 - 30 Nov. 1988
Gee Kwang Lim, Robert A. Freeman, and Delbert Tesar Apr. 1989 217 p
(Grant NAG9-188)
(NASA-CR-184969; NAS 1.26:184969) Avail: NTIS HC A10/MF A01 CSCL 13I

The kinematics and dynamics of a Stewart Platform type parallel structure robot (NASA's Dynamic Docking Test System) were modeled using the method of kinematic influence coefficients (KIC) and isomorphic transformations of system dependence from one set of generalized coordinates to another. By specifying the end-effector (platform) time trajectory, the required generalized input forces which would theoretically yield the desired motion were determined. It was found that the relationship between the platform motion and the actuators motion was nonlinear. In addition, the contribution to the total generalized forces, required at the actuators, from the acceleration related terms were found to be more significant than the velocity related terms. Hence, the curve representing the total required actuator force generally resembled the curve for the acceleration related force. Another observation revealed that the acceleration related effective inertia matrix I sub dd had the tendency to decouple, with the elements on the main diagonal of I sub dd being larger than the off-diagonal elements, while the velocity related inertia power array P sub ddd did not show such tendency. This tendency results in the acceleration related force curve of a given actuator resembling the acceleration profile of that particular actuator. Furthermore, it was indicated that the effective inertia matrix for the legs is more decoupled than that for the platform. These observations provide essential information for further research to develop an effective control strategy for real-time control of the Dynamic Docking Test System. Author

N89-23876*# Texas A&M Univ., College Station. Turbomachinery Lab.
FRICTION FACTOR DATA FOR FLAT PLATE TESTS OF SMOOTH AND HONEYCOMB SURFACES M.S. Thesis
Tae Woong Ha May 1989 100 p
(Grant NAG3-181)
(NASA-CR-184977; NAS 1.26:184977; TL-SEAL-1-89) Avail: NTIS HC A05/MF A01 CSCL 20C

Friction factors for honeycomb surfaces were measured with a flat plate tester. The flat plate test apparatus was described and a method was discussed for determining the friction factor experimentally. The friction factor model was developed for the flat plate test based on the Fanno Line Flow. The comparisons of the friction factor were plotted for smooth surfaces and six-honeycomb surfaces with three-clearances, 6.9 bar to 17.9 bar range of inlet pressures, and 5,000 to 100,000 range of the Reynolds number. The optimum geometries for the maximum friction factor were found as a function of cell width to cell depth and cell width to clearance ratios. Author

N89-23877# Sandia National Labs., Albuquerque, NM. Thermomechanical and Physical Div.
WHITE PAPER: EXPERIMENTAL AND COMPUTATIONAL STUDIES OF VERY HIGH VELOCITY IMPACTS
T. G. Trucano and J. R. Asay 1989 5 p Presented at the LTH-T Quarterly Review, Santa Barbara, CA, 14 Feb. 1989
(Contract DE-AC04-76DP-00789)
(DE89-007643; SAND-89-0404C; CONF-890272-1) Avail: NTIS HC A02/MF A01

The following research is proposed: (1) Perform four to six new time-resolved lethality experiments on cadmium at projectile velocities 7 km/s, greater than that of our previous work at 5.2 km/s. The increased velocity will substantially increase the mass percentage of vaporization. Through simulation of these experiments, computer codes can be validated for hypervelocity impact when vaporization occurs. (2) Perform an additional four to six 1-D lethality experiments on zinc. This material undergoes substantial vaporization under the experimental conditions, and would expand our knowledge about the sensitivity of KEW lethality to shock-induced vaporization. (3) Perform two to four ballistic impact experiments with the ballistics gun at Sandia to provide a full validation of computational capabilities used in simulating the 1-D experiments. These experiments would probe phenomenology that is similar to the 1-D experiments, but with multi-dimensional debris propagation. This will extend the confidence in computer modeling to conditions analagous to KEW lethality applications. DOE

N89-23878# Oak Ridge National Lab., TN.
NONINTRUSIVE METHODS FOR MONITORING THE OPERATIONAL READINESS OF SOLENOID-OPERATED VALVES
Robert C. Kryter 1989 12 p Presented at the NPAR Review Group Meeting, Rockville, MD, 21 Mar. 1989 Sponsored in part by US Nuclear Regulatory Commission
(Contract DE-AC05-84OR-21400)
(DE89-008732; CONF-890373-4-Vugraphs) Avail: NTIS HC A03/MF A01

Solenoid-operated valves (SOVs) are being studied at Oak Ridge National Laboratory as part of the USNRC Nuclear Plant Aging Research (NPAR) Program. The primary objective of the study is to identify, evaluate, and recommend methods for inspection, surveillance, monitoring, and maintenance of SOVs that can ensure their operational readiness--that is, their ability to perform required safety functions under all anticipated operating conditions. An earlier (Phase I) study described SOV failure modes and causes and identified measurable parameters that might be used to monitor the various degradations that lead to functional failure. The present (Phase II) study focuses on devising and then demonstrating the effectiveness of techniques and/or equipment with which to measure the previously identified performance parameters (or others) and thus detect and trend the progress of any degradation that may be occurring. DOE

N89-23879# Department of Energy, Washington, DC.
ELECTRIC AND HYBRID VEHICLES PROGRAM: REPORT TO CONGRESS Annual Report No. 12, fiscal year 1988
Feb. 1989 39 p
(DE89-008988; DOE/CE-0247) Avail: NTIS HC A03/MF A01

This twelfth annual report on the implementation of the Electric and Hybrid Vehicle Research, Development and Demonstration Act of 1976 (Public Law 94-413, as amended by Public Law 95-238, and Public Law 96-185), referred to as the Act, complies with the reporting requirements established in Section 14 of the Act. In addition to informing Congress of the progress and plans of the Department of Energy's Electric and Hybrid Vehicles Program, this report is intended to serve as a communication link between the Department and all of the public and private interests involved in making the program a success. During FY88, significant progress was made toward fulfilling the intent of the Congress in the Act. There has been continuing interest shown by both the automobile manufacturing and supply sectors of our economy in electric and hybrid vehicles. The three major domestic automobile manufacturers are all devoting some effort towards electric vehicles. Their participation includes cost-shared contracts with the Department of Energy and the Electric Power Research Institute as well as independently funded activities. Research and development efforts in batteries and propulsion components continue to achieve significant progress in providing industry with technology options that will result in vehicles that will be more economically competitive and more acceptable. DOE

N89-23880*# National Aeronautics and Space Administration. Langley Research Center, Hampton, VA.
TENSILE FILM CLAMPS AND MOUNTING BLOCK FOR THE RHEOVIBRON AND AUTOVIBRON VISCOELASTOMETER Patent Application
Diane M. Stoakley, inventor (to NASA), Anne K. StClair, inventor (to NASA), and Bruce D. Little, inventor (to NASA) 4 Nov. 1988 17 p Sponsored by NASA. Langley Research Center
(NASA-Case-LAR-13696-1; NAS 1.71:LAR-13696-1; US-Patent-Appl-SN-267146) Avail: NTIS HC A03/MF A01 CSCL 13I

A set of film clamps and a mounting block for use in the determination of tensile modulus and damping properties of films in a manually operated or automated Rheovibron is diagrammed. These clamps and mounting block provide uniformity of sample gripping and alignment in the instrument. Operator dependence and data variability are greatly reduced. NASA

N89-23881# Air Force Inst. of Tech., Wright-Patterson AFB, OH. School of Engineering.
MULTIPLE MODEL-BASED ROBOT CONTROL: DEVELOPMENT AND INITIAL EVALUATION M.S. Thesis
Larry D. Tellman Dec. 1988 145 p
(AD-A205725; AD-E501079; AFIT/GE/ENG/88D-55) Avail: NTIS HC A07/MF A01 CSCL 12/9

A new form of adaptive model-based robot control has been developed and experimentally evaluated. The Multiple Model Based Control (MMBC) technique utilizes knowledge of nominal manipulator dynamics and principles of Bayesian estimation to provide payload-independent trajectory tracking accuracy. The MMBC is formed by augmenting a model-based controller, which employs feedforward dynamic compensation and constant gain PD feedback, with a payload estimate provided by a Multiple Model Adaptive Estimator. Extensive simulation studies demonstrated the MMBC's ability to adapt to variations in manipulator payload quickly and accurately. Initial experimental evaluations on the first three links of a PUMA-560 validated the algorithm's potential. GRA

N89-23882# Air Force Wright-Patterson Aeronautical Labs., Wright-Patterson AFB, OH. Lubrication Branch.
CORRELATION OF PORTABLE WEAR METAL ANALYZER (PWMA-2) AND BAIRD A/E35U-3 SPECTROMETER OIL ANALYSIS DATA Final Report, 11 Oct. - 18 Nov. 1988
Robert L. Wright Nov. 1988 33 p
(AF Proj. 3048)
(AD-A205957; AFWAL-TR-88-2152) Avail: NTIS HC A03/MF A01 CSCL 07/2

Tables for correlation of the Perkin-Elmer portable wear metal analyzer, version two (PWMA-2) readings (in ppm) with the Baird A/E35U-3 atomic emission spectrometer readings (also in ppm) were prepared by curve fitting of data from aircraft, bearing test rig, and organometallic oil samples analyzed on both instruments. Each of the nine wear metal elements (Iron, Silicon, Aluminum, Chromium, Copper, Magnesium, Nickel, Silicon, Titanium) was separately fitted to linear, logarithmic, power law, and low order polynomial curves. Power law curve fits were best for almost all the elements, especially in the important low concentration range (0 to 5 ppm), where Air Force jet turbine engines typically operate. The power law curve was applied to all elements to construct the correlation tables with a general uncertainty in table values equal to about 0.5 to 1 ppm or 10 percent, whichever is greater. The coefficients of determination for the power law curve fits ranged from 0.935 for Al to 0.993 for Fe. The fit for silicon was very poor for any type of curve (best coefficient of determination = 0.564

for power curve fit) and therefore Si was not included in the tables because the confidence level for its values is very low trace metals. GRA

N89-23883# Massachusetts Inst. of Tech., Cambridge. Dept. of Chemical Engineering.
PATH DEPENDENT MORPHOLOGIES OF A DIBLOCK COPOLYMER OF POLYSTYRENE/HYDROGENATED POLYBUTADIENE
R. E. Cohen, P. L. Cheng, K. Dozinas, P. Kofinas, and C. V. Berney 15 Mar. 1989 16 p
(Contract N00014-87-K-0517)
(AD-A206504; TR-7) Avail: NTIS HC A03/MF A01 CSCL 07/6

Variations in solvent-casting pathways and in bulk annealing conditions led to a variety of morphologies for a single SEB diblock copolymer; some of these are kinetically trapped structures while others are consistent with expectations of equilibrium thermodynamics. Independent control of the morphological scale (microphase-separated vs. disordered) and degree/perfection of crystallinity was demonstrated. These degrees of freedom offer both opportunities and problems for those attempting to develop meaningful structure/processing/properties relationships for semicrystalline block copolymers and for blends in which they are meant to act as emulsifiers. GRA

N89-23586# Ljubljana Univ. (Yugoslavia). Jozef Stefan Inst.
THE WEAR OF CUTTING TOOLS: THE CONTRIBUTION OF ABRASIVE WEAR
Sasa Novak and Marija Komac *In* Kernforschungsanlage Juelich GmbH, The 8th German-Yugoslav Meeting on Materials Science and Development: Ceramics and Metals 1988 p 157-164 (For primary document see N89-23569 17-23)
Copyright Avail: NTIS HC A21/MF A01

N89-23893*# European Space Agency. European Space Research and Technology Center, ESTEC, Noordwijk (Netherlands).
THE EVOLUTION OF SPACE MECHANISMS IN THE ESA R AND D PROGRAM
D. Wyn-Roberts *In* NASA, Marshall Space Flight Center, The 23rd Aerospace Mechanisms Symposiums Mar. 1989 p 1-16 (For primary document see N89-23892 17-39)
Avail: NTIS HC A15/MF A01 CSCL 13I

N89-23895*# National Aeronautics and Space Administration. Lyndon B. Johnson Space Center, Houston, TX.
THE DESIGN AND ANALYSIS OF A DOUBLE SWIVEL TOGGLE RELEASE MECHANISM FOR THE ORBITER STABILIZED PAYLOAD DEPLOYMENT SYSTEM
Guy L. King and Ted Tsai *In* NASA, Marshall Space Flight Center, The 23rd Aerospace Mechanisms Symposium Mar. 1989 p 39-57 (For primary document see N89-23892 17-39)
Avail: NTIS HC A15/MF A01 CSCL 13I

N89-23897*# AEC-Able Engineering Co., Inc., Goleta, CA.
CAROUSEL DEPLOYMENT MECHANISM FOR COILABLE LATTICE TRUSS
Robert M. Warden and P. Alan Jones *In* NASA, Marshall Space Flight Center, The 23rd Aerospace Mechanisms Symposium Mar. 1989 p 77-100 (For primary document see N89-23892 17-39)
Avail: NTIS HC A15/MF A01 CSCL 13I

N89-23906*# Oak Ridge National Lab., TN.
TRACTION-DRIVE FORCE TRANSMISSION FOR TELEROBOTIC JOINTS
D. M. Williams and D. P. Kuban *In* NASA, Marshall Space Flight Center, The 23rd Aerospace Mechanisms Symposium Mar. 1989 p 207-222 (For primary document see N89-23892 17-39)
Avail: NTIS HC A15/MF A01 CSCL 13I

N89-23907*# Jet Propulsion Lab., California Inst. of Tech., Pasadena.
FLIGHT TELEROBOT MECHANISM DESIGN: PROBLEMS AND CHALLENGES
John B. Dahlgren and Edwin P. Kan *In* NASA, Marshall Space Flight Center, The 23rd Aerospace Mechanisms Symposium Mar. 1989 p 223-239 (For primary document see N89-23892 17-39)
Avail: NTIS HC A15/MF A01 CSCL 13I

N89-23912*# Naval Research Lab., Washington, DC.
PRACTICAL EXPERIENCES WITH WORM GEARING FOR SPACECRAFT POWER TRANSMISSION APPLICATIONS
William Purdy and William McCown (Rexnord Aerospace Mechanisms, Torrance, CA.) *In* NASA, Marshall Space Flight Center, The 23rd Aerospace Mechanisms Symposium Mar. 1989 p 291-307 (For primary document see N89-23892 17-39)
Avail: NTIS HC A15/MF A01 CSCL 20K

N89-23914*# European Space Tribology Lab., Risley (England).
THE IN-VACUO TORQUE PERFORMANCE OF DRY-LUBRICATED BALL BEARINGS AT CRYOGENIC TEMPERATURES
S. G. Gould and E. W. Roberts *In* NASA, Marshall Space Flight Center, The 23rd Aerospace Mechanisms Symposium Mar. 1989 , p 319-333 (For primary document see N89-23892 17-39)
Avail: NTIS HC A15/MF A01 CSCL 13I

38 QUALITY ASSURANCE AND RELIABILITY

Includes product sampling procedures and techniques; and quality control.

N89-23884# National Inst. of Standards and Technology, Gaithersburg, MD.
INSTITUTE FOR MATERIALS SCIENCE AND ENGINEERING, NONDESTRUCTIVE EVALUATION: TECHNICAL ACTIVITIES 1988 Annual Report
H. Thomas Yolken, ed. Oct. 1988 72 p
(PB89-151625; NISTIR-88/3839) Avail: NTIS HC A04/MF A01 CSCL 09D

Technical activities in nondestructive evaluation (NDE) that were carried out by or for the National Institute of Standards and Technology (NIST; formerly the National Bureau of Standards) in fiscal year 1988 (October 1, 1987, through September 30, 1988) are reviewed. The reviews in the annual report are arranged in the following sections that reflect the NDE Program's four major activity areas: NDE for Ceramic and Metal Powder Production and Consolidation; NDE for Formability of Metals; NDE for Composites Processing and Interfaces; and NDE Standards and Methods. Each of the sections is preceded by an introduction.
Author

N89-23885# Honeywell, Inc., Bloomington, MN. Computer Sciences Center.
A DESIGNERS' GUIDE TO RELIABLE DISTRIBUTED SYSTEMS: AN EXAMPLE DESIGN. VOLUME 1 Final Technical Report, Sep. 1982 - Aug. 1984
Anand R. Tripathi, Jonathan Silverman, William T. Wood, Elaine N. Frankowski, Pong-Sheng Wang, Shiva Azadegan, Shiv Seth, Rita Wu, and Helmut K. Berg Aug. 1988 354 p Prepared in cooperation with Information Research Associates, Inc., Austin, TX, and Texas Univ., Austin
(Contract F30602-82-C-0154; AF Proj. 2530)
(AD-A206039; RADC-TR-168-Vol-1) Avail: NTIS HC A16/MF A01 CSCL 12/5

This report describes an effort to develop a system designers guidebook for designing reliable distributed command and control systems. The guidebook contains a synthesis of reliable system

design principles and methods to evaluate distributed system designs for performance, reliability and functional correctness. The approach to developing the system designers guidebook in this effort is example driver. We develop a detailed design of a reliable distributed operating system and evaluate its performance. GRA

N89-23886# Honeywell, Inc., Bloomington, MN. Computer Sciences Center.
A DESIGNERS' GUIDE TO RELIABLE DISTRIBUTED SYSTEMS: AN EXAMPLE DESIGN. VOLUME 2 Final Technical Report, Sep. 1982 - Aug. 1984
Anand R. Tripathi, Jonathan Silverman, William T. Wood, Elaine N. Frankowski, Pong-Sheng Wang, Shiva Azadegan, Shiv Seth, Rita Wu, and Helmut K. Berg Aug. 1988 298 p Prepared in cooperation with Information Research Associates, Inc., Austin, TX, and Texas Univ., Austin
(Contract F30602-82-C-0154; AF Proj. 2530)
(AD-A206040; RADC-TR-168-Vol-2) Avail: NTIS HC A13/MF A01 CSCL 12/5

This report describes an effort to develop a system designers guidebook for designing reliable distributed command and control systems. The guidebook contains a synthesis of reliable system design principles and methods to evaluate distributed system designs for performance, reliability and functional correctness. The approach to developing the system designers guidebook in this effort is example driver. We develop a detailed design of a reliable distributed operating system and evaluate its performance. GRA

N89-23887# Army Missile Command, Redstone Arsenal, AL. Systems Analysis Div.
SYSTEM MEAN-TIME-BETWEEN-FAILURE VERSUS LIFE-CYCLE LOGISTICS COST SUBJECT TO THE INTRODUCTION OF LINE-REPLACEABLE-UNIT REDUNDANCY Final Report
Patrick B. Lawler, Jr. 18 Mar. 1988 140 p
(AD-A206324; AD-E951232; AMSMI/TR-OR-SA-88-01) Avail: NTIS HC A07/MF A01 CSCL 15/5

This document presents an examination of ten alternate system designs in which redundancy is employed to achieve various values of system Mean-Time-Between-Failure (MTBF). In serial system designs where line-replaceable-units (LRU's) possess exponentially distributed times to failure, life-cycle logistics cost is inversely proportional to system MTBF. In this analysis, this phenomena was found to be contradicted. Life-cycle logistics cost is directly proportional to system MTBF, in the presents of LRU redundancy and no preventive or scheduled maintenance. GRA

N89-23888# Army Belvoir Research and Development Center, Fort Belvoir, VA.
ENVIRONMENTAL STRESS SCREENING (ESS) GUIDE Final Technical Report
William H. Horner Jan. 1989 121 p
(AD-A206350; BRDEC-2477) Avail: NTIS HC A06/MF A01 CSCL 14/2

The increasing complexity of mechanical equipment and miniaturization of electronic equipment has made traditional methods of defect detection less efficient. One of the most effective techniques used to identify and eliminate these defects is ESS. ESS is the process of applying environmental stresses, in conjunction with functional testing, in order to stimulate the failure mechanisms of defects to the point of detection. Most of these defects are caused by flawed parts and poor assembly workmanship. The stress levels of applied stimuli must be as harsh as possible to precipitate the defects without causing damage to or reducing the useful life of properly manufactured hardware. Application of environmental stresses will accelerate the latent (or undetected) defects to become patent (detected), with functional testing required to detect failures. Functional testing can be performed either during or after the application of stress. The advantage of functional testing during stress application is that it allows the detection of intermittent failures. This guide provides a step-by-step approach to the planning, implementing, and monitoring of an ESS program for Army Materiel Command Troop Support Command (TROSCOM) hardware contracts and repair activities. This guide does not replace logical thinking on the part of the user, but presents the various elements of an ESS Program and advise the user in their selection and use. GRA

N89-23889# Aerospatiale, Cannes La Bocca (France).
EVALUATION OF TESTS AND DESIGN FACTORS
C. Vidal, T. deMollerat, and M. Klein (European Space Agency. European Space Research and Technology Center, ESTEC, Noordwijk, Netherlands) Paris, France 1988 13 p
(Rept-882-440-109; ETN-89-94502) Avail: NTIS HC A03/MF A01

A method for the definition of factor of safety ensuring structural reliability is presented. The procedure encompasses both theoretical reliability and practical aspects, combining design requirements, qualifications and acceptance tests. After studying statistical variations, a set for factor of safety is proposed for unmanned spacecraft up to 2000 kg. Extensions over 2000 kg and to manned spacecraft are possible. A computer implementation is also described. ESA

39 STRUCTURAL MECHANICS

Includes structural element design and weight analysis; fatigue; and thermal stress.

For applications see *05 Aircraft Design, Testing and Performance* and *18 Spacecraft Design, Testing and Performance*.

N89-23890*# Texas Univ., San Antonio. Div. of Engineering.
FATIGUE CRACK GROWTH MODEL RANDOM2 USER MANUAL, APPENDIX 1 Annual Report
Lola Boyce and Thomas B. Lovelace Jan. 1989 37 p
(Grant NAG3-867)
(NASA-CR-184939; NAS 1.26:184939) Avail: NTIS HC A03/MF A01 CSCL 20K

The FORTRAN program RANDOM2 is documented. RANDOM2 is based on fracture mechanics using a probabilistic fatigue crack growth model. It predicts the random lifetime of an engine component to reach a given crack size. Included in this user manual are details regarding the theoretical background of RANDOM2, input data, instructions and a sample problem illustrating the use of RANDOM2. Appendix A gives information on the physical quantities, their symbols, FORTRAN names, and both SI and U.S. Customary units. Appendix B includes photocopies of the actual computer printout corresponding to the sample problem. Appendices C and D detail the IMSL, Ver. 10(1), subroutines and functions called by RANDOM2 and a SAS/GRAPH(2) program that can be used to plot both the probability density function (p.d.f.) and the cumulative distribution function (c.d.f.). Author

N89-23891*# Texas Univ., San Antonio. Div. of Engineering.
FATIGUE STRENGTH REDUCTION MODEL: RANDOM3 AND RANDOM4 USER MANUAL, APPENDIX 2 Annual Report
Lola Boyce and Thomas B. Lovelace Jan. 1989 80 p
(Grant NAG3-867)
(NASA-CR-184940; NAS 1.26:184940) Avail: NTIS HC A05/MF A01 CSCL 20K

The FORTRAN programs RANDOM3 and RANDOM4 are documented. They are based on fatigue strength reduction, using a probabilistic constitutive model. They predict the random lifetime of an engine component to reach a given fatigue strength. Included in this user manual are details regarding the theoretical backgrounds of RANDOM3 and RANDOM4. Appendix A gives information on the physical quantities, their symbols, FORTRAN names, and both SI and U.S. Customary units. Appendix B and C include photocopies of the actual computer printout corresponding to the sample problems. Appendices D and E detail the IMSL, Version 10(1), subroutines and functions called by RANDOM3 and RANDOM4 and SAS/GRAPH(2) programs that can be used to

plot both the probability density functions (p.d.f.) and the cumulative distribution functions (c.d.f.). A.D.

N89-23892*# National Aeronautics and Space Administration. Marshall Space Flight Center, Huntsville, AL.
THE 23RD AEROSPACE MECHANISMS SYMPOSIUM
Washington Mar. 1989 342 p Symposium held in Huntsville, AL, 3-5 May 1989; sponsored by NASA, Washington, California Inst. of Tech., Pasadena, and LMSC, Sunnyvale, CA
(NASA-CP-3032; M-611; NAS 1.55:3032) Avail: NTIS HC A15/MF A01 CSCL 20K

Technological areas covered include space lubrication, bearings, aerodynamic devices, spacecraft latches, deployment, positioning, and pointing. Devices for Space Station docking and manipulator and teleoperator mechanisms are also described. For individual titles, see N89-23893 through N89-23914.

N89-23893*# European Space Agency. European Space Research and Technology Center, ESTEC, Noordwijk (Netherlands).
THE EVOLUTION OF SPACE MECHANISMS IN THE ESA R AND D PROGRAM **c37**
D. Wyn-Roberts *In* NASA, Marshall Space Flight Center, The 23rd Aerospace Mechanisms Symposiums Mar. 1989 p 1-16 (For primary document see N89-23892 17-39)
Avail: NTIS HC A15/MF A01 CSCL 13I

The status of recently completed and already ongoing technology developments, as well as some of the most important future developments of the European Space Agency are discussed. Among the subjects considered are Scientific Satellites, Columbus space station development, applications spacecraft for communications, Earth observation and meteorology, and the Ariane V and Hermes space transportation systems. Author

N89-23894*# Sandia National Labs., Albuquerque, NM.
A UNIDIRECTIONAL ROTARY SOLENOID AS APPLIED TO STRONGLINKS **c33**
Eugene W. Kenderdine *In* NASA, Marshall Space Flight Center, The 23rd Aerospace Mechanisms Symposium Mar. 1989 p 17-37 (For primary document see N89-23892 17-39)
Avail: NTIS HC A15/MF A01 CSCL 20K

The design goals and results of an advanced development stronglink are discussed. Special emphasis is placed on a new rotary solenoid concept to provide improved security during the handling, storage, transporting, and deployment of weapons to prevent accidental detonation of the weapons in the event of abnormal environments, such as impact, fire, crush, etc. Author

N89-23895*# National Aeronautics and Space Administration. Lyndon B. Johnson Space Center, Houston, TX.
THE DESIGN AND ANALYSIS OF A DOUBLE SWIVEL TOGGLE RELEASE MECHANISM FOR THE ORBITER STABILIZED PAYLOAD DEPLOYMENT SYSTEM **c37**
Guy L. King and Ted Tsai *In* NASA, Marshall Space Flight Center, The 23rd Aerospace Mechanisms Symposium Mar. 1989 p 39-57 (For primary document see N89-23892 17-39)
Avail: NTIS HC A15/MF A01 CSCL 13I

The NASA Stabilized Payload Deployment System (SPDS) is discussed. The lightweight and heavy-duty system rolls payloads over the orbiter's side rather than ejecting them upward. The system will enhance the orbiter capability of carrying larger and heavier payloads. The design, function, and analysis of a new three-pin double swivel toggle release mechanism which is crucial to the successful deployment of the SPDS are described. Author

N89-23896*# National Aeronautics and Space Administration. Marshall Space Flight Center, Huntsville, AL.
DESIGN, FABRICATION AND TEST OF A 4750 NEWTON-METER-SECOND DOUBLE GIMBAL CONTROL MOMENT GYROSCOPE **c35**
Lewis Cook, Paul Golley, Henning Krome, Joseph Blondin, Charles Gurrisi, and John Kolvek (Allied Signal Corp., Teterboro, NJ.) *In* *its* The 23rd Aerospace Mechanisms Symposium Mar. 1989 p 59-76 (For primary document see N89-23892 17-39)
Avail: NTIS HC A15/MF A01 CSCL 14B

The development of a prototype Control Moment Gyroscope (CMG) is discussed. Physical characteristics and the results of functional testing are presented to demonstrate the level of system performance obtained. Particular attention is given to how the man-rated mission requirement influenced the choice of the materials, fabrication, and design details employed. Comparisons are made of the measured system responses against the prediction generated by computer simulation. Author

N89-23897*# AEC-Able Engineering Co., Inc., Goleta, CA.
CAROUSEL DEPLOYMENT MECHANISM FOR COILABLE LATTICE TRUSS **c37**
Robert M. Warden and P. Alan Jones *In* NASA, Marshall Space Flight Center, The 23rd Aerospace Mechanisms Symposium Mar. 1989 p 77-100 (For primary document see N89-23892 17-39)
Avail: NTIS HC A15/MF A01 CSCL 13I

The development of a mechanism for instrumentation and solar-array deployment is discussed. One part of the technology consists of a smart motor which can operate in either an analog mode to provide high speed and torque, or in the stepper mode to provide accurate positioning. The second technology consists of a coilable lattice mast which is deployed and rotated about its axis with a common drive system. A review of the design and function of the system is presented. Structural and thermal test data are included. Author

N89-23898*# I.A.M. Rinaldo Piaggio, Finale Ligure (Italy).
DESIGN AND TESTING OF A DEPLOYABLE, RETRIEVABLE BOOM FOR SPACE APPLICATIONS **c18**
P. Becchi and S. DellAmico *In* NASA, Marshall Space Flight Center, The 23rd Aerospace Mechanisms Symposium Mar. 1989 p 101-112 (For primary document see N89-23892 17-39)
Avail: NTIS HC A15/MF A01 CSCL 22B

The Deployable Retrievable Boom which was developed as a part of the joint U.S.-Italian Tethered Satellite System (TSS) is described. The design mission of the boom is to support, deploy, and retrieve an experiment package for the study of the electromagnetic field surrounding the satellite. The mechanism includes a jettisoning provision and deployable harness for the supported payloads connection. The boom is based on a tubular telescopic concept. Particular emphasis is placed on the payload harness connection capability and safety provisions. Author

N89-23899*# Dornier-Werke G.m.b.H., Friedrichshafen (Germany, F.R.).
DESIGN AND VERIFICATION OF MECHANISMS FOR A LARGE FOLDABLE ANTENNA **c32**
Hans Jurgen Luhmann, Carl Christian Etzler, and Rudolf Wagner *In* NASA, Marshall Space Flight Center, The 23rd Aerospace Mechanisms Symposium Mar. 1989 p 113-126 (For primary document see N89-23892 17-39)
Avail: NTIS HC A15/MF A01 CSCL 20N

The characteristics of the Synthetic Aperture Radar (SAR) antenna aboard the ESA Remote Sensing Satellite (ERS-1) are presented. The antenna is folded into a dense package for launch and is deployed in orbit. The design requirements and constraints, their impact on the design, and the resulting features of the mechanisms are discussed. Author

N89-23900*# Honeywell Space and Aviation Systems, Durham, NC.
EDDY CURRENT DAMPER **c33**
R. C. Ellis, R. A. Fink, and R. W. Rich *In* NASA, Marshall Space Flight Center, The 23rd Aerospace Mechanisms Symposium Mar. 1989 p 127-137 (For primary document see N89-23892 17-39)
Avail: NTIS HC A15/MF A01 CSCL 09A

A high torque capacity eddy current damper used as a rate limiting device for a large solar array deployment mechanism is

discussed. The eddy current damper eliminates the problems associated with the outgassing or leaking of damping fluids. It also provides performance advantages such as damping torque rates, which are truly linear with respect to input speed, continuous 360 degree operation in both directions of rotation, wide operating temperature range, and the capability of convenient adjustment of damping rates by the user without disassembly or special tools. Author

N89-23901*# Lockheed Missiles and Space Co., Palo Alto, CA.
DEVELOPMENT OF A PRECISION, WIDE-DYNAMIC-RANGE ACTUATOR FOR USE IN ACTIVE OPTICAL SYSTEMS **c74**
K. R. Lorell, J-N. Aubrun, D. F. Zacharie, and E. O. Perez *In* NASA, Marshall Space Flight Center, The 23rd Aerospace Mechanisms Symposium Mar. 1989 p 139-156 (For primary document see N89-23892 17-39)
Avail: NTIS HC A15/MF A01 CSCL 20F

The design, operation, and performance of a wide-dynamic-range optical-quality actuator are discussed. The actuator uses a closed-loop control system to maintain accurate positioning and has an rms noise performance of 20 nm. A unique force offloading mechanism allows the actuator coil to dissipate less than 3 mW under quiescent conditions. The operation of an experimental segmented optical system that uses 18 of the actuators is examined to show how they are integrated into an actual system. Author

N89-23902*# General Dynamics Corp., San Diego, CA. Space Systems Div.
PYRO THRUSTER FOR PERFORMING ROCKET BOOSTER ATTACHMENT, DISCONNECT, AND JETTISON FUNCTIONS **c20**
Stephen Hornyak *In* NASA, Marshall Space Flight Center, The 23rd Aerospace Mechanisms Symposium Mar. 1989 p 157-167 (For primary document see N89-23892 17-39)
Avail: NTIS HC A15/MF A01 CSCL 21H

The concept of a pyro thruster, combining an automatic structural attachment with quick disconnect and thrusting capability, is described. The purpose of the invention is to simplify booster installation, disengagement, and jettison functions for the U.S. Air Force Advanced Launch Systems (ALS) program. Author

N89-23903*# Jet Propulsion Lab., California Inst. of Tech., Pasadena.
DESIGN AND DEVELOPMENT OF A HIGH-STIFFNESS, HIGH-RESOLUTION TORQUE SENSOR **c35**
Michael M. Socha and Boris J. Lurie *In* NASA, Marshall Space Flight Center, The 23rd Aerospace Mechanisms Symposium Mar. 1989 p 169-180 (For primary document see N89-23892 17-39)
Avail: NTIS HC A15/MF A01 CSCL 14B

A sensor has been designed and tested for precise pointing applications. The device is able to sense extremely small rotary motion and is immune to cross-axis forces. The hardware and design characteristics of the torque sensor are presented. Test data, integrated control methodology, and future applications are included. Author

N89-23904*# National Aeronautics and Space Administration. Marshall Space Flight Center, Huntsville, AL.
ASTRONAUT TOOL DEVELOPMENT: AN ORBITAL REPLACEABLE UNIT-PORTABLE HANDHOLD **c54**
John W. Redmon, Jr. *In its* The 23rd Aerospace Mechanisms Symposium Mar. 1989 p 181-193 (For primary document see N89-23892 17-39)
Avail: NTIS HC A15/MF A01 CSCL 05H

A tool to be used during astronaut Extra-Vehicular Activity (EVA) replacement of spent or defective electrical/electronic component boxes is described. The generation of requirements and design philosophies are detailed, as well as specifics relating to mechanical development, interface verifications, testing, and astronaut feedback. Findings are presented in the form of: (1) a design which is universally applicable to spacecraft component replacement, and (2) guidelines that the designer of orbital replacement units might incorporate to enhance spacecraft on-orbit maintainability and EVA mission safety. Author

N89-23905*# National Aeronautics and Space Administration. Langley Research Center, Hampton, VA.
DOUBLE LEAD SPIRAL PLATEN PARALLEL JAW END EFFECTOR **c18**
David C. Beals *In* NASA, Marshall Space Flight Center, The 23rd Aerospace Mechanisms Symposium Mar. 1989 p 195-206 (For primary document see N89-23892 17-39)
Avail: NTIS HC A15/MF A01 CSCL 22B

The double lead spiral platen parallel jaw end effector is an extremely powerful, compact, and highly controllable end effector that represents a significant improvement in gripping force and efficiency over the LaRC Puma (LP) end effector. The spiral end effector is very simple in its design and has relatively few parts. The jaw openings are highly predictable and linear, making it an ideal candidate for remote control. The finger speed is within acceptable working limits and can be modified to meet the user needs; for instance, greater finger speed could be obtained by increasing the pitch of the spiral. The force relaxation is comparable to the other tested units. Optimization of the end effector design would involve a compromise of force and speed for a given application. Author

N89-23906*# Oak Ridge National Lab., TN.
TRACTION-DRIVE FORCE TRANSMISSION FOR TELEROBOTIC JOINTS **c37**
D. M. Williams and D. P. Kuban *In* NASA, Marshall Space Flight Center, The 23rd Aerospace Mechanisms Symposium Mar. 1989 p 207-222 (For primary document see N89-23892 17-39)
Avail: NTIS HC A15/MF A01 CSCL 13I

A mechanism which meets the requirements of a teleoperated manipulator and those of an autonomous robot is discussed. The mechanism is a traction-drive differential that uses variable preload mechanisms. The differential provides compact design, with dextrous motion range and torque density similar to geared systems. The traction drive offers high stiffness to backlash for good robotic performance. The variable-loading mechanism (VLM) minimizes the drive-train friction for improved teleoperation. This combination provides a mechanism to allow advanced manipulation with either teleoperated control or autonomous robotic operation. The design principles of both major components of the joint mechanism are described. Author

N89-23907*# Jet Propulsion Lab., California Inst. of Tech., Pasadena.
FLIGHT TELEROBOT MECHANISM DESIGN: PROBLEMS AND CHALLENGES **c37**
John B. Dahlgren and Edwin P. Kan *In* NASA, Marshall Space Flight Center, The 23rd Aerospace Mechanisms Symposium Mar. 1989 p 223-239 (For primary document see N89-23892 17-39)
Avail: NTIS HC A15/MF A01 CSCL 13I

Problems and challenges of designing flight telerobot mechanisms are discussed. Specific experiences are drawn from the following system developments: (1) the Force Reflecting Hand Controller, (2) the Smart End Effector, (3) the force-torque sensor, and a generic multi-degrees-of-freedom manipulator. Author

N89-23908*# Teldix Luftfahrt-Ausruestungs G.m.b.H., Heidelberg (Germany, F.R.).
A FAMILY OF BAPTAs FOR GEO AND LEO APPLICATIONS **c44**
W. Auer *In* NASA, Marshall Space Flight Center, The 23rd Aerospace Mechanisms Symposium Mar. 1989 p 241-253 (For primary document see N89-23892 17-39)
Avail: NTIS HC A15/MF A01 CSCL 10A

The application of a Bearing and Power Transfer Assembly (BAPTA) to a Solar Array Drive for communications satellites is presented. The basic principles which were used as guidelines for

design and development are developed and the three main subassemblies are described in detail. The results of vibration qualification and thermal vacuum life tests are included. Author

N89-23909*# Honeywell, Inc., Phoenix, AZ. Satellite Systems Div.
SIGNAL AND POWER ROLL RING TESTING UPDATE **c33**
Dennis W. Smith *In* NASA, Marshall Space Flight Center, The 23rd Aerospace Mechanisms Symposium Mar. 1989 p 255-266 (For primary document see N89-23892 17-39)
Avail: NTIS HC A15/MF A01 CSCL 20K

The development of the roll ring as a long-life, low-torque alternative to the slip ring is discussed. A roll ring consists of one or more circular flexures captured by their own spring force in the annular space between two concentric conductors or contact rings. The advantages of roll rings over other types of electrical transfer devices are: extremely low drag torque, high transfer efficiencies in high-power configurations, extremely low wear debris generation, long life, and low weight for high-power applications. Author

N89-23910*# Ford Aerospace and Communications Corp., Palo Alto, CA.
DESIGN OF A 60 GHz BEAM WAVEGUIDE ANTENNA POSITIONER **c32**
Kenneth S. Emerick *In* NASA, Marshall Space Flight Center, The 23rd Aerospace Mechanisms Symposium Mar. 1989 p 267-278 (For primary document see N89-23892 17-39)
Avail: NTIS HC A15/MF A01 CSCL 20K

A development model antenna positioner mechanism with an integral 60 GHz radio frequency beam waveguide is discussed. The system features a 2-ft diameter carbon-fiber reinforced epoxy antenna reflector and support structure, and a 2-degree-of-freedom elevation over azimuth mechanism providing hemispherical field of view. Emphasis is placed on the constraints imposed on the mechanism by the radio frequency subsystems and how they impacted the mechanical configuration. Author

N89-23911*# National Aeronautics and Space Administration. Lewis Research Center, Cleveland, OH.
AGE DISTRIBUTION AMONG NASA SCIENTISTS AND ENGINEERS **c80**
Michael L. Ciancone *In* NASA, Marshall Space Flight Center, The 23rd Aerospace Mechanisms Symposium Mar. 1989 p 279-287 (For primary document see N89-23892 17-39)
Avail: NTIS HC A15/MF A01 CSCL 20K

The loss of technical expertise through attrition in NASA and the aerospace industry is discussed. This report documents historical age-related information for scientific and engineering personnel in general and the NASA Lewis Research Center in particular, for 1968 through 1987. Recommendations are made to promote discussion and to establish the groundwork for action. Author

N89-23912*# Naval Research Lab., Washington, DC.
PRACTICAL EXPERIENCES WITH WORM GEARING FOR SPACECRAFT POWER TRANSMISSION APPLICATIONS **c37**
William Purdy and William McCown (Rexnord Aerospace Mechanisms, Torrance, CA.) *In* NASA, Marshall Space Flight Center, The 23rd Aerospace Mechanisms Symposium Mar. 1989 p 291-307 (For primary document see N89-23892 17-39)
Avail: NTIS HC A15/MF A01 CSCL 20K

Experiences of several organizations using worm gearing for spacecraft are discussed. Practical aspects and subtleties of using worm gearing for design and operation is included. Knowledge gained from these applications is analyzed, and guidelines for usage are proposed. Author

N89-23913*# National Aeronautics and Space Administration. Langley Research Center, Hampton, VA.
A TWO-AXIS LASER BORESIGHT SYSTEM FOR A SHUTTLE EXPERIMENT **c36**
Joseph F. DeLorme *In* NASA, Marshall Space Flight Center, The 23rd Aerospace Mechanisms Symposium Mar. 1989 p 309-318 (For primary document see N89-23892 17-39)
Avail: NTIS HC A15/MF A01 CSCL 20E

A two-axis gimballed laser pointing mechanism is being developed for the Lidar In-space Technology Experiment (LITE) to be flown on the National Space Transportation System (NSTS) Space Shuttle in February 1993. This report describes the design requirements and goals, the configuration, analysis, and testing plans for this laser pointing device. Author

N89-23914*# European Space Tribology Lab., Risley (England).
THE IN-VACUO TORQUE PERFORMANCE OF DRY-LUBRICATED BALL BEARINGS AT CRYOGENIC TEMPERATURES **c37**
S. G. Gould and E. W. Roberts *In* NASA, Marshall Space Flight Center, The 23rd Aerospace Mechanisms Symposium Mar. 1989 p 319-333 (For primary document see N89-23892 17-39)
Avail: NTIS HC A15/MF A01 CSCL 13I

The performance of dry-lubricated, angular contact ball bearings in vacuum at a temperature of 20 degrees K has been investigated, and is compared with the in-vacuo performance at room temperatures. Bearings were lubricated using dry-lubricant techniques which have been previously established for space applications involving operations at or near room temperature. Comparative tests were undertaken using three lubricants: molybdenum disulphide, lead, and PTFE. Results obtained using the three lubricants are presented. Author

N89-23915# Technische Hogeschool, Eindhoven (Netherlands).
NUMERICAL IMPLEMENTATION OF THE SCHAPERY MODEL FOR NONLINEAR VISCO-ELASTICITY Ph.D. Thesis
H. F. L. Rooijackers 23 Sep. 1988 116 p
(PB89-144950) Avail: NTIS HC A06/MF A01 CSCL 20K

Plastics are applied in heavily loaded, critical structure parts. The deformations, in these cases, are mostly large, resulting in a highly nonlinear visco-elastic material behavior. In other words: the material behavior is described by a nonlinear relation between stresses and strain history. For such applications, the necessary, accurate analysis of the mechanical behavior cannot be done analytically anymore but must be performed numerically, for instance using the finite element method. In the thesis, a constitutive equation for nonlinear visco-elasticity is derived, starting from irreversible thermodynamics. Finally, the three-dimensional formulation of the Schapery model is obtained: a single integral model using internal variables to take history effects into account. This model, which is known from literature, is capable of the description of anisotropic material behavior. Author

N89-23916# Army Missile Command, Redstone Arsenal, AL. Structures Directorate.
MODAL ANALYSIS AND TESTING OF MISSILE SYSTEMS Summary Report, for period ending Sep. 1988
Larry C. Mixon, John A. Schaeffel, Jr., Peter L. Green, Roque L. Salas, and Russell Garner Dec. 1988 77 p
(AD-A204051; AD-E951297; AMSMI/TR-RD-ST-88-9) Avail: NTIS HC A05/MF A01 CSCL 16/4

This study was performed to establish the effectiveness of using modal tests to verify the accuracy of NASTRAN Finite Element Models (FEMs) of missiles. The structure used in this study was a mock-up of the FOG-M (Fiber Optics Guided Missile) system. While the missile was not a flight version, the structural characteristics and internal subcomponents were sufficiently close to the FOG-M to allow meaningful conclusions concerning the testing and analysis techniques. The study also permitted a comparison between two different methods of testing, i.e., normal mode and random response. Also, sensitivity analyses were conducted on the NASTRAN mathematical model to identify peculiarities associated with a subroutine used to compute eigenvectors and eigenvalues and to study the requirement for additional nodes when modeling the wings and fins. Eight modes of vibration were measured and correlated with the FEM models. Excellent to good correlation was obtained for the critical first

bending modes of the airframe, wings, and fins. Excellent to good correlation was obtained for the wings and fins higher mode shapes, but differences in most frequencies were noted for the higher modes of vibration. A Lessons Learned Chapter is provided that documents all difficulties experienced, and suggestions were provided for future test and analysis efforts. Finally, recommendations are offered on how this effort can most effectively be extended to a flight model of the FOG-M. GRA

N89-23917# Helsinki Univ. of Technology, Espoo (Finland).
APPLICATION OF AN EXACT FINITE ELEMENT METHOD TO ANALYSIS OF STATICS OF THIN ELASTIC SHELLS OF REVOLUTION WITH AXISYMMETRIC LOADING Ph.D. Thesis
Hannu Outinen 1988 27 p
(ISBN-952-900-399-4; ETN-89-94217) Avail: NTIS HC A03/MF A01

An exact finite element method was developed for the analysis of the statics of thin, linearly elastic shells of revolution with axisymmetric loading. Fundamental shells, which are circular plate, cylindrical shell, conical shell, spherical shell, and circular toroidal shell, are the finite elements used. The stiffness matrices and equivalent nodal forces are determined by using exact solutions of differential equations of the classical shell theory. The solutions are defined by elementary functions or power series. The method is adapted to a computer program tested numerically in application problems. ESA

N89-23918*# Case Western Reserve Univ., Cleveland, OH. Dept. of Civil Engineering.
FINITE ELEMENT MODELING OF FRICTIONALLY RESTRAINED COMPOSITE INTERFACES Final Report
Roberto Ballarini and Shamim Ahmed Apr. 1989 23 p
(Grant NAG3-856)
(NASA-CR-182281; NAS 1.26:182281) Avail: NTIS HC A03/MF A01 CSCL 20K

The use of special interface finite elements to model frictional restraint in composite interfaces is described. These elements simulate Coulomb friction at the interface, and are incorporated into a standard finite element analysis of a two-dimensional isolated fiber pullout test. Various interfacial characteristics, such as the distribution of stresses at the interface, the extent of slip and delamination, load diffusion from fiber to matrix, and the amount of fiber extraction or depression are studied for different friction coefficients. The results are compared to those obtained analytically using a singular integral equation approach, and those obtained by assuming a constant interface shear strength. The usefulness of these elements in micromechanical modeling of fiber-reinforced composite materials is highlighted. Author

N89-23919*# Analytical Services and Materials, Inc., Hampton, VA.
CRACK-FACE DISPLACEMENTS FOR EMBEDDED ELLIPTIC AND SEMI-ELLIPTICAL SURFACE CRACKS
I. S. Raju May 1989 31 p
(Contract NAS1-18599)
(NASA-CR-181822; NAS 1.26:181822) Avail: NTIS HC A03/MF A01 CSCL 20K

Analytical expressions for the crack-face displacements of an embedded elliptic crack in infinite solid subjected to arbitrary tractions are obtained. The tractions on the crack faces are assumed to be expressed in a polynomial form. These displacements expressions complete the exact solution of Vijayakumar and Atluri, and Nishioki and Atluri. For the special case of an embedded crack in an infinite solid subjected to uniform pressure loading, the present displacements agree with those by Green and Sneddon. The displacement equations derived were used with the finite-element alternating method (FEAM) for the analysis of a semi-elliptic surface crack in a finite solid subjected to remote tensile loading. The maximum opening displacements obtained with FEAM are compared to those with the finite-element method with singularity elements. The maximum crack opening displacements by the two methods showed good agreement. Author

N89-23920*# Boeing Helicopter Co., Philadelphia, PA.
GROUND SHAKE TEST OF THE BOEING MODEL 360 HELICOPTER AIRFRAME Final Report
D. A. Reed and R. Gabel Mar. 1989 298 p
(Contract NAS1-17497)
(NASA-CR-181766; NAS 1.26:181766; D210-12328-3) Avail: NTIS HC A13/MF A01 CSCL 20K

Boeing Helicopters, together with other U.S. Helicopter manufacturers, is engaged in a finite element applications program designed to emplace in the U.S. a superior capability to utilize finite element analysis models in support of helicopter airframe structurel design. This program was given the acronym DAMVIBS (Design Analysis Methods for VIBrationS). The test plan is reviewed and results are presented for a shake test of the Boeing Model 360 helicopter. Results of the test will serve as the basis for validation of a finite element vibration model of the helicopter. Author

N89-23921# Pennsylvania Univ., Philadelphia.
MECHANISMS OF DIFFUSION-CONTROLLED BRITTLE FRACTURE Progress Report, 1 Apr. 1988 - 31 Mar. 1989
Charles J. McMahon, Jr. 13 Feb. 1989 15 p
(Contract DE-FG02-87ER-45290)
(DE89-008728; DOE/ER-45290/2) Avail: NTIS HC A03/MF A01

During the past year the major accomplishments have been the completion of the first UHV testing chamber and the demonstration of the cracking phenomenon in a Cu-8 wt percent Sn alloy. The latter alloy was fabricated in our laboratory and was selected because of reports in the Japanese literature of reduced ductility due to intergranular fracture in such an alloy in the range 300 to 600 C and because of the well-documented surface-cavity of tin in this alloy system. Tin, of course, is a powerful embrittling element in iron and steel. In confirmation of the hypothesis, the slow brittle fracture phenomenon has been produced in this alloy at temperatures as low as 250 C. DOE

N89-23922# Sandia National Labs., Albuquerque, NM. Applied Mechanics Div.
PREDICTION AND MEASUREMENT OF DAMPING OF A LAMINATED BEAM WITH A CONSTRAINED VISCOELASTIC LAYER
D. J. Segalman and Philip Reamy Feb. 1989 33 p
(Contract DE-AC04-76DP-00789)
(DE89-009002; SAND-88-2551) Avail: NTIS HC A03/MF A01

Analytic predictions for damped natural frequencies of a simple viscoelastic structure are compared with measured values. The structure studied is an aluminum channel incorporating a constrained layer of highly viscoelastic polymer. The predictive technique employs a general and systematic method for calculating damping and stiffness matrices using only measured material properties and structure geometry. These matrices are then used to predict the dynamic properties of the structure. This work constitutes the first step in the experimental verification of the analytic method. Future work will demonstrate and test some of the unique capabilities of the analytic method including the ability to predict even the complex modes of viscoelastic structures. The experimental and analytic results are in the form of frequency response functions, and the frequencies and damping of the natural modes. The natural frequencies agreed to within 5 percent, as expected, and the damping values agreed to within the uncertainty in the properties of the viscoelastic damping material. The measured and predicted mode shapes, as compared using the Modal Assurance Criterion (MAC), also agreed closely. Agreement between the predicted and measured response of the structure studied is very good, and indicating that the analytic technique used is a viable method for modeling viscoelastically damped structures. DOE

N89-23923# Edgerton, Germeshausen and Grier, Inc., Idaho Falls, ID.
APPLICATIONS OF A DIGITAL ACOUSTIC-EMISSION DATA-ACQUISITION WORKSTATION

John A. Johnson, Nancy M. Carlson, and Randall T. Allemeier 1988 8 p Presented at the Review of Progress in Quantitative Nondestructive Evaluation, La Jolla, CA, 31 Jul. 1988
(Contract DE-AC07-76ID-01570)
(DE89-009648; EGG-M-88151; CONF-880760-11) Avail: NTIS HC A02/MF A01

An eight-channel, data-acquisition system is used to acquire and analyze acoustic-emission (AE) data from aluminum surface-crack specimens. The system is calibrated using known source locations and laser-generated ultrasound to determine the transducer locations by finding the arrival time of the longitudinal wave and then doing a nonlinear, least-squares fit. From these transducer locations, the origin of AE sources can be determined using a similar procedure. Automated methods for determining source location by finding the first signal above noise on each channel and identifying this signal as the longitudinal wave arrival are developed for processing the vast amount of data generated during a typical experiment. The application of these methods to data acquired during tensile testing is discussed. A goal of this research is to sense acoustic events to enable the prediction of conditions for initiation of crack growth. The predictions will be based on models being developed by Parks and McClintock that calculate the effects of specific crack growth conditions. DOE

N89-23924*# National Aeronautics and Space Administration. Langley Research Center, Hampton, VA.
LOCATING DAMAGED MEMBERS IN A TRUSS STRUCTURE USING MODAL TEST DATA: A DEMONSTRATION EXPERIMENT
Suzanne Weaver Smith (Virginia Polytechnic Inst. and State Univ., Blacksburg.) and Paul E. McGowan Apr. 1989 9 p Presented at the 30th Structures, Structural Dynamics and Materials Conference, Mobile, AL, 3-5 Apr. 1989
(NASA-TM-101595; NAS 1.15:101595) Avail: NTIS HC A02/MF A01 CSCL 20K

On-orbit assessment of large flexible space truss structures can be accomplished, in principle, with dynamic response information, structural identification methods, and model correlation techniques which produce an adjusted mathematical model. In a previously developed approach for damage location, an optimal update of the structure model is formed using the response data, then examined to locate damaged members. An experiment designed to demonstrate and verify the performance of the on-orbit assessment approach uses a laboratory scale model truss structure which exhibits characteristics expected for large space truss structures. Vibration experiments were performed to generate response data for the damaged truss. The damage location approach, analytical work performed in support of the vibration tests, the measured response of the test article, and some preliminary results are described. Author

N89-23925*# Lehigh Univ., Bethlehem, PA.
CRACKING OF A LAYERED MEDIUM ON AN ELASTIC FOUNDATION UNDER THERMAL SHOCK
Abd El-Fattah A. Rizk and Fazil Erdogan Aug. 1988 345 p
(Grant NAG1-713)
(NASA-CR-185316; NAS 1.26:185316) Avail: NTIS HC A15/MF A01 CSCL 20K

The cladded pressure vessel under thermal shock conditions which is simulated by using two simpler models was studied. The first model (Model 1) assumes that, if the crack size is very small compared to the vessel thickness, the problem can be treated as a semi-infinite elastic medium bonded to a very thin layer of different material. However, if the crack size is of the same order as the vessel thickness, the curvature effects may not be negligible. In this case it is assumed that the relatively thin walled hollow cylinder with cladding can be treated as a composite beam on an elastic foundation (Model 2). In both models, the effect of surface cooling rate is studied by assuming the temperature boundary condition to be a ramp function. The calculated results include the transient temperature, thermal stresses in the uncracked medium and stress intensity factors which are presented as a function of time, and the duration of cooling ramp. The stress intensity factors are also presented as a function of the size and the location of the crack. The problem is solved for two bonded materials of different thermal and mechanical properties. The mathematical formulation results in two singular integral equations which are solved numerically. The results are given for two material pairs, namely an austenitic steel layer welded on a ferritic steel substrate, and a ceramic coating on ferritic steel. In the case of the yielded clad, the stress intensity factors for a crack under the clad are determined by using a plastic strip model and are compared with elastic clad results. Author

N89-23926*# Lehigh Univ., Bethlehem, PA.
THE CRACK PROBLEM IN BONDED NONHOMOGENEOUS MATERIALS
Fazil Erdogan, A. C. Kaya (Middle East Technical Univ., Ankara, Turkey), and P. F. Joseph Nov. 1988 27 p
(Grant NAG1-713)
(NASA-CR-184897; NAS 1.26:184897) Avail: NTIS HC A03/MF A01 CSCL 20K

The plane elasticity problem for two bonded half planes containing a crack perpendicular to the interface was considered. The effect of very steep variations in the material properties near the diffusion plane on the singular behavior of the stresses and stress intensity factors were studied. The two materials were thus, assumed to have the shear moduli mu(o) and mu(o) exp (Beta x), x=0 being the diffusion plane. Of particular interest was the examination of the nature of stress singularity near a crack tip terminating at the interface where the shear modulus has a discontinuous derivative. The results show that, unlike the crack problem in piecewise homogeneous materials for which the singularity is of the form r/alpha, 0 less than alpha less than 1, in this problem the stresses have a standard square-root singularity regardless of the location of the crack tip. The nonhomogeneity constant Beta has, however, considerable influence on the stress intensity factors. Author

N89-23927*# Lehigh Univ., Bethlehem, PA.
THE MODE 3 CRACK PROBLEM IN BONDED MATERIALS WITH A NONHOMOGENEOUS INTERFACIAL ZONE
Fazil Erdogan, A. C. Kaya (Middle East Technical Univ., Ankara, Turkey), and P. F. Joseph Oct. 1988 33 p
(Grant NAG1-713)
(NASA-CR-185315; NAS 1.26:185315) Avail: NTIS HC A03/MF A01 CSCL 20K

The mode 3 crack problem for two bonded homogeneous half planes was considered. The interfacial zone was modelled by a nonhomogeneous strip in such a way that the shear modulus is a continuous function throughout the composite medium and has discontinuous derivatives along the boundaries of the interfacial zone. The problem was formulated for cracks perpendicular to the nominal interface and was solved for various crack locations in and around the interfacial region. The asymptotic stress field near the tip of a crack terminating at an interface was examined and it was shown that, unlike the corresponding stress field in piecewise homogeneous materials, in this case the stresses have the standard square root singularity and their angular variation was identical to that of a crack in a homogeneous medium. With application to the subcritical crack growth process in mind, the results given include mostly the stress intensity factors for some typical crack geometries and various material combinations.
Author

N89-23928*# Lehigh Univ., Bethlehem, PA.
CRACKING OF COATED MATERIALS UNDER TRANSIENT THERMAL STRESSES
A. A. Rizk and Fazil Erdogan Jun. 1988 56 p
(Grants NAG1-713; NSF MSM-86-13611)
(NASA-CR-184898; NAS 1.26:184898) Avail: NTIS HC A04/MF A01 CSCL 20K

The crack problem for a relatively thin layer bonded to a very thick substrate under thermal shock conditions is considered. The effect of surface cooling rate is studied by assuming the temperature boundary condition to be a ramp function. Among

the crack geometries considered are the edge crack in the coating layer, the broken layer, the edge crack going through the interface, the undercoat crack in the substrate and the embedded crack crossing the interface. The primary calculated quantity is the stress intensity factor at various singular points and the main variables are the relative sizes and locations of cracks, the time, and the duration of the cooling ramp. The problem is solved and rather extensive results are given for two material pairs, namely a stainless steel layer welded on a ferritic medium and a ceramic coating on a steel substrate. Author

N89-23929# Naval Postgraduate School, Monterey, CA.
COMPUTERIZED MEASUREMENT OF THERMOACOUSTICALLY GENERATED TEMPERATURE GRADIENTS M.S. Thesis
Milton D. Kite Dec. 1988 54 p
(AD-A205353) Avail: NTIS HC A04/MF A01 CSCL 20/13

The computerized measurement of thermoacoustically generated temperature gradients in short, thin plates is reported. The computerized data acquisition system is delineated. The temperature difference developed across a stack of short plates was measured as a function of the longitudinal position of the plates in a resonant tube for acoustic pressure amplitudes of 0.5 to 6.6 kPa, and static (or mean) pressure readings of 100 through 440 kPa, in argon and helium for the first through the third harmonic frequencies of the tube. Measured data were compared with predictions based on work done by Wheatley and others (J. Wheatley, et al., Journal of the Acoustical Society of America, v. 74, pp. 153 to 170, 1983) and results reported by Muzzerall (Master's Thesis in Engineering Acoustics, Naval Postgraduate School, Monterey, CA, September 1987). For low acoustic and static pressures, there is good agreement between measured data and theory. As pressures increase there is a general degradation of agreement up to the point at which it appears saturation of the thermoacoustic effect occurs. GRA

N89-23930# Illinois Univ., Chicago. Dept. of Civil Engineering Mechanics and Metallurgy.
GEOMETRICAL FOUNDATIONS OF MESOMECHANICS AND LAGRANGIAN FORMALISM Final Report
A. Chudnovsky and B. Kunin 5 Jan. 1989 35 p
(Grant AF-AFOSR-0034-88; AF Proj. 2302)
(AD-A205589; AFOSR-89-0307TR) Avail: NTIS HC A03/MF A01 CSCL 20/11

Results of a scouting program of research in foundations of mesomechanics are presented. A special case of Weyl's geometry was employed to derive equations of thermoelasticity on pure geometrical ground; this demonstrates the potential of using Weyl's geometry as a model of the geometry of the material space. Experimental methods of finding fractal dimensions of fracture surfaces were examined (for various materials) together with a method of fracture profile simulation; the results contribute to developing experimental techniques of studying metric properties of the material space. A new dynamic crack propagation equation was derived on the basis of the least action principle; this is a first step of applying the Lagrangian formalism to deriving equations of continuous damage evolution. GRA

N89-23931# Army Armament Research, Development and Engineering Center, Watervliet, NY.
OVERVIEW OF ASTM SYMPOSIUM ON ANALYTICAL AND EXPERIMENTAL METHODS FOR RESIDUAL STRESS EFFECTS IN FATIGUE Final Memorandum Report
R. L. Champoux (Ceramic Binder Systems, Inc., Butte, MT.), J. H. Underwood, and J. A. Kapp Feb. 1989 15 p
(AD-A205622; ARCCB-MR-89004) Avail: NTIS HC A02/MF A01 CSCL 11/4

An overview of the ASTM Symposium on Analytical and Experimental Methods for Residual Stress Effects in Fatigue is presented. The background and objective for the symposium are described and the technical papers presented at the symposium and published in the proceedings are summarized. The papers are in two general categories: (1) Effects of residual stress near the surface of a specimen or component -- particularly shot peening applications, and (2) Effects of bulk residual stresses--particularly autofrettaged pressure vessels and piping. GRA

N89-23932# Air Force Inst. of Tech., Wright-Patterson AFB, OH. School of Engineering.
QUADRATIC OPTIMAL CONTROL THEORY FOR VISCOELASTICALLY DAMPED STRUCTURES USING A FRACTIONAL DERIVATIVE VISCOELASTICITY MODEL M.S. Thesis
Richard N. Walker Dec. 1988 110 p
(AD-A206008; AFIT/GA/AA/88D-12) Avail: NTIS HC A06/MF A01 CSCL 20/11

The objective of this thesis is to develop a control law for structures incorporating both passive damping via viscoelastic materials modelled by a fractional calculus stress strain law and active damping by applied forces and torques. To achieve this, quadratic optimal control theory is modified to accommodate systems with fractional derivatives in the state vector. Specifically, linear regulator theory is modified. GRA

N89-23933# Texas A&M Univ., College Station. Mechanics and Materials Center.
EXPERIMENTAL AND THEORETICAL DETERMINATION OF THE THERMOMECHANICAL RESPONSE OF INELASTIC STRUCTURAL MATERIALS TO HIGH ENERGY THERMAL INPUTS Semiannual Technical Report, Jul. - Dec. 1988
D. H. Allen and M. S. Pilant Dec. 1988 74 p
(Contract F49620-86-K-0016)
(AD-A206100; MM-5485-88-10; AFOSR-89-0140TR) Avail: NTIS HC A04/MF A01 CSCL 20/11

The general objective of this research is to improve on existing theoretical models for predicting the response of inelastic aerospace structural components subjected to hostile thermal environments with emphasis on transient temperature conditions, radiation boundary conditions, extremely rapid heating rates, and possible phase change of the materials involved. For materials subjected to the conditions under study herein it is necessary to perform extremely complex experiments in order to determine the precise form of the theoretical constitutive equations. Finally, it is necessary to implement the resulting equations to boundary value problem solving algorithms in order to model the response of structural components with stress, strain, and temperature gradient fields. GRA

N89-23934# Air Force Inst. of Tech., Wright-Patterson AFB, OH. School of Engineering.
FRACTIONAL CALCULUS FORMULATION OF THE QUASI-STATIC VISCOELASTIC PROBLEM M.S. Thesis
Joseph B. McCullough, III Mar. 1989 71 p
(AD-A206136; AFIT/GA/AA/89M-02) Avail: NTIS HC A04/MF A01 CSCL 20/11

The purpose of this study was to demonstrate the use of fractional derivatives to capture the frequency and temperature dependency of viscoelastic material behavior. To model the frequency dependency of viscoelastic material, fractional derivatives were included in the complex modulus. Solution techniques were performed in the Laplace domain to allow for easy manipulation of the fractional derivative terms. To incorporate the temperature dependency of viscoelastic material in the complex modulus model, the method of reduced variables was employed with the use of the WLF equation. With the frequency and temperature dependency built into complex modulus, a finite element formulation was devised that incorporated elastic and viscoelastic response of a truss structure. The formulation was limited to the use of the complex modulus in the transition region, the region where the damping ability of viscoelastic material is maximized. Quasi-static motion was also assumed, which limited the response to low frequencies. GRA

N89-23935# Army Lab. Command, Watertown, MA. Material Technology Lab.
A COMBINED ISOTROPIC-KINEMATIC HARDENING MODEL FOR LARGE DEFORMATION METAL PLASTICITY Final Report M.S. Thesis
Charles S. White Dec. 1988 254 p
(AD-A206352; MTL-TR-88-46) Avail: NTIS HC A12/MF A01 CSCL 20/11

The need for increased accuracy in material modeling has been driven in recent years by advanced in computing capability and the complexity of problems which now may be analyzed. Current material models are unable to represent many of the important multi-dimensional effects of the plastic deformation of metals to large strain. These effects can become very important at the level of deformation reached in metal processing operations, shear band formation, penetration mechanisms, and crack tip processes. An experimental program was conducted to produce a number of different types of tests on several materials. The types of tests included: tension, large strain compression, symmetric cyclic, single reverse and large strain torsion. Materials tested were type 316 stainless steel and 1100-0 aluminum. Also data for 3 carbon steels was analyzed. The model captures key features of small strain uniaxial cyclic behavior very well including the additional hardening due to nonproportional cycling in tension-torsion. The predictions of the finite torsion results are not as close. The inclusion of plastic spin does not affect these results. GRA

N89-23936# Stuttgart Univ. (Germany, F.R.).
NUMERICAL METHODS TO TREAT COLLISIONLIKE PHENOMENA IN SOLIDS Ph.D. Thesis [NUMERISCHE VERFAHREN ZUR BEHANDLUNG STOSSARTIGER VORGAENGE IN FESTKOERPERN]
Reynaldo TaylordeLima 1988 106 p In GERMAN Sponsored by the Deutschen Akademischen Austauschdient, Germany, F.R. and the Pontifica Univ. Catolica do Rio de Janeiro, Brazil
(ETN-89-93944) Avail: NTIS HC A06/MF A01

The solution of hyperbolic collisionlike problems of solid state mechanics using the finite element method was investigated. The conventional methods for the structural dynamics were analyzed, with emphasis on wave propagation; their disadvantages in the treatment of collisionlike phenomena are discussed. As an alternative, finite difference methods were investigated and interpreted using the theory of hyperbolic equation systems in the conservation form. This experience was applied to the finite element method, and Taylor-Galerkin algorithms for wave propagation in elastic media were deduced. A Taylor-Galerkin algorithm for propagation of elastoplastic and shock waves in solids was derived. Simple examples demonstrate the applicability of the algorithm as well as the advantages with respect to the conventional methods of structural dynamics. ESA

N89-23937# Karlsruhe Univ. (Germany, F.R.). Fakultaet fuer Maschinenbau.
DYNAMIC INTERACTION BETWEEN FLUIDS AND SOLIDS Ph.D. Thesis [DYNAMISCHE FLUID-FESTKOERPER-WECHSEWIRKUNG]
Peter Seelinger 1987 117 p In GERMAN
(ETN-89-93948) Avail: NTIS HC A06/MF A01

Fundamental theoretical investigations of the dynamic interaction between fluids and solid bodies were performed. Model equations were developed for the description of the most important phenomena, based on the continuum-mechanics fundamentals of the dynamic flud-solid-body systems; special value was set on a uniform description of fluids and solid bodies. The two usual description methods (material and spatial) are discussed. The material description method is preferentially used for the mechanics of elastic solid bodies, while the spatial description method is preferentially applied to fluid mechanics. Examples of vibration problems and stability problems demonstrate that several interaction problems can be treated more comprehensively than before. ESA

N89-23938# Motoren- und Turbinen-Union Muenchen G.m.b.H. (Germany, F.R.).
CYCLIC CRACK PROPAGATION CHARACTERISTICS OF THE POWDER METALLURGICAL NICKEL-BASE ALLOY UDIMET 720 AT ELEVATED TEMPERATURES AND DIFFERENT DWELL TIMES Final Report
E. Affeldt, H. Floege, and M. Kraus Apr. 1988 29 p
(Contract BMFT-03-K-01012)
(ETN-89-94426) Avail: NTIS HC A03/MF A01

The microstructure and the crack growth behavior of HIPed, and HIPed and forged billets of the powder alloy U720LC were evaluated. Grain size and structure, and defect distribution were investigated using standard metallographic techniques. Crack propagation testing was performed using compact tension and surface crack specimens in order to compare the behavior of long and short cracks at room temperature, 673 K and 873 K. The crack growth rate in both materials increases with increasing temperature, decreasing frequency, and through the introduction of hold time. The crack growth rate also depends on microstructure, being greater for the HIP+forged material. The influence of temperature and microstructure was attributed to changes in crack closure, in surface roughness, and deformation mode. ESA

N89-23939# Aerospatiale, Cannes La Bocca (France). Cryogenic Lab.
SHAKING IN CRYOGENIC CONDITIONS
S. Taride Paris, France 1988 5 p
(Rept-882-440-101; ETN-89-94494) Avail: NTIS HC A02/MF A01

Vibration test facilities designed to test the optical cryo-mechanisms of ISOCAM, one of the four optical experiments on board the ISO astronomical spacecraft are described. The developed cyrostat is able to perform up to 23 g sine or random vibrations at temperatures below 4 K, on the whole of the ISOCAM instrument under clean vacuum environment. ESA

N89-23940# Aerospatiale, Cannes La Bocca (France).
TELESCOPE STRUCTURE FOR CRYOGENIC APPLICATION
J. A. Massoni Paris, France 1988 8 p In FRENCH; ENGLISH summary
(Rept-882-440-112; ETN-89-94505) Avail: NTIS HC A02/MF A01

The cryogenic infrared optical system of the Infrared Space Observatory (ISO) satellite is described. The cryogenic cooling is provided by a cryostat operating at 1.8 K with liquid helium. The telescope itself is a 60 cm Ritchey Chretien with a wavelength range 2 to 200 microns. It collimates infrared radiation for the benefit of all four focal plane experiments. ESA

42 GEOSCIENCES (GENERAL)

No abstracts in this category.

43 EARTH RESOURCES AND REMOTE SENSING

Includes remote sensing of earth resources by aircraft and spacecraft; photogrammetry; and aerial photography.

For instrumentation see *35 Instrumentation and Photography.*

N89-23941# Institut fuer Angewandte Geodaesie, Frankfurt am Main (Germany, F.R.).
REPORTS ON CARTOGRAPHY AND GEODESY. SERIES 1, NUMBER 101 [NACHRICHTEN AUS DEM KARTEN- UND VERMESSUNGSWESEN. REIHE 1, HEFT NR. 101]

1988 133 p In GERMAN; ENGLISH summary
(ISSN-0469-4236; ETN-89-93779) Avail: NTIS HC A07/MF A01

Hardware and software for graphic information systems; developments in the field of digital cartographic models; the status of the topographic-cartographic information system ATKIS; and the use of digital urban maps in land information systems are presented. Developments in automatic digitizing of cadastral mapping; the ARC-INFO geographic information system; the universal photogrammetric-cartographic system PHOCUS; and the ANA Tech system for digitizing drawings and cadastral maps are discussed. Geocoded data sets of imaging satellites; the computer assisted layout of graphic settlement representations; the computer assisted generalization of buildings for the construction of digital landscape models; and computer assisted generalization of transport line representations were studied. For individual titles, see N89-23942 through N89-23955.

N89-23942# Institut fuer Angewandte Geodaesie, Frankfurt am Main (Germany, F.R.).
DEFINITION AND FILLING OF INFORMATION SYSTEMS: CHALLENGE FOR A PHOTOGRAMMETRIC SERVICE ENTERPRISE [DEFINITION UND FUELLUNG VON INFORMATIONSSYSTEMEN: HERAUSFORDERUNG AN EIN PHOTOGRAMMETRISCHES DIENSTLEISTUNGSUNTERNEHMEN]
Hans-Dieter Arnold and Ralf Schroth *In its* Reports on Cartography and Geodesy. Series 1, Number 101 1988 p 7-16 In GERMAN; ENGLISH summary (For primary document see N89-23941 17-43)
Avail: NTIS HC A07/MF A01

Hardware and software components for graphic data processing and their applications, as well as data acquisition methods are presented. The hardware and software necessary to establish information systems for complex planning aims and decision making in all areas of the economy and administration are discussed; the specific task must first be defined in order to collect the basic data necessary to operate the systems. The equipment necessary for filling of systems, in particular in graphic data processing, is described. A review of aims demonstrates the broad spectrum of ways of obtaining information and shows the differences with traditional photogrammetry. A process for obtaining information is presented and examples are given. ESA

N89-23943# Institut fuer Angewandte Geodaesie, Frankfurt am Main (Germany, F.R.).
COMPUTER AIDED PRODUCTION OF A 1:25,000 RELIEF MODEL OF BERLIN AND SURROUNDINGS [RECHNERGESTUETZTE HERSTELLUNG EINES GELAENDERELIEFS UND UMGEBUNG 1:25,000]
Fred Christ *In its* Reports on Cartography and Geodesy. Series 1, Number 101 1988 p 17-22 In GERMAN; ENGLISH summary (For primary document see N89-23941 17-43)
Avail: NTIS HC A07/MF A01

Developments in digital cartographic models, as well as the computer aided production of a three-dimensional relief model of Berlin and of a two-dimensional relief map of Berlin with hypsometric shadings are presented. ESA

N89-23944# Institut fuer Angewandte Geodaesie, Frankfurt am Main (Germany, F.R.).
THE OFFICIAL TOPOGRAPHIC-CARTOGRAPHIC INFORMATION SYSTEM (ATKIS) OF THE GEODESY GROUP OF THE LAENDER OF THE FEDERAL REPUBLIC OF GERMANY: STATUS AFTER ONE YEAR OF DEVELOPMENT [DAS ADV-VORHABEN ATKIS - STAND NACH EINEM JAHR ENTWICKLUNGSARBEIT]
Rolf Harbeck *In its* Reports on Cartography and Geodesy. Series 1, Number 101 1988 p 23-30 In GERMAN; ENGLISH summary (For primary document see N89-23941 17-43)
Avail: NTIS HC A07/MF A01

The ATKIS topographic-cartographic system was extended with regard to its scientific bases, its resources, and the data model for storing the topographic information. Priority was given to the establishment of a digital topographic data set in the form of digital landscape models (DLM's). The feature type catalog, which serves to structure the landscape and define the contents of the DLM, is available as a draft version. Legal aspects of managing digital topographic data sets are dealt with. ESA

N89-23945# Institut fuer Angewandte Geodaesie, Frankfurt am Main (Germany, F.R.).
THE DIGITAL URBAN MAP AS A BASIS FOR A LAND INFORMATION SYSTEM IN LOCAL ADMINISTRATION [DIE DIGITALE STADTKARTE ALS GRUNDLAGE EINES LANDINFORMATIONSSYSTEMS IN DER KOMMUNALEN VERWALTUNG]
Karl Haslinger *In its* Reports on Cartography and Geodesy. Series 1, Number 101 1988 p 31-35 In GERMAN; ENGLISH summary (For primary document see N89-23941 17-43)
Avail: NTIS HC A07/MF A01

The use of digital urban maps in land information systems is discussed. The complex task imposed by the increasing environmental demands is greatly facilitated by a land information system, in particular in urban areas where large batches of information with extremely complex interdependence in a very small area occur. Land information systems are based on a digital cadastre (legal representation) and on an urban map (natural and artificial representation); this division is advantageous because of administrative division of responsibility and of technical requirements of revision. The production and updating of urban maps using analytic photogrammetry (taking geodetic additions into consideration) combined with graphic coding, has many advantages. The division of objects into dots, lines, network, and area allows their correlations to be described with descriptive data from specialized data bases. ESA

N89-23946# Institut fuer Angewandte Geodaesie, Frankfurt am Main (Germany, F.R.).
AUTOMATIC DIGITIZING OF CADASTRAL MAPS [AUTOMATISCHE DIGITALISIERUNG VON LIEGENSCHAFTSKARTEN]
Andreas Illert *In its* Reports on Cartography and Geodesy. Series 1, Number 101 1988 p 37-45 In GERMAN; ENGLISH summary (For primary document see N89-23941 17-43)
Avail: NTIS HC A07/MF A01

Developments in automatic digitizing for cadastral mapping are reviewed. The original map sheet is digitized by a raster-scan device. Data processing continues using the raster-to-vector conversion computer program RAVEL which transforms the raster image into a set of vector features in chains-and-nodes structure. From these data, texts and symbols are extracted using methods of numerical pattern recognition. The whole image is classified by structural techniques. ESA

N89-23947# Institut fuer Angewandte Geodaesie, Frankfurt am Main (Germany, F.R.).
ARC-INFO: A GEOGRAPHIC INFORMATION SYSTEM [ARC-INFO: EIN GEOGRAPHISCHES INFORMATIONSSYSTEM]
Hartwig Junius *In its* Reports on Cartography and Geodesy. Series 1, Number 101 1988 p 47-59 In GERMAN; ENGLISH summary (For primary document see N89-23941 17-43)
Avail: NTIS HC A07/MF A01

The ARC-INFO software package for the establishment of areal information systems is presented. The package contains modules for collecting and managing graphic data, as well as analytic functions and processes for the production of thematic maps. The basic data model can be considered as geo-relational. Dot, line, or areal planimetric reference systems can be selected for application within the system. Specialized data are allocated as attributes to these reference systems in the relational data base INFO. The analytic functions include the various intersection functions which are the outstanding characteristic of this system and which complement the data base evaluation functions. The areas of application are indicated in three examples. ESA

N89-23948# Institut fuer Angewandte Geodaesie, Frankfurt am Main (Germany, F.R.).
CARTOGRAPHIC SIGNATURES IN PHOCUS [KARTOGRAPHISCHE SIGNATUREN IN PHOCUS]
Wolfgang Kresse *In its* Reports on Cartography and Geodesy. Series 1, Number 101 1988 p 61-67 In GERMAN; ENGLISH summary (For primary document see N89-23941 17-43)
Avail: NTIS HC A07/MF A01

The universal Zeiss photogrammetric-cartographic system PHOCUS is presented. The most important characteristics of the PHOCUS graphics: independence of object geometries stored in the data base and a high level of independency from equipment are described. The usual map specifications can be generated with PHOCUS cartographic signatures. ESA

N89-23949# Institut fuer Angewandte Geodaesie, Frankfurt am Main (Germany, F.R.).
DIGITIZING OF DRAWINGS AND CADASTRAL MAPS USING A SCANNER SYSTEM [DIGITALISIERUNG VON ZEICHNUNGEN UND BESTANDSPLAENEN MIT SCANNERSYSTEM]
Juergen Kunsemueller *In its* Reports on Cartography and Geodesy. Series 1, Number 101 1988 p 69-73 In GERMAN; ENGLISH summary (For primary document see N89-23941 17-43)
Avail: NTIS HC A07/MF A01

The ANA Tech system for computer assisted vectorization as a preliminary stage to CAD map design is presented. The system provides a bridge between the manual drawing and the CAD system. The digitizing of existing drawings is automated and hence substantially simplified. The ANA Tech system uses the high-resolution Eagle scanner. The excellent hard and software technology makes the system cost effective. The system has a broad application domain. ESA

N89-23950# Institut fuer Angewandte Geodaesie, Frankfurt am Main (Germany, F.R.).
GEOCODED DATA SETS OF IMAGING SATELLITES [GEOCODIERTE DATENSAETZE ABBILDENDER SATELLITEN]
Hans-Joachim Lotz-Iwen and Gunter Schreier *In its* Reports on Cartography and Geodesy. Series 1, Number 101 1988 p 75-81 In GERMAN; ENGLISH summary (For primary document see N89-23941 17-43)
Avail: NTIS HC A07/MF A01

The geocoded presentation of data sets of imaging satellites is discussed. Geocoded data sets of imaging satellites are high precision images of thematic information of the Earth surface using cartographic projections. Digital data of the remote sensing system LANDSAT TM is transformed into a cartographic standard projection using digital image processing methods. The data of the synthetic aperture radar sensor are planned to be available in geocoded presentation in the framework of the European ERS-1 remote sensing satellite. ESA

N89-23951# Institut fuer Angewandte Geodaesie, Frankfurt am Main (Germany, F.R.).
COMPUTER ASSISTED LAYOUT OF GRAPHIC SETTLEMENT REPRESENTATIONS [RECHNERGESTUETZTE GESTALTUNG ANSCHAULICHER SIEDLUNGSDARSTELLUNGEN]
Peter Mesenburg *In its* Reports on Cartography and Geodesy. Series 1, Number 101 1988 p 83-90 In GERMAN; ENGLISH summary (For primary document see N89-23941 17-43)
Avail: NTIS HC A07/MF A01

Methods of computer assisted layout of plane representations of areal facts were investigated. Due to the many possibilities of varying representations according to a particular problem, central perspective projection was chosen as the definitive representation method. Aspects of representation geometry and the program concept are described and explained using a concrete example of graphic settlement representation. ESA

N89-23952# Institut fuer Angewandte Geodaesie, Frankfurt am Main (Germany, F.R.).
TOOLS FOR THE COMPUTER ASSISTED GENERALIZATION OF SETTLEMENTS FOR THE CONSTRUCTION OF DIGITAL LANDSCAPE MODELS [BAUSTEINE ZUR AUTOMATIONSGESTUETZTEN GENERALISIERUNG VON SIEDLUNGEN FUER DIE EINRICHTUNG DIGITALER LANDSCHAFTSMODELLE]
Uwe Meyer *In its* Reports on Cartography and Geodesy. Series 1, Number 101 1988 p 91-100 In GERMAN; ENGLISH summary (For primary document see N89-23941 17-43)
Avail: NTIS HC A07/MF A01

The computer assisted generalization of buildings for the construction of digital landscape models (DLM) in the framework of a cartographic information system is discussed. Tools for the computer assisted generalization as well as a method for typifying buildings are presented. Using a building class catalog, all objects are classified by a template-matching procedure and associated to the following DLM. ESA

N89-23953# Institut fuer Angewandte Geodaesie, Frankfurt am Main (Germany, F.R.).
COMPUTER ASSISTED GENERALIZATION OF TRANSPORT LINE REPRESENTATIONS [AUTOMATIONSGESTUETZTE GENERALISIERUNG VON VERKEHRSWEGEDARSTELLUNGEN]
Bernd M. Powitz *In its* Reports on Cartography and Geodesy. Series 1, Number 101 1988 p 101-110 In GERMAN; ENGLISH summary (For primary document see N89-23941 17-43)
Avail: NTIS HC A07/MF A01

Program modules and algorithms for the automatic generalization and subsequent batch revision of commercial and transport line representations are being developed. The respective middle axes of the transport network are stored as digital object information. These characteristic series of dots, which are independent of scale, form the basis for automated signature deviation. The deviation of double-line transport axes can lead to undesirable line intersections and signature overlapping, in particular at junctions and crossings. The vectorial transport line representations already available are screened and subsequently revised automatically using local and dot-related screening operations. The corrected data are then transformed back into vectorial coordinates, whereby the transport lines are presented at the required scale. The program system supplies a generalized picture of the transport network which requires only minimal manual revision for graphic output. ESA

N89-23954# Institut fuer Angewandte Geodaesie, Frankfurt am Main (Germany, F.R.).
HYBRID CARTOGRAPHIC DATA PROCESSING IN A GEOGRAPHIC INFORMATION SYSTEM [HYBRIDE KARTOGRAPHISCHE DATENVERARBEITUNG IN EINEM LANDESINFORMATIONSSYSTEM]
Bernd Sonne *In its* Reports on Cartography and Geodesy. Series 1, Number 101 1988 p 111-120 In GERMAN; ENGLISH summary (For primary document see N89-23941 17-43)
Avail: NTIS HC A07/MF A01

Aspects of hybrid graphic information systems are outlined. Hybrid data processing, i.e., the processing and management of vector data, images and their corresponding attributes in a common system, is increasingly important in the field of cartography. Components of the hardware and software configuration which describe the concept of a hybrid information system are presented. ESA

N89-23955# Institut fuer Angewandte Geodaesie, Frankfurt am Main (Germany, F.R.).
AUTOMATIC EXTRACTION OF AREAS FROM OVERLAYS OF THE SERIES DGK 5 (Bo) [AUTOMATISCHE EXTRAKTION VON FLAECHEN AUS DECKFOLIEN DER DGK 5 (BO)]
Jun Yang *In its* Reports on Cartography and Geodesy. Series 1, Number 101 1988 p 121-132 In GERMAN; ENGLISH

summary (For primary document see N89-23941 17-43)
Avail: NTIS HC A07/MF A01

The automatic digitizing of ground map overlays of the series DGK 5 was investigated. The maps are digitized using a scanner, and the data are then converted into vector format. Dotted boundary lines of areas of utilization are recognized by classification, followed by automatic extraction of the areas indicated by the boundary lines. Recognition of texts, figures, and symbols, necessary to describe the types of utilization, is achieved using numerical and non-numerical classification methods. ESA

N89-23956*# Alaska Univ., Fairbanks. Geophysical Inst.
REMOTE SENSING OF GLOBAL SNOWPACK ENERGY AND MASS BALANCE: IN-SITU MEASUREMENTS ON THE SNOW OF INTERIOR AND ARCTIC ALASKA Semiannual Report
Carl S. Benson Mar. 1989 11 p
(Grant NAG5-887)
(NASA-CR-180078; NAS 1.26:180078) Avail: NTIS HC A03/MF A01 CSCL 08L

Observations led to a study of the physical properties of snow and the processes which operate on it. These observations included microwave brightness temperatures in interior Alaska which revealed: (1) up to three times more variability from one cell (1/2 degree latitude x 1/2 degree longitude) to the next in winter than in summer (5 to 15 K in winter and about 5 K in summer); (2) the overall range of temperature from week to week is about seven times greater in winter than in summer; (3) the microwave brightness temperature is about 25 K less than air temperature during summer but 35 to 60 K less during winter; and (4) the presence of snow cover appears to contribute to increasing the difference between air temperature and brightness temperature. The role of irregular substrate under the snow in enhancing convection has been studied with particular attention to variations in snow cover on water surfaces and in forested regions. LANDSAT imagery has been obtained to prepare a classification of ground surface types of the area. The extreme conditions of the 1988 to 1989 winter are discussed with respect to comparing the microwave data sets from 1985, and before, up to the present. The use of the Mt. Wrangell area as aerial photogrammetric controls for glacier measurements is given attention. A.D.

N89-23957# Research Inst. of National Defence, Linkoeping (Sweden). Dept. of Information Technology.
SHORTEST PATHS IN A DIGITIZED MAP USING A TILE-BASED DATA STRUCTURE
Peter Holmes and Erland Jungert Oct. 1988 14 p Presented at the 3rd International Conference on Engineering Graphics and Descriptive Geometry, Vienna, 1988
(PB89-143432; FOA-B-30129-3.4; ISSN-0281-0263) Avail: NTIS HC A03/MF A01 CSCL 08B

The problem addressed here is that of finding the shortest paths between two points within a digitized map. The map contains obstacles which may not be traversed. For this reason, the problem statement is analogous to that of finding shortest paths within a simple polygon containing holes. The approach described herein consists of both heuristic and algorithmic aspects. The heuristic component includes an inference engine for performing spatial reasoning, which operates in tandem with A (*) graph search. The output of the heuristic component is a plan which guides the algorithmic components through final processing states. As a methodology for system structure, this organization of components forms a powerful framework for exploring various problems encountered in geometrical/spatial analysis. Author

N89-23958# Technische Hogeschool, Delft (Netherlands). Dept. of Geodesy.
ON THE CONNECTION OF GEODETIC POINTFIELDS IN RETrig AND RELATED TESTS FOR MODEL ERRORS
A. J. M. Kosters Feb. 1988 109 p
(PB89-146112; Rept-88-1) Avail: NTIS HC A06/MF A01 CSCL 08E

A general view on connection problems in geodesy is presented with worked out practical examples from the Readjustment of the European Triangulation (RETrig). The connection of point fields can be defined as combining different coordinate sets, with limited overlap, which were determined by different point positioning methods and/or with respect to a different datum. Examples of this are numerous in practical geodesy. For the thesis, two types of connection problems related to RETrig are important. The two are: combining two neighboring RETrig-blocks, using their common points; combining satellite derived coordinates (viz. Doppler, SLR, VLBI and GPS) with terrestrial ellipsoidal coordinates. Special attention is paid to the use of 2- and 3-dimensional statistical tests on station coordinates and to the use of substitute covariance matrices for coordinates. Author

N89-23959# Lawrence Livermore National Lab., CA.
USE OF THE 1:2,000,000 DIGITAL LINE GRAPH DATA IN EMERGENCY RESPONSE
Hoyt Walker Jan. 1989 13 p Presented at the ASPRS/ACSM Auto-Carto 9th Annual Convention, Baltimore, MD, 2-7 Apr. 1989
(Contract W-7405-eng-48)
(DE89-006730; UCRL-99435; CONF-8904117-1) Avail: NTIS HC A03/MF A01

Environmental emergencies often have effects that are distributed over the earth's surface. As a result, maps are usually the most effective way to portray the impact of an emergency. The Atmospheric Release Advisory Capability (ARAC) at Lawrence Livermore National Laboratory is an emergency response organization that utilizes computer-assisted cartography. ARAC provides real-time assessments of the consequences of atmospheric releases of radioactive material. The products of this service are isopleths of the material concentration plotted over a base map of geographic features. Because ARAC's commitments encompass the entire United States, the ability to produce base maps anywhere in the United States is very important. At present ARAC is using data derived from the United States Geological Survey's 1:2,000,000 Digital Line Graph (DLG) database to meets its small-scale mapping needs. The DLG data set contains much of the information needed to serve in this emergency response application. However, certain enhancements are required to produce the necessary base maps. To create a data set suitable for ARAC, several preprocessing steps are needed. These include transforming the coordinate system, extracting relevant features as individual entities, correcting coding errors, and matching the edges along adjacent sectional files. DOE

N89-23960# Helsinki Univ. of Technology, Espoo (Finland). Instrument Lab.
DETERMINATION OF AREAL SNOW WATER EQUIVALENT USING SATELLITE IMAGES AND GAMMA RAY SPECTROMETRY Ph.D. Thesis
Risto Kuittinen 1988 143 p Sponsored by the Academy of Finland; Imatran Voiman Saatio, Finland; and Maa-ja Vestekniikian Tuki R.Y., Finland
(Ci-91; ISBN-951-666-275-7; ISSN-0355-2705; ETN-89-94220)
Avail: NTIS HC A07/MF A01

A method for near real time estimation of the areal snow water equivalent in the snow melt period is studied. The method involves direct estimation of the areal snow water equivalent and the use of satellite images, gamma ray spectrometry, and field measurements in estimating snow water equivalent. The method also involves estimation of snow melt by satellite images and field measurements. The areal distribution of the snow and the factors affecting it during the snow melt period are studied. A method for estimating the snow water equivalent on the basis of the area of bare spots on the ground interpreted from satellite images is introduced. The errors in estimating the snow water equivalent are between 20 and 45 mm for point estimates. The accuracy of gamma ray spectrometry and the factors affecting it in snow water equivalent measurements are studied. On the basis of these measurements, the representativeness of point snow water equivalent estimates is evaluated. A snow melt equation based on the degree-days and global radiation is also studied. Daily areal snow water equivalents are estimated for a river basin and

the results are compared with measured stream flows. The errors in daily areal snow water equivalents were between 15 and 35 mm. ESA

N89-23961*# Michigan Univ., Ann Arbor. Radiation Lab.
MAPPING FREEZE/THAW BOUNDARIES WITH SMMR DATA
B. W. Zuerndorfer, A. W. England, M. C. Dobson, and F. T. Ulaby [1989] 28 p
(Grant NAG5-852)
(NASA-CR-184991; NAS 1.26:184991) Avail: NTIS HC A03/MF A01 CSCL 08B

Nimbus 7 Scanning Multichannel Microwave Radiometer (SMMR) data are used to map daily freeze/thaw patterns in the upper Midwest for the Fall of 1984. The combination of a low 37 GHz radiobrightness and a negative 10.7, 18, and 37 GHz spectral gradient, Partial Derivative of Tb with Respect to f, appears to be an effective discriminant for classifying soil as frozen or thawed. The 37 GHz emissivity is less sensitive to soil moisture than are the lower frequency emissivities so that the 37 GHz radiobrightness appears to track soil surface temperature relatively well. The negative gradient for frozen ground is a consequence of volume scatter darkening at shorter microwave wavelengths. This shorter wavelength darkening is not seen in thawed moist soils. Author

N89-23962# Naval Civil Engineering Lab., Port Hueneme, CA. Utilities, Process and Geographic Systems Div.
GEOBOTANICAL REMOTE SENSING FOR DETERMINATION OF AGGREGATE SOURCE MATERIAL Final Report, Jul. 1986 - Sep. 1988
Timothy Minor, David Mouat, and Jeff Myers (National Aeronautics and Space Administration. Ames Research Center, Moffett Field, CA.) Dec. 1988 23 p
(AD-A205943; NCEL-TN-1792) Avail: NTIS HC A03/MF A01 CSCL 08/2

Aggregate source material suitable for facility and roadbed construction is often a very limited and highly valuable resource. The location of suitable source material is crucial to construction operations once facility requirements are established. The application of airborne and spaceborne remote sensing to terrain information requirements has proved attractive because of the rapid processing time and extensive spatial coverage associated with remotely gathered imagery. Source material identification may be improved by the remote sensing of vegetation associated with the material, particularly in areas of high vegetative cover. A research study employing remote sensing techniques was initiated to determine if vegetation could be used to discriminate parent materials for suitability as aggregate source material. Two test sites representing potential alluvial and residual source areas were selected in a semiarid region of Central California. Methods developed for the study included field observations of vegetation characteristics associated with the two parent material types along with the analysis of Thematic Mapper Simulator data flown over the test sites. The most useful images were those composites that included bands from two of the techniques (i.e., a Perpendicular Vegetation Index (PVI) band combined with principal components bands). GRA

N89-23963 Deutsche Geodaetische Kommission, Munich (Germany, F.R.).
ANALYSIS AND OPTIMIZATION OF GEODETIC NETWORKS BY SPECTRAL CRITERIA AND MECHANICAL ANALOGIES Thesis - Karlsruhe Univ. [ANALYSE UND OPTIMIERUNG GEODAETISCHER NETZE NACH SPEKTRALEN KRITERIEN UND MECHANISCHE ANALOGIEN]
Reiner Jaeger 1988 136 p In GERMAN; ENGLISH summary
(Ser-C-342; ISBN-3-7696-9390-6; ISSN-0065-5325;
ETN-89-93998) Copyright Avail: Fachinformationszentrum Karlsruhe, 7514 Eggensheim-Leopoldshafen 2, Fed. Republic of Germany

The analysis and optimization of geodetic networks with mathematical models describable as eigenvalue problems connected with the variance-covariance matrix of network coordinates is studied. The eigenvalues and eigenvectors serve as spectral criteria for network analysis and as spectral target functions for network optimization respectively. The analysis is closely linked to the kinetics, especially to the eigen-vibrations of elastic mechanical structures. Proceeding from the elastic continuum, the complete foundation of analogies between elastomechanics and geodetic network-compensation by least squares can be carried out in the step of its finite element discretization, being based fundamentally on equivalent principles of variations. Optimization leads to solving different associated inverse eigenvalue problems with respect to prescribed target-spectra. ESA

N89-23964# Technische Univ., Delft (Netherlands). Faculty of Geodesy.
THE SEARCH FOR EDGES IN REMOTE SENSING IMAGES USING A DIGITAL POLYGONAL MAP Thesis [HET SOEKEN NAAR RANDEN IN EEN DIGITAAL REMOTE SENSING BEELD MET BEHULP VAN EEN DIGITALE POLYGOON-KAART]
Ruud G. Verwaal Aug. 1988 107 p In DUTCH; ENGLISH summary
(ETN-89-94146) Avail: NTIS HC A06/MF A01

Edge detection in digital remote sensing images using an approximate position external information from a digital polygonal map was investigated. The map is transformed in the coordinate system of the digital images, and profiles perpendicular to the polygons are extracted in which the search for edges is performed. The global or local maximum value yields a selection criterion for the magnitude in edge detection. A threshold magnitude is also used. Aerial scanner images are used, and a polygonal map is digitized using aerial pictures. The study shows that the magnitude of the gray value is a primary parameter in edge detection. Texture affects a proper evaluation of line structures. ESA

N89-23965# Technische Univ., Delft (Netherlands). Werkeenheid der Fotogrammetrie en Remote Sensing.
INVESTIGATION OF SEVERAL METHODS FOR THE DETECTION OF OUTSTANDING POINTS IN A DIGITAL IMAGE Thesis [HET ONDERZOEKEN VAN VERSCHILLENDE METHODEN VOOR HET OPSPOREN VAN MARKANTE PUNTEN IN EEN DIGITAAL BEELD]
Geert vanderMolen Nov. 1988 79 p In DUTCH; ENGLISH summary
(ETN-89-94148) Avail: NTIS HC A05/MF A01

Methods for the detection of outstanding points in a digital image were investigated, and the point detectors were compared under different circumstances. The investigated point detectors are the Moravec, the Dreschler, and the Foerstner operator; the last one can be combined with the Sobel, the Roberts, or the Prewitt gradient. Operation, reliability, and precision of these five point detectors were determined using a synthetic image in which the points to be detected are exactly known, and which were distorted by several types of noise. Without noise, no large differences in the precision of the detectors are found; the Dreschler operator is the most reliable and the fastest detector. With noise, it is shown that the results depend on the type of noise. The operation of the point detectors depends on the type of smoothing filter. The Foerstner operator gives the best results in many cases, especially in combination with the Sobel or Prewitt gradient. ESA

N89-23966# Technische Univ., Delft (Netherlands). Faculty of Geodesy.
CALCULATION OF THE SURFACE OF A GEODETIC POLYGON ON AN ELLIPSOID OF REVOLUTION Thesis [HET BEREKENEN VAN DE OPPERVLAKTE VAN EEN GEODETISCHE VEELHOEK OP EEN OMWENTELINGSELLIPSOIDE]
Jurrien Heeger Aug. 1988 65 p In DUTCH
(ETN-89-94149) Avail: NTIS HC A04/MF A01

An algorithm for the calculation of the surface of an arbitrary polygon on an ellipsoid of revolution was developed. The differential equations and the calculation methods for a geodetic line are presented. The algorithm was developed on the basis of the method

of Levallois and Dupuy that uses the Wallis integrals for the calculation of the geodetic line. The surface of a geodetic polygon was expressed as a function of Wallis integrals; however it is shown that this formula is not suited for the direct calculation of the surface. Therefore the Wallis integrals were replaced by a function of azimuths and longitudes. The developed programs are suited for calculations on microcomputers. The algorithm could not be tested because there are not sufficient examples in the literature. ESA

N89-23967# Technische Univ., Delft (Netherlands). Faculty of Geodesy.
VECTORIZATION OF GRID LINES Thesis [VECTORISEREN VAN RASTERLIJNEN]
P. C. F. Lips Oct. 1988 77 p In DUTCH; ENGLISH summary
(ETN-89-94150) Avail: NTIS HC A05/MF A01

The vectorization of grid lines, extracted from gray value images, was investigated with a view to geographic information systems. The operations of edge detection and line following, necessary to extract the grid line structures from digital images are discussed. The artificially created test image on which the final vectorization algorithm is tested, is described. Polygonal approximation methods are presented and compared; nonsequential methods give better results. The algorithm was tested on a synthetic image, i.e., on ideal test data, and submited to precision analyses. The results of the tests are very positive. ESA

N89-23968# Technische Univ., Delft (Netherlands). Faculty of Geodesy.
DESIGN OF A METHODOLOGY FOR THE DETECTION OF ERRORS IN TERRESTRIAL NETWORKS Thesis [ONTWERP VAN EEN METHODIEK VOOR FOUTDETECTIE IN TERRESTRISCHE NETWERKEN]
L. V. Kollaard Aug. 1988 97 p In DUTCH; ENGLISH summary
(ETN-89-94151) Avail: NTIS HC A05/MF A01

A methodology for the detection of errors in geodetic observations in two-dimensional control networks was developed. Parameter estimation and error detection are outlined. The two stages during the data processing, the measuring stage and the administrative stage, are described. The proposed methodology can easily be implemented on a microcomputer. Some limitations of the methodology are linked with a possible lack of information, namely the singularity and the separability problem. The methodology reduces data production costs, but requires better qualified personnel. ESA

N89-23969# Beleidscommie Remote Sensing, Delft (Netherlands).
ON THE INTERNATIONAL COMMERCIALIZATION OF REMOTE SENSING Final Report [INTERNATIONALE COMMERCIALISERING REMOTE SENSING]
Jan. 1988 81 p In DUTCH Prepared in cooperation with NEDECO, Netherlands; EUROCONSULT B.V., Arnhem, Netherlands; and DHV Raadgevend Ingenieursbureau B.V., Amersfoort, Netherlands
(Contract BCRS-Proj.-CO-1.3)
(BCRS-88-02; ETN-89-94288) Avail: NTIS HC A05/MF A01

Results of Dutch remote sensing research that have possible commercial applications were inventoried and analyzed. The future demand for remote sensing products by international financing institutions was evaluated and a market analysis was performed. The analysis shows that, if the commercialization criteria are strictly applied to the present products, only a very low percentage can be commercialized. The available expertise can be valuable for the development of the operational use of remote sensing for various applications. ESA

N89-23970# Beleidscommie Remote Sensing, Delft (Netherlands).
METEOSAT THERMAL INERTIA MAPPING FOR STUDYING WETLAND DYNAMICS IN THE WEST-AFRICAN SAHEL Final Report
A. Rosema, J. L. Fiselier, and W. F. Rodenburg (Leiden Univ., Netherlands) Oct. 1988 45 p Original contains color illustrations
(Contract BCRS-Proj.-OP-3.3)
(BCRS-88-10A; ETN-89-94289) Avail: NTIS HC A03/MF A01

Meteosat noon and midnight imagery of various dates in 1978, 1983, and 1985 were used to study the dynamics of flooding in the Niger delta and the Lake Chad basin. Infrared imagery was processed to derive images and maps of evapotranspiration (ETP) and thermal inertia (TI). The TI products give the best information on the flooding phase and extension. The ETP images provide valuable supplementary information, in particular on the presence of water in the root zone. The flooded area was quantified by counting pixels, which have a TI above a given threshold; in this way the flooding cycle can be reconstructed and the maximum extension determined for each year. It is shown that Meteosat TI mapping can be used successfully to study the dynamics of flooding in Sahelian wetlands. ESA

N89-23971# Beleidscommie Remote Sensing, Delft (Netherlands).
THERMAL ANALYSIS FOR THE MONITORING AND PREDICTION OF FLOOD DYNAMICS IN WETLANDS Final Report [THERMISCHE ANALYSE VOOR DE MONITORING EN VOORSPELLING VAN DE OVERSTROMINGSDYNAMIEK VAN WETLANDS]
J. L. Fiselier and A. Rosema (Environmental Analysis and Remote Sensing, Delft, Netherlands) Oct. 1988 55 p In DUTCH; ENGLISH summary
(Contract BCRS-Proj.-OP-3.3)
(BCRS-88-10B; ETN-89-94290) Avail: NTIS HC A04/MF A01

Meteosat-based thermal inertia analysis was used for the mapping of flood dynamics in the Niger inner delta in Mali and the Logone floodplain in northern Cameroon. The remote sensing analysis is based on the heat transfer properties of the surface. Thermal inertia analysis generates a map that shows a more distinct flooding pattern than the visual picture. The maps were used to predict the hydrological impact of planned hydroagricultural schemes. Different weather conditions, especially wind speed, within the area of the image can lead to differences in thermal inertia and false interpretation. Thermal inertia analysis and interpretation are improved by continuous monitoring. Thermal inertia mapping appears a promising tool for monitoring flood dynamics of the larger Sahelian floodplains. ESA

N89-23972# Karlsruhe Univ. (Germany, F.R.). Dept. of Photogrammetry and Remote Sensing.
RESEARCH FOR OPTIMIZATION OF FUTURE MOMS SENSORS Final Report
H. Kaufmann, F. J. Behr, R. Geerken, H. Jacobs, K. Jung, T. Voegtle, and W. Weisbrich Apr. 1988 55 p In GERMAN; ENGLISH summary
(Contract BMFT-01-QS-86-206)
(ETN-89-94424) Avail: NTIS HC A04/MF A01

By means of spectroradiometer data and a developed software package for data evaluation, spectral bands and one panchromatic band for the MOMS-02 sensor were defined together with the hardware. The analysis of the relative and absolute geometric quality of MOMS-01 data as compared with LANDSAT Thematic Mapper and SPOT-HRV data is described. Within this context a correlation technique for optimized data merge was developed for combining MOMS data with data of other sensors. ESA

44 ENERGY PRODUCTION AND CONVERSION

Includes specific energy conversion systems, e.g., fuel cells; global sources of energy; geophysical conversion; and windpower.

For related information see also *07 Aircraft Propulsion and Power, 20 Spacecraft Propulsion and Power,* and *28 Propellants and Fuels.*

N89-23973# Portland State Univ., OR. Dept. of Chemistry.
IMPROVED ACID ELECTROLYTES: THE SYNTHESIS AND STRUCTURE OF FLUORINE CONTAINING SULFONIC ACIDS FOR FUEL CELLS Final Report, Jul. 1987 - 15 Aug. 1988
Gary L. Gard Sep. 1988 20 p
(Contract GRI-5084-260-1085)
(PB89-142616; GRI-88/0283) Avail: NTIS HC A03/MF A01 CSCL 10A

Seven new ether containing sulfonyl fluorides (precursors to sulfonic acids) were prepared from 1(CF2)2O(CF2)2SO2F and unsaturated olefins/alkynes. Two new ether sultones were prepared. A more efficient route for preparing either containing sulfonic acids were discovered. Additional quantities of mono/disulfonic acids were prepared and evaluated. Significant results for fuel cell electrolytes were achieved. Author

N89-23974# Stanford Univ., CA. Dept. of Chemistry.
ENERGY TRANSFER AND PHOTOCHEMISTRY IN BIOMIMETIC SOLAR CONVERSION Annual Report, Oct. 1987 - Sep. 1988
Steven G. Boxer Sep. 1988 12 p
(Contract GRI-5083-260-0824)
(PB89-142590; GRI-88/0248) Avail: NTIS HC A03/MF A01 CSCL 10A

Methods were developed for studying electron transfer reactions and electron transfer in biomimetic solar energy systems. During the past year, research focused on the use of applied electric fields to study the nature of photoexcited states which decay into ion pairs by electron transfer and direct control of electron transfer reaction dynamics by application of electric fields. The effects of electric fields on the absorption or emission spectrum of a molecule (the Stark effect) provides information on the change in dipole moment associated with the transition. The first Stark effect spectra have been obtained for a transition metal complex in a polymer film. The absorption Stark effect for a series of Ru complexes demonstrates the dipolar nature of the initially excited state. The rate of the initial electron transfer in phosynthetic reaction centers is slowed by application of an electric field. An analysis of the fluorescence anisotropy induced by the field provides detailed information on the mechanism of the initial charge-separation step in photosynthesis. Author

N89-23975# Agency of Industrial Science and Technology, Tokyo (Japan).
JAPAN'S SUNSHINE PROJECT 1987 ANNUAL SUMMARY OF COMPREHENSIVE RESEARCH
Apr. 1988 154 p In JAPANESE
(DE88-756448; AIST-8801) Avail: NTIS (US Sales Only) HC A08

Basic design of the 1 kW class oceanic temperature difference power generation system was in progress. Test models were constructed and tested for the evaporator and absorption mixing condensation heat exchanger. Basic researches were conducted on the effect of water intake and discharge behavior on the elements of oceanic temperature difference power generation system. Deep sea anchorage was also investigated. Tasks for practical system and component technology were examined for 10 MW class. A 1/15 scale model was built for joining parts of water intake pipe and floating body to establish their functions. Researches on thermoelectric elements are concurrently going on using a 30 W class thermoelectric generation based on oceanic temperature difference. Researches conducted in the fields of biomass energy included: solar energy conversion in living organism; and production of liquid fuel from wooden biomass. Element technology in the 1000 kW class wind power generation, e.g., rotor and tower were conducted. DOE

N89-23976# Pacific Northwest Labs., Richland, WA.
LOW-TEMPERATURE VOLUMETRIC RECEIVER CONCEPT
M. K. Drost Sep. 1988 16 p Presented at the AIChE Summer National Conference, Denver, CO, 21-24 Sep. 1988
(Contract DE-AC06-76RL-01830)
(DE89-008245; PNL-SA-15444; CONF-8809312-1) Avail: NTIS HC A03/MF A01

This document describes an alternative solar central receiver concept that offers the potential for a substantial reduction in the cost of electrical energy. The concept consists of a low temperature volumetric receiver which supplies 1100 F air to a Kalina cycle heat engine. Hot air can also be supplied to a packed bed of Dresser basalt where the hot air is used to heat the bed. The thermal energy stored in the bed can be extracted and supplied to the Kalina cycle during periods of low insolation. Previous investigations of the volumetric receiver concentrated on high temperature applications. The results showed that the volumetric concept could be very efficient, but the receiver was expensive and there were significant technical problems. Areas of technical uncertainty included fiber durability, the feasibility of inducing a preswirl and cost effective applications. The use of the volumetric receiver to produce low temperature will avoid the problems identified in the high temperature studies. The attractiveness of the low temperature concept is enhanced by the availability of the Kalina cycle. This heat engine was developed as a bottoming cycle for Brayton and Rankine cycle power plants. The key feature of the Kalina cycle is its ability to efficiently utilize the energy in a relatively low temperature heat source. The combination of the low temperature volumetric receiver and the Kalina cycle is particularly interesting. DOE

N89-23977# IAP Research, Inc., Dayton, OH.
LONG PULSE HOMOPOLAR GENERATOR Final Report, Apr. 1983 - Jun. 1987
Edward A. Knoth and David P. Bauer Aug. 1988 29 p
(Contract F33615-83-C-2303)
(AD-A205452; AFWAL-TR-88-2045) Avail: NTIS HC A03/MF A01 CSCL 10/2

The objective of this program was to develop a lightweight, long pulse homopolar generator. The generator is designed to deliver 250 kW at 10 kA for pulses greater than 10 seconds. This report reviews the truncated drum (rotor) design and the testing performed. The main design features, such as active excitation coil cooling, of the generator components are reviewed. GRA

N89-23978# Stuttgart Univ. (Germany, F.R.). Fakultaet Elektrotechnik.
RADIATION PHYSICS PROPERTIES OF SELECTIVE SOLAR ENERGY ABSORBER LAYERS Ph.D. Thesis [DIE STRAHLUNGSPHYSIKALISCHEN EIGENSCHAFTEN SELEKTIVER SOLARABSORBERSCHICHTEN]
Karl Johannes Gindele 1988 118 p In GERMAN
(ETN-89-93945) Avail: NTIS HC A06/MF A01

An optical measuring technique is presented, that allows the determination of the radiation physics characteristics of surfaces, especially of selective solar energy absorption layers. The main problem, i.e., the measurement of the directed, semispace reflection degree of diffusively reflecting probes in the IR, was solved by the development for a Fourier spectrometer of a reflection auxiliary with diffuse gold-coated Ulbricht splene. The accuracy of the measurement is largely determined by the accuracy with which the reflection degree of the standard is determined. The study of the optical properties of selective layers with those instruments gives a contribution to the understanding of the interaction between electromagnetic radiation and matter in metal-dielectric layers (cermets) and in rough surfaces. ESA

N89-23979# Aerospatiale, Cannes La Bocca (France).
THE THIRD GENERATION RIGID SOLAR ARRAY GSR3

A. Mamode, D. Gangloff (Centre National d'Etudes Spatiales, Toulouse, France), J. L. Bastard, and Ph. Auffray Paris, France 1988 7 p
(Rept-882-440-105; ETN-89-94498) Avail: NTIS HC A02/MF A01

A solar array design, which is well suited to future missions is described. It combines high performance to cost ratio and reliability, thanks to a very simple design. The prototype model is detailed. It is characterized by deployment mechanisms of a new type, modularity, versatility and high performance levels. It is selected as a suitable candidate for Spacebus, SPOT4, and Vesta projects. ESA

N89-23908*# Teldix Luftfahrt-Ausruestungs G.m.b.H., Heidelberg (Germany, F.R.).
A FAMILY OF BAPTAs FOR GEO AND LEO APPLICATIONS
W. Auer *In* NASA, Marshall Space Flight Center, The 23rd Aerospace Mechanisms Symposium Mar. 1989 p 241-253
(For primary document see N89-23892 17-39)
Avail: NTIS HC A15/MF A01 CSCL 10A

45 ENVIRONMENT POLLUTION

Includes atmospheric, noise, thermal, and water pollution.

N89-23980# Environmental Protection Agency, Research Triangle Park, NC.
SUMMARY OF SELECTED NEW INFORMATION ON EFFECTS OF OZONE ON HEALTH AND VEGETATION. DRAFT SUPPLEMENT TO AIR QUALITY CRITERIA FOR OZONE AND OTHER PHOTOCHEMICAL OXIDANTS
Daniel L. Costa, Lawrence J. Folinsbee, James A. Raub, Beverly E. Tilton, and David T. Tingey (Environmental Protection Agency, Corvallis, OR.) Nov. 1988 92 p
(PB89-135123; ECAO-R-019S; EPA/600/8-88/105A) Avail: NTIS HC A05/MF A01 CSCL 13B

Selected literature from 1986 through 1988 on the vegetation and health effects resulting from exposure to ozone is reviewed and summarized for the purpose of providing the Agency with information useful in identifying new data that may be relevant for developing primary and secondary National Ambient Air Quality Standards for Ozone. Author

N89-23981# Alliance Technologies Corp., Chapel Hill, NC.
AREA SOURCE DOCUMENTATION FOR THE 1985 NATIONAL ACID PRECIPITATION ASSESSMENT PROGRAM INVENTORY Final Report, May 1986 - Aug. 1987
Janice L. Demmy, Wienke M. Tax, and Thomas E. Warn Dec. 1988 267 p Sponsored by EPA, Research Triangle Park, NC
(Contract EPA-68-02-4274)
(PB89-151427; CH-88-05; EPA/600/8-88/106) Avail: NTIS HC A12/MF A01 CSCL 13B

The 1985 National Acid Precipitation Assessment Program (NAPAP) Emissions Inventory, a general understanding of the estimating procedures that will be used by NAPAP and EPA's Office of Air Quality Planning and Standards to generate 1985 emissions estimates for area source categories is provided to states and other participants and users. General methodology and assumptions are discussed, as well as the original source of algorithms, activity levels, and emission factors. Emission estimates are updated annually by a series of computer programs which multiply each current area source activity level by an emission factor that accounts for emissions removed by any control technology. County emissions estimates are then summed to produce national emissions estimates. Area sources are divided into stationary sources, mobile sources, solid waste disposal, miscellaneous area sources, and additional area sources. Author

N89-23982*# National Aeronautics and Space Administration. John F. Kennedy Space Center, Cocoa Beach, FL.
REVIEW OF WILDLIFE RESOURCES OF VANDENBERG AIR FORCE BASE, CALIFORNIA
David R. Breininger (Bionetics Corp., Cocoa Beach, FL.) Jan. 1989 71 p
(Contract NAS10-10285)
(NASA-TM-102146; NAS 1.15:102146) Avail: NTIS HC A04/MF A01 CSCL 13B

Wildlife resources are reviewed for purposes of developing a Base Biological Monitoring Program (BMP) for Vandenberg Air Force Base (VAFB) in Santa Barbara County, California. The review and recommendations were prepared by review of applicable scientific literature and environmental documents for VAFB, discussing information needs with natural resource management professionals at VAFB, and observations of base field conditions. This process found that there are 29 federally listed vertebrates (endangered, threatened, or Category 2) that occur or may occur in the vicinity of VAFB. There are also 63 other state listed or regionally declining species that may occur in the vicinity of VAFB. Habitats of VAFB represent a very valuable environmental resource for rare and declining wildlife in California. However, little information is available on VAFB wildlife resources other than lists of species that occur or are expected to occur. Recommendations are presented to initiate a long-term wildlife monitoring program at VAFB to provide information for environmental impact assessment and wise land use planning. Author

N89-23983# Kernforschungsanlage, Juelich (Germany, F.R.). Inst. fuer Chemie.
EVALUATION OF THE HISTORICAL SCHOENBEIN METHOD FOR THE DETERMINATION OF OZONE IN A FLOW CHAMBER [UEBERPRUEFUNG DER HISTORISCHEN SCHOENBEIN-METHODE ZUM NACHWEIS VON OZON IN EINEM STROEMUNGSROHR]
Frank Muehlheims, Andreas Volz, and Dieter Kley Jul. 1988 63 p In GERMAN; ENGLISH summary
(JUEL-2218; ISSN-0366-0885; ETN-89-93963) Avail: NTIS HC A04/MF A01

The Schoenbein method used during the last century for the determination of atmospheric ozone is evaluated. The method is tested in a flow tube for its response to ozone, wind speed, and relative humidity. The results indicate that the technique is ambiguous as higher ozone concentrations may produce less coloration for exposure times around 8 hr or more. The data are valid only under the assumption that Ozone concentration during last century was around or below 10 ppb. Quantitative assessments are difficult due to the poor standardization of the papers and the strong influence of humidity. ESA

N89-23984# Lawrence Livermore National Lab., CA.
A DESCRIPTION OF THE SLAB MODEL
Donald L. Ermak Mar. 1989 10 p Presented at the Joint Army-Navy-NASA-Air Force Safety and Environmental Protection, San Antonio, TX, 3 Apr. 1989
(Contract W-7405-eng-48)
(DE89-009962; UCRL-100028; CONF-8904128-3) Avail: NTIS HC A02/MF A01

SLAB is a computer model that simulates the atmospheric dispersion of a denser-than-air release. The current version of SLAB simulates the atmospheric dispersion of either a pure vapor or a liquid droplet---vapor mixture. Three types of sources are treated: a ground level evaporating pool, an elevated horizontal jet, and an instantaneous release. The evaporating pool source is assumed to be all vapor; although subsequent liquid droplet formation may occur within the cloud. The jet and instantaneous sources may be pure vapor or a mixture of vapor and liquid droplets. Dispersion of the released emission is calculated by solving the conservation equations of mass, momentum, energy, and species with the cloud modeled as either a steady state plume, a transient puff, or a combination of the two depending upon the duration of the release. In the case of a finite duration evaporating pool or horizontal jet release, cloud dispersion is initially described using

the plume mode while the source is active. Once the source is shut off, subsequent dispersion is calculated using the puff mode. For an instantaneous release, the puff dispersion mode is used for the entire calculation. SLAB is available in a PC version that requires only a few minutes of computing time on an IBM-AT computer to run a typical problem. DOE

N89-23985*# Jet Propulsion Lab., California Inst. of Tech., Pasadena.
ENVIRONMENTAL PROJECTS. VOLUME 3: ENVIRONMENTAL COMPLIANCE AUDIT Final Report
15 Sep. 1987 255 p
(NASA-CR-185019; JPL-Publ-87-4; NAS 1.26:185019) Avail: NTIS HC A12/MF A01 CSCL 13B

The Goldstone Deep Space Communications Complex is part of NASA's Deep Space Network, one of the world's largest and most sensitive scientific telecommunications and radio navigation networks. Activities at Goldstone are carried out in support of six large parabolic dish antennas. In support of the national goal of the preservation of the environment and the protection of human health and safety, NASA, JPL and Goldstone have adopted a position that their operating installations shall maintain a high level of compliance with Federal, state, and local laws governing the management of hazardous substances, abestos, and underground storage tanks. A JPL version of a document prepared as an environmental audit of Goldstone operations is presented. Both general and specific items of noncompliance at Goldstone are identified and recommendations are provided for corrective actions. Author

N89-23986# Florida Univ., Gainesville. Dept. of Soil Science.
ENVIRONMENTAL INTERACTIONS OF HYDRAZINE FUELS IN SOIL/WATER SYSTEMS Final Report, Mar. 1985 - Sep. 1987
Jimmy Street, Clifford Johnston, Robert Mansell, and Steve Bloom Oct. 1988 312 p
(Contract F08635-83-C-0136)
(AD-A206244; AFESC/ESL-TR-88-24) Avail: NTIS HC A14/MF A01 CSCL 13/2

Because the Air Force is the primary user of the rocket fuels, hydrazine (Hz), monomethylhydrazine (MMH), and 1,1-dimethylhydrazine (UDMH), it is responsible for the environmental implications associated with the transport, storage, and handling of these fuels. During handling, hydrazine fuels could inadvertently be released to the atmosphere and the surrounding aqueous and terrestrial environments. The studies are divided into the following five areas: aqueous and soil suspension studies, surface interaction studies, biological interaction studies, soil column studies, and soil transport modeling. The objective of this work is to determine the fate of hydrazine fuel released into an aqueous or soil environment. Aqueous degradation studies reveal that the extent of hydrazine degradation and the products formed are highly dependent upon several variables. Among these include the type of container used in the studies, the presence of certain metal ions, the ionic strength, the presence and type of pH buffer, the temperature, the presence of bacteria, and the amount of dissolved oxygen. Aqueous hydrazine degradation is particularly rapid in quartz vessels with copper ions ions and oxygen present. Degradation also increases with increasing ionic strength, pH buffer concentration, temperature, and bacteria content. GRA

N89-23539*# National Aeronautics and Space Administration. Lyndon B. Johnson Space Center, Houston, TX.
ENVIRONMENTAL DEFINITION OF THE EARTH'S NEUTRAL ATMOSPHERE
James T. Visentine *In* NASA, Langley Research Center, NASA/SDIO Space Environmental Effects on Materials Workshop, Part 1 May 1989 p 179-195 (For primary document see N89-23528 17-23)
Avail: NTIS HC A16/MF A01 CSCL 13B

46 GEOPHYSICS

Includes aeronomy; upper and lower atmosphere studies; ionospheric and magnetospheric physics; and geomagnetism.

For space radiation see *93 Space Radiation.*

N89-23987# Royal Inst. of Tech., Stockholm (Sweden). Dept. of Plasma Physics.
ELECTRIC FIELDS IN THE MAGNETOSPHERE: THE EVIDENCE FROM ISEE, S3-3, GEOS AND VIKING
Carl-Gunne Faelthammar Aug. 1988 42 p
(TRITA-EPP-88-11; ISSN-0348-7539) Avail: NTIS HC A03/MF A01

Electric field measurements on the satellites S3-3, GEOS-1, GEOS-2, ISEE-1 and Viking have extended the empirical knowledge of electric fields in space so as to include the outer regions of the magnetosphere. While the measurements confirm some of the theoretically expected properties of the electric fields, they also reveal unexpected features and a high degree of complexity and variability. The existence of a magnetospheric dawn-to-dusk electric field, as expected on the basis of extrapolation from low altitude measurements, is confirmed in an average sense. However, the actual field exhibits large spatial and temporal variations, including strong fields of inductive origin. At the magnetopause the average (dawn to dusk directed) tangential electric field component is typically obscured by irregular fluctuations of larger amplitude. The magnetic-field aligned component of the electric field, which is of particular importance for ionosphere-magnetosphere coupling and for auroral acceleration is even now very difficult to measure directly. However, the data from electric field measurements provide further support for the conclusion, based on a variety of evidence, that a non-vanishing magnetic-field aligned electric field exists in the auroral acceleration region. Author

N89-23988# Los Alamos National Lab., NM.
NON-NEWTONIAN GRAVITATIONAL FORCES AND THE GREENLAND ICE-SHEET EXPERIMENT
Richard J. Hughes, T. Goldman, and Michael Martin Nieto 1989 7 p Presented at the 8th Moriond Workshop on Tests of Fundamental Laws in Physics, Les Arcs, France, 1 Jan. 1989
(Contract W-7405-eng-36)
(DE89-009348; LA-UR-89-1011; CONF-890199-2) Avail: NTIS HC A02/MF A01

The results of an experiment to test Newton's Inverse-Square Law of Gravitation in the Greenland ice-cap were announced recently. The anomalous gravity gradient which was found can be explained either by an unrecognized anomaly in the density of the rocks under the ice sheet, or by the existence of a non-Newtonian component of the gravitational force. Here we focus on the latter possibility, and find that the force would be attractive, with a strength between about 2.4 percent and 3.5 percent that of Newtonian gravity, and a range between about 225 m and 5.4 km. DOE

N89-23989 Leeds Univ. (England).
STUDIES OF INTERNAL GRAVITY WAVES IN THE STABLY STRATIFIED TROPOSPHERE Ph.D. Thesis
Julia Margaret Rees 1988 318 p
Avail: Univ. Microfilms Order No. BRD-84382

In 1986, the British Antarctic Survey installed the State Antarctic Boundary Layer Experiment at Halley Base. The purpose of the experiment was to investigate the structure of the nocturnal boundary layer. It was found that during periods of stable stratification, wavelike phenomena were always detected in the surface layer. The characteristics of the waves were determined and possible mechanisms for their generation were identified. A fully nonlinear, two-dimensional finite difference Navier-Stokes model was developed to model the lower troposphere at Halley Base and to study the behavior of Kelvin-Helmholtz type instabilities. The model was used to investigate the radiation of shear-induced internal gravity waves away from the level at which they were generated. It was deduced that the short bursts of

large amplitude waves may be caused by regions of shear instability above the surface layer. Statistical methods were used to analyze data from meteorological instruments mounted on a triangular array of masts in order to determine some of the properties of the waves. The dispersion relation of the waves was deduced and their direction of propagation was related to local topographic features. The results indicate that the smaller amplitude waves were generated by topographic forcing. Theoretical methods were used to derive the cross-spectral phases associated with three different types of internal gravity waves. The results obtained were used to identify which types of waves tend to be dominant in the surface layer at Halley Base. It was found that when the surface layer is strongly stably stratified that the waves present are trapped, neutral modes and when the surface layer is only weakly stably stratified, locally generated instabilities dominate. In order to study the effect of the waves on the mean flow, data from slow ascent radiosondes released in the vicinity of Halley Base were analyzed. Dissert. Abstr.

N89-23990# Defense Mapping Agency, Washington, DC.
PROBLEMS ENCOUNTERED IN THE STOKES' NUMERICAL INTEGRATION OF TERRESTRIAL GRAVITY ANOMALIES
Gary R. Weigel 18 Jan. 1989 45 p
(AD-A205448) Avail: NTIS HC A03/MF A01 CSCL 08/5

Various sets of gravimetric geoid undulations were completed at 600 globally distributed Doppler station sites using geopotential coefficients and different cap sizes of terrestrial gravity data. The means and standard deviations of the residuals between these gravimetric undulations and corresponding Doppler-derived geometric undulations were then computed for each set and compared. The gravimetric undulations were determined using either the OSU 81 or WGS 84 set of geopotential coefficients, each complete to degree and order 180, or a combination of the OSU 81 model truncated to degree and order 36 and terrestrial gravity data consisting of a global set of 1 deg X 1 deg mean free air anomalies. The radii of the caps containing the terrestrial data were, by design, varied from 0 deg to 65 deg. The Doppler undulations were derived by subtracting the mean sea level elevations at the stations from the Doppler-determined ellipsoid heights. The smallest standard deviations of the geoid undulation residuals were obtained when using a cap size of 6 deg. Unexpectedly, as the cap size was increased from 6 deg, increasingly larger standard deviations were produced. This basic trend remained after the global set was divided into Eastern and Western Hemispheres. GRA

N89-23991# Utah State Univ., Logan. Center for Atmospheric and Space Sciences.
MESOSPHERIC WIND MEASUREMENT Final Technical Report, 30 Jun. 1986 - 29 Sep. 1988
29 Sep. 1988 3 p
(Grant AF-AFOSR-0241-86; AF Proj. 2917)
(AD-A205593; AFOSR-89-0283TR) Avail: NTIS HC A02/MF A01 CSCL 17/9

This grant involves the construction of MENTOR, an RF interferometer radar to study acoustic-gravity waves in the mesopause region of the earth's atmosphere, under the Department of Defense-University Research Instrumentation Program. The subcontractor for the construction of MENTOR has completed the radar and put it in the field. All the electronics are fielded in an 8 x 8 x 20 ft shipboard container, with the antenna arrays deployed close by. The electronics consists of a 50-kW transmitter, 8 receivers, and 150 Mips of on-line computer. The radar antenna consists of a 32-Yagi antenna array configured as 16 Yagis for transmit and 16 Yagis for receive. The transmit array is deployed on one side of the shipboard container and operated as a single in-phase beam; the 16 separate Yagis for receive are sampled as 8 rows of 4 Yagis each. GRA

N89-23992# Naval Postgraduate School, Monterey, CA.
THERMAL IMAGES OF SKY AND SEA-SURFACE BACKGROUND INFRARED RADIATION M.S. Thesis
Panagiotis Psihogios Dec. 1988 157 p
(AD-A205819) Avail: NTIS HC A08/MF A01 CSCL 17/5

Thermal images of the sky and the sea surface background radiance were analyzed using the AGA Thermovision 780 system. Calculated sky radiance was compared with that predicted by the computer code LOWTRAN 6. The Schwartz-Hon computer model for the emissivity of the sea surface was validated using the results from AGA measurements and LOWTRAN 6. The factors which affect the radiance measurements were determined, and the degree of influence they exert was estimated. The radiance emitted from an overcast sky was found to be higher than that emitted from a clear sky. The wind speed reduces significantly the infrared sky radiance. Emissivity of the sea surface depends upon the wave roughness, remaining almost constant with the viewing angle. The whole result showed that LOWTRAN 6 provides a good prediction of the atmospheric radiance with deviation from measurement generally within 10 percent with cases to 15 percent for the elevation angle range from 0 to 19 degrees and that the Schwartz-Hon model agrees well with observation showing deviation varying up to 14 percent in the elevation angle range from 5 to 10 degrees. GRA

N89-23993# Atmospheric and Environmental Research, Inc., Cambridge, MA.
INFERRING RELATIVE HUMIDITY PROFILES FROM 3DNEPH CLOUD DATA: TECHNIQUE DEVELOPMENT AND DATA IMPACT STUDY
Thomas Nehrkorn and Ross N. Hoffman 13 Dec. 1988 50 p
(Contract F19628-86-C-0141)
(AD-A205825; AFGL-TR-88-0327; SR-5) Avail: NTIS HC A03/MF A01 CSCL 04/1

We study the inference of humidity profiles from cloud data, using the 3DNEPH database as the source of the cloudiness information. The 3DNEPH (now RTNEPH) is a high resolution cloud database produced operationally by the USAF Global Weather Central. A colocation study of cloud data with radiosonde measurements of relative humidity over North America is used to develop and test a statistical method for inferring humidity profiles; a global data impact study is used to assess the utility of this moisture information. We review some previously developed methods for inferring humidity from cloud cover data, describe the database and processing used in our colocation study, and discuss the development and testing of the new method for inferring humidity. Regression equations were developed for the first two empirical orthogonal functions of relative humidity, using vertically compacted and horizontally averaged 3DNEPH cloud cover values as predictors. The regression equations were found to have smaller errors than existing level-to-level cloud to humidity conversion techniques in tests in which no attempt was made to tune the existing methods for optimal performance. The utility of the bogus RH data for operational data assimilation was studied in a global observing system experiment, using the AGGL global data assimilation system. The impact of the additional RH data was evident in analyses in the early part of the assimilation runs but was lost in the noise of the assimilation system at later times. GRA

N89-23994# Air Force Inst. of Tech., Wright-Patterson AFB, OH. School of Engineering.
AN ANALYSIS OF LIGHTNING LAUNCH CONSTRAINTS M.S. Thesis
Donald E. Holland Dec. 1988 162 p
(AD-A206084; AFIT/GSO/ENS/88D-1) Avail: NTIS HC A08/MF A01 CSCL 04/1

The purpose of this thesis was to review the current set of lightning launch constraints being used by NASA, the USAF and the U.S. Navy. The 3 primary objectives were to: (1) Assimilate current knowledge about triggered lightning to aerospace systems, and how lightning launch constraints are used to make launching safer; (2) Analyze cloud-to-ground lightning in the Cape Canaveral, Florida, area for spatial and diurnal distributions and for its impact on launch availability; (3) Develop a model to simulate all lightning events to better determine launch availabilities based on the first

constraint. The study found that lightning activity in the Cape area is not uniformly distributed in time or space. There is a well-known afternoon peak in activity, plus, there are areas where lightning occurs with much greater frequency--especially with low-level winds from the southwest. Since the launch constraints specify standoff distances and delay times from naturally occurring lightning, and launch availability is a function of time of year, time of day, and launch site. From the simulation model, equations were derived to define launch availability as a function of standoff distance and delay time for each summer month (Apr-Sep) and each 3-hour group (e.g. 0000-0300 Local Standard Time) in July and August. GRA

N89-23995*# Aerospace Corp., El Segundo, CA. Space Sciences Lab.
RELATIVISTIC ELECTRON PRECIPITATION PATTERNS IN LONGITUDE AND LATITUDE: A REPLY TO W. R. SHELDON
D. N. Baker, J. B. Blake, D. J. Gorney, P. R. Higbie, and R. W. Klebesadel (Los Alamos National Lab., NM.) 16 Feb. 1989 11 p Prepared in cooperation with Air Force Space Div. , Los Angeles, CA
(Contract F04701-85-C-0086)
(NASA-CR-185442; NAS 1.26:185442; AD-A206459; TR-0088(3940-06)-6; SD-TR-89-05) Avail: NTIS HC A03/MF A01 CSCL 04/1

In an earlier paper by the authors, a proposal was made that the precipitation of relativistic electrons from the outer magnetosphere into the Earth's atmosphere could have substantial effects on the chemistry of the middle atmosphere. It has been argued that our earlier estimates of precipitation fluxes may have underestimated the precipitation rates in isolated regions, such as the South Atlantic Anomaly, and overestimated the precipitation in other latitude and longitude sectors. Here, we discuss the factors which influence the longitudinal uniformity of relativistic electron precipitation and the implications of our earlier assumption of uniform precipitation. GRA

N89-23996# Karlsruhe Univ. (Germany, F.R.). Fakultaet fuer Physik.
ANALYSIS OF TURBULENT MOTION PHENOMENA IN THE MARITIME ATMOSPHERIC BOUNDARY LAYER Ph.D. Thesis [ANALYSE TURBULENTER BEWEGUNGSVORGAENGE IN DER MARITIMEN ATMOSPHAERISCHEN GRENZSCHICHT]
Ulrich Corsmeier 1987 198 p In GERMAN
(ETN-89-93949) Avail: NTIS HC A09/MF A01

The structure of the maritime boundary layer was investigated using statistical methods for turbulent structure (ensemble averaging) as well as single-structure analysis (conditional sampling) and based on the data of the measuring campaign JASIN (Joint-Air-Sea Interaction experiments), a subprogram of GARP. The evaluation of these data improved the knowledge of the structure of the turbulence in the mainly neutral to slightly unstable layered medium and upper maritime atmospheric boundary layer (maritime Ekman layer). The classical, closed, three-dimensional turbulence elements were less demonstrated than the existence of perturbing components in the wind field which suddenly occur in locally and temporatily limited regions of maximum wind shear. In the ideal case, closed vortex structures develop which can be demonstrated in fluctuation and correlation series. ESA

N89-23997 Royal Netherlands Meteorological Inst., De Bilt. Physical Meteorology Dept.
STRATOCUMULUS MODELING Ph.D. Thesis - Vrije Univ., Amsterdam, Netherlands
P. G. Duynkerke 1988 138 p
(KNMI-WR-88-2; ISSN-0169-1651; ETN-89-94152) Copyright Avail: Royal Netherlands Meteorological Inst., P.O. Box 201, 3730 AE De Bilt, Wilhelminalaan 10, Netherlands

The stratocumulus-topped atmospheric boundary layer (ABL), turbulent structure of a stratus-topped ABL, and diurnal variations of a marine stratocumulus layer are discussed. For individual titles, see N89-23998 through N89-24000.

N89-23998 Royal Netherlands Meteorological Inst., De Bilt.
CURRENT PROBLEMS IN THE STRATOCUMULUS-TOPPED ATMOSPHERIC BOUNDARY LAYER
P. G. Duynkerke and A. G. M. Driedonks *In its* Stratocumulus Modeling 1988 p 15-51 Submitted for publication (For primary document see N89-23997 17-46)
Copyright Avail: Royal Netherlands Meteorological Inst., P.O. Box 201, 3730 AE De Bilt, Wilhelminalaan 10, Netherlands

Knowledge of the turbulent structure of the atmospheric boundary layer (ABL) capped by a cloud deck is reviewed. The most important physical processes determining this structure are the longwave radiative cooling at cloud top, the shortwave radiative warming by absorption in the cloud, the surface buoyancy flux, and wind shear across the top of the ABL. Turbulence can cause entrainment against the buoyancy jump at cloud top. In cases where only long-wave radiative fluxes and surface buoyancy fluxes are important, the turbulent structure is relatively well understood. When shortwave radiative fluxes and/or wind shear are also important, the resulting turbulent structure may change considerably. A decoupling of the cloud from the sub-cloud layer or of the top of the cloud from the rest of the ABL is then regularly observed. In no case are the details of the entrainment at cloud top understood well enough to derive a relatively simple formulation that is consistent with observations. Cloud-top entrainment instability may lead to the breakup of a cloud deck (but also to cloud deepening). The role of mesoscale circulations in determining fractional cloudiness is not well understood. ESA

N89-23999 Royal Netherlands Meteorological Inst., De Bilt.
TURBULENT STRUCTURE OF A SHEAR-DRIVEN STRATUS-TOPPED ATMOSPHERIC BOUNDARY LAYER: A COMPARISON OF MODEL RESULTS WITH OBSERVATIONS
P. G. Duynkerke and A. G. M. Driedonks *In its* Stratocumulus Modeling 1988 p 74-93 Previously announced in IAA as A89-14383 (For primary document see N89-23997 17-46)
Copyright Avail: Royal Netherlands Meteorological Inst., P.O. Box 201, 3730 AE De Bilt, Wilhelminalaan 10, Netherlands

An observational study of the cloud-topped atmospheric boundary layer (ABL) during a strong gale reveals that the turbulent boundary layer was dominated by shear instead of convection. A one dimensional ensemble-averaged model is used to study this type of cloud-topped ABL. Turbulence closure is formulated by using an equation for both the turbulent kinetic energy and the viscous dissipation. The radiation model consists of an emissivity model for the longwave radiation and a two stream model for the shortwave radiation. Model results and observations indicate that the longwave radiative cooling at cloud top is mainly balanced by entrainment of warm air from above the inversion. A parameterization for the rainfall is included, and the effect of this on the liquid water content is studied. ESA

N89-24000 Royal Netherlands Meteorological Inst., De Bilt.
THE DIURNAL VARIATION OF A MARINE STRATOCUMULUS LAYER: A MODEL SENSITIVITY STUDY
P. G. Duynkerke *In its* Stratocumulus Modeling 1988 p 94-119 Submitted for publication (For primary document see N89-23997 17-46)
Copyright Avail: Royal Netherlands Meteorological Inst., P.O. Box 201, 3730 AE De Bilt, Wilhelminalaan 10, Netherlands

A one dimensional model which was previously tested against observational data is used to study the diurnal variation of a marine stratocumulus layer. The influence of the shortwave radiative heating during different seasons on the decoupling of the cloud layer from the sub-cloud layer is discussed. Results for a typical winter and summer situation are presented. It is shown that the decoupling can strongly affect the surface energy balance, suggesting that it is important to resolve the diurnal variation. A sensitivity study of the model for initial and boundary conditions is presented. The results are shown not to be very sensitive to initial and boundary conditions. ESA

47 METEOROLOGY AND CLIMATOLOGY

Includes weather forecasting and modification.

N89-24001# Agricultural Research Service, Beltsville, MD.
MICROCOMPUTER PROGRAM FOR DAILY WEATHER SIMULATION
D. A. Woolhiser, C. L. Hanson, and C. W. Richardson Dec. 1988 59 p
(PB89-144638; ARS-75) Avail: NTIS HC A04/MF A01 CSCL 04B

The microcomputer program CLIMATE.BAS provides easy access to rainfall probabilities or simulated daily weather data for a State or region. Parameters for individual stations located within the region can be accessed directly, or they can be estimated for points between stations. In addition to precipitation, daily maximum temperatures, minimum temperatures and radiation can be simulated using a weakly stationary generating process conditioned on the precipitation process which is described by Markov-chain/mixed-exponential model. The seasonal variations of parameters are described by Fourier series, providing a very parsimonious model. Author

N89-24002*# National Aeronautics and Space Administration. Goddard Space Flight Center, Greenbelt, MD.
A REDUCED VERSION OF THE NMC DERF 2 DATA SET
Siegfried Schubert, Fong-Chiau Chang, William K. M. Lau, and Robert Kistler (National Meteorological Center, Washington, DC.) Mar. 1989 35 p
(NASA-TM-100727; Rept-89B00097; NAS 1.15:100727) Avail: NTIS HC A03/MF A01 CSCL 04B

The National Meterological Center (NMC) Dynamical Extended Range Forecast (DERF 2) data represents a major computational effort to better ascertain the potential for extended range forecasts and to develop a strategy for performing operational extended range forecasts using dynamical models. A major stumbling block for using this data has been the sheer volume of data that must be processed to perform even simple calculations. The product of the data reduction described is a manageable data set that fits comfortably on five magnetic tapes or on one compact disc. The document outlines the data reduction process of the second phase of DERF data. It contains the description of the fields and the resolution of both the original and final fields. In order to assist the users of this data set, maps of selected fields, using both the original truncation at rhomboidal 30 and the truncation of the final data at triangular 20, are displayed. Author

N89-24003# Centre de Recherches et d'Etudes Oceanographiques, La Rochelle (France).
STUDY OF A METHOD TO DE-ALIAS WINDS FROM ERS-1 DATA Final Report
Alain Cavanie and Pascal Lecomte Paris, France ESA 1988 91 p
(Contract ESTEC-6874/87/GP/I(SC))
(CREO-6374; ESA-CR(P)-2743; ETN-89-94465) Avail: NTIS HC A05/MF A01

Principles for de-aliasing winds from ERS-1 data, methods, blunder point screening, software tests carried out, and their results are summarized. The scatterometer and the problems posed in going from normalized radar cross-section (Sigma0) to unambiguous winds are discussed. The search for possible solutions, which corresponds to finding local minima of a maximum likelihood function, is described. De-aliasing, that is, choosing between these different solutions, is summarized. Influence of rapid wind changes and ice-regions are studied and general concepts of off-line manual de-aliasing presented. The main objective is a real-time wind extraction/ambiguity removal algorithm proposal and the indication of the added value of an improved ambiguity removal algorithm to be used in the off-line mode. It is clear that the quality of wind extraction (inversion and de-aliasing) depends very much on that of the empirical C-band model as well as the precision of this calibration. Within the limits of the model, the procedure developed for three-beam zones is very successful as long as bias and noise remain within the limits specified by ESA. ESA

N89-24004 Missouri Univ., Columbia.
NORMAL MODE ENERGETICS OF THE GENERAL CIRCULATION DURING THE FGGE YEAR Ph.D. Thesis
Hiroshi Tanaka 1988 89 p
Avail: Univ. Microfilms Order No. DA8904466

Three-dimensional normal mode functions are applied to the analysis of the energetics of the general circulation during the first (global atmosperic research program) garp global experiment (FGGE) year. The geophysical fluid dynamics laboratory (GFDL) FGGE data are used for the computation of both the normal mode energetics and the standard spectral energetics. Comparison of the normal mode energetics with the standard spectral energetics in the zonal wavenumber domain indicates a general consistency of both schemes in the spectral energy transformations. Parameterizing the three-dimensional scale of atmospheric waves by eigenfrequencies of Laplace's tidal equation, it is found that the kinetic energy spectrum in the low-frequency Rossby modes approximately obeys the 3 power of the eigenfrequencies. In contrast, the kinetic energy spectrum in the high-frequency Rossby modes obeys the - 5/3 power and merges with the spectrum in the high-frequency gravity modes. The observed energy spectra in the vertical and meridional index domains coincide with the theoretical energy spectra deduced from the atmospheric baroclinic instability. The normal mode energetics of the global circulation is summarized in a barotropic and baroclinic decomposition for the zonal mean and eddy energies for the stationary and transient components of the flow. The energy generated in the zonal mean baroclinic component is first transformed to the eddy baroclinic component through the process of atmospheric baroclinic instability. It is then further transformed to eddy and zonal mean barotropic components by the nonlinear up-scale cascade of kinetic energy. The zonal mean kinetic energy thus maintains its barotropic structure by the activities of baroclinic waves. The time series of energy variables during the FGGE Northern Hemisphere winter clearly indicates a sequence of energy transformation from the zonal baroclinic component via the synoptic-scale baroclinic component, to the planetary-scale barotropic component.
Dissert. Abstr.

N89-24005# National Climatic Center, Asheville, NC.
CLIMATIC ATLAS OF THE OUTER CONTINENTAL SHELF WATERS AND COASTAL REGIONS OF ALASKA. VOLUME 1: GULF OF ALASKA, REVISION
William A. Brower, Jr., Ronald G. Baldwin, Claude N. Williams, Jr., James L. Wise, and Lynn D. Leslie (Alaska Univ., Anchorage.) 1988 544 p
(AD-A205289; NAVAIR-50-1C-551; MMS-87-0011) Avail: NTIS HC A23/MF A01 CSCL 04/2

This project updates the knowledge of climatological conditions presented in the 1977 publication of this three-volume atlas. Such environmental information for the three Alaskan marine and near-coastal areas is important for resource development of the outer continental shelf-The Gulf of Alaska (Volume 1), the Bering Sea (Volume 2), and The Chukchi and Beaufort Seas (Volume 3). The maps, graphs and tables in the atlas present a detailed climatic profile of the marine and coastal regions of Alaska. Statistics give the means, extremes, and percent frequency of concurrence of threshold values for the elements of wind, visibility, present weather, sea level pressure, air and sea surface temperature, clouds, waves, and such supplemental information as storm surges, tides, sea ice, cyclone tracks, surface currents, bathymetry, detailed weather, and aviation weather. Data came from 4.5 million surface marine observations and 8.5 million observations for 66 coastal and island stations within the area 40 deg -84 deg N and 110 deg W -160 deg E, and provide the best possible climatological picture of the outer continental shelf waters and coastal regions of Alaska.
GRA

N89-24006# Naval Air Systems Command, Washington, DC.
US NAVY REGIONAL CLIMATIC STUDY OF THE NORTHERN CALIFORNIA OPERATING AREA
Sep. 1988 546 p Original contains color illustrations

(AD-A205342; NAVAIR-50-1C-554) Avail: NTIS HC A23/MF A01 CSCL 04/2

Surface marine observation statistics are presented on monthly charts in the forms of graphs, tables and isopleth maps. Land station data appear graphically and in Station Climatic Summary tables. The marine data (mostly from ships of opportunity) were summarized and machine plotted by one-degree quadrangle. Data for the moored buoys were summarized independently and plotted at their locations so comparisons between the data sources could be made as the charts were being subjectively analyzed. The graphs and tables for the marine areas are also presented by one-degree quadrangles (for visibility, wave heights, and wind roses). The geographical area for the tables and wind roses had to be divided and presented on two pages of clarity. These graphs and tables represent the objective compilation of available ship data; the data were not adjusted for suspected bias (low observation count, heavy weighting of observations during a short time interval, biases in coding, etc.), and differences may be found when comparing the graphical data with isopleth analyses. The total number of observations for a given one-degree square should always be considered when interpreting the data, as there may be an insufficient number to permit representative statistics. GRA

N89-24007# Air Force Environmental Technical Applications Center, Scott AFB, IL.

SURFACE OBSERVATION CLIMATIC SUMMARIES (SOCS) FOR NASA SHUTTLE LANDING FACILITY, FLORIDA Summary Report, Mar. 1978 - Oct. 1988

Jan. 1989 774 p

(AD-A205362; USAFETAC/DS-88/206) Avail: NTIS HC A99/MF A01 CSCL 04/2

Surface observation climatic summaries (SOCS) provide statistical climatic summaries of surface weather observations taken and recorded at specified USAF, Civilian, and Foreign Observing Stations. Hourly observations are summarized from a 10-year period of record (POR). Summary of Day (SOD) information is summarized from all available data in the OL-A climatic database. GRA

N89-24008# Clemson Univ., SC. Dept. of Physics and Astronomy.

STUDIES OF FRONTAL ZONE DYNAMICS WITH A HIGH-RESOLUTION WIND PROFILING SYSTEM Final Report, May 1985 - Sep. 1988

M. F. Larson 15 Jan. 1989 19 p

(Grant AF-AFOSR-0216-85; AF Proj. 2310)

(AD-A205988; AFOSR-89-0241TR) Avail: NTIS HC A03/MF A01 CSCL 04/2

Vertical velocity and reflectivity data obtained with the SOUSY-VHF-Radar located have been compared with the operational analysis data from the European Centre for Medium-range Weather Forecasting, with radiosonde data, as well as the standard synoptic weather maps for the region. Also, the effects of precipitation on VHF and UHF wind profiler data have been investigated. Results have shown that the radar reflectivities at 6 m wavelength are enhanced at the height where the frontal inversion is located. The UHF echoes are dominated by precipitation, even when the rainfall is light, while VHF echoes have nearly equal contributions from precipitation and the clear air, even when the rainfall is heavy. Comparison of the radar vertical velocities and the radiosonde data have made it possible to show the vertical circulations around several fronts. The results are in general agreement with the expected patterns of ascent in the warm air and descent in the cold sectors, but the detailed structures are more complicated and show a banded structure and a significant indirect circulation in connection with the fronts. Comparison of the operational analysis vertical velocities shows that some of the same features are reproduced in both data sets, but there are discrepancies with differences of up to half a day between the times of the appearance of the vertical velocity structures connected with fronts and jet stream passages over the radar. GRA

N89-24009# Atmospheric and Environmental Research, Inc., Cambridge, MA.

ON THE USE OF MULTIPROCESSING COMPUTERS FOR GLOBAL NUMERICAL WEATHER PREDICTION Final Report, Aug. 1988 - Jan. 1989

Ross N. Hoffman and Thomas Nehrkorn 15 Feb. 1989 42 p

(Contract F49620-88-C-0105)

(AD-A205102; P248-FR; AFOSR-89-0272TR) Avail: NTIS HC A03/MF A01 CSCL 04/2

A preliminary exploration is made of the uses of multiprocessing computers for large scale NWP using spectral models. In general if global communication between processors is relatively fast and easy, then implementing spectral models is feasible. The global spectral model is recast in terms of latitude and wavenumber tasks. This approach has a number of advantages: The entire algorithm is macrotasked. Only a handful of crucial pointers need to be locked. The spectral transform calculations are localized so that arithmetic always follows the same ordering and all results are exactly reproducible. The latitude wavenumber tasking scheme is implemented and tested on the Sequent Balance, a shared memory multiple instruction multiple data device. It is argued that this scheme could be easily extended and applied to larger machines of this class and provide a good starting point for distributed memory machines. The potential of single instruction multiple data machines is huge. A proposed algorithm for this class of machine uses a processor for each horizontal grid point. GRA

N89-24010# Army Lab. Command, White Sands Missile Range, NM. Atmospheric Sciences Lab.

THE US ARMY YUMA PROVING GROUND, ARIZONA 33-YEAR CLIMATE CALENDAR AND TABLES ON ASSOCIATED WEATHER ELEMENTS 1954-1986. AMERICAN DESERT COUNTRY Final Report, 1954 - 1986

James C. Devine Jun. 1988 135 p

(AD-A206256; ASL-TR-0226) Avail: NTIS HC A07/MF A01 CSCL 04/2

This report contains an extremely well documented history of pure desert conditions over a 33-yr period (1954 through 1986). The desert region is in southwestern Arizona. In many cases this climate is similar to the Midwest regions. In addition to the general discussion of the terrain, climate, visibility, and other features of interest, extensive detail and analyses of most weather elements during this period are presented in the eight appendices. Of interest to some is the fact that this period covers three sunspot cycle periods of 11 yr each and one cycle of the 22-yr variety. The data is presented here in a manner that interested personnel may develop their own comparative graphs to determine what effect, if any, these cycles have on varied weather elements in desert country. GRA

48 OCEANOGRAPHY

Includes biological, dynamic, and physical oceanography; and marine resources.

For related information see also *43 Earth Resources and Remote Sensing.*

N89-24011# Woods Hole Oceanographic Institution, MA.

EXPLORING THE NORTH ATLANTIC OCEAN ON FLOPPY DISKS

James R. Luyten and Henry M. Stommel Dec. 1988 59 p

(Contract N00014-84-C-0134; NSF OCE-86-13810)

(AD-A205733; WHOI-88-59) Avail: NTIS HC A04/MF A01 CSCL 08/3

A selection of hydrographic station data in the Atlantic between 8 S and 70 N is packed on four 5 1/4 in. floppy disks. Sample utility programs for reading and plotting the data are also on the disks. We present this computer atlas in preliminary form for use by students and professionals, in the belief that easy access to this valuable historical data will be educational and stimulating. Criticism and comment are welcome. GRA

N89-24012# Virginia Polytechnic Inst. and State Univ., Blacksburg.
IMPROVED SEA SURFACE SCATTERING MODEL Final Report, Jul. 1987 - Jul. 1988
Gary S. Brown 15 Nov. 1988 30 p
(Contract N00014-87-K-0723; ARPA Order 6075)
(AD-A205745) Avail: NTIS HC A03/MF A01 CSCL 20/3

This report develops an integral equation for the fluctuating zero mean part of the field scattered by a randomly rough perfectly conducting surface. The development starts with Magnetic Field Integral Equation for the current and then Fourier transforms this equation to obtain an integral equation for the scattered field in transform space. The method of smoothing is then used to develop an integral equation for the fluctuating part of the scattered field. The born term is this integral equation of the second kind contains much more information than the classical Kirchhoff approximation. It is shown to reduce to the Kirchhoff approximation for gently sloping surface with large rms roughness and the Rice perturbation result for small surface roughness. This new Born term contains factors which appear to have the potential capability for going beyond existing approximations but further analytical and numerical work is required to quantify this hypothesis. GRA

N89-24013# GKSS-Forschungszentrum Geesthacht (Germany, F.R.). Inst. fuer Physik.
OPTICAL PROPERTIES OF OCEANIC SUSPENDED MATTER AND THEIR INTERPRETATION FOR REMOTE SENSING OF PHYTOPLANKTON Thesis - Technische Univ., Hamburg [DIE OPTISCHEN EIGENSCHAFTEN DER OZEANISCHEN SCHWEBSTOFFE UND IHRE BEDEUTUNG FUER DIE FERNERKUNDUNG VON PHYTOPLANKTON]
U. Kronfeld 1988 161 p In GERMAN; ENGLISH summary
(GKSS-88/E/40; ISSN-0344-9629; ETN-89-94410) Copyright Avail: NTIS HC A08/MF A01

Optical properties of suspended matter and disolved substances in sea water are studied by remote sensing for the determination of organic and inorganic substances concentration. Model computation is achieved by recording optical absorption of chlorophyll content algae or phytoplankton and of mineral substances such as yellow suspensions. The upword directed radiation spectra are determined by 11 stations of the German MARSEN program. Scattering functions and extinction coefficients are calculated for different algae species from particle size distributions and optical reflection indices. ESA

N89-24014# GKSS-Forschungszentrum Geesthacht (Germany, F.R.).
IMAGING PROCEDURE OF UNDERWATER BOTTOM TOPOGRAPHY BY AIR AND SATELLITE IMAGES IN THE RANGE OF MICROWAVE AND VISIBLE ELECTROMAGNETIC SPECTRA Thesis - Bremen Univ. [ABBILDUNG VON SUBMARINER BODENTOPOGRAPHIE AUF LUFT- UND SATELLITENBILDERN IM MIKROWELLENBEREICH UND IM SICHTBAREN BEREICH DES ELEKTROMAGNETISCHEN SPEKTRUMS]
I. Hennings 1988 183 p In GERMAN; ENGLISH summary
(GKSS-88/E/41; ISSN-0344-9629; ETN-89-94411) Copyright Avail: NTIS HC A09/MF A01

The imaging mechanism of underwater bottom topography in coastal waters with strong (tidal) currents by real and by synthetic aperture radar is investigated. A theoretical model is presented which describes the radar cross-section modulation and is tested with radar data. As an example satellite images of an Earth terrain camera and of a synthetic aparture radar from the same sea area are analyzed. The imaging in the satellite photograph is direct sunlight specularly reflected from the sea surface (sunglitter radiance). ESA

51 LIFE SCIENCES (GENERAL)

N89-24015*# Florida Univ., Gainesville. Dept. of Engineering Sciences.
ADVANCED SPACE DESIGN PROGRAM TO THE UNIVERSITIES SPACE RESEARCH ASSOCIATION AND THE NATIONAL AERONAUTICS AND SPACE ADMINISTRATION Final Report, 1987-1988 Academic Year
Gale E. Nevill, Jr. Jun. 1988 264 p
(Grant NGT-21-002-080)
(NASA-CR-180450; NAS 1.26:180450) Avail: NTIS HC A12/MF A01 CSCL 06C

The goal of the Fall 1987 class of EGM 4000 was the investigation of engineering aspects contributing to the development of NASA's Controlled Ecological Life Support System (CELSS). The areas investigated were the geometry of plant growth chambers, automated seeding of plants, remote sensing of plant health, and processing of grain into edible forms. The group investigating variable spacing of individual soybean plants designed growth trays consisting of three dimensional trapezoids arranged in a compact circular configuration. The automated seed manipulation and planting group investigated the electrical and mechanical properties of wheat seeds and developed three seeding concepts based upon these properties. The plant health and disease sensing group developed a list of reliable plant health indicators and investigated potential detection technologies. For individual titles, see N89-24016 through N89-24021.

N89-24016*# Florida Univ., Gainesville.
VARIABLE PLANT SPACING
Jim Bledsoe and Lee Weiss *In its* Advanced Space Design Program to the Universities Space Research Association and the National Aeronautics and Space Administration Jun. 1988 41 p (For primary document see N89-24015 17-51)
Avail: NTIS HC A12/MF A01 CSCL 06C

The goal of this project was to develop a system for varying the spacings between soybean plants as they grow to maximize the number of plants grown in a given volume. The project was studied to aid in the development of NASA's Controlled Ecological Life Support System (CELSS). The resulting design consists of plant trays which are three dimensional trapezoids arranged into circles in a compact geometrical configuration. These circles are stacked together in back to back pairs to form a long cylinder. In each growth tray, plants will be housed in individual containers containing a nutrient delivery system and a plant support mechanism. Between the containers, a half trellis has been designed to space the plants for maximum space efficiency. The design allows for localized seeding and harvesting mechanisms due to the chambers' geometrical configuration. In addition, the components have been designed for ease of cleaning and minimal maintenance. Next semester, the individual components will be constructed and tested to determine the success of the design. Author

N89-24017*# Florida Univ., Gainesville.
AUTOMATED SEED MANIPULATION AND PLANTING
Ray Garcia, Javier Herrera, Scott Holcomb, Paul Kelly, Scott Myers, Manny Rosendo, Herbert Sivitz, and Dave Wolsefer *In its* Advanced Space Design Program to the Universities Space Research Association and the National Aeronautics and Space Administration Jun. 1988 32 p (For primary document see N89-24015 17-51)
Avail: NTIS HC A12/MF A01 CSCL 06C

Activities for the Fall Semester, 1987 focused on investigating the mechanical/electrical properties of wheat seeds and forming various Seed Planting System (SPS) concepts based on those properties. The Electrical Division of the design group was formed to devise an SPS using electrostatic charge fields for seeding operations. Experiments concerning seed separation using electrical induction (rearranging of the charges within the seed) were conducted with promising results. The seeds, when exposed to the high voltage and low current field produced by a Van de

Graff generator, were observed to move back and forth between two electrodes. An SPS concept has been developed based on this phenomena, and will be developed throughout the Spring Semester, 1988. The Mechanical Division centered on SPS concepts involving valves, pumps, and fluids to separate and deliver seeds. An SPS idea utilizing the pressure difference caused by air as it rushes out of holes drilled in the wall of a closed container has been formulated and will be considered for future development. Also, a system of seed separation and delivery employing a combination of centrifugal force, friction, and air flow was considered. Author

N89-24018*# Florida Univ., Gainesville.
PLANT HEALTH SENSING
Ara Manukian, Colleen McKelvy, Michael Pearce, and Steph Syslo *In its* Advanced Space Design Program to the Universities Space Research Association and the National Aeronautics and Space Administration Jun. 1988 34 p (For primary document see N89-24015 17-51)
Avail: NTIS HC A12/MF A01 CSCL 06C

If plants are to be used as a food source for long term space missions, they must be grown in a stable environment where the health of the crops is continuously monitored. The sensor(s) to be used should detect any diseases or health problems before irreversible damage occurs. The method of analysis must be nondestructive and provide instantaneous information on the condition of the crop. In addition, the sensor(s) must be able to function in microgravity. This first semester, the plant health and disease sensing group concentrated on researching and consulting experts in many fields in attempts to find reliable plant health indicators. Once several indicators were found, technologies that could detect them were investigated. Eventually the three methods chosen to be implemented next semester were stimulus response monitoring, video image processing and chlorophyll level detection. Most of the other technologies investigated this semester are discussed here. They were rejected for various reasons but are included in the report because NASA may wish to consider pursuing them in the future. Author

N89-24019*# Florida Univ., Gainesville.
MICROGRAVITY PARTICLE REDUCTION SYSTEM c29
Vanessa Brandon, Michelle Joslin, Lili Mateo, and Tracey Tubbs *In its* Advanced Space Design Program to the Universities Space Research Association and the National Aeronautics and Space Administration Jun. 1988 20 p (For primary document see N89-24015 17-51)
Avail: NTIS HC A12/MF A01 CSCL 22A

The Controlled Ecological Life Support System (CELSS) project, sponsored by NASA, is assembling the knowledge required to design, construct, and operate a system which will grow and process higher plants in space for the consumption by crew members of a space station on a long term space mission. The problem of processing dry granular organic materials in microgravity is discussed. For the purpose of research and testing, wheat was chosen as the granular material to be ground into flour. Possible systems which were devised to transport wheat grains into the food processor, mill the wheat into flour, and transport the flour to the food preparation system are described. The systems were analyzed and compared and two satisfactory systems were chosen. Prototypes of the two preferred systems are to be fabricated next semester. They will be tested under simulated microgravity conditions and revised for maximum effectiveness. Author

N89-24020*# Florida Univ., Gainesville.
AUTOMATED SEED MANIPULATION AND PLANTING
Ray Garcia, Javier Herrera, Scott Holcomb, Paul Kelly, Scott Myers, Manny Rosendo, Herbert Sivitz, and Dave Wolsefer *In its* Advanced Space Design Program to the Universities Space Research Association and the National Aeronautics and Space Administration Jun. 1988 36 p (For primary document see N89-24015 17-51)
Avail: NTIS HC A12/MF A01 CSCL 06C

The Mechanical Division fabricated three seed separators utilizing pressure gradients to move and separate wheat seeds. These separators are called minnow buckets and use air, water, or a combination of both to generate the pressure gradient. Electrostatic fields were employed in the seed separator constructed by the Electrical Division. This separator operates by forcing a temporary electric dipole on the wheat seeds and using charged electrodes to attract and move the seeds. Seed delivery to the hydroponic growth tray is accomplished by the seed cassette. The cassette is compatible with all the seed separators, and it consists of a plastic tube threaded with millipore filter paper. During planting operations, the seeds are placed in an empty cassette. The loaded cassette is then placed in the growth tray and nutrient solution provided. The solution wets the filter paper and capillary action draws the nutrients up to feed the seeds. These seeding systems were tested and showed encouraging results. Seeds were effectively separated and the cassette can support the growth of wheat plants. Problems remaining to be investigated include improving the success of delivering the seeds to the cassette and providing adequate spacing between seeds for the electric separator. Author

N89-24021*# Florida Univ., Gainesville.
NON-DESTRUCTIVE PLANT HEALTH SENSING USING ABSORPTION SPECTROSCOPY
Jim Bledsoe, Ara Manukian, Michael Pearce, and Lee Weiss *In its* Advanced Space Design Program to the Universities Space Research Association and the National Aeronautics and Space Administration Jun. 1988 56 p (For primary document see N89-24015 17-51)
Avail: NTIS HC A12/MF A01 CSCL 06C

The sensor group of the 1988 EGM 4001 class, working on NASA's Controlled Ecological Life Support Systems (CELSS) project, investigated many different plant health indicators and the technologies used to test them. The project selected by the group was to measure chlorophyll levels using absorption spectroscopy. The spectrometer measures the amount of chlorophyll in a leaf by measuring the intensity of light of a specific wavelength that is passed through a leaf. The three wavelengths of light being used corresponded to the near-IR absorption peaks of chlorophyll a, chlorophyll b, and chlorophyll-free structures. Experimentation showed that the sensor is indeed measuring levels of chlorophyll a and b and their changes before the human eye can see any changes. The detector clamp causes little damage to the leaf and will give fairly accurate readings on similar locations on a leaf, freeing the clamp from having to remain on the same spot of a leaf for all measurements. External light affects the readings only slightly so that measurements may be taken in light or dark environments. Future designs and experimentation will concentrate on reducing the size of the sensor and adapting it to a wider range of plants. Author

N89-24022*# General Electric Co., Moffett Field, CA.
GAS-GRAIN SIMULATION FACILITY: FUNDAMENTAL STUDIES OF PARTICLE FORMATION AND INTERACTIONS. VOLUME 1: EXECUTIVE SUMMARY AND OVERVIEW
Guy Fogleman, ed., Judith L. Huntington, ed. (Search for Extraterrestrial Intelligence Inst., Los Altos, CA.), Deborah E. Schwartz, ed., and Mark L. Fonda, ed. Mar. 1989 38 p Presented at the Gas-Grain Simulation Facility Experiments Workshop, Sunnyvale, CA, 31 Aug. - 1 Sep. 1987; sponsored by the Exobiology Flight Program
(NASA-CP-10026-Vol-1; A-88256-Vol-1; NAS 1.55:10026-Vol-1)
Avail: NTIS HC A03/MF A01 CSCL 06C

An overview of the Gas-Grain Simulation Facility (GGSF) project and its current status is provided. The proceedings of the Gas-Grain Simulation Facility Experiments Workshop are recorded. The goal of the workshop was to define experiments for the GGSF--a small particle microgravity research facility. The workshop addressed the opportunity for performing, in Earth orbit, a wide variety of experiments that involve single small particles (grains) or clouds of particles. The first volume includes the executive summary, overview, scientific justification, history, and planned development of the Facility. A.D.

N89-24023*# General Electric Co., Moffett Field, CA.
GAS-GRAIN SIMULATION FACILITY: FUNDAMENTAL STUDIES OF PARTICLE FORMATION AND INTERACTIONS. VOLUME 2: ABSTRACTS, CANDIDATE EXPERIMENTS AND FEASIBILITY STUDY
Guy Fogleman, ed., Judith L. Huntington, ed. (Search for Extraterrestrial Intelligence Inst., Los Altos, CA.), Deborah E. Schwartz, ed., and Mark L. Fonda, ed. Mar. 1989 199 p Presented at the Gas-Grain Simulation Facility Experiments Workshop, Sunnyvale, CA, 31 Aug. - 1 Sep. 1987; sponsored by the Exobiology Flight Program
(NASA-CP-10026-Vol-2; A-88256-Vol-2; NAS 1.55:10026-Vol-2) Avail: NTIS HC A09/MF A01 CSCL 06C

An overview of the Gas-Grain Simulation Facility (GGSF) project and its current status is provided. The proceedings of the Gas-Grain Simulation Facility Experiments Workshop are recorded. The goal of the workshop was to define experiments for the GGSF--a small particle microgravity research facility. The workshop addressed the opportunity for performing, in Earth orbit, a wide variety of experiments that involve single small particles (grains) or clouds of particles. Twenty experiments from the fields of exobiology, planetary science, astrophysics, atmospheric science, biology, physics, and chemistry were described at the workshop and are outlined in Volume 2. Each experiment description included specific scientific objectives, an outline of the experimental procedure, and the anticipated GGSF performance requirements. Since these experiments represent the types of studies that will ultimately be proposed for the facility, they will be used to define the general science requirements of the GGSF. Also included in the second volume is a physics feasibility study and abstracts of example Gas-Grain Simulation Facility experiments and related experiments in progress. Author

52 AEROSPACE MEDICINE

Includes physiological factors; biological effects of radiation; and effects of weightlessness on man and animals.

N89-24024*# National Academy of Sciences - National Research Council, Washington, DC. Committee on Space Biology and Medicine.
A STRATEGY FOR SPACE BIOLOGY AND MEDICAL SCIENCE FOR THE 1980s AND 1990s
1987 214 p
(Contract NASw-3482)
(NASA-CR-184895; NAS 1.26:184895) Avail: NTIS HC A10/MF A01 CSCL 06C

A guideline is provided for developing NASA's long-term mission plans and a rational, coherent research program. Ten topical areas for research are addressed: developmental biology, gravitropism in plants, sensorimotor integration, bone and mineral metabolism, cardiovascular/pulmonary function, muscle remodeling, nutrition, human reproduction, space anemia, and human behavior. Scientific goals, objectives, and required measurements and facilities for each of the major areas of space biology and medicine are identified and described along with primary goals and objectives for each of these disciplines. Proposals are made concerning the use of scientific panels to oversee the implementation of the strategy, life sciences' need for continuous access to spaceflight opportunities, the advantages of a focused mission strategy, certain design features that will enhance spaceflight experimentation, and general facilities. Other topics that are considered include mission planning, crew selection and training, and interagency and international cooperation. A.D.

N89-24025# Navy Experimental Diving Unit, Panama City, FL.
OXYGEN CONSUMPTION RATE OF OPERATIONAL UNDERWATER SWIMMERS Final Report
M. E. Knafelc Jan. 1989 13 p
(AD-A205331; NEDU-1-89) Avail: NTIS HC A03/MF A01 CSCL 06/4

Prior to evaluating an underwater breathing apparatus (UBA), diver performance must be determined. Previous studies determining the oxygen consumption of swimming and resting divers were done in the laboratory and were limited in scope. Criticisms of those studies suggested that they may not have accurately simulated the underwater work expected of an operational diver. This study measured the oxygen consumption (VO2) sustained by experienced Special Warfare (SPECWAR) operators participating in training exercises. By using a closed-circuit oxygen underwater breathing apparatus, the decrease in the oxygen bottle pressure reflected the amount of oxygen consumed by the diver. These values are comparable to the results of the previous studies. Guidelines reflecting underwater oxygen consumption and estimating carbon dioxide production for calculating carbon dioxide canister duration should be based on the results of these studies. GRA

N89-24026# Armed Forces Radiobiology Research Inst., Bethesda, MD.
A LOW-ENERGY X-RAY IRRADIATOR FOR ELECTROPHYSIOLOGICAL STUDIES
D. A. Schauer, G. H. Zeman, and T. C. Pellmar Dec. 1988 35 p
(AD-A205388; AFRRI-TR88-2) Avail: NTIS HC A03/MF A01 CSCL 06/7

A 50 kVp molybdenum target/filter X-ray was installed inside a lead-shielded Faraday cage. High-dose rates of up to 1.54 Gy/min (17.4 keV weighted average photons) were used to conduct local in vitro irradiations of the hippocampal region of guinea pig brains. Electrophysiological recordings of subtle changes in neuronal activity indicate the system is suitable for this application. GRA

N89-24027# Naval Health Research Center, San Diego, CA. Behavior Psychopharmacology Dept.
THE RELATIONSHIP BETWEEN SUBJECTIVE AND OBJECTIVE MEASURES OF SLEEPINESS Interim Report
Laverne C. Johnson, Charles R. Freeman, Cheryl L. Spinweber, and Steven A. Gomez 7 Dec. 1988 17 p
(AD-A205861; NHRC-88-50) Avail: NTIS HC A03/MF A01 CSCL 06/4

The purpose of the present study was to examine the relationship among the Multiple Sleep Latency Test (MSLT), lapses during a tapping task, a visual analog scale (VAS) and the Stanford sleepiness scale (SSS). Subjects were 80 male adult nonsmokers (age 20.3 + or - 2.7 years). The MSLT, SSS, and the VAS were obtained at two-hour intervals beginning at 0700 h. On the MSLT, sleep latency was measured from lights out to first spindle, K-complex or rapid-eye-movement (REM) period. The tapping task (lapses) was administered each day at 0600 h, but became nonsignificant as the day progressed. Correlations of objective and subjective measures from scores summed over both days were not significant. The two objective measures were significantly correlated throughout the day and over days as were the subjective measures. This study reaffirms the importance of time of day in sleepiness, and suggests that subjective and objective measures cannot be used interchangeably and may measure different aspects of sleepiness. GRA

N89-24028# Tennessee Univ., Memphis. Dept. of Physiology and Biophysics.
MURAMYL PEPTIDE-ENHANCED SLEEP: PHARMACOLOGICAL OPTIMIZATION OF PERFORMANCE Annual Report, 1 Jun. 1987 - 31 May 1988
James M. Krueger 1 Jun. 1988 138 p
(Contract DAMD17-86-C-6194; DA Proj. 3M1-61102-BS-10)
(AD-A205974) Avail: NTIS HC A07/MF A01 CSCL 06/15

The broad objective of this research is to develop the information needed to ascertain whether muramyl peptides (MPs) and/or other endogenous sleep factors (SFs) may be useful as somnogenic agents. Several SFs have been identified that may be involved in the cascade of biomedical events involved in regulation of sleep, e.g., interleukin-1 (IL1). Thus, we think it possible that new more effective somnogenic agents could be developed using MPs and/or other putative SFs. In the second

year of this contract six experiments were performed: MP somnogenic activity relationships were determined. The preoptic area (POA) of the brain has been implicated in sleep regulation. Relationships between sleep and infectious disease are examined. Staphylococcus aureus greatly altered rabbit sleep patterns over the course of the infections. Endotoxin and its lipid A moiety are components of gram-negative bacteria that share with MPs the ability to induce increased IL1 production. Alpha-melanocyte-stimulating hormone (aMSH), proopiomelanocortin-derived peptide which acts as a physiological inhibitor of some of IL1 actions, inhibited normal sleep and also antagonized IL1-enhanced sleep. GRA

N89-24029# Army Research Inst. of Environmental Medicine, Natick, MA.

PATTERNS OF HUMAN DRINKING: EFFECTS OF EXERCISE, WATER TEMPERATURE AND FOOD CONSUMPTION Final Report, Feb. 1988 - Feb. 1989

Patricia C. Szlyk, Ingrid V. Sils, Ralph P. Francesconi, and Roger W. Hubbard 24 Jan. 1989 24 p

(AD-A206031; USARIEM-M23-89) Avail: NTIS HC A03/MF A01 CSCL 06/4

The effects of exercise, water temperature and food consumption on patterns of ad libitum drinking were studied in 33 men during 6 consecutive cycles of 30 min walking (4.8 km.h-1, 5 percent grade) and 30 min rest in a climatic chamber (40 C, 40 percent relative humidity). On two nonconsecutive days, subjects consumed 15 C (cool) water during one trial and 40 C (warm) water during the other. We previously reported that two groups of drinkers can be identified during work in the heat by the criterion of Body Weight (BW) loss during the trial. Thus, avid drinkers (D) drank sufficiently such that they lost less than 2 percent of their initial Bw when consuming cool water ad libitum, while Reluctant Drinkers (RD) lost more than 2 percent of their BW. When warm water was provided, fluid consumption was reduced by 29 percent and 54 percent in D and RD, respectively and BW deficits were comparably increased. Intake of cool water elicited cyclic drinking patterns with higher rates during walking than during rest periods in both D and RD, whereas consumption of warm water produced this cyclic pattern only after food ingestion during the third rest. Food consumption stimulated fluid intake and reduced BW losses in both trials. Compared to pre-prandial (hours 1-2.5) rates, average post-lunch drinking rates during the last 3h increased 14 percent in D and 19 percent in RD when consuming cool water, and by 46 percent and 74 percent, respectively with warm water. GRA

N89-24030# Army Research Inst. of Environmental Medicine, Natick, MA.

HUMAN TEMPERATURE REGULATION DURING EXERCISE AFTER ORAL PYRIDOSTIGMINE ADMINISTRATION

Margaret A. Kolka and Lou A. Stephenson Mar. 1989 19 p

(AD-A206032; USARIEM-M27-89) Avail: NTIS HC A03/MF A01 CSCL 06/15

Four healthy males exercised in two experiments at ambient temperatures of 22 C, 29 C and 36 C. The relative humidity was 30 percent in each environment. One experiment in each environment was done 150 minutes after oral (30 mg) pyridostigmine bromide (PYR) administration, and the second experiment was done on a separate day with no medication (CON). Red blood cell cholinesterase was -39 (+ or - 7) percent lower after PYR. Esophageal (Tes) and mean skin temperature (Tsk), forearm blood flow (FBF), forearm sweating, and skin blood flow (SkBF) were measured twice each minute during a 15-min rest period and during 30 minutes of seated cycle exercise at approx. 58 percent VO2 peak. Whole body sweating was determined from weight changes before and after exercise. PYR decreased heart rate at rest and during exercise at 29 C and 36 C. Resting SkBF was 40 percent lower at 29 C and 30 percent lower at 36 C after PYR. During exercise, SkBF was 40 percent lower at 29 C and 50 percent lower at 36 C after PYR compared to CON. There was no effect of PYR on heat production at rest or during exercise. Tsk was different in the three conditions by design, but was unchanged by PYR. Tes was not different at rest in any conditions, but was elevated during exercise at 36 C in PYR compared to CON. GRA

N89-24031# Colorado Univ., Denver. Cardiovascular Pulmonary Research Lab.

HUMAN ADAPTATION TO THE TIBETAN PLATEAU Midterm Report, 7 Aug. 1987 - 16 Feb. 1989

Lorna G. Moore 15 Feb. 1989 10 p

(Contract DAMD17-87-C-7202; DA Proj. 3E1-62787-A-879)

(AD-A206463) Avail: NTIS HC A02/MF A01 CSCL 06/10

Humans live at high altitude for longer periods of time on the Tibetan Plateau than elsewhere in the world, thus providing opportunity to investigate the physiologic effects of longer (years to generations) duration of high altitude exposure. This has military importance because persons are stationed at high altitude locations for extended periods and some of the symptoms of failure to adjust to high altitude require months or years for development. We have completed two field projects (Fall 1987 and 1988) which suggest that Tibetans (natives) possess superior O2 transport and/or utilization systems compared to acclimatized newcomers (Han Chinese). Studies conducted in the period covered by this report addressed the control of breathing and blood oxygenation during sleep. In 22 healthy young men (11 Tibetans, 11 Hans), measurements of the control of breathing and lung volume during wakefulness were examined together with nightime studies of breathing and brain blood flow during sleep. Similar, additional studies were carried out in 8, principally Han patients with chronic mountain sickness and 8 age-matched, healthy controls. The data analysis from these studies is not yet complete but suggests that the Tibetans' greater lung volume, ventilatory sensitivity to hypoxia and high frequency respiratory pattern may confer protection against sleep-disordered breathing and thus better pressure blood oxygenation during sleep. GRA

N89-24032# Krug International, San Antonio, TX. Technology Services Div.

ADDITIVITY OF RETINAL DAMAGE FOR MULTIPLE-PULSE LASER EXPOSURES Final Report, Oct. 1985 - Jan. 1988

Joseph A. Zuclich and Michael F. Blankenstein Dec. 1988 25 p

(Contract F33615-84-C-0600)

(AD-A206514; USAFSAM-TR-88-24) Avail: NTIS HC A03/MF A01 CSCL 06/10

This study has examined the cumulative effects of multiple-pulse laser exposures in contributing to retinal damage via a thermal mechanism. Three sets of experiments have been conducted to determine the variation of multiple-pulse thresholds: with the interval between pulses; with the number of pulses in the pulse train when the interpulse interval is held constant; and with the retinal image size when both number of pulses and interpulse interval are invariant. In addition, thermal model calculations were carried out to compare model predictions with the experimental data. Conclusions from the experimental data are: (1) The threshold for a multiple-pulse train is related to that for an individual pulse in the train by a function of the number of pulses, but is independent of pulse-repetition frequency and pulse train length. This observation is in general accordance both with the thermal model predictions and with previously empirical models. (2) The additivity of multiple pulses is quantitatively similar for collimated and expanded laser beams incident at the eye. (3) The repair or recovery of laser-induced reversible retinal damage (i.e., sub-threshold with respect to the ophthalmoscopic lesion endpoint) is slow, having a time constant of the order of days. GRA

53 BEHAVIORAL SCIENCES

Includes psychological factors; individual and group behavior; crew training and evaluation; and psychiatric research.

N89-24033*# McDonnell-Douglas Corp., Long Beach, CA.
CREW PROCEDURES AND WORKLOAD OF RETROFIT CONCEPTS FOR MICROWAVE LANDING SYSTEM
Leland G. Summers and Jon E. Jonsson May 1989 48 p
(Contract NAS1-18028)
(NASA-CR-181700; NAS 1.26:181700; MDC-K1413) Avail: NTIS HC A03/MF A01 CSCL 05I

Crew procedures and workload for Microwave Landing Systems (MLS) that could be retrofitted into existing transport aircraft were evaluated. Two MLS receiver concepts were developed. One is capable of capturing a runway centerline and the other is capable of capturing a segmented approach path. Crew procedures were identified and crew task analyses were performed using each concept. Crew workload comparisons were made between the MLS concepts and an ILS baseline using a task-timeline workload model. Workload indexes were obtained for each scenario. The results showed that workload was comparable to the ILS baseline for the MLS centerline capture concept, but significantly higher for the segmented path capture concept. Author

N89-24034# Naval Submarine Medical Research Lab., Groton, CT.
PSYCHOMETRIC FUNCTION RECONSTRUCTION FROM ADAPTIVE TRACKING PROCEDURES Interim Report
Marjorie R. Leek, Thomas E. Hanna, and Lynne Marshall 29 Nov. 1988 26 p
(AD-A205668; NSMRL-1095) Avail: NTIS HC A03/MF A01 CSCL 05/8

Adaptive psychophysical procedures have come into widespread use for the estimation of psychophysical performance. Their popularity arises from their speed of implementation and efficiency in the stimulus levels far removed from the selected target values are seldom presented. Thus, experimental time and subject energy can be devoted to a precise delineation of performance at and around the target or threshold region. However, sometimes it is valuable to be able to describe a subject's performance across a wide range of stimulus values by construction of a psychometric function showing how performance changes with changing stimulus values. Since adaptive tracking procedures are specifically assigned to avoid stimulus levels far from the target value, the psychometric function constructed from the data in the track may be precisely defined near the target where there are many trial presentations for each level, but be a poor reflection of performance at levels removed from the target. While some authors have attempted to analyze the trial-by-trial data produced by an adaptive track to construct a psychometric function, there is little evidence that the functions they report do, in fact, represent the underlying function governing subject performance. GRA

N89-24035# Navy Personnel Research and Development Center, San Diego, CA.
DEVELOPMENT AND EVALUATION OF INTEGRATING DETAILS: A COMPLEX SPATIAL PROBLEM SOLVING TEST Technical Report, Jan. 1986 - Jun. 1988
David L. Alderton Feb. 1989 58 p
(AD-A205860; NPRDC-TR-89-6) Avail: NTIS HC A04/MF A01 CSCL 05/9

This report summarizes the theory behind and the development, evaluation, and refinement of a complex spatial processing test, Integrating Details. In the course of revamping and making the Armed Services Vocational Aptitude Battery (ASVAB) adaptive, the opportunity exists for replacing or adding test to the battery. Tests of spatial ability, a major dimension of human intelligence, are not represented in the ASVAB so they are reasonable candidates for inclusion. The vast psychometric literature on spatial ability suggests that only complex spatial tests are likely to be valid for both school and job performance. Theoretical and empirical work from visual cognition and mental imagery provided further guidelines for the development of a complex spatial test. Methodological techniques from componential analysis were used to initiate the test and develop an information processing model for test item solution. The results suggest that Integrating Details is a complex spatial problem solving test, that is relatively independent of verbal ability, that the test is reliable and has substantial construct validity. Furthermore, analyses demonstrate that the ability measured by Integrating Details is substantially unique from those measured by the ASVAB and thus there is ample opportunity for the test to augment the predictive validity of the ASVAB. A final 40-item version of the test is recommended for advanced development and validation with military enlisted personnel. GRA

N89-24036# South Dakota Univ., Vermillion. Human Factors Lab.
QUASI-MONOCHROMATIC VISUAL ENVIRONMENTS AND THE RESTING POINT OF ACCOMMODATION
Edward Trautman, Vernon Ellingstad, Michael Lilienthal (Naval Training Systems Center, Orlando, FL.), and Mary A. Trautman 1988 81 p Sponsored by Navy
(AD-A205938; NTSC-TR-88-028) Avail: NTIS HC A05/MF A01 CSCL 06/4

This investigation explored the importance of color as a factor in deterioration of correct visual accommodation and involuntary regression to the resting point of accommodation. The involvement of voluntary control of accommodation processes was manipulated by requiring extended performance on a difficult visual task. Broad band red and green as well as white visual environments were presented in two related experiments. The first considered color, light level and time on task. The second attempted a more specific examination of color and time on task. Expected light level, time on task and chromatic aberration effects were evident. Declining light levels and extended time on task produced expected decrements in accommodation. Ambient color environments produced predictable differential accommodation. No statistically significant differences were revealed to support the possibility of color mediated differential regression to resting point of accommodation. GRA

N89-24037# Duke Univ., Durham, NC. Center for Decision Studies.
MONITORING INFORMATION PROCESSING AND DECISIONS: THE MOUSELAB SYSTEM
Eric J. Johnson, John W. Payne, James R. Bettman, and David A. Schkade Feb. 1989 56 p
(Contract N00014-80-C-0114; RR04209)
(AD-A205963; ONR-TR-89-4) Avail: NTIS HC A04/MF A01 CSCL 12/5

In order to better understand the cognitive processes underlying judgment and choice, decision researchers have begun to use a variety of process tracing techniques. The idea is to complement many traditional measures of judgment and choice with a high density of observations on the intermediate stages of processing. This report documents a procedure for monitoring the information acquisition stages of decision behavior. The procedure is based on a micro-computer controlled pointing device called a mouse. The procedure offers a number of flexible graphics and data recording routines. The relationship of the procedure to other process tracing techniques is discussed. GRA

N89-24038# City of Hope Medical Center, Duarte, CA.
LONG TERM SYNAPTIC PLASTICITY AND LEARNING IN NEURONAL NETWORKS Final Technical Report, 15 Aug. 1986 - 14 Nov. 1988
Thomas H. Brown 14 Jan. 1989 13 p
(Contract F49620-86-C-0099)
(AD-A205993; AFOSR-89-0361TR) Avail: NTIS HC A03/MF A01 CSCL 06/1

The purpose of this project was to understand rapidly induced and persistent forms of synaptic memory. The properties of the synaptic modifications underlying this plasticity could account for some of the adaptive and self organizing capabilities of simple

and well-defined neurobiological networks in the mammalian brain. These can be studied rigorously using neurophysiological and optical techniques. Sprearheading the project effort was the working hypothesis that long-term synaptic potentiation (LTP), a use-dependent enhancement of synaptic transmission, may mediate certain mnemonic functions of hippocampal circuitry and other forebrain structures. The project was organized around four categories of interrelated specific aims. First, new quantal analysis methods were developed and tested (Aim 2) using patch-clamp techniques to study charge fluctuations of synaptic transmission during LTP at the crayfish neuromuscular junction. Accomplishment of this aim was necessary in order to be able to transfer and apply the new method to analyze and learn the biophysical mechanisms underlying LTP in hippocampal synapses (Aim 1) a much more difficult preparation to study at this level. GRA

N89-24039# Army Research Inst. of Environmental Medicine, Natick, MA.
TREATMENT WITH TYROSINE, A NEUROTRANSMITTER PRECURSOR, REDUCES ENVIRONMENTAL STRESS IN HUMANS
Louis E. Banderet and Harris R. Lieberman 1988 17 p
(AD-A206035; USARIEM-M17-89) Avail: NTIS HC A03/MF A01 CSCL 06/15

Acutely stressful situations can disrupt behavior and deplete brain norepinephrine and dopamine, catecholaminergic neurotransmitters. In animals, administration of tyrosine, a food constituent and precursor of the catecholamines, reduces these behavioral and neurochemical deficits. Using a double-blind, placebo-controlled crossover design we investigated whether tyrosine (100 mg/kg) would protect humans from some of the adverse consequences of a 4.5 hour exposure to cold and hypoxia. Tyrosine significantly decreased symptoms, adverse moods, and performance impairments in subjects who exhibited average or greater responses to these environmental conditions. These results suggest that treatment with tyrosine should be evaluated in a variety of acutely stressful situations for beneficial behavioral effects. GRA

N89-24040# Washington Univ., Saint Louis, MO. Dept. of Neurology.
THE ATTENTION SYSTEM OF THE HUMAN BRAIN
Michael I. Posner and Steven E. Petersen 28 Feb. 1989 31 p
(Contract N00014-86-K-0289)
(AD-A206157; TR-89-1) Avail: NTIS HC A03/MF A01 CSCL 05/8

The concept of attention as central to human performance extends back to the start of experimental psychology, yet even a few years ago, it would not have been possible to outline in even a preliminary form a functional anatomy of the human attentional system. New developments in neuroscience have opened the study of higher cognition to physiological analysis, and have revealed a system of anatomical areas that appear to be basic to the selection of information for focal (conscious) processing. The importance of attention is its unique role in connecting the mental level of description of processes used in cognitive science with the anatomical level common in neuroscience. Sperry describes the central role that mental concepts play in understanding brain function. As is the case for sensory and motor systems of the brain, our knowledge of the anatomy of attention is incomplete. Nevertheless, we can now begin to identify some principles of organization that allow attention to function as a unified system for the control of mental processing. Although many of our points are still speculative and controversial, we believe they constitute a basis for more detailed studies of attention from a cognitive-neuroscience viewpoint. Perhaps even more important for furthering future studies, multiple methods of mental chronometry, brain lesions, electrophysiology, and several types of neuro-imaging have converged on common findings. GRA

N89-24041# Massachusetts Inst. of Tech., Cambridge. Artificial Intelligence Lab.
THE ROLE OF KNOWLEDGE IN VISUAL SHAPE REPRESENTATION Ph.D. Thesis
Eric Saund Oct. 1988 303 p
(Contract N00014-85-K-0124)
(AD-A206173; AI-TR-1092) Avail: NTIS HC A14/MF A01 CSCL 12/9

This thesis shows how knowledge about the visual world can be built into a shape representation in the form of a descriptive vocabulary making explicit the important spatial events and geometrical relationships comprising an object's shape. We offer two specific computational tools establishing a framework by which a shape representation may support a variety of later visual processing tasks: (1) By maintaining shape tokens on a Scale-Space Blackboard, information about configurations of shape events such as contours and regions can be manipulated symbolically, while the pictorial organization inherent to a shape's spatial geometry is preserved. (2) Through the device of dimensionality-reduction, configurations of shape tokens can be interpreted in terms of their membership within deformation classes; this provides leverage in distinguishing shapes on the basis of subtle variations reflecting deformations in their forms. The power in these tools derives from their contributions to capturing knowledge about the visual world. In contrast to building block approaches to shape representation we employ a large and extensible vocabulary of shape descriptions tailored to the constraints and regularities of particular shape worlds. GRA

N89-24042# Washington Univ., Saint Louis, MO. Dept. of Neurology and Neurological Surgery.
RELATING ATTENTION TO VISUAL MECHANISMS
Gordon L. Shulman 28 Feb. 1989 20 p
(Contract N00014-86-K-0289; RR04206)
(AD-A206452; ONR-TR-89-2) Avail: NTIS HC A03/MF A01 CSCL 06/4

The effect of attention on visual perception has been a subject of great controversy. Much research on attention over the last thirty years has been framed by the debate on this question between proponents of early and late selection. Late selection theorists have argued that all perceptual encoding, including recognition, and certain semantic analyses are accomplished in parallel, while early selection theorists have countered that only simple physical analyses can be conducted in parallel. More sophisticated analyses of shape that support object recognition and memory access are conducted by limited capacity systems. Although the terms perceptual and semantic include a wide variety of processes, there has been an unfortunate tendency to extrapolate conclusions to the entire collection of processes based on results from a few. For example, researchers have tacitly assumed that if any evidence for semantic processing of unattended material is found, then perceptual operations must be parallel. This inference, however, only applies to the perceptual operations relevant to the recognition of the experimental stimuli, which are generally upright block alphanumeric characters. Recognition of these stimuli does not require the resolution of a vast number of problems the visual system must solve: the analysis of motion, three-dimensional space, constancies of various sorts, etc. GRA

54 MAN/SYSTEM TECHNOLOGY AND LIFE SUPPORT

Includes human engineering; biotechnology; and space suits and protective clothing.

For related information see also *16 Space Transportation.*

N89-24043# Technische Hogeschool, Delft (Netherlands). Dept. of Mathematics and Informatics Computer Science.
DIRECT MANIPULATION AND OTHER STYLES OF MAN-MACHINE INTERACTION

J. M. Versendaal 1988 20 p
(PB89-146070; Rept-88-53) Copyright Avail: NTIS HC A03/MF A01 CSCL 05H

As new technologies are used in computer hardware, such as fast refresh graphics screens, and as people began to realize that common computer interaction could be difficult, a new and, to the user often a more comprehensible computer dialogue style has emerged. Using that dialogue style, users interact with the computer system by directly manipulating the object of interest presented on the screen. Schneiderman called this new dialogue style Direct Manipulation (DM). A precise description of DM along with conventional dialogue styles is given. DM interfaces often cause unique problems, compared with other dialogue styles. These problems, their causes and possible ways of solving them are discussed. Author

N89-24044*# National Aeronautics and Space Administration. Marshall Space Flight Center, Huntsville, AL.
SPACE STATION ECLSS SIMPLIFIED INTEGRATED TEST Final Report
Richard G. Schunk, Robert M. Bagdigian, Robyn L. Carrasquillo, Kathyrn Y. Ogle, and Paul O. Wieland Mar. 1989 42 p
(NASA-TM-100363; NAS 1.15:100363) Avail: NTIS HC A03/MF A01 CSCL 06K

A discussion of the Space Station Simplified Integrated Test (SIT) was conducted. The first in a series of three integrated Environmental Control and Life Support (ECLS) system tests, the primary objectives of the SIT were to verify proper operation of ECLS subsystems functioning in an integrated fashion as well as to gather preliminary performance data for the partial ECLS system used in the test. A description of the SIT configuration, a summary of events, a discussion of anomalies that occurred during the test, and detailed results and analysis from individual measurements and water and gas samples taken during the test are included. The preprototype ECLS hardware used in the test is reported providing an overall process description and theory of operation for each hardware item. Author

N89-24045# Georgia Inst. of Tech., Atlanta. Center for Human-Machine Systems Research.
AN ICAI (INTELLIGENT COMPUTER AIDED INSTRUCTION) ARCHITECTURE FOR TROUBLESHOOTING IN COMPLEX DYNAMIC SYSTEMS
Janet L. Fath, Christine M. Mitchell, and T. Govindaraj Dec. 1988 62 p
(Contract N00014-87-K-0482; RM3-3-M-20)
(AD-A205434; GIT-88-4) Avail: NTIS HC A04/MF A01 CSCL 23/2

AHAB is an architecture for simulator-based ICAI (Intelligent Computer Aided Instruction) programs to teach troubleshooting in complex, dynamic environments. The architecture posits three elements of a computerized instructor: The task model, the student model, and the instructional module. The task model is a prescriptive model of expert performance that uses symptomatic and topographic search strategies to provide students with directed problem-solving aids. The student model is a descriptive model of student performance in the context of task model. This student model compares the student and task models, critiques student performance in the context of the task model. This student model compares the student and task models, critiques student performance, and provide interactive performance feedback. Finally, the instructional module coordinates information presented by the instructional media, the task model, and the student model so that each student receives individualized instruction. Concept and meta-concept knowledge that supports these elements is contained in frames and production rules, respectively. GRA

N89-24046# Defence Research Establishment Ottawa, (Ontario). Protective Sciences Div.
THE CONCEPT AND THEORETICAL CONSIDERATIONS OF A COLD WEATHER CLOTHING SYSTEM
B. Cain, B. Farnsworth, and R. Osczevski Dec. 1988 41 p
(AD-A205476; DREO-998) Avail: NTIS HC A03/MF A01 CSCL 05/8

The concept and theoretical considerations of a clothing system for cold weather is discussed. The temperature range of interest was -40 to 10 C which was divided into an extreme-cold temperature range (-40 to -10 C) and a cold-wet temperature range (-10 to 10 C). An essential goal of the clothing system was to provide adequate thermal insulation for metabolic rates between 150 and 600 W while a desirable goal was to provide adequate thermal insulation for metabolic rates up to 1000 W. The clothing differs from conventional clothing mainly in its doctrine of use as insulation is added to or removed from the outside. This makes the clothing more versatile and more easily used. GRA

N89-24047# Center for Night Vision and Electro-Optics, Fort Belvoir, VA.
NIGHT VISION GOGGLES (AN/PVS-7) PERFORMANCE ISSUES AND ANSWERS Final Report, 1986 - 1988
Walter B. Morrow, Jr. Mar. 1989 47 p
(AD-A206117; AMSEL-NV-TR-0075) Avail: NTIS HC A03/MF A01 CSCL 17/5

During 1987, pursuant to a tasking by the Undersecretary of the Army through the Institute for Defense Analysis, the U.S. Army CECOM Center for Night Vision and Electro-Optics (C2NVEO) carried out a comprehensive series of studies to characterize the spectral content of night sky irradiance across the spectral sensitivity bands of second and third generation AN/PVS-7 Night Vision Goggles. This effort was then logically extended to the development of a detailed comparative performance analysis of night vision goggles within the true spectral characterization of the night sky environment. Several related issues were also of concern to the Undersecretary, including the effect of various bandpass and notch spectral filters with goggles, and finally the operational life and reliability of night vision goggles. GRA

N89-24048# Analytics, Inc., Willow Grove, PA.
DESIGN OF A MANPRINT TOOL FOR PREDICTING PERSONNEL AND TRAINING CHARACTERISTICS IMPLIED BY SYSTEM DESIGN Final Report, Jun. 1987 - Jan. 1988
Alfred O. Dick, Alvah C. Bittner, and Regina Harris Jan. 1989 314 p
(Contract MDA903-86-C-0413)
(AD-A206201; ARI-RN-89-04) Avail: NTIS HC A14/MF A01 CSCL 05/9

This report describes the development and design specifications for a software-based aid for Army system designers. The purpose of the aid is to evaluate a system design by determining the operator and maintainer characteristics required by that design to reach criterion system performance levels. The aid is an analytical, simulation-based approach that will predict the impact on total system performance of individual differences in cognitive and psychomotor performance and of new system technologies. The specification describes a system based on the Human Operator Simulator (HOS) 4. In this approach, HOS performance micromodels are to be built from the Army Research Institute's (ARI) Project A predictor data. Although the design specification described herein is not being developed any further by ARI, it may prove useful for other projects. GRA

N89-24049# Carnegie-Mellon Univ., Pittsburgh, PA. Software Engineering Inst.
HUMAN-MACHINE INTERACTION CONSIDERATIONS FOR INTERACTIVE SOFTWARE Final Technical Report
Len Bass and Joelle Coutaz (Grenoble-1 Univ., France) Feb. 1989 117 p
(Contract F19628-85-C-0003)
(AD-A206574; CMU/SEI-89-TR-4; ESD-TR-89-04) Avail: NTIS HC A06/MF A01 CSCL 23/2

This document introduces current concepts and techniques relevant to the design and implementation of user interfaces. A user interface refers to those aspects of a system that the user refers to, perceives, knows and understands. A user interface is implemented by code that mediates between a user and a system.

This document covers both aspects. The first chapter is an introduction to the psychology of human-computer interaction. It presents the theoretical models that have had a significant impact on the evolution of the field. These models offer a way to organize the design process and help understand the cognitive process involved in interacting with a computer. The rest of the document is concerned with the software design of user interfaces and shows how the principles established by the cognitive principles can be put into practice. Following a presentation on the abstractions involved in the organization of an interactive system, attention is then directed to the tools for constructing user interfaces: windowing systems, tool kits and user interface management systems. GRA

N89-24050# Aerospatiale, Paris (France).
THE ROLE OF PILOT AND AUTOMATIC ONBOARD SYSTEMS IN FUTURE RENDEZVOUS AND DOCKING OPERATIONS
W. Fehse, A. Tobias, A. Getzschmann, M. Caldichoury, P. Maute, and M. Attanasio (Aerospatiale, Cannes La Bocca, France) 1988 13 p Presented at the 39th International Astronautical Federation Congress, Bangalore, India, 8-15 Oct. 1988 Previously announced in IAA as A89-17642
(Rept-882-440-116; IAF-88-037; ETN-89-94509) Avail: NTIS HC A03/MF A01

In the frame of a Hermes mission to service the Columbus module, an analysis of the role of pilots is presented. The discussion includes requirements, tasks to be performed onboard during rendezvous operations, the possibility of interaction by a pilot with an automatic guidance navigation and control system, and the necessary non-machine interfaces. Proposals for specific man machine interface displays and their arrangement in the cockpit are presented. The conclusion is that the pilot must have continuous access to all necessary information and must have the possibility to intervene at each point in time. ESA

N89-23904*# National Aeronautics and Space Administration. Marshall Space Flight Center, Huntsville, AL.
ASTRONAUT TOOL DEVELOPMENT: AN ORBITAL REPLACEABLE UNIT-PORTABLE HANDHOLD
John W. Redmon, Jr. *In its* The 23rd Aerospace Mechanisms Symposium Mar. 1989 p 181-193 (For primary document see N89-23892 17-39)
Avail: NTIS HC A15/MF A01 CSCL 05H

55 SPACE BIOLOGY

Includes exobiology; planetary biology; and extraterrestrial life.

No abstracts in this category.

59 MATHEMATICAL AND COMPUTER SCIENCES (GENERAL)

No abstracts in this category.

60 COMPUTER OPERATIONS AND HARDWARE

Includes hardware for computer graphics, firmware, and data processing.

For components see *33 Electronics and Electrical Engineering.*

N89-24051# Federal Aviation Administration, Atlantic City, NJ.
HOST COMPUTER SYSTEM CAPACITY MANAGEMENT PROCEDURES Technical Note, 1987
Norman W. Watts, Paul Connolly, Robert Goettge, Gary Morfitt, Robert Wiseman, Gary Wright, and Frank Yazek Feb. 1988 48 p
(Contract FAA-T0503-M)
(AD-A193416; DOT/FAA/CT-TN87/43) Avail: NTIS HC A03/MF A01 CSCL 09/2

The Federal Aviation Administration's Advanced Automation Program Office recognized the need for monitoring and assessing the National Airspace System's operational performance and for long term planning during the life-cycle of the Host Computer System. The assessment of the operational performance involved the acquisition and analysis of field measurement data, while the long-term capacity planning entails execution of a Host Computer System analytical model using current and project traffic and other system loads. The procedures document defines the activities to be executed in: measuring and monitoring operational performance; measuring projecting system workloads; predicting system performance using an analytical performance model; and analyzing and reporting current and predicted future performance of the Host Computer System. Author

N89-24052# National Inst. of Standards and Technology, Gaithersburg, MD. Advanced Systems Div.
WAVEFRONT MATRIX MULTIPLICATION ON A DISTRIBUTED-MEMORY MULTIPROCESSOR
James R. Nechvatal Jan. 1989 71 p
(PB89-151807; NISTIR-88/4001) Avail: NTIS HC A04/MF A01 CSCL 09B

The problem of efficiently multiplying matrices on distributed-memory, message-passing computers is considered. Block decomposition and wavefront computing are employed to yield a communication-efficient solution. It also explores interconnections between distributed data structures, physical networks of nodes and virtual networks of nodes and processes. The notion of wavefront computing is extended to include pipelining of data between nodes of networks of processes as well as physical networks of nodes. Algorithms are developed in layers to facilitate porting between topologies and programming environments. It is shown how different topologies can be employed in a single application. A mathematical characterization of data-routing for efficient matrix multiplication on distributed-memory machines is developed, which exhibits a wavefront version of the Dekel/Nassimi/Sahni algorithm as a special case. The notion of granularity is discussed in this context and is used to distinguish between algorithms on grounds of communication complexity. Author

N89-24053# Naval Ocean Systems Center, San Diego, CA.
SIGNAL-NOISE/INTERFERER COMBINER UNIT PROGRAMMABLE (SINCUP) Report, period ending Oct. 1987
E. Martinez DePison Jan. 1989 11 p
(AD-A205367) Avail: NTIS HC A03/MF A01 CSCL 12/6

The Signal Noise Interferer Combiner Unit Programmable (SINCUP) has been developed to facilitate laboratory performance testing of Very Low Frequency (LF) receivers. To accomplish this, the unit allows the combining in controlled amounts of various real-world environmental and manmade interference with an information carrying signal. The externally modulated signal is combined with internally/externally generated Gaussian noise and/or with an internally/externally generated interferer. In order to test modern digital processing techniques, such as Adaptive Null Steering, Eigenvector Sorting, and Widrow-Hoff adaptive filters,

SINCUP is capable of generating and meeting much higher signal-to-noise plus interference rations than earlier channel simulators. The present software has been written to accommodate a dynamic signal-to-noise ratio (SNR) range from -60 to +60 dB. Higher dynamic range units could be implemented. GRA

61 COMPUTER PROGRAMMING AND SOFTWARE

Includes computer programs, routines, alogorithms, and specific applications, e.g., CAD/CAM.

N89-24054*# Old Dominion Univ., Norfolk, VA. Dept. of Computer Science.
SOFTWARE RELIABILITY STUDIES Progress Report, period ended 31 Mar. 1989
Larry W. Wilson Mar. 1989 11 p
(Grant NAG1-750)
(NASA-CR-184857; NAS 1.26:184857) Avail: NTIS HC A03/MF A01 CSCL 09B

The longterm goal of this research is to identify or create a model for use in analyzing the reliability of flight control software. The immediate tasks addressed are the creation of data useful to the study of software reliability and production of results pertinent to software reliability through the analysis of existing reliability models and data. The completed data creation portion of this research consists of a Generic Checkout System (GCS) design document created in cooperation with NASA and Research Triangle Institute (RTI) experimenters. This will lead to design and code reviews with the resulting product being one of the versions used in the Terminal Descent Experiment being conducted by the Systems Validations Methods Branch (SVMB) of NASA/Langley. An appended paper details an investigation of the Jelinski-Moranda and Geometric models for software reliability. The models were given data from a process that they have correctly simulated and asked to make predictions about the reliability of that process. It was found that either model will usually fail to make good predictions. These problems were attributed to randomness in the data and replication of data was recommended. A.D.

N89-24055*# National Aeronautics and Space Administration. Lewis Research Center, Cleveland, OH.
LABORATORY PROCESS CONTROL USING NATURAL LANGUAGE COMMANDS FROM A PERSONAL COMPUTER
Herbert A. Will and Michael A. Mackin Apr. 1989 14 p
(NASA-TM-101988; E-4690; NAS 1.15:101988) Avail: NTIS HC A03/MF A01 CSCL 09B

PC software is described which provides flexible natural language process control capability with an IBM PC or compatible machine. Hardware requirements include the PC, and suitable hardware interfaces to all controlled devices. Software required includes the Microsoft Disk Operating System (MS-DOS) operating system, a PC-based FORTRAN-77 compiler, and user-written device drivers. Instructions for use of the software are given as well as a description of an application of the system. Author

N89-24056# Technische Hogeschool, Delft (Netherlands). Dept. of Mathematics and Informatics Computer Science.
USER INTERFACE AND HIGHLY INTERACTIVE SYSTEMS: SURVEY OF CURRENT RESEARCH
J. M. Versendaal 1988 35 p
(PB89-146088; Rept-88-60) Copyright Avail: NTIS HC A03/MF A01 CSCL 09B

Highly interactive systems are those systems that have a strong emphasis on the dialogue between computer system and user. The state of the art in highly interactive system design is described, particularly in design of user-computer dialogues. Section 2 describes methodologies for interactive system design. Section 3 describes the current research with respect to user-computer dialogues. In section 4, management systems for user interfaces and interactive applications are discussed. Section 5 describes the object oriented approach for user interface and interactive system design. In the final section a brief summary and conclusions are given. Author

N89-24057# Aeronautical Research Labs., Melbourne (Australia).
SMOOFF: A FORTRAN SMOOTHING PROGRAM Aircraft Structures Technical Memo.
I. H. Grundy Jul. 1988 25 p
(AD-A204087; ARL-STRUC-TM-490; DODA-AR-005-528) Avail: NTIS HC A03/MF A01 CSCL 12/5

The FORTRAN program SMOOFF (SMOOthing by a Filtered Fourier transform) smooths a noisy function of two variables on a rectangular domain, by minimizing an appropriate functional subject to a least squares constraint. GRA

N89-24058*# Institute for Computer Applications in Science and Engineering, Hampton, VA.
COMPILING HIGH LEVEL CONSTRUCTS TO DISTRIBUTED MEMORY ARCHITECTURES Final Report
Piyush Mehrotra and John VanRosendale Mar. 1989 12 p
Submitted for publication
(Contract NAS1-18605)
(NASA-CR-181825; NAS 1.26:181825; ICASE-89-20) Avail: NTIS HC A03/MF A01 CSCL 09B

Current languages for nonshared memory architectures provide a relative low-level programming environment. A set of primitives such as load balance and data distribution, which allow the programmer to express data-parallel algorithms at a higher level while also permitting control over those aspects of the program critical to performance, are described. Given such a program specification, the compiler automatically generates a distributed program containing send and receive constructs to perform interprocess communication. Author

N89-24059# Boeing Computer Services Co., Richland, WA.
FOURTH GENERATION COMPUTER LANGUAGES
B. Lewis Jan. 1989 6 p Presented at the Association for Energy Systems Operations and Procedures Conference, Berkeley, CA, 17 Jan. 1989 Prepared in cooperation with Westinghouse Hanford Co., Richland, WA
(Contract DE-AC06-87RL-10930)
(DE89-008800; WHC-SA-0504; CONF-890194-1) Avail: NTIS HC A02/MF A01

The role of Fourth Generation Languages (4GL) has changed dramatically during the last five years. The 4GLs were initially limited to end-user needs in a homogeneous environment. Now their intent is to work in heterogeneous environments and far surpass traditional end-user roles. DOE

N89-24060*# Jet Propulsion Lab., California Inst. of Tech., Pasadena.
OBSERVATION MODEL AND PARAMETER PARTIALS FOR THE JPL GEODETIC GPS MODELING SOFTWARE GPSOMC
O. J. Sovers and J. S. Border 15 Dec. 1988 42 p
(NASA-CR-185021; JPL-Publ-87-21-Rev-1; NAS 1.26:185021)
Avail: NTIS HC A03/MF A01 CSCL 09B

The physical models employed in GPSOMC and the modeling module of the GIPSY software system developed at JPL for analysis of geodetic Global Positioning Satellite (GPS) measurements are described. Details of the various contributions to range and phase observables are given, as well as the partial derivatives of the observed quantities with respect to model parameters. A glossary of parameters is provided to enable persons doing data analysis to identify quantities in the current report with their counterparts in the computer programs. There are no basic model revisions, with the exceptions of an improved ocean loading model and some new options for handling clock parametrization. Such misprints as were discovered were corrected. Further revisions include modeling improvements and assurances that the model description is in accord with the current software. Author

N89-24061# Naval Postgraduate School, Monterey, CA.
A CAD (COMPUTER AIDED DESIGN) TOOL FOR CURRENT-MODE MULTIPLE-VALUED CMOS CIRCUITS M.S. Thesis
Hoon S. Lee Dec. 1988 123 p
(AD-A205327) Avail: NTIS HC A06/MF A01 CSCL 12/5

The contribution of this thesis is the development of a CAD (Computer Aided Design) tool for current mode multiple-valued logic (MVL) CMOS circuits. It is only the second known MVL CAD tool and the first CAD tool for MVL CMOS. The tool accepts a specification of the function to be realized by the user, procedures a minimal or near-minimal realization (if such a realization is possible), and produces a layout of programmable logic array integrated circuits that realizes the given function. The layout is in MAGIC format, suitable for submission to a chip manufacturer. The CAD tools is designed also to be an analysis tool for heuristic minimization algorithms. GRA

N89-24062# Technical Solutions, Inc., Mesilla Park, NM.
AUTOMATIC DOCUMENTATION METHODOLOGIES FOR SOFTWARE MAINTENANCE Technical Report, Sep. 1985 - Nov. 1988
L. D. Landis, P. M. Hyland, A. L. Gilbert, and A. J. Fine 15 Jan. 1989 170 p
(Contract DAAG29-85-C-0026)
(AD-A205672; ARO-22935.3-EL-S) Avail: NTIS HC A08/MF A01 CSCL 12/5

Given the non-trivial costs of software systems, it has become imperative to maintain software for a much longer period of time than was considered desirable in the past. Providing tools that will facilitate software maintenance helps to extend the useful lifetime of a software system. This report discusses a research project that was directed at providing a general-purpose, automatic documentation generator that could provide both the detailed and higher-level information that maintenance programmers perceive usefull. The project proceeded in three phases. The first phase consisted on an examination of the documentation methodologies currently available, and language requirements necessary to achieve these documentation methodologies. The second phase consisted of the development of the design for a documentation language which would be used as an intermediate representation in the documentation process. Finally, a research prototype was developed, in order to test the design and validate the research conclusions. GRA

N89-24063# Notre Dame Univ., IN. Dept. of Electrical and Computer Engineering.
[ADAPTIVE SIGNAL PROCESSING] Final Report, 1 May 1987 - 31 Dec. 1988
Yih-Fang Huang and Ruey-Wen Liu 8 Mar. 1989 87 p
(Contract N00014-87-K-0284)
(AD-A205787) Avail: NTIS HC A05/MF A01 CSCL 12/6

Recent advances in integrated circuits and signal processing technology have prompted the need of algorithms with higher degrees of modularity and pipeline-ability, resulting in higher degrees of concurrency and machine perception. It is generally believed in the research community that higher degrees of concurrency and machine perception will bring forth many breakthroughs in many signal processing areas, particularly in adaptive systems, speech and image processing and recognition. The objective of this research project is to develop an adaptive signal processing architecture with important features such as modularity, pipeline-ability, and intelligent use of information. The ground work upon which this research project rests is a recursive parameter estimation algorithm, i.e., the so-called OBE algorithm, which features a discerning update strategy. This discerning update is in sharp contrast to the continual update used by most existing algorithms. The estimation algorithm has been developed with a set-theoretic framework. In particular, starting with the assumption that the underlying noise (of the system being studied) is bounded in magnitude, a recursive least-squares type of estimation algorithm was obtained with a discerning update strategy. An important outcome of such discerning updates is that the resulting algorithm can be implemented with two modules: An information processor followed by an updating processor. GRA

N89-24064# California Univ., Los Angeles. Western Management Science Inst.
COMPUTER-BASED MODELING ENVIRONMENTS
Arthur M. Geoffrion Dec. 1988 18 p Sponsored in part by Navy; NSF; and Shell Development Co.
(AD-A205828; WMSI-WP-363) Avail: NTIS HC A03/MF A01 CSCL 12/5

This paper gives the author's views on the kind of computer-based modeling environment needed to properly support management science/operations research work, and on the design challenges that need to be met in order to bring such modeling environments into being. It is a written version of the main ideas of two addresses: a plenary at IFORS 87 in Buenos Aires, and the keynote at the 1988 Canadian Operations Research Society Meeting in Montreal (May, 1988). Modeling environments have the potential to greatly increase the productivity of model-based work through better tools, to improve the quality of model-based work through better support for good modeling style and work practices, and to improve the frequency of use of MS/Or by bringing about a more comfortable working relationship between MS/OR professionals and their constituencies. GRA

N89-24065# Cornell Univ., Ithaca, NY. Dept. of Computer Science.
THE ROLE OF ORDER IN DISTRIBUTED PROGRAMS
Kenneth Birman and Keith Marzullo Mar. 1989 23 p Sponsored by DARPA, Arlington, VA
(AD-A206037) Avail: NTIS HC A03/MF A01 CSCL 12/5

This document discusses the role of order in building distributed systems. It is our belief that a principle of event ordering underlies the wide range of operating systems mechanisms that have been put forward for building robust distributed software. Stated concisely, this principle is that one achieves correct distributed behavior by ordering classes of distributed events that conflict with one another. By focusing on order, one can obtain simplified descriptions and convincingly correct solutions to problems that might otherwise have looked extremely complex. Moreover, we observe that there are a limited number of ways to obtain order, and that the choice made impacts greatly on performance. GRA

N89-24066# Air Force Inst. of Tech., Wright-Patterson AFB, OH. School of Engineering.
A DATABASE MANAGEMENT SYSTEM FOR COMPUTER-AIDED DIGITAL CIRCUIT DESIGN M.S. Thesis
Sue A. Ehrhart Dec. 1988 101 p
(AD-A206047; AFIT/GCS/ENG/88D-4) Avail: NTIS HC A06/MF A01 CSCL 20/3

This thesis effort documents the design and implementation of a relational database and associated database management system (DBMS) for the AFIT digital circuit design environment, a graphics oriented tool that allows circuits to be designed at a uniform, chip-level of detail, checked for proper connections, and simulated. The approach to this effort included a survey of existing methods of Computer-Aided Design (CAD) data management, analysis of the data and data manipulation requirements of the design environment, design of a data manipulation language, and implementation of a DBMS to carry out the manipulations. GRA

N89-24067# Naval Postgraduate School, Monterey, CA.
DESIGN AND IMPLEMENTATION OF AN EXPERT USER INTERFACE FOR THE COMPUTER AIDED PROTOTYPING SYSTEM M.S. Thesis
Henry G. Raum Dec. 1988 91 p
(AD-A206113) Avail: NTIS HC A05/MF A01 CSCL 12/5

This thesis builds on previous work done in the development of the Computer Aided Prototyping System (CAPS) and the Prototype System Description Language (PSDL). The increases in the size and complexity of software projects have caused system designers to reevaluate traditional software engineering

methodologies. Rapid prototyping is a method that allows the validation of system requirements and design early in the development cycle. The need for this type of tool is particularly critical in the development of real-time embedded systems. CAPS is one such system. CAPS is a complex system that consists of many individual software tools. An expert user interface that guides the software designers through the development and execution of prototype is described in this thesis. GRA

N89-24068# Stanford Univ., CA. Center for Large Scale Scientific Computation.
A VISUAL OBJECT-ORIENTED UNIFICATION SYSTEM Interim Report
Joseph Oliger, Ramani Pichumani, and Dulce Ponceleon 16 Mar. 1989 38 p
(Contracts N00014-82-K-0335; N00014-86-K-0565; N00014-87-K-0384)
(AD-A206228; CLASSIC-89-23) Avail: NTIS HC A03/MF A01 CSCL 12/5

This report introduces a software design platform which departs from the style of most design tools by acting as an extension to, rather than a replacement for, existing design tools. The ultimate goal of this system is to unify and integrate the various functions provided by text editors, graphics editors, text formatters, hyper-text and structured decomposition tools. It uses a very general data structure which can manifest itself in a variety of visual forms while enabling the user to easily create and manipulate the objects it represents. This tool is useful for creating large, general purpose, hierarchically structured programs, data structures, documents, and other similar objects. Moreover, this system is designed to allow for a wide variety of functions to be performed on these data objects (such as graph traversal or functional mapping), both from within the environment as well as externally (for example, mapping concurrent computations onto parallel architectures using a post-processor). This system is also considered to be a springboard for investigating future directions in software design and information management. GRA

N89-24069# Syracuse Univ., NY.
AN EXPERIMENTAL INVESTIGATION INTO SOFTWARE RELIABILITY Final Report, Nov. 1985 - Jan. 1987
Amrit L. Goel Oct. 1988 124 p
(Contract F30602-81-C-0193)
(AD-A206293; RADC-TR-88-213) Avail: NTIS HC A06/MF A01 CSCL 12/5

This report presents the results of an experiment investigating the effect of FORTRAN and Ada languages on program reliability. The experimental design employed was a full factorial design, i.e., a design in two variables, each at two levels. The problem used in the experiment was the Launch Interceptor Program (LIP), a simple but realistic anti-missile system. Reliability comparisons between Ada and FORTRAN programs were based on the total number of errors as well as on errors found during various testing phases. Some comparisons were also based on error density, the number of errors per 100 non-comment lines of code. It was found that on the average, the Ada programs had about 70 percent fewer errors than the FORTRAN ones. If errors during unit testing were excluded, the Ada program had about 78 percent less errors. Similar differences were found for data based on error causes and error types. GRA

N89-24070# TRW Defense Systems Group., Fairfax, VA. Systems Div.
ADVANCED COMPUTING SYSTEMS: AN ADVANCED REASONING-BASED DEVELOPMENT PARADIGM FOR ADA TRUSTED SYSTEMS AND ITS APPLICATION TO MACH Quarterly Status Report, No. 1, 28 Nov. 1988 - 28 Feb. 1989
15 Mar. 1989 95 p
(Contract MDA972-89-C-0029; ARPA Order 6414)
(AD-A206308) Avail: NTIS HC A05/MF A01 CSCL 12/7

Objectives and basis of the process model; motivations (drivers) and constraints of the process model; an overview of primary risk issues; elements of the process model; and process model in the lifecycle are discussed. GRA

N89-24071# Naval Postgraduate School, Monterey, CA.
A GRAPHICAL EDITOR FOR THE COMPUTER AIDED PROTOTYPING SYSTEM M.S. Thesis
Roger K. Thorstenson Dec. 1988 139 p
(AD-A206443) Avail: NTIS HC A07/MF A01 CSCL 12/5

The Computer Aided Prototyping System (CAPS) is used to develop executable prototypes of large embedded software systems with hard real-time requirements. The system is based upon the Prototype System Description Language (PSDL) and a set of integrated software development tools. A graphical tool is needed to decompose the PSDL composite operator into a network which shows its component parts and their communication paths. The graphical description is part of the specification of the intended system's components. This thesis explores the requirements of such an editor and demonstrates that it can be developed. It shows that the editor can effectively be used to decompose operators and that it can produce and equivalent textual representation in PSDL. GRA

N89-24072# Stanford Univ., CA. Dept. of Computer Science.
DEDUCTIVE PROGRAMMING SYNTHESIS Final Report, 16 Sep. 1987 - 16 Sep. 1988
Zohar Manna Mar. 1989 7 p
(Contract N00039-84-C-0211)
(AD-A206451) Avail: NTIS HC A02/MF A01 CSCL 12/5

Some of the most efficient numerical algorithms rely on a binary-search strategy; according to this strategy, the interval in which the desired output is sought is divided roughly in half at each iteration. This technique is so useful that some authors have proposed that a general binary-search paradigm or schema be built into program synthesis systems and then specialized as required for particular applications. It is certainly valuable to store such schemata if they are of general application and difficult to discover. This approach, however, leaves open the question of how schemata are discovered in the first place. We have found that the concept of binary search appears quite naturally and easily in the derivations of some numerical programs. The concept arises as the result of a single resolution step, between a goal and itself, using our deductive-synthesis techniques. GRA

N89-24073# Colorado Univ., Denver.
FAST ALGORITHMS FOR PARTIAL DIFFERENTIAL EQUATIONS ON ADVANCED COMPUTERS Final Report, 1 Feb. 1986 - 1 May 1988
Thomas A. Manteuffel 2 Mar. 1989 14 p
(Grant AF-AFOSR-0061-86; AF Proj. 2304)
(AD-A206469; AFOSR-89-0352TR) Avail: NTIS HC A03/MF A01 CSCL 12/1

This report covers four areas of research. The first area is an analysis of preconditionings. We have examined the properties that a preconditioning must possess in order to yield an iterative method with convergence properties independent of the discretization parameters. The second area is an attempt to provide a framework for the construction of conjugate gradient methods. The third area of research is the analysis of the equations governing the transport of neutrally charged particles and the construction of iterative methods for the solution of discrete transport equations. The final area of research is supraconvergence which deals with accurately approximating the solution of partial differential equations on highly irregular meshes. The first topic is very theoretical in nature but will have important implications to the practical choice of preconditionings. The second area is also theoretical in nature, but leads immediately to the development of new iterative methods. The third area builds on the analysis of the continuous operators to yield insight into the behavior of discrete approximations. The final goal of this third project is the development of efficient numerical methods for the solution of discrete transport equations on massively parallel machines. The final area of research will lead to more efficient solution of differential equations on irregular meshes. GRA

N89-24074# Defence Research Establishment Ottawa, (Ontario). Chemical Protection Section.
COMPUTER-AIDED DESIGN AND BIO-ENGINEERING: A REVIEW OF THE LITERATURE
D. Hidson Jul. 1988 26 p
(AD-A206534; DREO-TN-88-31) Avail: NTIS HC A03/MF A01 CSCL 12/5

Today, almost every branch of engineering uses computers in one form or another and medical science, anthropometry and bioengineering are no exception. The use of computers has come relatively late to these disciplines as large amounts of computing power and sophisticated graphics are required for the complex data generated by the human body. If one is using computers to generate a graphical representation of the human body (as in anthropometric studies) or to determine the shape of the cockpit of a fighter aircraft, large quantities of data must be handled, as rarely are these variables expressable as simple geometric functions. One of the reasons for the delay of computer applications has been the lack of the capabilities of computer graphics to render these data in a useable and visible form. The recent advances in image generation and processing, in terms of complexity and speed, have enabled workers in these fields to adopt computers for tasks which would have seemed impossible only a few years ago. This paper contains a short review of some applications of computers in bio-engineering and the use of computer-aided design in anthropometrics, bio-engineering and medical science. GRA

N89-24075# Carnegie-Mellon Univ., Pittsburgh, PA. Software Engineering Inst.
THE STATE OF SOFTWARE ENGINEERING PRACTICE: A PRELIMINARY REPORT Final Technical Report
Watts S. Humphrey, David H. Kitson, and Tim C. Kasse Feb. 1989 37 p
(Contract F19628-85-C-0003)
(AD-A206573; CMU/SEI-89-TR-1; ESD-TR-89-01) Avail: NTIS HC A03/MF A01 CSCL 12/5

This is the first in a series of Software Engineering Institute reports to provide periodic updates on the state of software engineering practice in the DOD software community. The SEI has developed, and is refining, a process framework and assessment methodology for characterizing the processes used by software organizations to develop and evolve software products. This report provides a brief overview of the process framework and assessment approach, describes assessment results obtained to date, and discusses implications of the current state of the practice for both customers and suppliers of DOD software. GRA

N89-24076# Yale Univ., New Haven, CT. Dept. of Computer Science.
RUNTIME AGGREGATION OF RECURSION RELATIONS
Harry Berryman and Joel Salz 25 Jan. 1989 14 p
(Contract N00014-86-K-0310)
(AD-A206576; YALEU/DCS/TR-677) Avail: NTIS HC A03/MF A01 CSCL 12/7

In many modern algorithms, relatively regular problems are encoded using flexible general purpose data structures. To obtain satisfactory performance on distributed memory architectures, it is often necessary to reconstruct and exploit the underlying dependency structure. The authors present a method to partition loops that have runtime dependencies that resemble uniform recurrence equations. Loops of this type are often found, among other places, in solving sparse triangular linear systems for preconditioning in Krylov space iterative linear system solvers. GRA

N89-24077# Swedish Defence Research Establishment, Stockholm.
GRADA: A GRAPHICAL PACKAGE IN Ada
Nils Roman and Magnus Sjoland Nov. 1988 53 p In SWEDISH; ENGLISH summary
(FOA-C-20741-2.7; ISSN-0347-3694; ETN-89-94304) Avail: NTIS HC A04/MF A01

Graphics tools put together in Ada packages, which are general and can be used in several applications, were developed on a Vax 750 with a digital equipment compiler, constructed so that the interface to the graphical equipment is as small as possible. There are drivers for a color terminal, for a color screen, and a line drawing terminal. There is a possibility to generate postscript files. ESA

N89-24078# Aerospatiale, Cannes La Bocca (France).
GEMMES: A NEW TOOL FOR DYNAMIC MODELING
C. Garnier and P. Rideau Paris, France 1988 7 p
(Rept-882-440-114; ETN-89-94507) Avail: NTIS HC A02/MF A01

The GEMMES software provides an alternative to the currently used numerical simulation software. It computes the equations of mechanical systems in a symbolic, non-numerical form. The present version handles tree-like systems. It allows a description of the geometry of the mechanical system and of its flexible constituents. It has a Fortran interface that automatically generates a simulator of the system. In the case of tree like system GEMME is a very efficient tool. The case of closed loop systems is not yet throughly solved. ESA

62 COMPUTER SYSTEMS

Includes computer networks and special application computer systems.

N89-24079*# National Aeronautics and Space Administration. Langley Research Center, Hampton, VA.
APPLICATION OF A PC BASED, REAL-TIME, DATA-AQUISITION SYSTEM IN ROTORCRAFT WIND-TUNNEL TESTING
Matthew L. Wilbur Washington Jul. 1989 26 p Prepared in cooperation with Army Aviation Systems Command, Hampton, VA
(NASA-TM-4119; L-16565; NAS 1.15:4119;
AVSCOM-TM-89-B-003) Avail: NTIS HC A03/MF A01 CSCL 09B

Data has been acquired for a rotocraft test in the NASA Langley Transonic Dynamics Tunnel using a desktop data acquisition system. The system, which consists of an IBM Personal Computer AT (PC-AT) and an Omega Engineering OM-900 Stand-Alone Interface System, is well suited for acquiring high speed data on a limited number of channels. The data acquisition system and the interrupt driven software which provides the capability for near real-time cyclic data acquisition as well as data storage and display are described. Author

N89-24080# Environmental Protection Agency, Washington, DC. Architectural Management and Planning Branch.
LOCAL AREA NETWORK TECHNICAL GUIDELINES. VOLUME 1: LAN DESIGN AND PLANNING (LAN TSR PROCESS)
Jan. 1988 475 p
(PB89-139091; EPA/IRM-88/503-Vol-1) Avail: NTIS HC A20/MF A01 CSCL 09B

The manual provides an overview of the Local Area Network (LAN) of personal computers and their potential to improve the efficiency and productivity of the organization. It includes elaboration on the planning and purchasing of the LAN as well as details on LAN site preparation installation, and daily operations. Author

N89-24081# Massachusetts Inst. of Tech., Cambridge. Microsystems Research Center.
CRITERIA FOR ROBUST STABILITY IN A CLASS OF LATERAL INHIBITION NETWORKS COUPLED THROUGH RESISTIVE GRIDS
John L. Wyatt, Jr. and David L. Standley Nov. 1988 22 p
(Contract N00014-87-K-0825; NSF MIP-88-14612)

(AD-A204174; VLSI-M-88-493) Avail: NTIS HC A03/MF A01 CSCL 23/3

In the analog VLSI implementation of neural systems, it is sometimes convenient to build later inhibition networks by using a locally connected on-chip resistive grid to interconnect active elements. A serious problem of unwanted spontaneous oscillation often arises with these circuits and renders them unusable in practice. This paper reports on criteria that guarantee these and certain other systems will be stable, even though the values of designed elements in the resistive grid may be imprecise and the location and values of parasitic elements may be unknown. The method is based on a rigorous, somewhat novel mathematical analysis using Tellegen's theorem from electrical circuits and the idea of a Popov multiplier from control theory. The criteria are local in that no overall analysis of the interconnected system is required for their use, empirical in that they involve only measurable frequency response data on the individual cells, and robust in that they are insensitive to network topology and to unmodelled parasitic resistances and capacitances in the interconnect network. Certain results are robust in the additional sense that specified nonlinear elements in the grid do not effect the stability criteria. The results are designed to be applicable, with further development, to complex and incompletely modelled living neural systems. GRA

N89-24082*# Draper (Charles Stark) Lab., Inc., Cambridge, MA.
AVIONICS ARCHITECTURE STUDIES FOR THE ENTRY RESEARCH VEHICLE
M. J. Dzwonczyk, M. F. McKinney, S. J. Adams, and R. J. Gauthier May 1989 124 p Presented at the 8th AIAA-IEEE Digital Avionics System Conference, Oct. 1988
(Contract NAS1-18061)
(NASA-CR-181828; NAS 1.26:181828) Avail: NTIS HC A06/MF A01 CSCL 09B

This report is the culmination of a year-long investigation of the avionics architecture for NASA's Entry Research Vehicle (ERV). The Entry Research Vehicle is conceived to be an unmanned, autonomous spacecraft to be deployed from the Shuttle. It will perform various aerodynamic and propulsive maneuvers in orbit and land at Edwards AFB after a 5 to 10 hour mission. The design and analysis of the vehicle's avionics architecture are detailed here. The architecture consists of a central triply redundant ultra-reliable fault tolerant processor attached to three replicated and distributed MIL-STD-1553 buses for input and output. The reliability analysis is detailed here. The architecture was found to be sufficiently reliable for the ERV mission plan. Author

N89-24083# Oak Ridge National Lab., TN. Mathematical Sciences Section.
REDUCTION OF A GENERAL MATRIX TO TRIDIAGONAL FORM
G. A. Geist Mar. 1989 26 p
(Contract DE-AC05-84OR-21400)
(DE89-008980; ORNL/TM-10991) Avail: NTIS HC A03/MF A01

This report reviews recent research in finding eigenvalues of general matrices by first reducing the matrix to tridiagonal form and then applying LR iteration to this reduced form. The report also describes a new algorithm for solving this problem and shows why it is superior to the other approaches. While our results show the algorithm to be over three times faster than the EISPACK routines for finding eigenvalues, there are some matrices for which the algorithm fails. The report describes how to detect these matrices during the reduction process and how to attempt to proceed. DOE

N89-24084*# National Aeronautics and Space Administration. Lyndon B. Johnson Space Center, Houston, TX.
A METHOD OF UP-FRONT LOAD BALANCING FOR LOCAL MEMORY PARALLEL PROCESSORS Patent Application
Paul Thomas Baffes, inventor (to NASA) 12 Dec. 1988 29 p Sponsored by NASA. Johnson Space Center
(NASA-Case-MSC-21348-1; NAS 1.71:MSC-21348-1; US-Patent-Appl-SN-283106) Avail: NTIS HC A03/MF A01 CSCL 09B

In a parallel processing computer system with multiple processing units and shared memory, a method is disclosed for uniformly balancing the aggregate computational load in, and utilizing minimal memory by, a network having identical computations to be executed at each connection therein. Read-only and read-write memory are subdivided into a plurality of process sets, which function like artificial processing units. Said plurality of process sets is iteratively merged and reduced to the number of processing units without exceeding the balance load. Said merger is based upon the value of a partition threshold, which is a measure of the memory utilization. The turnaround time and memory savings of the instant method are functions of the number of processing units available and the number of partitions into which the memory is subdivided. Typical results of the preferred embodiment yielded memory savings of from sixty to seventy five percent. NASA

N89-24085# Naval Postgraduate School, Monterey, CA.
DESIGN OF MULTIPLE-VALUED PROGRAMMABLE LOGIC ARRAYS (PLA) M.S. Thesis
Yong H. Ko Dec. 1988 70 p
(AD-A205307) Avail: NTIS HC A04/MF A01 CSCL 09/1

The goal of this thesis is the development of a programmable logic array (PLA) that accepts multiple-valued inputs and produces multiple-valued outputs. The PLA is implemented in CMOS and multiple levels are encoded as current. It is programmed by choosing transistor geometries which control the current level at which the PLA reacts to inputs. An example of a 4-valued PLA is shown. As part of this research, a C program was written that produces a PLA layout. GRA

N89-24086# Naval Ocean Systems Center, San Diego, CA.
LIGHT CHANNEL 5 Gb/s OPTOELECTRONIC TDM (TIME DIVISION MULTIPLEXING) Presentation Report, period ending Oct. 1988
D. J. Albares, C. T. Chang, T. R. Ogden, G. A. Garcia, and M. N. McLandrich Feb. 1989 4 p
(AD-A205501) Avail: NTIS HC A02/MF A01 CSCL 12/7

An 8:1, 5 Gb/s, time division multiplexer has been implemented using optoelectronic or metal-semiconductor-metal switches for sampling. The device was fabricated on InP and the switches activated via optical fiber delay lines by pulses from a GaAlAs laser diode array. This device concept is applicable to chip and to board level computing multiplexing. Time division multiplexing (TDM), serializing parallel data for high speed transmission, is an important element in most concepts and implementations in computer networking as well as other areas of communications. An optoelectronic TDM (OE-TDM) approach(1) is advantageous in speed, power, and signal-control isolation. It was conceived initially to offer serial transmission off VLSI chips and recently has shown promise as a stand alone multiplexing technique. We report an improved multiplexer in InP giving an 8:1 multiplex ratio, a 26 dB signal-to-noise ratio, and a 5 Gb/s serial data rate while using a realistic parallel data level of 2 volts instead of the earlier 15 V(1). GRA

N89-24087# Air Force Inst. of Tech., Wright-Patterson AFB, OH. School of Engineering.
PRASE (PARALLEL RESOURCE ANALYSIS SOFTWARE ENVIRONMENT) INSTRUMENTATION SOFTWARE FOR THE INTEL IPSC HYPERCUBE M.S. Thesis
Mark A. Kahl Dec. 1988 211 p
(AD-A206046; AFIT/GCS/ENG/88D-11) Avail: NTIS HC A10/MF A01 CSCL 12/5

PRASE (Parallel Resource Analysis Software Environment), developed at the Air Force Institute of Technology to support local users, consists of a set of subroutines and programs that aid a user in monitoring parallel processing software targeted for an Intel iPSC Hypercube. PRASE was in many ways patterned after Seecube, an effort by Alva Couch and others at Tufts University in Massachusetts. Like Seecube, instrumentation code

must be embedded in a user's source code to facilitate data collection. After data has been collected, a translator may be used to translate PRASE data into Seecube format. This allows application-specific instrumentation. Preprocessors for both C and FORTRAN automatically embed necessary subroutine calls using a user defined configuration file. The data collection subroutines are written in C and can be called by both C and FORTRAN. Data collected during program execution can be held in Hypercube memory and written to disk at the end of a run, or dumped periodically to disk during a run which may aid in debugging. GRA

N89-24088# Massachusetts Inst. of Tech., Lexington. Lincoln Lab.
PROSPECTS FOR CLASSIFYING COMPLEX IMAGERY USING A SELF-ORGANIZING NEURAL NETWORK
M. M. Meron and K. G. Heinemann 11 Jan. 1989 31 p
(Contract F19628-85-C-0002)
(AD-A206208; ESD-TR-88-322) Avail: NTIS HC A03/MF A01 CSCL 12/9

The objective of this study is to evaluate the performance of Fukushima's Neocognitron model when it is applied to complex imagery. This system could discriminate between simple alphabetical characters represented in fields of 16 by 16 pixels, and that shift invariance can be achieved through a proper choice of design parameters. This work describes results for expanded Neocognitron architectures operating on complex images of 128 by 128 pixels. These neural network systems were simulated on a VAX-8600 minicomputer. Wire frame models of three different vehicles were used to test the properties which Fukushima had demonstrated. The expanded Neocognitron systems were able to classify these objects and to identify their critical features. After training, each object was placed at different positions in the plane, and the Neocognitron's shift invariance property was tested. With complex (128 X 128) imagery, it was difficult to achieve proper classification and maintain shift invariance using only a few levels. In another experiment, the Neocognitron trained on polar transforms of objects in the training set. Objects in the training set were rotated, and polar transforms of the rotated images were submitted as input. In this manner, the Neocognitron's shift invariance was exploited to recognize rotated imagery. GRA

63 CYBERNETICS

Includes feedback and control theory, artificial intelligence, robotics and expert systems.

For related information see also *54 Man/System Technology and Life Support.*

N89-24089# Oxford Univ. (England). Dept. of Engineering Science.
STATE-SPACE FORMULAE FOR DISCRETE-TIME H INFINITY OPTIMIZATION
D.-W. Gu, M. C. Tsai, S. D. OYoung, and I. Postlethwaite 1988 49 p
(OUEL-1718/88; ETN-89-94211) Avail: NTIS HC A03/MF A01

The main computational steps in H sup inf optimization are explained: coprime factorization; inner-outer factorization; spectral factorization; and a model-matching problem. Formulae for coprime factorizations are the same in discrete and continuous-time and are therefore not included. The solution of the discrete-time algebraic Riccati equation which is an essential ingredient of all the factorizations is given. The algorithms are suitable for implementation in computer aided control system design procedures. Since the resulting controller is in discrete-time form, it can be readily incorporated into a digital control system. ESA

N89-24090# Oxford Univ. (England). Dept. of Engineering Science.
ROBUST MULTIVARIABLE FEEDBACK DESIGN
B. Kouvaritakis and M. S. Trimboli 1988 57 p Sponsored by the United Kingdom Science and Engineering Research Council and the AF
(OUEL-1723/88; ETN-89-94212) Avail: NTIS HC A04/MF A01

A design methodology which exploits a simple geometric alignment property between the principal directions of matrices (MPDA), and utilizes the method of exact eigenvalue inclusion regions, in order to produce simple, robust PI controllers which optimize key design objectives at pertinent frequency values is proposed. The proportional part of the controller is designed to obtain optimal multivariable gain margins, while the integral component optimizes disturbance rejection and tracking accuracy at low frequencies. Characterizing the optimal low frequency controller is a simple vector alignment between the major principal directions of the controller and the corresponding minor principal directions of the plant. For the case of unstructured perturbations, this amounts to a (partial) RFA condition and hence justifies the technique. At the intermediate/high frequency realm, an optimal solution to the robust gain margin maximization problem elicits a compensated structure having a non-simple Jordan form. Of the two key factors in manipulation of exact eigenvalue inclusion regions, namely the positioning of nominal compensated eigenvalues, and the conditioning of the compensated eigenvector matrix, the latter is more significant role in disturbance rejection/tracking accuracy optimization, while the former is decisive for robust relative stability. ESA

N89-24091# Oxford Univ. (England). Dept. of Engineering Science.
MULTIVARIABLE NYQUIST SELF-TUNING: A GENERAL APPROACH
B. Kouvaritakis and J. A. Rossiter 1988 33 p Sponsored by the United Kingdom Science and Engineering Research Council and the Central Electricity Generating Board, United Kingdom
(OUEL-1734/88; ETN-89-94213) Avail: NTIS HC A03/MF A01

Fractional representations for the branches of the characteristic transfer functions are developed for a Nyquist type of multivariable self tuning methodology. Algorithms are developed for the computation of these representations and their implementation within a self-tuning feedback configuration. Stability is also considered. The results are illustrated by numerical examples. A design study based on the open-loop unstable chemical reactor is presented. ESA

N89-24092# Illinois Univ., Urbana. Coordinated Science Lab.
EXPLANATION-BASED THEORY REVISION: AN APPROACH TO THE PROBLEMS OF INCOMPLETE AND INCORRECT THEORIES Ph.D. Thesis
Shankar A. Rajamoney Dec. 1988 253 p
(Contract N00014-86-K-0309)
(AD-A205337; UILU-ENG-88-2264) Avail: NTIS HC A12/MF A01 CSCL 05/8

Knowledge intensive Artificial Intelligence systems rely on a model of the domain, called a domain theory, to fulfill their tasks. A domain theory consists of a encoding of the knowledge required by the system to draw inferences about situation of interest. Systems that rely on domain theory face two difficult problems. Their performance is directly related to the amount of knowledge in the domain theory. In order to insure a satisfactory level of performance, the expert who constructs the domain theory has the tedious chore of anticipating the wide variety of examples on which the system may be run. For most complex real-world domains it is impossible to anticipate and handcode all the required knowledge. The expert is forced to make approximations and assumptions. This results in brittle systems that tend to draw erroneous inferences and fail frequently. Systems that rely on a domain theory are limited to reasoning within the deductive closure of the knowledge in the domain theory. Since the knowledge content of the domain theory remains constant, these systems are incapable of modelling dynamic or under-specified domains in which new knowledge is being constantly acquired. Furthermore, large amounts of additional knowledge must be provided to the system if it is to process new examples. Consequently, such

systems tend to be inflexible and inextensible. This thesis describes a method called explanation-based theory revision for augmenting and correcting an inadequate domain theory. GRA

N89-24093# Naval Postgraduate School, Monterey, CA.
DESIGNING FEEDBACK COMPENSATORS BY USING THE ROOT-LOCUS METHOD M.S. Thesis
Levent Korkmaz Dec. 1988 127 p
(AD-A205354) Avail: NTIS HC A07/MF A01 CSCL 09/1

The purpose of this thesis is to find suitable ways to design feedback compensators for high order systems by using Root-Locus methods. As a starting point we will examine a motor amplidyne system and a position control system that were previously designed using Bode methods. Then we generalize the method and extend it to other systems. The final subject of this thesis is to design feedback compensators as filters by using state feedback coefficients to define zeros of the filter, then we extend this idea to build cascade filters. GRA

N89-24094# Massachusetts Inst. of Tech., Cambridge. Artificial Intelligence Lab.
THREE-DIMENSIONAL RECOGNITION OF SOLID OBJECTS FROM A TWO-DIMENSIONAL IMAGE Ph.D. Thesis
Daniel Huttenlocher Oct. 1988 165 p
(Contracts N00014-86-K-0685; N00014-85-K-0124)
(AD-A205667; AI-TR-1045) Avail: NTIS HC A08/MF A01 CSCL 12/9

This thesis addresses the problem of recognizing solid objects in the three-dimensional world, using two-dimensional shape information extracted from a single image. Objects can be partly occluded and can occur in cluttered scenes. A model based approach is taken, where stored models are matched to an image. The matching problem is separated into two stages, which employ different representations of objects. The first stage uses the smallest possible number of local features to find transformations from a model to an image. This minimizes the amount of search required in recognition. The second stage uses the entire edge contour of an object to verify each transformation. This reduces the chance of finding false matches. A new method is developed for computing transformations from a model to an image. It is shown that when perspective viewing is approximated by orthographic projection plus scale, three corresponding model and image points define a unique transformation, up to a reflection. The solution method based on this result only involves second order equations, and thus is fast and robust. Recognizing objects under projection requires features that are relatively stable over changes in viewpoint. Stable features are obtained by segmenting edge contours at zeroes of curvature, because these points are preserved under projection. Each feature defines either a point and an orientation or three points, so only one or two features are needed to compute a transformation. GRA

N89-24095# Duke Univ., Durham, NC. Center for Decision Studies.
THE IMPACT OF ACCURACY AND EFFORT FEEDBACK AND GOALS ON ADAPTIVE DECISION BEHAVIOR
Elizabeth H. Creyer, James R. Bettman, and John W. Payne Feb. 1989 37 p
(Contract N00014-80-C-0114; RR04209)
(AD-A205751; ONR-TR-89-3) Avail: NTIS HC A03/MF A01 CSCL 12/4

This paper examines the impact of accuracy and effort feedback on decision processes. The effects of emphasizing either a goal of maximizing accuracy relative to effort or minimizing effort relative to accuracy are also considered. Feedback on the accuracy of decisions leads to more normative like processing information and improved performance only in the most difficult problems, i.e., decisions with low dispersion in attribute weights. Explicit effort feedback has almost no impact on processing or performance. The impact of the goal manipulation on decision processes was found to be consistent with the shift in strategies predicted by an effort/accuracy model of strategy selection. In particular, a goal of emphasizing accuracy led to more normative-like processing, while emphasis on effort led to less extensive, more selective, and more attribute-based processing and poorer performance. These results provide perhaps the clearest evidence to date of the effect of goals on processing differences. Complex interactive relationships between types of feedback and goal structures suggest the need for additional study. GRA

N89-24096# Environmental Research Inst. of Michigan, Ann Arbor. Sensor Systems Div.
HEURISTICS FOR COOPERATIVE PROBLEM SOLVING Final Report
R. Franklin and L. Harmon Feb. 1989 75 p
(Contract DAAE07-87-C-R001; DARPA Order 5609)
(AD-A206371; ERIM-198900-2-F; TACOM-TR-13389) Avail: NTIS HC A04/MF A01 CSCL 12/9

This study examined the potential for cooperative machine intelligence. Cooperation is a common problem-solving technique in natural systems and occurs among even simple organisms. It is, therefore, a potentially powerful tool for extending the capabilities of relatively unsophisticated machines. A model of cooperation is presented which integrates problems requiring cooperative solutions, mechanisms for their implementation and the organizational requirements of cooperative groups. The biological and social science literature on cooperation is reviewed and found to yield little information about how cooperation is actually carried out in natural systems. Research in the field of distributed artificial intelligence is reviewed and critiqued. GRA

64 NUMERICAL ANALYSIS

Includes iteration, difference equations, and numerical approximation.

N89-24097# National Aeronautical Lab., Bangalore (India). Fluid Mechanics Div.
SOLUTION OF ONE-DIMENSIONAL EULER EQUATIONS BY THE IMPLICIT FINITE DIFFERENCE TECHNIQUE OF BEAM AND WARMING
Vimala Dutta Sep. 1988 18 p
(NAL-PD-FM-8816) Avail: NTIS HC A03/MF A01

A computer program was developed for the solution of one-dimensional Euler equations by the implicit finite difference method of beam and Warming. The initial and boundary conditions of a given one-dimensional inviscid flow problem form the basic input for the 1-D Euler solver. Two test cases - propagating shock wave and shock tube flow - are considered. Results show fairly good agreement with exact solutions. Author

N89-24098# National Aeronautical Lab., Bangalore (India). Director's Unit.
INTRODUCTION TO IRREDUCIBLE TENSOR METHODS, PART 1
R. Narasimha Aug. 1988 18 p
(NAL-PD-DU-8802) Avail: NTIS HC A03/MF A01

The use of irreducible tensors for effective implementation of a spectral scheme for solving the nonlinear Boltzmann equation has recently been shown. The theory of irreducible tensors appears to have potential for wide applications in other areas of fluid dynamics, and, more generally, in continuum mechanics, and forges links with the theory of dynamical systems. An introduction to the concept of irreducible tensors and associated group-theoretic methods is presented. Author

N89-24099# Technische Hogeschool, Delft (Netherlands). Dept. of Mathematics and Informatics Computer Science.
ASYMPTOTIC BEHAVIOR OF RANDOM DISCRETE EVENT SYSTEMS
J. A. C. Resing, R. E. deVries, G. Hooghiemstra, M. S. Keane, and G. J. Olsder 1988 32 p
(PB89-146146; ISSN-0922-5641; Rept-88-56) Copyright Avail: NTIS HC A03/MF A01 CSCL 12A

Some aspects of the asymptotic behavior of Discrete Event

Dynamic Systems (DEDS) are discussed in which the activity times are random variables. The main result is that a central limit theorem holds for DEDS and consequently that the cycle-time of the system is asymptotically normally distributed. Author

N89-24100# Technische Hogeschool, Delft (Netherlands). Dept. of Mathematics and Informatics Computer Science.
RIEMANNIAN GEOMETRY ON FAMILIES OF LINEAR SYSTEMS: THE DETERMINISTIC CASE
Bernard Hanzon 1988 68 p
(PB89-146062; Rept-88-62) Copyright Avail: NTIS HC A04/MF A01 CSCL 12A

In linear system identification and in the related problem of parametrization of linear systems, the geometry of families of linear systems plays an important role. Besides knowledge of the topology, one also needs knowledge of the Riemannian geometry of such families. A number of rather natural candidates for such a Riemannian geometry are presented, for families of i/o-stable systems with fixed McMillan degree. It turns out that the candidates can be determined by straightforward matrix calculations, which involve solving for Lyapunov equations. For a certain special case, the Riemannian geometry and the corresponding inner metric is completely determined. For the general case, the Riemannian geometry and the corresponding inner metric is completely determined. For the general case, a group of isometries is presented. It is shown that popular canonical forms like the observability and controllability canonical forms behave badly, in the sense that the Riemannian metric tensor degenerates, in the neighborhood of systems with smaller McMillan degree. Special emphasis is given to the state bundle over a family of linear systems of fixed order. Author

N89-24101# Technische Hogeschool, Delft (Netherlands). Dept. of Mathematics and Informatics Computer Science.
EFFICIENT METHOD FOR SOLVING FREE-BOUNDARY PROBLEMS
R. M. S. M. Schulkes and C. Cuvelier 1988 23 p
(PB89-146138; ISSN-0922-5641; Rept-88-63) Copyright Avail: NTIS HC A03/MF A01 CSCL 12A

A method for solving free-boundary problems is studied. It is shown how the influence of the unknown position of the free boundary can be reduced to the free boundary itself. This leads to an attractive numerical procedure for solving free-boundary problems. The method is then used to solve a capillary free boundary problem and numerical properties of the method are investigated. Author

N89-24102# Helsinki Univ. of Technology, Espoo (Finland). Electromagnetics Lab.
POLARIZABILITY AND EFFECTIVE PERMITTIVITY OF LAYERED AND CONTINUOUSLY INHOMOGENEOUS DIELECTRIC ELLIPSOIDS
Ari Sihvola and Ismo V. Lindell Dec. 1988 34 p
(PB89-146476; ISBN-951-754-707-2; ISSN-0784-848X; Rept-37) Avail: NTIS HC A03/MF A01 CSCL 12A

The polarizabilities of partially and continuously inhomogeneous dielectric ellipsoids are analyzed. Multilayer inclusions where the boundaries between the layers are confocal ellipsoids, are solved in a static field. Transmission line analogy is applied, resulting in matrices with which the field components and the polarizability can be solved. In case of the continous permittivity profile, a differential equation is derived for the scattered potential, and from the amplitude of this function, the polarizability results. The limitation in the continuous case is that the permittivity function of the ellipsoid depend only on one coordinate in the ellipsoid coordinate system. The theory is applied to calculating the microwave attenuation of melting hail at the frequency of 1 GHz, where the hydrometeors are modeled as two layer ellipsoids. GRA

N89-24103# International Centre for Theoretical Physics, Trieste (Italy).
NONLINEAR SINGULAR ELLIPTIC EQUATIONS
Minh Duc Duong (Ho Chi Minh City Univ., Vietnam) Sep. 1988 30 p Submitted for publication
(DE88-705691; IC-88/311) Avail: NTIS (US Sales Only) HC A03/MF A01

We improve the Poincare inequality, the Sobolev imbedding theorem and the Trudinger imbedding theorem and prove a Mountain pass theorem. Applying these results we study a nonlinear singular mixed boundary problem. DOE

N89-24104# Aeronautical Research Inst. of Sweden, Stockholm. Aerodynamics Dept.
NUMERICAL SOLUTION OF THE EULER EQUATIONS USING LOCAL GRID REFINEMENT
Lars-Erik Eriksson 25 Mar. 1988 24 p Sponsored by the Swedish Defence Material Administration Air Material Dept., Stockholm
(FFA-143; ETN-89-94223) Avail: NTIS HC A03/MF A01; Almqvist and Wiksell, Bocksellers, Printers, Publishers, Stockholm, Sweden, 100 Swedish crowns

Local grid refinement as a means to improve the accuracy of finite difference solutions to the Euler equations is investigated in two and three space dimensions. Alternative conservative interface conditions for the centered finite volume scheme with explicit multistage time stepping are described and applied to the computation of steady Euler solutions on locally refined o-type grids around wings. In 2-D a comparison between the two interface conditions shows that they perform equally well and are stable even when shocks intersect the interface. One of the interface conditions is also investigated in 3-D and computed examples show that it performs equally well in this case also. Stability is achieved even when shocks or vortices intersect the interface. ESA

N89-24105# Aeronautical Research Inst. of Sweden, Stockholm. Aerodynamics Dept.
A STABILITY ANALYSIS OF VARIOUS PATCHED GRID INTERFACE CONDITIONS FOR HYPERBOLIC EQUATIONS
Lars-Erik Eriksson and Man Mohan Rai 25 Mar. 1988 39 p Sponsored by the Swedish Defence Material Administration Air Material Dept., Stockholm
(FFA-144; ETN-89-94224) Avail: NTIS HC A03/MF A01; Almqvist and Wiksell, Bocksellers, Printers, Publishers, Stockholm, Sweden, 100 Swedish crowns

The stability of various conservative interface conditions for patched grids is investigated in two space dimensions using a numerical technique where the maximum growth of the solution to a linear hyperbolic model problem is computed for a sequence of successively finer grids. Two interface conditions for a centered finite-volume scheme with explicit Runge-Kutta time integration are analyzed and another interface condition for an implicit upwind finite-difference scheme is also analyzed. The results show that in the case of the centered finite-volume scheme it is possible to obtain both conservative and stable interface conditions consistent with the interior scheme for the simplest type of grid interface where the grid on one side is two or three times as fine as the grid on the other side. In the general case of a noninteger relation between the tangential grid spacings on both sides of the interface, stability can still be achieved if extra dissipation of a magnitude comparable to that introduced by an upwind scheme is added locally along the interface. The analysis of a corresponding interface condition for a second-order accurate implicit upwing finite-difference scheme demonstrates that both conservation and stability is achieved for a wide range of grid interfaces with both integer and noninteger grid spacing ratios. ESA

N89-24106# Joint Inst. for Nuclear Research, Dubna (USSR). Lab. of Theoretical Physics.
CAPTURE AND CONFINEMENT OF SOLUTIONS IN NONLINEAR INTEGRABLE SYSTEMS
V. K. Melnikov 1988 22 p In RUSSIAN; ENGLISH summary
(DE88-705823; JINR-R-2-88-232) Avail: NTIS (US Sales Only) HC A03/MF A01

The system describing the interaction of a long wave and a short wave packet on the x,y plane is considered. The solutions

are found to describe a solution that comes from infinity and that is captured into a conditionally periodical oscillatory regime. The solutions are also found that describe a soliton coming from infinity and then decaying into two solitons: one goes to infinity and the other is captured into a conditionally periodical oscillatory regime. The results obtained are relevant to some problems of hydrodynamics, plasma physics, solid state physics, etc. DOE

N89-24107# Joint Inst. for Nuclear Research, Dubna (USSR). Lab. of Theoretical Physics.
EQUATIONS FOR TWO-DIMENSIONAL DENSITY MATRIX. APPROXIMATE SOLUTIONS IN THE VICINITY OF THE CLASSICAL SOLUTION
Am Gil Lee and V. M. Maltsev 1988 8 p In RUSSIAN; ENGLISH summary
(DE88-705825; JINR-P-2-88-298) Avail: NTIS (US Sales Only) HC A02/MF A01

Equations of quantum field theory in the phase space are investigated. Introduction of two dimensional density matrix enables the formulation in closed form of the quantum field theory in the phase space. Hamiltonian expansion in the phase space was obtained in the vicinity of classical field. This enables approximate solutions in the vicinity of the classical solution. DOE

N89-24108# Fermi National Accelerator Lab., Batavia, IL.
ON THE ALGEBRAIC STRUCTURE OF INTEGRABLE SYSTEMS IN MULTIDIMENSIONS
J. M. Maillet and F. Nijhoff (Clarkson Univ., Potsdam, NY.) Sep. 1988 5 p Presented at the 17th International Colloquium on Group Theoretical Methods in Physics, St. Adele, Canada, 27 Jun. 1988
(Contract DE-AC02-76CH-03000)
(DE89-008697; FNAL/C-88/130-T; CONF-8806105-6) Avail: NTIS HC A02/MF A01

The d-simplex equations are multidimensional generalizations of the Yang-Baxter (triangle) equations. We discuss the algebraic structure of the hierarchy of the d-simplex equations and their relevance to the notion of quantum and classical integrability. A multidimensional generalization of the notion of lax pair is given. DOE

N89-24109# Illinois Univ., Urbana. Dept. of Computer Science.
DIFFERENTIAL ALGEBRAIC EQUATIONS, INDICES, AND INTEGRAL ALGEBRAIC EQUATIONS
C. W. Gear Apr. 1989 15 p
(Contract DE-FG02-87ER-25026; NSF DMS-87-03226)
(DE89-009584; DOE/ER-25026/26; UIUCDCS-R-89-1505; UILU-ENG-88-1724) Avail: NTIS HC A03/MF A01

In a recent report, Hairer defines the index of Differential Algebraic Equations (DAEs) by considering the effect of perturbations of the equations on the solutions. This index is called the perturbation index, pi. An earlier form of index used by a number of authors is determined by the number of differentiations of the DAEs that are required to generate an ordinary differential equation (ODE) satisfied by the solution. We will call this the differential index, di. Hairer gives an example whose differential index is one and perturbation index is two and other examples where they are identical. We will show that di less than or equal to pi less than or equal to di + 1 and that di = pi if the derivative components of the DAE are total differentials. This means that the differential components have a first integral. The integrals are a special case of a new type of integral equation we will call Integral Algebraic Equations (IAEs). DOE

N89-24110# Sandia National Labs., Albuquerque, NM. CAD Technology Div.
SOLID MODELING REQUIREMENTS FOR FINITE ELEMENT MODELING USING MAPPED MESH TECHNIQUES
Patrick F. Chavez Jan. 1989 26 p
(Contract DE-AC04-76DP-00789)
(DE89-009639; SAND-88-3478) Avail: NTIS HC A03/MF A01

A three-dimensional mesh generation project is progressing in the CAD Technology Division at Sandia National Laboratories. The project goals are to provide advanced geometric modeling capabilities with automatic discretization routines for finite element model creation. The project supports finite element analysis activities conducted at Sandia. Typical analyses performed include linear and non-linear structural, linear and non-linear thermal, and hydrodynamic calculations. The use of quadrilateral and hexahedral finite elements is the common thread in this broad spectrum of analysis. Our effort is designed to produce finite element models exclusively composed of quadrilateral or hexahedral elements. The mesh generation work is progressing from prototype development to a production environment. We desire to interface the mesh generator with other solid modelers that offer additional functionality and robustness. This paper identifies requirements that must be satisfied by solid modeling systems to support finite element mesh generation developments. Although these requirements are based on our finite element modeling effort, it is obvious that many of them are generic to a variety of applications. DOE

N89-24111*# National Aeronautics and Space Administration. Ames Research Center, Moffett Field, CA.
NUMERICAL SIMULATION OF FLOW THROUGH AN ARTIFICIAL HEART
Stuart E. Rogers, Paul Kutler, Dochan Kwak, and Cetin Kiris (Stanford Univ., CA.) Apr. 1989 16 p
(NASA-TM-102183; A-89099; NAS 1.15:102183) Avail: NTIS HC A03/MF A01 CSCL 12A

A solution procedure was developed that solves the unsteady, incompressible Navier-Stokes equations, and was used to numerically simulate viscous incompressible flow through a model of the Pennsylvania State artificial heart. The solution algorithm is based on the artificial compressibility method, and uses flux-difference splitting to upwind the convective terms; a line-relaxation scheme is used to solve the equations. The time-accuracy of the method is obtained by iteratively solving the equations at each physical time step. The artificial heart geometry involves a piston-type action with a moving solid wall. A single H-grid is fit inside the heart chamber. The grid is continuously compressed and expanded with a constant number of grid points to accommodate the moving piston. The computational domain ends at the valve openings where nonreflective boundary conditions based on the method of characteristics are applied. Although a number of simplifing assumptions were made regarding the geometry, the computational results agreed reasonably well with an experimental picture. The computer time requirements for this flow simulation, however, are quite extensive. Computational study of this type of geometry would benefit greatly from improvements in computer hardware speed and algorithm efficiency enhancements. Author

N89-24112*# Institute for Computer Applications in Science and Engineering, Hampton, VA.
INVERSE PROBLEM TECHNIQUES FOR BEAMS WITH TIP BODY AND TIME HYSTERESIS DAMPING
H. T. Banks, R. H. Fabiano, and Y. Wang (Brown Univ., Providence, RI.) Apr. 1989 27 p Submitted for publication
(Contracts NAS1-18107; NAS1-18605; NAG1-517; F49620-86-C-0111; NSF MCS-85-04316)
(NASA-CR-181833; NAS 1.26:181833; ICASE-89-22) Avail: NTIS HC A03/MF A01 CSCL 12A

A model for a flexible beam with time hysteresis (Boltzmann type viscoelasticity) damping and tip body is presented. A computational method for the estimation of the camping parameters is developed, and theoretical convergence/continuous dependence results are given. An example is presented in which experimental data is used, demonstrating the efficacy of the computational method and the plausibility of the model for predicting response in damped structures. Author

N89-24113*# Institute for Computer Applications in Science and Engineering, Hampton, VA.
OPERATOR INDUCED MULTIGRID ALGORITHMS USING SEMIREFINEMENT Final Report
Naomi Decker and John VanRosendale Apr. 1989 25 p

(Contract NAS1-18605)
(NASA-CR-181834; NAS 1.26:181834; ICASE-89-24) Avail: NTIS HC A03/MF A01 CSCL 12A

A variant of multigrid, based on zebra relaxation, and a new family of restriction/prolongation operators is described. Using zebra relaxation in combination with an operator-induced prolongation leads to fast convergence, since the coarse grid can correct all error components. The resulting algorithms are not only fast, but are also robust, in the sense that the convergence rate is insensitive to the mesh aspect ratio. This is true even though line relaxation is performed in only one direction. Multigrid becomes a direct method if an operator-induced prolongation is used, together with the induced coarse grid operators. Unfortunately, this approach leads to stencils which double in size on each coarser grid. The use of an implicit three point restriction can be used to factor these large stencils, in order to retain the usual five or nine point stencils, while still achieving fast convergence. This algorithm achieves a V-cycle convergence rate of 0.03 on Poisson's equation, using 1.5 zebra sweeps per level, while the convergence rate improves to 0.003 if optimal nine point stencils are used. Numerical results for two and three dimensional model problems are presented, together with a two level analysis explaining these results. Author

N89-24114*# Institute for Computer Applications in Science and Engineering, Hampton, VA.
SHAPE IDENTIFICATION TECHNIQUE FOR A TWO-DIMENSIONAL ELLIPTIC SYSTEM BY BOUNDARY INTEGRAL EQUATION METHOD Final Report
Fumio Kojima Apr. 1989 25 p Submitted for publication
(Contract NAS1-18605)
(NASA-CR-181831; NAS 1.26:181831; ICASE-89-26) Avail: NTIS HC A03/MF A01 CSCL 12A

The geometrical structure of the boundary shape for a two-dimensional boundary value problem is identified. The output least square identification method is considered for estimating partially unknown boundary shapes. A numerical parameter estimation technique using the spline collocation method is proposed. Author

N89-24115# Naval Postgraduate School, Monterey, CA.
NUMERICAL EXPERIENCE WITH A SUPERFAST REAL TOEPLITZ SOLVER Technical Report, 1 Oct. 1988 - 30 Jan. 1989
William Gragg and Gregory S. Ammar 22 Feb. 1989 22 p
(AD-A205374; NPS53-89-008) Avail: NTIS HC A03/MF A01 CSCL 12/1

We briefly describe the Generalized Schur Algorithm for the superfast solution of positive definite Toeplitz systems of equations and its relationship with Schur's algorithm and the Szego recursions. We then present some experimental results obtained with our FORTRAN implementation of this superfast Toeplitz solver. We will see that the algorithm displays favorable behavior in that the growth rates of the resulting residuals and errors are comparable with those of the Szego recursions. GRA

N89-24116# Naval Research Lab., Washington, DC. Industrial Engineering Services Branch.
ON THE EQUATION Xa + Ya = Za
Allen R. Miller 7 Feb. 1989 9 p
(AD-A205460; NRL-9178) Avail: NTIS HC A02/MF A01 CSCL 12/1

An equation is solved for a as a function of X, Y, and Z in terms of a Wright function with negative unit argument. An equivalent form of Fermat's last theorem is given using this function. GRA

N89-24117# Massachusetts Inst. of Tech., Cambridge. Lab. for Information and Decision Systems.
ON THE COMMUNICATION COMPLEXITY OF DISTRIBUTED ALGEBRAIC COMPUTATION
Zhi-Quan Luo and John N. Tsitsiklis Feb. 1989 40 p
(Contract N00014-85-K-0519)
(AD-A205784; LIDS-P-1851) Avail: NTIS HC A03/MF A01 CSCL 12/1

We consider a situation where two processors P sub 1 and P sub 2 are to evaluate a collection of functions function 1,...., function 8 of two vector variables x, y, under the assumption that processor P sub 1 (respectively, P sub 2) has access only to the value of the variable x (respectively, y) and the functional form of function 1,...., function 8. We provide some new bounds on the communication complexity (the amount of information that has to be exchanged between the processors) for this problem. An almost optimal bound is derived for the case of one-way communication when the functions function 1,...., function 8 are polynomials. We also derive some new lower bounds for the case of two-way communication which improve on earlier bounds by Abelson A 80. As an application, we consider the case where x and y are n x n matrices and f(x,y) is a particular entry of the inverse of x + y. Under certain restriction on the class of allowed communication protocols, we obtain an omega(n squared) lower bound, in contrast to the omega(n) lower bound obtained by applying Abelson's results. Our results are based on certain tools from classical algebraic geometry and field extension theory. GRA

N89-24118# Stanford Univ., CA. Dept. of Statistics.
TESTS FOR THE GAMMA DISTRIBUTION WITH ESTIMATED SHAPE PARAMETERS
R. A. Lockhart and M. A. Stephens 14 Mar. 1989 25 p
(Contract N00014-86-K-0156; NR Proj. 042267)
(AD-A205829; TR-414) Avail: NTIS HC A03/MF A01 CSCL 12/3

It is well known that the distributions of the goodness-of-fit statistics W squared, U squared, and A squared do not depend on location and scale parameters even when these parameters must be estimated. It has generally been assumed, however, that when shape parameters must be estimated the null distributions of these statistics would depend too severely on the unknown parameters to permit their use in practice. Exact asymptotic distributions of these statistics are presented for the two parameter gamma family distributions. Critical points are given in tables constructed so as to avoid any need for extrapolation. The results presented show that the tests can be expected to be useful in practice. GRA

N89-24119# Air Force Inst. of Tech., Wright-Patterson AFB, OH. School of Engineering.
DISCRETE EVENT SIMULATION MODEL DECOMPOSITION M.S. Thesis
Scott R. Matthes Dec. 1988 127 p
(AD-A206048; AFIT/GOR/ENS/88D-13) Avail: NTIS HC A07/MF A01 CSCL 12/5

Simulation models are currently being used for a multitude of purposes. Some simulation models are concise and well organized thereby facilitating their usage. However, some of these models may be quite lengthy and complex which causes development costs to rise beyond an acceptable level. The creation of an effective development environment has helped to eliminate this problem. Tools which are used to support modeling and analysis have been incorporated into this environment. Such an environment uses a model specification language which has condition specifications as its basic constructs. This research focused on interpreting a discrete event simulation model's condition specification primitives and their associated actions. A network representation was created using these Condition Action Pairs (CAPs) as network nodes. The arcs, or edges, of the network represent information being transferred such as specific attributes of the CAPs. This network representation was decomposed into smaller networks, or sub-networks, by taking advantage of the structure of the network. The structure of the network was translated via a software interface into an edge-incidence matrix (E-matrix). The E-matrix was then transformed into a pseudo-covariance matrix (C-matrix). GRA

N89-24120# Yale Univ., New Haven, CT. Dept. of Computer Science.
PRECONDITIONED KRYLOV SOLVERS AND METHODS FOR RUNTIME LOOP PARALLELIZATION
Doug Baxter, Joel Salz, Martin Schultz, and Stan Eisenstat Oct. 1988 32 p
(Contract N00014-86-K-0310)
(AD-A206388; YALEU/DCS/TR-655) Avail: NTIS HC A03/MF A01 CSCL 12/7

We make a detailed examination of the performance achieved by a Krylov space sparse linear system solver that uses incompletely factored matrices for preconditioners. We compared two related mechanisms for parallelizing the computationally critical sparse triangular solves and sparse numeric incomplete factorizations on a range of test problems. From these comparisons we drew several interesting conclusions about methods that can be used to parallelize loops of the type found here. The performance we obtain is brought into perspective by comparison with timing results from a Cray X/MP supercomputer. Performance on an Encore Multimax/320 with relatively modest computational capabilities comes within a small factor of the performance on a comparable code run on a Cray X/MP. GRA

N89-24121# Yale Univ., New Haven, CT. Dept. of Computer Science.
KRYLOV METHODS PRECONDITIONED WITH INCOMPLETELY FACTORED MATRICES ON THE CM-2
Harry Berryman, Joel Salz, and William Gropp Mar. 1989 13 p
(Contract N00014-86-K-0310)
(AD-A206389; YALEU/DCS/TR-685) Avail: NTIS HC A03/MF A01 CSCL 12/5

This work measured what might be regarded best case timings for the sparse matrix vector multiplies, sparse triangular solves, and inner products that constitute the iterative portion of Krylov space programs that use incompletely factored matrices for preconditioning. Timings are performed on a large three dimensional model problem over a cube shaped domain discretized with a seven point template. The highest computational rate we achieved for the sparse triangular solve was 13.1 MFlops on 4K processors. This would correspond to 210 MFlops on an appropriately scaled problem on a 64K processor machine. The highest computational speed we achieved for a matrix vector multiply was 64.2 MFlops. This would correspond to a speed of 1027.0 MFlops in a 64K processor machine. Thus, for appropriately structured problems, the CM-2 achieves impressive computational speeds. The computational speed obtained from the CM-2 is compared. GRA

N89-24122# California Univ., Irvine. Dept. of Information and Computer Science.
EXPLORING THE EPISODIC STRUCTURE OF ALGEBRA STORY PROBLEM SOLVING: REVISION Technical Report No. 7, period ending 31 Dec. 1988
Rogers Hall, Dennis Kibler, Etienne Wenger, and Chris Truxaw 1 Jan. 1989 54 p
(Contract N00014-85-K-0373)
(AD-A206403; UCI-ICS-TR-86-24-REV) Avail: NTIS HC A04/MF A01 CSCL 12/1

This paper analyzes the quantitative and situational structure of algebra story problems, uses these materials to propose an interpretive framework for written problem-solving protocols, and then presents an exploratory study of the episodic structure of algebra story problem solving in a sizable group of mathematically competent subjects. Analyses of written protocols compare the strategic, tactical, and conceptual content of solution attempts, looking within these attempts at the interplay between problem are complimentary activities, giving rise to a succession of problem solving episodes. While direct algebraic problem solving is sometimes effective, results suggest that the algebraic formalism may be of little help in comprehending the quantitative constraints posed in a problem text. Instead, competent problem solvers often reason within the situational context presented by a story problem, using various forms of model-based reasoning to identify, pursue, and verify quantitative constraints required for solution. The paper concludes by discussing the implications of these findings for acquiring mathematical concepts (e.g., related linear functions) and for supporting their acquisition through instruction. GRA

N89-24123# Bayreuth Univ. (Germany, F.R.).
APPROXIMATION OF STOCHASTIC INTEGRAL EQUATIONS USING MARTINGALE DIFFERENCE SCHEMES Ph.D. Thesis [APPROXIMATION VON STOCHASTISCHEN INTEGRALGLEICHUNGEN DURCH MARTINGALDIFFERENZSCHEMATA]
Karin Hoffmann 1987 150 p In GERMAN
(ETN-89-93951) Avail: NTIS HC A07/MF A01

A method for the treatment of (stochastic) differential and integral equations was mathematically justified. The assumption that the solutions of a series of stochastic differential equation alway converge, was proved under relatively general conditions by approximating the stochastic differential equations by stochastic difference equations. The essential difference between stochastic integral equations and ordinary integral equations are the integral terms which have martingales as integrators. The main result is a theorem concerning the diffusion approximation, i.e., an invariance principle for the solution of a diffusion equation. ESA

N89-24124# Universiteit Twente, Enschede (Netherlands). Faculty of Applied Mathematics.
KNOWLEDGE REPRESENTATION USING KNOWLEDGE GRAPHS: APPLICATION TO THEORIES ON MATHEMATICAL MODELING AND SOLVING WORD PROBLEMS [KENNISREPRESENTATIE MET BEHULP VAN KENNISGRAFEN: TOEPASSING OP THEORIEEN BETREFFENDE MATHEMATISCH MODELLEREN EN HET OPLOSSEN VAN TOEPASSINGSVRAAGSTUKKEN]
G. J. T. A. Bakx, R. G. Edens, and C. Hoede Apr. 1988 115 p In DUTCH; ENGLISH summary
(MEMO-707; ISSN-0921-1969; ETN-89-94259) Avail: NTIS HC A06/MF A01

The techniques of the project Knowledge Graphs were used for the representation and comparison of theories on mathematical modelling and solving word problems. Texts in the field of these knowledge domains were transformed into a process description for the ideal student using text analysis prescriptions, with emphasis on the temporal ordering of the actions in the process description. In this way the theories can be represented by author graphs as well as by flow diagrams. Flow diagrams referring to one knowledge domain are then compiled into an integrated flow diagram, for which integration procedures were developed. These integrated flow diagrams represent the knowledge in the field of mathematical modelling and solving word problems, as far as the considered texts are concerned. The theories on the two considered knowledge domains were compared by comparing flow diagrams. ESA

65 STATISTICS AND PROBABILITY

Includes data sampling and smoothing; Monte Carlo method; and stochastic processes.

N89-24125# Pennsylvania State Univ., University Park. Dept. of Statistics.
MULTIVARIATE ANALYSIS AND ITS APPLICATIONS Annual Report, 1 Oct. 1987 - 31 Dec. 1988
C. R. Rao 14 Feb. 1989 23 p
(Grant AF-AFOSR-0030-88; AF Proj. 2304)
(AD-A205585; AFOSR-89-0276TR) Avail: NTIS HC A03/MF A01 CSCL 12/3

During the period of October 1, 1987 through December 31, 1988, research was carried out in several new areas of multi-variate analysis of interest to the Air Force. They have applications in manufacturing technology, automation, expert systems, pattern recognition and machine intelligence. About 59 Technical Reports were issued for publication in journals and presented at

conferences. A list of the Technical Reports together with the abstracts is given in the Appendix to this report. A brief outline of some of the important contributions is given. GRA

N89-24126# Stanford Univ., CA. Dept. of Statistics.
APPROACHES FOR EMPIRICAL BAYES CONFIDENCE INTERVALS
Bradley P. Carlin and Alan E. Gelfand 2 Mar. 1989 32 p
(Contract N00014-86-K-0156)
(AD-A205775; TR-413) Avail: NTIS HC A03/MF A01 CSCL 12/3

Parametric empirical Bayes methods of point estimation date to the landmark paper of James and Stein (1961) are presented. Interval estimation through parametric empirical Bayes techniques has a somewhat shorter history, which is summarized in the recent paper of Laird and Louis (1987). In the exchangeable case, one obtains a naive EB confidence interval by simply taking appropriate percentiles of the estimated posterior distribution of the parameter, where the estimation of the prior parameters (hyperparameters) is accomplished through marginal distribution of the data. Unfortunately, these naive intervals tend to be too short, since they fail to account for the variability in the estimation of the hyperparameters. That is, they don't attain the desired coverage probability in the EB sense defined in Morris (1983a,b). They also provide no statement of conditional calibration (Rubin, 1984). This paper proposes a conditional bias correction method for developing EB intervals which corrects these deficiencies in the naive intervals. As an alternative, several authors have suggested use of the marginal posterior in this regard. We attempt to clarify its role in achieving EB coverage. Results of extensive simulation of coverage probability and interval length for these approaches are presented in the context of several illustrative examples. GRA

N89-24127# Air Force Inst. of Tech., Wright-Patterson AFB, OH. School of Engineering.
A DEMONSTRATION OF THE METHOD OF STOCHASTIC FINITE ELEMENT ANALYSIS M.S. Thesis
Paul R. Bryant Mar. 1989 98 p
(AD-A206135; AFIT/GA/AA/89M-01) Avail: NTIS HC A05/MF A01 CSCL 12/4

Finite element analysis has been used as a design tool for many years, with structural reliability being ensured through use of a liberal factor of safety. Unfortunately, the safety factor is a blanket insurance against all hazards, and a designer has no way to optimize a structure against any particular hazard. This is particularly troublesome in the fields of aero/astro design, where every bit of mass must serve to maximum utility. The method of Stochastic Finite Element Analysis allows a designer to model any loading or hazard condition as closely to reality as desired by using an appropriate probability distribution function. Through a Monte Carlo simulation, the finite element model is subject to the probability functions. The cumulative output is analyzed for trends in failure probability and the design is altered to enhance its reliability, repeating the process until the desired level of reliability is achieved. The resulting design is optimal for the imposed conditions, and compared to a structure designed with a traditional factor of safety approach, is either lighter or more reliable. This demonstration revealed that for similar reliabilities, a stochastically designed wing was 20 percent lighter than a wing strengthened by the factor of safety. The major drawback in applying the method of stochastic finite element analysis is that very large, complex models can require extraordinary amounts of computer resources. GRA

N89-24128# Stanford Univ., CA. Dept. of Statistics.
SECOND-ORDER MOMENTS OF A STATIONARY MARKOV CHAIN AND SOME APPLICATIONS
T. W. Anderson Feb. 1989 19 p
(Contract DAAL03-89-K-0033)
(AD-A206366; ARO-26394.1-MA) Avail: NTIS HC A03/MF A01 CSCL 12/3

The i-th state of a finite-state Markov chain can be indicated by a vector with 1 in the i-th position and O's in the other positions. The vector-valued process defined in this way is autoregressive in the wide sense. The second-order moments, moving average representation, and spectral density of this process are obtained. The numerical-valued chain is a linear function of the vector; a simple condition is derived for it to be first-order autoregressive in the wide sense. The stationary probabilities of the chain can be estimated by the means of observations on the vector-valued process; this estimator is asymptotically equivalent to the maximum likelihood estimator. GRA

66 SYSTEMS ANALYSIS

Includes mathematical modeling; network analysis; and operations research.

N89-24129*# Advanced Technology, Inc., Huntsville, AL.
LAUNCH COMMIT CRITERIA PERFORMANCE TRENDING ANALYSIS, PHASE 1, REVISION A. SRM AND QA MISSION SERVICES
10 May 1989 81 p
(Contract NAS8-37812)
(NASA-CR-184859; NAS 1.26:184859; TD-002-342-444-0002)
Avail: NTIS HC A05/MF A01 CSCL 12B

An assessment of quantitative methods and measures for measuring launch commit criteria (LCC) performance measurement trends is made. A statistical performance trending analysis pilot study was processed and compared to STS-26 mission data. This study used four selected shuttle measurement types (solid rocket booster, external tank, space shuttle main engine, and range safety switch safe and arm device) from the five missions prior to mission 51-L. After obtaining raw data coordinates, each set of measurements was processed to obtain statistical confidence bounds and mean data profiles for each of the selected measurement types. STS-26 measurements were compared to the statistical data base profiles to verify the statistical capability of assessing occurrences of data trend anomalies and abnormal time-varying operational conditions associated with data amplitude and phase shifts. A.D.

N89-24130# Air Force Inst. of Tech., Wright-Patterson AFB, OH. School of Engineering.
PARALLEL ADA IMPLEMENTATION OF A MULTIPLE MODEL KALMAN FILTER TRACKING SYSTEM: A SOFTWARE ENGINEERING APPROACH M.S. Thesis
Walter J. Lemanski Mar. 1989 120 p
(AD-A206094; AFIT/GCS/ENG/89M-2) Avail: NTIS HC A06/MF A01 CSCL 15/6

The success of the Strategic Defense Initiative depends directly on significant advances in both computer hardware and software development technologies. Parallel architectures and the Ada programming language have advantages that make them candidates for use in SDI command and control computer systems. This thesis examines those advantages in the context of an SDI-type application: The implementation of a Kalman filter tracking system. This research consists of three parts. The first is a set of software engineering guidelines developed for use in creating parallel designs suitable for implementation in Ada. These guidelines cover the design process from initial problem analysis to final detailed design. Methods of problem decomposition are discussed, as are language partitioning strategies. Justification is provided for using the Ada task construct for process boundaries, and Ada multitasking design issues are reviewed. A parallel software design methodology is also described. GRA

67 THEORETICAL MATHEMATICS

Includes topology and number theory.

N89-24131# Massachusetts Inst. of Tech., Cambridge. Dept. of Mathematics.
NUMERICAL CONFORMAL MAPPING AND APPLICATIONS Annual Report, 1 Dec. 1987 - 30 Nov. 1988
Lloyd N. Trefethen 18 Jan. 1989 15 p
(Grant AF-AFOSR-0102-87; AF Proj. 2304)
(AD-A205602; AFOSR-89-0350TR) Avail: NTIS HC A03/MF A01 CSCL 12/2

Progress was made in three principal areas: (1) Conformal mapping of highly elongated polygons. Conventional methods of conformal mapping break down when applied to highly distorted regions, as arise frequently in applications. In the first year of research under this grant, Prof. Trefethen and Louis Howell developed a modified Schwarz-Christoffel formula to handle highly elongated polygons. In the second year this work was completed and written up for publication in the SIAM Journal on Scientific and Statistical Computing; (2) Conformal mapping of circular polygons. Work by Trefethen and Howell is underway on the problem of extending Schwarz-Christoffel methods to the mapping of circular polygons bounded by straight sides and circular arcs; (3) Applications in numerical linear algebra. The efficient solution of large nonsymmetric linear algebra problems Ax = b is an important but incompletely understood area of numerical analysis. Because the eigenvalues of A are generally complex, some algorithms for this problem are based on conformal mapping, complex approximation, and other techniques of complex analysis. One particular algorithm combining both conformal mapping and complex approximation is discussed in a new paper by Trefethen, and this has led to an investigation in greater generality of the behavior of non-normal matrices with complex spectra. GRA

N89-24132# Boston Univ., MA. Dept. of Computer Science.
SYMBOLIC ANALYSIS OF MULTIVARIABLE MISSILE SYSTEMS Final Technical Report, 1 Jul. 1984 - 31 Dec. 1985
Chih-Fan Chen and Ming M. Chen 4 May 1988 166 p
(Contract DAAH01-84-C-0489)
(AD-A206326; AD-E951239; AMSMI/CR-RD-GC-88-1) Avail: NTIS HC A08/MF A01 CSCL 12/4

A new systematic procedure mainly based on the Grassmann algebra is established for evaluating a symbolic transfer function in particular and a transfer matrix in general. After illustrating the rules for symbolic determinant evaluation, we extend the method to multivariable continuous and hybrid systems by the decoupling techniques. P-constrained and V-constrained models have been studied on the one hand; dead time compensators and the Smith compensators are deeply investigated on the other as the generalization of the new computerized symbolic treatment technique. In the appendix, this Grassman algebra-based method is compared with the existing methods such as symbolic evaluation via Fourier transform, symbolic evaluation via number theoretic transform, etc. GRA

N89-24133# Yale Univ., New Haven, CT. Dept. of Computer Science.
A BLOCKED JACOBI METHOD FOR THE SYMMETRIC EIGENPROBLEM
David E. Foulser Feb. 1989 25 p
(Contract N00014-86-K-0310)
(AD-A206553; YALEU/DCS/RR-680) Avail: NTIS HC A03/MF A01 CSCL 12/2

A block matrix generalization of the Jacobi rotation method for computing the eigen decomposition of a symmetric matrix is presented. This Blocked Classical Jacobi (BCJ) algorithm selects for block rotation at each step the off-diagonal block(s) of largest mass. The BCJ algorithm exhibits substantially shorter runtimes than another blocked Jacobi method, but is slower than a scalar Jacobi algorithm on random matrices with i.i.d. uniform elements. A probabilistic analysis of the BCJ selection method is presented. Timings and other data are presented from experiments on random matrices. GRA

70 PHYSICS (GENERAL)

For precision time and time interval (PTTI) see *35 Instrumentation and Photography;* for geophysics, astrophysics or solar physics see *46 Geophysics, 90 Astrophysics,* or *92 Solar Physics.*

N89-24134# Technische Hogeschool, Delft (Netherlands). Dept. of Mathematics and Informatics Computer Science.
MODELING OF A CONTINUOUS OSCILLATOR BY OSCILLATORS WITH A FINITE NUMBER OF DEGREES OF FREEDOM
A. H. P. vanderBurgh 1988 18 p Presented at the European Conference on Mathematics in Industry (ECMI), Glasgow, Scotland, 28-31 Aug. 1988
(PB89-146120; ISSN-0922-5641; Rept-88-77) Copyright Avail: NTIS HC A03/MF A01 CSCL 20C

In an engineering approach, continuous systems are often modeled by systems with a finite number of degrees of freedom. This way of modeling is usually based on arguments and principles from mechanics or physics. A continuous system and a system with a finite number of degrees are considered. Both systems are oscillators in a uniform wind field. An attempt is made to answer the question if, on the basis of the behavior of the solutions of the equations of motion of the oscillators, the engineering way of modeling may be understood or justified. GRA

N89-24135# Massachusetts Inst. of Tech., Cambridge.
LIQUID DYNAMIC CAMPACTION OF Fe-Nd-B PERMANENT MAGNETS Final Report, 1 Sep. 1984 - 31 Dec. 1988
Nicholas J. Grant, R. C. OHandley, and N. J. Grant Feb. 1989 7 p
(Contract DAAG29-84-K-0171)
(AD-A205632; ARO-21286.11-MS) Avail: NTIS HC A02/MF A01 CSCL 07/2

The purpose of this work was to gain an improved understanding of the critical parameters of the rapid solidification process known as Liquid Dynamic Compaction (LDC). This was to be accomplished by a series of experiments on an important alloy system, Fe-Nd-B, known to show property instabilities with small variations in processing conditions. As a secondary objective it was considered desirable if in the course of the program we developed permanent magnets with improved properties. Both of these objectives were met. GRA

N89-24136# State Univ. of New York, Buffalo. Dept. of Chemistry.
EXACT WAVE FUNCTIONS AND COHERENT STATES OF A DAMPED DRIVEN HARMONIC OSCILLATOR
H. G. Oh, H. R. Lee, Thomas F. George, and C. I. Um (Korea Univ., Seoul, South Korea) Feb. 1989 38 p
(Contract N00014-86-K-0043)
(AD-A205785; UBUFFALO/DC/89/TR-93) Avail: NTIS HC A03/MF A01 CSCL 20/10

For a damped oscillator forced by a time-dependent field, the exact wave function is obtained by three different methods: (1) Path-integral, (2) Second quantization and (3) Dynamical invariant. The explicit form of the dynamical invariant involves a solution to a corresponding auxiliary equation. The coherent states, defined as eigenstates of a new destruction operator, form a nonorthogonal, over complete set and correspond to the minimum uncertainty states. These coherent states give the exact classical motion of the damped driven harmonic oscillator. GRA

N89-24137# Georgia Univ., Athens. Dept. of Physics and Astronomy.
MEMORY FUNCTIONS AND RELAXATION FUNCTIONS OF SOME SPIN SYSTEMS
Joao Florencio and M. H. Lee 1988 6 p
(Contract DAAL03-87-K-0110)
(AD-A206340; ARO-24166.5-MA) Avail: NTIS HC A02/MF A01 CSCL 20/5

The method of recurrence relations has proved to be a powerful tool in the understanding of time evolutions of many-body systems

such as an electron gas, classical harmonic chains, and spin systems on a lattice. The method is reviewed with its applications to the dynamics of spins in the one-dimensional XY and transverse Ising models, and the spin van der Waals model. GRA

N89-23605# Yugoslav Academy of Sciences and Arts, Zagreb. Faculty of Natural Sciences.
AMORPHOUS MAGNETS
Boran Leontic *In* Kernforschungsanlage Juelich GmbH, The 8th German-Yugoslav Meeting on Materials Science and Development: Ceramics and Metals 1988 p 331-339 (For primary document see N89-23569 17-23)
Copyright Avail: NTIS HC A21/MF A01

71 ACOUSTICS

Includes sound generation, transmission and attenuation. For noise pollution see *45 Environmental Pollution.*

N89-24138*# National Aeronautics and Space Administration. Lewis Research Center, Cleveland, OH.
NOISE OF A MODEL COUNTERROTATION PROPELLER WITH SIMULATED FUSELAGE AND SUPPORT PYLON AT TAKEOFF/APPROACH CONDITIONS
Richard P. Woodward and Christopher E. Hughes Apr. 1989 26 p Presented at the 12th Aeroacoustics Conference, San Antonio, TX, 10-12 Apr. 1989; sponsored by AIAA
(NASA-TM-101996; E-4700; NAS 1.15:101996; AIAA-89-1143)
Copyright Avail: NTIS HC A03/MF A01 CSCL 20A

Two modern high-speed advanced counterrotation propellers, F7/A7 and F7/A3 were tested in the NASA Lewis Research Centers's 9- by 15-foot Anechoic Wind Tunnel at simulated takeoff/approach conditions of 0.2 Mach number. Both rotors were of similar diameter on the F7/A7 propeller, while the aft rotor diameter of the F7/A3 propeller was 85 percent of the forward propeller to reduce tip vortex-aft rotor interaction. The two propellers were designed for similar performance. The propellers were tested in both the clean configuration, and installed configuration consisting of a simulated upstream nacelle support pylon and fuselage section. Acoustic measurements were made with an axially translating microphone probe, and with a polar microphone probe which was fixed to the propeller nacelle and could make both sideline and circumferential acoustic surveys. Aerodynamic measurements were also made to establish propeller operating conditions. The propellers were run at blade setting angles (fron angle/rear angle) of 41.1/39.4 deg for the F7/A7 propeller, and 41.1/46.4 deg for the F7/A3 propeller. The forward rotors were tested over a range of tip speeds from 165 to 259 m/sec (540 to 850 ft/sec), and both propellers were tested at the maximum rotor-rotor spacing, based on pitch change axis separation, of 14.99 cm (5.90 in.). The data presented in this paper are for 0 deg propeller axis angle of attack. Results are presented for the baseline, pylon-alone, and strut + fuselage configurations. The presence of the simulated fuselage resulted in higher rotor-alone tone levels in a direction normal to the advancing propeller blade near the fuselage. A corresponding rotor-alone tone reduction was often observed 180 deg circumferentially from this region of increased noise. A significant rotor-alone increase for both rotors was observed diametrically opposite the fuselage. In some cases, interaction tone levels were likewise affected by the simulated installation. Author

N89-24139*# General Electric Co., Cincinnati, OH. Advanced Engineering Technologies Dept.
HIGH SPEED TURBOPROP AEROACOUSTIC STUDY (SINGLE ROTATION). VOLUME 1: MODEL DEVELOPMENT Final Report
C. E. Whitfield, P. R. Gliebe, R. Mani, and P. Mungur May 1989 185 p
(Contract NAS3-23721)
(NASA-CR-182257-Vol-1; NAS 1.26:182257-Vol-1) Avail: NTIS HC A09/MF A01 CSCL 20A

A frequency-domain noncompact-source theory for the steady loading and volume-displacement (thickness) noise of high speed propellers has been developed and programmed. Both near field and far field effects have been considered. The code utilizes blade surface pressure distributions obtained from three-dimensional nonlinear aerodynamic flow field analysis programs as input for evaluating the steady loading noise. Simplified mathematical models of the velocity fields induced at the propeller disk by nearby wing and fuselage surfaces and by angle-of-attack operation have been developed to provide estimates of the unsteady loading imposed on the propeller by these potential field type interactions. These unsteady blade loadings have been coupled to a chordwise compact propeller unsteady loading noise model to provide predictions of unsteady loading noise caused by these installation effects. Finally, an analysis to estimate the corrections to be applied to the free-field noise predictions in order to arrive at the measurable fuselage sound pressure levels has been formulated and programmed. This analysis considers the effects of fuselage surface reflection and diffraction together with surface boundary layer refraction. The steady loading and thickness model and the unsteady loading model have been verified using NASA-supplied data for the SR-2 and SR-3 model propfans. In addition, the steady loading and thickness model has been compared with data from the SR-6 model propfan. These theoretical models have been employed in the evaluation of the SR-7 powered Gulfstream aircraft in terms of noise characteristics at representative takeoff, cruise, and approach operating conditions. In all cases, agreement between theory and experiment is encouraging. Author

N89-24140*# National Aeronautics and Space Administration. Langley Research Center, Hampton, VA.
ACOUSTIC RESPONSE OF A RECTANGULAR WAVEGUIDE WITH A STRONG TRANSVERSE TEMPERATURE GRADIENT
William E. Zorumski Mar. 1989 35 p Presented at the 27th AIAA Aerospace Sciences Meeting in Reno, NV, 9-12 Jan. 1989
(NASA-TM-101564; NAS 1.15:101564) Avail: NTIS HC A03/MF A01 CSCL 20A

An acoustic wave equation was developed for a perfect gas with spatially-variable temperature. The strong-gradient wave equation was used to analyze the response of a rectangular wave guide containing a thermally-stratified gas. It was assumed that the temperature gradient is constant, representing one-dimensional heat transfer with a constant coefficient of conductivity. The analysis of the waveguide shows that the resonant frequencies of the waveguide are shifted away from the values that would be expected from the average temperature of the waveguide. For small gradients, the frequency shift is proportional to the square of the gradient. The factor of proportionality is a quadratic function of the natural frequency of the waveguide with uniform temperature. An experiment is designed to verify the essential features of the strong-gradient theory. Author

N89-24141*# Douglas Aircraft Co., Inc., Long Beach, CA.
INTERIOR NOISE CONTROL GROUND TEST STUDIES FOR ADVANCED TURBOPROP AIRCRAFT APPLICATIONS Final Report
Myles A. Simpson, Mark R. Cannon, Paul L. Burge, and Robert P. Boyd Apr. 1989 149 p
(Contract NAS1-18037)
(NASA-CR-181819; NAS 1.26:181819) Avail: NTIS HC A07/MF A01 CSCL 20A

The measurement and analysis procedures are documented, and the results of interior noise control ground tests conducted on a DC-9 aircraft test section are summarized. The objectives of these tests were to study the fuselage response characteristics of treated and untreated aircraft with aft-mount advanced turboprop engines and to analyze the effectiveness of selected noise control treatments in reducing passenger cabin noise on these aircraft. The results of fuselage structural mode surveys, cabin cavity surveys and sound intensity surveys are presented. The performance of various structural and cabin sidewall treatments is assessed, based on measurements of the resulting interior noise levels under simulated advanced turboprop excitation. Author

72 ATOMIC AND MOLECULAR PHYSICS

Includes atomic structure, electron properties, and molecular spectra.

N89-24142*# Alabama Univ., Huntsville. Cosmic Ray Lab.
DIRECT ELECTRON-PAIR PRODUCTION BY HIGH ENERGY HEAVY CHARGED PARTICLES Final Report, Apr. 15, 1988 - 15 Oct. 1989
Y. Takahashi, J. C. Gregory, T. Hayashi, and B. L. Dong 1 May 1989 20 p
(Grant NAG8-065)
(NASA-CR-184958; NAS 1.26:184958) Avail: NTIS HC A03/MF A01 CSCL 20H

Direct electron pain production via virtual photons by moving charged particles is a unique electro-magnetic process having a substantial dependence on energy. Most electro-magnetic processes, including transition radiation, cease to be sensitive to the incident energy above 10 TeV/AMU. Thus, it is expected, that upon establishment of cross section and detection efficiency of this process, it may provide a new energy measuring technique above 10 TeV/AMU. Three accelerator exposures of emulsion chambers designed for measurements of direct electron-pains were performed. The objectives of the investigation were to provide the fundamental cross-section data in emulsion stacks to find the best-fit theoretical model, and to provide a calibration of measurements of direct electron-pairs in emulsion chamber configurations. This paper reports the design of the emulsion chambers, accelerator experiments, microscope measurements, and related considerations for future improvements of the measurements, and for possible applications to high energy cosmic ray experiments. Also discussed are the results from scanning 56m of emulsion tracks at 1200x magnification so that scanning efficiency is optimized. Measurements of the delta-ray range spectrum were also performed for much shorter track lengths, but with sufficiently large statistics in the number of measured delta-rays. A.D.

N89-24143# Technische Hogeschool, Delft (Netherlands).
STRONG AND ELECTROMAGNETIC INTERACTIONS IN HEAVY EXOTIC ATOMS Ph.D. Thesis
Cornelius Theodorus deLaat 31 Mar. 1988 122 p Prepared in coop. with Natl. Inst. voor Kernfysica en Hoge-Energiefysica, Amsterdam, Neth. Spons. by Stichting voor Fundamenteel Onderzoek der Materie, Amsterdam, Neth., and Nederlandse Organisatie voor Zuiver Wetenschappelijk Onderzoek, Ha
(PB89-145718) Avail: NTIS HC A06/MF A01 CSCL 20H

Phenomena that occur when a negatively charged particle interacts with an atom are studied. The contents include the following: improvements in experimental methods and analysis; theory of hadronic interactions in pionic atoms; systematics of 3d and 4f pionic levels in Ta-181, natural Rhenium, natural Platinum, Au-197, Pb-208, Bi-209, and Np-237; the quadrupole moment of Np-237. GRA

N89-24144# California Univ., Santa Barbara. Dept. of Chemistry.
ENERGY DISPOSAL IN ION-MOLECULE REACTIONS Final Report, 15 Nov. 1985 - 14 Nov. 1988
Michael T. Bowers 15 Jan. 1989 8 p
(Grant AF-AFOSR-0059-86; AF Proj. 2303)
(AD-A205987; AFOSR-89-0233TR) Avail: NTIS HC A02/MF A01 CSCL 07/2

Work was accomplished in three areas: (1) Kinetic Energy of Products of Simple Ion Molecule Reactions, (2) Generation and Reactivity of Carbon cluster Ions, and (3) Photodissociation Dynamics of Simple Ion Neutral Clusters. GRA

N89-24145# Technische Univ., Brunswick (Germany, F.R.). Naturwissenschaftlichen Fakultaet.
CORRELATED ATOMIC MOTIONS IN LIQUID ALUMINUM Ph.D. Thesis [KORRELATIONEN ATOMARER BEWEGUNGEN IN FLUESSIGEM ALUMINIUM]
Manfred Matzke 1988 154 p In GERMAN
(ETN-89-93943) Avail: NTIS HC A08/MF A01

The statics and dynamics of liquid Al just above the melting point were studied using simulation calculations in the range of small times (less than 10(-12) s) and small distances (less than 1 nm). The static calculations for 500 atoms were performed using the Monte Carlo method and an interaction potential from the literature; for the time-dependent investigations the molecular dynamics with equal input data was used. It is shown that liquid Al in the q-domain around 15 1/nm can be considered as an harmonic, amorphous system. Excitation spectra in the static case were calculated as eigenvalue spectra of the coupling matrix and composed with results from molecular dynamics. The dynamic calculations show that the longitudinal motion suggests cluster oscillations, while in the transversal part the diffusion behavior, expected for longer times, is already visible in the considered domain of small times. ESA

N89-24146# Kernforschungsanlage, Juelich (Germany, F.R.).
MICROSCOPIC THEORY OF ELECTRON SPIN RESONANCE IN HEISENBERG SPIN GLASSES AND THERMAL FLUCTUATIONS IN CLASSICAL SPIN MODELS WITH RANDOM FIELDS Thesis - Duesseldorf Univ. [MIKROSKOPISCHE THEORIE DER ELEKTRON SPIN RESONANZ IN HEISENBERG SPINGLAESERN UND THERMISCHE FLUKTUATIONEN IN KLASSISCHEN SPINMODELLEN MIT ZUFALLSFELDERN]
Ulrich Schulz Aug. 1988 184 p In GERMAN; ENGLISH summary
(JUEL-2227; ISSN-0366-0885; ETN-89-94408) Avail: NTIS HC A09/MF A01

A microscopic picture of the phenomenological theory of electron spin resonance (ESR) frequencies and its linewidths is described. A mode of coupling approach to the damping of these frequencies is developed. Numerical results of the mode coupling theory are presented. A class of classical spin models with random fields and hierarchy of exact identities for the static correlation functions is determined in real and replica space. Temperatures and randomness effects on scaling behavior are outlined. ESA

N89-23557*# National Aeronautics and Space Administration. Lyndon B. Johnson Space Center, Houston, TX.
ATOMIC OXYGEN
Lubert J. Leger and James T. Visentine *In* NASA, Langley Research Center, NASA/SDIO Space Environmental Effects on Materials Workshop, Part 2 May 1989 p 545-552 (For primary document see N89-23547 17-23)
Avail: NTIS HC A12/MF A01 CSCL 20H

73 NUCLEAR AND HIGH-ENERGY PHYSICS

Includes elementary and nuclear particles; and reactor theory.

For space radiation see *93 Space Radiation.*

N89-24147# General Electric Co., Philadelphia, PA. Valley Forge Space Center.
FINAL SAFETY ANALYSIS REPORT FOR THE GALILEO MISSION. VOLUME 1: REFERENCE DESIGN DOCUMENT
May 1988 176 p
(Contract DE-AC01-79ET-32043)
(DE89-007268; DOE/ET-32043/T26-Vol-1) Avail: NTIS HC A09

The Galileo mission uses nuclear power sources called Radioisotope Thermoelectric Generators (RTGs) to provide the spacecraft's primary electrical power. Because these generators contain nuclear material, a Safety Analysis Report (SAR) is required. A preliminary SAR and an updated SAR were previously issued that provided an evolving status report on the safety analysis. As a result of the Challenger accident, the launch dates for both Galileo and Ulysses missions were later rescheduled for November 1989 and October 1990, respectively. The decision was made by

agreement between the DOE and the NASA to have a revised safety evaluation and report (FSAR) prepared on the basis of these revised vehicle accidents and environments. The results of this latest revised safety evaluation are presented in this document (Galileo FSAR). Volume 1, this document, provides the background design information required to understand the analyses presented in Volumes 2 and 3. It contains descriptions of the RTGs, the Galileo spacecraft, the Space Shuttle, the Inertial Upper Stage (IUS), the trajectory and flight characteristics including flight contingency modes, and the launch site. There are two appendices in Volume 1 which provide detailed material properties for the RTG. DOE

N89-24148# Naval Research Lab., Washington, DC. Plasma Theory Branch.
SIMULATION STUDIES OF PARTICLE ACCELERATION POWERED BY MODULATED INTENSE RELATIVISTIC ELECTRON BEAMS Interim Report
J. Krall, V. Serlin, M. Friedman, and Y. Y. Lau 14 Mar. 1989 38 p Prepared in cooperation with Science Applications International Corp., McLean, VA
(AD-A206348; NRL-MR-6425) Avail: NTIS HC A03/MF A01 CSCL 20/7

A time dependent, fully electromagnetic particle code is used to simulate transfer of energy from an annular modulated intense relativistic electron beam to a low current electron beam via a disk-loaded structure. It is shown that an intense beam may be used to drive such an accelerator at high transformer ratio (R 10) to obtain accelerating gradients in the about 100 MV/m range, with power excess of 1 GW transferred from the primary to the secondary beam. GRA

N89-24149# Swedish Defence Research Establishment, Stockholm.
MOBILE NUCLEAR POWER SYSTEMS
Bengt Andersson Nov. 1988 68 p In SWEDISH; ENGLISH summary
(FOA-C-20743-4.1; ISSN-0347-3694; ETN-89-94305) Avail: NTIS HC A04/MF A01

Nuclear reactors where the energy comes from nuclear fission and isotopic generators utilizing the energy of the decay of suitable isotopes are discussed. The reactors are used as power sources on board nuclear submarines and other warships, as well as in space and in remote places. Their thermal power ranges from 30 KWth in a satellite to 175 MWth on board an aircraft carrier. Isotopic generators are suitable only for small power demands and are used on board satellites and spaceprobes, automatic weather stations, lighthouses, and marine installations for navigation and observation. ESA

74 OPTICS

Includes light phenomena; and optical devices.
For lasers see *36 Lasers and Masers.*

N89-24150# National Technical Systems, Long Beach, CA.
FIBER OPTIC LEAK DETECTION SYSTEM Final Report, Aug. 1985 - Dec. 1986
Paul Lieberman and Tyler Nakamura Aug. 1988 196 p
(Contract GRI-5085-252-1153)
(PB89-148886; NTS-TR-1524-1; GRI-88/0246) Avail: NTIS HC A09/MF A01 CSCL 20F

A fiber optic based gas pipe leak detection system was developed that can determine, from within an underground pipe, the presence, location, type, and rate of a gas leak. Two fiber optic systems along with two fiber modes (multi and single) were tested. To test the optical time domain reflection (OTDR) concept, a short duration light pulse was sent down a fiber optic cable experiencing a localized acoustic disturbance, simulating a gas leak. The disturbance causes a partial reflection of the light pulse to occur. The reflected signal comes back through the beamsplitter and is detected by a photomultiplier tube (PMT). The PMT yields voltage versus time data from which leak characteristics are deciphered. To test optical time domain transmission (OTDT), a continuous helium/neon laser, fiber optic cable, cross-polarizer, and PMT were used. The laser beam was directed down the fiber optic cable. With the crossed polarizers set for null at the detector, a disturbance of the fiber caused light to reach the PMT where voltage time history was recorded. Author

N89-24151# Lawrence Livermore National Lab., CA.
CHARACTERIZATION OF MULTILAYER COATED CONCAVE DIFFRACTION GRATINGS IN THE EXTREME ULTRAVIOLET
Jay Bixler, Troy Barbee, Jr., and Dan Dietrich Feb. 1989 13 p Presented at the Berkeley Colloquium on Extreme Ultraviolet Astronomy, Berkeley, CA, 19-20 Jan. 1989
(Contract W-7405-eng-48)
(DE89-008831; UCRL-100083; CONF-890189-5) Avail: NTIS HC A03/MF A01

We describe here our work to date on characterizing two multilayer coated concave diffraction gratings, one conventionally ruled, the other holographically ruled. We have obtained photographic spectra with both gratings which indicate good resolution properties and promising efficiencies. DOE

N89-24152# Lawrence Livermore National Lab., CA.
TEMPORALLY SMOOTH BROADBAND PULSES OBTAINED BY CROSS PHASE MODULATION IN AN OPTICAL FIBER
P. H. Chaffee, F. G. Patterson, and M. A. Henesian 25 Jan. 1989 11 p Presented at the CLEO '89: Conference on Lasers and Electro Optics, Baltimore, MD, 24 Apr. 1989
(Contract W-7405-eng-48)
(DE89-008891; UCRL-99999; CONF-890423-8) Avail: NTIS HC A03/MF A01

We have broadened the output spectrum of a single-mode, Q-switched Nd: YLF oscillator (lambda = 1.053 micrometer) by co-propagating it with a noisy, broadband pulse in a polarization preserving fiber. The intensity as a function of time remains smooth, despite the 10(4) increase in bandwidth. DOE

N89-24153*# National Aeronautics and Space Administration. Pasadena Office, CA.
A COMPACT FAST WIDE ANGLE BROAD BAND SPECTROMETER OPTICAL SYSTEM Patent Application
Norman A. Page, inventor (to NASA) and Mary L. White, inventor (to NASA) (Jet Propulsion Lab., California Inst. of Tech., Pasadena.) 29 Nov. 1988 13 p
(Contract NAS7-918)
(NASA-Case-NPO-17562-1-CU; NAS 1.71:NPO-17562-1-CU; US-Patent-Appl-SN-277596) Avail: NTIS HC A03/MF A01 CSCL 20F

An improved spectrometer particularly adapted for the infrared range includes a solid glass optical system for implementing a double pass arrangement. A pair of optical elements can be joined along one optical cemented surface to function both as a collimator and a camera in an extremely compact configuration. As a result, a high numerical aperture wide field of view and broad spectral range spectrometer is achieved. NASA

N89-24154# Indiana Univ., Bloomington. Dept. of Chemistry.
FIBER-OPTIC TIME-RESOLVED FLUORESCENCE SENSOR FOR THE SIMULTANEOUS DETERMINATION OF Al(+3), Ga(+3) AND In(+3)
Mary K. Carroll, Frank V. Bright, and Gary M. Hieftje 10 Feb. 1989 29 p
(Contract N00014-86-K-0366)
(AD-A205689) Avail: NTIS HC A03/MF A01 CSCL 20/6

A fiber-optic fluorescence sensor for simultaneous multi-elemental determination has been developed. The sensor is based on the formation of a complex between specific metal ions and a metal-ion chelator. Several chelator ion systems and several means of chelator immobilization were studied. The successful fiber-optic sensor design is based on a pool of chelator solution trapped behind a Nafion membrane. The chelator ultimately chosen, lumogallion, forms strongly fluorescent complexes with trivalent

aluminum, gallium, and indium ions. Because of the difference in fluorescence lifetimes of the various lumogallion complexes, time-resolved fluorometry enables simultaneous determination of these ions. GRA

N89-24155# Department of the Navy, Washington, DC.
UTILIZATION OF MAGNETOSTRICTIVE OPTICAL FIBERS IN MULTIPLE ORDER GRADIOMETERS Patent Application
Lloyd C. Bobb, inventor (to Navy) 20 Jun. 1988 18 p Filed 20 Jun. 1988
(AD-D013960; US-Patent-Appl-SN-208931; Navy-Case-68403) Avail: NTIS HC A03/MF A01 CSCL 17/6

Magnetometers disposed as magnetostrictive segments on optical fiber elements are incorporated in multiple order gradiometers to reduce the size, weight and cost thereof. In the preferred embodiments, such reductions are greatly enhanced by consolidating a plurality of magnetometers on individual optical fiber elements, which also serves to decrease the number of devices associated with the magnetometers in the multiple order gradiometers. GRA

N89-24156# Naval Postgraduate School, Monterey, CA.
THREE-DIMENSIONAL ANALYSIS OF OPTICAL TRANSITION RADIATION M.S. Thesis
Wilmer G. Longstaff Dec. 1988 144 p
(AD-A205935) Avail: NTIS HC A07/MF A01 CSCL 20/8

A three dimensional analysis of the intensity distribution of backward optical transition radiation has been performed. The effects of variations in electron energy and beam divergence and on material properties such as dielectric permittivities and the resultant coherence length upon the angular distribution and polarization of optical transition radiation has been investigated. A surprising observation important to the use of optical transition radiation as a diagnostic tool for high energy electron beams is the behavior of the perpendicular component of the intensity. In contrast to low energies where the parallel component dominates, at electron energies above 200 MeV, the perpendicular component dominates. This requires the use of a polarization filter to diagnose particle beam properties at high energies. GRA

N89-24157# BDM Corp., McLean, VA.
DIGITAL OPTICS FOR NUMERICAL COMPUTING: THE RESIDUE NUMBER SYSTEM FOR NUMERICAL OPTICAL COMPUTING Final Technical Report, Aug. 1987 - Mar. 1988
Mark L. Heinrich, Ravindra A. Athale, and Michael W. Haney Oct. 1988 71 p
(AD-A206229; RADC-TR-88-229) Avail: NTIS HC A04/MF A01 CSCL 20/6

The use of Residue Number System (RNS) in performing high accuracy numerical computing with digital optics is investigated. The analysis is focused on the position coded residue representation and the Look Up Table (LUT) approach to arithmetic operations. Two approaches to reducing the total number of LUT entries (the spatial complexity) proposed by Boeing Aerospace Corp. and Westinghouse are studied. Analytical expressions for the spatial complexity, time complexity, and element complexity as a function of the modulus are derived for the two approaches in performing the standard operations of multiplication, addition and for the multiply-accumulate unit. The report thus provides a hardware-independent method of studying the trade-offs between these two major approaches to RNS optical computing. Hardware options for optical implementations of interconnects and nonlinear switching elements are outlined. The intimate relation between the algorithms, architectures and the hardware and their combined impact on the system performance is outlined suggesting directions for future work. GRA

N89-24158# Army Missile Command, Redstone Arsenal, AL. Guidance and Control Directorate.
STRUCTURAL MODE FREQUENCIES OF FOG-M (FIBER OPTICS GUIDED-MISSILE) ACTUATOR/FIN Technical Report, Oct. - Dec. 1984
Gordon D. Welford Nov. 1988 41 p
(AD-A206327; AD-E951293; AMSMI/TR-RD-GC-88-22) Avail: NTIS HC A03/MF A01 CSCL 13/7

An earlier report examined the pneumatic servo stiffness as a potential cause of marginal fin flutter mode stability. In this analysis, the bending stiffness of the vane, vane/actuator shaft, vane and actuator bearing combination is examined. It is shown that there exists a predominant 50 Hz mode which is caused by the fin structure and the radial type spring of the fin base into which the actuator shaft is inserted. GRA

N89-24159 Max-Planck-Inst. fuer Physik und Astrophysik, Garching (Germany, F.R.). Inst. fuer Extraterrestrische Physik.
ASSESSMENT OF SURFACE TOPOGRAPHY BY X-RAY SCATTERING MEASUREMENTS
Bernd Aschenbach and Heinrich Braeuninger 9 Oct. 1988 22 p Presented at the International Congress on Optical Science and Engineering, Hamburg, Fed. Republic of Germany, Sep. 1988 Submitted for publication
(MPE-Preprint-134; ETN-89-94395) Copyright Avail: Fachinformationszentrum Karlsruhe, 7514 Eggenstein-Leopoldshafen 2, Fed. Republic of Germany

In the context of developing optics for X-ray astronomy, measurements of a variety of flat mirrors and telescopes revealed that the total integrated scatter (TIS) formalism, well known in the optical regime, also describes the surface scattering of soft X-rays. A quantitative formalism is derived to separate the spectrum of spatial surface wavelengths into components which can be treated in a geometrical optics approach and those which need exact diffraction treatment. The method is applied to predict the X-ray point spread function of telescopes from mechanical profile measurements. The agreement between prediction and mesurement is remarkably good. ESA

N89-24160# Aerospatiale, Cannes La Bocca (France).
THERMAL AND CRYOGENIC ASPECTS OF THE ISO OPTICAL SUBSYSTEM
B. Collaudin and L. DeSa Paris, France 1988 8 p
(Rept-882-440-113; ETN-89-94506) Avail: NTIS HC A02/MF A01

The ISO optical subsystem is described. It is composed of a cold telescope, a main baffle, and a sunshade. The telescope and the baffle are cooled down to 3 K by means of heat exchange with helium evaporated from a superfluid helium tank. The sunshade is cooled by radiation towards space, using a radiator. The analyses are performed using the modular structure of ESATAN software and subroutines and through numerical interface specification. The current design fulfills the requirements. ESA

N89-23901*# Lockheed Missiles and Space Co., Palo Alto, CA.
DEVELOPMENT OF A PRECISION, WIDE-DYNAMIC-RANGE ACTUATOR FOR USE IN ACTIVE OPTICAL SYSTEMS
K. R. Lorell, J.N. Aubrun, D. F. Zacharie, and E. O. Perez *In* NASA, Marshall Space Flight Center, The 23rd Aerospace Mechanisms Symposium Mar. 1989 p 139-156 (For primary document see N89-23892 17-39)
Avail: NTIS HC A15/MF A01 CSCL 20F

75 PLASMA PHYSICS

Includes magnetohydrodynamics and plasma fusion.

For ionospheric plasmas see *46 Geophysics*. For space plasmas see *90 Astrophysics*.

N89-24161# Nagoya Univ. (Japan). Inst. of Plasma Physics.
SHEATH AND PRESHEATH IN A COLLISIONLESS OPEN FIELD PLASMA
Kunihiro Sato, Fujio Miyawaki, and Wakumi Fukui Sep. 1988 34 p Prepared in cooperation with Himeji Inst. of Tech. (Japan)
(IPPJ-890; ISSN-0469-4732) Avail: NTIS HC A03/MF A01

The plasma-sheath equation for a collisionless plasma with a finite-temperature particle source in a nonuniform open magnetic

field is formulated. The analytic solution of this equation is obtained from the quasi-neutral approximation for the plasma outside the sheath. The potential formed in the plasma depends on the profile of the magnetic field strength; potential drop in the plasma region increases and the ion distribution function becomes wider as the magnetic field strength decreases in the direction of the plasma flow. Application of the generalized Bohm criterion shows that the solution of the plasma equation always satisfies this criterion when the magnetic field monotonically decreases in the outside direction. Comparison of the analytic solution with the numerical results of the plasma-sheath equation confirms that over the whole region (except the sheath) the analytic solution for various profiles of the magnetic field agrees well with the numerical results when the Debye length is sufficiently small. Author

N89-24162*# Smithsonian Astrophysical Observatory, Cambridge, MA.
SOLAR AND STELLAR CORONAL PLASMAS Semiannual Report Nos. 12-17, 1 May 1986 - 30 Apr. 1989
Leon Golub Apr. 1989 177 p
(Grant NAGw-112)
(NASA-CR-184909; NAS 1.26:184909) Avail: NTIS HC A09/MF A01 CSCL 20I

Progress in observational, theoretical, and radio studies of coronal plasmas is summarized. Specifically work completed in the area of solar and stellar magnetic fields, related photospheric phenomena and the relationships between magnetism, rotation, coronal and chromospheric emission in solar-like stars is described. Also outlined are theoretical studies carried out in the following areas, among others: (1) neutral beams as the dominant energy transport mechanism in two ribbon-flares; (2) magneto hydrodynamic and circuit models for filament eruptions; and (3) studies of radio emission mechanisms in transient events. Finally, radio observations designed for coronal activity studies of the sun and of solar-type coronae are described. A bibliography of publications and talks is provided along with reprints of selected articles. A.D.

N89-24163# Royal Inst. of Tech., Stockholm (Sweden). Dept. of Plasma Physics.
ELECTRODYNAMICS OF COSMICAL PLASMAS: SOME BASIC ASPECTS OF COSMOLOGICAL IMPORTANCE
Carl-Gunne Faelthammar Feb. 1989 28 p Presented at the IEEE International Workshop on Plasma Cosmology, La Jolla, CA, 20-22 Feb. 1989
(TRITA-EPP-89-02; ISSN-0348-7539) Avail: NTIS HC A03/MF A01

In cosmology, as in astrophysics, the overwhelmingly dominant state of matter is the plasma state. Therefore it is necessary to take into account the properties of this state of matter, which in crucial respects are different from those of unionized matter. Basic electrodynamic properties, as revealed by laboratory and space plasma experiments, and consequences of these are reviewed. Included are coupling between magnetic fields and the motion of matter, filamentary and cellular structure, anomalous momentum coupling and mechanisms of chemical separation. Some of these properties, important for the understanding of the present-day universe, must also have been important in the cosmological evolution of which today's universe is the result. As some of the crucial properties are still poorly understood, but being investigated by laboratory and space plasma experiments, the result of such experiments should also be very relevant to the development of cosmology. Author

N89-24164# Nagoya Univ. (Japan). Inst. of Plasma Physics.
EIKONAL APPROXIMATION IN PARTIAL WAVE VERSION
Wen-Jia Qian and Hajime Narumi Mar. 1989 12 p Submitted for publication
(IPPJ-899; ISSN-0469-4732) Avail: NTIS HC A03/MF A01

The eikonal approximation is formulated in a partial wave version. This makes it possible to evaluate the electron scattering from many-electron atomic systems in a direct manner with a formal procedure similar to the Coulomb-Born and distorted wave approximations. Author

N89-24165# Oxford Univ. (England). Dept. of Engineering Science.
INVESTIGATION OF THE BEHAVIOUR OF A COLLISIONLESS R-F SHEATH
A. F. Stekolnikov, N. St. J. Braithwaite (Open Univ., Milton, England), and J. E. Allen 1987 17 p
(OUEL-1695/87; ETN-89-94210) Avail: NTIS HC A03/MF A01

The spatial and temporal distributions of the potential and charged particle densities in the sheath of an argon plasma were calculated for several values of applied RF potential. The results show that the ion density and mean electron density distributions are insensitive to the amount of RF applied. The instantaneous electron density oscillates with the field frequency and shows a substantial variation during one cycle. At comparatively high amplitudes of RF potential (less than 10) the instantaneous value of the electron density can exceed the ion density. There is a marked decrease in the minimum instantaneous value of the potential in much of the sheath. The thickness of the space charge region is modulated by the RF-field and the mean sheath thickness increases as the amplitude of the RF-potential is increased. Although the model applies to the whole of the sheath the asymptotic nature of the solution does not allow absolute sheath dimensions to be determined. The absolute value of the displacement current density increases towards the wall where it is largest. The displacement current at the wall increases less rapidly than the RF potential. ESA

N89-24166# Texas Univ., Austin.
ANALYSIS OF THE IGNITION EXPERIMENT IGNITEX
R. Carrera, G. Y. Fu, J. Helton, L. Hively, E. Montalvo, C. Ordonez, M. N. Rosenbluth (California Univ., San Diego.), S. Tamor, and J. W. VanDam 1989 4 p Presented at the 16th European Conference on Controlled Fusion and Plasma Physics, Venice, Italy, 13 Mar. 1989
(Contract DE-AC05-84OR-21400)
(DE89-007847; CONF-890302-16) Avail: NTIS HC A02/MF A01

The realization of an ignition experiment in a laboratory will prove the scientific feasibility of controlled thermonuclear fusion. The fusion ignition experiment IGNITEX has the potential to produce and control a self-sustained fusion reaction with relative simplicity and low cost. Relevant plasma physics aspects of the experiment are analyzed in this paper. DOE

N89-24167# Los Alamos National Lab., NM. Applied Theoretical Physics Div.
ONSET CONDITIONS FOR THE DRIVEN LOWER HYBRID DRIFT INSTABILITY IN AN EXPANDING MAGNETIZED PLASMA Technical Report, Oct. 1988 - Jan. 1989
D. Winske 24 Jan. 1989 35 p
(Contract W-7405-eng-36)
(AD-A205505; LA-UR-89-275) Avail: NTIS HC A03/MF A01 CSCL 20/3

Conditions for the turn on of short wavelength flute modes on plasmas expanding across an external magnetic field are discussed. The experimental data concerning scaling of the instability onset as a function of magnetic field are reviewed, followed by a similar review of numerical simulation results. Theoretical conditions for the appearance of the fast growing, short wavelength lower hybrid drift instability are derived. Overall, the experiments and simulations in which a scaling can be deduced suggest the turn-on of the instability is a strong function of the magnetic field. These results are discussed in relation to the NRL laser experiment, which in contrast exhibits little dependence of the instability onset on the applied field. GRA

N89-24168*# Jet Propulsion Lab., California Inst. of Tech., Pasadena.
MPD THRUSTER EROSION RESEARCH Final Report, 1 Jan. - 31 Dec. 1987

David Q. King and John L. Callas 30 Nov. 1988 34 p
(Contract NAS7-918; AF-AFOSR-0046-87; AF Proj. 2308)
(NASA-CR-185314; NAS 1.26:185314; AD-A205644; JPL-D-6020; AFOSR-89-0331TR) Avail: NTIS HC A03/MF A01 CSCL 20/9

The multimegawatt MPD (Magnetoplasma Dynamic) thruster is an electric engine capable of orbital transfer and maneuvering of large payloads driven by a megawatt class space power supply. The MPD thruster is capable of specific impulses from 1,500 to 8,000 s. The high specific impulse means this system can perform missions using much less propellant than chemical systems. A five MW MPD electric system, propellant and payload from one shuttle launch must be replaced by the equivalent of four fully loaded Centaur G' stages. Thus, the savings in propellant and launch costs are very substantial. This report discusses 3 aspects of MPD thruster Physics: (1) A significant operational problem which has limited the useful operation of the device is discussed. This is severe erosion of the insulator at the cathode insulator junction. A technique which appears to solve the problem has been tested, and is described. (2) A preliminary analyses of anode sheath is presented. (3) Analysis of the discharges two dimensional nature is explored for the case where transverse gradients are considered but transverse velocity is assumed to be zero. This situation applies to high aspect ratio devices. The analyses concludes with a formalism that provides a means to qualitatively evaluate Ohmic dissipation from simple measurements of magnetic Hall effect on magnetosonic choking (where thermodynamics is ignored). GRA

N89-24169# Indiana Univ., Bloomington. Dept. of Chemistry.
NOISE CHARACTERISTICS OF AN INDUCTIVELY COUPLED PLASMA-MASS SPECTROMETER
Naoki Furuta, Curtis A. Monnig, Pengyuan Yang, and Gary M. Hieftje 10 Feb. 1989 17 p
(Contract N00014-86-K-0366)
(AD-A205686) Avail: NTIS HC A03/MF A01 CSCL 20/9

Noise amplitude spectra for the signal from an inductively coupled plasma-mass spectrometer (ICP-MS) were measured and compared with those obtained with inductively coupled plasma-atomic emission spectrometry (ICP-AES). For the ICP-MS, white noise was dominant in background spectra. An audio-frequency noise peak at 200-350 Hz was observed and behaved much like the one noted earlier in ICP-AES. Unlike in ICP-AES, however, the frequency at which this noise peak occurs is dependent upon the sampling depth in the plasma. GRA

N89-24170# Indiana Univ., Bloomington. Dept. of Chemistry.
FLOW-INJECTION ANALYSIS UTILIZING A SPECTRALLY SEGMENTED PHOTODIODE-ARRAY INDUCTIVELY COUPLED PLASMA EMISSION SPECTROMETER. 1: MICROCOLUMN PRECONCENTRATION FOR THE DETERMINATION OF MOLYBDENUM
Naoki Furuta, K. R. Brushwyler, and Gary M. Hieftje 10 Feb. 1989 28 p
(Contract N00014-86-K-0366)
(AD-A205687) Avail: NTIS HC A03/MF A01 CSCL 09/1

A flow injection analysis (FIA) system incorporating a microcolumn of activated alumina was used for the determination of molybdenum by inductively coupled plasma-atomic emission spectrometry (ICP-AES). The transient signal resulting from the injection of molybdenum was determined by a spectrally segmented photodiode-array spectro-meter. Linear calibration was established for molybdenum over a concentration range 0 to 1000 ng/ml. The detection capability was approximately 50 times better than offered by comparable continuous-nebulization systems. The detection limit for molybdenum was 0.2 ng/ml, and the relative standard deviations at 500 and 10 ng/ml were about 2 and 5 percent, respectively. The ability of the multichannel photodiode array spectrometer to correct for background shifts which occur during signal integration period provided improved precision and accuracy. Application to the analysis of molybdenum in standard sea water (NASS-2) was demonstrated. GRA

N89-24171# Indiana Univ., Bloomington. Dept. of Chemistry.
USE OF A SPECTRALLY SEGMENTED PHOTODIODE-ARRAY SPECTROMETER FOR INDUCTIVELY COUPLED PLASMA ATOMIC EMISSION SPECTROSCOPY
Naoki Furuta, K. R. Brushwyler, and Gary M. Hieftje 10 Feb. 1989 29 p
(Contract N00014-86-K-0366)
(AD-A205688) Avail: NTIS HC A03/MF A01 CSCL 09/1

The utility of a spectrally segmented photodiode array spectrometer was examined by using inductively coupled plasma atomic emission spectrometry (ICP-AES). The spectrometer used in this study is capable of high resolution (reciprocal linear dispersion of approximately 0.08 nm/mm at 300 nm) over a wide spectral range (190 to 145nm). The effect of using spectral-peak areas instead of peak heights as a signal definition was determined by using the emission signals from 10 molybdenum lines obtained at various photodiode array integration periods. In addition, a signal definition involving a summation over a range of 5 pixels offered the best signal-to-noise ratio when the noise was defined as the standard deviation of the residual values from the line fit to the sideband background level. A detection limit of 6ng/ml was determined in this way for molybdenum. The multichannel capability of the spectrometer was found to permit continuous background correction, thereby reducing errors caused by low-frequency noise or plasma drift. Detector linearity was found to extend over three orders of magnitude with a single integration period. GRA

N89-24172# Michigan Univ., Ann Arbor. Dept. of Nuclear Engineering.
POPULATION INVERSIONS IN ABLATION PLASMAS GENERATED BY INTENSE ELECTRON BEAMS Final Report, 1 Nov. 1985 - 31 Oct. 1988
R. M. Gilgenbach, T. Kammash, and M. L. Brake Nov. 1988 130 p
(Grant AF-AFOSR-0012-86; AF Proj. 2301)
(AD-A205716; AFOSR-89-0294TR) Avail: NTIS HC A07/MF A01 CSCL 20/9

Experiments during the past three years have concerned the generation and spectroscopic study of electron beam-driven carbon plasmas in order to explore the production of optical and ultraviolet radiation from nonequilibrium populations. The output of MELBA (Michigan Electron Long Beam Accelerator), has been connected to an electron beam diode consisting of an aluminum (or brass) cathode stalk and a carbon anode. Magnetic field coils have been designed, procured, and utilized to focus the electron beam. A side viewing port permitted spectroscopic diagnostics to view across the surface of the anode. Spectroscopic diagnosis has been performed using a 1 m spectrograph capable of operation from the vacuum ultraviolet through the visible. This spectrograph is coupled to a 1024 channel optical multichannel analyzer. Spectra taken during the initial 400 ns period of the e-beam pulse showed a low effective charge plasma with primarily molecular components (C2, CH) as well as atomic hydrogen and singly ionized carbon (CII). When the generator pulse was crowbarred after the first 400 ns, the spectra revealed a continuation of the low charge state plasma. GRA

N89-24173# Indiana Univ., Bloomington. Dept. of Chemistry.
PRELIMINARY EVALUATION OF A MINIATURIZED TORCH FOR INDUCTIVELY COUPLED PLASMA MASS SPECTROMETRY
Barbara S. Ross, George H. Vickers, Pengyuan Yang, and Gary M. Hieftje 10 Feb. 1989 18 p
(Contract N00014-86-K-0366)
(AD-A205746) Avail: NTIS HC A03/MF A01 CSCL 14/2

Preliminary studies have shown that a 13 mm (miniature) torch can be used successfully as an ion source for inductively coupled plasma mass spectrometry (ICP-MS) but with a tenfold loss in detection capability. The 13 mm torch can be operated at total argon flows of 9 l/min, lower than an optimized conventional ICP torch. The 13 mm torch produces nearly the same background and linear dynamic range as the conventional-sized torch. However,

there is approximately one order of magnitude degradation in sensitivity and detection limits and the production of doubly charged ions is more pronounced. GRA

N89-24174# Indiana Univ., Bloomington. Dept. of Chemistry.
SIMULTANEOUS MEASUREMENT OF SPATIALLY RESOLVED ELECTRON TEMPERATURES, ELECTRON NUMBER DENSITIES AND GAS TEMPERATURES BY LASER LIGHT SCATTERING FROM THE ICP
Mao Huang and Gary M. Hieftje 10 Feb. 1989 39 p
(Contract N00014-86-K-0366)
(AD-A205747) Avail: NTIS HC A03/MF A01 CSCL 20/9

Spatially resolved electron temperatures, electron number densities and gas-kinetic temperatures have been determined at five observation heights, nine radial positions, and two settings of RF input power in an aerosol-free argon ICP sustained with a commercial MAK torch. The measurements were obtained by means of simultaneous ruby-laser Thomson scattering the Rayleigh scattering. In the central channel of the ICP the electron temperature ranges from 7000 K to 8500 K, the gas kinetic temperature is about 1000 K from 1.9 to 7.0 x ten to the 15th power/cc. Among the measured parameters, the electron number density is most sensitive to the input RF power and is noticeable and the Saha equation. The overpopulation-electron recombination processes, resulting in a recombining plasma in the analytical zone. This non-LTE feature might be significant for excitation and ionization mechanisms in the ICP. GRA

N89-24175# Aerospatiale Aquitaine, Saint-Medard en Jalles (France). Dept. Plasmas Thermiques industriels.
PRODUCT DEVELOPMENT AT AEROSPATIALE [DEVELOPPEMENT DES PRODUITS A L'AEROSPATIALE]
Didier Pineau Paris, France 30 May 1988 4 p In FRENCH Presented at the Societe Francaise des Tjermiciens Journee d'Etudes on l'Essor Industriel des Plasmas, 1 Jun. 1988
(Rept-882-430-111; ETN-89-94492) Avail: NTIS HC A02/MF A01

The product development described includes tests and studies of plasma systems, interfaces of plasma torches with existing procedures, and turnkey industrial plasma facilities. The plasma torches are 1 to 5 MW power, while up to 10 MW are being developed. Industrial test laboratory facilities are mentioned. ESA

N89-24176 Max-Planck-Inst. fuer Plasmaphysik, Garching (Germany, F.R.).
TRANSPORT OF TEST PARTICLES IN A MAGNETIC FIELD WITH PERTURBED MAGNETIC SURFACES Thesis - Technische Univ., Munich [TRANSPORT VON TESTTEILCHEN IM MAGNETFELD MIT GESTOERTEN MAGNETISCHEN FLAECHEN]
Hardy Sander Sep. 1988 76 p In GERMAN; ENGLISH summary
(IPP-2/296; ETN-89-93989) Copyright Avail: Fachinformationszentrum Karlsruhe, 7514 Eggenstein-Leopoldshafen 2, Fed. Republic of Germany

The radial transport of circulating particles in a perturbed toroidal magnetic field configuration is calculated using the mapping technique. The specific models are stellarators with external perturbations and tokamaks with tearing modes. Coulomb collisions of the circulating particles are described by a Lorentz scattering model of random changes of the pitch angle. Particle orbits in a perturbed magnetic field lead to a deterministic map whereas the Coulomb collisions introduce an extra stochastic process. The diffusion in a single chain of islands is studied by launching a sample of particles on the inner closed magnetic surface and calculating the loss rate. The presence of islands enhances the loss rate. In a second case the enhanced loss in a tokamak with two different islands on different resonant surfaces are investigated thus simulating tearing modes in tokamaks. Transport of particles is a mixture of stochastic diffusion of field lines and a random walk induced by Coulomb collisions. ESA

N89-24177# Institut Franco-Allemand de Recherches, Saint-Louis (France).
NUMERICAL MODELING OF LASER PRODUCED PLASMAS AND LASER INDUCED PRESSURE EFFECTS [NUMERISCHE MODELLIERUNG LASERERZEUGTER PLASMEN UND LASERINDUZIERTER DRUCKWIRKUNGEN]
K. Daree 7 Dec. 1987 55 p In GERMAN Presented at the Seminar des Lehrstuhls fuer Lasertechnik, Aachen, Fed. Republic of Germany, 27 Nov. 1987
(ISL-CO-244/87; ETN-89-94110) Avail: NTIS HC A04/MF A01

Numerical methods for the modeling of laser produced plasmas and their induced pressure effects are described. A method is proposed for predicting one dimensional plasma expansion and the induced energy mass and pressure calculation. A two dimensional program is applied to laser induced combustion and detonation waves. For ambiant pressures below 200 to 300 Pa the laser induced detonation wave generates a plasma. Computations achieved for the same wave length 1.06 micron show that instead of the detonation wave, a vaporization of the target is obtained with the formation of a combustion wave. ESA

N89-23555*# National Aeronautics and Space Administration. Lewis Research Center, Cleveland, OH.
SURFACE PHENOMENA IN PLASMA ENVIRONMENTS
C. K. Purvis and D. C. Ferguson *In* NASA, Langley Research Center, NASA/SDIO Space Environmental Effects on Materials Workshop, Part 2 May 1989 p 511-534 (For primary document see N89-23547 17-23)
Avail: NTIS HC A12/MF A01 CSCL 20I

76 SOLID-STATE PHYSICS

Includes superconductivity.

For related information, see also *33 Electronics and Electrical Engineering* and *36 Lasers and Masers.*

N89-24178# National Aeronautical Lab., Bangalore (India). Materials Science Div.
STUDIES ON HIGH-Tc SUPERCONDUCTING MATERIALS
P. S. Gopalakrishnan and P. S. L. Narasimhan Aug. 1987 14 p
(NAL-TM-MT-8703) Avail: NTIS HC A03/MF A01

A superconducting material of reproducible quality of chemical composition YBa2Cu307-delta was prepared. Samples of this material were characterized for transition temperatures by electrical resistivity measurements. Crystallographic parameters of this material were determined. Thin samples prepared by lapping showed an anomalous behavior just before transition. Author

N89-24179 Stanford Univ., CA.
HETEROJUNCTION BAND LINE-UPS AND THE ALLOYING EFFECT IN COMPOUND SEMICONDUCTOR ALLOYS: A PHOTOEMISSION STUDY Ph.D. Thesis
Chih-Kang Shih 1988 175 p
Avail: Univ. Microfilms Order No. DA8826227

A method utilizing core level photoemission spectroscopy is developed to study the intrinsic alignment of the valence band maxima between compound semiconductors and their alloys. These intrinsic bulk band line-ups form an ideal reference system for the investigation of interface-specific effects in determining heterojunction band alignments. Moreover, they allow the positioning of the constituent bands in determining the electronic structure of a semiconductor alloy. Four experimental examples (HgCdTe, CdZnTe, HgZnTe, and GaInAs) utilizing this method and their comparison with heterojunction measurements by others are also discussed. The technique of angle-resolved photoemission spectroscopy is used to study the k-dependence of the alloy scattering problem. A detailed study was performed on the Hg(1-x)Cd(x)Te system. By using angle-resolved photoemission spectroscopy, the E(k) dispersions of HgTe and CdTe bands is considered as the virtual crystal band. Thus, in the alloy the deviation of the band structure from the prediction of virtual crystal

approxximation is due to the alloy scattering effect. It is found that for the electronic states composed of large amplitude of the cation s orbital, the experimental result agrees with the calculation using coherent potential approximation within the context of tight-binding theory. However, for the electronic states which are primarily Te p states, an anomalous alloy scattering behavior is observed. Possible explanations are discussed. Dissert. Abstr.

N89-24180# National Inst. of Standards and Technology, Gaithersburg, MD. Semiconductor Electronics Div.
SEMICONDUCTOR MEASUREMENT TECHNOLOGY: AUTOMATIC DETERMINATION OF THE INTERSTITIAL OXYGEN CONTENT OF SILICON WAFERS POLISHED ON BOTH SIDES Final Report
Warren K. Gladden, Stephen R. Slaughter, Walter M. Duncan (Texas Instruments, Inc., Dallas.), and Aslan Baghdadi Nov. 1988 73 p Prepared in cooperation with Texas Instruments, Inc., Dallas
(PB89-151831; NIST-SP-400-81; LC-88-600601) Avail: SOD HC $3.75 as 003-003-02915-7; NTIS MF A01 CSCL 20L

FORTRAN and PASCAL computer programs which implement an American Society for Testing and Materials (ASTM) test method for the automatic determination of the interstitial oxygen content of silicon are presented. The programs are to be used as illustrative examples by programmers wishing to implement the ASTM algorithm on their computers. Also included are sample data that can be used to test the computer programs. The sample data are included in two forms: in print, and on an MS-DOS floppy disk.
Author

N89-24181# International Centre for Theoretical Physics, Trieste (Italy).
THE DILUTED TRI-DIMENSIONAL SPIN-ONE ISING MODEL WITH CRYSTAL FIELD INTERACTIONS
M. Saber (Mohammed V Univ., Rabat, Morocco) Sep. 1988 25 p Submitted for publication
(DE88-705663; IC-88/261) Avail: NTIS (US Sales Only) HC A03/MF A01

The 3D spin-one Ising models with nearest neighbor ferromagnetic interactions with crystal-field exhibit tricritical behavior are examined. A new method that applies to a wide class of random systems is used to study the influence of site and bond dilution on this behavior. We have calculated temperature-crystal-field-concentration phase diagrams and determined, in particular, the influence of dilution on the zero temperature tricritical temperature. DOE

N89-24182# International Centre for Theoretical Physics, Trieste (Italy).
MEAN FIELD THEORY OF THE SPIN-1 ISING MODEL WITH A RANDOM CRYSTAL FIELD
A. Elkenz and M. Saber (Mohammed V Univ., Rabat, Morocco) Sep. 1988 11 p Submitted for publication
(DE88-705669; IC-88/274) Avail: NTIS (US Sales Only) HC A03/MF A01

A spin-1 Ising model with a random crystal field DELTA (sub 1) has been studied within the mean-field approximation. For the particular two-valued distribution P(DELTA sub 1) = 1/2 (delta (DELTA sub 1 - DELTA (1 + alpha)) + delta (DELTA sub 1 - DELTA (1 - alpha))), three types of diagrams have been found in the (DELTA,T) plane, the type depends on the parameter alpha.
DOE

N89-24183# International Centre for Theoretical Physics, Trieste (Italy).
ELECTRICAL TRANSPORT PROPERTIES OF Hg0.7Cd0.3Te
M. M. Abdul-Gader, S. Aboudy, S. N. Ershov, and T. N. Parker (Royal Holloway and Bedford New Coll., Egham, England) Sep. 1988 17 p Submitted for publication
(DE88-705689; IC-88/309) Avail: NTIS (US Sales Only) HC A03/MF A01

Measurements of the resistivity, Hall effect, and the magnetoresistance of a Hg sub 0.7 Cd sub 0.3 Te sample have been carried out in the temperature region 4.2 K to 77 K and for magnetic fields in the interval 0 to 40 kG. The resistivity, Hall coefficient of the sample were found to be almost constant with temperature below 15K regardless of the presence of magnetic field. Scattering due to ionized impurities or the presence of Te vacancies would be a possible candidate for such a behavior. However, the resistivity and/or the mobility show a monotonic increase, whereas the Hall coefficient drops when the temperature is increased above 15K indicating the dominance of lattice scattering mechanisms at high temperatures. The observed magnetoresistance was found to vary almost linearly with magnetic field which may be partly due to a magnetic-field dependence of the Fermi level. DOE

N89-24184# International Centre for Theoretical Physics, Trieste (Italy).
COHESIVE AND ANHARMONIC ELASTIC PROPERTIES OF MIXED FLUORITE CRYSTALS
R. K. Singh and C. N. Rao (Bhopal Univ., India) Sep. 1988 17 p Submitted for publication
(DE88-705690; IC-88/310) Avail: NTIS (US Sales Only) HC A03/MF A01

The cohesive and anharmonic elastic properties of four mixed fluorite crystals (Ca sub x Sr sub 1-x F sub 2, Sr sub x Ba sub 1-x F sub 2, Ba sub x Ca sub 1-x F sub 2 and Cd sub x Pb sub 1-x F sub 2) have been investigated by means of a three body potential (TBP) model which consists of the long range Coulomb and three body interactions and the short range van der Waals attraction and overlap repulsion effective upto the second neighbor ions. Due to the lack of measured data on cohesive energy, third order elastic constants and pressure derivatives of the second order elastic constants of mixed fluorites, the accuracy of the present results has been tested by comparing them with the so-called experimental results generated by the application of Vegard's law to their corresponding experimental values for the host fluorites. DOE

N89-24185# International Centre for Theoretical Physics, Trieste (Italy).
THE ELECTRONIC STRUCTURE OF GaAs SUB 1-x P SUB x AND GaSb SUB 1-x P SUB x CALCULATED USING THE RECURSION METHOD
M. El-Hasan and M. Tomak (Middle East Technical Univ., Ankara, Turkey) Oct. 1988 17 p Submitted for publication
(DE88-705702; IC-88/330) Avail: NTIS (US Sales Only) HC A03/MF A01

The electronic structure calculation of GaAs sub 1-x P sub x and GaSb sub 1-x P sub x alloys using the recursion method is reported. A five orbitals, sp sup 3 s*, per atom model is used in the tight-binding representation of the Hamiltonian. The local density of states are calculated for Ga, As, Sb and P-sites, in a cluster of 216 atoms, the results are reasonably in good agreement with previous calculations. DOE

N89-24186# California Univ., Berkeley. Lawrence Berkeley Lab. Materials and Chemical Sciences Div.
SITE OCCUPANCY/VALENCE MEASUREMENTS USING CHANNELLING AND RELATED EFFECTS IN MICROANALYSIS
Kannan M. Krishnan Dec. 1988 16 p Presented at the Magnetic Materials Workshop, Santa Rosa, CA, 14-18 Nov. 1988 Submitted for publication
(Contract DE-AC03-76SF-00098)
(DE89-007658; LBL-26580; CONF-8811176-1) Avail: NTIS HC A03/MF A01

The current status of a novel crystallographic technique to determine specific-site occupations of elemental additions in crystalline materials, using the channelling or Borrman effect in electron diffraction is discussed. This technique is based on the effect of incident beam orientations on the intensities of either the characteristic X-ray emissions or the characteristic electron energy-loss edges. In general, this technique is in good agreement with other well established methods such as X-ray and neutron diffraction but has superior spatial resolution. It involves no

adjustable parameters, external standards or special specimen preparations; can distinguish neighbors in the periodic table; is very accurate and is applicable to trace elemental concentrations. In the Energy-loss Electrons in Transmission formulation, the technique can also provide specific site valence information. Finally, the applicability to the study of site occupancies in magnetic materials (spinels, Sm2(Co,TM)17 alloys, {Y,RE)3Fe5O12 epitaxial films, etc.) has been well demonstrated. DOE

N89-24187# Kernforschungsanlage, Juelich (Germany, F.R.). Inst. fuer Grenzflaechenforschung und Vakuumphysik.
STRUCTURE AND GRID DYNAMICS OF ULTRATHIN EPITAXIAL Ag AND Fe FILMS ON Ni(100) AND Cu(100) SUBSTRATES Thesis - Technische Univ., Aachen [STRUKTUR UND GITTERDYNAMIK ULTRADUENNER EPITAKTISCHER SILBER- UND EISENFILME AUF Ni(100)- UND CU(100)-SUBSTRATEN]
Winfried Daum Jul. 1988 107 p In GERMAN; ENGLISH summary
(JUEL-2221; ISSN-0366-0885; ETN-89-93965) Avail: NTIS HC A06/MF A01

The surface phonon dispersions of ultrathin epitaxial Ag films on Ni(100) and Cu(100) substrates and epitaxial Fe films on a Cu(100) substrate were studied using inelastic scattering of slow electrons. The experimental data are compared with lattice dynamical model calculations and conclusions about the atomic force field within the films are drawn. For the epitaxial systems investigated the relation between structure, epitaxial growth, and microscopic surface stress is discussed. As the film thickness is increased the structural and surface lattice dynamical properties of the films pass into those of the (111) surface of bulk Ag. The specific influence of the substrate on the surface phonon dispersion decreases rapidly with increasing film thickness. The dispersion of the surface mode for the bilayer is essentially identical for both substrates. The transition from a two-dimensional to a three-dimensional Ag crystal with the (111) surface is reflected in the surface phonon dispersion curves. ESA

N89-24188# Helsinki Univ. of Technology, Espoo (Finland). Dept. of Technical Physics.
NUCLEAR MAGNETISM IN COPPER AND SILVER: THEORY AND EXPERIMENTS Ph.D. Thesis
Arne Oja 1988 47 p Sponsored by the Academy of Finland and the Finnish Cultural Foundation
(ISBN-952-900-084-7; ETN-89-94218) Avail: NTIS HC A03/MF A01

Metals of interest for a nuclear-ordering experiments are described. Indirect spin-spin interactions vary widely in these systems, giving rise to correspondingly large variations in the ordering temperatures. The methods used to obtain information about indirect interactions are discussed. Experiments on nuclear ordering in copper and in other metals are reviewed. Theoretical understanding of the ordered phases of copper is summarized. ESA

N89-24189# Helsinki Univ. of Technology, Espoo (Finland). Dept. of Technical Physics.
MAGNETIC SUSCEPTIBILITY AND NEUTRON DIFFRACTION EXPERIMENTS ON NUCLEAR ORDERING IN COPPER Ph.D. Thesis
Teppo Jyrkkio 1988 33 p Sponsored by the Academy of Finland; the Finnish Cultural Foundation, and the Emil Aaltonen Foundation, Finland
(ISBN-951-754-573-8; ETN-89-94219) Avail: NTIS HC A03/MF A01

Experimental curves of entropy and susceptibility versus temperature for copper nuclear spins down to the ordered state were obtained. Impurities and anomalous spin-lattice relaxation in copper at submilli-Kelvin temperatures were observed. Phase diagrams for spontaneous nuclear ordering in copper were derived. Nuclear antiferromagnetic ordering in copper was investigated. The feasibility of neutron diffraction experiments on ordered copper nuclei at nano-Kelvin temperature was studied. Neutron scattering experiments on nuclear magnets were carried out. Calibration and applications of polarized neutron thermometry at milli- and micro-Kelvin temperatures is described.Observation of nuclear antiferromagnetic order in copper by neutron diffraction at nano-Kelvin temparatures is reported. ESA

N89-24190# Brookhaven National Lab., Upton, NY.
QUASIELASTIC AND INELASTIC SPIN FLUCTUATIONS IN SUPERCONDUCTING La2-xSrxCuO4
R. J. Birgeneau, Y. Endoh, Yoshikazu Hidaka, K. Kakurai, M. A. Kastner, T. Murakami, G. Shirane, T. R. Thurston (Massachusetts Inst. of Tech., Cambridge.), and K. Yamada 1988 11 p Presented at the 2nd NEC Symposium on Fundamental Approach to New Material Phases, Tokyo, Japan, 24 Oct. 1988 Sponsored in part by US-Japan Cooperative Neutron Scattering Program; Japanese Ministry of Education, Science and Culture
(Contract DE-AC02-76CH-00016; NSF DMR-85-01856; NSF DMR-87-19217)
(DE89-008157; BNL-42266; CONF-8810256-1) Avail: NTIS HC A03/MF A01

We review the results of recent neutron scattering studies of the spin fluctuations in samples of La1.89Sr0.11CuO4 which are approximately 80 percent superconducting with T(sub c) = 10 K. The structure factor, S(Q), reflects three dimensional modulated spin correlations with an in-plane correlation length of order 18 + or - 6 A. The fluctuations evolve with temperature from being predominantly dynamic at high temperatures to mainly quasielastic (absolute value of delta E is less than 0.5 MeV) at low temperatures. No significant differences are observed in the normal and superconducting states. DOE

N89-24191# Oak Ridge National Lab., TN. Solid State Div.
ZINC OXIDE VARISTOR TIME RESPONSE
F. A. Modine, R. W. Major, S. I. Choi, L. B. Bergman, and M. N. Silver (North Carolina Univ., Chapel Hill.) Feb. 1989 15 p Presented at the American Ceramic Society Conference on Zinc Oxide Varistors: Science and Technology, Schenectady, NY, 5 Dec. 1988 Submitted for publication
(Contract DE-AC05-84OR-21400)
(DE89-008234; CONF-881275-1) Avail: NTIS HC A03/MF A01

The application of a voltage to a zinc oxide varistor produces transient currents that persist on a time scale extending from 10(-8) to 10(5) seconds at the least. The transient currents are characterized by a power-law time dependence (i.e., I = I sub o/t sup m, where m is a little less than unity) and a weak temperature dependence that is described by a thermal activation energy of about 100 meV or less. The time dependence is confirmed by an ac admittance that increases as a noninteger power of the frequency (i.e., Y = Y(j omega) sup m), with Fourier theory providing the connection between the time and frequency measurements. Also, the transient currents are accompanied by changes in the ac admittance measured at fixed frequencies that reveal similar time and temperature dependencies. The transient currents are not well understood, but they are typical of the non-Debye electrical response that is found in many materials. An explanation of the transients is obtained if a distribution of relaxation times is assumed. DOE

N89-24192# Oak Ridge National Lab., TN. Metals and Ceramics Div.
DEFORMATION TWINNING IN ORDERED INTERMETALLIC COMPOUNDS
M. H. Yoo, C. L. Fu, and J. K. Lee 1988 8 p Presented at the Fall Meeting of the Materials Research Society, Boston, MA, 28 Nov. 1988
(Contract DE-AC05-84OR-21400)
(DE89-008748; CONF-881155-53) Avail: NTIS HC A02/MF A01

Mechanistic understanding of deformation twinning in ordered superlattice structures is reviewed, and the inter-relationships between twinning and generalized plastic flow or fracture toughness are discussed. While general discussions refer to all the fcc-based and bcc-based cubic and noncubic ordered intermetallic alloys,

specific calculations of the energetic and kinetic aspects of deformation twinning are made for TiAl. The importance of the twin-slip conjugate relationship on high temperature mechanical properties is emphasized. Discussion is given of possible effects of macro- and micro-alloying on twinning propensity. DOE

N89-24193# Lawrence Livermore National Lab., CA.
SHOCK COMPACTION OF YBa2Cu3O7-x AND HoBa2Cu3O7-x POWDERS IN A METAL MATRIX
W. J. Nellis, C. L. Seaman, M. B. Maple, E. A. Early, J. B. Holt, M. Kamegai, G. S. Smith, D. G. Hinks, and D. Dabrowski (Argonne National Lab., IL.) Feb. 1989 18 p Presented at the International Symposium on High Temperature Superconducting Oxides: Processing and Related Properties, Las Vegas, NV, 27-28 Feb. 1989
(Contracts W-7405-eng-48; W-31-109-eng-38)
(DE89-008827; UCRL-100472; CONF-890216-1) Avail: NTIS HC A03/MF A01

Shock compaction of powders has several features with potential for processing high-J sub c oxide superconductors. Because compaction occurs by applying 100 kbar pressures on fast microsec timescales, compressive energy and heating are localized on powder particle boundaries. By using single-crystallite particles the method could be used to heat and bond grain boundaries while maintaining their interiors cool and stable. Shock processing of ceramic powders produces defects and fine grain size, which might increase flux pinning and J sub c. This paper summarizes results of compactions using single-phase orthorhombic powder specimens of YBa2Cu3O(7-x) or HoBa2Cu3O(7-x) mixed with 30 vol percent Ag. Each powder specimen weighed less than 0.2 g. Dynamic pressures in the range 29 to 217 kbar were generated by impact of a 5 g plastic projectile at velocities in the range 0.77 to 3.26 km/s. Projectiles were accelerated with a two-stage light-gas gun. Representative pressure histories were calculated with a two-dimensional finite-element computer code. X-ray diffraction, optical microscopy, magnetic susceptibility, and electrical resistance measurements were made on the recovered compacts. X-ray and magnetic data show these oxide powders to be robust to shock compaction, essentially maintaining their chemical and crystal structures, oxygen stoichiometry, and bulk superconductivity to shock pressures well above 100 kbar. The dependence of magnetic susceptibility on shock pressure is interpreted by a decrease in grain size which is consistent with the optical microscopy. At 167 kbar some tetragonal phase is formed. DOE

N89-24194# Massachusetts Inst. of Tech., Cambridge. Dept. of Materials Science and Engineering.
GRAIN BOUNDARIES Progress Report, 15 Jun. 1988 - 14 Jun. 1989
R. W. Balluffi and P. D. Bristowe Feb. 1989 12 p
(Contract DE-FG02-87ER-45310)
(DE89-008881; DOE/ER-45310/17) Avail: NTIS HC A03/MF A01

The present document is a progress report describing the work accomplished during the second year (June 15, 1988 to June 14, 1989) of our three-year grant to study grain boundaries which started 15 June 1987. The research that was proposed initially for this period consisted of the following: (1) study of the atomistic structure of grain boundaries by means by combined X-ray diffraction and computer modeling; and (2) study of grain boundary phase transitions by electron microscopy and computer modeling. DOE

N89-24195# Sandia National Labs., Albuquerque, NM.
MONITORING THIN FILM PROPERTIES WITH SURFACE ACOUSTIC WAVE DEVICES: DIFFUSION, SURFACE AREA AND PORE SIZE DISTRIBUTION
G. C. Frye, S. J. Martin, A. J. Ricco, and C. J. Brinker 1988 21 p Presented at the 196th American Chemical Society National Meeting, Los Angeles, CA, 25 Sep. 1988
(Contract DE-AC04-76DP-00789)
(DE89-009379; SAND-88-0943C; CONF-880912-28) Avail: NTIS HC A03/MF A01

The ability of surface acoustic wave (SAW) devices to monitor adsorption of N sub 2 onto the surfaces of porous films and diffusion of species into polymer films has been demonstrated. Calculations based on the N sub 2 adsorption isotherms illustrate how sol-gel solution chemistry can be used to tailor the surface area and pore size distribution of thin films. BET surface areas from unity to over 30 cm squared/cm squared of film have been obtained with median pore diameters from less than 0.4 nm to greater than 6 nm. SAW frequency transients occurring during the diffusion of small molecular species into polymer films have been used to obtain diffusion coefficients from 10 (-9) to 10 (-15) cm squared/sec. DOE

N89-24196# General Atomics Technologies Corp., San Diego, CA.
HIGH-TEMPERATURE CERAMIC SUPERCONDUCTORS Quarterly Progress Report No. 2, 1 Oct. - 31 Dec. 1988
K. S. Mazdiyasni, K. C. Chen, B. W. McQuillan, F. C. Montgomery, and Patti Tsai 6 Jan. 1989 29 p
(Contract N00014-88-C-0714)
(AD-A205321; GA-C19465) Avail: NTIS HC A03/MF A01 CSCL 20/3

This program has been divided into six tasks: (1) metal alkoxide synthesis and processing, (2) microstructural evaluation and property measurement, (3) electrical and magnetic property measurement, (4) superconductor ceramic processing, (5) component fabrication and demonstration, and (6) reporting. GRA

N89-24197# State Univ. of New York, Buffalo. Dept. of Chemistry.
PHOTOABSORPTION OF MOLECULES AT CORRUGATED THIN METAL FILMS
P. T. Leung, Young S. Kim, and Thomas F. George Feb. 1989 31 p
(Contract N00014-86-K-0043)
(AD-A205325; UBUFFALO/DC/89/TR-92) Avail: NTIS HC A03/MF A01 CSCL 07/2

A phenomenological study has been carried out for the photoabsorption of molecules in the vicinity of a corrugated thin metal film. In particular, perturbative results for a grating silver film have been obtained to first order in the corrugation parameter, where the effect of the incident field coupled with the long-range surface plasmon is observed. Based on the different coupling nature between the radiations from the incident plane wave and from the molecular dipole to the substate film, it is proposed that, through control of the various parameters of the film, enhanced selective photoabsorption may be achieved. GRA

N89-24198# State Univ. of New York, Buffalo. Dept. of Chemistry.
DECAY OF MOLECULES AT CORRUGATED THIN METAL FILMS
P. T. Leung, Young S. Kim, and Thomas F. George Feb. 1989 33 p
(Contract N00014-86-K-0043)
(AD-A205487; UBUFFALO/DC/89/TR-91) Avail: NTIS HC A03/MF A01 CSCL 09/1

The problem of the decay rate for molecules at corrugated thin metal films is considered theoretically via a classical phenomenological approach by generalizing a previous theory for a single rough surface. In particular, numerical results are worked out in detail for grating films with various possible arrangements of the two grating surfaces, and for both the cases with a supported and free-standing film. Effects due to cross-coupling into the long- and short-range surface plasmons are observed, and correlations to recent experiments performed by the Rochester group are made. GRA

N89-24199# Naval Postgraduate School, Monterey, CA.
ATOMIC RELAXATION AND VACANCY-INTERSTITIAL RECOMBINATION IN Zr AND Zr3Al M.S. Thesis
Vito M. Menzella Dec. 1988 96 p
(AD-A205664) Avail: NTIS HC A05/MF A01 CSCL 20/5

This thesis examines two problems associated with crystalline defects in the materials Zr and Zr3Al, by means of a molecular dynamics simulation. In the first problem, the relaxed configuration around a single vacancy, a di-vacancy and a tri-vacancy is computed by introducing the defect into a perfect lattice and dynamically relaxing the crystal until it attains equilibrium. The results are in qualitative agreement with static studies but show clearly that first and second neighbors have different relaxed states depending on their configuration in the initial crystal lattice. GRA

N89-24200# University of Southern California, Los Angeles. Dept. of Electrical Engineering and Electrophysics.
ATOMIC LAYER EPITAXY. ATOMIC LAYER EPITAXY OF 3-5 COMPOUND SEMICONDUCTORS BY THERMAL AND LASER-ASSISTED METALORGANIC CHEMICAL VAPOR DEPOSITION Final Report
Steven P. DenBaars 31 Jan. 1989 251 p
(Contract N00014-85-K-0331)
(AD-A205699) Avail: NTIS HC A12/MF A01 CSCL 20/2

Atomic Layer Epitaxy (ALE) is a promising variation of conventional vapor phase epitaxy which achieves uniform growth of ultra-thin epitaxial layers by a self-limiting monolayer by monolayer deposition process. By developing a new regime of metalorganic chemical vapor deposition (MOCVD) growth, in which saturated surface reactions control the growth, it is possible to alternately deposit monolayers of column 3 and column 5 elements so that only one monolayer of the 3-5 compound semiconductor is deposited in every cycle of the deposition. In this thesis, ALE growth of single crystal GaAs, as well as AlAs and GaAs/AlGaAs heterostructures and devices is demonstrated. We have been able to grow extremely uniform ultra-thin epitaxial layers and quantum wells (QWs) with thickness variations of less than one monolayer per cm over an entire sample in an optimized reactor using ALE. The observed dependence of the growth rate on temperature and trimethylgallium flux is modeled by first order adsorption kinetics utilizing measured reaction rate constants. The low temperature photoluminescence (PL) of ALE grown GaAs QW's exhibit narrow line intrinsic luminescence with linewidths comparable to the best reported values by conventional MOCVD. GRA

N89-24201# Air Force Inst. of Tech., Wright-Patterson AFB, OH. School of Engineering.
CHARACTERIZATION OF SEMICONDUCTOR DEVICE PROCESSING ETCHANT SOLUTIONS FOR GaAs AND p+ GaAs LAYERS EMPLOYED IN AlxGa(1-x)As/GaAs MODFETs AND RELATED HETEROJUNCTION DEVICES M.S. Thesis
Brett F. Mayhew 30 Nov. 1988 137 p
(AD-A205772; AFIT/GE/ENG/88D-26) Avail: NTIS HC A07/MF A01 CSCL 07/2

The etch rates of GaAs, p+ GaAs, Al(x)Ga(1-x)As and n-Al(x)Ga(1-x)As were examined with respect to solution composition and pH in an effort to determine a solution that will selectively etch only GaAs from the area between the gate-and-source and gate-and-drain of a p+ GaAs/Al(x)Ga-(1-x)As/GaAs Modulation-Doped Field-Effect Transistor. The measurement of the etch rates for GaAs and Al(x)Ga(1-x)As was approached from different perspectives. First, a method based upon corrosion testing, that determines etch rates from weight loss, was attempted. A second method involved the use of a Fischione Twin-Jet Electropolisher. Both techniques were verified against a known method of etch depth measurement using a profilometer. A selective etch would also be useful in the last step of the fabrication process of the (ES)MODFET. GRA

N89-24202# Department of the Army, Washington, DC.
SUPERCONDUCTING PYX STRUCTURES Patent Application
Herbert A. Leupold, inventor (to Army) 24 Feb. 1989 17 p
Filed 24 Feb. 1989
(AD-D013958; US-Patent-Appl-SN-316710) Avail: NTIS HC A03/MF A01 CSCL 20/3

A permanent magnet structure comprising one or more truncated hollow cylindrical flux source (HCFS) segments with the end faces of each segment covered by superconducting sheets is discussed. In the case of a plurality of axially aligned segments, the array may be arranged to provide a periodic magnet structure suitable for use in a wiggler. GRA

N89-24203# Illinois Univ., Urbana. Coordinated Science Lab.
SOME 3-5 HETEROJUNCTION STRUCTURES AND HIGH SPEED DEVICES Final Report, 1 Jan. - 31 Dec. 1988
Hadis Morkoc 17 Feb. 1989 62 p
(Grant AF-AFOSR-0111-86; AF Proj. 2305)
(AD-A205946; AFOSR-89-0325TR) Avail: NTIS HC A04/MF A01 CSCL 20/12

This effort explored the new phenomena in high speed semiconductor devices and structures intended for optoelectronics. A detailed investigation of the collector breakdown properties in GaAs/AlGaAs HBT's has revealed light emission at junctions edges for the first time. The spectral features when analyzed led to the determination of electron and hole threshold energies for ionization for the first time. Additional features observed may shed light into the processing mechanisms not otherwise conveniently accessible. Other areas, e. g., modulation doped FET's, extremely low resistance nonalloyed ohmic contacts, HBT's on InP, quantum wells, optical properties of bulk AlGaAs and InGaAs were among many projects that were explored. GRA

N89-24204# Oregon Graduate Center for Study and Research, Beaverton. Dept. of Materials Science and Engineering.
FUNDAMENTAL AND APPLIED STUDIES OF EXPLOSIVELY FABRICATED HIGH-TEMPERATURE SUPERCONDUCTING FIXTURES Quarterly Technical Report, 1 Sep. - 30 Nov. 1988
L. E. Murr 30 Nov. 1988 39 p
(Contract N00014-88-C-0684; DARPA Order 6560)
(AD-A205953) Avail: NTIS HC A03/MF A01 CSCL 20/3

We have explosively fabricated a wide variety of monolithic superconductor metal matrix fixtures in a variety of tooling plate geometries, including a design which allowed the channels to be evacuated prior to and during the fabrication process. Tooling plates and fabricated monoliths were utilized in both silver and copper. Channel schedules included pure high quality YBa2Cu307 superconducting powder having a size distribution of roughly 0.2 to 20 micro, and mixtures of superconducting (SC) powder with metal powders: 10, 20 and 30 percent silver powder primarily in the silver tooling plate, and the same volume fractions of metal powder loading in copper tooling plates. We were able to demonstrate that tape and ribbon could be easily cold rolled in a multiple pass rolling process from explosively-fabricated linear, monolithic precursors by as much as 95 percent (to a tape thickness of 0.15 mm). The silver tapes have the convenience of allowing for an annealing treatment or treatment series which can connect the superconducting tape core for supercurrent transport. GRA

N89-24205# Washington State Univ., Pullman. Dept. of Chemistry.
ASSIGNMENT OF THE CHARGE-TRANSFER EXCITED STATES OF BIS(N-HETEROCYCLIC) COMPLEXES OF COPPER(I) Interim Report
W. L. Parker and G. A. Crosby 21 Mar. 1989 20 p Submitted for publication
(Contract N00014-87-K-0444; NSF CHE-81-19060; NSF CHE-84-21282)
(AD-A206012; ONR-TR-7) Avail: NTIS HC A03/MF A01 CSCL 07/1

Charge-transfer (CT) excited states of metal complexes are provoking intense study, particularly within the context of attempts to design efficient solar energy conversion processes. Since several classes of molecules containing the copper(I) ion have been observed to emit light in fluid solution, attention has been shown to induce electron transfer reactions, complete group theoretic

assignments of the nature of the electronic states responsible for the visible absorption and emission spectra have not yet appeared. In this study we focus on the rigid matrix spectra of (Cu(NN)2) species (NN = substituted 2,2 prime-bipyridine or substituted 1,10-phenanthroline) and propose a group theoretical model to rationalize the results of extensive photophysical measurements on these interesting substances. GRA

N89-24206# Weizmann Inst. of Science, Rehovoth (Israel).
QUASI-LIQUID CRYSTALLINE MATERIALS WITH SPECIAL ELECTRO-OPTIC PROPERTIES Final Report, 1 Dec. 1985 - 30 Nov. 1988
Valeri Krongauz Dec. 1988 32 p
(Contract DAJA45-85-C-0030)
(AD-A206015) Avail: NTIS HC A03/MF A01 CSCL 07/6

Photo/thermochromic liquid crystals and liquid crystal polymers were synthesized by combination of spiropyran and mesogenic groups in one low molar mass molecule or macromolecules. The spiropyran-merocyanine conversion affects the mesophase structure and results in formation of non-centrosymmetric nonlinear optical material, generating second harmonics. Aggregation of merocyanine molecules leads to a new photomechanical effect in low molar mass compounds and to the rheo-optical and boundary spectral effects in the side chain liquid crystal copolymers containing spiropyran side groups. Polychromic phototransformations in the copolymers as well as accompanying structural changes enable use of the polymer films for optical information storage. GRA

N89-24207# Perkin-Elmer Corp., Danbury, CT. Applied Science and Technology Sector.
LATTICE SYMMETRIES AND THERMAL EXPANSION
G. M. Gallatin 29 Mar. 1989 9 p Presented at the SPIE Technical Symposium on Aerospace Sensing, Orlando, FL, Mar. 1989
(Contract N00014-86-C-0435)
(AD-A206045; TR-1) Avail: NTIS HC A02/MF A01 CSCL 20/2

It is well known that many of the thermomechanical properties of crystals are due to anharmonic effects in the motion of the atoms. The anharmonic terms in the potential energy which lead to this behavior depend, in part, on the symmetry of the crystal lattice. Thus the thermomechanical properties of the crystal, including the coefficient of thermal expansion, depend on the point group of the lattice. In order to study this symmetry dependence the path integral representation of the density matrix in the adiabatic approximation is used here to evaluate the thermal expectation value of the atomic positions. From this result the approximate scaling behavior of the atomic displacement with temperature, mass, bond strength (harmonic coupling), and anharmonic coupling is determined. The path integral calculation is fully quantum mechanical and can be used, in principle, to derive all the thermomechanical properties of the crystal within the adiabatic approximation. GRA

N89-24208# Stanford Univ., CA. Dept. of Materials Science and Engineering.
FUNDAMENTAL STUDIES OF THE MECHANICAL BEHAVIOR OF MICROELECTRONIC THIN FILM MATERIALS Final Technical Report, Jan. 1986 - Dec. 1988
William D. Nix Jan. 1989 50 p
(Grant AF-AFOSR-0051-86)
(AD-A206057; AFOSR-89-0365TR) Avail: NTIS HC A03/MF A01 CSCL 07/2

It is appropriate to note that before this research program began, very little work had been done in universities on the mechanical properties of microelectronic thin film materials. As a result, much of our early work involved the development of experimental techniques, such as sub micron indentation and wafer curvature measurement, to study stresses and mechanical properties of thin films on substrates. Interest in these developments is indicated by the accepted publications and invited oral presentations listed at the end of this report. The recent MRS Symposium on Thin Films: Stresses and Mechanical Properties was an outgrowth of the research work started under this grant. GRA

N89-24209# Pennsylvania Univ., Philadelphia. Dept. of Physics.
MOLECULAR OPTICS NONLINEAR OPTICAL PROCESSES IN ORGANIC AND POLYMERIC CRYSTALS AND FILMS Final Report, Jun. 1985 - Apr. 1988
A. G. Garito Apr. 1988 151 p
(Contract F49620-85-C-0105)
(AD-A206372; AFOSR-89-0360TR) Avail: NTIS HC A08/MF A01 CSCL 07/6

Experimental and theoretical studies have firmly established that the largest second and third order microscopic nonlinear optical susceptibilities occur in organic and polymer systems. This major development has resulted in studies in optical bistability, phase conjugate wave generation, and neural networks. The physical microscopic origin and mechanism of second and third order nonlinear optical responses in conjugate polymers has been investigated. New theoretical concepts relating to the many-body nature of highly charge-correlated pi-electron states have been developed. The nonlinear optical responses of new pi-electron topological structures have been calculated, optical bistability in nonlinear optical conjugated polymers has been demonstrated. GRA

N89-24210# Massachusetts Univ., Amherst. Dept. of Chemical Engineering.
IN SITU MECHANISTIC STUDIES OF MOCVD GROWTH OF 3/5 SEMICONDUCTORS Final Report, 1 Aug. 1985 - 30 Sep. 1988
William C. Conner 7 Feb. 1989 9 p
(Contract DAAG29-85-K-0204)
(AD-A206396; ARO-22392.5-MS) Avail: NTIS HC A02/MF A01 CSCL 07/2

Our initial studies of metal organic chemical vapor deposition for the growth of 3-5 semiconductors have developed in situ techniques to follow the growth process both in the gas phase and in the on the surface (in the sorbed state). The results have provided a more direct perspective of the mechanisms and kinetics of the reaction between group 5 alkyls and group 3 hydrides. Both Fourier transform infrated spectroscopy (FTIR) and detailed surface spectroscopy have been employed to study the course of the reaction and the nature of the solid products. We conclude that the crucial steps of the reaction occur on the surface of the solid substrate. Although gas phase decomposition of the group 5 organometallic occurs, the reactions leading to the formation of 3-5 bonds proceed on the surface. This leads us to focus on the availability of adsorbed atomic hydrogen as it relates to the removal of alkyls from the group 5 metal organic in the continuation of this research. GRA

N89-24211# American Society for Engineering Education, Washington, DC.
ALTERNATE ARSENIC AND ANTIMONY SOURCES FOR THE OMCVD FABRICATION OF SEMICONDUCTORS Final Technical Report
John C. Pazik 1988 42 p
(Contract N00014-88-J-1072)
(AD-A206483) Avail: NTIS HC A03/MF A01 CSCL 07/3

There has been considerable interest in the effect of sterically demanding ligands on the synthesis and properties of organometallic derivatives of the main group elements. Organometallic compounds incorporating such ligands have been shown to exhibit some unusual properties. Once isolated, the neo-Pentylarsenic (III) bromides were used as starting materials for synthesis of the primary and secondary arsines, AsNpH2 and AsNp2H. Since these compounds were of direct interest as OMCVD precursors for the growth of GaAs, vapor pressure measurements were made in addition to the characterization data described above. In addition the reactivity of the primary and secondary arsines with trimethylgallium was examined and resulted in the preparation

of the new compounds, Np(H)AsGaMe2 and Np2AsGaMe2. The properties of these new (arsenic) gallium were described and were compared to those of the (trimethylsily1) methyl analogs. GRA

N89-24212# Kernforschungsanlage, Juelich (Germany, F.R.).
INVESTIGATION OF ELECTRONIC STATES IN NONMAGNETIC SINGLE CRYSTALS WITH SPIN-RESOLVED PHOTOEMISSION Thesis - Technische Hochschule, Aachen [UNTERSUCHUNG ELEKTRONISCHER ZUSTAENDE IN UNMAGNETISCHEN EINKRISTALLEN MIT SPINAUFGELOESTER PHOTOEMISSION]
Joachim Garbe Aug. 1988 122 p In GERMAN; ENGLISH summary
(JUEL-2228; ISSN-0366-0885; ETN-89-94409) Avail: NTIS HC A06/MF A01

Electronic states in nonmagnetic single crystals using spin-resolved photoemission with circularly polarized light are investigated. Experiments are carried out on the symmetric Pt(111) surface with normally incident light to verify theoretical predictions for the spin polarization from the symmetry of the electronic wave functions and the relativistic dipole selection rules. Using the same scattering geometry experiments are performed with the low symmetric Pt(110) surface where the spin polarization can not be predicted by group theoretical methods. At the TaC(100) surface, spin and angle resolved photoemission with circularly polarized light of variable photon energy is examined. ESA

77 THERMODYNAMICS AND STATISTICAL PHYSICS

Includes quantum mechanics; theoretical physics; and Bose and Fermi statistics.

For related information see also *25 Inorganic and Physical Chemistry* and *34 Fluid Mechanics and Heat Transfer.*

N89-24213# National Inst. of Standards and Technology, Boulder, CO. Chemical Engineering Science Div.
MICROPOROUS FUMED-SILICA INSULATION BOARD AS A CANDIDATE STANDARD REFERENCE MATERIAL OF THERMAL RESISTANCE
David R. Smith and Jerome G. Hust Oct. 1988 25 p
(Contract ORNL-IA-21428)
(PB89-148373; NISTIR-88/3901) Avail: NTIS HC A03/MF A01 CSCL 20M

Measurements of apparent thermal conductivity of microporous fumed-silica insulation board are reported in order to provide a basis for certifying it as a Standard Reference Material (SRM) of thermal resistance. These data, for a pair of specimens having a mean density of 301 kg/cu m encompass a range of temperature from 321 to 723 K and environmental gas pressures at and below ambient atmospheric pressure (40 to 83.7 kPa). Detailed analyses and intercomparisons of previously published data are given. Correlations of thermal conductivity with temperature and with pressure are given which represent the data within a standard deviation of 0.2 percent. This fumed-silica material has a thermal conductivity of 19.68 mW/(mK) at 300 K and is suitable for use as an SRM of very low conductivity from room temperature up to temperatures beyond 720 K (450 C). Great care in handling this material is necessary because of its fragility. Author

N89-24214# Cornell Univ., Ithaca, NY.
EXPERIMENTAL AND THEORETICAL STUDIES OF DENSE FLUID MIXTURES Progress Report, 1 Sep. 1986 - 28 Sep. 1989
J. A. Zollweg Feb. 1989 4 p
(Contract DE-FG02-86ER-13623)
(DE89-008882; DOE/ER-13623/2) Avail: NTIS HC A02/MF A01

Experimental measurements of thermodynamic properties for pure fluids using equipment which we constructed have been carried out. The direct-weighing densimeter contains a pressure vessel which hangs in an oven from a high-capacity precision digital balance. It is capable of measurements at pressures to 200 MPa. The speed-of-sound apparatus is capable of measurements to 400 MPa using the pulse-echo-overlap technique. Equation of state calculations, using data which had been obtained earlier, were performed. DOE

N89-24215*# Fermi National Accelerator Lab., Batavia, IL. Astrophysics Center.
THE FORMATION OF TOPOLOGICAL DEFECTS IN PHASE TRANSITIONS
Hardy M. Hodges (Chicago Univ., IL.) Apr. 1989 33 p
(Grant NAGw-1340)
(NASA-CR-185318; NAS 1.26:185318; Fermilab-Pub-89/108-A)
Avail: NTIS HC A03/MF A01 CSCL 20H

It was argued, and fought through numerical work that the results of non-dynamical Monte Carlo computer simulations cannot be applied to describe the formation of topological defects when the correlation length at the Ginzburg temperature is significantly smaller than the horizon size. To test the current hypothesis that infinite strings at formation are essentially described by Brownian walks of size the correlation length at the Ginzburg temperature, fields at the Ginzburg temperature were equilibrated. Infinite structure do not exist in equilibrium for reasonable definitions of the Ginzburg temperature, and horizons must be included in a proper treatment. A phase transition, from small-scale to large-scale string or domain wall structure, is found to occur very close to the Ginzburg temperature, in agreement with recent work. The formation process of domain walls and global strings were investigated through the breaking of initially ordered states. To mimic conditions in the early Universe, cooling times are chosen so that horizons exist in the sample volume when topological structure formation occurs. The classical fields are evolved in real-time by the numerical solution of Langevin equations of motion on a three dimensional spatial lattice. The results indicate that it is possible for most of the string energy to be in small loops, rather than in long strings, at formation. Author

80 SOCIAL SCIENCES (GENERAL)

Includes educational matters.

N89-23911*# National Aeronautics and Space Administration. Lewis Research Center, Cleveland, OH.
AGE DISTRIBUTION AMONG NASA SCIENTISTS AND ENGINEERS
Michael L. Ciancone *In* NASA, Marshall Space Flight Center, The 23rd Aerospace Mechanisms Symposium Mar. 1989 p 279-287 (For primary document see N89-23892 17-39)
Avail: NTIS HC A15/MF A01 CSCL 20K

81 ADMINISTRATION AND MANAGEMENT

Includes management planning and research.

N89-24216*# National Aeronautics and Space Administration. Lewis Research Center, Cleveland, OH.
[COMPREHENSIVE REPORT OF AEROPROPULSION, SPACE PROPULSION, SPACE POWER, AND SPACE SCIENCE APPLICATIONS OF THE LEWIS RESEARCH CENTER] Annual Report, 1988
1988 167 p Original contains color illustrations
(NASA-TM-100925; NAS 1.15:100925) Avail: NTIS HC A08/MF A01 CSCL 05A

The research activities of the Lewis Research Center for 1988 are summarized. The projects included are within basic and applied technical disciplines essential to aeropropulsion, space propulsion, space power, and space science/applications. These disciplines are materials science and technology, structural mechanics, life prediction, internal computational fluid mechanics, heat transfer, instruments and controls, and space electronics. A.D.

N89-24217# Air Force Office of Scientific Research, Bolling AFB, Washington, DC.
US AIR FORCE RESEARCH TECHNOLOGY AREA PLAN, FY 1989 Final Report
Sep. 1988 109 p
(AD-A205304; AFOSR-89-0262TR) Avail: NTIS HC A06/MF A01 CSCL 05/1

The Research Technology Area Plan (TAP) describes the activities funded under the Defence Research Science Program. Thirteen projects are listed and briefly described. E.R.

N89-24218# Air Force Human Resources Lab., Brooks AFB, TX.
AIR FORCE HUMAN RESOURCES LABORATORY R AND D ACCOMPLISHMENTS AND SERVICES, FY86-FY88 Final Technical Paper, Oct. 1985 - Sep. 1988
Douglas E. Blair Feb. 1989 46 p
(AD-A205312; AFHRL-TR-88-53) Avail: NTIS HC A03/MF A01 CSCL 05/9

This document provides a brief description of research and development accomplishments of the Air Force Human Resources Laboratory and services provided to various customers from fiscal years 1986 to 1988. Some of these accomplishments resulted in interim products and/or capability/feasibility demonstrations which served as building blocks for developing the end products. GRA

82 DOCUMENTATION AND INFORMATION SCIENCE

Includes information management; information storage and retrieval technology; technical writing; graphic arts; and micrography.

For computer documentation see *61 Computer Programming and Software.*

N89-24219* National Aeronautics and Space Administration, Washington, DC.
PATENT ABSTRACTS BIBLIOGRAPHY: A CONTINUING BIBLIOGRAPHY. SECTION 2: INDEXES (SUPPLEMENT 34)
Jan. 1989 507 p
(NASA-SP-7039(34)-Sect-2; NAS 1.21:7039(34)-Sect-2) Avail: NTIS HC A22; NTIS standing order as PB89-911100, $29.00 domestic, $58.00 foreign CSCL 05B

A subject index is provided for over 4600 patents and patent applications for the period May 1969 through December 1988. Additional indexes list personal authors, corporate authors, contract numbers, NASA case numbers, U.S. patent class numbers, U.S. patent numbers, and NASA accession numbers. Author

N89-24220# Defense Logistics Services Center, Battle Creek, MI.
DEFENSE INTEGRATED DATA SYSTEM (DIDS) PROCEDURES MANUAL. VOLUME 8: DOCUMENT IDENTIFIER CODE (DIC) INPUT/OUTPUT (I/O) FORMATS (FIXED LENGTH), CHANGE 3
Oct. 1988 92 p Supplement to DOD-4100.39-M-Vol-8
(PB89-139414; DOD-4100.39-M-Vol-8-Change-3) Avail: NTIS HC A05/MF A01 CSCL 05B

Operating procedures for processing transactions in support of the Federal Catalog System are provided and logistics management information outlined. Procedures address major logistics areas such as supply management, item identification, Interchangeability and Substitutability (I and S), and standardization. Also included is general and administrative information. All DIC and record formats that are Input/Output to/from DLSC in fixed length format are furnished. Author

N89-24221# Defense Logistics Services Center, Battle Creek, MI.
DEFENSE INTEGRATED DATA SYSTEM (DIDS) PROCEDURES MANUAL. VOLUME 2: MULTIPLE APPLICATION PROCEDURES
Oct. 1988 132 p Supersedes PB86-237484
(PB89-139307; DOD-4100.39-M-Vol-2) Avail: NTIS HC A07/MF A01 CSCL 05B

Operating procedures are provided for processing transactions in support of the Federal Catalog System and logistics management information is outlined. Procedures address major logistics areas such as supply management, item identification, interchangeability and substitutability, and standardization. Also included is general and administrative information. The manual consist of 16 volumes. GRA

N89-24222# Environmental Protection Agency, Washington, DC. Office of Information Resources Management.
GEOGRAPHIC INFORMATION SYSTEMS (GIS) GUIDELINES DOCUMENT Final Report
Jan. 1988 131 p
(PB89-132062; EPA/IRM-88/8801) Avail: NTIS HC A01/MF A01 CSCL 05B

The document provides a comprehensive overview of the management and technical issues involved with Geographic Information Systems (GIS) technology at Environmental Protection Agency (EPA). The guidelines are designed to help determine the appropriateness of initiating GIS technology within the agency as well as to serve as a reference for potential EPA and State GIS applications. Author

N89-24223# European Space Agency, Paris (France).
ESABASE: A MOST VERSATILE AND FLEXIBLE SYSTEM ENGINEERING TOOL
Norman Longdon, ed. Sep. 1988 38 p Original contains color illustrations
(ESA-BR-54; ISSN-0250-1589; ETN-89-94236) Copyright Avail: NTIS HC A03/MF A01

The ESABASE is an engineering tool supporting a wide variety of space-specific analyses. It is a framework consisting of data management, processing and application steering utilities, that has a number of application programs connected to it. In ESABASE the space system is described (and documented) in an easily understood language, only once. Appropriate data are automatically extracted from this description and passed to the chosen application as needed. Any changes in the description are thus known by all applications concerned. The applications connected to the framework provide: mass analysis, thermal analysis, outgassing contamination analysis, radiation analysis, spacecraft charging analysis, pointing behavior analysis, occultation analysis, perturbation analysis, atomic oxygen recession analysis, plume-impingement analysis, electrical wiring monitoring (harness), and attitude and orbit control system analysis. ESA

N89-24224 California Univ., Los Angeles.
KNOWLEDGE REPRESENTATION USING STRUCTURED MODELING Ph.D. Thesis
Srikanth Chari 1988 241 p
Avail: Univ. Microfilms Order No. DA8824654

The knowledge representation capabilities of Structured Modeling (Geoffrion, 1987) are studied. According to Structured Modeling (SM), a model is defined in terms of elements, each of which is either postulated as primitive or is defined in terms of other previously defined elements. The research has two objectives: (1) to describe the core concepts of SM using predicate logic, and (2) to clarify the modeling capabilities of SM with respect to semantic data models. The first objective aims to provide a better understanding of SM building a bridge between SM and a well defined mathematical system. The correspondence between structured models and logic is discussed, while a system using predicates, functions, and clauses (more specifically Horn clauses) is proposed to represent structured models. It is demonstrated how any structured model or model schema can be represented in logic, and defines necessary and sufficient conditions (in clausal form) under which a set of clauses represents a structured model and a model schema. A PROLOG based implementation, developed to test the validity of the representation is described. The second objective, examining the modeling capabilities of SM, serves to

demonstrate that SM is capable of representing the major abstractions of interest to data modelers. For this purpose, the research first formally defines the fundamental components of semantic data models. The representation of these components using the core concepts of SM is discussed and the capabilities of Structured Modeling Language (SML) to express such information are examined. Dissert. Abstr.

N89-24225# Naval Postgraduate School, Monterey, CA.
MANAGING SOUND IN A RELATIONAL MULTIMEDIA DATABASE SYSTEM M.S. Thesis
Gregory R. Sawyer Dec. 1988 108 p
(AD-A205742) Avail: NTIS HC A06/MF A01 CSCL 12/7

Sound, in all of its varied forms, is an important and widely used medium for the transmission of information. The widespread use of computers has greatly increased the breadth and depth of our information processing abilities. Yet the limited sensory functionality of computers has traditionally dictated a predominantly alphanumeric or textual communications interface standard. This thesis concentrates on the effective manipulation (i.e., capture, storage and retrieval) of sound data in a relational database system. It introduces the concept of an abstract data type of type SOUND which permits a level of sophistication in data manipulations that is beyond the capabilities of current systems. Such sophistication is accomplished through the use of a set of data manipulation operations which effectively hide the representation of the SOUND data structure from the user. As a result, the current familiarity of the user's view of the database remains unchanged when extended to the multimedia information processing environment. GRA

N89-24226# Naval Postgraduate School, Monterey, CA.
A PROGRAM INTERFACE PROTOTYPE FOR A MULTIMEDIA DATABASE INCORPORATING IMAGES M.S. Thesis
Cathy A. Thomas Dec. 1988 120 p
(AD-A206439) Avail: NTIS HC A06/MF A01 CSCL 12/5

This thesis represents one aspect of an exploration of the integration of unformatted data types, such as image, sound and signal, with more conventional formatted types in a single database. The focus of this thesis is the implementation of a prototype of a database employing a relational model that incorporates both formatted and unformatted data types. Initial research was limited to integration of image data. The prototype provides storage and retrieval capabilities, as well as a modest query handling capability. GRA

N89-23538*# National Aeronautics and Space Administration. Goddard Space Flight Center, Greenbelt, MD.
EnviroNET: SPACE ENVIRONMENT FOR STRATEGIC DEFENSE INITIATIVE EXPERIMENTS
Michael Lauriente *In* NASA, Langley Research Center, NASA/SDIO Space Environmental Effects on Materials Workshop, Part 1 May 1989 p 161-175 (For primary document see N89-23528 17-23)
Avail: NTIS HC A16/MF A01 CSCL 05B

83 ECONOMICS AND COST ANALYSIS

Includes cost effectiveness studies.

No abstracts in this category.

84 LAW, POLITICAL SCIENCE AND SPACE POLICY

Includes NASA appropriation hearings; aviation law; space law and policy; international law; international cooperation; and patent policy.

No abstracts in this category.

85 URBAN TECHNOLOGY AND TRANSPORTATION

Includes applications of space technology to urban problems; technology transfer; technology assessment; and surface and mass transportation.

For related information see also *03 Air Transportation and Safety, 16 Space Transportation,* and *44 Energy Production and Conversion.*

N89-24227# Air Force Systems Command, Wright-Patterson AFB, OH. Foreign Technology Div.
SUMMARY OF ACHIEVEMENTS IN SCIENTIFIC RESEARCH
22 Sep. 1988 26 p Transl. into ENGLISH of Beijing Inst. of Opto-Electronic Technology (People's Republic of China), 1985 5 p
(AD-A199947; FTD-ID(RS)T-0517-88) Avail: NTIS HC A03/MF A01 CSCL 09/3

The institute's work is briefly described. Brief technical descriptions and specifications are given for the following pieces of optical hardware: seven types of lasers for various uses, a laser sensitivity detector for chemical agents, a laser scanning radius gauge, a laser atomized particle microphotography system, two high speed strobe lights, a flight object capture device, an automatic motor energy saver, a wavelength scanner controller, a punching machine numerical controller, a fine dividing circuit step motor driver, a laser light intensity distribution detector, a laser output stability detector, a high speed laser energy detector, a laser wavelength calibrator, an ultrasonic modulator intended for laser applications, a laser dye recirculation system, a fiber optic coupler, two magnifiers for optical set-up and adjustment, two crystals for laser applications, and an optical bench apparatus. A.D.

N89-24228# Pacific Northwest Labs., Richland, WA.
PUTTING SCIENCE AND TECHNOLOGY TO WORK: A CASEBOOK OF TRANSFERRED TECHNOLOGIES
Oct. 1988 20 p
(Contract DE-AC06-76RL-01830)
(DE89-009158; PNL-SA-16279) Avail: NTIS HC A03/MF A01

New knowledge, processes, and products regularly emerge from federally funded research and development programs such as those at Pacific Northwest Laboratory (PNL). Through technology transfer, PNL shares the benefits of national investments in scientific progress with all segments of society. Technologies and technical capabilities developed for the U.S. Department of Energy and other Federal agencies are then put to work, applied to the needs of business, industry, and state and local government. GRA

N89-24229# Lawrence Livermore National Lab., CA.
ENGINEERING THRUST AREAS, 1989
1989 31 p
(Contract W-7405-eng-48)
(DE89-009009; UCID-20366-89) Avail: NTIS HC A03/MF A01

The mission of the Engineering Research Program is to develop the tools and technology needed to support current and future Laboratory programs. To accomplish this mission Engineering Research has two important goals - to identify key technology areas important to the Laboratory and to conduct high quality

research and development in support of Engineering's and the Laboratory's mission. To help focus our efforts in achieving our goals we identify key technologies called thrust areas and select technical leaders in these technologies to lead each area. The thrust areas are an integrated Engineering activity and, rather than being primarily discipline based, are staffed by the research engineers from EE and ME and from other Laboratory organizations as appropriate. The thrust area leaders are accountable to me for the quality and progress of their research activities but have significant latitude to manage the resources allocated to their thrust area. They are expected to establish strong links to the Laboratory program leaders, to use outside as well as inside experts to review the quality and direction of the research, to use university contacts to supplement and complement their efforts, and to be certain that we are not duplicating the work of others. The thrust area leader is also responsible for carrying out the development work that follows from the Research program so that the results of the research can be applied as early as possible to the needs of the programs. This booklet contains capsule descriptions of the activities of each thrust area and illustrates how thrust area activities and technologies support Laboratory programs. DOE

88 SPACE SCIENCES (GENERAL)

N89-24230# European Space Agency, Paris (France). ESA Debris Working Group.
SPACE DEBRIS: A REPORT FROM THE ESA DEBRIS WORKING GROUP
Nov. 1988 74 p
(ESA-SP-1109; ISSN-079-6566; ETN-89-94237) Copyright Avail: NTIS HC A04/MF A01; ESA Publications Div., ESTEC, Noordwijk, Netherlands, 30 Dutch guilders

Available data on space debris; the natural environment; the situation in low Earth orbits; the situation in geostationary orbit; risks on the ground posed by reentering space objects; influence of space debris on ground-based and spaceborne astronony; preventive measures; and legal aspects are reviewed. ESA

N89-23529*# National Aeronautics and Space Administration. Lewis Research Center, Cleveland, OH.
OVERVIEW OF ENVIRONMENTAL FACTORS
C. K. Purvis *In* NASA, Langley Research Center, NASA/SDIO Space Environmental Effects on Materials Workshop, Part 1 May 1989 p 5-24 (For primary document see N89-23528 17-23)
Avail: NTIS HC A16/MF A01 CSCL 11G

N89-23543*# National Aeronautics and Space Administration. Lyndon B. Johnson Space Center, Houston, TX.
ORBITAL DEBRIS ENVIRONMENT AND DATA REQUIREMENTS
Donald J. Kessler *In* NASA, Langley Research Center, NASA/SDIO Space Environmental Effects on Materials Workshop, Part 1 May 1989 p 281-299 (For primary document see N89-23528 17-23)
Avail: NTIS HC A16/MF A01 CSCL 03B

N89-23548*# Aerospace Corp., Los Angeles, CA.
THE SPACE PARTICLE ENVIRONMENT
Alfred L. Vampola *In* NASA, Langley Research Center, NASA/SDIO Space Environmental Effects on Materials Workshop, Part 2 May 1989 p 367-382 (For primary document see N89-23547 17-23)
Avail: NTIS HC A12/MF A01 CSCL 03B

89 ASTRONOMY

Includes radio, gamma-ray, and infrared astronomy, and astrometry.

N89-24231*# Smithsonian Astrophysical Observatory, Cambridge, MA.
OBSERVATIONS OF THE ROTATIONAL TRANSITIONS OF OH FROM THE ORION MOLECULAR CLOUD Semiannual Report Nos. 6, 7, 8, and 9, 1 April 1987 - 31 March 1989
Gary J. Melnick, Reinhard Genzel, A. Poglitsch, G. J. Stacey, and John B. Lugten (California Univ., Berkeley.) Mar. 1989 33 p
(Grant NAG2-311)
(NASA-CR-184802; NAS 1.26:184802) Avail: NTIS HC A03/MF A01 CSCL 03A

A summary of observed rotationally excited, far infrared OH line emissions from Orion-KL made using the Kuiper Airborne Observatory is given, together with a list of the resulting publications, talks, and lectures based on this data. In addition, a paper is appended, particularly addressing the (16)OH and (18)OH emission from Orion-KL. The first detections of the (16)OH (2)pi(1/2) to (2)pi(3/2) J = 3/2(-) to 3/2(+) rotational cross-ladder transition (53.351 micrometer) and the (18)OH (2)pi(3/2) J = 5/2(+) to 3/2(-) rotational ground-state transition (120.1719 micrometer). It is found that both of these lines exhibit a P-Cygni profile. A.D.

N89-24232*# National Aeronautics and Space Administration, Washington, DC.
REPORTS OF PLANETARY ASTRONOMY, 1989
Jun. 1989 159 p
(NASA-TM-4120; NAS 1.15:4120) Avail: NTIS HC A08/MF A01 CSCL 03A

This is a compilation of abstracts of reports from Principal Investigators funded through NASA's Planetary Astronomy Office. It provides a summarization of work conducted in this program in 1989. Each report contains a brief statement on the strategy of investigation and lists significant accomplishments within the area of the author's funded grant or contract, plans for future work, and publications. Author

N89-24233*# Pittsburgh Univ., PA. Dept. of Physics and Astronomy.
THE ALLEGHENY OBSERVATORY SEARCH FOR PLANETARY SYSTEMS Final Technical Report, 1980 - 1988
George D. Gatewood 11 Apr. 1989 12 p
(Grant NAG2-53)
(NASA-CR-184990; NAS 1.26:184990) Avail: NTIS HC A03/MF A01 CSCL 03A

The accomplishments of the observatory's search for planetary systems are summarized. Among these were the construction, implementation, and regular use of the Multichannel Astrometric Photometer (MAP), and the design, fabrication and use of the second largest refractor objective built since 1950. The MAP parallax and planetary observing programs are described. Various developments concerning alternate solid state photodetectors and telescope instrumentation are summarized. The extreme accuracy of the system is described in relation to a study of the position and velocity of the members of the open cluster Upgren 1. The binary star system stringently tests the theory of stellar evolution since it is composed of an evolved giant F5 III and a subgiant F5 IV star. A study that attempts to measure the luminosities, surface temperatures, and masses of these stars is discussed. A.D.

N89-24234 California Univ., Berkeley.
SPECTRA AND DYNAMICS OF YOUNG STELLAR OBJECTS Ph.D. Thesis
Fred Chester Adams 1988 203 p
Avail: Univ. Microfilms Order No. DA8902017

Theoretical spectral energy distributions for an evolutionary sequence of young stellar objects, from protostars to pre-main-sequence stars were calculated. The theory of protostellar objects, characterized by a central star and disk embedded within an infalling envelope of dust and gas, can explain the observed

infrared spectra of embedded Infrared Astronomy Satellite (IRAS) sources associated with molecular cloud cores. The infrared mass infall rates for these objects are generally consistent with the measured gas temperatures in nearby molecular clouds. In addition, fitting the data requires cloud rotation rates in the range 0.3 to 3.0 km/s/pc, values which are consistent with available observations. Next, it was found that T Tauri stars with near- and mid-infrared excesses can be understood as young stars surrounded by nebular disks. The disks in T Tauri systems are found in two varieties: passive disks which have no intrinsic luminosity and merely intercept and re-radiate stellar photons, and active disks which have appreciable intrinsic luminosity. For the most extreme cases in the latter category, the T Tauri stars with flat infrared spectra, spectral diagnostics can be used to determine estimates for the radii and masses of the disks. The derived parameters show that self-gravity of these disks may be dynamically important and may provide one possible source for the observed activity. Dissert. Abstr.

N89-24235 Texas Univ., Austin.
A SEARCH FOR PULSATIONS IN PLANETARY NEBULAE NUCLEI Ph.D. Thesis
Butler Preston Ander Hine, III 1988 168 p
Avail: Univ. Microfilms Order No. DA8901332

The results of a survey of the central stars of planetary nebulae designed to detect g-mode pulsations driven by hydrogen and/or helium shell burning were presented. Using newly developed high-speed photometric instrumentation to overcome the inherent difficulties in observing these central stars in the presence of their nebulae, time-series photometric data for 51 central stars was obtained in an effort to detect the g-mode pulsations predicted by Kawaler and his colleagues. No periodic variations were detected for periods between 40 and 500 seconds, in the data down to a limit of approximately 0.5 (average) millimagnitudes. Since the theoretical calcuations require these pulsations in the presence of shell burning, it was concluded that either the shell burning sources are extinguished prior to this evolutionary state, or some mechanism is inhibiting the growth of these pulsations. If the shell burning source is indeed extinguished prior to the central star becoming a white dwarf, then this implies that white dwarfs are formed with hydrogen layer masses less than 10 to the minus 6th power solar mass. Dissert. Abstr.

N89-24236 Texas Univ., Austin.
A STUDY OF THE MOTION IN THE NEIGHBORHOOD OF THE TRIANGULAR LIBRATION POINT Ph.D. Thesis
Danny Gene Tuckness, Jr. 1988 173 p
Avail: Univ. Microfilms Order No. DA8901407

The effects of the mass parameter mu on the librational motion of a third body near the triangular libration point in the circular restricted problem of three bodies was treated. A definition of stable librational motion with variable mu depends on whether the orbit trajectory of the third body crosses a defined boundary within a defined amount of time for the value of mu given. The boundary and time limit used to define the stability of the third body are established. The maximum initial velocities and maximum initial displacements originating from L4 such that the third body will display stable librational motion are found. The linearized equations of motion of the third body are studied and a comparison with the non-linearized equations of motion is made. To demonstrate the use of this study to space applications there is an investigation of a possible origin of the Trojan asteroids around the L4 point of the Jupiter-Sun system. Dissert. Abstr.

N89-24237# College of Eastern Montana, Billings. Dept. of Physical Sciences.
STUDY OF THE INFRARED CELESTIAL BACKGROUND Final Report, 1 Feb. 1985 - 31 Jan. 1988
Alan F. Bentley 30 Sep. 1988 67 p
(Grant AF-AFOSR-0139-85; AF Proj. 2311)
(AD-A205649; AFOSR-89-0318TR) Avail: NTIS HC A04/MF A01 CSCL 03/1

The following revised objectives were formulated: to determine the nature of infrared sources observed; to carry out theoretical investigations on the nature and evolution of selected infrared sources; and to establish the statistical distribution of infra-sources in space to a sensitivity limit and spatial resolution consistent with available observing equipment and techniques. The research objectives follow: Research on infrared sources in the W40 complex was published. Results of radio and infrared observations of OH/IR stars in the Galaxy were published. A theoretical study of the possibilities for observation of galaxies in the process of formation in the early universe was published in the Proceedings of the Montana Academy of Science. The results of a series of observations made on Nova Vulpeculae 1984 2 were published. Preliminary results on our studies of the infrared properties of the nuclei of planetary nebulae were presented. A theoretical model has been constructed for transfer of cosmic ray energy to emission nebulae. GRA

N89-24238# Max-Planck-Inst. fuer Physik und Astrophysik, Garching (Germany, F.R.). Inst. fuer Extraterrestrische Physik.
TIME AND SPECTRAL VARIABILITY OF THE LOW MASS X-RAY BINARIES [ZEITLICHE UND SPEKTRALE VARIABILITAET DER MASSEARMEN ROENTGENDOPPELSTERNE]
Andreas Langmeier Aug. 1988 163 p In GERMAN
(MPE-Report-210; ISSN-0178-0719; ETN-89-93991) Copyright
Avail: NTIS HC A08/MF A01

The photometric and spectral variability of two low mass X-ray binary stars in the galactic center were investigated onboard the European X-ray observatory EXOSAT. The physics of low mass X-ray binaries is reviewed, and the X-ray satellite EXOSAT and its instruments are described. The observations of the two investigated systems, GX17+2 and 4V1705-44 are compared with the observations of other low mass X-ray binary stars. A coherent picture of the variability of the investigated binary stars is sketched, and the possible physical mechanisms of the variability are depicted. The X-ray spectra of both systems are described with an emission model. The spectra change with intensity. Both systems show fast aperiodic fluctuations with a red frequency spectrum, which can be described by an exponential law. The evolution and the amplitude of the mass accretion rate were determined. ESA

N89-24239 Max-Planck-Inst. fuer Physik und Astrophysik, Garching (Germany, F.R.). Inst. fuer Extraterrestrische Physik.
GRAZING INCIDENCE TELESCOPES FOR ESA'S X-RAY ASTRONOMY MISSION XMM
Bernd Aschenbach and Heinrich Braeuninger Sep. 1988 20 p
Presented at the 32nd SPIE Annual International Symposium, San Diego, CA, Aug. 1988 Submitted for publication
(Contract ESTEC-6945/86/NL/SK)
(MPE-Preprint-129; ISSN-0178-0719; ETN-89-94390) Copyright
Avail: Fachinformationszentrum Karlsruhe, 7514 Eggenstein-Leopoldshafen 2, Fed. Republic of Germany

The high throughput mission XMM is described. The heart of the scientific payload consists of a set of three highly nested Wolter type 1 telescopes. A review of the optical design and layout is given. The grazing incidence mirrors will be made by epoxy replication from a highly polished glass mandrel. This technique is tested producing flat mirror samples, of which X-ray measurement of reflectivity and scattering are presented. ESA

90 ASTROPHYSICS

Includes cosmology; celestial mechanics; space plasmas; and interstellar and interplanetary gases and dust.

For related information see also *75 Plasma Physics*.

N89-24240*# National Aeronautics and Space Administration, Washington, DC.
COMET HALLEY: THE VIEW FROM PIONEER VENUS
[1989] 6 p Original contains color illustrations

(NASA-NF-127; NAS 1.20:127) Avail: NTIS HC A02/MF A01 CSCL 03B

The plans to scan Halley's Comet at close range using the Pioneer Venus Orbiter are discussed. The composition of comets, their paths through space, and the history of comet encounters are examined. An ultraviolet spectrometer aboard the spacecraft will determine the composition of the gaseous coma and will measure the total gas production during its passage. The Pioneer Venus Orbiter will observe the comet for five weeks before solar interference with communications occurs as Venus passes on the far side of the Sun from Earth. Diagrams of the solar system and the relationship of the comet to the planets and the Sun are provided. Author

N89-24241 Texas Univ. at Dallas, Richardson.
THE GEOMETRY OF PLANE WAVES IN SPACES OF CONSTANT CURVATURE Ph.D. Thesis
Hung Viet Tran 1988 132 p
Avail: Univ. Microfilms Order No. DA8827016

The geometry of possible plane wave fronts in spaces of constant curvature was examined for three cases in which the cosmological constant is positive, zero, or negative. The cosmological constant and a second-order invariant determined by a congruence of null rays were used. The spaces under investigation were embedded in a flat five-dimensional space. The null hyperplanes passing through the origin of the flat five-dimensional space was studied. The embedded spaces are represented by quadrics in the five-dimensional space. The plane wave fronts are represented by the intersection of the quadric with null hyperplanes passing through the origin of the five-dimensional space. In Minkowski spaces (zero cosmological constant), the plane-fronted waves will intersect if and only if the second-order invariant mentioned above is non-zero. For deSitter spaces (positive cosmological constant), plane-fronted waves will always intersect. For anti-deSitter spaces (negative cosmological constant), plane-fronted waves may but need not intersect. Author

N89-24242 Cornell Univ., Ithaca, NY.
RELATIVISTIC AND NON-RELATIVISTIC MAGNETOHYDRODYNAMIC FLOWS AROUND COMPACT STARS Ph.D. Thesis
Clark Matthew Mobarry 1988 181 p
Avail: Univ. Microfilms Order No. DA8900818

A set of theoretical tools are developed for studying the magnetized accretion disks and astrophysical jets in active galaxies. A general theory is developed for the steady axisymmetric flow of an ideal general-relativistic fluid around a Schwarzschild black hole. The theory leads to a second-order partial differential equation, a Grad-Shafranov equation, for the magnetic flux function psi(R, theta). The magnetic surface functions of the Grad-Shafranov method are shown to be the Lagrange multipliers of an energy principle. Thus, the magnetic surface functions are not arbitrary functions, but must be chosen consistent with physically stable equilibria. From the energy principle, a numerical artificial friction method is developed to solve the general relativistic Grad-Shafranov equation with fluid flow. This method is suited for the internal boundaries between elliptic and hyperbolic behavior present in magnetospheres with fluid flow. The friction method is shown to be compatible with a theory for the slow dissipative evolution of a nearly ideal MagnetoHydroDynamic (MHD) fluid. A virial theorem is derived from the basic equations of general relativistic MHD. It is used to obtain an upper bound on the total energy in the electromagnetic field in terms of the total gravitational binding energy between the black hole and the matter (and energy) outside it. An analysis is made of the motion of a charged test particle in the electromagnetic field of a magnetized accretion disk surrounding a black hole. The results are consistent with stable orbits close to the event horizon. A semi-analytical model is developed for the evolution and dissipation of narrow magnetized jets from an active galaxy. This model exhibits the acceleration and expansion of the jets with increasing axial distance from the central object. Dissert. Abstr.

N89-24243# Los Alamos National Lab., NM.
ON THE MEASUREMENT OF COSMOGENIC NUCLIDES IN COMETARY MATERIALS
G. F. Herzog, P. A. J. Englert, R. C. Reedy, K. Nishiizumi, C. P. Kohl, and J. R. Arnold (California Univ., San Diego.) 1989 15 p Presented at the Workshop on the Analysis of Returned Comet Nucleus Samples, Milpitas, CA, 16 Jan. 1989
(Contract W-7405-eng-36)
(DE89-009248; LA-UR-89-1110; CONF-890195-1) Avail: NTIS HC A03/MF A01

Determinations of the cosmogenic nuclide concentrations in cometary material will help to define the recent surface history of the comet and its exposure to cosmic rays. In particular, the rates for the removal or mixing of surface material could be studied, and any variations in cosmic-ray intensity implied by the data could be used to infer orbital changes during the last few million years. The measurement of the shorter-lived isotopes poses technical challenges that should be addressed now. The measurement of longer-lived isotopes will be straightforward, provided that rates of mass loss are not too high. DOE

N89-24244 Texas Univ., Austin.
A LINEAR ANALYSIS OF THE STABILITY OF STRONG SHOCKS AND THE EVOLUTION AND DISTRIBUTION OF MATERIALS IN A COLD DARK MATTER DOMINATED UNIVERSE Ph.D. Thesis
Dongsu Ryu 1988 262 p
Avail: Univ. Microfilms Order No. DA8901391

The analysis of a rippling instability for strong decelerating shock waves is given. The fundamental mode of nonradial stabilities for adiabatic wind-driven shocks was analyzed. Also the stability of isothermal shock waves was studied by approximating the dynamical evolution of high density regions behind the shock waves. The results predict that isothermal blast shocks are overstable for post-shock density contrasts greater than approx. 10 and isothermal wind-driven shocks are overstable for density contrasts greather than approx. 25. Calculations using fluid codes were done for three cosmological problems. Firstly, nonlinear gravitational clustering in a universe dominated by a coherently oscillating scalar field, which is a candidate of the cold dark matter, was studied. Secondly, the evolution of the intergalactic medium was calculated in a universe dominated by a cold dark matter. The gravitational force was calculated by interpolating the initial gravitational potential, and galaxies have formed only if the baryonic matter density is high. Finally, the evolution and distribution of the intergalactic medium, as well as the dark matter and galaxies, were studied in a universe dominated by a cold dark matter. The dark matter and galaxies were followed with an N-body code, while the intergalactic medium has been followed with a fluid code. Dissert. Abstr.

N89-24245 Boston Univ., MA.
A SELF CONSISTANT MODEL OF THE THREE PHASE INTERSTELLAR MEDIUM IN DISK GALAXIES Ph.D. Thesis
Zhong Wang 1989 236 p
Avail: Univ. Microfilms Order No. DA8904167

A number of physical processes were analyzed concerning velocity and spatial distributions, ionization structure, pressure variation, mass and energy balance, and equation of state of the diffuse interstellar gas in a three phase model. The effects of this model on the formation of molecular clouds and the evolution of disk galaxies were considered. The primary purpose was to incorporate self-consistently the interstellar conditions in a typical late-type galaxy, and to relate these to various observed large-scale phenomena. Ideal situations were modeled both analytically and numerically, and the results were compared with observational data of the Milky Way Galaxy and other nearby disk galaxies. Several main conclusions were: (1) the highly ionized gas found in the lower galactic halo is shown to be consistent with a model in which the gas is photoionized by the diffuse ultraviolet radiation (the observed distributions of ions such as CIV, SiIV and NV, and the extended neutral hydrogen disk layer can both be explained naturally if gas clouds move in ballistic orbits in the direction

perpendicular to the disk); (2) in a quasi-static and self-regulatory configuration, the photoelectric effects of interstellar grains are primarily responsible for heating the cold (t approx. = 100 K) gas; the warm (T approx. = 8,000 K) gas may be heated by supernova remnants and other mechanisms (both phases are extremely steady in their thermal temperatures, and each contribute roughly half of the total gas mass within a wide range of interstellar conditions) and (3) the large-scale atomic and molecular gas distributions in a sample of 15 disk galaxies can be well explained if molecular cloud formation and star formation follow a modified Schmidt Law. Dissert. Abstr.

N89-24246# Wyoming Univ., Laramie. Dept. of Physics and Astronomy.
GROUND-BASED INFRARED OBSERVATIONS OF SOURCES DISCOVERED BY THE AFGL, FIRRSE AND IRAS INFRARED SURVEYS Final Report, 15 Jul. 1984 - 14 Jul. 1987
E. J. Spillar 30 Jun. 1988 4 p
(Grant AF-AFOSR-0058-85; AF Proj. 2311)
(AD-A206335; AFOSR-89-0345TR) Avail: NTIS HC A02/MF A01 CSCL 03/2

The contracts research objective was to understand the infrared sources discovered by the AFGL, FIRRSE and IRAS Infrared Surveys. Work has continued on young stellar objects with a variety of collaborators. In particular, extensive infrared and radio observations have yielded new information on the true nature of this highly energetic outflow object. Particular results are the lack of a disk and the resolution of accelerated shells. High resolution maps have been made of several other young stellar objects in an effort to understand the energetics and nature of the objects. The group has continued its investigation of comets. Comets investigated include Giacobini-Zinner and Halley. Emphasis has been on understanding the emission from the dust in these objects. Because of the changing illumination of these dust grains, and the well understood geometry of comets, these objects provide unique information on interstellar dust. GRA

N89-23558*# National Aeronautics and Space Administration. Lyndon B. Johnson Space Center, Houston, TX.
MICROMETEOROIDS AND DEBRIS
Andrew Potter *In* NASA, Langley Research Center, NASA/SDIO Space Environmental Effects on Materials Workshop, Part 2 May 1989 p 553-557 (For primary document see N89-23547 17-23)
Avail: NTIS HC A12/MF A01 CSCL 03B

91 LUNAR AND PLANETARY EXPLORATION

Includes planetology; and manned and unmanned flights.

For spacecraft design or space stations see *18 Spacecraft Design, Testing and Performance.*

N89-24247# Academy of Sciences (USSR), Novosibirsk. Inst. Yadernoj Fiziki.
APPLICATION OF THE METHOD OF X-RAY FLUORESCENCE ANALYSIS WITH SYNCHROTRON RADIATION TO STUDY LUNAR MATTER
L. S. Tarasov, A. F. Kudryashova, V. B. Baryshev, G. N. Kulipanov, and A. N. Skrinskij 1988 30 p In RUSSIAN
(DE88-705782; IYaF-88-82) Avail: NTIS (US Sales Only) HC A03/MF A01

Possibilties of X-ray fluorescence analysis using synchrotron radiation are considered, microamounts of lunar samples being studied as examples. It is shown that the method permits to determine the composition of particles with the mass from 2 to 0.05 mg when the content of elements is at the level of 1 x 10(-4) and higher. Systematic geochemical data on the distribution of Sr, Y, Ce, La and other elements in lunar minerals and rocks are obtained. A great geochemical value of data on strontium distribution in the rocks is pointed out. DOE

N89-24248# Heidelberg Univ. (Germany, F.R.). Naturwissenschaftlich-Mathematischen Gesamtfakultaet.
CALIBRATION MEASUREMENTS ON MICROMETEORITE DETECTORS FOR THE MISSIONS ULYSSES, GALILEO AND GIOTTO Ph.D. Thesis [KALIBRATIONSMESSUNGEN AN MIKROMETEORITENDETEKTOREN FUER DIE MISSIONEN ULYSSES, GALILEO UND GIOTTO]
Jochen Ralf Goeller 1988 121 p In GERMAN
(ETN-89-93947) Avail: NTIS HC A06/MF A01

Measurements were performed for the calibration of the ULYSSES and the DIDSY IPM-P dust detector using a dust accelertor. The experiments were performed under as realistic conditions as possible with a view to the simulation of dust impact and the calculation of calibration curves. For the DIDSY IPM-P sensor A the mass dependence of the impact charges and the speed dependence of the impact charge were determined; for the sensor B the passage threshold of the Mylar foil, and the behavior of impact charges were determined. For the ULYSSES sensor the dependence of the measured quantities on the impact angle and the material of the dust particles. Accurate predictions concerning the ion energy distribution are not possible without a change of the experimental parameters. ESA

92 SOLAR PHYSICS

Includes solar activity, solar flares, solar radiation and sunspots.

For related information see *93 Space Radiation.*

N89-24249# Tufts Univ., Medford, MA. Dept. of Physics and Astronomy.
VERY LARGE ARRAY OBSERVATIONS OF THE SUN WITH RELATED OBSERVATIONS USING THE SMM (SOLAR MAXIMUM MISSION) SATELLITE Final Technical Report, 1 Jan. 1983 - 31 Aug. 1988
Kenneth R. Lang 12 Oct. 1988 327 p
(Grant AF-AFOSR-0019-83; AF Proj. 2311)
(AD-A203874; AFOSR-89-0044TR-APP) Avail: NTIS HC A15/MF A01 CSCL 03/2

Reprints of journal articles published during 1983 to 1988 by Tufts University are presented. Some representative titles are: Multiple Wavelength Observations of Flaring Active Regions; Very Large Array Observations of Solar Active Regions 3. Multiple Wavelength Observations. High-Resolution Observations of Solar Radio Bursts at 2, 6, and 20 cm Wavelength; The Circularly Polarized Sun at 12.6 cm Wavelength; Bright, Rapid, Highly Polarized Radio Spikes from the M Dwarf AD. Leonis; Possible Detection of Thermal Cyclotron Lines from Small Sources within Solar Active Regions. Observations of Preburst Heating and Magnetic Field Changes in a 20 cm Loop; The Structure of a Solar Active Region from RATAN-600 and Very Large Array Observations; The Solar-Stellar Connection; Short Term Prediction of Solar Bursts - Radio Wavelength Precursors; VLA Observations of Flare Build Up in Coronal Loops on the Sun and Solar Type Stars; VLA Observations of Narrow-Band Decimetric Burst Emission; VLA Observations of Solar Active Regions at Closely Spaced Frequencies: Evidence for Thermal Cyclotron Line Emission; VLA Observations of Compact, Variable Sources on the Sun; Flare Stars and Solar Bursts; High Resolution In Time and Frequency; Coronal Plasmas On The Sun and Nearby Stars; Coronal Diagnostics; Narrow-Band; Millisecond Radio Spikes From the Dwarf M Flare Star AD Leonis; VLA Observations of a Solar Noise Storm. GRA

N89-24250# National Geophysical Data Center, Boulder, CO.
SOLAR-GEOPHYSICAL DATA NUMBER 531, PART 1. DATA FOR OCTOBER, SEPTEMBER 1988 AND LATE DATA Prompt Reports, Nov. 1988
H. E. Coffey and J. A. McKinnon Nov. 1988 150 p
(PB89-139943; SGD-531-Pt-1) Avail: NTIS HC A07/MF A01 CSCL 03B

Solar-geophysical information is presented in tabular and

graphic form. Categories include data for October 1988 (advance and worldwide IUDS alert periods, solar activity indices, solar flares, solar radio emission, Stanford mean solar magnetic field); data for September 1988 (solar active regions, sudden ionospheric disturbances, solar radio spectral observations, cosmic ray measurements by neutron monitor, geomagnetic indices, radio propagation indices); and late data (Pioneer 12 interplanetary magnetic field magnitudes December 1987, cosmic ray measurements by neutron monitor July to August 1988, radio propagation indices August 1988). GRA

N89-24251*# Joint Inst. for Lab. Astrophysics, Boulder, CO.
REDISTRIBUTION IN ASTROPHYSICALLY IMPORTANT HYDROGEN LINES
J. Cooper, R. J. Ballagh (Otago Univ., Dunedin, New Zealand), and I. Hubeny 22 May 1989 8 p
(Grant NGL-06-003-057)
(NASA-CR-181375; NAS 1.26:181375) Avail: NTIS HC A02/MF A01 CSCL 03B

Under typical solar chromospheric conditions for hydrogen radiators, strong collisions due to both electrons and ions are well separated in time, so that a binary collision theory for collisional redistribution is applicable. However, a simple impact approximation may not be used, but rather a unified type theory is required in which frequency dependent line shape parameters are used to describe both impact and quasi-static regions of the spectrum. In addition, correlated terms which describe absorption and emission during a collision are important, and, in fact, without correlated terms describing both transfer of excitation and emission during the same collision unphysical predictions (such as negative intensities) would be obtained. In this paper theory is specifically developed for the coupled Lyman-alpha, Lyman-beta, Hydrogen-alpha system, and equations of statistical equilibrium and absorption and emission coefficients are given. All correlated events are examined and emission during a collision is found to be important in the line wings. Stimulated emission and absorption is also included within a broadband approximation. The major approximation is to ignore lower state interaction. It is found that for Lyman-beta Raman-coupling with Hydrogen-alpha occurs and the overall scattering of radiation in the line wings is mostly coherent. In contrast, for Hydrogen-alpha, incoherent redistribution due to lower state radiative decay (which occurs even in the absence of collisions) is found to dominate the coherent scattering. Finally, in the Lyman series the dominant incoherent contribution is associated with cascade transitions and inelastic collisions between different principal quantum states. Author

N89-24252# Air Force Geophysics Lab., Hanscom AFB, MA.
IMAGE PROCESSING OF CORONAL PICTURES
Raymond N. Smartt, Olga Koutchmy, Serge Koutchmy, Christian Nitschelm, and Julius Sykora 28 Feb. 1989 13 p
(AD-A205326; AFGL-TR-89-0060) Avail: NTIS HC A03/MF A01 CSCL 03/1

Coronal images contain many complex, superposed, faint, optically-thin structures: rays, loops, curved streamers, etc. The spatial resolution is often limited by the signal/noise ratio in the recording medium while the dynamic range in intensity is severely dominated by the radial gradient. The results obtained with a new simple image processing algorithm are applied to several typical eclipse and coronographic pictures. This 2D filter (second order difference operator in k-direction) shows superior quality by improving the signal/noise ratio, reducing the dynamic range and enhancing faint coronal structures. A comparison with results obtained with more commonly used 2D filters is also presented. The algorithm used here are briefly described, together with discussions of enhanced coronal images of coronal physics interest. GRA

N89-24253# Louisiana State Univ., Baton Rouge. Dept. of Physics and Astronomy.
SOLAR FLARES AND MAGNETOSPHERIC PARTICLES: INVESTIGATIONS BASED UPON THE ONR-602 AND ONR-604 EXPERIMENTS Annual Letter Report, for period ending 30 Nov. 1988
John P. Wefel 30 Nov. 1988 49 p
(Contract N00014-83-K-0365)
(AD-A205599) Avail: NTIS HC A03/MF A01 CSCL 04/1

Data from the ONR-602 experiment, obtained in a low altitude, polar orbit are being analyzed to investigate the composition, intensity levels and time variations of energetic charged particles both trapped within the Earth's magnetosphere and incident upon the magnetosphere from interplanetary space, particularly solar flare particles. The effort involves both data analysis/interpretation and detailed modeling of the near-Earth environment. The research focusses on the global zones of low energy particle precipitation, including the South Atlantic Anomaly region from which access to the radiation belts is obtained, and the solar particle events of May to Nov., 1982. In addition, scientific/technical support is being provided to the ONR-604 experiment to be launched on the CRRES mission. The results of these investigations will enhance our understanding of the geospace radiation environment and its effects on men, materials and electronic systems in space. GRA

N89-24254# Stanford Univ., CA. Center for Space Science and Astrophysics.
GEOMAGNETIC DISTURBANCES Final Report, 1 Oct. 1985 - 30 Sep. 1988
Philip H. Scherrer Jan. 1989 32 p
(Contract N00014-86-K-0085)
(AD-A206052) Avail: NTIS HC A03/MF A01 CSCL 03/2

Investigations have included observations and analysis of the solar and interplanetary quantities relevant to geomagnetic activity. The operation of the Wilcox Solar Observatory and analysis of the synoptic observations of magnetic fields has constituted a significant part of the effort. Emphasis has been to attempt to understand the timing and severity of geomagnetic disturbances by understanding the solar mechanisms responsible for the origin of solar wind variations. GRA

N89-23562*# National Aeronautics and Space Administration. Langley Research Center, Hampton, VA.
SOLAR RADIATION
Wayne S. Slemp *In its* NASA/SDIO Space Environmental Effects on Materials Workshop, Part 2 May 1989 p 573-575 (For primary document see N89-23547 17-23)
Avail: NTIS HC A12/MF A01 CSCL 03B

93 SPACE RADIATION

Includes cosmic radiation; and inner and outer earth's radiation belts.

For biological effects of radiation see *52 Aerospace Medicine*. For theory see *73 Nuclear and High-Energy Physics*.

N89-24255*# National Aeronautics and Space Administration. Langley Research Center, Hampton, VA.
A HIERARCHY OF TRANSPORT APPROXIMATIONS FOR HIGH ENERGY HEAVY (HZE) IONS
John W. Wilson, Stanley L. Lamkin, Farhat Hamidullah, Barry D. Ganapol (Arizona Univ., Tucson.), and Lawrence W. Townsend Washington Jul. 1989 39 p
(NASA-TM-4118; L-16572; NAS 1.15:4118) Avail: NTIS HC A03/MF A01 CSCL 03B

The transport of high energy heavy (HZE) ions through bulk materials is studied neglecting energy dependence of the nuclear cross sections. A three term perturbation expansion appears to be adequate for most practical applications for which penetration depths are less than 30 g per sq cm of material. The differential

energy flux is found for monoenergetic beams and for realistic ion beam spectral distributions. An approximate formalism is given to estimate higher-order terms. Author

N89-24256# Los Alamos National Lab., NM.
AN ULTRA-SOFT EINSTEIN X-RAY SURVEY
F. A. Cordova, J. Kartje, T. Rodriguez-Bell, K. O. Mason, and F. R. Harnden, Jr. (Harvard-Smithsonian Center for Astrophysics, Cambridge, MA.) 1989 14 p Presented at the Berkeley Colloquium on Extreme Ultraviolet Astronomy, Berkeley, CA, 19-20 Jan. 1989
(Contract W-7405-eng-36)
(DE89-007993; LA-UR-89-598; CONF-890189-4) Avail: NTIS HC A03/MF A01

We describe preliminary results of a survey of ultra-soft sources using the data base acquired with the Imaging Proportional Counter on the Einstein Observatory. Of the approx. 7700 detections of sources in this data base with signal-to-noise ratios greater than or equal to 3 in the energy band 0.16 to 3.5 keV, approx. 3% fit the selection criteria for sources that may have extremely soft X-ray components; i.e., they have a very low ratio of medium energy band (0.56 to 1.08 keV) to soft energy band (0.16 to 0.56 keV) counts. Preliminary results of our searches for counterparts of the ultra-soft sources, done with catalogs and optical and radio observations, reveal that the Ultra-Soft Survey is populated by, among other objects, isolated degenerate dwarf stars, particular subclasses of cataclysmic variable binaries, low-mass X-ray binaries in the LMC, some SAO stars of late spectral type, and several Hyades and dMe stars. With observations utilizing the Very Large Array, we identified one bright, Ultra-Soft Survey object with the radio pulsar PSR 0656 + 14. A particularly exciting result is the finding, thus far, of numerous active galactic nuclei among the Ultra-Soft Survey sources. Two-thirds of these AGN do not have any detectable X-ray emission above 1 keV. The remainder appear to have both an ultra-soft and a hard component. The soft component can be characterized by a power law with an energy spectral index, alpha sub E, greater than 2. The soft AGN are mostly low-redshift sources with V magnitudes ranging from 17 to 20. All of these AGN are viewed along lines of sight in which the equivalent hydrogen column density is less than 6 x 10(20)/cm. We present a table of the Ultra-Soft Survey sources for which we have identified probable optical counterparts. These objects presage the classes of source that EUVE and the Wide-Field Camera on ROSAT are likely to find in their all-sky, extreme ultraviolet surveys. DOE

N89-24257# Los Alamos National Lab., NM. Earth and Space Sciences Div.
A SEARCH FOR EUV EMISSION FROM CATACLYSMIC VARIABLES
Ronald S. Polidan (Arizona Univ., Tucson.) and Christopher W. Mauche 1989 13 p Presented at the Berkeley Colloquium on Extreme Ultraviolet Astronomy, Berkeley, CA, 19-20 Jan. 1989
(Contract W-7405-eng-36)
(DE89-008012; LA-UR-89-639; CONF-890189-2) Avail: NTIS HC A03/MF A01

Voyager far- and extreme-ultraviolet (500 to 1200 A) spectrophotometric observations of five cataclysmic variables (the dwarf novae SS Cyg and VW Hyi and the novalike variables V3885 Sgr, RW Sex, and IX Vel) are combined with neutral hydrogen column densities derived from the curve-of-growth analysis of interstellar absorption lines in high-resolution IUE spectra to place upper limits on the emitted flux in the 600 to 700 A EUV band. No EUV emission was observed in any of the five cataclysmic variables. Relatively high neutral hydrogen column densities (greater than 10(19)/cm) in SS Cyg, V3885 Sgr, RW Sex, and IX Vel preclude any discussion of their intrinsic EUV emission. For VW Hyi, the low neutral hydrogen column, and excellent Voyager data place severe upper limits on the intrinsic EUV flux of this cataclysmic variable. The derived EUV limits for VW Hyi are compared to predictions from various models and Voyager observations of EUV emission from nearby hot white dwarfs. DOE

N89-24258# Lawrence Livermore National Lab., CA. Dept. of Physics.
COMPACT SOURCE ORIGIN OF COSMIC RAY ANTIPROTONS
Charles D. Dermer Feb. 1989 5 p Presented at the Particle Astrophysics Workshop, Berkeley, CA, 8-10 Dec. 1988
(Contract W-7405-eng-48)
(DE89-008044; UCRL-100343; CONF-881212-1) Avail: NTIS HC A02/MF A01

The flux of cosmic ray antiprotons with kinetic energies between approx. 1 and 15 GeV is approx. 5 times greater than the flux predicted on the basis of the leaky-box model. This excess is attributed to secondary antineutron production in compact sources. Because the antineutrons are not confined by the magnetic field of the compact source, they leave the interaction site, decay in interstellar space and account for the apparent excess cosmic ray antiproton flux. The escape and decay of neutrons produced in association with the antineutrons is a source of cosmic ray protons. Observations of the angular variation of the intensity and spectral shape of 100 MeV photon rays produced by neutron-decay protons in the reaction p + p yields pion (0) yields 2 photons could reveal compact-source cosmic ray production sites. COS-B observations of spectral hardening near point sources, and future high-resolution observations of galactic point sources by Gamma-1 and the Egret telescope onboard the Gamma Ray Observatory may provide supporting evidence for this model. DOE

N89-24259 California Univ., Berkeley.
SPECTRAL OBSERVATIONS OF THE EXTREME ULTRAVIOLET BACKGROUND Ph.D. Thesis
Simon Ezra Labov 1988 174 p
Avail: Univ. Microfilms Order No. DA8902173

Observations in the far ultraviolet and soft X-ray bands suggest that the interstellar medium contains gas at temperatures between 10(5) and 10(6) K. If large volumes of local interstellar space are filled with this hot plasma, observable emission lines will be produced in the extreme ultraviolet (EUV). A unique grazing incidence spectrometer was designed to study the diffuse emission between 80 and 650 A with 10 to 30 A resolution. Interplanetary He(I) 584 A emission and geocoronal He(II) 304 A emission were detected, and other features were also observed which may originate in the hot ionized interstellar gas. One feature is consistent with O(V) emission at 630 A. This emission, when combined with upper limits for other lines, restricts the temperature to 5.5 less than log T less than 5.7, in agreement with temperatures derived from O(VI) absorption studies. A power law distribution of temperatures is only consistent with the data if the power law coefficient is negative, such as predicted for saturated evaporation of clouds in a hot medium. In this case, the O(VI) absorption data confines the filling factor of the emission to f less than or equal to 4.0 pct and the pressure to more than 37,000 cm(-3) K, substantially above ambient interstellar pressure. Such a pressure enhancement has been predicted for clouds undergoing saturated evaporation. Further, this O(V) emission is consistent with the local interstellar ionization levels suggested by solar backscatter observations. A feature centered at about 100 A is best fitted by a cluster of Fe(XVIII) and Fe(XIX) lines from gas at log T = 6.6 to 6.8. The higher temperature solution is consistent with previous low resolution soft X-ray observations. A feature found in the data at 108 A is consistent with Fe(X) and Fe(XI) emission from gas at log T = 6, the same temperature derived from soft X-ray background observations. Dissert. Abstr.

N89-24260*# National Aeronautics and Space Administration. Marshall Space Flight Center, Huntsville, AL.
RAPID FITTING OF PARTICLE CASCADE DEVELOPMENT DATA FROM X-RAY FILM DENSITOMETRY MEASUREMENTS
E. Roberts, Carl M. Benson, and Walter F. Fountain Jun. 1989 18 p
(NASA-TM-100368; NAS 1.15:100368) Avail: NTIS HC A03/MF A01 CSCL 03B

A semiautomatic method of fitting transition curves to X-ray film optical density measurements of electromagnetic particle cascades is described. Several hundred singly and multiple

interacting cosmic ray events from the JACEE 8 balloon flights were analyzed using this procedure. In addition to greatly increased speed compared to the previous manual method, the semiautomatic method offers increased accuracy through maximum likelihood fitting. Author

99 GENERAL

No abstracts in this category.

☆ U.S. GOVERNMENT PRINTING OFFICE: 1989—241-445/00108

Typical Subject Index Listing

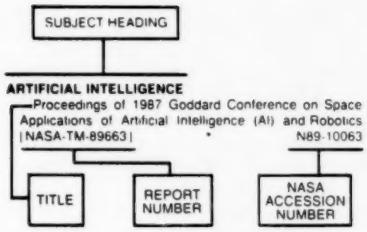

The subject heading is the key to the subject content of the document. Titles, report numbers, and accession numbers of pertinent documents are provided under each subject heading. When the title is insufficiently descriptive of the document content, a title extension has been added, separated from the title by three hyphens. The report number helps to indicate the type of document cited (e.g., NASA report, NASA translation, NASA contractor report). The NASA accession number is the number by which the document abstracts are arranged in this journal and by which the document is sold or requested. The titles, with title extensions if present, are arranged under each subject heading in ascending accession number order. The subject headings have been selected from the latest revision of the *NASA Thesaurus* (NASA SP-7064).

A

ABLATION
Direct laser/materials interaction: Laser ablation of superconductor materials and laser welding
[DE89-006560] N89-23857
ABLATIVE MATERIALS
Reentry materials in the atmosphere
[REPT-882-430-102] N89-23629
ABORTED MISSIONS
Simulator evaluation of a display for a Takeoff Performance Monitoring System
[NASA-TP-2908] N89-23469
ABRASION RESISTANCE
The wear of cutting tools: The contribution of abrasive wear N89-23586
ABRASIVES
High speed abrasive belt grinding
[AD-A205618] N89-23741
ABSORPTION SPECTROSCOPY
X-ray absorption spectroscopy of electrochemically generated species
[AD-A205572] N89-23647
Non-destructive plant health sensing using absorption spectroscopy N89-24021
ABSORPTIVITY
Optical properties of oceanic suspended matter and their interpretation for remote sensing of phytoplankton
[GKSS-88/E/40] N89-24013
ABSTRACTS
Reports of planetary astronomy, 1989
[NASA-TM-4120] N89-24232
ACCELERATION (PHYSICS)
Study on a highly sensitive electro-static suspended accelerometer (1)
[NAL-TR-1005] N89-23504
ACCELEROMETERS
Study on a highly sensitive electro-static suspended accelerometer (1)
[NAL-TR-1005] N89-23504
ACCIDENT PREVENTION
A unidirectional rotary solenoid as applied to stronglinks N89-23894
ACCLIMATIZATION
Human adaptation to the Tibetan Plateau
[AD-A206463] N89-24031
ACCRETION DISKS
Relativistic and non-relativistic magnetohydrodynamic flows around compact stars N89-24242
ACCURACY
Autonomous navigation and control
[AD-A205898] N89-23441
An improved strategy for determining earth satellite orbits by radio
[AD-A205826] N89-23497
The impact of accuracy and effort feedback and goals on adaptive decision behavior
[AD-A205751] N89-24095
ACETONITRILE
Polyethylene glycol-poly(2-methyl-5-vinyl tetrazole) polymer blend: A desensitizing binder for propellants and explosives
[AD-A206563] N89-23716
ACID RAIN
Area source documentation for the 1985 National Acid Precipitation Assessment Program Inventory
[PB89-151427] N89-23981
ACIDS
Improved acid electrolytes: The synthesis and structure of fluorine containing sulfonic acids for fuel cells
[PB89-142616] N89-23973
ACOUSTIC ATTENUATION
Flow-turning losses in solid rocket motors
[AD-A206099] N89-23525
ACOUSTIC DUCTS
Flow-turning losses in solid rocket motors
[AD-A206099] N89-23525
ACOUSTIC EMISSION
Testing chromium adhesion using acoustic emission
[AD-A205621] N89-23666
Institute for Materials Science and Engineering, nondestructive evaluation: Technical activities 1988
[PB89-151625] N89-23884
Applications of a digital acoustic-emission data-acquisition workstation
[DE89-009648] N89-23923
ACOUSTIC EXCITATION
Bifurcating jets at high Reynolds numbers
[AD-A205718] N89-23829
ACOUSTIC FREQUENCIES
Acoustic response of a rectangular waveguide with a strong transverse temperature gradient
[NASA-TM-101564] N89-24140
ACOUSTIC PROPAGATION
An investigation of the temperature dependence of the ultrasonic properties of AS4/lexan and XAS/lexan composites
[NASA-CR-184845] N89-23619
ACOUSTIC PROPERTIES
Acoustic response of a rectangular waveguide with a strong transverse temperature gradient
[NASA-TM-101564] N89-24140
ACOUSTIC SCATTERING
An investigation of the temperature dependence of the ultrasonic properties of AS4/lexan and XAS/lexan composites
[NASA-CR-184845] N89-23619
ACOUSTICS
Applications of a digital acoustic-emission data-acquisition workstation
[DE89-009648] N89-23923
ACOUSTO-OPTICS
A statistical analysis of the output signals of an acousto-optic spectrum analyzer for CW (Continuous-Wave) signals
[AD-A205404] N89-23763
ACRYLIC RESINS
Mechanical behavior of PMMA-impregnated silica gels
[AD-A205975] N89-23703
ACTIVATED CARBON
The dynamic behavior of water vapor on activated carbon
[AD-A206124] N89-23628
ACTIVATION
Mechanism of the initiation of the cationic polymerization of styrenes by silanes and activated covalent esters
[AD-A206502] N89-23708
ACTIVATION ENERGY
The glass transition temperature (Tg) as a parameter for monitoring the cure of an amine-cured epoxy system at constant heating rates
[AD-A206098] N89-23705
ACTIVE CONTROL
Detailed design of a Ride Quality Augmentation System for commuter aircraft
[NASA-CR-4230] N89-23470
ACTIVE GALAXIES
Relativistic and non-relativistic magnetohydrodynamic flows around compact stars N89-24242
ACTUATORS
Missile actuator simulation and an investigation into the accuracy of Runge-Kutta numerical integration
[AD-A206325] N89-23458
Actuator rate saturation compensator
[AD-D013962] N89-23474
Modeling and simulation of a Stewart platform type parallel structure robot
[NASA-CR-184969] N89-23875
Development of a precision, wide-dynamic-range actuator for use in active optical systems N89-23901
Practical experiences with worm gearing for spacecraft power transmission applications N89-23912
Structural mode frequencies of FOG-M (Fiber Optics Guided-Missile) actuator/fin
[AD-A206327] N89-24158
ADA (PROGRAMMING LANGUAGE)
Advanced computing systems: An advanced reasoning-based development paradigm for Ada trusted systems and its application to MACH
[AD-A206308] N89-24070
GRADA: A graphical package in Ada
[FOA-C-20741-2.7] N89-24077
Parallel ada implementation of a multiple model Kalman filter tracking system: A software engineering approach
[AD-A206094] N89-24130
ADAPTATION
Psychometric function reconstruction from adaptive tracking procedures
[AD-A205668] N89-24034
ADDITIVES
Sintering and HIPing with additives N89-23575
Corrosion and lubricity testing of nonflammable USAF formulated CTFE (Chlorotrifluoroethylene) base hydraulic fluid
[AD-A205467] N89-23695
ADHESION
The adhesion between glass and enamel N89-23598
Testing chromium adhesion using acoustic emission
[AD-A205621] N89-23666
ADHESIVE BONDING
Break dimensioning of space structural assemblies and its experimental validation
[REPT-882-430-109] N89-23508
Composites in complex assemblies
[REPT-882-430-110] N89-23509
ADHESIVES
Processable polyimide adhesive and matrix composite resin
[NASA-CASE-LAR-14101-1] N89-23692
ADIABATIC CONDITIONS
Study on a twin valveless pulse burner (temperature characteristics during pulse combustion)
[NAL-TR-973] N89-23873
Lattice symmetries and thermal expansion
[AD-A206045] N89-24207
ADIABATIC EQUATIONS
The dynamic behavior of water vapor on activated carbon
[AD-A206124] N89-23628

ADSORBENTS
The dynamic behavior of water vapor on activated carbon
[AD-A206124] N89-23628
ADSORPTION
Simple adsorbates on transition metal surfaces: A joint chemical and physical approach
[AD-A205726] N89-23689
Solid-vapor adsorption refrigeration system development
[PB89-140859] N89-23733
Monitoring thin film properties with surface acoustic wave devices: Diffusion, surface area and pore size distribution
[DE89-009379] N89-24195
Atomic layer epitaxy. Atomic layer epitaxy of 3-5 compound semiconductors by thermal and laser-assisted metalorganic chemical vapor deposition
[AD-A205699] N89-24200
ADVANCED VERY HIGH RESOLUTION RADIOMETER
The absolute radiometric calibration of the advanced very high resolution radiometer
[NASA-CR-185057] N89-23852
AEROASSIST
Optimal aeroassisted coplanar orbital transfer using an energy model
[NASA-CR-181778] N89-23495
AERODYNAMIC BALANCE
A closed-form trim solution yielding minimum trim drag for airplanes with multiple longitudinal-control effectors
[NASA-TP-2907] N89-23468
AERODYNAMIC CHARACTERISTICS
Transonic aerodynamic characteristics of a proposed Assured Crew Return Capability (ACRC) lifting-body configuration
[NASA-TM-4117] N89-23412
High angle-of-attack aerodynamic characteristics of crescent and elliptic wings
[NASA-CR-184992] N89-23418
Development of harmonic panel methods for aeroelastic applications to elastic bodies and body-fin combinations in supersonic flow
[AD-A205739] N89-23423
Preliminary design of a modular unmanned research vehicle. Volume 2: Subsystem technical development design study
[AD-A205678] N89-23454
AERODYNAMIC DRAG
Navier-Stokes solution for a NACA 0012 airfoil with mass flux (fan)
[AD-A205771] N89-23424
Drag and noise measurements on underwater vehicles with a riblet surface coating
[AD-A205500] N89-23825
AERODYNAMIC FORCES
Computational study of high supersonic flow over boattails with centered propulsive jets
[AD-A206364] N89-23431
Modelling aircraft dynamics
[AD-A204086] N89-23449
AERODYNAMIC HEATING
Numerical simulation of hypersonic flow around a space plane. 1: Basic development
[NAL-TR-976T] N89-23409
Experimental study of pressure and heating rate on a swept cylindrical leading edge resulting from swept shock wave interference
[NASA-CR-185326] N89-23411
SRB ascent aerodynamic heating design criteria reduction study, volume 1
[NASA-CR-183580] N89-23515
AERODYNAMIC INTERFERENCE
Experimental study of pressure and heating rate on a swept cylindrical leading edge resulting from swept shock wave interference
[NASA-CR-185326] N89-23411
AERODYNAMIC LOADS
Transonic operational characteristics and performance
[NAL-TR-968] N89-23408
Experimental study of pressure and heating rate on a swept cylindrical leading edge resulting from swept shock wave interference
[NASA-CR-185326] N89-23411
Optimum aeroelastic characteristics for composite supermaneuverable aircraft
[AD-A205503] N89-23452
High speed turboprop aeroacoustic study (single rotation). Volume 1: Model development
[NASA-CR-182257-VOL-1] N89-24139
AERODYNAMIC NOISE
Drag and noise measurements on underwater vehicles with a riblet surface coating
[AD-A205500] N89-23825
High speed turboprop aeroacoustic study (single rotation). Volume 1: Model development
[NASA-CR-182257-VOL-1] N89-24139
AERODYNAMIC STABILITY
Optimum aeroelastic characteristics for composite supermaneuverable aircraft
[AD-A205503] N89-23452
Exploitation of multiple solutions of the Navier-Stokes equations to achieve radically improved flight
[AD-A205939] N89-23831
AERODYNAMIC STALLING
High angle-of-attack aerodynamic characteristics of crescent and elliptic wings
[NASA-CR-184992] N89-23418
Aircraft Accident Report: AVAir Inc., Flight 3378, Fairchild Metro 3, SA227 AC, N622AV, Cary, North Carolina, February 19, 1988
[PB88-910412] N89-23436
AERODYNAMICS
NASA aeronautics research and technology
[NASA-EP-259] N89-23406
AEROELASTICITY
Optimum aeroelastic characteristics for composite supermaneuverable aircraft
[AD-A205503] N89-23452
AERONAUTICAL ENGINEERING
NASA aeronautics research and technology
[NASA-EP-259] N89-23406
AEROSOLS
Design of a chamber for CBW aerosol studies with relative humidity and particle concentration control
[AD-A205623] N89-23481
Synthesis of novel acid electrolytes for phosphoric acid fuel cells
[PB89-148944] N89-23786
Vaporization and recondensation in propagation and imaging of laser beams
[DE89-008014] N89-23858
Gas-Grain Simulation Facility: Fundamental studies of particle formation and interactions. Volume 1: Executive summary and overview
[NASA-CP-10026-VOL-1] N89-24022
Gas-Grain Simulation Facility: Fundamental studies of particle formation and interactions. Volume 2: Abstracts, candidate experiments and feasibility study
[NASA-CP-10026-VOL-2] N89-24023
AEROSPACE ENGINEERING
JPRS report: Science and technology. USSR: Space
[JPRS-USP-89-004] N89-23484
Agenda of the Fourth Annual Summer Conference, NASA/USRA University Advanced Design Program
[NASA-TM-101750] N89-23493
Comprehensive report of aeropropulsion, space propulsion, space power, and space science applications of the Lewis Research Center
[NASA-TM-100925] N89-24216
Patent abstracts bibliography: A continuing bibliography. Section 2: Indexes (supplement 34)
[NASA-SP-7039(34)-SECT-2] N89-24219
AEROSPACE ENVIRONMENTS
Effects of space radiation on electronic microcircuits N89-23549
AEROSPACE MEDICINE
Medical and biological support for a manned expedition to Mars N89-23492
A strategy for space biology and medical science for the 1980s and 1990s
[NASA-CR-184895] N89-24024
AEROSPACE PLANES
Numerical simulation of hypersonic flow around a space plane. 1: Basic development
[NAL-TR-976T] N89-23409
AEROSPACE SAFETY
Annual review of aircraft accident data, US Air Carrier operations: Calendar year 1986
[PB89-151021] N89-23434
Expert systems applied to spacecraft fire safety
[NASA-CR-182266] N89-23501
AEROSPACE SYSTEMS
On-orbit observations of single-event upset in harris HM-6508 RAMSs (Random Access Memories): An update
[AD-A206266] N89-23506
Spacecraft contamination experience N89-23545
The 23rd Aerospace Mechanisms Symposium
[NASA-CP-3032] N89-23892
An analysis of lightning launch constraints
[AD-A206084] N89-23994
AEROSPACE VEHICLES
Environmental definition of the earth's neutral atmosphere N89-23539
The long-term effects of the micrometeoroid and orbital debris environments on materials used in space N89-23542
Space vehicle thermal testing: Principles, practices and effectiveness N89-23550
Ultraviolet radiation effects N89-23551
Effects of thermal cycling on composite materials for space structures N89-23552
Experimental and theoretical determination of the thermomechanical response of inelastic structural materials to high energy thermal inputs
[AD-A206100] N89-23933
AEROTHERMODYNAMICS
Aerothermodynamic analysis of a Coanda/Refraction Jet Engine Test Facility
[AD-A205937] N89-23462
AFTERBODIES
Computational study of high supersonic flow over boattails with centered propulsive jets
[AD-A206364] N89-23431
Transonic Navier-Stokes solutions of three-dimensional afterbody flows
[NASA-TM-4111] N89-23433
AGGREGATES
Geobotanical remote sensing for determination of aggregate source material
[AD-A205943] N89-23962
AGING (BIOLOGY)
Age distribution among NASA scientists and engineers N89-23911
AGING (MATERIALS)
The structural basis for fatigue initiation in glassy polymers
[DE89-009292] N89-23689
Effect of physical annealing on the dynamic mechanical properties of a high T(g) amine-cured epoxy systems
[AD-A205980] N89-23704
AIR
Spontaneous ignition of atomized kerosine/air mixtures in a high pressure flowing system
[NAL-TR-966] N89-23635
On steel superficial hardening by concentrated electron beam in the air
[DE88-705781] N89-23658
AIR CONDITIONING EQUIPMENT
The application of self-tuning control techniques to a multivariable process
[OUEL-1737/88] N89-23737
Evaluation of three commercial microclimate cooling systems
[AD-A206318] N89-23744
AIR COOLING
Effect of internal convection and internal radiation on the structural temperatures of Space Shuttle Orbiter
[NASA-TM-100414] N89-23819
AIR FLOW
An instrument for the simultaneous measurement of velocity, temperature and density in unseeded air flows
[AD-A205588] N89-23453
Bifurcating jets at high Reynolds numbers
[AD-A205718] N89-23829
Friction factor data for flat plate tests of smooth and honeycomb surfaces
[NASA-CR-184977] N89-23876
AIR LAND INTERACTIONS
Mapping freeze/thaw boundaries with SMMR data
[NASA-CR-184991] N89-23961
AIR NAVIGATION
Loran C field strength contours: Contiguous US
[DOT/FAA/CT-TN89/16] N89-23437
The 4D-TECS integration for NASA TSRV airplane
[NASA-CR-4231] N89-23471
AIR QUALITY
Summary of selected new information on effects of ozone on health and vegetation. Draft supplement to air quality criteria for ozone and other photochemical oxidants
[PB89-135123] N89-23980
AIR TRAFFIC
Comparison of interpolation algorithms for speed control in air traffic management
[AD-A206314] N89-23444
AIR TRAFFIC CONTROL
National Airspace System Search and Rescue operational concept (NAS-SR-1329)
[DOT/FAA/DS-89/07] N89-23435
Generation of architectures for distributed intelligence systems
[AD-A205783] N89-23440
Comparison of interpolation algorithms for speed control in air traffic management
[AD-A206314] N89-23444
Host computer system capacity management procedures
[AD-A193416] N89-24051
AIR WATER INTERACTIONS
Analysis of turbulent motion phenomena in the maritime atmospheric boundary layer
[ETN-89-93949] N89-23996
AIRBORNE EQUIPMENT
Design of the ELDORA airborne Doppler radar
[PB89-144804] N89-23749

AIRBORNE SURVEILLANCE RADAR
Battlefield radar imaging through airborne millimetric wave SAR (Synthetic Aperture Radar)
[ETN-89-94228] N89-23751
AIRBORNE/SPACEBORNE COMPUTERS
Avionics architecture studies for the entry research vehicle
[NASA-CR-181828] N89-24082
AIRCRAFT ACCIDENT INVESTIGATION
Aircraft Accident Report: AVAir Inc., Flight 3378, Fairchild Metro 3, SA227 AC, N622AV, Cary, North Carolina, February 19, 1988
[PB88-910412] N89-23436
AIRCRAFT ACCIDENTS
Annual review of aircraft accident data, US Air Carrier operations: Calendar year 1986
[PB89-151021] N89-23434
AIRCRAFT COMPARTMENTS
Interior noise control ground test studies for advanced turboprop aircraft applications
[NASA-CR-181819] N89-24141
AIRCRAFT CONFIGURATIONS
Numerical simulation of hypersonic flow around a space plane. 1: Basic development
[NAL-TR-976T] N89-23409
A methodology for determining the survivability of fixed-wing aircraft against small arms
[AD-A205730] N89-23455
AIRCRAFT CONSTRUCTION MATERIALS
Composite materials nondestructive tests: Choice of methods depending on requirements
[REPT-882-430-105] N89-23630
AIRCRAFT CONTROL
Control design of an unstable non-minimum phase aircraft subject to control surface saturation
[AD-A206024] N89-23475
AIRCRAFT DESIGN
NASA aeronautics research and technology
[NASA-EP-259] N89-23406
Preliminary design of a modular unmanned research vehicle. Volume 2: Subsystem technical development design study
[AD-A205678] N89-23454
USAF (US Air Force) durability design handbook: Guidelines for the analysis and design of durable aircraft structures
[AD-A206286] N89-23457
Center of gravity control on Airbus aircraft: Fuel, range and loading
[REPT-882-111-101] N89-23460
A330/340 hydraulic system
[REPT-882-111-102] N89-23461
A closed-form trim solution yielding minimum trim drag for airplanes with multiple longitudinal-control effectors
[NASA-TP-2907] N89-23468
Control design of an unstable non-minimum phase aircraft subject to control surface saturation
[AD-A206024] N89-23475
Multivariable flight control design with parameter uncertainty for the AFTI/F-16
[AD-A206068] N89-23476
Agenda of the Fourth Annual Summer Conference, NASA/USRA University Advanced Design Program
[NASA-TM-101750] N89-23493
AIRCRAFT ENGINES
NASA aeronautics research and technology
[NASA-EP-259] N89-23406
Investigations on the cracking behavior of joints in airfields and roads: Field investigations and laboratory simulations
[PB89-141279] N89-23479
Comprehensive report of aeropropulsion, space propulsion, space power, and space science applications of the Lewis Research Center
[NASA-TM-100925] N89-24216
AIRCRAFT INSTRUMENTS
Development of the extended kalman filter for the advanced Completely Integrated Reference Instrumentation System (CIRIS)
[AD-A206083] N89-23443
AIRCRAFT LANDING
Comparison of interpolation algorithms for speed control in air traffic management
[AD-A206314] N89-23444
Heliport night parking area criteria test plan
[DOT/FAA/CT-TN88/45] N89-23480
AIRCRAFT MAINTENANCE
An analysis of Electronic Aids to Maintenance (EAM) for the Light Helicopter Family (LHX)
[AD-A205440] N89-23407
AIRCRAFT MANEUVERS
An investigation into the application of dynamic programming to determine optimal controls for tracking a cruise missile maneuver by CMMCA (Cruise Missile Mission Control Aircraft)
[AD-A205970] N89-23456
Heliport night parking area criteria test plan
[DOT/FAA/CT-TN88/45] N89-23480
AIRCRAFT NOISE
Noise and sonic boom impact technology. PCBOOM computer program for sonic boom research, volume 1
[AD-A206290] N89-23429
High speed turboprop aeroacoustic study (single rotation). Volume 1: Model development
[NASA-CR-182257-VOL-1] N89-24139
AIRCRAFT PERFORMANCE
Numerical simulation of hypersonic flow around a space plane. 1: Basic development
[NAL-TR-976T] N89-23409
Method and system for monitoring and displaying engine performance parameters
[NASA-CASE-LAR-14049-1] N89-23466
AIRCRAFT RELIABILITY
Flight testing of the Southern Cross replica aircraft
[AD-A205303] N89-23451
AIRCRAFT SAFETY
Annual review of aircraft accident data, US Air Carrier operations: Calendar year 1986
[PB89-151021] N89-23434
AIRCRAFT SPIN
Modelling aircraft dynamics
[AD-A204086] N89-23449
AIRCRAFT STABILITY
Detailed design of a Ride Quality Augmentation System for commuter aircraft
[NASA-CR-4230] N89-23470
AIRCRAFT STRUCTURES
A correlation study of X-29A aircraft and associated analytical developments N89-23450
Investigations on the cracking behavior of joints in airfields and roads: Field investigations and laboratory simulations
[PB89-141279] N89-23479
AIRCRAFT SURVIVABILITY
A methodology for determining the survivability of fixed-wing aircraft against small arms
[AD-A205730] N89-23455
AIRCRAFT WAKES
The low frequency oscillation in the flow over a NACA0012 airfoil with an iced leading edge
[NASA-TM-102018] N89-23417
AIRFOIL OSCILLATIONS
The low frequency oscillation in the flow over a NACA0012 airfoil with an iced leading edge
[NASA-TM-102018] N89-23417
AIRFOIL PROFILES
Numerical solution of periodic vortical flows about a thin airfoil
[NASA-TM-101998] N89-23413
The low frequency oscillation in the flow over a NACA0012 airfoil with an iced leading edge
[NASA-TM-102018] N89-23417
Computation of dynamics and control of unsteady vortical flows N89-23822
AIRFOILS
Navier-Stokes solution for a NACA 0012 airfoil with mass flux (fan)
[AD-A205771] N89-23424
Numerical study of the influence of leading and trailing edge flaps on the performance of airfoils
[AD-A206138] N89-23428
Donor acceptor polymerization chemistry as a vehicle to low energy cure of matrix resins: Evolution of the 2-Tg concept to produce Tg polymers at ambient temperatures
[AD-A206287] N89-23706
An experimental study of laminar flow control airfoil with suction through perforated surface at low speed
[NAL-TR-967] N89-23806
AIRFRAME MATERIALS
Quench sensitivity of airframe aluminium alloys
[PB89-146039] N89-23656
AIRFRAMES
USAF (US Air Force) durability design handbook: Guidelines for the analysis and design of durable aircraft structures
[AD-A206286] N89-23457
AIRPORT LIGHTS
Heliport night parking area criteria test plan
[DOT/FAA/CT-TN88/45] N89-23480
AIRPORTS
Comparison of interpolation algorithms for speed control in air traffic management
[AD-A206314] N89-23444
Response of pavement to freeze-thaw cycles: Lebanon, New Hampshire, regional airport
[AD-A205559] N89-23740
ALASKA
KRMS (K-band Radiometric Mapping System) SSM/I validation March 1988 quick look report
[NASA-CR-185320] N89-23766
Remote sensing of global snowpack energy and mass balance: In-situ measurements on the snow of interior and Arctic Alaska
[NASA-CR-180078] N89-23956
Climatic atlas of the outer continental shelf waters and coastal regions of Alaska. Volume 1: Gulf of Alaska, revision
[AD-A205289] N89-24005
ALGEBRA
On the algebraic structure of integrable systems in multidimensions
[DE89-008697] N89-24108
Differential algebraic equations, indices, and integral algebraic equations
[DE89-009584] N89-24109
On the communication complexity of distributed algebraic computation
[AD-A205784] N89-24117
Exploring the episodic structure of algebra story problem solving: Revision
[AD-A206403] N89-24122
Symbolic analysis of multivariable missile systems
[AD-A206326] N89-24132
ALGORITHMS
Comparison of interpolation algorithms for speed control in air traffic management
[AD-A206314] N89-23444
Code optimization of speckle reduction algorithms for image processing of rocket motor holograms
[AD-A205306] N89-23524
Enhanced tracking of ballistic targets using forward looking infrared measurements
[AD-A205727] N89-23769
Generating circuit tests by exploiting designed behavior
[AD-A206175] N89-23800
Multiple model-based robot control: Development and initial evaluation
[AD-A205725] N89-23881
Shortest paths in a digitized map using a tile-based data structure
[PB89-143432] N89-23957
Calculation of the surface of a geodetic polygon on an ellipsoid of revolution
[ETN-89-94149] N89-23966
On the use of multiprocessing computers for global numerical weather prediction
[AD-A206102] N89-24009
Wavefront matrix multiplication on a distributed-memory multiprocessor
[PB89-151807] N89-24052
Compiling high level constructs to distributed memory architectures
[NASA-CR-181825] N89-24058
A CAD (Computer Aided Design) tool for current-mode multiple-valued CMOS circuits
[AD-A205327] N89-24061
Adaptive signal processing
[AD-A205787] N89-24063
Deductive programming synthesis
[AD-A206451] N89-24072
Runtime aggregation of recursion relations
[AD-A206576] N89-24076
Reduction of a general matrix to tridiagonal form
[DE89-008980] N89-24083
Numerical experience with a superfast real Toeplitz solver
[AD-A205374] N89-24115
Numerical conformal mapping and applications
[AD-A205602] N89-24131
A blocked Jacobi method for the symmetric Eigenproblem
[AD-A206553] N89-24133
Digital optics for numerical computing: The residue number system for numerical optical computing
[AD-A206229] N89-24157
Semiconductor measurement technology: Automatic determination of the interstitial oxygen content of silicon wafers polished on both sides
[PB89-151831] N89-24180
Image processing of coronal pictures
[AD-A205326] N89-24252
ALIGNMENT
Tensile film clamps and mounting block for the rheovibron and autovibron viscoelastometer
[NASA-CASE-LAR-13696-1] N89-23880
ALTITUDE SICKNESS
Human adaptation to the Tibetan Plateau
[AD-A206463] N89-24031
ALUMINIDES
Intermetallic phases for high temperature applications N89-23612
Theoretical analysis of compatibility of several reinforcement materials with NiAl and FeAl matrices
[NASA-CR-182291] N89-23622

Theoretical studies of Ni3Al and NiAl with impurities
[DE89-006556] N89-23655

ALUMINUM

Sintering of Si3N4 in the presence of additives from Y2O3-SiO2-Al2O3 system N89-23581
A combined isotropic-kinematic hardening model for large deformation metal plasticity
[AD-A206352] N89-23935
Correlated atomic motions in liquid aluminum
[ETN-89-93943] N89-24145
Fiber-optic time-resolved fluorescence sensor for the simultaneous determination of Al(+3), Ga(+3) and In(+3)
[AD-A205689] N89-24154

ALUMINUM ALLOYS

Quench sensitivity of airframe aluminium alloys
[PB89-146039] N89-23656
Iron-niobium-aluminum alloy having high-temperature corrosion resistance
[DE89-009600] N89-23663
Fabrication of unidirectional fiber reinforced 6061 aluminum alloy using high pressure squeeze casting
[AD-A205717] N89-23668
Ambient temperature properties of PM (Powder Metal) aluminum-titanium alloys
[AD-A205997] N89-23671

ALUMINUM COMPOUNDS

Preparation and thermal expansion of Al2TiO5-TiO5-TiO2 sintered bodies N89-23578

ALUMINUM GALLIUM ARSENIDES

High-power single spatial mode AlGaAs channeled-substrate-planar semiconductor diode lasers for spaceborne communications
[NASA-CR-4238] N89-23660
Characterization of semiconductor device processing etchant solutions for GaAs and p+ GaAs layers employed in AlxGa(1-x)As/GaAs MODFETs and related heterojunction devices
[AD-A205772] N89-24201
Some 3-5 heterojunction structures and high speed devices
[AD-A205946] N89-24203

ALUMINUM NITRIDES

Thermal transport in pressureless sintered aluminum nitride N89-23590

ALUMINUM OXIDES

Injection molding of whisker-reinforced Al2O3-ZrO2 ceramics N89-23574
Microstructure development in alumina N89-23579
Sintering of CaO and MgO in the presence of nonequilibrium liquid phase N89-23580
Phase transformation of Zr(x)Hf(1-x)O2 in alumina matrix N89-23588
Preparation, characterization and thermal diffusivity of Al2TiO5 N89-23591
Dilatometric analysis of Al-, Ba-, Ca-titanate N89-23592
Temperature dependence of interfacial energies between solid oxides and liquid metals N89-23599
Characterization of a phase boundary in Ni-Al2O3 sintered under pressure N89-23600
Fabrication and properties of alumina-zirconia composites
[PB89-147532] N89-23620
Ceramic tribology: Methodology and mechanisms of alumina wear
[PB89-148357] N89-23679
Study of adherent oxide scales
[AD-A205799] N89-23700
Transmission losses in hollow aluminum oxide waveguide at 10.6 microns
[FOA-C-30518-3.1] N89-23804

AMBIENT TEMPERATURE

Ambient temperature properties of PM (Powder Metal) aluminum-titanium alloys
[AD-A205997] N89-23671

AMINES

Treatment with tyrosine, a neurotransmitter precursor, reduces environmental stress in humans
[AD-A206035] N89-24039

AMMONIA

Solid-vapor adsorption refrigeration system development
[PB89-140859] N89-23733

AMMUNITION

A methodology for determining the survivability of fixed-wing aircraft against small arms
[AD-A205730] N89-23455

AMPLIDYNES

Designing feedback compensators by using the root-locus method
[AD-A205354] N89-24093

ANALOG TO DIGITAL CONVERTERS

Phase accuracy experiments with a direct-sampling coherent detector
[AD-A205458] N89-23764
Monolithic GaAs digitizer for space-based laser pulse spreading effect
[NASA-CR-183430] N89-23855
Automatic digitizing of cadastral maps N89-23946

ANALYSIS (MATHEMATICS)

Comparison of computational analysis with flight tests of a 40mm solid-fuel ramjet projectile
[AD-A206536] N89-23459

ANALYSIS OF VARIANCE

Analysis and optimization of geodetic networks by spectral criteria and mechanical analogies
[SER-C-342] N89-23963

ANALYZERS

An evaluation of coplanar line for application in microwave integrated circuitry
[AD-A205305] N89-23795
Correlation of Portable Wear Metal Analyzer (PWMA-2) and Baird A/E35U-3 spectrometer oil analysis data
[AD-A205957] N89-23882

ANGLE OF ATTACK

High angle-of-attack aerodynamic characteristics of crescent and elliptic wings
[NASA-CR-184992] N89-23418
Flowfield measurements in the vortex wake of a missile at high angle of attack in turbulence
[AD-A205696] N89-23422
Modelling aircraft dynamics
[AD-A204086] N89-23449
Characteristics of a five-hole spherical pitot tube
[NAL-TR-971] N89-23463

ANISOTROPY

Numerical implementation of the Schapery model for nonlinear visco-elasticity
[PB89-144950] N89-23915

ANNEALING

Effect of physical annealing on the dynamic mechanical properties of a high T(g) amine-cured epoxy systems
[AD-A205980] N89-23704
Sequentially evaporated thin Y-Ba-Cu-O superconducting films on microwave substrates
[NASA-TM-102068] N89-23791

ANNIHILATION REACTIONS

Parametric study of radiative cooling of solid antihydrogen
[AD-A206092] N89-23742

ANODES

Megavolt, multi-kiloamp K(sub)a-band gyrotron oscillator experiment
[AD-A206271] N89-23801

ANOMALIES

On-orbit observations of single-event upset in harris HM-6508 RAMSs (Random Access Memories): An update
[AD-A206266] N89-23506
Trends in environmentally induced spacecraft anomalies N89-23536

ANTENNA ARRAYS

The effect of mutual coupling on the side lobe performance of Chebyshev arrays, volume 1
[AD-A205724] N89-23768
Design and verification of mechanisms for a large foldable antenna N89-23899
Design of a 60 GHz beam waveguide antenna positioner N89-23910

ANTENNA COMPONENTS

Design of a 60 GHz beam waveguide antenna positioner N89-23910

ANTENNA DESIGN

Small UHF microstrip radiating element
[REPT-882-440-103] N89-23780
Mechanical/electrical distortion model for reflector antennas
[REPT-882-440-104] N89-23781
TELE-X antenna module thermal control
[REPT-882-440-106] N89-23782
Near field testing of the electronically despun antenna of the Meteosat satellite
[REPT-882-440-108] N89-23783
ESA-D: An integrated software for antenna design and analysis
[REPT-882-440-111] N89-23784

ANTENNA RADIATION PATTERNS

The performance of Space-Based Radars (SBR) orbiting on elliptical orbits
[AD-A205951] N89-23772
Near field testing of the electronically despun antenna of the Meteosat satellite
[REPT-882-440-108] N89-23783

ANTHRACENE

In situ fluorescence monitoring of the viscosities of particle-filled polymers in flow
[PB89-146278] N89-23680

ANTHROPOMETRY

Computer-aided design and bio-engineering: A review of the literature
[AD-A206534] N89-24074

ANTIMISSILE DEFENSE

Parallel ada implementation of a multiple model Kalman filter tracking system: A software engineering approach
[AD-A206094] N89-24130

ANTIMISSILE MISSILES

Pif-Paf piloting of tactical missiles
[REPT-882-320-104] N89-23462

ANTIMONY

Alternate arsenic and antimony sources for the OMCVD fabrication of semiconductors
[AD-A206483] N89-24211

ANTIMONY ALLOYS

Critical assessment of the thermodynamic properties of antimony-copper alloys
[PB89-147524] N89-23657

ANTIPROTONS

Compact source origin of cosmic ray antiprotons
[DE89-008044] N89-24258

APERTURES

A compact fast wide angle broad band spectrometer optical system
[NASA-CASE-NPO-17562-1-CU] N89-24153

APOGEES

The performance of Space-Based Radars (SBR) orbiting on elliptical orbits
[AD-A205951] N89-23772

APPLICATION SPECIFIC INTEGRATED CIRCUITS

An application specific integrated circuit for dual-axis motion control
[DE89-007974] N89-23790

APPLICATIONS PROGRAMS (COMPUTERS)

Enhancements to a new free wake hover analysis
[NASA-CR-177523] N89-23414
Flosolver: A parallel computer for fluid dynamics
[NAL-TM-AE-8803] N89-23805
Fatigue crack growth model RANDOM2 user manual, appendix 1
[NASA-CR-184939] N89-23890
Fatigue strength reduction model: RANDOM3 and RANDOM4 user manual, appendix 2
[NASA-CR-184940] N89-23891
A description of the slab model
[DE89-009962] N89-23984
Microcomputer program for daily weather simulation
[PB89-144638] N89-24001
SMOOFF: A FORTRAN smoothing program
[AD-A204087] N89-24057
Solution of one-dimensional Euler equations by the implicit finite difference technique of Beam and Warming
[NAL-PD-FM-8816] N89-24097

APPROACH

Noise of a model counterrotation propeller with simulated fuselage and support pylon at takeoff/approach conditions
[NASA-TM-101996] N89-24138

APPROXIMATION

Numerical study of the influence of leading and trailing edge flaps on the performance of airfoils
[AD-A206138] N89-23428
An iterative technique to correct probe position errors in planar near-field to far-field transformations
[PB89-153886] N89-23750
Equations for two-dimensional density matrix. Approximate solutions in the vicinity of the classical solution
[DE88-705825] N89-24107
A hierarchy of transport approximations for high energy heavy (HZE) ions
[NASA-TM-4118] N89-24255

APTITUDE

Development and evaluation of integrating details: A complex spatial problem solving test
[AD-A205860] N89-24035

ARC JET ENGINES

Test facility and preliminary performance of a 100 kW class MPD thruster
[NASA-TM-102021] N89-23520
Arcjet nozzle design impacts
[NASA-TM-102050] N89-23522

ARC WELDING

The effect of welding process on the microstructure of HY-130 steel weldments
[AD-A205692] N89-23667

ARCHITECTURE (COMPUTERS)

Generation of architectures for distributed intelligence systems
[AD-A205783] N89-23440
A designers' guide to reliable distributed systems: An example design. Volume 1
[AD-A208039] N89-23885
A designers' guide to reliable distributed systems: An example design. Volume 2
[AD-A208040] N89-23886

An ICAI (Intelligent Computer Aided Instruction) architecture for troubleshooting in complex dynamic systems
[AD-A205434] N89-24045
Compiling high level constructs to distributed memory architectures
[NASA-CR-181825] N89-24058
Fourth generation computer languages
[DE89-008800] N89-24059
Adaptive signal processing
[AD-A205787] N89-24063
A visual object-oriented unification system
[AD-A206228] N89-24068
Runtime aggregation of recursion relations
[AD-A206576] N89-24076
Avionics architecture studies for the entry research vehicle
[NASA-CR-181828] N89-24082
Solid modeling requirements for finite element modeling using mapped mesh techniques
[DE89-009639] N89-24110

ARCTIC REGIONS
KRMS (K-band Radiometric Mapping System) SSM/I validation March 1988 quick look report
[NASA-CR-185320] N89-23766
Remote sensing of global snowpack energy and mass balance: In-situ measurements on the snow of interior and Arctic Alaska
[NASA-CR-180078] N89-23956

AREA
Automatic extraction of areas from overlays of the series DGK 5 (Bo) N89-23955

ARGON
Experimental thermal conductivity, thermal diffusivity and specific heat values of argon and nitrogen
[PB89-148407] N89-23637

ARGON LASERS
Functional assessment of laser irradiation
[AD-A206230] N89-23871

ARGON PLASMA
Ionization investigation of sputtered titanium and of titanium ion transport process in an argon discharge glow using laser induced fluorescence
[JUEL-2219] N89-23660
Investigation of the behaviour of a collisionless R-F sheath
[OUEL-1695/87] N89-24165
Preliminary evaluation of a miniaturized torch for inductively coupled plasma mass spectrometry
[AD-A205746] N89-24173
Simultaneous measurement of spatially resolved electron temperatures. Electron number densities and gas temperatures by laser light scattering from the ICP
[AD-A205747] N89-24174

ARIANE LAUNCH VEHICLE
The evolution of space mechanisms in the ESA R and D program N89-23893

ARITHMETIC
Digital optics for numerical computing: The residue number system for numerical optical computing
[AD-A206229] N89-24157

ARIZONA
The US Army Yuma Proving Ground, Arizona 33-year climate calendar and tables on associated weather elements 1954-1986. American desert country
[AD-A206256] N89-24010

ARMED FORCES (UNITED STATES)
US Air Force research technology area plan, FY 1989
[AD-A205304] N89-24217
Air Force Human Resources Laboratory R and D accomplishments and services, FY86-FY88
[AD-A205312] N89-24218

ARRAYS
Recursive gate-arrays
[AD-A205335] N89-23796

ARSENIC
Alternate arsenic and antimony sources for the OMCVD fabrication of semiconductors
[AD-A206483] N89-24211

ARTIFICIAL INTELLIGENCE
Generation of architectures for distributed intelligence systems
[AD-A205783] N89-23440
Flight telerobot mechanism design: Problems and challenges N89-23907
Explanation-based theory revision: An approach to the problems of incomplete and incorrect theories
[AD-A205337] N89-24092
Heuristics for cooperative problem solving
[AD-A206371] N89-24096
Knowledge representation using Structured Modeling N89-24224

ARTIFICIAL SATELLITES
Study on a highly sensitive electro-static suspended accelerometer (1)
[NAL-TR-1005] N89-23504
NASA space communications R and D (Research and Development): Issues, derived benefits, and future directions
[NASA-CR-184831] N89-23746

ASPECT RATIO
Flutter of a low-aspect-ratio rectangular wing
[NASA-TM-4116] N89-23447

ASSEMBLIES
Break dimensioning of space structural assemblies and its experimental validation
[REPT-882-430-109] N89-23508

ASTEROIDS
Reports of planetary astronomy, 1989
[NASA-TM-4120] N89-24232

ASTROMETRY
The Allegheny Observatory search for planetary systems
[NASA-CR-184990] N89-24233

ASTRONOMICAL MODELS
A self consistant model of the three phase interstellar medium in disk galaxies N89-24245

ASTRONOMICAL OBSERVATORIES
The Allegheny Observatory search for planetary systems
[NASA-CR-184990] N89-24233

ASTRONOMICAL PHOTOMETRY
The Allegheny Observatory search for planetary systems
[NASA-CR-184990] N89-24233

ASTRONOMICAL SATELLITES
Thermal and cryogenic aspects of the ISO optical subsystem
[REPT-882-440-113] N89-24160

ASTRONOMY
Reports of planetary astronomy, 1989
[NASA-TM-4120] N89-24232

ASYMPTOTIC PROPERTIES
Asymptotic behavior of random discrete event systems
[PB89-146146] N89-24099

ASYMPTOTIC SERIES
Asymptotic behavior of random discrete event systems
[PB89-146146] N89-24099

ATLANTIC OCEAN
Exploring the North Atlantic Ocean on floppy disks
[AD-A205733] N89-24011

ATMOSPHERIC ATTENUATION
Link availability and rain attenuation exceedance characteristics for EHF (Extremely High Frequency) satellite communications with arbitrary link parameters in Canada
[AD-A205403] N89-23762

ATMOSPHERIC BOUNDARY LAYER
Analysis of turbulent motion phenomena in the maritime atmospheric boundary layer
[ETN-89-93949] N89-23996
Current problems in the stratocumulus-topped atmospheric boundary layer N89-23998
Turbulent structure of a shear-driven stratus-topped atmospheric boundary layer: A comparison of model results with observations N89-23999

ATMOSPHERIC CIRCULATION
Analysis of turbulent motion phenomena in the maritime atmospheric boundary layer
[ETN-89-93949] N89-23996

ATMOSPHERIC CORRECTION
The absolute radiometric calibration of the advanced very high resolution radiometer
[NASA-CR-185057] N89-23852

ATMOSPHERIC ELECTRICITY
An analysis of lightning launch constraints
[AD-A206084] N89-23994

ATMOSPHERIC GENERAL CIRCULATION MODELS
Normal mode energetics of the general circulation during the FGGE year N89-24004

ATMOSPHERIC MODELS
Environmental definition of the earth's neutral atmosphere N89-23539
A description of the slab model
[DE89-009962] N89-23984
Stratocumulus modeling
[KNMI-WR-88-2] N89-23997
Turbulent structure of a shear-driven stratus-topped atmospheric boundary layer: A comparison of model results with observations N89-23999
The diurnal variation of a marine stratocumulus layer: A model sensitivity study N89-24000
On the use of multiprocessing computers for global numerical weather prediction
[AD-A206102] N89-24009

ATMOSPHERIC MOISTURE
Corrosion of silicon carbide ceramics at high temperatures in water vapor-containing atmospheres N89-23594
Evaluation of the historical Schoenbein method for the determination of ozone in a flow chamber
[JUEL-2218] N89-23983

ATMOSPHERIC PHYSICS
Thermal images of sky and sea-surface background infrared radiation
[AD-A205819] N89-23992

ATMOSPHERIC PRESSURE
The US Army Yuma Proving Ground, Arizona 33-year climate calendar and tables on associated weather elements 1954-1986. American desert country
[AD-A206256] N89-24010

ATMOSPHERIC TEMPERATURE
An instrument for the simultaneous measurement of velocity, temperature and density in unseeded air flows
[AD-A205588] N89-23453

ATMOSPHERIC TURBULENCE
Current problems in the stratocumulus-topped atmospheric boundary layer N89-23998
Turbulent structure of a shear-driven stratus-topped atmospheric boundary layer: A comparison of model results with observations N89-23999

ATMOSPHERICS
Loran C field strength contours: Contiguous US
[DOT/FAA/CT-TN89/16] N89-23437

ATOMIC INTERACTIONS
Correlated atomic motions in liquid aluminum
[ETN-89-93943] N89-24145
Eikonal approximation in partial wave version
[IPPJ-899] N89-24164

ATOMIC STRUCTURE
Electron spectroscopy for chemical analysis: Sample analysis
[NASA-CR-183568] N89-23634
Strength and structure of Ga(1-x)In(x)As alloys
[AD-A205415] N89-23644
A first-principles calculation of the resistivity and thermopower in strong-scattering alloys
[DE89-008565] N89-23661
Population inversions in ablation plasmas generated by intense electron beams
[AD-A205716] N89-24172
Heterojunction band line-ups and the alloying effect in compound semiconductor alloys: A photoemission study N89-24179
The electronic structure of GaAs sub 1-x P sub x and GaSb sub 1-x P sub x calculated using the recursion method
[DE88-705702] N89-24185
Structure and grid dynamics of ultrathin epitaxial Ag and Fe films on Ni(100) and Cu(100) substrates
[JUEL-2221] N89-24187
In situ mechanistic studies of MOCVD growth of 3/5 semiconductors
[AD-A206396] N89-24210

ATOMIZING
Cooling rate, undercooling and rapid solidification by atomization N89-23609
Spontaneous ignition of atomized kerosine/air mixtures in a high pressure flowing system
[NAL-TR-966] N89-23635

ATOMS
Atomic imaging and microanalysis of ceramics
[DE89-008172] N89-23684

ATTENTION
Relating attention to visual mechanisms
[AD-A206452] N89-24042

ATTENUATION COEFFICIENTS
Transmission losses in hollow aluminum oxide waveguide at 10.6 microns
[FOA-C-30518-3.1] N89-23804

ATTITUDE CONTROL
Control design of an unstable non-minimum phase aircraft subject to control surface saturation
[AD-A206024] N89-23475
Study on a highly sensitive electro-static suspended accelerometer (1)
[NAL-TR-1005] N89-23504

ATTITUDE GYROS
Design, fabrication and test of a 4750 Newton-meter-second double Gimbal control moment gyroscope N89-23896

ATTITUDE STABILITY
An analysis of the attitude stability of a space station subject to parametric excitation of periodic mass motion
[AD-A206009] N89-23505

AUDIO FREQUENCIES
Noise characteristics of an inductively coupled plasma-mass spectrometer
[AD-A205686] N89-24169

AURORAL ZONES
Electric fields in the magnetosphere: The evidence from ISEE, S3-3, GEOS and Viking
[TRITA-EPP-88-11] N89-23987

AUSFORMING
Behavior of metals during hot rolling processes. Part 1: Mathematical models N89-23613
Behavior of metals during hot rolling processes. Part 2: Experimental methods for flow stress determination and calculation of the two-dimensional temperature-field in the roll gap N89-23614
AUTOCORRELATION
Radar waveforms derived from orthogonal matrices [AD-A205459] N89-23765
Correlated atomic motions in liquid aluminum [ETN-89-93943] N89-24145
AUTOMATIC CONTROL
Center of gravity control on Airbus aircraft: Fuel, range and loading [REPT-882-111-101] N89-23460
A research facility for film cooling investigations with emphasis on the instrumentation system [NAL-TM-PR-8704] N89-23477
Traction-drive force transmission for telerobotic joints N89-23906
Automatic digitizing of cadastral maps N89-23946
Automated seed manipulation and planting N89-24017
AUTOMATIC FLIGHT CONTROL
Detailed design of a Ride Quality Augmentation System for commuter aircraft [NASA-CR-4230] N89-23470
Software reliability studies [NASA-CR-184857] N89-24054
AUTOMATIC PILOTS
The 4D-TECS integration for NASA TSRV airplane [NASA-CR-4231] N89-23471
Analytical transfer functions in parallel configurations [AD-A205714] N89-23472
AUTOMATIC TEST EQUIPMENT
Generating circuit tests by exploiting designed behavior [AD-A206175] N89-23800
AUTONOMOUS NAVIGATION
System study: Radiation hardened autonomous navigation [AD-A205604] N89-23439
Autonomous navigation and control [AD-A205898] N89-23441
AUTONOMOUS SPACECRAFT CLOCKS
Observation model and parameter partials for the JPL geodetic GPS modeling software GPSOMC [NASA-CR-185021] N89-24060
AVIONICS
Avionics architecture studies for the entry research vehicle [NASA-CR-181828] N89-24082
AXIAL FLOW
Bifurcating jets at high Reynolds numbers [AD-A205718] N89-23829
AXISYMMETRIC BODIES
Transonic Navier-Stokes solutions of three-dimensional afterbody flows [NASA-TM-4111] N89-23433
AXISYMMETRIC FLOW
Numerical studies of the effects of jet-induced mixing on liquid-vapor interface condensation [NASA-CR-182285] N89-23818

B

BACKGROUND RADIATION
Thermal images of sky and sea-surface background infrared radiation [AD-A205819] N89-23992
Study of the infrared celestial background [AD-A205649] N89-24237
BACKWARD FACING STEPS
Effect of wall cooling on the stability of compressible subsonic flows over smooth humps and backward-facing steps [NASA-CR-184960] N89-23812
BACTERIA
Cellular and molecular approaches to polymer synthesis by bacteria [AD-A206395] N89-23707
BALL BEARINGS
The in-vacuo torque performance of dry-lubricated ball bearings at cryogenic temperatures N89-23914
BALLISTIC TRAJECTORIES
Enhanced tracking of ballistic targets using forward looking infrared measurements [AD-A205727] N89-23769
BANACH SPACE
Nonlinear singular elliptic equations [DE88-705691] N89-24103
BAND STRUCTURE OF SOLIDS
Heterojunction band line-ups and the alloying effect in compound semiconductor alloys: A photoemission study N89-24179
BARIUM OXIDES
Studies on high-Tc superconducting materials [NAL-TM-MT-8703] N89-24178
Shock compaction of YBa2Cu3O7-x and HoBa2Cu3O7-x powders in a metal matrix [DE89-008827] N89-24193
BARIUM TITANATES
Dilatometric analysis of Al-, Ba-, Ca-titanate N89-23592
BARS
Information about hot flow-stress curves and the resulting structural changes N89-23616
BASE FLOW
Computational study of high supersonic flow over boattails with centered propulsive jets [AD-A206364] N89-23431
BASES (CHEMICAL)
Investigation of alpha-SiC hot corrosion in the presence of basic slag N89-23595
BATCH PROCESSING
Performance analysis of Kalman filters [PB89-146104] N89-23787
BAYES THEOREM
Approaches for empirical Bayes confidence intervals [AD-A205775] N89-24126
BEACONS
System study: Radiation hardened autonomous navigation [AD-A205604] N89-23439
BEAM WAVEGUIDES
A segmented mirror antenna for radiometers [NASA-TM-102045] N89-23753
BEAMS (SUPPORTS)
Prediction and measurement of damping of a laminated beam with a constrained viscoelastic layer [DE89-009002] N89-23922
Inverse problem techniques for beams with tip body and time hysteresis damping [NASA-CR-181833] N89-24112
BEAUFORT SEA (NORTH AMERICA)
KRMS (K-band Radiometric Mapping System) SSM/I validation March 1988 quick look report [NASA-CR-185320] N89-23766
BEHAVIOR
The impact of accuracy and effort feedback and goals on adaptive decision behavior [AD-A205751] N89-24095
BENDING MOMENTS
Modal analysis and testing of missile systems [AD-A204051] N89-23916
BENDING VIBRATION
Flutter of a low-aspect-ratio rectangular wing [NASA-TM-4116] N89-23447
Modal analysis and testing of missile systems [AD-A204051] N89-23916
BENZENE
Sorption of selected volatile organic constituents of jet fuels and solvents on natural sorbents from gas and solutions phases [AD-A204073] N89-23711
BERING SEA
KRMS (K-band Radiometric Mapping System) SSM/I validation March 1988 quick look report [NASA-CR-185320] N89-23766
BIBLIOGRAPHIES
Metrology for Electromagnetic Technology: A bibliography of NBS (National Bureau of Standards) publications, January 1970 - August 1988 [PB89-147847] N89-23748
Patent abstracts bibliography: A continuing bibliography. Section 2: Indexes (supplement 34) [NASA-SP-7039(34)-SECT-2] N89-24219
BIG BANG COSMOLOGY
Electrodynamics of cosmical plasmas: Some basic aspects of cosmological importance [TRITA-EPP-89-02] N89-24163
BIMETALS
Novel organoboranes as intermediates for ceramic precursors and high-energy fuels [AD-A206101] N89-23713
BINARY ALLOYS
A first-principles calculation of the resistivity and thermopower in strong-scattering alloys [DE89-008565] N89-23661
BINARY MIXTURES
Solidification of binary substances in rectangular and cylindrical cavities [DE89-008883] N89-23640
BINARY STARS
Time and spectral variability of the low mass X-ray binaries [MPE-REPORT-210] N89-24238
BIOASTRONAUTICS
A strategy for space biology and medical science for the 1980s and 1990s [NASA-CR-184895] N89-24024
BIOCHEMISTRY
Treatment with tyrosine, a neurotransmitter precursor, reduces environmental stress in humans [AD-A206035] N89-24039
BIODEGRADATION
The mechanisms of biodegradation of synthetic polymers [AD-A205628] N89-23699
Cellular and molecular approaches to polymer synthesis by bacteria [AD-A206395] N89-23707
Environmental interactions of hydrazine fuels in Soil/Water systems [AD-A206244] N89-23986
BIODYNAMICS
Biological results obtained by D1-mission N89-23732
BIOENGINEERING
Computer-aided design and bio-engineering: A review of the literature [AD-A206534] N89-24074
BIOGENY
Model of early self-replication based on covalent complementarity for a copolymer of glycerate-3-phosphate and glycerol-3-phosphate [NASA-CR-182912] N89-23693
BIOLOGICAL EFFECTS
Summary of 1st Summer School on Microgravity [DFVLR-IB-333-87/2] N89-23719
Biological results obtained by D1-mission N89-23732
Summary of selected new information on effects of ozone on health and vegetation. Draft supplement to air quality criteria for ozone and other photochemical oxidants [PB89-135123] N89-23980
BIOLOGICAL EVOLUTION
Model of early self-replication based on covalent complementarity for a copolymer of glycerate-3-phosphate and glycerol-3-phosphate [NASA-CR-182912] N89-23693
BIOMETRICS
Biological results obtained by D1-mission N89-23732
BIONICS
Environmental interactions of hydrazine fuels in Soil/Water systems [AD-A206244] N89-23986
Heuristics for cooperative problem solving [AD-A206371] N89-24096
BIOPHYSICS
Long term synaptic plasticity and learning in neuronal networks [AD-A205993] N89-24038
BIOSYNTHESIS
Cellular and molecular approaches to polymer synthesis by bacteria [AD-A206395] N89-23707
BIPOLAR TRANSISTORS
Some 3-5 heterojunction structures and high speed devices [AD-A205946] N89-24203
BLACK BODY RADIATION
Thermal images of sky and sea-surface background infrared radiation [AD-A205819] N89-23992
BLOOD CIRCULATION
Human temperature regulation during exercise after oral pyridostigmine administration [AD-A206032] N89-24030
BLOOD FLOW
Numerical simulation of flow through an artificial heart [NASA-TM-102183] N89-24111
BLOOD PRESSURE
Human adaptation to the Tibetan Plateau [AD-A206463] N89-24031
BLOWDOWN WIND TUNNELS
Ejector effects on a supersonic nozzle at low altitude and Mach number [AD-A206049] N89-23427
BOATTAILS
Computational study of high supersonic flow over boattails with centered propulsive jets [AD-A206364] N89-23431
BODIES OF REVOLUTION
Application of an exact finite element method to analysis of statics of thin elastic shells of revolution with axisymmetric loading [ISBN-952-900-399-4] N89-23917
BODY TEMPERATURE
Evaluation of three commercial microclimate cooling systems [AD-A206318] N89-23744

Patterns of human drinking: Effects of exercise, water temperature and food consumption
[AD-A206031] N89-24029

BODY WEIGHT
Patterns of human drinking: Effects of exercise, water temperature and food consumption
[AD-A206031] N89-24029

BODY-WING CONFIGURATIONS
Development of harmonic panel methods for aeroelastic applications to elastic bodies and body-fin combinations in supersonic flow
[AD-A205739] N89-23423

BOLTZMANN TRANSPORT EQUATION
Introduction to irreducible tensor methods, part 1
[NAL-PD-DU-8802] N89-24098

BONDING
Surface treatment using metal foil liner N89-23533

BOOMS (EQUIPMENT)
Design and testing of a deployable, retrievable boom for space applications N89-23898

BOOSTER ROCKET ENGINES
Pyro thruster for performing rocket booster attachment, disconnect, and jettison functions N89-23902

BORESIGHTS
A two-axis laser boresight system for a shuttle experiment N89-23913

BORON
Liquid dynamic compaction of Fe-Nd-B permanent magnets
[AD-A205632] N89-24135

BORON CARBIDES
Molded bodies having a high degree of hardness and a high degree of toughness for machining metals, carbides, ceramics and glasses
[DE89-008820] N89-23686

BOUNDARIES
Fundamental studies of beta phase decomposition modes in titanium alloys
[AD-A205296] N89-23665

BOUNDARY INTEGRAL METHOD
Shape identification technique for a two-dimensional elliptic system by boundary integral equation method
[NASA-CR-181831] N89-24114

BOUNDARY LAYER CONTROL
Navier-Stokes solution for a NACA 0012 airfoil with mass flux (fan)
[AD-A205771] N89-23424
Flow control for unsteady and separated flows and turbulent mixing
[AD-A205989] N89-23426
An experimental study of laminar flow control airfoil with suction through perforated surface at low speed
[NAL-TR-967] N89-23806

BOUNDARY LAYER EQUATIONS
On the Lagrangian description of unsteady boundary layer separation. Part 1: General theory
[NASA-TM-102026] N89-23821
Three-dimensional structure of boundary layers in transition to turbulence
[AD-A205587] N89-23828

BOUNDARY LAYER FLOW
A numerical scheme to solve unsteady and variable density low Mach number flows N89-23419
On the Lagrangian description of unsteady boundary layer separation. Part 1: General theory
[NASA-TM-102026] N89-23821
Three dimensional high speed boundary layer flows
[AD-A206145] N89-23837

BOUNDARY LAYER PLASMAS
Sheath and presheath in a collisionless open field plasma
[IPPJ-890] N89-24161

BOUNDARY LAYER SEPARATION
An experimental study of the effect of streamwise vortices on unsteady turbulent boundary-layer separation
[AD-A205462] N89-23420
Comparison of computational analysis with flight tests of a 40mm solid-fuel ramjet projectile
[AD-A206536] N89-23459

BOUNDARY LAYER STABILITY
Effect of wall cooling on the stability of compressible subsonic flows over smooth humps and backward-facing steps
[NASA-CR-184960] N89-23812
Rayleigh-Taylor instability of a viscous film overlying a passive fluid
[AD-A205578] N89-23827
Three-dimensional structure of boundary layers in transition to turbulence
[AD-A205587] N89-23828

BOUNDARY LAYER TRANSITION
An experimental study of laminar flow control airfoil with suction through perforated surface at low speed
[NAL-TR-967] N89-23806
Three-dimensional structure of boundary layers in transition to turbulence
[AD-A205587] N89-23828

BOUNDARY LAYERS
Studies of internal gravity waves in the stably stratified troposphere N89-23989

BOUNDARY VALUE PROBLEMS
Numerical solution of periodic vortical flows about a thin airfoil
[NASA-TM-101998] N89-23413
Effects of initial conditions on the development of supersonic turbulent free shear layers
[AD-A205607] N89-23421
Open boundary conditions for the Navier-Stokes equation
[FFA-145] N89-23816
Computation of flow around maneuvering submerged bodies
[AD-A205994] N89-23833
Efficient method for solving free-boundary problems
[PB89-146138] N89-24101
Shape identification technique for a two-dimensional elliptic system by boundary integral equation method
[NASA-CR-181831] N89-24114

BRAIN
Muramyl peptide-enhanced sleep: Pharmacological optimization of performance
[AD-A205974] N89-24028
Long term synaptic plasticity and learning in neuronal networks
[AD-A205993] N89-24038

BRAIN CIRCULATION
Human adaptation to the Tibetan Plateau
[AD-A206463] N89-24031

BRIGHTNESS TEMPERATURE
Remote sensing of global snowpack energy and mass balance: In-situ measurements on the snow of interior and Arctic Alaska
[NASA-CR-180078] N89-23956

BRITTLENESS
Mechanisms of diffusion-controlled brittle fracture
[DE89-008728] N89-23921

BROADBAND
Temporally smooth broadband pulses obtained by cross phase modulation in an optical fiber
[DE89-008891] N89-24152
A compact fast wide angle broad band spectrometer optical system
[NASA-CASE-NPO-17562-1-CU] N89-24153

BURNING RATE
Burning rate constant of fuel droplet under high pressure
[NAL-TR-1001] N89-23639

C

CADASTRAL MAPPING
The digital urban map as a basis for a land information system in local administration N89-23945
Automatic digitizing of cadastral maps N89-23946
Digitizing of drawings and cadastral maps using a scanner system N89-23949

CADMIUM TELLURIDES
High pressure studies on infrared detector materials
[NAL-TM-MT-8701] N89-23677

CALCIUM OXIDES
Sintering of CaO and MgO in the presence of nonequilibrium liquid phase N89-23580
Dilatometric analysis of Al-, Ba-, Ca-titanate N89-23592

CALIBRATING
Liquid-in-glass thermometer calibration service
[PB89-128888] N89-23846
The absolute radiometric calibration of the advanced very high resolution radiometer
[NASA-CR-185057] N89-23852
Approaches for empirical Bayes confidence intervals
[AD-A205775] N89-24126

CALIFORNIA
US Navy regional climatic study of the northern California operating area
[AD-A205342] N89-24006

CALORIMETERS
The structural basis for fatigue initiation in glassy polymers
[DE89-009292] N89-23689

CANADA
KRMS (K-band Radiometric Mapping System) SSM/I validation March 1988 quick look report
[NASA-CR-185320] N89-23766

CANOPIES (VEGETATION)
Geobotanical remote sensing for determination of aggregate source material
[AD-A205943] N89-23962

CARBON
High-temperature LDV seed particle development
[NASA-CR-182265] N89-23851
Energy disposal in ion-molecule reactions
[AD-A205987] N89-24144

CARBON DIOXIDE
Oxygen consumption rate of operational underwater swimmers
[AD-A205331] N89-24025

CARBON DIOXIDE LASERS
Nonlinear spectroscopy of multicomponent droplets and two- and three-dimensional measurements in flames
[AD-A205449] N89-23645
Transmission losses in hollow aluminum oxide waveguide at 10.6 microns
[FOA-C-30518-3.1] N89-23804
A vector scanning processing technique for pulsed laser velocimetry
[NASA-TM-102048] N89-23850
High-temperature LDV seed particle development
[NASA-CR-182265] N89-23851

CARBON FIBER REINFORCED PLASTICS
An investigation of the temperature dependence of the ultrasonic properties of AS4/lexan and XAS/lexan composites
[NASA-CR-184845] N89-23619

CARBON FIBERS
Preparation and properties of high strength carbon fibers N89-23589
Carbon fiber thermal conductivity measurement and analysis
[AD-A205682] N89-23625
High performance refractory composite materials
[REPT-882-430-106] N89-23631

CARBON STEELS
Wear resistant sintered steel with high carbide content N89-23607
The effect of welding process on the microstructure of HY-130 steel weldments
[AD-A205692] N89-23667

CARBON-CARBON COMPOSITES
The protection against oxidation of carbon materials. Thermodynamic and experimental study: A literature survey — carbon fibers
[REPT-882-430-108] N89-23633

CARRIER FREQUENCIES
Phase accuracy experiments with a direct-sampling coherent detector
[AD-A205458] N89-23764
Radar waveforms derived from orthogonal matrices
[AD-A205459] N89-23765

CARRIER TO NOISE RATIOS
Investigation of mutual interference between digitally modulated signals
[BBC-RD-1988/13] N89-23745

CASCADE FLOW
Mechanisms of secondary flows and losses within a three dimensional turbine stator cascade
[NAL-TR-970T] N89-23807
Investigation of incompressible cascade flows using a viscous/inviscid interactive code
[AD-A205972] N89-23832
Automatic analysis of holographic interferograms N89-23848

CASCADE WIND TUNNELS
A research facility for film cooling investigations with emphasis on the instrumentation system
[NAL-TM-PR-8704] N89-23477

CASE HISTORIES
Summary of selected new information on effects of ozone on health and vegetation. Draft supplement to air quality criteria for ozone and other photochemical oxidants
[PB89-135123] N89-23960

CAST ALLOYS
Mechanical properties of rapidly solidified iron-based alloys N89-23611

CASTING
Investigations on low cement and ultra low cement refractory castables N89-23593
Fabrication of unidirectional fiber reinforced 6061 aluminum alloy using high pressure squeeze casting
[AD-A205717] N89-23668

CATACLYSMIC VARIABLES
A search for EUV emission from cataclysmic variables
[DE89-008012] N89-24257

CATALOGS (PUBLICATIONS)
Defense Integrated Data System (DIDS) procedures manual. Volume 8: Document Identifier Code (DIC) Input/Output (I/O) formats (fixed length), change 3
[PB89-139414] N89-24220

CATALYSTS
Methanol vehicle catalyst evaluation, phase 3
[PB89-136139] N89-23874

CATALYTIC ACTIVITY
Pulsating catalytic combustion of gaseous fuels N89-23643
CATECHOLAMINE
Treatment with tyrosine, a neurotransmitter precursor, reduces environmental stress in humans [AD-A206035] N89-24039
CATHODES
Laser photoelectric effect at surface of discharge cathode [AD-A205741] N89-23869
Development of high power CARM (Cyclotron Auto-Resonance Maser) oscillators [AD-A206270] N89-23872
MPD thruster erosion research [NASA-CR-185314] N89-24168
CAVITIES
Solidification of binary substances in rectangular and cylindrical cavities [DE89-008883] N89-23640
Coupled integral equation solution for two dimensional bistatic TE scatter from a conducting cavity-backed infinite plane [AD-A206096] N89-23775
Acoustic response of a rectangular waveguide with a strong transverse temperature gradient [NASA-TM-101564] N89-24140
CAVITY RESONATORS
Attenuation measurement of very low-loss dielectric waveguides by the cavity resonator method in the millimeter/submillimeter wavelength range [AD-A206458] N89-23803
CELESTIAL GEODESY
Study of the infrared celestial background [AD-A205849] N89-24237
CELESTIAL MECHANICS
Comet Halley: The view from Pioneer Venus [NASA-NF-127] N89-24240
CELLS (BIOLOGY)
Cellular and molecular approaches to polymer synthesis by bacteria [AD-A206395] N89-23707
CEMENTS
Investigations on low cement and ultra low cement refractory castables N89-23593
CENTER OF GRAVITY
Center of gravity control on Airbus aircraft: Fuel, range and loading [REPT-882-111-101] N89-23460
CERAMIC COATINGS
Cracking of coated materials under transient thermal stresses [NASA-CR-184898] N89-23928
CERAMIC FIBERS
Silicon-carbide made of silicon-organic compounds N89-23572
Theoretical analysis of compatibility of several reinforcement materials with NiAl and FeAl matrices [NASA-CR-182291] N89-23622
Preparation and evaluation of silicon nitride matrices for silicon nitride-SiC fiber composites [NASA-CR-184798] N89-23678
CERAMIC MATRIX COMPOSITES
Ceramic Project of the Max-Planck Society N89-23571
Investigations of mullite-zirconia composites N89-23577
Preparation and thermal expansion of Al2TiO5-TiO5-TiO2 sintered bodies N89-23578
Sintering of Si3N4 in the presence of additives from Y2O3-SiO2-Al2O3 system N89-23581
Strengthening of silicon nitride ceramics N89-23585
Phase transformation of Zr(x)Hf(1-x)O2 in alumina matrix N89-23588
High performance refractory composite materials [REPT-882-430-106] N89-23631
Preparation and evaluation of silicon nitride matrices for silicon nitride-SiC fiber composites [NASA-CR-184798] N89-23678
CERAMICS
The 8th German-Yugoslav Meeting on Materials Science and Development: Ceramics and Metals [JUEL-SPEZ-446] N89-23569
Ceramic Project of the Max-Planck Society N89-23571
Silicon-carbide made of silicon-organic compounds N89-23572
Injection molding of whisker-reinforced Al2O3-ZrO2 ceramics N89-23574
Fatigue in ceramics N89-23583
Young's modulus of elasticity: Measured values for multiphase metals and their calculation via the bound concept N89-23584
Preparation, characterization and thermal diffusivity of Al2TiO5 N89-23591
Corrosion of silicon carbide ceramics at high temperatures in water vapor-containing atmospheres N89-23594
Neutral primary beam SIMS analysis of ceramic materials N89-23601
Electron conducting ceramics as sensor material for noise thermometry N89-23603
Microstructure and phase development in multicomponent ZnO based varistor ceramics N89-23604
Ultrafine microstructure composites prepared by chemical vapor deposition [AD-A206061] N89-23627
Ceramic tribology: Methodology and mechanisms of alumina wear [PB89-148357] N89-23679
Research needs in ceramic machining [PB89-148191] N89-23681
Atomic imaging and microanalysis of ceramics [DE89-008172] N89-23684
Molded bodies having a high degree of hardness and a high degree of toughness for machining metals, carbides, ceramics and glasses [DE89-006820] N89-23686
Microwave processing of ceramics [DE89-009350] N89-23690
Dynamic fatigue of ultralow-expansion glass for space mirrors, reissue A [AD-A205401] N89-23694
Heterocycles based on group 3, 4, and 5 elements precursors for novel glasses and ceramics [AD-A205586] N89-23696
Novel organoboranes as intermediates for ceramic precursors and high-energy fuels [AD-A206101] N89-23713
Design and construction of a state-of-the-art high temperature tribometer [PB89-148332] N89-23847
Institute for Materials Science and Engineering, nondestructive evaluation: Technical activities 1988 [PB89-151625] N89-23884
High-temperature ceramic superconductors [AD-A205321] N89-24196
CERTIFICATION
Qualification Motor no. 8 (QM-8), volume 1 [NASA-CR-183650] N89-23523
CHAD
Meteosat thermal inertia mapping for studying wetland dynamics in the West-African Sahel [BCRS-88-10A] N89-23970
CHANNEL FLOW
Free shear layer and swirl flow heat transfer enhancement [PB89-145106] N89-23810
CHANNEL NOISE
Investigation of mutual interference between digitally modulated signals [BBC-RD-1988/13] N89-23745
Signal-Noise/Interferer Combiner Unit Programmable (SINCUP) [AD-A205367] N89-24053
CHAOS
Coherence and chaos phenomena in Josephson oscillators for superconducting electronics [AD-A205469] N89-23798
The dimension of attractors underlying turbulent Poiseuille flow [AD-A206021] N89-23835
CHARACTERIZATION
Characterization of a phase boundary in Ni-Al2O3 sintered under pressure N89-23600
CHARGE TRANSFER
Assignment of the charge-transfer excited states of bis(N-heterocyclic) complexes of copper(I) [AD-A206012] N89-24205
CHARGED PARTICLES
Path dependent morphologies of a diblock copolymer of Polystyrene/Hydrogenated polybutadiene [AD-A206504] N89-23883
Fast algorithms for partial differential equations on advanced computers [AD-A206469] N89-24073
Solar flares and magnetospheric particles: Investigations based upon the ONR-602 and ONR-604 experiments [AD-A205599] N89-24253
CHARTS
KRMS (K-band Radiometric Mapping System) SSM/I validation March 1988 quick look report [NASA-CR-185320] N89-23766
CHEBYSHEV APPROXIMATION
The effect of mutual coupling on the side lobe performance of Chebyshev arrays, volume 1 [AD-A205724] N89-23768
CHELATION
Fiber-optic time-resolved fluorescence sensor for the simultaneous determination of Al(+3), Ga(+3) and In(+3) [AD-A205689] N89-24154
CHEMICAL ANALYSIS
Electron spectroscopy for chemical analysis: Sample analysis [NASA-CR-183568] N89-23634
Theta pinch discharges for solids vaporization and elemental chemical analysis [DE89-008888] N89-23641
Sample preparation techniques for evaluating methanol and formaldehyde emissions from methanol fueled vehicles and engines [PB89-136147] N89-23734
Fiber-optic time-resolved fluorescence sensor for the simultaneous determination of Al(+3), Ga(+3) and In(+3) [AD-A205689] N89-24154
CHEMICAL ATTACK
Environmental effects in niobium base alloys and other selected intermetallic compounds [AD-A206072] N89-23673
CHEMICAL BONDS
Novel organoboranes as intermediates for ceramic precursors and high-energy fuels [AD-A206101] N89-23713
CHEMICAL COMPOSITION
Electronic and ionic transport in polymers [AD-A206530] N89-23709
CHEMICAL EFFECTS
Summary of selected new information on effects of ozone on health and vegetation. Draft supplement to air quality criteria for ozone and other photochemical oxidants [PB89-135123] N89-23980
CHEMICAL ELEMENTS
Theta pinch discharges for solids vaporization and elemental chemical analysis [DE89-008888] N89-23641
CHEMICAL EVOLUTION
Model of early self-replication based on covalent complementarity for a copolymer of glycerate-3-phosphate and glycerol-3-phosphate [NASA-CR-182912] N89-23693
CHEMICAL LASERS
Numerical simulation of the dissociation of I2 by O2 (1 Delta) in a two dimensional parallel jet [AD-A206137] N89-23870
CHEMICAL REACTIONS
Simple adsorbates on transition metal surfaces: A joint chemical and physical approach [AD-A205726] N89-23669
Novel organoboranes as intermediates for ceramic precursors and high-energy fuels [AD-A206101] N89-23713
Improved acid electrolytes: The synthesis and structure of fluorine containing sulfonic acids for fuel cells [PB89-142616] N89-23973
Atomic layer epitaxy. Atomic layer epitaxy of 3-5 compound semiconductors by thermal and laser-assisted metalorganic chemical vapor deposition [AD-A205699] N89-24200
CHEMICAL WARFARE
Design of a chamber for CBW aerosol studies with relative humidity and particle concentration control [AD-A205623] N89-23481
CHINA
Summary of achievements in scientific research [AD-A199947] N89-24227
CHIPS (ELECTRONICS)
Criteria for robust stability in a class of lateral inhibition networks coupled through resistive grids [AD-A204174] N89-24081
CHIRP SIGNALS
Study of spread spectrum multiple access systems for satellite communications with overlay on current services: Executive summary [NASA-CR-180827-EXEC-SUMM] N89-23756
Study of spread spectrum multiple access systems for satellite communications with overlay on current services [NASA-CR-180827] N89-23757
CHLORINE
Microstructure-permeability relation in MnZn ferrites prepared of iron oxide with chlorine impurities N89-23602
CHLORINE FLUORIDES
Corrosion and lubricity testing of nonflammable USAF formulated CTFE (Chlorotrifluoroethylene) base hydraulic fluid [AD-A205487] N89-23695
Low energy consumption hydraulic techniques [AD-A206285] N89-23743

CHLOROPHYLLS
Non-destructive plant health sensing using absorption spectroscopy N89-24021
CHOLINESTERASE
Human temperature regulation during exercise after oral pyridostigmine administration
[AD-A206032] N89-24030
CHROMIUM
Testing chromium adhesion using acoustic emission
[AD-A205621] N89-23666
CHROMIUM OXIDES
Study of adherent oxide scales
[AD-A205799] N89-23700
CHROMOSPHERE
Redistribution in astrophysically important hydrogen lines
[NASA-CR-181375] N89-24251
CHUKCHI SEA
KRMS (K-band Radiometric Mapping System) SSM/I validation March 1988 quick look report
[NASA-CR-185320] N89-23766
CIRCUIT BOARDS
AN/TAC-1 demultiplexer circuit card assembly
[AD-A205744] N89-23770
CIRCUITS
Generating circuit tests by exploiting designed behavior
[AD-A206175] N89-23800
CITIES
Computer aided production of a 1:25,000 relief model of Berlin and surroundings N89-23943
The digital urban map as a basis for a land information system in local administration N89-23945
CLADDING
Interfacial reactions during cladding of steel by hot rolling N89-23615
CLAMPS
Tensile film clamps and mounting block for the rheovibron and autovibron viscoelastometer
[NASA-CASE-LAR-13696-1] N89-23880
CLAYS
Sorption of selected volatile organic constituents of jet fuels and solvents on natural sorbents from gas and solutions phases
[AD-A204073] N89-23711
CLIMATE
Climatic atlas of the outer continental shelf waters and coastal regions of Alaska. Volume 1: Gulf of Alaska, revision
[AD-A205289] N89-24005
Surface Observation Climatic Summaries (SOCS) for NASA Shuttle Landing Facility, Florida
[AD-A205362] N89-24007
The US Army Yuma Proving Ground, Arizona 33-year climate calendar and tables on associated weather elements 1954-1986. American desert country
[AD-A206256] N89-24010
CLIMATOLOGY
Climatic atlas of the outer continental shelf waters and coastal regions of Alaska. Volume 1: Gulf of Alaska, revision
[AD-A205289] N89-24005
US Navy regional climatic study of the northern California operating area
[AD-A205342] N89-24006
Surface Observation Climatic Summaries (SOCS) for NASA Shuttle Landing Facility, Florida
[AD-A205362] N89-24007
CLIMBING FLIGHT
SRB ascent aerodynamic heating design criteria reduction study, volume 1
[NASA-CR-183580] N89-23515
CLOCKS
AN/TAC-1 demultiplexer circuit card assembly
[AD-A205744] N89-23770
CLOSED ECOLOGICAL SYSTEMS
Space Station CMIF extended duration metabolic control test
[NASA-TM-100362] N89-23503
Advanced space design program to the Universities Space Research Association and the National Aeronautics and Space Administration
[NASA-CR-180450] N89-24015
Variable plant spacing N89-24016
Automated seed manipulation and planting N89-24017
Plant health sensing N89-24018
Microgravity particle reduction system N89-24019
Automated seed manipulation and planting N89-24020
Non-destructive plant health sensing using absorption spectroscopy N89-24021
Space station ECLSS simplified integrated test
[NASA-TM-100363] N89-24044
CLOTHING
The concept and theoretical considerations of a cold weather clothing system
[AD-A205476] N89-24046
CLOUD COVER
Inferring relative humidity profiles from 3DNEPH cloud data: Technique development and data impact study
[AD-A205825] N89-23993
Current problems in the stratocumulus-topped atmospheric boundary layer N89-23998
Surface Observation Climatic Summaries (SOCS) for NASA Shuttle Landing Facility, Florida
[AD-A205362] N89-24007
CLOUD PHYSICS
Stratocumulus modeling
[KNMI-WR-88-2] N89-23997
Current problems in the stratocumulus-topped atmospheric boundary layer N89-23998
Turbulent structure of a shear-driven stratus-topped atmospheric boundary layer: A comparison of model results with observations N89-23999
The diurnal variation of a marine stratocumulus layer: A model sensitivity study N89-24000
CLOUDS
Gas-Grain Simulation Facility: Fundamental studies of particle formation and interactions. Volume 1: Executive summary and overview
[NASA-CP-10026-VOL-1] N89-24022
Gas-Grain Simulation Facility: Fundamental studies of particle formation and interactions. Volume 2: Abstracts, candidate experiments and feasibility study
[NASA-CP-10026-VOL-2] N89-24023
CLOUDS (METEOROLOGY)
Inferring relative humidity profiles from 3DNEPH cloud data: Technique development and data impact study
[AD-A205825] N89-23993
CLUSTERS
A linear analysis of the stability of strong shocks and the evolution and distribution of materials in a cold dark matter dominated universe N89-24244
CLUTTER
Sea spike modeling
[AD-A205355] N89-23760
CMOS
A CAD (Computer Aided Design) tool for current-mode multiple-valued CMOS circuits
[AD-A205327] N89-24061
Design of multiple-valued programmable logic arrays (PLA)
[AD-A205307] N89-24085
COAL DERIVED LIQUIDS
Production of jet fuels from coal-derived liquids. Volume 8: Heteroatom removal by catalytic processing
[AD-A205470] N89-23712
COANDA EFFECT
Aerothermodynamic analysis of a Coanda/Refraction Jet Engine Test Facility
[AD-A205937] N89-23482
COASTAL WATER
Imaging procedure of underwater bottom topography by air and satellite images in the range of microwave and visible electromagnetic spectra
[GKSS-88/E/41] N89-24014
COASTS
Climatic atlas of the outer continental shelf waters and coastal regions of Alaska. Volume 1: Gulf of Alaska, revision
[AD-A205289] N89-24005
US Navy regional climatic study of the northern California operating area
[AD-A205342] N89-24006
COATING
Drag and noise measurements on underwater vehicles with a riblet surface coating
[AD-A205500] N89-23825
Radiation physics properties of selective solar energy absorber layers
[ETN-89-93945] N89-23978
COATINGS
Some examples of the degradation of properties of materials in space N89-23535
Ultrafine microstructure composites prepared by chemical vapor deposition
[AD-A206061] N89-23627
Effect of n on 1 laser treatment on damage threshold of selected optical coating
[DE89-008830] N89-23861
Characterization of multilayer coated concave diffraction gratings in the extreme ultraviolet
[DE89-008831] N89-24151
COCKPITS
Computer-aided design and bio-engineering: A review of the literature
[AD-A206534] N89-24074
CODING
Code optimization of speckle reduction algorithms for image processing of rocket motor holograms
[AD-A205306] N89-23524
Radar waveforms derived from orthogonal matrices
[AD-A205459] N89-23765
Investigation of incompressible cascade flows using a viscous/inviscid interactive code
[AD-A205972] N89-23832
COEFFICIENT OF FRICTION
Finite element modeling of frictionally restrained composite interfaces
[NASA-CR-182281] N89-23918
COGENERATION
Process integration methodology for natural gas-fueled heat pumps and cogeneration systems
[PB89-140867] N89-23811
COGNITION
Development and evaluation of integrating details: A complex spatial problem solving test
[AD-A205860] N89-24035
The attention system of the human brain
[AD-A206157] N89-24040
COHERENT LIGHT
Functional assessment of laser irradiation
[AD-A206230] N89-23871
Three-dimensional analysis of optical transition radiation
[AD-A205935] N89-24156
COHERENT RADAR
Coherent laser radar
[FOA-C-30512-3.1] N89-23778
COHERENT RADIATION
Summaries of papers presented at Short Wavelength Coherent Radiation: Generation and Applications Topical Meeting held in Cape Cod, Massachusetts on September 26-29, 1988
[AD-A205471] N89-23867
COHESION
Cohesive and anharmonic elastic properties of mixed fluorite crystals
[DE88-705690] N89-24184
COLD WEATHER
The concept and theoretical considerations of a cold weather clothing system
[AD-A205476] N89-24046
COLD WEATHER TESTS
Qualification Motor no. 8 (QM-8), volume 1
[NASA-CR-183650] N89-23523
COLLISIONLESS PLASMAS
Sheath and presheath in a collisionless open field plasma
[IPPJ-890] N89-24161
Investigation of the behaviour of a collisionless R-F sheath
[OUEL-1695/87] N89-24165
COLOR TELEVISION
Tuner for the first intermediate frequency of receivers for direct satellite reception
[ETN-89-93766] N89-23788
COLOR VISION
Quasi-monochromatic visual environments and the resting point of accommodation
[AD-A205938] N89-24036
COLUMBUS SPACE STATION
The two approaches for the thermal control of the Columbus resource module and Polar Platform
[REPT-882-440-110] N89-23511
The evolution of space mechanisms in the ESA R and D program N89-23893
COMBUSTIBLE FLOW
Fundamental studies on spray combustion and turbulent combustion
[AD-A206438] N89-23651
COMBUSTION
Fundamental studies on spray combustion and turbulent combustion
[AD-A206438] N89-23651
COMBUSTION CHAMBERS
Experiment on a cylindrical scramjet combustor. 2: Simulated flight Mach number 6.7
[NAL-TR-969] N89-23464
Design, fabrication and test of the RL10 derivative II chamber/primary nozzle
[NASA-CR-179595] N89-23519
Pulsating catalytic combustion of gaseous fuels N89-23643
Study on a twin valveless pulse burner (temperature characteristics during pulse combustion)
[NAL-TR-973] N89-23873
COMBUSTION EFFICIENCY
Experiment on a cylindrical scramjet combustor. 2: Simulated flight Mach number 6.7
[NAL-TR-969] N89-23464
Pulsating catalytic combustion of gaseous fuels N89-23643

Study on a twin valveless pulse burner (temperature characteristics during pulse combustion)
[NAL-TR-973] N89-23873

COMBUSTION STABILITY
Flow-turning losses in solid rocket motors
[AD-A206099] N89-23525
Pulsating catalytic combustion of gaseous fuels N89-23643

COMBUSTION TEMPERATURE
Study on a twin valveless pulse burner (temperature characteristics during pulse combustion)
[NAL-TR-973] N89-23873

COMET HEADS
Comet Halley: The view from Pioneer Venus
[NASA-NF-127] N89-24240

COMET TAILS
Comet Halley: The view from Pioneer Venus
[NASA-NF-127] N89-24240

COMETS
On the measurement of cosmogenic nuclides in cometary materials
[DE89-009248] N89-24243

COMFORT
Space station ECLSS simplified integrated test
[NASA-TM-100363] N89-24044

COMMAND AND CONTROL
A designers' guide to reliable distributed systems: An example design. Volume 1
[AD-A206039] N89-23885
Parallel ada implementation of a multiple model Kalman filter tracking system: A software engineering approach
[AD-A206094] N89-24130

COMMERCE
On the international commercialization of remote sensing
[BCRS-88-02] N89-23969

COMMINUTION
Microgravity particle reduction system N89-24019

COMMUNICATION NETWORKS
Link availability and rain attenuation exceedance characteristics for EHF (Extremely High Frequency) satellite communications with arbitrary link parameters in Canada
[AD-A205403] N89-23762

COMMUNICATION SATELLITES
A family of BAPTAs for GEO and LEO applications N89-23908

COMMUTER AIRCRAFT
Detailed design of a Ride Quality Augmentation System for commuter aircraft
[NASA-CR-4230] N89-23470

COMPACT GALAXIES
Relativistic and non-relativistic magnetohydrodynamic flows around compact stars N89-24242

COMPACTING
Liquid dynamic campaction of Fe-Nd-B permanent magnets
[AD-A205632] N89-24135
Shock compaction of YBa2Cu3O7-x and HoBa2Cu3O7-x powders in a metal matrix
[DE89-008827] N89-24193

COMPENSATORS
Actuator rate saturation compensator
[AD-D013962] N89-23474
Designing feedback compensators by using the root-locus method
[AD-A205354] N89-24093

COMPILERS
An investigation into the application of dynamic programming to determine optimal controls for tracking a cruise missile maneuver by CMMCA (Cruise Missile Mission Control Aircraft)
[AD-A205970] N89-23456

COMPLEX COMPOUNDS
X-ray absorption spectroscopy of electrochemically generated species
[AD-A205572] N89-23647

COMPLEX SYSTEMS
An ICAI (Intelligent Computer Aided Instruction) architecture for troubleshooting in complex dynamic systems
[AD-A205434] N89-24045

COMPLEX VARIABLES
On the equation Xa + Ya = Za
[AD-A205460] N89-24116

COMPLEXITY
On the communication complexity of distributed algebraic computation
[AD-A205784] N89-24117

COMPONENT RELIABILITY
Fatigue crack growth model RANDOM2 user manual, appendix 1
[NASA-CR-184939] N89-23890
Fatigue strength reduction model: RANDOM3 and RANDOM4 user manual, appendix 2
[NASA-CR-184940] N89-23891

COMPOSITE MATERIALS
Composites in complex assemblies
[REPT-882-430-110] N89-23509
Fabrication and properties of alumina-zirconia composites
[PB89-147532] N89-23620
Ultrafine microstructure composites prepared by chemical vapor deposition
[AD-A206061] N89-23627
Composite materials nondestructive tests: Choice of methods depending on requirements
[REPT-882-430-105] N89-23630
Challenges of nondestructive testing of composite materials
[REPT-882-430-107] N89-23632
Electronic and ionic transport in polymers
[AD-A206530] N89-23709
Institute for Materials Science and Engineering, nondestructive evaluation: Technical activities 1988
[PB89-151625] N89-23884

COMPOSITE STRUCTURES
Optimum aeroelastic characteristics for composite supermaneuverable aircraft
[AD-A205503] N89-23452
Composites in complex assemblies
[REPT-882-430-110] N89-23509
Composite materials nondestructive tests: Choice of methods depending on requirements
[REPT-882-430-105] N89-23630

COMPRESSIBLE BOUNDARY LAYER
Boundary layer and heat transfer behind a piston in a shock tube. Part 1: Theoretical considerations of laminar and turbulent boundary layer behind a piston in a tube
[ISL-R-111/87-PT-1] N89-23841

COMPRESSIBLE FLOW
Turbulent shear stress measurement in hypersonic flow
[AD-A206453] N89-23432
Three-dimensional laser anemometer study of compressible flow through orifice plates
[PB89-145098] N89-23808
Effect of wall cooling on the stability of compressible subsonic flows over smooth humps and backward-facing steps
[NASA-CR-184960] N89-23812
On the Lagrangian description of unsteady boundary layer separation. Part 1: General theory
[NASA-TM-102026] N89-23821

COMPUTATION
A closed-form trim solution yielding minimum trim drag for airplanes with multiple longitudinal-control effectors
[NASA-TP-2907] N89-23468

COMPUTATIONAL FLUID DYNAMICS
Numerical solution of periodic vortical flows about a thin airfoil
[NASA-TM-101998] N89-23413
A numerical scheme to solve unsteady and variable density low Mach number flows N89-23419
Navier-Stokes solution for a NACA 0012 airfoil with mass flux (fan)
[AD-A205771] N89-23424
Computational study of high supersonic flow over boattails with centered propulsive jets
[AD-A206364] N89-23431
Advances in computational design and analysis of airbreathing propulsion systems
[NASA-TM-101987] N89-23465
Design of water tunnel to measure wall pressure signatures due to tunnel blockage and wake effects
[AD-A206025] N89-23483
Flosolver: A parallel computer for fluid dynamics
[NAL-TM-AE-8803] N89-23805
Advanced computational techniques for hypersonic propulsion
[NASA-TM-102005] N89-23809
Some applications of the qualitative theory of differential equations in fluid dynamics
[ETN-89-94143] N89-23814
A numerical study of viscous vortex rings using a spectral method
[NASA-TM-101041] N89-23820
Computation of dynamics and control of unsteady vortical flows N89-23822
Exploitation of multiple solutions of the Navier-Stokes equations to achieve radically improved flight
[AD-A205939] N89-23831
A simple approximate method to evaluate the 3-D aerodynamic field around a streamline and to determine the validity of the quasi-three dimensional hypothesis
[ETN-89-94366] N89-23844
Solution of one-dimensional Euler equations by the implicit finite difference technique of Beam and Warming
[NAL-PD-FM-8816] N89-24097
Numerical solution of the Euler equations using local grid refinement
[FFA-143] N89-24104
Numerical simulation of flow through an artificial heart
[NASA-TM-102183] N89-24111
Modeling of a continuous oscillator by oscillators with a finite number of degrees of freedom
[PB89-146120] N89-24134

COMPUTATIONAL GRIDS
Investigation of three-dimensional mesh generation with precise controls
[AD-A205967] N89-23773
Numerical solution of the Euler equations using local grid refinement
[FFA-143] N89-24104
A stability analysis of various patched grid interface conditions for hyperbolic equations
[FFA-144] N89-24105
Solid modeling requirements for finite element modeling using mapped mesh techniques
[DE89-009639] N89-24110
Operator induced multigrid algorithms using semirefinement
[NASA-CR-181834] N89-24113

COMPUTER AIDED DESIGN
A correlation study of X-29A aircraft and associated analytical developments N89-23450
Advances in computational design and analysis of airbreathing propulsion systems
[NASA-TM-101987] N89-23465
Flight control system for the CRCA (Control Reconfigurable Combat Aircraft) using a command generator tracker with PI (Proportional-Plus-Integral) feedback and Kalman filter, volume 1
[AD-A205723] N89-23473
Control design of an unstable non-minimum phase aircraft subject to control surface saturation
[AD-A206024] N89-23475
Break dimensioning of space structural assemblies and its experimental validation
[REPT-882-430-109] N89-23508
Assembling the ISO thermal model with ESAT AN
[REPT-882-440-107] N89-23510
ESA-D: An integrated software for antenna design and analysis
[REPT-882-440-111] N89-23784
An application specific integrated circuit for dual-axis motion control
[DE89-007974] N89-23790
Design of a 100 MW X-band klystron
[DE89-008939] N89-23793
The FLUIDNET development and application to preliminary sizing of fluid loop systems
[REPT-882-440-102] N89-23845
Ground shake test of the Boeing Model 360 helicopter airframe
[NASA-CR-181766] N89-23920
Design of a MANPRINT tool for predicting personnel and training characteristics implied by system design
[AD-A206201] N89-24048
A CAD (Computer Aided Design) tool for current-mode multiple-valued CMOS circuits
[AD-A205327] N89-24061
A database management system for computer-aided digital circuit design
[AD-A206047] N89-24066
Design and implementation of an expert user interface for the computer aided prototyping system
[AD-A206113] N89-24067
Computer-aided design and bio-engineering: A review of the literature
[AD-A206534] N89-24074
ESABASE: A most versatile and flexible system engineering tool
[ESA-BR-54] N89-24223

COMPUTER AIDED MANUFACTURING
USAF (US Air Force) durability design handbook: Guidelines for the analysis and design of durable aircraft structures
[AD-A206286] N89-23457

COMPUTER AIDED MAPPING
Reports on Cartography and Geodesy. Series 1, number 101
[ISSN-0469-4236] N89-23941
Computer aided production of a 1:25,000 relief model of Berlin and surroundings N89-23943
The Official Topographic-Cartographic Information System (ATKIS) of the Geodesy Group of the Laender of the Federal Republic of Germany: Status after one year of development N89-23944
The digital urban map as a basis for a land information system in local administration N89-23945
Automatic digitizing of cadastral maps N89-23946
Cartographic signatures in PHOCUS N89-23948
Digitizing of drawings and cadastral maps using a scanner system N89-23949
Computer assisted layout of graphic settlement representations N89-23951

Tools for the computer assisted generalization of settlements for the construction of digital landscape models N89-23952
Computer assisted generalization of transport line representations N89-23953
Hybrid cartographic data processing in a geographic information system N89-23954
Automatic extraction of areas from overlays of the series DGK 5 (Bo) N89-23955
Shortest paths in a digitized map using a tile-based data structure
[PB89-143432] N89-23957
Use of the 1:2,000,000 Digital Line Graph data in emergency response
[DE89-006730] N89-23959
The search for edges in remote sensing images using a digital polygonal map
[ETN-89-94146] N89-23964

COMPUTER ASSISTED INSTRUCTION
An ICAI (Intelligent Computer Aided Instruction) architecture for troubleshooting in complex dynamic systems
[AD-A205434] N89-24045

COMPUTER DESIGN
Design and implementation of an expert user interface for the computer aided prototyping system
[AD-A206113] N89-24067

COMPUTER GRAPHICS
Advances in computational design and analysis of airbreathing propulsion systems
[NASA-TM-101987] N89-23465
Reports on Cartography and Geodesy. Series 1, number 101
[ISSN-0469-4236] N89-23941
Definition and filling of information systems: Challenge for a photogrammetric service enterprise N89-23942
Monitoring information processing and decisions: The MOUSELAB system
[AD-A205963] N89-24037
A graphical editor for the computer aided prototyping system
[AD-A206443] N89-24071
Computer-aided design and bio-engineering: A review of the literature
[AD-A206534] N89-24074
GRADA: A graphical package in Ada
[FOA-C-20741-2.7] N89-24077
GEMMES: A new tool for dynamic modeling
[REPT-882-440-114] N89-24078
ESABASE: A most versatile and flexible system engineering tool
[ESA-BR-54] N89-24223

COMPUTER NETWORKS
EnviroNET: Space environment for Strategic Defense Initiative experiments N89-23538
Computer-based modeling environments
[AD-A205828] N89-24064
Light channel 5 Gb/s optoelectronic TDM (Time Division Multiplexing)
[AD-A205501] N89-24086
Managing sound in a relational multimedia database system
[AD-A205742] N89-24225

COMPUTER PROGRAM INTEGRITY
An experimental investigation into software reliability
[AD-A206293] N89-24069

COMPUTER PROGRAMMING
A designers' guide to reliable distributed systems: An example design. Volume 1
[AD-A206039] N89-23885
A designers' guide to reliable distributed systems: An example design. Volume 2
[AD-A206040] N89-23886
User interface and highly interactive systems: Survey of current research
[PB89-146088] N89-24056
The role of order in distributed programs
[AD-A206037] N89-24065
A visual object-oriented unification system
[AD-A206228] N89-24068
Deductive programming synthesis
[AD-A206451] N89-24072
The state of software engineering practice: A preliminary report
[AD-A206573] N89-24075
Design of multiple-valued programmable logic arrays (PLA)
[AD-A205307] N89-24085

COMPUTER PROGRAMS
Numerical study of the influence of leading and trailing edge flaps on the performance of airfoils
[AD-A206138] N89-23428
Noise and sonic boom impact technology. PCBOOM computer program for sonic boom research, volume 1
[AD-A206290] N89-23429
Noise and sonic boom impact technology. PCBOOM computer program for sonic boom research. Volume 2: Program Users/Computer operations manual
[AD-A206291] N89-23430
Aerothermodynamic analysis of a Coanda/Refraction Jet Engine Test Facility
[AD-A205937] N89-23482
Continuous, low thrust coplanar orbit transfers with varying eccentricity
[AD-A206022] N89-23498
A numerical routine for defining rocket exhaust characteristics and impingement effects
[AD-A206323] N89-23526
EnviroNET: Space environment for Strategic Defense Initiative experiments N89-23538
Composite blade structural analyzer (COBSTRAN) user's manual
[NASA-TM-101461] N89-23621
A user's guide to the Molecular Modeling, Analysis and Display System (MMADS), 2nd edition
[AD-A205674] N89-23648
The effect of mutual coupling on the side lobe performance of Chebyshev arrays, volume 1
[AD-A205724] N89-23768
Derivation of a Godunov one dimensional fluid dynamics code
[AD-A205463] N89-23824
ARC-INFO: A geographic information system N89-23947
Calculation of the surface of a geodetic polygon on an ellipsoid of revolution
[ETN-89-94149] N89-23966
Thermal images of sky and sea-surface background infrared radiation
[AD-A205819] N89-23992
Exploring the North Atlantic Ocean on floppy disks
[AD-A205733] N89-24011
Human-machine interaction considerations for interactive software
[AD-A206574] N89-24049
Signal-Noise/Interferer Combiner Unit Programmable (SINCUP)
[AD-A205367] N89-24053
Automatic documentation methodologies for software maintenance
[AD-A205672] N89-24062
The role of order in distributed programs
[AD-A206037] N89-24065
An experimental investigation into software reliability
[AD-A206293] N89-24069
Advanced computing systems: An advanced reasoning-based development paradigm for Ada trusted systems and its application to MACH
[AD-A206308] N89-24070
PRASE (Parallel Resource Analysis Software Environment) instrumentation software for the Intel iPSC hypercube
[AD-A206046] N89-24087
Parallel ada implementation of a multiple model Kalman filter tracking system: A software engineering approach
[AD-A206094] N89-24130
Semiconductor measurement technology: Automatic determination of the interstitial oxygen content of silicon wafers polished on both sides
[PB89-151831] N89-24180
A program interface prototype for a multimedia database incorporating images
[AD-A206439] N89-24226

COMPUTER STORAGE DEVICES
On the use of multiprocessing computers for global numerical weather prediction
[AD-A206102] N89-24009

COMPUTER SYSTEMS DESIGN
Flosolver: A parallel computer for fluid dynamics
[NAL-TM-AE-8803] N89-23805
Direct manipulation and other styles of man-machine interaction
[PB89-146070] N89-24043
Human-machine interaction considerations for interactive software
[AD-A206574] N89-24049
User interface and highly interactive systems: Survey of current research
[PB89-146088] N89-24056
The state of software engineering practice: A preliminary report
[AD-A206573] N89-24075

COMPUTER SYSTEMS PERFORMANCE
Flosolver: A parallel computer for fluid dynamics
[NAL-TM-AE-8803] N89-23805
Host computer system capacity management procedures
[AD-A193416] N89-24051
Runtime aggregation of recursion relations
[AD-A206576] N89-24076
Local area network technical guidelines. Volume 1: LAN design and planning (LAN TSR process)
[PB89-139091] N89-24080

COMPUTER SYSTEMS PROGRAMS
Flosolver: A parallel computer for fluid dynamics
[NAL-TM-AE-8803] N89-23805
ARC-INFO: A geographic information system N89-23947
Host computer system capacity management procedures
[AD-A193416] N89-24051
Automatic documentation methodologies for software maintenance
[AD-A205672] N89-24062
GRADA: A graphical package in Ada
[FOA-C-20741-2.7] N89-24077
ESABASE: A most versatile and flexible system engineering tool
[ESA-BR-54] N89-24223

COMPUTER SYSTEMS SIMULATION
A demonstration of the method of stochastic finite element analysis
[AD-A206135] N89-24127

COMPUTER TECHNIQUES
Comparison of interpolation algorithms for speed control in air traffic management
[AD-A206314] N89-23444
Missile actuator simulation and an investigation into the accuracy of Runge-Kutta numerical integration
[AD-A206325] N89-23458
Investigation of three-dimensional mesh generation with precise controls
[AD-A205967] N89-23773
A designers' guide to reliable distributed systems: An example design. Volume 2
[AD-A206040] N89-23886
Computerized measurement of thermoacoustically generated temperature gradients
[AD-A205353] N89-23929
An ICAI (Intelligent Computer Aided Instruction) architecture for troubleshooting in complex dynamic systems
[AD-A205434] N89-24045
The role of order in distributed programs
[AD-A206037] N89-24065
Design and implementation of an expert user interface for the computer aided prototyping system
[AD-A206113] N89-24067
A graphical editor for the computer aided prototyping system
[AD-A206443] N89-24071
Fast algorithms for partial differential equations on advanced computers
[AD-A206469] N89-24073
Computer-aided design and bio-engineering: A review of the literature
[AD-A206534] N89-24074
The state of software engineering practice: A preliminary report
[AD-A206573] N89-24075
PRASE (Parallel Resource Analysis Software Environment) instrumentation software for the Intel iPSC hypercube
[AD-A206046] N89-24087
Preconditioned Krylov solvers and methods for runtime loop parallelization
[AD-A206388] N89-24120
Krylov methods preconditioned with incompletely factored matrices on the CM-2
[AD-A206389] N89-24121
Parallel ada implementation of a multiple model Kalman filter tracking system: A software engineering approach
[AD-A206094] N89-24130

COMPUTERIZED SIMULATION
An instrument for the simultaneous measurement of velocity, temperature and density in unseeded air flows
[AD-A205588] N89-23453
A methodology for determining the survivability of fixed-wing aircraft against small arms
[AD-A205730] N89-23455
Missile actuator simulation and an investigation into the accuracy of Runge-Kutta numerical integration
[AD-A206325] N89-23458
Advances in computational design and analysis of airbreathing propulsion systems
[NASA-TM-101987] N89-23465
Investigations on the cracking behavior of joints in airfields and roads: Field investigations and laboratory simulations
[PB89-141279] N89-23479
FILMCAL: An ESR (Electron Spin Resonance) simulation program for transition metals in phthalocyanine films
[AD-A206441] N89-23676
An iterative technique to correct probe position errors in planar near-field to far-field transformations
[PB89-153886] N89-23750

Navigation shift correction by radar cartography. Optimization and validation by simulation
[REPT-882-320-103] N89-23755
ASR-9 weather channel test report, executive s ummary
[DOT/FAA/PS-89/6-EXEC-SUMM] N89-23758
Investigation of optical compression techniques for dither coding
[AD-A206140] N89-23776
High energy semiconductor switch
[DE89-007399] N89-23789
Advanced computational techniques for hypersonic propulsion
[NASA-TM-102005] N89-23809
Two-dimensional numerical simulation of a Stirling engine heat exchanger
[NASA-TM-102057] N89-23823
Bifurcating jets at high Reynolds numbers
[AD-A205718] N89-23829
Computation of flow around manauvering submerged bodies
[AD-A205994] N89-23833
A numerical investigation of thin-film heat transfer gages
[AD-A206134] N89-23853
Modeling and simulation of a Stewart platform type parallel structure robot
[NASA-CR-184969] N89-23875
White paper: Experimental and computational studies of very high velocity impacts
[DE89-007643] N89-23877
A description of the slab model
[DE89-009962] N89-23984
An analysis of lightning launch constraints
[AD-A206084] N89-23994
Microcomputer program for daily weather simulation
[PB89-144638] N89-24001
Design of a MANPRINT tool for predicting personnel and training characteristics implied by system design
[AD-A206201] N89-24048
Computer-based modeling environments
[AD-A205828] N89-24064
GRADA: A graphical package in Ada
[FOA-C-20741-2.7] N89-24077
Designing feedback compensators by using the root-locus method
[AD-A205354] N89-24093
Discrete event simulation model decomposition
[AD-A206048] N89-24119
A demonstration of the method of stochastic finite element analysis
[AD-A206135] N89-24127
Simulation studies of particle acceleration powered by modulated intense relativistic electron beams
[AD-A206348] N89-24148
Grain boundaries
[DE89-006881] N89-24194

CONCENTRATION (COMPOSITION)
Design of a chamber for CBW aerosol studies with relative humidity and particle concentration control
[AD-A205623] N89-23481
Evaluation of the historical Schoenbein method for the determination of ozone in a flow chamber
[JUEL-2218] N89-23983
On the measurement of cosmogenic nuclides in cometary materials
[DE89-009248] N89-24243

CONCRETES
Investigations on the cracking behavior of joints in airfields and roads: Field investigations and laboratory simulations
[PB89-141279] N89-23479

CONCURRENT PROCESSING
Flosolver: A parallel computer for fluid dynamics
[NAL-TM-AE-8803] N89-23805

CONDENSING
Numerical studies of the effects of jet-induced mixing on liquid-vapor interface condensation
[NASA-CR-182285] N89-23818
Vaporization and recondensation in propagation and imaging of laser beams
[DE89-006014] N89-23858

CONDUCTIVE HEAT TRANSFER
Thermal transport in pressureless sintered aluminum nitride N89-23590

CONDUCTIVITY
Measuring conductivities of highly conductive membranes
[AD-A206043] N89-23649

CONFERENCES
NASA/SDIO Space Environmental Effects on Materials Workshop, part 1
[NASA-CP-3035-PT-1] N89-23526
The 8th German-Yugoslav Meeting on Materials Science and Development: Ceramics and Metals
[JUEL-SPEZ-446] N89-23569
Report on the partial support of the 1988 Gordon Conference on Polymers (West)
[AD-A205834] N89-23701
Summary of 1st Summer School on Microgravity
[DFVLR-IB-333-87/2] N89-23719
Intelligent processing of materials
[PB89-151823] N89-23735
The 23rd Aerospace Mechaniams Symposium
[NASA-CP-3032] N89-23892

CONFIDENCE LIMITS
Approaches for empirical Bayes confidence intervals
[AD-A205775] N89-24126
Launch commit criteria performance trending analysis, phase 1, revision A. SRM and QA mission services
[NASA-CR-184859] N89-24129

CONFORMAL MAPPING
Numerical conformal mapping and applications
[AD-A205602] N89-24131

CONFUSION
Active radar jamming
[FOA-C-30506-3.6] N89-23777

CONICAL NOZZLES
Arcjet nozzle design impacts
[NASA-TM-102050] N89-23522

CONSERVATION LAWS
Nonlinear systems of conservation laws
[AD-A205837] N89-23830

CONSOLIDATION
Physico-mathematical investigation of the consolidation of iron powder N89-23617
Spray deposition: A fundamental study of droplet impingement, spreading and consolidation
[AD-A206065] N89-23672

CONTAINERLESS MELTS
Nucleation and undercooling N89-23726

CONTINENTAL SHELVES
Climatic atlas of the outer continental shelf waters and coastal regions of Alaska. Volume 1: Gulf of Alaska, revision
[AD-A205289] N89-24005

CONTINUOUS RADIATION
A statistical analysis of the output signals of an acousto-optic spectrum analyzer for CW (Continuous-Wave) signals
[AD-A205404] N89-23783

CONTINUUM MECHANICS
Dynamic interaction between fluids and solids
[ETN-89-93948] N89-23937
Analysis and optimization of geodetic networks by spectral criteria and mechanical analogies
[SER-C-342] N89-23963

CONTOUR SENSORS
Research for optimization of future MOMS sensors
[ETN-89-94424] N89-23972

CONTOURS
The role of knowledge in visual shape representation
[AD-A206173] N89-24041

CONTRAROTATING PROPELLERS
Average-passage simulation of counter-rotating propfan propulsion systems as applied to cruise missiles
[NASA-TM-102043] N89-23416
Noise of a model counterrotation propeller with simulated fuselage and support pylon at takeoff/approach conditions
[NASA-TM-101996] N89-24138

CONTROL CONFIGURED VEHICLES
Flight control system for the CRCA (Control Reconfigurable Combat Aircraft) using a command generator tracker with PI (Proportional-Plus-Integral) feedback and Kalman filter, volume 1
[AD-A205723] N89-23473

CONTROL MOMENT GYROSCOPES
Design, fabrication and test of a 4750 Newton-meter-second double Gimbal control moment gyroscope N89-23896

CONTROL SURFACES
Control design of an unstable non-minimum phase aircraft subject to control surface saturation
[AD-A206024] N89-23475

CONTROL SYSTEMS DESIGN
Advances in computational design and analysis of airbreathing propulsion systems
[NASA-TM-101987] N89-23485
The functional mock-up test of the flight control system of the NAL QSTOL research aircraft ASKA
[NAL-TR-972] N89-23487
The 4D-TECS integration for NASA TSRV airplane
[NASA-CR-4231] N89-23471
Flight control system for the CRCA (Control Reconfigurable Combat Aircraft) using a command generator tracker with PI (Proportional-Plus-Integral) feedback and Kalman filter, volume 1
[AD-A205723] N89-23473
The application of self-tuning control techniques to a multivariable process
[OUEL-1737/88] N89-23737
Digital control of the Kuiper Airborne Observatory telescope
[NASA-TM-101082] N89-23785
Two-dimensional confined jet thrust vector control: Operating mechanisms and performance
[AD-A206011] N89-23834
Development of a precision, wide-dynamic-range actuator for use in active optical systems N89-23901
Space station ECLSS simplified integrated test
[NASA-TM-100363] N89-24044
Robust multivariable feedback design
[OUEL-1723/88] N89-24090
Multivariable Nyquist self-tuning: A general approach
[OUEL-1734/88] N89-24091

CONTROL THEORY
Multivariable flight control design with parameter uncertainty for the AFTI/F-16
[AD-A206068] N89-23476
Continuous, low thrust coplanar orbit transfers with varying eccentricity
[AD-A206022] N89-23498
Quadratic optimal control theory for viscoelastically damped structures using a fractional derivative viscoelasticity model
[AD-A206008] N89-23932
State-space formulae for discrete-time H infinity optimization
[OUEL-1718/88] N89-24089

CONTROLLERS
Digital control of the Kuiper Airborne Observatory telescope
[NASA-TM-101082] N89-23785
An application specific integrated circuit for dual-axis motion control
[DE89-007974] N89-23790

CONVECTION
Effect of internal convection and internal radiation on the structural temperatures of Space Shuttle Orbiter
[NASA-TM-100414] N89-23819

CONVECTIVE FLOW
An experimental study of the effect of streamwise vortices on unsteady turbulent boundary-layer separation
[AD-A205462] N89-23420
Numerical simulation of flow through an artificial heart
[NASA-TM-102183] N89-24111

CONVECTIVE HEAT TRANSFER
SRB ascent aerodynamic heating design criteria reduction study, volume 1
[NASA-CR-183580] N89-23515
Effect of internal convection and internal radiation on the structural temperatures of Space Shuttle Orbiter
[NASA-TM-100414] N89-23819

CONVERGENCE
Numerical study of the influence of leading and trailing edge flaps on the performance of airfoils
[AD-A206138] N89-23428
An iterative technique to correct probe position errors in planar near-field to far-field transformations
[PB89-153886] N89-23750
Operator induced multigrid algorithms using semirefinement
[NASA-CR-181834] N89-24113

COOLING
Cooling rate, undercooling and rapid solidification by atomization N89-23609
Fire propagation in concurrent flows
[PB89-151781] N89-23636
Macrosegregation and nucleation in undercooled Pb-Sn alloys
[NASA-TM-102023] N89-23664

COOLING SYSTEMS
SIRTF Telescope Instrument Changeout and Cryogen Replenishment (STICCR) Study
[NASA-CR-177380] N89-23512
Solid-vapor adsorption refrigeration system development
[PB89-140859] N89-23733
Evaluation of three commercial microclimate cooling systems
[AD-A206318] N89-23744

COORDINATION
NASA space communications R and D (Research and Development): Issues, derived benefits, and future directions
[NASA-CR-184831] N89-23746

COPLANARITY
Optimal aeroassisted coplanar orbital transfer using an energy model
[NASA-CR-181778] N89-23495
Continuous, low thrust coplanar orbit transfers with varying eccentricity
[AD-A206022] N89-23498

COPOLYMERS
Structure/permeability relationships of silicon-containing polyimides
[NASA-CR-4237] N89-23683

Model of early self-replication based on covalent complementarity for a copolymer of glycerate-3-phosphate and glycerol-3-phosphate
[NASA-CR-182912] N89-23693
Donor acceptor polymerization chemistry as a vehicle to low energy cure of matrix resins: Evolution of the 2-Tg concept to produce Tg polymers at ambient temperatures
[AD-A206287] N89-23706
Path dependent morphologies of a diblock copolymer of Polystyrene/Hydrogenated polybutadiene
[AD-A206504] N89-23883

COPPER
Stress relief cracking in copper-precipitation strengthened HSLA-100 steel
[AD-A205936] N89-23670
Environmental interactions of hydrazine fuels in Soil/Water systems
[AD-A206244] N89-23986
Nuclear magnetism in copper and silver: Theory and experiments
[ISBN-952-900-084-7] N89-24188
Magnetic susceptibility and neutron diffraction experiments on nuclear ordering in copper
[ISBN-951-754-573-8] N89-24189
Assignment of the charge-transfer excited states of bis(N-heterocyclic) complexes of copper(I)
[AD-A206012] N89-24205

COPPER ALLOYS
Mechanical properties of gas atomized Cu-Ti and Cu-Ti-B alloys N89-23610
Critical assessment of the thermodynamic properties of antimony-copper alloys
[PB89-147524] N89-23657

COPPER OXIDES
Studies on high-Tc superconducting materials
[NAL-TM-MT-8703] N89-24178
Quasielastic and inelastic spin fluctuations in superconducting La2-xSrxCuO4
[DE89-008157] N89-24190
Shock compaction of YBa2Cu3O7-x and HoBa2Cu3O7-x powders in a metal matrix
[DE89-008827] N89-24193

CORONAL HOLES
Solar and stellar coronal plasmas
[NASA-CR-184909] N89-24162

CORRELATION
Correlation of Portable Wear Metal Analyzer (PWMA-2) and Baird A/E35U-3 spectrometer oil analysis data
[AD-A205957] N89-23882

CORRELATION DETECTION
Improvement of navigation measurement procedures by the combined application of correlation techniques and parameter estimation
[ETN-89-93946] N89-23445

CORROSION RESISTANCE
Corrosion of silicon carbide ceramics at high temperatures in water vapor-containing atmospheres N89-23594
Iron-niobium-aluminum alloy having high-temperature corrosion resistance
[DE89-009600] N89-23663

CORROSION TESTS
Corrosion and lubricity testing of nonflammable USAF formulated CTFE (Chlorotrifluoroethylene) base hydraulic fluid
[AD-A205467] N89-23695

COSMIC DUST
Gas-Grain Simulation Facility: Fundamental studies of particle formation and interactions. Volume 1: Executive summary and overview
[NASA-CP-10026-VOL-1] N89-24022
Gas-Grain Simulation Facility: Fundamental studies of particle formation and interactions. Volume 2: Abstracts, candidate experiments and feasibility study
[NASA-CP-10026-VOL-2] N89-24023
Ground-based infrared observations of sources discovered by the AFGL, FIRRSE and IRAS infrared surveys
[AD-A206335] N89-24246

COSMIC PLASMA
Electrodynamics of cosmical plasmas: Some basic aspects of cosmological importance
[TRITA-EPP-89-02] N89-24163

COSMIC RAY SHOWERS
Rapid fitting of particle cascade development data from X-ray film densitometry measurements
[NASA-TM-100368] N89-24260

COSMIC RAYS
Direct electron-pair production by high energy heavy charged particles
[NASA-CR-184958] N89-24142
Solar-geophysical data number 531, part 1. Data for October, September 1988 and late data
[PB89-139943] N89-24250
Compact source origin of cosmic ray antiprotons
[DE89-008044] N89-24258

COSMOLOGY
On the measurement of cosmogenic nuclides in cometary materials
[DE89-009248] N89-24243

COST ANALYSIS
Reducing launch operations costs: New technologies and practices
[PB89-136402] N89-23500

COST REDUCTION
Reducing launch operations costs: New technologies and practices
[PB89-136402] N89-23500
Low-temperature volumetric receiver concept
[DE89-008245] N89-23976

COUETTE FLOW
The dimension of attractors underlying turbulent Poiseuille flow
[AD-A206021] N89-23835

COVALENCE
Mechanism of the initiation of the cationic polymerization of styrenes by silanes and activated covalent esters
[AD-A206502] N89-23708

COVALENT BONDS
Model of early self-replication based on covalent complementarity for a copolymer of glycerate-3-phosphate and glycerol-3-phosphate
[NASA-CR-182912] N89-23693

COVARIANCE
On the connection of geodetic pointfields in RETrig
[PB89-146112] N89-23958

CRACK ARREST
Cracking of coated materials under transient thermal stresses
[NASA-CR-184898] N89-23928

CRACK CLOSURE
Response of pavement to freeze-thaw cycles: Lebanon, New Hampshire, regional airport
[AD-A205559] N89-23740

CRACK GEOMETRY
The mode 3 crack problem in bonded materials with a nonhomogeneous interfacial zone
[NASA-CR-185315] N89-23927

CRACK INITIATION
Crack-face displacements for embedded elliptic and semi-elliptical surface cracks
[NASA-CR-181822] N89-23919

CRACK OPENING DISPLACEMENT
Crack-face displacements for embedded elliptic and semi-elliptical surface cracks
[NASA-CR-181822] N89-23919

CRACK PROPAGATION
USAF (US Air Force) durability design handbook: Guidelines for the analysis and design of durable aircraft structures
[AD-A206286] N89-23457
Environment-induced crack growth processes in nickel-base alloys
[DE89-008253] N89-23659
Testing chromium adhesion using acoustic emission
[AD-A205621] N89-23666
Dynamic fatigue of ultralow-expansion glass for space mirrors, reissue A
[AD-A205401] N89-23694
Environmental stress crazing and cracking of transparent polymers
[AD-A205624] N89-23697
Fatigue crack growth model RANDOM2 user manual, appendix 1
[NASA-CR-184939] N89-23890
Crack-face displacements for embedded elliptic and semi-elliptical surface cracks
[NASA-CR-181822] N89-23919
Applications of a digital acoustic-emission data-acquisition workstation
[DE89-009648] N89-23923
The crack problem in bonded nonhomogeneous materials
[NASA-CR-184897] N89-23926
The mode 3 crack problem in bonded materials with a nonhomogeneous interfacial zone
[NASA-CR-185315] N89-23927
Cracking of coated materials under transient thermal stresses
[NASA-CR-184898] N89-23928
Geometrical foundations of mesomechanics and Lagrangian formalism
[AD-A205589] N89-23930
Overview of ASTM symposium on analytical and experimental methods for residual stress effects in fatigue
[AD-A205622] N89-23931
Cyclic crack propagation characteristics of the powder metallurgical nickel-base alloy Udimet 720 at elevated temperatures and different dwell times
[ETN-89-94426] N89-23938

CRACK TIPS
The crack problem in bonded nonhomogeneous materials
[NASA-CR-184897] N89-23926
The mode 3 crack problem in bonded materials with a nonhomogeneous interfacial zone
[NASA-CR-185315] N89-23927

CRACKING (CHEMICAL ENGINEERING)
Production of jet fuels from coal-derived liquids. Volume 8: Heteroatom removal by catalytic processing
[AD-A205470] N89-23712

CRACKING (FRACTURING)
Environment-induced crack growth processes in nickel-base alloys
[DE89-008253] N89-23659
Stress relief cracking in copper-precipitation strengthened HSLA-100 steel
[AD-A205936] N89-23670
Fatigue crack growth model RANDOM2 user manual, appendix 1
[NASA-CR-184939] N89-23890
Cracking of a layered medium on an elastic foundation under thermal shock
[NASA-CR-185316] N89-23925
Cracking of coated materials under transient thermal stresses
[NASA-CR-184898] N89-23928

CRACKS
Investigations on the cracking behavior of joints in airfields and roads: Field investigations and laboratory simulations
[PB89-141279] N89-23479
Mechanisms of diffusion-controlled brittle fracture
[DE89-008728] N89-23921

CRASHES
Annual review of aircraft accident data, US Air Carrier operations: Calendar year 1986
[PB89-151021] N89-23434

CRAY COMPUTERS
Preconditioned Krylov solvers and methods for runtime loop parallelization
[AD-A206388] N89-24120
Krylov methods preconditioned with incompletely factored matrices on the CM-2
[AD-A206389] N89-24121

CREW PROCEDURES (INFLIGHT)
Aircraft Accident Report: AVAir Inc., Flight 3378, Fairchild Metro 3, SA227 AC, N622AV, Cary, North Carolina, February 19, 1988
[PB88-910412] N89-23436
Crew procedures and workload of retrofit concepts for microwave landing system
[NASA-CR-181700] N89-24033

CREW WORKSTATIONS
An evaluation of the F/FB/EF-111 crew/voice message system
[AD-A205998] N89-23774

CRITERIA
Launch commit criteria performance trending analysis, phase 1, revision A. SRM and QA mission services
[NASA-CR-184859] N89-24129

CRITICAL TEMPERATURE
The formation of topological defects in phase transitions
[NASA-CR-185318] N89-24215

CROP VIGOR
Advanced space design program to the Universities Space Research Association and the National Aeronautics and Space Administration
[NASA-CR-180450] N89-24015
Plant health sensing N89-24018

CROSS CORRELATION
Radar waveforms derived from orthogonal matrices
[AD-A205459] N89-23765

CROSS COUPLING
Decay of molecules at corrugated thin metal films
[AD-A205487] N89-24198

CROSS FLOW
Flowfield measurements in the vortex wake of a missile at high angle of attack in turbulence
[AD-A205698] N89-23422

CRUISE MISSILES
Average-passage simulation of counter-rotating propfan propulsion systems as applied to cruise missiles
[NASA-TM-102043] N89-23416
An investigation into the application of dynamic programming to determine optimal controls for tracking a cruise missile maneuver by CMMCA (Cruise Missile Mission Control Aircraft)
[AD-A205970] N89-23456

CRYOGENIC COOLING
SIRTF Telescope Instrument Changeout and Cryogen Replenishment (STICCR) Study
[NASA-CR-177380] N89-23512
Parametric study of radiative cooling of solid antihydrogen
[AD-A206092] N89-23742
CRYOGENIC EQUIPMENT
Shaking in cryogenic conditions
[REPT-882-440-101] N89-23939
Telescope structure for cryogenic application
[REPT-882-440-112] N89-23940
Thermal and cryogenic aspects of the ISO optical subsystem
[REPT-882-440-113] N89-24160
CRYOGENIC TEMPERATURE
The in-vacuo torque performance of dry-lubricated ball bearings at cryogenic temperatures N89-23914
Magnetic susceptibility and neutron diffraction experiments on nuclear ordering in copper
[ISBN-951-754-573-8] N89-24189
CRYOGENIC WIND TUNNELS
Hot-jet simulation in cryogenic wind tunnels
[NASA-RP-1220] N89-23448
CRYSTAL DEFECTS
Atomic relaxation and vacancy-interstitial recombination in Zr and Zr3Al
[AD-A205664] N89-24199
CRYSTAL DISLOCATIONS
Fundamental studies of beta phase decomposition modes in titanium alloys
[AD-A205296] N89-23665
Deformation twinning in ordered intermetallic compounds
[DE89-008748] N89-24192
CRYSTAL GROWTH
Semiconductors and monocrystal growth: Collection of charts, formulas and references N89-23729
Atomic layer epitaxy. Atomic layer epitaxy of 3-5 compound semiconductors by thermal and laser-assisted metalorganic chemical vapor deposition
[AD-A205699] N89-24200
CRYSTAL LATTICES
Theoretical studies of Ni3Al and NiAl with impurities
[DE89-006556] N89-23655
Studies on high-Tc superconducting materials
[NAL-TM-MT-8703] N89-24178
The diluted tri-dimensional spin-one Ising model with crystal field interactions
[DE88-705663] N89-24181
Mean field theory of the spin-1 Ising model with a random crystal field
[DE88-705669] N89-24182
Structure and grid dynamics of ultrathin epitaxial Ag and Fe films on Ni(100) and Cu(100) substrates
[JUEL-2221] N89-24187
Atomic relaxation and vacancy-interstitial recombination in Zr and Zr3Al
[AD-A205664] N89-24199
Lattice symmetries and thermal expansion
[AD-A206045] N89-24207
CRYSTAL STRUCTURE
Theoretical studies of Ni3Al and NiAl with impurities
[DE89-006556] N89-23655
Twin boundaries, interfaces and modulated structures in martensites
[DE89-009064] N89-23662
Fundamental studies of beta phase decomposition modes in titanium alloys
[AD-A205296] N89-23665
Atomic imaging and microanalysis of ceramics
[DE89-008172] N89-23684
Site occupancy/valence measurements using channelling and related effects in microanalysis
[DE89-007658] N89-24186
Structure and grid dynamics of ultrathin epitaxial Ag and Fe films on Ni(100) and Cu(100) substrates
[JUEL-2221] N89-24187
Quasielastic and inelastic spin fluctuations in superconducting La2-xSrxCuO4
[DE89-008157] N89-24190
Quasi-liquid crystalline materials with special electro-optic properties
[AD-A206015] N89-24206
Lattice symmetries and thermal expansion
[AD-A206045] N89-24207
CRYSTALLIZATION
Atomic imaging and microanalysis of ceramics
[DE89-008172] N89-23684
Research activity report concerning solidification technology under microgravity
[ETN-89-93868] N89-23718
Organic monocrystals N89-23730
Quasi-liquid crystalline materials with special electro-optic properties
[AD-A206015] N89-24206
CRYSTALLOGRAPHY
Site occupancy/valence measurements using channelling and related effects in microanalysis
[DE89-007658] N89-24186
CRYSTALS
Molecular optics nonlinear optical processes in organic and polymeric crystals and films
[AD-A206372] N89-24209
CURING
Epoxylite 8822 hardness study
[DE89-008961] N89-23687
CURRENT DISTRIBUTION
Current distribution in a three-dimensional IC analyzed by a perturbation method. Part 1: A simple steady state theory
[NASA-CR-185022] N89-23494
CURRENT SHEETS
A vector scanning processing technique for pulsed laser velocimetry
[NASA-TM-102048] N89-23850
CURVATURE
The geometry of plane waves in spaces of constant curvature N89-24241
CURVE FITTING
Correlation of Portable Wear Metal Analyzer (PWMA-2) and Baird A/E35U-3 spectrometer oil analysis data
[AD-A205957] N89-23882
Rapid fitting of particle cascade development data from X-ray film densitometry measurements
[NASA-TM-100368] N89-24260
CYCLIC COMPOUNDS
Novel organoboranes as intermediates for ceramic precursors and high-energy fuels
[AD-A206101] N89-23713
CYCLIC LOADS
Fatigue in ceramics N89-23583
CYCLOHEXANE
Sorption of selected volatile organic constituents of jet fuels and solvents on natural sorbents from gas and solutions phases
[AD-A204073] N89-23711
CYCLOTRON RESONANCE DEVICES
Megavolt, multi-kiloamp K(sub)a-band gyrotron oscillator experiment
[AD-A206271] N89-23801
Operation of a quasi-optical gyrotron with variable mirror separation
[AD-A206347] N89-23854
CYLINDERS
Experimental study of pressure and heating rate on a swept cylindrical leading edge resulting from swept shock wave interference
[NASA-CR-185326] N89-23411

D

DAMAGE
Strength and structure of Ga(1-x)In(x)As alloys
[AD-A205415] N89-23644
DAMAGE ASSESSMENT
Locating damaged members in a truss structure using modal test data: A demonstration experiment
[NASA-TM-101595] N89-23924
DAMPING
Eddy current damper N89-23900
DARK MATTER
A linear analysis of the stability of strong shocks and the evolution and distribution of materials in a cold dark matter dominated universe N89-24244
DATA ACQUISITION
A research facility for film cooling investigations with emphasis on the instrumentation system
[NAL-TM-PR-8704] N89-23477
Intelligent processing of materials
[PB89-151823] N89-23735
KRMS (K-band Radiometric Mapping System) SSM/I validation March 1988 quick look report
[NASA-CR-185320] N89-23766
Applications of a digital acoustic-emission data-acquisition workstation
[DE89-009648] N89-23923
Application of a PC based, real-time, data-aquisition system in rotorcraft wind-tunnel testing
[NASA-TM-4119] N89-24079
PRASE (Parallel Resource Analysis Software Environment) instrumentation software for the Intel iPSC hypercube
[AD-A206046] N89-24087
DATA BASE MANAGEMENT SYSTEMS
A database management system for computer-aided digital circuit design
[AD-A206047] N89-24066
A visual object-oriented unification system
[AD-A206228] N89-24068
ESABASE: A most versatile and flexible system engineering tool
[ESA-BR-54] N89-24223
A program interface prototype for a multimedia database incorporating images
[AD-A206439] N89-24226
DATA BASES
Atomic oxygen effects on spacecraft materials: The state of the art of our knowledge N89-23541
High-latitude field-strength measurements of standard broadcast band skywave transmissions monitored at Fairbanks, Alaska
[PB89-134829] N89-23747
Inferring relative humidity profiles from 3DNEPH cloud data: Technique development and data impact study
[AD-A205825] N89-23993
Discrete event simulation model decomposition
[AD-A206048] N89-24119
Managing sound in a relational multimedia database system
[AD-A205742] N89-24225
DATA COLLECTION PLATFORMS
Battlefield radar imaging through airborne millimetric wave SAR (Synthetic Aperture Radar)
[ETN-89-94228] N89-23751
DATA COMPRESSION
Investigation of optical compression techniques for dither coding
[AD-A206140] N89-23776
DATA LINKS
Link availability and rain attenuation exceedance characteristics for EHF (Extremely High Frequency) satellite communications with arbitrary link parameters in Canada
[AD-A205403] N89-23762
DATA MANAGEMENT
An experimental investigation into software reliability
[AD-A206293] N89-24069
Approaches for empirical Bayes confidence intervals
[AD-A205775] N89-24126
DATA PROCESSING
AN/TAC-1 demultiplexer circuit card assembly
[AD-A205744] N89-23770
Hybrid cartographic data processing in a geographic information system N89-23954
Investigation of several methods for the detection of outstanding points in a digital image
[ETN-89-94148] N89-23965
A reduced version of the NMC DERF 2 data set
[NASA-TM-100727] N89-24002
Study of a method to de-alias winds from ERS-1 data
[CREO-8374] N89-24003
Human adaptation to the Tibetan Plateau
[AD-A206463] N89-24031
Monitoring information processing and decisions: The MOUSELAB system
[AD-A205963] N89-24037
Defense Integrated Data System (DIDS) procedures manual. Volume 8: Document Identifier Code (DIC) Input/Output (I/O) formats (fixed length), change 3
[PB89-139414] N89-24220
DATA REDUCTION
A reduced version of the NMC DERF 2 data set
[NASA-TM-100727] N89-24002
DATA SIMULATION
Microcomputer program for daily weather simulation
[PB89-144838] N89-24001
DATA STORAGE
Exploring the North Atlantic Ocean on floppy disks
[AD-A205733] N89-24011
DATA STRUCTURES
Shortest paths in a digitized map using a tile-based data structure
[PB89-143432] N89-23957
Compiling high level constructs to distributed memory architectures
[NASA-CR-181825] N89-24058
A program interface prototype for a multimedia database incorporating images
[AD-A206439] N89-24226
DATA TRANSMISSION
Direct dissemination of data from ESA's future in-orbit infrastructure
[DDD-CP/TE-RE-7450] N89-23754
Light channel 5 Gb/s optoelectronic TDM (Time Division Multiplexing)
[AD-A205501] N89-24086
Managing sound in a relational multimedia database system
[AD-A205742] N89-24225
DAYTIME
The relationship between subjective and objective measures of sleepiness
[AD-A205861] N89-24027

DC 9 AIRCRAFT
Interior noise control ground test studies for advanced turboprop aircraft applications
[NASA-CR-181819] N89-24141
DECAY
A numerical routine for defining rocket exhaust characteristics and impingement effects
[AD-A206323] N89-23526
DECAY RATES
Decay of molecules at corrugated thin metal films
[AD-A205487] N89-24198
DECEPTION
Active radar jamming
[FOA-C-30506-3.6] N89-23777
DECISION MAKING
Generation of architectures for distributed intelligence systems
[AD-A205783] N89-23440
Monitoring information processing and decisions: The MOUSELAB system
[AD-A205963] N89-24037
The impact of accuracy and effort feedback and goals on adaptive decision behavior
[AD-A205751] N89-24095
DECOMPOSITION
Fundamental studies of beta phase decomposition modes in titanium alloys
[AD-A205296] N89-23885
DEEP SPACE NETWORK
Environmental projects. Volume 3: Environmental compliance audit
[NASA-CR-185019] N89-23985
DEFECTS
Environmental Stress Screening (ESS) guide
[AD-A206350] N89-23888
The formation of topological defects in phase transitions
[NASA-CR-185318] N89-24215
DEFENSE INDUSTRY
NASA space communications R and D (Research and Development): Issues, derived benefits, and future directions
[NASA-CR-184831] N89-23746
DEFENSE PROGRAM
Defense Integrated Data System (DIDS) procedures manual. Volume 2: Multiple application procedures
[PB89-139307] N89-24221
DEFORMATION
Strength and structure of Ga(1-x)In(x)As alloys
[AD-A205415] N89-23644
DEGREES OF FREEDOM
Modeling of a continuous oscillator by oscillators with a finite number of degrees of freedom
[PB89-146120] N89-24134
DELAMINATING
Mode 2 delamination fatigue resistance of composites N89-23624
Finite element modeling of frictionally restrained composite interfaces
[NASA-CR-182281] N89-23918
DENDRITIC CRYSTALS
Model systems — metal alloys N89-23728
DENSE PLASMAS
Nonlinear spectroscopy of multicomponent droplets and two- and three-dimensional measurements in flames
[AD-A205449] N89-23645
DENSIFICATION
Preparation and evaluation of silicon nitride matrices for silicon nitride-SiC fiber composites
[NASA-CR-184796] N89-23678
DENSITY DISTRIBUTION
Experimental and theoretical studies of dense fluid mixtures
[DE89-008882] N89-24214
DENSITY MEASUREMENT
Development of a CARS device for a feasibility study of density and temperature measurements at high time dependent resolution
[ISL-R-117/87] N89-23654
DEPLOYMENT
The 23rd Aerospace Mechanisms Symposium
[NASA-CP-3032] N89-23892
The third generation rigid solar array GSR3
[REPT-882-440-105] N89-23979
DEPOSITION
Spray deposition: A fundamental study of droplet impingement, spreading and consolidation
[AD-A206065] N89-23672
DESERTS
The US Army Yuma Proving Ground, Artzona 33-year climate calendar and tables on associated weather elements 1954-1986. American desert country
[AD-A206256] N89-24010
DESIGN ANALYSIS
Preliminary design of a modular unmanned research vehicle. Volume 2: Subsystem technical development design study
[AD-A205678] N89-23454
Advances in computational design and analysis of airbreathing propulsion systems
[NASA-TM-101967] N89-23465
Multivariable flight control design with parameter uncertainty for the AFTI/F-16
[AD-A206068] N89-23476
Buran designer Semenov interviewed N89-23488
SIRTF Telescope Instrument Changeout and Cryogen Replenishment (STICCR) Study
[NASA-CR-177380] N89-23512
A method to design blended rolled edges for compact range reflectors
[NASA-CR-184976] N89-23736
ESA-D: An integrated software for antenna design and analysis
[REPT-882-440-111] N89-23784
Li/FeS battery design for an electric van
[DE89-009808] N89-23794
Design, fabrication and test of a 4750 Newton-meter-second double Gimbal control moment gyroscope N89-23896
The third generation rigid solar array GSR3
[REPT-882-440-105] N89-23979
DETECTION
Co-aligning the RAIDS (Remote Atmospheric and Ionospheric Detection System) instruments
[AD-A205456] N89-23513
Fiber optic leak detection system
[PB89-148888] N89-24150
DETECTORS
Plant health sensing N89-24018
DETONATION WAVES
Analogy between explosive wave and front wave near curved walls
[ISL-CO-209/87] N89-23840
DIELECTRIC POLARIZATION
Polarizability and effective permittivity of layered and continuously inhomogeneous dielectric ellipsoids
[PB89-146476] N89-24102
DIELECTRIC PROPERTIES
An elastomeric electrical isolation membrane
[AD-D013966] N89-23702
Attenuation measurement of very low-loss dielectric waveguides by the cavity resonator method in the millimeter/submillimeter wavelength range
[AD-A206458] N89-23803
Polarizability and effective permittivity of layered and continuously inhomogeneous dielectric ellipsoids
[PB89-146476] N89-24102
DIELECTRICS
Dielectrics for long term space exposure and spacecraft charging: A briefing N89-23553
The effects of dielectric and metal loading on the dispersion characteristics for contrawound helix circuits used in high power traveling-wave tubes
[AD-A205345] N89-23797
Attenuation measurement of very low-loss dielectric waveguides by the cavity resonator method in the millimeter/submillimeter wavelength range
[AD-A206458] N89-23803
DIFFERENCE EQUATIONS
Approximation of stochastic integral equations using Martingale difference schemes
[ETN-89-93951] N89-24123
DIFFERENTIAL EQUATIONS
Some applications of the qualitative theory of differential equations in fluid dynamics
[ETN-89-94143] N89-23814
Fast algorithms for partial differential equations on advanced computers
[AD-A206469] N89-24073
Efficient method for solving free-boundary problems
[PB89-146138] N89-24101
Differential algebraic equations, indices, and integral algebraic equations
[DE89-009584] N89-24109
Sheath and presheath in a collisionless open field plasma
[IPPJ-890] N89-24161
DIFFRACTION
Characterization of multilayer coated concave diffraction gratings in the extreme ultraviolet
[DE89-008831] N89-24151
DIFFUSION
Diffusion N89-23724
Mechanisms of diffusion-controlled brittle fracture
[DE89-008728] N89-23921
Monitoring thin film properties with surface acoustic wave devices: Diffusion, surface area and pore size distribution
[DE89-009379] N89-24195
DIFFUSION FLAMES
A numerical scheme to solve unsteady and variable density low Mach number flows N89-23419
An experimental study of opposed flow diffusion flame extinction over a thin fuel in microgravity
[NASA-CR-182185] N89-23638
DIGITAL COMPUTERS
An evaluation of the F/FB/EF-111 crew/voice message system
[AD-A205998] N89-23774
Digital optics for numerical computing: The residue number system for numerical optical computing
[AD-A206229] N89-24157
DIGITAL DATA
The digital urban map as a basis for a land information system in local administration N89-23945
Investigation of several methods for the detection of outstanding points in a digital image
[ETN-89-94148] N89-23985
Managing sound in a relational multimedia database system
[AD-A205742] N89-24225
DIGITAL ELECTRONICS
A database management system for computer-aided digital circuit design
[AD-A206047] N89-24066
DIGITAL SIMULATION
Analytical transfer functions in parallel configurations
[AD-A205714] N89-23472
DIGITAL SYSTEMS
Investigation of mutual interference between digitally modulated signals
[BBC-RD-1988/13] N89-23745
Phase accuracy experiments with a direct-sampling coherent detector
[AD-A205458] N89-23764
AN/TAC-1 demultiplexer circuit card assembly
[AD-A205744] N89-23770
Digital control of the Kuiper Airborne Observatory telescope
[NASA-TM-101082] N89-23785
Generating circuit tests by exploiting designed behavior
[AD-A206175] N89-23800
Signal-Noise/Interferer Combiner Unit Programmable (SINCUP)
[AD-A205367] N89-24053
A database management system for computer-aided digital circuit design
[AD-A206047] N89-24066
DIGITAL TECHNIQUES
Automatic digitizing of cadastral maps N89-23946
Digitizing of drawings and cadastral maps using a scanner system N89-23949
Tools for the computer assisted generalization of settlements for the construction of digital landscape models N89-23952
Automatic extraction of areas from overlays of the series DGK 5 (Bo) N89-23955
Shortest paths in a digitized map using a tile-based data structure
[PB89-143432] N89-23957
DILATOMETRY
Dilatometric analysis of Al-, Ba-, Ca-titanate N89-23592
DILUTION
The diluted tri-dimensional spin-one Ising model with crystal field interactions
[DE88-705663] N89-24181
DIRECT CURRENT
Magnification of starting torques of dc motors by maximum power point trackers in photovoltaic systems
[NASA-TM-102040] N89-23792
DISCRETE FUNCTIONS
Fast algorithms for partial differential equations on advanced computers
[AD-A206469] N89-24073
Asymptotic behavior of random discrete event systems
[PB89-146146] N89-24099
DISCRIMINANT ANALYSIS (STATISTICS)
On the problem of optimal signal detection in discrete-time, correlated, non-Gaussian noise
[AD-A205859] N89-23771
Multivariate analysis and its applications
[AD-A205585] N89-24125
DISK GALAXIES
A self consistant model of the three phase interstellar medium in disk galaxies N89-24245
DISK OPERATING SYSTEM (DOS)
Laboratory process control using natural language commands from a personal computer
[NASA-TM-101988] N89-24055

DISPERSING
The effects of dielectric and metal loading on the dispersion characteristics for contrawound helix circuits used in high power traveling-wave tubes
[AD-A205345] N89-23797
DISPLAY DEVICES
Method and system for monitoring and displaying engine performance parameters
[NASA-CASE-LAR-14049-1] N89-23466
Simulator evaluation of a display for a Takeoff Performance Monitoring System
[NASA-TP-2908] N89-23469
DISPOSAL
Propellant reuse/recovery technology
[AD-A206306] N89-23714
DISTORTION
Impact of the geoplasma on a spaceborne GPS receiver system: A preliminary study
[AD-A205965] N89-23442
Numerical conformal mapping and applications
[AD-A205602] N89-24131
DISTRIBUTED PARAMETER SYSTEMS
A designers' guide to reliable distributed systems: An example design. Volume 1
[AD-A206039] N89-23885
A designers' guide to reliable distributed systems: An example design. Volume 2
[AD-A206040] N89-23886
DISTRIBUTED PROCESSING
Wavefront matrix multiplication on a distributed-memory multiprocessor
[PB89-151807] N89-24052
Compiling high level constructs to distributed memory architectures
[NASA-CR-181825] N89-24058
The role of order in distributed programs
[AD-A206037] N89-24065
Runtime aggregation of recursion relations
[AD-A206576] N89-24076
A method of up-front load balancing for local memory parallel processors
[NASA-CASE-MSC-21348-1] N89-24084
DISTRIBUTION FUNCTIONS
A description of the slab model
[DE89-009962] N89-23984
DIURNAL VARIATIONS
High-latitude field-strength measurements of standard broadcast band skywave transmissions monitored at Fairbanks, Alaska
[PB89-134829] N89-23747
An analysis of lightning launch constraints
[AD-A206084] N89-23994
The diurnal variation of a marine stratocumulus layer: A model sensitivity study N89-24000
DIVING (UNDERWATER)
Oxygen consumption rate of operational underwater swimmers
[AD-A205331] N89-24025
DOMAIN WALL
The formation of topological defects in phase transitions
[NASA-CR-185318] N89-24215
DOPPLER EFFECT
Problems encountered in the Stokes' numerical integration of terrestrial gravity anomalies
[AD-A205448] N89-23990
DOPPLER RADAR
Design of the ELDORA airborne Doppler radar
[PB89-144604] N89-23749
DRAG REDUCTION
Navier-Stokes solution for a NACA 0012 airfoil with mass flux (fan)
[AD-A205771] N89-23424
Drag and noise measurements on underwater vehicles with a riblet surface coating
[AD-A205500] N89-23825
DRAWINGS
Digitizing of drawings and cadastral maps using a scanner system N89-23949
DROPS (LIQUIDS)
Burning rate constant of fuel droplet under high pressure
[NAL-TR-1001] N89-23639
Nonlinear spectroscopy of multicomponent droplets and two- and three-dimensional measurements in flames
[AD-A205449] N89-23845
Fundamental studies on spray combustion and turbulent combustion
[AD-A206436] N89-23651
Spray deposition: A fundamental study of droplet impingement, spreading and consolidation
[AD-A206065] N89-23672
DRUGS
Muramyl peptide-enhanced sleep: Pharmacological optimization of performance
[AD-A205974] N89-24028
DUCTED FLOW
Flow-turning losses in solid rocket motors
[AD-A206099] N89-23525
DUCTILITY
Mechanical properties of rapidly solidified iron-based alloys N89-23611
Theoretical studies of Ni3Al and NiAl with impurities
[DE89-006556] N89-23655
DURABILITY
USAF (US Air Force) durability design handbook: Guidelines for the analysis and design of durable aircraft structures
[AD-A206286] N89-23457
DUST COLLECTORS
Calibration measurements on micrometeorite detectors for the missions ULYSSES, Galileo and Giotto
[ETN-89-93947] N89-24248
DYNAMIC CHARACTERISTICS
The dynamic behavior of water vapor on activated carbon
[AD-A206124] N89-23628
Dynamic fatigue of ultralow-expansion glass for space mirrors, reissue A
[AD-A205401] N89-23694
Coherence and chaos phenomena in Josephson oscillators for superconducting electronics
[AD-A205469] N89-23798
DYNAMIC CONTROL
Signal-Noise/Interferer Combiner Unit Programmable (SINCUP)
[AD-A205367] N89-24053
DYNAMIC LOADS
Modal analysis and testing of missile systems
[AD-A204051] N89-23916
DYNAMIC MODELS
Modelling aircraft dynamics
[AD-A204086] N89-23449
A reduced version of the NMC DERF 2 data set
[NASA-TM-100727] N89-24002
DYNAMIC PRESSURE
Flutter of a low-aspect-ratio rectangular wing
[NASA-TM-4116] N89-23447
DYNAMIC PROGRAMMING
An investigation into the application of dynamic programming to determine optimal controls for tracking a cruise missile maneuver by CMMCA (Cruise Missile Mission Control Aircraft)
[AD-A205970] N89-23456
DYNAMIC RESPONSE
The dynamic behavior of water vapor on activated carbon
[AD-A206124] N89-23628
GEMMES: A new tool for dynamic modeling
[REPT-662-440-114] N89-24078
DYNAMIC STRUCTURAL ANALYSIS
A correlation study of X-29A aircraft and associated analytical developments N89-23450
Prediction and measurement of damping of a laminated beam with a constrained viscoelastic layer
[DE89-009002] N89-23922

E

EARLY STARS
Ground-based infrared observations of sources discovered by the AFGL, FIRRSE and IRAS infrared surveys
[AD-A206335] N89-24246
EARPHONES
Intelligibility in noise of three LPC (Linear Predictive Coders) voice channels with active noise reduction headsets
[AD-A205613] N89-23767
EARTH (PLANET)
Problems encountered in the Stokes' numerical integration of terrestrial gravity anomalies
[AD-A205448] N89-23990
EARTH ATMOSPHERE
Co-aligning the RAIDS (Remote Atmospheric and Ionospheric Detection System) instruments
[AD-A205456] N89-23513
A description of the slab model
[DE89-009962] N89-23984
EARTH IONOSPHERE
Co-aligning the RAIDS (Remote Atmospheric and Ionospheric Detection System) instruments
[AD-A205456] N89-23513
An overview of charging environments N89-23554
Autofocus of SAR imagery degraded by ionospheric-induced phase errors
[DE89-008278] N89-23752
EARTH MAGNETOSPHERE
The space particle environment N89-23548
An overview of charging environments N89-23554
Electric fields in the magnetosphere: The evidence from ISEE, S3-3, GEOS and Viking
[TRITA-EPP-88-11] N89-23987
Relativistic electron precipitation patterns in longitude and latitude: A reply to W. R. Sheldon
[NASA-CR-185442] N89-23995
EARTH OBSERVATIONS (FROM SPACE)
The evolution of space mechanisms in the ESA R and D program N89-23893
EARTH OBSERVING SYSTEM (EOS)
The search for edges in remote sensing images using a digital polygonal map
[ETN-89-94146] N89-23964
EARTH ORBITAL ENVIRONMENTS
NASA/SDIO Space Environmental Effects on Materials Workshop, part 1
[NASA-CP-3035-PT-1] N89-23528
Overview of environmental factors N89-23529
Structural materials for space applications N89-23530
Radiation effects in spacecraft electronics N89-23531
Environmental effects on spacecraft materials N89-23532
EnviroNET: Space environment for Strategic Defense Initiative experiments N89-23538
Environmental definition of the earth's neutral atmosphere N89-23539
Atomic oxygen effects on materials N89-23540
Atomic oxygen effects on spacecraft materials: The state of the art of our knowledge N89-23541
Orbital debris environment and data requirements N89-23543
Spacecraft contamination experience N89-23545
Effects of the contamination environment on surfaces and materials N89-23546
Undercutting of defects in thin film protective coatings on polymer surfaces exposed to atomic oxygen
[NASA-TM-101986] N89-23691
EARTH ORBITS
An improved strategy for determining earth satellite orbits by radio
[AD-A205826] N89-23497
Continuous, low thrust coplanar orbit transfers with varying eccentricity
[AD-A206022] N89-23498
On-orbit observations of single-event upset in harris HM-6508 RAMSs (Random Access Memories): An update
[AD-A206266] N89-23506
Space debris: A report from the ESA Debris Working Group
[ESA-SP-1109] N89-24230
EDDY CURRENTS
Eddy current damper N89-23900
EDGES
A method to design blended rolled edges for compact range reflectors
[NASA-CR-184976] N89-23736
EDITING ROUTINES (COMPUTERS)
A graphical editor for the computer aided prototyping system
[AD-A206443] N89-24071
EDUCATION
Air Force Human Resources Laboratory R and D accomplishments and services, FY86-FY88
[AD-A205312] N89-24218
EFFERENT NERVOUS SYSTEMS
A low-energy X-ray irradiator for electrophysiological studies
[AD-A205388] N89-24026
EFFLUENTS
Use of the 1:2,000,000 Digital Line Graph data in emergency response
[DE89-006730] N89-23959
EIGENVALUES
Reduction of a general matrix to tridiagonal form
[DE89-008980] N89-24083
EIGENVECTORS
A blocked Jacobi method for the symmetric Eigenproblem
[AD-A206553] N89-24133
Exact wave functions and coherent states of a damped driven harmonic oscillator
[AD-A205785] N89-24136
EIKONAL EQUATION
Eikonal approximation in partial wave version
[IPPJ-899] N89-24164
EJECTORS
Ejector effects on a supersonic nozzle at low altitude and Mach number
[AD-A206049] N89-23427
EKMAN LAYER
Analysis of turbulent motion phenomena in the maritime atmospheric boundary layer
[ETN-89-93949] N89-23996

ELASTIC BODIES
Development of harmonic panel methods for aeroelastic applications to elastic bodies and body-fin combinations in supersonic flow
[AD-A205739] N89-23423
ELASTIC MEDIA
Cracking of a layered medium on an elastic foundation under thermal shock
[NASA-CR-185316] N89-23925
ELASTIC PROPERTIES
Experimental and theoretical determination of the thermomechanical response of inelastic structural materials to high energy thermal inputs
[AD-A206100] N89-23933
Cohesive and anharmonic elastic properties of mixed fluorite crystals
[DE88-705690] N89-24184
ELASTIC SHELLS
Application of an exact finite element method to analysis of statics of thin elastic shells of revolution with axisymmetric loading
[ISBN-952-900-399-4] N89-23917
ELASTOMERS
An elastomeric electrical isolation membrane
[AD-D013966] N89-23702
ELASTOSTATICS
Optimum aeroelastic characteristics for composite supermaneuverable aircraft
[AD-A205503] N89-23452
Fractional calculus formulation of the quasi-static viscoelastic problem
[AD-A206136] N89-23934
ELECTRIC BATTERIES
Electric and Hybrid Vehicles Program: Report to Congress
[DE89-008988] N89-23879
ELECTRIC CONNECTORS
An elastomeric electrical isolation membrane
[AD-D013966] N89-23702
ELECTRIC CURRENT
Current distribution in a three-dimensional IC analyzed by a perturbation method. Part 1: A simple steady state theory
[NASA-CR-185022] N89-23494
ELECTRIC FIELDS
Current distribution in a three-dimensional IC analyzed by a perturbation method. Part 1: A simple steady state theory
[NASA-CR-185022] N89-23494
Study on a highly sensitive electro-static suspended accelerometer (1)
[NAL-TR-1005] N89-23504
Dielectrics for long term space exposure and spacecraft charging: A briefing N89-23553
High electric field phenomena in insulation
[AD-A205525] N89-23799
Energy transfer and photochemistry in biomimetic solar conversion
[PB89-142590] N89-23974
Electric fields in the magnetosphere: The evidence from ISEE, S3-3, GEOS and Viking
[TRITA-EPP-88-11] N89-23987
ELECTRIC GENERATORS
Long pulse homopolar generator
[AD-A205452] N89-23977
ELECTRIC HYBRID VEHICLES
Li/FeS battery design for an electric van
[DE89-009808] N89-23794
Electric and Hybrid Vehicles Program: Report to Congress
[DE89-008988] N89-23879
ELECTRIC MOTOR VEHICLES
Li/FeS battery design for an electric van
[DE89-009808] N89-23794
Electric and Hybrid Vehicles Program: Report to Congress
[DE89-008988] N89-23879
ELECTRIC MOTORS
High energy semiconductor switch
[DE89-007399] N89-23789
Electric and Hybrid Vehicles Program: Report to Congress
[DE89-008988] N89-23879
Carousel deployment mechanism for collable lattice truss N89-23897
Signal and power roll ring testing update N89-23909
ELECTRIC NETWORKS
Criteria for robust stability in a class of lateral inhibition networks coupled through resistive grids
[AD-A204174] N89-24081
ELECTRIC POWER SUPPLIES
Solar dynamic power for space station freedom
[NASA-TM-102016] N89-23516
Signal and power roll ring testing update N89-23909
ELECTRIC POWER TRANSMISSION
Signal and power roll ring testing update N89-23909
ELECTRIC PULSES
A unidirectional rotary solenoid as applied to stronglinks N89-23894
ELECTRICAL ENGINEERING
Designing feedback compensators by using the root-locus method
[AD-A205354] N89-24093
ELECTRICAL FAULTS
Dielectrics for long term space exposure and spacecraft charging: A briefing N89-23553
ELECTRICAL INSULATION
An elastomeric electrical isolation membrane
[AD-D013966] N89-23702
High electric field phenomena in insulation
[AD-A205525] N89-23799
ELECTRICAL PROPERTIES
Measuring conductivities of highly conductive membranes
[AD-A206043] N89-23649
Semiconductors and monocrystal growth: Collection of charts, formulas and references N89-23729
ELECTRICAL RESISTIVITY
Electron conducting ceramics as sensor material for noise thermometry N89-23603
Light weight polymer matrix composite material
[NASA-CASE-LEW-14734-1] N89-23623
Viscosity and conductance of MEICl/AlCl3 melts containing nonaqueous solvents
[AD-A205468] N89-23646
A first-principles calculation of the resistivity and thermopower in strong-scattering alloys
[DE89-008585] N89-23661
High pressure studies on infrared detector materials
[NAL-TM-MT-8701] N89-23677
Metallically conducting polymers: The limiting effect of conjugation defects on the electrical conductivity, a polyacetylene example
[ETN-89-93950] N89-23710
Studies on high-Tc superconducting materials
[NAL-TM-MT-8703] N89-24178
Electrical transport properties of Hg0.7Cd0.3Te
[DE88-705689] N89-24183
ELECTRICITY
Low-temperature volumetric receiver concept
[DE89-008245] N89-23976
ELECTRO-OPTICS
Semiconductors and monocrystal growth: Collection of charts, formulas and references N89-23729
Quasi-liquid crystalline materials with special electro-optic properties
[AD-A206015] N89-24206
ELECTROCHEMICAL CELLS
Measuring conductivities of highly conductive membranes
[AD-A206043] N89-23649
ELECTROCHEMISTRY
X-ray absorption spectroscopy of electrochemically generated species
[AD-A205572] N89-23647
Nano- and microstructures in chemistry, electrochemistry, and materials science
[AD-A206296] N89-23650
ELECTRODE MATERIALS
Electrode carrying wire for GTAW welding
[NASA-CASE-MFS-29491-1] N89-23738
ELECTRODEPOSITION
Control of the composition of electrodeposited alloys by the use of certain types of additives
[AD-A206370] N89-23675
ELECTRODES
Production of metal powders by rotating electrode process N89-23608
ELECTRODYNAMICS
Electrodynamics of cosmical plasmas: Some basic aspects of cosmological importance
[TRITA-EPP-89-02] N89-24163
ELECTROENCEPHALOGRAPHY
A low-energy X-ray irradiator for electrophysiological studies
[AD-A205388] N89-24026
ELECTROLYSIS
Space station propulsion test bed
[NASA-CR-183615] N89-23521
ELECTROLYTES
Synthesis of novel acid electrolytes for phosphoric acid fuel cells
[PB89-148944] N89-23786
Improved acid electrolytes: The synthesis and structure of fluorine containing sulfonic acids for fuel cells
[PB89-142616] N89-23973
Patterns of human drinking: Effects of exercise, water temperature and food consumption
[AD-A206031] N89-24029
ELECTROMAGNETIC ABSORPTION
Imaging procedure of underwater bottom topography by air and satellite images in the range of microwave and visible electromagnetic spectra
[GKSS-88/E/41] N89-24014
ELECTROMAGNETIC COUPLING
The effect of mutual coupling on the side lobe performance of Chebyshev arrays, volume 1
[AD-A205724] N89-23768
Simulation studies of particle acceleration powered by modulated intense relativistic electron beams
[AD-A206348] N89-24148
Photoabsorption of molecules at corrugated thin metal films
[AD-A205325] N89-24197
ELECTROMAGNETIC FIELDS
Electromagnetic remote sensing. Low frequency electromagnetics
[AD-A205402] N89-23761
Long pulse homopolar generator
[AD-A205452] N89-23977
ELECTROMAGNETIC INTERACTIONS
Coupled integral equation solution for two dimensional bistatic TE scatter from a conducting cavity-backed infinite plane
[AD-A206096] N89-23775
Strong and electromagnetic interactions in heavy exotic atoms
[PB89-145718] N89-24143
Rapid fitting of particle cascade development data from X-ray film densitometry measurements
[NASA-TM-100368] N89-24260
ELECTROMAGNETIC NOISE
Performance of radar receivers in the presence of noise and intentional interference
[AD-A205328] N89-23759
Near-far resistant linear multiuser detection
[AD-A206363] N89-23802
Signal-Noise/Interferer Combiner Unit Programmable (SINCUP)
[AD-A205367] N89-24053
Noise characteristics of an inductively coupled plasma-mass spectrometer
[AD-A205686] N89-24169
ELECTROMAGNETIC PROPERTIES
Metrology for Electromagnetic Technology: A bibliography of NBS (National Bureau of Standards) publications, January 1970 - August 1988
[PB89-147847] N89-23748
ELECTROMAGNETIC PULSES
Pulse shaping on the Nova laser system
[DE89-008026] N89-23859
ELECTROMAGNETIC SCATTERING
Coupled integral equation solution for two dimensional bistatic TE scatter from a conducting cavity-backed infinite plane
[AD-A206096] N89-23775
Improved sea surface scattering model
[AD-A205745] N89-24012
Polarizability and effective permittivity of layered and continuously inhomogeneous dielectric ellipsoids
[PB89-146476] N89-24102
ELECTROMAGNETIC WAVE TRANSMISSION
Lossy layers: Theory and methods of measurement
[FOA-C-30513-3.2] N89-23779
ELECTROMAGNETISM
Electromagnetic remote sensing. Low frequency electromagnetics
[AD-A205402] N89-23761
Coupled integral equation solution for two dimensional bistatic TE scatter from a conducting cavity-backed infinite plane
[AD-A206096] N89-23775
Engineering thrust areas, 1989
[DE89-009009] N89-24229
ELECTROMAGNETS
Electromagnetic railgun hydrogen pellet injector: Progress and prospect
[DE89-009536] N89-23499
ELECTRON BEAMS
On steel superficial hardening by concentrated electron beam in the air
[DE88-705781] N89-23658
The chirped-pulse free-electron laser
[DE89-009041] N89-23862
Development of high power CARM (Cyclotron Auto-Resonance Maser) oscillators
[AD-A206270] N89-23872
Three-dimensional analysis of optical transition radiation
[AD-A205935] N89-24156
Population inversions in ablation plasmas generated by intense electron beams
[AD-A205716] N89-24172

ELECTRON DENSITY (CONCENTRATION)
Simultaneous measurement of spatially resolved electron temperatures. Electron number densities and gas temperatures by laser light scattering from the ICP
[AD-A205747] N89-24174
ELECTRON DIFFRACTION
Site occupancy/valence measurements using channelling and related effects in microanalysis
[DE89-007658] N89-24186
ELECTRON DIFFUSION
Control of the composition of electrodeposited alloys by the use of certain types of additives
[AD-A206370] N89-23675
ELECTRON EMISSION
Direct electron-pair production by high energy heavy charged particles
[NASA-CR-184958] N89-24142
ELECTRON ENERGY
The chirped-pulse free-electron laser
[DE89-009041] N89-23882
Simultaneous measurement of spatially resolved electron temperatures. Electron number densities and gas temperatures by laser light scattering from the ICP
[AD-A205747] N89-24174
ELECTRON GAS
Memory functions and relaxation functions of some spin systems
[AD-A206340] N89-24137
Simultaneous measurement of spatially resolved electron temperatures. Electron number densities and gas temperatures by laser light scattering from the ICP
[AD-A205747] N89-24174
ELECTRON MICROSCOPES
Steel hardness effects in boundary lubricated sliding: An in-situ SEM (Scanning Electron Microscope) study
[AD-A206156] N89-23674
ELECTRON MICROSCOPY
The effect of welding process on the microstructure of HY-130 steel weldments
[AD-A205692] N89-23667
Grain boundaries
[DE89-006881] N89-24194
ELECTRON PARAMAGNETIC RESONANCE
FILMCAL: An ESR (Electron Spin Resonance) simulation program for transition metals in phthalocyanine films
[AD-A206441] N89-23676
Microscopic theory of electron spin resonance in Heisenberg spin glasses and thermal fluctuations in classical spin models with random fields
[JUEL-2227] N89-24146
ELECTRON PRECIPITATION
Relativistic electron precipitation patterns in longitude and latitude: A reply to W. R. Sheldon
[NASA-CR-185442] N89-23995
ELECTRON PROBES
Electron spectroscopy for chemical analysis: Sample analysis
[NASA-CR-183568] N89-23634
ELECTRON PUMPING
IDA (Institute for Defense Analyses) gamma-ray laser: Investigation of the feasibility of developing a laser using nuclear transitions
[AD-A205318] N89-23864
IDA (Institute for Defense Analyses) gamma-ray laser: Investigation of developing a laser using nuclear transitions
[AD-A205319] N89-23865
ELECTRON SCATTERING
Eikonal approximation in partial wave version
[IPPJ-899] N89-24164
ELECTRON SPIN
Microscopic theory of electron spin resonance in Heisenberg spin glasses and thermal fluctuations in classical spin models with random fields
[JUEL-2227] N89-24146
Investigation of electronic states in nonmagnetic single crystals with spin-resolved photoemission
[JUEL-2228] N89-24212
ELECTRON STATES
Investigation of electronic states in nonmagnetic single crystals with spin-resolved photoemission
[JUEL-2228] N89-24212
ELECTRON TRANSFER
Electronic and ionic transport in polymers
[AD-A206530] N89-23709
Metallically conducting polymers: The limiting effect of conjugation defects on the electrical conductivity, a polyacetylene example
[ETN-89-93950] N89-23710
Energy transfer and photochemistry in biomimetic solar conversion
[PB89-142590] N89-23974
Assignment of the charge-transfer excited states of bis(N-heterocyclic) complexes of copper(I)
[AD-A206012] N89-24205
ELECTRONIC COUNTERMEASURES
A statistical analysis of the output signals of an acousto-optic spectrum analyzer for CW (Continuous-Wave) signals
[AD-A205404] N89-23763
Active radar jamming
[FOA-C-30506-3.6] N89-23777
ELECTRONIC EQUIPMENT
An analysis of Electronic Aids to Maintenance (EAM) for the Light Helicopter Family (LHX)
[AD-A205440] N89-23407
Summary of achievements in scientific research
[AD-A199947] N89-24227
ELECTROPHYSIOLOGY
A low-energy X-ray irradiator for electrophysiological studies
[AD-A205386] N89-24026
The attention system of the human brain
[AD-A206157] N89-24040
ELLIPSOIDS
Calculation of the surface of a geodetic polygon on an ellipsoid of revolution
[ETN-89-94149] N89-23966
Polarizability and effective permittivity of layered and continuously inhomogeneous dielectric ellipsoids
[PB89-146476] N89-24102
ELLIPTIC DIFFERENTIAL EQUATIONS
Nonlinear singular elliptic equations
[DE88-705691] N89-24103
ELLIPTICAL ORBITS
The performance of Space-Based Radars (SBR) orbiting on elliptical orbits
[AD-A205951] N89-23772
EMBEDDED COMPUTER SYSTEMS
Design and implementation of an expert user interface for the computer aided prototyping system
[AD-A206113] N89-24067
EMBRITTLEMENT
Mechanisms of diffusion-controlled brittle fracture
[DE89-008728] N89-23921
EMERGENCIES
Use of the 1:2,000,000 Digital Line Graph data in emergency response
[DE89-006730] N89-23959
EMISSION SPECTRA
Energy transfer and photochemistry in biomimetic solar conversion
[PB89-142590] N89-23974
Noise characteristics of an inductively coupled plasma-mass spectrometer
[AD-A205686] N89-24169
Flow-injection analysis utilizing a spectrally segmented photodiode-array inductively coupled plasma emission spectrometer. 1: Microcolumn preconcentration for the determination of molybdenum
[AD-A205687] N89-24170
Population inversions in ablation plasmas generated by intense electron beams
[AD-A205716] N89-24172
Observations of the rotational transitions of OH from the Orion molecular cloud
[NASA-CR-184802] N89-24231
Time and spectral variability of the low mass X-ray binaries
[MPE-REPORT-210] N89-24238
Very large array observations of the sun with related observations using the SMM (Solar Maximum Mission) satellite
[AD-A203874] N89-24249
An ultra-soft Einstein X-ray survey
[DE89-007993] N89-24256
A search for EUV emission from cataclysmic variables
[DE89-008012] N89-24257
Spectral observations of the extreme ultraviolet background N89-24259
EMISSIVITY
Mapping freeze/thaw boundaries with SMMR data
[NASA-CR-184991] N89-23961
Thermal images of sky and sea-surface background infrared radiation
[AD-A205819] N89-23992
ENAMELS
The adhesion between glass and enamel N89-23598
END EFFECTORS
Double lead spiral platen parallel jaw end effector N89-23905
Flight telerobot mechanism design: Problems and challenges N89-23907
ENDANGERED SPECIES
Review of wildlife resources of Vandenberg Air Force Base, California
[NASA-TM-102146] N89-23982
ENDOTOXINS
Muramyl peptide-enhanced sleep: Pharmacological optimization of performance
[AD-A205974] N89-24028
ENERGY CONSERVATION
The thermal resistance of flat powder-filled evacuated panels
[DE89-008243] N89-23685
ENERGY CONSUMPTION
Low energy consumption hydraulic techniques
[AD-A206285] N89-23743
ENERGY CONVERSION EFFICIENCY
Low-temperature volumetric receiver concept
[DE89-008245] N89-23976
ENERGY DISSIPATION
Solid-vapor adsorption refrigeration system development
[PB89-140859] N89-23733
ENERGY LEVELS
Strong and electromagnetic interactions in heavy exotic atoms
[PB89-145718] N89-24143
ENERGY POLICY
Radiation physics properties of selective solar energy absorber layers
[ETN-89-93945] N89-23978
ENERGY SPECTRA
Normal mode energetics of the general circulation during the FGGE year N89-24004
An ultra-soft Einstein X-ray survey
[DE89-007993] N89-24256
ENERGY STORAGE
Measuring conductivities of highly conductive membranes
[AD-A206043] N89-23649
Parametric study of radiative cooling of solid antihydrogen
[AD-A206092] N89-23742
ENERGY TRANSFER
Optimal aeroassisted coplanar orbital transfer using an energy model
[NASA-CR-181778] N89-23495
On the nature of Navier-Stokes turbulence
[NASA-TM-101983] N89-23813
IDA (Institute for Defense Analyses) gamma-ray laser: Investigation of the feasibility of developing a laser using nuclear transitions
[AD-A205318] N89-23864
IDA (Institute for Defense Analyses) gamma-ray laser: Investigation of developing a laser using nuclear transitions
[AD-A205319] N89-23865
Simulation studies of particle acceleration powered by modulated intense relativistic electron beams
[AD-A206348] N89-24148
ENGINE AIRFRAME INTEGRATION
Average-passage simulation of counter-rotating propfan propulsion systems as applied to cruise missiles
[NASA-TM-102043] N89-23416
ENGINE DESIGN
Qualification Motor no. 8 (QM-8), volume 1
[NASA-CR-183650] N89-23523
Results from baseline tests of the SPRE 1 and comparison with code model predictions
[NASA-TM-102044] N89-23527
ENGINE MONITORING INSTRUMENTS
Method and system for monitoring and displaying engine performance parameters
[NASA-CASE-LAR-14049-1] N89-23466
ENGINE PARTS
Ceramic Project of the Max-Planck Society N89-23571
Fatigue crack growth model RANDOM2 user manual, appendix 1
[NASA-CR-184939] N89-23890
Fatigue strength reduction model: RANDOM3 and RANDOM4 user manual, appendix 2
[NASA-CR-184940] N89-23891
ENGINE TESTING LABORATORIES
Test facility and preliminary performance of a 100 kW class MPD thruster
[NASA-TM-102021] N89-23520
ENGINE TESTS
Aerothermodynamic analysis of a Coanda/Refraction Jet Engine Test Facility
[AD-A205937] N89-23482
Design, fabrication and test of the RL10 derivative II chamber/primary nozzle
[NASA-CR-179595] N89-23519
Test facility and preliminary performance of a 100 kW class MPD thruster
[NASA-TM-102021] N89-23520
Space station propulsion test bed
[NASA-CR-183615] N89-23521
Results from baseline tests of the SPRE 1 and comparison with code model predictions
[NASA-TM-102044] N89-23527

ENVIRONMENT MANAGEMENT
Review of wildlife resources of Vandenberg Air Force Base, California
[NASA-TM-102146] N89-23982
ENVIRONMENT MODELS
Environmental interactions of hydrazine fuels in Soil/Water systems
[AD-A206244] N89-23986
ENVIRONMENTAL CONTROL
Space Station CMIF extended duration metabolic control test
[NASA-TM-100362] N89-23503
Space station ECLSS simplified integrated test
[NASA-TM-100363] N89-24044
ENVIRONMENTAL MONITORING
Review of wildlife resources of Vandenberg Air Force Base, California
[NASA-TM-102146] N89-23982
Environmental projects. Volume 3: Environmental compliance audit
[NASA-CR-185019] N89-23985
Geographic Information Systems (GIS) guidelines document
[PB89-132062] N89-24222
ENVIRONMENTAL QUALITY
Space station ECLSS simplified integrated test
[NASA-TM-100363] N89-24044
ENVIRONMENTAL SURVEYS
Environmental interactions of hydrazine fuels in Soil/Water systems
[AD-A206244] N89-23986
ENVIRONMENTAL TESTS
Undercutting of defects in thin film protective coatings on polymer surfaces exposed to atomic oxygen
[NASA-TM-101986] N89-23691
ENZYMES
The mechanisms of biodegradation of synthetic polymers
[AD-A205628] N89-23699
EPIDEMIOLOGY
Summary of selected new information on effects of ozone on health and vegetation. Draft supplement to air quality criteria for ozone and other photochemical oxidants
[PB89-135123] N89-23980
EPITAXY
Structure and grid dynamics of ultrathin epitaxial Ag and Fe films on Ni(100) and Cu(100) substrates
[JUEL-2221] N89-24187
EPOXY COMPOUNDS
Epoxylite 8822 hardness study
[DE89-008961] N89-23687
EPOXY RESINS
Effect of physical annealing on the dynamic mechanical properties of a high T(g) amine-cured epoxy systems
[AD-A205980] N89-23704
EQUATIONS OF MOTION
Optimal aeroassisted coplanar orbital transfer using an energy model
[NASA-CR-181778] N89-23495
Numerical study of orbital trajectories about Phobos
[AD-A205822] N89-23496
Increasing the margin of stability of arbitrarily finite modes of flexible large space structures with damping
[AD-A206487] N89-23507
Exact wave functions and coherent states of a damped driven harmonic oscillator
[AD-A205785] N89-24136
EQUATIONS OF STATE
White paper: Experimental and computational studies of very high velocity impacts
[DE89-007643] N89-23877
Experimental and theoretical studies of dense fluid mixtures
[DE89-008882] N89-24214
EROSION
MPD thruster erosion research
[NASA-CR-185314] N89-24168
ERROR ANALYSIS
An improved strategy for determining earth satellite orbits by radio
[AD-A205826] N89-23497
ERROR DETECTION CODES
Design of a methodology for the detection of errors in terrestrial networks
[ETN-89-94151] N89-23968
ERRORS
An experimental investigation into software reliability
[AD-A206293] N89-24069
ERS-1 (ESA SATELLITE)
Study of a method to de-alias winds from ERS-1 data
[CREO-6374] N89-24003
ERYTHROCYTES
Human temperature regulation during exercise after oral pyridostigmine administration
[AD-A206032] N89-24030
ESA SATELLITES
TELE-X antenna module thermal control
[REPT-882-440-106] N89-23782
Telescope structure for cryogenic application
[REPT-882-440-112] N89-23940
ESTIMATES
Improvement of navigation measurement procedures by the combined application of correlation techniques and parameter estimation
[ETN-89-93946] N89-23445
ESTIMATING
Tests for the gamma distribution with estimated shape parameters
[AD-A205829] N89-24118
ETCHANTS
Characterization of semiconductor device processing etchant solutions for GaAs and p+ GaAs layers employed in AlxGa(1-x)As/GaAs MODFETs and related heterojunction devices
[AD-A205772] N89-24201
ETCHING
Characterization of semiconductor device processing etchant solutions for GaAs and p+ GaAs layers employed in AlxGa(1-x)As/GaAs MODFETs and related heterojunction devices
[AD-A205772] N89-24201
ETHANE
Sorption of selected volatile organic constituents of jet fuels and solvents on natural sorbents from gas and solutions phases
[AD-A204073] N89-23711
ETHYLENE
Corrosion and lubricity testing of nonflammable USAF formulated CTFE (Chlorotrifluoroethylene) base hydraulic fluid
[AD-A205467] N89-23695
Sorption of selected volatile organic constituents of jet fuels and solvents on natural sorbents from gas and solutions phases
[AD-A204073] N89-23711
EULER EQUATIONS OF MOTION
Flosolver: A parallel computer for fluid dynamics
[NAL-TM-AE-8803] N89-23805
Open boundary conditions for the Navier-Stokes equation
[FFA-145] N89-23816
Solution of one-dimensional Euler equations by the implicit finite difference technique of Beam and Warming
[NAL-PD-FM-8816] N89-24097
Numerical solution of the Euler equations using local grid refinement
[FFA-143] N89-24104
EULER-LAGRANGE EQUATION
An analysis of the attitude stability of a space station subject to parametric excitation of periodic mass motion
[AD-A206009] N89-23505
On the Lagrangian description of unsteady boundary layer separation. Part 1: General theory
[NASA-TM-102026] N89-23821
EUROPEAN AIRBUS
Center of gravity control on Airbus aircraft: Fuel, range and loading
[REPT-882-111-101] N89-23460
A330/340 hydraulic system
[REPT-882-111-102] N89-23461
EUROPEAN SPACE PROGRAMS
The two approaches for the thermal control of the Columbus resource module and Polar Platform
[REPT-882-440-110] N89-23511
Mission conditions and hardware concepts N89-23720
Microgravity User Support Center (MUSC) N89-23721
Direct dissemination of data from ESA's future in-orbit infrastructure
[DDD-CP/TE-RE-7450] N89-23754
ESA-D: An integrated software for antenna design and analysis
[REPT-882-440-111] N89-23784
The evolution of space mechanisms in the ESA R and D program N89-23893
Shaking in cryogenic conditions
[REPT-882-440-101] N89-23939
Grazing incidence telescopes for ESA's X-ray astronomy mission XMM
[MPE-PREPRINT-129] N89-24239
EUTECTIC ALLOYS
Macrosegregation and nucleation in undercooled Pb-Sn alloys
[NASA-TM-102023] N89-23664
EVALUATION
The relationship between subjective and objective measures of sleepiness
[AD-A205861] N89-24027
EVAPORATION
Sequentially evaporated thin Y-Ba-Cu-O superconducting films on microwave substrates
[NASA-TM-102068] N89-23791
EXCITATION
Assignment of the charge-transfer excited states of bis(N-heterocyclic) complexes of copper(I)
[AD-A206012] N89-24205
EXHAUST EMISSION
Methanol vehicle catalyst evaluation, phase 3
[PB89-136139] N89-23874
Area source documentation for the 1985 National Acid Precipitation Assessment Program inventory
[PB89-151427] N89-23981
EXHAUST FLOW SIMULATION
Hot-jet simulation in cryogenic wind tunnels
[NASA-RP-1220] N89-23448
EXOBIOLOGY
A strategy for space biology and medical science for the 1980s and 1990s
[NASA-CR-184895] N89-24024
EXPERIMENT DESIGN
Heliport night parking area criteria test plan
[DOT/FAA/CT-TN88/45] N89-23480
In situ fluorescence monitoring of the viscosities of particle-filled polymers in flow
[PB89-146278] N89-23680
White paper: Experimental and computational studies of very high velocity impacts
[DE89-007643] N89-23877
EXPERT SYSTEMS
Expert systems applied to spacecraft fire safety
[NASA-CR-182266] N89-23501
Intelligent processing of materials
[PB89-151823] N89-23735
Design and implementation of an expert user interface for the computer aided prototyping system
[AD-A206113] N89-24067
EXPLOSIVE FORMING
Fundamental and applied studies of explosively fabricated high-temperature superconducting fixtures
[AD-A205953] N89-24204
EXPLOSIVES
Polyethylene glycol-poly(2-methyl-5-vinyl tetrazole) polymer blend: A desensitizing binder for propellants and explosives
[AD-A206563] N89-23716
EXPOSURE
Environmental effects in niobium base alloys and other selected intermetallic compounds
[AD-A206072] N89-23673
Additivity of retinal damage for multiple-pulse laser exposures
[AD-A206514] N89-24032
EXTRASOLAR PLANETS
The Allegheny Observatory search for planetary systems
[NASA-CR-184990] N89-24233
EXTRATERRESTRIAL ENVIRONMENTS
NASA/SDIO Space Environmental Effects on Materials Workshop, part 2
[NASA-CP-3035-PT-2] N89-23547
An overview of charging environments N89-23554
Influence of charging environments on spacecraft materials and system performance N89-23556
Trapped radiation N89-23560
Working group written presentation: Spacecraft charging N89-23568
EXTRATERRESTRIAL RADIATION
Effects of space radiation on electronic microcircuits N89-23549
Solar flares and magnetospheric particles: Investigations based upon the ONR-602 and ONR-604 experiments
[AD-A205599] N89-24253
EXTRAVEHICULAR ACTIVITY
Astronaut tool development: An orbital replaceable unit-portable handhold N89-23904
EXTREME ULTRAVIOLET RADIATION
Research studies on extreme ultraviolet and soft X-ray lasers
[AD-A205625] N89-23868
Characterization of multilayer coated concave diffraction gratings in the extreme ultraviolet
[DE89-008831] N89-24151
A search for EUV emission from cataclysmic variables
[DE89-008012] N89-24257
Spectral observations of the extreme ultraviolet background N89-24259
EXTREMELY HIGH FREQUENCIES
Link availability and rain attenuation exceedance characteristics for EHF (Extremely High Frequency) satellite communications with arbitrary link parameters in Canada
[AD-A205403] N89-23762

KRMS (K-band Radiometric Mapping System) SSM/I validation March 1988 quick look report
[NASA-CR-185320] N89-23766
EYE (ANATOMY)
Functional assessment of laser irradiation
[AD-A206230] N89-23871

F

F-16 AIRCRAFT
Multivariable flight control design with parameter uncertainty for the AFTI/F-16
[AD-A206068] N89-23476
FABRICATION
Design, fabrication and test of the RL10 derivative II chamber/primary nozzle
[NASA-CR-179595] N89-23519
Spacecraft contamination experience N89-23545
Fabrication and properties of alumina-zirconia composites
[PB89-147532] N89-23620
Fabrication of unidirectional fiber reinforced 6061 aluminum alloy using high pressure squeeze casting
[AD-A205717] N89-23668
Molded bodies having a high degree of hardness and a high degree of toughness for machining metals, carbides, ceramics and glasses
[DE89-008620] N89-23686
High-temperature ceramic superconductors
[AD-A205321] N89-24196
Characterization of semiconductor device processing etchant solutions for GaAs and p+ GaAs layers employed in AlxGa(1-x)As/GaAs MODFETs and related heterojunction devices
[AD-A205772] N89-24201
Fundamental and applied studies of explosively fabricated high-temperature superconducting fixtures
[AD-A205953] N89-24204
Alternate arsenic and antimony sources for the OMCVD fabrication of semiconductors
[AD-A206483] N89-24211
FACSIMILE COMMUNICATION
Investigation of optical compression techniques for dither coding
[AD-A206140] N89-23776
FACTORIAL DESIGN
An experimental investigation into software reliability
[AD-A206293] N89-24069
FACTORIZATION
State-space formulae for discrete-time H infinity optimization
[OUEL-1718/88] N89-24089
FAILURE
Preparation and properties of high strength carbon fibers N89-23589
FAILURE ANALYSIS
Break dimensioning of space structural assemblies and its experimental validation
[REPT-882-430-109] N89-23508
Testing chromium adhesion using acoustic emission
[AD-A205621] N89-23666
Fatigue crack growth model RANDOM2 user manual, appendix 1
[NASA-CR-184939] N89-23890
Software reliability studies
[NASA-CR-184857] N89-24054
FAILURE MODES
Radiation effects in spacecraft electronics N89-23531
Nonintrusive methods for monitoring the operational readiness of solenoid-operated valves
[DE89-008732] N89-23878
FAIRCHILD-HILLER AIRCRAFT
Aircraft Accident Report: AVAir Inc., Flight 3378, Fairchild Metro 3, SA227 AC, N622AV, Cary, North Carolina, February 19, 1988
[PB88-910412] N89-23436
FAR FIELDS
An iterative technique to correct probe position errors in planar near-field to far-field transformations
[PB89-153886] N89-23750
FAR INFRARED RADIATION
Observations of the rotational transitions of OH from the Orion molecular cloud
[NASA-CR-184802] N89-24231
FATIGUE (BIOLOGY)
Evaluation of three commercial microclimate cooling systems
[AD-A206318] N89-23744
FATIGUE (MATERIALS)
Fatigue in ceramics N89-23583
Mode 2 delamination fatigue resistance of composites N89-23624
The structural basis for fatigue initiation in glassy polymers
[DE89-009292] N89-23689
Dynamic fatigue of ultralow-expansion glass for space mirrors, reissue A
[AD-A205401] N89-23694
FATIGUE LIFE
Mode 2 delamination fatigue resistance of composites N89-23624
Fatigue crack growth model RANDOM2 user manual, appendix 1
[NASA-CR-184939] N89-23890
Fatigue strength reduction model: RANDOM3 and RANDOM4 user manual, appendix 2
[NASA-CR-184940] N89-23891
Overview of ASTM symposium on analytical and experimental methods for residual stress effects in fatigue
[AD-A205622] N89-23931
FAULT TOLERANCE
Avionics architecture studies for the entry research vehicle
[NASA-CR-181828] N89-24082
FEASIBILITY ANALYSIS
A chamber experiment for the feasibility study of an artificial plasma reflector for OTH radar applications
[NASA-CR-184912] N89-23478
Development of a CARS device for a feasibility study of density and temperature measurements at high time dependent resolution
[ISL-R-117/87] N89-23654
Proof of the feasibility of coherent and incoherent schemes for pumping a gamma-ray laser
[AD-A205371] N89-23866
FEEDBACK
Designing feedback compensators by using the root-locus method
[AD-A205354] N89-24093
The impact of accuracy and effort feedback and goals on adaptive decision behavior
[AD-A205751] N89-24095
FEEDBACK CONTROL
Flight control system for the CRCA (Control Reconfigurable Combat Aircraft) using a command generator tracker with PI (Proportional-Plus-Integral) feedback and Kalman filter, volume 1
[AD-A205723] N89-23473
Multivariable flight control design with parameter uncertainty for the AFTI/F-16
[AD-A206068] N89-23476
Multiple model-based robot control: Development and initial evaluation
[AD-A205725] N89-23881
Robust multivariable feedback design
[OUEL-1723/88] N89-24090
Multivariable Nyquist self-tuning: A general approach
[OUEL-1734/88] N89-24091
FERRITES
Microstructure-permeability relation in MnZn ferrites prepared of iron oxide with chlorine impurities N89-23602
On the correlation between microstructure and magnetic induction of porous iron and iron-Ni(0.4)Zn(0.6)Fe2O4 composites N89-23606
FERROMAGNETIC MATERIALS
Memory functions and relaxation functions of some spin systems
[AD-A206340] N89-24137
FERROMAGNETISM
Amorphous magnets N89-23605
Mean field theory of the spin-1 Ising model with a random crystal field
[DE88-705669] N89-24182
FIBER COMPOSITES
Composite blade structural analyzer (COBSTRAN) user's manual
[NASA-TM-101461] N89-23621
Light weight polymer matrix composite material
[NASA-CASE-LEW-14734-1] N89-23623
Carbon fiber thermal conductivity measurement and analysis
[AD-A205682] N89-23625
Preparation and evaluation of silicon nitride matrices for silicon nitride-SiC fiber composites
[NASA-CR-184798] N89-23678
Finite element modeling of frictionally restrained composite interfaces
[NASA-CR-182281] N89-23918
FIBER OPTICS
AN/TAC-1 demultiplexer circuit card assembly
[AD-A205744] N89-23770
Fiber optic leak detection system
[PB89-148886] N89-24150
Fiber-optic time-resolved fluorescence sensor for the simultaneous determination of Al(+3), Ga(+3) and In(+3)
[AD-A205689] N89-24154
Utilization of magnetostrictive optical fibers in multiple order gradiometers
[AD-D013960] N89-24155
Structural mode frequencies of FOG-M (Fiber Optics Guided-Missile) actuator/fin
[AD-A206327] N89-24158
FICKS EQUATION
Diffusion N89-23724
FIELD EFFECT TRANSISTORS
Some 3-5 heterojunction structures and high speed devices
[AD-A205946] N89-24203
FIELD OF VIEW
A compact fast wide angle broad band spectrometer optical system
[NASA-CASE-NPO-17562-1-CU] N89-24153
FIELD STRENGTH
Loran C field strength contours: Contiguous US
[DOT/FAA/CT-TN89/16] N89-23437
High-latitude field-strength measurements of standard broadcast band skywave transmissions monitored at Fairbanks, Alaska
[PB89-134829] N89-23747
FIELD THEORY (PHYSICS)
Equations for two-dimensional density matrix. Approximate solutions in the vicinity of the classical solution
[DE88-705825] N89-24107
FIGHTER AIRCRAFT
Multivariable flight control design with parameter uncertainty for the AFTI/F-16
[AD-A206068] N89-23476
Computer-aided design and bio-engineering: A review of the literature
[AD-A206534] N89-24074
FILM COOLING
A research facility for film cooling investigations with emphasis on the instrumentation system
[NAL-TM-PR-8704] N89-23477
FINITE DIFFERENCE THEORY
A numerical investigation of thin-film heat transfer gages
[AD-A206134] N89-23853
Numerical methods to treat collisionlike phenomena in solids
[ETN-89-93944] N89-23936
Solution of one-dimensional Euler equations by the implicit finite difference technique of Beam and Warming
[NAL-PD-FM-8816] N89-24097
Numerical solution of the Euler equations using local grid refinement
[FFA-143] N89-24104
FINITE ELEMENT METHOD
Modal analysis and testing of missile systems
[AD-A204051] N89-23916
Application of an exact finite element method to analysis of statics of thin elastic shells of revolution with axisymmetric loading
[ISBN-952-900-399-4] N89-23917
Finite element modeling of frictionally restrained composite interfaces
[NASA-CR-182281] N89-23918
Crack-face displacements for embedded elliptic and semi-elliptical surface cracks
[NASA-CR-181822] N89-23919
Ground shake test of the Boeing Model 360 helicopter airframe
[NASA-CR-181766] N89-23920
Experimental and theoretical determination of the thermomechanical response of inelastic structural materials to high energy thermal inputs
[AD-A206100] N89-23933
Fractional calculus formulation of the quasi-static viscoelastic problem
[AD-A206136] N89-23934
Numerical methods to treat collisionlike phenomena in solids
[ETN-89-93944] N89-23936
Solid modeling requirements for finite element modeling using mapped mesh techniques
[DE89-009639] N89-24110
A demonstration of the method of stochastic finite element analysis
[AD-A206135] N89-24127
FINS
Transonic aerodynamic characteristics of a proposed Assured Crew Return Capability (ACRC) lifting-body configuration
[NASA-TM-4117] N89-23412
Missile actuator simulation and an investigation into the accuracy of Runge-Kutta numerical integration
[AD-A206325] N89-23458

Structural mode frequencies of FOG-M (Fiber Optics Guided-Missile) actuator/fin
[AD-A206327] N89-24158

FIRE PREVENTION
Expert systems applied to spacecraft fire safety
[NASA-CR-182266] N89-23501

FIRES
Expert systems applied to spacecraft fire safety
[NASA-CR-182266] N89-23501

FIXED WINGS
A methodology for determining the survivability of fixed-wing aircraft against small arms
[AD-A205730] N89-23455

FLAME PROPAGATION
Fire propagation in concurrent flows
[PB89-151781] N89-23636
An experimental study of opposed flow diffusion flame extinction over a thin fuel in microgravity
[NASA-CR-182185] N89-23638

FLAME RETARDANTS
Corrosion and lubricity testing of nonflammable USAF formulated CTFE (Chlorotrifluoroethylene) base hydraulic fluid
[AD-A205467] N89-23695

FLAMEOUT
An experimental study of opposed flow diffusion flame extinction over a thin fuel in microgravity
[NASA-CR-182185] N89-23638

FLAMMABILITY
An experimental study of opposed flow diffusion flame extinction over a thin fuel in microgravity
[NASA-CR-182185] N89-23638

FLAT PLATES
A segmented mirror antenna for radiometers
[NASA-TM-102045] N89-23753

FLEXIBLE BODIES
Inverse problem techniques for beams with tip body and time hysteresis damping
[NASA-CR-181833] N89-24112

FLEXIBLE SPACECRAFT
Increasing the margin of stability of arbitrarily finite modes of flexible large space structures with damping
[AD-A206487] N89-23507

FLIGHT CHARACTERISTICS
Modelling aircraft dynamics
[AD-A204086] N89-23449
A correlation study of X-29A aircraft and associated analytical developments N89-23450
Flight testing of the Southern Cross replica aircraft
[AD-A205303] N89-23451

FLIGHT CONDITIONS
Heliport night parking area criteria test plan
[DOT/FAA/CT-TN88/45] N89-23480

FLIGHT CONTROL
Aircraft Accident Report: AVAir Inc., Flight 3378, Fairchild Metro 3, SA227 AC, N622AV, Cary, North Carolina, February 19, 1988
[PB88-910412] N89-23436
A330/340 hydraulic system
[REPT-882-111-102] N89-23461
The functional mock-up test of the flight control system of the NAL QSTOL research aircraft ASKA
[NAL-TR-972] N89-23467
The 4D-TECS integration for NASA TSRV airplane
[NASA-CR-4231] N89-23471
Flight control system for the CRCA (Control Reconfigurable Combat Aircraft) using a command generator tracker with PI (Proportional-Plus-Integral) feedback and Kalman filter, volume 1
[AD-A205723] N89-23473
Actuator rate saturation compensator
[AD-D013962] N89-23474
Control design of an unstable non-minimum phase aircraft subject to control surface saturation
[AD-A206024] N89-23475
Multivariable flight control design with parameter uncertainty for the AFTI/F-16
[AD-A206068] N89-23476
An evaluation of the F/FB/EF-111 crew/voice message system
[AD-A205998] N89-23774
Crew procedures and workload of retrofit concepts for microwave landing system
[NASA-CR-181700] N89-24033

FLIGHT HAZARDS
Space debris: A report from the ESA Debris Working Group
[ESA-SP-1109] N89-24230

FLIGHT SAFETY
Annual review of aircraft accident data, US Air Carrier operations: Calendar year 1986
[PB89-151021] N89-23434
Heliport night parking area criteria test plan
[DOT/FAA/CT-TN88/45] N89-23480

FLIGHT SIMULATION
Modelling aircraft dynamics
[AD-A204086] N89-23449
Experiment on a cylindrical scramjet combustor. 2: Simulated flight Mach number 6.7
[NAL-TR-969] N89-23464
The functional mock-up test of the flight control system of the NAL QSTOL research aircraft ASKA
[NAL-TR-972] N89-23467

FLIGHT TEST VEHICLES
Flight testing of the Southern Cross replica aircraft
[AD-A205303] N89-23451

FLIGHT TESTS
Flight testing of the Southern Cross replica aircraft
[AD-A205303] N89-23451
Comparison of computational analysis with flight tests of a 40mm solid-fuel ramjet projectile
[AD-A206536] N89-23459
Details of Buran shuttle flight N89-23486
Design features, flight monitoring of Buran N89-23487
Commentary on flight of Buran shuttle by designers Glushko and Semenov N89-23489

FLIR DETECTORS
Enhanced tracking of ballistic targets using forward looking infrared measurements
[AD-A205727] N89-23769

FLOOD PREDICTIONS
Thermal analysis for the monitoring and prediction of flood dynamics in wetlands
[BCRS-88-10B] N89-23971

FLOODS
Meteosat thermal inertia mapping for studying wetland dynamics in the West-African Sahel
[BCRS-88-10A] N89-23970
Thermal analysis for the monitoring and prediction of flood dynamics in wetlands
[BCRS-88-10B] N89-23971

FLOUR (FOOD)
Microgravity particle reduction system N89-24019

FLOW CHARACTERISTICS
On the nature of Navier-Stokes turbulence
[NASA-TM-101983] N89-23813
Evaluation of the historical Schoenbein method for the determination of ozone in a flow chamber
[JUEL-2218] N89-23983

FLOW DISTRIBUTION
Numerical simulation of hypersonic flow around a space plane. 1: Basic development
[NAL-TR-976T] N89-23409
Numerical solution of periodic vortical flows about a thin airfoil
[NASA-TM-101998] N89-23413
Average-passage simulation of counter-rotating propfan propulsion systems as applied to cruise missiles
[NASA-TM-102043] N89-23416
The low frequency oscillation in the flow over a NACA0012 airfoil with an iced leading edge
[NASA-TM-102018] N89-23417
A numerical scheme to solve unsteady and variable density low Mach number flows N89-23419
An experimental study of the effect of streamwise vortices on unsteady turbulent boundary-layer separation
[AD-A205462] N89-23420
Flowfield measurements in the vortex wake of a missile at high angle of attack in turbulence
[AD-A205896] N89-23422
Investigation of the flowfield created by the interaction of a sonic jet and a co-flowing supersonic stream
[AD-A205823] N89-23425
Comparison of computational analysis with flight tests of a 40mm solid-fuel ramjet projectile
[AD-A206536] N89-23459
Characteristics of a five-hole spherical pitot tube
[NAL-TR-971] N89-23463
Mechanisms of secondary flows and losses within a three dimensional turbine stator cascade
[NAL-TR-970T] N89-23807
Some applications of the qualitative theory of differential equations in fluid dynamics
[ETN-89-94143] N89-23814
Derivation of a Godunov one dimensional fluid dynamics code
[AD-A205463] N89-23824
Investigation of incompressible cascade flows using a viscous/inviscid interactive code
[AD-A205972] N89-23832
Computation of flow around maneuvering submerged bodies
[AD-A205994] N89-23833
Analogy between explosive wave and front wave near curved walls
[ISL-CO-209/87] N89-23840
High speed turboprop aeroacoustic study (single rotation). Volume 1: Model development
[NASA-CR-182257-VOL-1] N89-24139

FLOW EQUATIONS
A numerical scheme to solve unsteady and variable density low Mach number flows N89-23419
Some applications of the qualitative theory of differential equations in fluid dynamics
[ETN-89-94143] N89-23814
Open boundary conditions for the Navier-Stokes equation
[FFA-145] N89-23816
Derivation of a Godunov one dimensional fluid dynamics code
[AD-A205463] N89-23824

FLOW GEOMETRY
Numerical simulation of flow through an artificial heart
[NASA-TM-102183] N89-24111

FLOW MEASUREMENT
Measuring conductivities of highly conductive membranes
[AD-A206043] N89-23649
Open boundary conditions for the Navier-Stokes equation
[FFA-145] N89-23816
Comparison of split-film and x-film measurements in 2-D flow
[AD-A206023] N89-23836
Turbulence near a free surface in a plane jet
[AD-A206269] N89-23838
Numerical solution of the Euler equations using local grid refinement
[FFA-143] N89-24104

FLOW STABILITY
Fire propagation in concurrent flows
[PB89-151781] N89-23636

FLOW THEORY
The dimension of attractors underlying turbulent Poiseuille flow
[AD-A206021] N89-23835
Dynamic interaction between fluids and solids
[ETN-89-93948] N89-23937

FLOW VELOCITY
Numerical solution of periodic vortical flows about a thin airfoil
[NASA-TM-101998] N89-23413
Characteristics of a five-hole spherical pitot tube
[NAL-TR-971] N89-23463
Comparison of split-film and x-film measurements in 2-D flow
[AD-A206023] N89-23836
A vector scanning processing technique for pulsed laser velocimetry
[NASA-TM-102048] N89-23850

FLOW VISUALIZATION
Model systems --- metal alloys N89-23728
Telescience and image processing for PODI: An analysis and a proposal for a simulation set-up
[NLR-TR-88005-U] N89-23815
Bifurcating jets at high Reynolds numbers
[AD-A205718] N89-23829
Automatic analysis of holographic interferograms N89-23848

FLUENCE
Atomic oxygen effects on materials N89-23540

FLUID DYNAMICS
Derivation of a Godunov one dimensional fluid dynamics code
[AD-A205463] N89-23824
Investigation of incompressible cascade flows using a viscous/inviscid interactive code
[AD-A205972] N89-23832
Dynamic interaction between fluids and solids
[ETN-89-93948] N89-23937

FLUID FILMS
Rayleigh-Taylor instability of a viscous film overlying a passive fluid
[AD-A205578] N89-23827

FLUID FLOW
Telescience and image processing for PODI: An analysis and a proposal for a simulation set-up
[NLR-TR-88005-U] N89-23815
Exploitation of multiple solutions of the Navier-Stokes equations to achieve radically improved flight
[AD-A205939] N89-23831
Modeling of a continuous oscillator by oscillators with a finite number of degrees of freedom
[PB89-146120] N89-24134

FLUID MECHANICS
Flow control for unsteady and separated flows and turbulent mixing
[AD-A205989] N89-23426
Mathematical analysis of strong fluid mechanical effects in reacting and nonreacting gases
[AD-A206336] N89-23839

FLUID PRESSURE
Low energy consumption hydraulic techniques
[AD-A206285] N89-23743

FLUID-SOLID INTERACTIONS
Dynamic interaction between fluids and solids
[ETN-89-93948] N89-23937
FLUIDS
Experimental and theoretical studies of dense fluid mixtures
[DE89-008882] N89-24214
FLUORESCENCE
In situ fluorescence monitoring of the viscosities of particle-filled polymers in flow
[PB89-146278] N89-23680
Fiber-optic time-resolved fluorescence sensor for the simultaneous determination of Al(+3), Ga(+3) and In(+3)
[AD-A205689] N89-24154
Decay of molecules at corrugated thin metal films
[AD-A205487] N89-24198
FLUORINATION
Synthesis of novel acid electrolytes for phosphoric acid fuel cells
[PB89-148944] N89-23786
FLUORITE
Cohesive and anharmonic elastic properties of mixed fluorite crystals
[DE88-705690] N89-24184
FLUORO COMPOUNDS
Improved acid electrolytes: The synthesis and structure of fluorine containing sulfonic acids for fuel cells
[PB89-142616] N89-23973
FLUTTER ANALYSIS
Flutter of a low-aspect-ratio rectangular wing
[NASA-TM-4116] N89-23447
FOILS (MATERIALS)
Fundamental studies of beta phase decomposition modes in titanium alloys
[AD-A205296] N89-23665
FOLDING FIN AIRCRAFT ROCKET VEHICLE
Structural mode frequencies of FOG-M (Fiber Optics Guided-Missile) actuator/fin
[AD-A206327] N89-24158
FOLDING STRUCTURES
Design and testing of a deployable, retrievable boom for space applications N89-23898
Design and verification of mechanisms for a large foldable antenna N89-23899
FOOD INTAKE
Patterns of human drinking: Effects of exercise, water temperature and food consumption
[AD-A206031] N89-24029
FOOD PRODUCTION (IN SPACE)
Advanced space design program to the Universities Space Research Association and the National Aeronautics and Space Administration
[NASA-CR-180450] N89-24015
Variable plant spacing N89-24016
Automated seed manipulation and planting N89-24017
Plant health sensing N89-24018
Microgravity particle reduction system N89-24019
Automated seed manipulation and planting N89-24020
FORCED CONVECTION
An experimental study of opposed flow diffusion flame extinction over a thin fuel in microgravity
[NASA-CR-182185] N89-23638
FORMALDEHYDE
Sample preparation techniques for evaluating methanol and formaldehyde emissions from methanol fueled vehicles and engines
[PB89-136147] N89-23734
FORMALISM
Geometrical foundations of mesomechanics and Lagrangian formalism
[AD-A205589] N89-23930
FORMAT
A program interface prototype for a multimedia database incorporating images
[AD-A206439] N89-24226
FORTRAN
PRASE (Parallel Resource Analysis Software Environment) instrumentation software for the Intel iPSC hypercube
[AD-A206046] N89-24087
FOURIER ANALYSIS
Operator induced multigrid algorithms using semirefinement
[NASA-CR-181834] N89-24113
FOURIER TRANSFORMATION
An iterative technique to correct probe position errors in planar near-field to far-field transformations
[PB89-153886] N89-23750
SMOOFF: A FORTRAN smoothing program
[AD-A204087] N89-24057
Symbolic analysis of multivariable missile systems
[AD-A206326] N89-24132
FOVEA
Functional assessment of laser irradiation
[AD-A206230] N89-23871
FRACTOGRAPHY
USAF (US Air Force) durability design handbook: Guidelines for the analysis and design of durable aircraft structures
[AD-A206286] N89-23457
FRACTURE MECHANICS
Theoretical studies of Ni3Al and NiAl with impurities
[DE89-006556] N89-23655
Dynamic fatigue of ultralow-expansion glass for space mirrors, reissue A
[AD-A205401] N89-23694
Geometrical foundations of mesomechanics and Lagrangian formalism
[AD-A205589] N89-23930
Cyclic crack propagation characteristics of the powder metallurgical nickel-base alloy Udimet 720 at elevated temperatures and different dwell times
[ETN-89-94426] N89-23938
FRACTURE STRENGTH
Preparation and evaluation of silicon nitride matrices for silicon nitride-SiC fiber composites
[NASA-CR-184798] N89-23678
Environmental stress crazing and cracking of transparent polymers
[AD-A205624] N89-23697
Fatigue strength reduction model: RANDOM3 and RANDOM4 user manual, appendix 2
[NASA-CR-184940] N89-23891
Deformation twinning in ordered intermetallic compounds
[DE89-008748] N89-24192
FRACTURING
Mechanisms of diffusion-controlled brittle fracture
[DE89-008728] N89-23921
FREE ELECTRON LASERS
The chirped-pulse free-electron laser
[DE89-009041] N89-23862
FREE FLOW
Computing induced velocity perturbations due to a helicopter fuselage in a free stream
[NASA-TM-4113] N89-23410
Free shear layer and swirl flow heat transfer enhancement
[PB89-145106] N89-23810
Numerical simulation of the dissociation of I2 by O2 (1 Delta) in a two dimensional parallel jet
[AD-A206137] N89-23870
FREE JETS
Spectrometric studies of gas phase collision processes
[AD-A205570] N89-23826
FREE-PISTON ENGINES
Results from baseline tests of the SPRE 1 and comparison with code model predictions
[NASA-TM-102044] N89-23527
FREEZING
Response of pavement to freeze-thaw cycles: Lebanon, New Hampshire, regional airport
[AD-A205559] N89-23740
Mapping freeze/thaw boundaries with SMMR data
[NASA-CR-184991] N89-23961
FRICTION
Strength and structure of Ga(1-x)In(x)As alloys
[AD-A205415] N89-23644
Ceramic tribology: Methodology and mechanisms of alumina wear
[PB89-148357] N89-23679
Design and construction of a state-of-the-art high temperature tribometer
[PB89-148332] N89-23847
FRICTION FACTOR
Friction factor data for flat plate tests of smooth and honeycomb surfaces
[NASA-CR-184977] N89-23676
FRONTAL WAVES
Analogy between explosive wave and front wave near curved walls
[ISL-CO-209/87] N89-23840
FRONTS (METEOROLOGY)
Studies of frontal zone dynamics with a high-resolution wind profiling system
[AD-A205988] N89-24008
FUEL CELLS
Improved acid electrolytes: The synthesis and structure of fluorine containing sulfonic acids for fuel cells
[PB89-142616] N89-23973
FUEL COMBUSTION
Burning rate constant of fuel droplet under high pressure
[NAL-TR-1001] N89-23639
FUEL FLOW
An experimental study of opposed flow diffusion flame extinction over a thin fuel in microgravity
[NASA-CR-182185] N89-23638
FUEL INJECTION
Spontaneous ignition of atomized kerosine/air mixtures in a high pressure flowing system
[NAL-TR-966] N89-23635
FUEL TANKS
Center of gravity control on Airbus aircraft: Fuel, range and loading
[REPT-882-111-101] N89-23480
FUEL TESTS
Methanol vehicle catalyst evaluation, phase 3
[PB89-136139] N89-23874
FUELS
Pulsating catalytic combustion of gaseous fuels N89-23643
FUNCTIONAL DESIGN SPECIFICATIONS
A330/340 hydraulic system
[REPT-882-111-102] N89-23461
FUNCTIONS (MATHEMATICS)
On the equation Xa + Ya = Za
[AD-A205460] N89-24116
Exploring the episodic structure of algebra story problem solving: Revision
[AD-A206403] N89-24122
Second-order moments of a stationary Markov chain and some applications
[AD-A206366] N89-24128
A blocked Jacobi method for the symmetric Eigenproblem
[AD-A206553] N89-24133
FUSELAGES
Computing induced velocity perturbations due to a helicopter fuselage in a free stream
[NASA-TM-4113] N89-23410

G

GALACTIC EVOLUTION
A self consistant model of the three phase interstellar medium in disk galaxies N89-24245
GALACTIC NUCLEI
A search for pulsations in planetary nebulae nuclei N89-24235
Study of the infrared celestial background
[AD-A205649] N89-24237
GALILEO PROJECT
Final safety analysis report for the Galileo Mission. Volume 1: Reference design document
[DE89-007268] N89-24147
Calibration measurements on micrometeorite detectors for the missions ULYSSES, Galileo and Giotto
[ETN-89-93947] N89-24248
GALLIUM
Fiber-optic time-resolved fluorescence sensor for the simultaneous determination of Al(+3), Ga(+3) and In(+3)
[AD-A205689] N89-24154
GALLIUM ARSENIDE LASERS
High-power single spatial mode AlGaAs channeled-substrate-planar semiconductor diode lasers for spaceborne communications
[NASA-CR-4238] N89-23860
GALLIUM ARSENIDES
Strength and structure of Ga(1-x)In(x)As alloys
[AD-A205415] N89-23644
Monolithic GaAs digitizer for space-based laser pulse spreading effect
[NASA-CR-183430] N89-23855
The electronic structure of GaAs sub 1-x P sub x and GaSb sub 1-x P sub x calculated using the recursion method
[DE88-705702] N89-24185
Characterization of semiconductor device processing etchant solutions for GaAs and p+ GaAs layers employed in AlxGa(1-x)As/GaAs MODFETs and related heterojunction devices
[AD-A205772] N89-24201
Alternate arsenic and antimony sources for the OMCVD fabrication of semiconductors
[AD-A206483] N89-24211
GALLIUM PHOSPHIDES
The electronic structure of GaAs sub 1-x P sub x and GaSb sub 1-x P sub x calculated using the recursion method
[DE88-705702] N89-24185
GAMMA RAY LASERS
IDA (Institute for Defense Analyses) gamma-ray laser: Investigation of the feasibility of developing a laser using nuclear transitions
[AD-A205318] N89-23864

IDA (Institute for Defense Analyses) gamma-ray laser: Investigation of developing a laser using nuclear transitions
[AD-A205319] N89-23865
Proof of the feasibility of coherent and incoherent schemes for pumping a gamma-ray laser
[AD-A205371] N89-23866

GAMMA RAY SPECTROMETERS
Determination of areal snow water equivalent using satellite images and gamma ray spectrometry
[CI-91] N89-23960

GAS ANALYSIS
Space Station CMIF extended duration metabolic control test
[NASA-TM-100362] N89-23503
Development of an optical multigas detector
[PB89-148878] N89-23849
Evaluation of the historical Schoenbein method for the determination of ozone in a flow chamber
[JUEL-2218] N89-23983

GAS ATOMIZATION
Cooling rate, undercooling and rapid solidification by atomization N89-23609
Mechanical properties of gas atomized Cu-Ti and Cu-Ti-B alloys N89-23610
Fundamental studies on spray combustion and turbulent combustion
[AD-A206438] N89-23651

GAS COMPOSITION
Development of an optical multigas detector
[PB89-148878] N89-23849

GAS DISSOCIATION
Numerical simulation of the dissociation of I2 by O2 (1 Delta) in a two dimensional parallel jet
[AD-A206137] N89-23870

GAS FLOW
Some applications of the qualitative theory of differential equations in fluid dynamics
[ETN-89-94143] N89-23814

GAS INJECTION
A research facility for film cooling investigations with emphasis on the instrumentation system
[NAL-TM-PR-8704] N89-23477

GAS METERS
Development of an optical multigas detector
[PB89-148878] N89-23849

GAS PIPES
Fiber optic leak detection system
[PB89-148886] N89-24150

GAS STREAMS
Spray deposition: A fundamental study of droplet impingement, spreading and consolidation
[AD-A206065] N89-23672

GAS TEMPERATURE
Simultaneous measurement of spatially resolved electron temperatures. Electron number densities and gas temperatures by laser light scattering from the ICP
[AD-A205747] N89-24174

GAS TUNGSTEN ARC WELDING
Electrode carrying wire for GTAW welding
[NASA-CASE-MFS-29491-1] N89-23738
Internal wire guide for GTAW welding
[NASA-CASE-MFS-29489-1] N89-23739

GAS TURBINES
Environmental effects in niobium base alloys and other selected intermetallic compounds
[AD-A206072] N89-23673

GAS WELDING
The effect of welding process on the microstructure of HY-130 steel weldments
[AD-A205692] N89-23667

GAS-GAS INTERACTIONS
Mathematical analysis of strong fluid mechanical effects in reacting and nonreacting gases
[AD-A206336] N89-23839

GAS-LIQUID INTERACTIONS
Fundamental studies on spray combustion and turbulent combustion
[AD-A206438] N89-23651

GAS-METAL INTERACTIONS
Oxygen interaction with metal surfaces: Surface science approach N89-23596

GAS-SOLID INTERFACES
Boundary layer and heat transfer behind a piston in a shock tube. Part 2: Experimental study of heat transfer at the piston in a tube
[ISL-R-115/87-PT-2] N89-23842

GASEOUS DIFFUSION
Structure/permeability relationships of silicon-containing polyimides
[NASA-CR-4237] N89-23683

GATES (CIRCUITS)
Recursive gate-arrays
[AD-A205335] N89-23796

GELATION
The glass transition temperature (Tg) as a parameter for monitoring the cure of an amine-cured epoxy system at constant heating rates
[AD-A206098] N89-23705

GEOBOTANY
Geobotanical remote sensing for determination of aggregate source material
[AD-A205943] N89-23962

GEODESIC LINES
Calculation of the surface of a geodetic polygon on an ellipsoid of revolution
[ETN-89-94149] N89-23966

GEODESY
Reports on Cartography and Geodesy. Series 1, number 101
[ISSN-0469-4236] N89-23941
The Official Topographic-Cartographic Information System (ATKIS) of the Geodesy Group of the Laender of the Federal Republic of Germany: Status after one year of development N89-23944
On the connection of geodetic pointfields in RETrig
[PB89-146112] N89-23958

GEODETIC COORDINATES
On the connection of geodetic pointfields in RETrig
[PB89-146112] N89-23958
Vectorization of grid lines
[ETN-89-94150] N89-23967
Design of a methodology for the detection of errors in terrestrial networks
[ETN-89-94151] N89-23968

GEODETIC SATELLITES
Geocoded data sets of imaging satellites N89-23950
Observation model and parameter partials for the JPL geodetic GPS modeling software GPSOMC
[NASA-CR-185021] N89-24060

GEODETIC SURVEYS
Analysis and optimization of geodetic networks by spectral criteria and mechanical analogies
[SER-C-342] N89-23963

GEOGRAPHIC INFORMATION SYSTEMS
Reports on Cartography and Geodesy. Series 1, number 101
[ISSN-0469-4236] N89-23941
The Official Topographic-Cartographic Information System (ATKIS) of the Geodesy Group of the Laender of the Federal Republic of Germany: Status after one year of development N89-23944
The digital urban map as a basis for a land information system in local administration N89-23945
ARC-INFO: A geographic information system N89-23947
Hybrid cartographic data processing in a geographic information system N89-23954
Shortest paths in a digitized map using a tile-based data structure
[PB89-143432] N89-23957
The search for edges in remote sensing images using a digital polygonal map
[ETN-89-94146] N89-23964
Geographic Information Systems (GIS) guidelines document
[PB89-132062] N89-24222

GEOIDS
Problems encountered in the Stokes' numerical integration of terrestrial gravity anomalies
[AD-A205448] N89-23990

GEOMAGNETISM
Surface phenomena in plasma environments N89-23555
Geomagnetic disturbances
[AD-A206052] N89-24254

GEOMETRY
The role of knowledge in visual shape representation
[AD-A206173] N89-24041
Riemannian geometry on families of linear systems: The deterministic case
[PB89-146062] N89-24100
On the communication complexity of distributed algebraic computation
[AD-A205784] N89-24117
The geometry of plane waves in spaces of constant curvature N89-24241

GEOPHYSICS
Solar-geophysical data number 531, part 1. Data for October, September 1988 and late data
[PB89-139943] N89-24250

GEOPOTENTIAL
Problems encountered in the Stokes' numerical integration of terrestrial gravity anomalies
[AD-A205448] N89-23990

GERMANY
Computer aided production of a 1:25,000 relief model of Berlin and surroundings N89-23943

GIBBS FREE ENERGY
Critical assessment of the thermodynamic properties of antimony-copper alloys
[PB89-147524] N89-23657

GIOTTO MISSION
Calibration measurements on micrometeorite detectors for the missions ULYSSES, Galileo and Giotto
[ETN-89-93947] N89-24248

GLACIERS
Remote sensing of global snowpack energy and mass balance: In-situ measurements on the snow of interior and Arctic Alaska
[NASA-CR-180078] N89-23956

GLASS
The adhesion between glass and enamel N89-23598
Molded bodies having a high degree of hardness and a high degree of toughness for machining metals, carbides, ceramics and glasses
[DE89-008820] N89-23686
The structural basis for fatigue initiation in glassy polymers
[DE89-009292] N89-23689
Dynamic fatigue of ultralow-expansion glass for space mirrors, reissue A
[AD-A205401] N89-23694
Heterocycles based on group 3, 4, and 5 elements precursors for novel glasses and ceramics
[AD-A205586] N89-23696
The glass transition temperature (Tg) as a parameter for monitoring the cure of an amine-cured epoxy system at constant heating rates
[AD-A206098] N89-23705
Numerical solution of the three dimensional heat flow equation generated by a moving source
[ISL-R-116/87] N89-23843

GLASS FIBER REINFORCED PLASTICS
Effects of thermal cycling on composite materials for space structures N89-23552

GLASS TRANSITION TEMPERATURE
The glass transition temperature (Tg) as a parameter for monitoring the cure of an amine-cured epoxy system at constant heating rates
[AD-A206098] N89-23705

GLOBAL POSITIONING SYSTEM
Impact of the geoplasma on a spaceborne GPS receiver system: A preliminary study
[AD-A205965] N89-23442
Development of the extended kalman filter for the advanced Completely Integrated Reference Instrumentation System (CIRIS)
[AD-A206083] N89-23443
Global Positioning System (GPS) positioning at sea
[ETN-89-94145] N89-23446
Observation model and parameter partials for the JPL geodetic GPS modeling software GPSOMC
[NASA-CR-185021] N89-24060

GLOW DISCHARGES
Laser photoelectric effect at surface of discharge cathode
[AD-A205741] N89-23869

GLYCOLYSIS
Model of early self-replication based on covalent complementarity for a copolymer of glycerate-3-phosphate and glycerol-3-phosphate
[NASA-CR-182912] N89-23693

GOALS
The impact of accuracy and effort feedback and goals on adaptive decision behavior
[AD-A205751] N89-24095

GOERTLER INSTABILITY
Numerical simulation of Goertler/Tollmein-Schlichting wave-interaction
[NASA-CR-181823] N89-23817

GOGGLES
Night vision goggles (AN/PVS-7) performance issues and answers
[AD-A206117] N89-24047

GOODNESS OF FIT
Tests for the gamma distribution with estimated shape parameters
[AD-A205829] N89-24118

GOVERNMENT/INDUSTRY RELATIONS
Putting science and technology to work: A casebook of transferred technologies
[DE89-009158] N89-24228

GRAIN BOUNDARIES
Theoretical studies of Ni3Al and NiAl with impurities
[DE89-006556] N89-23655
Twin boundaries, interfaces and modulated structures in martensites
[DE89-009064] N89-23662
Fundamental studies of beta phase decomposition modes in titanium alloys
[AD-A205296] N89-23665
Atomic imaging and microanalysis of ceramics
[DE89-008172] N89-23684

Mechanisms of diffusion-controlled brittle fracture
[DE89-008726] N89-23921
Grain boundaries
[DE89-008881] N89-24194

GRAIN SIZE
Microstructure development in SiC N89-23582
High-temperature LDV seed particle development
[NASA-CR-182265] N89-23851

GRAINS
Gas-Grain Simulation Facility: Fundamental studies of particle formation and interactions. Volume 1: Executive summary and overview
[NASA-CP-10026-VOL-1] N89-24022
Gas-Grain Simulation Facility: Fundamental studies of particle formation and interactions. Volume 2: Abstracts, candidate experiments and feasibility study
[NASA-CP-10026-VOL-2] N89-24023

GRAINS (FOOD)
Advanced space design program to the Universities Space Research Association and the National Aeronautics and Space Administration
[NASA-CR-180450] N89-24015

GRAPHITE
Light weight polymer matrix composite material
[NASA-CASE-LEW-14734-1] N89-23623

GRAPHITE-EPOXY COMPOSITES
Effects of thermal cycling on composite materials for space structures N89-23552
Analysis of the NAVAIRDEVCEN self-priming topcoat on graphite/epoxy composites
[AD-A205961] N89-23626

GRAPHS (CHARTS)
Knowledge representation using knowledge graphs: Application to theories on mathematical modeling and solving word problems
[MEMO-707] N89-24124

GRATINGS (SPECTRA)
Characterization of multilayer coated concave diffraction gratings in the extreme ultraviolet
[DE89-008831] N89-24151
A compact fast wide angle broad band spectrometer optical system
[NASA-CASE-NPO-17562-1-CU] N89-24153
Decay of molecules at corrugated thin metal films
[AD-A205487] N89-24198

GRAVITATIONAL EFFECTS
Biological results obtained by D1-mission N89-23732
Gas-Grain Simulation Facility: Fundamental studies of particle formation and interactions. Volume 1: Executive summary and overview
[NASA-CP-10026-VOL-1] N89-24022

GRAVITATIONAL FIELDS
Non-Newtonian gravitational forces and the Greenland ice-sheet experiment
[DE89-009348] N89-23988
A linear analysis of the stability of strong shocks and the evolution and distribution of materials in a cold dark matter dominated universe N89-24244

GRAVITY ANOMALIES
Problems encountered in the Stokes' numerical integration of terrestrial gravity anomalies
[AD-A205448] N89-23990

GRAVITY WAVES
Studies of internal gravity waves in the stably stratified troposphere N89-23989
Mesospheric wind measurement
[AD-A205593] N89-23991

GRAZING INCIDENCE TELESCOPES
Grazing incidence telescopes for ESA's X-ray astronomy mission XMM
[MPE-PREPRINT-129] N89-24239

GRID GENERATION (MATHEMATICS)
Investigation of three-dimensional mesh generation with precise controls
[AD-A205967] N89-23773

GRINDING MACHINES
High speed abrasive belt grinding
[AD-A205618] N89-23741

GROUND EFFECT (AERODYNAMICS)
Enhancements to a new free wake hover analysis
[NASA-CR-177523] N89-23414

GROUND STATE
Nuclear magnetism in copper and silver: Theory and experiments
[ISBN-952-900-084-7] N89-24188

GROUND STATIONS
Environmental projects. Volume 3: Environmental compliance audit
[NASA-CR-185019] N89-23985

GROUND TESTS
An instrument for the simultaneous measurement of velocity, temperature and density in unseeded air flows
[AD-A205586] N89-23453
Ground shake test of the Boeing Model 360 helicopter airframe
[NASA-CR-181766] N89-23920

GROUND WIND
An analysis of lightning launch constraints
[AD-A206084] N89-23994

GROUP THEORY
Introduction to irreducible tensor methods, part 1
[NAL-PD-DU-8802] N89-24098

GUIDANCE (MOTION)
Autonomous navigation and control
[AD-A205898] N89-23441

GUIDE VANES
Average-passage simulation of counter-rotating propfan propulsion systems as applied to cruise missiles
[NASA-TM-102043] N89-23416

H

H LINES
Redistribution in astrophysically important hydrogen lines
[NASA-CR-181375] N89-24251

HABITABILITY
Medical and biological support for a manned expedition to Mars N89-23492

HABITATS
Review of wildlife resources of Vandenberg Air Force Base, California
[NASA-TM-102146] N89-23982

HALF PLANES
The crack problem in bonded nonhomogeneous materials
[NASA-CR-184897] N89-23926

HALL EFFECT
Electrical transport properties of Hg0.7Cd0.3Te
[DE88-705689] N89-24183

HALLEY'S COMET
Comet Halley: The view from Pioneer Venus
[NASA-NF-127] N89-24240

HARDNESS
Advanced layer materials N89-23587
Wear resistant sintered steel with high carbide content N89-23607
Mechanical properties of gas atomized Cu-Ti and Cu-Ti-B alloys N89-23610
Strength and structure of Ga(1-x)In(x)As alloys
[AD-A205415] N89-23644
Molded bodies having a high degree of hardness and a high degree of toughness for machining metals, carbides, ceramics and glasses
[DE89-008820] N89-23686
Epoxylite 8822 hardness study
[DE89-008961] N89-23687

HARMONIC OSCILLATORS
Exact wave functions and coherent states of a damped driven harmonic oscillator
[AD-A205785] N89-24136

HARMONICS
Development of harmonic panel methods for aeroelastic applications to elastic bodies and body-fin combinations in supersonic flow
[AD-A205739] N89-23423
Memory functions and relaxation functions of some spin systems
[AD-A206340] N89-24137
Quasi-liquid crystalline materials with special electro-optic properties
[AD-A206015] N89-24206

HAZARDS
Propellant reuse/recovery technology
[AD-A206306] N89-23714
A demonstration of the method of stochastic finite element analysis
[AD-A206135] N89-24127

HEALTH
Summary of selected new information on effects of ozone on health and vegetation. Draft supplement to air quality criteria for ozone and other photochemical oxidants
[PB89-135123] N89-23980

HEAT EXCHANGERS
Japan's Sunshine Project 1987 annual summary of comprehensive research
[DE88-756448] N89-23975

HEAT FLUX
A numerical investigation of thin-film heat transfer gages
[AD-A206134] N89-23853

HEAT MEASUREMENT
The structural basis for fatigue initiation in glassy polymers
[DE89-009292] N89-23689

HEAT PUMPS
Process integration methodology for natural gas-fueled heat pumps and cogeneration systems
[PB89-140867] N89-23811

HEAT RESISTANT ALLOYS
Intermetallic phases for high temperature applications N89-23612

HEAT SINKS
Reentry materials in the atmosphere
[REPT-882-430-102] N89-23629

HEAT TRANSFER
Carbon fiber thermal conductivity measurement and analysis
[AD-A205682] N89-23625
Free shear layer and swirl flow heat transfer enhancement
[PB89-145106] N89-23810
Two-dimensional numerical simulation of a Stirling engine heat exchanger
[NASA-TM-102057] N89-23823
Boundary layer and heat transfer behind a piston in a shock tube. Part 1: Theoretical considerations of laminar and turbulent boundary layer behind a piston in a tube
[ISL-R-111/87-PT-1] N89-23841
Boundary layer and heat transfer behind a piston in a shock tube. Part 2: Experimental study of heat transfer at the piston in a tube
[ISL-R-115/87-PT-2] N89-23842
Automatic analysis of holographic interferograms N89-23848
A numerical investigation of thin-film heat transfer gages
[AD-A206134] N89-23853
Computerized measurement of thermoacoustically generated temperature gradients
[AD-A205353] N89-23929
Low-temperature volumetric receiver concept
[DE89-008245] N89-23976

HEAT TRANSMISSION
Numerical solution of the three dimensional heat flow equation generated by a moving source
[ISL-R-116/87] N89-23843

HEAVY IONS
A hierarchy of transport approximations for high energy heavy (HZE) ions
[NASA-TM-4118] N89-24255

HEAVY NUCLEI
Direct electron-pair production by high energy heavy charged particles
[NASA-CR-184958] N89-24142
Strong and electromagnetic interactions in heavy exotic atoms
[PB89-145718] N89-24143

HELICOPTER WAKES
Enhancements to a new free wake hover analysis
[NASA-CR-177523] N89-23414

HELICOPTERS
An analysis of Electronic Aids to Maintenance (EAM) for the Light Helicopter Family (LHX)
[AD-A205440] N89-23407
Ground shake test of the Boeing Model 360 helicopter airframe
[NASA-CR-181766] N89-23920
Application of a PC based, real-time, data-aquisition system in rotorcraft wind-tunnel testing
[NASA-TM-4119] N89-24079

HELIPORTS
Heliport night parking area criteria test plan
[DOT/FAA/CT-TN88/45] N89-23480

HEPTANES
Burning rate constant of fuel droplet under high pressure
[NAL-TR-1001] N89-23639

HERMES MANNED SPACEPLANE
The FLUIDNET development and application to preliminary sizing of fluid loop systems
[REPT-882-440-102] N89-23845
The evolution of space mechanisms in the ESA R and D program N89-23893
The role of pilot and automatic onboard systems in future rendezvous and docking operations
[REPT-882-440-116] N89-24050

HETEROCYCLIC COMPOUNDS
Heterocycles based on group 3, 4, and 5 elements precursors for novel glasses and ceramics
[AD-A205586] N89-23696

HETEROJUNCTION DEVICES
Characterization of semiconductor device processing etchant solutions for GaAs and p+ GaAs layers employed in AlxGa(1-x)As/GaAs MODFETs and related heterojunction devices
[AD-A205772] N89-24201
Some 3-5 heterojunction structures and high speed devices
[AD-A205946] N89-24203

HETEROJUNCTIONS
Heterojunction band line-ups and the alloying effect in compound semiconductor alloys: A photoemission study N89-24179

HEURISTIC METHODS
Shortest paths in a digitized map using a tile-based data structure
[PB89-143432] N89-23957
Heuristics for cooperative problem solving
[AD-A206371] N89-24096
HIGH ALTITUDE BREATHING
Human adaptation to the Tibetan Plateau
[AD-A206463] N89-24031
HIGH ENERGY FUELS
Novel organoboranes as intermediates for ceramic precursors and high-energy fuels
[AD-A206101] N89-23713
HIGH ENERGY OXIDIZERS
Novel organoboranes as intermediates for ceramic precursors and high-energy fuels
[AD-A206101] N89-23713
HIGH FIELD MAGNETS
Eddy current damper N89-23900
HIGH LEVEL LANGUAGES
Design and implementation of an expert user interface for the computer aided prototyping system
[AD-A206113] N89-24067
Advanced computing systems: An advanced reasoning-based development paradigm for Ada trusted systems and its application to MACH
[AD-A206308] N89-24070
HIGH POLYMERS
Donor acceptor polymerization chemistry as a vehicle to low energy cure of matrix resins: Evolution of the 2-Tg concept to produce Tg polymers at ambient temperatures
[AD-A206287] N89-23706
HIGH POWER LASERS
Nonlinear spectroscopy of multicomponent droplets and two- and three-dimensional measurements in flames
[AD-A205449] N89-23645
High-power single spatial mode AlGaAs channeled-substrate-planar semiconductor diode lasers for spaceborne communications
[NASA-CR-4238] N89-23860
Experimental and theoretical determination of the thermomechanical response of inelastic structural materials to high energy thermal inputs
[AD-A206100] N89-23933
HIGH PRESSURE
Burning rate constant of fuel droplet under high pressure
[NAL-TR-1001] N89-23639
High pressure studies on infrared detector materials
[NAL-TM-MT-8701] N89-23677
HIGH RESOLUTION
Ultra-high resolution VUV-XUV laser: Application to the hyperfine study of krypton
[DE89-009059] N89-23863
Use of a spectrally segmented photodiode-array spectrometer for inductively coupled plasma atomic emission spectroscopy
[AD-A205688] N89-24171
HIGH STRENGTH STEELS
Behavior of metals during hot rolling processes. Part 1: Mathematical models N89-23613
Stress relief cracking in copper-precipitation strengthened HSLA-100 steel
[AD-A205936] N89-23670
HIGH TEMPERATURE
Design and construction of a state-of-the-art high temperature tribometer
[PB89-148332] N89-23847
High-temperature LDV seed particle development
[NASA-CR-182265] N89-23851
HIGH TEMPERATURE ENVIRONMENTS
Iron-niobium-aluminum alloy having high-temperature corrosion resistance
[DE89-009600] N89-23663
HIGH TEMPERATURE PLASMAS
Nonlinear spectroscopy of multicomponent droplets and two- and three-dimensional measurements in flames
[AD-A205449] N89-23645
HIGH TEMPERATURE SUPERCONDUCTORS
Studies on high-Tc superconducting materials
[NAL-TM-MT-8703] N89-24178
High-temperature ceramic superconductors
[AD-A205321] N89-24196
Fundamental and applied studies of explosively fabricated high-temperature superconducting fixtures
[AD-A205953] N89-24204
HIPPOCAMPUS
A low-energy X-ray irradiator for electrophysiological studies
[AD-A205388] N89-24026
HOLMIUM
Shock compaction of YBa2Cu3O7-x and HoBa2Cu3O7-x powders in a metal matrix
[DE89-008827] N89-24193
HOLOGRAPHIC INTERFEROMETRY
Model systems --- metal alloys N89-23728
Automatic analysis of holographic interferograms N89-23848
Summaries of papers presented at Short Wavelength Coherent Radiation: Generation and Applications Topical Meeting held in Cape Cod, Massachusetts on September 26-29, 1988
[AD-A205471] N89-23867
HOLOGRAPHY
Code optimization of speckle reduction algorithms for image processing of rocket motor holograms
[AD-A205306] N89-23524
HOMOGENEITY
Fabrication and properties of alumina-zirconia composites
[PB89-147532] N89-23620
HOMOGENIZING
Fabrication and properties of alumina-zirconia composites
[PB89-147532] N89-23620
HOMOPOLAR GENERATORS
Long pulse homopolar generator
[AD-A205452] N89-23977
HONEYCOMB STRUCTURES
Friction factor data for flat plate tests of smooth and honeycomb surfaces
[NASA-CR-184977] N89-23876
HORIZONTAL ORIENTATION
On the use of multiprocessing computers for global numerical weather prediction
[AD-A206102] N89-24009
HOT CORROSION
Investigation of alpha-SiC hot corrosion in the presence of basic slag N89-23595
HOT ISOSTATIC PRESSING
Sintering and HIPing with additives N89-23575
Preparation and evaluation of silicon nitride matrices for silicon nitride-SiC fiber composites
[NASA-CR-184798] N89-23678
HOT-WIRE ANEMOMETERS
Turbulent shear stress measurement in hypersonic flow
[AD-A206453] N89-23432
HOVERING
Enhancements to a new free wake hover analysis
[NASA-CR-177523] N89-23414
HUMAN BEHAVIOR
Treatment with tyrosine, a neurotransmitter precursor, reduces environmental stress in humans
[AD-A206035] N89-24039
HUMAN BEINGS
Human adaptation to the Tibetan Plateau
[AD-A206463] N89-24031
The attention system of the human brain
[AD-A206157] N89-24040
HUMAN PERFORMANCE
Evaluation of three commercial microclimate cooling systems
[AD-A206318] N89-23744
Age distribution among NASA scientists and engineers N89-23911
The relationship between subjective and objective measures of sleepiness
[AD-A205861] N89-24027
Patterns of human drinking: Effects of exercise, water temperature and food consumption
[AD-A206031] N89-24029
Psychometric function reconstruction from adaptive tracking procedures
[AD-A205668] N89-24034
Development and evaluation of integrating details: A complex spatial problem solving test
[AD-A205860] N89-24035
HUMAN RESOURCES
Air Force Human Resources Laboratory R and D accomplishments and services, FY86-FY88
[AD-A205312] N89-24218
HUMIDITY
Design of a chamber for CBW aerosol studies with relative humidity and particle concentration control
[AD-A205623] N89-23481
HUMIDITY MEASUREMENT
Inferring relative humidity profiles from 3DNEPH cloud data: Technique development and data impact study
[AD-A205825] N89-23993
HYDRAULIC EQUIPMENT
A330/340 hydraulic system
[REPT-882-111-102] N89-23461
Low energy consumption hydraulic techniques
[AD-A206285] N89-23743
The FLUIDNET development and application to preliminary sizing of fluid loop systems
[REPT-882-440-102] N89-23845
HYDRAULIC FLUIDS
Corrosion and lubricity testing of nonflammable USAF formulated CTFE (Chlorotrifluoroethylene) base hydraulic fluid
[AD-A205467] N89-23695
Low energy consumption hydraulic techniques
[AD-A206285] N89-23743
The FLUIDNET development and application to preliminary sizing of fluid loop systems
[REPT-882-440-102] N89-23845
HYDRAULIC TEST TUNNELS
Design of water tunnel to measure wall pressure signatures due to tunnel blockage and wake effects
[AD-A206025] N89-23483
HYDRAZINES
Spectroscopic studies of metal-ligand-surface interactions
[AD-A206460] N89-23652
Environmental interactions of hydrazine fuels in Soil/Water systems
[AD-A206244] N89-23986
HYDROCARBON COMBUSTION
Burning rate constant of fuel droplet under high pressure
[NAL-TR-1001] N89-23639
HYDROCARBONS
Spectroscopic studies of metal-ligand-surface interactions
[AD-A206460] N89-23652
HYDROGEN FUELS
Parametric study of radiative cooling of solid antihydrogen
[AD-A206092] N89-23742
HYDROGEN OXYGEN ENGINES
Study of the PBE cycle 100kN LH2/LO2 rocket engine
[NAL-TR-965] N89-23514
Design, fabrication and test of the RL10 derivative II chamber/primary nozzle
[NASA-CR-179595] N89-23519
Space station propulsion test bed
[NASA-CR-183615] N89-23521
HYDROGEN PLASMA
Population inversions in ablation plasmas generated by intense electron beams
[AD-A205716] N89-24172
HYDROGENATION
Production of jet fuels from coal-derived liquids. Volume 8: Heteroatom removal by catalytic processing
[AD-A205470] N89-23712
HYDROLYSIS
Fabricable polymers with excellent heat, oxidative and hydrolytic stability
[AD-A205627] N89-23698
Mechanism of the initiation of the cationic polymerization of styrenes by silanes and activated covalent esters
[AD-A206502] N89-23708
HYDROXYL RADICALS
Human temperature regulation during exercise after oral pyridostigmine administration
[AD-A206032] N89-24030
Observations of the rotational transitions of OH from the Orion molecular cloud
[NASA-CR-184802] N89-24231
HYPERBOLIC DIFFERENTIAL EQUATIONS
A stability analysis of various patched grid interface conditions for hyperbolic equations
[FFA-144] N89-24105
HYPERCUBE MULTIPROCESSORS
A method of up-front load balancing for local memory parallel processors
[NASA-CASE-MSC-21348-1] N89-24084
HYPERFINE STRUCTURE
Ultra-high resolution VUV-XUV laser: Application to the hyperfine study of krypton
[DE89-009059] N89-23863
HYPERGEOMETRIC FUNCTIONS
On the equation Xa + Ya = Za
[AD-A205460] N89-24116
HYPERSONIC BOUNDARY LAYER
Experimental study of pressure and heating rate on a swept cylindrical leading edge resulting from swept shock wave interference
[NASA-CR-185326] N89-23411
Turbulent shear stress measurement in hypersonic flow
[AD-A206453] N89-23432
HYPERSONIC COMBUSTION
Advanced computational techniques for hypersonic propulsion
[NASA-TM-102005] N89-23809
HYPERSONIC FLIGHT
Advanced computational techniques for hypersonic propulsion
[NASA-TM-102005] N89-23809

HYPERSONIC FLOW
Numerical simulation of hypersonic flow around a space plane. 1: Basic development
[NAL-TR-976T] N89-23409
Turbulent shear stress measurement in hypersonic flow
[AD-A206453] N89-23432
An instrument for the simultaneous measurement of velocity, temperature and density in unseeded air flows
[AD-A205588] N89-23453

HYPERSONIC HEAT TRANSFER
Experimental study of pressure and heating rate on a swept cylindrical leading edge resulting from swept shock wave interference
[NASA-CR-185326] N89-23411

HYPERSONIC SHOCK
Experimental study of pressure and heating rate on a swept cylindrical leading edge resulting from swept shock wave interference
[NASA-CR-185326] N89-23411

HYPERSONIC WIND TUNNELS
Nozzles for test system plasma generators --- Hermes
[REPT-882-430-104] N89-23502

HYPERVELOCITY GUNS
Long pulse homopolar generator
[AD-A205452] N89-23977

HYPERVELOCITY IMPACT
Micrometeoroids and debris N89-23558
Working group written presentation: Meteoroid/orbital debris effects on materials N89-23565

HYPOXIA
Human adaptation to the Tibetan Plateau
[AD-A206463] N89-24031
Treatment with tyrosine, a neurotransmitter precursor, reduces environmental stress in humans
[AD-A206035] N89-24039

I

ICE FORMATION
The low frequency oscillation in the flow over a NACA0012 airfoil with an iced leading edge
[NASA-TM-102018] N89-23417

IDEAL GAS
Acoustic response of a rectangular waveguide with a strong transverse temperature gradient
[NASA-TM-101564] N89-24140

IGNITION
Comparison of computational analysis with flight tests of a 40mm solid-fuel ramjet projectile
[AD-A206536] N89-23459
Spontaneous ignition of atomized kerosine/air mixtures in a high pressure flowing system
[NAL-TR-966] N89-23835
Analysis of the ignition experiment IGNITEX
[DE89-007847] N89-24156

IMAGE ANALYSIS
Automatic analysis of holographic interferograms N89-23848
Investigation of several methods for the detection of outstanding points in a digital image
[ETN-89-94148] N89-23965

IMAGE PROCESSING
Code optimization of speckle reduction algorithms for image processing of rocket motor holograms
[AD-A205306] N89-23524
Autofocus of SAR imagery degraded by ionospheric-induced phase errors
[DE89-008278] N89-23752
Telescience and image processing for PODI: An analysis and a proposal for a simulation set-up
[NLR-TR-88005-U] N89-23815
Automatic analysis of holographic interferograms N89-23848
Geocoded data sets of imaging satellites N89-23950
The role of knowledge in visual shape representation
[AD-A206173] N89-24041
SMOOFF: A FORTRAN smoothing program
[AD-A204087] N89-24057
Engineering thrust areas, 1989
[DE89-009009] N89-24229
Image processing of coronal pictures
[AD-A205326] N89-24252

IMAGE RESOLUTION
Investigation of optical compression techniques for dither coding
[AD-A206140] N89-23776

IMAGE ROTATION
Prospects for classifying complex imagery using a self-organizing neural network
[AD-A206208] N89-24088

IMAGES
Code optimization of speckle reduction algorithms for image processing of rocket motor holograms
[AD-A205306] N89-23524
Relating attention to visual mechanisms
[AD-A206452] N89-24042

IMAGING RADAR
Geocoded data sets of imaging satellites N89-23950
Imaging procedure of underwater bottom topography by air and satellite images in the range of microwave and visible electromagnetic spectra
[GKSS-88/E/41] N89-24014

IMAGING TECHNIQUES
Atomic imaging and microanalysis of ceramics
[DE89-008172] N89-23684
Vaporization and recondensation in propagation and imaging of laser beams
[DE89-008014] N89-23858
A program interface prototype for a multimedia database incorporating images
[AD-A206439] N89-24226

IMPACT DAMAGE
Microparticle impacts in space: Results from Solar Max and shuttle witness plate inspections N89-23544
Working group written presentation: Meteoroid/orbital debris effects on materials N89-23565
Working group written presentation: Trapped radiation effects N89-23566

IMPACT LOADS
White paper: Experimental and computational studies of very high velocity impacts
[DE89-007643] N89-23877

IMPINGEMENT
A numerical routine for defining rocket exhaust characteristics and impingement effects
[AD-A206323] N89-23526

IMPURITIES
Microstructure-permeability relation in MnZn ferrites prepared of iron oxide with chlorine impurities N89-23602
Theoretical studies of Ni3Al and NiAl with impurities
[DE89-006556] N89-23655

INCIDENT RADIATION
A compact fast wide angle broad band spectrometer optical system
[NASA-CASE-NPO-17562-1-CU] N89-24153
Photoabsorption of molecules at corrugated thin metal films
[AD-A205325] N89-24197

INCOHERENT SCATTERING
Proof of the feasibility of coherent and incoherent schemes for pumping a gamma-ray laser
[AD-A205371] N89-23866

INCOMPRESSIBLE FLOW
Investigation of incompressible cascade flows using a viscous/inviscid interactive code
[AD-A205972] N89-23832

INDEPENDENT VARIABLES
Improvement of navigation measurement procedures by the combined application of correlation techniques and parameter estimation
[ETN-89-93946] N89-23445

INDEXES (DOCUMENTATION)
Defense Integrated Data System (DIDS) procedures manual. Volume 8: Document Identifier Code (DIC) Input/Output (I/O) formats (fixed length), change 3
[PB89-139414] N89-24220

INDIUM
Fiber-optic time-resolved fluorescence sensor for the simultaneous determination of Al(+3), Ga(+3) and In(+3)
[AD-A205689] N89-24154

INDIUM ARSENIDES
Strength and structure of Ga(1-x)In(x)As alloys
[AD-A205415] N89-23644

INDUSTRIAL PLANTS
Process integration methodology for natural gas-fueled heat pumps and cogeneration systems
[PB89-140867] N89-23811
Product development at Aerospatiale --- industrial plasmas
[REPT-882-430-111] N89-24175

INELASTIC SCATTERING
Quasielastic and inelastic spin fluctuations in superconducting La2-xSrxCuO4
[DE89-008157] N89-24190

INERTIAL CONFINEMENT FUSION
Temporally smooth broadband pulses obtained by cross phase modulation in an optical fiber
[DE89-008891] N89-24152

INERTIAL NAVIGATION
Development of the extended kalman filter for the advanced Completely Integrated Reference Instrumentation System (CIRIS)
[AD-A206083] N89-23443

INFECTIOUS DISEASES
Muramyl peptide-enhanced sleep: Pharmacological optimization of performance
[AD-A205974] N89-24028

INFERENCE
Explanation-based theory revision: An approach to the problems of incomplete and incorrect theories
[AD-A205337] N89-24092

INFLUENCE COEFFICIENT
Enhancements to a new free wake hover analysis
[NASA-CR-177523] N89-23414

INFORMATION DISSEMINATION
intelligent processing of materials
[PB89-151823] N89-23735

INFORMATION SYSTEMS
Direct dissemination of data from ESA's future in-orbit infrastructure
[DDD-CP/TE-RE-7450] N89-23754
Definition and filling of information systems: Challenge for a photogrammetric service enterprise N89-23942

INFORMATION THEORY
Explanation-based theory revision: An approach to the problems of incomplete and incorrect theories
[AD-A205337] N89-24092

INFRARED ASTRONOMY
Assembling the ISO thermal model with ESAT AN
[REPT-882-440-107] N89-23510
Telescope structure for cryogenic application
[REPT-882-440-112] N89-23940
Thermal and cryogenic aspects of the ISO optical subsystem
[REPT-882-440-113] N89-24160
Observations of the rotational transitions of OH from the Orion molecular cloud
[NASA-CR-184802] N89-24231
Study of the infrared celestial background
[AD-A205649] N89-24237
Ground-based infrared observations of sources discovered by the AFGL, FIRRSE and IRAS infrared surveys
[AD-A206335] N89-24246

INFRARED ASTRONOMY SATELLITE
Ground-based infrared observations of sources discovered by the AFGL, FIRRSE and IRAS infrared surveys
[AD-A206335] N89-24246

INFRARED DETECTORS
High pressure studies on infrared detector materials
[NAL-TM-MT-8701] N89-23677

INFRARED IMAGERY
Thermal images of sky and sea-surface background infrared radiation
[AD-A205819] N89-23992

INFRARED PHOTOGRAPHY
Mapping freeze/thaw boundaries with SMMR data
[NASA-CR-184991] N89-23961

INFRARED RADIATION
Spectroscopic studies of metal-ligand-surface interactions
[AD-A206460] N89-23652
Thermal images of sky and sea-surface background infrared radiation
[AD-A205819] N89-23992

INFRARED SPECTRA
Spectroscopic studies of metal-ligand-surface interactions
[AD-A206460] N89-23652
Observations of the rotational transitions of OH from the Orion molecular cloud
[NASA-CR-184802] N89-24231
Spectra and dynamics of young stellar objects N89-24234

INFRARED SPECTROSCOPY
Polyethylene glycol-poly(2-methyl-5-vinyl tetrazole) polymer blend: A desensitizing binder for propellants and explosives
[AD-A206563] N89-23716

INFRARED TELESCOPES
Telescope structure for cryogenic application
[REPT-882-440-112] N89-23940
Thermal and cryogenic aspects of the ISO optical subsystem
[REPT-882-440-113] N89-24160

INFRARED TRACKING
Enhanced tracking of ballistic targets using forward looking infrared measurements
[AD-A205727] N89-23769

INHIBITORS
Criteria for robust stability in a class of lateral inhibition networks coupled through resistive grids
[AD-A204174] N89-24081

INHOMOGENEITY
The crack problem in bonded nonhomogeneous materials
[NASA-CR-184897] N89-23926
The mode 3 crack problem in bonded materials with a nonhomogeneous interfacial zone
[NASA-CR-185315] N89-23927

INJECTION MOLDING
Injection molding of whisker-reinforced Al2O3-ZrO2 ceramics N89-23574
INJECTORS
Electromagnetic railgun hydrogen pellet injector: Progress and prospect
[DE89-009536] N89-23499
INLET FLOW
Advanced computational techniques for hypersonic propulsion
[NASA-TM-102005] N89-23809
INLET PRESSURE
Friction factor data for flat plate tests of smooth and honeycomb surfaces
[NASA-CR-184977] N89-23876
INSTRUMENT COMPENSATION
Digital control of the Kuiper Airborne Observatory telescope
[NASA-TM-101082] N89-23785
INSTRUMENT LANDING SYSTEMS
Instrument landing system mathematical modeling study for Orlando International Airport Runway 35L localizer, Orlando, Florida. Final airside docking plan (Scheme 3A)
[AD-A205351] N89-23438
INTEGRAL EQUATIONS
An iterative technique to correct probe position errors in planar near-field to far-field transformations
[PB89-153886] N89-23750
Improved sea surface scattering model
[AD-A205745] N89-24012
Approximation of stochastic integral equations using Martingale difference schemes
[ETN-89-93951] N89-24123
Sheath and presheath in a collisionless open field plasma
[IPPJ-890] N89-24161
INTEGRATED CIRCUITS
Current distribution in a three-dimensional IC analyzed by a perturbation method. Part 1: A simple steady state theory
[NASA-CR-185022] N89-23494
On-orbit observations of single-event upset in harris HM-6508 RAMSs (Random Access Memories): An update
[AD-A206266] N89-23506
Effects of space radiation on electronic microcircuits N89-23549
An evaluation of coplanar line for application in microwave integrated circuitry
[AD-A205305] N89-23785
Adaptive signal processing
[AD-A205787] N89-24063
INTELLIGENCE
Development and evaluation of integrating details: A complex spatial problem solving test
[AD-A205860] N89-24035
INTELLIGIBILITY
Intelligibility in noise of three LPC (Linear Predictive Coders) voice channels with active noise reduction headsets
[AD-A205613] N89-23767
INTERACTIONAL AERODYNAMICS
Average-passage simulation of counter-rotating propfan propulsion systems as applied to cruise missiles
[NASA-TM-102043] N89-23416
Investigation of the flowfield created by the interaction of a sonic jet and a co-flowing supersonic stream
[AD-A205823] N89-23425
High speed turboprop aeroacoustic study (single rotation). Volume 1: Model development
[NASA-CR-182257-VOL-1] N89-24139
INTERACTIVE CONTROL
User interface and highly interactive systems: Survey of current research
[PB89-146088] N89-24056
INTERFACES
Fundamental and practical studies of metal contacts on mercury zinc telluride
[AD-A206560] N89-23653
Report on the partial support of the 1988 Gordon Conference on Polymers (West)
[AD-A205834] N89-23701
Application of a PC based, real-time, data-aquisition system in rotorcraft wind-tunnel testing
[NASA-TM-4119] N89-24079
Discrete event simulation model decomposition
[AD-A206048] N89-24119
Managing sound in a relational multimedia database system
[AD-A205742] N89-24225
INTERFACIAL ENERGY
Temperature dependence of interfacial energies between solid oxides and liquid metals N89-23599
INTERFACIAL TENSION
Finite element modeling of frictionally restrained composite interfaces
[NASA-CR-182281] N89-23918
INTERFERENCE
Investigation of mutual interference between digitally modulated signals
[BBC-RD-1988/13] N89-23745
INTERGALACTIC MEDIA
A linear analysis of the stability of strong shocks and the evolution and distribution of materials in a cold dark matter dominated universe N89-24244
INTERGRANULAR CORROSION
Environment-induced crack growth processes in nickel-base alloys
[DE89-008253] N89-23659
INTERIOR BALLISTICS
Boundary layer and heat transfer behind a piston in a shock tube. Part 2: Experimental study of heat transfer at the piston in a tube
[ISL-R-115/87-PT-2] N89-23842
INTERMEDIATE FREQUENCIES
Tuner for the first intermediate frequency of receivers for direct satellite reception
[ETN-89-93766] N89-23788
INTERMETALLICS
Intermetallic phases for high temperature applications N89-23612
Theoretical analysis of compatibility of several reinforcement materials with NiAl and FeAl matrices
[NASA-CR-182291] N89-23622
Theoretical studies of Ni3Al and NiAl with impurities
[DE89-006556] N89-23655
Environmental effects in niobium base alloys and other selected intermetallic compounds
[AD-A206072] N89-23673
Deformation twinning in ordered intermetallic compounds
[DE89-008748] N89-24192
INTERNATIONAL COOPERATION
Materials science cooperation in 1987 N89-23570
INTERPLANETARY DUST
Calibration measurements on micrometeorite detectors for the missions ULYSSES, Galileo and Giotto
[ETN-89-93947] N89-24248
INTERPLANETARY SPACE
Solar flares and magnetospheric particles: Investigations based upon the ONR-602 and ONR-604 experiments
[AD-A205599] N89-24253
INTERPLANETARY SPACECRAFT
Orbit parameters given N89-23491
INTERPOLATION
Comparison of interpolation algorithms for speed control in air traffic management
[AD-A206314] N89-23444
INTERPROCESSOR COMMUNICATION
Flosolver: A parallel computer for fluid dynamics
[NAL-TM-AE-8803] N89-23805
Signal-Noise/Interferer Combiner Unit Programmable (SINCUP)
[AD-A205367] N89-24053
INTERSTELLAR GAS
Observations of the rotational transitions of OH from the Orion molecular cloud
[NASA-CR-184802] N89-24231
A self consistant model of the three phase interstellar medium in disk galaxies N89-24245
INTERSTITIALS
Semiconductor measurement technology: Automatic determination of the interstitial oxygen content of silicon wafers polished on both sides
[PB89-151831] N89-24180
INVARIANT IMBEDDINGS
Nonlinear singular elliptic equations
[DE88-705691] N89-24103
The geometry of plane waves in spaces of constant curvature N89-24241
INVENTORIES
Area source documentation for the 1985 National Acid Precipitation Assessment Program Inventory
[PB89-151427] N89-23981
INVISCID FLOW
Investigation of incompressible cascade flows using a viscous/inviscid interactive code
[AD-A205972] N89-23832
Three dimensional high speed boundary layer flows
[AD-A206145] N89-23837
Solution of one-dimensional Euler equations by the implicit finite difference technique of Beam and Warming
[NAL-PD-FM-8816] N89-24097
IODIDES
Synthesis of novel acid electrolytes for phosphoric acid fuel cells
[PB89-148944] N89-23786
IODINE LASERS
Numerical simulation of the dissociation of I2 by O2 (1 Delta) in a two dimensional parallel jet
[AD-A206137] N89-23870
ION BEAMS
A hierarchy of transport approximations for high energy heavy (HZE) ions
[NASA-TM-4118] N89-24255
ION DENSITY (CONCENTRATION)
Ionization investigation of sputtered titanium and of titanium ion transport process in an argon discharge glow using laser induced fluorescence
[JUEL-2219] N89-23660
ION DISTRIBUTION
Ionization investigation of sputtered titanium and of titanium ion transport process in an argon discharge glow using laser induced fluorescence
[JUEL-2219] N89-23660
ION EMISSION
Chloride analysis in HAN-based liquid propellants by inductively coupled plasma spectroscopy
[AD-A206564] N89-23717
ION EXCHANGING
Electronic and ionic transport in polymers
[AD-A206530] N89-23709
ION PROBES
Neutral primary beam SIMS analysis of ceramic materials N89-23601
ION SHEATHS
Sheath and presheath in a collisionless open field plasma
[IPPJ-890] N89-24161
ION SOURCES
Preliminary evaluation of a miniaturized torch for inductively coupled plasma mass spectrometry
[AD-A205746] N89-24173
IONIC REACTIONS
Energy disposal in ion-molecule reactions
[AD-A205987] N89-24144
IONIZATION
Ionization investigation of sputtered titanium and of titanium ion transport process in an argon discharge glow using laser induced fluorescence
[JUEL-2219] N89-23660
IONOSPHERIC DISTURBANCES
Impact of the geoplasma on a spaceborne GPS receiver system: A preliminary study
[AD-A205965] N89-23442
Solar-geophysical data number 531, part 1. Data for October, September 1988 and late data
[PB89-139943] N89-24250
IRON
Physico-mathematical investigation of the consolidation of iron powder N89-23617
Liquid dynamic campaction of Fe-Nd-B permanent magnets
[AD-A205632] N89-24135
Structure and grid dynamics of ultrathin epitaxial Ag and Fe films on Ni(100) and Cu(100) substrates
[JUEL-2221] N89-24187
IRON ALLOYS
Mechanical properties of rapidly solidified iron-based alloys N89-23611
Intermetallic phases for high temperature applications N89-23612
Theoretical analysis of compatibility of several reinforcement materials with NiAl and FeAl matrices
[NASA-CR-182291] N89-23622
Iron-niobium-aluminum alloy having high-temperature corrosion resistance
[DE89-009600] N89-23663
IRRADIANCE
The absolute radiometric calibration of the advanced very high resolution radiometer
[NASA-CR-185057] N89-23852
Night vision goggles (AN/PVS-7) performance issues and answers
[AD-A206117] N89-24047
IRREVERSIBLE PROCESSES
Numerical implementation of the Schapery model for nonlinear visco-elasticity
[PB89-144950] N89-23915
ISING MODEL
Memory functions and relaxation functions of some spin systems
[AD-A206340] N89-24137
The diluted tri-dimensional spin-one Ising model with crystal field interactions
[DE88-705663] N89-24181
Mean field theory of the spin-1 Ising model with a random crystal field
[DE88-705669] N89-24182

ISOTHERMS
The glass transition temperature (Tg) as a parameter for monitoring the cure of an amine-cured epoxy system at constant heating rates
[AD-A206098] N89-23705
ITERATION
An iterative technique to correct probe position errors in planar near-field to far-field transformations
[PB89-153886] N89-23750
Runtime aggregation of recursion relations
[AD-A206576] N89-24076
ITERATIVE SOLUTION
Reduction of a general matrix to tridiagonal form
[DE89-008980] N89-24083
Efficient method for solving free-boundary problems
[PB89-146138] N89-24101

J

JAMMING
Active radar jamming
[FOA-C-30506-3.6] N89-23777
JET CONTROL
Two-dimensional confined jet thrust vector control: Operating mechanisms and performance
[AD-A206011] N89-23834
JET ENGINE FUELS
Sorption of selected volatile organic constituents of jet fuels and solvents on natural sorbents from gas and solutions phases
[AD-A204073] N89-23711
Production of jet fuels from coal-derived liquids. Volume 8: Heteroatom removal by catalytic processing
[AD-A205470] N89-23712
JET ENGINES
Aerothermodynamic analysis of a Coanda/Refraction Jet Engine Test Facility
[AD-A205937] N89-23482
JET FLOW
Hot-jet simulation in cryogenic wind tunnels
[NASA-RP-1220] N89-23448
Derivation of a Godunov one dimensional fluid dynamics code
[AD-A205463] N89-23624
JET MIXING FLOW
Investigation of the flowfield created by the interaction of a sonic jet and a co-flowing supersonic stream
[AD-A205823] N89-23425
A numerical routine for defining rocket exhaust characteristics and impingement effects
[AD-A206323] N89-23526
Numerical studies of the effects of jet-induced mixing on liquid-vapor interface condensation
[NASA-CR-182285] N89-23818
JET PROPULSION
Computational study of high supersonic flow over boattails with centered propulsive jets
[AD-A206364] N89-23431
JET THRUST
Method and system for monitoring and displaying engine performance parameters
[NASA-CASE-LAR-14049-1] N89-23466
Two-dimensional confined jet thrust vector control: Operating mechanisms and performance
[AD-A206011] N89-23834
JOINTS (JUNCTIONS)
Investigations on the cracking behavior of joints in airfields and roads: Field investigations and laboratory simulations
[PB89-141279] N89-23479
Microwave processing of ceramics
[DE89-009350] N89-23690
Design and development of a high-stiffness, high-resolution torque sensor N89-23903
JOSEPHSON JUNCTIONS
Coherence and chaos phenomena in Josephson oscillators for superconducting electronics
[AD-A205469] N89-23798
JUDGMENTS
Monitoring information processing and decisions: The MOUSELAB system
[AD-A205963] N89-24037

K

KALMAN FILTERS
Development of the extended kalman filter for the advanced Completely Integrated Reference Instrumentation System (CIRIS)
[AD-A206083] N89-23443
Flight control system for the CRCA (Control Reconfigurable Combat Aircraft) using a command generator tracker with PI (Proportional-Plus-Integral) feedback and Kalman filter, volume 1
[AD-A205723] N89-23473
Enhanced tracking of ballistic targets using forward looking infrared measurements
[AD-A205727] N89-23769
Performance analysis of Kalman filters
[PB89-146104] N89-23787
KAOLINITE
Sorption of selected volatile organic constituents of jet fuels and solvents on natural sorbents from gas and solutions phases
[AD-A204073] N89-23711
KAPTON (TRADEMARK)
Electron spectroscopy for chemical analysis: Sample analysis
[NASA-CR-183568] N89-23634
Undercutting of defects in thin film protective coatings on polymer surfaces exposed to atomic oxygen
[NASA-TM-101956] N89-23691
KEROSENE
Spontaneous ignition of atomized kerosine/air mixtures in a high pressure flowing system
[NAL-TR-966] N89-23635
KINEMATICS
Modeling and simulation of a Stewart platform type parallel structure robot
[NASA-CR-184969] N89-23875
KINETIC ENERGY
Turbulence near a free surface in a plane jet
[AD-A206269] N89-23838
Design, fabrication and test of a 4750 Newton-meter-second double Gimbal control moment gyroscope N89-23896
Normal mode energetics of the general circulation during the FGGE year N89-24004
Energy disposal in ion-molecule reactions
[AD-A205987] N89-24144
KINETIC HEATING
The glass transition temperature (Tg) as a parameter for monitoring the cure of an amine-cured epoxy system at constant heating rates
[AD-A206098] N89-23705
KINETICS
Simultaneous measurement of spatially resolved electron temperatures. Electron number densities and gas temperatures by laser light scattering from the ICP
[AD-A205747] N89-24174
KLYSTRONS
Design of a 100 MW X-band klystron
[DE89-008939] N89-23793
KNOWLEDGE BASES (ARTIFICIAL INTELLIGENCE)
Expert systems applied to spacecraft fire safety
[NASA-CR-182266] N89-23501
KNOWLEDGE REPRESENTATION
The role of knowledge in visual shape representation
[AD-A206173] N89-24041
Knowledge representation using knowledge graphs: Application to theories on mathematical modeling and solving word problems
[MEMO-707] N89-24124
Knowledge representation using Structured Modeling N89-24224
KRYPTON
Ultra-high resolution VUV-XUV laser: Application to the hyperfine study of krypton
[DE89-009059] N89-23863

L

LAGRANGE COORDINATES
Bifurcating jets at high Reynolds numbers
[AD-A205718] N89-23829
LAMINAR BOUNDARY LAYER
On the Lagrangian description of unsteady boundary layer separation. Part 1: General theory
[NASA-TM-102026] N89-23821
Boundary layer and heat transfer behind a piston in a shock tube. Part 1: Theoretical considerations of laminar and turbulent boundary layer behind a piston in a tube
[ISL-R-111/87-PT-1] N89-23841
LAMINAR FLOW
An experimental study of laminar flow control airfoil with suction through perforated surface at low speed
[NAL-TR-967] N89-23806
The dimension of attractors underlying turbulent Poiseuille flow
[AD-A206021] N89-23835
LAMINATES
Mode 2 delamination fatigue resistance of composites N89-23624
Prediction and measurement of damping of a laminated beam with a constrained viscoelastic layer
[DE89-009002] N89-23922
Cracking of a layered medium on an elastic foundation under thermal shock
[NASA-CR-185316] N89-23925
LAND ICE
Non-Newtonian gravitational forces and the Greenland ice-sheet experiment
[DE89-009348] N89-23988
LAND USE
Computer assisted layout of graphic settlement representations N89-23951
LANDING SITES
Buran dimensions, landing sit facilities N89-23485
LANGEVIN FORMULA
The formation of topological defects in phase transitions
[NASA-CR-185318] N89-24215
LANTHANUM COMPOUNDS
Quasielastic and inelastic spin fluctuations in superconducting La2-xSrxCuO4
[DE89-008157] N89-24190
LARGE SPACE STRUCTURES
Increasing the margin of stability of arbitrarily finite modes of flexible large space structures with damping
[AD-A206487] N89-23507
Locating damaged members in a truss structure using modal test data: A demonstration experiment
[NASA-TM-101595] N89-23924
LASER ALTIMETERS
Monolithic GaAs digitizer for space-based laser pulse spreading effect
[NASA-CR-183430] N89-23855
LASER ANEMOMETERS
Three-dimensional laser anemometer study of compressible flow through orifice plates
[PB89-145098] N89-23808
A vector scanning processing technique for pulsed laser velocimetry
[NASA-TM-102048] N89-23850
LASER APPLICATIONS
High energy efficient solid state laser sources
[NASA-CR-181782] N89-23856
Effect of n on 1 laser treatment on damage threshold of selected optical coating
[DE89-008830] N89-23861
Simultaneous measurement of spatially resolved electron temperatures. Electron number densities and gas temperatures by laser light scattering from the ICP
[AD-A205747] N89-24174
Atomic layer epitaxy. Atomic layer epitaxy of 3-5 compound semiconductors by thermal and laser-assisted metalorganic chemical vapor deposition
[AD-A205699] N89-24200
LASER BEAMS
High-temperature LDV seed particle development
[NASA-CR-182265] N89-23851
Vaporization and recondensation in propagation and imaging of laser beams
[DE89-008014] N89-23858
LASER DAMAGE
Functional assessment of laser irradiation
[AD-A206230] N89-23871
Additivity of retinal damage for multiple-pulse laser exposures
[AD-A206514] N89-24032
LASER DOPPLER VELOCIMETERS
Three-dimensional laser anemometer study of compressible flow through orifice plates
[PB89-145098] N89-23808
High-temperature LDV seed particle development
[NASA-CR-182265] N89-23851
LASER HEATING
Numerical solution of the three dimensional heat flow equation generated by a moving source
[ISL-R-116/87] N89-23843
Experimental and theoretical determination of the thermomechanical response of inelastic structural materials to high energy thermal inputs
[AD-A206100] N89-23933
LASER INTERFEROMETRY
Summaries of papers presented at Short Wavelength Coherent Radiation: Generation and Applications Topical Meeting held in Cape Cod, Massachusetts on September 26-29, 1988
[AD-A205471] N89-23867
LASER MICROSCOPY
Summaries of papers presented at Short Wavelength Coherent Radiation: Generation and Applications Topical Meeting held in Cape Cod, Massachusetts on September 26-29, 1988
[AD-A205471] N89-23867

LASER MODES
High-power single spatial mode AlGaAs channeled-substrate-planar semiconductor diode lasers for spaceborne communications
[NASA-CR-4238] N89-23860
LASER OUTPUTS
High-power single spatial mode AlGaAs channeled-substrate-planar semiconductor diode lasers for spaceborne communications
[NASA-CR-4238] N89-23860
Effect of n on 1 laser treatment on damage threshold of selected optical coating
[DE89-008830] N89-23861
Laser photoelectric effect at surface of discharge cathode
[AD-A205741] N89-23869
Functional assessment of laser irradiation
[AD-A206230] N89-23871
Additivity of retinal damage for multiple-pulse laser exposures
[AD-A206514] N89-24032
LASER PLASMAS
Nonlinear spectroscopy of multicomponent droplets and two- and three-dimensional measurements in flames
[AD-A205449] N89-23645
Onset conditions for the driven lower hybrid drift instability in an expanding magnetized plasma
[AD-A205505] N89-24167
Numerical modeling of laser produced plasmas and laser induced pressure effects
[ISL-CO-244/87] N89-24177
LASER PUMPING
High energy efficient solid state laser sources
[NASA-CR-181782] N89-23856
Proof of the feasibility of coherent and incoherent schemes for pumping a gamma-ray laser
[AD-A205371] N89-23866
LASER SPECTROSCOPY
Ionization investigation of sputtered titanium and of titanium ion transport process in an argon discharge glow using laser induced fluorescence
[JUEL-2219] N89-23660
Research studies on extreme ultraviolet and soft X-ray lasers
[AD-A205625] N89-23868
LASER TARGET INTERACTIONS
Numerical modeling of laser produced plasmas and laser induced pressure effects
[ISL-CO-244/87] N89-24177
LASER WELDING
Direct laser/materials interaction: Laser ablation of superconductor materials and laser welding
[DE89-006560] N89-23857
LATCH-UP
Current distribution in a three-dimensional IC analyzed by a perturbation method. Part 1: A simple steady state theory
[NASA-CR-185022] N89-23494
Effects of space radiation on electronic microcircuits N89-23549
LATITUDE
Relativistic electron precipitation patterns in longitude and latitude: A reply to W. R. Sheldon
[NASA-CR-185442] N89-23995
LAUNCH VEHICLES
An analysis of lightning launch constraints
[AD-A206084] N89-23994
LAYOUTS
Computer assisted layout of graphic settlement representations N89-23951
LEAD ALLOYS
Macrosegregation and nucleation in undercooled Pb-Sn alloys
[NASA-TM-102023] N89-23664
LEADING EDGE FLAPS
Numerical study of the influence of leading and trailing edge flaps on the performance of airfoils
[AD-A206138] N89-23428
LEADING EDGE SWEEP
Experimental study of pressure and heating rate on a swept cylindrical leading edge resulting from swept shock wave interference
[NASA-CR-185326] N89-23411
LEADING EDGES
The low frequency oscillation in the flow over a NACA0012 airfoil with an iced leading edge
[NASA-TM-102018] N89-23417
LEAKAGE
Fiber optic leak detection system
[PB89-148886] N89-24150
LEARNING
Long term synaptic plasticity and learning in neuronal networks
[AD-A205993] N89-24038
LEAST SQUARES METHOD
SMOOFF: A FORTRAN smoothing program
[AD-A204087] N89-24057
Shape identification technique for a two-dimensional elliptic system by boundary integral equation method
[NASA-CR-181831] N89-24114
LETHALITY
White paper: Experimental and computational studies of very high velocity impacts
[DE89-007643] N89-23877
LEXAN (TRADEMARK)
An investigation of the temperature dependence of the ultrasonic properties of AS4/lexan and XAS/lexan composites
[NASA-CR-184845] N89-23619
LIBRATIONAL MOTION
A study of the motion in the neighborhood of the triangular libration point N89-24236
LIFE (DURABILITY)
Reentry materials in the atmosphere
[REPT-882-430-102] N89-23629
System Mean-Time-Between-Failure versus life-cycle logistics cost subject to the introduction of Line-Replaceable-Unit redundancy
[AD-A206324] N89-23887
LIFE CYCLE COSTS
System Mean-Time-Between-Failure versus life-cycle logistics cost subject to the introduction of Line-Replaceable-Unit redundancy
[AD-A206324] N89-23887
LIFT
High angle-of-attack aerodynamic characteristics of crescent and elliptic wings
[NASA-CR-184992] N89-23418
LIFT DEVICES
A closed-form trim solution yielding minimum trim drag for airplanes with multiple longitudinal-control effectors
[NASA-TP-2907] N89-23468
LIFTING REENTRY VEHICLES
Transonic aerodynamic characteristics of a proposed Assured Crew Return Capability (ACRC) lifting-body configuration
[NASA-TM-4117] N89-23412
LIGANDS
Solid-vapor adsorption refrigeration system development
[PB89-140859] N89-23733
Alternate arsenic and antimony sources for the OMCVD fabrication of semiconductors
[AD-A206483] N89-24211
LIGHT (VISIBLE RADIATION)
Biological results obtained by D1-mission N89-23732
LIGHT EMISSION
Co-aligning the RAIDS (Remote Atmospheric and Ionospheric Detection System) instruments
[AD-A205456] N89-23513
LIGHT MODULATION
Some 3-5 heterojunction structures and high speed devices
[AD-A205946] N89-24203
LIGHT SCATTERING
Simultaneous measurement of spatially resolved electron temperatures. Electron number densities and gas temperatures by laser light scattering from the ICP
[AD-A205747] N89-24174
LIGHTNING
An analysis of lightning launch constraints
[AD-A206084] N89-23994
LINE SPECTRA
Observations of the rotational transitions of OH from the Orion molecular cloud
[NASA-CR-184802] N89-24231
LINEAR ACCELERATORS
Design of a 100 MW X-band klystron
[DE89-008939] N89-23793
LINEAR ARRAYS
Near-far resistant linear multiuser detection
[AD-A206363] N89-23802
LINEAR EQUATIONS
GEMMES: A new tool for dynamic modeling
[REPT-882-440-114] N89-24078
Exploring the episodic structure of algebra story problem solving: Revision
[AD-A206403] N89-24122
Numerical conformal mapping and applications
[AD-A205602] N89-24131
LINEAR FILTERS
Performance analysis of Kalman filters
[PB89-146104] N89-23787
LINEAR SYSTEMS
Riemannian geometry on families of linear systems: The deterministic case
[PB89-146062] N89-24100
LINEAR VIBRATION
Nonlinear systems of conservation laws
[AD-A205837] N89-23830
LINEARITY
Multivariate analysis and its applications
[AD-A205585] N89-24125
LININGS
Surface treatment using metal foil liner N89-23533
Internal wire guide for GTAW welding
[NASA-CASE-MFS-29489-1] N89-23739
LIQUID AIR CYCLE ENGINES
Study of the PBE cycle 100kN LH2/LO2 rocket engine
[NAL-TR-965] N89-23514
LIQUID ALLOYS
Spray deposition: A fundamental study of droplet impingement, spreading and consolidation
[AD-A206065] N89-23672
Liquid dynamic compaction of Fe-Nd-B permanent magnets
[AD-A205632] N89-24135
LIQUID CHROMATOGRAPHY
Sample preparation techniques for evaluating methanol and formaldehyde emissions from methanol fueled vehicles and engines
[PB89-136147] N89-23734
LIQUID CRYSTALS
Quasi-liquid crystalline materials with special electro-optic properties
[AD-A206015] N89-24206
LIQUID HELIUM
SIRTF Telescope Instrument Changeout and Cryogen Replenishment (STICCR) Study
[NASA-CR-177380] N89-23512
LIQUID METALS
Temperature dependence of interfacial energies between solid oxides and liquid metals N89-23599
Diffusion N89-23724
Correlated atomic motions in liquid aluminum
[ETN-89-93943] N89-24145
LIQUID PHASES
Sintering of CaO and MgO in the presence of nonequilibrium liquid phase N89-23580
Sintering of Si3N4 in the presence of additives from Y2O3-SiO2-Al2O3 system N89-23581
LIQUID ROCKET PROPELLANTS
Chloride analysis in HAN-based liquid propellants by inductively coupled plasma spectroscopy
[AD-A206564] N89-23717
LIQUID SURFACES
Environmental interactions of hydrazine fuels in Soil/Water systems
[AD-A206244] N89-23986
LIQUID-SOLID INTERFACES
Interfacial reactions during cladding of steel by hot rolling N89-23615
LIQUID-VAPOR INTERFACES
Numerical studies of the effects of jet-induced mixing on liquid-vapor interface condensation
[NASA-CR-182285] N89-23618
LITERATURE
Environmental effects on spacecraft materials N89-23532
LITHIUM SULFUR BATTERIES
Li/FeS battery design for an electric van
[DE89-009808] N89-23794
LOAD DISTRIBUTION (FORCES)
Finite element modeling of frictionally restrained composite interfaces
[NASA-CR-182281] N89-23918
LOADS (FORCES)
Study on a highly sensitive electro-static suspended accelerometer (1)
[NAL-TR-1005] N89-23504
The effects of dielectric and metal loading on the dispersion characteristics for contrawound helix circuits used in high power traveling-wave tubes
[AD-A205345] N89-23797
Modeling and simulation of a Stewart platform type parallel structure robot
[NASA-CR-184969] N89-23875
Crack-face displacements for embedded elliptic and semi-elliptical surface cracks
[NASA-CR-181822] N89-23919
LOCAL AREA NETWORKS
Local area network technical guidelines. Volume 1: LAN design and planning (LAN TSR process)
[PB89-139091] N89-24080
LOG PERIODIC ANTENNAS
Instrument landing system mathematical modeling study for Orlando International Airport Runway 35L localizer, Orlando, Florida. Final airside docking plan (Scheme 3A)
[AD-A205351] N89-23438
LOGIC
Knowledge representation using Structured Modeling N89-24224

LOGIC CIRCUITS
A CAD (Computer Aided Design) tool for current-mode multiple-valued CMOS circuits
[AD-A205327] N89-24061
A database management system for computer-aided digital circuit design
[AD-A206047] N89-24066
Design of multiple-valued programmable logic arrays (PLA)
[AD-A205307] N89-24065
LOGIC PROGRAMMING
Explanation-based theory revision: An approach to the problems of incomplete and incorrect theories
[AD-A205337] N89-24092
LOGISTICS
System Mean-Time-Between-Failure versus life-cycle logistics cost subject to the introduction of Line-Replaceable-Unit redundancy
[AD-A206324] N89-23887
LOGISTICS MANAGEMENT
Defense Integrated Data System (DIDS) procedures manual. Volume 2: Multiple application procedures
[PB89-139307] N89-24221
LONG DURATION EXPOSURE FACILITY
The Long Duration Exposure Facility material experiments N89-23534
LONG DURATION SPACE FLIGHT
Space Station CMIF extended duration metabolic control test
[NASA-TM-100362] N89-23503
LONG TERM EFFECTS
The long-term effects of the micrometeoroid and orbital debris environments on materials used in space N89-23542
LONG WAVE RADIATION
Proof of the feasibility of coherent and incoherent schemes for pumping a gamma-ray laser
[AD-A205371] N89-23866
Capture and confinement of solutions in nonlinear integrable systems
[DE88-705823] N89-24106
LONGITUDE
Relativistic electron precipitation patterns in longitude and latitude: A reply to W. R. Sheldon
[NASA-CR-185442] N89-23995
LOOK ANGLES (ELECTRONICS)
The performance of Space-Based Radars (SBR) orbiting on elliptical orbits
[AD-A205951] N89-23772
LORAN C
Loran C field strength contours: Contiguous US
[DOT/FAA/CT-TN89/16] N89-23437
LOSSY MEDIA
Lossy layers: Theory and methods of measurement
[FOA-C-30513-3.2] N89-23779
LOW ALTITUDE
Ejector effects on a supersonic nozzle at low altitude and Mach number
[AD-A206049] N89-23427
LOW FREQUENCIES
The low frequency oscillation in the flow over a NACA0012 airfoil with an iced leading edge
[NASA-TM-102018] N89-23417
Electromagnetic remote sensing. Low frequency electromagnetics
[AD-A205402] N89-23761
An evaluation of coplanar line for application in microwave integrated circuitry
[AD-A205305] N89-23795
Use of a spectrally segmented photodiode-array spectrometer for inductively coupled plasma atomic emission spectroscopy
[AD-A205688] N89-24171
LOW GRAVITY MANUFACTURING
Research activity report concerning solidification technology under microgravity
[ETN-89-93988] N89-23718
Summary of 1st Summer School on Microgravity
[DFVLR-IB-333-87/2] N89-23719
Convection N89-23723
Diffusion N89-23724
Phase transformation N89-23725
Nucleation and undercooling N89-23726
Model systems --- metal alloys N89-23728
Organic monocrystals N89-23730
LOW TEMPERATURE
The concept and theoretical considerations of a cold weather clothing system
[AD-A205476] N89-24046
LOW TEMPERATURE ENVIRONMENTS
Treatment with tyrosine, a neurotransmitter precursor, reduces environmental stress in humans
[AD-A206035] N89-24039
LOW VISIBILITY
Heliport night parking area criteria test plan
[DOT/FAA/CT-TN88/45] N89-23480
LUBRICANTS
Corrosion and lubricity testing of nonflammable USAF formulated CTFE (Chlorotrifluoroethylene) base hydraulic fluid
[AD-A205467] N89-23695
The 23rd Aerospace Mechanisms Symposium
[NASA-CP-3032] N89-23892
LUBRICATION
Steel hardness effects in boundary lubricated sliding: An in-situ SEM (Scanning Electron Microscope) study
[AD-A206156] N89-23674
Ceramic tribology: Methodology and mechanisms of alumina wear
[PB89-148357] N89-23679
The in-vacuo torque performance of dry-lubricated ball bearings at cryogenic temperatures N89-23914
LUMINOSITY
Ground-based infrared observations of sources discovered by the AFGL, FIRRSE and IRAS infrared surveys
[AD-A206335] N89-24248
LUMINOUS INTENSITY
Laser photoelectric effect at surface of discharge cathode
[AD-A205741] N89-23889
LUNAR BASES
Photovoltaic power system considerations for future lunar bases
[NASA-TM-102019] N89-23517
LUNAR SOIL
Application of the method of X-ray fluorescence analysis with synchrotron radiation to study lunar matter
[DE88-705782] N89-24247
LYMAN SPECTRA
Redistribution in astrophysically important hydrogen lines
[NASA-CR-181375] N89-24251

M

MACH NUMBER
A numerical scheme to solve unsteady and variable density low Mach number flows N89-23419
Ejector effects on a supersonic nozzle at low altitude and Mach number
[AD-A206049] N89-23427
Computational study of high supersonic flow over boattails with centered propulsive jets
[AD-A206364] N89-23431
Experiment on a cylindrical scramjet combustor. 2: Simulated flight Mach number 6.7
[NAL-TR-969] N89-23464
MACHINING
Research needs in ceramic machining
[PB89-148191] N89-23681
Molded bodies having a high degree of hardness and a high degree of toughness for machining metals, carbides, ceramics and glasses
[DE89-008820] N89-23686
High speed abrasive belt grinding
[AD-A205618] N89-23741
MAGNESIUM OXIDES
Sintering of CaO and MgO in the presence of nonequilibrium liquid phase N89-23580
MAGNETIC CORES
Amorphous magnets N89-23605
On the correlation between microstructure and magnetic induction of porous iron and iron-Ni(0.4)Zn(0.6)Fe2O4 composites N89-23606
MAGNETIC DISKS
Exploring the North Atlantic Ocean on floppy disks
[AD-A205733] N89-24011
MAGNETIC DISTURBANCES
Geomagnetic disturbances
[AD-A206052] N89-24254
MAGNETIC FIELD CONFIGURATIONS
Transport of test particles in a magnetic field with perturbed magnetic surfaces
[IPP-2/296] N89-24176
MAGNETIC FIELDS
Design of a 100 MW X-band klystron
[DE89-008939] N89-23793
Operation of a quasi-optical gyrotron with variable mirror separation
[AD-A206347] N89-23854
Onset conditions for the driven lower hybrid drift instability in an expanding magnetized plasma
[AD-A205505] N89-24167
Solar-geophysical data number 531, part 1. Data for October, September 1988 and late data
[PB89-139943] N89-24250
MAGNETIC INDUCTION
On the correlation between microstructure and magnetic induction of porous iron and iron-Ni(0.4)Zn(0.6)Fe2O4 composites N89-23606
Electromagnetic remote sensing. Low frequency electromagnetics
[AD-A205402] N89-23761
MAGNETIC MEASUREMENT
High-temperature ceramic superconductors
[AD-A205321] N89-24196
MAGNETIC PERMEABILITY
Microstructure-permeability relation in MnZn ferrites prepared of iron oxide with chlorine impurities N89-23602
Magnetic susceptibility and neutron diffraction experiments on nuclear ordering in copper
[ISBN-951-754-573-8] N89-24189
MAGNETIC PROPERTIES
High-temperature ceramic superconductors
[AD-A205321] N89-24196
MAGNETIC STORMS
High-latitude field-strength measurements of standard broadcast band skywave transmissions monitored at Fairbanks, Alaska
[PB89-134829] N89-23747
MAGNETOHYDRODYNAMIC FLOW
Relativistic and non-relativistic magnetohydrodynamic flows around compact stars N89-24242
MAGNETOHYDRODYNAMIC STABILITY
Onset conditions for the driven lower hybrid drift instability in an expanding magnetized plasma
[AD-A205505] N89-24167
MAGNETOMETERS
Utilization of magnetostrictive optical fibers in multiple order gradiometers
[AD-D013960] N89-24155
MAGNETOPAUSE
Electric fields in the magnetosphere: The evidence from ISEE, S3-3, GEOS and Viking
[TRITA-EPP-88-11] N89-23987
MAGNETORESISTIVITY
Electrical transport properties of Hg0.7Cd0.3Te
[DE88-705689] N89-24183
MAGNETOSPHERE-IONOSPHERE COUPLING
Electric fields in the magnetosphere: The evidence from ISEE, S3-3, GEOS and Viking
[TRITA-EPP-88-11] N89-23987
Electrodynamics of cosmical plasmas: Some basic aspects of cosmological importance
[TRITA-EPP-89-02] N89-24163
MAGNETOSPHERIC ION DENSITY
The space particle environment N89-23548
MAGNETOSTATICS
Electromagnetic remote sensing. Low frequency electromagnetics
[AD-A205402] N89-23761
MAGNETOSTRICTION
Utilization of magnetostrictive optical fibers in multiple order gradiometers
[AD-D013960] N89-24155
MAGNETS
Amorphous magnets N89-23605
MAINTENANCE
Returned Solar Max hardware degradation study results N89-23537
Donor acceptor polymerization chemistry as a vehicle to low energy cure of matrix resins: Evolution of the 2-Tg concept to produce Tg polymers at ambient temperatures
[AD-A206287] N89-23706
System Mean-Time-Between-Failure versus life-cycle logistics cost subject to the introduction of Line-Replaceable-Unit redundancy
[AD-A206324] N89-23887
MAN MACHINE SYSTEMS
Generation of architectures for distributed intelligence systems
[AD-A205783] N89-23440
Payload experts in D1-mission N89-23722
Direct manipulation and other styles of man-machine interaction
[PB89-146070] N89-24043
The role of pilot and automatic onboard systems in future rendezvous and docking operations
[REPT-882-440-116] N89-24050
Signal-Noise/Interferer Combiner Unit Programmable (SINCUP)
[AD-A205367] N89-24053
MAN-COMPUTER INTERFACE
Direct manipulation and other styles of man-machine interaction
[PB89-146070] N89-24043
Human-machine interaction considerations for interactive software
[AD-A206574] N89-24049
User interface and highly interactive systems: Survey of current research
[PB89-146088] N89-24056

MANAGEMENT INFORMATION SYSTEMS
Advanced computing systems: An advanced reasoning-based development paradigm for Ada trusted systems and its application to MACH
[AD-A206308] N89-24070
Defense Integrated Data System (DIDS) procedures manual. Volume 2: Multiple application procedures
[PB89-139307] N89-24221
MANAGEMENT METHODS
Computer-based modeling environments
[AD-A205828] N89-24064
MANAGEMENT PLANNING
Generation of architectures for distributed intelligence systems
[AD-A205783] N89-23440
Reducing launch operations costs: New technologies and practices
[PB89-136402] N89-23500
Geographic Information Systems (GIS) guidelines document
[PB89-132062] N89-24222
MANAGEMENT SYSTEMS
A database management system for computer-aided digital circuit design
[AD-A206047] N89-24066
MANEUVERABILITY
Computation of flow around maneuvering submerged bodies
[AD-A205994] N89-23833
MANGANESE COMPOUNDS
Microstructure-permeability relation in MnZn ferrites prepared of iron oxide with chlorine impurities
N89-23602
MANIPULATORS
An application specific integrated circuit for dual-axis motion control
[DE89-007974] N89-23790
Modeling and simulation of a Stewart platform type parallel structure robot
[NASA-CR-184969] N89-23875
The 23rd Aerospace Mechanisms Symposium
[NASA-CP-3032] N89-23892
Traction-drive force transmission for telerobotic joints
N89-23906
Automated seed manipulation and planting
N89-24020
MANNED MARS MISSIONS
Medical and biological support for a manned expedition to Mars N89-23492
MANNED ORBITAL LABORATORIES
Agenda of the Fourth Annual Summer Conference, NASA/USRA University Advanced Design Program
[NASA-TM-101750] N89-23493
MANNED SPACE FLIGHT
JPRS report: Science and technology. USSR: Space
[JPRS-USP-89-004] N89-23484
Medical and biological support for a manned expedition to Mars N89-23492
MANY BODY PROBLEM
Memory functions and relaxation functions of some spin systems
[AD-A206340] N89-24137
MANY ELECTRON EFFECTS
Eikonal approximation in partial wave version
[IPPJ-899] N89-24164
MAPPING
KRMS (K-band Radiometric Mapping System) SSM/I validation March 1988 quick look report
[NASA-CR-185320] N89-23766
MARANGONI CONVECTION
Convection N89-23723
MARINE METEOROLOGY
The diurnal variation of a marine stratocumulus layer: A model sensitivity study N89-24000
MARINE PROPULSION
Mobile nuclear power systems
[FOA-C-20743-4.1] N89-24149
MARKET RESEARCH
On the international commercialization of remote sensing
[BCRS-88-02] N89-23969
MARKETING
NASA space communications R and D (Research and Development): Issues, derived benefits, and future directions
[NASA-CR-184831] N89-23746
MARKOV CHAINS
Microcomputer program for daily weather simulation
[PB89-144638] N89-24001
MARKOV PROCESSES
Second-order moments of a stationary Markov chain and some applications
[AD-A206366] N89-24128
MARS ATMOSPHERE
Orbit parameters given N89-23491
Medical and biological support for a manned expedition to Mars N89-23492
MARS SAMPLE RETURN MISSIONS
Preliminary assessment of rover power systems for the Mars Rover Sample Return Mission
[NASA-TM-102003] N89-23518
MARS SURFACE
Orbit parameters given N89-23491
MARTENSITE
Twin boundaries, interfaces and modulated structures in martensites
[DE89-009064] N89-23662
MARTINGALES
Approximation of stochastic integral equations using Martingale difference schemes
[ETN-89-93951] N89-24123
MASERS
Development of high power CARM (Cyclotron Auto-Resonance Maser) oscillators
[AD-A206270] N89-23872
MASS
A study of the motion in the neighborhood of the triangular libration point N89-24236
MASS FLOW
Transonic operational characteristics and performance
[NAL-TR-968] N89-23408
Navier-Stokes solution for a NACA 0012 airfoil with mass flux (fan)
[AD-A205771] N89-23424
MASS SPECTROMETERS
Neutral primary beam SIMS analysis of ceramic materials N89-23601
Noise characteristics of an inductively coupled plasma-mass spectrometer
[AD-A205686] N89-24169
MASS SPECTROSCOPY
Neutral primary beam SIMS analysis of ceramic materials N89-23601
Preliminary evaluation of a miniaturized torch for inductively coupled plasma mass spectrometry
[AD-A205746] N89-24173
MASS TRANSFER
An analysis of the attitude stability of a space station subject to parametric excitation of periodic mass motion
[AD-A206009] N89-23505
MATERIALS HANDLING
Automated seed manipulation and planting
N89-24017
Automated seed manipulation and planting
N89-24020
MATERIALS RECOVERY
Intelligent processing of materials
[PB89-151823] N89-23735
MATERIALS SCIENCE
Materials science cooperation in 1987 N89-23570
MATHEMATICAL MODELS
Computing induced velocity perturbations due to a helicopter fuselage in a free stream
[NASA-TM-4113] N89-23410
Development of harmonic panel methods for aeroelastic applications to elastic bodies and body-fin combinations in supersonic flow
[AD-A205739] N89-23423
Numerical study of the influence of leading and trailing edge flaps on the performance of airfoils
[AD-A206138] N89-23428
Instrument landing system mathematical modeling study for Orlando International Airport Runway 35L localizer, Orlando, Florida. Final airside docking plan (Scheme 3A)
[AD-A205351] N89-23438
Autonomous navigation and control
[AD-A205898] N89-23441
Optimal aeroassisted coplanar orbital transfer using an energy model
[NASA-CR-181778] N89-23495
Assembling the ISO thermal model with ESAT AN
[REPT-882-440-107] N89-23510
Trapped particle flux models at NSSDC/WDC-A-R/S
N89-23561
Behavior of metals during hot rolling processes. Part 1: Mathematical models N89-23613
The dynamic behavior of water vapor on activated carbon
[AD-A206124] N89-23628
Solidification of binary substances in rectangular and cylindrical cavities
[DE89-008883] N89-23640
Autofocus of SAR imagery degraded by ionospheric-induced phase errors
[DE89-008278] N89-23752
Sea spike modeling
[AD-A205355] N89-23760
Mechanical/electrical distortion model for reflector antennas
[REPT-882-440-104] N89-23781
Performance analysis of Kalman filters
[PB89-146104] N89-23787
Numerical simulation of Goertler/Tollmein-Schlichting wave-interaction
[NASA-CR-181823] N89-23817
Numerical studies of the effects of jet-induced mixing on liquid-vapor interface condensation
[NASA-CR-182285] N89-23818
Two-dimensional numerical simulation of a Stirling engine heat exchanger
[NASA-TM-102057] N89-23823
Mathematical analysis of strong fluid mechanical effects in reacting and nonreacting gases
[AD-A206336] N89-23839
A simple approximate method to evaluate the 3-D aerodynamic field around a streamline and to determine the validity of the quasi-three dimensional hypothesis
[ETN-89-94366] N89-23844
A numerical investigation of thin-film heat transfer gages
[AD-A206134] N89-23853
Numerical simulation of the dissociation of I2 by O2 (1 Delta) in a two dimensional parallel jet
[AD-A206137] N89-23870
Finite element modeling of frictionally restrained composite interfaces
[NASA-CR-182281] N89-23918
Crack-face displacements for embedded elliptic and semi-elliptical surface cracks
[NASA-CR-181822] N89-23919
Locating damaged members in a truss structure using modal test data: A demonstration experiment
[NASA-TM-101595] N89-23924
Quadratic optimal control theory for viscoelastically damped structures using a fractional derivative viscoelasticity model
[AD-A206008] N89-23932
A combined isotropic-kinematic hardening model for large deformation metal plasticity
[AD-A206352] N89-23935
On the connection of geodetic pointfields in RETng
[PB89-146112] N89-23958
Stratocumulus modeling
[KNMI-WR-88-2] N89-23997
Turbulent structure of a shear-driven stratus-topped atmospheric boundary layer: A comparison of model results with observations N89-23999
The diurnal variation of a marine stratocumulus layer: A model sensitivity study N89-24000
Improved sea surface scattering model
[AD-A205745] N89-24012
Computer-based modeling environments
[AD-A205828] N89-24064
GEMMES: A new tool for dynamic modeling
[REPT-882-440-114] N89-24078
Asymptotic behavior of random discrete event systems
[PB89-146146] N89-24099
Solid modeling requirements for finite element modeling using mapped mesh techniques
[DE89-009639] N89-24110
Numerical simulation of flow through an artificial heart
[NASA-TM-102183] N89-24111
Inverse problem techniques for beams with tip body and time hysteresis damping
[NASA-CR-181833] N89-24112
Discrete event simulation model decomposition
[AD-A206048] N89-24119
Knowledge representation using knowledge graphs: Application to theories on mathematical modeling and solving word problems
[MEMO-707] N89-24124
A demonstration of the method of stochastic finite element analysis
[AD-A206135] N89-24127
Symbolic analysis of multivariable missile systems
[AD-A206326] N89-24132
Modeling of a continuous oscillator by oscillators with a finite number of degrees of freedom
[PB89-146120] N89-24134
High speed turboprop aeroacoustic study (single rotation). Volume 1: Model development
[NASA-CR-182257-VOL-1] N89-24139
Eikonal approximation in partial wave version
[IPPJ-899] N89-24164
Numerical modeling of laser produced plasmas and laser induced pressure effects
[ISL-CO-244/87] N89-24177
MATHEMATICAL PROGRAMMING
Analysis and optimization of geodetic networks by spectral criteria and mechanical analogies
[SER-C-342] N89-23963
MATRICES (MATHEMATICS)
Wavefront matrix multiplication on a distributed-memory multiprocessor
[PB89-151807] N89-24052

Reduction of a general matrix to tridiagonal form
[DE89-008980] N89-24083
Riemannian geometry on families of linear systems: The deterministic case
[PB89-146062] N89-24100
Equations for two-dimensional density matrix. Approximate solutions in the vicinity of the classical solution
[DE88-705825] N89-24107
Numerical experience with a superfast real Toeplitz solver
[AD-A205374] N89-24115
Krylov methods preconditioned with incompletely factored matrices on the CM-2
[AD-A206389] N89-24121

MATRIX MATERIALS
Surface treatment using metal foil liner N89-23533
An investigation of the temperature dependence of the ultrasonic properties of AS4/Iexan and XAS/Iexan composites
[NASA-CR-184845] N89-23619
Theoretical analysis of compatibility of several reinforcement materials with NiAl and FeAl matrices
[NASA-CR-182291] N89-23622
Preparation and evaluation of silicon nitride matrices for silicon nitride-SiC fiber composites
[NASA-CR-184798] N89-23678
Donor acceptor polymerization chemistry as a vehicle to low energy cure of matrix resins: Evolution of the 2-Tg concept to produce Tg polymers at ambient temperatures
[AD-A206287] N89-23706

MATRIX THEORY
A blocked Jacobi method for the symmetric Eigenproblem
[AD-A206553] N89-24133

MAXIMUM LIKELIHOOD ESTIMATES
Second-order moments of a stationary Markov chain and some applications
[AD-A206366] N89-24128

MEASURING INSTRUMENTS
Effects of the contamination environment on surfaces and materials N89-23546
A numerical investigation of thin-film heat transfer gages
[AD-A206134] N89-23853
Summary of achievements in scientific research
[AD-A199947] N89-24227

MECHANICAL DEVICES
Eddy current damper N89-23900
Astronaut tool development: An orbital replaceable unit-portable handhold N89-23904
Flight telerobot mechanism design: Problems and challenges N89-23907

MECHANICAL DRIVES
A family of BAPTAs for GEO and LEO applications N89-23908
Practical experiences with worm gearing for spacecraft power transmission applications N89-23912

MECHANICAL MEASUREMENT
Design and development of a high-stiffness, high-resolution torque sensor N89-23903

MECHANICAL PROPERTIES
Flowfield measurements in the vortex wake of a missile at high angle of attack in turbulence
[AD-A205696] N89-23422
Effect of physical annealing on the dynamic mechanical properties of a high T(g) amine-cured epoxy systems
[AD-A205980] N89-23704
Electronic and ionic transport in polymers
[AD-A206530] N89-23709
Lattice symmetries and thermal expansion
[AD-A206045] N89-24207

MECHANICAL TWINNING
Deformation twinning in ordered intermetallic compounds
[DE89-008748] N89-24192

MEDICAL SCIENCE
A strategy for space biology and medical science for the 1980s and 1990s
[NASA-CR-184895] N89-24024

MELTING
Metallic solidification N89-23727
Response of pavement to freeze-thaw cycles: Lebanon, New Hampshire, regional airport
[AD-A205559] N89-23740
Mapping freeze/thaw boundaries with SMMR data
[NASA-CR-184991] N89-23961

MEMBRANES
Measuring conductivities of highly conductive membranes
[AD-A206043] N89-23649
Structure/permeability relationships of silicon-containing polyimides
[NASA-CR-4237] N89-23683

MEMORY
Long term synaptic plasticity and learning in neuronal networks
[AD-A205993] N89-24038

MEMORY (COMPUTERS)
Wavefront matrix multiplication on a disributed-memory multiprocessor
[PB89-151807] N89-24052
Compiling high level constructs to distributed memory architectures
[NASA-CR-181825] N89-24058
A method of up-front load balancing for local memory parallel processors
[NASA-CASE-MSC-21348-1] N89-24084

MENTAL PERFORMANCE
The attention system of the human brain
[AD-A206157] N89-24040

MERCURY CADMIUM TELLURIDES
Fundamental and practical studies of metal contacts on mercury zinc telluride
[AD-A206560] N89-23653
High pressure studies on infrared detector materials
[NAL-TM-MT-8701] N89-23677
Electrical transport properties of Hg0.7Cd0.3Te
[DE88-705689] N89-24183

MERCURY TELLURIDES
Fundamental and practical studies of metal contacts on mercury zinc telluride
[AD-A206560] N89-23653
High pressure studies on infrared detector materials
[NAL-TM-MT-8701] N89-23677

MESOPAUSE
Mesospheric wind measurement
[AD-A205593] N89-23991

MESSAGE PROCESSING
An evaluation of the F/FB/EF-111 crew/voice message system
[AD-A205998] N89-23774
Wavefront matrix multiplication on a distributed-memory multiprocessor
[PB89-151807] N89-24052
Compiling high level constructs to distributed memory architectures
[NASA-CR-181825] N89-24058
On the communication complexity of distributed algebraic computation
[AD-A205784] N89-24117

METAL BONDING
In situ mechanistic studies of MOCVD growth of 3/5 semiconductors
[AD-A206396] N89-24210

METAL COATINGS
Testing chromium adhesion using acoustic emission
[AD-A205621] N89-23665

METAL FATIGUE
USAF (US Air Force) durability design handbook: Guidelines for the analysis and design of durable aircraft structures
[AD-A206286] N89-23457
Fatigue crack growth model RANDOM2 user manual, appendix 1
[NASA-CR-184939] N89-23890
Fatigue strength reduction model: RANDOM3 and RANDOM4 user manual, appendix 2
[NASA-CR-184940] N89-23891
Cyclic crack propagation characteristics of the powder metallurgical nickel-base alloy Udimet 720 at elevated temperatures and different dwell times
[ETN-89-94426] N89-23936

METAL FILMS
Control of the composition of electrodeposited alloys by the use of certain types of additives
[AD-A206370] N89-23675
Photoabsorption of molecules at corrugated thin metal films
[AD-A205325] N89-24197
Decay of molecules at corrugated thin metal films
[AD-A205487] N89-24198

METAL FOILS
Surface treatment using metal foil liner N89-23533

METAL IONS
Spectroscopic studies of metal-ligand-surface interactions
[AD-A206460] N89-23652
Chloride analysis in HAN-based liquid propellants by inductively coupled plasma spectroscopy
[AD-A206564] N89-23717
Environmental interactions of hydrazine fuels in Soil/Water systems
[AD-A206244] N89-23986

METAL MATRIX COMPOSITES
Effects of thermal cycling on composite materials for space structures N89-23552
Theoretical analysis of compatibility of several reinforcement materials with NiAl and FeAl matrices
[NASA-CR-182291] N89-23622
Fabrication of unidirectional fiber reinforced 6061 aluminum alloy using high pressure squeeze casting
[AD-A205717] N89-23668
Shock compaction of YBa2Cu3O7-x and HoBa2Cu3O7-x powders in a metal matrix
[DE89-008827] N89-24193

METAL OXIDE SEMICONDUCTORS
Microstructure and phase development in multicomponent ZnO based varistor ceramics N89-23604

METAL POWDER
Production of metal powders by rotating electrode process N89-23608
Physico-mathematical investigation of the consolidation of iron powder N89-23617
Ambient temperature properties of PM (Powder Metal) aluminum-titanium alloys
[AD-A205997] N89-23671
Institute for Materials Science and Engineering, nondestructive evaluation: Technical activities 1988
[PB89-151625] N89-23884
Fundamental and applied studies of explosively fabricated high-temperature superconducting fixtures
[AD-A205953] N89-24204

METAL PROPELLANTS
An experimental investigation in the behavior of metallized solid propellants
[AD-A206510] N89-23715

METAL SURFACES
Oxygen interaction with metal surfaces: Surface science approach N89-23596
Stability and instability of anodically formed layers on metallic surfaces N89-23597
Spectroscopic studies of metal-ligand-surface interactions
[AD-A206460] N89-23652
Simple adsorbates on transition metal surfaces: A joint chemical and physical approach
[AD-A205726] N89-23669
Environmental interactions of hydrazine fuels in Soil/Water systems
[AD-A206244] N89-23986

METAL WORKING
Fabrication of unidirectional fiber reinforced 6061 aluminum alloy using high pressure squeeze casting
[AD-A205717] N89-23668
Institute for Materials Science and Engineering, nondestructive evaluation: Technical activities 1988
[PB89-151625] N89-23884

METALLIC GLASSES
Metallic solidification N89-23727

METALLIC PLASMAS
Chloride analysis in HAN-based liquid propellants by inductively coupled plasma spectroscopy
[AD-A206564] N89-23717

METALLIZING
An experimental investigation in the behavior of metallized solid propellants
[AD-A206510] N89-23715

METALLOGRAPHY
Control of the composition of electrodeposited alloys by the use of certain types of additives
[AD-A206370] N89-23675

METALS
The 8th German-Yugoslav Meeting on Materials Science and Development: Ceramics and Metals
[JUEL-SPEZ-446] N89-23569
Molded bodies having a high degree of hardness and a high degree of toughness for machining metals, carbides, ceramics and glasses
[DE89-008820] N89-23686
The effects of dielectric and metal loading on the dispersion characteristics for contrawound helix circuits used in high power traveling-wave tubes
[AD-A205345] N89-23797

METEORITES
Overview of environmental factors N89-23529

METEORITIC DAMAGE
Micrometeoroids and debris N89-23558

METEOROLOGICAL PARAMETERS
Microcomputer program for daily weather simulation
[PB89-144638] N89-24001
A reduced version of the NMC DERF 2 data set
[NASA-TM-100727] N89-24002
Surface Observation Climatic Summaries (SOCS) for NASA Shuttle Landing Facility, Florida
[AD-A205362] N89-24007
The US Army Yuma Proving Ground, Arizona 33-year climate calendar and tables on associated weather elements 1954-1986. American desert country
[AD-A206256] N89-24010

METEOROLOGICAL RADAR
Design of the ELDORA airborne Doppler radar
[PB89-144604] N89-23749

ASR-9 weather channel test report, executive s ummary
[DOT/FAA/PS-89/6-EXEC-SUMM] N89-23758
Studies of frontal zone dynamics with a high-resolution wind profiling system
[AD-A205988] N89-24008
METEOSAT SATELLITE
Near field testing of the electronically despun antenna of the Meteosat satellite
[REPT-882-440-108] N89-23783
Meteosat thermal inertia mapping for studying wetland dynamics in the West-African Sahel
[BCRS-88-10A] N89-23970
METHODOLOGY
Design of a methodology for the detection of errors in tarrestrial networks
[ETN-89-94151] N89-23968
METHYL ALCOHOL
Sample preparation techniques for evaluating methanol and formaldehyde emissions from methanol fueled vehicles and engines
[PB89-136147] N89-23734
Methanol vehicle catalyst evaluation, phase 3
[PB89-136139] N89-23874
METHYL COMPOUNDS
Polyethylene glycol-poly(2-methyl-5-vinyl tetrazole) polymer blend: A desensitizing binder for propellants and explosives
[AD-A206563] N89-23716
METROLOGY
Metrology for Electromagnetic Technology: A bibliography of NBS (National Bureau of Standards) publications, January 1970 - August 1988
[PB89-147847] N89-23748
MICROANALYSIS
Atomic imaging and microanalysis of ceramics
[DE89-008172] N89-23684
Site occupancy/valence measurements using channelling and related effects in microanalysis
[DE89-007658] N89-24186
Application of the method of X-ray fluorescence analysis with synchrotron radiation to study lunar matter
[DE88-705782] N89-24247
MICROCLIMATOLOGY
Evaluation of three commercial microclimate cooling systems
[AD-A206318] N89-23744
MICROCOMPUTERS
Noise and sonic boom impact technology. PCBOOM computer program for sonic boom research, volume 1
[AD-A206290] N89-23429
Noise and sonic boom impact technology. PCBOOM computer program for sonic boom research. Volume 2: Program Users/Computer operations manual
[AD-A206291] N89-23430
Microcomputer program for daily weather simulation
[PB89-144638] N89-24001
Monitoring information processing and decisions: The MOUSELAB system
[AD-A205963] N89-24037
MICROELECTRONICS
Effects of space radiation on electronic microcircuits N89-23549
Nano- and microstructures in chemistry, electrochemistry, and materials science
[AD-A206296] N89-23650
Fundamental studies of the mechanical behavior of microelectronic thin film materials
[AD-A206057] N89-24208
Engineering thrust areas, 1989
[DE89-009009] N89-24229
MICROHARDNESS
Preparation and evaluation of silicon nitride matrices for silicon nitride-SiC fiber composites
[NASA-CR-184798] N89-23678
MICROMETEORITES
Calibration measurements on micrometeorite detectors for the missions ULYSSES, Galileo and Giotto
[ETN-89-93947] N89-24248
MICROMETEOROIDS
NASA/SDIO Space Environmental Effects on Materials Workshop, part 1
[NASA-CP-3035-PT-1] N89-23528
The long-term effects of the micrometeoroid and orbital debris environments on materials used in space N89-23542
Orbital debris environment and data requirements N89-23543
NASA/SDIO Space Environmental Effects on Materials Workshop, part 2
[NASA-CP-3035-PT-2] N89-23547
Micrometeoroids and debris N89-23558
Working group written presentation: Meteoroid/orbital debris effects on materials N89-23565
MICROMINIATURIZATION
Summaries of papers presented at Short Wavelength Coherent Radiation: Generation and Applications Topical Meeting held in Cape Cod, Massachusetts on September 26-29, 1988
[AD-A205471] N89-23867
MICROORGANISMS
The mechanisms of biodegradation of synthetic polymers
[AD-A205628] N89-23699
Drag and noise measurements on underwater vehicles with a riblet surface coating
[AD-A205500] N89-23825
MICROPOROSITY
Microporous fumed-silica insulation board as a candidate Standard Reference Material of thermal resistance
[PB89-148373] N89-24213
MICROPROCESSORS
An application specific integrated circuit for dual-axis motion control
[DE89-007974] N89-23790
MICROSTRIP TRANSMISSION LINES
Small UHF microstrip radiating element
[REPT-882-440-103] N89-23780
MICROSTRUCTURE
Microstructure development in alumina N89-23579
Microstructure development in SiC N89-23582
Strengthening of silicon nitride ceramics N89-23585
Microstructure-permeability relation in MnZn ferrites prepared of iron oxide with chlorine impurities N89-23602
Microstructure and phase development in multicomponent ZnO based varistor ceramics N89-23604
On the correlation between microstructure and magnetic induction of porous iron and iron-Ni(0.4)Zn(0.6)Fe2O4 composites N89-23606
Carbon fiber thermal conductivity measurement and analysis
[AD-A205682] N89-23625
Ultrafine microstructure composites prepared by chemical vapor deposition
[AD-A206061] N89-23627
Nano- and microstructures in chemistry, electrochemistry, and materials science
[AD-A206296] N89-23650
Ambient temperature properties of PM (Powder Metal) aluminum-titanium alloys
[AD-A205997] N89-23671
Preparation and evaluation of silicon nitride matrices for silicon nitride-SiC fiber composites
[NASA-CR-184798] N89-23678
Atomic imaging and microanalysis of ceramics
[DE89-008172] N89-23684
Report on the partial support of the 1988 Gordon Conference on Polymers (West)
[AD-A205834] N89-23701
Mechanisms of diffusion-controlled brittle fracture
[DE89-008728] N89-23921
Shock compaction of YBa2Cu3O7-x and HoBa2Cu3O7-x powders in a metal matrix
[DE89-008827] N89-24193
Grain boundaries
[DE89-008881] N89-24194
MICROWAVE CIRCUITS
An evaluation of coplanar line for application in microwave integrated circuitry
[AD-A205305] N89-23795
MICROWAVE EMISSION
Population inversions in ablation plasmas generated by intense electron beams
[AD-A205716] N89-24172
MICROWAVE EQUIPMENT
Engineering thrust areas, 1989
[DE89-009009] N89-24229
MICROWAVE IMAGERY
Remote sensing of global snowpack energy and mass balance: In-situ measurements on the snow of interior and Arctic Alaska
[NASA-CR-180078] N89-23956
MICROWAVE LANDING SYSTEMS
Instrument landing system mathematical modeling study for Orlando International Airport Runway 35L localizer, Orlando, Florida. Final airside docking plan (Scheme 3A)
[AD-A205351] N89-23438
Crew procedures and workload of retrofit concepts for microwave landing system
[NASA-CR-181700] N89-24033
MICROWAVE OSCILLATORS
Megavolt, multi-kiloamp K{sub }a-band gyrotron oscillator experiment
[AD-A206271] N89-23801
MICROWAVES
An improved strategy for determining earth satellite orbits by radio
[AD-A205826] N89-23497
Microwave processing of ceramics
[DE89-009350] N89-23690
KRMS (K-band Radiometric Mapping Sysiem) SSM/I validation March 1988 quick look report
[NASA-CR-185320] N89-23766
An evaluation of coplanar line for application in microwave integrated circuitry
[AD-A205305] N89-23795
MIDAIR COLLISIONS
Annual review of aircraft accident data, US Air Carrier operations: Calendar year 1986
[PB89-151021] N89-23434
MILITARY OPERATIONS
Battlefield radar imaging through airborne millimetric wave SAR (Synthetic Aperture Radar)
[ETN-89-94228] N89-23751
Design of a MANPRINT tool for predicting personnel and training characteristics implied by system design
[AD-A206201] N89-24048
MILITARY TECHNOLOGY
IDA (Institute for Defense Analyses) gamma-ray laser: Investigation of the feasibility of developing a laser using nuclear transitions
[AD-A205318] N89-23864
IDA (Institute for Defense Analyses) gamma-ray laser: Investigation of developing a laser using nuclear transitions
[AD-A205319] N89-23865
MILLIMETER WAVES
Battlefield radar imaging through airborne millimetric wave SAR (Synthetic Aperture Radar)
[ETN-89-94228] N89-23751
Attenuation measurement of very low-loss dielectric waveguides by the cavity resonator method in the millimeter/submillimeter wavelength range
[AD-A206458] N89-23803
MILLING MACHINES
Research needs in ceramic machining
[PB89-148191] N89-23681
MINIATURIZATION
Preliminary evaluation of a miniaturized torch for inductively coupled plasma mass spectrometry
[AD-A205746] N89-24173
MINKOWSKI SPACE
The geometry of plane waves in spaces of constant curvature N89-24241
MIRRORS
Dynamic fatigue of ultralow-expansion glass for space mirrors, reissue A
[AD-A205401] N89-23694
A segmented mirror antenna for radiometers
[NASA-TM-102045] N89-23753
Operation of a quasi-optical gyrotron with variable mirror separation
[AD-A206347] N89-23854
Assessment of surface topography by X-ray scattering measurements
[MPE-PREPRINT-134] N89-24159
MISSILE COMPONENTS
Missile actuator simulation and an investigation into the accuracy of Runge-Kutta numerical integration
[AD-A206325] N89-23458
Structural mode frequencies of FOG-M (Fiber Optics Guided-Missile) actuator/fin
[AD-A206327] N89-24158
MISSILE CONFIGURATIONS
Average-passage simulation of counter-rotating propfan propulsion systems as applied to cruise missiles
[NASA-TM-102043] N89-23416
MISSILE CONTROL
An investigation into the application of dynamic programming to determine optimal controls for tracking a cruise missile maneuver by CMMCA (Cruise Missile Mission Control Aircraft)
[AD-A205970] N89-23456
Pif-Paf piloting of tactical missiles
[REPT-882-320-104] N89-23462
MISSILE DEFENSE
Pif-Paf piloting of tactical missiles
[REPT-882-320-104] N89-23462
MISSILE DESIGN
Pif-Paf piloting of tactical missiles
[REPT-882-320-104] N89-23462
Modal analysis and testing of missile systems
[AD-A204051] N89-23916
MISSILE SYSTEMS
Navigation shift correction by radar cartography. Optimization and validation by simulation
[REPT-882-320-103] N89-23755
Symbolic analysis of multivariable missile systems
[AD-A206326] N89-24132

MISSILE TRACKING
An investigation into the application of dynamic programming to determine optimal controls for tracking a cruise missile maneuver by CMMCA (Cruise Missile Mission Control Aircraft)
[AD-A205970] N89-23456
Enhanced tracking of ballistic targets using forward looking infrared measurements
[AD-A205727] N89-23760
MISSILE TRAJECTORIES
Computational study of high supersonic flow over boattails with centered propulsive jets
[AD-A206364] N89-23431
Enhanced tracking of ballistic targets using forward looking infrared measurements
[AD-A205727] N89-23760
MISSILE VIBRATION
Modal analysis and testing of missile systems
[AD-A204051] N89-23916
MISSILES
Flowfield measurements in the vortex wake of a missile at high angle of attack in turbulence
[AD-A205696] N89-23422
Missile actuator simulation and an investigation into the accuracy of Runge-Kutta numerical integration
[AD-A206325] N89-23458
Symbolic analysis of multivariable missile systems
[AD-A206326] N89-24132
MIXED CRYSTALS
Cohesive and anharmonic elastic properties of mixed fluorite crystals
[DE86-705690] N89-24184
MODAL RESPONSE
Modal analysis and testing of missile systems
[AD-A204051] N89-23916
MODEL REFERENCE ADAPTIVE CONTROL
Multiple model-based robot control: Development and initial evaluation
[AD-A205725] N89-23881
MODELS
Assignment of the charge-transfer excited states of bis(N-heterocyclic) complexes of copper(I)
[AD-A206012] N89-24205
MODFETS
Characterization of semiconductor device processing etchant solutions for GaAs and p+ GaAs layers employed in AlxGa(1-x)As/GaAs MODFETs and related heterojunction devices
[AD-A205772] N89-24201
MODULES
Adaptive signal processing
[AD-A205787] N89-24063
MODULUS OF ELASTICITY
Young's modulus of elasticity: Measured values for multiphase metals and their calculation via the bound concept N89-23584
Theoretical analysis of compatibility of several reinforcement materials with NiAl and FeAl matrices
[NASA-CR-182291] N89-23622
MOISTURE CONTENT
Determination of areal snow water equivalent using satellite images and gamma ray spectrometry
[CI-91] N89-23960
MOLECULAR ABSORPTION
Assignment of the charge-transfer excited states of bis(N-heterocyclic) complexes of copper(I)
[AD-A206012] N89-24205
MOLECULAR CLOUDS
Observations of the rotational transitions of OH from the Orion molecular cloud
[NASA-CR-184802] N89-24231
A self consistant model of the three phase interstellar medium in disk galaxies N89-24245
MOLECULAR COLLISIONS
Spectrometric studies of gas phase collision processes
[AD-A205570] N89-23826
MOLECULAR INTERACTIONS
Energy disposal in ion-molecule reactions
[AD-A205987] N89-24144
MOLECULAR RELAXATION
Spectrometric studies of gas phase collision processes
[AD-A205570] N89-23826
MOLECULAR STRUCTURE
Light weight polymer matrix composite material
[NASA-CASE-LEW-14734-1] N89-23623
Structure/permeability relationships of silicon-containing polyimides
[NASA-CR-4237] N89-23683
Atomic relaxation and vacancy-interstitial recombination in Zr and Zr3Al
[AD-A205664] N89-24199
MOLECULES
A user's guide to the Molecular Modeling, Analysis and Display System (MMADS), 2nd edition
[AD-A205674] N89-23648
Parametric study of radiative cooling of solid antihydrogen
[AD-A206092] N89-23742
Photoabsorption of molecules at corrugated thin metal films
[AD-A205325] N89-24197
Decay of molecules at corrugated thin metal films
[AD-A205487] N89-24198
MOLTEN SALT ELECTROLYTES
Viscosity and conductance of MEICI/AICI3 melts containing nonaqueous solvents
[AD-A205468] N89-23646
MOLYBDENUM
Flow-injection analysis utilizing a spectrally segmented photodiode-array inductively coupled plasma emission spectrometer. 1: Microcolumn preconcentration for the determination of molybdenum
[AD-A205687] N89-24170
Use of a spectrally segmented photodiode-array spectrometer for inductively coupled plasma atomic emission spectroscopy
[AD-A205688] N89-24171
MOMENTUM TRANSFER
Comparison of split-film and x-film measurements in 2-D flow
[AD-A206023] N89-23836
Turbulence near a free surface in a plane jet
[AD-A206269] N89-23838
MONITORS
Simulator evaluation of a display for a Takeoff Performance Monitoring System
[NASA-TP-2908] N89-23469
Plant health sensing N89-24018
Non-destructive plant health sensing using absorption spectroscopy N89-24021
Monitoring information processing and decisions: The MOUSELAB system
[AD-A205963] N89-24037
Monitoring thin film properties with surface acoustic wave devices: Diffusion, surface area and pore size distribution
[DE89-009379] N89-24195
MONOMERS
Mechanical behavior of PMMA-impregnated silica gels
[AD-A205975] N89-23703
Donor acceptor polymerization chemistry as a vehicle to low energy cure of matrix resins: Evolution of the 2-Tg concept to produce Tg polymers at ambient temperatures
[AD-A206287] N89-23706
MONTE CARLO METHOD
Young's modulus of elasticity: Measured values for multiphase metals and their calculation via the bound concept N89-23584
A demonstration of the method of stochastic finite element analysis
[AD-A206135] N89-24127
The formation of topological defects in phase transitions
[NASA-CR-185318] N89-24215
MONTMORILLONITE
Sorption of selected volatile organic constituents of jet fuels and solvents on natural sorbents from gas and solutions phases
[AD-A204073] N89-23711
MORPHOLOGY
Solidification of binary substances in rectangular and cylindrical cavities
[DE89-008883] N89-23640
Strength and structure of Ga(1-x)In(x)As alloys
[AD-A205415] N89-23644
MOTION STABILITY
An analysis of the attitude stability of a space station subject to parametric excitation of periodic mass motion
[AD-A206009] N89-23505
Nonlinear systems of conservation laws
[AD-A205837] N89-23830
MOTORS
Magnification of starting torques of dc motors by maximum power point trackers in photovoltaic systems
[NASA-TM-102040] N89-23792
MSM (SEMICONDUCTORS)
Light channel 5 Gb/s optoelectronic TDM (Time Division Multiplexing)
[AD-A205501] N89-24086
MTBF
System Mean-Time-Between-Failure versus life-cycle logistics cost subject to the introduction of Line-Replaceable-Unit redundancy
[AD-A206324] N89-23887
MULLITES
Investigations of mullite-zirconia composites N89-23577
MULTIPHASE FLOW
Nonlinear systems of conservation laws
[AD-A205837] N89-23830
MULTIPLE ACCESS
Study of spread spectrum multiple access systems for satellite communications with overlay on current services: Executive summary
[NASA-CR-180827-EXEC-SUMM] N89-23756
Study of spread spectrum multiple access systems for satellite communications with overlay on current services
[NASA-CR-180827] N89-23757
Near-far resistant linear multiuser detection
[AD-A206363] N89-23802
MULTIPLEXING
AN/TAC-1 demultiplexer circuit card assembly
[AD-A205744] N89-23770
MULTIPLICATION
Wavefront matrix multiplication on a distributed-memory multiprocessor
[PB89-151807] N89-24052
MULTIPROCESSING (COMPUTERS)
On the use of multiprocessing computers for global numerical weather prediction
[AD-A206102] N89-24009
Wavefront matrix multiplication on a distributed-memory multiprocessor
[PB89-151807] N89-24052
Krylov methods preconditioned with incompletely factored matrices on the CM-2
[AD-A206389] N89-24121
MULTISPECTRAL BAND SCANNERS
Geobotanical remote sensing for determination of aggregate source material
[AD-A205943] N89-23962
Research for optimization of future MOMS sensors
[ETN-89-94424] N89-23972
MULTIVARIATE STATISTICAL ANALYSIS
Evaluation of tests and design factors — structures
[REPT-882-440-109] N89-23889
Multivariate analysis and its applications
[AD-A205585] N89-24125
Symbolic analysis of multivariable missile systems
[AD-A206326] N89-24132

N

NACELLES
Transonic operational characteristics and performance
[NAL-TR-968] N89-23408
NASA PROGRAMS
NASA aeronautics research and technology
[NASA-EP-259] N89-23406
Patent abstracts bibliography: A continuing bibliography. Section 2: Indexes (supplement 34)
[NASA-SP-7039(34)-SECT-2] N89-24219
NASA SPACE PROGRAMS
Reducing launch operations costs: New technologies and practices
[PB89-136402] N89-23500
NASTRAN
Modal analysis and testing of missile systems
[AD-A204051] N89-23916
NATIONAL AIRSPACE SYSTEM
National Airspace System Search and Rescue operational concept (NAS-SR-1329)
[DOT/FAA/DS-89/07] N89-23435
Host computer system capacity management procedures
[AD-A193416] N89-24051
NATURAL GAS
Process integration methodology for natural gas-fueled heat pumps and cogeneration systems
[PB89-140867] N89-23811
NATURAL LANGUAGE (COMPUTERS)
Laboratory process control using natural language commands from a personal computer
[NASA-TM-101988] N89-24055
NAVIER-STOKES EQUATION
Numerical simulation of hypersonic flow around a space plane. 1: Basic development
[NAL-TR-976T] N89-23409
Navier-Stokes solution for a NACA 0012 airfoil with mass flux (fan)
[AD-A205771] N89-23424
Transonic Navier-Stokes solutions of three-dimensional afterbody flows
[NASA-TM-4111] N89-23433
Flosolver: A parallel computer for fluid dynamics
[NAL-TM-AE-8803] N89-23805
On the nature of Navier-Stokes turbulence
[NASA-TM-101983] N89-23813

Open boundary conditions for the Navier-Stokes equation
[FFA-145] N89-23818
A numerical study of viscous vortex rings using a spectral method
[NASA-TM-101041] N89-23820
Exploitation of multiple solutions of the Navier-Stokes equations to achieve radically improved flight
[AD-A205939] N89-23831
Computation of flow around maneuvering submerged bodies
[AD-A205994] N89-23833
Numerical simulation of flow through an artificial heart
[NASA-TM-102183] N89-24111

NAVIGATION AIDS
Loran C field strength contours: Contiguous US
[DOT/FAA/CT-TN89/16] N89-23437
System study: Radiation hardened autonomous navigation
[AD-A205604] N89-23439
Navigation shift correction by radar cartography. Optimization and validation by simulation
[REPT-882-320-103] N89-23755
Performance analysis of Kalman filters
[PB89-146104] N89-23787

NEAR FIELDS
An iterative technique to correct probe position errors in planar near-field to far-field transformations
[PB89-153886] N89-23750

NEBULAE
Study of the infrared celestial background
[AD-A205649] N89-24237

NEODYMIUM
Liquid dynamic compaction of Fe-Nd-B permanent magnets
[AD-A205632] N89-24135

NEODYMIUM LASERS
Pulse shaping on the Nova laser system
[DE89-008026] N89-23859

NETWORK ANALYSIS
Criteria for robust stability in a class of lateral inhibition networks coupled through resistive grids
[AD-A204174] N89-24081

NEURAL NETS
Criteria for robust stability in a class of lateral inhibition networks coupled through resistive grids
[AD-A204174] N89-24081
A method of up-front load balancing for local memory parallel processors
[NASA-CASE-MSC-21348-1] N89-24084
Prospects for classifying complex imagery using a self-organizing neural network
[AD-A206208] N89-24088
Molecular optics nonlinear optical processes in organic and polymeric crystals and films
[AD-A206372] N89-24209

NEUROMUSCULAR TRANSMISSION
Treatment with tyrosine, a neurotransmitter precursor, reduces environmental stress in humans
[AD-A206035] N89-24039

NEURONS
A low-energy X-ray irradiator for electrophysiological studies
[AD-A205368] N89-24026

NEUROPHYSIOLOGY
Long term synaptic plasticity and learning in neuronal networks
[AD-A205993] N89-24038

NEUROTRANSMITTERS
Treatment with tyrosine, a neurotransmitter precursor, reduces environmental stress in humans
[AD-A206035] N89-24039

NEUTRAL ATMOSPHERES
Environmental definition of the earth's neutral atmosphere N89-23539

NEUTRAL SHEETS
Electric fields in the magnetosphere: The evidence from ISEE, S3-3, GEOS and Viking
[TRITA-EPP-88-11] N89-23987

NEUTRON DIFFRACTION
Magnetic susceptibility and neutron diffraction experiments on nuclear ordering in copper
[ISBN-951-754-573-8] N89-24189

NEUTRON FLUX DENSITY
Nuclear magnetism in copper and silver: Theory and experiments
[ISBN-952-900-084-7] N89-24188

NEUTRON SCATTERING
Quasielastic and inelastic spin fluctuations in superconducting La2-xSrxCuO4
[DE89-008157] N89-24190

NEWTON THEORY
Non-Newtonian gravitational forces and the Greenland ice-sheet experiment
[DE89-009348] N89-23988

NICKEL ALLOYS
Intermetallic phases for high temperature applications N89-23612
Theoretical analysis of compatibility of several reinforcement materials with NiAl and FeAl matrices
[NASA-CR-182291] N89-23622
Theoretical studies of Ni3Al and NiAl with impurities
[DE89-006556] N89-23655
Environment-induced crack growth processes in nickel-base alloys
[DE89-008253] N89-23659

NICKEL COMPOUNDS
Characterization of a phase boundary in Ni-Al2O3 sintered under pressure N89-23600

NIGER
Meteosat thermal inertia mapping for studying wetland dynamics in the West-African Sahel
[BCRS-88-10A] N89-23970

NIGHT FLIGHTS (AIRCRAFT)
Heliport night parking area criteria test plan
[DOT/FAA/CT-TN88/45] N89-23480

NIGHT SKY
Night vision goggles (AN/PVS-7) performance issues and answers
[AD-A206117] N89-24047

NIGHT VISION
Night vision goggles (AN/PVS-7) performance issues and answers
[AD-A206117] N89-24047

NIOBIUM ALLOYS
Iron-niobium-aluminum alloy having high-temperature corrosion resistance
[DE89-009600] N89-23663
Environmental effects in niobium base alloys and other selected intermetallic compounds
[AD-A206072] N89-23673

NITROGEN
Experimental thermal conductivity, thermal diffusivity and specific heat values of argon and nitrogen
[PB89-148407] N89-23637

NOBLE METALS
Methanol vehicle catalyst evaluation, phase 3
[PB89-136139] N89-23874

NOISE GENERATORS
Noise of a model counterrotation propeller with simulated fuselage and support pylon at takeoff/approach conditions
[NASA-TM-101996] N89-24138

NOISE INTENSITY
Noise of a model counterrotation propeller with simulated fuselage and support pylon at takeoff/approach conditions
[NASA-TM-101996] N89-24138

NOISE MEASUREMENT
Noise characteristics of an inductively coupled plasma-mass spectrometer
[AD-A205686] N89-24169

NOISE PREDICTION (AIRCRAFT)
Status of sonic boom methodology and understanding
[NASA-CP-3027] N89-23415
High speed turboprop aeroacoustic study (single rotation). Volume 1: Model development
[NASA-CR-182257-VOL-1] N89-24139
Interior noise control ground test studies for advanced turboprop aircraft applications
[NASA-CR-181819] N89-24141

NOISE PROPAGATION
High speed turboprop aeroacoustic study (single rotation). Volume 1: Model development
[NASA-CR-182257-VOL-1] N89-24139

NOISE REDUCTION
Intelligibility in noise of three LPC (Linear Predictive Coders) voice channels with active noise reduction headsets
[AD-A205613] N89-23767
Drag and noise measurements on underwater vehicles with a riblet surface coating
[AD-A205500] N89-23825
Interior noise control ground test studies for advanced turboprop aircraft applications
[NASA-CR-181819] N89-24141

NOISE SPECTRA
Use of a spectrally segmented photodiode-array spectrometer for inductively coupled plasma atomic emission spectroscopy
[AD-A205688] N89-24171

NOISE TEMPERATURE
Electron conducting ceramics as sensor material for noise thermometry N89-23603

NOISE TOLERANCE
Interior noise control ground test studies for advanced turboprop aircraft applications
[NASA-CR-181819] N89-24141

NONAQUEOUS ELECTROLYTES
Viscosity and conductance of MEICI/AICI3 melts containing nonaqueous solvents
[AD-A205468] N89-23646

NONDESTRUCTIVE TESTS
An investigation of the temperature dependence of the ultrasonic properties of AS4/Ixan and XAS/Ixan composites
[NASA-CR-184845] N89-23619
Composite materials nondestructive tests: Choice of methods depending on requirements
[REPT-882-430-105] N89-23630
Challenges of nondestructive testing of composite materials
[REPT-882-430-107] N89-23632
NMR characterization of porous structures: Ceramics and sandstones: Renewal proposal
[DE89-009148] N89-23642
Intelligent processing of materials
[PB89-151823] N89-23735
Institute for Materials Science and Engineering, nondestructive evaluation: Technical activities 1988
[PB89-151625] N89-23884
Environmental Stress Screening (ESS) guide
[AD-A206350] N89-23888
Engineering thrust areas, 1989
[DE89-009009] N89-24229

NONEQUILIBRIUM THERMODYNAMICS
Numerical implementation of the Schapery model for nonlinear visco-elasticity
[PB89-144950] N89-23915

NONFLAMMABLE MATERIALS
Corrosion and lubricity testing of nonflammable USAF formulated CTFE (Chlorotrifluoroethylene) base hydraulic fluid
[AD-A205467] N89-23695
Low energy consumption hydraulic techniques
[AD-A206285] N89-23743

NONLINEAR EQUATIONS
Introduction to irreducible tensor methods, part 1
[NAL-PD-DU-8802] N89-24098
Nonlinear singular elliptic equations
[DE88-705691] N89-24103

NONLINEAR OPTICS
Quasi-liquid crystalline materials with special electro-optic properties
[AD-A206015] N89-24206

NONLINEAR SYSTEMS
Rayleigh-Taylor instability of a viscous film overlying a passive fluid
[AD-A205578] N89-23827
Nonlinear systems of conservation laws
[AD-A205837] N89-23830
Symbolic analysis of multivariable missile systems
[AD-A206326] N89-24132

NONLINEARITY
Numerical simulation of Goertler/Tollmein-Schlichting wave-interaction
[NASA-CR-181823] N89-23817
Numerical implementation of the Schapery model for nonlinear visco-elasticity
[PB89-144950] N89-23915

NONNEWTONIAN FLOW
Non-Newtonian gravitational forces and the Greenland ice-sheet experiment
[DE89-009348] N89-23988

NONNEWTONIAN FLUIDS
In situ fluorescence monitoring of the viscosities of particle-filled polymers in flow
[PB89-146278] N89-23680

NONRELATIVISTIC MECHANICS
Relativistic and non-relativistic magnetohydrodynamic flows around compact stars N89-24242

NORMAL DENSITY FUNCTIONS
Sea spike modeling
[AD-A205355] N89-23760
Asymptotic behavior of random discrete event systems
[PB89-146146] N89-24099

NOVA LASER SYSTEM
Pulse shaping on the Nova laser system
[DE89-008026] N89-23859

NOZZLE DESIGN
Nozzles for test system plasma generators --- Hermes
[REPT-882-430-104] N89-23502
Design, fabrication and test of the RL10 derivative II chamber/primary nozzle
[NASA-CR-179595] N89-23519
Arcjet nozzle design impacts
[NASA-TM-102050] N89-23522
Advanced computational techniques for hypersonic propulsion
[NASA-TM-102005] N89-23809

NOZZLE FLOW
Transonic Navier-Stokes solutions of three-dimensional afterbody flows
[NASA-TM-4111] N89-23433
Advanced computational techniques for hypersonic propulsion
[NASA-TM-102005] N89-23809
Two-dimensional confined jet thrust vector control: Operating mechanisms and performance
[AD-A206011] N89-23834
NUCLEAR ELECTRIC POWER GENERATION
Mobile nuclear power systems
[FOA-C-20743-4.1] N89-24149
NUCLEAR FUSION
Mobile nuclear power systems
[FOA-C-20743-4.1] N89-24149
Analysis of the ignition experiment IGNITEX
[DE89-007847] N89-24166
NUCLEAR MAGNETIC RESONANCE
NMR characterization of porous structures: Ceramics and sandstones: Renewal proposal
[DE89-009148] N89-23642
NUCLEAR POWER PLANTS
Nonintrusive methods for monitoring the operational readiness of solenoid-operated valves
[DE89-008732] N89-23878
NUCLEAR SPIN
Nuclear magnetism in copper and silver: Theory and experiments
[ISBN-952-900-084-7] N89-24188
NUCLEAR STRUCTURE
IDA (Institute for Defense Analyses) gamma-ray laser: Investigation of the feasibility of developing a laser using nuclear transitions
[AD-A205318] N89-23864
IDA (Institute for Defense Analyses) gamma-ray laser: Investigation of developing a laser using nuclear transitions
[AD-A205319] N89-23865
Nuclear magnetism in copper and silver: Theory and experiments
[ISBN-952-900-084-7] N89-24188
NUCLEAR WEAPONS
A unidirectional rotary solenoid as applied to stronglinks N89-23894
NUCLEATION
Twin boundaries, interfaces and modulated structures in martensites
[DE89-009064] N89-23662
Macrosegregation and nucleation in undercooled Pb-Sn alloys
[NASA-TM-102023] N89-23664
Nucleation and undercooling N89-23726
Gas-Grain Simulation Facility: Fundamental studies of particle formation and interactions. Volume 1: Executive summary and overview
[NASA-CP-10026-VOL-1] N89-24022
NUCLIDES
On the measurement of cosmogenic nuclides in cometary materials
[DE89-009248] N89-24243
NUMERICAL ANALYSIS
Investigation of three-dimensional mesh generation with precise controls
[AD-A205967] N89-23773
The effects of dielectric and metal loading on the dispersion characteristics for contrawound helix circuits used in high power traveling-wave tubes
[AD-A205345] N89-23797
Deductive programming synthesis
[AD-A206451] N89-24072
Exploring the episodic structure of algebra story problem solving: Revision
[AD-A206403] N89-24122
Numerical conformal mapping and applications
[AD-A205602] N89-24131
NUMERICAL INTEGRATION
Missile actuator simulation and an investigation into the accuracy of Runge-Kutta numerical integration
[AD-A206325] N89-23458
NUMERICAL STABILITY
A stability analysis of various patched grid interface conditions for hyperbolic equations
[FFA-144] N89-24105
Numerical experience with a superfast real Toeplitz solver
[AD-A205374] N89-24115
NUMERICAL WEATHER FORECASTING
A reduced version of the NMC DERF 2 data set
[NASA-TM-100727] N89-24002
On the use of multiprocessing computers for global numerical weather prediction
[AD-A206102] N89-24009
NYQUIST DIAGRAM
Multivariable Nyquist self-tuning: A general approach
[OUEL-1734/88] N89-24091

O

OBLIQUE SHOCK WAVES
Numerical simulation of Goertler/Tollmein-Schlichting wave-interaction
[NASA-CR-181823] N89-23817
OCEAN BOTTOM
Imaging procedure of underwater bottom topography by air and satellite images in the range of microwave and visible electromagnetic spectra
[GKSS-88/E/41] N89-24014
OCEAN MODELS
Improved sea surface scattering model
[AD-A205745] N89-24012
Observation model and parameter partials for the JPL geodetic GPS modeling software GPSOMC
[NASA-CR-185021] N89-24060
OCEAN SURFACE
Sea spike modeling
[AD-A205355] N89-23760
Analysis of turbulent motion phenomena in the maritime atmospheric boundary layer
[ETN-89-93949] N89-23996
Improved sea surface scattering model
[AD-A205745] N89-24012
OCEAN TEMPERATURE
Japan's Sunshine Project 1987 annual summary of comprehensive research
[DE88-756448] N89-23975
OCEAN THERMAL ENERGY CONVERSION
Japan's Sunshine Project 1987 annual summary of comprehensive research
[DE88-756448] N89-23975
OCEANOGRAPHIC PARAMETERS
Analysis of turbulent motion phenomena in the maritime atmospheric boundary layer
[ETN-89-93949] N89-23996
US Navy regional climatic study of the northern California operating area
[AD-A205342] N89-24006
Exploring the North Atlantic Ocean on floppy disks
[AD-A205733] N89-24011
OILS
Steel hardness effects in boundary lubricated sliding: An in-situ SEM (Scanning Electron Microscope) study
[AD-A206156] N89-23674
OMNIDIRECTIONAL ANTENNAS
Small UHF microstrip radiating element
[REPT-882-440-103] N89-23780
ON-LINE SYSTEMS
An ICAI (Intelligent Computer Aided Instruction) architecture for troubleshooting in complex dynamic systems
[AD-A205434] N89-24045
OPERATING SYSTEMS (COMPUTERS)
EnviroNET: Space environment for Strategic Defense Initiative experiments N89-23538
Defense Integrated Data System (DIDS) procedures manual. Volume 8: Document Identifier Code (DIC) Input/Output (I/O) formats (fixed length), change 3
[PB89-139414] N89-24220
OPERATIONAL HAZARDS
An analysis of lightning launch constraints
[AD-A206084] N89-23994
OPERATIONS RESEARCH
Computer-based modeling environments
[AD-A205828] N89-24064
OPERATOR PERFORMANCE
Design of a MANPRINT tool for predicting personnel and training characteristics implied by system design
[AD-A206201] N89-24048
OPERATORS (MATHEMATICS)
Operator induced multigrid algorithms using semirefinement
[NASA-CR-181834] N89-24113
Exact wave functions and coherent states of a damped driven harmonic oscillator
[AD-A205785] N89-24136
OPTICAL COMPUTERS
Digital optics for numerical computing: The residue number system for numerical optical computing
[AD-A206229] N89-24157
OPTICAL DATA PROCESSING
Digital optics for numerical computing: The residue number system for numerical optical computing
[AD-A206229] N89-24157
OPTICAL EQUIPMENT
Development of a precision, wide-dynamic-range actuator for use in active optical systems N89-23901
Fiber-optic time-resolved fluorescence sensor for the simultaneous determination of Al(+3), Ga(+3) and In(+3)
[AD-A205689] N89-24154
Summary of achievements in scientific research
[AD-A199947] N89-24227
OPTICAL FIBERS
Temporally smooth broadband pulses obtained by cross phase modulation in an optical fiber
[DE89-008891] N89-24152
Utilization of magnetostrictive optical fibers in multiple order gradiometers
[AD-D013960] N89-24155
OPTICAL MEASURING INSTRUMENTS
Contamination N89-23559
Development of an optical multigas detector
[PB89-148878] N89-23849
OPTICAL PROPERTIES
Semiconductors and monocrystal growth: Collection of charts, formulas and references N89-23729
Radiation physics properties of selective solar energy absorber layers
[ETN-89-93945] N89-23978
Optical properties of oceanic suspended matter and their interpretation for remote sensing of phytoplankton
[GKSS-88/E/40] N89-24013
Three-dimensional recognition of solid objects from a two-dimensional image
[AD-A205667] N89-24094
Temporally smooth broadband pulses obtained by cross phase modulation in an optical fiber
[DE89-008891] N89-24152
Quasi-liquid crystalline materials with special electro-optic properties
[AD-A206015] N89-24206
Molecular optics nonlinear optical processes in organic and polymeric crystals and films
[AD-A206372] N89-24209
OPTICAL RADAR
Coherent laser radar
[FOA-C-30512-3.1] N89-23778
A two-axis laser boresight system for a shuttle experiment N89-23913
OPTICAL REFLECTION
Fiber optic leak detection system
[PB89-148886] N89-24150
OPTICAL SWITCHING
Fatigue-resistant photochromic plastics
[DE89-007336] N89-23682
OPTICAL TRANSITION
Three-dimensional analysis of optical transition radiation
[AD-A205935] N89-24156
OPTICAL WAVEGUIDES
Transmission losses in hollow aluminum oxide waveguide at 10.6 microns
[FOA-C-30518-3.1] N89-23804
OPTIMAL CONTROL
An investigation into the application of dynamic programming to determine optimal controls for tracking a cruise missile maneuver by CMMCA (Cruise Missile Mission Control Aircraft)
[AD-A205970] N89-23456
Optimal aeroassisted coplanar orbital transfer using an energy model
[NASA-CR-181778] N89-23495
Increasing the margin of stability of arbitrarily finite modes of flexible large space structures with damping
[AD-A206487] N89-23507
Design and development of a high-stiffness, high-resolution torque sensor N89-23903
Quadratic optimal control theory for viscoelastically damped structures using a fractional derivative viscoelasticity model
[AD-A206008] N89-23932
State-space formulae for discrete-time H infinity optimization
[OUEL-1718/88] N89-24089
OPTIMIZATION
A closed-form trim solution yielding minimum trim drag for airplanes with multiple longitudinal-control effectors
[NASA-TP-2907] N89-23468
Continuous, low thrust coplanar orbit transfers with varying eccentricity
[AD-A206022] N89-23498
Performance analysis of Kalman filters
[PB89-146104] N89-23787
Analysis and optimization of geodetic networks by spectral criteria and mechanical analogies
[SER-C-342] N89-23963
Reduction of a general matrix to tridiagonal form
[DE89-008980] N89-24083
State-space formulae for discrete-time H infinity optimization
[OUEL-1718/88] N89-24089
On the communication complexity of distributed algebraic computation
[AD-A205784] N89-24117
ORBIS
Mission conditions and hardware concepts N89-23720

ORBIT CALCULATION
Numerical study of orbital trajectories about Phobos
[AD-A205822] N89-23496
An improved strategy for determining earth satellite orbits by radio
[AD-A205826] N89-23497
ORBIT TRANSFER VEHICLES
Agenda of the Fourth Annual Summer Conference, NASA/USRA University Advanced Design Program
[NASA-TM-101750] N89-23493
ORBITAL SERVICING
SIRTF Telescope Instrument Changeout and Cryogen Replenishment (STICCR) Study
[NASA-CR-177380] N89-23512
Returned Solar Max hardware degradation study results N89-23537
ORDER-DISORDER TRANSFORMATIONS
A first-principles calculation of the resistivity and thermopower in strong-scattering alloys
[DE89-008565] N89-23661
Lattice symmetries and thermal expansion
[AD-A206045] N89-24207
ORGANIC CHEMISTRY
A user's guide to the Molecular Modeling, Analysis and Display System (MMADS), 2nd edition
[AD-A205674] N89-23648
Synthesis of novel acid electrolytes for phosphoric acid fuel cells
[PB89-148944] N89-23786
ORGANIC MATERIALS
Molecular optics nonlinear optical processes in organic and polymeric crystals and films
[AD-A206372] N89-24209
ORGANOMETALLIC COMPOUNDS
Alternate arsenic and antimony sources for the OMCVD fabrication of semiconductors
[AD-A206483] N89-24211
ORIFICE FLOW
Three-dimensional laser anemometer study of compressible flow through orifice plates
[PB89-145098] N89-23808
ORIFICES
Three-dimensional laser anemometer study of compressible flow through orifice plates
[PB89-145098] N89-23808
ORTHOGONALITY
Radar waveforms derived from orthogonal matrices
[AD-A205459] N89-23765
OSCILLATIONS
Modeling of a continuous oscillator by oscillators with a finite number of degrees of freedom
[PB89-146120] N89-24134
OSCILLATORS
Coherence and chaos phenomena in Josephson oscillators for superconducting electronics
[AD-A205469] N89-23798
High energy efficient solid state laser sources
[NASA-CR-181782] N89-23856
Development of high power CARM (Cyclotron Auto-Resonance Maser) oscillators
[AD-A206270] N89-23872
Modeling of a continuous oscillator by oscillators with a finite number of degrees of freedom
[PB89-146120] N89-24134
OVER-THE-HORIZON RADAR
A chamber experiment for the feasibility study of an artificial plasma reflector for OTH radar applications
[NASA-CR-184912] N89-23478
OVERPRESSURE
Noise and sonic boom impact technology. PCBOOM computer program for sonic boom research, volume 1
[AD-A206290] N89-23429
Noise and sonic boom impact technology. PCBOOM computer program for sonic boom research. Volume 2: Program Users/Computer operations manual
[AD-A206291] N89-23430
OXIDATION
Atomic oxygen N89-23557
Working group written presentation: Atomic oxygen N89-23564
Study of adherent oxide scales
[AD-A205799] N89-23700
OXIDATION RESISTANCE
The protection against oxidation of carbon materials. Thermodynamic and experimental study: A literature survey — carbon fibers
[REPT-882-430-108] N89-23633
Undercutting of defects in thin film protective coatings on polymer surfaces exposed to atomic oxygen
[NASA-TM-101986] N89-23691
Fabricable polymers with excellent heat, oxidative and hydrolytic stability
[AD-A205627] N89-23698
OXYGEN
Oxygen interaction with metal surfaces: Surface science approach N89-23596
OXYGEN ANALYZERS
Semiconductor measurement technology: Automatic determination of the interstitial oxygen content of silicon wafers polished on both sides
[PB89-151831] N89-24180
OXYGEN ATOMS
NASA/SDIO Space Environmental Effects on Materials Workshop, part 1
[NASA-CP-3035-PT-1] N89-23528
Structural materials for space applications N89-23530
Atomic oxygen effects on materials N89-23540
Atomic oxygen effects on spacecraft materials: The state of the art of our knowledge N89-23541
NASA/SDIO Space Environmental Effects on Materials Workshop, part 2
[NASA-CP-3035-PT-2] N89-23547
Atomic oxygen N89-23557
Working group written presentation: Atomic oxygen N89-23564
Undercutting of defects in thin film protective coatings on polymer surfaces exposed to atomic oxygen
[NASA-TM-101986] N89-23691
OXYGEN CONSUMPTION
Oxygen consumption rate of operational underwater swimmers
[AD-A205331] N89-24025
OXYGEN PRODUCTION
Cellular and molecular approaches to polymer synthesis by bacteria
[AD-A206395] N89-23707
OZONE
Summary of selected new information on effects of ozone on health and vegetation. Draft supplement to air quality criteria for ozone and other photochemical oxidants
[PB89-135123] N89-23980
OZONOMETRY
Evaluation of the historical Schoenbein method for the determination of ozone in a flow chamber
[JUEL-2218] N89-23983

P

PACIFIC OCEAN
US Navy regional climatic study of the northern California operating area
[AD-A205342] N89-24006
PAINTS
Analysis of the NAVAIRDEVCEN self-priming topcoat on graphite/epoxy composites
[AD-A205961] N89-23626
PAIR PRODUCTION
Direct electron-pair production by high energy heavy charged particles
[NASA-CR-184958] N89-24142
PANEL FLUTTER
Development of harmonic panel methods for aeroelastic applications to elastic bodies and body-fin combinations in supersonic flow
[AD-A205739] N89-23423
PANELS
The thermal resistance of flat powder-filled evacuated panels
[DE89-008243] N89-23685
PARALLEL COMPUTERS
Flosolver: A parallel computer for fluid dynamics
[NAL-TM-AE-8803] N89-23805
PARALLEL PLATES
Two-dimensional numerical simulation of a Stirling engine heat exchanger
[NASA-TM-102057] N89-23823
PARALLEL PROCESSING (COMPUTERS)
Advances in computational design and analysis of airbreathing propulsion systems
[NASA-TM-101987] N89-23465
Flosolver: A parallel computer for fluid dynamics
[NAL-TM-AE-8803] N89-23805
A method of up-front load balancing for local memory parallel processors
[NASA-CASE-MSC-21348-1] N89-24084
PRASE (Parallel Resource Analysis Software Environment) instrumentation software for the Intel iPSC hypercube
[AD-A206046] N89-24087
Prospects for classifying complex imagery using a self-organizing neural network
[AD-A206208] N89-24088
Preconditioned Krylov solvers and methods for runtime loop parallelization
[AD-A206388] N89-24120
Parallel ada implementation of a multiple model Kalman filter tracking system: A software engineering approach
[AD-A206094] N89-24130
PARALLEL PROGRAMMING
Preconditioned Krylov solvers and methods for runtime loop parallelization
[AD-A206388] N89-24120
PARAMETER IDENTIFICATION
Adaptive signal processing
[AD-A205787] N89-24063
PARAMETERIZATION
Multiple model-based robot control: Development and initial evaluation
[AD-A205725] N89-23881
Riemannian geometry on families of linear systems: The deterministic case
[PB89-146062] N89-24100
Approaches for empirical Bayes confidence intervals
[AD-A205775] N89-24126
PARTIAL DIFFERENTIAL EQUATIONS
Three-dimensional structure of boundary layers in transition to turbulence
[AD-A205587] N89-23828
Observation model and parameter partials for the JPL geodetic GPS modeling software GPSOMC
[NASA-CR-185021] N89-24060
Fast algorithms for partial differential equations on advanced computers
[AD-A206469] N89-24073
PARTICLE ACCELERATION
Simulation studies of particle acceleration powered by modulated intense relativistic electron beams
[AD-A206348] N89-24148
PARTICLE ACCELERATORS
Simulation studies of particle acceleration powered by modulated intense relativistic electron beams
[AD-A206348] N89-24148
PARTICLE BEAMS
Three-dimensional analysis of optical transition radiation
[AD-A205935] N89-24156
PARTICLE COLLISIONS
Microparticle impacts in space: Results from Solar Max and shuttle witness plate inspections N89-23544
Effects of the contamination environment on surfaces and materials N89-23546
Transport of test particles in a magnetic field with perturbed magnetic surfaces
[IPP-2/296] N89-24178
PARTICLE DENSITY (CONCENTRATION)
Rapid fitting of particle cascade development data from X-ray film densitometry measurements
[NASA-TM-100368] N89-24260
PARTICLE ENERGY
Direct electron-pair production by high energy heavy charged particles
[NASA-CR-184958] N89-24142
PARTICLE FLUX DENSITY
Trapped particle flux models at NSSDC/WDC-A-R/S N89-23561
Compact source origin of cosmic ray antiprotons
[DE89-008044] N89-24258
PARTICLE INTERACTIONS
Viscosity and conductance of MEICI/AICI3 melts containing nonaqueous solvents
[AD-A205468] N89-23646
Gas-Grain Simulation Facility: Fundamental studies of particle formation and interactions. Volume 1: Executive summary and overview
[NASA-CP-10026-VOL-1] N89-24022
Gas-Grain Simulation Facility: Fundamental studies of particle formation and interactions. Volume 2: Abstracts, candidate experiments and feasibility study
[NASA-CP-10026-VOL-2] N89-24023
PARTICLE MOTION
The space particle environment N89-23548
Working group written presentation: Trapped radiation effects N89-23566
PARTICLE PRODUCTION
Compact source origin of cosmic ray antiprotons
[DE89-008044] N89-24258
PARTICLE SIZE DISTRIBUTION
Design of a chamber for CBW aerosol studies with relative humidity and particle concentration control
[AD-A205623] N89-23481
Propellant reuse/recovery technology
[AD-A206306] N89-23714
An experimental investigation in the behavior of metallized solid propellants
[AD-A206510] N89-23715
PARTICLE SPIN
Memory functions and relaxation functions of some spin systems
[AD-A206340] N89-24137
The diluted tri-dimensional spin-one Ising model with crystal field interactions
[DE88-705663] N89-24181

Mean field theory of the spin-1 Ising model with a random crystal field
[DE88-705669] N89-24182
Quasielastic and inelastic spin fluctuations in superconducting La2-xSrxCuO4
[DE89-008157] N89-24190
PARTICLES
Gas-Grain Simulation Facility: Fundamental studies of particle formation and interactions. Volume 1: Executive summary and overview
[NASA-CP-10026-VOL-1] N89-24022
Gas-Grain Simulation Facility: Fundamental studies of particle formation and interactions. Volume 2: Abstracts, candidate experiments and feasibility study
[NASA-CP-10026-VOL-2] N89-24023
PARTICULATES
Gas-Grain Simulation Facility: Fundamental studies of particle formation and interactions. Volume 1: Executive summary and overview
[NASA-CP-10026-VOL-1] N89-24022
Gas-Grain Simulation Facility: Fundamental studies of particle formation and interactions. Volume 2: Abstracts, candidate experiments and feasibility study
[NASA-CP-10026-VOL-2] N89-24023
PATENT POLICY
Patent abstracts bibliography: A continuing bibliography. Section 2: Indexes (supplement 34)
[NASA-SP-7039(34)-SECT-2] N89-24219
PATTERN RECOGNITION
Automatic extraction of areas from overlays of the series DGK 5 (Bo) N89-23955
The search for edges in remote sensing images using a digital polygonal map
[ETN-89-94146] N89-23964
The role of knowledge in visual shape representation
[AD-A206173] N89-24041
PAVEMENTS
Response of pavement to freeze-thaw cycles: Lebanon, New Hampshire, regional airport
[AD-A205559] N89-23740
PAYLOAD CONTROL
The design and analysis of a double swivel toggle release mechanism for the Orbiter stabilized payload deployment system N89-23895
Carousel deployment mechanism for collable lattice truss N89-23897
Design and testing of a deployable, retrievable boom for space applications N89-23898
Design and verification of mechanisms for a large foldable antenna N89-23899
A family of BAPTAs for GEO and LEO applications N89-23908
Design of a 60 GHz beam waveguide antenna positioner N89-23910
PAYLOAD DELIVERY (STS)
The design and analysis of a double swivel toggle release mechanism for the Orbiter stabilized payload deployment system N89-23895
PAYLOAD RETRIEVAL (STS)
Design and testing of a deployable, retrievable boom for space applications N89-23898
PELLETS
Electromagnetic railgun hydrogen pellet injector: Progress and prospect
[DE89-009536] N89-23499
PEPTIDES
Muramyl peptide-enhanced sleep: Pharmacological optimization of performance
[AD-A205974] N89-24028
PERCEPTION
Relating attention to visual mechanisms
[AD-A206452] N89-24042
PERFORMANCE PREDICTION
Host computer system capacity management procedures
[AD-A193416] N89-24051
PERFORMANCE TESTS
Nozzles for test system plasma generators — Hermes
[REPT-882-430-104] N89-23502
Study of the PBE cycle 100kN LH2/LO2 rocket engine
[NAL-TR-965] N89-23514
Design, fabrication and test of the RL10 derivative II chamber/primary nozzle
[NASA-CR-179595] N89-23519
Atomic oxygen effects on spacecraft materials: The state of the art of our knowledge N89-23541
Corrosion and lubricity testing of nonflammable USAF formulated CTFE (Chlorotrifluoroethylene) base hydraulic fluid
[AD-A205467] N89-23695
Li/FeS battery design for an electric van
[DE89-009808] N89-23794
Generating circuit tests by exploiting designed behavior
[AD-A206175] N89-23800
Signal-Noise/Interferer Combiner Unit Programmable (SINCUP)
[AD-A205367] N89-24053
Automatic documentation methodologies for software maintenance
[AD-A205672] N89-24062
Preconditioned Krylov solvers and methods for runtime loop parallelization
[AD-A206388] N89-24120
Characterization of semiconductor device processing etchant solutions for GaAs and p+ GaAs layers employed in AlxGa(1-x)As/GaAs MODFETs and related heterojunction devices
[AD-A205772] N89-24201
PERMANENT MAGNETS
Liquid dynamic compaction of Fe-Nd-B permanent magnets
[AD-A205632] N89-24135
Superconducting PYX structures
[AD-D013958] N89-24202
PERMEABILITY
Structure/permeability relationships of silicon-containing polyimides
[NASA-CR-4237] N89-23683
PERMITTIVITY
Polarizability and effective permittivity of layered and continuously inhomogeneous dielectric ellipsoids
[PB89-146476] N89-24102
PERSONAL COMPUTERS
Laboratory process control using natural language commands from a personal computer
[NASA-TM-101988] N89-24055
Application of a PC based, real-time, data-aquisition system in rotorcraft wind-tunnel testing
[NASA-TM-4119] N89-24079
Local area network technical guidelines. Volume 1: LAN design and planning (LAN TSR process)
[PB89-139091] N89-24080
PERSONNEL MANAGEMENT
Air Force Human Resources Laboratory R and D accomplishments and services, FY86-FY88
[AD-A205312] N89-24218
PERTURBATION
Computing induced velocity perturbations due to a helicopter fuselage in a free stream
[NASA-TM-4113] N89-23410
Rayleigh-Taylor instability of a viscous film overlying a passive fluid
[AD-A205578] N89-23827
Improved sea surface scattering model
[AD-A205745] N89-24012
PERTURBATION THEORY
Current distribution in a three-dimensional IC analyzed by a perturbation method. Part 1: A simple steady state theory
[NASA-CR-185022] N89-23494
Differential algebraic equations, indices, and integral algebraic equations
[DE89-009584] N89-24109
PHASE DIAGRAMS
Critical assessment of the thermodynamic properties of antimony-copper alloys
[PB89-147524] N89-23657
Phase transformation N89-23725
PHASE ERROR
Autofocus of SAR imagery degraded by ionospheric-induced phase errors
[DE89-008278] N89-23752
PHASE MODULATION
Temporally smooth broadband pulses obtained by cross phase modulation in an optical fiber
[DE89-008691] N89-24152
PHASE SHIFT KEYING
Investigation of mutual interference between digitally modulated signals
[BBC-RD-1988/13] N89-23745
PHASE TRANSFORMATIONS
Phase transformation of Zr(x)Hf(1-x)O2 in alumina matrix N89-23588
Characterization of a phase boundary in Ni-Al2O3 sintered under pressure N89-23600
Twin boundaries, interfaces and modulated structures in martensites
[DE89-009064] N89-23662
Phase transformation N89-23725
Metallic solidification N89-23727
Experimental and theoretical determination of the thermomechanical response of inelastic structural materials to high energy thermal inputs
[AD-A206100] N89-23933
Studies on high-Tc superconducting materials
[NAL-TM-MT-8703] N89-24178
Grain boundaries
[DE89-008881] N89-24194
The formation of topological defects in phase transitions
[NASA-CR-185318] N89-24215
PHOSPHORIC ACID FUEL CELLS
Synthesis of novel acid electrolytes for phosphoric acid fuel cells
[PB89-148944] N89-23786
PHOTOABSORPTION
Photoabsorption of molecules at corrugated thin metal films
[AD-A205325] N89-24197
PHOTOCHEMICAL REACTIONS
Ultraviolet radiation effects N89-23551
Energy transfer and photochemistry in biomimetic solar conversion
[PB89-142590] N89-23974
Fiber-optic time-resolved fluorescence sensor for the simultaneous determination of Al(+3), Ga(+3) and In(+3)
[AD-A205689] N89-24154
PHOTOCHROMISM
Fatigue-resistant photochromic plastics
[DE89-007336] N89-23682
PHOTODIODES
Use of a spectrally segmented photodiode-array spectrometer for inductively coupled plasma atomic emission spectroscopy
[AD-A205688] N89-24171
PHOTODISSOCIATION
Energy disposal in ion-molecule reactions
[AD-A205987] N89-24144
PHOTOELECTRIC EFFECT
Laser photoelectric effect at surface of discharge cathode
[AD-A205741] N89-23869
PHOTOELECTRIC EMISSION
Heterojunction band line-ups and the alloying effect in compound semiconductor alloys: A photoemission study N89-24179
Investigation of electronic states in nonmagnetic single crystals with spin-resolved photoemission
[JUEL-2228] N89-24212
PHOTOELECTRIC MATERIALS
High pressure studies on infrared detector materials
[NAL-TM-MT-8701] N89-23677
PHOTOELECTRON SPECTROSCOPY
Heterojunction band line-ups and the alloying effect in compound semiconductor alloys: A photoemission study N89-24179
PHOTOGRAMMETRY
Reports on Cartography and Geodesy. Series 1, number 101
[ISSN-0469-4236] N89-23941
Definition and filling of information systems: Challenge for a photogrammetric service enterprise N89-23942
Cartographic signatures in PHOCUS N89-23948
Remote sensing of global snowpack energy and mass balance: In-situ measurements on the snow of interior and Arctic Alaska
[NASA-CR-180078] N89-23956
PHOTOMAPPING
The search for edges in remote sensing images using a digital polygonal map
[ETN-89-94146] N89-23964
PHOTOMETERS
Fiber-optic time-resolved fluorescence sensor for the simultaneous determination of Al(+3), Ga(+3) and In(+3)
[AD-A205689] N89-24154
The Allegheny Observatory search for planetary systems
[NASA-CR-184990] N89-24233
A search for pulsations in planetary nebulae nuclei N89-24235
PHOTOVOLTAIC CELLS
Solar dynamic power for space station freedom
[NASA-TM-102016] N89-23516
Photovoltaic power system considerations for future lunar bases
[NASA-TM-102019] N89-23517
Magnification of starting torques of dc motors by maximum power point trackers in photovoltaic systems
[NASA-TM-102040] N89-23792
PHTHALOCYANIN
FILMCAL: An ESR (Electron Spin Resonance) simulation program for transition metals in phthalocyanine films
[AD-A206441] N89-23676
PHYSICAL CHEMISTRY
A user's guide to the Molecular Modeling, Analysis and Display System (MMADS), 2nd edition
[AD-A205674] N89-23648
PHYSICAL EXERCISE
Patterns of human drinking: Effects of exercise, water temperature and food consumption
[AD-A206031] N89-24029

PHYSIOLOGICAL RESPONSES
Evaluation of three commercial microclimate cooling systems
[AD-A206318] N89-23744
PILOT PERFORMANCE
The role of pilot and automatic onboard systems in future rendezvous and docking operations
[REPT-882-440-116] N89-24050
PILOTLESS AIRCRAFT
Preliminary design of a modular unmanned research vehicle. Volume 2: Subsystem technical development design study
[AD-A205678] N89-23454
PIONEER VENUS 1 SPACECRAFT
Comet Halley: The view from Pioneer Venus
[NASA-NF-127] N89-24240
PIONS
Strong and electromagnetic interactions in heavy exotic atoms
[PB89-145718] N89-24143
PIPELINING (COMPUTERS)
Wavefront matrix multiplication on a distributed-memory multiprocessor
[PB89-151807] N89-24052
PISTONS
Boundary layer and heat transfer behind a piston in a shock tube. Part 1: Theoretical considerations of laminar and turbulent boundary layer behind a piston in a tube
[ISL-R-111/87-PT-1] N89-23841
PITCHING MOMENTS
High angle-of-attack aerodynamic characteristics of crescent and elliptic wings
[NASA-CR-184992] N89-23418
PITOT TUBES
Characteristics of a five-hole spherical pitot tube
[NAL-TR-971] N89-23463
PLANAR STRUCTURES
An evaluation of coplanar line for application in microwave integrated circuitry
[AD-A205305] N89-23795
PLANE STRESS
The crack problem in bonded nonhomogeneous materials
[NASA-CR-184897] N89-23926
PLANE WAVES
Effects of initial conditions on the development of supersonic turbulent free shear layers
[AD-A205607] N89-23421
The geometry of plane waves in spaces of constant curvature N89-24241
PLANETARY NEBULAE
A search for pulsations in planetary nebulae nuclei N89-24235
PLANETARY SYSTEMS
The Allegheny Observatory search for planetary systems
[NASA-CR-184990] N89-24233
PLANETS
Reports of planetary astronomy, 1989
[NASA-TM-4120] N89-24232
PLANNING
US Air Force research technology area plan, FY 1989
[AD-A205304] N89-24217
PLANTS (BOTANY)
Plant health sensing N89-24018
Non-destructive plant health sensing using absorption spectroscopy N89-24021
PLASMA ANTENNAS
A chamber experiment for the feasibility study of an artificial plasma reflector for OTH radar applications
[NASA-CR-184912] N89-23478
PLASMA CONTROL
Analysis of the ignition experiment IGNITEX
[DE89-007847] N89-24166
PLASMA DENSITY
A chamber experiment for the feasibility study of an artificial plasma reflector for OTH radar applications
[NASA-CR-184912] N89-23478
Investigation of the behaviour of a collisionless R-F sheath
[OUEL-1695/87] N89-24165
PLASMA DIAGNOSTICS
Investigation of the behaviour of a collisionless R-F sheath
[OUEL-1695/87] N89-24165
PLASMA DIODES
Development of high power CARM (Cyclotron Auto-Resonance Maser) oscillators
[AD-A206270] N89-23872
Population inversions in ablation plasmas generated by intense electron beams
[AD-A205716] N89-24172
PLASMA DRIFT
Onset conditions for the driven lower hybrid drift instability in an expanding magnetized plasma
[AD-A205505] N89-24167
Use of a spectrally segmented photodiode-array spectrometer for inductively coupled plasma atomic emission spectroscopy
[AD-A205688] N89-24171
PLASMA ENGINES
Test facility and preliminary performance of a 100 kW class MPD thruster
[NASA-TM-102021] N89-23520
PLASMA GENERATORS
Nozzles for test system plasma generators --- Hermes
[REPT-882-430-104] N89-23502
PLASMA GUNS
Product development at Aerospatiale --- industrial plasmas
[REPT-882-430-111] N89-24175
PLASMA HEATING
Development of high power CARM (Cyclotron Auto-Resonance Maser) oscillators
[AD-A206270] N89-23872
PLASMA INTERACTIONS
Surface phenomena in plasma environments N89-23555
Spacecraft charging N89-23563
Working group written presentation: Atomic oxygen N89-23564
Electrodynamics of cosmical plasmas: Some basic aspects of cosmological importance
[TRITA-EPP-89-02] N89-24163
PLASMA PHYSICS
Analysis of the ignition experiment IGNITEX
[DE89-007847] N89-24166
PLASMA POWER SOURCES
MPD thruster erosion research
[NASA-CR-185314] N89-24168
PLASMA PROPULSION
Test facility and preliminary performance of a 100 kW class MPD thruster
[NASA-TM-102021] N89-23520
PLASMA RADIATION
Flow-injection analysis utilizing a spectrally segmented photodiode-array inductively coupled plasma emission spectrometer. 1: Microcolumn preconcentration for the determination of molybdenum
[AD-A205687] N89-24170
PLASMA SHEATHS
Sheath and presheath in a collisionless open field plasma
[IPPJ-890] N89-24161
Investigation of the behaviour of a collisionless R-F sheath
[OUEL-1695/87] N89-24165
PLASMA SPECTRA
Flow-injection analysis utilizing a spectrally segmented photodiode-array inductively coupled plasma emission spectrometer. 1: Microcolumn preconcentration for the determination of molybdenum
[AD-A205687] N89-24170
Use of a spectrally segmented photodiode-array spectrometer for inductively coupled plasma atomic emission spectroscopy
[AD-A205688] N89-24171
PLASMA TORCHES
Preliminary evaluation of a miniaturized torch for inductively coupled plasma mass spectrometry
[AD-A205746] N89-24173
Product development at Aerospatiale --- industrial plasmas
[REPT-882-430-111] N89-24175
PLASMAS (PHYSICS)
Chloride analysis in HAN-based liquid propellants by inductively coupled plasma spectroscopy
[AD-A206564] N89-23717
Transport of test particles in a magnetic field with perturbed magnetic surfaces
[IPP-2/296] N89-24176
PLASMASPHERE
Electric fields in the magnetosphere: The evidence from ISEE, S3-3, GEOS and Viking
[TRITA-EPP-88-11] N89-23987
PLASMONS
Decay of molecules at corrugated thin metal films
[AD-A205487] N89-24196
PLASTIC COATINGS
Analysis of the NAVAIRDEVCEN self-priming topcoat on graphite/epoxy composites
[AD-A205961] N89-23626
PLASTIC DEFORMATION
Behavior of metals during hot rolling processes. Part 2: Experimental methods for flow stress determination and calculation of the two-dimensional temperature-field in the roll gap N89-23614
Interfacial reactions during cladding of steel by hot rolling N89-23615
A combined isotropic-kinematic hardening model for large deformation metal plasticity
[AD-A206352] N89-23935
PLASTIC PROPELLANTS
Polyethylene glycol-poly(2-methyl-5-vinyl tetrazole) polymer blend: A desensitizing binder for propellants and explosives
[AD-A206563] N89-23716
PLASTIC PROPERTIES
Numerical implementation of the Schapery model for nonlinear visco-elasticity
[PB89-144950] N89-23915
PLUMES
A numerical routine for defining rocket exhaust characteristics and impingement effects
[AD-A206323] N89-23526
PNEUMATIC EQUIPMENT
Missile actuator simulation and an investigation into the accuracy of Runge-Kutta numerical integration
[AD-A206325] N89-23458
Structural mode frequencies of FOG-M (Fiber Optics Guided-Missile) actuator/fin
[AD-A206327] N89-24158
POINT SPREAD FUNCTIONS
Assessment of surface topography by X-ray scattering measurements
[MPE-PREPRINT-134] N89-24159
POINTING CONTROL SYSTEMS
A two-axis laser boresight system for a shuttle experiment N89-23913
POLARITY
Actuator rate saturation compensator
[AD-D013962] N89-23474
POLARIZED ELECTROMAGNETIC RADIATION
Three-dimensional analysis of optical transition radiation
[AD-A205935] N89-24156
POLARIZED RADIATION
Three-dimensional analysis of optical transition radiation
[AD-A205935] N89-24156
POLICIES
Reducing launch operations costs: New technologies and practices
[PB89-136402] N89-23500
Orbital debris environment and data requirements N89-23543
POLLUTION CONTROL
Environmental projects. Volume 3: Environmental compliance audit
[NASA-CR-185019] N89-23985
POLLUTION MONITORING
Area source documentation for the 1985 National Acid Precipitation Assessment Program inventory
[PB89-151427] N89-23981
POLYACETYLENE
Metallically conducting polymers: The limiting effect of conjugation defects on the electrical conductivity, a polyacetylene example
[ETN-89-93950] N89-23710
POLYBUTADIENE
In situ fluorescence monitoring of the viscosities of particle-filled polymers in flow
[PB89-146278] N89-23680
Fabricable polymers with excellent heat, oxidative and hydrolytic stability
[AD-A205627] N89-23698
Path dependent morphologies of a diblock copolymer of Polystyrene/Hydrogenated polybutadiene
[AD-A206504] N89-23883
POLYCARBONATES
The structural basis for fatigue initiation in glassy polymers
[DE89-009292] N89-23689
POLYESTERS
Fatigue-resistant photochromic plastics
[DE89-007336] N89-23682
POLYETHYLENES
Fabricable polymers with excellent heat, oxidative and hydrolytic stability
[AD-A205627] N89-23698
Polyethylene glycol-poly(2-methyl-5-vinyl tetrazole) polymer blend: A desensitizing binder for propellants and explosives
[AD-A206563] N89-23716
POLYGONS
Calculation of the surface of a geodetic polygon on an ellipsoid of revolution
[ETN-89-94149] N89-23966
POLYIMIDES
Structure/permeability relationships of silicon-containing polyimides
[NASA-CR-4237] N89-23683
Undercutting of defects in thin film protective coatings on polymer surfaces exposed to atomic oxygen
[NASA-TM-101986] N89-23691
Processable polyimide adhesive and matrix composite resin
[NASA-CASE-LAR-14101-1] N89-23692

POLYMER CHEMISTRY
Electron spectroscopy for chemical analysis: Sample analysis
[NASA-CR-183568] N89-23634
Donor acceptor polymerization chemistry as a vehicle to low energy cure of matrix resins: Evolution of the 2-Tg concept to produce Tg polymers at ambient temperatures
[AD-A206287] N89-23706
Cellular and molecular approaches to polymer synthesis by bacteria
[AD-A206395] N89-23707
POLYMER MATRIX COMPOSITES
Light weight polymer matrix composite material
[NASA-CASE-LEW-14734-1] N89-23623
Processable polyimide adhesive and matrix composite resin
[NASA-CASE-LAR-14101-1] N89-23692
POLYMER PHYSICS
Metallically conducting polymers: The limiting effect of conjugation defects on the electrical conductivity, a polyacetylene example
[ETN-89-93950] N89-23710
POLYMERIC FILMS
High electric field phenomena in insulation
[AD-A205525] N89-23799
Tensile film clamps and mounting block for the rheovibron and autovibron viscoelastometer
[NASA-CASE-LAR-13696-1] N89-23680
POLYMERIZATION
Water-processable conducting polymers
[DE89-009251] N89-23688
Fabricable polymers with excellent heat, oxidative and hydrolytic stability
[AD-A205627] N89-23698
The mechanisms of biodegradation of synthetic polymers
[AD-A205628] N89-23699
Report on the partial support of the 1988 Gordon Conference on Polymers (West)
[AD-A205834] N89-23701
Donor acceptor polymerization chemistry as a vehicle to low energy cure of matrix resins: Evolution of the 2-Tg concept to produce Tg polymers at ambient temperatures
[AD-A206287] N89-23706
Electronic and ionic transport in polymers
[AD-A206530] N89-23709
POLYMETHYL METHACRYLATE
Environmental stress crazing and cracking of transparent polymers
[AD-A205624] N89-23697
POLYPROPYLENE
High electric field phenomena in insulation
[AD-A205525] N89-23799
POLYSTATION DOPPLER TRACKING SYSTEM
Turbulent shear stress measurement in hypersonic flow
[AD-A206453] N89-23432
POLYSTYRENE
Fabricable polymers with excellent heat, oxidative and hydrolytic stability
[AD-A205627] N89-23698
POLYURETHANE RESINS
Analysis of the NAVAIRDEVCEN self-priming topcoat on graphite/epoxy composites
[AD-A205961] N89-23626
POROSITY
NMR characterization of porous structures: Ceramics and sandstones: Renewal proposal
[DE89-009148] N89-23642
POROUS MATERIALS
NMR characterization of porous structures: Ceramics and sandstones: Renewal proposal
[DE89-009148] N89-23642
Nonlinear systems of conservation laws
[AD-A205837] N89-23830
Monitoring thin film properties with surface acoustic wave devices: Diffusion, surface area and pore size distribution
[DE89-009379] N89-24195
PORTABLE EQUIPMENT
Correlation of Portable Wear Metal Analyzer (PWMA-2) and Baird A/E35U-3 spectrometer oil analysis data
[AD-A205957] N89-23882
POSITION (LOCATION)
Investigation of several methods for the detection of outstanding points in a digital image
[ETN-89-94148] N89-23965
POSITION ERRORS
System study: Radiation hardened autonomous navigation
[AD-A205604] N89-23439
Impact of the geoplasma on a spaceborne GPS receiver system: A preliminary study
[AD-A205965] N89-23442
An iterative technique to correct probe position errors in planar near-field to far-field transformations
[PB89-153886] N89-23750
POSITIONING DEVICES (MACHINERY)
Design and verification of mechanisms for a large foldable antenna N89-23899
Design of a 60 GHz beam waveguide antenna positioner N89-23910
POTABLE WATER
Patterns of human drinking: Effects of exercise, water temperature and food consumption
[AD-A206031] N89-24029
POWDER (PARTICLES)
Ceramic Project of the Max-Planck Society N89-23571
Fabrication and properties of alumina-zirconia composites
[PB89-147532] N89-23620
The thermal resistance of flat powder-filled evacuated panels
[DE89-008243] N89-23685
Shock compaction of YBa2Cu3O7-x and HoBa2Cu3O7-x powders in a metal matrix
[DE89-008827] N89-24193
POWDER METALLURGY
Sintering of CaO and MgO in the presence of nonequilibrium liquid phase N89-23580
Production of metal powders by rotating electrode process N89-23608
Cooling rate, undercooling and rapid solidification by atomization N89-23609
Ambient temperature properties of PM (Powder Metal) aluminum-titanium alloys
[AD-A205997] N89-23671
POWER SPECTRA
Performance of radar receivers in the presence of noise and intentional interference
[AD-A205328] N89-23759
PRE-MAIN SEQUENCE STARS
Spectra and dynamics of young stellar objects N89-24234
PRECIPITATION (METEOROLOGY)
Surface Observation Climatic Summaries (SOCS) for NASA Shuttle Landing Facility, Florida
[AD-A205362] N89-24007
PRECIPITATION HARDENING
Stress relief cracking in copper-precipitation strengthened HSLA-100 steel
[AD-A205936] N89-23670
PREDICTION ANALYSIS TECHNIQUES
A numerical routine for defining rocket exhaust characteristics and impingement effects
[AD-A206323] N89-23526
The dimension of attractors underlying turbulent Poiseuille flow
[AD-A206021] N89-23835
Fatigue crack growth model RANDOM2 user manual, appendix 1
[NASA-CR-184939] N89-23890
Fatigue strength reduction model: RANDOM3 and RANDOM4 user manual, appendix 2
[NASA-CR-184940] N89-23891
On the use of multiprocessing computers for global numerical weather prediction
[AD-A206102] N89-24009
PREPARATION
Sample preparation techniques for evaluating methanol and formaldehyde emissions from methanol fueled vehicles and engines
[PB89-136147] N89-23734
PRESSURE DISTRIBUTION
Experimental study of pressure and heating rate on a swept cylindrical leading edge resulting from swept shock wave interference
[NASA-CR-185326] N89-23411
Low energy consumption hydraulic techniques
[AD-A206285] N89-23743
PRESSURE EFFECTS
Design of water tunnel to measure wall pressure signatures due to tunnel blockage and wake effects
[AD-A206025] N89-23483
Structure/permeability relationships of silicon-containing polyimides
[NASA-CR-4237] N89-23683
A self consistant model of the three phase interstellar medium in disk galaxies N89-24245
PRESSURE MEASUREMENT
Ejector effects on a supersonic nozzle at low altitude and Mach number
[AD-A206049] N89-23427
PRESSURE REDUCTION
Study of the PBE cycle 100kN LH2/LO2 rocket engine
[NAL-TR-965] N89-23514
Mechanisms of secondary flows and losses within a three dimensional turbine stator cascade
[NAL-TR-970T] N89-23807
PREVENTION
Effects of the contamination environment on surfaces and materials N89-23546
PROBABILITY DENSITY FUNCTIONS
Sea spike modeling
[AD-A205355] N89-23760
Launch commit criteria performance trending analysis, phase 1, revision A. SRM and QA mission services
[NASA-CR-184859] N89-24129
PROBABILITY DISTRIBUTION FUNCTIONS
A methodology for determining the survivability of fixed-wing aircraft against small arms
[AD-A205730] N89-23455
Fast algorithms for partial differential equations on advanced computers
[AD-A206469] N89-24073
Tests for the gamma distribution with estimated shape parameters
[AD-A205829] N89-24118
Multivariate analysis and its applications
[AD-A205585] N89-24125
Launch commit criteria performance trending analysis, phase 1, revision A. SRM and QA mission services
[NASA-CR-184859] N89-24129
PROBABILITY THEORY
Approaches for empirical Bayes confidence intervals
[AD-A205775] N89-24126
Second-order moments of a stationary Markov chain and some applications
[AD-A206366] N89-24128
A blocked Jacobi method for the symmetric Eigenproblem
[AD-A206553] N89-24133
PROBLEM SOLVING
Development and evaluation of integrating details: A complex spatial problem solving test
[AD-A205860] N89-24035
An ICAI (Intelligent Computer Aided Instruction) architecture for troubleshooting in complex dynamic systems
[AD-A205434] N89-24045
The role of order in distributed programs
[AD-A206037] N89-24065
Explanation-based theory revision: An approach to the problems of incomplete and incorrect theories
[AD-A205337] N89-24092
Heuristics for cooperative problem solving
[AD-A206371] N89-24096
Numerical experience with a superfast real Toeplitz solver
[AD-A205374] N89-24115
On the equation Xa + Ya = Za
[AD-A205460] N89-24116
Preconditioned Krylov solvers and methods for runtime loop parallelization
[AD-A206388] N89-24120
Exploring the episodic structure of algebra story problem solving: Revision
[AD-A206403] N89-24122
Knowledge representation using knowledge graphs: Application to theories on mathematical modeling and solving word problems
[MEMO-707] N89-24124
PROCESS CONTROL (INDUSTRY)
Strengthening of silicon nitride ceramics N89-23585
Preparation and properties of high strength carbon fibers N89-23589
Challenges of nondestructive testing of composite materials
[REPT-882-430-107] N89-23632
Microwave processing of ceramics
[DE89-009350] N89-23690
Process integration methodology for natural gas-fueled heat pumps and cogeneration systems
[PB89-140867] N89-23811
PRODUCT DEVELOPMENT
Product development at Aerospatiale — industrial plasmas
[REPT-882-430-111] N89-24175
PRODUCTION COSTS
High speed abrasive belt grinding
[AD-A205618] N89-23741
PRODUCTION ENGINEERING
Slip casting of fused silica N89-23573
Production of metal powders by rotating electrode process N89-23608
PRODUCTIVITY
Local area network technical guidelines. Volume 1: LAN design and planning (LAN TSR process)
[PB89-139091] N89-24080
PROGRAM VERIFICATION (COMPUTERS)
Software reliability studies
[NASA-CR-184857] N89-24054

PROGRAMMING LANGUAGES
Compiling high level constructs to distributed memory architectures
[NASA-CR-181825] N89-24058
Fourth generation computer languages
[DE89-008800] N89-24059
PROJECT MANAGEMENT
Mission conditions and hardware concepts N89-23720
Microgravity User Support Center (MUSC) N89-23721
Payload experts in D1-mission N89-23722
Age distribution among NASA scientists and engineers N89-23911
PROJECTILES
Comparison of computational analysis with flight tests of a 40mm solid-fuel ramjet projectile
[AD-A206536] N89-23459
White paper: Experimental and computational studies of very high velocity impacts
[DE89-007643] N89-23877
PROJECTS
Putting science and technology to work: A casebook of transferred technologies
[DE89-009158] N89-24228
PROP-FAN TECHNOLOGY
Average-passage simulation of counter-rotating propfan propulsion systems as applied to cruise missiles
[NASA-TM-102043] N89-23416
PROPELLANT BINDERS
Polyethylene glycol-poly(2-methyl-5-vinyl tetrazole) polymer blend: A desensitizing binder for propellants and explosives
[AD-A206563] N89-23716
PROPELLANT COMBUSTION
An experimental investigation in the behavior of metallized solid propellants
[AD-A206510] N89-23715
PROPELLANT TRANSFER
Center of gravity control on Airbus aircraft: Fuel, range and loading
[REPT-882-111-101] N89-23460
PROPELLANTS
Propellant reuse/recovery technology
[AD-A206306] N89-23714
Polyethylene glycol-poly(2-methyl-5-vinyl tetrazole) polymer blend: A desensitizing binder for propellants and explosives
[AD-A206563] N89-23716
PROPELLER BLADES
High speed turboprop aeroacoustic study (single rotation). Volume 1: Model development
[NASA-CR-182257-VOL-1] N89-24139
PROPELLER FANS
Average-passage simulation of counter-rotating propfan propulsion systems as applied to cruise missiles
[NASA-TM-102043] N89-23416
PROPELLERS
High speed turboprop aeroacoustic study (single rotation). Volume 1: Model development
[NASA-CR-182257-VOL-1] N89-24139
PROPULSION
Advanced computational techniques for hypersonic propulsion
[NASA-TM-102005] N89-23809
PROPULSION SYSTEM CONFIGURATIONS
Average-passage simulation of counter-rotating propfan propulsion systems as applied to cruise missiles
[NASA-TM-102043] N89-23416
Advances in computational design and analysis of airbreathing propulsion systems
[NASA-TM-101987] N89-23465
PROPULSION SYSTEM PERFORMANCE
Design, fabrication and test of the RL10 derivative II chamber/primary nozzle
[NASA-CR-179595] N89-23519
Test facility and preliminary performance of a 100 kW class MPD thruster
[NASA-TM-102021] N89-23520
Space station propulsion test bed
[NASA-CR-183615] N89-23521
PROTECTIVE CLOTHING
Evaluation of three commercial microclimate cooling systems
[AD-A206318] N89-23744
The concept and theoretical considerations of a cold weather clothing system
[AD-A205476] N89-24046
PROTECTIVE COATINGS
Advanced layer materials N89-23587
The protection against oxidation of carbon materials. Thermodynamic and experimental study: A literature survey — carbon fibers
[REPT-882-430-108] N89-23633
Undercutting of defects in thin film protective coatings on polymer surfaces exposed to atomic oxygen
[NASA-TM-101986] N89-23691
PROTEINS
Organic monocrystals N89-23730
PROTOSTARS
Spectra and dynamics of young stellar objects N89-24234
PROTOTYPES
A graphical editor for the computer aided prototyping system
[AD-A206443] N89-24071
A program interface prototype for a multimedia database incorporating images
[AD-A206439] N89-24226
PSYCHOLOGICAL TESTS
Design of a MANPRINT tool for predicting personnel and training characteristics implied by system design
[AD-A206201] N89-24048
PSYCHOLOGY
The attention system of the human brain
[AD-A206157] N89-24040
PSYCHOMETRICS
Psychometric function reconstruction from adaptive tracking procedures
[AD-A205668] N89-24034
Development and evaluation of integrating details: A complex spatial problem solving test
[AD-A205860] N89-24035
PSYCHOMOTOR PERFORMANCE
Psychometric function reconstruction from adaptive tracking procedures
[AD-A205668] N89-24034
Design of a MANPRINT tool for predicting personnel and training characteristics implied by system design
[AD-A206201] N89-24048
PSYCHOPHYSICS
Psychometric function reconstruction from adaptive tracking procedures
[AD-A205668] N89-24034
PSYCHOPHYSIOLOGY
Psychometric function reconstruction from adaptive tracking procedures
[AD-A205668] N89-24034
PULSE COMMUNICATION
Phase accuracy experiments with a direct-sampling coherent detector
[AD-A205458] N89-23764
PULSE COMPRESSION
Radar waveforms derived from orthogonal matrices
[AD-A205459] N89-23765
PULSED LASERS
A vector scanning processing technique for pulsed laser velocimetry
[NASA-TM-102048] N89-23850
Pulse shaping on the Nova laser system
[DE89-008026] N89-23859
The chirped-pulse free-electron laser
[DE89-009041] N89-23862
PYLONS
Noise of a model counterrotation propeller with simulated fuselage and support pylon at takeoff/approach conditions
[NASA-TM-101996] N89-24138
PYROLYSIS
High-temperature LDV seed particle development
[NASA-CR-182265] N89-23851
PYROTECHNICS
Pyro thruster for performing rocket booster attachment, disconnect, and jettison functions N89-23902
PYRROLES
Water-processable conducting polymers
[DE89-009251] N89-23688

Q

QUADRATIC EQUATIONS
Quadratic optimal control theory for viscoelastically damped structures using a fractional derivative viscoelasticity model
[AD-A206008] N89-23932
QUADRUPOLES
Strong and electromagnetic interactions in heavy exotic atoms
[PB89-145718] N89-24143
QUALIFICATIONS
Qualification Motor no. 8 (QM-8), volume 1
[NASA-CR-183650] N89-23523
QUALITY CONTROL
Composite materials nondestructive tests: Choice of methods depending on requirements
[REPT-882-430-105] N89-23630
Challenges of nondestructive testing of composite materials
[REPT-882-430-107] N89-23632
Environmental Stress Screening (ESS) guide
[AD-A206350] N89-23868
QUANTITATIVE ANALYSIS
Application of the method of X-ray fluorescence analysis with synchrotron radiation to study lunar matter
[DE88-705782] N89-24247
QUANTUM ELECTRONICS
Atomic layer epitaxy. Atomic layer epitaxy of 3-5 compound semiconductors by thermal and laser-assisted metalorganic chemical vapor deposition
[AD-A205699] N89-24200
QUANTUM THEORY
Equations for two-dimensional density matrix. Approximate solutions in the vicinity of the classical solution
[DE88-705825] N89-24107
Lattice symmetries and thermal expansion
[AD-A206045] N89-24207
QUENCHING (COOLING)
An experimental study of opposed flow diffusion flame extinction over a thin fuel in microgravity
[NASA-CR-182185] N89-23638
Quench sensitivity of airframe aluminium alloys
[PB89-146039] N89-23656

R

RADAR
On the problem of optimal signal detection in discrete-time, correlated, non-Gaussian noise
[AD-A205859] N89-23771
RADAR ANTENNAS
The performance of Space-Based Radars (SBR) orbiting on elliptical orbits
[AD-A205951] N89-23772
Mesospheric wind measurement
[AD-A205593] N89-23991
RADAR CROSS SECTIONS
Coupled integral equation solution for two dimensional bistatic TE scatter from a conducting cavity-backed infinite plane
[AD-A206096] N89-23775
RADAR DATA
Study of a method to de-alias winds from ERS-1 data
[CREO-6374] N89-24003
RADAR ECHOES
Active radar jamming
[FOA-C-30506-3.6] N89-23777
Studies of frontal zone dynamics with a high-resolution wind profiling system
[AD-A205988] N89-24008
RADAR IMAGERY
Battlefield radar imaging through airborne millimetric wave SAR (Synthetic Aperture Radar)
[ETN-89-94228] N89-23751
Autofocus of SAR imagery degraded by ionospheric-induced phase errors
[DE89-008278] N89-23752
RADAR MAPS
Navigation shift correction by radar cartography. Optimization and validation by simulation
[REPT-882-320-103] N89-23755
RADAR NAVIGATION
Navigation shift correction by radar cartography. Optimization and validation by simulation
[REPT-882-320-103] N89-23755
RADAR RECEIVERS
Performance of radar receivers in the presence of noise and intentional interference
[AD-A205328] N89-23759
Mesospheric wind measurement
[AD-A205593] N89-23991
RADAR REFLECTORS
A chamber experiment for the feasibility study of an artificial plasma reflector for OTH radar applications
[NASA-CR-184912] N89-23478
RADAR RESOLUTION
Sea spike modeling
[AD-A205355] N89-23760
RADAR SIGNATURES
Imaging procedure of underwater bottom topography by air and satellite images in the range of microwave and visible electromagnetic spectra
[GKSS-88/E/41] N89-24014
RADIANT FLUX DENSITY
Spectrometric studies of gas phase collision processes
[AD-A205570] N89-23826
RADIATION BELTS
The space particle environment N89-23548
Trapped radiation N89-23560
Trapped particle flux models at NSSDC/WDC-A-R/S N89-23561

Solar flares and magnetospheric particles: Investigations based upon the ONR-602 and ONR-604 experiments [AD-A205599] N89-24253
RADIATION COUNTERS
Direct electron-pair production by high energy heavy charged particles [NASA-CR-184958] N89-24142
RADIATION DAMAGE
Effect of n on 1 laser treatment on damage threshold of selected optical coating [DE89-008830] N89-23861
RADIATION DISTRIBUTION
Three-dimensional analysis of optical transition radiation [AD-A205935] N89-24156
RADIATION EFFECTS
NASA/SDIO Space Environmental Effects on Materials Workshop, part 1 [NASA-CP-3035-PT-1] N89-23526
Overview of environmental factors N89-23529
Structural materials for space applications N89-23530
Radiation effects in spacecraft electronics N89-23531
Trends in environmentally induced spacecraft anomalies N89-23536
Returned Solar Max hardware degradation study results N89-23537
Atomic oxygen effects on materials N89-23540
NASA/SDIO Space Environmental Effects on Materials Workshop, part 2 [NASA-CP-3035-PT-2] N89-23547
Ultraviolet radiation effects N89-23551
Dielectrics for long term space exposure and spacecraft charging: A briefing N89-23553
An overview of charging environments N89-23554
Atomic oxygen N89-23557
Trapped radiation N89-23560
Trapped particle flux models at NSSDC/WDC-A-R/S N89-23561
Solar radiation N89-23562
Spacecraft charging N89-23563
Working group written presentation: Atomic oxygen N89-23564
Working group written presentation: Trapped radiation effects N89-23566
Working group written presentation: Solar radiation N89-23567
Working group written presentation: Spacecraft charging N89-23568
On steel superficial hardening by concentrated electron beam in the air [DE88-705781] N89-23658
High electric field phenomena in insulation [AD-A205525] N89-23799
Effect of n on 1 laser treatment on damage threshold of selected optical coating [DE89-008830] N89-23861
A low-energy X-ray irradiator for electrophysiological studies [AD-A205388] N89-24028
RADIATION HARDENING
System study: Radiation hardened autonomous navigation [AD-A205604] N89-23439
On steel superficial hardening by concentrated electron beam in the air [DE88-705781] N89-23658
RADIATION MEASUREMENT
On the measurement of cosmogenic nuclides in cometary materials [DE89-009248] N89-24243
RADIATION SOURCES
Summaries of papers presented at Short Wavelength Coherent Radiation: Generation and Applications Topical Meeting held in Cape Cod, Massachusetts on September 26-29, 1988 [AD-A205471] N89-23857
An ultra-soft Einstein X-ray survey [DE89-007993] N89-24256
RADIATION SPECTRA
Ultraviolet radiation effects N89-23551
RADIATIVE HEAT TRANSFER
Effect of internal convection and internal radiation on the structural temperatures of Space Shuttle Orbiter [NASA-TM-100414] N89-23819
RADIO COMMUNICATION
AN/TAC-1 demultiplexer circuit card assembly [AD-A205744] N89-23770
RADIO DIRECTION FINDERS
Navigation shift correction by radar cartography. Optimization and validation by simulation [REPT-882-320-103] N89-23755
RADIO FREQUENCIES
Investigation of the behaviour of a collisionless R-F sheath [OUEL-1695/87] N89-24165
RADIO NAVIGATION
Improvement of navigation measurement procedures by the combined application of correlation techniques and parameter estimation [ETN-89-93946] N89-23445
RADIO RECEIVERS
Tuner for the first intermediate frequency of receivers for direct satellite reception [ETN-89-93766] N89-23788
Near-far resistant linear multiuser detection [AD-A206363] N89-23802
RADIO TRANSMISSION
Loran C field strength contours: Contiguous US [DOT/FAA/CT-TN89/16] N89-23437
RADIOACTIVE CONTAMINANTS
Use of the 1:2,000,000 Digital Line Graph data in emergency response [DE89-006730] N89-23959
RADIOISOTOPE BATTERIES
Preliminary assessment of rover power systems for the Mars Rover Sample Return Mission [NASA-TM-102003] N89-23518
Final safety analysis report for the Galileo Mission. Volume 1: Reference design document [DE89-007268] N89-24147
RADIOMETERS
A segmented mirror antenna for radiometers [NASA-TM-102045] N89-23753
RADIOMETRIC CORRECTION
The absolute radiometric calibration of the advanced very high resolution radiometer [NASA-CR-185057] N89-23852
RADIOMETRIC RESOLUTION
The absolute radiometric calibration of the advanced very high resolution radiometer [NASA-CR-185057] N89-23852
RADIOSONDES
Studies of frontal zone dynamics with a high-resolution wind profiling system [AD-A205988] N89-24008
RAILGUN ACCELERATORS
Electromagnetic railgun hydrogen pellet injector: Progress and prospect [DE89-009536] N89-23499
RAIN
Link availability and rain attenuation exceedance characteristics for EHF (Extremely High Frequency) satellite communications with arbitrary link parameters in Canada [AD-A205403] N89-23762
RAMAN SPECTRA
Nonlinear spectroscopy of multicomponent droplets and two- and three-dimensional measurements in flames [AD-A205449] N89-23645
Spectroscopic studies of metal-ligand-surface interactions [AD-A206460] N89-23652
RAMAN SPECTROSCOPY
Development of a CARS device for a feasibility study of density and temperature measurements at high time dependent resolution [ISL-R-117/87] N89-23654
RAMJET ENGINES
Comparison of computational analysis with flight tests of a 40mm solid-fuel ramjet projectile [AD-A206536] N89-23459
RANDOM ACCESS MEMORY
Signal-Noise/Interferer Combiner Unit Programmable (SINCUP) [AD-A205367] N89-24053
RANDOM NOISE
Investigation of mutual interference between digitally modulated signals [BBC-RD-1988/13] N89-23745
Near-far resistant linear multiuser detection [AD-A206363] N89-23802
RANDOM PROCESSES
Microscopic theory of electron spin resonance in Heisenberg spin glasses and thermal fluctuations in classical spin models with random fields [JUEL-2227] N89-24146
RANDOM VARIABLES
Asymptotic behavior of random discrete event systems [PB89-146146] N89-24099
RANDOM VIBRATION
Environmental Stress Screening (ESS) guide [AD-A206350] N89-23888
RATINGS
Simulator evaluation of a display for a Takeoff Performance Monitoring System [NASA-TP-2908] N89-23469
REACTION BONDING
Preparation and evaluation of silicon nitride matrices for silicon nitride-SiC fiber composites [NASA-CR-184798] N89-23678
REACTION KINETICS
Fundamental studies on spray combustion and turbulent combustion [AD-A206438] N89-23651
Study of adherent oxide scales [AD-A205799] N89-23700
Nucleation and undercooling N89-23726
Atomic layer epitaxy. Atomic layer epitaxy of 3-5 compound semiconductors by thermal and laser-assisted metalorganic chemical vapor deposition [AD-A205699] N89-24200
In situ mechanistic studies of MOCVD growth of 3/5 semiconductors [AD-A206396] N89-24210
REACTION TIME
The relationship between subjective and objective measures of sleepiness [AD-A205861] N89-24027
REACTIVITY
Energy disposal in ion-molecule reactions [AD-A205987] N89-24144
REACTOR SAFETY
Final safety analysis report for the Galileo Mission. Volume 1: Reference design document [DE89-007268] N89-24147
REAL TIME OPERATION
Application of a PC based, real-time, data-aquisition system in rotorcraft wind-tunnel testing [NASA-TM-4119] N89-24079
RECEIVERS
Impact of the geoplasma on a spaceborne GPS receiver system: A preliminary study [AD-A205965] N89-23442
RECLAMATION
Propellant reuse/recovery technology [AD-A206306] N89-23714
RECOGNITION
Relating attention to visual mechanisms [AD-A206452] N89-24042
RECTANGULAR WAVEGUIDES
Acoustic response of a rectangular waveguide with a strong transverse temperature gradient [NASA-TM-101564] N89-24140
RECTANGULAR WINGS
Flutter of a low-aspect-ratio rectangular wing [NASA-TM-4116] N89-23447
RECURSIVE FUNCTIONS
Recursive gate-arrays [AD-A205335] N89-23796
Runtime aggregation of recursion relations [AD-A206576] N89-24076
Numerical experience with a superfast real Toeplitz solver [AD-A205374] N89-24115
The electronic structure of GaAs sub 1-x P sub x and GaSb sub 1-x P sub x calculated using the recursion method [DE88-705702] N89-24185
REDUCED GRAVITY
An experimental study of opposed flow diffusion flame extinction over a thin fuel in microgravity [NASA-CR-182185] N89-23638
Research activity report concerning solidification technology under microgravity [ETN-89-93988] N89-23718
Summary of 1st Summer School on Microgravity [DFVLR-IB-333-87/2] N89-23719
Mission conditions and hardware concepts N89-23720
Microgravity User Support Center (MUSC) N89-23721
Payload experts in D1-mission N89-23722
Convection N89-23723
Diffusion N89-23724
Phase transformation N89-23725
Nucleation and undercooling N89-23726
Metallic solidification N89-23727
Model systems — metal alloys N89-23728
Semiconductors and monocrystal growth: Collection of charts, formulas and references N89-23729
Organic monocrystals N89-23730
Microgravity conditions of a spacecraft N89-23731
Biological results obtained by D1-mission N89-23732
Telescience and image processing for PODI: An analysis and a proposal for a simulation set-up [NLR-TR-88005-U] N89-23815
Advanced space design program to the Universities Space Research Association and the National Aeronautics and Space Administration [NASA-CR-180450] N89-24015
Microgravity particle reduction system N89-24019

Gas-Grain Simulation Facility: Fundamental studies of particle formation and interactions. Volume 1: Executive summary and overview
[NASA-CP-10026-VOL-1] N89-24022
Gas-Grain Simulation Facility: Fundamental studies of particle formation and interactions. Volume 2: Abstracts, candidate experiments and feasibility study
[NASA-CP-10026-VOL-2] N89-24023

REDUNDANCY
A closed-form trim solution yielding minimum trim drag for airplanes with multiple longitudinal-control effectors
[NASA-TP-2907] N89-23468
System Mean-Time-Between-Failure versus life-cycle logistics cost subject to the introduction of Line-Replaceable-Unit redundancy
[AD-A206324] N89-23887

REENTRY SHIELDING
Nozzles for test system plasma generators --- Hermes
[REPT-882-430-104] N89-23502
Reentry materials in the atmosphere
[REPT-882-430-102] N89-23629
High performance refractory composite materials
[REPT-882-430-106] N89-23631

REENTRY VEHICLES
Reentry materials in the atmosphere
[REPT-882-430-102] N89-23629

REFLECTANCE
Studies of frontal zone dynamics with a high-resolution wind profiling system
[AD-A205988] N89-24008

REFLECTOR ANTENNAS
A segmented mirror antenna for radiometers
[NASA-TM-102045] N89-23753

REFLECTORS
A method to design blended rolled edges for compact range reflectors
[NASA-CR-184976] N89-23736
Mechanical/electrical distortion model for reflector antennas
[REPT-882-440-104] N89-23781

REFRACTING TELESCOPES
The Allegheny Observatory search for planetary systems
[NASA-CR-184990] N89-24233

REFRACTORIES
Investigations on low cement and ultra low cement refractory castables N89-23593

REFRACTORY MATERIALS
Theoretical analysis of compatibility of several reinforcement materials with NiAl and FeAl matrices
[NASA-CR-182291] N89-23622
High performance refractory composite materials
[REPT-882-430-106] N89-23631
The protection against oxidation of carbon materials. Thermodynamic and experimental study: A literature survey --- carbon fibers
[REPT-882-430-108] N89-23633

REGENERATIVE FUEL CELLS
Photovoltaic power system considerations for future lunar bases
[NASA-TM-102019] N89-23517

REGRESSION ANALYSIS
Inferring relative humidity profiles from 3DNEPH cloud data: Technique development and data impact study
[AD-A205825] N89-23993

REGULATIONS
Environmental projects. Volume 3: Environmental compliance audit
[NASA-CR-185019] N89-23985

REINFORCING FIBERS
Theoretical analysis of compatibility of several reinforcement materials with NiAl and FeAl matrices
[NASA-CR-182291] N89-23622
Fabrication of unidirectional fiber reinforced 6061 aluminum alloy using high pressure squeeze casting
[AD-A205717] N89-23668
Finite element modeling of frictionally restrained composite interfaces
[NASA-CR-182281] N89-23918

REINFORCING MATERIALS
Theoretical analysis of compatibility of several reinforcement materials with NiAl and FeAl matrices
[NASA-CR-182291] N89-23622

RELATIVISTIC EFFECTS
Relativistic and non-relativistic magnetohydrodynamic flows around compact stars N89-24242

RELATIVISTIC ELECTRON BEAMS
Simulation studies of particle acceleration powered by modulated intense relativistic electron beams
[AD-A206348] N89-24148

RELAXATION TIME
Zinc oxide varistor time response
[DE89-008234] N89-24191

RELIABILITY
An experimental investigation into software reliability
[AD-A206293] N89-24069

RELIABILITY ANALYSIS
Evaluation of tests and design factors --- structures
[REPT-882-440-109] N89-23889
Avionics architecture studies for the entry research vehicle
[NASA-CR-181828] N89-24082

RELIEF MAPS
Computer aided production of a 1:25,000 relief model of Berlin and surroundings N89-23943

REMOTE CONTROL
Double lead spiral platen parallel jaw end effector N89-23905
Traction-drive force transmission for telerobotic joints N89-23906
Flight telerobot mechanism design: Problems and challenges N89-23907

REMOTE MANIPULATOR SYSTEM
The design and analysis of a double swivel toggle release mechanism for the Orbiter stabilized payload deployment system N89-23895

REMOTE SENSING
Co-aligning the RAIDS (Remote Atmospheric and Ionospheric Detection System) instruments
[AD-A205456] N89-23513
Electromagnetic remote sensing. Low frequency electromagnetics
[AD-A205402] N89-23761
Remote sensing of global snowpack energy and mass balance: In-situ measurements on the snow of interior and Arctic Alaska
[NASA-CR-180078] N89-23956
Determination of areal snow water equivalent using satellite images and gamma ray spectrometry
[CI-91] N89-23960
Geobotanical remote sensing for determination of aggregate source material
[AD-A205943] N89-23962
The search for edges in remote sensing images using a digital polygonal map
[ETN-89-94146] N89-23964
Investigation of several methods for the detection of outstanding points in a digital image
[ETN-89-94148] N89-23965
Vectorization of grid lines
[ETN-89-94150] N89-23967
On the international commercialization of remote sensing
[BCRS-88-02] N89-23969
Optical properties of oceanic suspended matter and their interpretation for remote sensing of phytoplankton
[GKSS-88/E/40] N89-24013

REMOTE SENSORS
Research for optimization of future MOMS sensors
[ETN-89-94424] N89-23972

REPLICAS
Flight testing of the Southern Cross replica aircraft
[AD-A205303] N89-23451
Grazing incidence telescopes for ESA's X-ray astronomy mission XMM
[MPE-PREPRINT-129] N89-24239

REQUIREMENTS
Continuous, low thrust coplanar orbit transfers with varying eccentricity
[AD-A206022] N89-23498

RESCUE OPERATIONS
National Airspace System Search and Rescue operational concept (NAS-SR-1329)
[DOT/FAA/DS-89/07] N89-23435

RESEARCH
US Air Force research technology area plan, FY 1989
[AD-A205304] N89-24217

RESEARCH AIRCRAFT
The functional mock-up test of the flight control system of the NAL QSTOL research aircraft ASKA
[NAL-TR-972] N89-23467
The 4D-TECS integration for NASA TSRV airplane
[NASA-CR-4231] N89-23471

RESEARCH AND DEVELOPMENT
NASA aeronautics research and technology
[NASA-EP-259] N89-23406
Materials science cooperation in 1987 N89-23570
IDA (Institute for Defense Analyses) gamma-ray laser: Investigation of the feasibility of developing a laser using nuclear transitions
[AD-A205318] N89-23864
IDA (Institute for Defense Analyses) gamma-ray laser: Investigation of developing a laser using nuclear transitions
[AD-A205319] N89-23865
The evolution of space mechanisms in the ESA R and D program N89-23893
The state of software engineering practice: A preliminary report
[AD-A206573] N89-24075
Air Force Human Resources Laboratory R and D accomplishments and services, FY86-FY88
[AD-A205312] N89-24218
Putting science and technology to work: A casebook of transferred technologies
[DE89-009158] N89-24228

RESEARCH FACILITIES
A research facility for film cooling investigations with emphasis on the instrumentation system
[NAL-TM-PR-8704] N89-23477
Microgravity User Support Center (MUSC) N89-23721
The evolution of space mechanisms in the ESA R and D program N89-23893

RESEARCH MANAGEMENT
US Air Force research technology area plan, FY 1989
[AD-A205304] N89-24217

RESEARCH VEHICLES
Preliminary design of a modular unmanned research vehicle. Volume 2: Subsystem technical development design study
[AD-A205678] N89-23454

RESIDUAL STRESS
Overview of ASTM symposium on analytical and experimental methods for residual stress effects in fatigue
[AD-A205622] N89-23931

RESIN MATRIX COMPOSITES
Mode 2 delamination fatigue resistance of composites N89-23624
Processable polyimide adhesive and matrix composite resin
[NASA-CASE-LAR-14101-1] N89-23692
Donor acceptor polymerization chemistry as a vehicle to low energy cure of matrix resins: Evolution of the 2-Tg concept to produce Tg polymers at ambient temperatures
[AD-A206287] N89-23706

RESINS
Attenuation measurement of very low-loss dielectric waveguides by the cavity resonator method in the millimeter/submillimeter wavelength range
[AD-A206458] N89-23803

RESISTORS
Zinc oxide varistor time response
[DE89-008234] N89-24191

RESONANT FREQUENCIES
Analytical transfer functions in parallel configurations
[AD-A205714] N89-23472
Computerized measurement of thermoacoustically generated temperature gradients
[AD-A205353] N89-23929

RESPIRATION
Oxygen consumption rate of operational underwater swimmers
[AD-A205331] N89-24025

RETINA
Additivity of retinal damage for multiple-pulse laser exposures
[AD-A206514] N89-24032

REUSABLE ROCKET ENGINES
Design, fabrication and test of the RL10 derivative II chamber/primary nozzle
[NASA-CR-179595] N89-23519

REYNOLDS NUMBER
Free shear layer and swirl flow heat transfer enhancement
[PB89-145106] N89-23810

RHEOLOGY
Quasi-liquid crystalline materials with special electro-optic properties
[AD-A206015] N89-24206

RIBLETS
Drag and noise measurements on underwater vehicles with a riblet surface coating
[AD-A205500] N89-23825

RIDING QUALITY
Detailed design of a Ride Quality Augmentation System for commuter aircraft
[NASA-CR-4230] N89-23470

RING LASERS
High energy efficient solid state laser sources
[NASA-CR-181782] N89-23856

RL-10 ENGINES
Design, fabrication and test of the RL10 derivative II chamber/primary nozzle
[NASA-CR-179595] N89-23519

ROADS
Investigations on the cracking behavior of joints in airfields and roads: Field investigations and laboratory simulations
[PB89-141279] N89-23479

ROBOTICS
Multiple model-based robot control: Development and initial evaluation
[AD-A205725] N89-23881

Double lead spiral platen parallel jaw end effector N89-23905
Traction-drive force transmission for telerobotic joints N89-23906
Flight telerobot mechanism design: Problems and challenges N89-23907

ROBOTS
An application specific integrated circuit for dual-axis motion control [DE89-007974] N89-23790
Modeling and simulation of a Stewart platform type parallel structure robot [NASA-CR-184969] N89-23875
Multiple model-based robot control: Development and initial evaluation [AD-A205725] N89-23881

ROBUSTNESS (MATHEMATICS)
The role of order in distributed programs [AD-A206037] N89-24065
Robust multivariable feedback design [OUEL-1723/88] N89-24090

ROCKET ENGINE DESIGN
Design, fabrication and test of the RL10 derivative II chamber/primary nozzle [NASA-CR-179595] N89-23519
Space station propulsion test bed [NASA-CR-183615] N89-23521

ROCKET ENGINES
Code optimization of speckle reduction algorithms for image processing of rocket motor holograms [AD-A205306] N89-23524
An experimental investigation in the behavior of metallized solid propellants [AD-A206510] N89-23715

ROCKET EXHAUST
A numerical routine for defining rocket exhaust characteristics and impingement effects [AD-A206323] N89-23526

ROCKET NOZZLES
Ejector effects on a supersonic nozzle at low altitude and Mach number [AD-A206049] N89-23427
Design, fabrication and test of the RL10 derivative II chamber/primary nozzle [NASA-CR-179595] N89-23519

ROCKET THRUST
Ejector effects on a supersonic nozzle at low altitude and Mach number [AD-A206049] N89-23427

ROTARY WINGS
Enhancements to a new free wake hover analysis [NASA-CR-177523] N89-23414

ROTATION
Production of metal powders by rotating electrode process N89-23608

ROTOR AERODYNAMICS
Enhancements to a new free wake hover analysis [NASA-CR-177523] N89-23414

ROTOR BLADES (TURBOMACHINERY)
Composite blade structural analyzer (COBSTRAN) user's manual [NASA-TM-101461] N89-23621

ROTOR BODY INTERACTIONS
Noise of a model counterrotation propeller with simulated fuselage and support pylon at takeoff/approach conditions [NASA-TM-101996] N89-24138

ROTOR DYNAMICS
Computing induced velocity perturbations due to a helicopter fuselage in a free stream [NASA-TM-4113] N89-23410

ROTORS
Signal and power roll ring testing update N89-23909
Application of a PC based, real-time, data-aquisition system in rotorcraft wind-tunnel testing [NASA-TM-4119] N89-24079

ROVING VEHICLES
Preliminary assessment of rover power systems for the Mars Rover Sample Return Mission [NASA-TM-102003] N89-23518

RUN TIME (COMPUTERS)
Runtime aggregation of recursion relations [AD-A206576] N89-24076

RUNGE-KUTTA METHOD
Missile actuator simulation and an investigation into the accuracy of Runge-Kutta numerical integration [AD-A206325] N89-23458

RUNWAYS
Instrument landing system mathematical modeling study for Orlando International Airport Runway 35L localizer, Orlando, Florida. Final airside docking plan (Scheme 3A) [AD-A205351] N89-23438
Investigations on the cracking behavior of joints in airfields and roads: Field investigations and laboratory simulations [PB89-141279] N89-23479

RYDBERG SERIES
Ultra-high resolution VUV-XUV laser: Application to the hyperfine study of krypton [DE89-009059] N89-23863

S

SAFETY
Corrosion and lubricity testing of nonflammable USAF formulated CTFE (Chlorotrifluoroethylene) base hydraulic fluid [AD-A205467] N89-23695
A demonstration of the method of stochastic finite element analysis [AD-A206135] N89-24127

SAFETY DEVICES
A unidirectional rotary solenoid as applied to stronglinks N89-23894

SAFETY FACTORS
Evaluation of tests and design factors --- structures [REPT-882-440-109] N89-23889

SAFETY MANAGEMENT
A unidirectional rotary solenoid as applied to stronglinks N89-23894

SAMPLING
Sample preparation techniques for evaluating methanol and formaldehyde emissions from methanol fueled vehicles and engines [PB89-136147] N89-23734

SATELLITE ATTITUDE CONTROL
An analysis of the attitude stability of a space station subject to parametric excitation of periodic mass motion [AD-A206009] N89-23505

SATELLITE COMMUNICATION
Study of spread spectrum multiple access systems for satellite communications with overlay on current services: Executive summary [NASA-CR-180827-EXEC-SUMM] N89-23756
Study of spread spectrum multiple access systems for satellite communications with overlay on current services [NASA-CR-180827] N89-23757
Link availability and rain attenuation exceedance characteristics for EHF (Extremely High Frequency) satellite communications with arbitrary link parameters in Canada [AD-A205403] N89-23762

SATELLITE DESIGN
TELE-X antenna module thermal control [REPT-882-440-106] N89-23782
Near field testing of the electronically despun antenna of the Meteosat satellite [REPT-882-440-108] N89-23783
Shaking in cryogenic conditions [REPT-882-440-101] N89-23939

SATELLITE DOPPLER POSITIONING
On the connection of geodetic pointfields in RETrig [PB89-146112] N89-23958

SATELLITE IMAGERY
The absolute radiometric calibration of the advanced very high resolution radiometer [NASA-CR-185057] N89-23852
Geocoded data sets of imaging satellites N89-23950
Remote sensing of global snowpack energy and mass balance: In-situ measurements on the snow of interior and Arctic Alaska [NASA-CR-180078] N89-23956
Determination of areal snow water equivalent using satellite images and gamma ray spectrometry [CI-91] N89-23960

SATELLITE LIFETIME
Arcjet nozzle design impacts [NASA-TM-102050] N89-23522

SATELLITE NAVIGATION SYSTEMS
Global Positioning System (GPS) positioning at sea [ETN-89-94145] N89-23446
Observation model and parameter partials for the JPL geodetic GPS modeling software GPSOMC [NASA-CR-185021] N89-24060

SATELLITE ORBITS
Orbit parameters given N89-23491
An improved strategy for determining earth satellite orbits by radio [AD-A205826] N89-23497
Co-aligning the RAIDS (Remote Atmospheric and Ionospheric Detection System) instruments [AD-A205456] N89-23513

SATELLITE POWER TRANSMISSION (TO EARTH)
Study of spread spectrum multiple access systems for satellite communications with overlay on current services: Executive summary [NASA-CR-180827-EXEC-SUMM] N89-23756

SATELLITE TELEVISION
Tuner for the first intermediate frequency of receivers for direct satellite reception [ETN-89-93766] N89-23788

SCALE (CORROSION)
Study of adherent oxide scales [AD-A205799] N89-23700

SCALING LAWS
Lattice symmetries and thermal expansion [AD-A206045] N89-24207

SCANNING
A vector scanning processing technique for pulsed laser velocimetry [NASA-TM-102048] N89-23850
Digitizing of drawings and cadastral maps using a scanner system N89-23949

SCATTERING
A first-principles calculation of the resistivity and thermopower in strong-scattering alloys [DE89-008565] N89-23661
Sea spike modeling [AD-A205355] N89-23760
Transport of test particles in a magnetic field with perturbed magnetic surfaces [IPP-2/296] N89-24176

SCATTEROMETERS
Study of a method to de-alias winds from ERS-1 data [CREO-6374] N89-24003

SCHLIEREN PHOTOGRAPHY
Telescience and image processing for PODI: An analysis and a proposal for a simulation set-up [NLR-TR-88005-U] N89-23815

SCIENTIFIC SATELLITES
The evolution of space mechanisms in the ESA R and D program N89-23893

SCIENTISTS
Age distribution among NASA scientists and engineers N89-23911

SEA LEVEL
Problems encountered in the Stokes' numerical integration of terrestrial gravity anomalies [AD-A205448] N89-23990

SEA WATER
Optical properties of oceanic suspended matter and their interpretation for remote sensing of phytoplankton [GKSS-88/E/40] N89-24013

SEALING
Friction factor data for flat plate tests of smooth and honeycomb surfaces [NASA-CR-184977] N89-23876

SEARCHING
National Airspace System Search and Rescue operational concept (NAS-SR-1329) [DOT/FAA/DS-89/07] N89-23435
Deductive programming synthesis [AD-A206451] N89-24072

SECONDARY FLOW
Mechanisms of secondary flows and losses within a three dimensional turbine stator cascade [NAL-TR-970T] N89-23807

SECONDARY INJECTION
Two-dimensional confined jet thrust vector control: Operating mechanisms and performance [AD-A206011] N89-23834

SEEDS
Automated seed manipulation and planting N89-24017
Automated seed manipulation and planting N89-24020

SELECTIVE SURFACES
Radiation physics properties of selective solar energy absorber layers [ETN-89-93945] N89-23978

SELECTIVITY
Structure/permeability relationships of silicon-containing polyimides [NASA-CR-4237] N89-23683

SELENIDES
High pressure studies on infrared detector materials [NAL-TM-MT-8701] N89-23677

SELF ORGANIZING SYSTEMS
Prospects for classifying complex imagery using a self-organizing neural network [AD-A206208] N89-24088

SEMANTICS
Relating attention to visual mechanisms [AD-A206452] N89-24042

SEMICONDUCTOR DEVICES
Fundamental and practical studies of metal contacts on mercury zinc telluride [AD-A206560] N89-23653
Semiconductor measurement technology: Automatic determination of the interstitial oxygen content of silicon wafers polished on both sides [PB89-151831] N89-24180

Characterization of semiconductor device processing etchant solutions for GaAs and p+ GaAs layers employed in AlxGa(1-x)As/GaAs MODFETs and related heterojunction devices
[AD-A205772] N89-24201

SEMICONDUCTOR LASERS
High-power single spatial mode AlGaAs channeled-substrate-planar semiconductor diode lasers for spaceborne communications
[NASA-CR-4238] N89-23860

SEMICONDUCTORS (MATERIALS)
High pressure studies on infrared detector materials
[NAL-TM-MT-8701] N89-23677
Semiconductors and monocrystal growth: Collection of charts, formulas and references N89-23729
High energy semiconductor switch
[DE89-007399] N89-23789
Heterojunction band line-ups and the alloying effect in compound semiconductor alloys: A photoemission study N89-24179
Semiconductor measurement technology: Automatic determination of the interstitial oxygen content of silicon wafers polished on both sides
[PB89-151831] N89-24180
In situ mechanistic studies of MOCVD growth of 3/5 semiconductors
[AD-A206396] N89-24210
Alternate arsenic and antimony sources for the OMCVD fabrication of semiconductors
[AD-A206483] N89-24211

SENSITIVITY
Quench sensitivity of airframe aluminium alloys
[PB89-146039] N89-23656

SENSORS
Design and development of a high-stiffness, high-resolution torque sensor N89-23903

SENSORY PERCEPTION
The attention system of the human brain
[AD-A206157] N89-24040

SEPARATED FLOW
High angle-of-attack aerodynamic characteristics of crescent and elliptic wings
[NASA-CR-184992] N89-23418
Flow control for unsteady and separated flows and turbulent mixing
[AD-A205989] N89-23426
Some applications of the qualitative theory of differential equations in fluid dynamics
[ETN-89-94143] N89-23814

SEPARATORS
Automated seed manipulation and planting N89-24020

SEQUENCING
Analytical transfer functions in parallel configurations
[AD-A205714] N89-23472
Laboratory process control using natural language commands from a personal computer
[NASA-TM-101988] N89-24055

SERVICE LIFE
USAF (US Air Force) durability design handbook: Guidelines for the analysis and design of durable aircraft structures
[AD-A206286] N89-23457
SIRTF Telescope Instrument Changeout and Cryogen Replenishment (STICCR) Study
[NASA-CR-177380] N89-23512
Study of adherent oxide scales
[AD-A205799] N89-23700
Fatigue crack growth model RANDOM2 user manual, appendix 1
[NASA-CR-184939] N89-23890
Fatigue strength reduction model: RANDOM3 and RANDOM4 user manual, appendix 2
[NASA-CR-184940] N89-23891
MPD thruster erosion research
[NASA-CR-185314] N89-24168

SERVOMECHANISMS
Actuator rate saturation compensator
[AD-D013962] N89-23474
Carousel deployment mechanism for collable lattice truss N89-23897
Structural mode frequencies of FOG-M (Fiber Optics Guided-Missile) actuator/fin
[AD-A206327] N89-24158

SHAPES
Tests for the gamma distribution with estimated shape parameters
[AD-A205829] N89-24118

SHEAR FLOW
Turbulent shear stress measurement in hypersonic flow
[AD-A206453] N89-23432

SHEAR LAYERS
Effects of initial conditions on the development of supersonic turbulent free shear layers
[AD-A205607] N89-23421
Investigation of the flowfield created by the interaction of a sonic jet and a co-flowing supersonic stream
[AD-A205823] N89-23425
Computational study of high supersonic flow over boattails with centered propulsive jets
[AD-A206364] N89-23431
Free shear layer and swirl flow heat transfer enhancement
[PB89-145106] N89-23810

SHEAR PROPERTIES
Effects of initial conditions on the development of supersonic turbulent free shear layers
[AD-A205607] N89-23421

SHEAR STRAIN
The crack problem in bonded nonhomogeneous materials
[NASA-CR-184897] N89-23926

SHEAR STRESS
Turbulent shear stress measurement in hypersonic flow
[AD-A206453] N89-23432
Comparison of split-film and x-film measurements in 2-D flow
[AD-A206023] N89-23836
Turbulence near a free surface in a plane jet
[AD-A206269] N89-23838

SHOCK RESISTANCE
Investigation of alpha-SiC hot corrosion in the presence of basic slag N89-23595

SHOCK TUBES
Boundary layer and heat transfer behind a piston in a shock tube. Part 1: Theoretical considerations of laminar and turbulent boundary layer behind a piston in a tube
[ISL-R-111/87-PT-1] N89-23841
Boundary layer and heat transfer behind a piston in a shock tube. Part 2: Experimental study of heat transfer at the piston in a tube
[ISL-R-115/87-PT-2] N89-23842
Solution of one-dimensional Euler equations by the implicit finite difference technique of Beam and Warming
[NAL-PD-FM-8816] N89-24097

SHOCK WAVE INTERACTION
Experimental study of pressure and heating rate on a swept cylindrical leading edge resulting from swept shock wave interference
[NASA-CR-185326] N89-23411
Effects of initial conditions on the development of supersonic turbulent free shear layers
[AD-A205607] N89-23421

SHOCK WAVE PROPAGATION
Solution of one-dimensional Euler equations by the implicit finite difference technique of Beam and Warming
[NAL-PD-FM-8816] N89-24097

SHOCK WAVES
Investigation of the flowfield created by the interaction of a sonic jet and a co-flowing supersonic stream
[AD-A205823] N89-23425
A linear analysis of the stability of strong shocks and the evolution and distribution of materials in a cold dark matter dominated universe N89-24244

SHORT TAKEOFF AIRCRAFT
Navier-Stokes solution for a NACA 0012 airfoil with mass flux (fan)
[AD-A205771] N89-23424
The functional mock-up test of the flight control system of the NAL QSTOL research aircraft ASKA
[NAL-TR-972] N89-23467

SHORT WAVE RADIATION
Summaries of papers presented at Short Wavelength Coherent Radiation: Generation and Applications Topical Meeting held in Cape Cod, Massachusetts on September 26-29, 1988
[AD-A205471] N89-23867
Capture and confinement of solutions in nonlinear integrable systems
[DE88-705823] N89-24106

SIDELOBES
The effect of mutual coupling on the side lobe performance of Chebyshev arrays, volume 1
[AD-A205724] N89-23768

SIDESLIP
Characteristics of a five-hole spherical pitot tube
[NAL-TR-971] N89-23463

SIGNAL DETECTION
On the problem of optimal signal detection in discrete-time, correlated, non-Gaussian noise
[AD-A205859] N89-23771
Noise characteristics of an inductively coupled plasma-mass spectrometer
[AD-A205686] N89-24169

SIGNAL DETECTORS
Use of a spectrally segmented photodiode-array spectrometer for inductively coupled plasma atomic emission spectroscopy
[AD-A205688] N89-24171

SIGNAL PROCESSING
Study of spread spectrum multiple access systems for satellite communications with overlay on current services
[NASA-CR-180827] N89-23757
A statistical analysis of the output signals of an acousto-optic spectrum analyzer for CW (Continuous-Wave) signals
[AD-A205404] N89-23763
Phase accuracy experiments with a direct-sampling coherent detector
[AD-A205458] N89-23764
Adaptive signal processing
[AD-A205787] N89-24063

SIGNAL RECEPTION
Performance of radar receivers in the presence of noise and intentional interference
[AD-A205328] N89-23759

SIGNAL REFLECTION
Performance of radar receivers in the presence of noise and intentional interference
[AD-A205328] N89-23759

SIGNAL TO NOISE RATIOS
Performance of radar receivers in the presence of noise and intentional interference
[AD-A205328] N89-23759
Intelligibility in noise of three LPC (Linear Predictive Coders) voice channels with active noise reduction headsets
[AD-A205813] N89-23767
Signal-Noise/Interferer Combiner Unit Programmable (SINCUP)
[AD-A205367] N89-24053
Image processing of coronal pictures
[AD-A205326] N89-24252
An ultra-soft Einstein X-ray survey
[DE89-007993] N89-24256

SIGNATURES
Cartographic signatures in PHOCUS N89-23948

SILANES
Mechanism of the initiation of the cationic polymerization of styrenes by silanes and activated covalent esters
[AD-A206502] N89-23708

SILICA GEL
Mechanical behavior of PMMA-impregnated silica gels
[AD-A205975] N89-23703

SILICON CARBIDES
Silicon-carbide made of silicon-organic compounds N89-23572
Microstructure development in SiC N89-23582
Corrosion of silicon carbide ceramics at high temperatures in water vapor-containing atmospheres N89-23594
Investigation of alpha-SiC hot corrosion in the presence of basic slag N89-23595
Preparation and evaluation of silicon nitride matrices for silicon nitride-SiC fiber composites
[NASA-CR-184798] N89-23678

SILICON DIOXIDE
Slip casting of fused silica N89-23573
Undercutting of defects in thin film protective coatings on polymer surfaces exposed to atomic oxygen
[NASA-TM-101986] N89-23691
Mechanical behavior of PMMA-impregnated silica gels
[AD-A205975] N89-23703
Microporous fumed-silica insulation board as a candidate Standard Reference Material of thermal resistance
[PB89-148373] N89-24213

SILICON NITRIDES
Sintering of Si3N4 in the presence of additives from Y2O3-SiO2-Al2O3 system N89-23581
Strengthening of silicon nitride ceramics N89-23585
Preparation and evaluation of silicon nitride matrices for silicon nitride-SiC fiber composites
[NASA-CR-184798] N89-23678

SILICON TRANSISTORS
Semiconductor measurement technology: Automatic determination of the interstitial oxygen content of silicon wafers polished on both sides
[PB89-151831] N89-24180

SILICONES
Structure/permeability relationships of silicon-containing polyimides
[NASA-CR-4237] N89-23883

SILOXANES
Mechanism of the initiation of the cationic polymerization of styrenes by silanes and activated covalent esters
[AD-A206502] N89-23708

SILVER
Some examples of the degradation of properties of materials in space N89-23535
Structure and grid dynamics of ultrathin epitaxial Ag and Fe films on Ni(100) and Cu(100) substrates
[JUEL-2221] N89-24187

Nuclear magnetism in copper and silver: Theory and experiments
[ISBN-952-900-084-7] N89-24188

SILVER CHLORIDES
Chloride analysis in HAN-based liquid propellants by inductively coupled plasma spectroscopy
[AD-A206564] N89-23717

SIMPLEX METHOD
On the algebraic structure of integrable systems in multidimensions
[DE89-008697] N89-24108

SIMULATION
Atomic oxygen effects on spacecraft materials: The state of the art of our knowledge N89-23541
Geometrical foundations of mesomechanics and Lagrangian formalism
[AD-A205589] N89-23930

SIMULATORS
Transonic operational characteristics and performance
[NAL-TR-968] N89-23408
Simulator evaluation of a display for a Takeoff Performance Monitoring System
[NASA-TP-2908] N89-23489

SINGLE CRYSTALS
Semiconductors and monocrystal growth: Collection of charts, formulas and references N89-23729
Organic monocrystals N89-23730
Investigation of electronic states in nonmagnetic single crystals with spin-resolved photoemission
[JUEL-2226] N89-24212

SINGLE EVENT UPSETS
Effects of space radiation on electronic microcircuits N89-23549

SINTERING
Sintering and HIPing with additives N89-23575
Preparing and sintering of yttria-stabilized zirconia N89-23576
Preparation and thermal expansion of Al2TiO5-TiO5-TiO2 sintered bodies N89-23578
Microstructure development in alumina N89-23579
Sintering of CaO and MgO in the presence of nonequilibrium liquid phase N89-23580
Sintering of Si3N4 in the presence of additives from Y2O3-SiO2-Al2O3 system N89-23581
Microstructure development in SiC N89-23582
Thermal transport in pressureless sintered aluminum nitride N89-23590
Wear resistant sintered steel with high carbide content N89-23607
Preparation and evaluation of silicon nitride matrices for silicon nitride-SiC fiber composites
[NASA-CR-184798] N89-23578
Microwave processing of ceramics
[DE89-009350] N89-23690

SKIN FRICTION
Three dimensional high speed boundary layer flows
[AD-A206145] N89-23837

SKY RADIATION
Thermal images of sky and sea-surface background infrared radiation
[AD-A205819] N89-23892

SLAGS
Investigation of alpha-SiC hot corrosion in the presence of basic slag N89-23595

SLEEP
The relationship between subjective and objective measures of sleepiness
[AD-A205861] N89-24027
Muramyl peptide-enhanced sleep: Pharmacological optimization of performance
[AD-A205974] N89-24028

SLIP CASTING
Slip casting of fused silica N89-23573

SMALL PERTURBATION FLOW
Flosolver: A parallel computer for fluid dynamics
[NAL-TM-AE-8803] N89-23805

SNOW
Determination of areal snow water equivalent using satellite images and gamma ray spectrometry
[CI-91] N89-23960

SNOW COVER
Remote sensing of global snowpack energy and mass balance: In-situ measurements on the snow of interior and Arctic Alaska
[NASA-CR-180078] N89-23956

SOFTWARE ENGINEERING
Software reliability studies
[NASA-CR-184857] N89-24054
Laboratory process control using natural language commands from a personal computer
[NASA-TM-101988] N89-24055
Automatic documentation methodologies for software maintenance
[AD-A205872] N89-24062
The state of software engineering practice: A preliminary report
[AD-A206573] N89-24075
PRASE (Parallel Resource Analysis Software Environment) instrumentation software for the Intel iPSC hypercube
[AD-A206046] N89-24087

SOFTWARE TOOLS
A CAD (Computer Aided Design) tool for current-mode multiple-valued CMOS circuits
[AD-A205327] N89-24061
Design and implementation of an expert user interface for the computer aided prototyping system
[AD-A206113] N89-24067
A visual object-oriented unification system
[AD-A206228] N89-24068
The state of software engineering practice: A preliminary report
[AD-A206573] N89-24075

SOIL MOISTURE
Mapping freeze/thaw boundaries with SMMR data
[NASA-CR-184991] N89-23961

SOILS
Sorption of selected volatile organic constituents of jet fuels and solvents on natural sorbents from gas and solutions phases
[AD-A204073] N89-23711

SOLAR ACTIVITY
High-latitude field-strength measurements of standard broadcast band skywave transmissions monitored at Fairbanks, Alaska
[PB89-134829] N89-23747
Solar and stellar coronal plasmas
[NASA-CR-184909] N89-24162
Solar-geophysical data number 531, part 1. Data for October, September 1988 and late data
[PB89-139943] N89-24250
Solar flares and magnetospheric particles: Investigations based upon the ONR-602 and ONR-604 experiments
[AD-A205599] N89-24253

SOLAR ARRAYS
Photovoltaic power system considerations for future lunar bases
[NASA-TM-102019] N89-23517
Carousel deployment mechanism for collable lattice truss N89-23897
Eddy current damper N89-23900
A family of BAPTAs for GEO and LEO applications N89-23906
The third generation rigid solar array GSR3
[REPT-882-440-105] N89-23979

SOLAR CELLS
Some examples of the degradation of properties of materials in space N89-23535

SOLAR COLLECTORS
Low-temperature volumetric receiver concept
[DE89-008245] N89-23976

SOLAR CORONA
Solar and stellar coronal plasmas
[NASA-CR-184909] N89-24162
Very large array observations of the sun with related observations using the SMM (Solar Maximum Mission) satellite
[AD-A203874] N89-24249
Image processing of coronal pictures
[AD-A205326] N89-24252
Geomagnetic disturbances
[AD-A206052] N89-24254

SOLAR COSMIC RAYS
Solar flares and magnetospheric particles: Investigations based upon the ONR-602 and ONR-604 experiments
[AD-A205599] N89-24253

SOLAR CYCLES
The US Army Yuma Proving Ground, Arizona 33-year climate calendar and tables on associated weather elements 1954-1986. American desert country
[AD-A206256] N89-24010
Geomagnetic disturbances
[AD-A206052] N89-24254

SOLAR DYNAMIC POWER SYSTEMS
Solar dynamic power for space station freedom
[NASA-TM-102016] N89-23516

SOLAR ENERGY
Energy transfer and photochemistry in biomimetic solar conversion
[PB89-142590] N89-23974

SOLAR ENERGY ABSORBERS
Radiation physics properties of selective solar energy absorber layers
[ETN-89-93945] N89-23976

SOLAR FLARES
Very large array observations of the sun with related observations using the SMM (Solar Maximum Mission) satellite
[AD-A203874] N89-24249
Solar flares and magnetospheric particles: Investigations based upon the ONR-602 and ONR-604 experiments
[AD-A205599] N89-24253

SOLAR MAXIMUM MISSION
Returned Solar Max hardware degradation study results N89-23537
Microparticle impacts in space: Results from Solar Max and shuttle witness plate inspections N89-23544

SOLAR OBSERVATORIES
Very large array observations of the sun with related observations using the SMM (Solar Maximum Mission) satellite
[AD-A203874] N89-24249

SOLAR PHYSICS
Solar-geophysical data number 531, part 1. Data for October, September 1988 and late data
[PB89-139943] N89-24250

SOLAR RADIATION
Trends in environmentally induced spacecraft anomalies N89-23536
Solar radiation N89-23562
Working group written presentation: Solar radiation N89-23567

SOLAR RADIO BURSTS
Very large array observations of the sun with related observations using the SMM (Solar Maximum Mission) satellite
[AD-A203874] N89-24249

SOLAR RADIO EMISSION
Very large array observations of the sun with related observations using the SMM (Solar Maximum Mission) satellite
[AD-A203874] N89-24249
Solar-geophysical data number 531, part 1. Data for October, September 1988 and late data
[PB89-139943] N89-24250

SOLAR SPECTRA
Redistribution in astrophysically important hydrogen lines
[NASA-CR-181375] N89-24251

SOLAR TERRESTRIAL INTERACTIONS
Trends in environmentally induced spacecraft anomalies N89-23536

SOLAR WIND
Geomagnetic disturbances
[AD-A206052] N89-24254

SOLENOIDS
Nonintrusive methods for monitoring the operational readiness of solenoid-operated valves
[DE89-008732] N89-23878

SOLID PROPELLANT ROCKET ENGINES
Pif-Paf piloting of tactical missiles
[REPT-882-320-104] N89-23482
Flow-turning losses in solid rocket motors
[AD-A206099] N89-23525

SOLID ROCKET PROPELLANTS
An experimental investigation in the behavior of metallized solid propellants
[AD-A206510] N89-23715

SOLID STATE LASERS
High energy efficient solid state laser sources
[NASA-CR-181782] N89-23856

SOLID-SOLID INTERFACES
Finite element modeling of frictionally restrained composite interfaces
[NASA-CR-182281] N89-23918

SOLIDIFICATION
Cooling rate, undercooling and rapid solidification by atomization N89-23609
Mechanical properties of rapidly solidified iron-based alloys N89-23611
Solidification of binary substances in rectangular and cylindrical cavities
[DE89-008883] N89-23640
Spray deposition: A fundamental study of droplet impingement, spreading and consolidation
[AD-A206065] N89-23672
Research activity report concerning solidification technology under microgravity
[ETN-89-93988] N89-23718
Metallic solidification N89-23727

SOLIDS
Theta pinch discharges for solids vaporization and elemental chemical analysis
[DE89-008888] N89-23641
Numerical methods to treat collisionlike phenomena in solids
[ETN-89-93944] N89-23936
Three-dimensional recognition of solid objects from a two-dimensional image
[AD-A205667] N89-24094

SOLITARY WAVES
Capture and confinement of solutions in nonlinear integrable systems
[DE88-705823] N89-24106

SOLUTIONS
Fiber-optic time-resolved fluorescence sensor for the simultaneous determination of Al(+3), Ga(+3) and In(+3)
[AD-A205689] N89-24154
SOLVENTS
Viscosity and conductance of MEICl/AlCl3 melts containing nonaqueous solvents
[AD-A205468] N89-23646
Sorption of selected volatile organic constituents of jet fuels and solvents on natural sorbents from gas and solutions phases
[AD-A204073] N89-23711
SONIC BOOMS
Status of sonic boom methodology and understanding
[NASA-CP-3027] N89-23415
Noise and sonic boom impact technology. PCBOOM computer program for sonic boom research, volume 1
[AD-A206290] N89-23429
Noise and sonic boom impact technology. PCBOOM computer program for sonic boom research. Volume 2: Program Users/Computer operations manual
[AD-A206291] N89-23430
SORBENTS
Sorption of selected volatile organic constituents of jet fuels and solvents on natural sorbents from gas and solutions phases
[AD-A204073] N89-23711
SORPTION
Sorption of selected volatile organic constituents of jet fuels and solvents on natural sorbents from gas and solutions phases
[AD-A204073] N89-23711
SOUND PRESSURE
Computerized measurement of thermoacoustically generated temperature gradients
[AD-A205353] N89-23929
SOUND TRANSMISSION
Noise and sonic boom impact technology. PCBOOM computer program for sonic boom research, volume 1
[AD-A206290] N89-23429
Interior noise control ground test studies for advanced turboprop aircraft applications
[NASA-CR-181819] N89-24141
Managing sound in a relational multimedia database system
[AD-A205742] N89-24225
SOUND WAVES
Flow-turning losses in solid rocket motors
[AD-A206099] N89-23525
Mesospheric wind measurement
[AD-A205593] N89-23991
Experimental and theoretical studies of dense fluid mixtures
[DE89-008882] N89-24214
SOVIET SATELLITES
Orbit parameters given N89-23491
SOVIET SPACECRAFT
Buran dimensions, landing sit facilities N89-23485
Details of Buran shuttle flight N89-23486
Design features, flight monitoring of Buran N89-23487
Buran designer Semenov interviewed N89-23488
Commentary on flight of Buran shuttle by designers Glushko and Semenov N89-23489
Buran space shuttle described by engineer N89-23490
SOYBEANS
Variable plant spacing N89-24016
SPACE BASED RADAR
The performance of Space-Based Radars (SBR) orbiting on elliptical orbits
[AD-A205951] N89-23772
SPACE COMMUNICATION
NASA space communications R and D (Research and Development): Issues, derived benefits, and future directions
[NASA-CR-184831] N89-23746
SPACE DEBRIS
NASA/SDIO Space Environmental Effects on Materials Workshop, part 1
[NASA-CP-3035-PT-1] N89-23528
Overview of environmental factors N89-23529
Structural materials for space applications N89-23530
The long-term effects of the micrometeoroid and orbital debris environments on materials used in space N89-23542
Orbital debris environment and data requirements N89-23543
Micrometeoroids and debris N89-23558
Working group written presentation: Meteoroid/orbital debris effects on materials N89-23565
Space debris: A report from the ESA Debris Working Group
[ESA-SP-1109] N89-24230
SPACE ENVIRONMENT SIMULATION
Microgravity conditions of a spacecraft N89-23731
SPACE ERECTABLE STRUCTURES
Carousel deployment mechanism for collable lattice truss N89-23897
SPACE EXPLORATION
NASA space communications R and D (Research and Development): Issues, derived benefits, and future directions
[NASA-CR-184831] N89-23746
SPACE HABITATS
Agenda of the Fourth Annual Summer Conference, NASA/USRA University Advanced Design Program
[NASA-TM-101750] N89-23493
SPACE INFRARED TELESCOPE FACILITY
SIRTF Telescope Instrument Changeout and Cryogen Replenishment (STICCR) Study
[NASA-CR-177380] N89-23512
SPACE LABORATORIES
Gas-Grain Simulation Facility: Fundamental studies of particle formation and interactions. Volume 1: Executive summary and overview
[NASA-CP-10026-VOL-1] N89-24022
SPACE MAINTENANCE
Astronaut tool development: An orbital replaceable unit-portable handhold N89-23904
SPACE NAVIGATION
Autonomous navigation and control
[AD-A205898] N89-23441
SPACE PLASMAS
Overview of environmental factors N89-23529
Surface phenomena in plasma environments N89-23555
Contamination N89-23559
Electrodynamics of cosmical plasmas: Some basic aspects of cosmological importance
[TRITA-EPP-89-02] N89-24163
SPACE PLATFORMS
Design and development of a high-stiffness, high-resolution torque sensor N89-23903
SPACE POWER REACTORS
Final safety analysis report for the Galileo Mission. Volume 1: Reference design document
[DE89-007266] N89-24147
SPACE SHUTTLE BOOSTERS
SRB ascent aerodynamic heating design criteria reduction study, volume 1
[NASA-CR-183580] N89-23515
Qualification Motor no. 8 (QM-8), volume 1
[NASA-CR-183650] N89-23523
SPACE SHUTTLE MISSIONS
Launch commit criteria performance trending analysis, phase 1, revision A. SRM and QA mission services
[NASA-CR-184859] N89-24129
SPACE SHUTTLE ORBITERS
Effect of internal convection and internal radiation on the structural temperatures of Space Shuttle Orbiter
[NASA-TM-100414] N89-23819
SPACE SHUTTLE PAYLOADS
Microparticle impacts in space: Results from Solar Max and shuttle witness plate inspections N89-23544
The design and analysis of a double swivel toggle release mechanism for the Orbiter stabilized payload deployment system N89-23895
SPACE SHUTTLES
Details of Buran shuttle flight N89-23486
Commentary on flight of Buran shuttle by designers Glushko and Semenov N89-23489
Buran space shuttle described by engineer N89-23490
Trapped particle flux models at NSSDC/WDC-A-R/S N89-23561
The design and analysis of a double swivel toggle release mechanism for the Orbiter stabilized payload deployment system N89-23895
A two-axis laser boresight system for a shuttle experiment N89-23913
SPACE STATION PAYLOADS
Gas-Grain Simulation Facility: Fundamental studies of particle formation and interactions. Volume 1: Executive summary and overview
[NASA-CP-10026-VOL-1] N89-24022
SPACE STATION POWER SUPPLIES
Solar dynamic power for space station freedom
[NASA-TM-102016] N89-23516
Comprehensive report of aeropropulsion, space propulsion, space power, and space science applications of the Lewis Research Center
[NASA-TM-100925] N89-24216
SPACE STATION PROPULSION
Space station propulsion test bed
[NASA-CR-183615] N89-23521
SPACE STATION STRUCTURES
Double lead spiral platen parallel jaw end effector N89-23905
Locating damaged members in a truss structure using modal test data: A demonstration experiment
[NASA-TM-101595] N89-23924
SPACE STATIONS
Agenda of the Fourth Annual Summer Conference, NASA/USRA University Advanced Design Program
[NASA-TM-101750] N89-23493
Expert systems applied to spacecraft fire safety
[NASA-CR-182266] N89-23501
Space Station CMIF extended duration metabolic control test
[NASA-TM-100362] N89-23503
An analysis of the attitude stability of a space station subject to parametric excitation of periodic mass motion
[AD-A206009] N89-23505
The 23rd Aerospace Mechanisms Symposium
[NASA-CP-3032] N89-23892
Signal and power roll ring testing update N89-23909
SPACE TOOLS
Astronaut tool development: An orbital replaceable unit-portable handhold N89-23904
SPACE TRANSPORTATION
The design and analysis of a double swivel toggle release mechanism for the Orbiter stabilized payload deployment system N89-23895
SPACE TRANSPORTATION SYSTEM
Design and testing of a deployable, retrievable boom for space applications N89-23898
Pyro thruster for performing rocket booster attachment, disconnect, and jettison functions N89-23902
SPACE WEAPONS
White paper: Experimental and computational studies of very high velocity impacts
[DE89-007643] N89-23877
A unidirectional rotary solenoid as applied to stronglinks N89-23894
SPACEBORNE EXPERIMENTS
The Long Duration Exposure Facility material experiments N89-23534
Returned Solar Max hardware degradation study results N89-23537
Gas-Grain Simulation Facility: Fundamental studies of particle formation and interactions. Volume 1: Executive summary and overview
[NASA-CP-10026-VOL-1] N89-24022
Gas-Grain Simulation Facility: Fundamental studies of particle formation and interactions. Volume 2: Abstracts, candidate experiments and feasibility study
[NASA-CP-10026-VOL-2] N89-24023
SPACECRAFT CHARGING
NASA/SDIO Space Environmental Effects on Materials Workshop, part 1
[NASA-CP-3035-PT-1] N89-23528
Dielectrics for long term space exposure and spacecraft charging: A briefing N89-23553
An overview of charging environments N89-23554
Surface phenomena in plasma environments N89-23555
Influence of charging environments on spacecraft materials and system performance N89-23556
Spacecraft charging N89-23563
Working group written presentation: Spacecraft charging N89-23568
SPACECRAFT COMPONENTS
Practical experiences with worm gearing for spacecraft power transmission applications N89-23912
The in-vacuo torque performance of dry-lubricated ball bearings at cryogenic temperatures N89-23914
SPACECRAFT CONFIGURATIONS
Transonic aerodynamic characteristics of a proposed Assured Crew Return Capability (ACRC) lifting-body configuration
[NASA-TM-4117] N89-23412
SPACECRAFT CONSTRUCTION MATERIALS
Overview of environmental factors N89-23529
Structural materials for space applications N89-23530
Environmental effects on spacecraft materials N89-23532
Atomic oxygen effects on materials N89-23540
Atomic oxygen effects on spacecraft materials: The state of the art of our knowledge N89-23541
The long-term effects of the micrometeoroid and orbital debris environments on materials used in space N89-23542
Effects of the contamination environment on surfaces and materials N89-23546
Atomic oxygen N89-23557
Working group written presentation: Solar radiation N89-23567
SPACECRAFT CONTAMINATION
NASA/SDIO Space Environmental Effects on Materials Workshop, part 1
[NASA-CP-3035-PT-1] N89-23528
Spacecraft contamination experience N89-23545

Effects of the contamination environment on surfaces and materials N89-23546
Contamination N89-23559
SPACECRAFT CONTROL
Design, fabrication and test of a 4750 Newton-meter-second double Gimbal control moment gyroscope N89-23896
SPACECRAFT DEFENSE
Dynamic fatigue of ultralow-expansion glass for space mirrors, reissue A
[AD-A205401] N89-23694
SPACECRAFT DESIGN
Design features, flight monitoring of Buran N89-23487
Buran designer Semenov interviewed N89-23488
Commentary on flight of Buran shuttle by designers Glushko and Semenov N89-23489
Agenda of the Fourth Annual Summer Conference, NASA/USRA University Advanced Design Program
[NASA-TM-101750] N89-23493
Assembling the ISO thermal model with ESAT AN
[REPT-882-440-107] N89-23510
Some examples of the degradation of properties of materials in space N89-23535
Spacecraft contamination experience N89-23545
Microgravity conditions of a spacecraft N89-23731
The FLUIDNET development and application to preliminary sizing of fluid loop systems
[REPT-882-440-102] N89-23845
The third generation rigid solar array GSR3
[REPT-882-440-105] N89-23979
The role of pilot and automatic onboard systems in future rendezvous and docking operations
[REPT-882-440-116] N89-24050
ESABASE: A most versatile and flexible system engineering tool
[ESA-BR-54] N89-24223
SPACECRAFT DOCKING
The 23rd Aerospace Mechanisms Symposium
[NASA-CP-3032] N89-23892
SPACECRAFT ELECTRONIC EQUIPMENT
Radiation effects in spacecraft electronics N89-23531
SPACECRAFT ENVIRONMENTS
An overview of charging environments N89-23554
Influence of charging environments on spacecraft materials and system performance N89-23556
Space station ECLSS simplified integrated test
[NASA-TM-100363] N89-24044
SPACECRAFT GLOW
Atomic oxygen N89-23557
SPACECRAFT GUIDANCE
Optimal aeroassisted coplanar orbital transfer using an energy model
[NASA-CR-181778] N89-23495
SPACECRAFT LANDING
Buran dimensions, landing sit facilities N89-23485
Surface Observation Climatic Summaries (SOCS) for NASA Shuttle Landing Facility, Florida
[AD-A205362] N89-24007
SPACECRAFT LAUNCHING
Buran space shuttle described by engineer N89-23490
Reducing launch operations costs: New technologies and practices
[PB89-136402] N89-23500
Launch commit criteria performance trending analysis, phase 1, revision A. SRM and QA mission services
[NASA-CR-184859] N89-24129
SPACECRAFT ORBITS
Numerical study of orbital trajectories about Phobos
[AD-A205822] N89-23496
Influence of charging environments on spacecraft materials and system performance N89-23556
Atomic oxygen N89-23557
Trapped radiation N89-23560
Spacecraft charging N89-23563
Working group written presentation: Atomic oxygen N89-23564
Working group written presentation: Meteoroid/orbital debris effects on materials N89-23565
Space debris: A report from the ESA Debris Working Group
[ESA-SP-1109] N89-24230
SPACECRAFT POWER SUPPLIES
Preliminary assessment of rover power systems for the Mars Rover Sample Return Mission
[NASA-TM-102003] N89-23518
Results from baseline tests of the SPRE 1 and comparison with code model predictions
[NASA-TM-102044] N89-23527
MPD thruster erosion research
[NASA-CR-185314] N89-24168
Comprehensive report of aeropropulsion, space propulsion, space power, and space science applications of the Lewis Research Center
[NASA-TM-100925] N89-24216
SPACECRAFT PROPULSION
Comprehensive report of aeropropulsion, space propulsion, space power, and space science applications of the Lewis Research Center
[NASA-TM-100925] N89-24216
SPACECRAFT REENTRY
Optimal aeroassisted coplanar orbital transfer using an energy model
[NASA-CR-181778] N89-23495
Effect of internal convection and internal radiation on the structural temperatures of Space Shuttle Orbiter
[NASA-TM-100414] N89-23819
SPACECRAFT SHIELDING
Design features, flight monitoring of Buran N89-23487
SPACECRAFT STABILITY
Increasing the margin of stability of arbitrarily finite modes of flexible large space structures with damping
[AD-A206487] N89-23507
SPACECRAFT STRUCTURES
Increasing the margin of stability of arbitrarily finite modes of flexible large space structures with damping
[AD-A206487] N89-23507
Break dimensioning of space structural assemblies and its experimental validation
[REPT-882-430-109] N89-23508
Composites in complex assemblies
[REPT-882-430-110] N89-23509
EnviroNET: Space environment for Strategic Defense Initiative experiments N89-23538
SPACECRAFT SURVIVABILITY
Micrometeoroids and debris N89-23558
Trapped radiation N89-23560
Working group written presentation: Spacecraft charging N89-23568
SPACECRAFT TEMPERATURE
The FLUIDNET development and application to preliminary sizing of fluid loop systems
[REPT-882-440-102] N89-23845
SPACECRAFT TRAJECTORIES
Numerical study of orbital trajectories about Phobos
[AD-A205822] N89-23496
SPACELAB PAYLOADS
Summary of 1st Summer School on Microgravity
[DFVLR-IB-333-87/2] N89-23719
Payload experts in D1-mission N89-23722
Biological results obtained by D1-mission N89-23732
SPACING
Variable plant spacing N89-24016
SPATIAL DEPENDENCIES
Shortest paths in a digitized map using a tile-based data structure
[PB89-143432] N89-23957
SPATIAL DISTRIBUTION
Orbital debris environment and data requirements N89-23543
Development and evaluation of integrating details: A complex spatial problem solving test
[AD-A205860] N89-24035
The role of knowledge in visual shape representation
[AD-A206173] N89-24041
SPATIAL MARCHING
Computation of flow around maneuvering submerged bodies
[AD-A205994] N89-23833
SPATIAL RESOLUTION
An instrument for the simultaneous measurement of velocity, temperature and density in unseeded air flows
[AD-A205588] N89-23453
Investigation of optical compression techniques for dither coding
[AD-A206140] N89-23778
Image processing of coronal pictures
[AD-A205326] N89-24252
SPECIFIC HEAT
Experimental thermal conductivity, thermal diffusivity and specific heat values of argon and nitrogen
[PB89-148407] N89-23637
SPECIFIC IMPULSE
Design, fabrication and test of the RL10 derivative II chamber/primary nozzle
[NASA-CR-179595] N89-23519
MPD thruster erosion research
[NASA-CR-185314] N89-24168
SPECIFICATIONS
Li/FeS battery design for an electric van
[DE89-009808] N89-23794
SPECTRAL BANDS
Geobotanical remote sensing for determination of aggregate source material
[AD-A205943] N89-23962
Research for optimization of future MOMS sensors
[ETN-89-94424] N89-23972
Night vision goggles (AN/PVS-7) performance issues and answers
[AD-A206117] N89-24047
Spectral observations of the extreme ultraviolet background N89-24259
SPECTRAL EMISSION
Mapping freeze/thaw boundaries with SMMR data
[NASA-CR-184991] N89-23961
SPECTRAL ENERGY DISTRIBUTION
Second-order moments of a stationary Markov chain and some applications
[AD-A206366] N89-24128
Spectra and dynamics of young stellar objects N89-24234
SPECTRAL METHODS
A numerical study of viscous vortex rings using a spectral method
[NASA-TM-101041] N89-23820
Introduction to irreducible tensor methods, part 1
[NAL-PD-DU-8802] N89-24098
SPECTRAL RESOLUTION
Research for optimization of future MOMS sensors
[ETN-89-94424] N89-23972
SPECTRAL SIGNATURES
Research for optimization of future MOMS sensors
[ETN-89-94424] N89-23972
SPECTROMETERS
Electron spectroscopy for chemical analysis: Sample analysis
[NASA-CR-183568] N89-23634
Correlation of Portable Wear Metal Analyzer (PWMA-2) and Baird A/E35U-3 spectrometer oil analysis data
[AD-A205957] N89-23882
A compact fast wide angle broad band spectrometer optical system
[NASA-CASE-NPO-17562-1-CU] N89-24153
Noise characteristics of an inductively coupled plasma-mass spectrometer
[AD-A205686] N89-24169
Flow-injection analysis utilizing a spectrally segmented photodiode-array inductively coupled plasma emission spectrometer. 1: Microcolumn preconcentration for the determination of molybdenum
[AD-A205687] N89-24170
SPECTRORADIOMETERS
Research for optimization of future MOMS sensors
[ETN-89-94424] N89-23972
SPECTROSCOPY
Spectroscopic studies of metal-ligand-surface interactions
[AD-A206460] N89-23652
Chloride analysis in HAN-based liquid propellants by inductively coupled plasma spectroscopy
[AD-A206564] N89-23717
SPECTRUM ANALYSIS
A statistical analysis of the output signals of an acousto-optic spectrum analyzer for CW (Continuous-Wave) signals
[AD-A205404] N89-23763
SPECULAR REFLECTION
Code optimization of speckle reduction algorithms for image processing of rocket motor holograms
[AD-A205306] N89-23524
SPEED CONTROL
Comparison of interpolation algorithms for speed control in air traffic management
[AD-A206314] N89-23444
Practical experiences with worm gearing for spacecraft power transmission applications N89-23912
SPHERES
High-temperature LDV seed particle development
[NASA-CR-182265] N89-23851
SPIN DYNAMICS
Memory functions and relaxation functions of some spin systems
[AD-A206340] N89-24137
SPIN GLASS
Microscopic theory of electron spin resonance in Heisenberg spin glasses and thermal fluctuations in classical spin models with random fields
[JUEL-2227] N89-24146
SPIN REDUCTION
Near field testing of the electronically despun antenna of the Meteosat satellite
[REPT-882-440-108] N89-23783
SPIN RESONANCE
FILMCAL: An ESR (Electron Spin Resonance) simulation program for transition metals in phthalocyanine films
[AD-A206441] N89-23676
SPIN-LATTICE RELAXATION
Nuclear magnetism in copper and silver: Theory and experiments
[ISBN-952-900-084-7] N89-24188

SPOILERS
Computation of dynamics and control of unsteady vortical flows N89-23822
SPRAYERS
Fundamental studies on spray combustion and turbulent combustion
[AD-A206438] N89-23651
Spray deposition: A fundamental study of droplet impingement, spreading and consolidation
[AD-A206065] N89-23672
SPREAD SPECTRUM TRANSMISSION
Study of spread spectrum multiple access systems for satellite communications with overlay on current services: Executive summary
[NASA-CR-180827-EXEC-SUMM] N89-23756
Study of spread spectrum multiple access systems for satellite communications with overlay on current services
[NASA-CR-180827] N89-23757
Near-far resistant linear multiuser detection
[AD-A206363] N89-23802
SPREADING
Spray deposition: A fundamental study of droplet impingement, spreading and consolidation
[AD-A206065] N89-23672
Monolithic GaAs digitizer for space-based laser pulse spreading effect
[NASA-CR-183430] N89-23855
SPUTTERING
Ionization investigation of sputtered titanium and of titanium ion transport process in an argon discharge glow using laser induced fluorescence
[JUEL-2219] N89-23660
STABILITY AUGMENTATION
Detailed design of a Ride Quality Augmentation System for commuter aircraft
[NASA-CR-4230] N89-23470
STABILIZATION
Digital control of the Kuiper Airborne Observatory telescope
[NASA-TM-101082] N89-23785
STABILIZERS (AGENTS)
Fatigue-resistant photochromic plastics
[DE89-007336] N89-23682
STAGNATION PRESSURE
Experiment on a cylindrical scramjet combustor. 2: Simulated flight Mach number 6.7
[NAL-TR-969] N89-23464
STAGNATION TEMPERATURE
Experiment on a cylindrical scramjet combustor. 2: Simulated flight Mach number 6.7
[NAL-TR-969] N89-23464
STAINLESS STEELS
Cracking of coated materials under transient thermal stresses
[NASA-CR-184898] N89-23928
A combined isotropic-kinematic hardening model for large deformation metal plasticity
[AD-A206352] N89-23935
STANDARDS
Liquid-in-glass thermometer calibration service
[PB89-128888] N89-23846
Nonintrusive methods for monitoring the operational readiness of solenoid-operated valves
[DE89-008732] N89-23876
Microporous fumed-silica insulation board as a candidate Standard Reference Material of thermal resistance
[PB89-148373] N89-24213
STAR FORMATION
A self consistant model of the three phase interstellar medium in disk galaxies N89-24245
STARS
Study of the infrared celestial background
[AD-A205649] N89-24237
STATE VECTORS
State-space formulae for discrete-time H infinity optimization
[OUEL-1718/88] N89-24089
STATIC AERODYNAMIC CHARACTERISTICS
Optimum aeroelastic characteristics for composite supermaneuverable aircraft
[AD-A205503] N89-23452
STATIC PRESSURE
Characteristics of a five-hole spherical pitot tube
[NAL-TR-971] N89-23463
Computerized measurement of thermoacoustically generated temperature gradients
[AD-A205353] N89-23929
STATIC TESTS
Qualification Motor no. 8 (QM-8), volume 1
[NASA-CR-183650] N89-23523
STATISTICAL ANALYSIS
Trends in environmentally induced spacecraft anomalies N89-23536
A statistical analysis of the output signals of an acousto-optic spectrum analyzer for CW (Continuous-Wave) signals
[AD-A205404] N89-23763
STATISTICAL CORRELATION
Correlated atomic motions in liquid aluminum
[ETN-89-93943] N89-24145
STATISTICAL MECHANICS
The diluted tri-dimensional spin-one Ising model with crystal field interactions
[DE88-705663] N89-24161
STATISTICAL TESTS
Tests for the gamma distribution with estimated shape parameters
[AD-A205829] N89-24118
STATORS
Mechanisms of secondary flows and losses within a three dimensional turbine stator cascade
[NAL-TR-970T] N89-23807
STEELS
Behavior of metals during hot rolling processes. Part 2: Experimental methods for flow stress determination and calculation of the two-dimensional temperature-field in the roll gap N89-23614
Interfacial reactions during cladding of steel by hot rolling N89-23615
On steel superficial hardening by concentrated electron beam in the air
[DE88-705781] N89-23658
Steel hardness effects in boundary lubricated sliding: An in-situ SEM (Scanning Electron Microscope) study
[AD-A206156] N89-23674
STELLAR ACTIVITY
Solar and stellar coronal plasmas
[NASA-CR-184909] N89-24162
STELLAR CORONAS
Solar and stellar coronal plasmas
[NASA-CR-184909] N89-24162
STELLAR EVOLUTION
Spectra and dynamics of young stellar objects N89-24234
A search for pulsations in planetary nebulae nuclei N89-24235
Time and spectral variability of the low mass X-ray binaries
[MPE-REPORT-210] N89-24238
STELLAR MASS ACCRETION
Time and spectral variability of the low mass X-ray binaries
[MPE-REPORT-210] N89-24238
STELLAR OSCILLATIONS
A search for pulsations in planetary nebulae nuclei N89-24235
STELLAR PHYSICS
Time and spectral variability of the low mass X-ray binaries
[MPE-REPORT-210] N89-24238
STELLAR RADIATION
A search for EUV emission from cataclysmic variables
[DE89-008012] N89-24257
STELLAR SPECTRA
Ground-based infrared observations of sources discovered by the AFGL, FIRRSE and IRAS infrared surveys
[AD-A206335] N89-24246
Spectral observations of the extreme ultraviolet background N89-24259
STELLAR SPECTROPHOTOMETRY
A search for EUV emission from cataclysmic variables
[DE89-008012] N89-24257
STIFFNESS MATRIX
Prediction and measurement of damping of a laminated beam with a constrained viscoelastic layer
[DE89-009002] N89-23922
STIRLING ENGINES
Results from baseline tests of the SPRE 1 and comparison with code model predictions
[NASA-TM-102044] N89-23527
Two-dimensional numerical simulation of a Stirling engine heat exchanger
[NASA-TM-102057] N89-23823
STOCHASTIC PROCESSES
Approximation of stochastic integral equations using Martingale difference schemes
[ETN-89-93951] N89-24123
A demonstration of the method of stochastic finite element analysis
[AD-A206135] N89-24127
STOICHIOMETRY
Direct laser/materials interaction: Laser ablation of superconductor materials and laser welding
[DE89-006560] N89-23857
STRAIN DISTRIBUTION
Twin boundaries, interfaces and modulated structures in martensites
[DE89-009064] N89-23662
STRAIN GAGES
Design and development of a high-stiffness, high-resolution torque sensor N89-23903
STRAIN HARDENING
A combined isotropic-kinematic hardening model for large deformation metal plasticity
[AD-A206352] N89-23935
STRANGE ATTRACTORS
The dimension of attractors underlying turbulent Poiseuille flow
[AD-A206021] N89-23835
STRATIFIED FLOW
Studies of internal gravity waves in the stably stratified troposphere N89-23989
Acoustic response of a rectangular waveguide with a strong transverse temperature gradient
[NASA-TM-101564] N89-24140
STRATOCUMULUS CLOUDS
Stratocumulus modeling
[KNMI-WR-88-2] N89-23997
Current problems in the stratocumulus-topped atmospheric boundary layer N89-23998
Turbulent structure of a shear-driven stratus-topped atmospheric boundary layer: A comparison of model results with observations N89-23999
The diurnal variation of a marine stratocumulus layer: A model sensitivity study N89-24000
STRESS (PHYSIOLOGY)
Evaluation of three commercial microclimate cooling systems
[AD-A206318] N89-23744
Human temperature regulation during exercise after oral pyridostigmine administration
[AD-A206032] N89-24030
STRESS ANALYSIS
Turbulent shear stress measurement in hypersonic flow
[AD-A206453] N89-23432
Behavior of metals during hot rolling processes. Part 2: Experimental methods for flow stress determination and calculation of the two-dimensional temperature-field in the roll gap N89-23614
Information about hot flow-stress curves and the resulting structural changes N89-23616
Composite blade structural analyzer (COBSTRAN) user's manual
[NASA-TM-101461] N89-23621
Stress relief cracking in copper-precipitation strengthened HSLA-100 steel
[AD-A205936] N89-23670
Environmental Stress Screening (ESS) guide
[AD-A206350] N89-23888
Modal analysis and testing of missile systems
[AD-A204051] N89-23916
Cracking of a layered medium on an elastic foundation under thermal shock
[NASA-CR-185316] N89-23925
Cracking of coated materials under transient thermal stresses
[NASA-CR-184898] N89-23928
Dynamic interaction between fluids and solids
[ETN-89-93948] N89-23937
STRESS CORROSION
Environment-induced crack growth processes in nickel-base alloys
[DE89-008253] N89-23659
STRESS CYCLES
Fatigue strength reduction model: RANDOM3 and RANDOM4 user manual, appendix 2
[NASA-CR-184940] N89-23891
STRESS DISTRIBUTION
Finite element modeling of frictionally restrained composite interfaces
[NASA-CR-182281] N89-23918
The mode 3 crack problem in bonded materials with a nonhomogeneous interfacial zone
[NASA-CR-185315] N89-23927
STRESS INTENSITY FACTORS
The crack problem in bonded nonhomogeneous materials
[NASA-CR-184897] N89-23926
STRESS MEASUREMENT
Turbulent shear stress measurement in hypersonic flow
[AD-A206453] N89-23432
Comparison of split-film and x-film measurements in 2-D flow
[AD-A206023] N89-23836
STRESS RELAXATION
The structural basis for fatigue initiation in glassy polymers
[DE89-009292] N89-23689
STRESS RELIEVING
Stress relief cracking in copper-precipitation strengthened HSLA-100 steel
[AD-A205936] N89-23670

STRESS-STRAIN RELATIONSHIPS
Numerical implementation of the Schapery model for nonlinear visco-elasticity
[PB89-144950] N89-23915
Quadratic optimal control theory for viscoelastically damped structures using a fractional derivative viscoelasticity model
[AD-A206008] N89-23932
A combined isotropic-kinematic hardening model for large deformation metal plasticity
[AD-A206352] N89-23935
STRESSES
Environmental stress crazing and cracking of transparent polymers
[AD-A205624] N89-23697
STRING THEORY
The formation of topological defects in phase transitions
[NASA-CR-185318] N89-24215
STRONG INTERACTIONS (FIELD THEORY)
Strong and electromagnetic interactions in heavy exotic atoms
[PB89-145718] N89-24143
STRONGLY COUPLED PLASMAS
Chloride analysis in HAN-based liquid propellants by inductively coupled plasma spectroscopy
[AD-A206564] N89-23717
Noise characteristics of an inductively coupled plasma-mass spectrometer
[AD-A205666] N89-24169
Use of a spectrally segmented photodiode-array spectrometer for inductively coupled plasma atomic emission spectroscopy
[AD-A205688] N89-24171
Preliminary evaluation of a miniaturized torch for inductively coupled plasma mass spectrometry
[AD-A205746] N89-24173
Simultaneous measurement of spatially resolved electron temperatures, Electron number densities and gas temperatures by laser light scattering from the ICP
[AD-A205747] N89-24174
STRONTIUM COMPOUNDS
Quasielastic and inelastic spin fluctuations in superconducting La2-xSrxCuO4
[DE89-008157] N89-24190
STRUCTURAL ANALYSIS
USAF (US Air Force) durability design handbook: Guidelines for the analysis and design of durable aircraft structures
[AD-A206286] N89-23457
Composites in complex assemblies
[REPT-882-430-110] N89-23509
Composite blade structural analyzer (COBSTRAN) user's manual
[NASA-TM-101461] N89-23621
Composite materials nondestructive tests: Choice of methods depending on requirements
[REPT-882-430-105] N89-23630
Application of an exact finite element method to analysis of statics of thin elastic shells of revolution with axisymmetric loading
[ISBN-952-900-399-4] N89-23917
Ground shake test of the Boeing Model 360 helicopter airframe
[NASA-CR-181766] N89-23920
Locating damaged members in a truss structure using modal test data: A demonstration experiment
[NASA-TM-101595] N89-23924
STRUCTURAL DESIGN
A correlation study of X-29A aircraft and associated analytical developments N89-23450
Double lead spiral platen parallel jaw end effector N89-23905
Locating damaged members in a truss structure using modal test data: A demonstration experiment
[NASA-TM-101595] N89-23924
STRUCTURAL DESIGN CRITERIA
Evaluation of tests and design factors — structures
[REPT-882-440-109] N89-23889
STRUCTURAL ENGINEERING
A demonstration of the method of stochastic finite element analysis
[AD-A206135] N89-24127
STRUCTURAL FAILURE
Break dimensioning of space structural assemblies and its experimental validation
[REPT-882-430-109] N89-23508
STRUCTURAL RELIABILITY
Evaluation of tests and design factors — structures
[REPT-882-440-109] N89-23889
STRUCTURAL STABILITY
Locating damaged members in a truss structure using modal test data: A demonstration experiment
[NASA-TM-101595] N89-23924
STRUCTURAL WEIGHT
An analysis of Electronic Aids to Maintenance (EAM) for the Light Helicopter Family (LHX)
[AD-A205440] N89-23407
STRUTS
Transonic operational characteristics and performance
[NAL-TR-968] N89-23408
STYRENES
Mechanism of the initiation of the cationic polymerization of styrenes by silanes and activated covalent esters
[AD-A206502] N89-23708
Path dependent morphologies of a diblock copolymer of Polystyrene/Hydrogenated polybutadiene
[AD-A206504] N89-23883
SUBMERGED BODIES
Computation of flow around maneuvering submerged bodies
[AD-A205994] N89-23833
SUBMILLIMETER WAVES
Attenuation measurement of very low-loss dielectric waveguides by the cavity resonator method in the millimeter/submillimeter wavelength range
[AD-A206458] N89-23803
SUBSONIC FLOW
Effect of wall cooling on the stability of compressible subsonic flows over smooth humps and backward-facing steps
[NASA-CR-184960] N89-23812
SUBSONIC WIND TUNNELS
A research facility for film cooling investigations with emphasis on the instrumentation system
[NAL-TM-PR-8704] N89-23477
SUBSTRATES
Sequentially evaporated thin Y-Ba-Co-O superconducting films on microwave substrates
[NASA-TM-102068] N89-23791
SUCTION
An experimental study of laminar flow control airfoil with suction through perforated surface at low speed
[NAL-TR-967] N89-23806
SULFONES
Improved acid electrolytes: The synthesis and structure of fluorine containing sulfonic acids for fuel cells
[PB89-142616] N89-23973
SULFONIC ACID
Improved acid electrolytes: The synthesis and structure of fluorine containing sulfonic acids for fuel cells
[PB89-142616] N89-23973
SUNSPOT CYCLE
High-latitude field-strength measurements of standard broadcast band skywave transmissions monitored at Fairbanks, Alaska
[PB89-134829] N89-23747
The US Army Yuma Proving Ground, Arizona 33-year climate calendar and tables on associated weather elements 1954-1986. American desert country
[AD-A206256] N89-24010
SUNSPOTS
The US Army Yuma Proving Ground, Arizona 33-year climate calendar and tables on associated weather elements 1954-1986. American desert country
[AD-A206256] N89-24010
SUPERCONDUCTING FILMS
Direct laser/materials interaction: Laser ablation of superconductor materials and laser welding
[DE89-006560] N89-23857
SUPERCONDUCTING MAGNETS
High-temperature ceramic superconductors
[AD-A205321] N89-24196
Superconducting PYX structures
[AD-D013958] N89-24202
SUPERCONDUCTIVITY
Sequentially evaporated thin Y-Ba-Co-O superconducting films on microwave substrates
[NASA-TM-102068] N89-23791
Coherence and chaos phenomena in Josephson oscillators for superconducting electronics
[AD-A205469] N89-23798
Fundamental and applied studies of explosively fabricated high-temperature superconducting fixtures
[AD-A205953] N89-24204
SUPERCONDUCTORS
Metrology for Electromagnetic Technology: A bibliography of NBS (National Bureau of Standards) publications, January 1970 - August 1988
[PB89-147847] N89-23748
Quasielastic and inelastic spin fluctuations in superconducting La2-xSrxCuO4
[DE89-008157] N89-24190
SUPERHIGH FREQUENCIES
Design of a 100 MW X-band klystron
[DE89-008939] N89-23793
SUPERLATTICES
Deformation twinning in ordered intermetallic compounds
[DE89-008748] N89-24192
SUPERSONIC COMBUSTION RAMJET ENGINES
Effects of initial conditions on the development of supersonic turbulent free shear layers
[AD-A205807] N89-23421
Experiment on a cylindrical scramjet combustor. 2: Simulated flight Mach number 6.7
[NAL-TR-969] N89-23464
SUPERSONIC FLIGHT
Status of sonic boom methodology and understanding
[NASA-CP-3027] N89-23415
Noise and sonic boom impact technology. PCBOOM computer program for sonic boom research, volume 1
[AD-A206290] N89-23429
SUPERSONIC FLOW
Development of harmonic panel methods for aeroelastic applications to elastic bodies and body-fin combinations in supersonic flow
[AD-A205739] N89-23423
Investigation of the flowfield created by the interaction of a sonic jet and a co-flowing supersonic stream
[AD-A205823] N89-23425
SUPERSONIC NOZZLES
Ejector effects on a supersonic nozzle at low altitude and Mach number
[AD-A206049] N89-23427
SUPPORTS
Tensile film clamps and mounting block for the rheovibron and autovibron viscoelastometer
[NASA-CASE-LAR-13696-1] N89-23880
SURFACE ACOUSTIC WAVE DEVICES
Monitoring thin film properties with surface acoustic wave devices: Diffusion, surface area and pore size distribution
[DE89-009379] N89-24195
SURFACE COOLING
Effect of wall cooling on the stability of compressible subsonic flows over smooth humps and backward-facing steps
[NASA-CR-184960] N89-23812
SURFACE CRACKS
Environmental stress crazing and cracking of transparent polymers
[AD-A205624] N89-23697
Crack-face displacements for embedded elliptic and semi-elliptical surface cracks
[NASA-CR-181822] N89-23919
Applications of a digital acoustic-emission data-acquisition workstation
[DE89-009648] N89-23923
SURFACE DEFECTS
Undercutting of defects in thin film protective coatings on polymer surfaces exposed to atomic oxygen
[NASA-TM-101986] N89-23691
SURFACE DISTORTION
Mechanical/electrical distortion model for reflector antennas
[REPT-882-440-104] N89-23781
SURFACE FINISHING
Advanced layer materials N89-23587
Undercutting of defects in thin film protective coatings on polymer surfaces exposed to atomic oxygen
[NASA-TM-101986] N89-23691
High speed abrasive belt grinding
[AD-A205618] N89-23741
Assessment of surface topography by X-ray scattering measurements
[MPE-PREPRINT-134] N89-24159
SURFACE LAYERS
Stability and instability of anodically formed layers on metallic surfaces N89-23597
Cracking of a layered medium on an elastic foundation under thermal shock
[NASA-CR-185316] N89-23925
SURFACE NAVIGATION
Global Positioning System (GPS) positioning at sea
[ETN-89-94145] N89-23446
SURFACE PROPERTIES
An experimental study of laminar flow control airfoil with suction through perforated surface at low speed
[NAL-TR-967] N89-23806
Friction factor data for flat plate tests of smooth and honeycomb surfaces
[NASA-CR-184977] N89-23876
SURFACE REACTIONS
Returned Solar Max hardware degradation study results N89-23537
EnviroNET: Space environment for Strategic Defense Initiative experiments N89-23538
Environmental definition of the earth's neutral atmosphere N89-23539
Atomic oxygen effects on materials N89-23540
Atomic oxygen effects on spacecraft materials: The state of the art of our knowledge N89-23541
The long-term effects of the micrometeoroid and orbital debris environments on materials used in space N89-23542

Surface phenomena in plasma environments N89-23555
Influence of charging environments on spacecraft materials and system performance N89-23556
Oxygen interaction with metal surfaces: Surface science approach N89-23596
Stability and instability of anodically formed layers on metallic surfaces N89-23597

SURFACE STABILITY
Stability and instability of anodically formed layers on metallic surfaces N89-23597

SURFACE TEMPERATURE
Effect of internal convection and internal radiation on the structural temperatures of Space Shuttle Orbiter [NASA-TM-100414] N89-23819
Mapping freeze/thaw boundaries with SMMR data [NASA-CR-184991] N89-23961

SURFACE TO AIR MISSILES
Flowfield measurements in the vortex wake of a missile at high angle of attack in turbulence [AD-A205696] N89-23422

SURFACE WAVES
The effect of welding process on the microstructure of HY-130 steel weldments [AD-A205692] N89-23667

SURFACTANTS
Water-processable conducting polymers [DE89-009251] N89-23688

SURGES
Zinc oxide varistor time response [DE89-008234] N89-24191

SURVEILLANCE RADAR
ASR-9 weather channel test report, executive s ummary [DOT/FAA/PS-89/6-EXEC-SUMM] N89-23758

SURVEYS
Environmental effects on spacecraft materials N89-23532

SWEEP ANGLE
Experimental study of pressure and heating rate on a swept cylindrical leading edge resulting from swept shock wave interference [NASA-CR-185326] N89-23411

SWEPT WINGS
High angle-of-attack aerodynamic characteristics of crescent and elliptic wings [NASA-CR-184992] N89-23418

SWIRLING
Free shear layer and swirl flow heat transfer enhancement [PB89-145106] N89-23810

SWITCHES
High energy semiconductor switch [DE89-007399] N89-23789
Light channel 5 Gb/s optoelectronic TDM (Time Division Multiplexing) [AD-A205501] N89-24086

SYMBOLIC PROGRAMMING
Symbolic analysis of multivariable missile systems [AD-A206326] N89-24132

SYNAPSES
Long term synaptic plasticity and learning in neuronal networks [AD-A205993] N89-24038

SYNCHRONISM
An instrument for the simultaneous measurement of velocity, temperature and density in unseeded air flows [AD-A205588] N89-23453

SYNCHRONOUS PLATFORMS
A segmented mirror antenna for radiometers [NASA-TM-102045] N89-23753

SYNCHROTRON RADIATION
Application of the method of X-ray fluorescence analysis with synchrotron radiation to study lunar matter [DE88-705782] N89-24247

SYNTHESIS (CHEMISTRY)
In situ fluorescence monitoring of the viscosities of particle-filled polymers in flow [PB89-146278] N89-23680
Heterocycles based on group 3, 4, and 5 elements precursors for novel glasses and ceramics [AD-A205586] N89-23696
Report on the partial support of the 1988 Gordon Conference on Polymers (West) [AD-A205834] N89-23701
Cellular and molecular approaches to polymer synthesis by bacteria [AD-A206395] N89-23707
Novel organoboranes as intermediates for ceramic precursors and high-energy fuels [AD-A206101] N89-23713
Synthesis of novel acid electrolytes for phosphoric acid fuel cells [PB89-148944] N89-23786
Improved acid electrolytes: The synthesis and structure of fluorine containing sulfonic acids for fuel cells [PB89-142616] N89-23973

SYNTHETIC APERTURE RADAR
Battlefield radar imaging through airborne millimetric wave SAR (Synthetic Aperture Radar) [ETN-89-94228] N89-23751
Autofocus of SAR imagery degraded by ionospheric-induced phase errors [DE89-008278] N89-23752
Design and verification of mechanisms for a large foldable antenna N89-23899
Imaging procedure of underwater bottom topography by air and satellite images in the range of microwave and visible electromagnetic spectra [GKSS-88/E/41] N89-24014

SYNTHETIC FUELS
Sample preparation techniques for evaluating methanol and formaldehyde emissions from methanol fueled vehicles and engines [PB89-136147] N89-23734

SYSTEM IDENTIFICATION
Riemannian geometry on families of linear systems: The deterministic case [PB89-146062] N89-24100

SYSTEMS ANALYSIS
Summary of 1st Summer School on Microgravity [DFVLR-IB-333-87/2] N89-23719
Microgravity conditions of a spacecraft N89-23731
System Mean-Time-Between-Failure versus life-cycle logistics cost subject to the introduction of Line-Replaceable-Unit redundancy [AD-A206324] N89-23887
Preconditioned Krylov solvers and methods for runtime loop parallelization [AD-A206388] N89-24120
Symbolic analysis of multivariable missile systems [AD-A206326] N89-24132

SYSTEMS ENGINEERING
JPRS report: Science and technology. USSR: Space [JPRS-USP-89-004] N89-23484
Buran space shuttle described by engineer N89-23490
The two approaches for the thermal control of the Columbus resource module and Polar Platform [REPT-882-440-110] N89-23511
Spacecraft contamination experience N89-23545
Monolithic GaAs digitizer for space-based laser pulse spreading effect [NASA-CR-183430] N89-23855
Design and implementation of an expert user interface for the computer aided prototyping system [AD-A206113] N89-24067
Advanced computing systems: An advanced reasoning-based development paradigm for Ada trusted systems and its application to MACH [AD-A206308] N89-24070

SYSTEMS INTEGRATION
Development of the extended kalman filter for the advanced Completely Integrated Reference Instrumentation System (CIRIS) [AD-A206083] N89-23443
The 4D-TECS integration for NASA TSRV airplane [NASA-CR-4231] N89-23471
A graphical editor for the computer aided prototyping system [AD-A206443] N89-24071
On the algebraic structure of integrable systems in multidimensions [DE89-008697] N89-24108
Defense Integrated Data System (DIDS) procedures manual. Volume 2: Multiple application procedures [PB89-139307] N89-24221

SYSTEMS MANAGEMENT
Automatic documentation methodologies for software maintenance [AD-A205672] N89-24062

SYSTEMS STABILITY
Criteria for robust stability in a class of lateral inhibition networks coupled through resistive grids [AD-A204174] N89-24081

T

TAKEOFF
Simulator evaluation of a display for a Takeoff Performance Monitoring System [NASA-TP-2908] N89-23469
Noise of a model counterrotation propeller with simulated fuselage and support pylon at takeoff/approach conditions [NASA-TM-101996] N89-24138

TARGET ACQUISITION
Enhanced tracking of ballistic targets using forward looking infrared measurements [AD-A205727] N89-23769

TARGET RECOGNITION
Coherent laser radar [FOA-C-30512-3.1] N89-23778

TASK COMPLEXITY
Crew procedures and workload of retrofit concepts for microwave landing system [NASA-CR-181700] N89-24033

TASKS
The relationship between subjective and objective measures of sleepiness [AD-A205861] N89-24027
Development and evaluation of integrating details: A complex spatial problem solving test [AD-A205860] N89-24035

TAXIING
Instrument landing system mathematical modeling study for Orlando International Airport Runway 35L localizer, Orlando, Florida. Final airside docking plan (Scheme 3A) [AD-A205351] N89-23438

TAYLOR INSTABILITY
Rayleigh-Taylor instability of a viscous film overlying a passive fluid [AD-A205578] N89-23827

TAYLOR SERIES
An iterative technique to correct probe position errors in planar near-field to far-field transformations [PB89-153886] N89-23750

TDR SATELLITES
Direct dissemination of data from ESA's future in-orbit infrastructure [DDD-CP/TE-RE-7450] N89-23754

TEAMS
Age distribution among NASA scientists and engineers N89-23911

TECHNOLOGY ASSESSMENT
Research needs in ceramic machining [PB89-148191] N89-23681

TECHNOLOGY TRANSFER
Development of harmonic panel methods for aeroelastic applications to elastic bodies and body-fin combinations in supersonic flow [AD-A205739] N89-23423
Putting science and technology to work: A casebook of transferred technologies [DE89-009158] N89-24228

TECHNOLOGY UTILIZATION
Putting science and technology to work: A casebook of transferred technologies [DE89-009158] N89-24228

TEFLON (TRADEMARK)
Some examples of the degradation of properties of materials in space N89-23535

TELECOMMUNICATION
Phase accuracy experiments with a direct-sampling coherent detector [AD-A205458] N89-23764
Near-far resistant linear multiuser detection [AD-A206363] N89-23802
On the communication complexity of distributed algebraic computation [AD-A205784] N89-24117

TELEOPERATORS
An application specific integrated circuit for dual-axis motion control [DE89-007974] N89-23790
The 23rd Aerospace Mechanisms Symposium [NASA-CP-3032] N89-23892

TELESCOPES
Digital control of the Kuiper Airborne Observatory telescope [NASA-TM-101082] N89-23785
Development of a precision, wide-dynamic-range actuator for use in active optical systems N89-23901
A two-axis laser boresight system for a shuttle experiment N89-23913

TELEVISION RECEIVERS
Tuner for the first intermediate frequency of receivers for direct satellite reception [ETN-89-93766] N89-23788

TEMPERATURE CONTROL
Assembling the ISO thermal model with ESAT AN [REPT-882-440-107] N89-23510
The two approaches for the thermal control of the Columbus resource module and Polar Platform [REPT-882-440-110] N89-23511
Space vehicle thermal testing: Principles, practices and effectiveness N89-23550
TELE-X antenna module thermal control [REPT-882-440-106] N89-23782

TEMPERATURE DEPENDENCE
Temperature dependence of interfacial energies between solid oxides and liquid metals N89-23599

An investigation of the temperature dependence of the ultrasonic properties of AS4/lexan and XAS/lexan composites
[NASA-CR-184845] N89-23619
TEMPERATURE DISTRIBUTION
Behavior of metals during hot rolling processes. Part 2: Experimental methods for flow stress determination and calculation of the two-dimensional temperature-field in the roll gap N89-23814
Automatic analysis of holographic interferograms N89-23848
Study on a twin valveless pulse burner (temperature characteristics during pulse combustion)
[NAL-TR-973] N89-23873
TEMPERATURE EFFECTS
Some examples of the degradation of properties of materials in space N89-23535
Atomic oxygen effects on materials N89-23540
Space vehicle thermal testing: Principles, practices and effectiveness N89-23550
Effects of thermal cycling on composite materials for space structures N89-23552
Effect of physical annealing on the dynamic mechanical properties of a high T(g) amine-cured epoxy systems
[AD-A205980] N89-23704
Response of pavement to freeze-thaw cycles: Lebanon, New Hampshire, regional airport
[AD-A205559] N89-23740
Experimental and theoretical determination of the thermomechanical response of inelastic structural materials to high energy thermal inputs
[AD-A206100] N89-23933
Microscopic theory of electron spin resonance in Heisenberg spin glasses and thermal fluctuations in classical spin models with random fields
[JUEL-2227] N89-24146
TEMPERATURE GRADIENTS
Space vehicle thermal testing: Principles, practices and effectiveness N89-23550
Computerized measurement of thermoacoustically generated temperature gradients
[AD-A205353] N89-23929
Japan's Sunshine Project 1987 annual summary of comprehensive research
[DE88-756448] N89-23975
Acoustic response of a rectangular waveguide with a strong transverse temperature gradient
[NASA-TM-101564] N89-24140
TEMPERATURE MEASUREMENT
Electron conducting ceramics as sensor material for noise thermometry N89-23603
Experimental thermal conductivity, thermal diffusivity and specific heat values of argon and nitrogen
[PB89-148407] N89-23637
Development of a CARS device for a feasibility study of density and temperature measurements at high time dependent resolution
[ISL-R-117/87] N89-23654
TENSILE DEFORMATION
Information about hot flow-stress curves and the resulting structural changes N89-23616
TENSILE PROPERTIES
Tensile film clamps and mounting block for the rheovibron and autovibron viscoelastometer
[NASA-CASE-LAR-13696-1] N89-23880
TENSILE STRENGTH
Mechanical properties of rapidly solidified iron-based alloys N89-23611
TENSILE STRESS
Information about hot flow-stress curves and the resulting structural changes N89-23616
TENSILE TESTS
Information about hot flow-stress curves and the resulting structural changes N89-23616
Applications of a digital acoustic-emission data-acquisition workstation
[DE89-009648] N89-23923
TENSOR ANALYSIS
Riemannian geometry on families of linear systems: The deterministic case
[PB89-146062] N89-24100
TENSORS
Introduction to irreducible tensor methods, part 1
[NAL-PD-DU-8802] N89-24098
TERNARY ALLOYS
Deformation twinning in ordered intermetallic compounds
[DE89-008748] N89-24192
TERRAIN
The Official Topographic-Cartographic Information System (ATKIS) of the Geodesy Group of the Laender of the Federal Republic of Germany: Status after one year of development N89-23944
Tools for the computer assisted generalization of settlements for the construction of digital landscape models N89-23952
TEST FACILITIES
Aerothermodynamic analysis of a Coanda/Refraction Jet Engine Test Facility
[AD-A205937] N89-23482
Design of water tunnel to measure wall pressure signatures due to tunnel blockage and wake effects
[AD-A206025] N89-23483
Shaking in cryogenic conditions
[REPT-882-440-101] N89-23939
TEST FIRING
Qualification Motor no. 8 (QM-8), volume 1
[NASA-CR-183650] N89-23523
TEST STANDS
Test facility and preliminary performance of a 100 kW class MPD thruster
[NASA-TM-102021] N89-23520
Space station propulsion test bed
[NASA-CR-183615] N89-23521
TEST VEHICLES
Methanol vehicle catalyst evaluation, phase 3
[PB89-136139] N89-23874
TETHERED SATELLITES
Design and testing of a deployable, retrievable boom for space applications N89-23898
THEMATIC MAPPING
Geocoded data sets of imaging satellites N89-23950
Mapping freeze/thaw boundaries with SMMR data
[NASA-CR-184991] N89-23961
Geobotanical remote sensing for determination of aggregate source material
[AD-A205943] N89-23962
Meteosat thermal inertia mapping for studying wetland dynamics in the West-African Sahel
[BCRS-88-10A] N89-23970
THERMAL BOUNDARY LAYER
Boundary layer and heat transfer behind a piston in a shock tube. Part 2: Experimental study of heat transfer at the piston in a tube
[ISL-R-115/87-PT-2] N89-23842
THERMAL CONDUCTIVITY
Carbon fiber thermal conductivity measurement and analysis
[AD-A205682] N89-23625
Experimental thermal conductivity, thermal diffusivity and specific heat values of argon and nitrogen
[PB89-148407] N89-23637
Microporous fumed-silica insulation board as a candidate Standard Reference Material of thermal resistance
[PB89-148373] N89-24213
THERMAL CONTROL COATINGS
Working group written presentation: Solar radiation N89-23567
THERMAL CYCLING TESTS
Space vehicle thermal testing: Principles, practices and effectiveness N89-23550
Effects of thermal cycling on composite materials for space structures N89-23552
Study of adherent oxide scales
[AD-A205799] N89-23700
Environmental Stress Screening (ESS) guide
[AD-A206350] N89-23888
THERMAL DEGRADATION
High electric field phenomena in insulation
[AD-A205525] N89-23799
THERMAL DIFFUSION
Experimental thermal conductivity, thermal diffusivity and specific heat values of argon and nitrogen
[PB89-148407] N89-23637
THERMAL DIFFUSIVITY
Preparation, characterization and thermal diffusivity of Al2TiO5 N89-23591
THERMAL ENVIRONMENTS
SRB ascent aerodynamic heating design criteria reduction study, volume 1
[NASA-CR-183580] N89-23515
Space vehicle thermal testing: Principles, practices and effectiveness N89-23550
Effects of thermal cycling on composite materials for space structures N89-23552
THERMAL EXPANSION
Preparation and thermal expansion of Al2TiO5-TiO5-TiO2 sintered bodies N89-23578
Dilatometric analysis of Al-, Ba-, Ca-titanate N89-23592
Theoretical analysis of compatibility of several reinforcement materials with NiAl and FeAl matrices
[NASA-CR-182291] N89-23622
Lattice symmetries and thermal expansion
[AD-A206045] N89-24207
THERMAL INSULATION
The thermal resistance of flat powder-filled evacuated panels
[DE89-008243] N89-23685
The concept and theoretical considerations of a cold weather clothing system
[AD-A205476] N89-24046
Microporous fumed-silica insulation board as a candidate Standard Reference Material of thermal resistance
[PB89-148373] N89-24213
THERMAL MAPPING
Meteosat thermal inertia mapping for studying wetland dynamics in the West-African Sahel
[BCRS-88-10A] N89-23970
Thermal analysis for the monitoring and prediction of flood dynamics in wetlands
[BCRS-88-10B] N89-23971
THERMAL PLASMAS
Influence of charging environments on spacecraft materials and system performance N89-23556
THERMAL PROTECTION
SRB ascent aerodynamic heating design criteria reduction study, volume 1
[NASA-CR-183580] N89-23515
Reentry materials in the atmosphere
[REPT-882-430-102] N89-23629
High performance refractory composite materials
[REPT-882-430-106] N89-23631
THERMAL RADIATION
NASA/SDIO Space Environmental Effects on Materials Workshop, part 2
[NASA-CP-3035-PT-2] N89-23547
Effect of internal convection and internal radiation on the structural temperatures of Space Shuttle Orbiter
[NASA-TM-100414] N89-23819
THERMAL RESISTANCE
The thermal resistance of flat powder-filled evacuated panels
[DE89-008243] N89-23685
The concept and theoretical considerations of a cold weather clothing system
[AD-A205476] N89-24046
Microporous fumed-silica insulation board as a candidate Standard Reference Material of thermal resistance
[PB89-148373] N89-24213
THERMAL SHOCK
Cracking of a layered medium on an elastic foundation under thermal shock
[NASA-CR-185316] N89-23925
THERMAL STABILITY
Fabricable polymers with excellent heat, oxidative and hydrolytic stability
[AD-A205627] N89-23698
THERMAL STRESSES
Cracking of coated materials under transient thermal stresses
[NASA-CR-184898] N89-23928
Experimental and theoretical determination of the thermomechanical response of inelastic structural materials to high energy thermal inputs
[AD-A206100] N89-23933
THERMOCHROMATIC MATERIALS
Quasi-liquid crystalline materials with special electro-optic properties
[AD-A206015] N89-24206
THERMODYNAMIC PROPERTIES
Critical assessment of the thermodynamic properties of antimony-copper alloys
[PB89-147524] N89-23657
Experimental and theoretical studies of dense fluid mixtures
[DE89-006882] N89-24214
THERMODYNAMICS
White paper: Experimental and computational studies of very high velocity impacts
[DE89-007643] N89-23877
THERMOELASTICITY
Geometrical foundations of mesomechanics and Lagrangian formalism
[AD-A205589] N89-23930
THERMOELECTRIC GENERATORS
Preliminary assessment of rover power systems for the Mars Rover Sample Return Mission
[NASA-TM-102003] N89-23518
Final safety analysis report for the Galileo Mission. Volume 1: Reference design document
[DE89-007268] N89-24147
THERMOELECTRIC MATERIALS
High pressure studies on infrared detector materials
[NAL-TM-MT-8701] N89-23677
THERMOELECTRIC POWER GENERATION
Japan's Sunshine Project 1987 annual summary of comprehensive research
[DE88-756448] N89-23975
THERMOMETERS
Liquid-in-glass thermometer calibration service
[PB89-128888] N89-23846
THERMOPLASTIC RESINS
Mode 2 delamination fatigue resistance of composites N89-23624
Environmental stress crazing and cracking of transparent polymers
[AD-A205624] N89-23697

THERMOREGULATION
Human temperature regulation during exercise after oral pyridostigmine administration
[AD-A206032] N89-24030
THETA PINCH
Theta pinch discharges for solids vaporization and elemental chemical analysis
[DE89-008888] N89-23641
THIN AIRFOILS
Numerical solution of periodic vortical flows about a thin airfoil
[NASA-TM-101998] N89-23413
THIN FILMS
Steel hardness effects in boundary lubricated sliding: An in-situ SEM (Scanning Electron Microscope) study
[AD-A206156] N89-23674
Sequentially evaporated thin Y-Ba-Co-O superconducting films on microwave substrates
[NASA-TM-102068] N89-23791
A numerical investigation of thin-film heat transfer gages
[AD-A206134] N89-23853
Structure and grid dynamics of ultrathin epitaxial Ag and Fe films on Ni(100) and Cu(100) substrates
[JUEL-2221] N89-24187
Monitoring thin film properties with surface acoustic wave devices: Diffusion, surface area and pore size distribution
[DE89-009379] N89-24195
Photoabsorption of molecules at corrugated thin metal films
[AD-A205325] N89-24197
Fundamental studies of the mechanical behavior of microelectronic thin film materials
[AD-A206057] N89-24208
THIN PLATES
Fundamental studies of beta phase decomposition modes in titanium alloys
[AD-A205296] N89-23665
Computerized measurement of thermoacoustically generated temperature gradients
[AD-A205353] N89-23929
THIN WALLED SHELLS
Application of an exact finite element method to analysis of statics of thin elastic shells of revolution with axisymmetric loading
[ISBN-952-900-399-4] N89-23917
THREE BODY PROBLEM
Cohesive and anharmonic elastic properties of mixed fluorite crystals
[DE88-705690] N89-24184
A study of the motion in the neighborhood of the triangular libration point N89-24236
THREE DIMENSIONAL BOUNDARY LAYER
Three-dimensional structure of boundary layers in transition to turbulence
[AD-A205587] N89-23828
THREE DIMENSIONAL FLOW
Three-dimensional structure of boundary layers in transition to turbulence
[AD-A205587] N89-23828
Numerical solution of the three dimensional heat flow equation generated by a moving source
[ISL-R-116/87] N89-23843
A simple approximate method to evaluate the 3-D aerodynamic field around a streamline and to determine the validity of the quasi-three dimensional hypothesis
[ETN-89-94366] N89-23844
THREE DIMENSIONAL MODELS
Transonic Navier-Stokes solutions of three-dimensional afterbody flows
[NASA-TM-4111] N89-23433
Numerical implementation of the Schapery model for nonlinear visco-elasticity
[PB89-144950] N89-23915
THREE DIMENSIONAL MOTION
Bifurcating jets at high Reynolds numbers
[AD-A205718] N89-23829
THRESHOLDS (PERCEPTION)
Three-dimensional recognition of solid objects from a two-dimensional image
[AD-A205667] N89-24094
THROTTLING
The 4D-TECS integration for NASA TSRV airplane
[NASA-CR-4231] N89-23471
THRUST AUGMENTATION
Ejector effects on a supersonic nozzle at low altitude and Mach number
[AD-A206049] N89-23427
THRUST CONTROL
Continuous, low thrust coplanar orbit transfers with varying eccentricity
[AD-A206022] N89-23498
THRUST MEASUREMENT
Arcjet nozzle design impacts
[NASA-TM-102050] N89-23522
THRUST VECTOR CONTROL
A closed-form trim solution yielding minimum trim drag for airplanes with multiple longitudinal-control effectors
[NASA-TP-2907] N89-23468
Two-dimensional confined jet thrust vector control: Operating mechanisms and performance
[AD-A206011] N89-23834
TILES
Design features, flight monitoring of Buran N89-23487
TIME
Automatic documentation methodologies for software maintenance
[AD-A205672] N89-24062
TIME DEPENDENCE
Epoxylite 8822 hardness study
[DE89-008961] N89-23687
TIME DIVISION MULTIPLEXING
Light channel 5 Gb/s optoelectronic TDM (Time Division Multiplexing)
[AD-A205501] N89-24086
TIME MEASUREMENT
An instrument for the simultaneous measurement of velocity, temperature and density in unseeded air flows
[AD-A205588] N89-23453
TIN ALLOYS
Macrosegregation and nucleation in undercooled Pb-Sn alloys
[NASA-TM-102023] N89-23664
TITAN LAUNCH VEHICLES
Pyro thruster for performing rocket booster attachment, disconnect, and jettison functions N89-23902
TITANIUM
Ionization investigation of sputtered titanium and of titanium ion transport process in an argon discharge glow using laser induced fluorescence
[JUEL-2219] N89-23660
Correlation of Portable Wear Metal Analyzer (PWMA-2) and Baird A/E35U-3 spectrometer oil analysis data
[AD-A205957] N89-23882
TITANIUM ALLOYS
Fundamental studies of beta phase decomposition modes in titanium alloys
[AD-A205296] N89-23665
Ambient temperature properties of PM (Powder Metal) aluminum-titanium alloys
[AD-A205997] N89-23671
TITANIUM BORIDES
Mechanical properties of gas atomized Cu-Ti and Cu-Ti-B alloys N89-23610
TITANIUM CARBIDES
The wear of cutting tools: The contribution of abrasive wear N89-23586
TITANIUM OXIDES
Preparation and thermal expansion of Al2TiO5-TiO5-TiO2 sintered bodies N89-23578
Preparation, characterization and thermal diffusivity of Al2TiO5 N89-23591
TOKAMAK DEVICES
Transport of test particles in a magnetic field with perturbed magnetic surfaces
[IPP-2/296] N89-24176
TOLERANCES (PHYSIOLOGY)
Functional assessment of laser irradiation
[AD-A206230] N89-23871
Human adaptation to the Tibetan Plateau
[AD-A206463] N89-24031
Additivity of retinal damage for multiple-pulse laser exposures
[AD-A206514] N89-24032
TOLLMIEN-SCHLICHTING WAVES
Numerical simulation of Goertler/Tollmein-Schlichting wave-interaction
[NASA-CR-181823] N89-23817
TOLUENE
Sorption of selected volatile organic constituents of jet fuels and solvents on natural sorbents from gas and solutions phases
[AD-A204073] N89-23711
TOOLS
The wear of cutting tools: The contribution of abrasive wear N89-23586
Advanced layer materials N89-23587
TOPOGRAPHY
Tools for the computer assisted generalization of settlements for the construction of digital landscape models N89-23952
Computer assisted generalization of transport line representations N89-23953
TOPOLOGY
The formation of topological defects in phase transitions
[NASA-CR-185318] N89-24215
TORCHES
Electrode carrying wire for GTAW welding
[NASA-CASE-MFS-29491-1] N89-23738
Internal wire guide for GTAW welding
[NASA-CASE-MFS-29489-1] N89-23739
TORQUE
Magnification of starting torques of dc motors by maximum power point trackers in photovoltaic systems
[NASA-TM-102040] N89-23792
TORQUEMETERS
Design and development of a high-stiffness, high-resolution torque sensor N89-23903
TOUGHNESS
Molded bodies having a high degree of hardness and a high degree of toughness for machining metals, carbides, ceramics and glasses
[DE89-008820] N89-23686
TRACKING (POSITION)
System study: Radiation hardened autonomous navigation
[AD-A205804] N89-23439
Magnification of starting torques of dc motors by maximum power point trackers in photovoltaic systems
[NASA-TM-102040] N89-23792
Psychometric function reconstruction from adaptive tracking procedures
[AD-A205668] N89-24034
Parallel ada implementation of a multiple model Kalman filter tracking system: A software engineering approach
[AD-A206094] N89-24130
TRAILING EDGE FLAPS
Numerical study of the influence of leading and trailing edge flaps on the performance of airfoils
[AD-A206136] N89-23428
TRAINING SIMULATORS
Design of a MANPRINT tool for predicting personnel and training characteristics implied by system design
[AD-A206201] N89-24048
TRAJECTORY CONTROL
Optimal aeroassisted coplanar orbital transfer using an energy model
[NASA-CR-181778] N89-23495
TRAJECTORY OPTIMIZATION
Multiple model-based robot control: Development and initial evaluation
[AD-A205725] N89-23881
TRANSDUCERS
Applications of a digital acoustic-emission data-acquisition workstation
[DE89-009648] N89-23923
TRANSFER FUNCTIONS
Analytical transfer functions in parallel configurations
[AD-A205714] N89-23472
TRANSFER ORBITS
Optimal aeroassisted coplanar orbital transfer using an energy model
[NASA-CR-181778] N89-23495
Continuous, low thrust coplanar orbit transfers with varying eccentricity
[AD-A206022] N89-23498
TRANSIENT LOADS
Cracking of coated materials under transient thermal stresses
[NASA-CR-184898] N89-23928
TRANSISTOR LOGIC
Design of multiple-valued programmable logic arrays (PLA)
[AD-A205307] N89-24085
TRANSITION METALS
P-T diagrams of transition elements N89-23618
X-ray absorption spectroscopy of electrochemically generated species
[AD-A205572] N89-23647
Simple adsorbates on transition metal surfaces: A joint chemical and physical approach
[AD-A205726] N89-23669
FILMCAL: An ESR (Electron Spin Resonance) simulation program for transition metals in phthalocyanine films
[AD-A206441] N89-23676
TRANSITION PRESSURE
P-T diagrams of transition elements N89-23618
TRANSITION TEMPERATURE
P-T diagrams of transition elements N89-23618
The glass transition temperature (Tg) as a parameter for monitoring the cure of an amine-cured epoxy system at constant heating rates
[AD-A206098] N89-23705
Studies on high-Tc superconducting materials
[NAL-TM-MT-8703] N89-24178
TRANSLATIONAL MOTION
Numerical solution of the three dimensional heat flow equation generated by a moving source
[ISL-R-116/87] N89-23843
TRANSMISSION LINES
AN/TAC-1 demultiplexer circuit card assembly
[AD-A205744] N89-23770
TRANSMISSION LOSS
Lossy layers: Theory and methods of measurement
[FOA-C-30513-3.2] N89-23779

TRANSMISSIONS (MACHINE ELEMENTS)
Traction-drive force transmission for telerobotic joints N89-23906
TRANSMITTANCE
Contamination N89-23559
Fatigue-resistant photochromic plastics [DE89-007336] N89-23682
TRANSMITTERS
Near-far resistant linear multiuser detection [AD-A206363] N89-23802
TRANSONIC FLIGHT
Exploitation of multiple solutions of the Navier-Stokes equations to achieve radically improved flight [AD-A205939] N89-23831
TRANSONIC FLOW
Transonic Navier-Stokes solutions of three-dimensional afterbody flows [NASA-TM-4111] N89-23433
Exploitation of multiple solutions of the Navier-Stokes equations to achieve radically improved flight [AD-A205939] N89-23831
TRANSONIC FLUTTER
Flutter of a low-aspect-ratio rectangular wing [NASA-TM-4116] N89-23447
TRANSONIC WIND TUNNELS
Transonic operational characteristics and performance [NAL-TR-968] N89-23408
Transonic aerodynamic characteristics of a proposed Assured Crew Return Capability (ACRC) lifting-body configuration [NASA-TM-4117] N89-23412
TRANSPONDERS
Design of a 60 GHz beam waveguide antenna positioner N89-23910
TRANSPORT AIRCRAFT
Flight testing of the Southern Cross replica aircraft [AD-A205303] N89-23451
TRANSPORT PROPERTIES
Electronic and ionic transport in polymers [AD-A206530] N89-23709
Electrical transport properties of Hg0.7Cd0.3Te [DE88-705689] N89-24183
TRANSPORT THEORY
A hierarchy of transport approximations for high energy heavy (HZE) ions [NASA-TM-4118] N89-24255
TRANSPORTATION NETWORKS
Computer assisted generalization of transport line representations N89-23953
TRANSVERSE OSCILLATION
Free shear layer and swirl flow heat transfer enhancement [PB89-145106] N89-23810
TRAPPED PARTICLES
Working group written presentation: Trapped radiation effects N89-23566
Path dependent morphologies of a diblock copolymer of Polystyrene/Hydrogenated polybutadiene [AD-A206504] N89-23883
Solar flares and magnetospheric particles: Investigations based upon the ONR-602 and ONR-604 experiments [AD-A205599] N89-24253
TREND ANALYSIS
Launch commit criteria performance trending analysis, phase 1, revision A. SRM and QA mission services [NASA-CR-184859] N89-24129
TRENDS
Trends in environmentally induced spacecraft anomalies N89-23536
TRIBOLOGY
Ceramic tribology: Methodology and mechanisms of alumina wear [PB89-148357] N89-23679
Design and construction of a state-of-the-art high temperature tribometer [PB89-148332] N89-23847
TROPOSPHERE
Studies of internal gravity waves in the stably stratified troposphere N89-23989
Observation model and parameter partials for the JPL geodetic GPS modeling software GPSOMC [NASA-CR-185021] N89-24060
TRUSSES
Carousel deployment mechanism for collable lattice truss N89-23897
Locating damaged members in a truss structure using modal test data: A demonstration experiment [NASA-TM-101595] N89-23924
Fractional calculus formulation of the quasi-static viscoelastic problem [AD-A206136] N89-23934
TUBE HEAT EXCHANGERS
Two-dimensional numerical simulation of a Stirling engine heat exchanger [NASA-TM-102057] N89-23823
TUNERS
Tuner for the first intermediate frequency of receivers for direct satellite reception [ETN-89-93766] N89-23788
TUNGSTEN CARBIDES
The wear of cutting tools: The contribution of abrasive wear N89-23586
TUNING
The application of self-tuning control techniques to a multivariable process [OUEL-1737/88] N89-23737
Multivariable Nyquist self-tuning: A general approach [OUEL-1734/88] N89-24091
TURBINE BLADES
A research facility for film cooling investigations with emphasis on the instrumentation system [NAL-TM-PR-8704] N89-23477
Composite blade structural analyzer (COBSTRAN) user's manual [NASA-TM-101461] N89-23621
Mechanisms of secondary flows and losses within a three dimensional turbine stator cascade [NAL-TR-970T] N89-23807
TURBINES
Transonic operational characteristics and performance [NAL-TR-968] N89-23408
TURBOMACHINERY
A simple approximate method to evaluate the 3-D aerodynamic field around a streamline and to determine the validity of the quasi-three dimensional hypothesis [ETN-89-94366] N89-23844
TURBOPROP AIRCRAFT
High speed turboprop aeroacoustic study (single rotation). Volume 1: Model development [NASA-CR-182257-VOL-1] N89-24139
Interior noise control ground test studies for advanced turboprop aircraft applications [NASA-CR-181819] N89-24141
TURBOPROP ENGINES
High speed turboprop aeroacoustic study (single rotation). Volume 1: Model development [NASA-CR-182257-VOL-1] N89-24139
TURBULENCE
On the nature of Navier-Stokes turbulence [NASA-TM-101983] N89-23813
Three-dimensional structure of boundary layers in transition to turbulence [AD-A205587] N89-23828
Vaporization and recondensation in propagation and imaging of laser beams [DE89-008014] N89-23858
TURBULENCE EFFECTS
Fire propagation in concurrent flows [PB89-151781] N89-23636
TURBULENCE MODELS
Transonic Navier-Stokes solutions of three-dimensional afterbody flows [NASA-TM-4111] N89-23433
TURBULENT BOUNDARY LAYER
An experimental study of the effect of streamwise vortices on unsteady turbulent boundary-layer separation [AD-A205462] N89-23420
Effects of initial conditions on the development of supersonic turbulent free shear layers [AD-A205607] N89-23421
Flow control for unsteady and separated flows and turbulent mixing [AD-A205989] N89-23426
Three dimensional high speed boundary layer flows [AD-A206145] N89-23837
Boundary layer and heat transfer behind a piston in a shock tube. Part 1: Theoretical considerations of laminar and turbulent boundary layer behind a piston in a tube [ISL-R-111/87-PT-1] N89-23841
TURBULENT FLOW
Turbulent shear stress measurement in hypersonic flow [AD-A206453] N89-23432
Fundamental studies on spray combustion and turbulent combustion [AD-A206438] N89-23651
The dimension of attractors underlying turbulent Poiseuille flow [AD-A206021] N89-23835
Comparison of split-film and x-film measurements in 2-D flow [AD-A206023] N89-23836
Analysis of turbulent motion phenomena in the maritime atmospheric boundary layer [ETN-89-93949] N89-23996
TURBULENT JETS
Turbulence near a free surface in a plane jet [AD-A206269] N89-23838
TURBULENT MIXING
Flow control for unsteady and separated flows and turbulent mixing [AD-A205989] N89-23426
TURBULENT WAKES
Flowfield measurements in the vortex wake of a missile at high angle of attack in turbulence [AD-A205696] N89-23422
TURNING FLIGHT
An investigation into the application of dynamic programming to determine optimal controls for tracking a cruise missile maneuver by CMMCA (Cruise Missile Mission Control Aircraft) [AD-A205970] N89-23456
TWO DIMENSIONAL FLOW
Computation of dynamics and control of unsteady vortical flows N89-23822
Comparison of split-film and x-film measurements in 2-D flow [AD-A206023] N89-23836
TYROSINE
Treatment with tyrosine, a neurotransmitter precursor, reduces environmental stress in humans [AD-A206035] N89-24039

U

U.S.S.R. SPACE PROGRAM
JPRS report: Science and technology. USSR: Space [JPRS-USP-89-004] N89-23484
Details of Buran shuttle flight N89-23486
Buran designer Semenov interviewed N89-23488
Medical and biological support for a manned expedition to Mars N89-23492
UDIMET ALLOYS
Cyclic crack propagation characteristics of the powder metallurgical nickel-base alloy Udimet 720 at elevated temperatures and different dwell times [ETN-89-94426] N89-23938
ULTRAHIGH FREQUENCIES
Small UHF microstrip radiating element [REPT-882-440-103] N89-23780
ULTRAPURE METALS
Oxygen interaction with metal surfaces: Surface science approach N89-23596
ULTRASONIC FLAW DETECTION
An investigation of the temperature dependence of the ultrasonic properties of AS4/Iexan and XAS/Iexan composites [NASA-CR-184845] N89-23619
ULTRASONIC TESTS
An investigation of the temperature dependence of the ultrasonic properties of AS4/Iexan and XAS/Iexan composites [NASA-CR-184845] N89-23619
ULTRAVIOLET ABSORPTION
Ultraviolet radiation effects N89-23551
ULTRAVIOLET LASERS
Ultra-high resolution VUV-XUV laser: Application to the hyperfine study of krypton [DE89-009059] N89-23863
Research studies on extreme ultraviolet and soft X-ray lasers [AD-A205625] N89-23868
ULTRAVIOLET MICROSCOPY
Summaries of papers presented at Short Wavelength Coherent Radiation: Generation and Applications Topical Meeting held in Cape Cod, Massachusetts on September 26-29, 1988 [AD-A205471] N89-23867
ULTRAVIOLET RADIATION
Co-aligning the RAIDS (Remote Atmospheric and Ionospheric Detection System) instruments [AD-A205456] N89-23513
Ultraviolet radiation effects N89-23551
Solar radiation N89-23562
Working group written presentation: Solar radiation N89-23567
ULTRAVIOLET SPECTROMETERS
Comet Halley: The view from Pioneer Venus [NASA-NF-127] N89-24240
ULTRAVIOLET SPECTROSCOPY
Spectral observations of the extreme ultraviolet background N89-24259
ULYSSES MISSION
Calibration measurements on micrometeorite detectors for the missions ULYSSES, Galileo and Giotto [ETN-89-93947] N89-24248
UNCONTROLLED REENTRY (SPACECRAFT)
Space debris: A report from the ESA Debris Working Group [ESA-SP-1109] N89-24230

UNDERWATER BREATHING APPARATUS
Oxygen consumption rate of operational underwater swimmers
[AD-A205331] N89-24025
UNDERWATER PHYSIOLOGY
Oxygen consumption rate of operational underwater swimmers
[AD-A205331] N89-24025
UNDERWATER VEHICLES
Drag and noise measurements on underwater vehicles with a riblet surface coating
[AD-A205500] N89-23825
UNITED STATES
Loran C field strength contours: Contiguous US
[DOT/FAA/CT-TN89/16] N89-23437
UNSTEADY FLOW
A numerical scheme to solve unsteady and variable density low Mach number flows N89-23419
An experimental study of the effect of streamwise vortices on unsteady turbulent boundary-layer separation
[AD-A205462] N89-23420
Development of harmonic panel methods for aeroelastic applications to elastic bodies and body-fin combinations in supersonic flow
[AD-A205739] N89-23423
Flow control for unsteady and separated flows and turbulent mixing
[AD-A205989] N89-23426
Pulsating catalytic combustion of gaseous fuels N89-23643
On the Lagrangian description of unsteady boundary layer separation. Part 1: General theory
[NASA-TM-102026] N89-23821
Computation of dynamics and control of unsteady vortical flows N89-23822
Study on a twin valveless pulse burner (temperature characteristics during pulse combustion)
[NAL-TR-973] N89-23873
A search for pulsations in planetary nebulae nuclei N89-24235
USER MANUALS (COMPUTER PROGRAMS)
Composite blade structural analyzer (COBSTRAN) user's manual
[NASA-TM-101461] N89-23621
Fatigue crack growth model RANDOM2 user manual, appendix 1
[NASA-CR-184939] N89-23890
Fatigue strength reduction model: RANDOM3 and RANDOM4 user manual, appendix 2
[NASA-CR-184940] N89-23891
Defense Integrated Data System (DIDS) procedures manual. Volume 8: Document Identifier Code (DIC) Input/Output (I/O) formats (fixed length), change 3
[PB89-139414] N89-24220
USER REQUIREMENTS
Direct dissemination of data from ESA's future in-orbit infrastructure
[DDD-CP/TE-RE-7450] N89-23754
Human-machine interaction considerations for interactive software
[AD-A206574] N89-24049
A graphical editor for the computer aided prototyping system
[AD-A206443] N89-24071

V

VALENCE
Site occupancy/valence measurements using channelling and related effects in microanalysis
[DE89-007658] N89-24186
VALVES
Low energy consumption hydraulic techniques
[AD-A206285] N89-23743
Nonintrusive methods for monitoring the operational readiness of solenoid-operated valves
[DE89-008732] N89-23878
VAPOR DEPOSITION
Ultrafine microstructure composites prepared by chemical vapor deposition
[AD-A206061] N89-23627
Atomic layer epitaxy. Atomic layer epitaxy of 3-5 compound semiconductors by thermal and laser-assisted metalorganic chemical vapor deposition
[AD-A205699] N89-24200
In situ mechanistic studies of MOCVD growth of 3/5 semiconductors
[AD-A206396] N89-24210
VAPOR EPITAXY
Atomic layer epitaxy. Atomic layer epitaxy of 3-5 compound semiconductors by thermal and laser-assisted metalorganic chemical vapor deposition
[AD-A205699] N89-24200
VAPOR PHASES
Sorption of selected volatile organic constituents of jet fuels and solvents on natural sorbents from gas and solutions phases
[AD-A204073] N89-23711
Spectrometric studies of gas phase collision processes
[AD-A205570] N89-23826
In situ mechanistic studies of MOCVD growth of 3/5 semiconductors
[AD-A206396] N89-24210
VAPORIZING
Theta pinch discharges for solids vaporization and elemental chemical analysis
[DE89-008888] N89-23641
Vaporization and recondensation in propagation and imaging of laser beams
[DE89-008014] N89-23858
VAPORS
A description of the slab model
[DE89-009962] N89-23984
VARIABILITY
Time and spectral variability of the low mass X-ray binaries
[MPE-REPORT-210] N89-24238
VARIANCE (STATISTICS)
On the problem of optimal signal detection in discrete-time, correlated, non-Gaussian noise
[AD-A205859] N89-23771
VARISTORS
Microstructure and phase development in multicomponent ZnO based varistor ceramics N89-23604
Zinc oxide varistor time response
[DE89-008234] N89-24191
VECTOR ANALYSIS
A vector scanning processing technique for pulsed laser velocimetry
[NASA-TM-102048] N89-23850
Krylov methods preconditioned with incompletely factored matrices on the CM-2
[AD-A206389] N89-24121
VECTORS (MATHEMATICS)
Vectorization of grid lines
[ETN-89-94150] N89-23967
VELOCITY DISTRIBUTION
Computing induced velocity perturbations due to a helicopter fuselage in a free stream
[NASA-TM-4113] N89-23410
On the communication complexity of distributed algebraic computation
[AD-A205784] N89-24117
VELOCITY MEASUREMENT
Turbulent shear stress measurement in hypersonic flow
[AD-A206453] N89-23432
An instrument for the simultaneous measurement of velocity, temperature and density in unseeded air flows
[AD-A205588] N89-23453
VENTILATION
Space station ECLSS simplified integrated test
[NASA-TM-100363] N89-24044
VERTICAL LANDING
Heliport night parking area criteria test plan
[DOT/FAA/CT-TN88/45] N89-23480
VERY LARGE ARRAY (VLA)
Very large array observations of the sun with related observations using the SMM (Solar Maximum Mission) satellite
[AD-A203874] N89-24249
VERY LARGE SCALE INTEGRATION
Recursive gate-arrays
[AD-A205335] N89-23796
VESTS
Evaluation of three commercial microclimate cooling systems
[AD-A206318] N89-23744
VIBRATION DAMPING
Digital control of the Kuiper Airborne Observatory telescope
[NASA-TM-101082] N89-23785
Tensile film clamps and mounting block for the rheovibron and autovibron viscoelastometer
[NASA-CASE-LAR-13696-1] N89-23880
Exact wave functions and coherent states of a damped driven harmonic oscillator
[AD-A205785] N89-24136
VIBRATION MEASUREMENT
Modal analysis and testing of missile systems
[AD-A204051] N89-23916
VIBRATION SIMULATORS
Shaking in cryogenic conditions
[REPT-882-440-101] N89-23939
VIBRATION TESTS
Ground shake test of the Boeing Model 360 helicopter airframe
[NASA-CR-181766] N89-23920
Shaking in cryogenic conditions
[REPT-882-440-101] N89-23939
VIBRATIONAL SPECTRA
Spectroscopic studies of metal-ligand-surface interactions
[AD-A206460] N89-23652
VIBRATIONAL STRESS
Shaking in cryogenic conditions
[REPT-882-440-101] N89-23939
VISCOELASTIC DAMPING
Prediction and measurement of damping of a laminated beam with a constrained viscoelastic layer
[DE89-009002] N89-23922
Quadratic optimal control theory for viscoelastically damped structures using a fractional derivative viscoelasticity model
[AD-A206008] N89-23932
Fractional calculus formulation of the quasi-static viscoelastic problem
[AD-A206136] N89-23934
Inverse problem techniques for beams with tip body and time hysteresis damping
[NASA-CR-181833] N89-24112
VISCOELASTICITY
Numerical implementation of the Schapery model for nonlinear visco-elasticity
[PB89-144950] N89-23915
Prediction and measurement of damping of a laminated beam with a constrained viscoelastic layer
[DE89-009002] N89-23922
Fractional calculus formulation of the quasi-static viscoelastic problem
[AD-A206136] N89-23934
VISCOSITY
Viscosity and conductance of MEICl/AlCl3 melts containing nonaqueous solvents
[AD-A205468] N89-23648
In situ fluorescence monitoring of the viscosities of particle-filled polymers in flow
[PB89-146278] N89-23680
VISCOUS FLOW
A numerical study of viscous vortex rings using a spectral method
[NASA-TM-101041] N89-23820
Rayleigh-Taylor instability of a viscous film overlying a passive fluid
[AD-A205578] N89-23827
Computation of flow around maneuvering submerged bodies
[AD-A205994] N89-23833
Three dimensional high speed boundary layer flows
[AD-A206145] N89-23837
VISUAL ACCOMMODATION
Quasi-monochromatic visual environments and the resting point of accommodation
[AD-A205938] N89-24036
VISUAL ACUITY
Quasi-monochromatic visual environments and the resting point of accommodation
[AD-A205938] N89-24036
VISUAL DISCRIMINATION
Three-dimensional recognition of solid objects from a two-dimensional image
[AD-A205667] N89-24094
VISUAL FIELDS
Three-dimensional recognition of solid objects from a two-dimensional image
[AD-A205667] N89-24094
VISUAL PERCEPTION
Quasi-monochromatic visual environments and the resting point of accommodation
[AD-A205938] N89-24036
Three-dimensional recognition of solid objects from a two-dimensional image
[AD-A205667] N89-24094
VISUAL STIMULI
Relating attention to visual mechanisms
[AD-A206452] N89-24042
VOICE COMMUNICATION
Intelligibility in noise of three LPC (Linear Predictive Coders) voice channels with active noise reduction headsets
[AD-A205613] N89-23767
An evaluation of the F/FB/EF-111 crew/voice message system
[AD-A205998] N89-23774
VORTEX RINGS
A numerical study of viscous vortex rings using a spectral method
[NASA-TM-101041] N89-23820
Bifurcating jets at high Reynolds numbers
[AD-A205718] N89-23829

VORTICES
Numerical solution of periodic vortical flows about a thin airfoil
[NASA-TM-101998] N89-23413
High angle-of-attack aerodynamic characteristics of crescent and elliptic wings
[NASA-CR-184992] N89-23418
An experimental study of the effect of streamwise vortices on unsteady turbulent boundary-layer separation
[AD-A205462] N89-23420
Numerical simulation of Goertler/Tollmein-Schlichting wave-interaction
[NASA-CR-181823] N89-23817
Computation of dynamics and control of unsteady vortical flows N89-23822
VORTICITY EQUATIONS
Numerical study of the influence of leading and trailing edge flaps on the performance of airfoils
[AD-A206138] N89-23428
A numerical study of viscous vortex rings using a spectral method
[NASA-TM-101041] N89-23820

W

WAFERS
Fundamental studies of the mechanical behavior of microelectronic thin film materials
[AD-A206057] N89-24208
WALL FLOW
Analogy between explosive wave and front wave near curved walls
[ISL-CO-209/87] N89-23840
WALL PRESSURE
Design of water tunnel to measure wall pressure signatures due to tunnel blockage and wake effects
[AD-A206025] N89-23483
WATER
Water-processable conducting polymers
[DE89-009251] N89-23688
WATER COLOR
Optical properties of oceanic suspended matter and their interpretation for remote sensing of phytoplankton
[GKSS-88/E/40] N89-24013
WATER PRESSURE
Design of water tunnel to measure wall pressure signatures due to tunnel blockage and wake effects
[AD-A206025] N89-23483
WATER TREATMENT
Space Station CMIF extended duration metabolic control test
[NASA-TM-100362] N89-23503
WATER VAPOR
Corrosion of silicon carbide ceramics at high temperatures in water vapor-containing atmospheres N89-23594
The dynamic behavior of water vapor on activated carbon
[AD-A206124] N89-23628
WAVE DIFFRACTION
A method to design blended rolled edges for compact range reflectors
[NASA-CR-184976] N89-23736
WAVE DISPERSION
A description of the slab model
[DE89-009962] N89-23984
WAVE EQUATIONS
Increasing the margin of stability of arbitrarily finite modes of flexible large space structures with damping
[AD-A206487] N89-23507
Acoustic response of a rectangular waveguide with a strong transverse temperature gradient
[NASA-TM-101564] N89-24140
WAVE FRONTS
Wavefront matrix multiplication on a distributed-memory multiprocessor
[PB89-151807] N89-24052
WAVE FUNCTIONS
Exact wave functions and coherent states of a damped driven harmonic oscillator
[AD-A205785] N89-24136
Eikonal approximation in partial wave version
[IPPJ-899] N89-24164
WAVE INTERACTION
Numerical simulation of Goertler/Tollmein-Schlichting wave-interaction
[NASA-CR-181823] N89-23817
Three-dimensional structure of boundary layers in transition to turbulence
[AD-A205587] N89-23828
Mathematical analysis of strong fluid mechanical effects in reacting and nonreacting gases
[AD-A206336] N89-23839
Capture and confinement of solutions in nonlinear integrable systems
[DE88-705823] N89-24106
WAVE PACKETS
Capture and confinement of solutions in nonlinear integrable systems
[DE88-705823] N89-24106
WAVE PROPAGATION
Analogy between explosive wave and front wave near curved walls
[ISL-CO-209/87] N89-23840
Molecular optics nonlinear optical processes in organic and polymeric crystals and films
[AD-A206372] N89-24209
WAVEGUIDES
An evaluation of coplanar line for application in microwave integrated circuitry
[AD-A205305] N89-23795
Attenuation measurement of very low-loss dielectric waveguides by the cavity resonator method in the millimeter/submillimeter wavelength range
[AD-A206458] N89-23803
Design and verification of mechanisms for a large foldable antenna N89-23899
WEAPON SYSTEMS
An analysis of Electronic Aids to Maintenance (EAM) for the Light Helicopter Family (LHX)
[AD-A205440] N89-23407
WEAR
Correlation of Portable Wear Metal Analyzer (PWMA-2) and Baird A/E35U-3 spectrometer oil analysis data
[AD-A205957] N89-23882
WEAR INHIBITORS
The wear of cutting tools: The contribution of abrasive wear N89-23586
WEAR RESISTANCE
Wear resistant sintered steel with high carbide content N89-23607
Ceramic tribology: Methodology and mechanisms of alumina wear
[PB89-148357] N89-23679
Design and construction of a state-of-the-art high temperature tribometer
[PB89-148332] N89-23847
WEATHER
Use of the 1:2,000,000 Digital Line Graph data in emergency response
[DE89-006730] N89-23959
Inferring relative humidity profiles from 3DNEPH cloud data: Technique development and data impact study
[AD-A205825] N89-23993
Climatic atlas of the outer continental shelf waters and coastal regions of Alaska. Volume 1: Gulf of Alaska, revision
[AD-A205289] N89-24005
Surface Observation Climatic Summaries (SOCS) for NASA Shuttle Landing Facility, Florida
[AD-A205362] N89-24007
WEATHER FORECASTING
ASR-9 weather channel test report, executive s ummary
[DOT/FAA/PS-89/6-EXEC-SUMM] N89-23758
Microcomputer program for daily weather simulation
[PB89-144638] N89-24001
WEIGHT REDUCTION
Photovoltaic power system considerations for future lunar bases
[NASA-TM-102019] N89-23517
WEIGHTLESSNESS
Payload experts in D1-mission N89-23722
WEIGHTLESSNESS SIMULATION
Microgravity conditions of a spacecraft N89-23731
WELDABILITY
Stress relief cracking in copper-precipitation strengthened HSLA-100 steel
[AD-A205936] N89-23670
WELDING
Overview of ASTM symposium on analytical and experimental methods for residual stress effects in fatigue
[AD-A205622] N89-23931
WETLANDS
Meteosat thermal inertia mapping for studying wetland dynamics in the West-African Sahel
[BCRS-88-10A] N89-23970
Thermal analysis for the monitoring and prediction of flood dynamics in wetlands
[BCRS-88-10B] N89-23971
WETTING
Temperature dependence of interfacial energies between solid oxides and liquid metals N89-23599
WHEAT
Automated seed manipulation and planting N89-24017
Automated seed manipulation and planting N89-24020
WHISKERS (CRYSTALS)
Injection molding of whisker-reinforced Al2O3-ZrO2 ceramics N89-23574
WIGGLER MAGNETS
The chirped-pulse free-electron laser
[DE89-009041] N89-23862
Superconducting PYX structures
[AD-D013958] N89-24202
WILDLIFE
Review of wildlife resources of Vandenberg Air Force Base, California
[NASA-TM-102146] N89-23982
WIND MEASUREMENT
Mesospheric wind measurement
[AD-A205593] N89-23991
Study of a method to de-alias winds from ERS-1 data
[CREO-6374] N89-24003
WIND PROFILES
Study of a method to de-alias winds from ERS-1 data
[CREO-6374] N89-24003
Studies of frontal zone dynamics with a high-resolution wind profiling system
[AD-A205988] N89-24008
WIND TUNNEL APPARATUS
A research facility for film cooling investigations with emphasis on the instrumentation system
[NAL-TM-PR-8704] N89-23477
WIND TUNNEL MODELS
Model systems --- metal alloys N89-23728
WIND TUNNEL TESTS
Transonic operational characteristics and performance
[NAL-TR-968] N89-23408
Experimental study of pressure and heating rate on a swept cylindrical leading edge resulting from swept shock wave interference
[NASA-CR-185326] N89-23411
High angle-of-attack aerodynamic characteristics of crescent and elliptic wings
[NASA-CR-184992] N89-23418
Hot-jet simulation in cryogenic wind tunnels
[NASA-RP-1220] N89-23448
A research facility for film cooling investigations with emphasis on the instrumentation system
[NAL-TM-PR-8704] N89-23477
Application of a PC based, real-time, data-aquisition system in rotorcraft wind-tunnel testing
[NASA-TM-4119] N89-24079
WIND TUNNEL WALLS
Ejector effects on a supersonic nozzle at low altitude and Mach number
[AD-A206049] N89-23427
WIND VELOCITY
Studies of frontal zone dynamics with a high-resolution wind profiling system
[AD-A205988] N89-24008
WING PLANFORMS
High angle-of-attack aerodynamic characteristics of crescent and elliptic wings
[NASA-CR-184992] N89-23418
WINGS
Optimum aeroelastic characteristics for composite supermaneuverable aircraft
[AD-A205503] N89-23452
WIRE
Electrode carrying wire for GTAW welding
[NASA-CASE-MFS-29491-1] N89-23738
Internal wire guide for GTAW welding
[NASA-CASE-MFS-29489-1] N89-23739
WORKLOADS (PSYCHOPHYSIOLOGY)
Crew procedures and workload of retrofit concepts for microwave landing system
[NASA-CR-181700] N89-24033
The role of pilot and automatic onboard systems in future rendezvous and docking operations
[REPT-882-440-116] N89-24050
WORKSTATIONS
Applications of a digital acoustic-emission data-acquisition workstation
[DE89-009648] N89-23923
WRANGELL MOUNTAINS (AK)
Remote sensing of global snowpack energy and mass balance: In-situ measurements on the snow of interior and Arctic Alaska
[NASA-CR-180078] N89-23956

X

X RAY ABSORPTION
X-ray absorption spectroscopy of electrochemically generated species
[AD-A205572] N89-23647
X RAY ANALYSIS
Application of the method of X-ray fluorescence analysis with synchrotron radiation to study lunar matter
[DE88-705782] N89-24247

X RAY ASTRONOMY
Grazing incidence telescopes for ESA's X-ray astronomy mission XMM
[MPE-PREPRINT-129] N89-24239
X RAY DENSITY MEASUREMENT
Rapid fitting of particle cascade development data from X-ray film densitometry measurements
[NASA-TM-100368] N89-24260
X RAY DIFFRACTION
Grain boundaries
[DE89-008881] N89-24194
X RAY FLUORESCENCE
Application of the method of X-ray fluorescence analysis with synchrotron radiation to study lunar matter
[DE88-705782] N89-24247
X RAY IRRADIATION
A low-energy X-ray irradiator for electrophysiological studies
[AD-A205388] N89-24026
X RAY LASERS
Research studies on extreme ultraviolet and soft X-ray lasers
[AD-A205625] N89-23868
X RAY SCATTERING
Assessment of surface topography by X-ray scattering measurements
[MPE-PREPRINT-134] N89-24159
X RAY SOURCES
Summaries of papers presented at Short Wavelength Coherent Radiation: Generation and Applications Topical Meeting held in Cape Cod, Massachusetts on September 26-29, 1988
[AD-A205471] N89-23867
X RAY SPECTRA
Spectral observations of the extreme ultraviolet background N89-24259
X RAY SPECTROSCOPY
X-ray absorption spectroscopy of electrochemically generated species
[AD-A205572] N89-23647
X RAY STARS
Time and spectral variability of the low mass X-ray binaries
[MPE-REPORT-210] N89-24238
X RAY TELESCOPES
Assessment of surface topography by X-ray scattering measurements
[MPE-PREPRINT-134] N89-24159
Grazing incidence telescopes for ESA's X-ray astronomy mission XMM
[MPE-PREPRINT-129] N89-24239
X RAYS
An ultra-soft Einstein X-ray survey
[DE89-007993] N89-24256
X-29 AIRCRAFT
A correlation study of X-29A aircraft and associated analytical developments N89-23450
XYLENE
Sorption of selected volatile organic constituents of jet fuels and solvents on natural sorbents from gas and solutions phases
[AD-A204073] N89-23711

Y

YTTRIUM
Sintering of Si3N4 in the presence of additives from Y2O3-SiO2-Al2O3 system N89-23581
YTTRIUM COMPOUNDS
Preparing and sintering of yttria-stabilized zirconia N89-23576
Shock compaction of YBa2Cu3O7-x and HoBa2Cu3O7-x powders in a metal matrix
[DE89-008827] N89-24193
YTTRIUM OXIDES
Studies on high-Tc superconducting materials
[NAL-TM-MT-8703] N89-24178

Z

ZINC
Fundamental and practical studies of metal contacts on mercury zinc telluride
[AD-A206560] N89-23653
ZINC COMPOUNDS
Microstructure-permeability relation in MnZn ferrites prepared of iron oxide with chlorine impurities N89-23602
ZINC OXIDES
Injection molding of whisker-reinforced Al2O3-ZrO2 ceramics N89-23574
Microstructure and phase development in multicomponent ZnO based varistor ceramics N89-23604
Zinc oxide varistor time response
[DE89-008234] N89-24191
ZINC TELLURIDES
Fundamental and practical studies of metal contacts on mercury zinc telluride
[AD-A206560] N89-23653
ZIRCONIUM
Temperature dependence of interfacial energies between solid oxides and liquid metals N89-23599
ZIRCONIUM COMPOUNDS
Investigations of mullite-zirconia composites N89-23577
ZIRCONIUM OXIDES
Preparing and sintering of yttria-stabilized zirconia N89-23576
Fabrication and properties of alumina-zirconia composites
[PB89-147532] N89-23620
ZONAL FLOW (METEOROLOGY)
Normal mode energetics of the general circulation during the FGGE year N89-24004

Typical Personal Author Index Listing

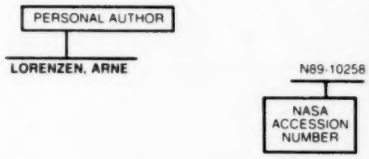

Listings in this index are arranged alphabetically by personal author. The NASA accession number denotes the number by which the citation is identified.

A

AARONSON, H. I. N89-23665
ABBOT, RICHARD I. N89-23497
ABBOTT, TERENCE S. N89-23466
ABDUL-GADER, M. M. N89-24183
ABEYOUNIS, WILLIAM K. N89-23433
ABOUDY, S. N89-24183
ABRAMOFF, BENNET N89-23703
ACOSTA, R. N89-23753
ADAMCZYK, JOHN J. N89-23416
ADAMS, D. M. N89-23762
ADAMS, FRED CHESTER N89-24234
ADAMS, S. J. N89-24082
ADCOCK, JAMES L. N89-23786
AFFELDT, E. N89-23938
AGATONOVIC, RATOMIR N89-23617
AHMADI, ALI REZA N89-23450
AHMED, SHAMIM N89-23918
AIELLO, ROBERT A. N89-23621
AKTAN, ALI I. N89-23675
AL-MAAITAH, AYMAN A. N89-23812
ALBARES, D. J. N89-24086
ALBERS, R. C. N89-23655
ALDERTON, DAVID L. N89-24035
ALDISSI, MAHMOUD N89-23688
ALLEMEIER, RANDALL T. N89-23923
ALLEN, D. H. N89-23933
ALLEN, J. E. N89-24165
ALLEN, PHILIP B. N89-23661
ALLEN, WENDY L. N89-23740
ALTHOFF, SUSAN L. N89-23410
AMMAR, GREGORY S. N89-24115
AMORUSO, MICHAEL J. N89-23472
ANDERSON, T. W. N89-24128
ANDERSSON, BENGT N89-24149
ANDRE, S. N89-23845
APELIAN, D. N89-23672
APPELBAUM, JOSEPH N89-23517
N89-23792
ARMES, STEVEN P. N89-23688
ARNOLD, HANS-DIETER N89-23942
ARNOLD, J. R. N89-24243
ARSOV, LJUBOMIR D. N89-23597
ASAI, KEISUKE N89-23408
N89-23448
ASAY, J. R. N89-23877
ASCHENBACH, BERND N89-24159
N89-24239
ATANASOV, ATANAS N89-23490
ATASSI, HAFIZ M. N89-23413
ATHALE, RAVINDRA A. N89-24157
ATTANASIO, M. N89-24050
AUBRUN, J-N. N89-23901
AUCEL, S. N89-23511
AUER, W. N89-23908
AUFFRAY, PH. N89-23979
AXELSON, SCOTT R. N89-23678
AZADEGAN, SHIVA N89-23885
N89-23886

B

BAFFES, PAUL THOMAS N89-24084
BAGDIGIAN, ROBERT M. N89-23503
N89-24044
BAGHDADI, ASLAN N89-24180
BAK, JOSEPH N89-23741
BAKER, D. N. N89-23995
BAKKER, PIETER GERRIT N89-23814
BAKX, G. J. T. A. N89-24124
BALASCO, A. A. N89-23714
BALDWIN, RONALD G. N89-24005
BALKO, BOHDAN N89-23864
N89-23865
BALLAGH, R. J. N89-24251
BALLARINI, ROBERTO N89-23918
BALLING, P. N89-23783
BALLUFFI, R. W. N89-24194
BANDERET, LOUIS E. N89-24039
BANKS, BRUCE A. N89-23540
BANKS, H. T. N89-24112
BARBEE, TROY, JR. N89-24151
BARBIER, P. N89-23630
BARLOW, G. N89-23794
BARNABA, J. M. N89-23774
BARSANTI, M. L. N89-23854
BARSCH, GERALD R. N89-23662
BARYSHEV, V. B. N89-24247
BASS, LEN N89-24049
BASTARD, J. L. N89-23979
BAUER, DAVID P. N89-23977
BAXTER, DOUG N89-24120
BEALS, DAVID C. N89-23905
BECCHI, P. N89-23898
BEEKER, GREGORY L. N89-23498
BEHR, F. J. N89-23972
BENSON, CARL M. N89-24260
BENSON, CARL S. N89-23956
BENTLEY, ALAN F. N89-24237
BENTS, DAVID J. N89-23518
BENTSON, JAMES N89-23452
BERG, HELMUT K. N89-23885
N89-23886
BERGMAN, L. B. N89-24191
BERNEY, C. V. N89-23883
BERQUIST, AKE N89-23779
BERRY, JOHN D. N89-23410
BERRYMAN, HARRY N89-24076
N89-24121
BETTMAN, JAMES R. N89-24037
N89-24095
BETZ, FREDERICK E. N89-23535
BEU, DANIELLE N89-23675
BHAGAT, RAM B. N89-23668
BHASIN, K. B. N89-23791
BIBEAU, C. N89-23859
BILITZA, D. N89-23561
BINNENBRUCK, H. N89-23720
BIRGENEAU, R. J. N89-24190
BIRMAN, KENNETH N89-24065
BISHOP, DWIGHT E. N89-23429
BITTNER, ALVAH C. N89-24048
BIXLER, JAY N89-24151
BIZJAK, IVAN N89-23616
BLACK, W. M. N89-23801
BLAIR, DOUGLAS E. N89-24218
BLAKE, J. B. N89-23506
N89-23995
BLANKENSTEIN, MICHAEL F. N89-24032
BLEDSOE, JIM N89-24016
N89-24021
BLONDIN, JOSEPH N89-23896
BLOOM, STEVE N89-23986
BOBB, LLOYD C. N89-24155
BOISSET, J. P. N89-23780
N89-23781
N89-23784
BOLLER, SCOTT A. N89-23849
BONAFEDE, JOSEPH A. N89-23853
BORCHARDT, GUENTER N89-23601
N89-23615
BORDER, J. S. N89-24060
BORING, A. M. N89-23655
BORSON, E. N. N89-23545
BOSIC, DUSAN N89-23610
BOSKOVIC, SNEZANA N89-23581
BOULDIN, D. W. N89-23790
BOWEN, R. C. N89-23714
BOWERS, MICHAEL T. N89-24144
BOWLES, KENNETH J. N89-23623
BOXER, STEVEN G. N89-23974
BOYCE, LOLA N89-23890
N89-23891
BOYD, ROBERT P. N89-24141
BOYLES, PAUL D. N89-23424
BRADY, JOYCE A. N89-23540
BRAEUNINGER, HEINRICH N89-24159
N89-24239
BRAITHWAITE, N. ST. J. N89-24165
BRAKE, M. L. N89-24172
BRANDON, VANESSA N89-24019
BREININGER, DAVID R. N89-23982
BRIGHT, FRANK V. N89-24154
BRILEY, G. L. N89-23521
BRILEY, W. R. N89-23833
BRINKER, C. J. N89-24195
BRISTOWE, P. D. N89-24194
BRIXY, H. N89-23603
BROWER, WILLIAM A., JR. N89-24005
BROWN, GARY S. N89-24012
BROWN, RANDALL H. N89-23661
BROWN, THOMAS H. N89-24038
BRUEMMER, S. M. N89-23659
BRUSHWYLER, K. R. N89-24170
N89-24171
BRYANT, PAUL R. N89-24127
BUDD, A. J. N89-23444
BUILTEMAN, H. N89-23512
BUR, A. J. N89-23680
BURCHARDS, H. D. N89-23611
BURGE, PAUL L. N89-24141
BURNSIDE, WALTER D. N89-23736
BURRI, G. N89-23600
BUTLER, G. B. N89-23706
BUTLER, WILLIAM H. N89-23661
BYER, ROBERT L. N89-23856

C

CADARETTE, BRUCE S. N89-23744
CADOT, J. P. N89-23783
CAI, ZHIHUA N89-23649
N89-23650
CAIN, B. N89-24046
CAIN, WILLIAM N. N89-23797
CAIRELLI, JAMES E. N89-23527
CALABRESE, S. J. N89-23674
CALARESE, WLADIMIRO N89-23432
CALDICHOURY, M. N89-24050
CALLAS, JOHN L. N89-24168
CALLENAS, ANDERS N89-23804
CAMERON, J. A. N89-23699
CAMPBELL, ROMEL N89-23472
CANNON, MARK R. N89-24141
CANRIGHT, DAVID N89-23827
CANTRELL, B. H. N89-23771
CANTWELL, B. J. N89-23820
CAPSIMALIS, G. P. N89-23666
CARLETTI, U. N89-23751
CARLIN, BRADLEY P. N89-24126
CARLIN, D. B. N89-23860
CARLSON, NANCY M. N89-23923
CARRASQUILLO, ROBYN L. N89-23503
N89-24044
CARRERA, R. N89-24166
CARROLL, MARY K. N89-24154
CARTER, W. B. N89-23634
CARUSO, S. C. N89-23831
CATON, JEFFREY L. N89-23834
CAVANIE, ALAIN N89-24003
CEROVIC, D. N89-23580
CHAFFEE, P. H. N89-23659
N89-24152
CHAMPOUX, R. L. N89-23931
CHANG, C. T. N89-24086
CHANG, FONG-CHIAU N89-24002

CHANG, RICHARD K. N89-23645
CHARI, SRIKANTH N89-24224
CHAVEZ, PATRICK F. N89-24110
CHAWLA, KALPANA N89-23822
CHELOTTI, J. N. N89-23845
CHEN, CHIH-FAN N89-24132
CHEN, K. C. N89-24196
CHEN, MING M. N89-24132
CHEN, S. P. N89-23655
CHENG, I. F. N89-23650
CHENG, P. L. N89-23883
CHIANG, C. N89-23796
CHIANG, C.-H. N89-23651
CHILDS, ROBERT E. N89-23431
CHILENSKAS, A. A. N89-23794
CHINZEI, NOBUO N89-23464
CHOI, S. I. N89-24191
CHRIST, FRED N89-23943
CHRISTENSON, M. S. N89-23640
CHRISTIANSEN, P. L. N89-23798
CHU, NORI Y. C. N89-23682
CHUDNOVSKY, A. N89-23930
CIANCONE, MICHAEL L. N89-23911
CLAUSSEN, N. N89-23574
COFFEY, H. E. N89-24250
COHEN, LESLIE N89-23864
N89-23865
COHEN, R. E. N89-23883
COLE, STANLEY R. N89-23447
COLLAUDIN, B. N89-24160
COLLINS, CARL B. N89-23866
COMPTON, WILLIAM B., III N89-23433
CONNER, WILLIAM C. N89-24210
CONNOLLY, J. C. N89-23860
CONNOLLY, PAUL N89-24051
COOK, LEWIS N89-23896
COOPER, J. N89-24251
CORDOVA, F. A. N89-24256
CORSMEIER, ULRICH N89-23998
COSTA, DANIEL L. N89-23980
COULSON, N. G. N89-23451
COULTER, D. N89-23586
COUNSELMAN, CHARLES C., III N89-23497
COUR-PALAIS, BURTON G. N89-23542
COUTAZ, JOELLE N89-24049
COWLEY, STEPHEN J. N89-23821
CRAIN, W. K. N89-23515
CREMERS, D. A. N89-23857
CREYER, ELIZABETH H. N89-24095
CROMWELL, E. N89-23863
CROSBY, G. A. N89-24205
CRUICKSHANK, ALEXANDER M. N89-23701
CURRAN, FRANCIS M. N89-23522
CUVELIER, C. N89-24101

D

DABROWSKI, D. N89-24193
DADDIO, E. N89-23751
DAHLGREN, JOHN B. N89-23907
DARDEN, CHRISTINE M. N89-23415
DAREE, K. N89-24177
DAUM, WINFRIED N89-24187
DECKER, MADELYN M. N89-23717
DECKER, NAOMI N89-24113
DECRISTOFANO, BARRY S. N89-23744
DEGROH, HENRY C., III N89-23664
DEISSLER, ROBERT G. N89-23813
DELAAT, CORNELIUS THEODORUS ADRIANUS MARIA
N89-24143
DELANA, BRETT S. N89-23747
DELLAMICO, S. N89-23898
DELORME, JOSEPH F. N89-23913
DEMMY, JANICE L. N89-23981
DEMOLLERAT, T. N89-23889
DENBAARS, STEVEN P. N89-24200
DEPISON, E. MARTINEZ N89-24053
DERMER, CHARLES D. N89-24258
DESA, L. N89-24160
DESHPANDE, M. D. N89-23805
DEVINE, JAMES C. N89-24010
DEVRIES, R. E. N89-24099
DEWEESE, MARY E. N89-23748
DICK, ALFRED O. N89-24048
DIETRICH, DAN N89-24151
DING, Y. N89-23852
DIXON, R. D. N89-23857
DO, CHOON H. N89-23706
DOBSON, M. C. N89-23961
DOLLING, D. S. N89-23421
DONALDSON, KENT E. N89-23470
DONG, B. L. N89-24142
DONLEY, SHAWN T. N89-23474
DOWNING, DAVID R. N89-23470
DOZINAS, K. N89-23883
DRIEDONKS, A. G. M. N89-23998
N89-23999
DROFENIK, MIHA N89-23602
DROST, M. K. N89-23976
DUCHEMIN, J.-M. N89-23844
DUDENHOEFER, JAMES E. N89-23823
DUNCAN, WALTER M. N89-24180
DUONG, MINH DUC N89-24103
DURAND, BENOIT J. N89-23425
DUTTA, VIMALA N89-24097
DUYNKERKE, P. G. N89-23997
N89-23998
N89-23999
N89-24000
DYER, GERALD N89-23738
N89-23739
DYMEK, CHESTER J., JR. N89-23646
DZWONCZYK, M. J. N89-24082

E

EARLY, E. A. N89-24193
EATON, J. K. N89-23426
EATON, ROBERT A. N89-23740
EDENS, R. G. N89-24124
EDMONDS, LARRY D. N89-23494
EDWARDS, ROBERT V. N89-23850
EHRHART, SUE A. N89-24066
EICHEL, PAUL H. N89-23752
EICHHORN, A. N89-23654
EISCH, JOHN J. N89-23713
EISEMAN, PETER R. N89-23773
EISENSTAT, STAN N89-24120
EL-HASAN, M. N89-24185
ELDER, RICHARD C. N89-23647
ELKENZ, A. N89-24182
ELLINGSTAD, VERNON N89-24036
ELLIS, R. C. N89-23900
EMERICK, KENNETH S. N89-23910
ENDOH, Y. N89-24190
ENG, ANTHONY T. N89-23626
ENGEL, C. D. N89-23515
ENGLAND, A. W. N89-23961
ENGLERT, P. A. J. N89-24243
ENNS, J. B. N89-23705
EPPLER, DUANE T. N89-23766
EPPLEY, KENNETH N89-23793
ERDOGAN, FAZIL N89-23925
N89-23926
N89-23927
N89-23928
ERIKSSON, LARS-ERIK N89-24104
N89-24105
ERMAK, DONALD L. N89-23984
ERSHOV, S. N. N89-24183
ESTLER, R. C. N89-23857
ETTENBERG, M. N89-23860
ETZLER, CARL CHRISTIAN N89-23899
EVANS, S. A. N89-23521

F

FABER, KATHERINE T. N89-23644
FABIANO, R. H. N89-24112
FAELTHAMMAR, CARL-GUNNE N89-23987
N89-24163
FAIRBANKS, RONALD R. N89-23775
FAMINI, GEORGE R. N89-23648
FANDEL, THOMAS N89-23577
FARINA, A. N89-23751
FARLEY, GUY J. N89-23763
FARMER, L. DENNIS N89-23766
FARNSWORTH, B. N89-24046
FARSHCHI, M. N89-23831
FATH, JANET L. N89-24045
FAUBERT, D. N89-23772
FEHSE, W. N89-24050
FENN, J. B. N89-23826
FERGUSON, D. C. N89-23555
FERKUL, PAUL V. N89-23638
FERNANDEZ-POLLO, A. C. N89-23636
FETAHAGIC, TARIC N89-23582
N89-23595
FINE, A. J. N89-24062
FINK, R. A. N89-23900
FISCHER, R. P. N89-23854
FISELIER, J. L. N89-23970
N89-23971
FISK, TIMOTHY E. N89-23836
FITZER, E. N89-23572
FLIFLET, A. W. N89-23801
N89-23854
N89-23872
FLOEGE, H. N89-23938
FLOOD, DENNIS J. N89-23517
FLORENCIO, JOAO N89-24137
FOERTHMANN, RUDIGER N89-23594
FOGLEMAN, GUY N89-24022
N89-24023
FOLINSBEE, LAWRENCE J. N89-23980
FONDA, MARK L. N89-24022
N89-24023
FOULSER, DAVID E. N89-24133
FOUNTAIN, WALTER F. N89-24260
FRANCESCONI, RALPH P. N89-24029
FRANK, D. N89-23512
FRANKLIN, R. N89-24096
FRANKLIN, THOMAS C. N89-23675
FRANKOWSKI, ELAINE N. N89-23885
N89-23886
FRAZIER, WILLIAM E. N89-23671
FREDERICKSON, A. R. N89-23553
FREDERICKSON, EDWARD W. N89-23407
FREDERKING, T. H. K. N89-23512
FREEMAN, CHARLES R. N89-24027
FREEMAN, GARTH B. N89-23627
FREEMAN, ROBERT A. N89-23875
FRIDAY, DAVID K. N89-23628
FRIEBELE, E. J. N89-23566
FRIEDMAN, EUGENE M. N89-23472
FRIEDMAN, M. N89-24148
FRISH, MICHAEL B. N89-23851
FROST, C. L. N89-23515
FRUSH, CHARLES L. N89-23749
FRYE, G. C. N89-24195
FU, C. L. N89-24192
FU, G. Y. N89-24166
FUKUI, WAKUMI N89-24161
FULLER, R. C. N89-23707
FUNKE, PAUL N89-23613
N89-23616
FURUHARA, T. N89-23665
FURUTA, NAOKI N89-24169
N89-24170
N89-24171

G

GABEL, R. N89-23920
GABRIEL, S. B. N89-23554
GAL-ED, REUVEN N89-23643
GALLATIN, G. M. N89-24207
GANAPOL, BARRY D. N89-24255
GANGLOFF, D. N89-23979
GARBE, JOACHIM N89-24212
GARCIA-FOGEDA, PABLO N89-23423
GARCIA, G. A. N89-24086
GARCIA, RAY N89-24017
N89-24020
GARD, GARY L. N89-23973
GARECHT, D. M. N89-23523
GARITO, A. G. N89-24209
GARNER, RUSSELL N89-23916
GARNIER, C. N89-24078
GARRETT, H. B. N89-23554
GARUFI, FRANK N89-23437
GARVEY, RAY N89-23533
GASIC, M. N89-23573
GATES, RICHARD S. N89-23679
GATEWOOD, GEORGE D. N89-24233
GAUTHIER, R. J. N89-24082
GAZENKO, O. G. N89-23492
GEAR, C. W. N89-24109
GEERKEN, R. N89-23972
GEIST, G. A. N89-24083
GELFAND, ALAN E. N89-24126
GENG, STEVEN M. N89-23527
GENZEL, REINHARD N89-24231
GEOFFRION, ARTHUR M. N89-24064
GEORGE, ALBERT R. N89-23415
GEORGE, THOMAS F. N89-24136
N89-24197
N89-24198
GERARD, GEOVING J. N89-23627
GERLACH, KARL N89-23765
GERSTL, S. A. W. N89-23858
GETZSCHMANN, A. N89-24050
GHIGLIA, DENNIS C. N89-23752
GIDLEY, DAVID W. N89-23689
GIERARD, ROBERT A. N89-23768
GILBERT, A. L. N89-24062
GILGENBACH, R. M. N89-24172
GILLCRIST, MARC C. N89-23825
GILLEN, G. N89-23672
GILLHAM, JOHN K. N89-23704
N89-23705
GINDELE, KARL JOHANNES N89-23978
GLADDEN, WARREN K. N89-24180
GLASS, CHRISTOPHER E. N89-23411

GLIEBE, P. R. N89-24139
GLUCK, DONALD F. N89-23550
GLUSHKO, V. N89-23489
GODEC, GREG E. N89-23646
GOEL, AMRIT L. N89-24069
GOELLER, JOCHEN RALF N89-24248
GOETTGE, ROBERT N89-24051
GOLD, S. H. N89-23801
N89-23872
GOLDMAN, T. N89-23988
GOLKOVSKIJ, M. G. N89-23658
GOLLEY, PAUL N89-23896
GOLUB, LEON N89-24162
GOMEZ, STEVEN A. N89-24027
GONG, LESLIE N89-23819
GOODMAN, J. M. N89-23442
GOODRICH, KENNETH H. N89-23468
GOPALAKRISHNAN, P. S. N89-24178
GORJAN, D. N89-23574
GORNEY, D. J. N89-23995
GORY, J. F. N89-23845
GOTTHARD, R. N89-23600
GOULD, S. G. N89-23914
GOVINDAN, T. R. N89-23833
GOVINDARAJ, T. N89-24045
GRAGG, WILLIAM N89-24115
GRANATSTEIN, V. L. N89-23801
GRANT, N. J. N89-24135
GRANT, NICHOLAS J. N89-24135
GRATHWOHL, GEORG N89-23583
GRAVES, R. S. N89-23685
GREEN, PETER L. N89-23916
GREENE, J. B. N89-23743
GREGORY, J. C. N89-24142
GREIL, PETER N89-23585
N89-23590
GREINER, M. N89-23810
GROPP, WILLIAM N89-24121
GROSS, GARRY L. N89-23474
GROVER, JOHN M. N89-23455
GRUNDY, I. H. N89-24057
GU, D.-W. N89-24089
GUI, ZHENXING N89-23869
GUPTA, INDER J. N89-23736
GURRISI, CHARLES N89-23896
GUYVARCH, J. P. N89-23755
GYARMATI, E. N89-23594

H

HA, TAE WOONG N89-23876
HA, TRI T. N89-23756
N89-23757
HAAG, THOMAS W. N89-23520
N89-23522
HAEUSSER, HELMUT HEINZ N89-23603
HAFEEZ, FARAN N89-23428
HAFFNER, J. W. N89-23532
HALL, CHRISTOPHER D. N89-23454
HALL, H. K., JR. N89-23698
HALL, ROGERS N89-24122
HALPERIN, W. P. N89-23642
HALYO, NESIM N89-23495
HAMACHER, H. N89-23731
HAMIDULLAH, FARHAT N89-24255
HAND, K. J. N89-23566
HANEY, MICHAEL W. N89-24157
HANIGOFSKY, JOHN A. N89-23627
HANNA, THOMAS E. N89-24034
HANSON, C. L. N89-24001
HANZON, BERNARD N89-24100
HARBECK, ROLF N89-23944
HARDESTY, D. L. N89-23801
HARDY, D. A. N89-23566
HARGRAEVES, T. A. N89-23854
HARMON, L. N89-24096
HARNDEN, F. R., JR. N89-24256
HARRIS, REGINA N89-24048
HARRIS, S. E. N89-23868
HASHIMOTO, RYOHEI N89-23514
HASLINGER, KARL N89-23945
HASSOUN, JOHN A. N89-23774
HAUSER, JOSEPH A. N89-23535
HAY, P. J. N89-23655
HAYASHI, SHIGERU N89-23635
HAYASHI, T. N89-24142
HAYES, WALLACE D. N89-23415
HEAVNER, LEONARD G. N89-23456
HEEGER, JURRIEN N89-23966
HEINEMAN, WILLIAM R. N89-23647
HEINEMANN, K. G. N89-24088
HEINRICH, MARK L. N89-24157
HEINZEL, VOLKER N89-23686
HELTON, J. N89-24166
HENESIAN, M. A. N89-24152
HENNING, BJORN N89-23782
HENNINGS, I. N89-24014
HERLACH, D. M. N89-23726
N89-23727
HERRERA, JAVIER N89-24017
N89-24020
HERSH, ALAN S. N89-23525
HERZOG, G. F. N89-24243
HESSELINK, LAMBERTUS N89-23426
HETLAND, M. D. N89-23712
HEYDLAUFF, BRUCE N89-23766
HIDAKA, YOSHIKAZU N89-24190
HIDSON, D. N89-24074
HIEFTJE, GARY M. N89-24154
N89-24169
N89-24170
N89-24171
N89-24173
N89-24174
HIGBIE, P. R. N89-23995
HIGBY, P. N89-23566
HILDEBRAND, PETER H. N89-23749
HILDMAN, B. O. N89-23729
HINE, BUTLER PRESTON ANDERSON, III N89-24235
HINKS, D. G. N89-24193
HIRTH, JOHN P. N89-23644
HIVELY, L. N89-24166
HO, J. N89-23481
HODGES, HARDY M. N89-24215
HOEDE, C. N89-24124
HOFFMAN, ROSS N. N89-23993
N89-24009
HOFFMANN, KARIN N89-24123
HOFFMANN, ROALD N89-23669
HOLCOMB, SCOTT N89-24017
N89-24020
HOLLAND, DONALD E. N89-23994
HOLLECK, H. N89-23587
HOLMES, PETER N89-23957
HOLT, J. B. N89-24193
HOLZHAUER, W. N89-23674
HOOGHIEMSTRA, G. N89-24099
HORDONNEAU, A. N89-23629
N89-23631
HORIUCHI, SHOUJI N89-23635
HORNER, WILLIAM H. N89-23888
HORNYAK, STEPHEN N89-23902
HOSOE, NOBUYUKI N89-23408
HOST, M. N89-23718
HOUSHMAND, B. N89-23753
HSIEH, ALEX J. N89-23697
HSU, HUEY S. N89-23663
HSU, STEPHEN M. N89-23679
N89-23847
HUANG, MAO N89-24174
HUANG, S. J. N89-23699
HUANG, YIH-FANG N89-24063
HUBBARD, ROGER W. N89-24029
HUBENY, I. N89-24251
HUBER, BERNARD N89-23460
HUGHES, CHRISTOPHER E. N89-24138
HUGHES, RICHARD J. N89-23988
HUMPHREY, WATTS S. N89-24075
HUMPHREYS, W. W. N89-23420
HUNDLEY, M. L. N89-23714
HUNSUCKER, ROBERT D. N89-23747
HUNTER, J. C. N89-23848
HUNTINGTON, JUDITH L. N89-24022
N89-24023
HUSSAINI, M. Y. N89-23817
HUST, JEROME G. N89-24213
HUTTENLOCHER, DANIEL N89-24094
HYLAND, P. M. N89-24062

I

IBRAHIM, MOUNIR B. N89-23823
ILIN, YE. A. N89-23492
ILLERT, ANDREAS N89-23946
INAGAKI, TOSHIHARU N89-23463
INCROPERA, F. P. N89-23640
INGER, GEORGE R. N89-23837
INTIHAR, HEDA N89-23602
ISHIDA, YOJI N89-23806

J

JACOBS, H. N89-23972
JAEGER, REINER N89-23963
JAEKLE, D. N89-23512
JAKE, C. A. N89-23714
JAKOWATZ, CHARLES V., JR. N89-23752
JARRETT, B. R. N89-23764
JASMAKOVSKI, B. N89-23576
JAUCH, U. N89-23599
JEAN, F. N89-23844
JEFFREY, J. R. N89-23743
JEONG, JAE S. N89-23795
JERNEMALM, VEINE N89-23777
JI, Q. H. N89-23478
JOHNSON, CLIFFORD T. N89-23711
JOHNSON, ERIC J. N89-24037
JOHNSON, JOHN A. N89-23923
JOHNSON, LAVERNE C. N89-24027
JOHNSON, MIKE N89-23706
JOHNSON, RICHARD L. N89-23454
JOHNSTON, C. T. N89-23652
JOHNSTON, CLIFFORD N89-23986
JOHNSTON, J. P. N89-23426
JONES, JAMES L., JR. N89-23534
JONES, P. ALAN N89-23897
JONES, R. H. N89-23659
JONSSON, JON E. N89-24033
JOSEPH, P. F. N89-23926
N89-23927
JOSLIN, MICHELLE N89-24019
JOTA, F. G. N89-23737
JUNG, K. N89-23972
JUNGERT, ERLAND N89-23957
JUNIUS, HARTWIG N89-23947
JYRKKIO, TEPPO N89-24189

K

KAESER, DANA S. N89-23524
KAHL, MARK A. N89-24087
KAINER, KARL URLICH N89-23611
KAKURAI, K. N89-24190
KAMEGAI, M. N89-24193
KAMINER, I. N89-23471
KAMMASH, T. N89-24172
KAN, EDWIN P. N89-23907
KANDA, TAKESHI N89-23514
KANMURI, AKIO N89-23514
KAPP, J. A. N89-23931
KARANOVIC, LJ. N89-23604
KARASAWA, TOSHIO N89-23408
KARTJE, J. N89-24256
KASHIWAGI, TAKASHI N89-23501
KASSE, TIM C. N89-24075
KASTNER, M. A. N89-24190
KATZ, JOEL D. N89-23690
KAUFMANN, H. N89-23972
KAUP, T. N89-23718
KAYA, A. C. N89-23926
N89-23927
KAYSSER, WOLFGANG A. N89-23575
N89-23609
N89-23610
N89-23612
KEANE, M. S. N89-24099
KEDO, V. D. N89-23658
KEEFE, LAURENCE N89-23835
KELLER, DONALD N89-23740
KELLY, PAUL N89-24017
N89-24020
KENDERDINE, EUGENE W. N89-23894
KENNEDY, W. J., JR. N89-23681
KERR, M. P. N89-23772
KESCHTKAR, HOSSEIN-ALI N89-23686
KESKINEN, KARI N89-23620
KESSLER, DONALD J. N89-23543
KEUTHEN, MATHIAS N89-23572
KEVORKIJAN, VARUZAN N89-23595
KHANNA, S. M. N89-23762
KIBLER, DENNIS N89-24122
KICEVIC, DUSAN N89-23573
KIEFT, LAWRENCE VANDE N89-23716
KIM, H. D. N89-23579
KIM, KYEKYOON N89-23499
KIM, YOUNG S. N89-24197
N89-24198
KINARD, WILLIAM H. N89-23534
KING, DAVID Q. N89-24168
KING, GUY L. N89-23895
KING, J. H. N89-23561
KINKEAD, A. K. N89-23801
KIRIS, CETIN N89-24111
KIRKPATRICK, D. A. N89-23801
N89-23872
KISS, SANDOR J. N89-23580
KISTLER, ROBERT N89-24002
KITE, MILTON D. N89-23929
KITSON, DAVID H. N89-24075
KLAUS, E. ERWIN N89-23679
N89-23847
KLAUSMANN, R. N89-23607
KLEBESADEL, R. W. N89-23995
KLEIN, H. N89-23725

KLEIN, LISA C. N89-23703
KLEIN, M. N89-23889
KLEY, DIETER N89-23983
KLINEBERG, JOHN M. N89-23465
KNAFELC, M. E. N89-24025
KNOTH, EDWARD A. N89-23977
KNUDSON, C. L. N89-23712
KO, WILLIAM L. N89-23819
KO, YONG H. N89-24085
KOCZAK, MICHAEL J. N89-23671
KOFINAS, P. N89-23883
KOHL, C. P. N89-24243
KOIKE, AKIRA N89-23408
KOJIMA, FUMIO N89-24114
KOLAR, DRAGO N89-23569
N89-23582
N89-23602
KOLASINSKI, W. A. N89-23549
N89-23566
KOLKA, MARGARET A. N89-24030
KOLKMAN, H. J. N89-23656
KOLLAARD, L. V. N89-23968
KOLVEK, JOHN N89-23896
KOMAC, MARIJA N89-23586
KOMAC, MILOS N89-23595
KOMURO, TOMOYUKI N89-23464
KONOVALOV, B. N89-23488
KOONTZ, STEVEN L. N89-23541
KOPER, JUDITH L. N89-23474
KOPPMANN, RALF N89-23660
KORKMAZ, LEVENT N89-24093
KOSEC, MARIJA N89-23569
KOSMAC, TOMAZ N89-23574
KOSSIAVAS, G. N89-23780
KOSTERS, A. J. M. N89-23958
KOSTIC, B. N89-23573
KOSTIC, EMILIJA N89-23580
KOSTIC, PETAR N89-23604
KOUTCHMY, OLGA N89-24252
KOUTCHMY, SERGE N89-24252
KOUVARITAKIS, B. N89-24090
N89-24091
KRALL, J. N89-24148
KRANZMANN, AXEL N89-23590
KRATZER, R. H. N89-23696
KRAUS, M. N89-23938
KRAWCZYNSKI, JOHANNA N89-23569
N89-23570
KRENGEL, RONALD N89-23614
KRESSE, WOLFGANG N89-23948
KRETSCHMER, FRANK F., JR. N89-23765
KRISHNAN, KANNAN M. N89-24186
KROENERT, W. N89-23577
N89-23593
KROME, HENNING N89-23896
KRONFELD, U. N89-24013
KRONGAUZ, VALERI N89-24206
KROO, I. M. N89-23426
KRUEGER, JAMES M. N89-24028
KRUEGER, PAUL J. N89-23770
KRYTER, ROBERT C. N89-23878
KUBAN, D. P. N89-23906
KUBO, SHIN N89-23409
KUDOU, KENJI N89-23464
KUDRYASHOVA, A. F. N89-24247
KUHN, RODNEY N89-23435
KUIJPERS, E. A. N89-23815
KUITTINEN, RISTO N89-23960
KULIPANOV, G. N. N89-24247
KUNG, A. H. N89-23863
KUNIN, B. N89-23930
KUNSEMUELLER, JUERGEN N89-23949
KUO, CHIN-CHUAN N89-23760
KUO, S. P. N89-23478
KUTLER, PAUL N89-24111
KWAK, DOCHAN N89-24111

L

LAAG, RAINHARD N89-23610
N89-23612
LABOV, SIMON EZRA N89-24259
LABUS, THOMAS L. N89-23516
LACKEY, W. J. N89-23627
LAFON, T. N89-23845
LAGHARI, J. R. N89-23799
LALLMAN, FREDERICK J. N89-23468
LAMATSCH, PETER J. N89-23454
LAMKIN, STANLEY L. N89-24255
LANDIS, L. D. N89-24062
LANG, KENNETH R. N89-24249
LANGMEIER, ANDREAS N89-24238
LANTERI, ALAIN N89-23782
LAO, BENNIG N89-23855
LARSON, M. F. N89-24008
LASIECKA, I. N89-23507
LAU, WILLIAM K. M. N89-24002
LAU, Y. Y. N89-24148
LAUFER, GABRIEL N89-23453
LAURIENTE, MICHAEL N89-23538
LAUTENBACH, KURT A. N89-23483
LAWLER, PATRICK B., JR. N89-23887
LAWLEY, A. N89-23672
LAWSON, J. K. N89-23859
LAZURE, B. N89-23462
LEAHY, BRIAN T. N89-23687
LECOMTE, PASCAL N89-24003
LEE, A. N89-23680
LEE, AM GIL N89-24107
LEE, H. R. N89-24136
LEE, HOON S. N89-24061
LEE, J. K. N89-24192
LEE, M. H. N89-24137
LEE, R. C. N89-23801
LEE, S. W. N89-23753
LEE, Y. T. N89-23863
LEEK, MARJORIE R. N89-24034
LEFLOCH, C. N89-23632
LEGER, LUBERT J. N89-23557
N89-23564
LEMANSKI, WALTER J. N89-24130
LEMEN, JULIE B. N89-23407
LENZ, ROBERT W. N89-23707
LEONARD, A. N89-23829
LEONARD, JOSEPH M. N89-23648
LEONTIC, BORAN N89-23605
LEROUX, RENE N89-23502
LESLIE, LYNN D. N89-24005
LETALICK, DIETMAR N89-23778
LEUNG, P. T. N89-24197
N89-24198
LEUPOLD, HERBERT A. N89-24202
LEVIS, ALEXANDER H. N89-23440
LEVY, R. N89-23833
LEWIS, B. N89-24059
LEWIS, G. K. N89-23857
LEWIS, RICHARD L. N89-23750
LIEBERMAN, HARRIS R. N89-24039
LIEBERMAN, PAUL N89-24150
LILIENTHAL, MICHAEL N89-24036
LIM, GEE KWANG N89-23875
LIMPEL, M. N89-23602
LIN, CHIN-SHUN N89-23818
LINDE, G. J. N89-23764
LINDE, S. N89-23479
LINDELL, ISMO V. N89-24102
LINDQUIST, JOHN W. N89-23407
LINTULA, PEKKA N89-23620
LIPS, P. C. F. N89-23967
LITTKE, W. N89-23730
LITTLE, BRUCE D. N89-23880
LIU, C. K. N89-23512
LIU, CHAO N89-23649
LIU, D. D. N89-23423
LIU, RUEY-WEN N89-24063
LOCKHART, R. A. N89-24118
LOHE, S. N. N89-23743
LONG, MARSHALL B. N89-23645
LONGDON, NORMAN N89-24223
LONGSTAFF, WILMER G. N89-24156
LORELL, K. R. N89-23901
LOTZ-IWEN, HANS-JOACHIM N89-23950
LOVELACE, THOMAS B. N89-23890
N89-23891
LOVELY, RONALD G. N89-23516
LOWELL, CARL E. N89-23623
LOWRY, R. E. N89-23680
LUGTEN, JOHN B. N89-24231
LUHMANN, HANS JURGEN N89-23899
LUNG, MING-HUNG N89-23422
LUO, ZHI-QUAN N89-24117
LUPAS, R. N89-23802
LURIE, BORIS J. N89-23903
LUTZ, E. N89-23574
LUYTEN, JAMES R. N89-24011
LYMAN, J. L. N89-23857

M

MAAG, CARL R. N89-23546
N89-23559
MACKIN, MICHAEL A. N89-24055
MACLACHLAN, MICHAEL J. N89-23742
MADDILA, S. N89-23796
MAHLE, JOHN J. N89-23628
MAIGRET, JEAN-PIERRE N89-23508
MAILLET, J. M. N89-24108
MAJDA, ANDREW J. N89-23839
MAJOR, R. W. N89-24191
MALIK, M. R. N89-23817
MALTSEV, V. M. N89-24107
MAMODE, A. N89-23979
MANDEL, R. N89-23506
MANHEIMER, W. M. N89-23801
N89-23854
MANI, R. N89-24139
MANICKAM, M. D. N89-23477
MANN, ULRICH N89-23788
MANNA, ZOHAR N89-24072
MANNING, S. D. N89-23457
MANSELL, ROBERT N89-23986
MANTENIEKS, MARIS A. N89-23520
MANTEUFFEL, THOMAS A. N89-24073
MANUKIAN, ARA N89-24018
N89-24021
MAPLE, M. B. N89-24193
MARABLE, R. W. N89-23519
MARAOUI, ANDRE N89-23482
MARINKOVIC, SLOBADAN N89-23589
MAROLDA, VICTOR N89-23702
MARRO, L. N89-23781
N89-23784
MARSHALL, LYNNE N89-24034
MARTIN, C. A. N89-23449
MARTIN, C. R. N89-23850
MARTIN, CHARLES R. N89-23649
MARTIN, MICHEL N89-23508
MARTIN, S. J. N89-24195
MARYNICK, DENNIS S. N89-23709
MARZULLO, KEITH N89-24065
MASON, K. O. N89-24256
MASON, MARY L. N89-23433
MASSONI, J. A. N89-23940
MASUMURA, S. M. N89-23676
MASUYA, GORO N89-23464
MATEO, LILI N89-24019
MATHES, M. N89-23718
MATHESON, E. M. N89-23774
MATHUR, P. N89-23672
MATTHES, SCOTT R. N89-24119
MATYJASZEWSKI, K. N89-23708
MATZKE, MANFRED N89-24145
MAUCHE, CHRISTOPHER W. N89-24257
MAUDAL, SVERRE N89-23754
MAUTE, P. N89-24050
MAVROPOULOS, PANAGIOTIS G. N89-23759
MAYHEW, BRETT F. N89-24201
MAZDIYASNI, K. S. N89-24196
MCCABE, DOUGLAS A. N89-23454
MCCORMACK, ANN C. N89-23785
MCCOWAN, R. B. N89-23872
MCCOWN, WILLIAM N89-23912
MCCULLOUGH, JOSEPH B., III N89-23934
MCDANIEL, L. H. N89-23714
MCELROY, D. L. N89-23685
MCFEE, JOHN E. N89-23761
MCGOWAN, PAUL E. N89-23924
MCKAY, DAVID S. N89-23544
MCKELVY, COLLEEN N89-24018
MCKINLEY, RICHARD L. N89-23787
MCKINNEY, M. F. N89-24082
MCKINNON, J. A. N89-24250
MCLANDRICH, M. N. N89-24086
MCMAHON, CHARLES J., JR. N89-23921
MCNUTT, STEVEN A. N89-23670
MCNUTT, TERESA M. N89-23667
MCQUILLAN, B. W. N89-24196
MEHROTRA, PIYUSH N89-24058
MEIER, G. H. N89-23673
MELNICK, GARY J. N89-24231
MELNIKOV, V. K. N89-24106
MENON, M. M. N89-24088
MENZELLA, VITO M. N89-24199
MERROW, JAMES E. N89-23540
MERWIN, OLIVER J. N89-23475
MESENBURG, PETER N89-23951
MESSERSCHMID, E. N89-23722
MEYER, HUBERT W., JR. N89-23824
MEYER, UWE N89-23952
MIDDLETON, DAVID B. N89-23469
MIHELCIC, JUDITH A. N89-23691
MILLER, ALLEN R. N89-24116
MILLER, JEFFREY A. N89-23870
MILLER, P. E. N89-23478
MILOSEVIC, OLIVERA N89-23604
MILOSEVSKI, MILOSAV N89-23591
N89-23592
MILUN, MILORAD N89-23596
MINOR, TIMOTHY N89-23962
MIRALLES-WILHELM, F. N89-23651
MISHRA, INDU B. N89-23716
MISRA, AJAY K. N89-23622
MITCHELL, CHRISTINE M. N89-24045
MITKOV, M. N89-23575
N89-23610
MITSUBORI, SUSUMU N89-23408

MIXON, LARRY C. N89-23916
MIYAWAKI, FUJIO N89-24161
MOBARRY, CLARK MATTHEW N89-24242
MODINE, F. A. N89-24191
MOIN, PARVIZ N89-23835
MONNIG, CURTIS A. N89-24169
MONTALVO, E. N89-24166
MONTGOMERY, F. C. N89-24196
MOODY, SCOTT J. N89-23458
MOORE, GERALD T. N89-23862
MOORE, LORNA G. N89-24031
MORABITO, C. N89-23751
MORDFIN, LEONARD N89-23735
MORDIKE, BARRY LESLIE N89-23611
MORFITT, GARY N89-24051
MORGAN, GENE N89-23738
N89-23739
MORKOC, HADIS N89-24203
MORRIS, STEPHEN N89-23827
MORRISON, GERALD L. N89-23808
MORROW, WALTER B., JR. N89-24047
MOU, Y. N89-23665
MOUAT, DAVID N89-23962
MOUTONNET, J. P. N89-23783
MUEHLHEIMS, FRANK N89-23983
MUELLER, PAUL J., III N89-23454
MUENCHAUSEN, R. E. N89-23857
MULAC, RICHARD A. N89-23416
MUNGUR, P. N89-24139
MURAKAMI, ATSUO N89-23464
MURAKAMI, T. N89-24190
MURR, L. E. N89-24204
MUTH, LORANT A. N89-23750
MYERS, JEFF N89-23962
MYERS, SCOTT N89-24017
N89-24020

N

NAKAHARA, J. H. N89-23696
NAKAMURA, TYLER N89-24150
NAOUMIDIS, ARISTIDES N89-23594
NARASIMHA, R. N89-24098
NARASIMHAN, P. S. L. N89-24178
NARUMI, HAJIME N89-24164
NAST, T. C. N89-23512
NAUMANN, K. W. N89-23840
NAYFEH, ALI, H. N89-23812
NECHVATAL, JAMES R. N89-24052
NEHRKORN, THOMAS N89-23993
N89-24009
NELEVIC, L. N89-23608
NELLIS, W. J. N89-24193
NEVILL, GALE E., JR. N89-24015
NEWLAND, J. D. N89-23745
NICHOLSON, DONALD M. N89-23661
NICOLL, JEFFREY F. N89-23865
NIELSEN, P. H. N89-23781
NIETO, MICHAEL MARTIN N89-23988
NIETODECASTRO, C. A. N89-23637
NIIOKA, TAKASHI N89-23639
NIJHOFF, F. N89-24108
NIKITIN, ALEKSANDR N89-23490
NIKOLOPOULOS, PANAJOTIS N89-23599
NISHIIZUMI, K. N89-24243
NITSCHELM, CHRISTIAN N89-24252
NIX, WILLIAM D. N89-24208
NIXON, CHARLES W. N89-23767
NIXON, DAVID N89-23831
NOERDLINGER, PETER D. N89-23441
NOGAR, N. S. N89-23857
NOGUCHI, MASAYOSHI N89-23806
NORDSTROM, JAN N89-23816
NOURSE, ROSWELL W. N89-23526
NOUSE, HIROYUKI N89-23807
NOVAK, SASA N89-23586
NOVAKOVIC, RADA N89-23617
N89-23618
NUSCA, MICHAEL J. N89-23459

O

OBERACKER, R. N89-23607
OGAWA, TOSHIO N89-23467
OGDEN, T. R. N89-24086
OGLE, KATHRYN Y. N89-23503
OGLE, KATHYRN Y. N89-24044
OGUADA, RICHARD A. N89-23711
OH, H. G. N89-24136
OHANDLEY, R. C. N89-24135
OJA, ARNE N89-24188
OKADA, NORIAKI N89-23467
OLIGER, JOSEPH N89-24068
OLSDER, G. J. N89-24099
OLSEN, DAVID N89-23766
ONDRACEK, GERHARD N89-23578
N89-23584
N89-23599
ORDONEZ, C. N89-24166
OSCZEVSKI, R. N89-24046
OSHAUGHNESSY, P. R. N89-23471
OSKAY, VURAL N89-23459
OTTO, G. N89-23719
N89-23724
OUSLEY, GILBERT W. N89-23537
OUTINEN, HANNU N89-23917
OVCHAROV, V. N89-23487
OWEN, F. K. N89-23432
OYIBO, GABRIEL A. N89-23452
OYOUNG, S. D. N89-24089

P

PACE, M. D. N89-23676
PACIOREK, K. L. N89-23696
PAGE, NORMAN A. N89-24153
PANGRAZI, R. N89-23751
PAPIERNIK, A. N89-23780
PARAMENTIER, R. D. N89-23798
PAREKH, D. E. N89-23829
PARKER, T. N. N89-24183
PARKER, W. L. N89-24205
PARKES, JAMES E. N89-23520
PARMLEY, R. T. N89-23512
PATTERSON, F. G. N89-24152
PAVICEVIC, MIODRAG K. N89-23600
PAVLOVIC, V. N89-23589
PAVLOVSKI, BLAGOJ N89-23576
PAWLOWSKI, BRIAN J. N89-23476
PAYNE, JOHN W. N89-24037
N89-24095
PAYSON, STEVEN S. N89-23473
PAZIK, JOHN C. N89-24211
PEARCE, MICHAEL N89-24018
N89-24021
PEHOWSKI, S. E. N89-23743
PEJANOVIC, STANKO N89-23589
PELLMAR, T. C. N89-24026
PEREZ, E. O. N89-23901
PERKINS, R. A. N89-23637
PERSON, LEE H., JR. N89-23466
N89-23469
PERSON, W. B. N89-23652
PERVAN, PETAR N89-23596
PETERSEN, STEVEN E. N89-24040
PETROVIC, V. N89-23604
N89-23608
PETZOW, GUENTER N89-23571
N89-23575
N89-23590
N89-23609
PICHUMANI, RAMANI N89-24068
PICKERELL, THOMAS N89-23435
PIDGEON, WILLIAM M. N89-23734
PIERCE, ALLAN D. N89-23415
PIERCE, N. J. N89-23743
PIERCE, VICKY G. N89-23851
PILANT, M. S. N89-23933
PILTCH, M. N89-23657
PINEAU, DIDIER N89-24175
PIOTROWSKI, GREGORY K. N89-23874
PLESNIA, M. A. N89-23838
PLOTKA, MARVIN S. N89-23480
POGLITSCH, A. N89-24231
POLIDAN, RONALD S. N89-24257
POMERANTZ, MARTIN N89-23709
PONCELEON, DULCE N89-24068
PONTOPPIDAN, K. N89-23781
N89-23784
POPPINGA, BONNO N89-23788
POSNER, MICHAEL I. N89-24040
POSTLETHWAITE, I. N89-24089
POTAPCZUK, M. G. N89-23417
POTTER, ANDREW N89-23558
N89-23565
POULAIN, B. N89-23511
POVINELLI, LOUIS A. N89-23809
POWELL, CLEMANS A. N89-23415
POWELL, J. D. N89-23426
POWITZ, BERND M. N89-23953
PRATT, J. R. N89-23683
PRATT, J. RICHARD N89-23692
PRATT, TIMOTHY N89-23756
N89-23757
PRIEBE, H.-R. N89-23615
PRINZ, DIANNE K. N89-23513
PROGAR, DONALD J. N89-23692
PSIHOGIOS, PANAGIOTIS N89-23992
PURDY, WILLIAM N89-23912
PURVIS, C. K. N89-23529
N89-23555

Q

QIAN, WEN-JIA N89-24164
QUACKENBUSH, TODD R. N89-23414
QUINN, JARUS W. N89-23867
QUINN, ROBERT D. N89-23819
QUINN, WILLIAM F. N89-23740

R

RAGAB, SAAD A. N89-23812
RAI, MAN MOHAN N89-24105
RAITANO, PAUL N89-23520
RAJAMONEY, SHANKAR A. N89-24092
RAJESHWAR, KRISHNAN N89-23709
RAJU, I. S. N89-23919
RAMBERG, S. E. N89-23838
RAMBONE, JAMES D. N89-23438
RAMESH, R. N89-23684
RAMESH, T. G. N89-23677
RANGEL, R. H. N89-23651
RAO, C. N. N89-24184
RAO, C. R. N89-24125
RAO, P. S. N89-23711
RASKOVIC, V. N89-23589
RAUB, JAMES A. N89-23980
RAUM, HENRY G. N89-24067
RAYMOND, JAMES P. N89-23531
READY, DENNIS N89-23644
REAMY, PHILIP N89-23922
REBROV, M. N89-23485
N89-23486
REDMON, JOHN W., JR. N89-23904
REED, D. A. N89-23920
REED, MATTHEW P. N89-23734
REEDY, R. C. N89-24243
REES, JULIA MARGARET N89-23989
REIDY, LAUREL W. N89-23825
REIJNEN, PIET N89-23579
REMANE, EDMUND N89-23606
RENHORN, INGMAR N89-23778
N89-23804
RESING, J. A. C. N89-24099
REX, S. N89-23718
N89-23728
REYNOLDS, JOHN R. N89-23709
REYNOLDS, W. C. N89-23420
N89-23426
N89-23829
RHUE, R. D. N89-23711
RICCO, A. J. N89-24195
RICH, R. W. N89-23900
RICHARDSON, C. W. N89-24001
RIDEAU, P. N89-24078
RINDT, J. R. N89-23712
RISBERG, R. L. N89-23789
RISTIC, M. M. N89-23617
N89-23618
RIZK, A. A. N89-23928
RIZK, ABD EL-FATTAH A. N89-23925
RIZZO, DAVID R. N89-23769
ROBBINS, DAVID O. N89-23871
ROBERTS, E. N89-24260
ROBERTS, E. W. N89-23914
ROBERTS, L. N89-23426
ROCABOY, A. N89-23510
ROCKENFELLER, UWE N89-23733
RODENBURG, W. F. N89-23970
RODER, H. M. N89-23637
RODRIGUEZ-BELL, T. N89-24256
ROECKER, H. N89-23598
ROGERS, STUART E. N89-24111
ROGNES, BERNT N89-23754
ROHRER, N. J. N89-23791
ROMAN, NILS N89-24077
ROOIJACKERS, H. F. L. N89-23915
RORHLT, LARS N89-23754
ROSE, CHARLIE N89-23439
ROSEMA, A. N89-23970
N89-23971
ROSENBLUTH, M. N. N89-24166
ROSENDO, MANNY N89-24017
N89-24020
ROSS, BARBARA S. N89-24173
ROSSITER, ALAN P. N89-23811
ROSSITER, J. A. N89-24091
ROTH, S. C. N89-23680
RUTLEDGE, SHARON K. N89-23540
N89-23691
RYAN, DANIEL J. N89-23687
RYTKOENEN, TUIJA N89-23620

RYU, DONGSU N89-24244
RZESNITZEK, KLAUS N89-23609

S

SABER, M. N89-24181
N89-24182
SAITOH, TAKASHI N89-23635
SAKAI, TOSHIHO N89-23463
SALAS, ROQUE L. N89-23916
SALIMOV, R. A. N89-23658
SALVETTI, AUGUSTINE N89-23430
SALZ, JOEL N89-24076
N89-24120
N89-24121
SALZMANN, M. A. N89-23787
SAMPLE, ROBERT J. N89-23668
SAMUELSEN, G. S. N89-23651
SANDER, HARDY N89-24176
SANDVIK, AGNAR N89-23754
SANGSTON, K. J. N89-23771
SANTORO, R. T. N89-23566
SARASAMMA, V. R. N89-23805
SARJEANT, W. J. N89-23799
SARMA, G. S. R. N89-23723
SARRAFZADEH, M. N89-23796
SATO, JUNICHI N89-23639
SATO, KUNIHIRO N89-24161
SATTERLEE, P. E., JR. N89-23790
SAUND, ERIC N89-24041
SAUVAN, M. N89-23780
SAWKA, MICHAEL N. N89-23744
SAWYER, D. M. N89-23561
SAWYER, GREGORY R. N89-24225
SCHAEFER-SIEBERT, DIETRICH N89-23710
SCHAEFFEL, JOHN A., JR. N89-23916
SCHAUER, D. A. N89-24026
SCHELLHORN, M. N89-23843
SCHERRER, PHILIP H. N89-24254
SCHERRER, S. N89-23601
SCHKADE, DAVID A. N89-24037
SCHMID, H. N89-23600
SCHMIDT, J. N89-23512
SCHMITZ, G. J. N89-23718
N89-23728
SCHNEIDER, JON C. N89-23416
SCHRA, L. N89-23656
SCHREIER, GUNTER N89-23950
SCHROTH, RALF N89-23942
SCHUB, INGEBORG N89-23686
SCHUBERT, SIEGFRIED N89-24002
SCHUHMACHER, UWE N89-23593
SCHULKES, R. M. S. M. N89-24101
SCHULTZ, MARTIN N89-24120
SCHULZ, BRIGITTE N89-23591
N89-23592
SCHULZ, HANS N89-23587
SCHULZ, ULRICH N89-24146
SCHUNK, RICHARD G. N89-23503
N89-24044
SCHWARTZ, DEBORAH E. N89-24022
N89-24023
SCOTT, JAMES R. N89-23413
SEAMAN, C. L. N89-24193
SEAVER, CHRISTOPHER A. N89-23427
SECUNDE, RICHARD R. N89-23516
SEELINGER, PETER N89-23937
SEGALMAN, D. J. N89-23922
SEIDE, OTMAR N89-23598
SEIDMAN, HARRY N89-23430
SEILER, F. N89-23841
N89-23842
SELTVEIT, A. N89-23593
SEMENOV, YU. N89-23488
N89-23489
SERLIN, V. N89-24148
SETH, SHIV N89-23885
N89-23886
SHAFFER, TIMOTHY D. N89-23709
SHAU, Y. R. N89-23421
SHEARER, MICHAEL N89-23830
SHEN, GUIRONG N89-23869
SHIH, CHIH-KANG N89-24179
SHIMABUKUKO, F. I. N89-23803
SHIMODAIRA, KAZUO N89-23635
SHIRANE, G. N89-24190
SHIRLEY, MARK H. N89-23800
SHUBHA, V. N89-23677
SHULMAN, GORDON L. N89-24042
SIGNORELLI, L. N89-23461
SIGULINSKI, FEODOR N89-23588
SIHVOLA, ARI N89-24102
SILS, INGRID V. N89-24029
SILVER, M. N. N89-24191
SILVERMAN, JONATHAN N89-23885
N89-23886
SIMPSON, MYLES A. N89-24141
SINGER, S. N89-23792
SINGH, R. K. N89-24184
SINHA, U. N. N89-23805
SIRIGNANO, W. A. N89-23651
SIVITZ, HERBERT N89-24017
N89-24020
SJOLAND, MAGNUS N89-24077
SKAAR, ERIC C. N89-23681
SKOVGAARD, O. N89-23798
SKRINSKIJ, A. N. N89-24247
SKUPINSKI, ROBERT C. N89-23527
SLATER, P. N. N89-23852
SLAUGHTER, STEPHEN R. N89-24180
SLEMP, WAYNE S. N89-23551
N89-23562
N89-23567
SLIWA, STEVEN M. N89-23468
SMARTT, RAYMOND N. N89-24252
SMEGGIL, JOHN G. N89-23700
SMITH, B. T. N89-23619
SMITH, DAVID R. N89-24213
SMITH, DENNIS W. N89-23909
SMITH, G. S. N89-24193
SMITH, JANE S. N89-23695
SMITH, MARK A. N89-23706
SMITH, MICHAEL J. N89-23715
SMITH, RICHARD L. N89-23501
SMITH, SUZANNE WEAVER N89-23924
SNIR, ZEEV N89-23832
SNYDER, B. N89-23810
SNYDER, PHILIP K. N89-23785
SOCHA, MICHAEL M. N89-23903
SOLIMAN, MOHAMED AHMED FAHMY N89-23419
SOLOMON, JOSEPH K. N89-23443
SONNE, BERND N89-23954
SOTIROPOULOU, D. N89-23599
SOVERS, O. J. N89-24060
SOVEY, JAMES S. N89-23520
SOVIE, AMY J. N89-23522
SPALART, PHILIPPE R. N89-23820
SPARROW, DAVID A. N89-23864
N89-23865
SPECK, D. R. N89-23859
SPECKMAN, KAREN N. N89-23744
SPEECE, DANA J. N89-23694
SPICER, W. E. N89-23653
SPILLAR, E. J. N89-24246
SPINWEBER, CHERYL L. N89-24027
SRINIVASAN, KRISHNA N89-23624
SRIVATSAN, RAGHAVACHARI N89-23469
SRULIJES, J. N89-23841
STACEY, G. J. N89-24231
STAMENKOVIC, IVAN N89-23578
STANAWAY, S. K. N89-23820
STANDLEY, DAVID L. N89-24081
STAPLES, EDWARD N89-23855
STCLAIR, ANNE K. N89-23880
STCLAIR, TERRY L. N89-23692
STEFANOVIC, D. N89-23617
STEIN, BLAND A. N89-23528
N89-23547
STEINVALL, OVE N89-23778
STEKOLNIKOV, A. F. N89-24165
STEPHENS, M. A. N89-24118
STEPHENSON, LOU A. N89-24030
STERN, S. A. N89-23683
STERRETT, MARK E. N89-23687
STEVENS, N. JOHN N89-23556
N89-23563
N89-23568
STOAKLEY, DIANE M. N89-23880
STOJANOVSKA, L. N89-23576
STOMMEL, HENRY M. N89-24011
STONE, D. A. N89-23652
STREET, JIMMY N89-23986
STRUMBERGER, V. N89-23595
STUCKEY, WAYNE K. N89-23560
N89-23566
STUDER, F. A. N89-23751
SUCY, M. N89-23801
SUENAGA, HISASHI N89-23408
SUIKAT, REINER N89-23470
SULLIVAN, C. A. N89-23872
SUMMERS, LELAND G. N89-24033
SUZUKI, KOICHI N89-23408
SWEAN, T. F., JR. N89-23838
SYKORA, JULIUS N89-24252
SYSLO, STEPH N89-24018
SZLYK, PATRICIA C. N89-24029

T

TADA, AKIRA N89-23467
TAI, FRANK M. N89-23441
TAKAHASHI, MAMORU N89-23639
TAKAHASHI, Y. N89-24142
TAMOR, S. N89-24166
TANAKA, HIROSHI N89-24004
TARASOV, L. S. N89-24247
TARIDE, S. N89-23939
TASKINEN, PEKKA N89-23657
TAX, WIENKE M. N89-23981
TAYLOR, DEBORAH B. N89-23495
TAYLORDELIMA, REYNALDO N89-23936
TEETS, ROBERT B. N89-23496
TEICHMAN, LOUIS A. N89-23528
N89-23547
TEILLET, P. M. N89-23852
TELLMAN, LARRY D. N89-23881
TENNEY, DARREL R. N89-23530
TEPPO, OSMO N89-23657
TESAR, DELBERT N89-23875
TEUNISSEN, P. J. G. N89-23787
TEW, ROY C. N89-23823
THART, W. G. J. N89-23656
THOMAS, CATHY A. N89-24226
THOMAS, G. N89-23684
THOMAS, IAN M. N89-23861
THOMAS, JAMES L. N89-23433
THOMPSON, A. W. N89-23673
THOMPSON, JOHN R. N89-23627
THORNWALD, HERBERT N89-23828
THORSTENSON, ROGER K. N89-24071
THUEMMLER, FRITZ ERNST N89-23607
THURSTON, T. R. N89-24190
TIERNEY, M. J. N89-23650
TILTON, BEVERLY E. N89-23980
TINGEY, DAVID T. N89-23980
TIONG, K. K. N89-23478
TIPTON, T. L. N89-23652
TOBIAS, A. N89-24050
TODARO, M. E. N89-23666
TOMAK, M. N89-24185
TOMPKINS, STEPHEN S. N89-23552
N89-23566
TOTTEN, VENITA N89-23675
TOWNSEND, LAWRENCE W. N89-24255
TRAN, HUNG VIET N89-24241
TRAUTMAN, EDWARD N89-24036
TRAUTMAN, MARY A. N89-24036
TREFETHEN, LLOYD N. N89-24131
TRENT, WILLIAM N89-23435
TRICKL, T. N89-23863
TRIGGIANI, R. N89-23507
TRIMBOLI, M. S. N89-24090
TRIOLO, JACK J. N89-23537
TRIPATHI, ANAND R. N89-23885
N89-23886
TROUT, T. K. N89-23680
TROXEL, SETH W. N89-23758
TRUCANO, T. G. N89-23877
TRUXAW, CHRIS N89-24122
TSAI, M. C. N89-24089
TSAI, PATTI N89-24196
TSAI, TED N89-23895
TSITSIKLIS, JOHN N. N89-24117
TSO, JIN N89-23525
TUBBS, TRACEY N89-24019
TUCKNESS, DANNY GENE, JR. N89-24236
TURK, RADOMIR N89-23615
N89-23616
TURNER, R. N89-23810

U

UCHIDA, TADAO N89-23467
ULABY, F. T. N89-23961
UM, C. I. N89-24136
UNDERWOOD, J. H. N89-23931
USKOKOVIC, DRAGOLJUB N89-23604
N89-23608

V

VAIDYANATHAN, R. N89-23683
VAJSMAN, A. F. N89-23658
VALA, M. T. N89-23652
VALCO, G. J. N89-23791
VAMPOLA, ALFRED L. N89-23548
N89-23560
N89-23566
VANDAM, C. P. N89-23418
VANDAM, J. W. N89-24166
VANDERBURGH, A. H. P. N89-24134
VANDERMOLEN, GEERT N89-23985
VANDOMMELEN, LEON L. N89-23821
VANDYKE, L. S. N89-23650
VANROSENDALE, JOHN N89-24058
N89-24113

VANSELOW, JANICE J. N89-23697
VANTKLOOSTER, K. N89-23783
VARKKING, M. J. J. N89-23863
VASSERMAN, S. B. N89-23658
VECKO, TATJANA N89-23615
VEFSNMO, EIRIK N89-23754
VERSENDAAL, J. M. N89-24043
N89-24056
VERWAAL, RUUD G. N89-23964
VICKERS, GEORGE H. N89-24173
VIDAL, C. N89-23889
VIGNOLLET, MICHEL N89-23509
VISENTINE, JAMES T. N89-23539
N89-23557
N89-23564
VISSER, HANS N89-23446
VOEGTLE, T. N89-23972
VOLKMANN, D. N89-23732
VOLZ, ANDREAS N89-23983
VONMALLINCKRODT, D. N89-23603
VOTER, A. F. N89-23655

W

WACHSPRESS, DANIEL A. N89-23414
WAGENER, K. B. N89-23706
WAGNER, RUDOLF N89-23899
WAKAMATSU, YOSHIO N89-23514
WALKER, HOYT N89-23959
WALKER, RICHARD N. N89-23932
WALLS, JOHN E. N89-23438
WALTHER, CRAIG N89-23749
WANDELT, KLAUS N89-23596
WANG, F. W. N89-23680
WANG, PONG-SHENG N89-23885
N89-23886
WANG, RUNWEN N89-23869
WANG, Y. N89-24112
WANG, ZHONG N89-24245
WARDEN, ROBERT M. N89-23897
WARE, GEORGE M. N89-23412
WARN, THOMAS E. N89-23981
WARNER, J. D. N89-23791
WATERS, W. M. N89-23764
WATTS, NORMAN W. N89-24051
WEBER, ARTHUR L. N89-23693
WEBER, S. N89-23601
WEFEL, JOHN P. N89-24253
WEI, JINXIAN N89-23625
WEIGEL, GARY R. N89-23990
WEILAND, T. L. N89-23859
WEISBRICH, W. N89-23972
WEISS, LEE N89-24016
N89-24021
WEISS, ROSANNE M. N89-23480
WEISSHAAR, T. A. N89-23452
WELFORD, GORDON D. N89-24158
WENGER, ETIENNE N89-24122
WERNET, MARK P. N89-23850
WHITE, CHARLES S. N89-23935
WHITE, MARY L. N89-24153
WHITFIELD, C. E. N89-24139
WIDEN, ANDERS N89-23778
WIELAND, PAUL O. N89-23503
N89-24044
WILBUR, MATTHEW L. N89-24079
WILDER, JOHN G. N89-23861
WILKINS, JOHN N89-23669
WILKINSON, DANIEL C. N89-23536
WILL, HERBERT A. N89-24055
WILLIAMS, CLAUDE N., JR. N89-24005
WILLIAMS, D. M. N89-23906
WILLIAMS, THOMAS E. N89-23505
WILLSON, W. G. N89-23712
WILSON, JOHN W. N89-24255
WILSON, LARRY W. N89-24054
WINDELBERG, DIRK N89-23584
WINSKE, D. N89-24167
WIRTZ, R. A. N89-23810
WISANRAKKIT, GUY N89-23704
N89-23705
WISE, JACQUELYN N89-23846
WISE, JAMES L. N89-24005
WISEMAN, ROBERT N89-24051
WITTIG, MANFRED N89-23445
WITTMANN, K. N89-23721
WOLSEFER, DAVE N89-24017
N89-24020
WOOD, WILLIAM T. N89-23885
N89-23886
WOODWARD, RICHARD P. N89-24138
WOOLHISER, D. A. N89-24001
WRIGHT, GARY N89-24051
WRIGHT, ROBERT L. N89-23882
WU, RITA N89-23885
N89-23886
WYATT, JOHN L., JR. N89-24081
WYN-ROBERTS, D. N89-23893

Y

YAMADA, HIDESHI N89-23635
YAMADA, K. N89-24190
YAMAKAWA, MASANORI N89-23639
YAMAMOTO, ATSUMASA N89-23807
YAMAMOTO, YUKIMITSU N89-23409
YAMATO, HIROYUKI N89-23467
YANAGI, RYOJI N89-23807
YANG, J. N. N89-23457
YANG, JUN N89-23955
YANG, PENGYUAN N89-24169
N89-24173
YARBROUGH, D. W. N89-23685
YAZEK, FRANK N89-24051
YEE, ALBERT F. N89-23689
YEH, C. N89-23803
YELLETS, JEFFREY P. N89-23847
YOLKEN, H. THOMAS N89-23735
N89-23884
YOO, M. H. N89-24192
YOUNG, J. F. N89-23868

Z

ZACHARIE, D. F. N89-23901
ZAMAN, K. B. M. Q. N89-23417
ZARDECKI, A. N89-23858
ZDUJIC, MIODRAG N89-23608
ZEMAN, G. H. N89-24026
ZHANG, SHUNYE N89-23869
ZHANG, Y. S. N89-23478
ZIMMERMAN, M. N89-23753
ZIMMERMANN, S. D. N89-23790
ZOLLWEG, J. A. N89-24214
ZORUMSKI, WILLIAM E. N89-24140
ZUCLICH, JOSEPH A. N89-24032
ZUERNDORFER, B. W. N89-23961

Typical Corporate Source Index Listing

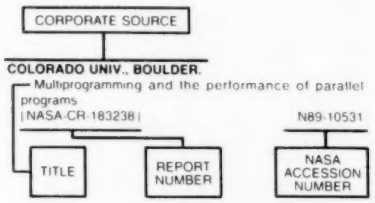

Listings in this index are arranged alphabetically by corporate source. The title of the document provides the user with a brief description of the subject matter. The report number helps to indicate the type of document cited (e.g., NASA report, translation, NASA contractor report). The NASA accession number denotes the number by which the citation is identified. The titles are arranged under each corporate source in ascending accession number order.

A

AACHENER CENTRUM FUER ERSTARRUNG UNTER SCHWERELOSIGKEIT E.V. (GERMANY, F.R.).
Research activity report concerning solidification technology under microgravity
[ETN-89-93988] N89-23718
Model systems N89-23728

ACADEMY OF SCIENCES (USSR), NOVOSIBIRSK.
On steel superficial hardening by concentrated electron beam in the air
[DE88-705781] N89-23658
Application of the method of X-ray fluorescence analysis with synchrotron radiation to study lunar matter
[DE88-705782] N89-24247

ADVANCED TECHNOLOGY, INC., HUNTSVILLE, AL.
Launch commit criteria performance trending analysis, phase 1, revision A. SRM and QA mission services
[NASA-CR-184859] N89-24129

AEC-ABLE ENGINEERING CO., INC., GOLETA, CA.
Carousel deployment mechanism for collable lattice truss N89-23897

AERONAUTICAL RESEARCH INST. OF SWEDEN, STOCKHOLM.
Open boundary conditions for the Navier-Stokes equation
[FFA-145] N89-23816
Numerical solution of the Euler equations using local grid refinement
[FFA-143] N89-24104
A stability analysis of various patched grid interface conditions for hyperbolic equations
[FFA-144] N89-24105

AERONAUTICAL RESEARCH LABS., MELBOURNE (AUSTRALIA).
Modelling aircraft dynamics
[AD-A204086] N89-23449
SMOOFF: A FORTRAN smoothing program
[AD-A204087] N89-24057

AERONAUTICAL SYSTEMS DIV., WRIGHT-PATTERSON AFB, OH.
An evaluation of the F/FB/EF-111 crew/voice message system
[AD-A205998] N89-23774

AEROSPACE CORP., EL SEGUNDO, CA.
On-orbit observations of single-event upset in harris HM-6508 RAMSs (Random Access Memories): An update
[AD-A206266] N89-23506
Spacecraft contamination experience N89-23545
Effects of space radiation on electronic microcircuits N89-23549
Space vehicle thermal testing: Principles, practices and effectiveness N89-23550
Dynamic fatigue of ultralow-expansion glass for space mirrors, reissue A
[AD-A205401] N89-23694
Attenuation measurement of very low-loss dielectric waveguides by the cavity resonator method in the millimeter/submillimeter wavelength range
[AD-A206458] N89-23803
Relativistic electron precipitation patterns in longitude and latitude: A reply to W. R. Sheldon
[NASA-CR-185442] N89-23995

AEROSPACE CORP., LOS ANGELES, CA.
The space particle environment N89-23548
Trapped radiation N89-23560

AEROSPACE MEDICAL RESEARCH LABS., WRIGHT-PATTERSON AFB, OH.
Intelligibility in noise of three LPC (Linear Predictive Coders) voice channels with active noise reduction headsets
[AD-A205613] N89-23767

AEROSPATIALE, CANNES LA BOCCA (FRANCE).
Assembling the ISO thermal model with ESAT AN
[REPT-882-440-107] N89-23510
The two approaches for the thermal control of the Columbus resource module and Polar Platform
[REPT-882-440-110] N89-23511
Small UHF microstrip radiating element
[REPT-882-440-103] N89-23780
Mechanical/electrical distortion model for reflector antennas
[REPT-882-440-104] N89-23781
TELE-X antenna module thermal control
[REPT-882-440-106] N89-23782
Near field testing of the electronically despun antenna of the Meteosat satellite
[REPT-882-440-108] N89-23783
ESA-D: An integrated software for antenna design and analysis
[REPT-882-440-111] N89-23784
The FLUIDNET development and application to preliminary sizing of fluid loop systems
[REPT-882-440-102] N89-23845
Evaluation of tests and design factors
[REPT-882-440-109] N89-23889
Shaking in cryogenic conditions
[REPT-882-440-101] N89-23939
Telescope structure for cryogenic application
[REPT-882-440-112] N89-23940
The third generation rigid solar array GSR3
[REPT-882-440-105] N89-23979
GEMMES: A new tool for dynamic modeling
[REPT-882-440-114] N89-24078
Thermal and cryogenic aspects of the ISO optical subsystem
[REPT-882-440-113] N89-24160

AEROSPATIALE, CHATILLON (FRANCE).
Pif-Paf piloting of tactical missiles
[REPT-882-320-104] N89-23462

AEROSPATIALE, PARIS (FRANCE).
The role of pilot and automatic onboard systems in future rendezvous and docking operations
[REPT-882-440-116] N89-24050

AEROSPATIALE, TOULOUSE (FRANCE).
Center of gravity control on Airbus aircraft: Fuel, range and loading
[REPT-882-111-101] N89-23460
A330/340 hydraulic system
[REPT-882-111-102] N89-23461

AEROSPATIALE AQUITAINE, SAINT-MEDARD EN JALLES (FRANCE).
Nozzles for test system plasma generators
[REPT-882-430-104] N89-23502
Break dimensioning of space structural assemblies and its experimental validation
[REPT-882-430-109] N89-23508
Composites in complex assemblies
[REPT-882-430-110] N89-23509
Reentry materials in the atmosphere
[REPT-882-430-102] N89-23629
Composite materials nondestructive tests: Choice of methods depending on requirements
[REPT-882-430-105] N89-23630
High performance refractory composite materials
[REPT-882-430-106] N89-23631
Challenges of nondestructive testing of composite materials
[REPT-882-430-107] N89-23632
The protection against oxidation of carbon materials. Thermodynamic and experimental study: A literature survey
[REPT-882-430-108] N89-23633
Product development at Aerospatiale
[REPT-882-430-111] N89-24175

AGENCY OF INDUSTRIAL SCIENCE AND TECHNOLOGY, TOKYO (JAPAN).
Japan's Sunshine Project 1987 annual summary of comprehensive research
[DE88-756448] N89-23975

AGRICULTURAL RESEARCH SERVICE, BELTSVILLE, MD.
Microcomputer program for daily weather simulation
[PB89-144638] N89-24001

AIR FORCE ACADEMY, CO.
Viscosity and conductance of MEICl/AlCl3 melts containing nonaqueous solvents
[AD-A205468] N89-23646

AIR FORCE ENVIRONMENTAL TECHNICAL APPLICATIONS CENTER, SCOTT AFB, IL.
Surface Observation Climatic Summaries (SOCS) for NASA Shuttle Landing Facility, Florida
[AD-A205362] N89-24007

AIR FORCE GEOPHYSICS LAB., HANSCOM AFB, MA.
Dielectrics for long term space exposure and spacecraft charging: A briefing N89-23553
Image processing of coronal pictures
[AD-A205326] N89-24252

AIR FORCE HUMAN RESOURCES LAB., BROOKS AFB, TX.
Air Force Human Resources Laboratory R and D accomplishments and services, FY86-FY88
[AD-A205312] N89-24218

AIR FORCE INST. OF TECH., WRIGHT-PATTERSON AFB, OH.
Navier-Stokes solution for a NACA 0012 airfoil with mass flux (fan)
[AD-A205771] N89-23424
Investigation of the flowfield created by the interaction of a sonic jet and a co-flowing supersonic stream
[AD-A205823] N89-23425
Ejector effects on a supersonic nozzle at low altitude and Mach number
[AD-A206049] N89-23427
Numerical study of the influence of leading and trailing edge flaps on the performance of airfoils
[AD-A206138] N89-23428
Development of the extended kalman filter for the advanced Completely Integrated Reference Instrumentation System (CIRIS)
[AD-A206083] N89-23443
Preliminary design of a modular unmanned research vehicle. Volume 2: Subsystem technical development design study
[AD-A205678] N89-23454
A methodology for determining the survivability of fixed-wing aircraft against small arms
[AD-A205730] N89-23455
An investigation into the application of dynamic programming to determine optimal controls for tracking a cruise missile maneuver by CMMCA (Cruise Missile Mission Control Aircraft)
[AD-A205970] N89-23456
Flight control system for the CRCA (Control Reconfigurable Combat Aircraft) using a command generator tracker with PI (Proportional-Plus-Integral) feedback and Kalman filter, volume 1
[AD-A205723] N89-23473
Control design of an unstable non-minimum phase aircraft subject to control surface saturation
[AD-A206024] N89-23475
Multivariable flight control design with parameter uncertainty for the AFTI/F-16
[AD-A206068] N89-23476

Design of water tunnel to measure wall pressure signatures due to tunnel blockage and wake effects
[AD-A206025] N89-23483
Numerical study of orbital trajectories about Phobos
[AD-A205822] N89-23496
Continuous, low thrust copianar orbit transfers with varying eccentricity
[AD-A206022] N89-23498
An analysis of the attitude stability of a space station subject to parametric excitation of periodic mass motion
[AD-A206009] N89-23505
Parametric study of radiative cooling of solid antihydrogen
[AD-A206092] N89-23742
The effect of mutual coupling on the side lobe performance of Chebyshev arrays, volume 1
[AD-A205724] N89-23768
Enhanced tracking of ballistic targets using forward looking infrared measurements
[AD-A205727] N89-23769
Coupled integral equation solution for two dimensional bistatic TE scatter from a conducting cavity-backed infinite plane
[AD-A206096] N89-23775
Two-dimensional confined jet thrust vector control: Operating mechanisms and performance
[AD-A206011] N89-23834
Comparison of split-film and x-film measurements in 2-D flow
[AD-A206023] N89-23836
A numerical investigation of thin-film heat transfer gages
[AD-A206134] N89-23853
Numerical simulation of the dissociation of I2 by O2 (1 Delta) in a two dimensional parallel jet
[AD-A206137] N89-23870
Multiple model-based robot control: Development and initial evaluation
[AD-A205725] N89-23881
Quadratic optimal control theory for viscoelastically damped structures using a fractional derivative viscoelasticity model
[AD-A206008] N89-23932
Fractional calculus formulation of the quasi-static viscoelastic problem
[AD-A206136] N89-23934
An analysis of lightning launch constraints
[AD-A206084] N89-23994
A database management system for computer-aided digital circuit design
[AD-A206047] N89-24066
PRASE (Parallel Resource Analysis Software Environment) instrumentation software for the Intel iPSC hypercube
[AD-A206046] N89-24087
Discrete event simulation model decomposition
[AD-A206048] N89-24119
A demonstration of the method of stochastic finite element analysis
[AD-A206135] N89-24127
Parallel ada implementation of a multiple model Kalman filter tracking system: A software engineering approach
[AD-A206094] N89-24130
Characterization of semiconductor device processing etchant solutions for GaAs and p+ GaAs layers employed in AlxGa(1-x)As/GaAs MODFETs and related heterojunction devices
[AD-A205772] N89-24201

AIR FORCE OFFICE OF SCIENTIFIC RESEARCH, BOLLING AFB, WASHINGTON, DC.
US Air Force research technology area plan, FY 1989
[AD-A205304] N89-24217

AIR FORCE SPACE DIV., LOS ANGELES, CA.
Relativistic electron precipitation patterns in longitude and latitude: A reply to W. R. Sheldon
[NASA-CR-185442] N89-23995

AIR FORCE SYSTEMS COMMAND, WRIGHT-PATTERSON AFB, OH.
Carbon fiber thermal conductivity measurement and analysis
[AD-A205682] N89-23825
Laser photoelectric effect at surface of discharge cathode
[AD-A205741] N89-23869
Summary of achievements in scientific research
[AD-A199947] N89-24227

AIR FORCE WRIGHT-PATTERSON AERONAUTICAL LABS., WRIGHT-PATTERSON AFB, OH.
Correlation of Portable Wear Metal Analyzer (PWMA-2) and Baird A/E35U-3 spectrometer oil analysis data
[AD-A205957] N89-23882

AIRCRAFT RESEARCH AND DEVELOPMENT UNIT, EDINBURG (AUSTRALIA).
Flight testing of the Southern Cross replica aircraft
[AD-A205303] N89-23451

ALABAMA UNIV., HUNTSVILLE.
Direct electron-pair production by high energy heavy charged particles
[NASA-CR-184958] N89-24142

ALASKA UNIV., FAIRBANKS.
High-latitude field-strength measurements of standard broadcast band skywave transmissions monitored at Fairbanks, Alaska
[PB89-134829] N89-23747
Remote sensing of global snowpack energy and mass balance: In-situ measurements on the snow of interior and Arctic Alaska
[NASA-CR-180078] N89-23956

ALFRED UNIV., NY.
Preparation and evaluation of silicon nitride matrices for silicon nitride-SiC fiber composites
[NASA-CR-184798] N89-23678

ALLIANCE TECHNOLOGIES CORP., CHAPEL HILL, NC.
Area source documentation for the 1985 National Acid Precipitation Assessment Program Inventory
[PB89-151427] N89-23981

AMERASIA TECHNOLOGY, INC., WESTLAKE VILLAGE, CA.
Monolithic GaAs digitizer for space-based laser pulse spreading effect
[NASA-CR-183430] N89-23855

AMERICAN OPTICAL CO., SOUTHBRIDGE, MA.
Fatigue-resistant photochromic plastics
[DE89-007336] N89-23682

AMERICAN SOCIETY FOR ENGINEERING EDUCATION, WASHINGTON, DC.
Alternate arsenic and antimony sources for the OMCVD fabrication of semiconductors
[AD-A206483] N89-24211

ANALATOM, INC., SUNNYVALE, CA.
An instrument for the simultaneous measurement of velocity, temperature and density in unseeded air flows
[AD-A205588] N89-23453

ANALEX CORP., CLEVELAND, OH.
Numerical studies of the effects of jet-induced mixing on liquid-vapor interface condensation
[NASA-CR-182285] N89-23818

ANALYTICAL SERVICES AND MATERIALS, INC., HAMPTON, VA.
Crack-face displacements for embedded elliptic and semi-elliptical surface cracks
[NASA-CR-181822] N89-23919

ANALYTICS, INC., WILLOW GROVE, PA.
Design of a MANPRINT tool for predicting personnel and training characteristics implied by system design
[AD-A206201] N89-24048

APPLIED RESEARCH LAB., STATE COLLEGE, PA.
Fabrication of unidirectional fiber reinforced 6061 aluminum alloy using high pressure squeeze casting
[AD-A205717] N89-23668

ARGONNE NATIONAL LAB., IL.
Li/FeS battery design for an electric van
[DE89-009808] N89-23794

ARIZONA STATE UNIV., TEMPE.
Development of harmonic panel methods for aeroelastic applications to elastic bodies and body-fin combinations in supersonic flow
[AD-A205739] N89-23423

ARIZONA UNIV., TUCSON.
Fabricable polymers with excellent heat, oxidative and hydrolytic stability
[AD-A205827] N89-23698
The absolute radiometric calibration of the advanced very high resolution radiometer
[NASA-CR-185057] N89-23852

ARMED FORCES RADIOBIOLOGY RESEARCH INST., BETHESDA, MD.
A low-energy X-ray irradiator for electrophysiological studies
[AD-A205388] N89-24026

ARMY ARMAMENT RESEARCH, DEVELOPMENT AND ENGINEERING CENTER, PICATINNY ARSENAL, NJ.
Analytical transfer functions in parallel configurations
[AD-A205714] N89-23472

ARMY ARMAMENT RESEARCH, DEVELOPMENT AND ENGINEERING CENTER, WATERVLIET, NY.
Testing chromium adhesion using acoustic emission
[AD-A205621] N89-23666
High speed abrasive belt grinding
[AD-A205618] N89-23741
Overview of ASTM symposium on analytical and experimental methods for residual stress effects in fatigue
[AD-A205622] N89-23931

ARMY AVIATION SYSTEMS COMMAND, HAMPTON, VA.
Application of a PC based, real-time, data-aquisition system in rotorcraft wind-tunnel testing
[NASA-TM-4119] N89-24079

ARMY BELVOIR RESEARCH AND DEVELOPMENT CENTER, FORT BELVOIR, VA.
Corrosion and lubricity testing of nonflammable USAF formulated CTFE (Chlorotrifluoroethylene) base hydraulic fluid
[AD-A205467] N89-23695
Environmental Stress Screening (ESS) guide
[AD-A206350] N89-23888

ARMY COLD REGIONS RESEARCH AND ENGINEERING LAB., HANOVER, NH.
Response of pavement to freeze-thaw cycles: Lebanon, New Hampshire, regional airport
[AD-A205559] N89-23740

ARMY LAB. COMMAND, WATERTOWN, MA.
Environmental stress crazing and cracking of transparent polymers
[AD-A205624] N89-23697
A combined isotropic-kinematic hardening model for large deformation metal plasticity
[AD-A206352] N89-23935

ARMY LAB. COMMAND, WHITE SANDS MISSILE RANGE, NM.
The US Army Yuma Proving Ground, Arizona 33-year climate calendar and tables on associated weather elements 1954-1986. American desert country
[AD-A206256] N89-24010

ARMY MISSILE COMMAND, REDSTONE ARSENAL, AL.
Missile actuator simulation and an investigation into the accuracy of Runge-Kutta numerical integration
[AD-A206325] N89-23458
A numerical routine for defining rocket exhaust characteristics and impingement effects
[AD-A206323] N89-23526
System Mean-Time-Between-Failure versus life-cycle logistics cost subject to the introduction of Line-Replaceable-Unit redundancy
[AD-A206324] N89-23887
Modal analysis and testing of missile systems
[AD-A204051] N89-23916
Structural mode frequencies of FOG-M (Fiber Optics Guided-Missile) actuator/fin
[AD-A206327] N89-24158

ARMY RESEARCH INST. OF ENVIRONMENTAL MEDICINE, NATICK, MA.
Evaluation of three commercial microclimate cooling systems
[AD-A206318] N89-23744
Patterns of human drinking: Effects of exercise, water temperature and food consumption
[AD-A206031] N89-24029
Human temperature regulation during exercise after oral pyridostigmine administration
[AD-A206032] N89-24030
Treatment with tyrosine, a neurotransmitter precursor, reduces environmental stress in humans
[AD-A206035] N89-24039

ATMOSPHERIC AND ENVIRONMENTAL RESEARCH, INC., CAMBRIDGE, MA.
Inferring relative humidity profiles from 3DNEPH cloud data: Technique development and data impact study
[AD-A205825] N89-23993
On the use of multiprocessing computers for global numerical weather prediction
[AD-A206102] N89-24009

B

BALL AEROSPACE SYSTEMS DIV., BOULDER, CO.
System study: Radiation hardened autonomous navigation
[AD-A205604] N89-23439

BALLISTIC RESEARCH LABS., ABERDEEN PROVING GROUND, MD.
Comparison of computational analysis with flight tests of a 40mm solid-fuel ramjet projectile
[AD-A206536] N89-23459
Polyethylene glycol-poly(2-methyl-5-vinyl tetrazole) polymer blend: A desensitizing binder for propellants and explosives
[AD-A206563] N89-23716
Chloride analysis in HAN-based liquid propellants by inductively coupled plasma spectroscopy
[AD-A206564] N89-23717
Derivation of a Godunov one dimensional fluid dynamics code
[AD-A205463] N89-23824

BAYLOR UNIV., WACO, TX.
Control of the composition of electrodeposited alloys by the use of certain types of additives
[AD-A206370] N89-23675

BAYREUTH UNIV. (GERMANY, F.R.).
Approximation of stochastic integral equations using Martingale difference schemes
[ETN-89-93951] N89-24123

BDM CORP., MCLEAN, VA.
Digital optics for numerical computing: The residue number system for numerical optical computing
[AD-A206229] N89-24157
BELEIDSCOMMIE REMOTE SENSING, DELFT (NETHERLANDS).
On the international commercialization of remote sensing
[BCRS-88-02] N89-23969
Meteosat thermal inertia mapping for studying wetland dynamics in the West-African Sahel
[BCRS-88-10A] N89-23970
Thermal analysis for the monitoring and prediction of flood dynamics in wetlands
[BCRS-88-10B] N89-23971
BELGRADE UNIV. (YUGOSLAVIA).
Characterization of a phase boundary in Ni-Al2O3 sintered under pressure N89-23600
BOEING COMMERCIAL AIRPLANE CO., SEATTLE, WA.
The 4D-TECS integration for NASA TSRV airplane
[NASA-CR-4231] N89-23471
BOEING COMPUTER SERVICES CO., RICHLAND, WA.
Fourth generation computer languages
[DE89-008800] N89-24059
BOEING HELICOPTER CO., PHILADELPHIA, PA.
Ground shake test of the Boeing Model 360 helicopter airframe
[NASA-CR-181766] N89-23920
BOLT, BERANEK, AND NEWMAN, INC., CANOGA PARK, CA.
Noise and sonic boom impact technology. PCBOOM computer program for sonic boom research, volume 1
[AD-A206290] N89-23429
Noise and sonic boom impact technology. PCBOOM computer program for sonic boom research. Volume 2: Program Users/Computer operations manual
[AD-A206291] N89-23430
BONN UNIV. (GERMANY, F.R.).
Biological results obtained by D1-mission N89-23732
BOSTON UNIV., MA.
Symbolic analysis of multivariable missile systems
[AD-A206326] N89-24132
A self consistant model of the three phase interstellar medium in disk galaxies N89-24245
BRITISH BROADCASTING CORP., KINGSWOOD (ENGLAND).
Investigation of mutual interference between digitally modulated signals
[BBC-RD-1988/13] N89-23745
BROOKHAVEN NATIONAL LAB., UPTON, NY.
Quasielastic and inelastic spin fluctuations in superconducting La2-xSrxCuO4
[DE89-008157] N89-24190

C

CALIFORNIA UNIV., BERKELEY.
Fire propagation in concurrent flows
[PB89-151781] N89-23636
Spectra and dynamics of young stellar objects N89-24234
Spectral observations of the extreme ultraviolet background N89-24259
CALIFORNIA UNIV., BERKELEY. LAWRENCE BERKELEY LAB.
Atomic imaging and microanalysis of ceramics
[DE89-008172] N89-23684
Ultra-high resolution VUV-XUV laser: Application to the hyperfine study of krypton
[DE89-009059] N89-23863
Site occupancy/valence measurements using channelling and related effects in microanalysis
[DE89-007658] N89-24186
CALIFORNIA UNIV., DAVIS.
High angle-of-attack aerodynamic characteristics of crescent and elliptic wings
[NASA-CR-184992] N89-23418
A numerical scheme to solve unsteady and variable density low Mach number flows N89-23419
CALIFORNIA UNIV., IRVINE.
Fundamental studies on spray combustion and turbulent combustion
[AD-A206438] N89-23651
Exploring the episodic structure of algebra story problem solving: Revision
[AD-A206403] N89-24122
CALIFORNIA UNIV., LOS ANGELES.
Attenuation measurement of very low-loss dielectric waveguides by the cavity resonator method in the millimeter/submillimeter wavelength range
[AD-A206458] N89-23803
Computer-based modeling environments
[AD-A205328] N89-24064
Knowledge representation using Structured Modeling N89-24224
CALIFORNIA UNIV., SANTA BARBARA.
Energy disposal in ion-molecule reactions
[AD-A205987] N89-24144
CARNEGIE-MELLON UNIV., PITTSBURGH, PA.
Fundamental studies of beta phase decomposition modes in titanium alloys
[AD-A205296] N89-23665
Mechanism of the initiation of the cationic polymerization of styrenes by silanes and activated covalent esters
[AD-A206502] N89-23708
Human-machine interaction considerations for interactive software
[AD-A206574] N89-24049
The state of software engineering practice: A preliminary report
[AD-A206573] N89-24075
CASE WESTERN RESERVE UNIV., CLEVELAND, OH.
An experimental study of opposed flow diffusion flame extinction over a thin fuel in microgravity
[NASA-CR-182185] N89-23638
Finite element modeling of frictionally restrained composite interfaces
[NASA-CR-182281] N89-23918
CENTER FOR NIGHT VISION AND ELECTRO-OPTICS, FORT BELVOIR, VA.
Night vision goggles (AN/PVS-7) performance issues and answers
[AD-A206117] N89-24047
CENTER FOR RESEARCH AND DEVELOPMENT OF MATERIALS, SARAJEVO (YUGOSLAVIA).
Microstructure development in SiC N89-23582
CENTRE DE RECHERCHES ET D'ETUDES OCEANOGRAPHIQUES, LA ROCHELLE (FRANCE).
Study of a method to de-alias winds from ERS-1 data
[CREO-6374] N89-24003
CHEMICAL RESEARCH AND DEVELOPMENT CENTER, ABERDEEN PROVING GROUND, MD.
A user's guide to the Molecular Modeling, Analysis and Display System (MMADS), 2nd edition
[AD-A205674] N89-23648
CHRISTOPHER NEWPORT COLL., NEWPORT NEWS, VA.
An investigation of the temperature dependence of the ultrasonic properties of AS4/Ixan and XAS/Ixan composites
[NASA-CR-184845] N89-23619
CINCINNATI UNIV., OH.
X-ray absorption spectroscopy of electrochemically generated species
[AD-A205572] N89-23647
CITY OF HOPE MEDICAL CENTER, DUARTE, CA.
Long term synaptic plasticity and learning in neuronal networks
[AD-A205993] N89-24038
CITY UNIV., LONDON (ENGLAND).
Automatic analysis of holographic interferograms N89-23848
CLEMSON UNIV., SC.
Research needs in ceramic machining
[PB89-148191] N89-23681
Studies of frontal zone dynamics with a high-resolution wind profiling system
[AD-A205988] N89-24008
COLLEGE OF EASTERN MONTANA, BILLINGS.
Study of the infrared celestial background
[AD-A205649] N89-24237
COLORADO UNIV., BOULDER.
Computation of dynamics and control of unsteady vortical flows N89-23822
COLORADO UNIV., DENVER.
Human adaptation to the Tibetan Plateau
[AD-A206463] N89-24031
Fast algorithms for partial differential equations on advanced computers
[AD-A206469] N89-24073
COLUMBIA UNIV., NEW YORK, NY.
Investigation of three-dimensional mesh generation with precise controls
[AD-A205967] N89-23773
COMPLERE, INC., PALO ALTO, CA.
Turbulent shear stress measurement in hypersonic flow
[AD-A206453] N89-23432
COMPUTAS EXPERT SYSTEMS A/S, KOKKEDAL (DENMARK).
Direct dissemination of data from ESA's future in-orbit infrastructure
[DDD-CP/TE-RE-7450] N89-23754
COMPUTER RESOURCE MANAGEMENT, INC., VIENNA, VA.
National Airspace System Search and Rescue operational concept (NAS-SR-1329)
[DOT/FAA/DS-89/07] N89-23435
CONNECTICUT UNIV., STORRS.
The mechanisms of biodegradation of synthetic polymers
[AD-A205628] N89-23699
CONTINUUM DYNAMICS, INC., PRINCETON, NJ.
Enhancements to a new free wake hover analysis
[NASA-CR-177523] N89-23414
CORNELL UNIV., ITHACA, NY.
Simple adsorbates on transition metal surfaces: A joint chemical and physical approach
[AD-A205726] N89-23669
The role of order in distributed programs
[AD-A206037] N89-24065
Experimental and theoretical studies of dense fluid mixtures
[DE89-008882] N89-24214
Relativistic and non-relativistic magnetohydrodynamic flows around compact stars N89-24242

D

DAVID SARNOFF RESEARCH CENTER, PRINCETON, NJ.
High-power single spatial mode AlGaAs channeled-substrate-planar semiconductor diode lasers for spaceborne communications
[NASA-CR-4238] N89-23860
DEFENCE RESEARCH ESTABLISHMENT OTTAWA, (ONTARIO).
Link availability and rain attenuation exceedance characteristics for EHF (Extremely High Frequency) satellite communications with arbitrary link parameters in Canada
[AD-A205403] N89-23762
A statistical analysis of the output signals of an acousto-optic spectrum analyzer for CW (Continuous-Wave) signals
[AD-A205404] N89-23763
The performance of Space-Based Radars (SBR) orbiting on elliptical orbits
[AD-A205951] N89-23772
The concept and theoretical considerations of a cold weather clothing system
[AD-A205476] N89-24046
Computer-aided design and bio-engineering: A review of the literature
[AD-A206534] N89-24074
DEFENCE RESEARCH ESTABLISHMENT SUFFIELD, RALSTON (ALBERTA).
Design of a chamber for CBW aerosol studies with relative humidity and particle concentration control
[AD-A205623] N89-23481
Electromagnetic remote sensing. Low frequency electromagnetics
[AD-A205402] N89-23761
DEFENSE LOGISTICS SERVICES CENTER, BATTLE CREEK, MI.
Defense Integrated Data System (DIDS) procedures manual. Volume 8: Document Identifier Code (DIC) Input/Output (I/O) formats (fixed length), change 3
[PB89-139414] N89-24220
Defense Integrated Data System (DIDS) procedures manual. Volume 2: Multiple application procedures
[PB89-139307] N89-24221
DEFENSE MAPPING AGENCY, WASHINGTON, DC.
Problems encountered in the Stokes' numerical integration of terrestrial gravity anomalies
[AD-A205448] N89-23990
DELTA INFORMATION SYSTEMS, INC., HORSHAM, PA.
Investigation of optical compression techniques for dither coding
[AD-A206140] N89-23776
DEPARTMENT OF ENERGY, WASHINGTON, DC.
Electric and Hybrid Vehicles Program: Report to Congress
[DE89-008988] N89-23879
DEPARTMENT OF THE ARMY, WASHINGTON, DC.
Superconducting PYX structures
[AD-D013958] N89-24202
DEPARTMENT OF THE NAVY, WASHINGTON, DC.
Actuator rate saturation compensator
[AD-D013962] N89-23474
An elastomeric electrical isolation membrane
[AD-D013966] N89-23702
Utilization of magnetostrictive optical fibers in multiple order gradiometers
[AD-D013960] N89-24155
DEUTSCHE FORSCHUNGS- UND VERSUCHSANSTALT FUER LUFT- UND RAUMFAHRT, COLOGNE (GERMANY, F.R.).
Summary of 1st Summer School on Microgravity
[DFVLR-IB-333-87/2] N89-23719
Mission conditions and hardware concepts N89-23720

Microgravity User Support Center (MUSC) N89-23721
Convection N89-23723
Diffusion N89-23724
Phase transformation N89-23725
Nucleation and undercooling N89-23726
Metallic solidification N89-23727
Semiconductors and monocrystal growth: Collection of charts, formulas and references N89-23729
Microgravity conditions of a spacecraft N89-23731

DEUTSCHE GEODAETISCHE KOMMISSION, MUNICH (GERMANY, F.R.).
Analysis and optimization of geodetic networks by spectral criteria and mechanical analogies
[SER-C-342] N89-23963

DHV RAADGEVEND INGENIEURSBUREAU B.V., AMERSFOORT (NETHERLANDS).
On the international commercialization of remote sensing
[BCRS-88-02] N89-23969

DORNIER-WERKE G.M.B.H., FRIEDRICHSHAFEN (GERMANY, F.R.).
Design and verification of mechanisms for a large foldable antenna N89-23899

DOUGLAS AIRCRAFT CO., INC., LONG BEACH, CA.
Interior noise control ground test studies for advanced turboprop aircraft applications
[NASA-CR-181819] N89-24141

DRAPER (CHARLES STARK) LAB., INC., CAMBRIDGE, MA.
Avionics architecture studies for the entry research vehicle
[NASA-CR-181828] N89-24082

DREXEL UNIV., PHILADELPHIA, PA.
Spray deposition: A fundamental study of droplet impingement, spreading and consolidation
[AD-A206065] N89-23672

DUKE UNIV., DURHAM, NC.
Monitoring information processing and decisions: The MOUSELAB system
[AD-A205963] N89-24037
The impact of accuracy and effort feedback and goals on adaptive decision behavior
[AD-A205751] N89-24095

E

EDGERTON, GERMESHAUSEN AND GRIER, INC., IDAHO FALLS, ID.
Applications of a digital acoustic-emission data-acquisition workstation
[DE89-009648] N89-23923

EG AND G MOUND APPLIED TECHNOLOGIES, MIAMISBURG, OH.
Epoxylite 8822 hardness study
[DE89-008961] N89-23687

ENVIRONMENTAL PROTECTION AGENCY, ANN ARBOR, MI.
Sample preparation techniques for evaluating methanol and formaldehyde emissions from methanol fueled vehicles and engines
[PB89-136147] N89-23734
Methanol vehicle catalyst evaluation, phase 3
[PB89-136139] N89-23874

ENVIRONMENTAL PROTECTION AGENCY, RESEARCH TRIANGLE PARK, NC.
Summary of selected new information on effects of ozone on health and vegetation. Draft supplement to air quality criteria for ozone and other photochemical oxidants
[PB89-135123] N89-23980

ENVIRONMENTAL PROTECTION AGENCY, WASHINGTON, DC.
Local area network technical guidelines. Volume 1: LAN design and planning (LAN TSR process)
[PB89-139091] N89-24080
Geographic Information Systems (GIS) guidelines document
[PB89-132062] N89-24222

ENVIRONMENTAL RESEARCH INST. OF MICHIGAN, ANN ARBOR.
Heuristics for cooperative problem solving
[AD-A206371] N89-24096

EUROCONSULT B.V., ARNHEM (NETHERLANDS).
On the international commercialization of remote sensing
[BCRS-88-02] N89-23969

EUROPEAN SPACE AGENCY, PARIS (FRANCE).
ESABASE: A most versatile and flexible system engineering tool
[ESA-BR-54] N89-24223
Space debris: A report from the ESA Debris Working Group
[ESA-SP-1109] N89-24230

EUROPEAN SPACE AGENCY. EUROPEAN SPACE RESEARCH AND TECHNOLOGY CENTER, ESTEC, NOORDWIJK (NETHERLANDS).
The evolution of space mechanisms in the ESA R and D program N89-23893

EUROPEAN SPACE TRIBOLOGY LAB., RISLEY (ENGLAND).
The in-vacuo torque performance of dry-lubricated ball bearings at cryogenic temperatures N89-23914

F

FEDERAL AVIATION ADMINISTRATION, ATLANTIC CITY, NJ.
Loran C field strength contours: Contiguous US
[DOT/FAA/CT-TN89/16] N89-23437
Instrument landing system mathematical modeling study for Orlando International Airport Runway 35L localizer, Orlando, Florida. Final airside docking plan (Scheme 3A)
[AD-A205351] N89-23438
Heliport night parking area criteria test plan
[DOT/FAA/CT-TN88/45] N89-23480
Host computer system capacity management procedures
[AD-A193416] N89-24051

FERMI NATIONAL ACCELERATOR LAB., BATAVIA, IL.
On the algebraic structure of integrable systems in multidimensions
[DE89-008697] N89-24108
The formation of topological defects in phase transitions
[NASA-CR-185318] N89-24215

FLORIDA STATE UNIV., GAINESVILLE.
Sorption of selected volatile organic constituents of jet fuels and solvents on natural sorbents from gas and solutions phases
[AD-A204073] N89-23711

FLORIDA UNIV., GAINESVILLE.
Spectroscopic studies of metal-ligand-surface interactions
[AD-A206460] N89-23652
Donor acceptor polymerization chemistry as a vehicle to low energy cure of matrix resins: Evolution of the 2-Tg concept to produce Tg polymers at ambient temperatures
[AD-A206287] N89-23706
Environmental interactions of hydrazine fuels in Soil/Water systems
[AD-A206244] N89-23986
Advanced space design program to the Universities Space Research Association and the National Aeronautics and Space Administration
[NASA-CR-180450] N89-24015
Variable plant spacing N89-24016
Automated seed manipulation and planting N89-24017
Plant health sensing N89-24018
Microgravity particle reduction system N89-24019
Automated seed manipulation and planting N89-24020
Non-destructive plant health sensing using absorption spectroscopy N89-24021

FORD AEROSPACE AND COMMUNICATIONS CORP., PALO ALTO, CA.
Design of a 60 GHz beam waveguide antenna positioner N89-23910

FREIBURG UNIV. (GERMANY, F.R.).
Organic monocrystals N89-23730

G

GENERAL ATOMICS TECHNOLOGIES CORP., SAN DIEGO, CA.
High-temperature ceramic superconductors
[AD-A205321] N89-24196

GENERAL DYNAMICS CORP., FORT WORTH, TX.
USAF (US Air Force) durability design handbook: Guidelines for the analysis and design of durable aircraft structures
[AD-A206286] N89-23457

GENERAL DYNAMICS CORP., SAN DIEGO, CA.
Pyro thruster for performing rocket booster attachment, disconnect, and jettison functions N89-23902

GENERAL ELECTRIC CO., CINCINNATI, OH.
High speed turboprop aeroacoustic study (single rotation). Volume 1: Model development
[NASA-CR-182257-VOL-1] N89-24139

GENERAL ELECTRIC CO., MOFFETT FIELD, CA.
Gas-Grain Simulation Facility: Fundamental studies of particle formation and interactions. Volume 1: Executive summary and overview
[NASA-CP-10026-VOL-1] N89-24022
Gas-Grain Simulation Facility: Fundamental studies of particle formation and interactions. Volume 2: Abstracts, candidate experiments and feasibility study
[NASA-CP-10026-VOL-2] N89-24023

GENERAL ELECTRIC CO., PHILADELPHIA, PA.
Final safety analysis report for the Galileo Mission. Volume 1: Reference design document
[DE89-007268] N89-24147

GEO-CENTERS, INC., FORT WASHINGTON, MD.
The dynamic behavior of water vapor on activated carbon
[AD-A206124] N89-23628

GEORGIA INST. FOR RESEARCH, ATLANTA.
Ultrafine microstructure composites prepared by chemical vapor deposition
[AD-A206061] N89-23627

GEORGIA INST. OF TECH., ATLANTA.
Pulsating catalytic combustion of gaseous fuels N89-23643
An ICAI (Intelligent Computer Aided Instruction) architecture for troubleshooting in complex dynamic systems
[AD-A205434] N89-24045

GEORGIA TECH RESEARCH INST., ATLANTA.
Electron spectroscopy for chemical analysis: Sample analysis
[NASA-CR-183568] N89-23634

GEORGIA UNIV., ATHENS.
Memory functions and relaxation functions of some spin systems
[AD-A206340] N89-24137

GKSS-FORSCHUNGSZENTRUM GEESTHACHT (GERMANY, F.R.).
Optical properties of oceanic suspended matter and their interpretation for remote sensing of phytoplankton
[GKSS-88/E/40] N89-24013
Imaging procedure of underwater bottom topography by air and satellite images in the range of microwave and visible electromagnetic spectra
[GKSS-88/E/41] N89-24014

GORDON RESEARCH CONFERENCES, INC., KINGSTON, RI.
Report on the partial support of the 1988 Gordon Conference on Polymers (West)
[AD-A205834] N89-23701

H

HEIDELBERG UNIV. (GERMANY, F.R.).
Calibration measurements on micrometeorite detectors for the missions ULYSSES, Galileo and Giotto
[ETN-89-93947] N89-24248

HELSINKI UNIV. OF TECHNOLOGY, ESPOO (FINLAND).
Fabrication and properties of alumina-zirconia composites
[PB89-147532] N89-23620
Critical assessment of the thermodynamic properties of antimony-copper alloys
[PB89-147524] N89-23657
Application of an exact finite element method to analysis of statics of thin elastic shells of revolution with axisymmetric loading
[ISBN-952-900-399-4] N89-23917
Determination of areal snow water equivalent using satellite images and gamma ray spectrometry
[CI-91] N89-23960
Polarizability and effective permittivity of layered and continuously inhomogeneous dielectric ellipsoids
[PB89-146476] N89-24102
Nuclear magnetism in copper and silver: Theory and experiments
[ISBN-952-900-084-7] N89-24188
Magnetic susceptibility and neutron diffraction experiments on nuclear ordering in copper
[ISBN-951-754-573-8] N89-24189

HERSH ACOUSTICAL ENGINEERING, CHATSWORTH, CA.
Flow-turning losses in solid rocket motors
[AD-A206099] N89-23525

HIMEJI INST. OF TECH. (JAPAN).
Sheath and presheath in a collisionless open field plasma
[IPPJ-890] N89-24161

HONEYWELL, INC., BLOOMINGTON, MN.
A designers' guide to reliable distributed systems: An example design. Volume 1
[AD-A206039] N89-23885
A designers' guide to reliable distributed systems: An example design. Volume 2
[AD-A206040] N89-23886

HONEYWELL, INC., PHOENIX, AZ.
Signal and power roll ring testing update N89-23909

HONEYWELL SPACE AND AVIATION SYSTEMS, DURHAM, NC.
Eddy current damper N89-23900

HORIZONS TECHNOLOGY, INC., OAKTON, VA.
An analysis of Electronic Aids to Maintenance (EAM) for the Light Helicopter Family (LHX)
[AD-A205440] N89-23407

I

I.A.M. RINALDO PIAGGIO, FINALE LIGURE (ITALY).
Design and testing of a deployable, retrievable boom for space applications N89-23898
IAP RESEARCH, INC., DAYTON, OH.
Long pulse homopolar generator
[AD-A205452] N89-23977
ICI-TENSA SERVICES, HOUSTON, TX.
Process integration methodology for natural gas-fueled heat pumps and cogeneration systems
[PB89-140867] N89-23811
ILLINOIS UNIV., CHICAGO.
Geometrical foundations of mesomechanics and Lagrangian formalism
[AD-A205589] N89-23930
ILLINOIS UNIV., URBANA.
Electromagnetic railgun hydrogen pellet injector: Progress and prospect
[DE89-009536] N89-23499
Theta pinch discharges for solids vaporization and elemental chemical analysis
[DE89-008888] N89-23641
Recursive gate-arrays
[AD-A205335] N89-23796
Explanation-based theory revision: An approach to the problems of incomplete and incorrect theories
[AD-A205337] N89-24092
Differential algebraic equations, indices, and integral algebraic equations
[DE89-009584] N89-24109
Some 3-5 heterojunction structures and high speed devices
[AD-A205946] N89-24203
INDIANA UNIV., BLOOMINGTON.
Fiber-optic time-resolved fluorescence sensor for the simultaneous determination of Al(+3), Ga(+3) and In(+3)
[AD-A205689] N89-24154
Noise characteristics of an inductively coupled plasma-mass spectrometer
[AD-A205686] N89-24169
Flow-injection analysis utilizing a spectrally segmented photodiode-array inductively coupled plasma emission spectrometer. 1: Microcolumn preconcentration for the determination of molybdenum
[AD-A205687] N89-24170
Use of a spectrally segmented photodiode-array spectrometer for inductively coupled plasma atomic emission spectroscopy
[AD-A205688] N89-24171
Preliminary evaluation of a miniaturized torch for inductively coupled plasma mass spectrometry
[AD-A205746] N89-24173
Simultaneous measurement of spatially resolved electron temperatures. Electron number densities and gas temperatures by laser light scattering from the ICP
[AD-A205747] N89-24174
INFORMATION AND CONTROL SYSTEMS, INC., HAMPTON, VA.
Optimal aeroassisted coplanar orbital transfer using an energy model
[NASA-CR-181778] N89-23495
INFORMATION RESEARCH ASSOCIATES, INC., AUSTIN, TX.
A designers' guide to reliable distributed systems: An example design. Volume 1
[AD-A206039] N89-23885
A designers' guide to reliable distributed systems: An example design. Volume 2
[AD-A206040] N89-23886
INSTITUT FRANCO-ALLEMAND DE RECHERCHES, SAINT-LOUIS (FRANCE).
Development of a CARS device for a feasibility study of density and temperature measurements at high time dependent resolution
[ISL-R-117/87] N89-23654
Analogy between explosive wave and front wave near curved walls
[ISL-CO-209/87] N89-23840
Boundary layer and heat transfer behind a piston in a shock tube. Part 1: Theoretical considerations of laminar and turbulent boundary layer behind a piston in a tube
[ISL-R-111/87-PT-1] N89-23841
Boundary layer and heat transfer behind a piston in a shock tube. Part 2: Experimental study of heat transfer at the piston in a tube
[ISL-R-115/87-PT-2] N89-23842
Numerical solution of the three dimensional heat flow equation generated by a moving source
[ISL-R-116/87] N89-23843
Numerical modeling of laser produced plasmas and laser induced pressure effects
[ISL-CO-244/87] N89-24177
INSTITUT FUER ANGEWANDTE GEODAESIE, FRANKFURT AM MAIN (GERMANY, F.R.).
Reports on Cartography and Geodesy. Series 1, number 101
[ISSN-0469-4236] N89-23941
Definition and filling of information systems: Challenge for a photogrammetric service enterprise N89-23942
Computer aided production of a 1:25,000 relief model of Berlin and surroundings N89-23943
The Official Topographic-Cartographic Information System (ATKIS) of the Geodesy Group of the Laender of the Federal Republic of Germany: Status after one year of development N89-23944
The digital urban map as a basis for a land information system in local administration N89-23945
Automatic digitizing of cadastral maps N89-23946
ARC-INFO: A geographic information system N89-23947
Cartographic signatures in PHOCUS N89-23948
Digitizing of drawings and cadastral maps using a scanner system N89-23949
Geocoded data sets of imaging satellites N89-23950
Computer assisted layout of graphic settlement representations N89-23951
Tools for the computer assisted generalization of settlements for the construction of digital landscape models N89-23952
Computer assisted generalization of transport line representations N89-23953
Hybrid cartographic data processing in a geographic information system N89-23954
Automatic extraction of areas from overlays of the series DGK 5 (Bo) N89-23955
INSTITUT ZA NUKLEARNE NAUKE BORIS KIDRIC, BELGRADE (YUGOSLAVIA).
Slip casting of fused silica N89-23573
Sintering of CaO and MgO in the presence of nonequilibrium liquid phase N89-23580
Sintering of Si3N4 in the presence of additives from Y2O3-SiO2-Al2O3 system N89-23581
Phase transformation of Zr(x)Hf(1-x)O2 in alumina matrix N89-23588
Preparation and properties of high strength carbon fibers N89-23589
INSTITUTE FOR COMPUTER APPLICATIONS IN SCIENCE AND ENGINEERING, HAMPTON, VA.
Numerical simulation of Goertler/Tollmein-Schlichting wave-interaction
[NASA-CR-181823] N89-23817
Compiling high level constructs to distributed memory architectures
[NASA-CR-181825] N89-24058
Inverse problem techniques for beams with tip body and time hysteresis damping
[NASA-CR-181833] N89-24112
Operator induced multigrid algorithms using semirefinement
[NASA-CR-181834] N89-24113
Shape identification technique for a two-dimensional elliptic system by boundary integral equation method
[NASA-CR-181831] N89-24114
INSTITUTE FOR DEFENSE ANALYSES, ALEXANDRIA, VA.
IDA (Institute for Defense Analyses) gamma-ray laser: Investigation of the feasibility of developing a laser using nuclear transitions
[AD-A205318] N89-23864
IDA (Institute for Defense Analyses) gamma-ray laser: Investigation of developing a laser using nuclear transitions
[AD-A205319] N89-23865
INTERNATIONAL CENTRE FOR THEORETICAL PHYSICS, TRIESTE (ITALY).
Nonlinear singular elliptic equations
[DE88-705691] N89-24103
The diluted tri-dimensional spin-one Ising model with crystal field interactions
[DE88-705663] N89-24181
Mean field theory of the spin-1 Ising model with a random crystal field
[DE88-705669] N89-24182
Electrical transport properties of Hg0.7Cd0.3Te
[DE88-705689] N89-24183
Cohesive and anharmonic elastic properties of mixed fluorite crystals
[DE88-705690] N89-24184
The electronic structure of GaAs sub 1-x P sub x and GaSb sub 1-x P sub x calculated using the recursion method
[DE88-705702] N89-24185
IOWA STATE UNIV. OF SCIENCE AND TECHNOLOGY, AMES.
Three dimensional high speed boundary layer flows
[AD-A206145] N89-23837

J

JAYCOR, VIENNA, VA.
Operation of a quasi-optical gyrotron with variable mirror separation
[AD-A206347] N89-23854
JET PROPULSION LAB., CALIFORNIA INST. OF TECH., PASADENA.
Current distribution in a three-dimensional IC analyzed by a perturbation method. Part 1: A simple steady state theory
[NASA-CR-185022] N89-23494
Effects of the contamination environment on surfaces and materials N89-23546
An overview of charging environments N89-23554
Contamination N89-23559
Design and development of a high-stiffness, high-resolution torque sensor N89-23903
Flight telerobot mechanism design: Problems and challenges N89-23907
Environmental projects. Volume 3: Environmental compliance audit
[NASA-CR-185019] N89-23985
Observation model and parameter partials for the JPL geodetic GPS modeling software GPSOMC
[NASA-CR-185021] N89-24060
MPD thruster erosion research
[NASA-CR-185314] N89-24168
JOINT INST. FOR LAB. ASTROPHYSICS, BOULDER, CO.
Redistribution in astrophysically important hydrogen lines
[NASA-CR-181375] N89-24251
JOINT INST. FOR NUCLEAR RESEARCH, DUBNA (USSR).
Capture and confinement of solutions in nonlinear integrable systems
[DE88-705823] N89-24106
Equations for two-dimensional density matrix. Approximate solutions in the vicinity of the classical solution
[DE88-705825] N89-24107
JOINT PUBLICATIONS RESEARCH SERVICE, ARLINGTON, VA.
JPRS report: Science and technology. USSR: Space
[JPRS-USP-89-004] N89-23484
Buran dimensions, landing sit facilities N89-23485
Details of Buran shuttle flight N89-23486
Design features, flight monitoring of Buran N89-23487
Buran designer Semenov interviewed N89-23488
Commentary on flight of Buran shuttle by designers Glushko and Semenov N89-23489
Buran space shuttle described by engineer N89-23490
Orbit parameters given N89-23491
Medical and biological support for a manned expedition to Mars N89-23492

K

KANSAS UNIV., LAWRENCE.
A correlation study of X-29A aircraft and associated analytical developments N89-23450
KANSAS UNIV. CENTER FOR RESEARCH, INC., LAWRENCE.
Detailed design of a Ride Quality Augmentation System for commuter aircraft
[NASA-CR-4230] N89-23470
KARLSRUHE UNIV. (GERMANY, F.R.).
Silicon-carbide made of silicon-organic compounds N89-23572
Fatigue in ceramics N89-23583
Wear resistant sintered steel with high carbide content N89-23607
Metallically conducting polymers: The limiting effect of conjugation defects on the electrical conductivity, a polyacetylene example
[ETN-89-93950] N89-23710
Dynamic interaction between fluids and solids
[ETN-89-93948] N89-23937
Research for optimization of future MOMS sensors
[ETN-89-94424] N89-23972
Analysis of turbulent motion phenomena in the maritime atmospheric boundary layer
[ETN-89-93949] N89-23996

KERNFORSCHUNGSANLAGE, JUELICH (GERMANY, F.R.).
The 8th German-Yugoslav Meeting on Materials Science and Development: Ceramics and Metals
[JUEL-SPEZ-446] N89-23569
Materials science cooperation in 1987 N89-23570
Preparation and thermal expansion of Al2TiO5-TiO5-TiO2 sintered bodies N89-23578
Young's modulus of elasticity: Measured values for multiphase metals and their calculation via the bound concept N89-23584
Corrosion of silicon carbide ceramics at high temperatures in water vapor-containing atmospheres N89-23594
Ionization investigation of sputtered titanium and of titanium ion transport process in an argon discharge glow using laser induced fluorescence
[JUEL-2219] N89-23660
Evaluation of the historical Schoenbein method for the determination of ozone in a flow chamber
[JUEL-2218] N89-23983
Microscopic theory of electron spin resonance in Heisenberg spin glasses and thermal fluctuations in classical spin models with random fields
[JUEL-2227] N89-24146
Structure and grid dynamics of ultrathin epitaxial Ag and Fe films on Ni(100) and Cu(100) substrates
[JUEL-2221] N89-24187
Investigation of electronic states in nonmagnetic single crystals with spin-resolved photoemission
[JUEL-2228] N89-24212
KERNFORSCHUNGSZENTRUM G.M.B.H., KARLSRUHE (GERMANY, F.R.).
Advanced layer materials N89-23587
Preparation, characterization and thermal diffusivity of Al2TiO5 N89-23591
Dilatometric analysis of Al-, Ba-, Ca-titanate N89-23592
On the correlation between microstructure and magnetic induction of porous iron and iron-Ni(0.4)Zn(0.6)Fe2O4 composites N89-23606
KRUG INTERNATIONAL, SAN ANTONIO, TX.
Additivity of retinal damage for multiple-pulse laser exposures
[AD-A206514] N89-24032

L

LAWRENCE LIVERMORE NATIONAL LAB., CA.
Pulse shaping on the Nova laser system
[DE89-008026] N89-23859
Effect of n on 1 laser treatment on damage threshold of selected optical coating
[DE89-008830] N89-23861
Use of the 1:2,000,000 Digital Line Graph data in emergency response
[DE89-006730] N89-23959
A description of the slab model
[DE89-009962] N89-23984
Characterization of multilayer coated concave diffraction gratings in the extreme ultraviolet
[DE89-008831] N89-24151
Temporally smooth broadband pulses obtained by cross phase modulation in an optical fiber
[DE89-008891] N89-24152
Shock compaction of YBa2Cu3O7-x and HoBa2Cu3O7-x powders in a metal matrix
[DE89-008827] N89-24193
Engineering thrust areas, 1989
[DE89-009009] N89-24229
Compact source origin of cosmic ray antiprotons
[DE89-008044] N89-24258
LEEDS UNIV. (ENGLAND).
Studies of internal gravity waves in the stably stratified troposphere N89-23989
LEHIGH UNIV., BETHLEHEM, PA.
Cracking of a layered medium on an elastic foundation under thermal shock
[NASA-CR-185316] N89-23925
The crack problem in bonded nonhomogeneous materials
[NASA-CR-184897] N89-23926
The mode 3 crack problem in bonded materials with a nonhomogeneous interfacial zone
[NASA-CR-185315] N89-23927
Cracking of coated materials under transient thermal stresses
[NASA-CR-184898] N89-23928
LITTLE (ARTHUR D.), INC., CAMBRIDGE, MA.
Propellant reuse/recovery technology
[AD-A206306] N89-23714
LJUBLJANA UNIV. (YUGOSLAVIA).
Injection molding of whisker-reinforced Al2O3-ZrO2 ceramics N89-23574
The wear of cutting tools: The contribution of abrasive wear N89-23586
Investigation of alpha-SiC hot corrosion in the presence of basic slag N89-23595
Microstructure-permeability relation in MnZn ferrites prepared of iron oxide with chlorine impurities N89-23602
Interfacial reactions during cladding of steel by hot rolling N89-23615
Information about hot flow-stress curves and the resulting structural changes N89-23616
LOCKHEED MISSILES AND SPACE CO., PALO ALTO, CA.
SIRTF Telescope Instrument Changeout and Cryogen Replenishment (STICCR) Study
[NASA-CR-177380] N89-23512
Development of a precision, wide-dynamic-range actuator for use in active optical systems N89-23901
LOCKHEED MISSILES AND SPACE CO., SUNNYVALE, CA.
On-orbit observations of single-event upset in harris HM-6508 RAMSs (Random Access Memories): An update
[AD-A206266] N89-23506
LOEWE OPTA G.M.B.H., KRONACH (GERMANY, F.R.).
Tuner for the first intermediate frequency of receivers for direct satellite reception
[ETN-89-93766] N89-23788
LOS ALAMOS NATIONAL LAB., NM.
Theoretical studies of Ni3Al and NiAl with impurities
[DE89-006558] N89-23655
Water-processable conducting polymers
[DE89-009251] N89-23688
Microwave processing of ceramics
[DE89-009350] N89-23690
Direct laser/materials interaction: Laser ablation of superconductor materials and laser welding
[DE89-006560] N89-23857
Vaporization and recondensation in propagation and imaging of laser beams
[DE89-008014] N89-23858
Non-Newtonian gravitational forces and the Greenland ice-sheet experiment
[DE89-009348] N89-23988
Onset conditions for the driven lower hybrid drift instability in an expanding magnetized plasma
[AD-A205505] N89-24167
On the measurement of cosmogenic nuclides in cometary materials
[DE89-009248] N89-24243
An ultra-soft Einstein X-ray survey
[DE89-007993] N89-24256
A search for EUV emission from cataclysmic variables
[DE89-008012] N89-24257
LOUISIANA STATE UNIV., BATON ROUGE.
Solar flares and magnetospheric particles: Investigations based upon the ONR-602 and ONR-604 experiments
[AD-A205599] N89-24253

M

MASSACHUSETTS INST. OF TECH., CAMBRIDGE.
Generation of architectures for distributed intelligence systems
[AD-A205783] N89-23440
An improved strategy for determining earth satellite orbits by radio
[AD-A205826] N89-23497
Generating circuit tests by exploiting designed behavior
[AD-A206175] N89-23800
Path dependent morphologies of a diblock copolymer of Polystyrene/Hydrogenated polybutadiene
[AD-A206504] N89-23883
The role of knowledge in visual shape representation
[AD-A206173] N89-24041
Criteria for robust stability in a class of lateral inhibition networks coupled through resistive grids
[AD-A204174] N89-24081
Three-dimensional recognition of solid objects from a two-dimensional image
[AD-A205667] N89-24094
On the communication complexity of distributed algebraic computation
[AD-A205784] N89-24117
Numerical conformal mapping and applications
[AD-A205602] N89-24131
Liquid dynamic compaction of Fe-Nd-B permanent magnets
[AD-A205632] N89-24135
Grain boundaries
[DE89-006881] N89-24194
MASSACHUSETTS INST. OF TECH., LEXINGTON.
ASR-9 weather channel test report, executive summary
[DOT/FAA/PS-89/6-EXEC-SUMM] N89-23758
Prospects for classifying complex imagery using a self-organizing neural network
[AD-A206208] N89-24088
MASSACHUSETTS UNIV., AMHERST.
Cellular and molecular approaches to polymer synthesis by bacteria
[AD-A206395] N89-23707
In situ mechanistic studies of MOCVD growth of 3/5 semiconductors
[AD-A206396] N89-24210
MAX-PLANCK-GESELLSCHAFT, PLOEN (GERMANY, F.R.).
Oxygen interaction with metal surfaces: Surface science approach N89-23596
MAX-PLANCK-INST. FUER METALLFORSCHUNG, STUTTGART (GERMANY, F.R.).
Ceramic Project of the Max-Planck Society N89-23571
Sintering and HIPing with additives N89-23575
Strengthening of silicon nitride ceramics N89-23585
Thermal transport in pressureless sintered aluminum nitride N89-23590
Cooling rate, undercooling and rapid solidification by atomization N89-23609
Mechanical properties of gas atomized Cu-Ti and Cu-Ti-B alloys N89-23610
Intermetallic phases for high temperature applications N89-23612
MAX-PLANCK-INST. FUER PHYSIK UND ASTROPHYSIK, GARCHING (GERMANY, F.R.).
Assessment of surface topography by X-ray scattering measurements
[MPE-PREPRINT-134] N89-24159
Time and spectral variability of the low mass X-ray binaries
[MPE-REPORT-210] N89-24238
Grazing incidence telescopes for ESA's X-ray astronomy mission XMM
[MPE-PREPRINT-129] N89-24239
MAX-PLANCK-INST. FUER PLASMAPHYSIK, GARCHING (GERMANY, F.R.).
Transport of test particles in a magnetic field with perturbed magnetic surfaces
[IPP-2/296] N89-24176
MCDONNELL AIRCRAFT CO., SAINT LOUIS, MO.
Low energy consumption hydraulic techniques
[AD-A206285] N89-23743
MCDONNELL-DOUGLAS CORP., LONG BEACH, CA.
Crew procedures and workload of retrofit concepts for microwave landing system
[NASA-CR-181700] N89-24033
METRAFLU, ECULLY (FRANCE).
A simple approximate method to evaluate the 3-D aerodynamic field around a streamline and to determine the validity of the quasi-three dimensional hypothesis
[ETN-89-94366] N89-23844
MICHIGAN UNIV., ANN ARBOR.
The structural basis for fatigue initiation in glassy polymers
[DE89-009292] N89-23689
Mapping freeze/thaw boundaries with SMMR data
[NASA-CR-184991] N89-23961
Population inversions in ablation plasmas generated by intense electron beams
[AD-A205716] N89-24172
MICROCOSM, INC., TORRANCE, CA.
Autonomous navigation and control
[AD-A205898] N89-23441
MISSION RESEARCH CORP., NEWINGTON, VA.
Operation of a quasi-optical gyrotron with variable mirror separation
[AD-A206347] N89-23854
MISSION RESEARCH CORP., SAN DIEGO, CA.
Radiation effects in spacecraft electronics N89-23531
MISSOURI UNIV., COLUMBIA.
Normal mode energetics of the general circulation during the FGGE year N89-24004
MITRE CORP., BEDFORD, MA.
AN/TAC-1 demultiplexer circuit card assembly
[AD-A205744] N89-23770
MORTON THIOKOL, BRIGHAM CITY, UT.
Qualification Motor no. 8 (QM-8), volume 1
[NASA-CR-183650] N89-23523
MOTOREN- UND TURBINEN-UNION MUENCHEN G.M.B.H. (GERMANY, F.R.).
Cyclic crack propagation characteristics of the powder metallurgical nickel-base alloy Udimet 720 at elevated temperatures and different dwell times
[ETN-89-94426] N89-23938

N

NAGOYA UNIV. (JAPAN).
Sheath and presheath in a collisionless open field plasma
[IPPJ-890] N89-24161
Eikonal approximation in partial wave version
[IPPJ-899] N89-24164

NAPLES UNIV. (ITALY).
The diluted tri-dimensional spin-one Ising model with crystal field interactions
[DE88-705863] N89-24181

NATIONAAL INST. VOOR KERNFYSICA EN HOGE ENERGIEFYSICA, AMSTERDAM (NETHERLANDS).
Strong and electromagnetic interactions in heavy exotic atoms
[PB89-145718] N89-24143

NATIONAL ACADEMY OF SCIENCES - NATIONAL RESEARCH COUNCIL, WASHINGTON, DC.
NASA space communications R and D (Research and Development): Issues, derived benefits, and future directions
[NASA-CR-184831] N89-23746
A strategy for space biology and medical science for the 1980s and 1990s
[NASA-CR-184895] N89-24024

NATIONAL AERONAUTICAL LAB., BANGALORE (INDIA).
A research facility for film cooling investigations with emphasis on the instrumentation system
[NAL-TM-PR-8704] N89-23477
High pressure studies on infrared detector materials
[NAL-TM-MT-8701] N89-23677
Flosolver: A parallel computer for fluid dynamics
[NAL-TM-AE-8803] N89-23805
Solution of one-dimensional Euler equations by the implicit finite difference technique of Beam and Warming
[NAL-PD-FM-8816] N89-24097
Introduction to irreducible tensor methods, part 1
[NAL-PD-DU-8802] N89-24098
Studies on high-Tc superconducting materials
[NAL-TM-MT-8703] N89-24178

NATIONAL AERONAUTICS AND SPACE ADMINISTRATION, WASHINGTON, DC.
NASA aeronautics research and technology
[NASA-EP-259] N89-23406
Patent abstracts bibliography: A continuing bibliography. Section 2: Indexes (supplement 34)
[NASA-SP-7039(34)-SECT-2] N89-24219
Reports of planetary astronomy, 1989
[NASA-TM-4120] N89-24232
Comet Halley: The view from Pioneer Venus
[NASA-NF-127] N89-24240

NATIONAL AERONAUTICS AND SPACE ADMINISTRATION. AMES RESEARCH CENTER, MOFFETT FIELD, CA.
Digital control of the Kuiper Airborne Observatory telescope
[NASA-TM-101082] N89-23785
Effect of internal convection and internal radiation on the structural temperatures of Space Shuttle Orbiter
[NASA-TM-100414] N89-23819
A numerical study of viscous vortex rings using a spectral method
[NASA-TM-101041] N89-23820
Numerical simulation of flow through an artificial heart
[NASA-TM-102183] N89-24111

NATIONAL AERONAUTICS AND SPACE ADMINISTRATION. GODDARD SPACE FLIGHT CENTER, GREENBELT, MD.
Returned Solar Max hardware degradation study results N89-23537
EnviroNET: Space environment for Strategic Defense Initiative experiments N89-23538
Trapped particle flux models at NSSDC/WDC-A-R/S N89-23561
A reduced version of the NMC DERF 2 data set
[NASA-TM-100727] N89-24002

NATIONAL AERONAUTICS AND SPACE ADMINISTRATION. JOHN F. KENNEDY SPACE CENTER, COCOA BEACH, FL.
Agenda of the Fourth Annual Summer Conference, NASA/USRA University Advanced Design Program
[NASA-TM-101750] N89-23493
Review of wildlife resources of Vandenberg Air Force Base, California
[NASA-TM-102146] N89-23982

NATIONAL AERONAUTICS AND SPACE ADMINISTRATION. LYNDON B. JOHNSON SPACE CENTER, HOUSTON, TX.
Environmental definition of the earth's neutral atmosphere N89-23539
Atomic oxygen effects on spacecraft materials: The state of the art of our knowledge N89-23541
The long-term effects of the micrometeoroid and orbital debris environments on materials used in space N89-23542
Orbital debris environment and data requirements N89-23543
Microparticle impacts in space: Results from Solar Max and shuttle witness plate inspections N89-23544
Atomic oxygen N89-23557
Micrometeoroids and debris N89-23558
Working group written presentation: Atomic oxygen N89-23564
Working group written presentation: Meteoroid/orbital debris effects on materials N89-23565
The design and analysis of a double swivel toggle release mechanism for the Orbiter stabilized payload deployment system N89-23895
A method of up-front load balancing for local memory parallel processors
[NASA-CASE-MSC-21348-1] N89-24084

NATIONAL AERONAUTICS AND SPACE ADMINISTRATION. LANGLEY RESEARCH CENTER, HAMPTON, VA.
Computing induced velocity perturbations due to a helicopter fuselage in a free stream
[NASA-TM-4113] N89-23410
Transonic aerodynamic characteristics of a proposed Assured Crew Return Capability (ACRC) lifting-body configuration
[NASA-TM-4117] N89-23412
Status of sonic boom methodology and understanding
[NASA-CP-3027] N89-23415
Transonic Navier-Stokes solutions of three-dimensional afterbody flows
[NASA-TM-4111] N89-23433
Flutter of a low-aspect-ratio rectangular wing
[NASA-TM-4116] N89-23447
Hot-jet simulation in cryogenic wind tunnels
[NASA-RP-1220] N89-23448
Method and system for monitoring and displaying engine performance parameters
[NASA-CASE-LAR-14049-1] N89-23486
A closed-form trim solution yielding minimum trim drag for airplanes with multiple longitudinal-control effectors
[NASA-TP-2907] N89-23488
Simulator evaluation of a display for a Takeoff Performance Monitoring System
[NASA-TP-2908] N89-23489
NASA/SDIO Space Environmental Effects on Materials Workshop, part 1
[NASA-CP-3035-PT-1] N89-23528
Structural materials for space applications N89-23530
The Long Duration Exposure Facility material experiments N89-23534
NASA/SDIO Space Environmental Effects on Materials Workshop, part 2
[NASA-CP-3035-PT-2] N89-23547
Ultraviolet radiation effects N89-23551
Effects of thermal cycling on composite materials for space structures N89-23552
Solar radiation N89-23562
Working group written presentation: Trapped radiation effects N89-23566
Working group written presentation: Solar radiation N89-23567
Processable polyimide adhesive and matrix composite resin
[NASA-CASE-LAR-14101-1] N89-23692
Numerical simulation of Goertler/Tollmein-Schlichting wave-interaction
[NASA-CR-181823] N89-23817
Tensile film clamps and mounting block for the rheovibron and autovibron viscoelastometer
[NASA-CASE-LAR-13686-1] N89-23880
Double lead spiral platen parallel jaw end effector N89-23905
A two-axis laser boresight system for a shuttle experiment N89-23913
Locating damaged members in a truss structure using modal test data: A demonstration experiment
[NASA-TM-101595] N89-23924
Application of a PC based, real-time, data-aquisition system in rotorcraft wind-tunnel testing
[NASA-TM-4119] N89-24079
Acoustic response of a rectangular waveguide with a strong transverse temperature gradient
[NASA-TM-101564] N89-24140
A hierarchy of transport approximations for high energy heavy (HZE) ions
[NASA-TM-4118] N89-24255

NATIONAL AERONAUTICS AND SPACE ADMINISTRATION. LEWIS RESEARCH CENTER, CLEVELAND, OH.
Numerical solution of periodic vortical flows about a thin airfoil
[NASA-TM-101998] N89-23413
Average-passage simulation of counter-rotating propfan propulsion systems as applied to cruise missiles
[NASA-TM-102043] N89-23416
The low frequency oscillation in the flow over a NACA0012 airfoil with an iced leading edge
[NASA-TM-102018] N89-23417
Advances in computational design and analysis of airbreathing propulsion systems
[NASA-TM-101987] N89-23465
Solar dynamic power for space station freedom
[NASA-TM-102016] N89-23516
Photovoltaic power system considerations for future lunar bases
[NASA-TM-102019] N89-23517
Preliminary assessment of rover power systems for the Mars Rover Sample Return Mission
[NASA-TM-102003] N89-23518
Test facility and preliminary performance of a 100 kW class MPD thruster
[NASA-TM-102021] N89-23520
Arcjet nozzle design impacts
[NASA-TM-102050] N89-23522
Results from baseline tests of the SPRE 1 and comparison with code model predictions
[NASA-TM-102044] N89-23527
Overview of environmental factors N89-23529
Atomic oxygen effects on materials N89-23540
Surface phenomena in plasma environments N89-23555
Composite blade structural analyzer (COBSTRAN) user's manual
[NASA-TM-101461] N89-23621
Light weight polymer matrix composite material
[NASA-CASE-LEW-14734-1] N89-23623
Macrosegregation and nucleation in undercooled Pb-Sn alloys
[NASA-TM-102023] N89-23664
Undercutting of defects in thin film protective coatings on polymer surfaces exposed to atomic oxygen
[NASA-TM-101966] N89-23691
A segmented mirror antenna for radiometers
[NASA-TM-102045] N89-23753
Sequentially evaporated thin Y-Ba-Cu-O superconducting films on microwave substrates
[NASA-TM-102068] N89-23791
Magnification of starting torques of dc motors by maximum power point trackers in photovoltaic systems
[NASA-TM-102040] N89-23792
Advanced computational techniques for hypersonic propulsion
[NASA-TM-102005] N89-23809
On the nature of Navier-Stokes turbulence
[NASA-TM-101983] N89-23813
On the Lagrangian description of unsteady boundary layer separation. Part 1: General theory
[NASA-TM-102026] N89-23821
Two-dimensional numerical simulation of a Stirling engine heat exchanger
[NASA-TM-102057] N89-23823
A vector scanning processing technique for pulsed laser velocimetry
[NASA-TM-102048] N89-23850
Age distribution among NASA scientists and engineers N89-23911
Laboratory process control using natural language commands from a personal computer
[NASA-TM-101988] N89-24055
Noise of a model counterrotation propeller with simulated fuselage and support pylon at takeoff/approach conditions
[NASA-TM-101996] N89-24138
Comprehensive report of aeropropulsion, space propulsion, space power, and space science applications of the Lewis Research Center
[NASA-TM-100925] N89-24216

NATIONAL AERONAUTICS AND SPACE ADMINISTRATION. MARSHALL SPACE FLIGHT CENTER, HUNTSVILLE, AL.
Space Station CMIF extended duration metabolic control test
[NASA-TM-100362] N89-23503
Electrode carrying wire for GTAW welding
[NASA-CASE-MFS-29491-1] N89-23738
Internal wire guide for GTAW welding
[NASA-CASE-MFS-29489-1] N89-23739
The 23rd Aerospace Mechanisms Symposium
[NASA-CP-3032] N89-23892
Design, fabrication and test of a 4750 Newton-meter-second double Gimbal control moment gyroscope N89-23896
Astronaut tool development: An orbital replaceable unit-portable handhold N89-23904
Space station ECLSS simplified integrated test
[NASA-TM-100363] N89-24044

Rapid fitting of particle cascade development data from X-ray film densitometry measurements
[NASA-TM-100368] N89-24260

NATIONAL AERONAUTICS AND SPACE ADMINISTRATION. PASADENA OFFICE, CA.
A compact fast wide angle broad band spectrometer optical system
[NASA-CASE-NPO-17562-1-CU] N89-24153

NATIONAL AEROSPACE LAB., AMSTERDAM (NETHERLANDS).
Quench sensitivity of airframe aluminium alloys
[PB89-146039] N89-23656
Telescience and image processing for PODI: An analysis and a proposal for a simulation set-up
[NLR-TR-88005-U] N89-23815

NATIONAL AEROSPACE LAB., TOKYO (JAPAN).
Transonic operational characteristics and performance
[NAL-TR-968] N89-23408
Numerical simulation of hypersonic flow around a space plane. 1: Basic development
[NAL-TR-976T] N89-23409
Characteristics of a five-hole spherical pitot tube
[NAL-TR-971] N89-23463
Experiment on a cylindrical scramjet combustor. 2: Simulated flight Mach number 6.7
[NAL-TR-969] N89-23464
The functional mock-up test of the flight control system of the NAL QSTOL research aircraft ASKA
[NAL-TR-972] N89-23467
Study on a highly sensitive electro-static suspended accelerometer (1)
[NAL-TR-1005] N89-23504
Study of the PBE cycle 100kN LH2/LO2 rocket engine
[NAL-TR-965] N89-23514
Spontaneous ignition of atomized kerosine/air mixtures in a high pressure flowing system
[NAL-TR-966] N89-23635
Burning rate constant of fuel droplet under high pressure
[NAL-TR-1001] N89-23639
An experimental study of laminar flow control airfoil with suction through perforated surface at low speed
[NAL-TR-967] N89-23806
Mechanisms of secondary flows and losses within a three dimensional turbine stator cascade
[NAL-TR-970T] N89-23807
Study on a twin valveless pulse burner (temperature characteristics during pulse combustion)
[NAL-TR-973] N89-23873

NATIONAL BUREAU OF STANDARDS, BOULDER, CO.
Metrology for Electromagnetic Technology: A bibliography of NBS (National Bureau of Standards) publications, January 1970 - August 1988
[PB89-147847] N89-23748

NATIONAL CENTER FOR ATMOSPHERIC RESEARCH, BOULDER, CO.
Design of the ELDORA airborne Doppler radar
[PB89-144604] N89-23749

NATIONAL CLIMATIC CENTER, ASHEVILLE, NC.
Climatic atlas of the outer continental shelf waters and coastal regions of Alaska. Volume 1: Gulf of Alaska, revision
[AD-A205289] N89-24005

NATIONAL GEOPHYSICAL DATA CENTER, BOULDER, CO.
Solar-geophysical data number 531, part 1. Data for October, September 1988 and late data
[PB89-139943] N89-24250

NATIONAL INST. OF STANDARDS AND TECHNOLOGY, BOULDER, CO.
Experimental thermal conductivity, thermal diffusivity and specific heat values of argon and nitrogen
[PB89-148407] N89-23637
An iterative technique to correct probe position errors in planar near-field to far-field transformations
[PB89-153866] N89-23750
Microporous fumed-silica insulation board as a candidate Standard Reference Material of thermal resistance
[PB89-146373] N89-24213

NATIONAL INST. OF STANDARDS AND TECHNOLOGY, GAITHERSBURG, MD.
Expert systems applied to spacecraft fire safety
[NASA-CR-182266] N89-23501
Ceramic tribology: Methodology and mechanisms of alumina wear
[PB89-148357] N89-23679
In situ fluorescence monitoring of the viscosities of particle-filled polymers in flow
[PB89-146278] N89-23680
Intelligent processing of materials
[PB89-151823] N89-23735
Liquid-in-glass thermometer calibration service
[PB89-128888] N89-23848
Design and construction of a state-of-the-art high temperature tribometer
[PB89-148332] N89-23847
Institute for Materials Science and Engineering, nondestructive evaluation: Technical activities 1988
[PB89-151625] N89-23684
Wavefront matrix multiplication on a distributed-memory multiprocessor
[PB89-151807] N89-24052
Semiconductor measurement technology: Automatic determination of the interstitial oxygen content of silicon wafers polished on both sides
[PB89-151831] N89-24180

NATIONAL OCEANIC AND ATMOSPHERIC ADMINISTRATION, BOULDER, CO.
Trends in environmentally induced spacecraft anomalies N89-23536

NATIONAL TECHNICAL SYSTEMS, LONG BEACH, CA.
Development of an optical multigas detector
[PB89-148878] N89-23849
Fiber optic leak detection system
[PB89-148886] N89-24150

NATIONAL TRANSPORTATION SAFETY BOARD, WASHINGTON, DC.
Annual review of aircraft accident data, US Air Carrier operations: Calendar year 1986
[PB89-151021] N89-23434
Aircraft Accident Report: AVAir Inc., Flight 3378, Fairchild Metro 3, SA227 AC, N622AV, Cary, North Carolina, February 19, 1988
[PB88-910412] N89-23436

NAVAL AIR DEVELOPMENT CENTER, WARMINSTER, PA.
Analysis of the NAVAIRDEVCEN self-priming topcoat on graphite/epoxy composites
[AD-A205961] N89-23626
Ambient temperature properties of PM (Powder Metal) aluminum-titanium alloys
[AD-A205997] N89-23671

NAVAL AIR SYSTEMS COMMAND, WASHINGTON, DC.
US Navy regional climatic study of the northern California operating area
[AD-A205342] N89-24006

NAVAL CIVIL ENGINEERING LAB., PORT HUENEME, CA.
Geobotanical remote sensing for determination of aggregate source material
[AD-A205943] N89-23962

NAVAL HEALTH RESEARCH CENTER, SAN DIEGO, CA.
The relationship between subjective and objective measures of sleepiness
[AD-A205861] N89-24027

NAVAL OCEAN RESEARCH AND DEVELOPMENT ACTIVITY, BAY SAINT LOUIS, MS.
KRMS (K-band Radiometric Mapping System) SSM/I validation March 1988 quick look report
[NASA-CR-185320] N89-23766

NAVAL OCEAN RESEARCH AND DEVELOPMENT ACTIVITY, HANOVER, NH.
KRMS (K-band Radiometric Mapping System) SSM/I validation March 1988 quick look report
[NASA-CR-185320] N89-23766

NAVAL OCEAN SYSTEMS CENTER, SAN DIEGO, CA.
Drag and noise measurements on underwater vehicles with a riblet surface coating
[AD-A205500] N89-23825
Signal-Noise/Interferer Combiner Unit Programmable (SINCUP)
[AD-A205367] N89-24053
Light channel 5 Gb/s optoelectronic TDM (Time Division Multiplexing)
[AD-A205501] N89-24086

NAVAL POLAR OCEANOGRAPHY CENTER, SUITLAND, MD.
KRMS (K-band Radiometric Mapping System) SSM/I validation March 1988 quick look report
[NASA-CR-185320] N89-23766

NAVAL POSTGRADUATE SCHOOL, MONTEREY, CA.
Flowfield measurements in the vortex wake of a missile at high angle of attack in turbulence
[AD-A205696] N89-23422
Aerothermodynamic analysis of a Coanda/Refraction Jet Engine Test Facility
[AD-A205937] N89-23482
Code optimization of speckle reduction algorithms for image processing of rocket motor holograms
[AD-A205305] N89-23524
The effect of welding process on the microstructure of HY-130 steel weldments
[AD-A205692] N89-23667
Stress relief cracking in copper-precipitation strengthened HSLA-100 steel
[AD-A205936] N89-23670
An experimental investigation in the behavior of metallized solid propellants
[AD-A206510] N89-23715
Performance of radar receivers in the presence of noise and intentional interference
[AD-A205328] N89-23759
Sea spike modeling
[AD-A205355] N89-23760
An evaluation of coplanar line for application in microwave integrated circuitry
[AD-A205305] N89-23795
Rayleigh-Taylor instability of a viscous film overlying a passive fluid
[AD-A205578] N89-23827
Investigation of incompressible cascade flows using a viscous/inviscid interactive code
[AD-A205972] N89-23832
Computerized measurement of thermoacoustically generated temperature gradients
[AD-A205353] N89-23929
Thermal images of sky and sea-surface background infrared radiation
[AD-A205819] N89-23992
A CAD (Computer Aided Design) tool for current-mode multiple-valued CMOS circuits
[AD-A205327] N89-24061
Design and implementation of an expert user interface for the computer aided prototyping system
[AD-A206113] N89-24067
A graphical editor for the computer aided prototyping system
[AD-A206443] N89-24071
Design of multiple-valued programmable logic arrays (PLA)
[AD-A205307] N89-24085
Designing feedback compensators by using the root-locus method
[AD-A205354] N89-24093
Numerical experience with a superfast real Toeplitz solver
[AD-A205374] N89-24115
Three-dimensional analysis of optical transition radiation
[AD-A205935] N89-24156
Atomic relaxation and vacancy-interstitial recombination in Zr and Zr3Al
[AD-A205664] N89-24199
Managing sound in a relational multimedia database system
[AD-A205742] N89-24225
A program interface prototype for a multimedia database incorporating images
[AD-A206439] N89-24226

NAVAL RESEARCH LAB., WASHINGTON, DC.
Impact of the geoplasma on a spaceborne GPS receiver system: A preliminary study
[AD-A205965] N89-23442
Co-aligning the RAIDS (Remote Atmospheric and Ionospheric Detection System) instruments
[AD-A205456] N89-23513
Some examples of the degradation of properties of materials in space N89-23535
FILMCAL: An ESR (Electron Spin Resonance) simulation program for transition metals in phthalocyanine films
[AD-A206441] N89-23676
Phase accuracy experiments with a direct-sampling coherent detector
[AD-A205458] N89-23764
Radar waveforms derived from orthogonal matrices
[AD-A205459] N89-23765
On the problem of optimal signal detection in discrete-time, correlated, non-Gaussian noise
[AD-A205859] N89-23771
Megavolt, multi-kiloamp K(sub)a-band gyrotron oscillator experiment
[AD-A206271] N89-23801
Turbulence near a free surface in a plane jet
[AD-A206269] N89-23838
Operation of a quasi-optical gyrotron with variable mirror separation
[AD-A206347] N89-23854
Development of high power CARM (Cyclotron Auto-Resonance Maser) oscillators
[AD-A206270] N89-23872
Practical experiences with worm gearing for spacecraft power transmission applications N89-23912
On the equation Xa + Ya = Za
[AD-A205460] N89-24116
Simulation studies of particle acceleration powered by modulated intense relativistic electron beams
[AD-A206348] N89-24148

NAVAL SUBMARINE MEDICAL RESEARCH LAB., GROTON, CT.
Psychometric function reconstruction from adaptive tracking procedures
[AD-A205668] N89-24034

NAVAL WEAPONS CENTER, CHINA LAKE, CA.
KRMS (K-band Radiometric Mapping System) SSM/I validation March 1988 quick look report
[NASA-CR-185320] N89-23766
NAVY EXPERIMENTAL DIVING UNIT, PANAMA CITY, FL.
Oxygen consumption rate of operational underwater swimmers
[AD-A205331] N89-24025
NAVY PERSONNEL RESEARCH AND DEVELOPMENT CENTER, SAN DIEGO, CA.
Development and evaluation of integrating details: A complex spatial problem solving test
[AD-A205860] N89-24035
NEDECO (NETHERLANDS).
On the international commercialization of remote sensing
[BCRS-88-02] N89-23969
NEVADA UNIV., RENO.
Free shear layer and swirl flow heat transfer enhancement
[PB89-145106] N89-23810
NEW MEXICO UNIV., ALBUQUERQUE.
The chirped-pulse free-electron laser
[DE89-009041] N89-23862
NIELSEN ENGINEERING AND RESEARCH, INC., MOUNTAIN VIEW, CA.
Computational study of high supersonic flow over boattails with centered propulsive jets
[AD-A206364] N89-23431
Exploitation of multiple solutions of the Navier-Stokes equations to achieve radically improved flight
[AD-A205939] N89-23831
NORTH CAROLINA UNIV., CHAPEL HILL.
Nonlinear systems of conservation laws
[AD-A205837] N89-23830
NORTH DAKOTA UNIV., GRAND FORKS.
Production of jet fuels from coal-derived liquids. Volume 8: Heteroatom removal by catalytic processing
[AD-A205470] N89-23712
NORTHWESTERN UNIV., EVANSTON, IL.
NMR characterization of porous structures: Ceramics and sandstones: Renewal proposal
[DE89-009148] N89-23642
NOTRE DAME UNIV., IN.
Adaptive signal processing
[AD-A205787] N89-24063

O

OAK RIDGE GASEOUS DIFFUSION PLANT, TN.
Molded bodies having a high degree of hardness and a high degree of toughness for machining metals, carbides, ceramics and glasses
[DE89-008820] N89-23686
OAK RIDGE NATIONAL LAB., TN.
Surface treatment using metal foil liner N89-23533
A first-principles calculation of the resistivity and thermopower in strong-scattering alloys
[DE89-008565] N89-23661
Iron-niobium-aluminum alloy having high-temperature corrosion resistance
[DE89-009600] N89-23663
The thermal resistance of flat powder-filled evacuated panels
[DE89-008243] N89-23685
Nonintrusive methods for monitoring the operational readiness of solenoid-operated valves
[DE89-008732] N89-23878
Traction-drive force transmission for telerobotic joints N89-23906
Reduction of a general matrix to tridiagonal form
[DE89-008980] N89-24083
Zinc oxide varistor time response
[DE89-008234] N89-24191
Deformation twinning in ordered intermetallic compounds
[DE89-008748] N89-24192
OFFICE OF TECHNOLOGY ASSESSMENT, WASHINGTON, DC.
Reducing launch operations costs: New technologies and practices
[PB89-136402] N89-23500
OHIO STATE UNIV., COLUMBUS.
Strength and structure of Ga(1-x)In(x)As alloys
[AD-A205415] N89-23644
A method to design blended rolled edges for compact range reflectors
[NASA-CR-184976] N89-23736
OHIO WESLEYAN UNIV., DELAWARE.
Functional assessment of laser irradiation
[AD-A206230] N89-23871
OLD DOMINION UNIV., NORFOLK, VA.
Experimental study of pressure and heating rate on a swept cylindrical leading edge resulting from swept shock wave interference
[NASA-CR-185326] N89-23411
Software reliability studies
[NASA-CR-184857] N89-24054
OPTICAL SOCIETY OF AMERICA, WASHINGTON, DC.
Summaries of papers presented at Short Wavelength Coherent Radiation: Generation and Applications Topical Meeting held in Cape Cod, Massachusetts on September 26-29, 1988
[AD-A205471] N89-23867
OREGON GRADUATE CENTER FOR STUDY AND RESEARCH, BEAVERTON.
Fundamental and applied studies of explosively fabricated high-temperature superconducting fixtures
[AD-A205953] N89-24204
OXFORD UNIV. (ENGLAND).
The application of self-tuning control techniques to a multivariable process
[OUEL-1737/88] N89-23737
State-space formulae for discrete-time H infinity optimization
[OUEL-1718/88] N89-24089
Robust multivariable feedback design
[OUEL-1723/88] N89-24090
Multivariable Nyquist self-tuning: A general approach
[OUEL-1734/88] N89-24091
Investigation of the behaviour of a collisionless R-F sheath
[OUEL-1695/87] N89-24165

P

PACIFIC NORTHWEST LABS., RICHLAND, WA.
Environment-induced crack growth processes in nickel-base alloys
[DE89-008253] N89-23659
Low-temperature volumetric receiver concept
[DE89-008245] N89-23976
Putting science and technology to work: A casebook of transferred technologies
[DE89-009158] N89-24228
PATRAS UNIV. (GREECE).
Temperature dependence of interfacial energies between solid oxides and liquid metals N89-23599
PENNSYLVANIA STATE UNIV., UNIVERSITY PARK.
Twin boundaries, interfaces and modulated structures in martensites
[DE89-009064] N89-23662
Multivariate analysis and its applications
[AD-A205585] N89-24125
PENNSYLVANIA UNIV., PHILADELPHIA.
Mechanisms of diffusion-controlled brittle fracture
[DE89-008728] N89-23921
Molecular optics nonlinear optical processes in organic and polymeric crystals and films
[AD-A206372] N89-24209
PERKIN-ELMER CORP., DANBURY, CT.
Lattice symmetries and thermal expansion
[AD-A206045] N89-24207
PHYSICAL SCIENCES, INC., ANDOVER, MA.
High-temperature LDV seed particle development
[NASA-CR-182265] N89-23851
PITTSBURGH UNIV., PA.
Environmental effects in niobium base alloys and other selected intermetallic compounds
[AD-A206072] N89-23673
The Allegheny Observatory search for planetary systems
[NASA-CR-184990] N89-24233
POLYTECHNIC UNIV., FARMINGDALE, NY.
Optimum aeroelastic characteristics for composite supermaneuverable aircraft
[AD-A205503] N89-23452
A chamber experiment for the feasibility study of an artificial plasma reflector for OTH radar applications
[NASA-CR-184912] N89-23478
PORTLAND STATE UNIV., OR.
Improved acid electrolytes: The synthesis and structure of fluorine containing sulfonic acids for fuel cells
[PB89-142616] N89-23973
PRATT AND WHITNEY AIRCRAFT, WEST PALM BEACH, FL.
Design, fabrication and test of the RL10 derivative II chamber/primary nozzle
[NASA-CR-179595] N89-23519
PRINCETON UNIV., NJ.
Effect of physical annealing on the dynamic mechanical properties of a high T(g) amine-cured epoxy systems
[AD-A205980] N89-23704
The glass transition temperature (Tg) as a parameter for monitoring the cure of an amine-cured epoxy system at constant heating rates
[AD-A206098] N89-23705
Near-far resistant linear multiuser detection
[AD-A206363] N89-23802
Mathematical analysis of strong fluid mechanical effects in reacting and nonreacting gases
[AD-A206336] N89-23839
PURDUE UNIV., WEST LAFAYETTE, IN.
Solidification of binary substances in rectangular and cylindrical cavities
[DE89-008883] N89-23640

R

RENAULT VEHICLES INDUSTRIELS (FRANCE).
SRB ascent aerodynamic heating design criteria reduction study, volume 1
[NASA-CR-183580] N89-23515
RENSSELAER POLYTECHNIC INST., TROY, NY.
Mode 2 delamination fatigue resistance of composites N89-23624
Steel hardness effects in boundary lubricated sliding: An in-situ SEM (Scanning Electron Microscope) study
[AD-A206156] N89-23674
RESEARCH INST. OF NATIONAL DEFENCE, LINKOEPING (SWEDEN).
Shortest paths in a digitized map using a tile-based data structure
[PB89-143432] N89-23957
RISBERG POWER ELECTRONICS, INC., NEW BERLIN, WI.
High energy semiconductor switch
[DE89-007399] N89-23789
ROCKWELL INTERNATIONAL CORP., CANOGA PARK, CA.
Space station propulsion test bed
[NASA-CR-183615] N89-23521
ROCKWELL INTERNATIONAL CORP., SEAL BEACH, CA.
Environmental effects on spacecraft materials N89-23532
ROCKY RESEARCH CORP., BOULDER CITY, NV.
Solid-vapor adsorption refrigeration system development
[PB89-140859] N89-23733
ROYAL INST. OF TECH., STOCKHOLM (SWEDEN).
Electric fields in the magnetosphere: The evidence from ISEE, S3-3, GEOS and Viking
[TRITA-EPP-88-11] N89-23987
Electrodynamics of cosmical plasmas: Some basic aspects of cosmological importance
[TRITA-EPP-89-02] N89-24163
ROYAL NETHERLANDS METEOROLOGICAL INST., DE BILT.
Stratocumulus modeling
[KNMI-WR-88-2] N89-23997
Current problems in the stratocumulus-topped atmospheric boundary layer N89-23998
Turbulent structure of a shear-driven stratus-topped atmospheric boundary layer: A comparison of model results with observations N89-23999
The diurnal variation of a marine stratocumulus layer: A model sensitivity study N89-24000
ROYAL SIGNALS AND RADAR ESTABLISHMENT, MALVERN (ENGLAND).
Comparison of interpolation algorithms for speed control in air traffic management
[AD-A206314] N89-23444
RUTGERS - THE STATE UNIV., NEW BRUNSWICK, NJ.
Mechanical behavior of PMMA-impregnated silica gels
[AD-A205975] N89-23703

S

SALK INSTITUTE FOR BIOLOGICAL STUDIES, SAN DIEGO, CA.
Model of early self-replication based on covalent complementarity for a copolymer of glycerate-3-phosphate and glycerol-3-phosphate
[NASA-CR-182912] N89-23693
SANDIA NATIONAL LABS., ALBUQUERQUE, NM.
Autofocus of SAR imagery degraded by ionospheric-induced phase errors
[DE89-008278] N89-23752
White paper: Experimental and computational studies of very high velocity impacts
[DE89-007643] N89-23877
A unidirectional rotary solenoid as applied to stronglinks N89-23894
Prediction and measurement of damping of a laminated beam with a constrained viscoelastic layer
[DE89-009002] N89-23922

Solid modeling requirements for finite element modeling using mapped mesh techniques
[DE89-009639] N89-24110
Monitoring thin film properties with surface acoustic wave devices: Diffusion, surface area and pore size distribution
[DE89-009379] N89-24195

SCIENCE APPLICATIONS INTERNATIONAL CORP., MCLEAN, VA.
Development of high power CARM (Cyclotron Auto-Resonance Maser) oscillators
[AD-A206270] N89-23872
Simulation studies of particle acceleration powered by modulated intense relativistic electron beams
[AD-A206348] N89-24148

SCIENTIFIC RESEARCH ASSOCIATES, INC., GLASTONBURY, CT.
Computation of flow around maneuvering submerged bodies
[AD-A205994] N89-23833

SELENIA S.P.A., ROME (ITALY).
Battlefield radar imaging through airborne millimetric wave SAR (Synthetic Aperture Radar)
[ETN-89-94228] N89-23751

SERBIAN ACADEMY OF SCIENCES AND ARTS, BELGRADE (YUGOSLAVIA).
Microstructure and phase development in multicomponent ZnO based varistor ceramics
N89-23604
Production of metal powders by rotating electrode process N89-23608
Physico-mathematical investigation of the consolidation of iron powder N89-23617
P-T diagrams of transition elements N89-23618

SKOPJE UNIV. (YUGOSLAVIA).
Preparing and sintering of yttria-stabilized zirconia
N89-23576
Stability and instability of anodically formed layers on metallic surfaces N89-23597

SMITHSONIAN ASTROPHYSICAL OBSERVATORY, CAMBRIDGE, MA.
Solar and stellar coronal plasmas
[NASA-CR-184909] N89-24162
Observations of the rotational transitions of OH from the Orion molecular cloud
[NASA-CR-184802] N89-24231

SOCIETE NATIONALE INDUSTRIELLE AEROSPATIALE, PARIS (FRANCE).
Navigation shift correction by radar cartography. Optimization and validation by simulation
[REPT-882-320-103] N89-23755

SOUTH DAKOTA UNIV., VERMILLION.
Quasi-monochromatic visual environments and the resting point of accommodation
[AD-A205938] N89-24036

STANFORD LINEAR ACCELERATOR CENTER, CA.
Design of a 100 MW X-band klystron
[DE89-008939] N89-23793

STANFORD UNIV., CA.
An experimental study of the effect of streamwise vortices on unsteady turbulent boundary-layer separation
[AD-A205462] N89-23420
Flow control for unsteady and separated flows and turbulent mixing
[AD-A205989] N89-23426
Fundamental and practical studies of metal contacts on mercury zinc telluride
[AD-A206560] N89-23653
Bifurcating jets at high Reynolds numbers
[AD-A205718] N89-23829
The dimension of attractors underlying turbulent Poiseuille flow
[AD-A206021] N89-23835
Turbulence near a free surface in a plane jet
[AD-A206269] N89-23838
High energy efficient solid state laser sources
[NASA-CR-181782] N89-23856
Research studies on extreme ultraviolet and soft X-ray lasers
[AD-A205625] N89-23866
Energy transfer and photochemistry in biomimetic solar conversion
[PB89-142590] N89-23974
A visual object-oriented unification system
[AD-A206228] N89-24068
Deductive programming synthesis
[AD-A206451] N89-24072
Tests for the gamma distribution with estimated shape parameters
[AD-A205829] N89-24118
Approaches for empirical Bayes confidence intervals
[AD-A205775] N89-24126
Second-order moments of a stationary Markov chain and some applications
[AD-A206366] N89-24128
Heterojunction band line-ups and the alloying effect in compound semiconductor alloys: A photoemission study
N89-24179
Fundamental studies of the mechanical behavior of microelectronic thin film materials
[AD-A206057] N89-24208
Geomagnetic disturbances
[AD-A206052] N89-24254

STATE UNIV. OF NEW YORK, ALBANY.
High electric field phenomena in insulation
[AD-A205525] N89-23799

STATE UNIV. OF NEW YORK, BINGHAMTON.
Novel organoboranes as intermediates for ceramic precursors and high-energy fuels
[AD-A206101] N89-23713

STATE UNIV. OF NEW YORK, BUFFALO.
Exact wave functions and coherent states of a damped driven harmonic oscillator
[AD-A205785] N89-24136
Photoabsorption of molecules at corrugated thin metal films
[AD-A205325] N89-24197
Decay of molecules at corrugated thin metal films
[AD-A205487] N89-24198

STUTTGART UNIV. (GERMANY, F.R.).
Improvement of navigation measurement procedures by the combined application of correlation techniques and parameter estimation
[ETN-89-93946] N89-23445
Payload experts in D1-mission N89-23722
Numerical methods to treat collisionlike phenomena in solids
[ETN-89-93944] N89-23936
Radiation physics properties of selective solar energy absorber layers
[ETN-89-93945] N89-23978

SVERDRUP TECHNOLOGY, INC., CLEVELAND, OH.
Theoretical analysis of compatibility of several reinforcement materials with NiAl and FeAl matrices
[NASA-CR-182291] N89-23622

SWEDISH DEFENCE RESEARCH ESTABLISHMENT, LINKOEPING.
Active radar jamming
[FOA-C-30506-3.6] N89-23777
Coherent laser radar
[FOA-C-30512-3.1] N89-23778
Lossy layers: Theory and methods of measurement
[FOA-C-30513-3.2] N89-23779
Transmission losses in hollow aluminum oxide waveguide at 10.6 microns
[FOA-C-30518-3.1] N89-23804

SWEDISH DEFENCE RESEARCH ESTABLISHMENT, STOCKHOLM.
GRADA: A graphical package in Ada
[FOA-C-20741-2.7] N89-24077
Mobile nuclear power systems
[FOA-C-20743-4.1] N89-24149

SWEDISH INST. FOR MATERIALS TESTING, BORAS.
Investigations on the cracking behavior of joints in airfields and roads: Field investigations and laboratory simulations
[PB89-141279] N89-23479

SYRACUSE UNIV., NY.
Structure/permeability relationships of silicon-containing polyimides
[NASA-CR-4237] N89-23683
An experimental investigation into software reliability
[AD-A206293] N89-24069

T

TECHNICAL SOLUTIONS, INC., MESILLA PARK, NM.
Automatic documentation methodologies for software maintenance
[AD-A205872] N89-24062

TECHNICAL UNIV. OF DENMARK, LYNGBY.
Coherence and chaos phenomena in Josephson oscillators for superconducting electronics
[AD-A205469] N89-23798

TECHNISCHE HOCHSCHULE, AACHEN (GERMANY, F.R.).
Investigations of mullite-zirconia composites
N89-23577
Microstructure development in alumina N89-23579
Investigations on low cement and ultra low cement refractory castables N89-23593
The adhesion between glass and enamel N89-23598
Electron conducting ceramics as sensor material for noise thermometry N89-23603

TECHNISCHE HOGESCHOOL, DELFT (NETHERLANDS).
Performance analysis of Kalman filters
[PB89-146104] N89-23787
On the connection of geodetic pointfields in RETrig
[PB89-146112] N89-23958
Direct manipulation and other styles of man-machine interaction
[PB89-146070] N89-24043
User interface and highly interactive systems: Survey of current research
[PB89-146088] N89-24056
Asymptotic behavior of random discrete event systems
[PB89-146146] N89-24099
Riemannian geometry on families of linear systems: The deterministic case
[PB89-146062] N89-24100
Efficient method for solving free-boundary problems
[PB89-146138] N89-24101
Modeling of a continuous oscillator by oscillators with a finite number of degrees of freedom
[PB89-146120] N89-24134
Strong and electromagnetic interactions in heavy exotic atoms
[PB89-145718] N89-24143

TECHNISCHE HOGESCHOOL, EINDHOVEN (NETHERLANDS).
Numerical implementation of the Schapery model for nonlinear visco-elasticity
[PB89-144950] N89-23915

TECHNISCHE UNIV., BRUNSWICK (GERMANY, F.R.).
Correlated atomic motions in liquid aluminum
[ETN-89-93943] N89-24145

TECHNISCHE UNIV., CLAUSTHAL-ZELLERFELD (GERMANY, F.R.).
Neutral primary beam SIMS analysis of ceramic materials N89-23601
Mechanical properties of rapidly solidified iron-based alloys N89-23611
Behavior of metals during hot rolling processes. Part 1: Mathematical models N89-23613
Behavior of metals during hot rolling processes. Part 2: Experimental methods for flow stress determination and calculation of the two-dimensional temperature-field in the roll gap N89-23614

TECHNISCHE UNIV., DELFT (NETHERLANDS).
Global Positioning System (GPS) positioning at sea
[ETN-89-94145] N89-23446
Some applications of the qualitative theory of differential equations in fluid dynamics
[ETN-89-94143] N89-23814
The search for edges in remote sensing images using a digital polygonal map
[ETN-89-94146] N89-23964
Investigation of several methods for the detection of outstanding points in a digital image
[ETN-89-94148] N89-23965
Calculation of the surface of a geodetic polygon on an ellipsoid of revolution
[ETN-89-94149] N89-23966
Vectorization of grid lines
[ETN-89-94150] N89-23967
Design of a methodology for the detection of errors in terrestrial networks
[ETN-89-94151] N89-23968

TELDIX LUFTFAHRT-AUSRUESTUNGS G.M.B.H., HEIDELBERG (GERMANY, F.R.).
A family of BAPTAs for GEO and LEO applications
N89-23908

TELEROBOTICS INTERNATIONAL, INC., KNOXVILLE, TN.
An application specific integrated circuit for dual-axis motion control
[DE89-007974] N89-23790

TENNESSEE UNIV., KNOXVILLE.
Synthesis of novel acid electrolytes for phosphoric acid fuel cells
[PB89-148944] N89-23786

TENNESSEE UNIV., MEMPHIS.
Muramyl peptide-enhanced sleep: Pharmacological optimization of performance
[AD-A205974] N89-24028

TEXAS A&M UNIV., COLLEGE STATION.
Measuring conductivities of highly conductive membranes
[AD-A206043] N89-23649
Nano- and microstructures in chemistry, electrochemistry, and materials science
[AD-A206296] N89-23650
Three-dimensional laser anemometer study of compressible flow through orifice plates
[PB89-145098] N89-23808
Friction factor data for flat plate tests of smooth and honeycomb surfaces
[NASA-CR-184977] N89-23876
Experimental and theoretical determination of the thermomechanical response of inelastic structural materials to high energy thermal inputs
[AD-A206100] N89-23933

TEXAS UNIV., ARLINGTON.
Electronic and ionic transport in polymers
[AD-A206530] N89-23709
TEXAS UNIV., AUSTIN.
Effects of initial conditions on the development of supersonic turbulent free shear layers
[AD-A205607] N89-23421
Modeling and simulation of a Stewart platform type parallel structure robot
[NASA-CR-184969] N89-23875
A designers' guide to reliable distributed systems: An example design. Volume 1
[AD-A206039] N89-23885
A designers' guide to reliable distributed systems: An example design. Volume 2
[AD-A206040] N89-23886
Analysis of the ignition experiment IGNITEX
[DE89-007847] N89-24166
A search for pulsations in planetary nebulae nuclei N89-24235
A study of the motion in the neighborhood of the triangular libration point N89-24236
A linear analysis of the stability of strong shocks and the evolution and distribution of materials in a cold dark matter dominated universe N89-24244
TEXAS UNIV., DALLAS.
Proof of the feasibility of coherent and incoherent schemes for pumping a gamma-ray laser
[AD-A205371] N89-23866
TEXAS UNIV., SAN ANTONIO.
Fatigue crack growth model RANDOM2 user manual, appendix 1
[NASA-CR-184939] N89-23890
Fatigue strength reduction model: RANDOM3 and RANDOM4 user manual, appendix 2
[NASA-CR-184940] N89-23891
TEXAS UNIV. AT DALLAS, RICHARDSON.
The geometry of plane waves in spaces of constant curvature N89-24241
TRW DEFENSE SYSTEMS GROUP., FAIRFAX, VA.
Advanced computing systems: An advanced reasoning-based development paradigm for Ada trusted systems and its application to MACH
[AD-A206308] N89-24070
TRW SPACE TECHNOLOGY LABS., REDONDO BEACH, CA.
Influence of charging environments on spacecraft materials and system performance N89-23556
Spacecraft charging N89-23563
Working group written presentation: Spacecraft charging N89-23568
TUFTS UNIV., MEDFORD, MA.
Very large array observations of the sun with related observations using the SMM (Solar Maximum Mission) satellite
[AD-A203874] N89-24249

U

ULTRASYSTEMS, INC., IRVINE, CA.
Heterocycles based on group 3, 4, and 5 elements precursors for novel glasses and ceramics
[AD-A205586] N89-23696
UNITED ANALYSIS, INC., VIENNA, VA.
USAF (US Air Force) durability design handbook: Guidelines for the analysis and design of durable aircraft structures
[AD-A206286] N89-23457
UNITED TECHNOLOGIES RESEARCH CENTER, EAST HARTFORD, CT.
Study of adherent oxide scales
[AD-A205799] N89-23700
UNIVERSITEIT TWENTE, ENSCHEDE (NETHERLANDS).
Knowledge representation using knowledge graphs: Application to theories on mathematical modeling and solving word problems
[MEMO-707] N89-24124
UNIVERSITY OF SOUTHERN CALIFORNIA, LOS ANGELES.
Atomic layer epitaxy. Atomic layer epitaxy of 3-5 compound semiconductors by thermal and laser-assisted metalorganic chemical vapor deposition
[AD-A205699] N89-24200
UTAH STATE UNIV., LOGAN.
Mesospheric wind measurement
[AD-A205593] N89-23991
UTAH UNIV., SALT LAKE CITY.
The effects of dielectric and metal loading on the dispersion characteristics for contrawound helix circuits used in high power traveling-wave tubes
[AD-A205345] N89-23797

V

VIRGINIA POLYTECHNIC INST. AND STATE UNIV., BLACKSBURG.
Study of spread spectrum multiple access systems for satellite communications with overlay on current services: Executive summary
[NASA-CR-180827-EXEC-SUMM] N89-23756
Study of spread spectrum multiple access systems for satellite communications with overlay on current services
[NASA-CR-180827] N89-23757
Effect of wall cooling on the stability of compressible subsonic flows over smooth humps and backward-facing steps
[NASA-CR-184960] N89-23812
Three-dimensional structure of boundary layers in transition to turbulence
[AD-A205587] N89-23828
Improved sea surface scattering model
[AD-A205745] N89-24012
VIRGINIA UNIV., CHARLOTTESVILLE.
Increasing the margin of stability of arbitrarily finite modes of flexible large space structures with damping
[AD-A206487] N89-23507

W

WASHINGTON STATE UNIV., PULLMAN.
Assignment of the charge-transfer excited states of bis(N-heterocyclic) complexes of copper(I)
[AD-A206012] N89-24205
WASHINGTON UNIV., SAINT LOUIS, MO.
The attention system of the human brain
[AD-A206157] N89-24040
Relating attention to visual mechanisms
[AD-A206452] N89-24042
WEIZMANN INST. OF SCIENCE, REHOVOTH (ISRAEL).
Quasi-liquid crystalline materials with special electro-optic properties
[AD-A206015] N89-24206
WESTINGHOUSE HANFORD CO., RICHLAND, WA.
Fourth generation computer languages
[DE89-008800] N89-24059
WOODS HOLE OCEANOGRAPHIC INSTITUTION, MA.
Exploring the North Atlantic Ocean on floppy disks
[AD-A205733] N89-24011
WYOMING UNIV., LARAMIE.
Ground-based infrared observations of sources discovered by the AFGL, FIRRSE and IRAS infrared surveys
[AD-A206335] N89-24246

Y

YALE UNIV., NEW HAVEN, CT.
Nonlinear spectroscopy of multicomponent droplets and two- and three-dimensional measurements in flames
[AD-A205449] N89-23645
Spectrometric studies of gas phase collision processes
[AD-A205570] N89-23826
Runtime aggregation of recursion relations
[AD-A206576] N89-24078
Preconditioned Krylov solvers and methods for runtime loop parallelization
[AD-A206388] N89-24120
Krylov methods preconditioned with incompletely factored matrices on the CM-2
[AD-A206389] N89-24121
A blocked Jacobi method for the symmetric Eigenproblem
[AD-A206553] N89-24133
YUGOSLAV ACADEMY OF SCIENCES AND ARTS, ZAGREB.
Amorphous magnets N89-23605

Typical Contract Number Index Listing

Listings in this index are arranged alphanumerically by contract number. Under each contract number the NASA accession numbers denoting documents that have been produced as a result of research done under that contract are arranged in ascending order. The NASA accession number denotes the number by which the citation is identified.

AF PROJ. Q011 ..... N89-23776
AF PROJ. 2301 ..... N89-23799
N89-24172
AF PROJ. 2302 ..... N89-23930
AF PROJ. 2303 ..... N89-23647
N89-23701
N89-23713
N89-23826
N89-24144
AF PROJ. 2304 ..... N89-23773
N89-23830
N89-24073
N89-24125
N89-24131
AF PROJ. 2305 ..... N89-24203
AF PROJ. 2306 ..... N89-23665
AF PROJ. 2307 ..... N89-23835
N89-23837
AF PROJ. 2308 ..... N89-23645
N89-23651
N89-24168
AF PROJ. 2310 ..... N89-24008
AF PROJ. 2311 ..... N89-24237
N89-24246
N89-24249
AF PROJ. 2480 ..... N89-23712
AF PROJ. 2530 ..... N89-23665
N89-23886
AF PROJ. 2917 ..... N89-23991
AF PROJ. 3005 ..... N89-23831
AF PROJ. 3048 ..... N89-23882
AF-AFOSR-0012-86 ..... N89-24172
AF-AFOSR-0016-86 ..... N89-23651
AF-AFOSR-0019-83 ..... N89-24249
AF-AFOSR-0030-88 ..... N89-24125
AF-AFOSR-0034-88 ..... N89-23930
AF-AFOSR-0046-87 ..... N89-24168
AF-AFOSR-0051-86 ..... N89-24208
AF-AFOSR-0056-88 ..... N89-23635
AF-AFOSR-0058-85 ..... N89-24246
AF-AFOSR-0059-86 ..... N89-24144
AF-AFOSR-0061-86 ..... N89-24073
AF-AFOSR-0063-87 ..... N89-23799
AF-AFOSR-0089-88 ..... N89-23647
AF-AFOSR-0100-88 ..... N89-23645
AF-AFOSR-0102-87 ..... N89-24131
AF-AFOSR-0108-85 ..... N89-23713
AF-AFOSR-0108-88 ..... N89-23701
AF-AFOSR-0111-88 ..... N89-24203
AF-AFOSR-0139-85 ..... N89-24237
AF-AFOSR-0216-85 ..... N89-24008
AF-AFOSR-0241-86 ..... N89-23991
AF-AFOSR-0283-87 ..... N89-23830
AF-AFOSR-0303-84 ..... N89-23665
AF-AFOSR-0307-86 ..... N89-23773
AF-AFOSR-0321-87 ..... N89-23507
AF-AFOSR-0323-87 ..... N89-23826
AF-AFOSR-0357-85 ..... N89-23837
ARPA ORDER 4989 ..... N89-23802
ARPA ORDER 5526 ..... N89-23644
ARPA ORDER 5674 ..... N89-23653
ARPA ORDER 6075 ..... N89-24012
ARPA ORDER 6414 ..... N89-24070
ARPA ORDER 9132 ..... N89-23441
BCRS-PROJ.-CO-1.3 ..... N89-23969
BCRS-PROJ.-OP-3.3 ..... N89-23970
N89-23971
BMFT-FKZ-SLN87-01 ..... N89-23718
BMFT-01-QS-86-206 ..... N89-23972
BMFT-01-YH-8503-9 ..... N89-23788
BMFT-03-K-01012 ..... N89-23938
BMVG-T/R-760/F-0007/F-1707 ..... N89-23841
N89-23842
DA PROJ. 1C1-61102-A-71-A N89-23628
DA PROJ. 1L1-61102-BH-57 ..... N89-23798
DA PROJ. 1L1-62211-A-47-A N89-23410
DA PROJ. 3E1-62777-A-878 ..... N89-23871
DA PROJ. 3E1-62787-A-879 ..... N89-24031
DA PROJ. 3M1-61102-BS-10 ..... N89-24028
DA PROJ. 4A7-62730-AT-42 ..... N89-23740
DAAA15-87-D-0007 ..... N89-23628
DAAE07-87-C-R001 ..... N89-24096
DAAG09-85-G-0035 ..... N89-23407
DAAG29-84-K-0004 ..... N89-23423
DAAG29-84-K-0171 ..... N89-24135
DAAG29-85-C-0026 ..... N89-24062
DAAG29-85-K-0110 ..... N89-23898
DAAG29-85-K-0204 ..... N89-24210
DAAG29-85-K-0205 ..... N89-23675
DAAG29-85-K-0222 ..... N89-23699
DAAH01-84-C-0489 ..... N89-24132
DAAK11-85-D-0008 ..... N89-23714
DAAL03-86-C-0002 ..... N89-23431
DAAL03-86-K-0003 ..... N89-23839
DAAL03-86-K-0076 ..... N89-23674
DAAL03-87-K-0062 ..... N89-23802
DAAL03-87-K-0110 ..... N89-24137
DAAL03-89-K-0033 ..... N89-24128
DAJA45-85-C-0030 ..... N89-24206
DAJA45-85-C-0042 ..... N89-23798
DAMD17-75-C-5008 ..... N89-23871
DAMD17-81-C-1065 ..... N89-23871
DAMD17-86-C-6194 ..... N89-24028
DAMD17-87-C-7202 ..... N89-24031
DARPA ORDER 5609 ..... N89-24096
DARPA ORDER 6155 ..... N89-23673
DARPA ORDER 6560 ..... N89-24204
DCA100-7-C-0078 ..... N89-23776
DE-AC01-79ET-32043 ..... N89-24147
DE-AC02-76CH-00016 ..... N89-23661
N89-24190
DE-AC02-76CH-03000 ..... N89-24108
DE-AC03-76SF-00098 ..... N89-23684
N89-23863
N89-24186
DE-AC03-76SF-00515 ..... N89-23793
DE-AC03-87SF-17300 ..... N89-23682
DE-AC04-76DP-00789 ..... N89-23752
N89-23877
N89-23922
N89-24110
N89-24195
DE-AC04-88DP-43495 ..... N89-23887
DE-AC05-84OR-21400 ..... N89-23661
N89-23663
N89-23685
N89-23878
N89-24083
N89-24166
N89-24191
N89-24192
DE-AC05-84OT-21400 ..... N89-23686
DE-AC05-86ER-80399 ..... N89-23790
DE-AC06-76RL-01830 ..... N89-23659
N89-23976
N89-24228
DE-AC06-87RL-10930 ..... N89-24059
DE-AC07-76ID-01570 ..... N89-23923
DE-FG01-87CE-15319 ..... N89-23789
DE-FG02-84ER-13218 ..... N89-23641
DE-FG02-84ER-52111 ..... N89-23499
DE-FG02-85ER-45214 ..... N89-23662
DE-FG02-86ER-13623 ..... N89-24214
DE-FG02-86ER-45251 ..... N89-23642
DE-FG02-87ER-13759 ..... N89-23640
DE-FG02-87ER-25026 ..... N89-24109
DE-FG02-87ER-45290 ..... N89-23921
DE-FG02-87ER-45310 ..... N89-24194
DE-FG02-88ER-45366 ..... N89-23689
DE-FG04-87ER-13788 ..... N89-23862
DOT-FA79WA1-059 ..... N89-23740
DTFA01-80-Y-10546 ..... N89-23758
DTFA01-88-Y-01073 ..... N89-23435
EPA-68-02-4274 ..... N89-23981
ESA-7450/87/NL/PP(SC) N89-23754
ESTEC-6659/86/NL/PH N89-23784
ESTEC-6874/87/GP/I(SC) N89-24003
ESTEC-6945/86/NL/SK N89-24239
FAA-TO701-R N89-23480
FAA-T0503-M N89-24051
FAA-T0702-N N89-23437
FCC-0375 ..... N89-23747
F04611-81-C-0041 ..... N89-23525
F04701-85-C-0086 ..... N89-23506
N89-23694
N89-23803
N89-23995
F08635-83-C-0136 ..... N89-23652
N89-23711
N89-23986
F19628-85-C-0002 ..... N89-23758
N89-24088
F19628-85-C-0003 ..... N89-24049
N89-24075
F19628-86-C-0001 ..... N89-23770
F19628-86-C-0141 ..... N89-23993
F19628-86-K-0009 ..... N89-23497
F30602-81-C-0193 ..... N89-24069
F30602-82-C-0154 ..... N89-23885
N89-23886
F30602-84-C-0153 ..... N89-23797
F30602-87-C-0056 ..... N89-23441
F33615-83-C-2303 ..... N89-23977
F33615-84-C-0600 ..... N89-24032
F33615-84-C-2417 ..... N89-23743
F33615-84-C-3208 ..... N89-23457
F33615-85-C-5093 ..... N89-23706
F33615-86-C-0530 ..... N89-23429
N89-23430
F33615-87-C-3014 ..... N89-23432
F49620-84-K-0005 ..... N89-23829
F49620-85-C-0042 ..... N89-23696
F49620-85-C-0101 ..... N89-23868
F49620-85-C-0105 ..... N89-24209
F49620-85-C-0129 ..... N89-23644
F49620-86-C-0099 ..... N89-24038
F49620-86-C-0111 ..... N89-24112
F49620-86-K-0016 ..... N89-23933
F49620-86-K-0020 ..... N89-23420
N89-23426
N89-23829
F49620-87-C-0046 ..... N89-23452
F49620-87-K-0005 ..... N89-23828
F49620-88-C-0013 ..... N89-23673
F49620-88-C-0097 ..... N89-23831
F49620-88-C-0105 ..... N89-24009
F49620-88-C-0126 ..... N89-23453
GRI-5083-260-0824 ..... N89-23974
GRI-5084-251-1070 ..... N89-23849
GRI-5084-260-1085 ..... N89-23973
GRI-5084-260-1090 ..... N89-23786
GRI-5085-252-1153 ..... N89-24150
GRI-5086-233-1459 ..... N89-23811
GRI-5086-260-1340 ..... N89-23808
GRI-5087-233-1583 ..... N89-23733
GRI-5087-260-1562 ..... N89-23810
IAEA-3227 ..... N89-23596
IAEA-4527 ..... N89-23596
MDA903-84-C-0031 ..... N89-23864
N89-23865
MDA903-88-C-0413 ..... N89-24048
MDA972-89-C-0029 ..... N89-24070
MIPR-ARO-106-88 ..... N89-23868
MIPR-FY1455-86-N-0857 ..... N89-23712
NAGW-112 ..... N89-24162
NAGW-1340 ..... N89-24215
NAG1-182 ..... N89-23856

NAG1-345 ..... N89-23470
NAG1-431 ..... N89-23619
NAG1-517 ..... N89-24112
NAG1-713 ..... N89-23925
N89-23926
N89-23927
N89-23928
NAG1-714 ..... N89-23812
NAG1-732 ..... N89-23418
NAG1-750 ..... N89-24054
NAG2-53 ..... N89-24233
NAG2-311 ..... N89-24231
NAG3-181 ..... N89-23876
NAG3-419 ..... N89-23753
NAG3-856 ..... N89-23918
NAG3-867 ..... N89-23890
N89-23891
NAG5-852 ..... N89-23961
NAG5-859 ..... N89-23852
NAG5-887 ..... N89-23958
NAG5-1051 ..... N89-23478
NAG8-065 ..... N89-24142
NAG9-188 ..... N89-23875
NANB-7-D0737 ..... N89-23636
NASA ORDER C-32000-M N89-23501
NASA ORDER H-98048-B N89-23634
NASA-SAA-C-99066-G N89-23821
NASW-3482 ..... N89-24024
NASW-4154 ..... N89-23746
NAS1-17441 ..... N89-23860
NAS1-17493 ..... N89-23495
NAS1-17497 ..... N89-23920
NAS1-18000 ..... N89-23683
NAS1-18027 ..... N89-23471
NAS1-18028 ..... N89-24033
NAS1-18037 ..... N89-24141
NAS1-18061 ..... N89-24082
NAS1-18107 ..... N89-24112
NAS1-18599 ..... N89-23919
NAS1-18605 ..... N89-23817
N89-24058
N89-24112
N89-24113
N89-24114
NAS2-12051 ..... N89-23512
NAS2-12810 ..... N89-23414
NAS3-23721 ..... N89-24139
NAS3-24564 ..... N89-23818
NAS3-24738 ..... N89-23519
NAS3-24867 ..... N89-23756
N89-23757
NAS3-25266 ..... N89-23622
NAS3-25284 ..... N89-23651
NAS5-30266 ..... N89-23855
NAS7-918 ..... N89-24153
N89-24168
NAS8-30490 ..... N89-23523
NAS8-35322 ..... N89-23515
NAS8-36418 ..... N89-23521
NAS8-37812 ..... N89-24129
NAS10-10285 ..... N89-23982
NCC3-59 ..... N89-23678
NCC3-105 ..... N89-23791
NGL-06-003-057 ..... N89-24251
NGT-21-002-080 ..... N89-23493
N89-24015
NGT-50088 ..... N89-23638
NGT-80001 ..... N89-23493
NIVR-2405N N89-23815
NR PROJ. 042267 ..... N89-24118
NR PROJ. 4325201 ..... N89-23812
NSF ATM-87-09659 ..... N89-23749
NSF CHE-81-19060 ..... N89-24205
NSF CHE-84-21282 ..... N89-24205
NSF DMC-86-12943 ..... N89-23681
NSF DMR-85-01856 ..... N89-24190
NSF DMR-87-19217 ..... N89-24190
NSF DMS-87-03226 ..... N89-24109
NSF ECS-84-10902 ..... N89-23796
NSF MCS-85-04316 ..... N89-24112
NSF MIP-87-09074 ..... N89-23796
NSF MIP-88-14612 ..... N89-24081
NSF MSM-86-13611 ..... N89-23926
NSF OCE-86-13810 ..... N89-24011
NSG-1613 ..... N89-23736
NSG-7627 ..... N89-23693
N00014-80-C-0114 ..... N89-24037
N89-24095
N00014-82-K-0335 ..... N89-24068
N00014-82-K-0576 ..... N89-23669
N00014-82-K-0612 ..... N89-23649
N89-23650
N00014-83-K-0365 ..... N89-24253
N00014-84-C-0134 ..... N89-24011
N00014-84-C-0149 ..... N89-23796
N00014-84-K-0021 ..... N89-23704
N00014-84-K-0472 ..... N89-23705
N89-23672
N00014-85-C-0421 ..... N89-23700
N00014-85-C-2536 ..... N89-23439
N00014-85-C-2642 ..... N89-23531
N00014-85-K-0011 ..... N89-23812
N00014-85-K-0124 ..... N89-23800
N89-24041
N89-24094
N00014-85-K-0331 ..... N89-24200
N00014-85-K-0373 ..... N89-24122
N00014-85-K-0519 ..... N89-23440
N89-24117
N00014-86-C-0435 ..... N89-24207
N00014-86-C-2488 ..... N89-23866
N00014-86-F-0115 ..... N89-23680
N00014-86-K-0043 ..... N89-24136
N89-24197
N89-24198
N00014-86-K-0085 ..... N89-24254
N00014-86-K-0156 ..... N89-24118
N89-24126
N00014-86-K-0289 ..... N89-24040
N89-24042
N00014-86-K-0309 ..... N89-24092
N00014-86-K-0310 ..... N89-24076
N89-24120
N89-24121
N89-24133
N00014-86-K-0366 ..... N89-24154
N89-24169
N89-24170
N89-24171
N89-24173
N89-24174
N00014-86-K-0369 ..... N89-23707
N00014-86-K-0565 ..... N89-24068
N00014-86-K-0685 ..... N89-24094
N00014-86-K-0769 ..... N89-23709
N00014-86-K-0854 ..... N89-23653
N00014-87-K-0036 ..... N89-23627
N00014-87-K-0116 ..... N89-23708
N00014-87-K-0128 ..... N89-23421
N00014-87-K-0284 ..... N89-24063
N00014-87-K-0384 ..... N89-24068
N00014-87-K-0444 ..... N89-24205
N00014-87-K-0482 ..... N89-24045
N00014-87-K-0517 ..... N89-23883
N00014-87-K-0529 ..... N89-23703
N00014-87-K-0723 ..... N89-24012
N00014-87-K-0825 ..... N89-24081
N00014-88-C-0684 ..... N89-24204
N00014-88-C-0714 ..... N89-24196
N00014-88-J-1072 ..... N89-24211
N00014-88-J-1115 ..... N89-23887
N00024-85-C-6041 ..... N89-23668
N00039-84-C-0211 ..... N89-24072
N00167-86-C-0049 ..... N89-23833
ORNL-IA-21428 ..... N89-24213
RF PROJ. 5595 ..... N89-23808
RM3-3-M-20 ..... N89-24045
RR04206 ..... N89-24042
RR04209 ..... N89-24037
N89-24095
W-31-109-ENG-38 ..... N89-23794
N89-24193
W-7405-ENG-38 ..... N89-23655
N89-23668
N89-23690
N89-23857
N89-23858
N89-23988
N89-24167
N89-24243
N89-24256
N89-24257
W-7405-ENG-48 ..... N89-23859
N89-23861
N89-23959
N89-23984
N89-24151
N89-24152
N89-24193
N89-24229
N89-24258
159-41-06 ..... N89-23512
199-22-76-01 ..... N89-24255
307-50-00 ..... N89-23850
324-01-00 ..... N89-23851
352-03-03 ..... N89-23785
474-46-10 ..... N89-23691
474-52-10 ..... N89-23516
505-45-33-56 ..... N89-24033
505-55-41-04 ..... N89-23471
505-61-01-01 ..... N89-23448
505-61-11-01 ..... N89-24140
505-61-41-02 ..... N89-23470
505-61-51 ..... N89-23414
505-61-51-10 ..... N89-23410
505-62-01 ..... N89-24055
505-62-21 ..... N89-23413
N89-23417
N89-23465
N89-23809
N89-23821
505-63-1B N89-23621
505-63-01-05 ..... N89-23919
505-63-21-02 ..... N89-23447
505-63-31 ..... N89-23918
505-63-51-01 ..... N89-23920
505-63-51-03 ..... N89-24079
505-66-01-02 ..... N89-23468
N89-23469
505-69-61-03 ..... N89-23415
505-90-01 ..... N89-23416
N89-23813
505-90-21-01 ..... N89-23817
N89-24058
N89-24113
N89-24114
506-40-41-01 ..... N89-23412
506-41-11 ..... N89-23517
N89-23792
506-42-31 ..... N89-23520
506-42-32 ..... N89-23522
506-43-11-01 ..... N89-23683
506-43-21-04 ..... N89-23528
N89-23547
506-44-20 ..... N89-23791
506-44-21-01 ..... N89-23860
506-49-11-01 ..... N89-24082
510-01-01 ..... N89-23822
532-09-01 ..... N89-23819
535-03-01 ..... N89-24138
N89-24139
535-03-01-01 ..... N89-23433
535-03-11-04 ..... N89-24141
584-01-31 ..... N89-23858
585-01-31-05 ..... N89-23924
586-01-11 ..... N89-23518
N89-23527
N89-23823
643-10-01 ..... N89-23756
N89-23757
650-60-20 ..... N89-23753
674-03-03 ..... N89-23501
674-22-05 ..... N89-23638
674-25-05 ..... N89-23664
805-19-00-01 ..... N89-24022
N89-24023

Typical Report Number Index Listing

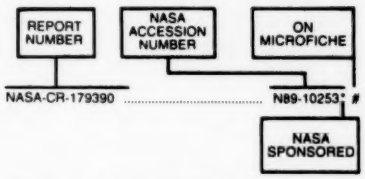

Listings in this index are arranged alphanumerically by report number. The NASA accession number denotes the number by which the citation is identified. An asterisk (*) indicates that the item is a NASA report. A pound sign (#) indicates that the item is available on microfiche.

A-88256-VOL-1 ..... N89-24022* #
A-88256-VOL-2 ..... N89-24023* #
A-88306 ..... N89-23820* #
A-89068 ..... N89-23785* #
A-89099 ..... N89-24111* #

AAMRL-TR-88-063 ..... N89-23767 #

ACT-104 ..... N89-23796 #

AD-A193416 ..... N89-24051 #
AD-A199947 ..... N89-24227 #
AD-A203874 ..... N89-24249 #
AD-A204051 ..... N89-23916 #
AD-A204073 ..... N89-23711 #
AD-A204086 ..... N89-23449 #
AD-A204087 ..... N89-24057 #
AD-A204174 ..... N89-24061 #
AD-A205289 ..... N89-24005 #
AD-A205296 ..... N89-23665 #
AD-A205303 ..... N89-23451 #
AD-A205304 ..... N89-24217 #
AD-A205305 ..... N89-23795 #
AD-A205306 ..... N89-23524 #
AD-A205307 ..... N89-24065 #
AD-A205312 ..... N89-24215 #
AD-A205318 ..... N89-23884 #
AD-A205319 ..... N89-23885 #
AD-A205321 ..... N89-24196 #
AD-A205325 ..... N89-24197 #
AD-A205326 ..... N89-24252 #
AD-A205327 ..... N89-24061 #
AD-A205328 ..... N89-23759 #
AD-A205331 ..... N89-24025 #
AD-A205335 ..... N89-23798 #
AD-A205337 ..... N89-24092 #
AD-A205342 ..... N89-24006 #
AD-A205345 ..... N89-23797 #
AD-A205351 ..... N89-23438 #
AD-A205353 ..... N89-23929 #
AD-A205354 ..... N89-24093 #
AD-A205355 ..... N89-23780 #
AD-A205362 ..... N89-24007 #
AD-A205367 ..... N89-24053 #
AD-A205371 ..... N89-23866 #
AD-A205374 ..... N89-24115 #
AD-A205388 ..... N89-24026 #
AD-A205401 ..... N89-23694 #
AD-A205402 ..... N89-23761 #
AD-A205403 ..... N89-23762 #
AD-A205404 ..... N89-23763 #
AD-A205415 ..... N89-23644 #
AD-A205434 ..... N89-24045 #
AD-A205440 ..... N89-23407 #
AD-A205448 ..... N89-23990 #
AD-A205449 ..... N89-23645 #
AD-A205452 ..... N89-23977 #
AD-A205456 ..... N89-23513 #
AD-A205458 ..... N89-23784 #
AD-A205459 ..... N89-23765 #
AD-A205460 ..... N89-24116 #
AD-A205462 ..... N89-23420 #
AD-A205463 ..... N89-23824 #
AD-A205467 ..... N89-23695 #
AD-A205468 ..... N89-23646 #
AD-A205469 ..... N89-23798 #
AD-A205470 ..... N89-23712 #
AD-A205471 ..... N89-23867 #
AD-A205476 ..... N89-24046 #
AD-A205487 ..... N89-24198 #
AD-A205500 ..... N89-23825 #
AD-A205501 ..... N89-24066 #
AD-A205503 ..... N89-23452 #
AD-A205505 ..... N89-24167 #
AD-A205525 ..... N89-23799 #
AD-A205559 ..... N89-23740 #
AD-A205570 ..... N89-23826 #
AD-A205572 ..... N89-23647 #
AD-A205578 ..... N89-23827 #
AD-A205585 ..... N89-24125 #
AD-A205586 ..... N89-23696 #
AD-A205587 ..... N89-23828 #
AD-A205588 ..... N89-23453 #
AD-A205589 ..... N89-23930 #
AD-A205593 ..... N89-23991 #
AD-A205599 ..... N89-24253 #
AD-A205602 ..... N89-24131 #
AD-A205604 ..... N89-23439 #
AD-A205606 ..... N89-23766* #
AD-A205607 ..... N89-23421 #
AD-A205613 ..... N89-23767 #
AD-A205618 ..... N89-23741 #
AD-A205621 ..... N89-23666 #
AD-A205622 ..... N89-23931 #
AD-A205623 ..... N89-23481 #
AD-A205624 ..... N89-23697 #
AD-A205625 ..... N89-23868 #
AD-A205627 ..... N89-23698 #
AD-A205628 ..... N89-23699 #
AD-A205632 ..... N89-24135 #
AD-A205644 ..... N89-24168* #
AD-A205649 ..... N89-24237 #
AD-A205664 ..... N89-24199 #
AD-A205667 ..... N89-24094 #
AD-A205668 ..... N89-24034 #
AD-A205672 ..... N89-24062 #
AD-A205674 ..... N89-23648 #
AD-A205676 ..... N89-23454 #
AD-A205682 ..... N89-23625 #
AD-A205686 ..... N89-24169 #
AD-A205687 ..... N89-24170 #
AD-A205688 ..... N89-24171 #
AD-A205689 ..... N89-24154 #
AD-A205692 ..... N89-23667 #
AD-A205696 ..... N89-23422 #
AD-A205699 ..... N89-24200 #
AD-A205714 ..... N89-23472 #
AD-A205716 ..... N89-24172 #
AD-A205717 ..... N89-23668 #
AD-A205718 ..... N89-23829 #
AD-A205723 ..... N89-23473 #
AD-A205724 ..... N89-23768 #
AD-A205725 ..... N89-23881 #
AD-A205726 ..... N89-23669 #
AD-A205727 ..... N89-23769 #
AD-A205730 ..... N89-23455 #
AD-A205733 ..... N89-24011 #
AD-A205739 ..... N89-23423 #
AD-A205741 ..... N89-23869 #
AD-A205742 ..... N89-24225 #
AD-A205744 ..... N89-23770 #
AD-A205745 ..... N89-24012 #
AD-A205746 ..... N89-24173 #
AD-A205747 ..... N89-24174 #
AD-A205751 ..... N89-24095 #
AD-A205771 ..... N89-23424 #
AD-A205772 ..... N89-24201 #
AD-A205775 ..... N89-24126 #
AD-A205783 ..... N89-23440 #
AD-A205784 ..... N89-24117 #
AD-A205785 ..... N89-24136 #
AD-A205787 ..... N89-24063 #
AD-A205799 ..... N89-23700 #
AD-A205819 ..... N89-23992 #
AD-A205822 ..... N89-23496 #
AD-A205823 ..... N89-23425 #
AD-A205825 ..... N89-23993 #
AD-A205826 ..... N89-23497 #
AD-A205828 ..... N89-24064 #
AD-A205829 ..... N89-24118 #
AD-A205834 ..... N89-23701 #
AD-A205837 ..... N89-23830 #
AD-A205859 ..... N89-23771 #
AD-A205860 ..... N89-24035 #
AD-A205861 ..... N89-24027 #
AD-A205898 ..... N89-23441 #
AD-A205935 ..... N89-24156 #
AD-A205936 ..... N89-23670 #
AD-A205937 ..... N89-23482 #
AD-A205938 ..... N89-24036 #
AD-A205939 ..... N89-23831 #
AD-A205943 ..... N89-23962 #
AD-A205946 ..... N89-24203 #
AD-A205951 ..... N89-23772 #
AD-A205953 ..... N89-24204 #
AD-A205957 ..... N89-23882 #
AD-A205961 ..... N89-23626 #
AD-A205963 ..... N89-24037 #
AD-A205965 ..... N89-23442 #
AD-A205967 ..... N89-23773 #
AD-A205970 ..... N89-23456 #
AD-A205972 ..... N89-23832 #
AD-A205974 ..... N89-24028 #
AD-A205975 ..... N89-23703 #
AD-A205980 ..... N89-23704 #
AD-A205987 ..... N89-24144 #
AD-A205988 ..... N89-24008 #
AD-A205989 ..... N89-23426 #
AD-A205993 ..... N89-24038 #
AD-A205994 ..... N89-23833 #
AD-A205997 ..... N89-23671 #
AD-A205998 ..... N89-23774 #
AD-A206008 ..... N89-23932 #
AD-A206009 ..... N89-23505 #
AD-A206011 ..... N89-23834 #
AD-A206012 ..... N89-24205 #
AD-A206015 ..... N89-24206 #
AD-A206021 ..... N89-23835 #
AD-A206022 ..... N89-23498 #
AD-A206023 ..... N89-23836 #
AD-A206024 ..... N89-23475 #
AD-A206025 ..... N89-23483 #
AD-A206031 ..... N89-24029 #
AD-A206032 ..... N89-24030 #
AD-A206035 ..... N89-24039 #
AD-A206037 ..... N89-24065 #
AD-A206039 ..... N89-23885 #
AD-A206040 ..... N89-23886 #
AD-A206043 ..... N89-23649 #
AD-A206045 ..... N89-24207 #
AD-A206046 ..... N89-24087 #
AD-A206047 ..... N89-24066 #
AD-A206048 ..... N89-24119 #
AD-A206049 ..... N89-23427 #
AD-A206052 ..... N89-24254 #
AD-A206057 ..... N89-24208 #
AD-A206061 ..... N89-23627 #
AD-A206065 ..... N89-23672 #
AD-A206068 ..... N89-23476 #
AD-A206072 ..... N89-23673 #
AD-A206083 ..... N89-23443 #
AD-A206084 ..... N89-23994 #
AD-A206092 ..... N89-23742 #
AD-A206094 ..... N89-24130 #
AD-A206096 ..... N89-23775 #
AD-A206098 ..... N89-23705 #
AD-A206099 ..... N89-23525 #
AD-A206100 ..... N89-23933 #
AD-A206101 ..... N89-23713 #
AD-A206102 ..... N89-24009 #
AD-A206113 ..... N89-24067 #
AD-A206117 ..... N89-24047 #
AD-A206124 ..... N89-23628 #
AD-A206134 ..... N89-23853 #
AD-A206135 ..... N89-24127 #
AD-A206136 ..... N89-23934 #
AD-A206137 ..... N89-23870 #

AD-A206136 ..... N89-23428 #
AD-A206140 ..... N89-23776 #
AD-A206145 ..... N89-23837 #
AD-A206156 ..... N89-23674 #
AD-A206157 ..... N89-24040 #
AD-A206173 ..... N89-24041 #
AD-A206175 ..... N89-23800 #
AD-A206201 ..... N89-24048 #
AD-A206208 ..... N89-24088 #
AD-A206228 ..... N89-24088 #
AD-A206229 ..... N89-24157 #
AD-A206230 ..... N89-23871 #
AD-A206244 ..... N89-23986 #
AD-A206256 ..... N89-24010 #
AD-A206266 ..... N89-23506 #
AD-A206269 ..... N89-23838 #
AD-A206270 ..... N89-23872 #
AD-A206271 ..... N89-23801 #
AD-A206285 ..... N89-23743 #
AD-A206286 ..... N89-23457 #
AD-A206287 ..... N89-23706 #
AD-A206290 ..... N89-23429 #
AD-A206291 ..... N89-23430 #
AD-A206293 ..... N89-24069 #
AD-A206296 ..... N89-23650 #
AD-A206306 ..... N89-23714 #
AD-A206308 ..... N89-24070 #
AD-A206314 ..... N89-23444 #
AD-A206318 ..... N89-23744 #
AD-A206323 ..... N89-23526 #
AD-A206324 ..... N89-23887 #
AD-A206325 ..... N89-23458 #
AD-A206326 ..... N89-24132 #
AD-A206327 ..... N89-24158 #
AD-A206335 ..... N89-24246 #
AD-A206336 ..... N89-23839 #
AD-A206340 ..... N89-24137 #
AD-A206347 ..... N89-23854 #
AD-A206348 ..... N89-24148 #
AD-A206350 ..... N89-23888 #
AD-A206352 ..... N89-23935 #
AD-A206363 ..... N89-23802 #
AD-A206364 ..... N89-23431 #
AD-A206366 ..... N89-24126 #
AD-A206370 ..... N89-23675 #
AD-A206371 ..... N89-24096 #
AD-A206372 ..... N89-24209 #
AD-A206388 ..... N89-24120 #
AD-A206389 ..... N89-24121 #
AD-A206395 ..... N89-23707 #
AD-A206396 ..... N89-24210 #
AD-A206403 ..... N89-24122 #
AD-A206438 ..... N89-23651 #
AD-A206439 ..... N89-24226 #
AD-A206441 ..... N89-23676 #
AD-A206443 ..... N89-24071 #
AD-A206451 ..... N89-24072 #
AD-A206452 ..... N89-24042 #
AD-A206453 ..... N89-23432 #
AD-A206456 ..... N89-23803 #
AD-A206459 ..... N89-23995* #
AD-A206460 ..... N89-23652 #
AD-A206463 ..... N89-24031 #
AD-A206469 ..... N89-24073 #
AD-A206483 ..... N89-24211 #
AD-A206487 ..... N89-23507 #
AD-A206502 ..... N89-23708 #
AD-A206504 ..... N89-23883 #
AD-A206510 ..... N89-23715 #
AD-A206514 ..... N89-24032 #
AD-A206530 ..... N89-23709 #
AD-A206534 ..... N89-24074 #
AD-A206536 ..... N89-23459 #
AD-A206553 ..... N89-24133 #
AD-A206560 ..... N89-23653 #
AD-A206563 ..... N89-23716 #
AD-A206564 ..... N89-23717 #
AD-A206573 ..... N89-24075 #
AD-A206574 ..... N89-24049 #
AD-A206576 ..... N89-24076 #

AD-D013956 ..... N89-24202 #
AD-D013960 ..... N89-24155 #
AD-D013962 ..... N89-23474 #
AD-D013966 ..... N89-23702 #

AD-E501074 ..... N89-23864 #
AD-E501075 ..... N89-23665 #
AD-E501078 ..... N89-23473 #
AD-E501079 ..... N89-23669 #
AD-E501079 ..... N89-23766 #
AD-E501079 ..... N89-23769 #
AD-E501079 ..... N89-23881 #
AD-E900856 ..... N89-23744 #
AD-E951232 ..... N89-23887 #
AD-E951239 ..... N89-24132 #
AD-E951249 ..... N89-23458 #
AD-E951293 ..... N89-24158 #
AD-E951294 ..... N89-23526 #
AD-E951297 ..... N89-23916 #

AFAL-TR-87-095 ..... N89-23525 #

AFESC/ESL-TR-88-02 ..... N89-23711 #
AFESC/ESL-TR-88-06 ..... N89-23652 #
AFESC/ESL-TR-88-24 ..... N89-23986 #

AFGL-TR-88-0129 ..... N89-23497 #
AFGL-TR-88-0327 ..... N89-23993 #
AFGL-TR-89-0060 ..... N89-24252 #

AFHRL-TR-88-53 ..... N89-24218 #

AFIT/GA/AA/88D-01 ..... N89-23498 #
AFIT/GA/AA/88D-12 ..... N89-23932 #
AFIT/GA/AA/88M-1 ..... N89-23853 #
AFIT/GA/AA/89M-01 ..... N89-24127 #
AFIT/GA/AA/89M-02 ..... N89-23934 #

AFIT/GAE/AA/88D-02 ..... N89-23424 #
AFIT/GAE/AA/88D-11 ..... N89-23425 #
AFIT/GAE/AA/88D-16 ..... N89-23836 #
AFIT/GAE/AA/88D-20 ..... N89-23483 #
AFIT/GAE/AA/88D-33 ..... N89-23427 #
AFIT/GAE/AA/89M-1 ..... N89-23834 #
AFIT/GAE/AA/89M-2 ..... N89-23426 #
AFIT/GAE/AA/89M-3 ..... N89-23870 #

AFIT/GCS/ENG/88D-4 ..... N89-24066 #
AFIT/GCS/ENG/88D-11 ..... N89-24087 #
AFIT/GCS/ENG/89M-2 ..... N89-24130 #

AFIT/GE/ENG/88D-26 ..... N89-24201 #
AFIT/GE/ENG/88D-55 ..... N89-23881 #
AFIT/GE/ENG/89M-1 ..... N89-23476 #
AFIT/GE/ENG/89M-4-VOL-1 ..... N89-23768 #
AFIT/GE/ENG/89M-5 ..... N89-23475 #
AFIT/GE/ENG/89M-5-VOL-1 ..... N89-23473 #
AFIT/GE/ENG/89M-7 ..... N89-23769 #
AFIT/GE/ENG/89M-8 ..... N89-23443 #

AFIT/GNE/ENP/89M-4 ..... N89-23742 #

AFIT/GOR/ENS/88D-13 ..... N89-24119 #

AFIT/GSE/AA/88D-2 ..... N89-23454 #

AFIT/GSO/AA/88D-2 ..... N89-23505 #
AFIT/GSO/AA/88D-16 ..... N89-23496 #

AFIT/GSO/ENS/88D-1 ..... N89-23994 #

AFIT/GST/ENS/89M-6 ..... N89-23456 #
AFIT/GST/ENS/89M-05 ..... N89-23455 #

AFIT/MA/GE/88D-1 ..... N89-23775 #

AFOSR-89-0044TR-APP ..... N89-24249 #
AFOSR-89-0076TR ..... N89-23830 #
AFOSR-89-0127TR ..... N89-23452 #
AFOSR-89-0140TR ..... N89-23933 #
AFOSR-89-0232TR ..... N89-23426 #
AFOSR-89-0233TR ..... N89-24144 #
AFOSR-89-0234TR ..... N89-23713 #
AFOSR-89-0235TR ..... N89-23665 #
AFOSR-89-0241TR ..... N89-24008 #
AFOSR-89-0261TR ..... N89-23701 #
AFOSR-89-0262TR ..... N89-24217 #
AFOSR-89-0265TR ..... N89-23644 #
AFOSR-89-0266TR ..... N89-23799 #
AFOSR-89-0267TR ..... N89-23645 #
AFOSR-89-0272TR ..... N89-24009 #
AFOSR-89-0275TR ..... N89-23420 #
AFOSR-89-0276TR ..... N89-24125 #
AFOSR-89-0281TR ..... N89-23696 #
AFOSR-89-0282TR ..... N89-23829 #
AFOSR-89-0283TR ..... N89-23991 #
AFOSR-89-0287TR ..... N89-23837 #
AFOSR-89-0294TR ..... N89-24172 #
AFOSR-89-0301TR ..... N89-23647 #
AFOSR-89-0303TR ..... N89-23828 #
AFOSR-89-0304TR ..... N89-23835 #
AFOSR-89-0307TR ..... N89-23930 #
AFOSR-89-0309TR ..... N89-23826 #
AFOSR-89-0310TR ..... N89-23453 #
AFOSR-89-0316TR ..... N89-24237 #
AFOSR-89-0319TR ..... N89-23773 #
AFOSR-89-0325TR ..... N89-24203 #
AFOSR-89-0328TR ..... N89-23507 #
AFOSR-89-0331TR ..... N89-24168* #
AFOSR-89-0345TR ..... N89-24246 #
AFOSR-89-0350TR ..... N89-24131 #
AFOSR-89-0352TR ..... N89-24073 #
AFOSR-89-0360TR ..... N89-24209 #
AFOSR-89-0361TR ..... N89-24038 #
AFOSR-89-0364TR ..... N89-23831 #
AFOSR-89-0365TR ..... N89-24208 #
AFOSR-89-0366TR ..... N89-23673 #
AFOSR-89-0436TR ..... N89-23651 #

AFRRI-TR88-2 ..... N89-24026 #

AFWAL-TR-87-2042-VOL-6 ..... N89-23712 #
AFWAL-TR-88-2045 ..... N89-23977 #
AFWAL-TR-88-2062 ..... N89-23743 #
AFWAL-TR-88-2152 ..... N89-23882 #
AFWAL-TR-88-3119 ..... N89-23457 #
AFWAL-TR-88-4249 ..... N89-23706 #

AI-TR-1045 ..... N89-24094 #
AI-TR-1092 ..... N89-24041 #
AI-TR-1099 ..... N89-23800 #

AIAA-89-1143 ..... N89-24138* #
AIAA-89-1744 ..... N89-23818* #
AIAA-89-2943 ..... N89-23416* #

AIST-8801 ..... N89-23975 #

AMSEL-NV-TR-0075 ..... N89-24047 #

AMSMI/CR-RD-GC-88-1 ..... N89-24132 #

AMSMI/TR-OR-SA-88-01 ..... N89-23887 #

AMSMI/TR-RD-GC-88-14 ..... N89-23458 #
AMSMI/TR-RD-GC-88-22 ..... N89-24158 #

AMSMI/TR-RD-ST-88-7 ..... N89-23526 #
AMSMI/TR-RD-ST-88-9 ..... N89-23916 #

AMXTH-TE-CR-88026 ..... N89-23714 #

ARAED-TR-88041 ..... N89-23472 #
ARAED-TR-89006 ..... N89-23472 #

ARCCB-MR-89004 ..... N89-23931 #

ARCCB-TR-89002 ..... N89-23741 #
ARCCB-TR-89005 ..... N89-23666 #

ARDU-TI-953 ..... N89-23451 #

ARI-RN-89-04 ..... N89-24048 #
ARI-RN-89-09 ..... N89-23407 #

ARL-AERO-TM-400 ..... N89-23449 #

ARL-STRUC-TM-490 ..... N89-24057 #

ARL/PSU/TR-88-015 ..... N89-23668 #

ARO-20928.8-EG ..... N89-23423 #
ARO-21286.11-MS ..... N89-24135 #
ARO-22392.5-MS ..... N89-24210 #
ARO-22536.5-CH ..... N89-23698 #
ARO-22677.11-LS ..... N89-23699 #
ARO-22727.13-CH ..... N89-23675 #
ARO-22842.25-PH ..... N89-23868 #
ARO-22935.3-EL-S ..... N89-24062 #
ARO-22943.12-MA ..... N89-23839 #
ARO-23525.27-EG ..... N89-23674 #
ARO-24166.5-MA ..... N89-24137 #
ARO-24543.9-EL ..... N89-23802 #
ARO-26394.1-MA ..... N89-24128 #

ARS-75 ..... N89-24001 #

ASD-TR-88-5037 ..... N89-23774 #

ASL-TR-0226 ..... N89-24010 #

ASU-CR-R-89021 ..... N89-23423 #

ATC-168-EXEC-SUMM ..... N89-23758 #

AVSCOM-TM-89-B-003 ..... N89-24079* #

AVSCOM-TR-89-B-001 ..... N89-23410* #

BBC-RD-1988/13 ..... N89-23745

BBN-6741-VOL-1 ..... N89-23429 #
BBN-6742-VOL-2 ..... N89-23430 #

BCRS-88-02 ..... N89-23969 #
BCRS-88-10A ..... N89-23970 #
BCRS-88-10B ..... N89-23971 #

BNL-42266 ..... N89-24190 #

BRDEC-2473 ..... N89-23695 #
BRDEC-2477 ..... N89-23888 #

BRL-TR-2975 ..... N89-23824 #
BRL-TR-2976 ..... N89-23717 #
BRL-TR-2983 ..... N89-23459 #
BRL-TR-2985 ..... N89-23716 #

CH-88-05 ..... N89-23981 #

CI-91 ..... N89-23960 #

CLASSIC-89-23 ..... N89-24068 #

CMU/SEI-89-TR-1 ..... N89-24075 #
CMU/SEI-89-TR-4 ..... N89-24049 #

CONF-880760-11 ..... N89-23923 #
CONF-880904-9 ..... N89-23863 #
CONF-880912-28 ..... N89-24195 #
CONF-881155-42 ..... N89-23655 #
CONF-881155-52 ..... N89-23861 #
CONF-881155-53 ..... N89-24192 #
CONF-881212-1 ..... N89-24258 #
CONF-881275-1 ..... N89-24191 #
CONF-890189-2 ..... N89-24257 #
CONF-890189-4 ..... N89-24256 #
CONF-890189-5 ..... N89-24151 #
CONF-890194-1 ..... N89-24059 #
CONF-890195-1 ..... N89-24243 #
CONF-890199-2 ..... N89-23988 #
CONF-890216-1 ..... N89-24193 #
CONF-890240-4 ..... N89-23794 #
CONF-890272-1 ..... N89-23877 #
CONF-890273-1 ..... N89-23685 #
CONF-890302-16 ..... N89-24186 #
CONF-890306-1 ..... N89-23690 #
CONF-890335-8-VUGRAPHS ..... N89-23793 #
CONF-890358-4 ..... N89-23858 #
CONF-890373-4-VUGRAPHS ..... N89-23876 #
CONF-890374-1 ..... N89-23752 #
CONF-890423-7 ..... N89-23859 #
CONF-890423-8 ..... N89-24152 #
CONF-890435-1 ..... N89-23857 #
CONF-8806105-6 ..... N89-24106 #
CONF-8809123-2 ..... N89-23682 #
CONF-8809312-1 ..... N89-23976 #
CONF-8810195-6 ..... N89-23684 #
CONF-8810231-9 ..... N89-23499 #
CONF-8810256-1 ..... N89-24190 #
CONF-8810296-4 ..... N89-23861 #
CONF-8810330-1 ..... N89-23659 #
CONF-8811176-1 ..... N89-24186 #
CONF-8904111-5 ..... N89-23790 #
CONF-8904117-1 ..... N89-23959 #
CONF-8904128-3 ..... N89-23984 #
CONF-8904138-1 ..... N89-23688 #

CRDEC-TR-030 ..... N89-23648 #
CRDEC-TR-045 ..... N89-23628 #

CREO-6374 ..... N89-24003 #

CRREL-SR-89-2 ..... N89-23740 #

DDD-CP/TE-RE-7450 ..... N89-23754 #

DE88-705663 ..... N89-24181 #
DE88-705669 ..... N89-24182 #
DE88-705689 ..... N89-24183 #
DE88-705690 ..... N89-24184 #
DE88-705691 ..... N89-24103 #
DE88-705702 ..... N89-24185 #
DE88-705781 ..... N89-23658 #
DE88-705782 ..... N89-24247 #
DE88-705823 ..... N89-24106 #
DE88-705825 ..... N89-24107 #
DE88-756448 ..... N89-23975 #
DE89-006556 ..... N89-23655 #
DE89-006560 ..... N89-23657 #
DE89-006730 ..... N89-23959 #
DE89-007268 ..... N89-24147 #
DE89-007336 ..... N89-23682 #
DE89-007399 ..... N89-23789 #
DE89-007643 ..... N89-23877 #
DE89-007658 ..... N89-24186 #
DE89-007847 ..... N89-24186 #
DE89-007974 ..... N89-23790 #
DE89-007993 ..... N89-24256 #
DE89-008012 ..... N89-24257 #
DE89-008014 ..... N89-23858 #
DE89-008026 ..... N89-23859 #
DE89-008044 ..... N89-24258 #
DE89-008157 ..... N89-24190 #
DE89-008172 ..... N89-23684 #
DE89-008234 ..... N89-24191 #
DE89-008243 ..... N89-23685 #
DE89-008245 ..... N89-23976 #
DE89-008253 ..... N89-23659 #
DE89-008278 ..... N89-23752 #
DE89-008565 ..... N89-23681 #
DE89-008697 ..... N89-24108 #
DE89-008728 ..... N89-23921 #
DE89-008732 ..... N89-23878 #
DE89-008748 ..... N89-24192 #
DE89-008800 ..... N89-24059 #
DE89-008820 ..... N89-23686 #
DE89-008827 ..... N89-24193 #
DE89-008830 ..... N89-23681 #
DE89-008831 ..... N89-24151 #
DE89-008881 ..... N89-24194 #
DE89-008882 ..... N89-24214 #
DE89-008883 ..... N89-23640 #
DE89-008888 ..... N89-23641 #
DE89-008891 ..... N89-24152 #
DE89-008939 ..... N89-23793 #
DE89-008961 ..... N89-23687 #
DE89-008980 ..... N89-24083 #
DE89-008988 ..... N89-23879 #
DE89-009002 ..... N89-23922 #
DE89-009009 ..... N89-24229 #
DE89-009041 ..... N89-23862 #
DE89-009059 ..... N89-23863 #
DE89-009064 ..... N89-23662 #
DE89-009148 ..... N89-23642 #
DE89-009158 ..... N89-24228 #
DE89-009248 ..... N89-24243 #
DE89-009251 ..... N89-23688 #
DE89-009292 ..... N89-23689 #
DE89-009348 ..... N89-23986 #
DE89-009350 ..... N89-23690 #
DE89-009379 ..... N89-24195 #
DE89-009536 ..... N89-23499 #
DE89-009584 ..... N89-24109 #
DE89-009600 ..... N89-23663 #
DE89-009639 ..... N89-24110 #
DE89-009648 ..... N89-23923 #
DE89-009808 ..... N89-23794 #
DE89-009982 ..... N89-23984 #

DFVLR-IB-333-87/2 ..... N89-23719 #

DOD-4100.39-M-VOL-2 ..... N89-24221 #
DOD-4100.39-M-VOL-8-CHANGE-3 ..... N89-24220 #

DODA-AR-003-256 ..... N89-23451 #
DODA-AR-005-528 ..... N89-24057 #
DODA-AR-005-534 ..... N89-23449 #

DOE/CE-0247 ..... N89-23879 #
DOE/CE-15319/T8 ..... N89-23789 #

DOE/ER-13218/23 ..... N89-23641 #
DOE/ER-13623/2 ..... N89-24214 #
DOE/ER-13759/2 ..... N89-23640 #
DOE/ER-13786/T1 ..... N89-23862 #
DOE/ER-25026/26 ..... N89-24109 #
DOE/ER-45214/T4 ..... N89-23662 #
DOE/ER-45251/T2 ..... N89-23642 #
DOE/ER-45290/2 ..... N89-23921 #
DOE/ER-45310/17 ..... N89-24194 #
DOE/ER-45366/1 ..... N89-23689 #

DOE/ET-32043/T26-VOL-1 ..... N89-24147 #

DOT/FAA/CT-TN87/43 ..... N89-24051 #
DOT/FAA/CT-TN88/45 ..... N89-23480 #
DOT/FAA/CT-TN89/4 ..... N89-23438 #
DOT/FAA/CT-TN89/16 ..... N89-23437 #

DOT/FAA/DS-89/07 ..... N89-23435 #

DOT/FAA/PS-89/1 ..... N89-23740 #
DOT/FAA/PS-89/6-EXEC-SUMM ..... N89-23758 #

DREO-TN-88-31 ..... N89-24074 #

DREO-991 ..... N89-23762 #
DREO-993 ..... N89-23763 #
DREO-995 ..... N89-23772 #
DREO-998 ..... N89-24046 #

DRES-SM-1271 ..... N89-23481 #

DRES-SP-124 ..... N89-23761 #

DRIC-BR-109213 ..... N89-23444 #

D210-12328-3 ..... N89-23920* #
E-4440 ..... N89-23638* #
E-4570 ..... N89-23621* #
E-4682 ..... N89-23813* #
E-4686 ..... N89-23691* #
E-4689 ..... N89-23485* #
E-4690 ..... N89-24055* #
E-4700 ..... N89-24138* #
E-4703 ..... N89-23413* #
E-4707 ..... N89-23518* #
E-4711 ..... N89-23809* #
E-4727 ..... N89-23417* #
E-4730 ..... N89-23516* #
E-4741 ..... N89-23792* #
E-4742 ..... N89-23520* #
E-4744 ..... N89-23517* #
E-4749 ..... N89-23818* #
E-4759 ..... N89-23664* #
E-4770 ..... N89-23821* #
E-4791 ..... N89-23416* #
E-4792 ..... N89-23527* #
E-4793 ..... N89-23753* #
E-4796 ..... N89-23622* #
E-4798 ..... N89-23850* #
E-4802 ..... N89-23522* #
E-4812 ..... N89-23501* #
E-4815 ..... N89-23823* #
E-4825 ..... N89-23791* #

ECAO-R-019S ..... N89-23980 #

EGG-M-88151 ..... N89-23923 #

EPA/AA/CTAB-88/10 ..... N89-23874 #

EPA/AA/TEB-88/02 ..... N89-23734 #

EPA/IRM-88/503-VOL-1 ..... N89-24080 #
EPA/IRM-88/8801 ..... N89-24222 #

EPA/600/8-88/105A ..... N89-23980 #
EPA/600/8-88/106 ..... N89-23981 #

ERIM-198900-2-F ..... N89-24096 #

ESA-BR-54 ..... N89-24223 #

ESA-CR(P)-2734 ..... N89-23754 #
ESA-CR(P)-2743 ..... N89-24003 #

ESA-SP-1109 ..... N89-24230 #

ESD-TR-88-290 ..... N89-23770 #
ESD-TR-88-322 ..... N89-24088 #
ESD-TR-89-01 ..... N89-24075 #
ESD-TR-89-04 ..... N89-24049 #

ESL-719493-6 ..... N89-23736* #

ETN-89-93758 ..... N89-23719 #
ETN-89-93766 ..... N89-23788 #
ETN-89-93779 ..... N89-23941 #
ETN-89-93943 ..... N89-24145 #
ETN-89-93944 ..... N89-23836 #
ETN-89-93945 ..... N89-23978 #
ETN-89-93946 ..... N89-23445 #
ETN-89-93947 ..... N89-24248 #
ETN-89-93948 ..... N89-23937 #
ETN-89-93949 ..... N89-23996 #
ETN-89-93950 ..... N89-23710 #
ETN-89-93951 ..... N89-24123 #
ETN-89-93956 ..... N89-23569 #
ETN-89-93963 ..... N89-23963 #
ETN-89-93964 ..... N89-23660 #
ETN-89-93965 ..... N89-24187 #
ETN-89-93968 ..... N89-23718 #
ETN-89-93989 ..... N89-24176
ETN-89-93991 ..... N89-24238 #
ETN-89-93998 ..... N89-23963
ETN-89-94109 ..... N89-23840 #
ETN-89-94110 ..... N89-24177 #
ETN-89-94114 ..... N89-23841 #
ETN-89-94115 ..... N89-23842 #
ETN-89-94116 ..... N89-23843 #
ETN-89-94117 ..... N89-23654 #
ETN-89-94143 ..... N89-23814 #
ETN-89-94145 ..... N89-23446 #
ETN-89-94146 ..... N89-23964 #
ETN-89-94148 ..... N89-23965 #
ETN-89-94149 ..... N89-23966 #
ETN-89-94150 ..... N89-23967 #
ETN-89-94151 ..... N89-23968 #
ETN-89-94152 ..... N89-23997
ETN-89-94196 ..... N89-23815 #
ETN-89-94210 ..... N89-24165 #
ETN-89-94211 ..... N89-24089 #
ETN-89-94212 ..... N89-24090 #

ETN-89-94213 ..... N89-24091 #
ETN-89-94214 ..... N89-23737 #
ETN-89-94217 ..... N89-23917 #
ETN-89-94218 ..... N89-24188 #
ETN-89-94219 ..... N89-24189 #
ETN-89-94220 ..... N89-23960 #
ETN-89-94223 ..... N89-24104 #
ETN-89-94224 ..... N89-24105 #
ETN-89-94225 ..... N89-23816 #
ETN-89-94228 ..... N89-23751 #
ETN-89-94236 ..... N89-24223 #
ETN-89-94237 ..... N89-24230 #
ETN-89-94259 ..... N89-24124 #
ETN-89-94266 ..... N89-23969 #
ETN-89-94269 ..... N89-23970 #
ETN-89-94290 ..... N89-23971 #
ETN-89-94304 ..... N89-24077 #
ETN-89-94305 ..... N89-24149 #
ETN-89-94306 ..... N89-23777 #
ETN-89-94309 ..... N89-23778 #
ETN-89-94310 ..... N89-23779 #
ETN-89-94311 ..... N89-23804 #
ETN-89-94366 ..... N89-23844 #
ETN-89-94390 ..... N89-24239
ETN-89-94395 ..... N89-24159
ETN-89-94408 ..... N89-24146 #
ETN-89-94409 ..... N89-24212 #
ETN-89-94410 ..... N89-24013 #
ETN-89-94411 ..... N89-24014 #
ETN-89-94424 ..... N89-23972 #
ETN-89-94426 ..... N89-23938 #
ETN-89-94460 ..... N89-23754 #
ETN-89-94465 ..... N89-24003 #
ETN-89-94477 ..... N89-23460 #
ETN-89-94478 ..... N89-23461 #
ETN-89-94481 ..... N89-23755 #
ETN-89-94482 ..... N89-23462 #
ETN-89-94484 ..... N89-23829 #
ETN-89-94485 ..... N89-23502 #
ETN-89-94486 ..... N89-23630 #
ETN-89-94487 ..... N89-23631 #
ETN-89-94488 ..... N89-23632 #
ETN-89-94489 ..... N89-23633 #
ETN-89-94490 ..... N89-23508 #
ETN-89-94491 ..... N89-23509 #
ETN-89-94492 ..... N89-24175 #
ETN-89-94494 ..... N89-23939 #
ETN-89-94495 ..... N89-23845 #
ETN-89-94496 ..... N89-23780 #
ETN-89-94497 ..... N89-23781 #
ETN-89-94498 ..... N89-23979 #
ETN-89-94499 ..... N89-23782 #
ETN-89-94500 ..... N89-23510 #
ETN-89-94501 ..... N89-23783 #
ETN-89-94502 ..... N89-23889 #
ETN-89-94503 ..... N89-23511 #
ETN-89-94504 ..... N89-23784 #
ETN-89-94505 ..... N89-23940 #
ETN-89-94506 ..... N89-24160 #
ETN-89-94507 ..... N89-24078 #
ETN-89-94509 ..... N89-24050 #

FCC-0375-88 ..... N89-23747 #

FERMILAB-PUB-89/106-A ..... N89-24215* #

FFA-143 ..... N89-24104 #
FFA-144 ..... N89-24105 #
FFA-145 ..... N89-23816 #

FJSRL-TR-88-0003 ..... N89-23646 #

FNAL/C-88/130-T ..... N89-24108 #

FOA-B-30129-3.4 ..... N89-23957 #

FOA-C-20741-2.7 ..... N89-24077 #
FOA-C-20743-4.1 ..... N89-24149 #
FOA-C-30506-3.6 ..... N89-23777 #
FOA-C-30512-3.1 ..... N89-23778 #
FOA-C-30513-3.2 ..... N89-23779 #
FOA-C-30518-3.1 ..... N89-23804 #

FR-19625 ..... N89-23519* #
FR-688107 ..... N89-23495* #

FTD-ID(RS)T-0517-88 ..... N89-24227 #
FTD-ID(RS)T-1067-88 ..... N89-23869 #
FTD-ID(RS)T-1075-88 ..... N89-23625 #

GA-C19485 ..... N89-24196 #

GINZTON-4442 ..... N89-23856* #

GIT-88-4 ..... N89-24045 #

GKSS-88/E/40 ..... N89-24013 #
GKSS-88/E/41 ..... N89-24014 #

GL-88-2 ..... N89-23453 #

GR-104 ..... N89-23810 #

GRI-88/0165 ..... N89-23811 #
GRI-88/0245 ..... N89-23849 #
GRI-88/0246 ..... N89-24150 #
GRI-88/0248 ..... N89-23974 #
GRI-88/0273 ..... N89-23733 #
GRI-88/0283 ..... N89-23973 #
GRI-88/0289 ..... N89-23808 #
GRI-88/0321 ..... N89-23810 #
GRI-88/0329 ..... N89-23786 #

GRL/8803 ..... N89-23866 #

GTRI-A-4699-2 ..... N89-23627 #

H-1486 ..... N89-23819* #

HSD-TR-88-014-VOL-1 ..... N89-23429 #
HSD-TR-88-014-VOL-2 ..... N89-23430 #

IAF-88-037 ..... N89-24050 #

IC-88/261 ..... N89-24181 #
IC-88/274 ..... N89-24182 #
IC-88/309 ..... N89-24183 #
IC-88/310 ..... N89-24184 #
IC-88/311 ..... N89-24103 #
IC-88/330 ..... N89-24185 #

ICASE-89-20 ..... N89-24058* #
ICASE-89-21 ..... N89-23817* #
ICASE-89-22 ..... N89-24112* #
ICASE-89-24 ..... N89-24113* #
ICASE-89-26 ..... N89-24114* #

ICOMP-89-8 ..... N89-23821* #

IDA-P-2004 ..... N89-23864 #
IDA-P-2083 ..... N89-23865 #

IDA/HQ-87-31897 ..... N89-23864 #
IDA/HQ-87-33002 ..... N89-23865 #

INT-PATENT-CLASS-C22C2906 ..... N89-23686 #
INT-PATENT-CLASS-C22C3200 ..... N89-23686 #

IPP-2/296 ..... N89-24176

IPPJ-890 ..... N89-24181 #
IPPJ-899 ..... N89-24184 #

ISBN-3-7696-9390-6 ..... N89-23963
ISBN-3-89336-001-8 ..... N89-23569 #
ISBN-91-7848-108-2 ..... N89-23479 #
ISBN-951-666-275-7 ..... N89-23960 #
ISBN-951-754-573-8 ..... N89-24189 #
ISBN-951-754-658-0 ..... N89-23620 #
ISBN-951-754-661-0 ..... N89-23657 #
ISBN-951-754-707-2 ..... N89-24102 #
ISBN-952-900-084-7 ..... N89-24186 #
ISBN-952-900-399-4 ..... N89-23917 #

ISL-CO-209/87 ..... N89-23840 #
ISL-CO-244/87 ..... N89-24177 #

ISL-R-111/87-PT-1 ..... N89-23841 #
ISL-R-115/87-PT-2 ..... N89-23842 #
ISL-R-116/87 ..... N89-23843 #
ISL-R-117/87 ..... N89-23654 #

ISSN-079-6566 ..... N89-24230 #
ISSN-0065-5325 ..... N89-23963
ISSN-0169-1651 ..... N89-23997
ISSN-0178-0719 ..... N89-24238 #
ISSN-0178-0719 ..... N89-24239
ISSN-0250-1589 ..... N89-24223 #
ISSN-0261-0263 ..... N89-23957 #
ISSN-0344-9629 ..... N89-24013 #
ISSN-0344-9629 ..... N89-24014 #
ISSN-0347-3694 ..... N89-24077 #
ISSN-0347-3694 ..... N89-24149 #
ISSN-0347-3708 ..... N89-23777 #
ISSN-0347-3708 ..... N89-23778 #
ISSN-0347-3708 ..... N89-23779 #
ISSN-0347-3708 ..... N89-23804 #
ISSN-0348-7539 ..... N89-23987 #
ISSN-0348-7539 ..... N89-24163 #
ISSN-0355-2705 ..... N89-23960 #
ISSN-0366-0885 ..... N89-23660 #
ISSN-0366-0885 ..... N89-23983 #
ISSN-0366-0885 ..... N89-24146 #
ISSN-0366-0885 ..... N89-24187 #
ISSN-0366-0885 ..... N89-24212 #
ISSN-0389-4010 ..... N89-23408 #
ISSN-0389-4010 ..... N89-23409 #
ISSN-0389-4010 ..... N89-23463 #
ISSN-0389-4010 ..... N89-23464 #
ISSN-0389-4010 ..... N89-23467 #
ISSN-0389-4010 ..... N89-23504 #
ISSN-0389-4010 ..... N89-23514 #
ISSN-0389-4010 ..... N89-23635 #
ISSN-0389-4010 ..... N89-23639 #
ISSN-0389-4010 ..... N89-23806 #
ISSN-0389-4010 ..... N89-23807 #
ISSN-0389-4010 ..... N89-23873 #
ISSN-0469-4236 ..... N89-23941 #
ISSN-0469-4732 ..... N89-24161 #
ISSN-0469-4732 ..... N89-24164 #
ISSN-0784-848X ..... N89-24102 #
ISSN-0785-5168 ..... N89-23620 #
ISSN-0921-1969 ..... N89-24124 #
ISSN-0922-5641 ..... N89-24099 #
ISSN-0922-5641 ..... N89-24101 #
ISSN-0922-5641 ..... N89-24134 #

IYAF-88-73 ..... N89-23658 #
IYAF-88-82 ..... N89-24247 #

JINR-P-2-88-298 ..... N89-24107 #

JINR-R-2-88-232 ..... N89-24106 #

JPL-D-6020 ..... N89-24168* #

JPL-PUBL-87-4 ..... N89-23985* #
JPL-PUBL-87-21-REV-1 ..... N89-24060* #
JPL-PUBL-87-28-PT-1 ..... N89-23494* #

JPRS-USP-89-004 ..... N89-23484 #

JUEL-SPEZ-446 ..... N89-23569 #

JUEL-2218 ..... N89-23983 #
JUEL-2219 ..... N89-23660 #
JUEL-2221 ..... N89-24187 #
JUEL-2227 ..... N89-24146 #
JUEL-2228 ..... N89-24212 #

K/TR-89/1 ..... N89-23686 #

KNMI-WR-88-2 ..... N89-23997

KU-FRL-6132-7 ..... N89-23470* #

L-16484 ..... N89-23468* #
L-16510 ..... N89-23469* #
L-16516 ..... N89-23433* #
L-16533 ..... N89-23410* #
L-16544 ..... N89-23447* #
L-16561 ..... N89-23412* #
L-16564 ..... N89-23448* #
L-16565 ..... N89-24079* #
L-16567 ..... N89-23415* #
L-16572 ..... N89-24255* #
L-16575-PT-1 ..... N89-23528* #
L-16575-PT-2 ..... N89-23547* #

LA-UR-89-218 ..... N89-23655 #
LA-UR-89-275 ..... N89-24167 #
LA-UR-89-300 ..... N89-23857 #
LA-UR-89-598 ..... N89-24256 #
LA-UR-89-622 ..... N89-23858 #
LA-UR-89-639 ..... N89-24257 #
LA-UR-89-995 ..... N89-23690 #
LA-UR-89-1011 ..... N89-23988 #
LA-UR-89-1110 ..... N89-24243 #
LA-UR-89-1125 ..... N89-23688 #

LBL-26319 ..... N89-23684 #
LBL-26580 ..... N89-24186 #
LBL-26760 ..... N89-23863 #

LC-88-600539 ..... N89-23500 #
LC-88-600579 ..... N89-23847 #
LC-88-600580 ..... N89-23846 #
LC-88-600582 ..... N89-23679 #
LC-88-600601 ..... N89-24180 #

LIDS-P-1849 ..... N89-23440 #
LIDS-P-1851 ..... N89-24117 #

M-611 ..... N89-23892* #

MDC-K1413 ..... N89-24033* #

MEMO-707 ..... N89-24124 #

MLM-3581 ..... N89-23687 #

MM-5485-88-10 ..... N89-23933 #

MMS-87-0011 ..... N89-24005 #

MPE-PREPRINT-129 ..... N89-24239
MPE-PREPRINT-134 ..... N89-24159

MPE-REPORT-210 ..... N89-24238 #

MTL-TR-88-46 ..... N89-23935 #
MTL-TR-89-12 ..... N89-23697 #

MTR-10362 ..... N89-23770 #

NADC-88067-60 ..... N89-23671 #
NADC-88102-60 ..... N89-23626 #

NAL-PD-DU-8802 ..... N89-24098 #

NAL-PD-FM-8816 ..... N89-24097 #

NAL-TM-AE-8803 ..... N89-23805 #

NAL-TM-MT-8701 ..... N89-23677 #
NAL-TM-MT-8703 ..... N89-24178 #

NAL-TM-PR-8704 ..... N89-23477 #

NAL-TR-965 ..... N89-23514 #
NAL-TR-966 ..... N89-23635 #
NAL-TR-967 ..... N89-23806 #
NAL-TR-968 ..... N89-23408 #
NAL-TR-969 ..... N89-23464 #
NAL-TR-970T ..... N89-23807 #
NAL-TR-971 ..... N89-23463 #
NAL-TR-972 ..... N89-23467 #
NAL-TR-973 ..... N89-23873 #
NAL-TR-976T ..... N89-23409 #
NAL-TR-1001 ..... N89-23639 #
NAL-TR-1005 ..... N89-23504 #

NAS 1.15:4111 ..... N89-23433* #
NAS 1.15:4113 ..... N89-23410* #
NAS 1.15:4116 ..... N89-23447* #
NAS 1.15:4117 ..... N89-23412* #
NAS 1.15:4118 ..... N89-24255* #
NAS 1.15:4119 ..... N89-24079* #
NAS 1.15:4120 ..... N89-24232* #
NAS 1.15:100362 ..... N89-23503* #
NAS 1.15:100363 ..... N89-24044* #
NAS 1.15:100368 ..... N89-24260* #
NAS 1.15:100414 ..... N89-23819* #
NAS 1.15:100727 ..... N89-24002* #
NAS 1.15:100925 ..... N89-24216* #
NAS 1.15:101041 ..... N89-23820* #
NAS 1.15:101082 ..... N89-23785* #
NAS 1.15:101461 ..... N89-23621* #
NAS 1.15:101564 ..... N89-24140* #
NAS 1.15:101595 ..... N89-23924* #
NAS 1.15:101750 ..... N89-23493* #
NAS 1.15:101983 ..... N89-23813* #
NAS 1.15:101986 ..... N89-23691* #
NAS 1.15:101987 ..... N89-23465* #
NAS 1.15:101988 ..... N89-24055* #
NAS 1.15:101996 ..... N89-24138* #
NAS 1.15:101998 ..... N89-23413* #
NAS 1.15:102003 ..... N89-23518* #
NAS 1.15:102005 ..... N89-23809* #
NAS 1.15:102016 ..... N89-23516* #
NAS 1.15:102018 ..... N89-23417* #
NAS 1.15:102019 ..... N89-23517* #
NAS 1.15:102021 ..... N89-23520* #
NAS 1.15:102023 ..... N89-23664* #
NAS 1.15:102026 ..... N89-23821* #
NAS 1.15:102040 ..... N89-23792* #
NAS 1.15:102043 ..... N89-23416* #
NAS 1.15:102044 ..... N89-23527* #
NAS 1.15:102045 ..... N89-23753* #
NAS 1.15:102048 ..... N89-23850* #
NAS 1.15:102050 ..... N89-23522* #
NAS 1.15:102057 ..... N89-23823* #
NAS 1.15:102068 ..... N89-23791* #
NAS 1.15:102146 ..... N89-23982* #
NAS 1.15:102183 ..... N89-24111* #
NAS 1.19:259 ..... N89-23406* #
NAS 1.20:127 ..... N89-24240* #
NAS 1.21:7039(34)-SECT-2 ..... N89-24219*
NAS 1.26:4230 ..... N89-23470* #
NAS 1.26:4231 ..... N89-23471* #
NAS 1.26:4237 ..... N89-23683* #
NAS 1.26:4238 ..... N89-23860* #
NAS 1.26:177380 ..... N89-23512* #
NAS 1.26:177523 ..... N89-23414* #
NAS 1.26:179595 ..... N89-23519* #
NAS 1.26:180078 ..... N89-23956* #
NAS 1.26:180450 ..... N89-24015* #
NAS 1.26:180827 ..... N89-23757* #
NAS 1.26:180827-EXEC-SUMM ..... N89-23756* #
NAS 1.26:181375 ..... N89-24251* #
NAS 1.26:181700 ..... N89-24033* #
NAS 1.26:181766 ..... N89-23920* #
NAS 1.26:181778 ..... N89-23495* #
NAS 1.26:181782 ..... N89-23856* #
NAS 1.26:181819 ..... N89-24141* #
NAS 1.26:181822 ..... N89-23919* #
NAS 1.26:181823 ..... N89-23817* #
NAS 1.26:181825 ..... N89-24058* #
NAS 1.26:181828 ..... N89-24082* #
NAS 1.26:181831 ..... N89-24114* #
NAS 1.26:181833 ..... N89-24112* #
NAS 1.26:181834 ..... N89-24113* #
NAS 1.26:182185 ..... N89-23638* #
NAS 1.26:182257-VOL-1 ..... N89-24139* #
NAS 1.26:182265 ..... N89-23851* #
NAS 1.26:182266 ..... N89-23501* #
NAS 1.26:182281 ..... N89-23918* #
NAS 1.26:182285 ..... N89-23818* #
NAS 1.26:182291 ..... N89-23622* #
NAS 1.26:182912 ..... N89-23693* #
NAS 1.26:183430 ..... N89-23855* #
NAS 1.26:183568 ..... N89-23634* #
NAS 1.26:183580 ..... N89-23515* #
NAS 1.26:183615 ..... N89-23521* #
NAS 1.26:183650 ..... N89-23523* #
NAS 1.26:184798 ..... N89-23678* #
NAS 1.26:184802 ..... N89-24231* #
NAS 1.26:184831 ..... N89-23746* #
NAS 1.26:184845 ..... N89-23619* #
NAS 1.26:184857 ..... N89-24054* #
NAS 1.26:184859 ..... N89-24129* #
NAS 1.26:184895 ..... N89-24024* #
NAS 1.26:184897 ..... N89-23926* #
NAS 1.26:184898 ..... N89-23928* #
NAS 1.26:184909 ..... N89-24162* #
NAS 1.26:184912 ..... N89-23478* #
NAS 1.26:184939 ..... N89-23890* #
NAS 1.26:184940 ..... N89-23891* #
NAS 1.26:184958 ..... N89-24142* #
NAS 1.26:184960 ..... N89-23812* #
NAS 1.26:184969 ..... N89-23875* #
NAS 1.26:184976 ..... N89-23736* #
NAS 1.26:184977 ..... N89-23876* #
NAS 1.26:184990 ..... N89-24233* #
NAS 1.26:184991 ..... N89-23961* #
NAS 1.26:184992 ..... N89-23418* #
NAS 1.26:185019 ..... N89-23985* #
NAS 1.26:185021 ..... N89-24060* #
NAS 1.26:185022 ..... N89-23494* #
NAS 1.26:185057 ..... N89-23852* #
NAS 1.26:185314 ..... N89-24168* #
NAS 1.26:185315 ..... N89-23927* #
NAS 1.26:185316 ..... N89-23925* #
NAS 1.26:185318 ..... N89-24215* #
NAS 1.26:185320 ..... N89-23766* #
NAS 1.26:185326 ..... N89-23411* #
NAS 1.26:185442 ..... N89-23995* #
NAS 1.55:3027 ..... N89-23415* #
NAS 1.55:3032 ..... N89-23892* #
NAS 1.55:3035-PT-1 ..... N89-23528* #
NAS 1.55:3035-PT-2 ..... N89-23547* #
NAS 1.55:10026-VOL-1 ..... N89-24022* #
NAS 1.55:10026-VOL-2 ..... N89-24023* #
NAS 1.60:2907 ..... N89-23468* #
NAS 1.60:2908 ..... N89-23469* #
NAS 1.61:1220 ..... N89-23448* #
NAS 1.71:LAR-13696-1 ..... N89-23880* #
NAS 1.71:LAR-14049-1 ..... N89-23466* #
NAS 1.71:LAR-14101-1 ..... N89-23692* #
NAS 1.71:LEW-14734-1 ..... N89-23623* #
NAS 1.71:MFS-29489-1 ..... N89-23739* #
NAS 1.71:MFS-29491-1 ..... N89-23738* #
NAS 1.71:MSC-21348-1 ..... N89-24084* #
NAS 1.71:NPO-17562-1-CU ..... N89-24153* #

NASA-CASE-LAR-13696-1 ..... N89-23880* #
NASA-CASE-LAR-14049-1 ..... N89-23466* #
NASA-CASE-LAR-14101-1 ..... N89-23692* #

NASA-CASE-LEW-14734-1 ..... N89-23623* #

NASA-CASE-MFS-29489-1 ..... N89-23739* #
NASA-CASE-MFS-29491-1 ..... N89-23738* #

NASA-CASE-MSC-21348-1 ..... N89-24084* #

NASA-CASE-NPO-17562-1-CU ..... N89-24153* #

NASA-CP-3027 ..... N89-23415* #
NASA-CP-3032 ..... N89-23892* #
NASA-CP-3035-PT-1 ..... N89-23528* #
NASA-CP-3035-PT-2 ..... N89-23547* #
NASA-CP-10026-VOL-1 ..... N89-24022* #
NASA-CP-10026-VOL-2 ..... N89-24023* #

NASA-CR-4230 ..... N89-23470* #
NASA-CR-4231 ..... N89-23471* #
NASA-CR-4237 ..... N89-23683* #
NASA-CR-4238 ..... N89-23860* #
NASA-CR-177380 ..... N89-23512* #
NASA-CR-177523 ..... N89-23414* #
NASA-CR-179595 ..... N89-23519* #
NASA-CR-180078 ..... N89-23956* #
NASA-CR-180450 ..... N89-24015* #
NASA-CR-180827 ..... N89-23757* #
NASA-CR-180827-EXEC-SUMM ..... N89-23756* #
NASA-CR-181375 ..... N89-24251* #
NASA-CR-181700 ..... N89-24033* #
NASA-CR-181766 ..... N89-23920* #
NASA-CR-181778 ..... N89-23495* #
NASA-CR-181782 ..... N89-23856* #
NASA-CR-181819 ..... N89-24141* #
NASA-CR-181822 ..... N89-23919* #
NASA-CR-181823 ..... N89-23817* #
NASA-CR-181825 ..... N89-24058* #
NASA-CR-181828 ..... N89-24082* #
NASA-CR-181831 ..... N89-24114* #
NASA-CR-181833 ..... N89-24112* #
NASA-CR-181834 ..... N89-24113* #
NASA-CR-182185 ..... N89-23638* #
NASA-CR-182257-VOL-1 ..... N89-24139* #
NASA-CR-182265 ..... N89-23851* #
NASA-CR-182266 ..... N89-23501* #
NASA-CR-182281 ..... N89-23918* #
NASA-CR-182285 ..... N89-23818* #
NASA-CR-182291 ..... N89-23622* #
NASA-CR-182912 ..... N89-23693* #
NASA-CR-183430 ..... N89-23855* #
NASA-CR-183568 ..... N89-23634* #
NASA-CR-183580 ..... N89-23515* #
NASA-CR-183615 ..... N89-23521* #
NASA-CR-183650 ..... N89-23523* #
NASA-CR-184798 ..... N89-23678* #
NASA-CR-184802 ..... N89-24231* #
NASA-CR-184831 ..... N89-23746* #
NASA-CR-184845 ..... N89-23619* #
NASA-CR-184857 ..... N89-24054* #
NASA-CR-184859 ..... N89-24129* #
NASA-CR-184895 ..... N89-24024* #
NASA-CR-184897 ..... N89-23926* #
NASA-CR-184898 ..... N89-23928* #
NASA-CR-184909 ..... N89-24162* #
NASA-CR-184912 ..... N89-23478* #
NASA-CR-184939 ..... N89-23890* #
NASA-CR-184940 ..... N89-23891* #
NASA-CR-184958 ..... N89-24142* #
NASA-CR-184960 ..... N89-23812* #
NASA-CR-184969 ..... N89-23875* #
NASA-CR-184976 ..... N89-23736* #
NASA-CR-184977 ..... N89-23876* #
NASA-CR-184990 ..... N89-24233* #
NASA-CR-184991 ..... N89-23961* #
NASA-CR-184992 ..... N89-23418* #
NASA-CR-185019 ..... N89-23985* #
NASA-CR-185021 ..... N89-24060* #
NASA-CR-185022 ..... N89-23494* #
NASA-CR-185057 ..... N89-23852* #
NASA-CR-185314 ..... N89-24168* #
NASA-CR-185315 ..... N89-23927* #
NASA-CR-185316 ..... N89-23925* #
NASA-CR-185318 ..... N89-24215* #
NASA-CR-185320 ..... N89-23766* #
NASA-CR-185326 ..... N89-23411* #
NASA-CR-185442 ..... N89-23995* #

NASA-EP-259 ..... N89-23406* #

NASA-NF-127 ..... N89-24240* #

NASA-RP-1220 ..... N89-23448* #

NASA-SP-7039(34)-SECT-2 ..... N89-24219*

NASA-TM-4111 ..... N89-23433* #
NASA-TM-4113 ..... N89-23410* #
NASA-TM-4116 ..... N89-23447* #
NASA-TM-4117 ..... N89-23412* #
NASA-TM-4118 ..... N89-24255* #
NASA-TM-4119 ..... N89-24079* #
NASA-TM-4120 ..... N89-24232* #
NASA-TM-100362 ..... N89-23503* #
NASA-TM-100363 ..... N89-24044* #
NASA-TM-100368 ..... N89-24260* #
NASA-TM-100414 ..... N89-23819* #
NASA-TM-100727 ..... N89-24002* #
NASA-TM-100925 ..... N89-24216* #
NASA-TM-101041 ..... N89-23820* #

NASA-TM-101082 N89-23785* #
NASA-TM-101461 N89-23621* #
NASA-TM-101564 N89-24140* #
NASA-TM-101595 N89-23924* #
NASA-TM-101750 N89-23493* #
NASA-TM-101983 N89-23813* #
NASA-TM-101986 N89-23691* #
NASA-TM-101987 N89-23465* #
NASA-TM-101988 N89-24055* #
NASA-TM-101996 N89-24138* #
NASA-TM-101998 N89-23413* #
NASA-TM-102003 N89-23518* #
NASA-TM-102005 N89-23809* #
NASA-TM-102016 N89-23516* #
NASA-TM-102018 N89-23417* #
NASA-TM-102019 N89-23517* #
NASA-TM-102021 N89-23520* #
NASA-TM-102023 N89-23664* #
NASA-TM-102026 N89-23821* #
NASA-TM-102040 N89-23792* #
NASA-TM-102043 N89-23416* #
NASA-TM-102044 N89-23527* #
NASA-TM-102045 N89-23753* #
NASA-TM-102048 N89-23850* #
NASA-TM-102050 N89-23522* #
NASA-TM-102057 N89-23823* #
NASA-TM-102068 N89-23791* #
NASA-TM-102146 N89-23982* #
NASA-TM-102183 N89-24111* #

NASA-TP-2907 N89-23468* #
NASA-TP-2908 N89-23469* #

NAVAIR-50-1C-551 N89-24005 #
NAVAIR-50-1C-554 N89-24006 #

NAVY-CASE-68403 N89-24155 #

NBSIR-88/3097 N89-23748 #

NCAR/TN-325+EDD N89-23749 #

NCEL-TN-1792 N89-23962 #

NCS-TIB-88-5 N89-23776 #

NEAR-TR-397 N89-23431 #
NEAR-TR-398 N89-23831 #

NEDU-1-89 N89-24025 #

NHRC-88-50 N89-24027 #

NIST-GCR-89-557 N89-23636 #

NIST-SP-400-81 N89-24180 #

NIST-TN-1323 N89-23750 #

NIST/SP-250/23 N89-23846 #
NIST/SP-755 N89-23847 #
NIST/SP-758 N89-23679 #

NISTIR-88/3839 N89-23884 #
NISTIR-88/3892 N89-23680 #
NISTIR-88/3901 N89-24213 #
NISTIR-88/3902 N89-23637 #
NISTIR-88/4001 N89-24052 #
NISTIR-89/4024 N89-23735 #

NLR-MP-88003-U N89-23656 #

NLR-TR-88005-U N89-23815 #

NORDA-TN-385 N89-23766* #

NPRDC-TR-89-6 N89-24035 #

NPS53-89-008 N89-24115 #
NPS53-89-012 N89-23827 #

NRL-MR-6290 N89-23442 #
NRL-MR-6367 N89-23838 #
NRL-MR-6388 N89-23872 #
NRL-MR-6400 N89-23513 #
NRL-MR-6417 N89-23676 #
NRL-MR-6419 N89-23801 #
NRL-MR-6422 N89-23854 #
NRL-MR-6425 N89-24148 #

NRL-9080 N89-23765 #
NRL-9177 N89-23771 #
NRL-9178 N89-24116 #
NRL-9182 N89-23764 #

NSF/ENG-88015 N89-23681 #

NSMRL-1095 N89-24034 #

NTS-TR-1524-1 N89-24150 #
NTS-TR-6005 N89-23849 #

NTSB/AAR-88/10 N89-23436 #

NTSB/ARC-89/01 N89-23434 #

NTSC-TR-88-028 N89-24036 #

ONR-TR-7 N89-24205 #
ONR-TR-35 N89-23650 #
ONR-TR-89-2 N89-24042 #
ONR-TR-89-3 N89-24095 #
ONR-TR-89-4 N89-24037 #

ORNL/TM-10991 N89-24083 #

OTA-TM-ISC-28 N89-23500 #

OUEL-1695/87 N89-24165 #
OUEL-1718/88 N89-24089 #
OUEL-1723/88 N89-24090 #
OUEL-1734/88 N89-24091 #
OUEL-1737/88 N89-23737 #

PATENTS-US-A7181630 N89-23663 #

PB88-910412 N89-23436 #
PB89-128888 N89-23846 #
PB89-132062 N89-24222 #
PB89-134829 N89-23747 #
PB89-135123 N89-23980 #
PB89-136139 N89-23874 #
PB89-136147 N89-23734 #
PB89-136402 N89-23500 #
PB89-139091 N89-24080 #
PB89-139307 N89-24221 #
PB89-139414 N89-24220 #
PB89-139943 N89-24250 #
PB89-140859 N89-23733 #
PB89-140867 N89-23811 #
PB89-141279 N89-23479 #
PB89-142590 N89-23974 #
PB89-142616 N89-23973 #
PB89-143432 N89-23957 #
PB89-144604 N89-23749 #
PB89-144638 N89-24001 #
PB89-144950 N89-23915 #
PB89-145098 N89-23808 #
PB89-145106 N89-23810 #
PB89-145718 N89-24143 #
PB89-146039 N89-23656 #
PB89-146062 N89-24100 #
PB89-146070 N89-24043 #
PB89-146088 N89-24056 #
PB89-146104 N89-23787 #
PB89-146112 N89-23958 #
PB89-146120 N89-24134 #
PB89-146138 N89-24101 #
PB89-146146 N89-24099 #
PB89-146278 N89-23680 #
PB89-146476 N89-24102 #
PB89-147524 [illegible]3657 #
PB89-147532 [illegible]3820 #
PB89-147847 N89-23748 #
PB89-148191 N89-23681 #
PB89-148332 N89-23847 #
PB89-148357 N89-23679 #
PB89-148373 N89-24213 #
PB89-148407 N89-23637 #
PB89-148878 N89-23849 #
PB89-148886 N89-24150 #
PB89-148944 N89-23786 #
PB89-151021 N89-23434 #
PB89-151427 N89-23981 #
PB89-151625 N89-23884 #
PB89-151781 N89-23636 #
PB89-151807 N89-24052 #
PB89-151823 N89-23735 #
PB89-151831 N89-24180 #
PB89-153886 N89-23750 #

PNL-SA-15444 N89-23976 #
PNL-SA-16273 N89-23659 #
PNL-SA-16279 N89-24228 #

POLY-AE-88-8 N89-23452 #

PSI-2062/TR-890 N89-23851* #

PUBL-89605-VOL-1 N89-23523* #

P248-FR N89-24009 #

R/D-4943-PH-01 N89-23798 #

RADC-TR-87-227 N89-23441 #
RADC-TR-88-213 N89-24069 #
RADC-TR-88-215 N89-23797 #
RADC-TR-88-229 N89-24157 #
RADC-TR-168-VOL-1 N89-23885 #
RADC-TR-168-VOL-2 N89-23886 #

REPT-37 N89-24102 #
REPT-88.2 N89-23787 #
REPT-88-1 N89-23958 #
REPT-88-53 N89-24043 #
REPT-88-56 N89-24099 #
REPT-88-60 N89-24056 #
REPT-88-62 N89-24100 #
REPT-88-63 N89-24101 #
REPT-88-77 N89-24134 #
REPT-89B00097 N89-24002* #
REPT-882-111-101 N89-23460 #
REPT-882-111-102 N89-23461 #
REPT-882-320-103 N89-23755 #
REPT-882-320-104 N89-23462 #
REPT-882-430-102 N89-23629 #
REPT-882-430-104 N89-23502 #
REPT-882-430-105 N89-23630 #
REPT-882-430-106 N89-23631 #
REPT-882-430-107 N89-23632 #
REPT-882-430-108 N89-23633 #
REPT-882-430-109 N89-23508 #
REPT-882-430-110 N89-23509 #
REPT-882-430-111 N89-24175 #
REPT-882-440-101 N89-23939 #
REPT-882-440-102 N89-23845 #
REPT-882-440-103 N89-23780 #
REPT-882-440-104 N89-23781 #
REPT-882-440-105 N89-23979 #
REPT-882-440-106 N89-23782 #
REPT-882-440-107 N89-23510 #
REPT-882-440-108 N89-23783 #
REPT-882-440-109 N89-23889 #
REPT-882-440-110 N89-23511 #
REPT-882-440-111 N89-23784 #
REPT-882-440-112 N89-23940 #
REPT-882-440-113 N89-24160 #
REPT-882-440-114 N89-24078 #
REPT-882-440-116 N89-24050 #

RI/RD89-104 N89-23521* #

RSRE-MEMO-4131 N89-23444 #

RTR-090-01 N89-23515* #

SAND-88-0943C N89-24195 #
SAND-88-2551 N89-23922 #
SAND-88-2720C N89-23752 #
SAND-88-3478 N89-24110 #
SAND-89-0404C N89-23877 #

SD-TR-86-49 N89-23694 #
SD-TR-89-05 N89-23995* #
SD-TR-89-07 N89-23506 #
SD-TR-89-10 N89-23803 #

SER-C-342 N89-23963

SGD-531-PT-1 N89-24250 #

SP-RAPP-1988:23 N89-23479 #

SR-1 N89-23497 #
SR-5 N89-23993 #

SRA-R88-920029-F N89-23833 #

SU-SLAC-PUB-4900 N89-23793 #

T-4277 N89-23512* #

TACOM-TR-13389 N89-24096 #

TD-002-342-444-0002 N89-24129* #

TF-35 N89-23829 #
TF-42 N89-23420 #

TKK-V-B40 N89-23657 #
TKK-V-B41 N89-23620 #

TL-SEAL-1-89 N89-23876* #

TR-1 N89-23703 #
TR-1 N89-24207 #
TR-4 N89-23672 #
TR-7 N89-23883 #

TR-9 ..... N89-23708 #
TR-19 ..... N89-23704 #
TR-34 ..... N89-23649 #
TR-89-1 ..... N89-24040 #
TR-413 ..... N89-24126 #
TR-414 ..... N89-24118 #
TR-0066(6409-11)-1 ..... N89-23694 #
TR-0066A(2925-06)-1 ..... N89-23803 #
TR-0088(3940-05)-5 ..... N89-23506 #
TR-0088(3940-06)-6 ..... N89-23995* #

TRITA-EPP-88-11 ..... N89-23987 #
TRITA-EPP-89-02 ..... N89-24163 #

TWR-17591-VOL-1 ..... N89-23523* #

UBUFFALO/DC/89/TR-91 ..... N89-24198 #
UBUFFALO/DC/89/TR-92 ..... N89-24197 #
UBUFFALO/DC/89/TR-93 ..... N89-24136 #

UCI-ICS-TR-86-24-REV ..... N89-24122 #

UCID-20366-89 ..... N89-24229 #

UCRL-99435 ..... N89-23959 #
UCRL-99951 ..... N89-23859 #
UCRL-99999 ..... N89-24152 #
UCRL-100028 ..... N89-23984 #
UCRL-100083 ..... N89-24151 #
UCRL-100343 ..... N89-24258 #
UCRL-100472 ..... N89-24193 #
UCRL-100617 ..... N89-23861 #

UILU-ENG-88-1724 ..... N89-24109 #
UILU-ENG-88-2262 ..... N89-23796 #
UILU-ENG-88-2264 ..... N89-24092 #

UIUCDCS-R-89-1505 ..... N89-24109 #

US-PATENT-APPL-SN-181630 ..... N89-23663 #
US-PATENT-APPL-SN-204152 ..... N89-23474 #
US-PATENT-APPL-SN-208931 ..... N89-24155 #
US-PATENT-APPL-SN-246703 ..... N89-23702 #
US-PATENT-APPL-SN-266045 ..... N89-23692* #
US-PATENT-APPL-SN-267146 ..... N89-23680* #
US-PATENT-APPL-SN-270189 ..... N89-23466* #
US-PATENT-APPL-SN-277596 ..... N89-24153* #
US-PATENT-APPL-SN-279624 ..... N89-23623* #
US-PATENT-APPL-SN-279625 ..... N89-23739* #
US-PATENT-APPL-SN-279677 ..... N89-23738* #
US-PATENT-APPL-SN-283106 ..... N89-24084* #
US-PATENT-APPL-SN-316710 ..... N89-24202 #

USAFETAC/DS-88/206 ..... N89-24007 #

USAFSAM-TR-88-24 ..... N89-24032 #

USARIEM-M17-89 ..... N89-24039 #
USARIEM-M19-89 ..... N89-23744 #
USARIEM-M23-89 ..... N89-24029 #
USARIEM-M27-89 ..... N89-24030 #

UTEC-MD-88-050 ..... N89-23797 #

UTRC/R89-917259-1 ..... N89-23700 #

UVA/525683/AM89/102 ..... N89-23507 #

VLSI-M-88-493 ..... N89-24081 #

WHC-SA-0504 ..... N89-24059 #

WHOI-88-59 ..... N89-24011 #

WMSI-WP-363 ..... N89-24064 #

WRDC-TR-89-3035 ..... N89-23432 #

YALEU/DCS/RR-680 ..... N89-24133 #

YALEU/DCS/TR-655 ..... N89-24120 #
YALEU/DCS/TR-677 ..... N89-24076 #
YALEU/DCS/TR-685 ..... N89-24121 #

FEDERAL REGIONAL DEPOSITORY LIBRARIES

ALABAMA

AUBURN UNIV. AT MONTGOMERY LIBRARY
Documents Department
Montgomery, AL 36193
(205) 271-9650

UNIV. OF ALABAMA LIBRARY
Documents Dept.-Box S
University, AL 35486
(205) 348-6046

ARIZONA

DEPT. OF LIBRARY, ARCHIVES AND PUBLIC RECORDS
Third Floor—State Cap.
1700 West Washington
Phoenix, AZ 85007
(602) 255-4121

UNIVERSITY OF ARIZONA LIB.
Government Documents Dept.
Tucson, AZ 85721
(602) 621-6433

ARKANSAS

ARKANSAS STATE LIBRARY
One Capitol Mall
Little Rock, AR 72201
(501) 371-2326

CALIFORNIA

CALIFORNIA STATE LIBRARY
Govt. Publications Section
P.O. Box 2037
Sacramento, CA 95809
(916) 324-4863

COLORADO

UNIV OF COLORADO LIB.
Government Pub. Division
Campus Box 184
Boulder, CO 80309
(303) 492-8834

DENVER PUBLIC LIBRARY
Govt. Pub. Department
1357 Broadway
Denver, CO 80203
(303) 571-2131

CONNECTICUT

CONNECTICUT STATE LIBRARY
Government Documents Unit
231 Capitol Avenue
Hartford, CT 06106
(203) 566-7029

FLORIDA

UNIV. OF FLORIDA LIBRARIES
Library West
Documents Department
Gainesville, FL 32611
(904) 392-0367

GEORGIA

UNIV. OF GEORGIA LIBRARIES
Government Reference Dept.
Athens, GA 30602
(404) 542-8949

HAWAII

UNIV. OF HAWAII LIBRARY
Govt. Documents Collection
2550 The Mall
Honolulu, HI 96822
(808) 948-8230

IDAHO

UNIV. OF IDAHO LIBRARY
Documents Section
Moscow, ID 83843
(208) 885-6344

ILLINOIS

ILLINOIS STATE LIBRARY
Information Services Branch
Centennial Building
Springfield, IL 62756
(217) 782-5185

INDIANA

INDIANA STATE LIBRARY
Serials Documents Section
140 North Senate Avenue
Indianapolis, IN 46204
(317) 232-3686

IOWA

UNIV. OF IOWA LIBRARIES
Govt. Documents Department
Iowa City, IA 52242
(319) 353-3318

KANSAS

UNIVERSITY OF KANSAS
Doc. Collect—Spencer Lib.
Lawrence, KS 66045-2800
(913) 864-4662

KENTUCKY

UNIV. OF KENTUCKY LIBRARIES
Govt. Pub. Department
Lexington, KY 40506-0039
(606) 257-3139

LOUISIANA

LOUISIANA STATE UNIVERSITY
Middleton Library
Govt. Docs. Dept.
Baton Rouge, LA 70803
(504) 388-2570

LOUISIANA TECHNICAL UNIV. LIBRARY
Documents Department
Ruston, LA 71272-0046
(318) 257-4962

MAINE

UNIVERSITY OF MAINE
Raymond H. Fogler Library
Tri-State Regional Documents Depository
Orono, ME 04469
(207) 581-1680

MARYLAND

UNIVERSITY OF MARYLAND
McKeldin Lib.—Doc. Div.
College Park, MD 20742
(301) 454-3034

MASSACHUSETTS

BOSTON PUBLIC LIBRARY
Government Docs. Dept.
Boston, MA 02117
(617) 536-5400 ext.226

MICHIGAN

DETROIT PUBLIC LIBRARY
Sociology Department
5201 Woodward Avenue
Detroit, MI 48202-4093
(313) 833-1409

MICHIGAN STATE LIBRARY
P.O. Box 30007
Lansing, MI 48909
(517) 373-1593

MINNESOTA

UNIVERSITY OF MINNESOTA
Government Pubs. Division
409 Wilson Library
309 19th Avenue South
Minneapolis, MN 55455
(612) 373-7870

MISSISSIPPI

UNIV. OF MISSISSIPPI LIB.
Documents Department
University, MS 38677
(601) 232-5857

MONTANA

UNIV. OF MONTANA
Mansfield Library
Documents Division
Missoula, MT 59812
(406) 243-6700

NEBRASKA

UNIVERSITY OF NEBRASKA - LINCOLN
Love Library
Documents Department
Lincoln, NE 68588-0410
(402) 472-2562

NEVADA

UNIVERSITY OF NEVADA LIB.
Govt. Pub. Department
Reno, NV 89557-0044
(702) 784-6579

NEW JERSEY

NEWARK PUBLIC LIBRARY
5 Washington Street
Newark, NJ 07101-0630
(201) 733-7812

NEW MEXICO

UNIVERSITY OF NEW MEXICO
Zimmerman Library
Government Pub. Dept.
Albuquerque, NM 87131
(505) 277-5441

NEW MEXICO STATE LIBRARY
Reference Department
325 Don Gaspar Avenue
Santa Fe, NM 87503
(505) 827-3826

NEW YORK

NEW YORK STATE LIBRARY
Empire State Plaza
Albany, NY 12230
(518) 474-5563

NORTH CAROLINA

UNIVERSITY OF NORTH CAROLINA AT CHAPEL HILL
Davis Library
BA/SS Documents Division
Chapel Hill, NC 27515
(919) 962-1151

NORTH DAKOTA

UNIVERSITY OF NORTH DAKOTA
Chester Fritz Library
Documents Department
Grand Forks, ND 58202
(701) 777-4629
In cooperation with North Dakota State Univ. Library

OHIO

STATE LIBRARY OF OHIO
Documents Department
65 South Front Street
Columbus, OH 43266-0334
(614) 462-7051

OKLAHOMA

OKLAHOMA DEPT. OF LIB.
Government Documents
200 NE 18th Street
Oklahoma City, OK 73105
(405) 521-2502, ext. 252

OKLAHOMA STATE UNIV. LIB.
Documents Department
Stillwater, OK 74078
(405) 624-6546

OREGON

PORTLAND STATE UNIV. LIB.
Documents Department
P.O. Box 1151
Portland, OR 97207
(503) 229-3673

PENNSYLVANIA

STATE LIBRARY OF PENN.
Government Pub. Section
P.O. Box 1601
Harrisburg, PA 17105
(717) 787-3752

TEXAS

TEXAS STATE LIBRARY
Public Services Department
P.O. Box 12927—Cap. Sta.
Austin, TX 78711
(512) 475-2996

TEXAS TECH. UNIV. LIBRARY
Govt. Documents Department
Lubbock, TX 79409
(806) 742-2268

UTAH

UTAH STATE UNIVERSITY
Merrill Library, U.M.C. 30
Logan, UT 84322
(801) 750-2682

VIRGINIA

UNIVERSITY OF VIRGINIA
Alderman Lib.—Public Doc.
Charlottesville, VA 22903-2498
(804) 924-3133

WASHINGTON

WASHINGTON STATE LIBRARY
Documents Section
Olympia, WA 98504
(206) 753-4027

WEST VIRGINIA

WEST VIRGINIA UNIV. LIB.
Documents Department
Morgantown, WV 26506-6069
(304) 293-3640

WISCONSIN

MILWAUKEE PUBLIC LIBRARY
814 West Wisconsin Avenue
Milwaukee, WI 53233
(414) 278-3065

ST. HIST LIB. OF WISCONSIN
Government Pub. Section
816 State Street
Madison, WI 53706
(608) 262-4347

WYOMING

WYOMING STATE LIBRARY
Supreme Ct. & Library Bld.
Cheyenne, WY 82002
(307) 777-5919

National Aeronautics and
Space Administration
Code NTT-4
Washington, D.C.
20546

Official Business

Penalty for Private Use, $300

SPECIAL FOURTH-CLASS RATE
POSTAGE & FEES PAID
NASA
PERMIT No G 27

NASA

POSTMASTER: If Undeliverable (Section 158
Postal Manual) Do Not Return